

SPRINGER
REFERENCE

Jyotishkumar Parameswaranpillai
Nishar Hameed
Jürgen Pionteck
Eamor M. Woo
Editors

Handbook of Epoxy Blends

 Springer

Handbook of Epoxy Blends

Jyotishkumar Parameswaranpillai
Nishar Hameed • Jürgen Pionteck
Eamor M. Woo
Editors

Handbook of Epoxy Blends

With 558 Figures and 82 Tables

 Springer

Editors

Jyotishkumar Parameswaranpillai
Department of Polymer Science and Rubber
Technology
Cochin University of Science and
Technology
Kochi, India

Nishar Hameed
Institute for Frontier Materials
Deakin University
Geelong, Victoria, Australia

Jürgen Pionteck
Leibniz-Institut für Polymerforschung
Dresden e.V.
Dresden, Germany

Eamor M. Woo
Department of Chemical Engineering
National Cheng Kung University
Taiwan, China

ISBN 978-3-319-40041-9

ISBN 978-3-319-40043-3 (eBook)

ISBN 978-3-319-40042-6 (print and electronic bundle)

DOI 10.1007/978-3-319-40043-3

Library of Congress Control Number: 2017938023

© Springer International Publishing AG 2017

This work is subject to copyright. All rights are reserved by the Publisher, whether the whole or part of the material is concerned, specifically the rights of translation, reprinting, reuse of illustrations, recitation, broadcasting, reproduction on microfilms or in any other physical way, and transmission or information storage and retrieval, electronic adaptation, computer software, or by similar or dissimilar methodology now known or hereafter developed.

The use of general descriptive names, registered names, trademarks, service marks, etc. in this publication does not imply, even in the absence of a specific statement, that such names are exempt from the relevant protective laws and regulations and therefore free for general use.

The publisher, the authors and the editors are safe to assume that the advice and information in this book are believed to be true and accurate at the date of publication. Neither the publisher nor the authors or the editors give a warranty, express or implied, with respect to the material contained herein or for any errors or omissions that may have been made. The publisher remains neutral with regard to jurisdictional claims in published maps and institutional affiliations.

Printed on acid-free paper

This Springer imprint is published by Springer Nature

The registered company is Springer International Publishing AG

The registered company address is: Gewerbestrasse 11, 6330 Cham, Switzerland

Preface

Epoxy resins, perhaps the most versatile thermosetting polymers, have been the center of research and industrial attraction since its commercial introduction, mainly due to good processability, cost effectiveness, high performance characteristics, and possibility of tremendous applications from automobiles to space crafts to sophisticated electronic components. Over the past several decades, academic and industrial research has been focused mainly to alleviate the intrinsic brittleness of epoxy resins, the main constraint which adversely restricts many of their potential applications as high performance engineering materials. The dedicated efforts from researchers in laboratories all over the world have unequivocally established that the incorporation of appropriate amount of judiciously selected functionalized elastomers or engineering thermoplastics or block copolymers can effectively improve the performance characteristics of these materials. Recently, this field has experienced an impressive renaissance mainly due to the introduction of sophisticated instruments to explore the nanostructured features of these materials and to establish structure-property correlations. This leads to an exponential upsurge in the number of papers, reviews, and patents in this field.

In the light of all these developments, we considered it important to edit a book encompassing all the pertinent developments happened in this area and to present a contemporary overview of the entire field. *Handbook of Epoxy Blends* is designed to provide not only a convenient source of information but also an intuitive insight into further advances and future directions of research to those who desire to specialize further in this field. By judicious editing, we have ensured that the book will be beneficial to the beginners, researchers, industrialists, and practitioners in this area of research. Moreover, in an attempt to scrutinize the topic from different perspectives, we also paid much attention to utilize the expertise of emerging scientists and established researchers in this area.

The book is divided into three parts. Each part brings together all the aspects concerning epoxy blends including the state-of-the-art, opportunities, challenges, preparation, processing, characterization, analytical and numerical approaches, and down-to-earth applications. In *Part 1*, 14 chapters are structured in a comprehensive manner to provide an integrated overview of all the pertinent aspects related to epoxy/rubber blends. *Part 2* provides a succinct organization of 13 chapters dealing

with epoxy/thermoplastic blends, and *Part 3* encompasses concise but comprehensive overview of epoxy/block copolymer blends in 10 chapters.

The editors are extremely grateful to the contributors of all chapters for their sincere support and commitment. We are indebted to Springer editorial office and publishing team for their kind support in the preparation and publication of this book. We wish that all class of readers will enjoy using this book and will find the book informative and instructive. We also hope that the book will serve as a valuable reference for those who work in this area and a guide for a novice in this field.

India

Australia

Germany

Taiwan

Jyotishkumar Parameswaranpillai

Nishar Hameed

Jürgen Pionteck

Eamor M. Woo

Contents

Volume 1

Part I Epoxy/Rubber Blends	1
1 Introduction to Rubber Toughened Epoxy Polymers	3
Shi-Ai Xu and Xiao-Xue Song	
2 Novel Techniques for the Preparation of Different Epoxy/Rubber Blends	29
Bluma Guenther Soares and Sebastien Livi	
3 Miscibility and Phase Separation of Epoxy/Rubber Blends	69
Shi-Ai Xu	
4 Morphology of Epoxy/Rubber Blends	101
P. Poornima Vijayan	
5 Spectroscopic Analysis of Epoxy/Rubber Blends	147
Zhengguang Heng, Yang Chen, Huawei Zou, and Mei Liang	
6 Rheology of Epoxy/Rubber Blends	185
Padmanabhan Krishnan	
7 Cure Kinetics of Epoxy/Rubber Polymer Blends	211
Debora Puglia and José Maria Kenny	
8 Dynamic Mechanical Thermal Analysis of Epoxy/Rubber Blends	239
Qinghua Zhang, Ren He, and Xiaoli Zhan	
9 Thermal Properties of Epoxy/Rubber Blends	249
Shoubing Chen, Tingmei Wang, and Qihua Wang	
10 Mechanical Properties of Epoxy/Rubber Blends	279
Hanieh Kargarzadeh, Ishak Ahmad, and Ibrahim Abdullah	
11 Water Sorption and Solvent Sorption Behavior of Epoxy/Rubber Polymer Blends	315
Padmanabhan Krishnan	

12 Ternary System of Epoxy/Rubber Blend Clay Nanocomposite . . .	339
Nor Yuliana Yuhana	
13 Particulate Composites Based on Epoxy/Rubber Blends	371
B. Kothandaraman	
14 Applications of Epoxy/Rubber Blends	399
B. T. Marouf and R. Bagheri	

Volume 2

Part II Epoxy/Thermoplastic Blends	427
15 Introduction to Epoxy/Thermoplastic Blends	429
Jinyan Wang, Rui Liu, and Xigao Jian	
16 Novel Techniques for the Preparation of Different Epoxy/Thermoplastic Blends	459
Xiaole Cheng and Jeffrey S. Wiggins	
17 Miscibility, Phase Separation, and Mechanism of Phase Separation in Epoxy/Thermoplastic Blends	487
Fenghua Chen, Yan Zhang, Tongchen Sun, and Charles C. Han	
18 Morphology of Epoxy/Thermoplastic Blends	523
Yingfeng Yu, Gebin Shen, and Zhuoyu Liu	
19 Light Scattering of Epoxy/Thermoplastic Blends	557
Anbazhagan Palanisamy and Nishar Hameed	
20 Spectroscopic Analysis of Epoxy/Thermoplastic Blends	583
Juan Carlos Cabanelas, Claire Antonelli, Verónica San Miguel, Berna Serrano, and Juan Baselga	
21 Rheology of Epoxy/Thermoplastic Blends	613
Leah M. Johnson and Nicolas D. Huffman	
22 Cure Kinetics of Epoxy/Thermoplastic Blends	649
Bejoy Francis	
23 Dynamic Mechanical Thermal Analysis of Epoxy/Thermoplastic Blends	675
Angel Romo-Uribe	
24 Thermal Properties of Epoxy/Thermoplastic Blends	707
Irthasa Aazem, Aklesh Kumar, Manisha Mohapatra, Jung Hwi Cho, Jarin Joyner, Peter Samora Owuor, Jyotishkumar Parameswaranpillai, Vijay Kumar Thakur, Jinu Jacob George, and Raghavan Prasanth	
25 Mechanical Properties of Epoxy/Thermoplastic Blends	743
Ana M. Díez-Pascual	

26 Applications of Epoxy/Thermoplastic Blends	775
Gianluca Cicala and Salvatore Mannino	
27 pVT Analysis of the Effect of Addition of Thermoplastics, Block-Copolymers, or Rubbers on the Curing Behavior and Shrinkage of Epoxy Resins	799
Jürgen Pionteck	
Part III Epoxy/Block-Copolymer Blends	825
28 Introduction to Epoxy/Block-Copolymer Blends	827
Seno Jose, Sajeev Martin George, and Jyotishkumar Parameswaranpillai	
29 Miscibility, Phase Separation, and Mechanism of Phase Separation of Epoxy/Block-Copolymer Blends	841
Hernan Garate, Noé J. Morales, Silvia Goyanes, and Norma B. D'Accorso	
30 Morphology of Epoxy/Block-Copolymer Blends	883
Galder Kortaberria	
31 Spectroscopic Analysis of Epoxy/Block-Copolymer Blends	919
Fenfeng Wang, Xin He, Qinqin Dang, Tao Li, and Pingchuan Sun	
32 Rheology of Epoxy/Block-Copolymer Blends	955
Junkal Gutierrez, Laida Cano, and Agnieszka Tercjak	
33 Cure Kinetics of Epoxy/Block-Copolymer Blends	979
Connie Ocando, Raquel Fernandez, M ^a Angeles Corcuera, and Arantxa Eceiza	
34 Dynamic Mechanical Thermal Analysis of Epoxy/Block-Copolymer Blends	1007
Sajeev Martin George, Nishar Hameed, Seno Jose, Jinu Jacob George, and Jyotishkumar Parameswaranpillai	
35 Thermal Properties of Epoxy/Block-Copolymer Blends	1041
Nisa V. Salim, Jyotishkumar Parameswaranpillai, Bronwyn L. Fox, and Nishar Hameed	
36 Mechanical Properties of Epoxy/Block-Copolymer Blends	1067
Lei Li and Sixun Zheng	
37 Water Sorption and Solvent Sorption of Epoxy/Block-Copolymer and Epoxy/Thermoplastic Blends	1097
Anbazhagan Palanisamy, Nisa V. Salim, Jyotishkumar Parameswaranpillai, and Nishar Hameed	
Index	1113

About the Editors



Dr. Jyotishkumar Parameswaranpillai is an INSPIRE Faculty at Department of Polymer Science and Rubber Technology of Cochin University of Science and Technology, Kerala, India. He received his Ph.D. in Polymer Science and Technology (Chemistry) from Mahatma Gandhi University, Kerala, India. He has published around 60 papers (including few book chapters) in high quality international peer-reviewed journals on polymer nanocomposites, polymer blends, elastomers, and biopolymers and has edited four books. Dr. Jyotishkumar received a number of prestigious awards which include INSPIRE Faculty Award of

Department of Science and Technology, Government of India; Kerala State Young Scientist Award 2016 of Government of Kerala, India; and Venus International Foundation award for the Best Young Faculty and Young Scientist for his outstanding contribution in polymer science.



Dr. Nishar Hameed is the Australian Research Council's Discovery Early Career Researcher at the Factory of the Future, Swinburne University of Technology, Australia. Prior to joining Swinburne, Nishar was a Research Fellow at Carbon Nexus, Deakin University, where he completed his Ph.D. in 2011 and Alfred Deakin Postdoctoral Research Fellowship in 2013. Nishar's research is mainly focused on the novel and faster processing of next generation polymers, carbon fibers, and composite materials. He has published more than 50 high impact journal papers, 6 book chapters, 2 edited books, and 2 patents. He has also held visiting appointments at

Rice University, University of California, Los Angeles, University of Southern Mississippi, University of Kentucky, CNRS Montpellier, Indian Institute of Technology Madras, and Indian Institute of Science Bangalore.



Jürgen Pionteck received his Ph.D. in Chemistry from the Technische Universität Dresden, Germany, in 1988, working on the development of organophosphorus compounds as primary antioxidants under the guidance of K. Schwetlick. Starting at the Leibniz Institute of Polymer Research Dresden, Germany, in 1988, where he was Head of the Polymer Blend Department from 1990 till 1998, he became interested in polymer synthesis, processing and characterization, polymer blends and composites, blend interfaces, and thermodynamics (1 year research stay with W. J. MacKnight at University of Massachusetts at Amherst, USA, in 1991/92). Nowadays, he is focused on functional composites, suitable for sensor applications, capacitors, and thermoelectric material. He is coauthor of more than 180 papers and book chapters, coeditor of the *Handbook of Antistatics* and coauthor of the Volume *Thermodynamic Properties – pVT-Data and Thermal Properties* of the *Landolt-Börnstein Numerical Data and Functional Relationships in Science and Technology – New Series* (Group VIII, Vol. 6A: Part 2). He was awarded with the Honorary Medal of the Polymer Institute Bratislava, Slovakia, and as Erudite Visiting Professor by the Government of Kerala, India.



Prof. Dr. Eamor M. Woo is currently Professor with Endowed Chair in Chemical Engineering Department of National Cheng Kung University (NCKU), Tainan, Taiwan.

He received his Ph.D. degree from the University of Texas at Austin (Austin, Texas, USA).

After several years of academic and industrial experiences in USA, he joined faculty in Department of Chemical Engineering of NCKU, Tainan, Taiwan, since 1992 to present, with research fields focusing on polymer morphology, crystallization, and structures characterization of biodegradable, bio-based plastics and green materials; phase behavior and phase separation; self-assembly of lamellae in spherulites; etc.

He has published over 245 refereed and highly cited papers, including several review articles (*Prog. Polym. Sci.*, *Crystals*, *Euro. Polym. J.*, etc.), and three book chapters (in *Handbook of Adhesives*, *Encyclopedia of Polymer Science and Technology*, etc.) and made over 250 conference presentations internationally, with many keynotes and plenary speeches in major conferences.

He has received numerous academic honors/awards including Research Excellence, Outstanding Researcher Award, etc., from Ministry of Science and Technology, Taiwan.

In professional services, he is Senior Editor for *Journal of Polymer Research* (a Springer-Nature journal). Currently, he also serves as Guest Editor for a special issue–2017 in *Crystals*.

Contributors

Irthasa Aazem Department of Polymer Science and Rubber Technology, Cochin University of Science and Technology, Cochin, Kerala, India

Ibrahim Abdullah Faculty of Science and Technology, School of Chemical Sciences and Food Technology, Polymer Research Center (PORCE), Universiti Kebangsaan Malaysia (UKM), Bangi, Selangor, Malaysia

Ishak Ahmad Faculty of Science and Technology, School of Chemical Sciences and Food Technology, Polymer Research Center (PORCE), Universiti Kebangsaan Malaysia (UKM), Bangi, Selangor, Malaysia

Claire Antonelli Department of Materials Science and Engineering and Chemical Engineering, Universidad Carlos III de Madrid, Leganes, Spain

R. Bagheri Polymeric Materials Research Group, Department of Materials Science and Engineering, Sharif University of Technology, Tehran, Iran

Juan Baselga Department of Materials Science and Engineering and Chemical Engineering, Universidad Carlos III de Madrid, Leganes, Spain

Juan Carlos Cabanelas Department of Materials Science and Engineering and Chemical Engineering, Universidad Carlos III de Madrid, Leganes, Spain

Laida Cano Group 'Materials + Technologies', Department of Chemical and Environmental Engineering, Engineering College of Gipuzkoa, University of the Basque Country, UPV/EHU, Donostia-San Sebastián, Spain

Fenghua Chen Laboratory of Advanced Polymer Materials, Institute of Chemistry, Chinese Academy of Sciences, Beijing, China

Shoubing Chen State Key Laboratory of Solid Lubrication, Lanzhou Institute of Chemical Physics, Chinese Academy of Sciences, Lanzhou, China

Yang Chen State Key Laboratory of Polymer Materials Engineering, Polymer Research Institute of Sichuan University, Sichuan University, Chengdu, China

Xiaole Cheng School of Polymers and High Performance Materials, Polymer Science and Engineering, University of Southern Mississippi, Hattiesburg, MS, USA

Jung Hwi Cho School of Engineering, Materials Science, Brown University, Providence, Rhode Island, USA

Gianluca Cicala Department for Industrial Engineering, University of Catania, Catania, Italy

M^a Angeles Corcuera Group ‘Materials + Technologies’, Department of Chemical and Environmental Engineering, Polytechnic School, University of the Basque Country, Donostia-San Sebastián, Spain

Norma B. D’Accorso CIHIDECAR-CONICET, Departamento de Química Orgánica, FCEyN-UBA, Ciudad Universitaria, Ciudad Autónoma de Buenos Aires, Argentina

Qinqin Dang Key Laboratory of Functional Polymer Materials of the Ministry of Education, College of Chemistry, Nankai University, Tianjin, China

Ana M. Díez-Pascual Analytical Chemistry, Physical Chemistry and Chemical Engineering Department, Faculty of Biology, Environmental Sciences and Chemistry, Alcalá University, Alcalá de Henares, Madrid, Spain

Arantxa Eceiza Group ‘Materials + Technologies’, Department of Chemical and Environmental Engineering, Polytechnic School, University of the Basque Country, Donostia-San Sebastián, Spain

Raquel Fernandez Group ‘Materials + Technologies’, Department of Chemical and Environmental Engineering, Polytechnic School, University of the Basque Country, Donostia-San Sebastián, Spain

Bronwyn L. Fox Factory of the Future, Swinburne University of Technology, Melbourne, Australia

Bejoy Francis Department of Chemistry, St. Berchmans College, Changanassery, Kottayam, Kerala, India

Hernan Garate YPF Tecnología S.A., Ensenada, Buenos Aires, Argentina
IFIBA-CONICET, LP&MC, Departamento de Física, FCEyN-UBA, Ciudad Universitaria, Ciudad Autónoma de Buenos Aires, Argentina
CIHIDECAR-CONICET, Departamento de Química Orgánica, FCEyN-UBA, Ciudad Universitaria, Ciudad Autónoma de Buenos Aires, Argentina

Sajeev Martin George Department of Chemistry, St. Thomas College, Palai/Arunapuram, Kerala, India

Jinu Jacob George Department of Polymer Science and Rubber Technology, Cochin University of Science and Technology, Cochin, Kerala, India

Silvia Goyanes IFIBA-CONICET, LP&MC, Departamento de Física, FCEyN-UBA, Ciudad Universitaria, Ciudad Autónoma de Buenos Aires, Argentina

Junkal Gutierrez Group ‘Materials + Technologies’, Department of Chemical and Environmental Engineering, Engineering College of Gipuzkoa, University of the Basque Country, UPV/EHU, Donostia-San Sebastián, Spain

Nishar Hameed Carbon Nexus, Institute for Frontier Materials, Deakin University, Geelong, VIC, Australia

Factory of the Future, Swinburne University of Technology, Melbourne, VIC, Australia

Charles C. Han Beijing National Laboratory for Molecular Sciences, State Key Laboratory of Polymer Physics and Chemistry, Joint Laboratory of Polymer Science and Materials, Institute of Chemistry, Chinese Academy of Sciences, Beijing, China
Institute for Advanced Study, Shenzhen University, Guangdong, China

Ren He College of Chemical and Biochemical Engineering, Zhejiang University, Hangzhou, China

Xin He Key Laboratory of Functional Polymer Materials of the Ministry of Education, College of Chemistry, Nankai University, Tianjin, China

Zhengguang Heng State Key Laboratory of Polymer Materials Engineering, Polymer Research Institute of Sichuan University, Sichuan University, Chengdu, China

Nicolas D. Huffman Advanced Materials and System Integration, Research Triangle Institute (RTI) International, Research Triangle Park, NC, USA

Xigao Jian State Key Laboratory of Fine Chemicals, Dalian University of Technology, Dalian, China

Department of Polymer Science and Materials, Dalian University of Technology, Dalian, China

Leah M. Johnson Advanced Materials and System Integration, Research Triangle Institute (RTI) International, Research Triangle Park, NC, USA

Seno Jose Department of Chemistry, Government College Kottayam, Kottayam, Kerala, India

Jarin Joyner Department of Materials Science and NanoEngineering, Rice University, Houston, TX, USA

Department of Mechanical Engineering and Materials Science, Rice University, Houston, TX, USA

Hanieh Kargarzadeh Faculty of Science and Technology, School of Chemical Sciences and Food Technology, Polymer Research Center (PORCE), Universiti Kebangsaan Malaysia (UKM), Bangi, Selangor, Malaysia

José Maria Kenny Civil and Environmental Engineering Department, Materials Engineering Center, UdR INSTM, University of Perugia, Terni, Italy

Galder Kortaberria ‘Materials + Technologies’ Group, Universidad del País Vasco/Euskal Herriko Unibertsitatea, Donostia, Spain

B. Kothandaraman Madras Institute of Technology, Anna University, Chennai, Tamil Nadu, India

Padmanabhan Krishnan VIT-University, Vellore, India

Aklesh Kumar Department of Polymer Science and Rubber Technology, Cochin University of Science and Technology, Cochin, Kerala, India

Lei Li Department of Polymer Science and Engineering and the State Key Laboratory of Metal Matrix Composites, Shanghai Jiao Tong University, Shanghai, China

Tao Li Key Laboratory of Functional Polymer Materials of the Ministry of Education, College of Chemistry, Nankai University, Tianjin, China

Mei Liang State Key Laboratory of Polymer Materials Engineering, Polymer Research Institute of Sichuan University, Sichuan University, Chengdu, China

Rui Liu State Key Laboratory of Fine Chemicals, Department of Polymer Science and Materials, Dalian University of Technology, Dalian, China

Zhuoyu Liu State Key Laboratory of Molecular Engineering of Polymers, Collaborative Innovation Center of Polymers and Polymer Composite Materials, Department of Macromolecular Science, Fudan University, Shanghai, China

Sebastien Livi Université de Lyon, Lyon, France

INSA Lyon, Villeurbanne, France

UMR 5223, Ingénierie des Matériaux Polymères, CNRS, Paris, France

Salvatore Mannino Department for Industrial Engineering, University of Catania, Catania, Italy

B. T. Marouf Department of Materials Science and Engineering, Faculty of Engineering, Urmia University, Urmia, Iran

Manisha Mohapatra Department of Polymer Science and Rubber Technology, Cochin University of Science and Technology, Cochin, Kerala, India

Noé J. Morales YPF Tecnología S.A., Ensenada, Buenos Aires, Argentina

Connie Ocando Laboratoire De Physique Des Surfaces Et Des Interfaces, Université De Mons-UMONS, Mons, Belgium

Peter Samora Owuor Department of Materials Science and NanoEngineering, Rice University, Houston, TX, USA

Department of Mechanical Engineering and Materials Science, Rice University, Houston, TX, USA

Anbazhagan Palanisamy Institute for Frontier Materials, Deakin University, Geelong, Australia

Jyotishkumar Parameswaranpillai Department of Polymer Science and Rubber Technology, Cochin University of Science and Technology, Cochin, Kerala, India

Jürgen Pionteck Leibniz-Institut für Polymerforschung Dresden e.V., Dresden, Germany

Raghavan Prasanth Department of Polymer Science and Rubber Technology, Cochin University of Science and Technology, Cochin, Kerala, India

Department of Materials Science and NanoEngineering, Rice University, Houston, TX, USA

Department of Mechanical Engineering and Materials Science, Rice University, Houston, TX, USA

Debora Puglia Civil and Environmental Engineering Department, Materials Engineering Center, UdR INSTM, University of Perugia, Terni, Italy

Angel Romo-Uribe Advanced Science and Technology, Johnson & Johnson Vision Care, Inc., Jacksonville, FL, USA

Nisa V. Salim Carbon Nexus, Institute for Frontier Materials, Deakin University, Geelong, VIC, Australia

Verónica San Miguel Department of Materials Science and Engineering and Chemical Engineering, Universidad Carlos III de Madrid, Leganes, Spain

Berna Serrano Department of Materials Science and Engineering and Chemical Engineering, Universidad Carlos III de Madrid, Leganes, Spain

Gebin Shen State Key Laboratory of Molecular Engineering of Polymers, Collaborative Innovation Center of Polymers and Polymer Composite Materials, Department of Macromolecular Science, Fudan University, Shanghai, China

Bluma Guenther Soares Programa de Engenharia Metalúrgica e de Materiais-COPPE, Centro de Tecnologia, Universidade Federal do Rio de Janeiro, Rio de Janeiro, Brazil

Xiao-Xue Song School of Materials Science and Engineering, East China University of Science and Technology, Shanghai, China

Tongchen Sun Aerospace Special Materials and Processing Technology Institute, Beijing, China

Pingchuan Sun Key Laboratory of Functional Polymer Materials of the Ministry of Education, College of Chemistry, Nankai University, Tianjin, China

Agnieszka Tercjak Group 'Materials + Technologies', Department of Chemical and Environmental Engineering, Engineering College of Gipuzkoa, University of the Basque Country, UPV/EHU, Donostia-San Sebastián, Spain

Vijay Kumar Thakur School of Aerospace, Transport and Manufacturing, Cranfield University, Cranfield, Bedfordshire, UK

P. Poornima Vijayan Center for Advanced Materials, Qatar University, Doha, Qatar

Fenfen Wang Key Laboratory of Functional Polymer Materials of the Ministry of Education, College of Chemistry, Nankai University, Tianjin, China

Jinyan Wang State Key Laboratory of Fine Chemicals, Dalian University of Technology, Dalian, China

Department of Polymer Science and Materials, Dalian University of Technology, Dalian, China

Qihua Wang State Key Laboratory of Solid Lubrication, Lanzhou Institute of Chemical Physics, Chinese Academy of Sciences, Lanzhou, China

Tingmei Wang State Key Laboratory of Solid Lubrication, Lanzhou Institute of Chemical Physics, Chinese Academy of Sciences, Lanzhou, China

Jeffrey S. Wiggins School of Polymers and High Performance Materials, Polymer Science and Engineering, University of Southern Mississippi, Hattiesburg, MS, USA

Shi-Ai Xu Department of Polymer Engineering and Science, School of Materials Science and Engineering, East China University of Science and Technology, Shanghai, China

Yingfeng Yu State Key Laboratory of Molecular Engineering of Polymers, Collaborative Innovation Center of Polymers and Polymer Composite Materials, Department of Macromolecular Science, Fudan University, Shanghai, China

Nor Yuliana Yuhana Department of Chemical and Process Engineering, Universiti Kebangsaan Malaysia, Bangi, Selangor, Malaysia

Xiaoli Zhan College of Chemical and Biochemical Engineering, Zhejiang University, Hangzhou, China

Qinghua Zhang College of Chemical and Biochemical Engineering, Zhejiang University, Hangzhou, China

Yan Zhang College of Engineering, and National Engineering and Technology Research Center of Wood-based Resources Comprehensive Utilization, Zhejiang Agriculture and Forestry University, Hangzhou, China

Sixun Zheng Department of Polymer Science and Engineering and the State Key Laboratory of Metal Matrix Composites, Shanghai Jiao Tong University, Shanghai, China

Huawei Zou State Key Laboratory of Polymer Materials Engineering, Polymer Research Institute of Sichuan University, Sichuan University, Chengdu, China

Part I

Epoxy/Rubber Blends

Introduction to Rubber Toughened Epoxy Polymers

1

Shi-Ai Xu and Xiao-Xue Song

Abstract

Epoxy resins are a class of thermosetting polymers widely used for structural application. However, as epoxy resins are inherently brittle because of their highly cross-linked structure, a great effort has been made to improve the fracture toughness. A widely used method for this purpose is the addition of second-phase polymeric particles, and over the past decades, great success has been achieved in this area. This chapter provides a comprehensive overview of the development in rubber-toughened epoxy. First, we review the history of rubber-toughened epoxy and different kinds of rubbers used for toughening epoxy. Then, we summarize the factors affecting the toughening effect and mechanisms accounting for rubber-toughened epoxy. Finally, we discuss some new trends in this field.

Keywords

Epoxy • Rubber/epoxy blends • Liquid rubber • Miscibility • Phase separation • Thermodynamics of phase separation • Phase diagram • Binodal curve • Spinodal curve • Upper critical solution temperature • Lower critical solution temperature • Critical conditions of phase separation • Mechanisms for phase separation • Spinodal separation • Nucleation and Growth separation • Solubility parameter • Cloud-point temperature • Critical interaction parameter • Morphology • Curing agent • Curing protocol • Scanning electron microscopy •

S.-A. Xu (✉)

Department of Polymer Engineering and Science, School of Materials Science and Engineering, East China University of Science and Technology, Shanghai, China
e-mail: saxu@ecust.edu.cn

X.-X. Song

School of Materials Science and Engineering, East China University of Science and Technology, Shanghai, China
e-mail: sxx0131@126.com

Transmission electron microscopy • Optical microscopy • Light transmittance •
Light scattering • Electron microscopy

Contents

Introduction	4
Rubbers Used for Toughening Epoxy	5
Liquid Rubber	5
Core-Shell Rubber	10
Block Copolymer Rubber	13
Influential Factors of Toughening Effect	13
Rubber Content	14
Particle Size	15
Matrix Characteristics	15
Toughening Mechanisms of Rubber/Epoxy System	16
New Trends	19
Bio-based Tougheners for Epoxy	19
Block Copolymer-Toughened Epoxy	22
Controlling of Morphology	23
Conclusions	23
References	24

Introduction

Epoxy resins are a class of versatile polymers containing two or more oxirane rings or epoxy groups in their molecular structure, which can be hardened into thermosetting plastics with the use of a suitable curing agent. Epoxy resins have found a wide range of applications as coatings, adhesives, electrical insulators, electronic encapsulation materials, and matrices for fibrous components due to their excellent adhesiveness, chemical resistance, and mechanical and physical properties (Liu et al. 2014). In general, cured epoxy resins have better stiffness, strength, heat resistance, solvent barrier properties, and creep resistance than thermoplastic polymers due to their highly cross-linked three-dimensional network structure (Xu et al. 2013). The pressure needed for the fabrication of epoxy resins is lower than that of other thermosetting resins. Shrinkage and residual stress are also much lower in the cured products than that in the unsaturated polyester resins cured by vinyl polymerization. Epoxy resin is available ranging from low viscous liquid to tack-free solid, and cured epoxy polymers can be applied in a wide range of temperatures by selecting an appropriate hardener with good control over the cross-linking degree (Ratna and Banthia 2004). These unique properties make epoxy one of the most widely studied thermosetting polymers with a wide range of industrial applications (Ratna and Banthia 2004; LeMay and Kelley 1986).

However, epoxy is essentially a rigid and brittle polymeric material because of its highly cross-linked structure and has very poor resistance to impact and crack initiation in the cured state. The fracture energy of epoxy is two and three orders of magnitude lower than that of engineering thermoplastics and metals, respectively (Bascom and Hunston 1989). This implies the need to toughen epoxy in order to

have a wider application. Over the past decades, great efforts have been made to improve the fracture toughness of epoxy (Bagheri et al. 2009). A widely used method for this purpose is to add rigid or soft particles as a second phase. Rigid particles used include inorganic or organic particles, and the resulting epoxy polymer is named “particulate-filled epoxy,” and soft particles used are basically compliant rubbery particles with a glass transition temperature (T_g) much lower than that under service conditions. The technique of incorporating rubbery second phase is known as “rubber-toughening” technique (Garg and Mai 1988).

This chapter reviews the history of rubber-toughened epoxy.

Rubbers Used for Toughening Epoxy

Liquid Rubber

Liquid rubber is one of the most successful tougheners for epoxy. The attempt to toughen epoxy resins was initiated by researchers from B. F. Goodrich Company and first reported by McGarry (McGarry 1970). Since then, extensive research has been devoted to understanding the toughening mechanisms of rubber-toughened epoxies (Bucknall and Partridge 1983; Kinloch et al. 1983; Yee and Pearson 1986; Bucknall and Gilbert 1989; Gilbert and Bucknall 1991), and several reviews have been published (Ratna and Banthia 2004; Bagheri et al. 2009; Garg and Mai 1988; Unnikrishnan and Thachil 2012). Butadiene-acrylonitrile-based rubbers are the principal liquid rubbers used for toughening epoxies, among which carboxyl-terminated butadiene-acrylonitrile (CTBN) with different contents of acrylonitrile (AN) has been most extensively used. Other elastomers from this family include amino-terminated butadiene-acrylonitrile (ATBN), epoxy-terminated butadiene-acrylonitrile (ETBN), and vinyl-terminated butadiene-acrylonitrile (VTBN) (Garg and Mai 1988).

CTBN

McGarry et al. used a liquid CTBN copolymer to modify diglycidyl ether of bisphenol A (DGEBA) epoxy cured with 2,4,6-tri(dimethylaminoethyl) phenol (DMP) (McGarry 1970; Sultan et al. 1971; Sultan and McGarry 1973). The results showed that the fracture toughness of modified epoxy was increased by an order of magnitude at the optimum rubber content (about 7.5 wt.%) (McGarry 1970). CTBN has been shown to be the most effective toughener for epoxy. In a typical process, CTBN is first dissolved in the epoxy, and after the addition of the curing agent, the rubbery phase precipitates to form the second-phase particles as the epoxy resin begins to cure and the molecular weight begins to increase (Bascom et al. 1975; Kim and Ma 1996; Bucknall and Partridge 1986; Verchère et al. 1989).

A good miscibility between rubber and epoxy is very important to achieve a satisfactory toughening effect. Bucknall and Partridge (1986) found that the miscibility between CTBN and epoxy depended largely on the type of epoxy resin used, and CTBN was more miscible with epoxy having similar solubility parameters. Verchère et al. (1989) found that the miscibility between epoxy monomers

(DGEBA) and rubbers (CTBN) was very sensitive to the molecular weight of the epoxy molecule, and even a small increase in the number-average molecular weight led to a significant shift in the miscibility gap to higher temperatures. Moreover, a lower content of AN in the CTBN resulted in poorer miscibility due to the change in solubility parameter. In contrast, CTBN with a higher content of AN had a larger solubility parameter, resulting in better miscibility with epoxy.

A strong interfacial bond between the particles and the matrix is also very important to achieve improved toughness. For CTBN, the carboxyl groups react easily with the oxirane rings of the epoxy, thus resulting in a good interfacial adhesion between the two phases (Barcia et al. 2002).

ATBN

Chikhi et al. (2002) used liquid ATBN containing 16% AN to toughen DGEBA epoxy cured by polyaminoimidazoline, and they found that the addition of ATBN led to an increase in the elongation at break and the appearance of yielding. The tensile modulus decreased slightly from 1.85 to about 1.34 GPa with increasing ATBN content, whereas the Izod impact strength was increased by three times with the addition of 12.5 phr ATBN compared to that of the unmodified epoxy.

Wise et al. (2000) compared the effects of CTBN and ATBN on the curing behavior of epoxy, and they concluded that the carboxyl end groups of CTBN strongly enhanced the curing rate through the impurity catalysis mechanism, whereas the ATBN retarded the reaction possibly by the dilution effects or changes in the dielectric constant of the reacting medium. Figure 1 illustrates the

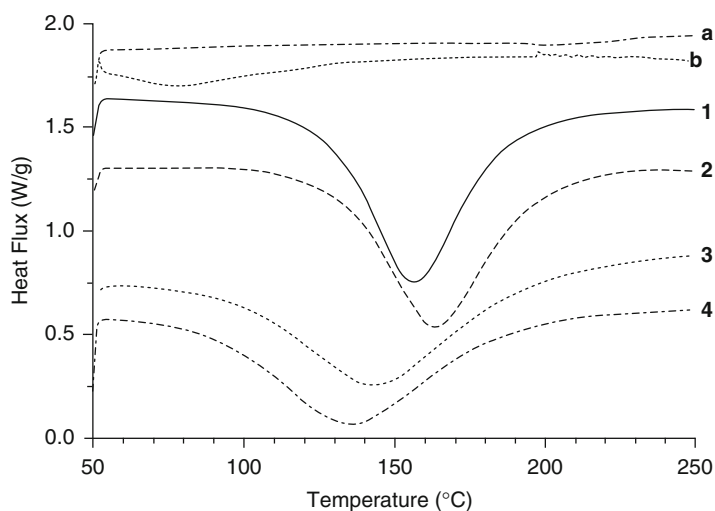


Fig. 1 Scanning DSC of aniline/DGEBA: 1 unfilled, 2 10 wt.% ATBN (16% AN), 3 10 wt.% CTBN (13% AN), and 4 20 wt.% CTBN (13% AN). (a, b) 25 wt.% CTBN (13% AN) in DGEBA and 55 wt.% ATBN (16% AN) in DGEBA without aniline (Reprinted from Wise et al. (2000), Copyright (2000), with permission from Elsevier)

accelerating and retarding effect of CTBN and ATBN on the curing reaction. The peak exotherm was shifted to lower temperatures with increasing CTBN concentration due to the enhanced reaction rate. However, ATBN did not catalyze the aniline-DGEBA reaction. It is clear that the reaction between DGEBA and CTBN (curve a) was small relative to the epoxy-amine reaction, while there was a measurable reaction between ATBN and DGEBA (curve b).

ETBN

Grishchuk et al. (2013) investigated the toughening effect of ETBN in epoxy hardened with 4,4-diaminodiphenyl methane in the presence of benzoxazine. As expected, the incorporation of ETBN greatly decreased the stiffness and T_g of the epoxy system, which was characteristic for plasticizers. Such stiffness reduction seemed to be typical for functionalized liquid rubber-toughened tetrafunctional epoxy systems. ETBN fulfilled its role as a toughening agent. The incorporation of ETBN enhanced fracture toughness (K_{Ic}) and in particular, fracture energy (G_{Ic}). As the content of ETBN increased, the fracture mechanical parameters were markedly enhanced, the size distribution became broader, and the morphology of the ETBN domains changed from a featureless type to a sea-island type. ETBN was micron scaled, dispersed, and participated in the polymerization with diamine, leading to rubber-rich domains covalently bonded to the matrix (Grishchuk et al. 2013).

Kunz et al. (1982) compared the morphology (dispersed phase composition, size distribution, and particle/matrix interface shapes) of epoxies modified with CTBN and ATBN and found that ATBN-modified epoxies had a diffuse-appearing interface between the dispersed rubber phase and the epoxy matrix, in contrast to the sharp boundaries of CTBN particle interfaces. This was because ATBN particles were highly irregular in shape, while CTBN particles were nearly spherical. However, both modifiers showed a bimodal particle size distribution.

The effect of CTBN and ETBN on the curing behavior of epoxy/novolac system was investigated by dynamic scanning calorimetry. Indeed, CTBN affected the kinetic parameters of cure compared to that of plain epoxy mixture, and significant difference was observed in the curing behavior of CTBN- and ETBN-modified systems. A clearly pronounced effect of CTBN content was noted. The initial curing rate was increased by a factor of two compared to that of unmodified epoxy/novolac system, whereas the rate constant k_2 of the CTBN-modified epoxy system was reduced due to the formation of CTBN domains. From the view of later processing, it was very advantageous that the reaction rate observed for ETBN/epoxy/novolac mixture was almost the same, as in non-modified system. A smaller activation energy was observed for CTBN/epoxy/novolac series. The activation energy for ETBN-modified epoxy at the early stage of curing was almost the same, but at the later stages, some increase was noted both in relation to the non-modified epoxy system (Szeluga et al. 2008).

Functionalized Polybutadiene Rubber

HTPB (hydroxyl-terminated polybutadiene) is a liquid polybutadiene rubber with hydroxyl end groups, which could be used to improve the toughness of

epoxy resins. However, HTPB has poor compatibility with epoxy resins (Barcia et al. 2002). In order to provide an effective interfacial adhesion, both HTPB and epoxy resin should be chemically bonded to each other. Ozturk et al. (2001) utilized a silane coupling agent to improve the compatibility between HTPB and epoxy matrix, and it was found that the thermal and mechanical properties of DGEBA-based epoxy resin with HTPB were increased by the silane coupling agent.

Some authors have epoxidized HTPB mainly to increase its polarity and consequently its compatibility with epoxy. Bussi and Ishida (1994) used internally epoxidized hydroxyl-terminated polybutadiene (ETPB) to improve the mechanical properties of DGEBA-based epoxy resins. Latha et al. (1994) also studied the toughening effect of epoxidized hydroxyl-terminated polybutadiene on epoxy resins cured with an amine. Lap shear strength (LSS) and T-peel strength were found to increase with increasing ETPB content up to 10 phr, which was attributed to the higher toughness produced by the dispersed rubber particles. At a higher ETPB content, the rubber phase became continuous and the flexibilisation effect predominated over the toughening effect of ETPB.

Epoxidized HTPB is an effective toughening agent for epoxy resins, as the introduction of epoxy groups into the double bonds of HTPB increases the miscibility with epoxy resin. This leads to phase separation of rubber domains in the epoxy matrix, thus making epoxidized HTPB an effective toughening agent (Gopala Krishnan et al. 2013).

HTPB functionalized with isocyanate groups was used to prepare DGEBA-based epoxy (Barcia et al. 2002). HTPB was first reacted with an appropriate amount of toluene diisocyanate (TDI), and the isocyanate end-capped HTPB (ITPB) was reacted with the epoxy to form a block copolymer (BCP). The results showed that this ETPB-modified epoxy was transparent and homogeneous with good impact resistance. A good impact performance was achieved even with 5% ETPB, which was better than that of the HTPB-modified epoxy (Table 1).

ETPB was synthesized and utilized to enhance the toughness of an epoxy system (Yahyaie et al. 2013), in both bulk and coating states. The scanning electron microscope (SEM) results showed that plastic void growth (Fig. 2a), cavitation (Fig. 2b), and shear yielding (Fig. 2c) were the main toughening mechanisms of

Table 1 Mechanical properties of cured epoxy samples (Barcia et al. 2002)

Epoxy resin (%)	HTPB (%)	ETPB ^a (%)	Impact strength (J/m ²)	Flexural yield stress (MPa)	Flexural modulus (MPa)
100	0	0	9.7±0.4	83.8	2536
95	5	0	11.4±0.3	72.0	2385
90	10	0	14.2±0.4	62.2	1912
85	15	0	11.2±0.4	60.0	1860
95	0	5	13.6±0.3	67.0	1753
90	0	10	15.3±0.4	70.0	1776
85	0	15	9.0±0.9	62.3	1523

^aETPB is the BCP obtained by end-capping the isocyanate-modified HTPB with epoxy

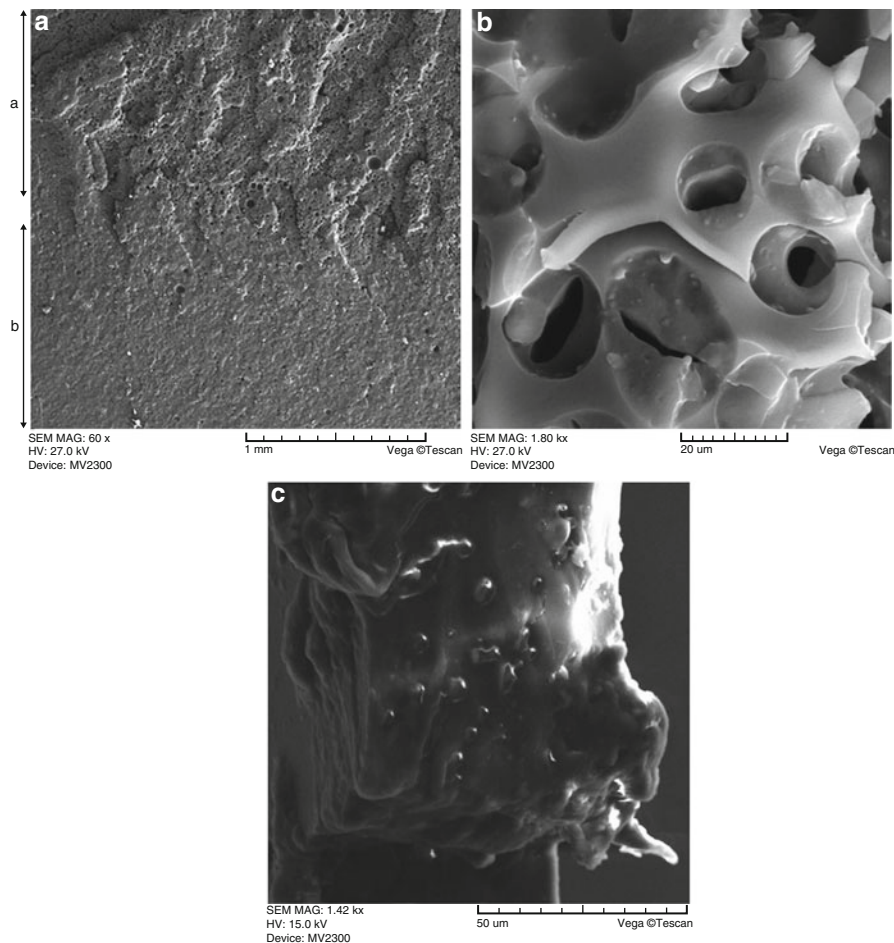


Fig. 2 Different mechanisms in ETPB-toughened epoxy (Reprinted from Yahyaie et al. (2013), Copyright (2013), with permission from Elsevier). (a) SEM micrographs of the fracture surface of rubber-modified sample: slow and fast growth zone (the volumetric expansion of rubbery phase indicated plastic void growth mechanism). (b) Cavitation of ETPB rubber particles in modified sample. (c) Shear yielding of ETPB-toughened epoxy sample

bulk epoxy systems. The mechanical properties of ETPB-modified epoxy resins increased with increasing ETPB content and reached a maximum at 7.5 wt.% and then decreased with further increase in ETPB content. However, crack arresting and shear yielding were the active mechanisms in thin films. The modification with ETPB could increase the chances of energy dissipation upon the application of an external force, mainly due to the plastic deformation of the matrix which increased the cohesion strength of the modified samples. The hardness of the samples decreased with increasing ETPB content, indicating that a portion of rubber was dissolved in the epoxy phase and plasticized the system.

Other Rubbers

Some acrylate-based liquid rubbers have also been used for toughening epoxy, such as poly(2-ethylhexyl acrylate) (PEHA) oligomers with terminal and pendant reactive groups such as carboxyl-terminated, amine-terminated, and carboxyl-randomized PEHAs (Ratna 2009; Karger-Kocsis 1993).

Core-Shell Rubber

Although the addition of liquid rubber can significantly improve the toughness of epoxy resins, it is inevitably accompanied by a significant loss in elastic modulus and yield strength. The liquid rubber is initially miscible with epoxy and undergoes a phase separation during curing, leading to the formation of a two-phase microstructure. It is known that the phase separation depends largely on the formulation and the processing and curing conditions, and incomplete phase separation can result in a significant lower T_g . However, it remains difficult to control the phase separation of rubber during curing, and failure to do so may result in an uneven particle size distribution. The differences in morphology and volume of the separated phase affect the mechanical performance of the product (Ratna and Banthia 2004). All these problems can be overcome by using insoluble preformed core-shell rubber (CSR) prepared by emulsion polymerization (Pearson and Yee 1991; Bagheri and Pearson 1996; Sue 1991; Gam et al. 2003; Nguyen-Thuc and Maazouz 2002; Mafi and Ebrahimi 2008; Giannakopoulos et al. 2010). Unlike phase-separated rubber, the size, morphology, composition, shell thickness and cross-link density of the rubbery cores can be controlled separately by using emulsion polymerization techniques, making it possible to produce rubber particles with a controlled particle size. Figure 3 shows high-resolution SEM images of fracture surfaces of epoxy with 9 wt.% of three different CS rubbers (see Table 2) obtained using a field emission gun scanning electron microscope (FEG-SEM) (Giannakopoulos et al. 2010). The use of CSR with rubbery materials as a core can (1) increase the toughness of epoxy resins without significant deterioration in thermomechanical properties (Maazouz et al. 1994), (2) reduce the internal stress of incorporated epoxy resins (Nakamura et al. 1986), and (3) cater easily to the design variables of core-shell particles (CSP), such as changing the compositions, cross-linking status, and particle size of CSPs (Lin and Shieh 1998a).

In general, the shell of CSR particles should be compatible with the epoxy matrix, and poly(methyl methacrylate) is often used (Giannakopoulos et al. 2010). Typical core materials used include butadiene (Qian et al. 1995), acrylate polyurethane (Jingqiang et al. 2004), and siloxane, which have been shown to increase the toughness of both bulk polymers and fiber composites (Pearson and Yee 1991; Lin and Shieh 1998b; Bécu-Longuet et al. 1999; Day et al. 2001). Hayes and Seferis (2001) reviewed the use of CSR particles in thermosetting polymers and composites, and the properties of polymers that could be affected by the incorporation of CSR particles.

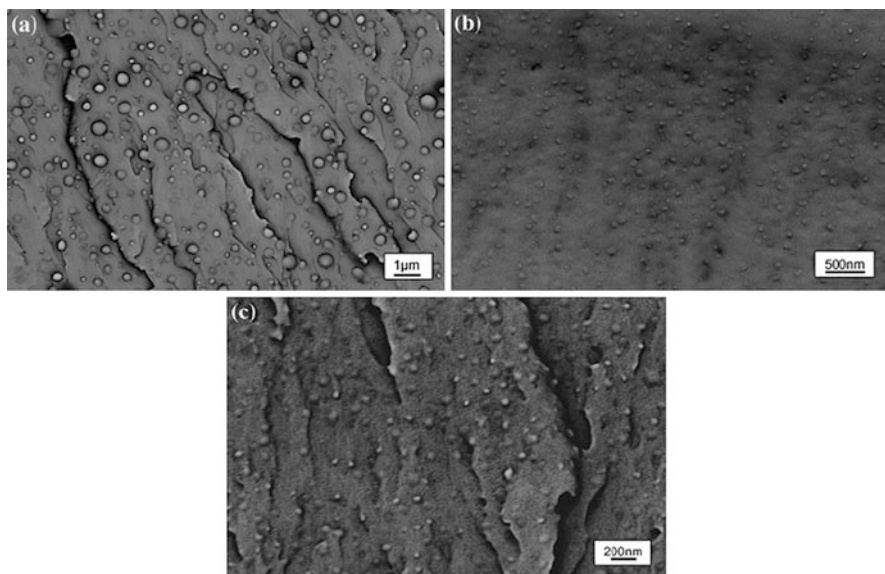


Fig. 3 FEG-SEM images of fracture surfaces of epoxy with 9 wt.% of three different CSR particles. (a) MX96; (b) MX-125; (c) MX156

Table 2 Compositions and properties of CSR particles

Type	Core	Core diameter (nm)	Shell	Diameter (nm)
MX 125	Styrene-butadiene copolymer	100	PMMA	85–115
MX 156	Polybutadiene	100	PMMA	85–115
MX 960	Polysiloxane	300	PMMA	250–350

The preformed particles can be incorporated into the epoxy matrix by mechanical mixing. CSPs with rubbery-type materials as a core prepared by two-stage emulsion polymerization were used to toughen epoxy resins (Maazouz et al. 1994; Sue et al. 1993a). The samples were prepared by directly dispersing CSPs in the epoxy matrix without undergoing phase separation. The size and content of CSPs and their interfacial bonding with the epoxy matrix strongly affected the toughening behaviors (Lin and Shieh 1998a). The particle size should be large enough to allow their deformation energy to be higher than their interfacial bonding to the epoxy matrix. Otherwise, no cavitation occurs during fracture (Dompas and Groeninckx 1994). Once the cavitation occurs, if the interparticle distance is short enough, the local yielding leads to the formation of a thin matrix ligament. As a result, the local material in the crack tip is transformed from brittle to tough, thus increasing the fracture toughness (Wu 1985).

Poly(butyl acrylate) (PBA)/poly(methyl methacrylate) (PMMA) CSPs with different core sizes prepared by seeded emulsion polymerization were dispersed in the epoxy resin. The SEM observation clearly showed that PBA cores were dispersed in the cured epoxy matrix, while PMMA shell seemed to dissolve in the matrix. The internal stress of cured epoxy resin decreased with the modification of the particles, and such a tendency was enhanced with a decrease in the particle size (Nakamura et al. 1986).

Sue et al. (1993b) found a modest improvement in the fracture toughness of a DGEBA/DDS system modified by CSR particles with a connected morphology compared to a well-dispersed microstructure. This is attributed to the additional toughness provided by the crack deflection around the locally clustered particles. The connected morphology enables shear bands to grow further at the crack tip.

The dispersibility of the particles can be improved by introducing cross-link into the shell or using comonomer like AN or glycidyl methacrylate (GMA) which increases the interfacial adhesion by polar or chemical interaction (Ratna and Banthia 2004).

Qian et al. (1995) prepared poly(butadiene-co-styrene) (PBS) core-poly(methyl methacrylate) (PMMA) shell particles using a two-step emulsion polymerization to toughen an epoxy polymer. The role of particle-epoxy interfaces was studied by systematically varying the shell composition of the CSPs such as PMMA, P[MMA-AN], P[MMA-GMA], and P[MMA-divinyl benzene(DVB)]. This resulted in a change in the nature of the particle-epoxy interfaces in terms of physical interactions and chemical bonding. The results showed that the morphology of the dispersed particles in the epoxy matrix played an important role in toughening epoxies. The degree of dispersion could be varied by incorporating AN and GMA comonomers in the PMMA shells or by cross-linking the shell. The cluster size could be further reduced by using MMA-AN or MMA-GMA copolymer as shell composition or 5% cross-linker (divinyl benzene). The nanoscale interactions of the rubber-matrix interface do not directly influence fracture toughness, but it can be used to control the blend morphology which has a dramatic effect on toughness.

Lin and Shieh (1998a, b) have prepared reactive CSPs with butyl acrylate (BA) as the core and MMA-GMA copolymer as the shell, which were then used as toughening agents for DGEBA epoxy. Various sizes of reactive CSPs were prepared by copolymerizing MMA with various concentrations of GMA in the shell area, which provided reactive epoxy groups. Ethylene glycol dimethacrylate (EG-DMA) was used to cross-link the core or the shell. When 100 mol% GMA was used in the second stage of the soapless emulsion polymerization, about 40% of GMA monomer did not participate in the reaction, indicating that the reactivity of GMA was much lower than that of MMA if it was used alone. Thus, a high content of GMA was not a good choice in the preparation of reactive CSPs, because it would reduce the T_g of CSP and the conversion degree in the shell region. Besides, the T_g of the BA core could be increased if cross-linked with EG-DMA (Lin and Shieh 1998a).

The toughening effect of CSPs was evaluated as a function of the cross-linking state of CSP, the number of epoxy groups in a particle, and the particle size and the

content of CSP in the epoxy resins. Shell cross-linked CSPs had a higher toughening effect than core cross-linked CSPs because they coagulated to a cluster locally and still maintained a good global dispersion. The toughening effect of CSP could be enhanced by introducing the epoxy groups in the shell region to react with the epoxy matrix because the excess deformation of CSP than the epoxy matrix prior to cavitation could trigger the plastic flow of the surrounding epoxy matrix. The GMA in the shell region of CSP was more reactive than the DGEBA epoxy resin, and thus could accelerate the curing reaction. The incorporation of reactive CSP with a particle size of $\leq 0.25 \mu\text{m}$ was able to increase the T_g of epoxy matrix if they were dispersed uniformly (Lin and Shieh 1998b).

Block Copolymer Rubber

Amphiphilic BCPs are effective in toughening epoxy resins (Hillmyer et al. 1997; Lipic et al. 1998; Grubbs et al. 2000a, b, 2001; Dean et al. 2001, 2003a, b; Guo et al. 2003; Wu et al. 2005; Jain and Bates 2003). BCPs usually consist of an epoxy-miscible block and an epoxy-immiscible block, and they can self-assemble into well-defined micro-/nanostructures in the form of spherical micelles, wormlike micelles, or vesicles, depending on the molecular weight, block length, and composition of the BCPs (Maazouz et al. 1994; Liu et al. 2008). The addition of a relatively small amount (5 wt.%) of BCPs led to a remarkable improvement in fracture toughness. Similar researches on triblock copolymer-toughened epoxies have also been reported in recent years.

Yang et al. (2009) synthesized poly(3-caprolactone)-block-poly(butadiene-co-acrylonitrile)-block-poly(3-caprolactone) triblock copolymer via the ring-opening polymerization of 3-caprolactone with dihydroxyl-terminated butadiene-co-acrylonitrile random copolymer. This triblock copolymer was then used to toughen epoxy thermosets via the formation of nanostructures, leading to a higher T_g and fracture toughness compared with the ternary blend consisting of epoxy, poly(butadiene-co-acrylonitrile), and poly(3-caprolactone).

Liu et al. (2010) used an amphiphilic poly(ethylene-alt-propylene)-b-poly(ethylene oxide) (PEP-PEO) block copolymer to blend with bisphenol A-based epoxy resins. The fracture toughness was improved by $>100\%$ over the neat epoxy with the incorporation of 5 wt.% BCP. The BCP is self-assembled into a wormlike micelle structure in cured resins, as shown in Fig. 4.

Influential Factors of Toughening Effect

There are many factors influencing the toughening effect on the rubber-toughened epoxy system, including rubber content, particle size, and matrix characteristics. However, it should be noted that some of these factors are changed simultaneously in some studies, and problems arise as it is difficult to change one factor without affecting others due to the interdependence of these factors.

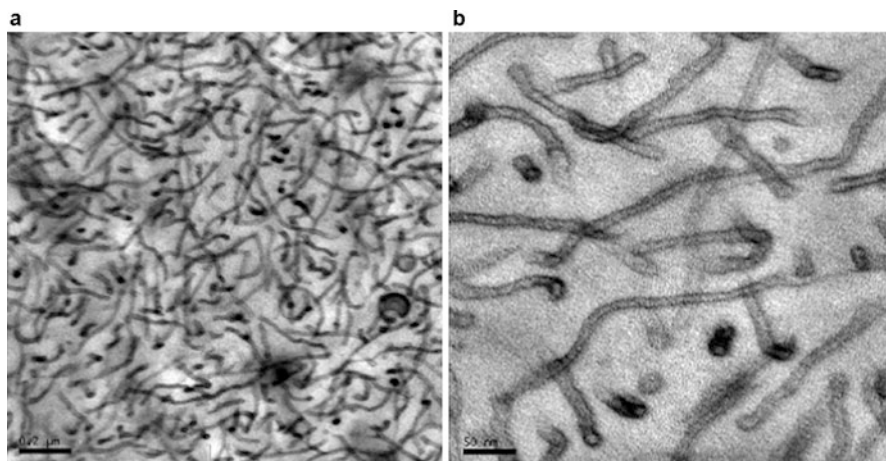


Fig. 4 TEM micrographs of BCP wormlike micelle-modified epoxy at (a) low and (b) high magnification (Reprinted with permission from Liu et al. (2010). Copyright (2010), American Chemical Society)

Rubber Content

The effect of rubber content on the fracture toughness has been extensively investigated (Hillmyer et al. 1997; Lipic et al. 1998; Grubbs et al. 2000a). Generally, the toughness of rubber-toughened epoxy increases with increasing rubber content and reaches a maximum at 10–15 phr of rubber. As the toughening effect is closely related to the molecular weight; the AN content; the number of carboxyl, hydroxyl, and hydroxyl groups per molecule; and the cross-linking density of cured epoxy, the optimal CTBN content differs greatly in different systems.

Xu et al. (2013) found that plane-strain energy toughness increased with increasing CTBN content and reached a maximum at 10 wt.% CTBN. Ratna and Banthia (2004) synthesized a series of liquid carboxyl-terminated poly(2-ethyl hexyl acrylate) (CTPEHA) with various molecular weights by bulk polymerization, and they found that the optimum properties were obtained at about 10–15 phr of CTPEHA. The interfacial area increased at first and then decreased where the CTBN concentration increased from 15 to 20 wt.%, indicating that the incorporation of about 15 wt.% elastomer resulted in better toughened properties. In addition, a cocontinuity state was attained with the addition of 20–25 wt.% CTBN. A further increase in the concentration of the elastomer led to phase inversion. Xu et al. (2013) also found that the morphology and distribution of CTBN in a phase-separated CTBN-modified epoxy resin was affected by the CTBN composition, and the resulting CTBN/epoxy blend exhibited delaminated structure when the CTBN content exceeded 20 wt.%.

Thomas et al. (2004) investigated the effect of CTBN loading on the mechanical and thermal properties of epoxy cured by nadic methyl anhydride. It was found that both impact strength and critical stress intensity factor increased with increasing

CTBN concentration. Fairly good results were obtained at a critical concentration of 15 wt.%. The fracture energy increased from 0.3 for virgin epoxy to 3.1 MPa m^{1/2} for the modified one. Similarly, the impact strength increased from 126 to 612 kJ/m². On average, the size of the elastomer domains ranged from 0.5 to 1 μm in diameter.

Kim and Ma (1996) evaluated the fracture toughness of epoxy modified by Hycar CTBN rubber with a molecular weight of 1300 and an AN content of 13%. The maximum fracture toughness was achieved at about 4 phr of CTBN and closely corresponded to that of stress whitening.

The toughness of rubber-modified epoxy increased with the rubber volume fraction up to about 0.2–0.3 (Lin and Chung 1994; Lowe et al. 1996), and a higher volume fraction resulted in phase inversion and loss of mechanical fracture. Phase inversion often occurred at a volume fraction higher than 20% (Lin and Chung 1994), but sometimes at a volume fraction lower than 5% (Boogh et al. 1999).

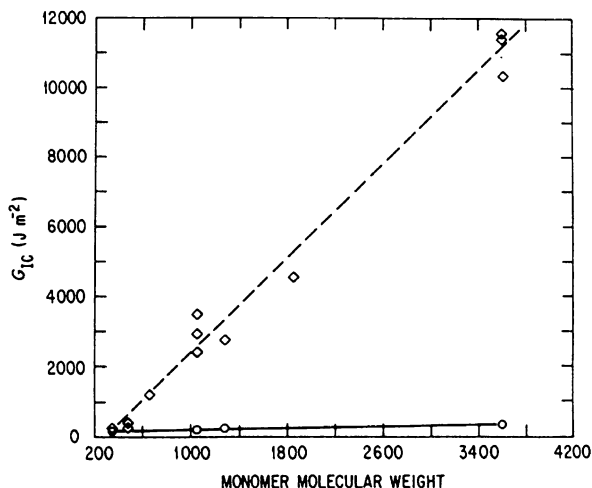
Particle Size

For rubber-toughened plastics, the particle size of the rubber phase is a critical factor determining the toughening effect. Particles of <1 μm exhibited lower impact resistance, particles of 3–5 μm exhibited optimum toughness, while particles of >5 μm again exhibited poor toughness. The same effect was observed in rubber-modified epoxy resins (McGarry 1970). Sultan and McGarry (1973) studied the effect of rubber-particle size on deformation mechanisms in glassy epoxy, and they concluded that particles of a few hundred angstroms caused epoxy matrix to exhibit shear banding and the macroscopic failure envelope of such a system followed a modified von Mises criterion. With larger particles the failure mode changed as shown by the macroscopic yield envelope and the associated activation energy.

Matrix Characteristics

The matrix as the host for the second rubbery phase plays a major role in toughening epoxies, according to the generally accepted toughening mechanism that considers the shear deformation of the matrix as the primary source of toughness (Kozii and Rozenberg 1992). Meeks (1974) is one of the first to demonstrate the importance of the structure of the cured epoxy on its toughenability. He found that tightly cross-linked structures with a relatively high T_g were not toughenable. Kinloch et al. (1987) changed the cross-link density of an epoxy system by changing the curing schedule and found much less toughenability in the tighter epoxy network. Pearson and Yee (1989) investigated the role of matrix ductility in the toughenability of elastomer-modified DGEBA-based epoxies. Matrix ductility was varied by using epoxies with different monomer molecular weights. The fracture toughness of the elastomer-modified epoxies was found to be highly

Fig. 5 Fracture energy is almost independent of the monomer molecular weight for the neat epoxy (*solid line*). For rubber-modified epoxy (*dashed line*), fracture energy increases with increasing epoxide monomer molecular weight, i.e., decreasing cross-link density (Pearson and Yee 1989)



dependent on the epoxide monomer weight, while that of the neat epoxies was almost independent of the monomer molecular weight, as shown in Fig. 5.

Levita et al. (1991) prepared a series of networks with different cross-link densities using bifunctional epoxide prepolymers of different molecular weights cross-linked with diaminodiphenyl sulphone and investigated their fracture behaviors. For comparison, the same set of resins modified with CTBN was also prepared. It was found that the relation between the fracture toughness and cross-linking density depended on the tip radius of the pre-crack on the samples. The fracture toughness decreased with increasing cross-link density for all samples with sharp crack. The reduction in toughness caused by cross-linking could be attributed either to the decrease of the volume of the plastic zone at the notch tip or to a lack of post-yield deformability. However, tests performed with blunt notches showed that fracture toughness reached a maximum at medium cross-link densities. Besides, the cross-link density had a much greater influence in the case of rubber-modified formulations. The stress intensity factor (K_{IC}) data for the neat resins and CTBN-modified system with blunt notches and sharp cracks are shown in Figs. 6 and 7, respectively. Chen and Jan (1995) claimed that high matrix ductility increased the size of plastic deformation zone and thus contributed to toughening.

Toughening Mechanisms of Rubber/Epoxy System

Since the pioneering work of McGarry, the toughening mechanism of rubber-modified epoxies has been a topic of extensive research (Ratna and Banthia 2004; Bagheri et al. 2009; Garg and Mai 1988; Unnikrishnan and Thachil 2012). Several toughening mechanisms have been proposed, including the crazing of the matrix, rubber-particle bridging, formation of a plastic zone in the matrix, rubber cavitation and induced shear deformation of the matrix, and crack bifurcation and/or

Fig. 6 Stress intensity factor, K_I , against cross-link density for the neat resins: (a) tip radius $500\ \mu\text{m}$ (K_{Ib}) and (b) sharp crack (K_{Ic}) (Levita et al. 1991)

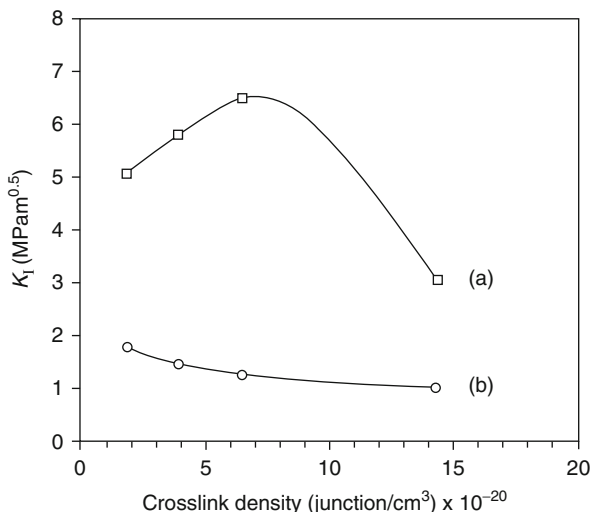
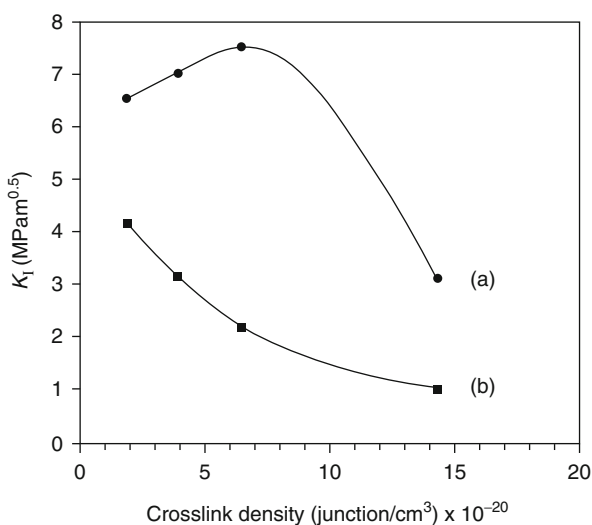


Fig. 7 Stress intensity factor, K_I , against cross-link density for rubber-modified resins: (a) tip radius $500\ \mu\text{m}$ (K_{Ib}) and (b) sharp crack (K_{Ic}) (Levita et al. 1991)



deflection by rubber particles. Yee et al. (2000) systematically reviewed toughening mechanisms and models for rubber-toughened epoxy.

Sultan and McGarry (1973) noted that the size of the cavities in the deformed epoxy was larger than the particle size of undeformed epoxy, which was incorrectly taken as the evidence for crazing of the matrix. Although later Bucknall et al. (1989) suggested shear flow as an additional toughening mechanism, crazing was considered to be the main toughening mechanism until doubt was cast by Yee et al. (2000). Now it is accepted that cavitation of the rubber particles and

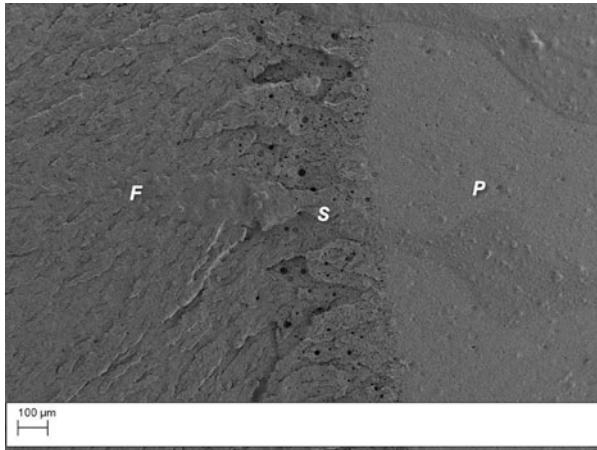


Fig. 8 SEM micrograph of the CT fracture surface of the binary CTBN/epoxy composite with 5 wt.% CTBN (Xu et al. 2013)

subsequent hole growth by matrix shear deformation are the most important toughening mechanism (Yee et al. 2000).

Although the cavitation of rubber particles itself does not consume much energy (Bagheri et al. 2009), it plays a key role in toughening epoxy, because it relieves the plane-strain constraint ahead of the crack tip, allowing the stress concentration associated with cavitated particles to activate extensive shear deformation of the matrix in the form of dilatational void growth, discrete shear bands between cavitated particles, or even diffuse shear yielding (Yee et al. 2000).

Rubber cavitation in rubber-modified epoxies was observed by many researchers. Xu et al. (2013) examined the fracture surfaces of the samples in the compact tension (CT) tests by field emission scanning electron microscopy (FE-SEM). Figure 8 shows the CT fracture surface of the binary epoxy composite containing 5 wt.% CTBN. There are three distinct areas (marked by P, S, and F, respectively) in the fracture surface, where area P is the sharp pre-crack zone produced by the fresh razor, area F is the fast crack-propagation zone, and area S is the stable crack-propagation zone corresponding to the part of load-crack opening displacement curve from zero to the maximum load. The sample fractured suddenly after the load reached the maximum, indicating that the stable crack-propagation zone is the main area consuming the energy in the CT tensile process although area S is much smaller than area F. Therefore, the mechanisms of the epoxy composites are definitely related to area S.

Figure 9 shows the enlarged images of the three zones shown in Fig. 8. It can be seen that the size of the black holes resulting from the pulling out of the CTBN rubber particles in area S is much larger than that in area P and F, and the average size of the holes is obviously larger than that of the CTBN rubber particles. Thus, the cavitation of rubber particles occurs in the stable crack-propagation zone, resulting in extensive shear deformation of the matrix in the form of dilatational

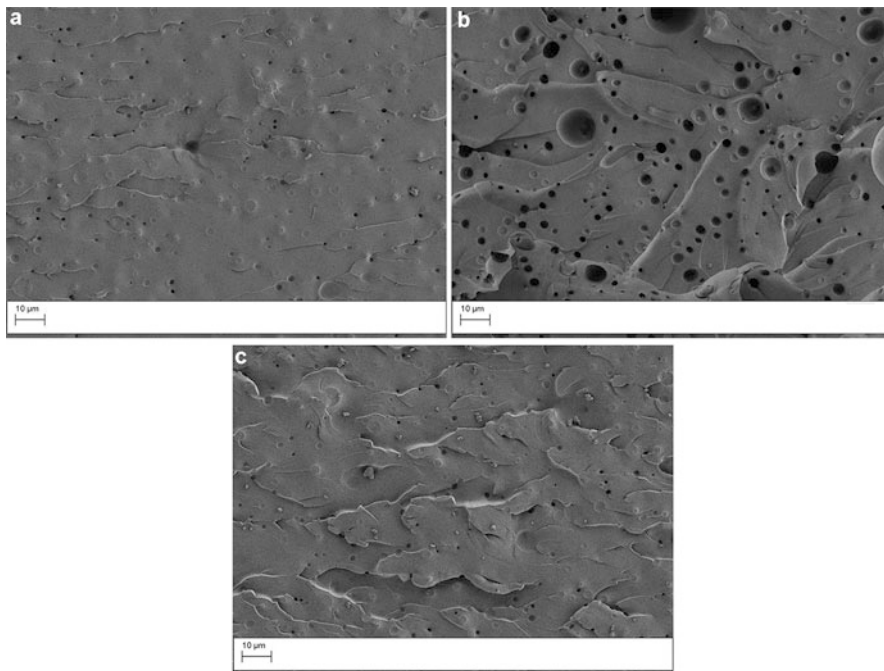


Fig. 9 SEM micrographs of different zones on the CT fracture surface of the binary CTBN/epoxy composite with 5 wt.% CTBN: (a) pre-crack zone, (b) stable crack zone, and (c) fast crack zone

void growth. The transverse contraction and the heat expansion coefficient of rubber particles are larger than that of epoxy matrix due to its larger Poisson's ratio. Thus, the rubber phase contracts more than the matrix phase upon cooling of the sample from curing temperature to room temperature, resulting in an increment of the free volume in the interface zone between the two phases. These two factors initiate and promote the cavitation of rubber particles.

New Trends

Bio-based Tougheners for Epoxy

As fossil fuels become scarcer, it is desirable to minimize the use of petroleum-based chemicals in the manufacture of polymeric materials. In recent years, increasing attention has been paid to the use of renewable natural materials for toughening epoxy (Liu et al. 2014). The conversion of natural materials into useful polymeric materials has been regarded as an effective means of saving fossil resources and protecting our living environment (Deng et al. 2015).

Mathew et al. (2010) prepared a low molecular weight liquid natural rubber possessing hydroxyl functionality (HLNR) by photo depolymerization of natural

rubber. The addition of HLNR to an anhydride hardener-epoxy resin mixture led to the formation of a two-phase microstructure in the cured systems, consisting of spherical particles of liquid natural rubber strongly bonded to the surrounding matrix. The toughness reached a maximum at 15 wt.% HLNR despite a marginal decrease in Young's modulus, tensile strength, and flexural properties, indicating that HLNR could be employed as an effective toughener for epoxy resin.

Sahoo et al. (2014) found that the addition of 20 phr of epoxidized soybean oil (ESO) led to enhanced toughness of the epoxy without an appreciable reduction of properties. In addition, the elongation at break and flexural strain increased with increasing ESO concentration. Further, ESO was transesterified to form epoxy methyl soyate (EMS), which was then blended with DGEBA epoxy. It was found that the thermomechanical and damping properties of the EMS-toughened epoxy system were greatly improved.

The epoxidized natural rubber (ENR) prepared by the epoxidation of natural rubber with peracetic, perbenzoic, and perphthalic acids in solutions is also qualified for toughening epoxy (Gan and Hamid 1997). Because of the presence of the reactive epoxide and vinyl groups in the backbone, ENR can be utilized in polymer modification and blending by reacting with common epoxy curing agents containing OH, NH, COOH, and C=C groups (Gan and Hamid 1997; Hashim and Kohjiya 1994). The introduction of the epoxy group allows ENR to have a higher T_g , oil resistance, and polarity than the natural rubber. By varying the epoxidation degree, ENR with different physical properties such as T_g , resilience, damping, polarity, oil swelling, and compatibility can be prepared (Gan and Hamid 1997; Baker et al. 1985).

Epoxidized natural rubber (ENR50) and its liquid version (LENR50) were applied to modify two sets of DGEBA-based epoxy resins. The ENR loading ranged from 1.6 to 5.9 wt.% and could be up to 12 wt.%. At the maximum LENR loading, the tensile toughness increased by 250%, and the impact toughness increased by 125% in comparison with that of the neat formulation. The improvements obtained with ENR were nearly as high as those from LENR. The SEM micrographs of fracture surfaces showed uniform dispersion of rubber particles in the submicrometer size range. LENR particles ranged from 0.33 to 0.47 μm , while ENR particles ranged from 0.48 to 0.67 μm , as shown in Fig. 10 (Cizravi and Subramaniam 1999).

ENR could affect the curing behavior and adhesive strength of the epoxy (DGEBA) and dicyandiamide/2-methyl imidazole system. The addition of ENR leads to greater exotherms as compared to that of neat epoxy, which could be attributed to the reaction of epoxide groups in the ENR during curing. ENR could react with curing agents applied in the epoxy system and release heat (Hashim and Kohjiya 1994). Consequently, the increase of the epoxide concentration from ENR results in more curing reactions and reaction heats. The presence of ENR facilitates the reaction with the curing agent more effectively at lower curing temperatures. The time to maximal curing rate, the glass transition temperature, the rate constant, and

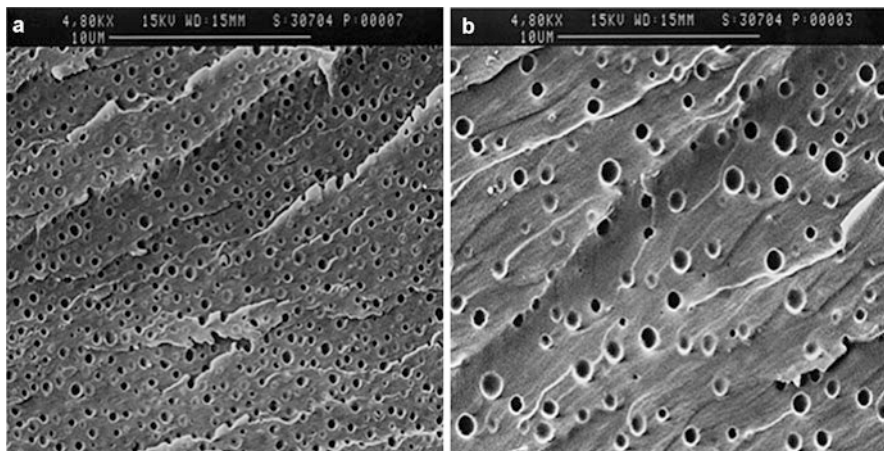


Fig. 10 SEM micrograph of the dispersion of (a) LENR50 with 10.1 wt.% loading and (b) ENR50 with 4.5 wt.% loading (Cizravi and Subramaniam 1999)

the reaction order of epoxy system change with the content of ENR added because of the reaction of ENR with the epoxy system. Because the addition of ENR affects the stoichiometric balance and the reaction mechanisms, the structure of the cross-linked resin and the conversion near to gel are changed. The particle size of the rubber phase increases with increasing curing temperature and ENR content. The volume fraction (V_f) of the separated rubber phase follows a similar trend except at high curing temperatures, implying that the dissolution of epoxy resin in ENR also depends on the curing temperature and the amount of ENR. The increase in V_f is attributed to the epoxy resin dissolved in ENR during curing. A higher curing temperature facilitates the dissolution of epoxy resin in ENR, while a lower curing temperature leads to a slow increase in viscosity. If there is enough time for rubber phase separation, there would be less dissolved epoxy in the rubber particles (Bussi and Ishida 1994). The increase in the miscible content of the low T_g constituent could shift the T_g of miscible blend to a lower temperature. The higher the epoxidized content, the lower the T_g because of the better miscibility. The addition of ENR leads to a decrease in the lap shear strength (LSS), which appears to be contradictory to the results obtained from the V_f and T_g in which a soft and flexible cured ENR/epoxy system should be reached because of the dissolution of ENR in the epoxy matrix. This could be attributed to the adverse affect of ENR on the cured structure of epoxy matrix. It is believed that ENR affects the stoichiometric ratio of epoxy and curing agents because of its participation in the curing reaction that causes a structural change in the cured epoxy matrix. This may lead to the formation of an interior cured system in ENR/epoxy system (Hong and Chan 2004).

ENRs with different concentrations of up to 20 wt.% were prepared and used as modifiers for an anhydride/epoxy mixture to develop a high-performance material

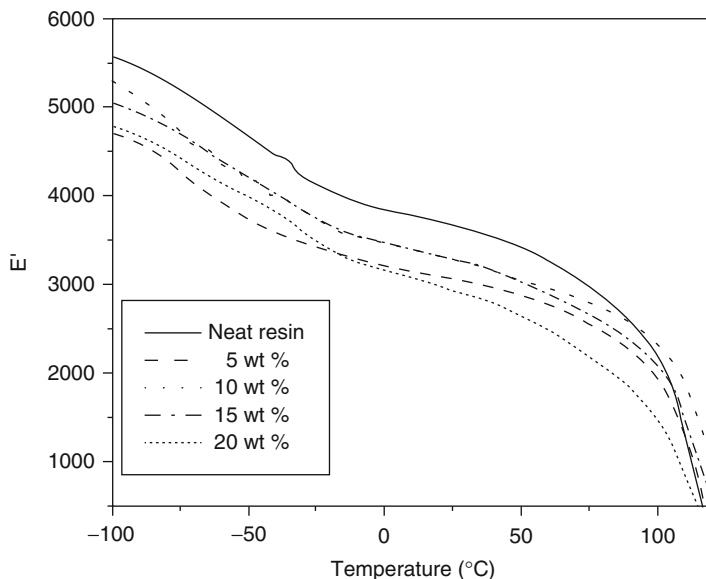


Fig. 11 Variation of E' of the DGEBA/ENR blends (Hong and Chan 2004)

with epoxy and liquid natural rubbers. It was shown that the storage modulus and T_g of ENR/epoxy blends decreased slightly with the addition of rubber due to the lower stiffness of ENR. Interestingly, the T_g of the epoxy phase shifted toward a slightly lower temperature with the addition of ENR, as shown in Fig. 11. The thermal stability of the epoxy matrix was retained as the initial and final decomposition temperatures were not affected by the blending of the epoxy with ENR. The domain size increased with increasing ENR content because of coalescence. The cured epoxy resin containing about 10 wt.% ENR showed the best balance of properties, and the impact strength was enhanced by 305%, indicating a better energy-transfer mechanism operating in the ENR/epoxy because of the excellent interfacial adhesion and bonding with the matrix. ENR droplets acted as the stress concentrators, resulting in plastic deformation in the surrounding matrix which could take up a significant amount of applied stress. As a result, the impact strength and fracture toughness were greater than those of unmodified epoxy (Mathew et al. 2014).

Block Copolymer-Toughened Epoxy

BCPs could self-assemble into nanoscale micellar structures in the epoxy matrix at low loadings, resulting in a dramatic increase in fracture resistance (Barcia et al. 2002; Chikhi et al. 2002; Wise et al. 2000; Grishchuk et al. 2013; Kunz et al. 1982). Moreover, BCPs have a minimal impact on the glass transition temperature and Young's modulus of epoxy. To obtain the optimum toughening

effect, it is important to synthesize BCPs with special structures and to control their micellar structures in self-assembling process.

Controlling of Morphology

In preparing rubber-toughened epoxies, liquid rubber and liquid epoxy are mechanically mixed to form a homogeneous solution. Upon curing, rubber particles precipitate as a second phase. The final microstructure of the blend is highly dependent on the phase separation in the curing process. A new trend is to control the morphology of the blend by changing the mixing sequence or the curing program.

Zhou et al. (2014) proposed a novel method for preparing CTBN/epoxy blend, in which an initiator was added to the liquid rubber-epoxy mixture to initiate the cross-linking reaction and then a curing agent was added to cure epoxy. The results showed that the impact strength of CTBN/epoxy blends was greatly improved without affecting the modulus. The yield strength, Young's modulus, and impact strength of the CTBN/epoxy blend prepared by the new method were increased by 2.7%, 5.5%, and 20.9%, respectively, compared with that of the traditional counterparts. However, unlike traditional CTBN/epoxy blend in which the dispersed particles were pure rubber phases, the rubber phase and matrix formed a local interpenetrating network in the pre-cross-linked CTBN/epoxy blend, resulting in an improvement of interfacial adhesion between the two phases and thus a great improvement in the mechanical properties.

In some literature, CTBN was pre-reacted with the epoxy before the addition of hardener in order to form an epoxy-terminated elastomer molecule (Verchere et al. 1990).

Conclusions

Epoxy resins can be toughened by blending with a suitable liquid rubber that is initially miscible with epoxy and undergoes a phase separation during curing, leading to the formation of a two-phase microstructure; or blending with preformed rubbery particles. The morphology of the separated phase depends largely on the curing conditions and the initial amount of rubber in the first case. Nevertheless, it is initially defined in the second case (Maazouz et al. 1994).

The fracture energy increases with the addition of rubbers, especially for the rubber with a high AN content. The same toughening effect is obtained with CSP but without any decrease in T_g of the epoxy network.

The parameters that influence the toughening efficiency of the rubber-toughened epoxy include (1) the inherent ductility of the epoxy matrix, e.g., the cross-link density of the epoxy matrix; (2) the properties of rubber particles, e.g., the size, morphology, and cross-link density of the rubber phase; and (3) the particle-epoxy interface (Qian et al. 1995). The fracture energy of toughened epoxy increases with increasing volume fraction of rubber (Lowe et al. 1996).

Large particles appear to be not as efficient as small ones in improving fracture energy. Large rubber particles outside the process zone act only as bridging particles, resulting in a modest increase in fracture energy, while small ones in the process zone are forced to cavitate by the large hydrostatic stress component in the process zone and thus contribute to increasing fracture energy. There is a critical interparticle distance below which the material is tough and above which the material is brittle. For a given volume fraction of rubber, the interparticle distance can be reduced by decreasing the particle size (Wu and Margolina 1990). The optimal particles size actually involves a bimodal distribution of both small and large particles. It is shown that rubber-modified networks having a bimodal distribution of particles exhibit higher fracture toughness than that of the matrix having a unimodal distribution of particles (Kunz et al. 1982; Kinloch and Hunston 1987).

The final properties of the multiphase polymer blends depend on the morphology of the system. The morphology of the separated phase depends largely on the curing conditions and the initial amount of rubber. The spherical liquid rubber domains can cause sufficient stress transfer and thereby prevent the material from catastrophic failure (Mathew et al. 2010).

Butadiene liquid rubber has been the most widely used toughener for epoxy. The carboxyl end groups strongly enhance the curing rate. However, as the butadiene component of the elastomers contains unsaturated bonds, it would be a site for premature thermal and/or oxidative instability, and such modified resins are not suitable for use at high temperatures (Okamoto 1983). Excessive cross-linking could take place with time, which would detract from the otherwise desirable improvements accomplished with these structures. However, there is the possibility of the presence of traces of carcinogenic free acrylonitrile, which might limit the use of these materials (Duseck et al. 1984). Recently, some saturated liquid rubbers such as polysulfide (Kemp et al. 1992), acrylate (Iijima et al. 1992), and polyurethane (Wang and Chen 1995) have been reported as replacements for CTBN.

The toughness of epoxy resins can be significantly improved at the expense of the high-temperature properties due to the dissolved liquid rubber. The glass transition temperature of the epoxy system decreases with the addition of liquid rubber, but remains constant with the addition of CSR. Nowadays, liquid rubbers with other inorganic fillers, such as nanoclay (Vijayan et al. 2013), silica nanoparticles (Sprenger 2013), and multiwalled carbon nanotubes (Mahmood et al. 2014), are used to modify the epoxy resins. The incorporation of both rubber and rigid inorganic fillers will generate a new kind of epoxy resins with remarkable properties, which has attracted the attention of many researchers. This opens a new research direction in this field.

References

- Bagheri R, Pearson RA (1996) Role of blend morphology in rubber-toughened polymers. *J Mater Sci* 31(15):3945–3954

- Bagheri R, Marouf BT, Pearson RA (2009) Rubber-toughened epoxies: a critical review. *Polym Rev* 49(3):201–225
- Baker CSL, Gelling IR, Newell R (1985) Epoxidized natural rubber. *Rubber Chem Technol* 58 (1):67–85
- Barcia FL, Abrahao MA, Soares BG (2002) Modification of epoxy resin by isocyanate-terminated polybutadiene. *J Appl Polym Sci* 83(4):838–849
- Bascom WD, Hunston DL (1989) Rubber toughened plastics. American Chemical Society, Washington, DC
- Bascom WD, Cottingham RL, Jones RL et al (1975) The fracture of epoxy- and elastomer-modified epoxy polymers in bulk and as adhesives. *J Appl Polym Sci* 19(9):2545–2562
- Bécu-Longuet L, Bonnet A, Pichot C et al (1999) Epoxy networks toughened by core-shell particles: influence of the particle structure and size on the rheological and mechanical properties. *J Appl Polym Sci* 72(6):849–858
- Boogh A, Pettersson B, Månson J-AE (1999) Hyperbranched polymers as tougheners for epoxy resins. *Polymer* 40:2249–2261
- Bucknall CB, Gilbert AH (1989) Toughening tetrafunctional epoxy resins using polyetherimide. *Polymer* 30(2):213–217
- Bucknall C, Partridge I (1983) Phase separation in epoxy resins containing polyethersulphone. *Polymer* 24(5):639–644
- Bucknall CB, Partridge IK (1986) Phase separation in crosslinked resins containing polymeric modifiers. *Polym Eng Sci* 26(1):54–62
- Bussi P, Ishida H (1994) Composition of the continuous phase in partially miscible blends of epoxy resin and epoxidized rubber by dynamic mechanical analysis. *Polymer* 35(5):956–966
- Chen TK, Jan YH (1995) Effect of matrix ductility on the fracture behavior of rubber toughened epoxy resins. *Polym Eng Sci* 35(9):778–785
- Chikhi N, Fellahi S, Bakar M (2002) Modification of epoxy resin using reactive liquid (ATBN) rubber. *Eur Polym J* 38(2):251–264
- Cizravi J, Subramaniam K (1999) Thermal and mechanical properties of epoxidized natural rubber modified epoxy matrices. *Polym Int* 48(9):889–895
- Day RJ, Lovell PA, Wazzan AA (2001) Toughened carbon/epoxy composites made by using core/shell particles. *Compos Sci Technol* 61(1):41–56
- Dean JM, Lipic PM, Grubbs RB et al (2001) Micellar structure and mechanical properties of block copolymer-modified epoxies. *J Polym Sci B* 39(23):2996–3010
- Dean JM, Grubbs RB, Saad W et al (2003a) Mechanical properties of block copolymer vesicle and micelle modified epoxies. *J Polym Sci B* 41(20):2444–2456
- Dean JM, Verghese NE, Pham HQ et al (2003b) Nanostructure toughened epoxy resins. *Macromolecules* 36(25):9267–9270
- Deng J, Liu X, Li C et al (2015) Synthesis and properties of a bio-based epoxy resin from 2,5-furandicarboxylic acid (FDCA). *RSC Adv* 5(21):15930–15939
- Dompas D, Groeninckx G (1994) Toughening behaviour of rubber-modified thermoplastic polymers involving very small rubber particles: 1. A criterion for internal rubber cavitation. *Polymer* 35(22):4743–4749
- Duseck K, Lendnicky F, Lunak S et al (1984) In rubber modified thermoset. American Chemistry Society, Washington, DC
- Gam KT, Miyamoto M, Nishimura R et al (2003) Fracture behavior of core-shell rubber-modified clay-epoxy nanocomposites. *Polym Eng Sci* 43(10):1635–1645
- Gan S-N, Hamid ZA (1997) Partial conversion of epoxide groups to diols in epoxidized natural rubber. *Polymer* 38(8):1953–1956
- Garg AC, Mai Y-W (1988) Failure mechanisms in toughened epoxy resins—a review. *Compos Sci Technol* 31(3):179–223
- Giannakopoulos G, Masania K, Taylor AC (2010) Toughening of epoxy using core-shell particles. *J Mater Sci* 46(2):327–338

- Gilbert AH, Bucknall CB (1991) Epoxy resin toughened with thermoplastic. *Makromol Chem Macromol Symp* 45(1):289–298
- Gopala Krishnan PS, Ayyaswamy K, Nayak SK (2013) Hydroxy terminated polybutadiene: chemical modifications and applications. *J Macromol Sci A* 50(1):128–138
- Grishchuk S, Sorochynska L, Vorster OC et al (2013) Structure, thermal, and mechanical properties of DDM-hardened epoxy/benzoxazine hybrids: effects of epoxy resin functionality and ETBN toughening. *J Appl Polym Sci* 127(6):5082–5093
- Grubbs RB, Broz ME, Dean JM et al (2000a) Selectively epoxidized polyisoprene-polybutadiene block copolymers. *Macromolecules* 33(7):2308–2310
- Grubbs RB, Dean JM, Broz ME et al (2000b) Reactive block copolymers for modification of thermosetting epoxy. *Macromolecules* 33(26):9522–9534
- Grubbs RB, Dean JM, Bates FS (2001) Methacrylic block copolymers through metal-mediated living free radical polymerization for modification of thermosetting epoxy. *Macromolecules* 34(25):8593–8595
- Guo Q, Dean JM, Grubbs RB et al (2003) Block copolymer modified novolac epoxy resin. *J Polym Sci B* 41(17):1994–2003
- Hashim AS, Kohjiya S (1994) Curing of epoxidized natural rubber with p-phenylenediamine. *J Polym Sci A Polym Chem* 32(6):1149–1157
- Hayes BS, Seferis JC (2001) Modification of thermosetting resins and composites through preformed polymer particles: a review. *Polym Compos* 22(4):451–467
- Hillmyer MA, Lipic PM, Hajduk DA et al (1997) Self-assembly and polymerization of epoxy resin-amphiphilic block copolymer nanocomposites. *J Am Chem Soc* 119(11):2749–2750
- Hong S-G, Chan C-K (2004) The curing behaviors of the epoxy/dicyanamide system modified with epoxidized natural rubber. *Thermochem Acta* 417(1):99–106
- Iijima T, Yoshioka N, Tomoi M (1992) Effect of cross-link density on modification of epoxy resins with reactive acrylic elastomers. *Eur Polym J* 28(6):573–581
- Jain S, Bates FS (2003) On the origins of morphological complexity in block copolymer surfactants. *Science* 300(5618):460–464
- Jingqiang S, Yafeng Z, Jindong Q et al (2004) Core-shell particles with an acrylate polyurethane core as tougheners for epoxy resins. *J Mater Sci* 39(20):6383–6384
- Karger-Kocsis J (1993) Instrumented impact fracture and related failure behavior in short- and long-glass-fiber-reinforced polypropylene. *Compos Sci Technol* 48(1–4):273–283
- Kemp TJ, Wilford A, Howarth OW et al (1992) Structural and materials properties of a polysulphide-modified epoxide resin. *Polymer* 33(9):1860–1871
- Kim HS, Ma P (1996) Correlation between stress-whitening and fracture toughness in rubber-modified epoxies. *J Appl Polym Sci* 61(4):659–662
- Kinloch AJ, Hunston DL (1987) Effect of volume fraction of dispersed rubbery phase on the toughness of rubber-toughened epoxy polymers. *J Mater Sci Lett* 6(2):137–139
- Kinloch AJ, Shaw SJ, Tod DA et al (1983) Deformation and fracture behaviour of a rubber-toughened epoxy: 1. Microstructure and fracture studies. *Polymer* 24(10):1341–1354
- Kinloch AJ, Finch CA, Hashemi S (1987) Effect of segmental molecular mass between crosslinks of the matrix phase on the toughness of rubber-modified epoxies. *Polym Commun* 28:322–325
- Kozii VV, Rozenberg BA (1992) Mechanisms of energy dissipation in elastomer-modified thermosetting polymer matrices and composites based on such polymers. *Polym Sci* 34:919–951
- Kunz SC, Sayre JA, Assink RA (1982) Morphology and toughness characterization of epoxy resins modified with amine and carboxyl terminated rubbers. *Polymer* 23(13):1897–1906
- Latha PB, Adhinarayanan K, Ramaswamy R (1994) Epoxidized hydroxy-terminated polybutadiene – synthesis, characterization and toughening studies. *Int J Adhes Adhes* 14(1):57–61
- LeMay JD, Kelley FN (1986) Structure and ultimate properties of epoxy resins. *Adv Polym Sci* 78:115–148

- Levita G, De Petris S, Marchetti A et al (1991) Crosslink density and fracture toughness of epoxy resins. *J Mater Sci* 26(9):2348–2352
- Lin KF, Chung UL (1994) Phase-inversion investigations of rubber-modified epoxies by electron microscopy and X-ray diffraction. *J Mater Sci* 29(5):1198–1202
- Lin K-F, Shieh Y-D (1998a) Core-shell particles to toughen epoxy resins. I. Preparation and characterization of core-shell particles. *J Appl Polym Sci* 69(10):2069–2078
- Lin K-F, Shieh Y-D (1998b) Core-shell particles designed for toughening the epoxy resins. II. Core-shell-particle-toughened epoxy resins. *J Appl Polym Sci* 70(12):2313–2322
- Lipic PM, Bates FS, Hillmyer MA (1998) Nanostructured thermosets from self-assembled amphiphilic block copolymer/epoxy resin mixtures. *J Am Chem Soc* 120(35):8963–8970
- Liu J, Sue H-J, Thompson ZJ et al (2008) Nanocavitation in self-assembled amphiphilic block copolymer-modified epoxy. *Macromolecules* 41(20):7616–7624
- Liu J, Thompson ZJ, Sue H-J et al (2010) Toughening of epoxies with block copolymer micelles of wormlike morphology. *Macromolecules* 43(17):7238–7243
- Liu Y, Wang J, Xu S (2014) Synthesis and curing kinetics of cardanol-based curing agents for epoxy resin by in situ depolymerization of paraformaldehyde. *J Polym Sci A Polym Chem* 52(4):472–480
- Lowe A, Kwon O-H, Mai Y-W (1996) Fatigue and fracture behaviour of novel rubber modified epoxy resins. *Polymer* 37(4):565–572
- Maazouz A, Sautereau H, Gerard JF (1994) Toughening of epoxy networks using pre-formed core-shell particles or reactive rubbers. *Polym Bull* 33(1):67–74
- Mafi ER, Ebrahimi M (2008) Role of core-shell rubber particle cavitation resistance on toughenability of epoxy resins. *Polym Eng Sci* 48(7):1376–1380
- Mahmood N, Khan AU, Stöckelhuber KW, et al (2014) Carbon nanotubes-filled thermoplastic polyurethane-urea and carboxylated acrylonitrile butadiene rubber blend nanocomposites. *J Appl Polym Sci* 131(11):40341
- Mathew VS, Sinturel C, George SC et al (2010) Epoxy resin/liquid natural rubber system: secondary phase separation and its impact on mechanical properties. *J Mater Sci* 45(7):1769–1781
- Mathew VS, George SC, Parameswaranpillai J et al (2014) Epoxidized natural rubber/epoxy blends: phase morphology and thermomechanical properties. *J Appl Polym Sci* 131(4):39906
- McGarry FJ (1970) Building design with fibre reinforced materials. *Proc R Soc A: Math Phys Eng Sci* 319(1536):59–68
- Meeks AC (1974) Fracture and mechanical properties of epoxy resin and rubber-modified epoxies. *Polymer* 15:675–681
- Nakamura Y, Tabata H, Suzuki H et al (1986) Internal stress of epoxy resin modified with acrylic core-shell particles prepared by seeded emulsion polymerization. *J Appl Polym Sci* 32(5):4865–4871
- Nguyen-Thuc BH, Maazouz A (2002) Morphology and rheology relationships of epoxy/core-shell particle blends. *Polym Eng Sci* 42(1):120–133
- Okamoto Y (1983) Thermal aging study of carboxyl-terminated polybutadiene and poly(butadiene-acrylonitrile)-reactive liquid polymers. *Polym Eng Sci* 23(4):222–225
- Ozturk A, Kaynak C, Tincer T (2001) Effects of liquid rubber modification on the behaviour of epoxy resin. *Eur Polym J* 37(12):2353–2363
- Pearson RA, Yee AF (1989) Toughening mechanisms in elastomer-modified epoxies. *J Mater Sci* 24(7):2571–2580
- Pearson RA, Yee AF (1991) Influence of particle size and particle size distribution on toughening mechanisms in rubber-modified epoxies. *J Mater Sci* 26(14):3828–3844
- Qian JY, Pearson RA, Dimonie VL et al (1995) Synthesis and application of core-shell particles as toughening agents for epoxies. *J Appl Polym Sci* 58(2):439–448
- Ratna D (2009) Handbook of thermoset resins. Smithers Rapra, London
- Ratna D, Banthia AK (2004) Rubber toughened epoxy. *Macromol Res* 12(1):11–21

- Sahoo SK, Mohanty S, Nayak SK (2014) Synthesis and characterization of bio-based epoxy blends from renewable resource based epoxidized soybean oil as reactive diluent. *Chin J Polym Sci* 33 (1):137–152
- Sprenger S (2013) Epoxy resins modified with elastomers and surface-modified silica nanoparticles. *Polymer* 54(18):4790–4797
- Sue H-J (1991) Study of rubber-modified brittle epoxy systems. Part II: toughening mechanisms under mode-I fracture. *Polym Eng Sci* 31(4):275–288
- Sue HJ, Garcia-Meitin EI, Orchard NA (1993a) Toughening of epoxies via craze-like damage. *J Polym Sci B* 31(5):595–608
- Sue HJ, Garcia-Meitin EI, Pickelman DM et al (1993b) Toughened plastics. American Chemistry Society, Washington, DC
- Sultan JN, McGarry FJ (1973) Effect of rubber particle size on deformation mechanisms in glassy epoxy. *Polym Eng Sci* 13(1):29–34
- Sultan JN, Liable RC, McGarry FJ (1971) Microstructure of two-phase polymers. *Polym Symp* 16:127–136
- Szeluga U, Kurzeja L, Galina H (2008) Curing of epoxy/novolac system modified with reactive liquid rubber and carbon filler. *Polym Bull* 60(4):555–567
- Thomas R, Abraham J, Thomas PS et al (2004) Influence of carboxyl-terminated (butadiene-co-acrylonitrile) loading on the mechanical and thermal properties of cured epoxy blends. *J Polym Sci B* 42(13):2531–2544
- Unnikrishnan KP, Thachil ET (2012) Toughening of epoxy resins. *Des Monomers Polym* 9 (2):129–152
- Verchère D, Sautereau H, Pascault JP et al (1989) Miscibility of epoxy monomers with carboxyl-terminated butadiene-acrylonitrile random copolymers. *Polymer* 30(1):107–115
- Verchere D, Sautereau H, Pascault JP et al (1990) Rubber-modified epoxies. I. Influence of carboxyl-terminated butadiene-acrylonitrile random copolymers (CTBN) on the polymerization and phase separation processes. *J Appl Polym Sci* 41(3–4):467–485
- Vijayan PP, Puglia D, Kenny JM et al (2013) Effect of organically modified nanoclay on the miscibility, rheology, morphology and properties of epoxy/carboxyl-terminated (butadiene-co-acrylonitrile) blend. *Soft Matter* 9(10):2899
- Wang H-H, Chen J-C (1995) Toughening of epoxy resin by reacting with functional terminated-polyurethanes. *J Appl Polym Sci* 57(6):671–677
- Wise CW, Cook WD, Goodwin AA (2000) CTBN rubber phase precipitation in model epoxy resins. *Polymer* 41(12):4625–4633
- Wu S (1985) Phase structure and adhesion in polymer blends: a criterion for rubber toughening. *Polymer* 26(12):1855–1863
- Wu S, Margolina A (1990) Reply to comments. *Polymer* 31(5):972–974
- Wu J, Thio YS, Bates FS (2005) Structure and properties of PBO-PEO diblock copolymer modified epoxy. *J Polym Sci B* 43(15):1950–1965
- Xu SA, Wang GT, Mai YW (2013) Effect of hybridization of liquid rubber and nanosilica particles on the morphology, mechanical properties, and fracture toughness of epoxy composites. *J Mater Sci* 48(9):3546–3556
- Yahyaie H, Ebrahimi M, Tahami HV et al (2013) Toughening mechanisms of rubber modified thin film epoxy resins. *Prog Org Coat* 76(1):286–292
- Yang X, Yi F, Xin Z et al (2009) Morphology and mechanical properties of nanostructured blends of epoxy resin with poly(ϵ -caprolactone) block poly(butadiene-co-acrylonitrile) block poly(ϵ -caprolactone) triblock copolymer. *Polymer* 50(16):4089–4100
- Yee AF, Pearson RA (1986) Toughening mechanisms in elastomer-modified epoxies, part I mechanical studies. *J Mater Sci* 21:2462–2474
- Yee AF, Du J, Thouless MD (2000) *Polymer blends*. Wiley, New York
- Zhou H-S, Song X-X, Xu S-A (2014) Mechanical and thermal properties of novel rubber-toughened epoxy blend prepared by in situ pre-crosslinking. *J Appl Polym Sci* 131(22):41110

Novel Techniques for the Preparation of Different Epoxy/Rubber Blends

2

Bluma Guenther Soares and Sebastien Livi

Abstract

Since longtime, academic and industrial research has been focused on the development of epoxy networks with excellent mechanical properties such as their fracture toughness and flexural and tensile properties by using rubber particles or low molar mass liquid rubbers. In fact, different routes have been developed to increase their resistance to damage such as the synthesis of new copolymers and block copolymers, the incorporation of unmodified or modified rubber particles, as well as the formation of graft interpenetrating polymer networks (graft-IPN). Nevertheless, the number of publications combining the keywords epoxy and rubber is considerable. Thus, various types of rubber have been studied as modifiers of epoxy networks, including functionalized or not butadiene–acrylonitrile rubber (NBR), polybutadiene (PBD), acrylate-based rubbers, natural rubber (NR), styrene–butadiene rubber (SBR), polydimethylsiloxane (PDMS), etc. For these reasons, this chapter gives an overview of the different preparation of epoxy–rubber networks and their final properties.

Keywords

Epoxy prepolymer • Thermosets • Rubber particles • Liquid rubber • Epoxy–rubber networks

B.G. Soares (✉)

Programa de Engenharia Metalúrgica e de Materiais-COPPE, Centro de Tecnologia, Universidade Federal do Rio de Janeiro, Rio de Janeiro, Brazil

e-mail: bluma@metalmat.ufjf.br

S. Livi

Université de Lyon, Lyon, France

INSA Lyon, Villeurbanne, France

UMR 5223, Ingénierie des Matériaux Polymères, CNRS, Paris, France

e-mail: sebastien.livi@insa-lyon.fr

Contents

Introduction	30
Preparation of Rubber–Epoxy Blends	32
Physical Blending	32
The Use of Epoxy–Rubber Adduct	32
The Use of Preformed Rubber Particles	35
Epoxy Modified with Rubber Nanoparticles	37
The Use of Preformed Cross-Linked Nanoparticles	38
Epoxy–Rubber Nanoparticle Blends Prepared by Microphase Separation During Curing Process	38
Main Elastomers Used to Modify Epoxy Networks	39
Butadiene–Acrylonitrile Rubber (NBR)-Based Modified Epoxy Resin	39
Liquid Polybutadiene-Based Modified Epoxy Resin	46
Natural Rubber as Modifier of Epoxy Resin	50
Polysiloxane as Modifier of Epoxy Resin	53
Acrylate Rubber as Modifier of Epoxy Resin	57
Conclusion Remarks	60
References	60

Introduction

Epoxy networks are considered one of the most versatile thermoset materials and are widely utilized for coatings, structural adhesives, and composites, as well as electrical and electronic materials, due to their excellent properties, such as low shrinkage during curing, good adhesion, high strength and stiffness, resistance to heat, creep and chemicals, and good thermal characteristics (Pascual et al. 2002). However, these materials are brittle and exhibit poor toughness which limit their applications in many areas. In fact, they have much lower fracture energies than thermoplastics (two orders of magnitude) or metals (three orders of magnitude), which considerably limits their resistance to damage. Thus, the academic and industrial research has been focused on developing new systems in order to improve the toughening of epoxy networks, which include the use of thermoplastics, rubbers, etc. As stated by several authors, the incorporation of rubber particles as additives has been extensively studied for modifying the deformation mechanism which occurs at the crack tip (Riew and Gillham 1984; Bagheri et al. 2009; Thomas et al. 2014). In this regard, low molar mass liquid rubbers are preferred to avoid excessive increase of viscosity, thus making easier the processability of the system. Moreover, such liquid rubbers must contain appropriate functional groups, such as hydroxyl, carboxyl, amino, epoxy, and isocyanate groups, which are able to chemically react with the oxirane and/or the hydroxyl groups of the epoxy prepolymer, providing an effective anchorage between rubber particles and epoxy matrix. However, the use of low molar mass liquid rubbers is somewhat restricted by their limited solubility and compatibility with the epoxy-curing agent mixtures leading to phase

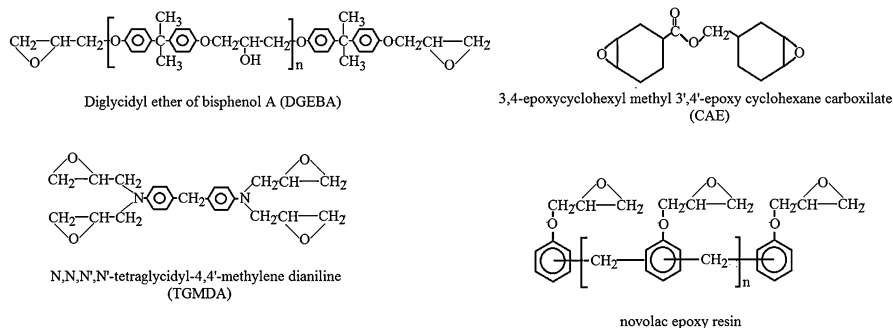


Fig. 1 Structure of the main epoxy prepolymer used for the preparation of epoxy-based thermo-setting materials

separation during curing process. In order to prepare epoxy–rubber blends, different procedures have been studied, and the most commonly used consists of blending rubber with epoxy prepolymer using mechanical mixing such as internal mixer (Brabender), screw, or twin-screw extruder. Other ways with or without solvent consist the use of high-speed mixing such as Ultra-turrax[®] or Rayneri. Another route well described in the literature is to prepare epoxy–rubber adduct by reacting the oxirane or hydroxyl groups of the epoxy prepolymer with the functional groups of the rubber.

Figure 1 illustrates the structure of the common epoxy prepolymers with the assigned reactive sites.

Relatively low amount of rubber particles (10–15%) well adhered to the epoxy matrix can dissipate the mechanical energy by cavitation and/or shear yielding, thus increasing the crack grow resistance of the corresponding modified epoxy networks, which is fundamental for achieving final products with outstanding fracture properties (Verchere et al. 1991; Ohashi et al. 1992). Several types of rubber have been investigated as epoxy network modifiers and include butadiene–acrylonitrile rubber (NBR), polybutadiene (PBD), acrylate-based rubbers, natural rubber (NR), styrene–butadiene rubber (SBR), and polydimethylsiloxane (PDMS), which are randomly and/or terminally functionalized with different groups. The final properties as well as the morphologies of the rubber-modified epoxy network depends on the chemical structure of the rubber, the nature of the functional groups in the rubber chain, the solubility, concentration, molecular weight and the method used for incorporating the rubber within the epoxy system, the nature of the curing agent, etc.

The present chapter describes an overview of the different procedures used to develop rubber-based epoxy blends and discusses more broadly the use of rubber or preformed rubber as particles as well as some modified epoxy systems. Moreover, this work also highlights the different families of elastomers conventionally used to modify epoxy networks.

Preparation of Rubber–Epoxy Blends

Physical Blending

Different ways have been investigated to prepare rubber–epoxy blends. The most commonly used procedure consists of blending rubber with epoxy prepolymer using mechanical mixing. For rubber with high molar mass, blending is usually assisted by an appropriate solvent to facilitate the incorporation of the rubber with the epoxy (Frounchi et al. 2000). However, in the case of low molar mass liquid rubber, the presence of solvent is not required. In this case, the epoxy prepolymer and the rubber are directly mixed using conventional mechanical mixing or high-speed mixing. Then, an appropriate curing agent is added and the mixture is transferred to mold to perform the curing process, whose protocol depends on the nature of the hardener (amine, phenol, acid, etc.). This methodology has been used since 1970 to incorporate liquid rubber into epoxy prepolymers and is indicated for rubbers which are soluble with the epoxy prepolymer, as carboxyl-terminated butadiene–acrylonitrile rubber (CTBN) (Sultan et al. 1971). During the curing process, the rubber begins to precipitate out from the epoxy matrix because of the increase in molar mass of the matrix and phase separates, initially in the form of rubber/epoxy co-continuous structure, which turns into separated rubber phase usually in the form of spherical particles (Williams et al. 1997; Yamanaka and Inoue 1990; Yamanaka et al. 1989; Chan and Rey 1997; Inoue 1995; Wise et al. 2000). This process is known as “reaction-induced phase separation process.” The morphology of these blends is influenced by the polarity of the rubber (Chen and Jan 1992; Zhao et al. 2015), composition (Mathew et al. 2014), molar mass of the rubber (Chen et al. 1994a), the nature of the hardener, and the curing schedule (Ratna 2001; Thomas et al. 2007), among others.

The Use of Epoxy–Rubber Adduct

To improve the interfacial adhesion between epoxy matrix and rubber particles, several authors have performed the previous reaction between the functionalized rubber and the epoxy matrix and employed the corresponding adduct on the preparation of rubber-modified epoxy network. The epoxy–rubber adduct can be prepared by reacting the active groups located in the epoxy prepolymer (oxirane or hydroxyl groups) with appropriate functional groups located randomly or at the end of the rubber chain component such as carboxyl, hydroxyl, amine, and isocyanate groups, among others.

Hydroxyl groups are not highly reactive toward oxirane groups. However, if an appropriate catalyst is employed, the reaction may be possible. These are the cases of the systems reported by Zhou and Cai (2012) who have successfully prepared the epoxy–rubber adduct by reacting hydroxyl-terminated polybutadiene (HTPB) with epoxy prepolymer at temperature higher than 100 °C, in the presence of 2,4,6-tri(dimethylaminomethyl)phenol as catalyst. The effectiveness of the reaction,

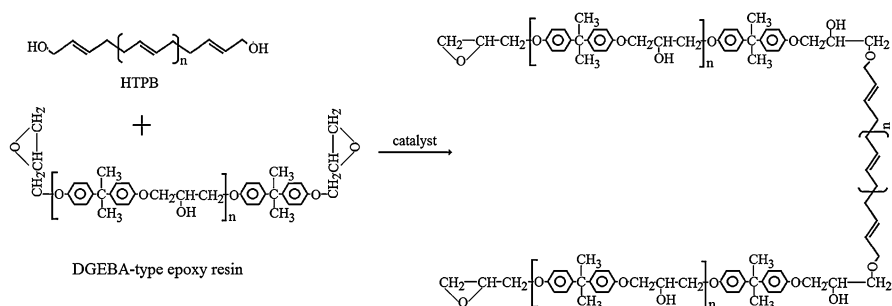


Fig. 2 Scheme for the reaction between epoxy and hydroxyl-terminated liquid rubber

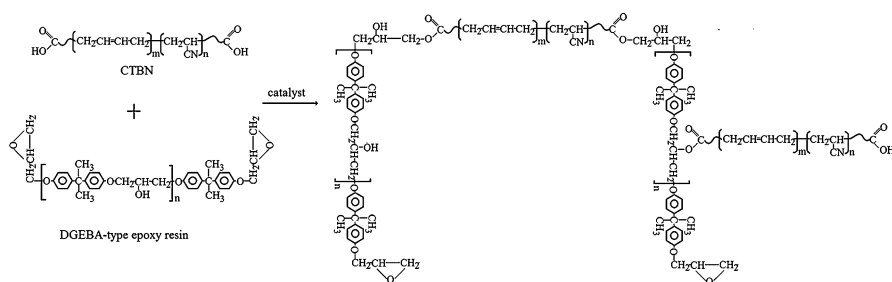


Fig. 3 Scheme for the reaction between epoxy and carboxyl-terminated liquid rubber

illustrated in Fig. 2, was confirmed by Fourier transform infrared spectroscopy (FTIR). Zhou and Zuo (2013) also developed the adduct between epoxy prepolymer and hydroxyl-terminated styrene–butadiene rubber (HTSBR) using similar methodology with benzyldimethylamine as catalyst. In both systems, the impact strength of the epoxy network increased with the addition of the rubber–epoxy adduct. The best compromise of mechanical performance has been achieved by using 10 phr (parts per hundred) of rubber.

The adduct resulted from the reaction between carboxyl-functionalized rubber and epoxy prepolymer, illustrated in Fig. 3, is considered as one of the most popular ways to achieve epoxy–rubber networks with a good balance between thermal and impact properties. Such approach has been used for the development of epoxy modified with carboxyl-randomized (CRBN) or carboxyl-terminated butadiene–acrylonitrile rubber (CTBN) (Vásquez et al. 1987), carboxyl-functionalized acrylate rubber (Ratna and Banthia 2000), and carboxyl-terminated polybutadiene (CTPB) (Barcia et al. 2003). The reaction of carboxyl group with oxirane groups proceeds slowly at 80 °C, without catalyst (Varley 2004). Thus, Rudakova et al. (2013, 2014) prepared the epoxy–rubber adduct without catalyst by reacting both components at 120 °C and cured. However, most of the studies reported in the literature employ triphenylphosphine (Vásquez et al. 1987; Ratna and Banthia 2000; Barcia et al. 2003) or hexadecyltrimethyl ammonium bromide (Minxian et al. 2009) as

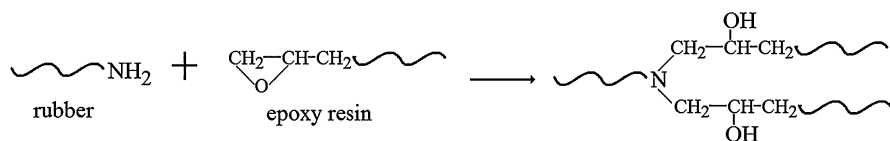


Fig. 4 Scheme for the reaction between epoxy and amino-terminated liquid rubber

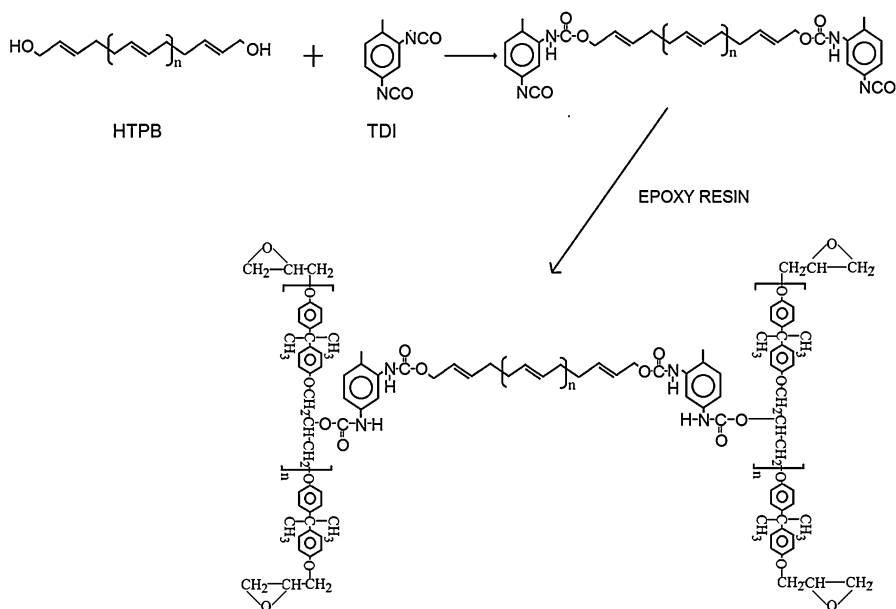


Fig. 5 Scheme for the reaction between epoxy and isocyanate-terminated liquid rubber (PBNCO)

catalyst. All modified epoxy networks presented phase-separated morphology. Details related to these systems will be discussed later.

Epoxy–rubber adduct has also been prepared using polybutadiene functionalized with *p*-aminobenzoic acid (Kar and Banthia 2005). The reaction, shown in Fig. 4, was performed at 200 °C due to the low reactivity of the aromatic amine toward nucleophilic attack. Then, the system was cured with triethylenetetramine (TETA), giving rise to epoxy networks with outstanding impact resistance with 15 phr of rubber, but lower glass transition temperature and modulus, as usually observed for CTBN-based epoxy systems.

The use of isocyanate-functionalized rubber also constitutes a very promising approach for developing toughened epoxy network, through the previous preparation of rubber–epoxy adduct, according to the scheme illustrated in Fig. 5 (Barcia et al. 2002, 2003; Soares et al. 2011). The corresponding rubber–epoxy system was cured with TETA, resulting in transparent materials, containing rubber particles dispersed in nanometric scale, even with rubber content as high as 20 phr (Soares et al. 2011).

The Use of Preformed Rubber Particles

Except for the isocyanate-functionalized liquid polybutadiene (PBNCO)/epoxy systems, the other abovementioned epoxy networks result in phase separation during the curing process, whose morphology and size of the rubber particles are difficult to control and depend on the rubber content, the chemical nature of the rubber and hardener, as well as the curing conditions. Moreover, regarding the liquid nitrile rubber and CTBN, part of the rubber, being soluble in the epoxy matrix before curing, should remain dissolved within the epoxy, contributing for a decreasing in glass transition temperature and mechanical strength (Williams et al. 1997). A common strategy to overcome these drawbacks is dispersing preformed rubbery particles with a predefined form into the epoxy matrix. This approach has been extensively investigated for more than three decades, using preformed core-shell rubber (CSR) particles. An interesting review on this subject was published in 2001 by Hayes and Seferis (2001). The CSR particles are usually constituted by a soft rubbery core within a hard shell and are typically prepared by emulsion polymerization. The dried particles are compounded with epoxy matrix, giving rise to materials with outstanding toughness characteristics without decreasing the thermal properties. This technique results in a well-controlled particle size and volume fraction of the CSR phase homogeneously dispersed within the epoxy matrix. The shell is formed by a glassy material to avoid losing the size and shape during compounding with epoxy matrix. Moreover, it should be compatible with the epoxy matrix, such as poly(methyl methacrylate) (PMMA) (Bagheri et al. 2009). Both core and shell parts of the particle can be cross-linked, contributing to the size and shape stabilization during blending with the epoxies. Usually, the cross-linking of the outer layer is carried out by polymerizing methyl methacrylate with a small amount of ethylene glycol dimethacrylate. Lin and Shieh (1998) studied the effect of cross-linking in both core and shell parts of the particle on the toughness effectiveness of modified epoxy networks and concluded that the cross-linked CSR particle presented higher toughening effect on epoxy network.

Different rubbers have been employed as the soft inner layer of the CSR particles. The most common are poly(butyl acrylate) (PBA), poly(styrene-co-butadiene) (SBR), and polysiloxane (PDMS). Several authors have used CSR particles comprising PBA core surrounded by an outer layer of cross-linked PMMA containing some amount of glycidyl methacrylate (GMA) (Bécu-Longuet et al. 1999). The presence of GMA at the shell part of the particle contributes for an improvement of the interfacial adhesion between particle and epoxy matrix, as the oxirane groups in the GMA comonomer can take part on the epoxy network during the curing process. An improvement of toughness without decreasing the glass transition temperature is usually observed for almost all systems employed. In epoxy network cured with *m*-phenylene-diamine, the addition of such core-shell particles resulted in an increase of T_g until the proportion of 10 phr of CSR particles (Lin and Shieh 1998).

Other studies have used PBA as core with PMMA cross-linked and functionalized with carboxyl groups as the shell, as this group can react with both oxirane and hydroxyl groups of the epoxy prepolymer, increasing the

particle–matrix adhesion (Maazouz et al. 1994; Ashida et al. 1999). CSR particles formed by cross-linked PBA as core and ion-cross-linked PMMA as shell were employed by Ashida et al. as toughening agents of epoxy networks (1999). The ion-cross-linked PMMA shell was obtained by adding a small content of methacrylic acid during the late stage of the MMA polymerization.

Poly(butadiene-co-styrene) (SBR) has been also used as core for the preparation of CSR particles constituted by PMMA as the outer layer to improve the properties of epoxy networks. Becu et al. (1997) compare the effect of two CSR particles based on PBA or SBR as the core and PMMA shell layer, which was slightly cross-linked and functionalized with carboxyl groups, as toughening agent for epoxy system cured with dicyandiamide (DDA), and obtained modified epoxy network with fracture toughness around 500% and 250%, respectively, higher than the neat epoxy network, without significant change in the T_g values. They also concluded that the particle comprising PBA core presented higher toughening effect for epoxy networks than that containing SBR as core.

Thuc and Maazouz have used similar SBR-based CSR in epoxy/isophorone diamine system and studied the effect of the functionalization of the PMMA shell part with carboxyl groups (2002). An agglomeration of the particles for non-functionalized particles was observed by the authors. Contrarily, an homogeneous distribution of the rubber particles and a significant increase in viscosity of the epoxy prepolymer were observed when COOH-functionalized CSR particles were used (Thuc and Maazouz 2002). Mousavi and Amraei (2015) recently employed SBR-based CSR particles without functionalization in the shell layer, in epoxy systems cured with dicyandiamide, obtaining materials with an improvement of 100% in fracture toughness, without affecting the glass transition temperature. However, this improvement was inferior when compared to earlier studies developed by Becu et al. (1997), highlighting the importance of the functionalized shell to attain better particle–matrix interaction and consequently outstanding toughening effect.

Roy et al. (2014) investigated the influence of core–shell particles formed by PDMS–epoxy microspheres of particle size in the range of 250–177 μm , as toughener for epoxy system. The cross-linked PDMS microsphere was coated with epoxy layer. The presence of 5% of the CSR-based PDMS resulted in improved impact strength and fracture energy of the modified epoxy network. Chen et al. (2013) also employed PDMS-based core–shell particles with 0.18 μm in epoxy system cured with an anhydride hardener. The authors observed a significant increase of fracture energy using 20 wt% of the CSR particle. The toughening was effective even at temperature as low as $-100\text{ }^\circ\text{C}$.

The use of multilayer CSR particle as modifier for epoxy networks has been also considered by some authors. Day et al. (2001) developed particles that consisted of cross-linked PMMA as the inner glassy core, surrounded by cross-linked PBA as the rubbery layer, and an outer layer comprising a PMMA–poly(ethyl acrylate)–co-GMA copolymer. The total diameter of these particles was around 0.5 μm . The authors have compared the efficiency of CSR particles with rubbery layer with different thickness and also a CSR particle with no GMA copolymer in the outer layer. The critical stress intensity factor, K_{1C} , increases as the rubber particle

content increase and the best results were achieved for systems containing CSR particles containing higher amount of rubbery shell and GMA in the outer shell layer.

CSR nanoparticles have been also incorporated into the epoxy matrix. Giannakopoulos et al. (2011) have compared the effect of three different CSR nanoparticles on the thermal and mechanical properties of epoxy network cured with methylhexahydrophthalic anhydride. The soft rubber core consisted of SBR, polybutadiene (PBD), or polydimethylsiloxane (PDMS), whereas PMMA was used as the hard outer shell. SBR/PMMA and PBD/PMMA CSR particles presented a diameter in the range of 85–115 nm, whereas the diameter of PDMS/PMMA particle corresponded to 250–350 nm. In all cases, the presence of CSR resulted in an increase of fracture toughness without affecting the glass transition temperature. They compared these systems with that involving CTBN pre-reacted with the epoxy matrix. The toughening effect of CTBN-based epoxy networks was better than those observed in the systems with CSR particles, but Tg value was lower.

Quan and Ivankovic (2015) have used acrylic/PMMA CSR nanoparticle, with 203 nm and 74 nm in diameter, in epoxy system cured with dicyandiamide and observed an increase of both Tg and ductility and a decrease of modulus and tensile strength of epoxy network. Smaller CSR particles were more effective in improving the thermal properties, i.e., higher Tg.

An interesting work reported by Thitsartarn et al. (2015) involves the use of a novel multilayer core–shell nanoparticle composed of three layers: octapolyhedral oligomeric silsesquioxane as the rigid inner core, surrounded by PBA as the soft segment covalently bonded to the inner core as a middle layer and terminated with the amino functional group. The use of as low as 1 wt% of this particle resulted in a significant improvement of impact resistance and tensile strength without affecting the modulus.

Most of the studies involving CSR particles and nanoparticles observed an improvement on toughening effect but a decrease of tensile strength. According to Roy et al. (2014), the decrease of mechanical performance is not so important for CSR prepared with PDMS as core, in comparison to other acrylate-based CSRs. Contrary to the liquid rubber-modified epoxy networks, most of the systems involving CSR particles do not present significant change in the Tg values, probably because of the presence of the glassy shell in these CSR particles. Some systems, as those epoxy networks modified with acrylic/PMMA CSR nanoparticle (Quan and Ivankovic 2015), even present an increase in the Tg values, which may be due to the nanosized particles.

Epoxy Modified with Rubber Nanoparticles

The modification of epoxy networks with rubber nanoparticles has been recently increased in interest because the interaction between rubber particle and epoxy matrix can be optimized as a consequence of a significant increasing in interfacial

area. Thus, some important properties as fracture toughness and impact resistance should be improved without altering processing, thermal and optical properties, and perhaps stiffness of the final product. Such a morphology requires specific techniques which may include the incorporation of preformed cross-linked nanoparticles, the induced microphase separation during the curing process, and a pre-cross-linking of the rubber component in situ in the presence of the epoxy matrix.

The Use of Preformed Cross-Linked Nanoparticles

Besides CSR nanoparticles discussed in the preceding section, previously cross-linked rubber nanoparticles have been used to modify the epoxy matrix for improving fracture toughness and other properties. Nanosized copoly(styrene-butyl acrylate-ethylene glycol dimethacrylate) (St-BA-EGDMA) particles were developed by Khoei et al. (2009) and used in epoxy formulations to improve the adhesion strength (Khoei and Hassani 2010). The particles were first dispersed in dimethylacetamide using ultrasonic wave to form a transparent dispersion, and the solution was incorporated within the epoxy resin. After removal of the solvent, piperidine as the curing agent was added, and the mixture was applied into metal substrates for adhesion testing. The material containing 20 wt% of rubber particle was transparent and presented a morphology characterized by nanoparticles with an average size of ca. 97 nm homogeneously dispersed in the epoxy matrix. An increase of around 30 °C in the T_g and a significant improvement on the adhesion properties for aluminum and copper substrate were observed by using 20% of nanoparticle. Similar approach has been employed for CTBN-modified epoxy network and it will be discussed later.

Le et al. (2010) modified DGEBA-based epoxy resin with commercial rubber nanoparticle with 55 nm in diameter and studied the effect of two different curing agents on the main properties: Jeffamine D-230 and DDS. They observed a maximum improvement of toughness of around 230% with the addition of 5 wt% of nanoparticle for the system cured with Jeffamine D-230 (230%) and around 190% with the addition of 10 wt% of nanoparticle in the case of the systems cured with DDS. The improved fracture toughness was achieved without significant changes in the tensile strength, modulus, and glass transition temperature. The outstanding performance of these nanostructured epoxy systems was attributed to a very high total particle surface area and low surface–surface interparticle distance.

Epoxy–Rubber Nanoparticle Blends Prepared by Microphase Separation During Curing Process

Rubber modifiers incorporating block copolymers also constitutes a promising way to develop toughened epoxy network. Such copolymers comprise the liquid rubber

end-capped with a polymer segment which is similar or miscible with the epoxy matrix. This structure allows the rubber segment to self-assemble into hierarchical substructure at the nanometer scale within the epoxy matrix, giving rise to networked materials with combined transparency and toughness. Some examples in the literature involving liquid rubbers (HTPB, PDMS, and CTBN) as segments of block copolymers as modifiers for epoxy networks have been described and will be discussed later.

Main Elastomers Used to Modify Epoxy Networks

Butadiene–Acrylonitrile Rubber (NBR)-Based Modified Epoxy Resin

Butadiene–acrylonitrile rubber is a copolymer formed by butadiene and acrylonitrile. Functionalized liquid butadiene–acrylonitrile rubbers are considered as the most widely employed toughening agent for epoxy network and consist of hydroxy (HTBN)-, carboxyl (CTBN)-, and amino (ATBN)-terminated butadiene–acrylonitrile rubber and also carboxyl (CRBN) and epoxy (ERBN) randomly functionalized butadiene–acrylonitrile rubber. This popularity is based on its polar characteristics, which can be tuned by varying the acrylonitrile content in the copolymer and functionalization (Chen et al. 1994b), thus imparting some compatibility/miscibility with the epoxy prepolymer before the curing process. The miscibility of end-capped butadiene–acrylonitrile rubber follows the order (Chen et al. 1994a):

Amino → epoxy → carboxy → non – functionalized liquid nitrile rubber

Several strategies have been reported to incorporate this elastomer into the epoxy network and depend on the physical nature of the rubber. Some of these procedure will be discussed in this section.

Incorporation of Liquid Nitrile Rubber

The classical way to modify epoxy resin with rubber is blending low molar mass butadiene–acrylonitrile rubber, especially CTBN, with epoxy prepolymer by conventional mechanical mixing, because of its lower viscosity, which makes easier its dispersion within the epoxy matrix without the presence of solvent. Moreover, the functionalization promotes a better adhesion between epoxy matrix and the rubber and a more homogeneous dispersion, which are important for attaining better toughening and impact properties of the final product. In order to improve the adhesion between the blend components, CTBN is previously reacted with the epoxy matrix in the presence of triphenylphosphine, which was found to be an effective catalyst for the reaction between COOH and oxirane groups, according to Fig. 3 (Verchere et al. 1990). The corresponding adduct, usually called epoxy-terminated nitrile rubber (ETBN), is then employed on the preparation of the modified epoxy network.

As discussed before, CTBN and other functionalized liquid nitrile rubbers (ATBN, HTBN) are miscible in the epoxy prepolymer and phase separate during the curing step by a process known as “reaction-induced phase separation process.” The morphology is usually characterized by the presence of spherical rubber particles with diameter in the range of 0.5 until around 10 μm , depending on several parameter. In spite of the reaction between the carboxyl groups of the rubber component and the epoxy matrix, it is not complete, and a fraction of the rubber does not take part on the network and stay dissolved in the epoxy matrix, contributing to the decrease of T_g and modulus. Considering that, these modified networks usually present lower glass transition temperature and modulus.

Most of the studies involve the modification of DGEBA-type epoxy resin (Frigione et al. 1995; Bagheri et al. 2009). However, CTBN has been also employed on the modification of cycloaliphatic epoxy resin, epoxidized cardanol-based novolac resin, epoxy o-cresol novolac resin, etc., using different curing agents. Table 1 summarizes some of these systems prepared by mixing low molar mass nitrile rubber and epoxy resin.

Some factors influence on the phase-separated morphology of rubber-modified epoxy thermosetting materials, which in turn affect their thermal and mechanical properties. The most important factor is the chemical structure of the nitrile rubber and the epoxy matrix. Some authors observed a decrease in rubber particle size for modified epoxies containing CTBN with higher amount of acrylonitrile (Russell and Chartoff 2005; Klug and Seferis 1999; Verchere et al. 1989). Increasing acrylonitrile content in the copolymer increases the polarity of the rubber, resulting in an increase of the miscibility with the epoxy matrix. This characteristic promotes a phase separation at a later stage of the curing process, resulting in smaller particle size. Verchere et al. (1989) also observed an increase of miscibility of CTBN in epoxy matrix when the molar mass of the epoxy increases, which was attributed to an increase in the secondary OH group concentration in the epoxy chain contributing to an improvement on the rubber–epoxy interaction. The use of mixture of two kinds of CTBN with different acrylonitrile content led to a bimodal distribution of rubber particle inside the epoxy matrix and, according to the authors, is responsible for a significant increase in fracture toughness (Chen and Jan 1992).

The nature of hardener and the curing temperature also exert some influence on the morphology of the modified epoxy blends. Thomas et al. (2004, 2007) have studied the effect of CTBN on the morphology and thermal properties of epoxy/anhydride networks and obtained thermosetting materials with rubber particle homogeneously distributed within the epoxy matrix, with size in the range of 0.5–1.0 μm . The smaller elastomer domains compared with those obtained with amine-based hardener has been attributed to the fast-curing ability of anhydride, which minimize the chance of rubber domain coalescence during curing (Yamanaka et al. 1989). Thomas et al. (2007) have also observed a decrease of rubber particle size when the curing was performed at higher temperature. This phenomenon was explained by the decrease of the curing time with the temperature and the decrease of the viscosity of the medium, resulting in a lower degree of coalescence of particles and ultimately phase separation of smaller particles.

Table 1 Some examples of epoxy networks modified with CTBN

Epoxy resin type	Hardener	Rubber	Particle size ^d (µm)	Variation of Tg ^a (°C)	Improvement of K1c ^a (%)	Improvement of impact strength ^a (%)	Depression of modulus ^a (%)	References
DGEBA	Nadic methyl anhydride	CTBN (18%AN)	0.82	-70	170	142 (528 with 15%)	-30%	(Thomas et al. 2004)
Epoxy-cardanol-based novolac	Polyamine	CTBN (26% AN)	-	-	-	106 (317 with 15%)	-	(Yadav et al. 2009)
Epoxy-cardanol-based novolac	Polyamine	CTBN (26% AN)	-	-	-	96 (247 with 15%)	-	(Yadav and Srivastava 2014)
CAE	DDS	CTBN (27% AN)	5-20	-43	-	62 (125 with 15%)	-	(Tripathi and Srivastava 2007a, 2009)
CAE/DGEBA (1:3)	DDS	CTBN	5.6	-4	250 (350 with 15%)	22 (170 with 20%)	-11%	(Tripathi and Srivastava 2008)
DGEBA	DDS	CTBN (27% AN)				40 (160 with 20%)		(Tripathi and Srivastava 2007b)
DGEBA	Piperidine	ETBN ^b (18% AN)	1-4			15 (38 with 20%)		(Ramos et al. 2005)
DGEBA	Phenolic resin	CTBN (27% AN)				214 (360 with 20 phr)		(Liu et al. 2012)
DGEBA	Polyetheramine (D-400)	ETBN ^b (27% AN)	0.5-1.5			100 (220 with 25%)		(Shi et al. 2009)

(continued)

Table 1 (continued)

Epoxy resin type	Hardener	Rubber	Particle size ^a (μm)	Variation of T_g^a ($^{\circ}\text{C}$)	Improvement of K_{Ic}^a (%)	Improvement of impact strength ^a (%)	Depression of modulus ^a (%)	References
DGEBA	DICY	CTBN (27% AN)	<1	+6 (15 phr)	75	35 (170 with 25 phr)	-16	(Akbari et al. 2013)
DGEBA	Anhydride	CTBN			43		-21%	(Dadfar and Ghadami 2013)
DGEBA	Cycloaliphatic amine	CTBN (10%AN)	0.39-6.4	-5		54		(Chonkaew and Sombatsompop 2012)
DGEBA	Anhydride	CTBN (18%AN)	0.82	-11				(Thomas et al. 2007)
Epoxy cresol novolac	DDM	CTBN (17% AN)	6			230		(Nigam et al. 1999)

^aData recorded from modified epoxy network containing 10% of rubber

^bAdduct between CTBN and epoxy resin

^c K_{Ic} = Critical stress intensity factor

ATBN has also been employed for toughening epoxy networks. The motivation of using this modifier rubber is the higher reactivity of amino groups toward epoxy group than carboxyl groups, which could render a stronger interaction between rubber and epoxy matrix through covalent bonds. Consequently, less amount of dissolved, non-reacted rubber should be present in the system, contributing to a smaller decrease of the T_g of the system when compared to the CTBN-based modified epoxy systems. Kunz et al. (1982) have compared the effect of CTBN and ATBN on the morphology of epoxy resin cured with a polyoxypropyleneamine (Jeffamine T-403). The amino-terminated rubber was prepared by reacting CTBN with *N*-aminoethyl-piperazine. ATBN was dispersed in the epoxy matrix with slightly smaller particle size than CTBN and present a diffuse boundary between dispersed and matrix phases. However, both systems prepared by mixing liquid rubbers and epoxy matrix presented similar mechanical properties.

ATBN was also effective in improving impact strength with minimum influence on the T_g of epoxy network cured with polyaminoimidazoline (Chikhi et al. 2002) or cycloaliphatic polyamine hardener (Abadyan et al. 2009a, b).

Recently, Dou et al. (2016) developed a strategy of improving mechanical properties of ATBN–epoxy networks by using mixtures of ATBN with different acrylonitrile contents. The system was cured with polyetheramine. DGEBA-type epoxy matrix was compounded with 39 phr of ATBN containing 10%, 18%, and 26% of AN and cured with polyetheramine, resulting in an increase of impact strength of the thermosetting materials of around 223%, 280%, and 615%, respectively, suggesting that higher amount of AN results in better compatibilization with epoxy matrix, giving rise to outstanding toughness. However, by using a mixture of ATBN with 10% and 26% in a proportion 8:31 phr, an increase of impact of 955% was observed.

ATBN was also employed as curing agent for DGEBA-type epoxy resin (He et al. 2012). High amount of ATBN (in the range of 59–82% of rubber) was necessary to achieve a good level of cross-linking density. The mixtures was cured at room temperature followed by annealing at different temperatures. Excellent mechanical properties were achieved, which were attributed to the phase-separated morphology characterized by the presence of hard epoxy domains dispersed in soft ATBN matrix. The epoxy hard domains act as rigid filler to enhance the strength.

Incorporation of Solid Rubber

High molar mass solid butadiene–acrylonitrile rubber (NBR) should be mixed with epoxy resin in solution. For example, Dehaghi et al. (2013) have dissolved NBR, in powdered form, in a mixture of solvent, including toluene/*n*-butanol/butyl acetate (40:20:40). The mixture was stirred by homogenizer for 15 min at 3000 rpm to form stable transparent dispersion. Then the solvent was evaporated and the mixture was cured. The modified epoxy system prepared by this way presented significant decrease of tensile strength but an increase in fracture energy.

Frounchi et al. (2000) have developed similar system. They have used the solution blending approach and performed the in situ cross-linking of NBR component using 2,6-bis(hydroxymethyl)phenol simultaneously to the curing process of

the epoxy matrix. The T_g of the system slightly increased with the addition of non-cross-linked rubber. The addition of the rubber cross-linking agent resulted in additional increase of T_g . A significant improvement on the impact resistance was observed mainly for the systems containing NBR with higher amount of acrylonitrile, as expected due to the higher compatibility. Also, the cross-linking of the rubber phase imparted additional impact toughness on the modified epoxy networks.

Nanostructured Rubber–Epoxy Blends Containing Nitrile Rubber

Nanostructured epoxy networks containing functionalized nitrile rubber have been also investigated, with the aim of developing toughened epoxy materials with minimum decrease of thermal, optical, and mechanical properties. Different approaches have been reported for this purpose and include blending an appropriate functionalized liquid rubber with epoxy matrix, the utilization of preformed nanoparticles, and the in situ preparation of rubber nanoparticles. In this section, some examples of nitrile rubber-based nanostructured epoxy–rubber blends will be emphasized.

Minfeng et al. (2008) observed smaller rubber particle size and stronger interfacial interaction for blends containing carboxyl-randomized butadiene–acrylonitrile rubber (CRBN) when compared with hydroxyl-terminated butadiene–acrylonitrile rubber (HTBN). The micrograph of epoxy resin modified with CRBN and cured with 4,4'-diaminodiphenylmethane (DDM) did not show distinct separated phase indicating that the rubber was dispersed in nanometric scale, whereas the particle size of epoxy modified with HTBN was in the range of 0.2–2 μm . The impact properties increased with the addition of the liquid rubber particles and achieved a maximum with 5% of rubber. At this composition, improvement of 55% and 67% related to the neat epoxy network was observed for systems modified with HTBN and CRBN, respectively.

Zhao et al. (2015) have studied the influence of the epoxidation of CTBN on the morphology of the epoxy–rubber blend cured with methyltetrahydrophthalic anhydride. The epoxidation was performed in the presence of hydrogen peroxide and formic acid, according to the scheme presented in Fig. 6. Whereas the traditional CTBN/epoxy blends were totally opaque, the epoxidation of the rubber resulted in transparent materials with rubber particles in nanoscale size, due to the better miscibility of the last one in epoxy matrix. The impact strength increased 100%, 135%, and 150% for the epoxy network containing 15% of non-epoxidized CTBN, with 10% of CTBN, with 0.16 mol/100 g and 15% of CTBN, and with 0.30 mol/100 g of epoxide groups, related to the neat epoxy network.

The use of preformed rubber nanoparticles has also been proved to be a very promising strategy for the development of nanostructured epoxy–rubber thermosetting materials. Zhao et al. (2013) compounded CTBN nanoparticle with epoxy resin

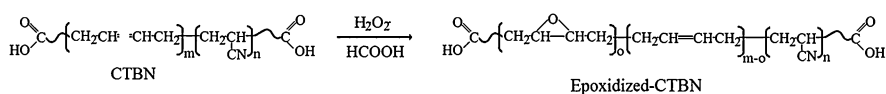


Fig. 6 Epoxidation reaction of CTBN

in a three-roll mill, obtaining well-dispersed particles with no agglomeration and particle size in the range of 90 nm. The system cured with diethyl toluene diamine presented outstanding tensile strength and toughness as compared with neat epoxy network.

Guan et al. (2015) incorporated powdered CTBN preformed latex nanoparticle in epoxy resin cured with 4-methylhexahydrophthalic anhydride using a high-speed mechanical mixing (5000 rpm, at 80 °C for 120 min) to break up the agglomerates and improve the particle dispersion. The epoxy dispersions containing these nanoparticles, with average diameter of ~90 nm, presented a significant increasing of viscosity. The corresponding cured material presented T_g values higher than the neat epoxy network and an increase of K_{IC} of about 69%, with 9.2 wt% of rubber.

Another interesting approach for the development of epoxy–rubber blends with stable morphology and rubber phase at a nanometric scale involves the cross-linking of rubber phase which has been previously dispersed in the rubber matrix. Hsu and Liang (2007) used this procedure to prepare interpenetrating CTBN/epoxy network structures with nanometric-sized morphology. The procedure consisted of blending a solution of liquid CTBN containing benzoyl peroxide or dicumyl peroxide in a mixture containing epoxy resin and the hardener. A polyglycidyl ether of o-cresol-formaldehyde novolac/4,4'-diaminodiphenyl sulfone (DDS) mixture was employed. After removal of the solvent, transparent and viscous mixture containing 20 wt% of CTBN were obtained. The system was heated to induce simultaneously the curing of the epoxy matrix by DDS and the vulcanization of the rubber phase by peroxide. The resulting IPN system contained vulcanized and interpenetrated rubber phase on a nanometric scale and displays outstanding fracture toughness without changing the T_g .

The team of Prof. Xu (Zhou and Xu 2014; Zhou et al. 2014) also performed the cross-linking of liquid CTBN inside the epoxy matrix. However, some differences in the procedure adopted by the authors, when compared with the system described above, resulted in a morphology characterized by rubber nanoparticles homogeneously distributed within the epoxy matrix. This new approach involves the dissolution of the CTBN in the epoxy matrix with the addition of peroxide. The mixture was heated at 85 °C for 5 h under stirring to initiate the cross-linking of CTBN. Then the curing agent for the epoxy resin was added to form the thermosetting material. During the pre-curing stage, the carboxyl groups of CTBN may react with epoxy, providing a good anchorage between rubber and matrix. As the rubber is homogeneously dispersed in the epoxy matrix, the cross-linked rubber remains in the form of spherical nanoparticles. By using this procedure, the addition of 5% of CTBN resulted in 2.5 times higher impact strength than the neat epoxy network cured with piperidine, without affecting yield stress and Young's modulus. Because the molar mass of CTBN after the pre-cross-linking stage is very high, some epoxy portion stays confined inside the rubber particle, giving rise to a localized interpenetrating polymer network inside the dispersed rubbery phase.

The incorporation of block segment miscible with epoxy matrix in the CTBN chain constitutes also a promising strategy for developing nanostructured CTBN-modified epoxy networks. In this context, Heng et al. (2015) have successfully prepared block copolymer constituted by liquid CTBN which was previously

modified with methoxypolyethylene glycol (CTBN-b-PEG) via the esterification reaction and used this copolymer in epoxy resin cured with 4,4'-methylenebis (2-chloroaniline) (MOCA), to enhance both toughness and tensile strength of the final material. The addition of up to 15% of the block copolymer resulted in transparent material with CTBN domains with average size of 10 nm, confirming the microphase-separated morphology. The authors also observed a significant depression of the glass transition temperature of the epoxy matrix with the addition of the block copolymer and suggested that the PEG segment in the block copolymer is miscible with epoxy/MOCA cured system, contributing for a plasticizing effect on the epoxy matrix. The T_g depression was around 60 °C with the addition of 20 wt% of the block copolymer. Nevertheless, the impact strength, the critical stress intensity factor, and tensile strength increase with the addition of CTBN-b-PEG reaching maximum values with the addition of 15% of the block copolymer.

Liquid Polybutadiene-Based Modified Epoxy Resin

Hydroxyl-terminated polybutadiene (HTPB), as well as the carboxyl-, epoxy-, and isocyanate-modified HTPB, has been used as epoxy modifier for improving toughness and other properties. Unlike CTBN, HTPB is immiscible with epoxy resin at room temperature because of the weak polarity of HTPB compared to CTBN. Except for some specific systems involving polybutadiene as core in CSR-based epoxy networks (Giannakopoulos et al. 2011), most of the studies reported involve mechanical mixing of liquid-functionalized rubber with epoxy resin rather than using preformed cured particles.

Incorporation of Liquid Polybutadiene Rubber

HTPB without additional functionalization has been evaluated as epoxy modifier because of its low moisture permeability, low T_g , and excellent resistance to aqueous acid and bases. Different approaches and curing systems have been investigated. The curing agent used for the development of the HTPB-modified epoxy networks exerts significant influence on the morphology of the corresponding thermoset material. The use of triethylenetetramine (TETA) as the curing agent results in a morphology characterized by large rubber particles and large particle size distribution, with particle size in between 0.1 and 75 μm , most of them situated in the range of 11–32 μm for blend containing 10 wt% of HTPB (Barcia et al. 2003).

Anhydride-based curing system is interesting because it has a very low viscosity at room temperature, which facilitates the processing of the mixtures. Moreover, the anhydride group is able to react with the hydroxyl groups of the HTPB, imparting better interaction between the rubber particle and the thermoset material (epoxy/hardener system). Kaynak's group (Ozturk et al. 2001; Kaynak et al. 2002) employed 1 and 1.5 wt% of HTPB in epoxy formulations. The authors affirmed that higher amount of rubber results in improper mixing because of the incompatibility between the components. They observed better mechanical performance when the HTPB was previously mixed with the hardener at room temperature for 1 h.

Table 2 Effect of blending procedure on the impact strength and morphology of epoxy resin modified with HTPB

Rubber content (%)	A (cured with TETA) (Barcia et al. 2003)		B (cured with anhydride) (Thomas et al. 2008)		C (cured with anhydride) (Zhou and Cai 2012)	
	Impact strength improvement (%)	Rubber particle size (μm)	Impact strength improvement (%)	Rubber particle size (μm)	Impact strength improvement (%)	Rubber particle size (μm)
5	17		25	0.82	45	
10	46	10–33	47	0.90	88	3–20
15	15		11	1.2	64	
20	–		3	1.5	36	

Thomas et al. (2008, 2010) employed methyl nadic anhydride as curing agent and observed a decrease of tensile strength and modulus as the amount of rubber increased. The impact strength and fracture toughness increased up to an amount of HTPB corresponding to 10 phr, achieving values 47% and 122% higher than the neat epoxy network, respectively. The number average diameter of rubber domains inside the epoxy matrix stayed in the range of 0.82–1.5 μm for blends containing 5–20 phr of HTPB. The authors also studied the effect of the curing temperature for blend containing 10 phr of HTPB and observed an increasing of impact strength as the curing temperature increases until 160 °C. At this conditions, the morphology was characterized by a homogeneous distribution of particle size, observed by scanning electronic microscopy (SEM).

In order to improve the adhesion between epoxy resin and HTPB, Zhou and Cai (2012) first reacted HTPB with epoxy resin at 130 °C for 1–2 h, using 2,4,6-tri(dimethylaminomethyl)phenol as catalyst (Fig. 2). Table 2 compares the percentage of increasing in impact strength for systems prepared by different procedures. In all these systems, the maximum increase in impact strength was achieved by using 10 phr of HTPB. Considering the conventional mixing approach, the nature of the curing agent did not exert great influence on the extent of the impact strength improvement. Both epoxy systems containing 10 phr of HTPB and cured with TETA or anhydride display similar impact strength in spite of the great difference in rubber particle size. However, the improvement was much better when HTPB has been previously reacted with epoxy resin (Zhou and Cai 2012), even though the system presented large particle size and particle size distribution. This result highlights the importance of a good interfacial adhesion for achieving better morphological and mechanical behavior.

The miscibility of HTPB in epoxy system was investigated by Meng et al. (2006) who have employed 4,4'-methylenebis-(2-chloroaniline) (MOCA), a high-temperature curing agent. Before curing, the mixture between HTPB and epoxy prepolymer were cloudy at room temperature but transparent at elevated temperatures. The mixture between HTPB/epoxy and MOCA was transparent at the beginning of the curing process performed at 150 °C. However, as the curing proceeded, the system becomes cloudy indicating a reaction-induced phase separation process.

In this case, spherical rubber particle with diameter around 2 μm and homogeneously dispersed inside the epoxy matrix was obtained.

Carboxyl-terminated PB (CTPB) has also been investigated as modifier for different epoxy systems. Some authors have performed a simple blending of the components and the hardener. For example, epoxy cresol novolac (ECN) resin was modified with CTPB and cured with diaminodiphenylmethane (DDM) (Nigam et al. 1998). In spite of the presence of carboxyl group, the CTPB presented gross phase-separated morphology, with an average particle size of 10 μm . A marginal increase of both flexural strength and modulus (15% and 3%, respectively) was observed with the addition of 10% of CTPB. By using epoxidized resol-based phenolic resin/polyamide system, the toughening effectiveness of CTPB was significant (Shukla and Srivastava 2006). Indeed, both impact strength and tensile strength increased by about 200% with the addition of 15 wt% of rubber.

Barcia et al. (2003) developed epoxy end-capped HTPB by reacting HTPB with maleic anhydride at 80 $^{\circ}\text{C}$ for 24 h, which was subsequently reacted with epoxy resin in the presence of triphenylphosphine as a catalyst, according to the scheme shown in Fig. 7. The epoxy network modified with 10 wt% of CTPB resulted in an increase of both impact strength and tensile yield stress of around 70% and 55%, respectively. Moreover, no significant variation on the T_g values has been observed. These results indicate that CTPB should be a promising toughening agent for epoxy resin because it can improve the impact properties without losing the mechanical and thermal properties. These behavior suggests that there is no rubber dissolved inside the epoxy matrix. The average particle size was in the range of 1.2–1.8 μm .

Liquid polybutadiene functionalized with amino group (ATPB) was also employed as toughening agent for DGEBA-type epoxy resin cured with TETA (Kar and Banthia 2005). The synthesis of ATPB was performed by reacting the

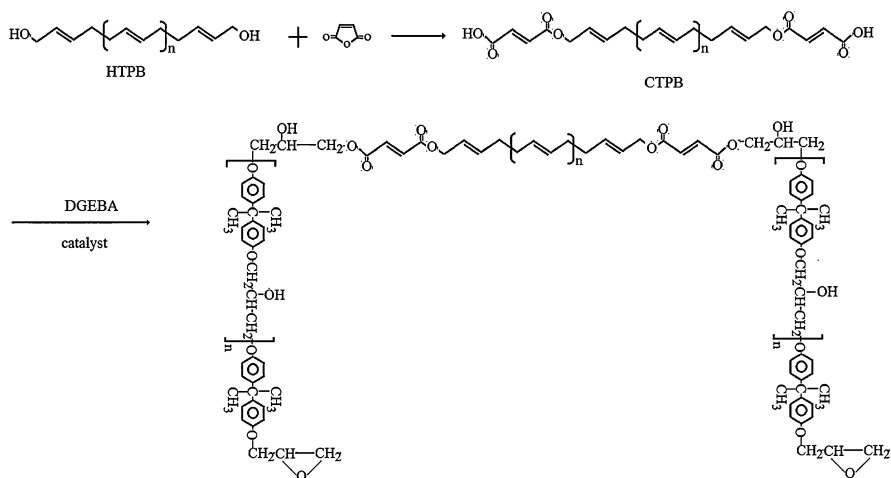


Fig. 7 Scheme for the preparation of epoxy prepolymer modified with CTPB

HTPB with *p*-amino benzoic acid. In order to promote the covalent bonding between ATPB and epoxy resin, both components were reacted at 200 °C for 5 h. This procedure is necessary because of the low reactivity of aromatic amine toward epoxy groups. After this treatment, the system was cured with TETA. The corresponding network presented a significant increasing of the impact strength with the amount of ATPB (around 250% with the addition of 15 phr of rubber), but a decreasing of the T_g .

The epoxidation of HTPB chains has also been considered more than two decades ago for improving the compatibility between HTPB and epoxy resin. Bussi and Ishida (1994a, b) employed epoxidized HTPB (E-HTPB) with different degrees of epoxidation in epoxy systems cured with bisphenol A. The epoxidation increases the polarity of the rubber, thus improving its miscibility with epoxy resin. From kinetics studies, the authors concluded that the internal oxirane groups of E-HTPB is less reactive than the oxirane groups of the epoxy resin. Therefore, the epoxidized HTPB does not take part on the network and the role of the internal oxirane groups is basically to increase the miscibility of HTPB (Bussi and Ishida 1994a). From dynamic mechanical analysis, the authors observed a considerable depression of the T_g values, mainly for E-HTPB samples with higher degree of epoxidation (Bussi and Ishida 1994b).

Latha et al. (1994) employed 2,4,6-tri(*N,N*-dimethylaminomethyl)phenol as the curing agent for a similar system and observed an improvement of impact strength and adhesive properties on aluminum substrate with the addition of 10 phr of epoxidized HTPB, without affecting the T_g . More recently, Lee et al. (2005) investigated the curing behavior of DGEBA-based epoxy resin with methylene dianiline (MDA) in the presence of epoxidized HTPB. They also observed that E-HTPB is miscible with epoxy resin. They have concluded that the E-HTPB is self-curable, through the reaction between the hydroxyl and oxirane groups. In presence of DGEBA, the hydroxyl groups located at the end of the E-HTPB would react favorably with the oxirane groups of DGEBA. In the presence of the curing agent, the reaction between the epoxy and hardener is dominant over the cross-reaction.

Tian et al. (2011) also modified HTPB with chain-extended urea, by the reaction with toluene diisocyanate (TDI) followed by dimethylamine, and used in epoxy formulations cured with dicyandiamide. The modified rubber accelerated the curing process probably because of the presence of carbamate group in the modified HTPB chain. The effect of the molar mass of HTPB on the main properties has been investigated. The best impact resistance was achieved by using modified HTPB with lower molar mass ($M_n = 1800$). By using 13 phr of this modified rubber, an increase of about 290% in impact strength related to the neat epoxy was observed. However, the glass transition temperature presented a significant decrease confirming the flexibilizing action of the modified rubber.

Nanostructured Rubber–Epoxy Blends Containing Polybutadiene Rubber

Nanostructured HTPB–epoxy blends have been successfully prepared by using the corresponding block copolymer containing segments similar or miscible with the epoxy matrix. In this sense, Meng et al. (2006) prepared poly

(ϵ -caprolactone)-*b*-polybutadiene-*b*-poly(ϵ -caprolactone) triblock copolymer (PCL-PB-PCL) via the ring-opening polymerization of ϵ -caprolactone in the presence of hydroxyl-terminated liquid polybutadiene (HTPB) and used this copolymer in DGEBA-based epoxy system cured with 4,4'-methylenebis(2-chloroaniline) (MOCA). PCL component is soluble in the epoxy/MOCA mixture at room temperature but HTPB is not. After curing at high temperature (150 °C), the system stayed transparent indicating no macroscopic phase separation. However, by transmission electron microscopy, the formation of heterogeneous morphology at the nanoscopic level was evident, even when 30 wt% of triblock copolymer was employed. Considering that the curing temperature is much higher than the corresponding upper critical solution temperature (UCST) of the system, the authors proposed that the formation of the nanoscopic structure is due to the reaction-induced microphase separation of the PB blocks rather than from a self-organized structure formed before curing.

Block copolymer prepared via coupling reaction of isocyanate-terminated HTPB (PBNCO) and epoxy resin (Fig. 5) also results in nanostructured rubber–epoxy networks (Barcia et al. 2002; Soares et al. 2011). The mixture of DGEBA with PBNCO was completely transparent indicating miscibility of the components. After curing with TETA, the corresponding networks remained completely transparent even with a proportion of rubber as high as 20 phr (Soares et al. 2011). From transmission electron microscopy, the nanostructure of the rubber domains, with average size of 5–10 nm, has been confirmed (Soares et al. 2011). Increasing the amount of rubber in the epoxy matrix, the number of spherical particles increased but the rubber domains were still small and more densely packed. Additionally, the T_g values did not present any significant change indicating that there is no soluble rubber inside the epoxy matrix. This modified epoxy system also presents the unique combination of toughening and stiffness properties, as the impact strength has been increased to around 250% with the addition of 10 phr of modified rubber, with also a slight increase of T_g and Young's modulus (Soares et al. 2011). The transparency of the functionalized epoxy network without decreasing of T_g confirm that the rubber material is not dissolved inside the rubber but rather it is dispersed in nanometer scale. This behavior may be attributed to the high reactivity of isocyanate groups toward hydroxyl and epoxy groups of the epoxy matrix, which promote the covalent reaction between the components, thus forming effective block copolymer constituted by polybutadiene in the middle, end-capped by DGEBA molecules, as illustrated in Fig. 5. Moreover, being the segment of the block copolymer constituted by epoxy resin chain, the block copolymer takes part of the epoxy network. Besides outstanding mechanical, optical, and thermal performance, the adhesive properties of these materials were evaluated using both butt joint and lap shear tests, indicating also a significant improvement of these properties (Barcia et al. 2004).

Natural Rubber as Modifier of Epoxy Resin

An approach to improve the toughening of epoxy prepolymer is the use of unmodified or modified elastomeric particles based on natural rubber (NR) which

have the ability to crystallize under stretching (Khan and Poh 2011). However, natural rubber has many disadvantages such as a low resistance to solvents and oils and a low air barrier properties (Roy et al. 1990). Thus, most of the published articles in the literature reports the chemical treatment or the depolymerization of the natural rubber (Roy et al. 1990). While other studies have focused on the combination of the natural rubber with nanoparticles such as carbon black, silica, and layered silicates or with different rubbers such as polybutadiene, styrene–butadiene rubber, etc. (Alex et al. 2011; Fang et al. 2013; Jin et al. 2015; Hofmann 1989), nevertheless, we have focused our research only on the chemical modification of NR.

For example, Kumar et al. have investigated the modification of epoxy prepolymer denoted DGEBA with maleated depolymerized natural rubber (MDPR) (Kumar and Kothandaraman 2008). In this work, they have synthesized MDPR with 2 phr (parts per hundred) of maleic anhydride, and they have prepared different epoxy–MDPR networks with epoxy prepolymer as major phase. They have used methylene dianiline as curing agent and triphenylphosphine as catalyst. Finally, epoxy networks have cured 3 h at 100 °C. In addition, the authors have also studied the influence of MDPR on the thermal and mechanical (tensile and flexural tests, impact resistance) properties. Thus, they have highlighted that the incorporation of MDPR into epoxy monomer led to an increase in the strain at break and flexural strain to failure without change of the glass transition temperature. Moreover, the impact strength values of the epoxy/MDPR obtained by Izod unnotched impact test are higher than the impact strength value of epoxy–amine networks without elastomeric particles (Kumar and Kothandaraman 2008).

Most of the published literature have focused on the epoxidation process of polydiene rubbers (Pummerer and Bukard 1922; Gelling 1985; Burfield et al. 1984; Perera et al. 1988). In 1922, Pummerer and Bukard were the first to epoxidize natural rubber which is not very successful (Pummerer and Bukard 1922). Other authors have also investigated the chemical modification of NR, but it was only in 1985 that Gelling et al. first patented a process to develop epoxidized NR (ENR) without the formation of secondary products by using different acid treatments (Davies et al. 1983; Burfield et al. 1984; Perera et al. 1988). Thus, due to its good reactivity and its better compatibility with epoxy prepolymer, ENR was used to reinforce epoxy networks (Tanjung et al. 2015; Guthner and Hammer 1993; Hong et al. 2005; Hong and Chan 2004; Chan and Rey 1997; Wise et al. 2000). In addition, it has been demonstrated that the use of ENR as toughening modifiers into epoxy resin can modify the curing reaction of the epoxy networks (Guthner and Hammer 1993; Hong et al. 2005). This phenomenon is due mainly to the presence of epoxy groups on the natural rubber. Indeed, Hong et al. have studied the curing behavior of epoxy/dicyandiamide networks with the presence of 2-methylimidazole as accelerator and with 5–15 phr of ENR50 (Epoxyrene 50, i.e., 50 mol% epoxidized) (Hong et al. 2005; Hong and Chan 2004). The authors have demonstrated that the incorporation of ENR combined with the dilution of the hardener induced a change in the reaction mechanisms. Moreover, as epoxidized NR has a lower glass transition temperature compared to epoxy networks, the structure and the conversion percentage of the cured epoxy matrices are modified (Hong and Chan 2004). When the

percentage of ENR is increased, the percentage of conversion significantly increases. They have also demonstrated a phase separation behavior of the epoxy/rubber systems by scanning electronic microscopy characterized by the formation of spherical rubber particles with domain sizes between 1 and 2.2 μm (Hong and Chan 2004). In addition, the authors have highlighted that an increase of the ENR content (>5 phr) led to a significant decrease of the lap shear strength (LSS).

Other authors such as Mathew et al. have investigated the effect of epoxidized natural rubber on the mechanical performances as well as the morphology of the epoxy matrix (Mathew et al. 2014). In this work, epoxy prepolymer (LAPOX B-11) was cured by an anhydride curing agent denoted nadic methyl anhydride with the presence of *N,N*-dimethylbenzylamine as a catalyst (Mathew et al. 2014). Finally, they have demonstrated that the epoxy systems composed of ENR particles led to an improvement of the fracture toughness as well as the impact strength. In addition, ENR droplets were observed into the epoxy matrix by SEM showing the variation of the size of the rubber particles in function of its content.

More recently, Chuayjuljit et al. have synthesized ENRs via in situ epoxidation method in order to obtain ENRs with 25, 40, 50, 60, 70, and 80 mol% of epoxide groups, and they have introduced 2, 5, 7, and 10 phr of these rubbers in epoxy resin cured with polyamide resin as curing agent (Chuayjuljit et al. 2006). Thus, they have demonstrated that the use of over 5 phr of ENR particles led to a decrease of the Young's modulus, the impact strength, and the flexural modulus (Chuayjuljit et al. 2006).

To decrease the viscosity and to improve the processing of the epoxy–rubber blends, the use of low molar mass liquid rubbers derived from natural rubber as a modifier of epoxy resin has been widely studied. For example, Thomas et al. have investigated the influence of different amounts of hydroxylated-terminated liquid natural rubber (HTLNR) on the mechanical properties of epoxy–anhydride networks. The authors have highlighted a reduction in the tensile strength combined with an increase of the fracture toughness when 10 phr of HTLNR was used (Thomas et al. 2008). Other studies have also demonstrated that the HTLNR droplets acted as stress concentrators leading to the plastic deformation in the epoxy matrix (Mathew et al. 2010, 2012). Recently, Mathew et al. have shown that the incorporation of 15 and 20 wt% of HTLNR in epoxy resin led to the best compromise in terms of final properties (Mathew et al. 2012). Indeed, the impact strength as well as the fracture toughness have been significantly improved.

In conclusion, the chemical modification such as the epoxidation or the depolymerization of the natural rubber (NR) is an excellent way to prepare epoxy–rubber networks with good mechanical properties. In fact, the use of HTLNR or ENR generally leads to an improvement of the fracture toughness with decreases of the flexural and tensile modulus. In fact, several parameters can play a role in the final properties of the polymer materials such as the concentration of rubber particles, the functionalization of ENR by epoxide groups, their distribution into epoxy matrix, and the choice of the hardener (polyamine, amine, anhydride, etc.). Thus, many studies are still required in order to find the best compromise.

Polysiloxane as Modifier of Epoxy Resin

In order to overcome the brittleness of epoxy matrices and improve their impact properties, other additives were used such as silicon rubber or polydimethylsiloxane (PDMS), commonly investigated as toughening agents (Huang and Kinloch 1992; Yorkgitis et al. 1985; Karger-Kocsis and Friedrich 1993). In fact, PDMS has many advantages such as UV insensitivity, low surface tension, an extremely low glass transition temperature (T_g of about $-120\text{ }^\circ\text{C}$) mainly due to the high flexibility of these chains, and low solubility parameters inducing an immiscibility in epoxy prepolymer before and after cross-linking reaction. In addition, the incorporation of PDMS leads to epoxy networks with an excellent thermal and oxygen stability. Thus, different routes have been explored and reported in the literature such as (i) the use of PDMS particles (Rey et al. 1999), (ii) the synthesis of block copolymers containing PDMS blocks (Hedrick et al. 1988a), (iii) the modification of the epoxy structure by inserting PDMS or polymethylphenylsiloxane (PMPS) as soft segments (Hedrick et al. 1988b), and (iv) the formation of a graft interpenetrating polymer networks (graft-IPN).

Use of Preformed Particles

Over the past 30 or 40 years, several authors have studied the distribution of preformed rubber particles into the epoxy prepolymer (Rey et al. 1999; Huang and Kinloch 1992; Maazouz et al. 1994). Although this method is easy, scalable, and transferable to industry, many challenges remain to be overcome such as the control of particle size and the quality of the filler dispersion as well as the increase in viscosity generated by their incorporation in the polymer matrix (Rey et al. 1999).

However, various works have reported the use of PDMS particles in the epoxy reactive systems. For example, Rey et al. have investigated the incorporation of different quantities (4, 8, and 15 wt%) of PDMS particles in physical and mechanical properties of epoxy-amine networks based on DGEBA/dicyandiamide (DDA) with the use of a catalyst denoted Durion (Rey et al. 1999). In this study, they have mixed PDMS in the reactive mixture by using two dispersion tools (Ultraturax and a twin-screw extruder) and the epoxy blends were cured 2 h at $120\text{ }^\circ\text{C}$. Thus, they have highlighted that a part of dissolved PDMS generates a decrease of the glass transition temperature as well as a decrease in shear modulus. In the opposite, an increase of the crack propagation resistance was obtained characterized by increases in fracture toughness (K_{Ic}) and fatigue crack propagation. Moreover, the best mechanical performance were observed when 8 wt% of PDMS was incorporated (Rey et al. 1999).

Other authors have synthesized and used polyether-grafted polysiloxane (FPMS) and epoxy-miscible polysiloxane particles (EMPP) as toughening agents of epoxy prepolymer (Ma et al. 2010). In the first case, they have used the good affinity of polyether with epoxy function to improve the miscibility of polysiloxane-modified particles with epoxy prepolymer. In the second case, they have synthesized

epoxy-miscible polysiloxane particles by hydrosilylation. Then, they have incorporated 10 wt% of FPMS and EMPP in epoxy-amine networks composed of DGEBA/4,4-diaminodiphenylmethane denoted DDM and cured at 80 °C during 5.5 h, 2 h at 150 °C, and 2 h at 180 °C. Thus, they have highlighted that the use of these modified particles led to an increase of the tensile and impact strength of the epoxy networks without reducing the glass transition temperature. However, they have demonstrated better mechanical results when EMPP particles were used. The outstanding mechanical performance for epoxy modified with epoxy-miscible polysiloxane particles (EMPP) was attributed to the morphology characterized by regular particles with diameter of 340 nm.

Ho and Wang (2001) have prepared dispersed silicon rubber-modified aralkyl-novolac epoxy via hydrosilylation. In addition, they have developed a process to introduce dispersed polysiloxane particles into phenol aralkyl-novolac epoxy prepolymer. Thus, they have demonstrated decreases of the flexural modulus and the coefficient of thermal expansion combined with a significant decrease of the T_g .

In summary, few works have reported the use of unmodified or modified PDMS particles as toughening agents of epoxy networks.

Use of Block Copolymers Based on PDMS Blocks

In recent years, academic research has focused on the synthesis of block copolymers containing PDMS blocks for use as surface or toughness modifiers or as structuring agents of epoxy networks (Gong et al. 2008; Xu and Zheng 2007). In fact, many authors have highlighted that the addition of block copolymers into epoxy prepolymer led to a ordered or disordered nanostructures via microphase separation mechanism (Buchholz and Mühlaupt 1992; Könczol et al. 1994). Huang et al. (2001) have studied the influence of polyether-polydimethylsiloxane-polyether (PER-PDMS-PER) as surface agents of epoxy matrix. They have synthesized six kinds of triblock copolymer by hydrosilylation of bis-dimethylsiloxy-terminated PDMS with allyl-terminated polyether and by varying the PDMS block length. Then, the authors have introduced PER-PDMS-PER copolymers (5 wt%) and an stoichiometric amount of curing agent (methylene dianiline (MDA)) into epoxy prepolymer at 90–100 °C. After a curing process of 1 h at 100 °C and 3 h at 150 °C, static friction coefficients and water contact angles were determined on epoxy networks. In conclusion, they have demonstrated that the use of triblock copolymer is a promising route to improve the contact angle values but not to increase the oil and water repellency of epoxy matrices.

Mühlaupt et al. have studied the influence of a branched poly(ϵ -caprolactone)-polydimethylsiloxane-poly(ϵ -caprolactone) (PCL-PDMS-PCL) into epoxy resin. They have highlighted that the use of a small amount of the block copolymer (5 wt%) induced a morphology composed of spherical PDMS particles (20 nm) combined with significant increases of Young's modulus and strength at break (Buchholz and Mühlaupt 1992; Könczol et al. 1994). Recently, Xu and Zheng (2007) have investigated the incorporation of linear ABA triblock copolymer (PCL-PDMS-PCL) and the resulting morphologies. More recently, other authors

such as Gong et al. (2008) have synthesized new block copolymer containing poly (hydroxyether of bisphenol A) and polydimethylsiloxane blocks denoted PH-alt-PDMS. They have introduced PH-alt-PDMS block copolymer in epoxy blends composed of DGEBA and diaminodiphenylmethane (DDM) and cured 2 h at 150 °C and 2 h at 180 °C. Then, the morphology as well as the critical stress intensity factors (K_{Ic}) were determined. They have demonstrated that the addition of block copolymer (5–20 wt%) leads to a significant increase of the K_{Ic} (1.5 MN/m^{3/2} for epoxy–amine network and 3.0 MN/m^{3/2} when 20 wt% of copolymer was used).

Other block copolymers such as ABC triblock copolymer composed of PDMS-PCL-PS have been used in epoxy thermosets (Fan et al. 2009). They have designed ABC copolymer in function of the chemical nature of the blocks. Thus, they have used PDMS blocks which are immiscible with epoxy before and after curing reaction, PS blocks inducing phase separation in epoxy prepolymer, and finally PCL blocks which are known to be miscible with epoxy before and after curing reaction. After, they have added 10, 20, 30, and 40 wt% of PDMS-PCL-PS in epoxy mixtures composed of DGEBA–4,4'-methylenebis(2-chloroaniline) (MOCA) and cured 2 h at 150 °C and 2 h at 180 °C.

In conclusion, the synthesis of block copolymers composed of PDMS blocks has been extensively studied. The resulting morphologies as well as the thermal and mechanical properties have been also investigated. Even if increases in toughness of the epoxy thermosets were obtained, significant amounts of block copolymers are required limiting their use in industry.

Incorporation of the PDMS or PMPS Soft Segments in Epoxy Structure

Another strategy developed in the literature was to introduce polymethylphenylsiloxane (PMPS) and polydimethylsiloxane (PDMS) as soft segments into epoxy structure (Lin and Huang 1994, 1996; Hou et al. 2000; Ochi and Shimaoka 1999; Ho and Wang 1996; Zhao et al. 2000) to improve the final properties of epoxy networks. Other authors such as Lin et al. have also demonstrated that the use of copolymers constituted of siloxane and sulfone segments containing epoxy prepolymer denoted ESBS led to materials with an excellent thermal behavior and nonflammability properties for applications requiring the use of high temperature (Lin and Huang 1994). In addition, an increase of the glass transition temperature can be obtained (Lin and Huang 1994).

Moreover, the same research group have studied the synthesis of epoxy prepolymer (based on DGEBA) with different siloxane contents and oligomers and their influence in the thermal and mechanical properties of these networks (Lin and Huang 1996). Thus, different copolymers such as siloxane-modified epoxy prepolymer (ESDG) have been developed and the epoxy networks were cured with 2 phr of 2,4,6-tris(dimethylaminomethyl)phenol denoted DMP-30 as curing agent at 120 °C during 1 h and post-cured at 150 °C during 2 h. In this work, epoxy equivalent weight (EEW) of the samples were determined by using the HCl/pyridine method (Lee and Yang 1992). Thus, epoxy networks based on PMPS–DGEBA with high thermal stability and high impact strengths were processed (Lin and Huang 1996).

Recently, epoxy–siloxane copolymer was synthesized from the hydrosilylation between allyl glycidyl ether and poly(methylhydrosiloxane) copolymer (Hou et al. 2000). Thus, epoxy–amine networks composed of DGEBA and dicyandiamide (DICY) with the benzyldimethylamine (BDMA) as catalyst have been prepared. Hou et al. (2000) have concluded that the cured epoxy containing 9.1 wt% of copolymer will be the best candidate to improve the toughness of the epoxy matrix due to better dispersion of the siloxane chains. In addition, they have highlighted that an increase of the siloxane segments in the copolymers led to an improvement of the thermal behavior of epoxy–amine systems.

More recently, other authors such as Rath et al. have developed epoxy systems based on the modification of aliphatic epoxy by introducing silicone segments through urethane route (Rath et al. 2009). In order to create this network, a number of synthetic steps are required: (i) synthesis of epoxy adipate prepolymer constituted of diglycidyl ether of neopentyl glycol and adipic acid using triphenylphosphine as catalyst, (ii) synthesis of TDI-capped hydroxyl-terminated polydimethylsiloxane based on toluene diisocyanate (TDI) and PDMS with hydroxyl functions at the end of chains, (iii) reaction between epoxy adipate prepolymer and TDI-capped hydroxyl-terminated polydimethylsiloxane to form silicone-modified epoxy prepolymer, and (iv) curing of this new network with amine hardener denoted *O,O'*-bis-(2-aminopropyl)polypropyleneglycol-block-polyethyleneglycol-block-polypropyleneglycol. Then, they have investigated the effect of the addition of 15 and 30 wt% of silicone-modified epoxy prepolymer on the morphology, the thermal and mechanical properties, as well as the surface wettability of the epoxy networks. The authors have highlighted a biphasic morphology with a homogeneous dispersion of PDMS rubber particles coupled with lower surface energy (Rath et al. 2009).

In conclusion, the incorporation of siloxane segments into the epoxy structure is a good way for the preparation of epoxy networks with good final properties. Nevertheless, many comparative studies between epoxy/PDMS particles, epoxy/block copolymers, and the networks based on the chemical modification of the epoxy structure are required in order to develop epoxy–rubber blends with excellent final properties.

Structuration by Graft Interpenetrating Polymer Networks (Graft-IPN)

The last route to prepare epoxy networks with polysiloxane as modifiers is to synthesize graft interpenetrating polymeric networks (Nguyen and Suh 1984; Frisch 1985; Velan and Bilal 2000). In 1997, Sung and Lin (1997) have demonstrated that it is possible to develop epoxy/PDMS graft-IPN by using 3-aminopropyltrimethoxysilane (γ -APS) as reactive coupling agent and MDA as curing agent. The authors have shown that the use of γ -APS led to faster epoxy–amine reaction and the presence of alkoxy groups in the silane induced the reaction with hydroxyl-terminated PDMS. Then, they have investigated the influence of the PDMS content (5–25 wt%) on the fracture behaviors as well as the mechanical properties of epoxy networks. The authors have highlighted epoxy networks composed of PDMS domains with sizes between 6 and 20 μm . In addition, they have demonstrated that an increase of the PDMS amount led to decreases of the tensile

and flexural strengths due to poor cohesive strength between epoxy resin and PDMS. However, they have shown an increase of the fracture energy. In another study, the same authors have incorporated a new component denoted polypropylene glycol into the epoxy/PDMS graft-IPN (Sung and Lin 1997). Thus, they have highlighted that this multicomponent system led to a better phase homogeneity with a single glass transition temperature for a PDMS/PPG ratio below 12%. Moreover, better energy damping properties have been revealed.

Other authors such as Velan et al. have also worked on similar systems based on DGEBA/PDMS with diethylenetriamine as hardener and γ -APS as cross-linking agent to develop polymer materials for electrical insulation, encapsulation, and aerospace applications (Velan and Bilal 2000). In fact, these PDMS–epoxy IPN led to better electrical and thermal properties coupled with high impact resistance.

More recently, Jia et al. (2007) have prepared epoxy/PDMS IPNs in a common solvent (toluene) and the resulting morphologies have been investigated by scanning electronic microscopy (SEM) and atomic force microscopy (AFM). In this work, two curing reactions take place simultaneously between (i) epoxy prepolymer (DGEBA) and the curing agent denoted methyltetrahydrophthalic anhydride (MTHPA) and (ii) between vinyl-terminated PDMS and hydride-terminated PDMS. Thus, the authors have highlighted a nanostructuring of PDMS with domain sizes between 10 and 50 nm. Nevertheless, no thermal and mechanical properties were studied.

In conclusion, various synthetic methods have been studied to develop nanostructured epoxy/PDMS graft-IPN with good thermal, electrical, and mechanical properties. However, few works on these multicomponent systems are reported in the literature limiting their use in many applications.

Acrylate Rubber as Modifier of Epoxy Resin

As for the polydimethylsiloxane and in order to generate two-phase systems wherein the rubber phase would improve the cracking resistance of the epoxy matrix without deterioration of their thermal and/or mechanical properties, acrylate chemistry has also been widely studied and used. In fact, different approaches have been reported in the literature, such as (i) the synthesis of acrylate-based liquid rubbers and (ii) the use of core–shell particles

Synthesis of Acrylate-Based Liquid Rubbers

As previously mentioned, the use of liquid rubber based on CTBN has been greatly investigated to improve the fracture toughness of epoxy networks (Achary et al. 1990). However due to the presence of unsaturated bonds in the butadiene segments, thermal degradation and oxidative instability may occur during the curing process at high temperature (Okamoto 1983). Thus, different authors have turned to acrylate-based liquid rubbers having better thermal and oxidative stability (Duseck et al. 1984; Ochi and Bell 1984; Gazit and Bell 1983; Nakamura et al. 1986; Lee et al. 1986; Iijima et al. 1991a, b; Khong et al. 2008).

In 1988, Tomoi et al. (1988) have prepared new copolymers based on acrylate rubbers with a pendant epoxy group by copolymerization of butyl acrylate (BA) with vinyl benzyl glycidyl ether (VBGE), and they have used this copolymer in epoxy–amine system composed of DGEBA/DDS. Thus, they have highlighted that the use of 20 wt% of the copolymer containing 74% of BA and 26% of VBGE led to an increase of 30% of the fracture toughness compared to cured unmodified epoxy networks. The authors have also demonstrated the formation of two-phase microstructures composed of rubber particles with diameter of 2 μm . In addition, the authors have observed that a change in the composition of the copolymer plays a key role on the final properties of the epoxy networks (Tomoi et al. 1988). Different authors have also demonstrated that carboxyl-terminated poly(*n*-butyl acrylate) liquid rubber and *n*-butyl acrylate (acrylic acid) copolymers are good toughening agents of epoxy–amine networks (Ochi and Bell 1984; Lee et al. 1986). For example, Lee et al. have synthesized *n*-butyl acrylate (nBA)/acrylic acid (AA) copolymers and used in epoxy systems composed of DGEBA/DICY (Lee et al. 1986). Moreover, they have studied the influence of the functionality of the copolymers (between 1.62 and 9.93) on the properties of epoxy networks. Thus, they have shown that the use of these copolymers induced an increase of the lap shear and T-peel strengths of the epoxy networks.

Other authors have also worked on the encapsulation of electronic devices with epoxy–acrylate rubber systems. For example, Ho et al. have modified epoxy prepolymer by vinylization and prepared acrylate rubber dispersion by vinyl in situ polymerization (Ho and Wang 1993). Then, they have used this dispersion to improve the toughness of epoxy systems based on cresol-formaldehyde novolac epoxy prepolymer and phenolic novolac resin as curing agent. In this work, the authors have obtained epoxy networks with excellent resistance to the thermal shock cycling test combined with an increase of the fracture toughness without reduction of T_g (Ho and Wang 1993). Nevertheless, decreases in the coefficient of the thermal expansion and in the flexural modulus have been observed. In addition, they have highlighted that 2-ethylhexylacrylate is the best modifier for these epoxy systems.

Recently, Ratna and Banthia (2000) have synthesized various acrylate-based liquid rubbers denoted 2-ethylhexylacrylate-acrylic acid with different molecular weights and functionality and have introduced these new copolymers in epoxy prepolymer cured with triethylenetetramine (TETA) as hardener with the presence of triphenylphosphine (PPh_3) as catalyst. Then, they have studied the effect of these liquid rubbers on the thermal and impact properties of epoxy–amine systems. Finally, they have demonstrated that the use of liquid rubber with a functionality of 5.19 led to a single-phase morphology, whereas a functionality of 1.68 was the best compromise characterized by an increase of the impact strength with slight decreases of the T_g and storage modulus. More recently, the same authors have also investigated the influence of carboxyl-terminated poly(2-ethylhexylacrylate) (CTPEHA) synthesized by bulk polymerization in the same epoxy–amine system (Ratna et al. 2001). Thus, they have highlighted that the incorporation of liquid

rubber up to 20 phr concentration induced increases of the impact and adhesive strengths combined with slight decreases of the tensile and flexural strength.

In 2004, other authors such as Kar and Banthia (2004) have synthesized CTPEHA and an epoxy-randomized PEHA denoted ERPEHA as tougheners of epoxy matrix based on DGEBA/TETA/PPh₃ systems cured 2 days at room temperature and post-cured at 80 °C during 2 h. They have obtained the best results in impact strength when the liquid rubber was introduced in 1:1 ratio, with respect to a concentration of 10 phr in epoxy-amine networks. More recently, various authors have also studied more complex mixtures where bisphenol A was added to the epoxy-rubber systems leading to an increase of the ductility of the strain at break combined with higher toughness efficiency (Khong et al. 2008).

In conclusion, as the preparation of epoxy systems requires to work at higher temperatures during significant times (several hours) and depending on the chemical nature of the hardener (amine, anhydride, phenol, polyamide, etc.), the use of acrylate-based liquid rubbers is an excellent alternative to CTBN through their better thermal and oxidative stability.

Use of Core-Shell Particles

In the field of acrylate rubbers, another strategy was reported in the literature such as the synthesis and the incorporation of core-shell particles in epoxy resin adhesives to increase their mechanical performances (Ashida et al. 1999; Lee et al. 1986; Nakamura et al. 1990). Thus, Ashida et al. have used acrylic particles composed of poly(butyl acrylate) (PBA) as core and poly(methyl methacrylate) (PMMA) as shell, and they have introduced these particles in epoxy-amine networks (Ashida et al. 1999). Moreover, they have demonstrated that the addition of a small amount of core-shell particles in epoxy matrix led to higher fracture toughness and adhesion strength because a bond is formed between epoxy prepolymer and these particles. In fact, the presence of epoxy resin around the core-shell particles has the effect of improving the level of energy absorption due to the plastic deformation of the epoxy matrix. Other authors have also highlighted that the particles swell with the epoxy resin during the curing process (Lee et al. 1986; Nakamura et al. 1990).

Kim et al. (1997) have developed poly(urethane acrylate)/poly(glycidyl methacrylate-co-acrylonitrile) core-shell particles of different sizes by emulsion polymerization. Indeed, they have modified the particles size (48–200 nm) by adding polyoxyethylene groups in the urethane acrylate molecules. Then, they have investigated the influence of the particles size on the impact strength of epoxy-amine networks. Thus, they have concluded that an increase of the shell thickness as well as an increase of the amount of particles induced an increase of the impact strength.

In summary, this last route is very promising because the use of a small amount of these core-shell particles can lead to significant increases of the mechanical performances of the epoxy-rubber networks and in particular concerning their fracture toughness. In addition, many of core-shell particles are currently commercially available which makes their use easier for industrial applications.

Conclusion Remarks

Nowadays, thermoset-based epoxy resins are most commonly used in a wide range of applications such as the automotive, aerospace, and also electronic devices, thanks to their excellent thermal, thermomechanical, and adhesive properties as well as their excellent process ability. However, these systems have many disadvantages, and in particular, their great brittleness limits their fracture resistance, fatigue behavior, and impact strength. Thus, many approaches have been developed and investigated in the literature in order to improve the fracture toughness and to modify the deformation mechanism of epoxy resins such as the incorporation of rubber particles, the synthesis of new copolymers or block copolymers containing rubber segments or blocks, the formation of graft interpenetrating polymer networks, or the use of low molar mass liquid rubbers. For these reasons, this chapter summarizes the different preparation of epoxy–rubber networks as well as their significant effect on their final properties.

References

- Abadyan M, Khademi V, Bagheri R, Haddadpour H, Kouchakzadeh MA, Farsadi M (2009a) Use of rubber modification technique to improve fracture-resistance of hoop wound composites. *Mater Des* 30:1976–1984
- Abadyan M, Bagheri R, Haddadpour H, Motamedi P (2009b) Investigation of the fracture resistance in hoop wound composites modified with two different reactive oligomers. *Mater Des* 30:3048–3055
- Achary PS, Latha PB, Ramaswamy R (1990) Room temperature curing of CTBN-toughened epoxy adhesive with elevated temperature service capability. *J Appl Polym Sci* 41:151–162
- Akbari R, Beheshty H, Shervin M (2013) Toughening of dicyandiamide-cured DGEBA-based epoxy resins by CTBN liquid rubber. *Iran Polym J* 22:313–324
- Alex R, Sasidharan KK, Kurian T, Chandra AK (2011) Carbon black master batch from fresh natural rubber latex. *Plast Rubber Compos* 40:420–424
- Ashida T, Katoh A, Handa K, Ochi M (1999) Structure and properties of epoxy resins modified with acrylic particles. *J Appl Polym Sci* 74:2955–2962
- Bagheri R, Marouf BT, Pearson RA (2009) Rubber-toughened epoxies: a critical review. *J Macromol Sci C Polym Rev J* 49:201–225
- Barcia FL, Abrahão MA, Soares BG (2002) Modification of epoxy resin by isocyanate-terminated polybutadiene. *J Appl Polym Sci* 83:838–849
- Barcia FL, Amaral TP, Soares BG (2003) Synthesis and properties of epoxy resin modified with epoxy-terminated liquid polybutadiene. *Polymer* 44:5811–5819
- Barcia FL, Soares BG, Sampaio E (2004) Adhesive properties of epoxy resin modified by end-functionalized liquid polybutadiene. *J Appl Polym Sci* 93:2370–2378
- Becu L, Maazouz A, Sautereau H, Gerard JF (1997) Fracture behavior of epoxy polymers modified with core-shell rubber particles. *J Appl Polym Sci* 65:2419–2431
- Bécu-Longuet L, Bonnet A, Pichot C, Sautereau H, Maazouz A (1999) Epoxy networks toughened by core-shell particles: influence of the particle structure and size on the rheological and mechanical properties. *J Appl Polym Sci* 72:849–858
- Buchholz U, Mühlaupt R (1992) Branched polysiloxane block copolymers as epoxy toughening agents. *ACS Polym Prepr* 33:205

- Burfield DR, Lim KL, Law KS (1984) Analysis of epoxidized natural rubber. A comparative study of dsc, nmr, elemental analysis and direct titration methods. *Polymer* 25:995–998
- Bussi P, Ishida H (1994a) Partially miscible blends of epoxy resin and epoxidized rubber: structural characterization of the epoxidized rubber and mechanical properties of the blends. *J Appl Polym Sci* 53:441–454
- Bussi P, Ishida H (1994b) Composition of the continuous phase in partially miscible blends of epoxy resin and epoxidized rubber by dynamic mechanical analysis. *Polymer* 35:956–966
- Chan PK, Rey AD (1997) Polymerization-induced phase separation. 2. Morphological analysis. *Macromolecules* 30:2135–2143
- Chen TK, Jan YH (1992) Fracture mechanism of toughened epoxy resin with bimodal rubber-particle size distribution. *J Mater Sci* 27:111–121
- Chen D, Pascault JP, Sautereau H, Ruseckaite RA, Williams RJJ (1994a) Rubber-modified epoxies: III. Influence of the rubber molecular weight on the phase separation process. *Polym Int* 33:253–261
- Chen D, Pascault JP, Bertsch RJ, Drake RS, Siebert AR (1994b) Synthesis, characterization and properties of reactive liquid rubbers based on butadiene-acrylonitrile copolymers. *J Appl Polym Sci* 51:1959
- Chen J, Kinloch AJ, Sprenger S, Taylor AC (2013) The mechanical properties and toughening mechanism of an epoxy polymer modified with polysiloxane-based core-shell particles. *Polymer* 54:4276–4289
- Chikhi N, Fellahi S, Bakar M (2002) Modification of epoxy resin using reactive liquid (ATBN) rubber. *Eur Polym J* 38:251–264
- Chonkaew W, Sombatsompop N (2012) Mechanical and tribological properties of epoxy modified by liquid carboxyl terminated poly(butadiene-co-acrylonitrile) rubber. *J Appl Polym Sci* 125:361–369
- Chuayjuljit S, Soatthiyanon N, Potiyaraj P (2006) Polymer blends of epoxy resin and epoxidized natural rubber. *J Appl Polym Sci* 102:452–459
- Dadfar MR, Ghadami F (2013) Effect of rubber modification on fracture toughness properties of glass reinforced hot cured epoxy composites. *Mater Des* 47:16–20
- Davies CKL, Wolfe SV, Gelling IR, Thomas AG (1983) Strain crystallization in random copolymers produced by epoxidation of cis 1,4-polyisoprene. *Polymer* 24:107–113
- Day RJ, Lovell PA, Wazzan AA (2001) Thermal and mechanical characterization of epoxy resins toughened using preformed particles. *Polym Int* 50:849–857
- Dehaghi HAA, Mazinani S, Zaarei D, Kalae M, Jabari H, Sedaghat N (2013) Thermal and morphological characteristics of solution blended epoxy/NBR compound. *J Therm Anal Calorim* 114:185–194
- Dou H, Tian B, Huang Y, Quan Y, Chen Q, Yin G (2016) Improved mechanical properties of ATBN-toughened epoxy networks by controlling the phase separation scale. *J Adhes Sci Technol* 30:642–6522
- Duseck K, Lendnický F, Lunak S, Mach M, Duskova D (1984) Rubber modified thermoset resin, *Advances in chemistry series* 208. ACS, Washington, DC, p 28
- Fan W, Wang L, Zheng S (2009) Nanostructures in thermosetting blends of epoxy resin with polydimethylsiloxane-block-poly(ϵ -caprolactone)-block-polystyrene ABC triblock copolymer. *Macromolecules* 42:327–336
- Fang L, Wei M, Warastthinon N, Shen J, Jian R, Schmidt D, Barry C, Mead J (2013) Preparation and properties of styrene-butadiene rubber/clay nanocomposites by using liquid rubber/clay masterbatches. *Rubber Chem Technol* 86:96
- Frigione ME, Mascia L, Acierno D (1995) Oligomeric and polymeric modifiers for toughening of epoxy resins. *Eur Polym J* 31:1021–1029
- Frisch HL (1985) Interpenetrating polymer networks. *Br Polym J* 17:149–153
- Frounchi M, Mehrabzadeh M, Parvary M (2000) Toughening epoxy resins with solid acrylonitrile-butadiene rubber. *Polym Int* 49:163–169

- Gazit S, Bell JP (1983) Synthesis and analysis of saturated, reactive n-butyl acrylate polymers for use in epoxy resin toughening. *ACS Symp Ser* 221(55):69
- Gelling IR (1985) Modification of natural rubber latex with peracetic acid. *Rubber Chem Technol* 58:86–96
- Giannakopoulos G, Masania K, Taylor AC (2011) Toughening of epoxy using core-shell particles. *J Mater Sci* 46:327–338
- Gong W, Zeng K, Wang L, Zheng S (2008) Poly(hydroxyether of bisphenol A)-block-polydimethylsiloxane alternating block copolymer and its nanostructured blends with epoxy resin. *Polymer* 49:3318–3326
- Guan LZ, Gong LX, Tang LC, Wu LB, Jiang JX, Lai GQ (2015) Mechanical properties and fracture behaviors of epoxy composites with phase-separation formed liquid rubber and preformed powdered rubber nanoparticles: a comparative study. *Polym Compos* 36:785–799
- Guthner T, Hammer B (1993) Curing of epoxy resins with dicyandiamide and urones. *J Appl Polym Sci* 50:1453–1459
- Hayes BS, Seferis JC (2001) Modification of thermosetting resins and composites through preformed polymer particles: a review. *Polym Compos* 22:451–467
- He D, Ding X, Chang P, Chen Q (2012) Effect of annealing on phase separation and mechanical properties of epoxy/ATBN adhesive. *Int J Adhes Adhes* 38:11–16
- Hedrick JL, Haidar B, Russel TP, Hofer DC (1988a) Synthesis and properties of segmented and block poly(hydroxyether-siloxane) copolymers. *Macromolecules* 21:1967–1977
- Hedrick JL, Hofer DC, Russel TP, Haidar B (1988b) Structural modifications of segmented poly(hydroxyether-siloxane) copolymers. *Polym Bull* 19:573–578
- Heng Z, Chen Y, Zou H, Liang M (2015) Simultaneously enhanced tensile strength and fracture toughness of epoxy resins by a poly(ethylene oxide)-block-carboxyl terminated butadiene-acrylonitrile rubber diblock copolymer. *RSC Adv* 5:42362–42368
- Ho TH, Wang CS (1993) Toughening of epoxy resins by modification with dispersed acrylate rubber for electronic packaging. *J Appl Polym Sci* 50:477–483
- Ho TH, Wang CS (1996) Modification of epoxy resins with polysiloxane thermoplastic polyurethane for electronic encapsulation. *Polymer* 37:2733–2742
- Ho TH, Wang CS (2001) Modification of epoxy resin with siloxane containing phenol aralkyl epoxy resin for electronic encapsulation application. *Eur Polym J* 37:267–274
- Hofmann W (1989) *Rubber technologist's handbook*. Hanser Publishers, New York, p 143. Chap 5
- Hong SG, Chan CK (2004) The curing behaviors of the epoxy/dicyanamide system modified with epoxidized natural rubber. *Thermochim Acta* 417:99–106
- Hong SG, Chan CK, Chuang CC, Keong CH, Hsueh YP (2005) The curing behavior and adhesion strength of the epoxidized natural rubber modified epoxy/dicyandiamide system. *J Polym Res* 12:295–303
- Hou SS, Chung YP, Chan CK, Kuo PL (2000) Function and performance of silicone copolymer. Part IV. Curing behavior and characterization of epoxy-siloxane copolymers blended with diglycidyl ether of bisphenol-A. *Polymer* 41:3263–3272
- Hsu YG, Liang CW (2007) Properties and behavior of CTBN-modified epoxy with IPN structure. *J Appl Polym Sci* 106:1576–1584
- Huang Y, Kinloch AJ (1992) Modelling of the toughening mechanisms in rubber-modified epoxy polymers. *J Mater Sci* 27:2753–2762
- Huang W, Yao Y, Huang Y, Yu Y (2001) Surface modification of epoxy resin by polyether-polydimethylsiloxanes-polyether triblock copolymers. *Polymer* 42:1763–1766
- Iijima T, Tomoi M, Suzuki A, Kakiuchi H (1991a) Toughening of epoxy resins by modification with reactive elastomers composed of butyl acrylate and glycidyl (meth) acrylate. *Eur Polym J* 27:851–858
- Iijima T, Horiba T, Tomoi M (1991b) Toughening of epoxy resins by modification with reactive elastomers composed of butyl acrylate, glycidyl methacrylate and acrylonitrile or styrene. *Eur Polym J* 27:1231–1238
- Inoue T (1995) Reaction-induced phase decomposition in polymer blends. *Prog Polym Sci* 20:119–153

- Jia LY, Zhang C, Du ZJ, Li CJ, Li HQ (2007) Preparation of interpenetrating polymer networks of epoxy/polydimethylsiloxane in a common solvent of the precursors. *Polym J* 39:593–597
- Jin Z, Luo Z, Yang S, Lu S (2015) Influence of complexing treatment and epoxy resin coating on the properties of aramid fiber reinforced natural rubber. *J Appl Polym Sci* 132:42122–42130
- Kar S, Banthia AK (2004) Use of acrylate-based liquid rubbers as toughening agents and adhesive property modifiers of epoxy resin. *J Appl Polym Sci* 92:3814–3821
- Kar S, Banthia AK (2005) Synthesis and evaluation of liquid amine-terminated polybutadiene rubber and its role in epoxy toughening. *J Appl Polym Sci* 96:2446–2453
- Karger-Kocsis J, Friedrich K (1993) Microstructure-related fracture toughness and fatigue crack growth behavior in toughened, anhydride-cured epoxy resins. *Compos Sci Technol* 48:263–272
- Kaynak C, Ozturk A, Tincer T (2002) Flexibility improvement of epoxy resin by liquid rubber modification. *Polym Int* 51:749–756
- Khan I, Poh BT (2011) Natural rubber-based pressure-sensitive adhesives: a review. *J Polym Environ* 19:793–811
- Khoe S, Hassani N (2010) Adhesion strength improvement of epoxy resin reinforced with nanoelastomeric copolymer. *Mater Sci Eng A* 527:6562–6567
- Khoe S, Mahdavian AR, Bairamy W, Ashjari M (2009) An investigation into the improvement of adhesive strength of polyimides by incorporation of elastomeric nanoparticles. *J Colloid Interface Sci* 336:872–878
- Khong J, Tang Y, Zhang X, Gu J (2008) Synergic effect of acrylate liquid rubber and bisphenol A on toughness of epoxy resins. *Polym Bull* 60:229–236
- Kim JW, Kim JY, Suh KD (1997) Preparation and physical properties of rubber modified epoxy resin using poly(urethane acrylate)/poly(glycidyl methacrylate-co-acrylonitrile) Core-Shell composite particles. *J Appl Polym Sci* 63:1589–1600
- Klug JH, Seferis JC (1999) Phase separation influence on the performance of CTBN-toughened epoxy adhesives. *Polym Eng Sci* 39:1837–1848
- Könczöl L, Döll W, Buchholz U, Mühlaupt R (1994) Ultimate properties of epoxy resins modified with a polysiloxane-polycaprolactone block copolymer. *J Appl Polym Sci* 54:815–826
- Kumar KD, Kothandaraman B (2008) Modification of (DGEBA) epoxy resin with maleated depolymerised natural rubber. *Express Polym Lett* 2:304–308
- Kunz SC, Sayre JA, Assink RA (1982) Morphology and toughness characterization of epoxy resins modified with amine and carboxyl terminated rubbers. *Polymer* 23:1897–1906
- Latha PB, Adhinarayanan K, Ramaswamy R (1994) Epoxidized hydroxyl-terminated polybutadiene – synthesis, characterization and toughening studies. *Int J Adhes Adhes* 14:57–61
- Le QH, Kuan HC, Dai JB, Zaman I, Luong L, Ma J (2010) Structure – property relations of 55 nm particle-toughened epoxy. *Polymer* 51:4867–4879
- Lee ST, Yang CP (1992) Synthesis and properties of cationic resins derived from polyether/polyester-modified epoxy resins. *J Appl Polym Sci* 46:991–1000
- Lee Y, Wang S, Chin W (1986) Liquid-rubber-modified epoxy adhesives cured with dicyandiamide. I. Preparation and characterization. *J Appl Polym Sci* 32:6317–6329
- Lee J, Yandek GR, Kyu T (2005) Reaction induced phase separation in mixtures of multifunctional polybutadiene and epoxy. *Polymer* 46:12511–12522
- Lin ST, Huang SK (1994) Synthesis and characterization of siloxane-modified epoxy resin. *J Polym Res* 1:151
- Lin ST, Huang SK (1996) Synthesis and impact properties of siloxane-DGEBA epoxy copolymers. *J Polym Sci A Polym Chem* 34:1907–1922
- Lin KF, Shieh YD (1998) Core-shell particles designed for toughening the epoxy resins. II. Core-shell-particle-toughened epoxy resins. *J Appl Polym Sci* 70:2313–2322
- Liu J, Jia X, Zhang S, Liu R, Liu X (2012) Preparation and characterization of carboxyl-terminated poly (butadiene-co-acrylonitrile) – epoxy resin prepolymers for fusion – bonded-epoxy powder coating. *J Wuhan Univ Technol-Mater Sci* 27:694–701
- Ma S, Liu WQ, Yu D, Wang ZF (2010) Modification of epoxy resin with polyether-grafted-polysiloxane and epoxy-miscible polysiloxane particles. *Macromol Res* 18:22–28

- Maazouz A, Sautereau H, Gérard JF (1994) Toughening of epoxy networks using pré-formed core-shell particle or reactive rubbers. *Polym Bull* 33:67–74
- Mathew VS, Sinturel C, George SC, Thomas S (2010) Epoxy resin/liquid natural rubber system: secondary phase separation and its impact on mechanical properties. *J Mater Sci* 45:1769–1781
- Mathew VS, Jyotishkumar P, George SC, Gopalakrishnan P, Delbreilh L, Saiter JM, Saikia PJ, Thomas S (2012) High performance HTLNR/epoxy blend – phase morphology and thermo-mechanical properties. *J Appl Polym Sci* 125:804–811
- Mathew VS, George SC, Parameswaranpillai J, Thomas S (2014) Epoxidized natural rubber/epoxy blends: phase morphology and thermomechanical properties. *J Appl Polym Sci* 131:39906–39914
- Meng F, Zheng S, Zhang W, Li H, Liang Q (2006) Nanostructured thermosetting blends of epoxy resin and amphiphilic poly(ϵ -caprolactone)-block-polybutadiene-block-poly(ϵ -caprolactone) triblock copolymer. *Macromolecules* 39:711–719
- Minfeng Z, Xudong S, Huiquan X, Genzhong J, Xuewen J, Baoyi W, Chenze Q (2008) Investigation of free volume and the interfacial, and toughening behavior for epoxy/rubber composites by positron annihilation. *Radiat Phys Chem* 77:245–251
- Minxian S, Zhixiong H, Yaming L, Guorui Y. (2009) Performance of CTBN (carbocyl-terminated poly(butadiene-co-acrylonitrile))-EP (diglycidyl ether of bisphenol-A (DGEBA)) prepolymers and CTBN-EP/polyetheramine (PEA) system. *J Wuhan Univ Tech Mater Sci Ed* 24:757–762
- Mousavi SR, Amraei IA (2015) Toughening of dicyandiamide-cured DGEBA-based epoxy resin using MBS core-shell rubber particles. *J Compos Mater* 49:2357–2363
- Nakamura Y, Tabata H, Suzuki H, Ito K, Okubo M, Matsumoto T (1986) Internal stress of epoxy resin modified with acrylic core-shell particles prepared by seeded emulsion polymerization. *J Appl Polym Sci* 32:4865–4871
- Nakamura Y, Yamaguchi M, Kitayama A, Iko K (1990) Internal stress of epoxy resin modified with acrylic polymers produced by in situ UV radiation polymerization. *J Appl Polym Sci* 39:1045–1060
- Nguyen LT, Suh NP (1984) Reaction injection molding of interpenetrating polymer networks. In: Riew CK, Gillham JK (eds). *Rubber modified thermoset resins*, vol. 208, chapter 19. American Chemical Society, pp. 311–319
- Nigam V, Setua DK, Mathur N (1998) Wide-angle X-ray scattering, fourier transform infrared spectroscopy, and scanning electron microscopy studies on the influence of the addition of liquid functional rubber into epoxy thermoset. *J Appl Polym Sci* 70:537–543
- Nigam V, Setua DK, Mathur N (1999) Characterization of liquid carboxy terminated copolymer of butadiene acrylonitrile modified epoxy resin. *Polym Eng Sci* 39:1425–1432
- Ochi M, Bell JP (1984) Rubber-modified epoxy resins containing high functionality acrylic elastomers. *J Appl Polym Sci* 29:1381–1391
- Ochi M, Shimaoka S (1999) Phase structure and toughness of silicone-modified epoxy resin with added silicone graft copolymer. *Polymer* 40:1305–1312
- Ohashi K, Hasegawa K, Fukuda A, Uede K (1992) Curing behavior of epoxy resin having hydroxymethyl group. *J Appl Polym Sci* 44:419
- Okamoto Y (1983) Thermal aging study of carboxyl-terminated polybutadiene and poly (butadiene-acrylonitrile)-reactive liquid polymers. *Polym Eng Sci* 23:222–225
- Ozturk A, Kaynak C, Tiner T (2001) Effects of liquid rubber modification on the behavior of epoxy resin. *Eur Polym J* 37:2353–2363
- Pascualt JP, Sautereau H, Verdu J, Williams RJJ (2002) *Thermosetting polymers*. Marcel Dekker, New York
- Perera MCS, Elix JA, Bradbury JH (1988) Furanized rubber studied by NMR spectroscopy. *J Polym Sci A Polym Chem* 26:637–651
- Pummerer R, Bukard PA (1922) *Über Kautschuk*. *Eur J Inorg Chem* 55:3458–3472
- Quan D, Ivankovic A (2015) Effect of core-shell rubber (CSR) nano-particles on mechanical properties and fracture toughness of an epoxy polymer. *Polymer* 66:16–28

- Ramos VD, Costa HM, Soares VLP, Nascimento RSV (2005) Modification of epoxy resin: a comparison of different types of elastomer. *Polym Test* 24:387–394
- Rath SK, Chavan JG, Sasane S, Srivastava A, Patri M, Samui AB, Chakraborty BC, Sawant SN (2009) Coatings of PDMS-modified epoxy via urethane linkage: segmental correlation length, phase morphology, thermomechanical and surface behavior. *Prog Org Coat* 65:366–374
- Ratna D (2001) Phase separation in liquid rubber modified epoxy mixture. Relationship between curing conditions, morphology and ultimate behavior. *Polymer* 42:4209–4218
- Ratna D, Banthia AK (2000) Toughening of epoxy resin by modification with 2-ethylhexylacrylate-acrylic acid copolymers. *Polym Int* 49:309–315
- Ratna D, Banthia AK, Deb PC (2001) Acrylate-based liquid rubber as impact modifier for epoxy resin. *J Appl Polym Sci* 80:1792–1801
- Rey L, Poisson N, Maazouz A, Sautereau H (1999) Enhancement of crack propagation resistance in epoxy resins by introducing poly(dimethylsiloxane) particles. *J Mater Sci* 34:1775–1781
- Riew CK, Gillham JK (eds) (1984) Rubber modified thermoset resins. American Chemical Society, Washington, DC
- Roy S, Gupta BR, Maiti BR (1990) Studies on the epoxidation of natural rubber. *J Elastomers Plast* 22:280–294
- Roy PK, Iqbal N, Kumar D (2014) Polysiloxane-based core-shell microspheres for toughening of epoxy resins. *J Polym Res* 21:348 (9 pp)
- Rudakova EV, Kovzhina AL, Evtyukov NZ, Mashlyakovskii LN, Tverdov AI, Otvalko ZA, Fomin SE, Ushakova ES (2013) Study of physic-mechanical properties of epoxy coatings modified with liquid rubbers with terminal carboxyl group. *Russ J Appl Chem* 86:1760–1766
- Rudakova EV, Ramsh AS, Mashlyakovskii LN, Kurliyand SK (2014) Structure and relaxation properties of cured films based on 4,4'-isopropylidenediphenol epoxy resin modified with liquid rubbers containing terminal carboxy groups. *Russ J Appl Chem* 87:1300–1307
- Russell B, Chartoff R (2005) The influence of cure conditions on the morphology and phase distribution in a rubber-modified epoxy resin using scanning electron microscopy and atomic force microscopy. *Polymer* 46:785–798
- Shi M, Huang Z, Li Y, Yang G (2009) Performance of CTBN (carboxyl-terminated poly (butadiene-co-acrylonitrile))-EP(diglycidyl ether of bisphenol A (DGEBA)) prepolymers and CTBN-EP/polyetheramine (PEA) system. *J Wuhan Univ Technol-Mater Sci* 24:757–762
- Shukla SK, Srivastava D (2006) Blends of modified epoxy resin and carboxyl-terminated polybutadiene. *J Appl Polym Sci* 100:1802–1808
- Soares BG, Dahmouche K, Lima VD, Silva AA, Caplan SPC, Barcia FL (2011) Characterization of nanostructured epoxy networks modified with isocyanate-terminated liquid polybutadiene. *J Colloid Interface Sci* 358:338–346
- Sultan JN, Liable RC, McGarry FJ (1971) Microstructure of two-phase polymers. *Polym Symp* 16:127–136
- Sung PH, Lin CY (1997) Polysiloxane modified epoxy polymer networks-II. Dynamic mechanical behavior of multicomponent graft-IPNs (Epoxy/polysiloxane/polypropylene glycol). *Eur Polym J* 33:231–233
- Tanjung FA, Hassan A, Hasan M (2015) Use of epoxidized natural rubber as a toughening agent in plastics. *J Appl Polym Sci* 132:42270–42279
- Thitsartarn W, Fan X, Sun Y, Yeo JCC, Yuan D, He C (2015) Simultaneous enhancement of strength and toughness of epoxy using POSS-rubber core-shell nanoparticles. *Compos Sci Technol* 118:63–71
- Thomas R, Abraham J, Thomas PS, Thomas S (2004) Influence of carboxyl-terminated (butadiene-co-acrylonitrile) loading on the mechanical and thermal properties of cured epoxy blends. *J Polym Sci Polym Phys Ed* 42:2531–2544
- Thomas R, Durix S, Sinturel C, Omonov T, Goossens S, Groeninckx G, Moldenaers P, Thomas S (2007) Cure kinetics, morphology and miscibility of modified DGEBA-based epoxy resin – effects of a liquid rubber inclusion. *Polymer* 48:1695–1710

- Thomas R, Yumei D, Yuelong H, Le Y, Moldenaers P, Weimin Y, Czigan Y, Thomas S (2008) Miscibility, morphology, thermal, and mechanical properties of a DGEBA based epoxy resin toughened with a liquid rubber. *Polymer* 49:278–294
- Thomas R, Boudenne A, Ibos L, Candau Y, Thomas S (2010) Thermophysical properties of CTBN and HTPB liquid rubber modified epoxy blends. *J Appl Polym Sci* 116:3232–3241
- Thomas S, Sinturel C, Thomas R (2014) Micro – and nanostructures epoxy/rubber blends. Wiley-VCH, Weinheim
- Thuc BHN, Maazouz A (2002) Morphology and rheology relationships of epoxy/core-shell particle blends. *Polym Eng Sci* 42:120–133
- Tian X, Geng Y, Yin D, Zhang B, Zhang Y (2011) Studies on the properties of a thermosetting epoxy modified with chain-extended ureas containing hydroxyl-terminated polybutadiene. *Polym Test* 30:16–22
- Tomoi M, Yamazaki H, Akada H, Kakiuchi H (1988) Modification of epoxy resins with acrylic rubbers containing a pendant epoxy group. *Die Angewandte Makromolekulare Chemie* 163:63–76
- Tripathi G, Srivastava D (2007a) Effect of carboxyl-terminated butadiene acrylonitrile copolymer concentration on mechanical and morphological features of binary blends of nonglycidyl-type epoxy resins. *Adv Polym Technol* 26:258–271
- Tripathi G, Srivastava D (2007b) Effect of carboxyl-terminated poly(butadiene-co-acrylonitrile) (CTBN) concentration on thermal and mechanical properties of binary blends of diglycidyl ether of bisphenol A (DGEBA) epoxy resin. *Mater Sci Eng A* 443:262–269
- Tripathi G, Srivastava D (2008) Studies on the physic-mechanical and thermal characteristics of blends of DGEBA epoxy, 3,4 epoxy cyclohexylmethyl 3',4'-epoxycyclohexane carboxylate and carboxyl terminated butadiene – co- acrylonitrile (CTBN). *Mater Sci Eng A* 496:483–493
- Tripathi G, Srivastava D (2009) Studies on blends of cycloaliphatic epoxy resin with varying concentrations of carboxyl terminated butadiene acrylonitrile copolymer I: thermal and morphological properties. *Bull Mater Sci* 32:199–204
- Varley RJ (2004) Toughening of epoxy resin systems using low-viscosity additives. *Polym Int* 53:78–84
- Vásquez A, Rojas AJ, Adabbo HE, Borrajo J, Williams RJJ (1987) Rubber – modified thermosets: prediction of the particle size distribution of dispersed domains. *Polymer* 28:1156–1164
- Velan TVT, Bilal IM (2000) Aliphatic amine cured PDMS-epoxy interpenetrating network system for high performance engineering applications-development and characterization. *Bull Mater Sci* 23:425–429
- Verchere D, Sautereau H, Pascault JP, Moschiar SM, Riccardi CC, Williams RJJ (1989) Miscibility of epoxy monomers with carboxyl-terminated butadiene-acrylonitrile random copolymers. *Polymer* 30:107–115
- Verchere D, Sautereau H, Pascault JP, Moschiar SM, Riccardi CC, Williams RJJ (1990) Rubber-modified epoxies. I. Influence of carboxyl-terminated butadiene-acrylonitrile random copolymer (CTBN) on the polymerization and phase separation processes. *J Appl Polym Sci* 41:467–485
- Verchere D, Pascault JP, Sautereau H, Moschiar SM, Riccardi CC, Williams RJJ (1991) Rubber-modified epoxies. II. Influence of the cure schedule and rubber concentration on the generated morphology. *J Appl Polym Sci* 42:701–716
- Williams RJJ, Rozenberg BA, Pascault JP (1997) Reaction – induced phase separation in modified thermosetting polymers. *Adv Polym Sci* 128:95–156
- Wise CW, Cook WD, Goodwin AA (2000) CTBN rubber phase precipitation in model epoxy resin. *Polymer* 41:4625–4633
- Xu Z, Zheng S (2007) Morphology and thermomechanical properties of nanostructured thermosetting blends of epoxy resin and poly(ϵ -caprolactone)-block-polydimethylsiloxane-block- poly(ϵ -caprolactone) triblock copolymer. *Polymer* 48:6134–6144
- Yadav R, Srivastava D (2014) Compatibility, thermal, mechanical and morphological properties of cardanol based epoxidized resin modified with liquid rubber. *Int J Plast Technol* 18:27–48

- Yadav R, Awasthi P, Srivastava D (2009) Studies on synthesis of modified epoxidized novolac resin from renewable resource material for application in surface coating. *J Appl Polym Sci* 114:1471–1484
- Yamanaka K, Inoue T (1990) Phase separation mechanism of rubber-modified epoxy. *J Mater Sci* 25:241
- Yamanaka K, Takagi Y, Inoue T (1989) Reaction-induced phase separation in rubber-modified epoxy resin. *Polymer* 30:1839–1844
- Yorkgitis EM, Eiss NS Jr, Tran C, Wilkes GL, McGrath JE (1985) Epoxy resins and composites I, siloxane-modified epoxy resins. *Adv Polym Sci* 72:79–109
- Zhao F, Sun Q, Fang DP, Yao KD (2000) Preparation and properties of polydimethylsiloxane-modified epoxy resins. *J Appl Polym Sci* 76:1683–1690
- Zhao Y, Chen ZK, Liu Y, Xiao HM, Feng QP, Fu SY (2013) Simultaneously enhanced cryogenic tensile strength and fracture toughness of epoxy resins by carboxylic nitrile-butadiene nano-rubber. *Compos Part A* 55:178–187
- Zhao K, Song XX, Liang CS, Wang J, Xu AS (2015) Morphology and properties of nanostructured epoxy blends toughened with epoxidized carboxyl-terminated liquid rubber. *Iran Polym J* 24:425–435
- Zhou W, Cai J (2012) Mechanical and dielectric properties of epoxy resin modified using reactive liquid rubber (HTPB). *J Appl Polym Sci* 124:4346–4351
- Zhou H, Xu S (2014) A new method to prepare rubber toughened epoxy with high modulus and high impact strength. *Mater Lett* 121:238–240
- Zhou W, Zuo J (2013) Mechanical, thermal and electrical properties of epoxy modified with a reactive hydroxyl-terminated polystyrene-butadiene liquid rubber. *J Reinf Plast Compos* 32:1359–1369
- Zhou H, Song XX, Xu SA (2014) Mechanical and thermal properties of novel rubber-toughened epoxy blend prepared by in situ pré-crosslinking. *J Appl Polym Sci* 131:41110 (7 pp)

Shi-Ai Xu

Abstract

The incorporation of functionalized liquid rubbers is one of the most successful methods to toughen epoxies. These rubbers are initially miscible with epoxy oligomers at a given temperature, however, the reaction-induced phase separation occurs because of the increment in the molecular weight of the epoxy matrix as the curing reaction proceeds, thereby resulting in the precipitation of rubber as a dispersed phase. The properties of the resultant epoxy/rubber blends depend largely on their final morphologies, which in turn are determined by the phase separation of the epoxy/rubber blends in the curing process. In this chapter, we first introduce the thermodynamics of phase separation based on the Flory-Huggins solution theory and then discuss the miscibility of epoxy oligomers with liquid rubbers and some factors affecting the phase separation of epoxy/rubber blends, such as the structural properties of rubber, curing agent, and curing procedure. We also discuss the techniques used to study phase separation. Finally, some critical comments and conclusions are given.

Keywords

Epoxy • Rubber/epoxy blends • Liquid rubber • Miscibility • Phase separation • Thermodynamics of phase separation • Phase diagram • Binodal curve • Spinodal curve • Upper critical solution temperature • Lower critical solution temperature • Critical conditions of phase separation • Mechanisms for phase separation • Spinodal separation • Nucleation and growth separation • Solubility parameter • Cloud-point temperature • Critical interaction parameter • Morphology • Curing agent • Curing protocol • Scanning electron microscopy • Transmission electron

S.-A. Xu (✉)

Department of Polymer Engineering and Science, School of Materials Science and Engineering,
East China University of Science and Technology, Shanghai, China
e-mail: saxu@ecust.edu.cn

microscopy • Optical microscopy • Light transmittance • Light scattering •
Electron microscopy

Contents

Introduction	70
Thermodynamics of Phase Separation	71
Phase Diagram of Polymer-Polymer System	71
Critical Conditions for Phase Separation	73
Mechanisms of Phase Separation	74
Miscibility of Epoxy Oligomer with Liquid Rubber	77
Phase Separation of Epoxy/Rubber Blends	82
Factors Affecting Phase Separation of Epoxy/Rubber System	83
Molecular Weight of Rubber	83
Functional Groups on Rubber	84
Curing Agents	85
Curing Protocols	87
Techniques for Studying Phase Separation of Epoxy/Rubber Blends	88
Optical Microscopy	89
Light Transmittance	91
Light Scattering	91
Electron Microscopy	92
Critical Comments	95
Conclusions	95
References	97

Introduction

Epoxy resins are among the most important thermosetting polymers and have been extensively used as structural adhesives, surface coatings, structural composites, and electrical laminates (Zhou et al. 2014; Ratna and Banthia 2004). However, as neat epoxies are brittle with poor resistance to crack growth, their applications as the matrices for high-performance composites are greatly limited (Heng et al. 2015). An efficient way to toughen these brittle polymers is to incorporate a dispersed rubbery phase, which can increase the fracture energy of the polymers by several folds. However, the general rigid rubber with a high molecular weight cannot be well dissolved and dispersed in the epoxy matrix due to significant differences in the chemical structure, polarity, and viscosity between them. Therefore, liquid rubber or preformed core-shell rubber has often been used to toughen epoxies (Yahyaie et al. 2013; Yee and Pearson 1986; Parker et al. 1990; Bascom et al. 1981; Sue 1991; Yee and Du 2000; Abadyan et al. 2012). An appealing feature of liquid rubber as a modifier is its good miscibility with the parent epoxy oligomers (Ratna 2001). Normally, liquid rubber and epoxy oligomer initially form a homogeneous solution by mechanical mixing, and upon curing, rubber particles precipitate as a second phase due to the increase in the molecular weight of the matrix (Wise et al. 2000; Tian et al. 2011). The morphology of rubber-toughened blends is determined by

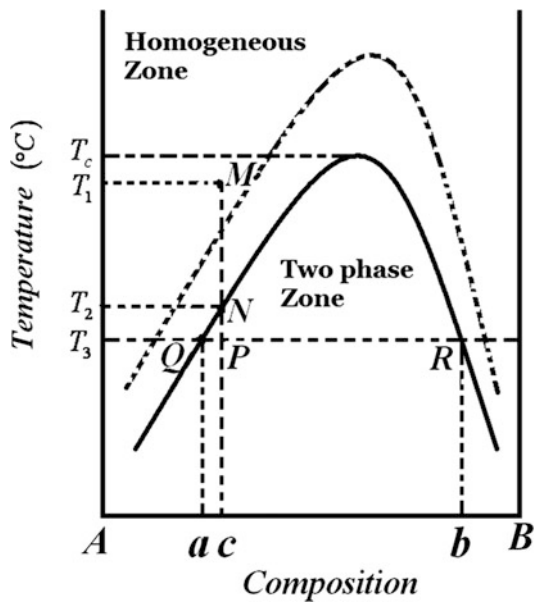
phase separation in the curing process, which in turn depends on the miscibility between the liquid rubber and epoxy, curing conditions, hardeners used, etc. In this chapter, the miscibility and phase separation of rubber-toughened epoxy blends are discussed.

Thermodynamics of Phase Separation

Phase Diagram of Polymer-Polymer System

Phase diagram offers a convenient way to follow the phase separation of the polymer-polymer system (Olabisi et al. 1979; Sperling 2006; Sanchez and Stone 2000; Jiang 1988). Phase separation is determined by the thermodynamics related to the miscibility between the two polymers. The miscibility of a mixture composed of two polymers (A and B) depends on the temperature, composition, and molecular weight of the two polymers. Figure 1 shows a typical phase diagram of a binary polymer system, where A and B on the abscissa represent pure polymer A and B , and the vertical coordinate is the temperature of the system. The solid line (also called the binodal curve) is a boundary between the homogeneous zone and the two-phase zone. The system is homogeneous in the region above the curve and separates into two phases in the region enclosed by the curve. If the composition of the mixture is c , and the initial temperature of the system is T_1 , the corresponding point M lies in the

Fig. 1 Phase diagram of a binary polymer system



homogeneous zone, indicating that the mixture is completely miscible at T_1 . As the temperature decreases to T_2 , the corresponding point N lies on the binodal curve, and thus the system is at the critical point between the homogeneous zone and the two-phase zone. As the temperature further decreases to T_3 , the corresponding point P lies in the two-phase zone, resulting in the occurrence of phase separation. After the system reaches thermodynamic equilibrium, it will separate into two phases corresponding to point Q and R , and the corresponding composition is denoted as a and b , respectively. In phase Q with a composition of a , polymer A is predominant over polymer B , whereas in phase R with a composition of b , the situation is reversed. The mass of the two phases (M_Q and M_R) can be calculated using the level principle:

$$\frac{M_Q}{M_R} = \frac{PR}{QP} \quad (1)$$

In the present case, the content of polymer A is higher than that of polymer B ; thus, the amount of phase Q is higher. Phase Q is generally continuous, and phase R is dispersed.

When the temperature of the system is higher than the upper critical solution temperature (UCST, T_c), the system is homogeneous, regardless of its composition. However, the system in the region surrounded by the binodal curve displays a two-phase structure. When the molecular weight of polymer A or polymer B increases, the binodal curve moves upward (as shown in dashed line).

Beside the UCST-type phase diagram discussed above, there are many other types of phase diagrams. Figure 2 shows a phase diagram with a lower critical solution temperature (LCST).

Fig. 2 LCST-type phase diagram of a binary polymer system

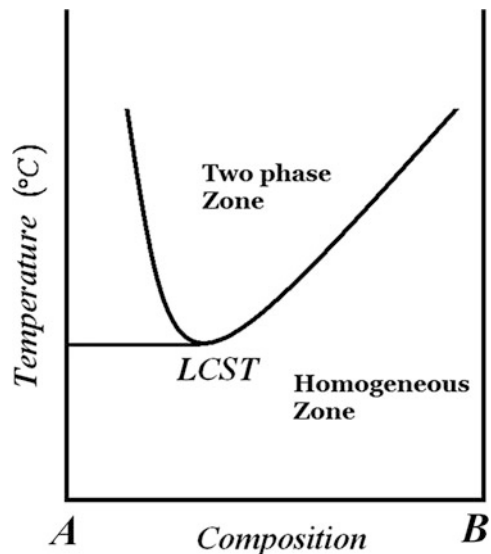
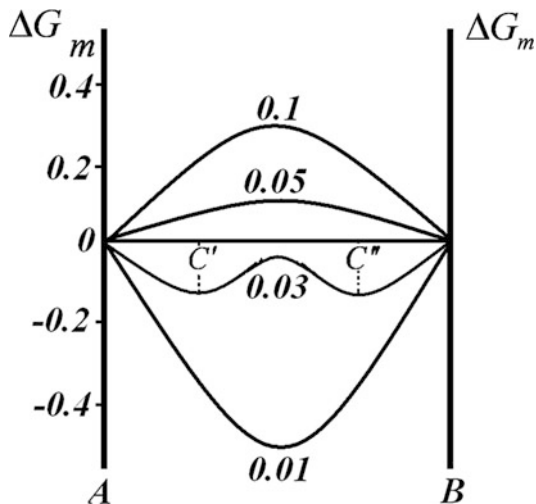


Fig. 3 Plots of ΔG_m versus the composition of the mixture with different χ



Critical Conditions for Phase Separation

The free energy of mixing (ΔG_m) for a binary polymer system can be derived from the quasi-lattice model proposed by Flory and Huggins:

$$\frac{\Delta G_m}{RT} = \frac{V_t}{V} \left(\frac{\Psi_1}{x_1} \ln \Psi_1 + \frac{\Psi_2}{x_2} \ln \Psi_2 + \chi \Psi_1 \Psi_2 \right) \quad (2)$$

where Ψ_1 and Ψ_2 are the volume fraction of polymer 1 and polymer 2; x_1 and x_2 are the segment number of polymer 1 and polymer 2, which is proportional to the molecular weight of the polymer; χ is the Flory-Huggins interaction parameter; V_t is the total volume of the system; V is the volume of the segment; R is the gas constant; and T is the absolute temperature.

Assuming that $x_1 = x_2 = 100$, the variation of ΔG_m with χ is shown in Fig. 3. It shows that at one extreme, if χ is very small (i.e., 0.01), $\chi \Psi_1 \Psi_2$ will also be very small, and ΔG_m is negative in the entire composition range and has only one minimum. Thus, the two polymers are miscible, and their mixture with any composition is homogeneous, whereas at the other extreme, if χ is very large (i.e., 0.1), $\chi \Psi_1 \Psi_2$ is large and ΔG_m is positive in the entire composition range and has only one maximum. Thus, the two polymers are immiscible, and their mixture cannot be homogeneous. However, if χ takes an intermediate value (i.e., 0.03), ΔG_m is negative in the entire composition range and has two minima. When the composition of the mixture is between C' and C'' , the free energy of the mixture will decrease as the mixture separates into two phases with a composition of C' and C'' .

The above conclusion is also true in the case of $x_1 \neq x_2$, but the ΔG_m curve is not symmetrical anymore in this case.

Thus, when the ΔG_m curve changes from having one minimum to having two minima, phase separation occurs in the mixture of two polymers. The critical point for phase separation is that when the two minima and one maximum coincide. As shown in Fig. 3, the ΔG_m curve with two minima must have two inflection points, and the mathematical discriminant for this case is that the second and the third order derivative of ΔG_m equals to zero:

$$\frac{\partial^2 \Delta G_m}{\partial^2 \Psi_1} = 0 \quad (3)$$

$$\frac{\partial^3 \Delta G_m}{\partial^3 \Psi_2} = 0 \quad (4)$$

Combining Eqs. 2, 3, and 4, the critical condition can be expressed as

$$\chi_c = \frac{1}{2} \left[\frac{1}{\sqrt{x_1}} + \frac{1}{\sqrt{x_2}} \right]^2 \quad (5)$$

Mechanisms of Phase Separation

The above discussion suggests that the mixture is immiscible if $\Delta G_m > 0$. However, even if ΔG_m is negative and it has two minima are present, the mixture is not always miscible in the entire composition range, and phase separation may occur in certain composition ranges.

Now we discuss how phase separation occurs.

Figure 4 shows the variation of the free energy of mixing with the composition of a binary polymer mixture, where *A* and *B* are two pure polymers. At T_1 , the ΔG_m curve has two minima, and the corresponding compositions are denoted as C_b^1 and C_b^2 , respectively. Accordingly, there are two inflection points on the curve, and the corresponding compositions are denoted as C_s^1 and C_s^2 , respectively. However, these minima and inflection points change as a function of temperature. For example, as the temperature increases from T_1 to T_2 , the curve moves up. Therefore, different compositions corresponding to the two minima and inflection points can be obtained at different temperatures. Now, temperature is used as the vertical coordinate, and the mixture composition as the horizontal coordinate. The points corresponding to the two minima, such as (T_1, C_b^1) and (T_1, C_b^2) , are connected with a smooth binodal curve, as shown at the bottom of Fig. 4. Similarly, those discrete points corresponding to the two inflection points at different temperatures are also connected with a smooth spinodal curve. In fact, the lower part of Fig. 4 is the phase diagram of a binary polymer blend. In the region surrounded by the binodal curve, the blend shows a two-phase structure. However, phase separation processes differ greatly in different composition ranges.

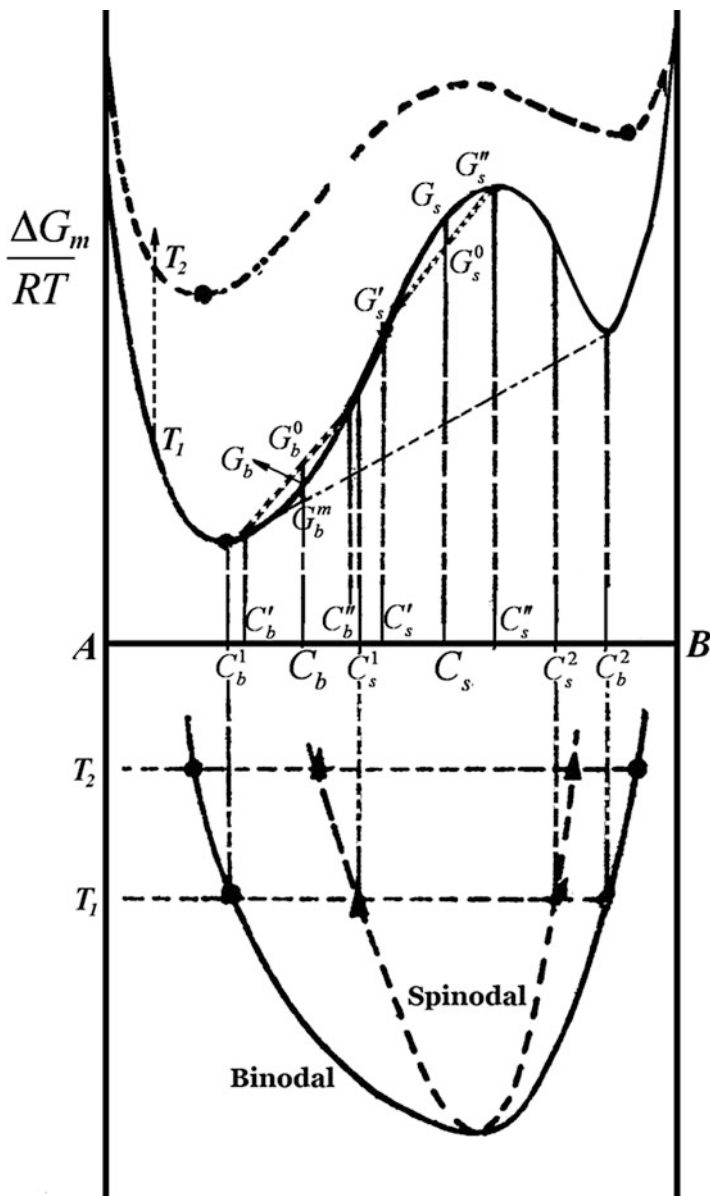


Fig. 4 Variation of the free energy of mixing with the composition of a binary polymer mixture and the spinodal and binodal curves

Spinodal Separation

When the composition of the system is between the two inflection points, i.e., the region surrounded by the spinodal curve, phase separation occurs by a spinodal

mechanism. Assuming that the composition of the system is C_s , it is seen from the upper part of Fig. 4 that the free energy of mixing is G_s . If phase separation is induced by small amplitude composition fluctuations, then according to the level principle, the compositions of the two resulting phases must be on the opposite sides of C_s , which are denoted as C'_s and C''_s , and the corresponding free energies are denoted as G'_s and G''_s , respectively. The total free energy of the separated system (G_s^o) is the linear additivity of the free energy of each phase, which is the value where the tie-line $G'_s - G''_s$ crosses the average composition (i.e., the initial composition). It can be seen that G_s^o is always lower than G_s , which means that the free energy will decrease compared with the original homogeneous system if the system separates into two phases owing to any small perturbation in composition about C_s . Hence, such a separation proceeds spontaneously without any energy barrier and continues slowly until the lowest free energy is achieved at C_b^1 and C_b^2 . Consequently, once phase separation occurs, the system cannot remain homogeneous spontaneously because that would require an uphill climb from the free energy trough. The composition of the two phases, G'_s and G''_s , changes successively in phase separation, and the final composition at equilibrium is denoted as C_b^1 and C_b^2 .

Nucleation and Growth

If the initial composition of the system intervenes between the minimum and its neighboring inflection, i.e., in the region surrounded by the binodal and spinodal curves, phase separation will occur by another mechanism.

If the overall composition is C_b , then the free energy of the system is G_b . Assuming that the system separates into two phases with a composition of C_b^1 and C_b^2 by concentration fluctuation, then the free energy of the heterogeneous system after separation is G_b^o . It is obvious that G_b^o is always larger than G_b , indicating that phase separation results in an increase in the free energy of the system. Thus, phase separation will not occur spontaneously, and the system is metastable and homogeneous. However, if the system separates into two phases whose compositions correspond to the two minima of ΔG_m (C_b^1 and C_b^2), the total free energy of the separated system is G_b^m , which is absolutely lower than G_b . In other words, the free energy decreases as the initial homogeneous system separates into two phases with a composition of C_b^1 and C_b^2 . However, phase separation cannot occur by perturbation in composition. Instead, it occurs by nucleation, which is the process of forming an initial fragment of a new and more stable phase within a metastable mother phase. This initial fragment is called a nucleus and its formation requires an increase in the free energy; thus, there must be a finite undercooling into the binodal region in order to develop a nucleus. Hence, an analogy can be drawn to crystallization kinetics. Generally, nucleation is a very slow process that takes a long time to complete. Once the nucleus has formed, polymer molecules will assemble on the surface of the nucleus in the same composition as the nucleus, driven by free energy reduction. This process makes the nucleus grow gradually, resulting in an increase in domain size of dispersed phase. In this case, the dispersed phases are not interconnected.

Figure 4 shows that if the initial composition of the system lies in the left region surrounded by the binodal and spinodal curves, polymer A is predominant, and the

nucleus in which polymer B predominates will form. The compositions of the nucleus and the matrix near the nucleus are close to C_b^2 and C_b^1 . As phase separation continues, the molecules of polymer B in the matrix will assemble into the nucleus, resulting in nucleus growth and the formation of dispersed phases.

In summary, for a mixture initially homogeneous at a given temperature, if the composition of the system falls over the region surrounded by the binodal and spinodal curves due to temperature change, the system is thermodynamically metastable and cannot separate into two phases spontaneously. Once the nucleus of the dispersed phase forms, phase separation occurs by the nucleation and growth mechanism. However, if the system falls over the region surrounded by the spinodal curve, it is thermodynamically unstable, and phase separation occurs spontaneously by the spinodal mechanism.

Miscibility of Epoxy Oligomer with Liquid Rubber

The miscibility between epoxy oligomer and liquid rubber has an important effect on the phase separation in the curing process. A popular aphorism used in organic chemistry for predicting the solubility is “like dissolves like,” where “like” is qualitatively defined as having similar chemical groups or polarities (Sperling 2006). In the early twentieth century, Hildebrand found that the miscibility between two compounds depended on the difference in the cohesive energy and proposed the concept of solubility parameter, which was defined as the square root of the cohesive energy density:

$$\delta = \sqrt{\frac{\Delta E}{\tilde{V}}} \quad (6)$$

where ΔE is the cohesive energy and \tilde{V} is the molar volume.

For a mixture composed of polymer A and polymer B, Hildebrand and Scott proposed on a quantitative basis that for regular solutions

$$\frac{\Delta H}{V_t} = (\delta_A - \delta_B)^2 \Psi_A \Psi_B \quad (7)$$

where ΔH is the enthalpy of mixing, V_t is the total volume of the mixture, and Ψ is the volume fraction of polymer A and polymer B in the mixture, respectively.

The solubility parameter can be calculated from a knowledge of the chemical structure of any compound using the group molar attraction constant, F , for each group:

$$\delta = \frac{\rho}{M} \sum_i F_i \quad (8)$$

where ρ is the density and M is the molecular weight. For a polymer, M is the molecular weight of monomeric unit.

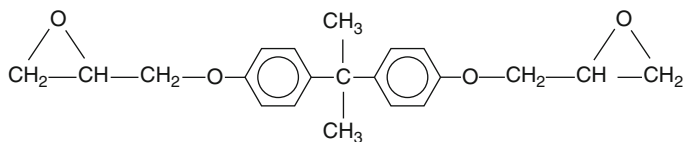
Group molar attraction constants have been tabulated for many chemical groups by Small (1953) and Hoy (1970) and in the handbook edited by Brandrup and Immergut (1989). However, it is noteworthy that as there is a minor difference in the F values, the calculated solubility parameters may be different using different data resources.

Epoxy oligomers and general rigid elastomers, such as natural rubber and butadiene rubber, are immiscible because of the difference in the chemical structure, polarity, and molecular weight. According to Eq. 5, for an epoxy oligomer/rubber system, the critical interaction parameter χ_c increases as the molecular weight of rubber decreases; thus, it is possible to form a homogeneous system at lower temperatures. This is the reason why liquid rubbers with a low molecular weight are chosen to toughen epoxies. Moreover, epoxy oligomer molecule is polar with a large cohesive energy and solubility parameter, while polybutadiene is nonpolar with a small solubility parameter. In order to enhance the miscibility between epoxy resins and rubber, liquid butadiene-acrylonitrile rubber is used. Functionalization of liquid rubber can increase not only the interfacial adhesion by the reaction between the functional groups on the liquid rubber and the epoxy or hardener but also the cohesive energy of the functionalized rubber, resulting in an increase in the solubility parameter of the functionalized rubber. Thus, carboxyl-terminated butadiene-acrylonitrile (CTBN) with different contents of acrylonitrile (AN) has been widely used to modify epoxy resins (Yee and Pearson 1986; Bucknall and Partridge 1983; Kinloch et al. 1983; Bucknall and Gilbert 1989; Gilbert and Bucknall 1991); Garg and Mai 1988; Mathew et al. 2014). Other elastomers such as amino-terminated butadiene-acrylonitrile (ATBN), epoxy-terminated butadiene-acrylonitrile (ETBN), epoxidized natural rubber, and functionalized liquid natural rubber have also been used (Yahyaie et al. 2013).

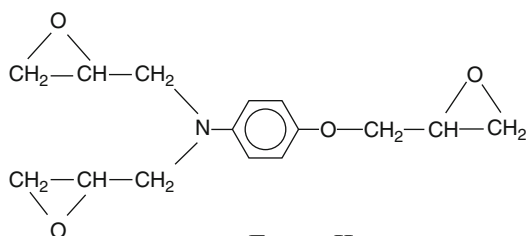
Surprisingly, little attention has been paid to the miscibility between epoxy resins and liquid rubber. The miscibility between them is generally determined by visual inspection. If the resulting solution is homogeneous and transparent, it is considered to be miscible.

Bucknall and Partridge (1986) investigated the miscibility between three liquid epoxy oligomers (di-, tri-, and tetrafunctional epoxies; Ciba-Geigy, UK) and CTBN using the solubility parameter approach, and the structural formulae of the three epoxies and CTBN are shown in Fig. 5.

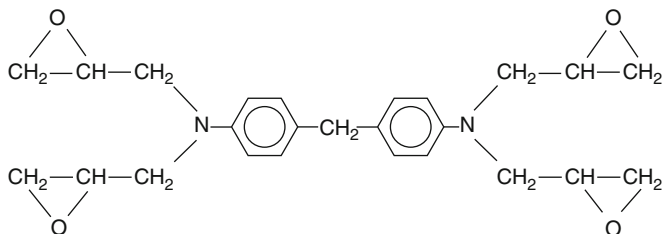
The solubility parameter values for each oligomer and CTBN were calculated by the Fedors method, which was similar to the well-known Small method, and the results are shown in Table 1. It clearly showed that the miscibility between CTBN and epoxy oligomers depended largely on the type of epoxy oligomers used. CTBN was more miscible with epoxy I which had a similar solubility parameter, and the incompatibility between epoxy II or epoxy III and CTBN was indicated by the difference in their respective δ values. Lee et al. (1982) found it necessary to use a more polar rubber and a two-step, pre-react method in order to achieve a uniform dispersion of rubber particles in an epoxy III system.



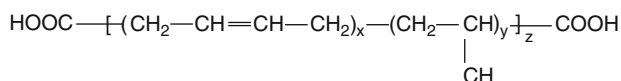
Epoxy I



Epoxy II



Epoxy III



CTBN

Fig. 5 Structural formulae of three liquid epoxy resins and CTBN (Bucknall and Partridge 1986)**Table 1** Calculated solubility parameters, molar volumes, and molecular weights for epoxy resins and CTBN at 25 °C (Bucknall and Partridge 1986)

Compound	δ (H)	Molar volume (cm ³ /mol)	Molecular weight (g/mol)
Epoxy I	10.0	272	380
Epoxy II	10.9	180	300
Epoxy III	11.0	285	530
CTBN	9.9	3127	3320

However, the concept of solubility parameter is suitable for nonpolar or weakly polar systems. For a mixture consisting of polar components, a good miscibility can be achieved only when the solubility parameter and polarity are close. The intermolecular forces include the dispersion force, dipole force, and hydrogen bond. If their contributions to cohesive energy are additive, then the condition for the miscibility between two compounds is that the solubility parameters of individual components should be the same, a condition which is rarely met.

The simple one-component solubility parameter method is extremely limited in dealing with polar compounds, while the three-component solubility parameter method is very difficult to apply. Some scholars have experimentally investigated the miscibility between epoxy oligomer and liquid rubber and phase behavior of the mixture using cloud-point measurements. Wang and Zupko (1981) studied the miscibility between diglycidyl ether of bisphenol A (DGEBA) epoxy monomers and CTBN with two different AN contents. UCST-type behaviors were observed, with the precipitation threshold located at a CTBN volume fraction of about 0.07. However, this location was incorrectly assigned to the difference in the molecular weights of both components and the corresponding variation of the combinatorial entropy of mixing (Verchère et al. 1989). Besides, the position of the miscibility gap was very sensitive to the AN content of CTBN. A decrease in the AN content from 17% to 10% led to an increase in the precipitation threshold temperature by about 73 °C, which was attributed to the increase in the difference in the solubility parameters between the two components as the AN content decreased (Verchère et al. 1989).

Montarnal et al. (1986) measured the cloud-point curves (CPC) of CTBN-DGEBA oligomer systems and found that the terminal carboxyl groups of CTBN could be capped with the epoxide groups of DGEBA, forming an adduct of CTBN with DGEBA. Compared with the pure CTBN-DGEBA system, the capped CTBN-DGEBA system showed a shift of miscibility gap to lower temperatures. Thus, the generated adduct could increase the miscibility of both components.

Wàtzquez et al. (1987) investigated the variation of the cloud-point temperatures with the CTBN content in DGEBA/DDS (diaminodiphenylsulfone) system. DGEBA and CTBN were assumed to be monodisperse, and the free energy of mixing was calculated by the Flory-Huggins equation. In order to avoid gelation, an epoxy/amine ratio of 3.5 was used. Finally, the interaction parameter was obtained as a function of temperature.

Vechère et al. (1989) investigated the effects of several formulation parameters (i.e., the molecular weight of the DGEBA monomer, CTBN type, and the use of an adduct of CTBN with DGEBA) on the miscibility gap of the system by measuring CPC using a light transmittance device. Figure 6 shows the CPC for the mixture of CTBN containing 8 wt% AN with epoxy monomers with different molecular masses (i.e., variable \bar{n} , the average value of the repeat unit numbers (n) calculated from the number-average molecular weight according to the structural formula of DGEBA, top of Fig. 6). Obviously, \bar{n} was proportional to the molecular mass of epoxy monomer. A UCST-type phase diagram was observed for every case, which was consistent with the results of Wang and Zupko (1981). Moreover, the location of

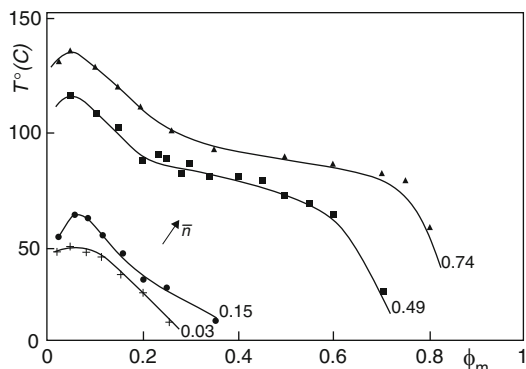
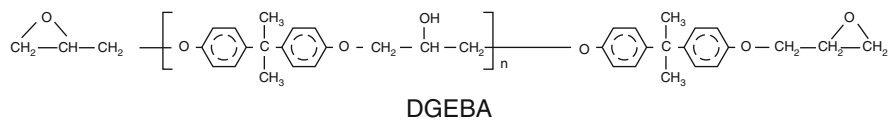


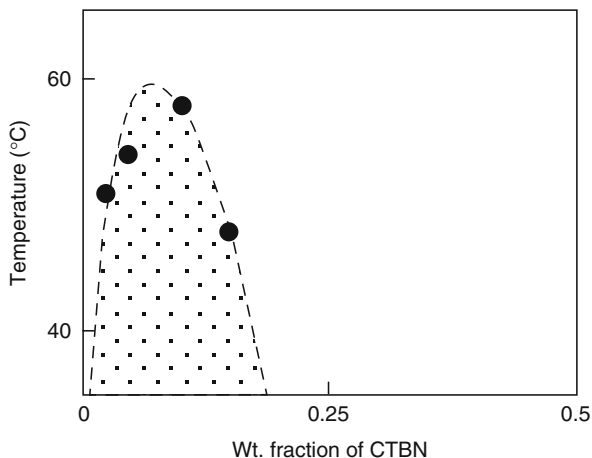
Fig. 6 Cloud-point temperature versus mass fraction of CTBN for mixtures of CTBN with epoxy monomers of different molar masses (different \bar{n} values) (Verchère et al. 1989)

miscibility gap was extremely sensitive to the molecular mass of the epoxy monomer. As the number-average molecular weight of epoxy monomers increased from 349 to 383 g/mol, the precipitation threshold temperature (the maximum of CPC) increased by about 14 °C. An increase in \bar{n} led to a change in the chemical composition of epoxy molecules, such as an increase in the concentration of the secondary OH groups, which in turn resulted in a negligible change in the solubility parameter. However, the change in the molecular mass was shown to be the main reason for the change in the miscibility gap location.

The use of CTBN containing less AN led to a decrease in miscibility, which could be explained by the change in the solubility parameter. However, using CTBN as an adduct with epoxy monomer led to an increase in miscibility due to the copolymer effect. The systems containing CTBN adducts with diamine copolymers showed a complex behavior with two maxima in CPCs.

Although cloud-point measurement is convenient to characterize phase behaviors of epoxy/CTBN system, the resultant CPC is not thermodynamically binodal at equilibrium because the parameters related to phase separation can be detected only when the phase separation proceeds to a certain extent. For example, when light scattering is used to follow the phase separation process, the scattering intensity will produce a significant change only when the dispersed phase reaches a certain size. Besides, the CPC location depends on the heating or cooling rate in the experiment. In order to obtain the binodal curve at equilibrium, Yamanaka and Inoue (1990) showed that the epoxy oligomer/pre-reacted CTBN mixture which was heterogeneous at room temperature became homogeneous as the temperature was increased to, e.g., 100 °C, while when the homogeneous mixture was linearly cooled at a constant rate, an onset of phase separation was observed under a light microscope

Fig. 7 UCST-type phase diagram of the epoxy oligomer/pre-reacted CTBN mixture (Yamanaka and Inoue 1990)



when the temperature was reduced to T_s (the temperature at which phase separation occurred). Obviously, T_s depended on the cooling rate, and a higher cooling rate resulted in a lower T_s . The intercept of T_s in the plot of T_s against the heating rate could be obtained, at which the heating rate was zero, and the intercept temperature corresponded to the binodal temperature. Figure 7 indicates that the epoxy oligomer/pre-reacted CTBN mixture showed a UCST-type phase diagram.

Phase Separation of Epoxy/Rubber Blends

Generally, the epoxy/CTBN mixture loaded with a curing agent is still a single-phase system before curing. As the temperature increases, the curing reaction proceeds, which results in an increase in molecular weight of epoxy. According to Eq. 5, this leads to a decrease in critical interaction parameter χ_c , which is the essential cause of phase separation. Quite different from the phase separation due to temperature variation, the phase separation of epoxy/rubber blends generally occurs at a constant temperature, and it is induced by the curing reaction that leads to an increment in molecular weight of epoxy. Hence, this is called reaction-induced phase separation.

Because the molecular weight of rubber basically remains unchanged in the curing process, Eq. 5 can be rewritten as

$$\chi_c = \frac{1}{2} \left[A + \frac{1}{\sqrt{x_2}} \right]^2 \quad (9)$$

where A is a constant depending on the molecular weight of rubber. Obviously, the critical interaction parameter χ_c decreases as the molecular weight of epoxy increases, which means that phase separation occurs when the actual interaction between epoxy and rubber exceeds χ_c .

The phase separation mechanism for epoxy/rubber blends has been experimentally investigated by many researchers. For instance, Yamanaka and Inoue (1990) investigated the phase separation of rubber in an epoxy matrix using light scattering and concluded that phase separation took place via the spinodal decomposition induced by the increase in the molecular weight of epoxy as the curing reaction proceeded. However, Chen and Lee (1995) showed that the phase separation proceeds via a nucleation and growth mechanism in a similar system using optical light microscopy. Such mechanism was also reported in the epoxy/rubber blends by Kiefer (Kiefer et al. 1996).

Factors Affecting Phase Separation of Epoxy/Rubber System

The phase separation behavior of a mixture consisting of epoxy monomer and rubber without a curing agent is similar to that of a general binary system, and phase separation is generally induced by temperature change. However, the phase separation of epoxy/rubber system cured at a constant temperature is generally induced by the increment in molecular weight of epoxy owing to the curing reaction. The curing reaction in epoxy system is very complicated, and many factors can affect the phase separation of the system.

Molecular Weight of Rubber

Although rubber does not participate in the curing reaction, its molecular weight has a significant effect on its miscibility with epoxy monomer before curing, which finally influences the phase separation of the curing system.

Chen et al. (1994) investigated the effect of rubber molecular weight on the reaction-induced phase separation in rubber-modified epoxies by cloud-point measurement. The liquid rubber used in this study was ETBN synthesized from three carboxy-terminated butadiene-acrylonitrile random copolymers: CTBN-8 L ($\bar{M}_n = 2030$), CTBN-8 ($\bar{M}_n = 3600$), and CTBN-8H ($\bar{M}_n = 6050$), where CTBN-8 is the standard commercial product HycarTM 1300 \times 8, “L” refers to a low molecular weight, and “H” refers to a high molecular weight, respectively. Figure 8 shows the CPCs for CTBN-8L, CTBN-8, and CTBN-8H mixed with the epoxy oligomer. It was shown that increasing the molecular weight of rubber from ETBN-8L to ETBN-8H led to a significant decrease in its miscibility with DGEBA due to the decrease in the entropic contribution to free energy. A similar decrease was also observed in the formulations containing the curing agent. Besides, an increase in molecular weight of rubber also led to a decrease in cloud-point conversion ($x_{cp} = 0.41$ for ETBN-8L and $x_{cp} = 0.12$ for ETBN-8H). The cloud-point viscosity, η_{cp} , decreased as x_{cp} decreased, which was the key factor determining the final morphologies. The times, conversions, and viscosities at the cloud point for different systems are listed in Table 2, where the cloud-point time, t_{cp} , was determined as the time at which a decrease in the transmitted light intensity was recorded; the cloud-point interval,

Fig. 8 Cloud-point curves for rubbers of different molecular weights mixed with DGEBA (Chen et al. 1994)

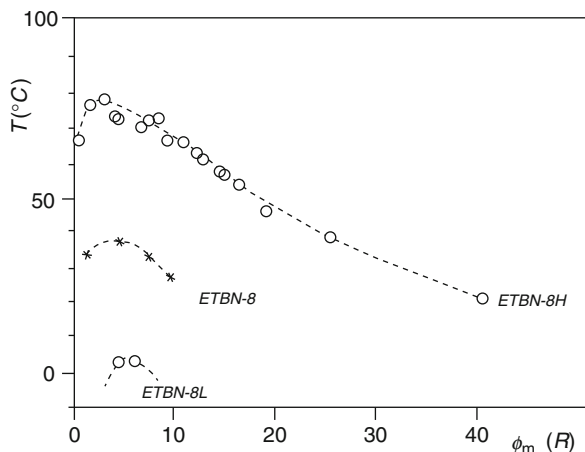


Table 2 Times, conversions, and viscosities at the cloud point (and cloud-point interval) for rubbers of different molecular weights measured at 50 °C (Chen et al. 1994)

System	t_{cp} (min)	Δt_{cp} (min)	x_{cp}	Δx_{cp}	η_{cp} (Pa·s)
ETBN-8 L	164	33.0	0.41	0.08	700
ETBN-8	133	8.3	0.29	0.02	102
ETBN-8H	12	7.0	0.12	0.01	11

Δt_{cp} , as the interval from the onset to the time at which the intensity of transmitted light was practically null; and t_{cp} and Δt_{cp} as the corresponding chemical conversions, x_{cp} and Δx_{cp} , using the kinetic curves, respectively.

The DGEBA-type epoxy modified by three different butadiene-acrylonitrile copolymers with a number-average molecular weight of 2030, 3600, and 6050 g/mol was cured with a cycloaliphatic diamine. The results indicated that increasing rubber molecular weight resulted in a decrease in the conversion and viscosity of the system at the cloud point, a primary morphology of a low concentration of particles with a large size, a more complete segregation of the rubber from the matrix leading to a smaller decrease in the glass transition temperature of the system, and a decrease in the toughening effect.

Functional Groups on Rubber

Wu et al. (2013) illuminated the role of phase domain size in toughening epoxy thermosets with a block ionomer, i.e., sulfonated polystyrene-block-poly(ethylene-co-butylene)-block-polystyrene (SSEBS) synthesized by sulfonation of SEBS with 67 wt% polystyrene. The morphology of epoxy/SSEBS blends can be controlled at a nanometer or micrometer scale by adjusting the sulfonation degree of SSEBS. There exists a critical sulfonation degree (10.8 mol%) for the formation of nanostructures in these epoxy/SSEBS blends, exceeding which only microphase separation occurs

and transparent nanostructured blends were formed. In the nanostructured blends containing SSEBS with a high sulfonation degree, the size of phase domains decreases with the sulfonation degree, leading to a decrease in fracture toughness. However, the toughness of macrophase-separated blends containing SSEBS with a low sulfonation degree is slightly improved. The epoxy blend with submicrometer phase domains in the range of 0.05–1.0 μm containing SSEBS with a moderate degree of sulfonation (5.8 mol%) has the maximum toughness.

Wise et al. (2000) compared the effects of different end groups of liquid rubber on the phase separation behaviors of epoxy/rubber blends cured with amine, and it was found that the carboxyl end groups of CTBN strongly accelerated the curing rate by the impurity catalysis mechanism, whereas the amino-terminated ATBN retarded the reaction. The glass transition behaviors of the blends were investigated by dynamic mechanical thermal analysis (DMTA), and the results showed that the height of the DMTA rubber peak was a linear function of the level of CTBN, indicating that ca. 3% of CTBN was dissolved in the cured epoxy matrix.

Romo-Urbe et al. (2014) also investigated the effect of the end groups of two liquid rubbers (silyl-dihydroxy terminated (PDMS-co-DPS-OH) and silyl-diglycidyl ether terminated (PDMS-DGE)) on the curing kinetics and morphology of DGEBA-based epoxy resin using shear rheometry. The results clearly suggested that the elastomers induced a catalytic effect on the curing reaction, and the gel point decreased with increasing curing temperature. The elastomers accelerated the curing reaction of DGEBA, leading to significantly shorter gel times. This was especially prominent for the hydroxyl-terminated elastomer in which the gel point at the highest curing temperature (110 $^{\circ}\text{C}$) was not detected due to the rapid curing reaction.

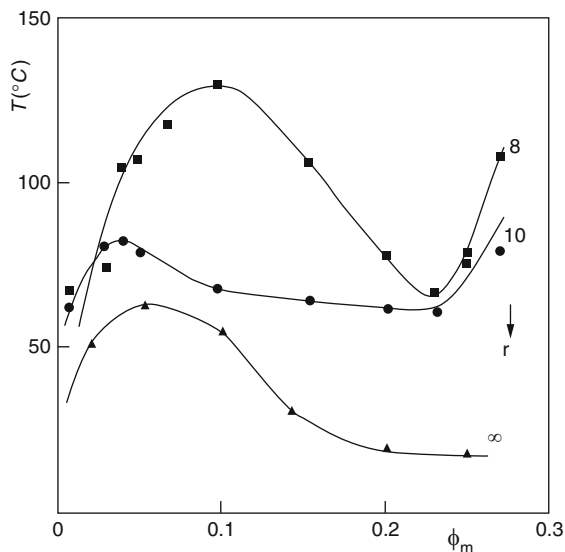
Ho and Wang (1994) used dispersed acrylate rubbers to reduce the stress of cresol-formaldehyde novolac epoxy resins cured with phenolic novolac resin for electronic encapsulation applications and found that the phase separation of the resultant acrylate elastomers from epoxy resin was greatly affected by the size of the alkyl group on the acrylate monomer.

Curing Agents

To achieve a desired performance, the epoxy oligomers must be converted into a cross-linked polymer in the presence of a suitable curing agent, which is generally an organic compound with at least two reactive groups in a molecule (Liu et al. 2014). The curing agent can react with the epoxy and is directly coupled into the cross-linked system as a structural member of the polymer (Mohan 2013), and thus the performance of epoxy resins can be strongly affected by the curing agent. Different epoxies with different properties can be obtained using different curing agents and curing procedures, thus making epoxies one of the most extensively used thermosetting polymers in structural applications (Rao and Pathak 2006; Liu et al. 2009).

In the fabrication process of epoxy/rubber blends, epoxy oligomer and liquid rubber are first mixed into a homogeneous solution and then loaded with the curing agent. After well mixing, the mixture is heated to a given temperature and then

Fig. 9 Cloud-point temperature (T) versus the mass fraction (ϕ_m) of CTBN for mixtures of EDA and DGEBA ($\bar{n} = 0.12$, see Fig. 6) copolymers with the adduct for various r ($r = \text{eq. epoxy/eq. amine}$) (Verchère et al. 1989)



cured. Therefore, the curing agent has an important effect on the phase separation behavior of epoxy/rubber blends. However, unlike the rubber component, the curing agent participates in the curing reaction of epoxy. Hence, the domain size of the rubber phase in the epoxy/rubber blends can be considerably affected by the curing agent used because it determines the kinetics of the curing reaction. Therefore, it is difficult to obtain generalized rules for the phase separation behavior of epoxy/rubber blends (Kim and Kim 1994).

The effect of curing agent on the phase separation of epoxy/rubber blends was systematically investigated by Verchère et al. (1989). Figure 9 shows the CPCs for different r values (r is defined as the equivalent ratio of the epoxy oligomer to the amine curing agent) and the curve obtained in the absence of diamine ($r \rightarrow \infty$). Increasing the diamine amount in the system (i.e., decreasing r) results in a significant increase in the location of miscibility gap. This may be attributed to the increase in the number-average molecular weight, the polydispersity, and the difference in the solubility parameter between the two components caused by increasing the amount of ethylene diamine (EDA). An interesting phenomenon is the presence of a minimum in the CPC, leading to an increase in the cloud-point temperature with the adduct amount when shifting to the right of the minimum. The adduct was prepared by reacting the carboxyl groups of CTBN with an excess of DGEBA using triphenylphosphine (TPP) as a catalyst. A similar trend was also observed when EDA was replaced by diaminodiphenylsulfone (Wätzquez et al. 1987), which could be qualitatively explained by that the adduct also reacted with diamine, thus increasing its molar mass. The larger the adduct amount in the formulation, the larger the expected increase in its molar volume.

However, less research attention has been paid to the phase separation of epoxy resins cured by anhydride, which is another major class of curing agents for epoxy.

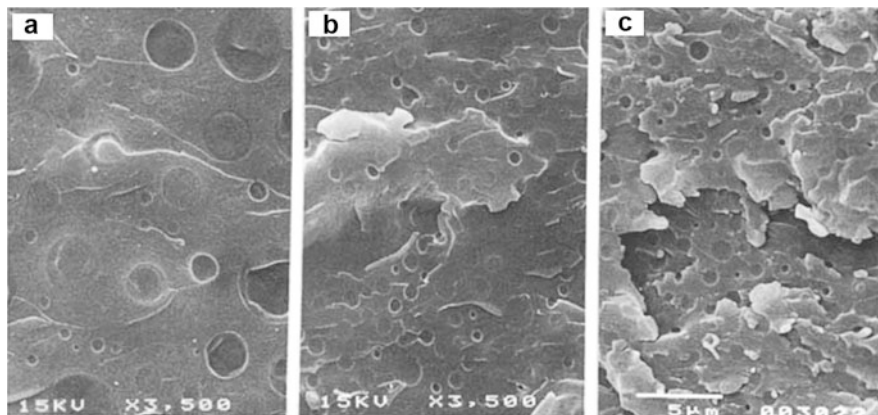


Fig. 10 SEM photographs of ATBN-modified epoxy blends cured at different temperatures: (a) 50 °C, (b) 70 °C, and (c) 110 °C (Kim and Kim 1994)

The rate of anhydride curing of the epoxy is extremely slow at low temperatures. Utilizing the great difference in the rate of curing reaction, Rohde et al. (2015) prepared interpenetrating polymer networks comprising anhydride-cured epoxy resin and polydicyclopentadiene, and the blend concurrently showed high tensile strength, modulus, toughness, and impact strength.

Curing Protocols

Kim et al. (Kim and Kim 1994) investigated the effect of curing temperature on the phase separation and morphology of epoxy blends modified by ATBN (Hycar 1300 \times 16, B. F. Goodrich) containing 16 wt% AN, and the morphology of the mixture cured at different temperatures is shown in Fig. 10. It was shown that the domain correlation length of the 15 wt% ATBN-epoxy system decreased as the isothermal curing temperature was increased, and larger spherical domains were observed in the SEM micrographs of epoxy blends cured at a lower temperature. This was in good agreement with the results of light scattering experiments. As the driving force for phase separation derived from supercooling became smaller as the curing temperature was increased, the conversion at the onset of phase separation was higher at higher curing temperatures at which the supercooling degree was lower. This led to a higher viscosity at the onset of phase separation at a higher curing temperature, resulting in difficulty of diffusion. Therefore, the degree of phase separation at a high curing temperature was low, and the average size of dispersed rubber particles was small.

Ratna (2001) has demonstrated that the phase separation behavior of epoxy blends modified by carboxyl-terminated poly(2-ethyl hexyl acrylate) (CTPEHA) liquid rubber depended on curing conditions. He observed the morphology of fully cured epoxy blends cured at different temperatures and found that the size of discrete

particles with a unimodal distribution increased with an increase in the curing temperature, and phase separation started in the gelation region. Thus, particle growth was not possible because of the diffusional restriction existing after the gelation of the epoxy matrix. The impact strength of the modified blends increased slowly with increasing curing temperature up to 140 °C and then decreased thereafter. The sample cured at 180 °C showed significantly lower toughness. A similar result was reported by De Graaf et al. (1995) in thermoplastic toughened epoxy systems.

Chan et al. (1984) also investigated the curing process and its effect on the development of the morphology and transition of two rubber-modified epoxy systems. A two-step curing process was used to obtain fully cured blends with different morphologies. More specifically, the resin was first isothermally cured at different temperatures until the curing reaction was terminated and then post-cured at a temperature above the maximum glass transition temperature of the system until the curing reaction was totally completed. Two commercial rubbers (pre-reacted carboxyl-terminated and amino-terminated rubbers) synthesized from the same butadiene-acrylonitrile copolymer were used, and all blends were loaded with 15 parts per hundred parts resin (phr) of rubber. It was found that the mechanical properties of ATBN-modified system were more sensitive to curing history than that of pre-reacted CTBN-modified system, because the volume fraction of the dispersed phase in the ATBN-modified system possessed a higher sensitivity to cure conditions.

Grillet et al. (1992) investigated the effect of a two-step process and different cure schedules on the morphology of a rubber-modified epoxy blend. A large difference was found for the same initial rubber content: the dispersed particles showed irregular contours with a broad diameter distribution when a two-step process was used. However, no matter which curing schedule was used, the volume fraction of the dissolved rubber in the epoxy matrix was the same.

Techniques for Studying Phase Separation of Epoxy/Rubber Blends

Many techniques have been used to study the miscibility of epoxy/rubber blends, including differential scanning calorimetry (DSC) (Jenninger et al. 2000), Fourier transform infrared (FTIR) spectroscopy (Akbari et al. 2013), and dynamic mechanical analysis (DMA) (Liu 2013). The microstructural evolution of the polymerization-induced phase separation process can be successfully monitored by scanning electron microscopy (SEM), transmission electron microscopy (TEM) (Guo et al. 2001), atomic force microscopy (AFM), optical microscopy (OM), rheological dynamic analysis, small-angle laser light scattering, and the combination of the aforementioned techniques (Mezzeng et al. 2001; Jyotishkumar et al. 2010; Liu et al. 2006; Choe et al. 2003; Bonnet et al. 1999; Tang et al. 2007; Amendt et al. 2010).

Optical Microscopy

Yamanaka and Inoue (1990) observed the phase separation behavior of a binary mixture of epoxy oligomer and pre-reacted CTBN by optical microscopy. CTBN was pre-reacted with an equal amount of epoxy oligomer at 150 °C for 2 h in a nitrogen atmosphere, and the epoxy oligomer and pre-reacted CTBN were fully mixed and spread on a cover glass. The mixture on the cover glass was inserted in a heating-cooling stage mounted on a light microscope and programmed to provide a linear temperature rise and fall. First, the temperature was increased to obtain a homogeneous single-phase mixture and then cooled. During the cooling process, an onset of phase separation was observed under the light microscope. Changing the weight fraction of CTBN in the mixture resulted in the occurrence of phase separation at different temperatures. A phase diagram was obtained by plotting the temperature versus the weight fraction of CTBN (Fig. 7). In addition, a mixture loaded with DDM was also prepared in the same way, and the ternary mixture on the cover glass was cured in a hot chamber at a constant temperature. The morphology development in the curing process was recorded by an optical microscope. Figure 11 shows the light micrographs taken at various curing stages. The system was homogeneous (Fig. 11a) immediately after the temperature jumped from room temperature to the curing temperature (100 °C, above UCST), and phase separation took place after a certain time lag, resulting in a fairly regular microscopic texture (Fig. 11b). However, the image contrast of the texture became strong and the periodic distance decreased slightly with cure time (Fig. 11c–e).

Chen and Lee (1995) also investigated the phase separation of a rubber-modified epoxy system during curing, and the morphological changes were recorded by real-time optical microscopy. A drop of the mixture was quickly placed on a glass slide while it was still warm and was covered with another glass slide. Both slides were

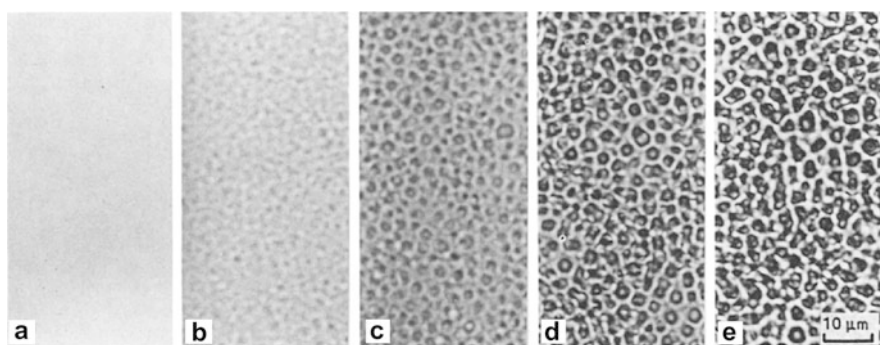


Fig. 11 Light micrographs at various curing stages at 100 °C. Epoxy/pre-reacted CTBN/DDM = 100/20/26. (a) 1 min, (b) 8 min, (c) 17 min, (d) 32 min, and (e) 360 min (Yamanaka and Inoue 1990)

clamped together, and two pieces of 0.01 mm thick steel spacers were placed between the top and bottom glass slides to control the sample thickness. This assembly was transferred to a hot stage that was programmed to provide a linear temperature rise and fall, as shown in Fig. 12. It was observed that the mixture remained homogeneous during the initial curing period; and a thermodynamically stable rubber-rich phase with a particle size of r_c or larger grew spontaneously at a certain reaction extent. The changing and fixation of the two-phase morphology

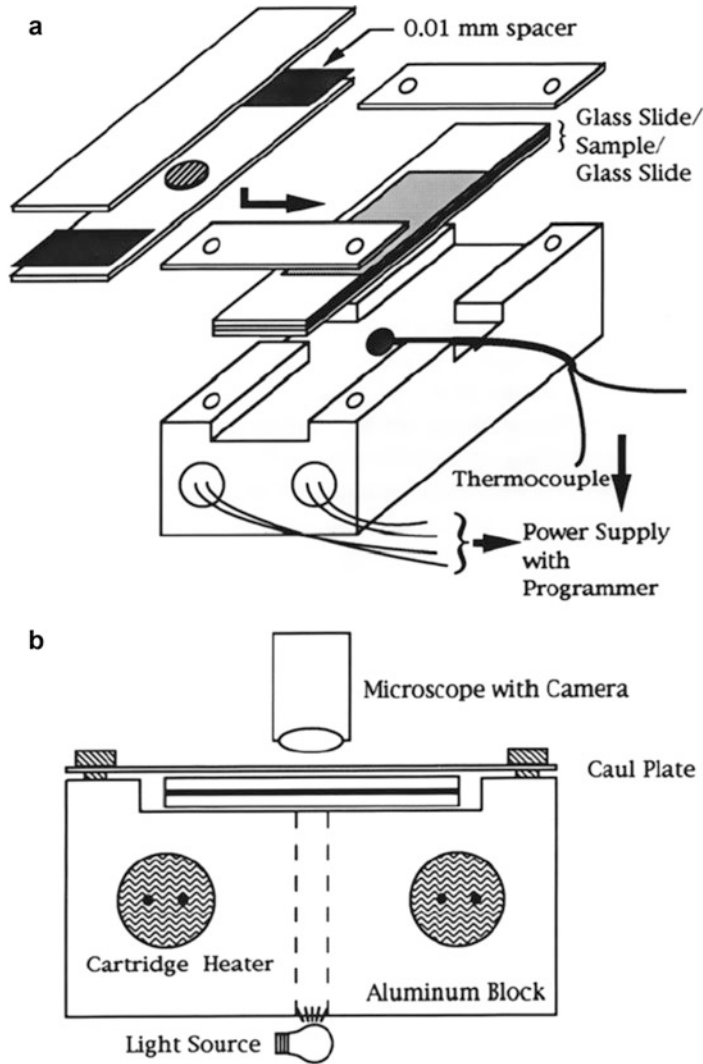


Fig. 12 The optical microscopy hot stage used to observe and record the real-time phase separation process (Chen and Lee 1995)

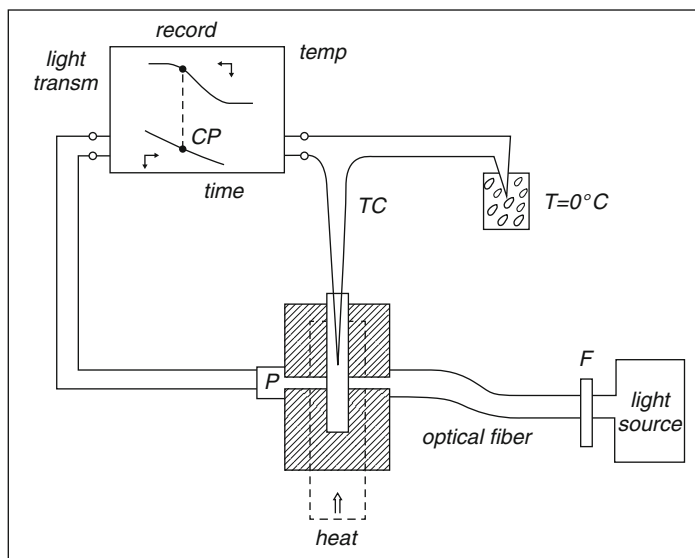


Fig. 13 Schematic diagram of the device used for the determination of CPC. *F* filter, *P* photodetector, *CP* cloud point (Verchère et al. 1989)

during curing were the result of molecular weight buildup in the matrix of the epoxy-rich phase. As curing reactions preceded phase separation, the increased viscosity could be expected to significantly retard the long-range migration of molecules in the subsequent phase separation.

Light Transmittance

Figure 13 shows a schematic diagram of the light transmission device used to obtain CPC (Verchère et al. 1989) based on the decrease in the fraction of transmitted light at the time of phase separation, due to the difference in the refractive index of both phases (1.57 for pure DGEBA and 1.51 for pure CTBN). The sample chamber containing a copper-constantan thermocouple (TC) was introduced into the metallic block heated by electrical resistance or circulating oil coming from a thermostat, which provided the possibility of heating or cooling at different rates. The sample was heated to a temperature about 20°C higher than the cloud point, maintained at that temperature for 5–10 min, and then decreased at a cooling rate of $1^{\circ}\text{C}/\text{min}$. The cloud point was determined from the resulting intensity versus time curve shown in Fig. 13.

Light Scattering

Although light scattering is not as intuitive as optical microscopy, it is more sensitive to follow the phase separation of epoxy/CTBN blends. Zhang et al. (1997)

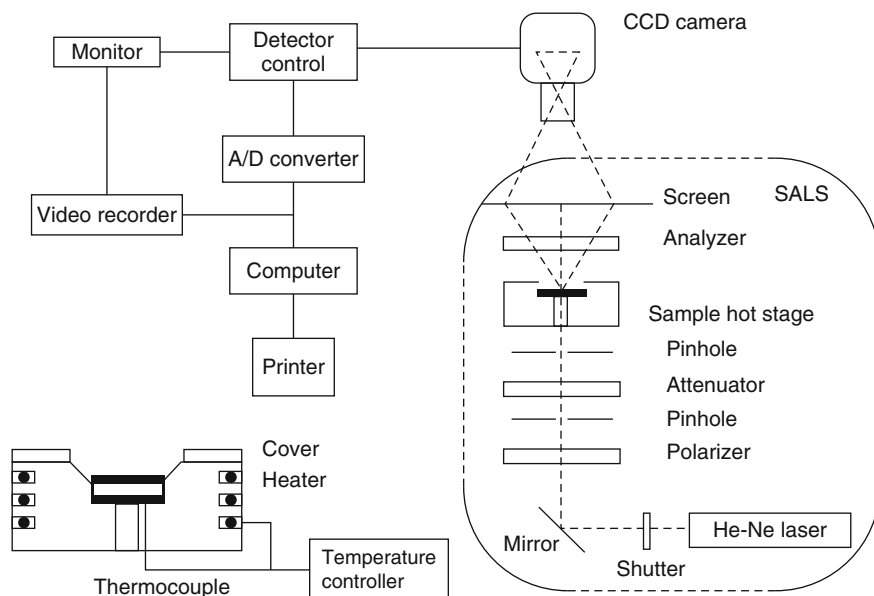


Fig. 14 Time-resolved small-angle light scattering apparatus (Zhang et al. 1997)

investigated the phase separation mechanisms and morphological development during the curing of epoxy with a novel liquid rubber using a laser light scattering apparatus (Fig. 14), which could record the change of the scattering profiles and patterns over time during phase separation. They found that as the cure reaction proceeded, the phase separation took place via the spinodal decomposition induced by the polymerization of epoxy resin.

Kim and Kim (1994) also investigated the phase separation behavior of ATBN-modified epoxy resin during the curing process by light scattering. Spinodal decomposition was shown to be the dominant phase separation mechanism of ATBN-DGEBA blends. Since the ATBN-DGEBA blends showed a UCST-type behavior, the degree of phase separation cured at a low temperature was higher than that cured at a high temperature. The domain correlation length decreased as the isothermal curing temperature was increased. The phase separation started at the early reaction stage when the ATBN content was about 10 wt%, which was in accordance with the phase diagram.

Electron Microscopy

Electron microscopy (SEM and TEM) is an effective means to characterize the morphology of the blends. SEM is often used to observe the final morphology of the cured epoxy blends (Ben Saleh et al. 2014; Thomas et al. 2004). Before observation, the sample is often etched by solvent to obtain a better contrast (Tanaka

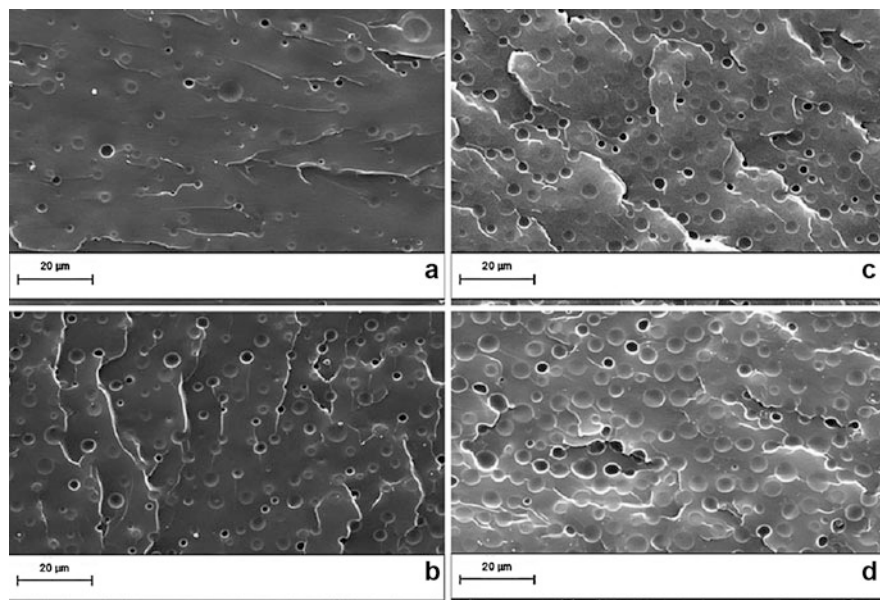


Fig. 15 SEM micrographs of the cryofractured surfaces of binary CTBN/epoxy blends with different CTBN contents. (a) 5 wt%, (b) 10 wt%, (c) 15 wt%, and (d) 20 wt% (Xu et al. 2013)

2000). Xu et al. (2013) explored the epoxy/CTBN blends with different CTBN contents. The samples were fractured in liquid nitrogen and then etched in toluene for 10 h so that the rubber particles dispersed in the matrix would be dissolved. The samples were washed with fresh toluene and dried in a vacuum oven overnight at room temperature. Finally, the surfaces were coated with a thin layer of gold before observation. Figure 15 shows the SEM micrographs of the binary CTBN/epoxy blend, where the holes were the CTBN phase etched by toluene. It was shown that the average particle size of CTBN rubber increased with CTBN content.

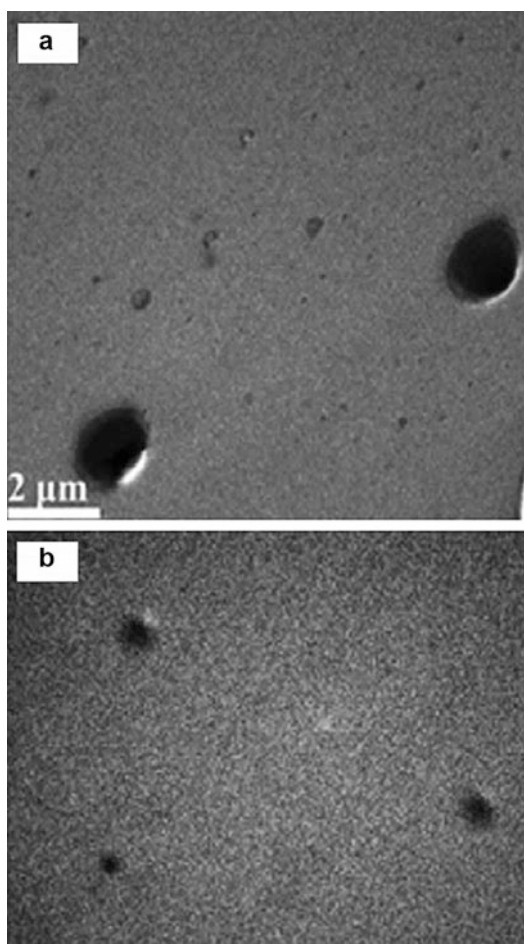
TEM is often used to observe the fine structure of epoxy/rubber blends. Mathew (Mathew et al. 2010) observed the morphology of epoxy blends toughened by liquid natural rubber functionalized with hydroxyl groups by SEM. The blends showed secondary phase separation, and the rubber particles dispersed in the epoxy matrix contained cross-linked epoxy particles. A schematic representation of the secondary phase separation of epoxy in the HLNr phase was shown. Unfortunately, the morphology was not confirmed by TEM.

Because rubber phase usually contains unsaturated bonds, rubber-modified epoxies are often stained with osmium tetroxide to enhance the contrast (Chan et al. 1984; Zhao et al. 2015a). Zhao et al. (2015a, b) used epoxidized liquid rubber prepared by epoxidization of liquid CTBN using hydrogen peroxide and formic acid to toughen epoxy and observed the morphological features of cured blends using TEM. The TEM samples were prepared using an ultramicrotome and stained with OsO_4 vapor for 20 min to enhance the contrast between the polybutadiene phase and

epoxy region. Figure 16 shows the microstructure of the cured blends with 10 wt% of liquid rubber, in which the dark area was the rubber phase stained with OsO_4 . For the blends with unmodified CTBN (Fig. 16a), the rubber particles were micro-sized with relatively clear boundaries, whereas for the blends modified by epoxidized CTBN with an epoxide value of 0.16, the rubber particles were nano-sized with blurred boundaries (Fig. 16b). These phenomena could be attributed to the miscibility between epoxidized CTBN and epoxy resin.

In addition to the above methods, small-angle X-ray scattering (Chen et al. 1993, 1994), small-angle neutron scattering (Dean et al. 2006), and cloud-point, dielectric relaxation spectroscopy, temperature-jump light-scattering, and rheometry measurements (Barham et al. 2001; Plummer et al. 2001; Serrano et al. 2009; Müller et al. 2007; Yu et al. 2004) have also been widely used to investigate polymerization-induced phase separation in thermosets.

Fig. 16 TEM images of cured blends containing 10 wt% rubber. (a) CTBN (unepoxidized); and (b) epoxidized CTBN (with an epoxide value of 0.16) (Zhao et al. 2015a)



Critical Comments

Despite a large number of studies investigating the phase separation of epoxy/rubber blends, some important issues remain to be elucidated.

1. Most previous studies have been based on the Flory-Huggins quasi-lattice model. Although this model is convenient and effective for calculating and predicting the phase separation behavior of epoxy/rubber blends, it is too simple and has many assumptions, resulting in a large difference between theoretical and experimental results.
2. The change in the molecular weight of epoxy during the curing process is often cited as the main reason for phase separation. In fact, the chemical composition of epoxy changes continuously during the curing process because the curing agent takes part in the curing reaction and is incorporated into the cured network, thus resulting in a continuous change in the solubility of epoxy. Moreover, the configuration of epoxy also evolves from initial linear molecule to branching, finally to three-dimensional cross-linking.
3. The change in the molecular weight and configuration of epoxy results in a remarkable change in the viscoelastic properties of the system, which play a crucial role in the phase separation. This type of phase separation is called “viscoelastic phase separation” (Tanaka 2000), which is characterized by some unique coarsening behaviors like phase inversion. However, the viscoelastic effect has rarely been considered in previous studies.
4. Many methods, including optical microscopy, light scattering, and light transmittance, have been used to characterize the phase separation process of epoxy/rubber blends. However, a potential problem with these methods is the time-lag effect. Thus, only cloud-point curves can be measured, and the real-time thermodynamic phase diagram cannot be obtained.
5. Previous studies have focused primarily on the systems cured by amines, and there is little coverage on the epoxy/rubber blends cured by anhydride-type curing agents.

Conclusions

The miscibility between epoxy monomer and liquid rubber CTBN at a given temperature depends on many factors such as the functionality number and molecular weight of epoxy monomer, the AN content, and the molecular weight and dispersity of CTBN. DGEBA and CTBN exhibit an UCST-type phase separation behavior.

The mixture of epoxy monomer with liquid rubber is a single-phase system immediately after the addition of a curing agent. As the curing reaction proceeds, phase separation is induced by the increase in the molecular weight of epoxy superimposed by possible variation of the interaction parameter, χ , with conversion, which is called reaction-induced decomposition. Depending on the initial

composition and curing conditions, phase separation occurs via the spinodal mechanism (Yamanaka and Inoue 1990; Chen and Lee 1995) or the nucleation and growth mechanism.

The electron microscopy reveals that in cured resin, the spherical rubber domains are dispersed somewhat regularly in an epoxy matrix, which may result from a specific situation, the competitive progress of the spinodal decomposition and polymerization, i.e., the coarsening process to irregular domain structure seems to be suppressed by network formation in the epoxy phase. It is also shown that curing at higher temperatures results in the suppression at an earlier stage of spinodal decomposition and, hence, shorter interdomain spacing.

To better understand the phase separation mechanism, one needs to follow the phase separation process over the entire particle size range. Thus, the use of a single technique, typically light scattering or small-angle X-ray scattering, will lead to conclusions only corresponding to a restricted observation window.

The preparation of high-performance epoxy/rubber blends requires a good understanding of the thermodynamics and kinetics of phase separation process and the influencing factors, including the kinetics of curing reaction and the diffusion kinetics of reactive constituents. However, these factors interplay with each other in epoxy/rubber system. For example, as curing reaction proceeds, the molecular weight and chemical structure of the matrix change continuously, and the increment in the viscosity of the system results in a decrease in the diffusion rate of the reactive species and consequently an increase in the driving force for phase separation. If phase separation occurs before gelation, the morphologies and properties of the resultant blends are determined by thermodynamic considerations (Yamanaka et al. 1989).

The morphological development of epoxy/rubber blends depends largely on the thermodynamics of phase separation (Zielinski et al. 1996; Park and Kim 1997). The thermodynamic analysis of phase separation allows us to better understand the phase behavior and to obtain the phase diagram of epoxy/rubber blends in the curing process, which is fundamental to explain and control morphological development. The phase diagram of epoxy/rubber blends is qualitatively different from that of other materials due to the inherent polydispersity of polymers (Soulé et al. 2007; Choi and Bae 1999). Several experimental variables that affect the thermodynamics and/or kinetics of reaction-induced phase separation process, such as the type and concentration of modifier (Koningsveld and Staverman 1968); molecular weight of components; reactivity of curing agent; curing conditions, especially temperature (Aquad et al. 2003; Stefani et al. 2001; Remiro et al. 2001; Girard-Reydet et al. 1997); initial miscibility between epoxy monomer and modifier; reaction rate; and viscosity, among others, could directly influence the morphologies developed.

The competition between the curing rates and phase separation determines the mechanism of the reaction-induced phase separation, i.e., nucleation and growth or spinodal demixing (Williams et al. 1997; Araki et al. 1998). Controlling this mechanism is crucial for the final morphologies and properties of the epoxy/rubber blends. The influence of some parameters like composition and cure temperature on

the final morphology has been investigated using scattering techniques (Inoue 1995; Girard-Reydet et al. 1998). However, it is very difficult to obtain the information about the continuously changing morphology in the course of reaction-induced phase separation with these ex situ methods. Girard-Reydet et al. (1998) deduced changes in morphology by means of in situ or real-time diffraction techniques using different observation windows. In situ dielectrical measurements also provide information about morphology using interfacial polarization due to phase separation (Bascom et al. 1981; Sue 1991). These real-time techniques, however, are limited to the rate of phase separation and the accompanying mechanism, without information about the competing rate of network formation.

References

- Abadyan M, Bagheri R, Kouchakzadeh MA (2012) *J Appl Polym Sci* 125:2467
- Akbari R, Beheshty MH, Shervin M (2013) Toughening of dicyandiamide-cured DGEBA-based epoxy resins by CTBN liquid rubber. *Iran Polym J* 22:313–324
- Amendt MA, Chen L, Hillmyer MA (2010) *Macromolecules* 43:3924
- Araki T, Tran-Cong Q, Shibayama M (1998) Structure and properties of multi-phase polymeric materials. Dekker, New York, p 155
- Auad ML, Borrajo J, Aranguren MI (2003) Morphology of rubber-modified vinyl ester resins cured at different temperatures. *J Appl Polym Sci* 89(1):274–283
- Barham B, Fossier K, Voge G, Waldow D (2001) *Macromolecules* 34:514
- Bascom W, Ting R, Moultn RJ, Riew CK, Siebert AR (1981) *J Mater Sci* 16:2657
- Ben Saleh AB, Mohd Ishak ZA, Hashim AS, Kamil WA, Ishiaku US (2014) Synthesis and characterization of liquid natural rubber as impact modifier for epoxy resin. *Phys Procedia* 55:129–137
- Bonnet A, Pascault JP, Sautereau H, Camberlin Y (1999) *Macromolecules* 32:8524
- Brandrup J, Immergut EH (1989) *Polymer handbook*, 3rd edn. Wiley, New York
- Bucknall CB, Gilbert AH (1989) Toughening tetrafunctional epoxy resins using polyetherimide. *Polymer* 30(2):213–217
- Bucknall C, Partridge I (1983) Phase separation in epoxy resins containing polyethersulphone. *Polymer* 24(5):639–644
- Bucknall CB, Partridge IK (1986) Phase separation in crosslinked resins containing polymeric modifiers. *Polym Eng Sci* 26(1):54–62
- Chan LC, Gillham JK, Kinloch AJ, Shaw SJ (1984) Chapter 15, Chapter 16: Rubber-modified epoxies morphology, transitions, and mechanical properties. In: Riew C et al (eds) *Rubber-modified thermoset resins*, Advances in chemistry. American Chemical Society, Washington, DC
- Chen JP, Lee YD (1995) A real-time study of the phase-separation process during polymerization of rubber-modified epoxy. *Polymer* 36(1):55–65
- Chen D, Sautereau H, Pascault JP, Vigier G (1993) Rubber modified epoxies: II. A reaction induced phase separation observed in situ and a posteriori with different methods. *Polym Int* 32:369
- Chen D, Pascault JP, Sautereau H, Ruseckaite RA, Williams RJJ (1994) Rubber-modified epoxies: III. Influence of the rubber molecular weight on the phase separation process. *Polym Int* 33:253–261
- Choe Y, Kim M, Kim W (2003) *Macromol Res* 11:267
- Choi JJ, Bae YC (1999) Liquid-liquid equilibria of polydisperse polymer systems. *Eur Polym J* 35(9):1703–1711

- De Graaf LA, Hempenious MA, Moller M (1995) *Polym Prepr* 36:787
- Dean KM, Cook WD, Lin MY (2006) Small angle neutron scattering and dynamic mechanical thermal analysis of dimethacrylate/epoxy IPNs. *Eur Polym J* 42:2872–2887
- Garg AC, Mai YW (1988) Failure mechanisms in toughened epoxy resins—a review. *Compos Sci Technol* 31(3):179–223
- Gilbert AH, Bucknal CB (1991) Epoxy resin toughened with thermoplastic. *Makromol Chem Macromol Symp* 45(1):289–298
- Girard-Reydet E, Vicard V, Pascaul JP, Sautereau H (1997) Polyetherimide modified epoxy networks: influence of cure conditions on morphology and mechanical properties. *J Appl Polym Sci* 65(12):2433–2445
- Girard-Reydet E, Sautereau H, Pascault JP, Keates P, Navard P, Thollet G, Vigier G (1998) *Polymer* 39:2269
- Grillet AC, Galy J, Pascault JP (1992) Influence of a two-step process and of different cure schedules on the generated morphology of a rubber-modified epoxy system based on aromatic diamines. *Polymer* 33(1):34–43
- Guo Q, Eigueiredo P, Thomann R, Gronski W (2001) Phase behavior, morphology and interfacial structure in thermoset thermoplastic elastomer blends of poly(propylene glycol)-type epoxy resin and polystyrene-*b*-polybutadiene. *Polymer* 42:10101–10110
- Heng Z, Chen Y, Zou H, Liang M (2015) Simultaneously enhanced tensile strength and fracture toughness of epoxy resins by a poly(ethylene oxide)-block-carboxyl terminated butadiene-acrylonitrile rubber dilock copolymer”. *RSC Adv* 5:42362
- Ho TH, Wang CS (1994) Dispersed acrylate rubber-modified epoxy resins for electronic encapsulation. *J Polym Res* 1(1):103–108
- Hoy KL (1970) *J Paint Technol* 46:76
- Inoue T (1995) *Prog Polym Sci* 20:119
- Jenninger W, Schawe JEK, Alig I (2000) Calorimetric studies of isothermal curing of phase separating epoxy networks. *Polymer* 41:1577–1588
- Jiang M (1988) Physical chemistry of polymer blends (Chinese). Sichuan Education Press, Chengdu
- Jyotishkumar P, Özdilek C, Moldenaers P, Sinturel C, Janke A, Pionteck J, Thomas S (2010) Dynamics of phase separation in poly(acrylonitrile-butadiene-styrene)-modified epoxy/DDS system: kinetics and viscoelastic effects. *J Phys Chem B* 114:13271–13281
- Kiefer J, Hilborn JG, Hedrick JL (1996) Chemically induced phase separation: a new technique for the synthesis of macroporous epoxy networks. *Polymer* 37(25):5715–5725
- Kim DS, Kim SC (1994) Rubber modified epoxy resin. II: phase separation behavior. *Polym Eng Sci* 34(21):1598–1604
- Kim BS, Chiba T, Inoue T (1993) *Polymer* 34:2809
- Kinloch AJ, Shaw SJ, Tod DA, Hunston DL (1983) Deformation and fracture behaviour of a rubber-toughened epoxy: 1. Microstructure and fracture studies. *Polymer* 24(83):1341–1354
- Koningsveld R, Staverman AJ (1968) Liquid-liquid phase separation in multicomponent polymer solutions. I. Statement of the problem and description of methods of calculation. *J Polym Sci A Polym Chem* 6(2):305–323
- Lee BL, Lizak CM, Riew CK, Moulton RJ (1982) Rubber toughening of tetrafunctional epoxy resin. BF Goodrich internal report
- Liu Y (2013) Polymerization-induced phase separation and resulting thermomechanical properties of thermosetting/reactive nonlinear polymer blends: a review. *J Appl Polym Sci* 127(5):3279–3292
- Liu XY, Zhan GZ, Yu YF, Li SJJ (2006) *J Polym Sci B Polym Phys* 44:3102
- Liu XQ, Xin WB, Zhang JW (2009) *Green Chem* 11:1018–1025
- Liu Y, Wang J, Xu S (2014) Synthesis and curing kinetics of cardanol-based curing agents for epoxy resin by in-situ depolymerisation of paraformaldehyde. *J Polym Sci A Polym Chem* 52(4):472–480
- Mathew VS, Sinturel C, George SC, Thomas S (2010) Epoxy resin/liquid natural rubber system: secondary phase separation and its impact on mechanical properties. *J Mater Sci* 45:1769–1781

- Mathew VS, George SC, Parameswaranpillai J, Thomas S (2014) Epoxidized natural rubber/epoxy blends: phase morphology and thermomechanical properties. *J Appl Polym Sci* 131(4):39906
- Mezzeng R, Plummer CJG, Boogh L, Månson JAE (2001) Morphology build-up in dendritic hyperbranched polymer modified epoxy resins: modelling and characterization. *Polymer* 42:305–317
- Mohan P (2013) *Polym Plast Technol Eng* 52:107–125
- Montarnal S, Pascault JP, Sautereau H (1986) In: *Mélanges de Polymères*. GFP, Trasbourg, p 279
- Müller Y, Häußler L, Pionteck J (2007) *Macromol Symp* 254:267
- Olabisi O, Robeson LM, Shaw MT (1979) *Polymer-polymer miscibility*. Academic, New York
- Park JW, Kim SC (1997) In: Kim SC, Sperling LH (eds) *IPNs around the world, science and engineering*. Springer, Chichester, p 27
- Parker DS, Sue HJ, Huang J, Yee AF (1990) Toughening mechanisms in core-shell rubber modified polycarbonate. *Polymer* 31:2267–2277
- Plummer CJG, Mezzenga R, Boogh L, Månson JAE (2001) *Polym Eng Sci* 41:43
- Rao BS, Pathak SK (2006) *J Appl Polym Sci* 100:3956–3965
- Ratna D (2001) Phase separation in liquid rubber modified epoxy mixture. Relationship between curing conditions, morphology and ultimate behavior. *Polymer* 42:4209–4218
- Ratna D, Banthia AK (2004) Rubber toughened epoxy. *Macromol Res* 12(1):11–21
- Remiro PM, Marieta C, Riccardi CC, Mondragon I (2001) Influence of curing conditions on the morphologies of a PMMA-modified epoxy matrix. *Polymer* 42(25):9909–9914
- Rohde BJ, Robertson ML, Krishnamoorti R (2015) Concurrent curing kinetics of an anhydride-cured epoxy resin and polydicyclopentadiene. *Polymer* 69:204–214
- Romo-Urbe A, Arcos-Casarrubias JA, Flores A, Valerio-CáRdenas C, González AE (2014) Influence of rubber on the curing kinetics of DGEBA epoxy and the effect on the morphology and hardness of the composites. *Polym Bull* 71:1241–1262
- Sanchez IC, Stone MT (2000) Chapter 2: Statistical thermodynamics of polymer solutions and blends. In: Paul DR, Bucknall CB (eds) *Polymer blends*. Wiley, New York
- Serrano E, Kortaberria G, Arruti P, Tercjak A, Mondragon I (2009) *Eur Polym J* 45:1046
- Small PA (1953) *J Appl Chem* 3:71
- Soulé ER, Elicabe GE, Borrajo J, Williams RJJ (2007) Analysis of the phase separation induced by a free-radical polymerization in solutions of polyisobutylene in isobornyl methacrylate. *Ind Eng Chem Res* 46:7535–7542
- Sperling LH (2006) *Introduction to physical polymer science*, 4th edn. Wiley, New York
- Stefani PM, Riccardi CC, Remiro PM, Mondragón I (2001) Morphology profiles generated by temperature gradient in PMMA modified epoxy system. *Polym Eng Sci* 41(11):2013–2021
- Sue H (1991) *J Polym Eng* 31:275
- Tanaka H (2000) Viscoelastic phase separation. *J Phys Condens Matter* 12(15):R207–R264
- Tang XL, Zhao L, Li L, Zhang HD, Wu PY (2007) *Acta Chim Sin* 65:2449
- Thomas R, Abraham J, Selvin P, Thomas S (2004) Influence of carboxyl-terminated (butadiene-coacrylonitrile) loading on the mechanical and thermal properties of cured epoxy blends. *J Polym Sci B Polym Phys* 42:2531–2544
- Tian X, Geng Y, Yin D, Zhang B, Zhang Y (2011) *Polym Test* 30:16
- Verchère D, Sautereau H, Pascault JP, Moschiar SM, Riccardi CC, Williams RJJ (1989) Miscibility of epoxy monomers with carboxyl-terminated butadiene acrylonitrile random copolymers. *Polymer* 30:107–115
- Wang TT, Zupko HM (1981) Phase separation behavior of rubber-modified epoxies. *J Appl Polym Sci* 26:2391–2401
- Wátzquez A, Rojas AJ, Adabbo HE, Borrajo J, Williams RJJ (1987) *Polymer* 28:1156
- Williams RJJ, Rozenberg BA, Pascault JP (1997) *Adv Polym Sci* 128:95
- Wise CW, Cook WD, Goodwin AA (2000) Rubber phase precipitation in model epoxy resins. *Polymer* 41:4625–4633
- Wu S, Guo Q, Kraska M, Bernd S, Mai YW (2013) Toughening epoxy thermosets with block ionomers: the role of phase domain size. *Macromolecules* 46:8190–8202

- Xu SA, Wang GT, Mai YW (2013) Effect of hybridization of liquid rubber and nanosilica particles on the morphology, mechanical properties, and fracture toughness of epoxy composites. *J Mater Sci* 48(9):3546–3556
- Yahyaie H, Ebrahimi M, Tahami HV, Mafi ER (2013) Toughening mechanisms of rubber modified thin film epoxy resins. *Prog Org Coat* 76:286–292
- Yamanaka K, Inoue T (1990) Phase separation mechanism of rubber-modified epoxy. *J Mater Sci* 25:241–245
- Yamanaka K, Takagi Y, Inoue T (1989) Reaction-induced phase separation in rubber-modified epoxy resins. *Polymer* 30:1839–1844
- Yee AF, Du J (2000) Toughening of epoxies. In: *Polymer blends*, Paul DR, Bucknall CB (eds) vol 2. Wiley, New York, p 225
- Yee AF, Pearson RA (1986) Toughening mechanisms in elastomer-modified epoxies. Part I Mechanical studies. *J Mater Sci* 21:2462–2474
- Yu YF, Wang MH, Gan WJ, Tao QS, Li SJ (2004) *J Phys Chem B* 108:6208
- Zhang J, Zhang H, Yan D, Zhou H, Yang Y (1997) Reaction-induced phase separation in rubber-modified epoxy resin. *Sci China B* 40(1):15–23
- Zhao K, Song XX, Liang CS, Wang J, Xu SA (2015a) Morphology and properties of nanostructured epoxy blends toughened with epoxidized carboxyl-terminated liquid rubber. *Iran Polym J* 24(5):425–435
- Zhao K, Wang J, Song XX, Liang CS, Xu SA (2015b) Curing kinetics of nanostructured epoxy blends toughened with epoxidized carboxyl-terminated liquid rubber. *Thermochim Acta* 605:8–15
- Zhou HS, Song XX, Xu SA (2014) Mechanical and thermal properties of novel rubber-toughened epoxy composite prepared via in-situ pre-crosslinking. *J Appl Polym Sci* 131(22):41110
- Zielinski JM, Vratsanos MS, Laurer JH, Spontak RJ (1996) Phase-separation on studies of heat-cured ATU-flexibilized epoxies. *Polymer* 37(1):75–84

P. Poornima Vijayan

Abstract

The investigations on the morphological features of epoxy/rubber blends are of great importance as the morphology controls the property and performance of these blends. The characterization techniques like optical microscopy (OM), scanning electron microscopy (SEM), atomic force microscopy (AFM), and transmission electron microscopy (TEM) are commonly used to evaluate the morphology and phase distribution of the dispersed rubber particles in the epoxy matrix. These characterization techniques are used to explore the morphological features in epoxy systems modified with different kinds of rubbers such as liquid rubbers, preformed core-shell rubber particles, in situ-formed rubber particles, etc. Moreover, several factors which affect the final two-phase morphology in the epoxy/rubber blends are also explored using these techniques. The fracture surface characteristics are also explored using morphological investigation of the fracture/fatigue surface of the epoxy/rubber blends to establish the toughening mechanism operating in them. While both OM and SEM are widely used to reveal the microstructure, AFM and TEM are used to trace out the nanostructure in such blends. The current chapter gives a detailed discussion on the use of such techniques to explore the morphology and the microscopic toughening phenomena operates in epoxy/rubber blends on the basis of published reports.

Keywords

Epoxy blends • Liquid rubber • Microscopic techniques

P.P. Vijayan (✉)

Center for Advanced Materials, Qatar University, Doha, Qatar

e-mail: poornimavijayan2007@gmail.com

Contents

Introduction	102
Techniques Used for Morphological Analysis	103
Optical Microscopy (OM)	103
Scanning Electron Microscopy (SEM)	113
Atomic Force Microscopy (AFM)	127
Transmission Electron Microscopy (TEM)	135
Conclusions	143
References	143

Introduction

The performance of epoxy/rubber blends is strongly influenced by their morphology (Manziona et al. 1981b; Verchere et al. 1991a). In liquid rubber-modified epoxy, the generation of morphology is based on the phenomenon called “reaction-induced phase separation” (Yamanaka et al. 1989). After adding the curing agent into the mixture of epoxy prepolymer and liquid rubber, the epoxy resin begins to cross-link. As the cross-linking progresses, the liquid rubber precipitates out from the epoxy phase as discrete particulate phase. The developed two-phase morphology consists of an elastomeric phase having diameter in micro- or nanometer range finely dispersed in the epoxy matrix. The two-phase morphology developed in the epoxy/rubber blends is affected by several factors such as the initial compatibility between the epoxy resin and the rubber, reaction of epoxy with the end group of the rubber, type and amount of the curing agent employed, cure history, degree of pre-reaction between the rubber and the resin prior to the curing reaction, rubber content, etc. Hence, the morphology in liquid rubber-modified epoxy can be tuned through control over these factors (Bagheri and Pearson 2000). Better control over the morphology in epoxy/liquid rubber blend is the key to ultimately balance their properties and performance. A large number of research reports were available in this area, and it is worthwhile to point out the major morphological findings in epoxy/rubber blends. The various morphological parameters in epoxy/liquid rubber blends like the total rubber content (Bartlet et al. 1985), the volume fraction of the rubber phase (Manziona et al. 1981a), the rubber particle size and distribution (Sultan and McGarry 1973; Pearson and Yee 1991), and the interparticle distance (Bagheri and Pearson 2000) were investigated by researchers. Nowadays, preformed core-shell rubber and in situ-formed rubber particles are used as toughening agents instead of liquid rubber. The core-shell rubber particles consist of a soft rubber core within a harder shell and are formed by emulsion polymerization prior to mixing with epoxy. Hence, in epoxy/preformed rubber blends unlike in epoxy/liquid rubber blend, the particle size and its distribution remain unchanged when the concentration is altered (He et al. 1999; Kinloch et al. 2014). While in conventional epoxy/rubber blends, liquid rubber forms 1–10 μm -sized particles upon curing; the preformed and in situ-formed rubber offered nanosized particles below 100 nm.

Different techniques including optical microscopy (OM), scanning electron microscopy (SEM), atomic force microscopy (AFM), and transmission electron

microscopy (TEM) were extensively used to characterize the morphology in epoxy/rubber blends. The current chapter aims to comprehend the use of various techniques to establish the morphological features in different epoxy/rubber blends. The role of different factors such as rubber content, nature of rubber, cure conditions, etc. on the morphological parameters of epoxy/rubber blends will be discussed based on the literature reports. The fracture toughness mechanism operate in epoxy/rubber blends can also be established with the help of these morphological techniques. Moreover, morphological studies to correlate the properties of epoxy/rubber blends will also be reviewed and presented.

Techniques Used for Morphological Analysis

While optical microscopy (OM) is used to investigate the miscibility between the blend components and the online monitoring of morphology changes during cure reaction, scanning electron microscopy (SEM), atomic force microscopy (AFM), and transmission electron microscopy (TEM) are used to determine the final morphology and phase distribution of the dispersed rubber particles in epoxy/rubber blends. Moreover, OM and SEM are used to investigate the microstructures of the fracture surfaces of epoxy/rubber blends to correlate the morphological parameters with the fracture properties and to elucidate the fracture mechanism.

Optical Microscopy (OM)

Optical microscopy is a simple technique to observe the miscibility between epoxy prepolymer and liquid rubber and the reaction-induced phase separation thereafter while varying the temperature. After the temperature jumps to the curing temperature, the homogenous resin/liquid rubber mixture starts to demix due to the increase in the molecular weight of epoxy, which resulted in the poor miscibility between liquid rubber and epoxy. The understanding of phase separation dynamics is of crucial importance in achieving an optimum phase structure in epoxy/liquid rubber blends. The optical images are also able to give supporting information to light-scattering observations about the mechanism of demixing. The early stage research on epoxy/liquid rubber blends was mainly focused on miscibility and phase-separation studies.

The phase behavior of epoxy prepolymer and carboxyl-terminated (butadiene-co-acrylonitrile) (CTBN) mixture was studied by Lee and Kyu (1990). Epoxy/CTBN mixture without curing agent showed an upper critical solution temperature (UCST) phase behavior, i.e., the mixture phase separates upon cooling but reverts to a single phase upon heating. Figure 1 shows the microscopic image of a highly interconnected phase structure in epoxy/20 wt.% CTBN mixture, when it was suddenly brought from a single-phase (53 °C) to an unstable two-phase region (23 °C). These interconnected phase structure is one of the familiar characteristics of phase separation by spinodal decomposition.

Fig. 1 An optical micrograph of 20 wt.% CTBN mixture revealing interconnected domains (Lee and Kyu 1990)



Also, the phase-separation behavior of epoxy/CTBN mixture in the presence of 4,4'-diaminodiphenylmethane (DDM) curing agent was investigated (Yamanaka and Inoue 1990). Figure 2 shows optical micrographs of the mixture at various stages of cure reaction in epoxy/CTBN mixture with DDM. Above UCST (100 °C) after a certain time lag, the homogenous epoxy/CTBN system (Fig. 2a) started to phase separate, resulting in a co-continuous structure which is characteristic of spinodal decomposition (Fig. 2b). At the late stage of spinodal decomposition, the phase connectivity will be interrupted to yield a droplet structure (Fig. 2c, d). Once the epoxy network has been established in the matrix, further curing will proceed without changing the position of the droplets (Fig. 2e). Later, a similar spinodal decomposition mechanism was observed for a mixture of epoxy and amine-terminated (butadiene-co-acrylonitrile) (ATBN) rubber with triethylene tetramine (TETA) curing agent (Kim and Kim 1994).

Later, the mechanism of demixing in epoxy/hydroxyl-terminated butadiene-acrylonitrile random copolymer (HTBN) mixture cured with methyltetrahydrophthalic anhydride was studied (Zhang et al. 1999). They confirmed the phase-separation mechanism as “nucleation growth coupled with spinodal decomposition” using optical microscopy coupled with light-scattering technique. The optical microscopic pictures (Fig. 3) evident the start of phase separation at 9 min of isothermal heating at 160 °C like a co-continuous structure and then it grows into droplets in a bimodal distribution at about 11 min. From 0 to 9 min of isothermal curing at 160 °C, the epoxy/HTBN system undergoes a nucleation growth mechanism as confirmed from light-scattering measurements. During this initial stage of phase separation, the

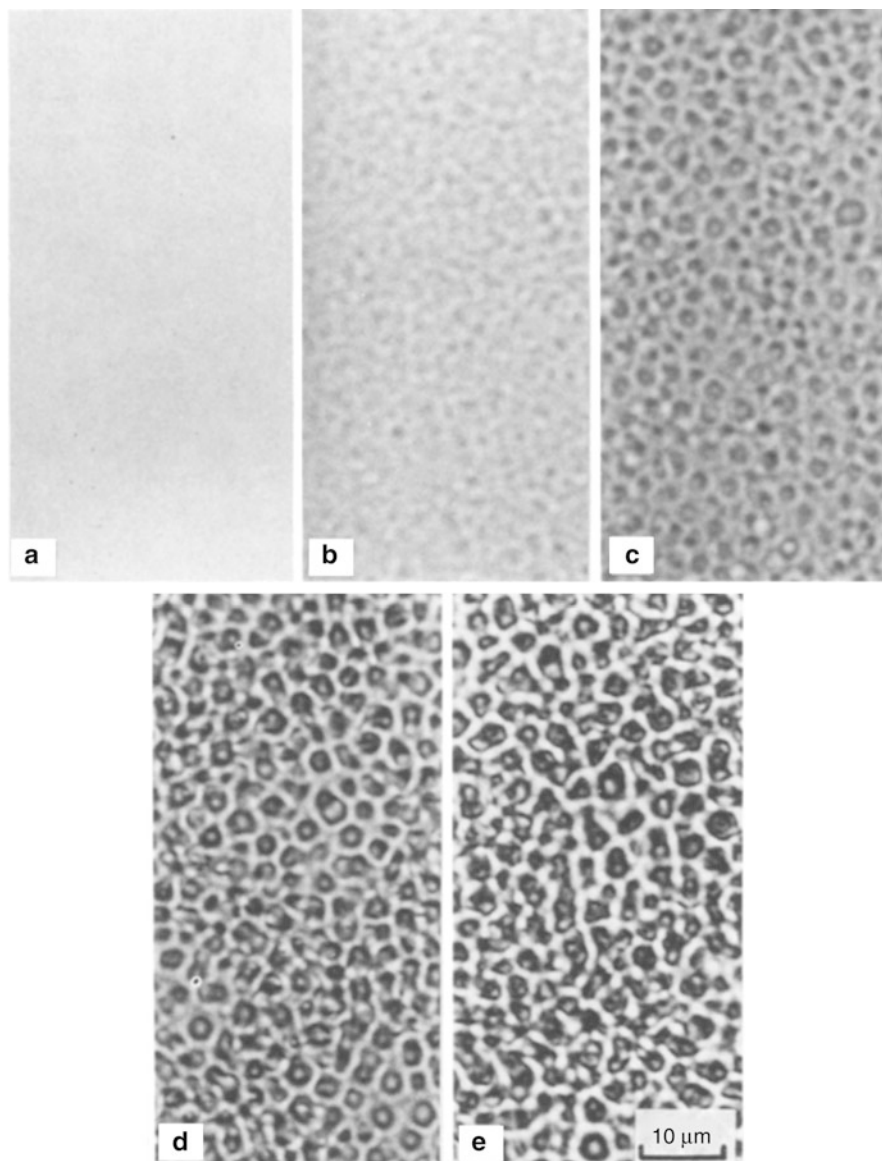


Fig. 2 Optical micrographs at various stages of curing at 100 °C for epoxy/pre-reacted CTBN/DDM = 100/20/26. (a) 1 min, (b) 8 min, (c) 17 min, (d) 32 min, (e) 360 min (Yamanaka and Inoue 1990)

size of the precipitated phase is so small that it goes beyond the visual observation range. Hence, these particles are not visible in optical microscope.

Ratna and Simon (2010) investigated the phase behavior of the epoxy/epoxy functional dendritic hyperbranched polymer (HBP) blend with tetraglycidyl diamino

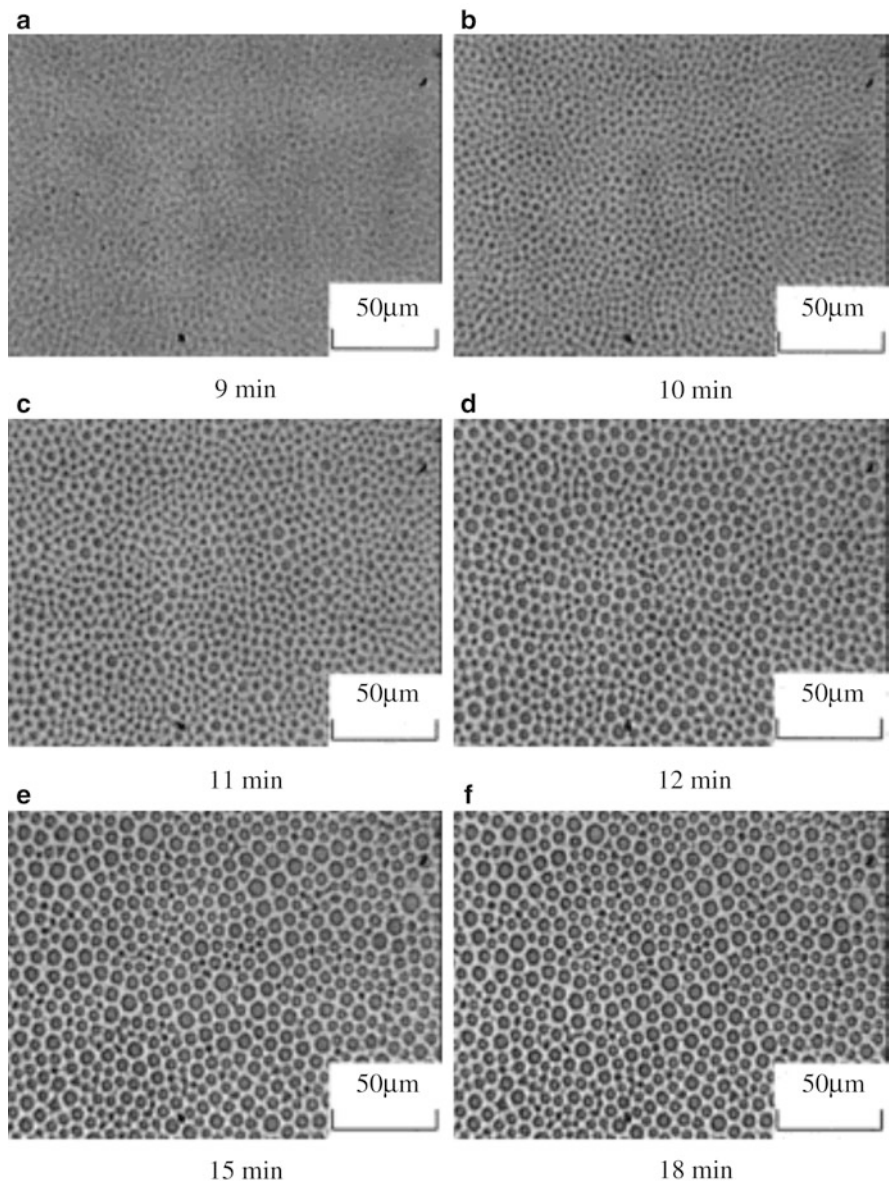


Fig. 3 Optical micrographs for the epoxy/HTBN system cured at 160 °C at different time intervals: (a) 9 min (b) 10 min (c) 11 min (d) 12 min, (e) 15 min, (f) 18 min (Zhang et al. 1999)

diphenyl methane (DETDA) as curing agent using optical microscope (Fig. 4). It was found that the HBP was not miscible with epoxy at room temperature, and as the temperature increased to 120 °C, the system became homogeneous indicating

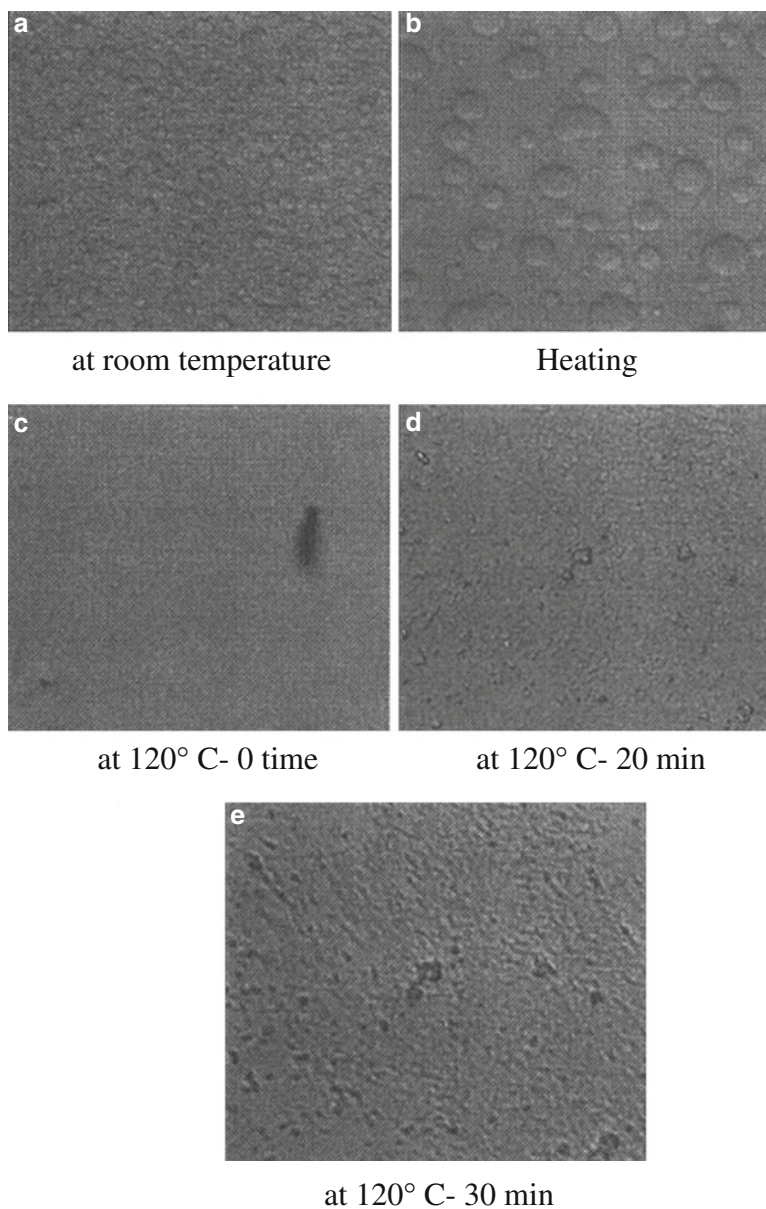


Fig. 4 Optical micrographs of epoxy/HBP/DETDA mixture (a) at room temperature (b) heating (c) at 120°C in zero time (d) at 120°C after 20 min and (e) at 120°C after 30 min (Ratna and Simon 2010)

miscibility of HBP with epoxy. However, as the blend was heated isothermally at 120°C, the epoxy resin began to cross-link, and phase separation occurred leading to the formation of a two-phase microstructure.

With the advancement of nanotechnology, it has been a practice to incorporate the nanofillers into the epoxy/rubber blends to further modify their properties. Recently, the role of nanofiller on miscibility between epoxy resin and CTBN was studied using optical microscopy (Vijayan et al. 2013). Vijayan et al. used optical microscopy to draw the phase diagram of epoxy and CTBN with and without nanoclay. They found that the presence of nanoclay reduced the miscibility between epoxy and CTBN as the UCST (upper critical solution temperature) phase diagram shifts toward a higher temperature with increase in nanoclay loading. The presence of nanofiller also altered the phase-separation kinetics in epoxy/CTBN blend (Vijayan et al. 2012). An organically modified clay facilitated a faster phase separation of CTBN from epoxy resin cured with anhydride due to the catalytic activity of the nanoclay (Fig. 5). The faster phase separation has been accompanied by smaller-sized CTBN domains in nanoclay filled epoxy/CTBN blends.

The different morphology generated in epoxy/liquid rubber blends as a function of chemical structure and functionality of epoxy resin was investigated by Naè (1986). They used diglycidyl ether of bisphenol A (DR), triglycidyl ether of tris (hydroxyphenyl) methane (TEN), and tetraglycidyl 4, 4' diamino diphenylmethane (TGDDM) as di-, tri-, and tetrafunctional epoxy, respectively. Pre-reacted CTBN (endcapped with a difunctional brominated epoxy) was used in order to limit the polymerization to epoxy/amine reactions. It was observed from the OM images that the difunctional resin showed homogeneously dispersed rubber particles in the epoxy matrix (Fig. 6a, d). At the same time, in tri- and tetrafunctional systems, the rubbery domains were in the shape of a shell and core (Fig. 6b, c, e, f). According to Naè et al., if the epoxy cross-links formed during the cure reaction are relatively close to each other, many rubbery segments were formed out of the main matrix and resulted in agglomerates. These agglomerates were in the form of “cells” which include a high concentration of rubber particles inside as seen in the trifunctional system (Fig. 6b, e). In a trifunctional system, the dimensions of the formed network cannot accommodate more than 6% rubber in it and therefore reject the rubber to form the observed cells. This agglomeration was proposed to be a reason for mechanical failure of this blend material.

Ratna and Banthia (2000) investigated the fracture surface of epoxy modified with carboxyl-terminated poly(2-ethylhexyl acrylate) (CTPEHA) liquid rubber as a function of the concentration of liquid rubber using OM. The fracture surfaces of CTPEHA-modified epoxy consisted of two distinct phases in which the globular particles are dispersed in a continuous epoxy matrix. They found that the number of phase-separated particles increased with an increase in the concentration of CTPEHA. It was found that the blend with 10 phr of CTPEHA contains rubber particles uniformly distributed throughout the matrix, and this was explained as the reason for the maximum impact and adhesion properties attained with 10 ± 5 phr CTPEHA.

Optical microscopy is also used to evaluate the fracture propagation in the damage surface, particularly for observing deformations that induce birefringence. Optically isotropic, stress-free materials appear dark when viewed between completely crossed polarizers, while deformed toughened epoxy is birefringent

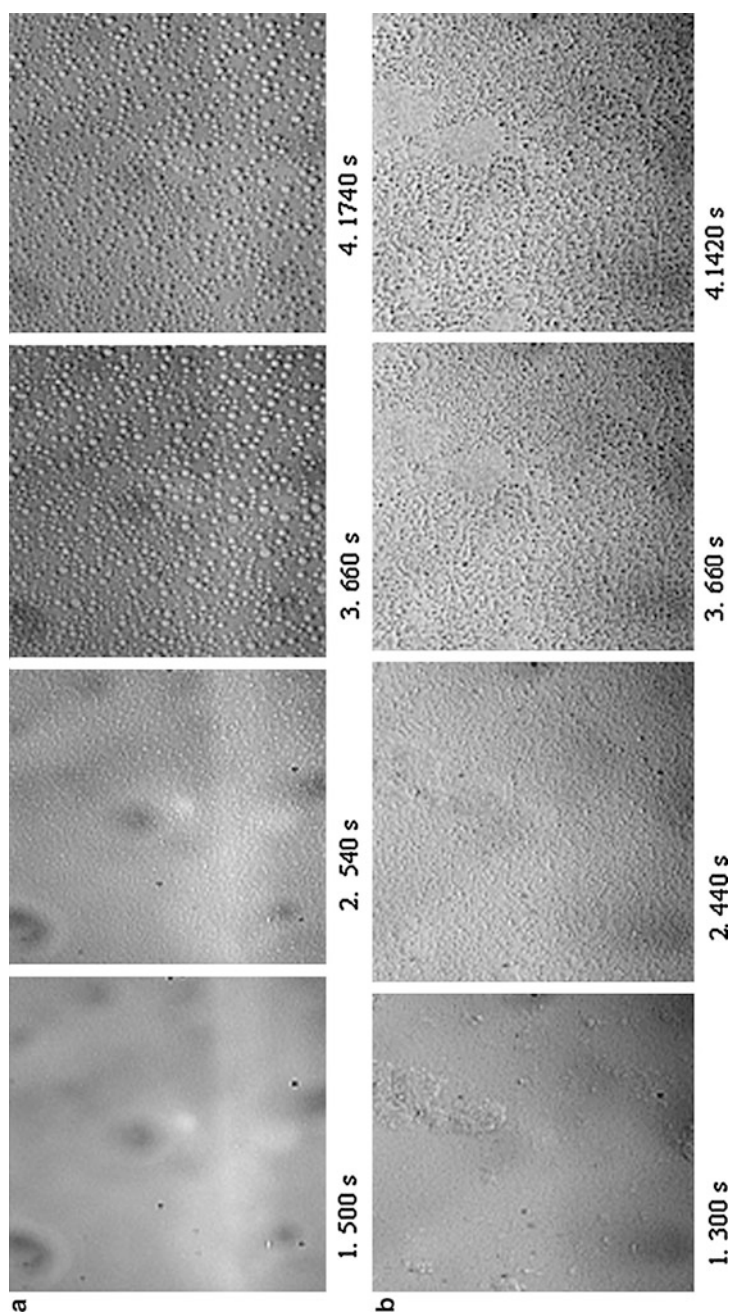


Fig. 5 Optical microscopic images of morphological evolution during cure of (a) epoxy/15 phr CTBN and (b) epoxy/3 phr nanoclay/15 phr CTBN at 130 °C ($200 \times 150 \mu\text{m}$) (Vijayan et al. 2012)

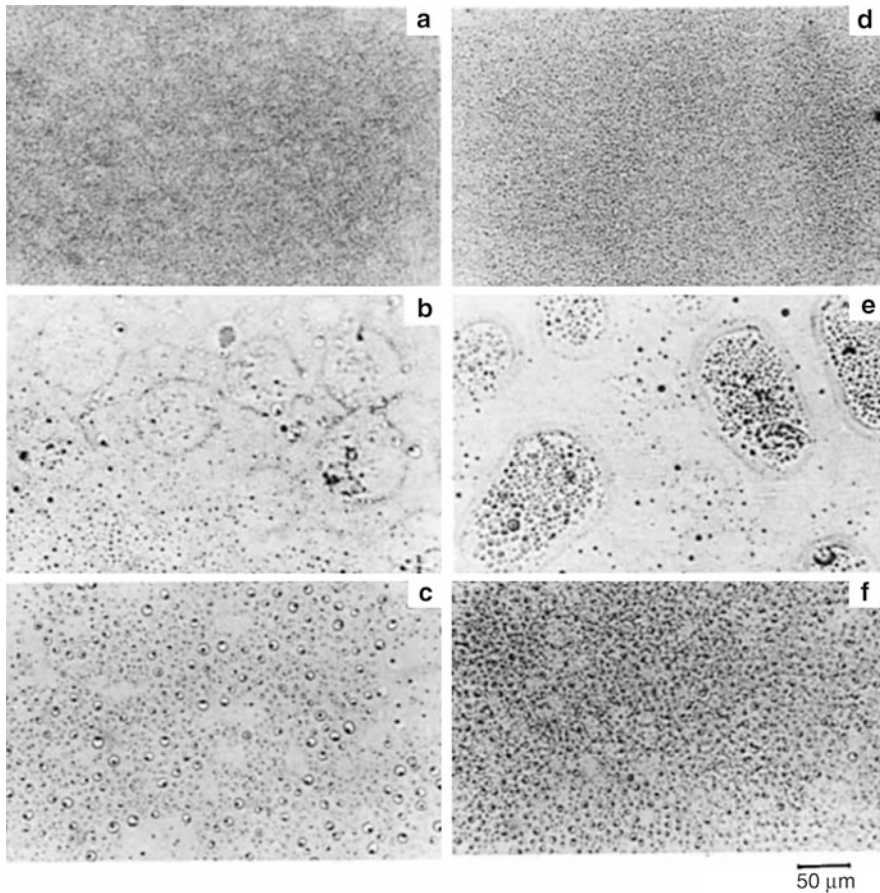
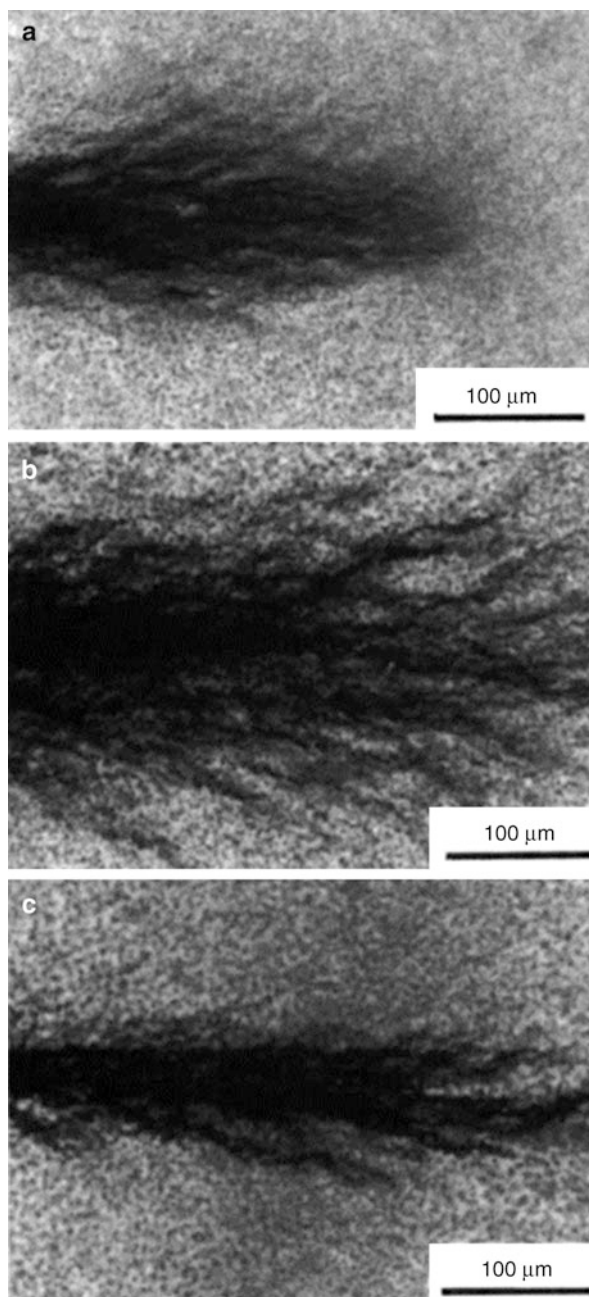


Fig. 6 Representative optical micrographs of (a) DR/4% rubber (b) TEN/4% rubber (c) TGDDM/4% rubber (d) DR/8% rubber (e) TEN/8% rubber (f) TGDDM/8% rubber (Naè 1986)

and transmits part of the light. OM of thin sections perpendicular to the fracture surface of epoxy/CTBN blend showed that the cavitated particles generate shear bands (Pearson and Yee 1986). Bagheri and Pearson (1995) investigated the shape and size of generated plastic zone during fracture of liquid rubber-modified epoxies using transmission optical microscopy (TOM). In this study, ductile and stiff interface was introduced around CTBN particles in an epoxy matrix through endcapping of the liquid rubber with flexible polypropylene glycol diepoxide (DGEP) epoxy chains and rigid diglycidyl ether of bisphenol A (DGEBA), respectively. It was observed that the nature of interface induced significant difference in size and shape of the plastic zone generated in epoxy/CTBN blends (Fig. 7). Epoxy modified with CTBN–DGEBA yielded a more feathery, less dense, and larger plastic zone size than in CTBN-modified epoxy. At the same time, in CTBN–DGEP-modified epoxy with

Fig. 7 TOM micrographs taken from the midplane of the crack tip damage zone in epoxies modified by (a) CTBN (b) CTBN–DGEBA and (c) CTBN–DGEP (Bagheri and Pearson 1995)

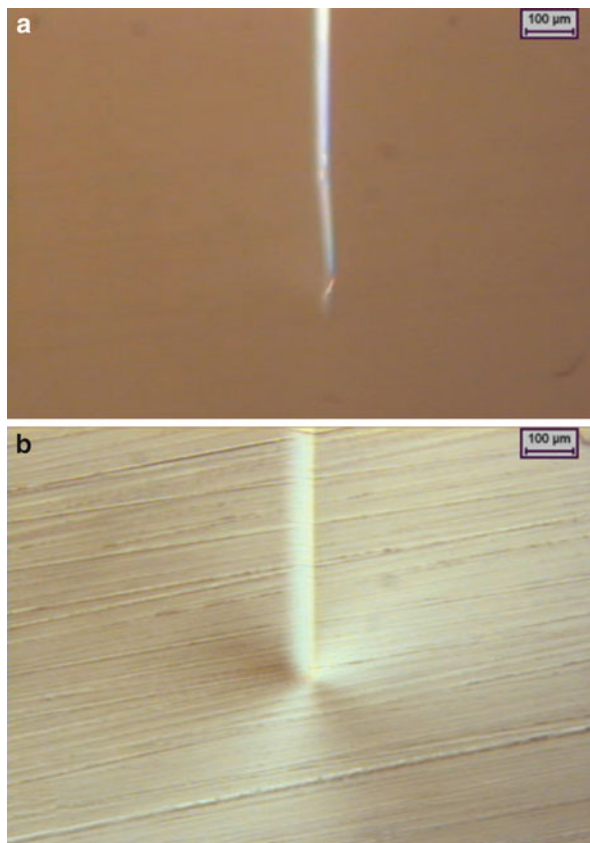


superior fracture toughness, the shape of the plastic zone was different from those of CTBN and CTBN–DGEBA-modified epoxies due to the difference in toughening mechanisms.

In another study, the subsurface fatigue damage of the epoxy/CTBN blend was examined using optical microscopy (Azimi et al. 1996). The optical micrographs confirmed the shear banding between cavitated rubber particles and the presence of a birefringent zone indicating the matrix yielding. The micrographs also showed lenticular features between rubber particles near the elastic/plastic interface which were reminiscent of crazes.

Ma et al. (2008) investigated the optical micrograph of the thin section taken in the midplane and near the crack tip of compact tension (CT) specimen of neat epoxy and epoxy blended with 15 wt.% rubber nanoparticle in situ formed in epoxy by the reaction of an oligomer diamine (piperidine) with epoxy (Fig. 8a, b). As shown in the figure, there was no evidence of any birefringent characteristics in the case of neat epoxy, implying no plastic deformation in the vicinity of the crack tip (Fig. 8a). At the same time in the case of epoxy/15 wt.% in situ-formed rubber nanoparticle blend, there was an obvious birefringent zone at the crack tip indicating plastic deformation in the vicinity of the crack tip. The difference in the fracture behavior was correspondent with the 500% enhanced energy release rate in rubber nanoparticle-modified epoxy when compared with neat epoxy.

Fig. 8 Optical micrograph of a thin section taken midplane and near the arrested crack tip of (a) the neat epoxy CT and (b) the CT sample containing 15 wt.% rubber nanoparticles under crossed polars (Ma et al. 2008)



Similarly, subcritical crack tip of epoxy toughened with both large CSR particles (acrylic rubber core surrounded by poly methyl methacrylate (PMMA) shell) and small CSR particles (butadiene–acrylic copolymer) were observed using TOM (Quan and Ivankovic 2015). The absence of plastic zone at the crack tip of neat epoxy is evident in the TOM images (Fig. 9a). As large CSR content was increased above 16 vol.%, the damage zone was found to be comprised of two zones, an outer larger gray zone surrounding an inner smaller dark zone closer to the crack tip with pronounced featherlike features. The dark zone was explained to consist of shear bands and voids, while the outer gray zone consists of only voids due to particles debonding. The TOM (Fig. 9) was used to measure the depth of fracture damage zone (FDZ), and it was found that the size of FDZ increased as the content of CSR increased up to 30 vol.% and then decreased for volume fraction greater than 30 vol.%. The sizes of damage zone were proportional to the values of fracture energy as seen in Fig. 10.

Scanning Electron Microscopy (SEM)

The two-phase morphology of epoxy/rubber blends, consisting of rubbery particles embedded in an epoxy matrix, was mostly studied using SEM analysis. Moreover, the mechanical properties of the epoxy/rubber blends were correlated with microstructure through SEM. The role of various factors like the nature of the rubber, rubber content, cure temperature, cure time, etc. on the morphology of epoxy/rubber blends was studied with the help of SEM. Some of the most important results among these studies are described below.

The compatibility of the rubber and epoxy can be controlled by the acrylonitrile content in the copolymers of butadiene- and acrylonitrile-based liquid rubber as well as the cure conditions. Manzione et al. (1981a) studied the effect of acrylonitrile content of CTBN on the morphology using SEM. Epoxy modified with carboxyl-terminated poly(butadiene-co-acrylonitrile) (CTBN(X8)) having acrylonitrile content of 17 wt.% showed a maximum in the average domain size at the intermediate cure temperature (120 °C) and a slight maximum in volume fraction of phase-separated rubber at the lowest cure temperature (90 °C) (Fig. 11a–c). At the same time, cured resin with CTBN(X15) having acrylonitrile content of 10 wt.%, i.e., less compatible with epoxy when compared to CTBN(X8), showed maxima in both domain size and volume fraction at the intermediate cure temperature (120 °C) (Fig. 11d–f). They proposed a generalized representation of morphology as a function of cure temperature and is presented in Fig. 11g. According to them, the volume fraction of phase-separated rubber is maximum at intermediate temperatures. Gelation halts phase separation and seals the morphology, and hence the temperature of gelation determines the morphology.

Later a similar study was carried out by Russell and Chartoff (2005) using SEM images of epoxy resin modified with CTBN having different acrylonitrile content. The relationship between the acrylonitrile content and the morphology is shown in Fig. 12. CTBN rubber having a low acrylonitrile content (10%) showed much larger

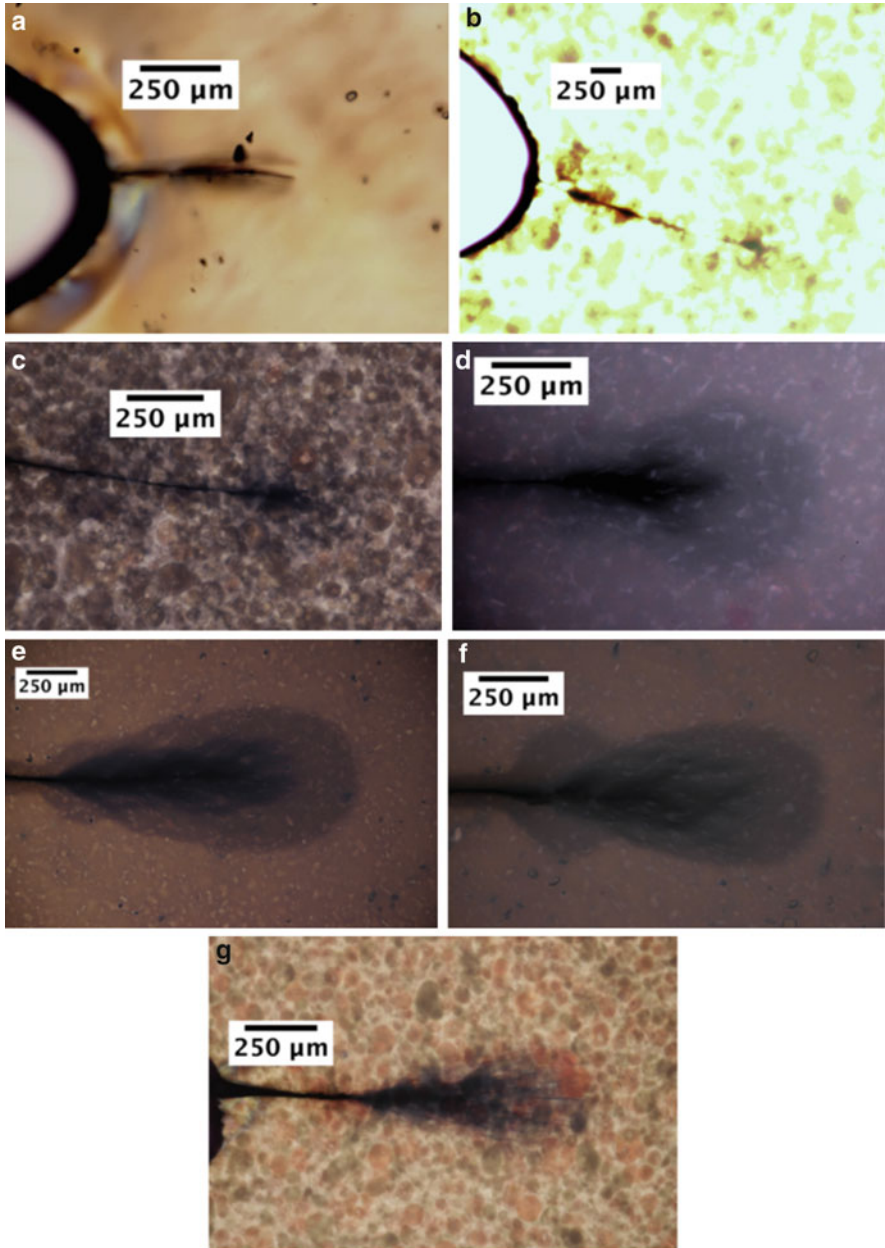


Fig. 9 TOM images of the subcritical crack tip of double-notched four-point bending (DN-4PB) samples of (a) epoxy (b) epoxy-8 vol.% large CSR particle, (c) epoxy-16 vol.% large CSR particle, (d) epoxy-22 vol.% large CSR particle, (e) epoxy-30 vol.% large CSR particle, (f) epoxy-38 vol.% large CSR particle, (g) epoxy-22 vol.% large CSR particle-16 vol.% small CSR particle (Quan and Ivankovic 2015)

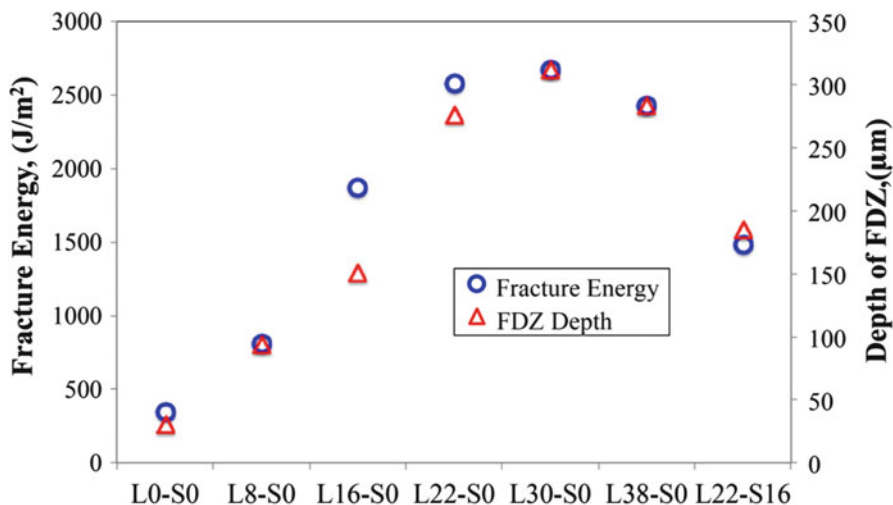


Fig. 10 Comparison of fracture energy and size of FDZ for epoxy (L0-S0), epoxy-8 vol.% large CSR particle (L8-S0), epoxy-16 vol.% large CSR particle (L16-S0), epoxy-22 vol.% large CSR particle (L22-S0), epoxy-30 vol.% large CSR particle (L30-S0), epoxy-38 vol.% large CSR particle (L38-S0), and epoxy-22 vol.% large CSR particle-16 vol.% small CSR particle (L22-S16) (Quan and Ivankovic 2015)

rubber particles and a broader particle size distribution than epoxy samples modified with CTBN rubber that has a higher acrylonitrile content (18%). The presence of higher level of the polar acrylonitrile units in CTBN required a higher degree of cure before phase precipitation of a CTBN phase (Wise et al. 2000). This might result in a smaller particle size because at higher degrees of cure the viscosity of the epoxy phase is higher, which would reduce the ease of CTBN diffusion and of particle agglomeration. Beyond the optimum acrylonitrile content (dependent on chemistry of the rubber), the solubility parameter of the rubber became so close to that of the epoxy that it could not phase separate from the matrix (Ratna and Banthia 2007). Hence it resulted in a reduction of the impact performance of the blend as phase separation is the necessary condition for toughening.

Verchere et al. (1991b) studied the morphological features in epoxy/epoxy-terminated butadiene-acrylonitrile random copolymer (ETBN) blend as a function of the cure schedule. It was observed that the concentration of dispersed rubber particles decreased with increase in the cure temperature.

The reactive end groups in the rubber were found to affect the dynamics of the reaction-induced phase separation and the final morphology of the blend. Researchers studied the role of the end group of the liquid rubber on morphology of the blend using SEM. While amine-terminated butadiene-acrylonitrile random copolymers (ATBN)-modified epoxies showed a diffuse-appearing interface between the dispersed rubber phase and the epoxy matrix, sharp interface boundaries was shown by CTBN-modified epoxies (Kunz et al. 1982). The visually diffuse interface in ATBN-modified epoxy was explained due to the segmental mixing of

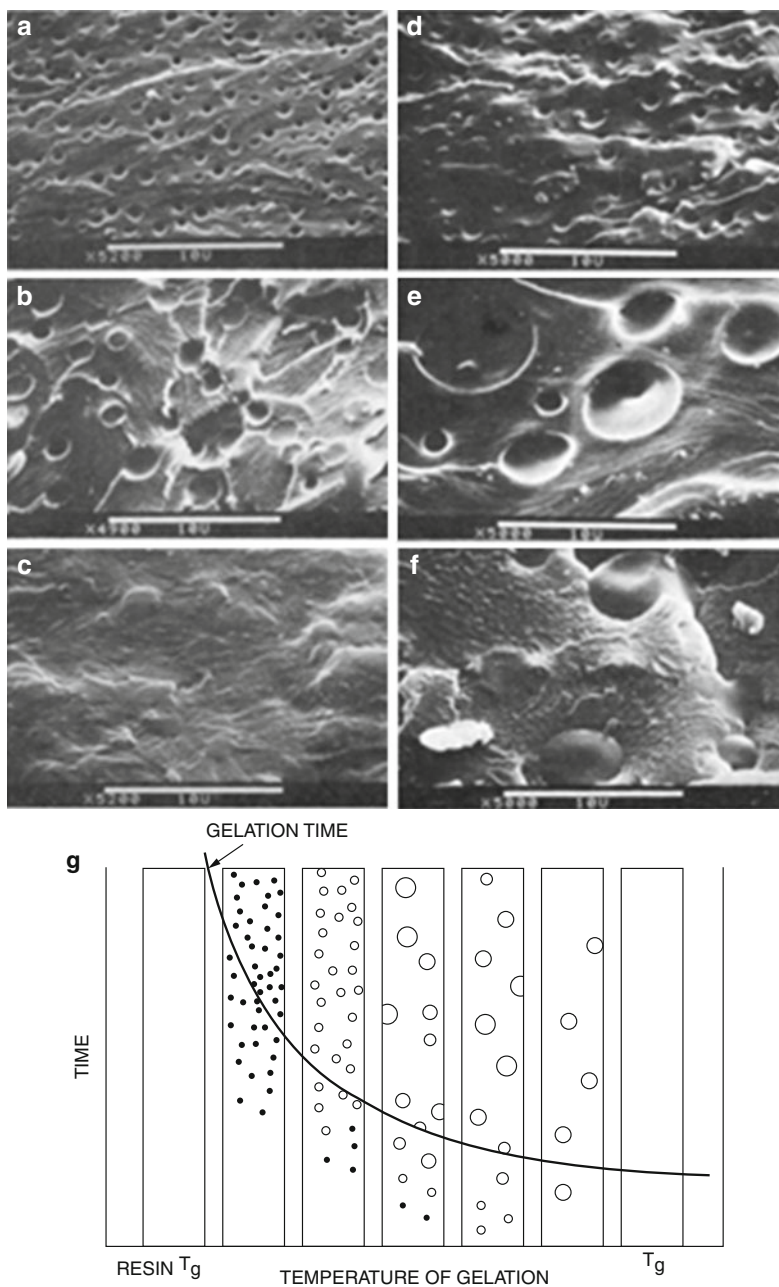


Fig. 11 SEM micrographs of rubber-modified epoxy cured at (a) 90, (b) 120, and (c) 150 using CTBN with acrylonitrile content of 17 wt.%; CTBN with acrylonitrile content of 10 wt.% cured at (d) 90, (e) 120, and (f) 150, (g) a proposed generalized schematic representation of morphology as a function of cure temperature (Manziona et al. 1981a)

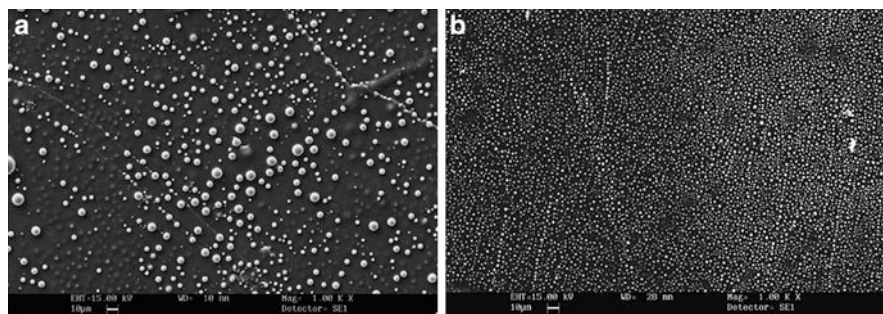


Fig. 12 SEM images of epoxy toughened with CTBN having acrylonitrile content of (a) 10% and (b) 18% (cured at 120 °C) (Russell and Chartoff 2005)

rubber and epoxy between the two phases which would provide an interphase region with a continuously varying relaxation spectrum. In another study, liquid rubbers with different end groups but the same main chain (carboxyl-, epoxy-, amine-terminated and nonfunctional butadiene–acrylonitrile random copolymers) were employed in the same epoxy system (Chen et al. 1994). The mean particle diameter calculated from SEM images was found to decrease in the order NFBN > ETBN > CTBN > ATBN. The reactive groups of the rubber were found to have a major role on the structure inside the particles, since most additive molecules are involved in the particles and most rubber-reactive end groups react inside the particle. In backscattered electron images (BSEI) obtained from osmium tetroxide-stained polished surfaces in the scanning electron microscope, epoxy amine copolymer island in each rubber particle was detected for NFBN-based system (Fig. 13).

The initial rubber composition was also found to affect the size of the phase-separated rubber particles (Thomas et al. 2004; Tripathi and Srivastava 2007). Thomas et al. (2004) carried out a detailed analysis on the variations of particle size and related parameters based on the rubber content on anhydride-cured epoxy/CTBN blends using SEM. The size of the phase-separated rubber was found to increase with increasing CTBN content from 5 wt.% to 20 wt.% (Fig. 14). This increase in size of the dispersed CTBN particle was due to the coalescence of the dispersed rubber particles, and this effect was more prominent at higher concentration of the CTBN. They calculated the interfacial area of the dispersed CTBN phase by using the formula $\frac{3\Phi}{r}$, where Φ is the volume fraction of dispersed phase and r is the domain radius. The variation of interfacial area per unit volume as a function of CTBN concentration is plotted in Fig. 15a. The interfacial area was found to increase first and then decreased above 15 wt.%. The percentage distribution versus particle size for 15 and 20 wt.% CTBN is shown in Fig. 15b. The size of the domain was observed to range mostly from 0.5 to 1 μm in diameter with slight bimodal distribution.

The relationships between microstructure and fracture behavior of toughened thermoset were widely studied. SEM is a widely accepted technique to investigate the nature of the fracture surface of epoxy/rubber blend to elucidate the fracture

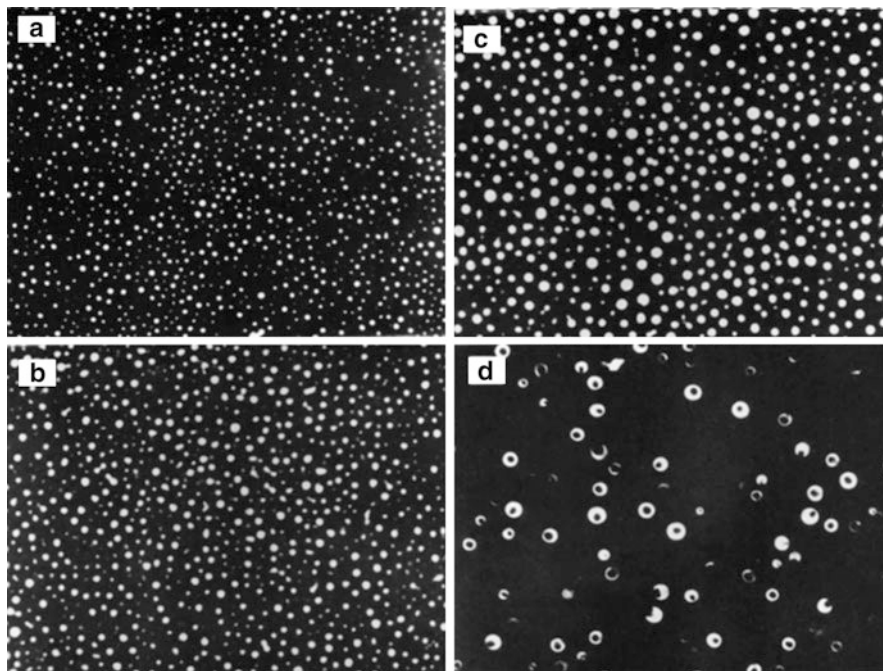


Fig. 13 Backscattered electron images (*BSEI*) of (a) epoxy/ATBN, (b) epoxy/CTBN, (c) epoxy/ETBN, and (d) epoxy/NFBN blends. The stained white part is rich in rubber (Chen et al. 1994)

mechanisms operate in the system (Bascom et al. 1975, 1981; Wise et al. 2000; Kinloch et al. 1983a, b). A detailed fractography analysis of epoxy/CTBN blend was done by Kinloch et al. (1983a) as a function of temperature and test rate. Three main types of crack growth have been identified based on the SEM analysis of fracture surface of epoxy/CTBN blend, and they are brittle stable (type C, at low temperature), brittle unstable (type B, at intermediate test temperatures), and ductile stable (type A, at relatively high temperatures/low rates). Figure 16 shows the SEM images of type C and type A of crack growth in modified and unmodified epoxy. As the test temperature was increased, the type of crack growth changed progressively from type C to type A in both unmodified and CTBN-modified epoxy. However, the fracture toughness for the modified epoxy was always significantly greater than that of the unmodified epoxy.

Various toughening mechanisms that operate in epoxy/rubber blends were discussed by various researchers, and well accepted among them are localized shear yielding (Kinloch et al. 1983b; Pearson and Yee 1986a) and plastic void growth in the epoxy matrix, initiated by cavitation or debonding of the rubber particles (Huang and Kinloch 1992; Yee et al. 1993). Localized shear yielding implies the shear banding within the epoxy matrix that is evident between the rubber particles, then the epoxy matrix is ductile enough to support plastic deformation. Matrix void growth occurs when the rubber particles either cavitate or debond from

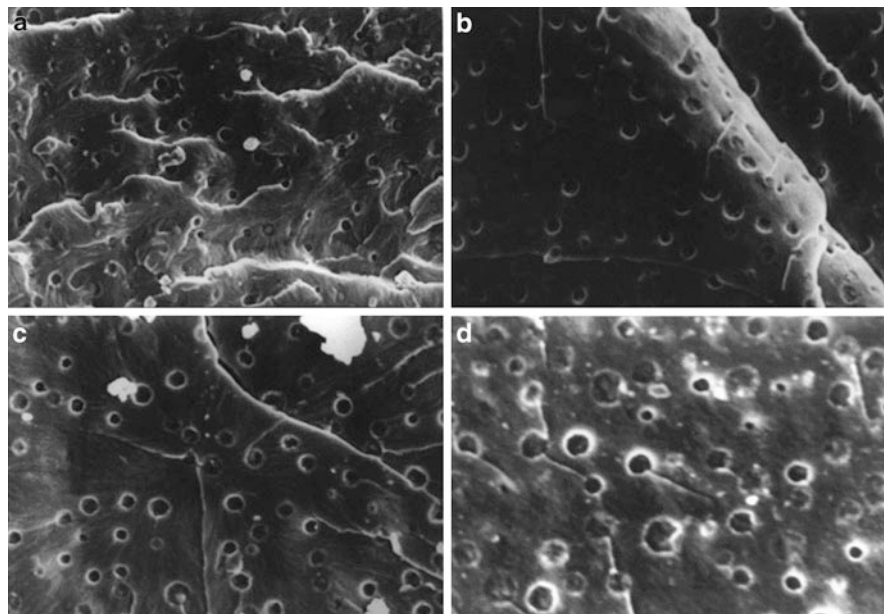


Fig. 14 SEM images of epoxy containing (a) 5 wt.% CTBN (magnification $\times 1,650$), (b) 10 wt.% CTBN (magnification $\times 1,925$), (c) 15 wt.% CTBN (magnification $\times 2,200$), and (d) 20 wt.% CTBN (magnification $\times 2,750$) (Thomas et al. 2004)

the matrix, before the onset of strain hardening of the matrix. The SEM images showing cavitation is given in Fig. 17. The rubber cavitation causes local constraint relief in the blend. This constraint relief delayed the crack initiation process in the matrix, and the surrounding epoxy matrix can undergo more plastic deformation and absorb more plastic energy.

The rubber particle size and distribution, the interparticle distance, the matrix cross-link density, etc. were found to influence the fracture mechanism and toughness (Bagheri et al. 2009). Pearson et al. (Pearson and Yee 1986) reported the SEM micrographs of the stress-whitened regions on the fracture surfaces of CTBN-modified epoxy as a function of rubber content (Fig. 18). They observed that as the rubber content increased, the voids became larger and more uniform in size. The matrix surrounding the voids exhibited notable plastic deformation and became larger as the particle–particle distance decreased.

Similarly, in epoxy/epoxidized natural rubber (ENR) blend, the observed trend in fracture toughness with rubber content was explained on the basis of fracture surface analysis using SEM (Mathew et al. 2014). The domain size of spherical ENR particles increased with increasing ENR content (Fig. 19), and the smaller rubber particles that were difficult to cavitate or debond from the epoxy matrix resulted in maximum fracture toughness for 10 wt.% ENR-modified blends.

Since the toughening mechanism is rubber particle size dependent, the mechanisms operated in nanosized rubber particle-toughened epoxy blend differ from that

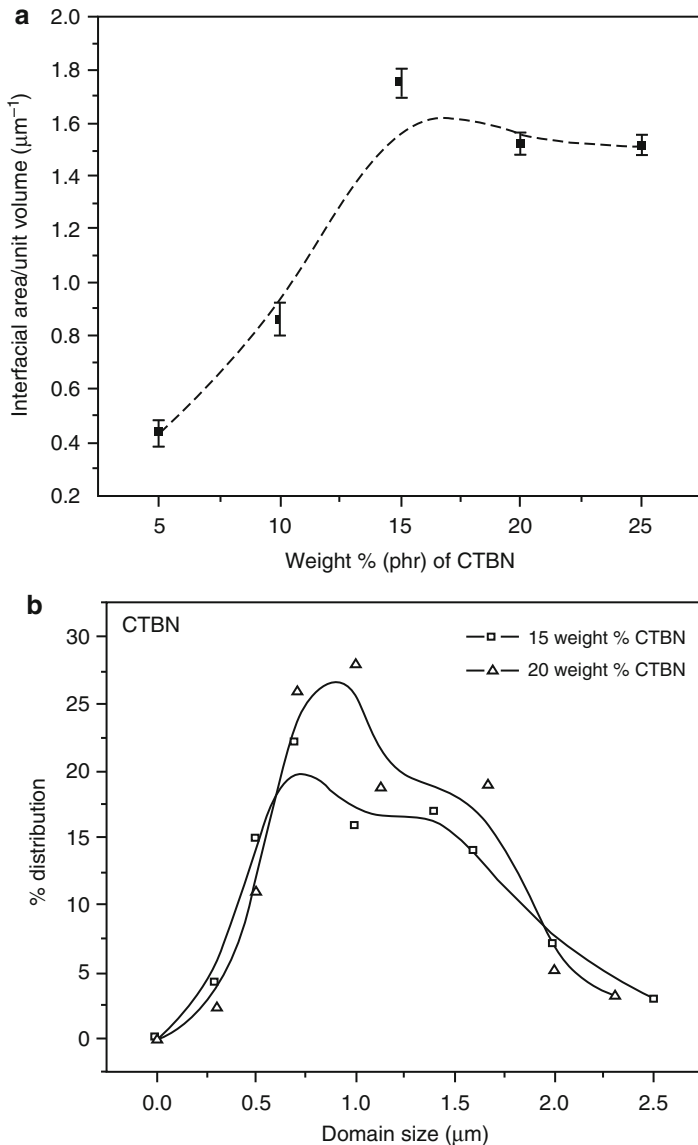


Fig. 15 (a) Interfacial area per unit volume as a function of wt.% of CTBN, (b) Percentage distribution of particles versus particle size for epoxy/CTBN blend with 15 and 20 wt.% CTBN (Thomas et al. 2004)

in micro-sized rubber particle-toughened epoxy. Both cryogenic (77 K)- and room temperature (RT)-toughening effect of carboxylic nitrile-butadiene nano-rubber (NR) particles on epoxy matrix was well understood from the SEM images (Fig. 20a, b) of the fracture surfaces (Zhao et al. 2013). The shear-yielded

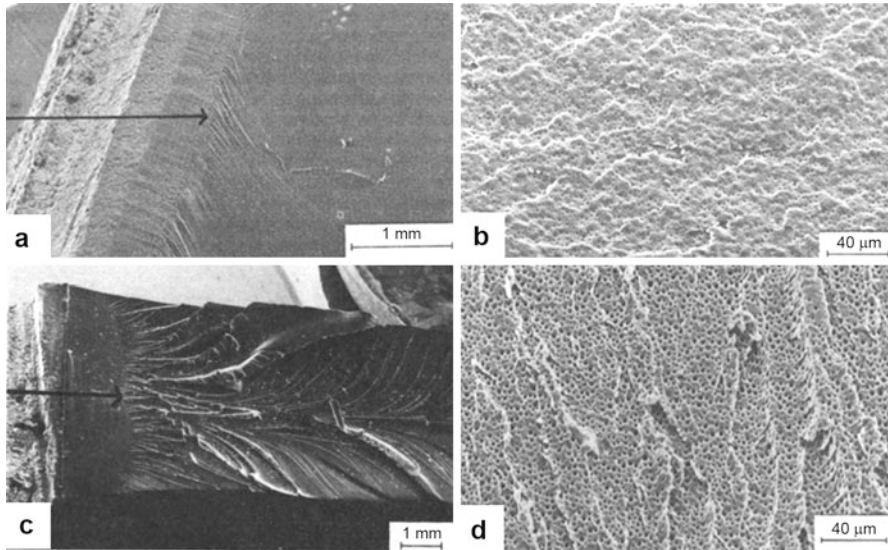
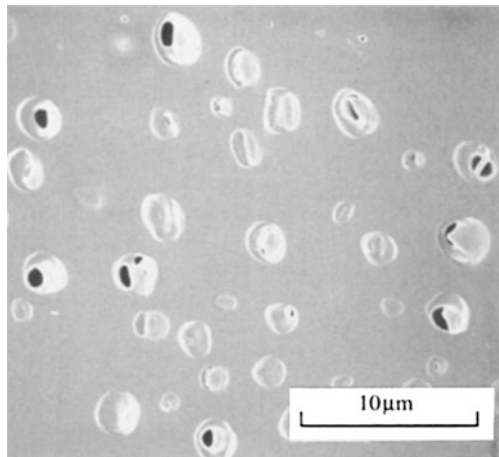


Fig. 16 Scanning electron micrograph of (a) brittle stable (type C) crack growth in unmodified epoxy, (b) brittle stable (type C) crack growth in rubber-modified epoxy of (c) ductile stable (type A) crack growth in unmodified epoxy and (d) ductile stable (type A) crack growth in rubber-modified epoxy (Kinloch et al. 1983a)

Fig. 17 Cavitation in the plastic zone as revealed in a scanning electron micrograph of a microtomed surface of epoxy/CTBN blend (Yee et al. 1993)



deformation was observed as the major toughening mechanism, and it produced blunting of the crack tip as seen in Fig. 20, bringing about the reduction of stress concentration near the crack tip which consequently improved the fracture toughness of nanosized rubber particle-toughened epoxy.

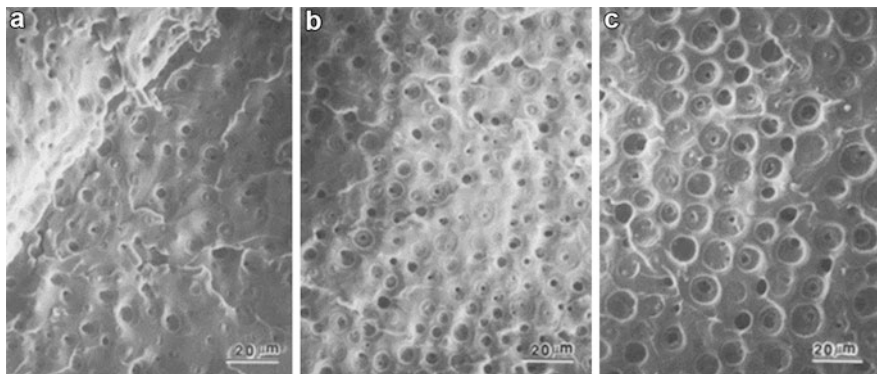


Fig. 18 SEM from the stress-whitened area of fractured specimen of (a) epoxy/10 phr CTBN (b) epoxy/20 phr CTBN and (c) epoxy/30 phr CTBN. The *white lines* are due to tearing of the material between two crack planes, causing a surface step (Pearson and Yee 1986)

Recently, Guan et al. (2014) reported a comparative study on the fracture behaviors of epoxy filled with submicron liquid rubber (LR) and preformed nanoscale-powered rubber (PR) using SEM images of their tensile fracture surfaces. The study showed that the enhanced fracture toughness of the epoxy/rubber blend was due to the local plastic deformations of matrix induced by debonding/cavitation of rubber particles regardless of the rubber type. Furthermore, the SEM fracture surfaces gave indication on the less plastic deformation of matrix induced by the PR nanoparticles to consume fracture energy than the corresponding LR particles due to the presence of agglomerates of PR nanoparticles in the matrix. The fracture morphology of epoxy simultaneously modified with multi-scale rubber particles – LR and PR – were also evaluated using SEM (Tang et al. 2013). SEM analysis gave evidence that both LR and PR together could help in intensifying the hydrodynamic forces around crack tip region, facilitating intensive cavitation/debonding of rubber, and thus yielding massive matrix plastic deformation including matrix void growth and shear banding. Relatively large stress-white zone and scalelike rough fracture surface, which are identified in SEM images (Fig. 21), also contribute more to the enhanced toughness in hybrid systems.

The crack growth behavior in CSR-modified epoxy was found to be dependent on crosshead rates and CSR content (Xiao and Ye 2000). Figure 22 shows the fracture surfaces of 15% CSR-modified epoxy at different crosshead rates. Two distinct regions with characteristics of stress-whitening and smooth surfaces can be clearly observed in Fig. 22. They estimated the length of this stress-whitened zone from the SEM images, and it was found to be decreased at a high crosshead rate or for a low rubber content (Table 1). They plotted lengths of averaged stress-whitened zone against fracture toughness (Fig. 23). The variation of stress-whitened zone length with the crosshead rate or rubber content is very well correlated with that of fracture toughness values (expressed in stress intensity factor, K_{IC}). Similar to liquid rubber-toughened epoxy, the major toughening mechanisms identified in CSR-modified epoxy system were rubber particle cavitation and its locally induced plastic deformation.

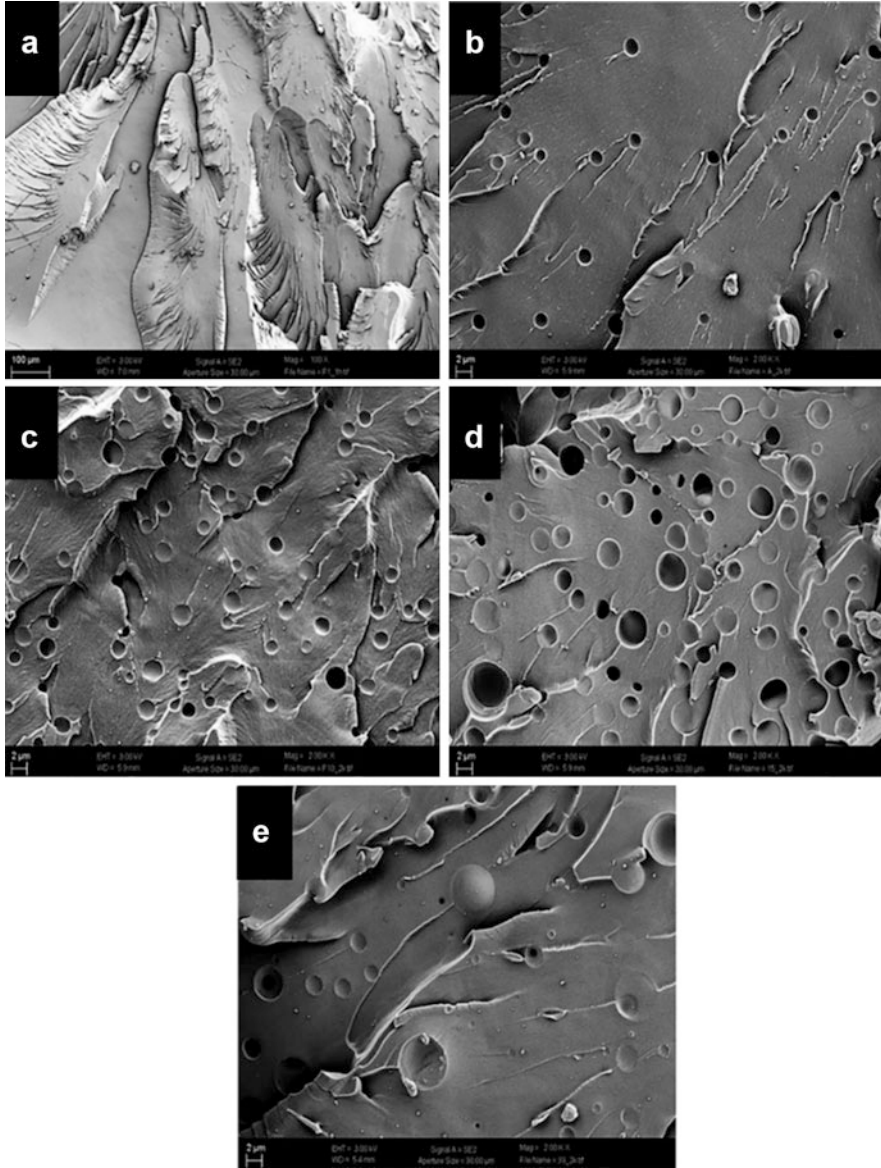


Fig. 19 Scanning electron micrographs of the (a) neat epoxy and (b) 5, (c) 10, (d) 15, and (e) 20 wt.% ENR/epoxy blend surfaces after fracture measurements (Mathew et al. 2014)

A detailed fracture surface analysis of preformed polysiloxane core-shell rubber (S-CSR) particle-modified epoxy was done by Chen et al. (2013) using field emission gun scanning electron microscopy (FEG-SEM). The toughening mechanisms induced by the S-CSR particles were identified as localized plastic shear band

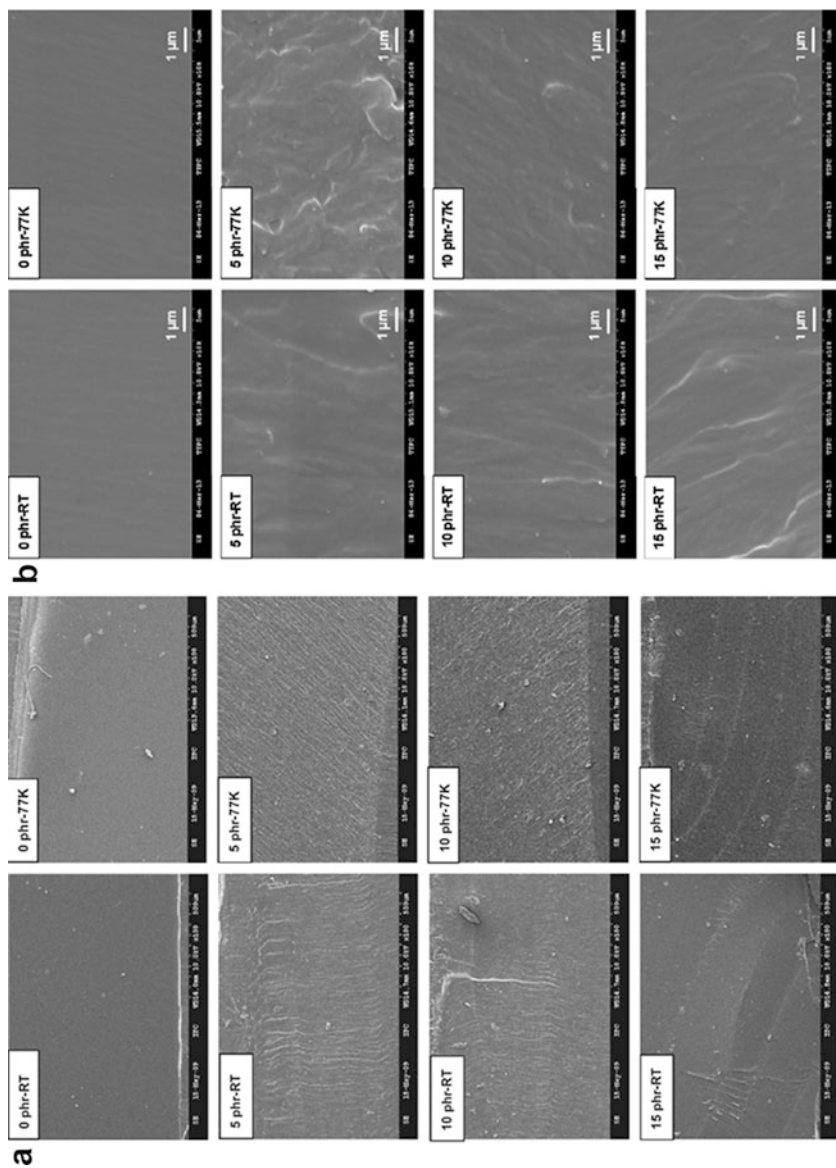


Fig. 20 (a) SEM images of the fracture surfaces of the NR-epoxy blends at RT and 77 K and (b) enlarged SEM images (Zhao et al. 2013)

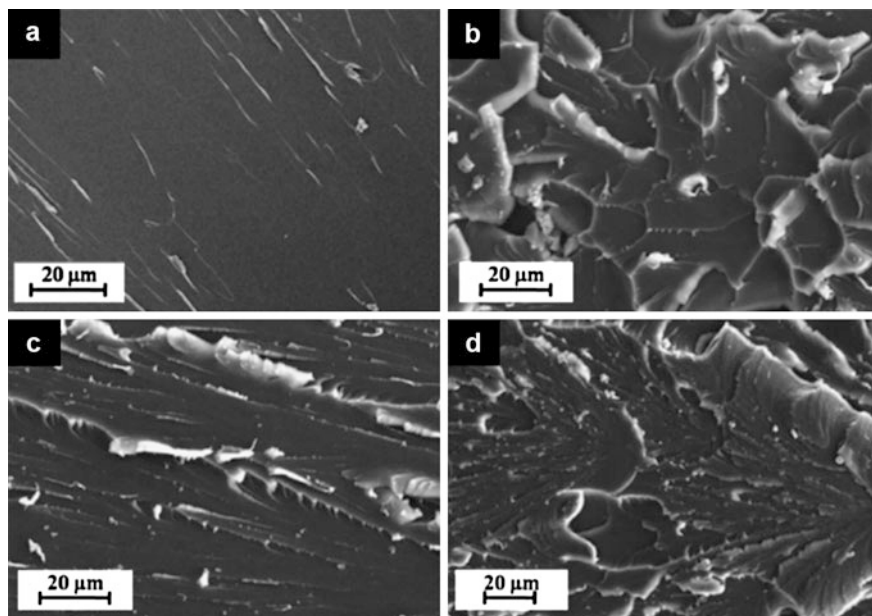


Fig. 21 Higher-magnified SEM graphs of fracture surfaces taken from the “hackle” zone: (a) neat epoxy, epoxy with (b) PR (9.2 wt.%), (c) LR (9.2 wt.%), and (d) PR (9.2 wt.%) LR (9.2 wt.%) (Tang et al. 2013)

yielding around the particles and cavitation of the particles followed by plastic void growth of the epoxy matrix (Fig. 24). Cavitation, as opposed to particle debonding, revealed the strong bonding between the S-CSR rubber particle and the surrounding matrix. The core-to-shell adhesion must also be relatively high for the S-CSR particles, as no debonding was observed. The fracture surfaces of the S-CSR particle-modified epoxy tested at low temperature were similar to the samples tested at room temperature. It was observed that all of the S-CSR particles are cavitated, even at $-109\text{ }^{\circ}\text{C}$, although the size of the cavities was reduced at low temperatures due to a lesser extent of plastic void growth in the epoxy polymer.

Recently, the fracture surface of CSR nanoparticle-modified epoxy system was studied using SEM (Quan and Ivankovic 2015). Two CSR particles of different sizes were used (large CSR, 300 nm and small CSR, 50 nm). The fracture surfaces of CSR particle-modified epoxy were covered with sea of voids, which were identified as circular features (Fig. 25). It was observed that the initiation of voids could result from three mechanisms: CSR shell debonding from matrix, CSR rubbery core cavitation, and CSR core debonding from CSR shell.

SEM was also used to prove the synergistic effect of multiphase particles in fracture toughness reported in nanofiller-modified epoxy/rubber blends. Liu et al. (2004) investigated the fracture surface of nanoclay-modified epoxy/CTBN blend. While in epoxy/CTBN blend, yielding and plastic deformation along with cavitation were evident (Fig. 26a); crack bifurcation was observed as the dominant

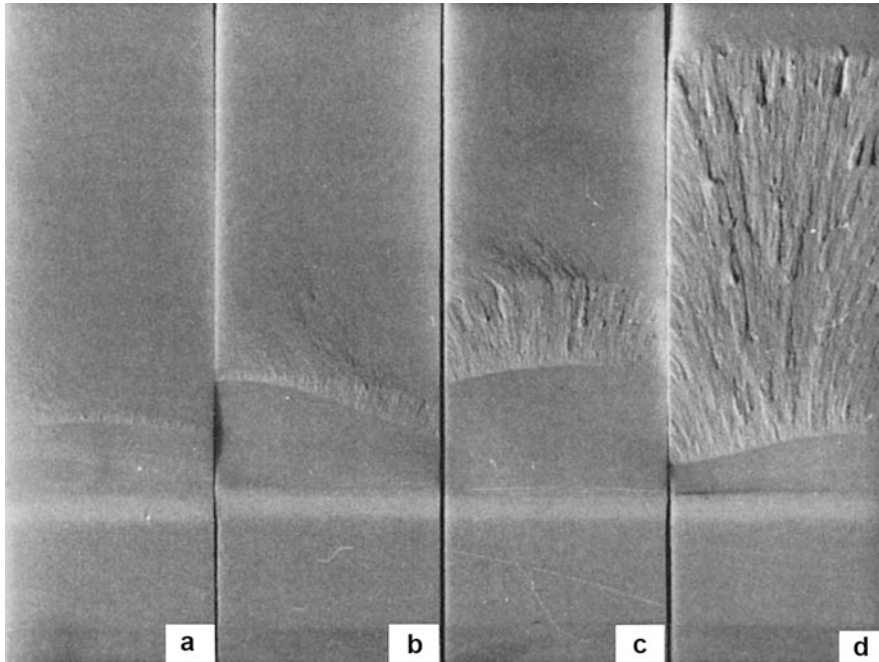


Fig. 22 Fracture surfaces of 15% CSR-modified epoxy specimens at different crosshead rates: (a) 500 mm/min, (b) 50 mm/min, (c) 5 mm/min, and (d) 0.5 mm/min (Xiao and Ye 2000)

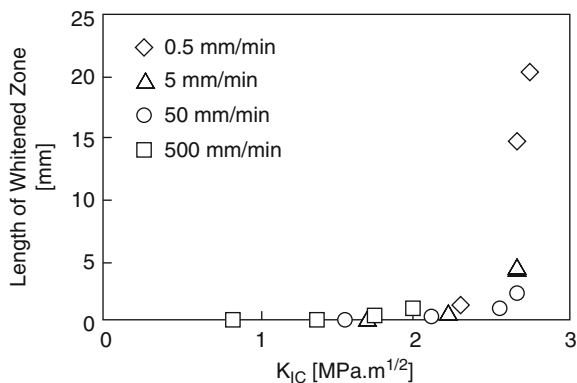
Table 1 The average length of stress-whitened zone as a function of CSR content and crosshead rate (Xiao and Ye 2000)

Crosshead rate [mm/min]	Length of stress-whitened zone [mm]			
	5%	10%	15%	20%
0.5	0.2	1.1	20.3	14.6
5	0.14	0.7	4.0	4.2
50	0.1	0.4	1.0	2.2
500	0.0	0.1	0.4	0.9

toughening mechanism in epoxy/clay nanocomposite (Fig. 26b). Fracture surfaces of nanoclay-modified epoxy/CTBN blend (Fig. 26c) showed both features of fracture surface of epoxy/CTBN blend and epoxy/clay nanocomposite.

At the same time, in nanosilica-modified epoxy/rubber blend, the nanosilica was found to enhance the plastic deformation in the process zone that enlarges the zone size in front of the crack tip (Fig. 27) (Liang and Pearson 2010). This enhancement involved an increase in shear band density between rubber particles in the plastic zone. The expanded plastic zone further shielded the crack tip and therefore improved the fracture toughness.

Fig. 23 Correlation between length of stress-whitened zone and fracture toughness for CSR-modified epoxy (Xiao and Ye 2000)



The fracture surface of glycidyl polyhedral oligomeric silsesquioxane (POSS)-modified epoxy/CTBN blend was analyzed using SEM (Konnola et al. 2015). The micrographs (Fig. 28) revealed that the rubber particles in hybrid were different from the usually observed smooth quasisphere in the epoxy/rubber blend due to the high cross-link density created by octafunctional POSS particles near rubber particles. Also the rubber particle size in the hybrid was found to be smaller than that in epoxy/CTBN blend due to the fact that the POSS particles prevent the coalescence of the CTBN phase.

Atomic Force Microscopy (AFM)

AFM is a surface analysis technique used to get additional and supporting details to SEM findings on phase morphology and failure mechanism in epoxy/rubber blends (Nigam et al. 2003). Using AFM technique, only those rubber particles that transfix the sample surface can be imaged. Since it is unlikely that an entire imaged rubber particle is on the sample surface, rubber particle size determined using AFM may sometimes lead to misleading conclusions. However, AFM can be effectively used in providing valuable information about the presence of nano-phase dispersed rubber particles, which are difficult to trace out in SEM images. AFM with the proper scanning conditions is capable of studying the nano-dispersed rubber phase in detail. Russell and Chartoff (2005) used AFM technique to find out the presence of rubber particles below 40 nm in size in epoxy/CTBN blends for the first time (Fig. 29). According to them, the portion of the rubber represented by these nanoscale particles has been assumed by previous researchers to be the dissolved portion in the epoxy phase rather than phase separated.

The rubber domains in isocyanate-functionalized polybutadiene (NCOTBP)-modified epoxy in nanoscale dimension were better detected by AFM technique (Fig. 30) (Soares et al. 2004). In the phase contrast AFM image (Fig. 30b) of epoxy modified with NCOTBP, the black domains correspond to the soft rubbery phase.

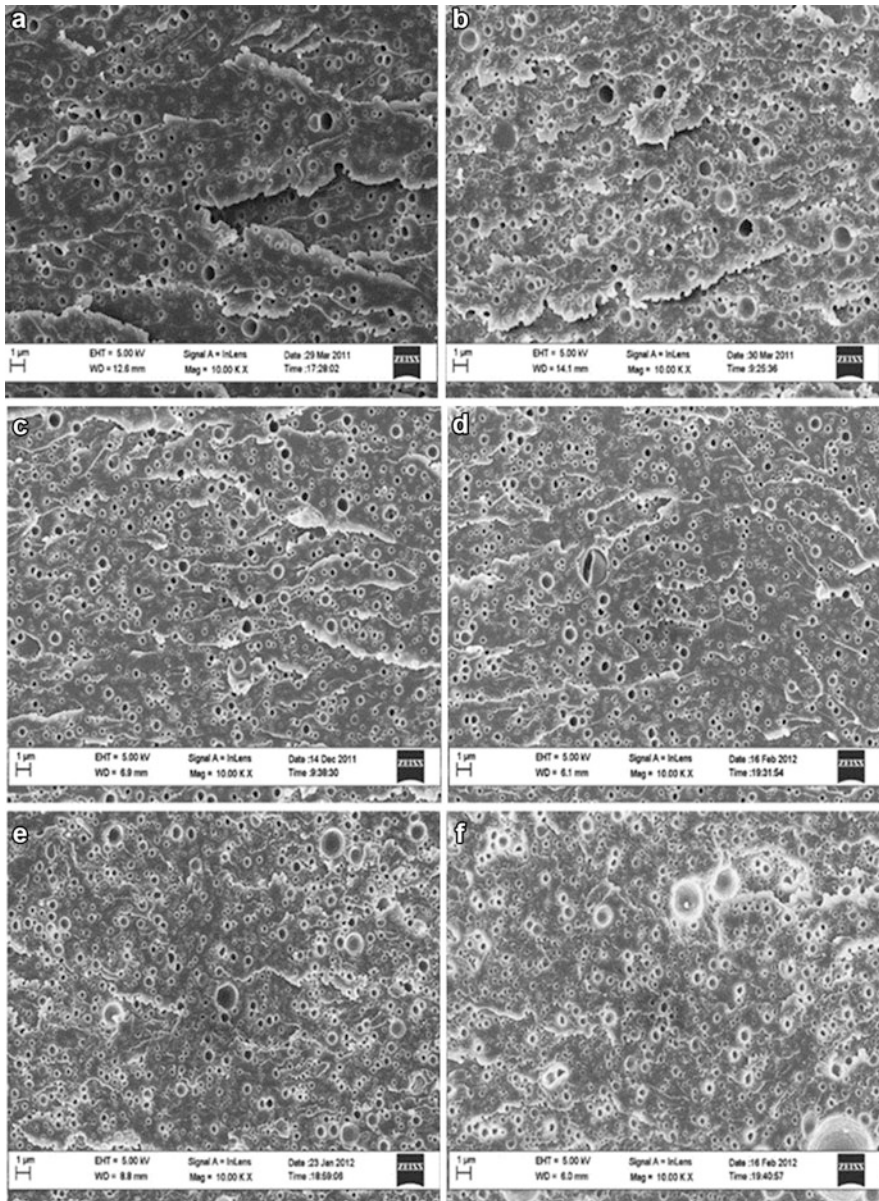


Fig. 24 FEG-SEM images of the fracture surface of the epoxy polymers modified with (a) 10 wt.% and (b) 20 wt.% of S-CSR particles at 20 °C; 10 wt.% S-CSR particle-modified epoxy polymer tested at (c) -55 °C and (d) -109 °C; 20 wt.% S-CSR particle-modified epoxy polymer tested at (e) -55 °C and (f) -109 °C (Chen et al. 2013)

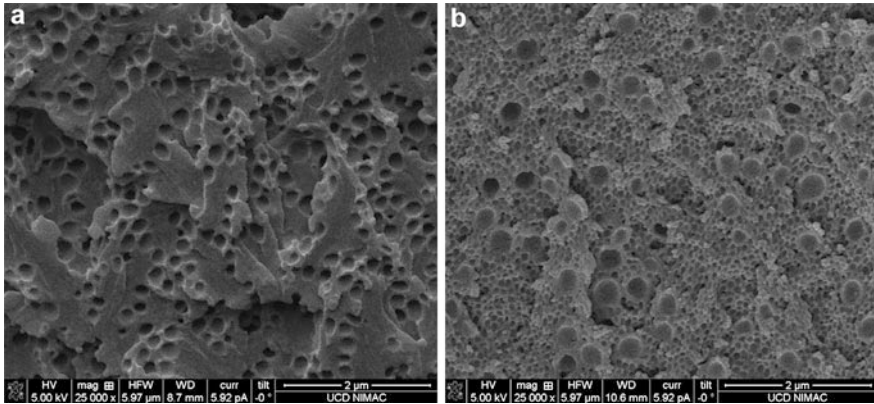


Fig. 25 SEM images of fracture surface for epoxy modified with (a) 22 vol.% of large CSR (b) 22 vol.% of large CSR and 16 vol.% of small CSR (Quan and Ivankovic 2015)

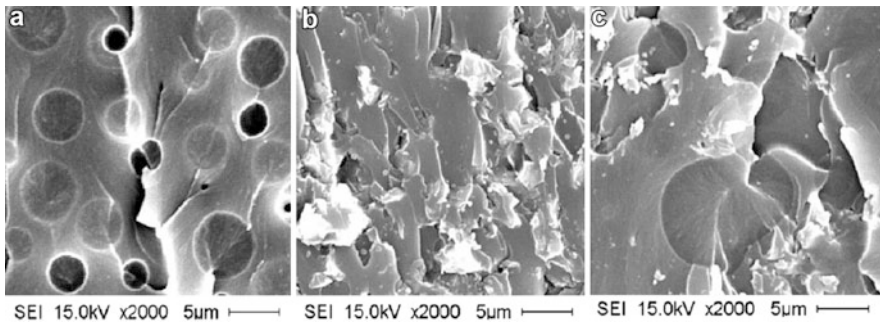
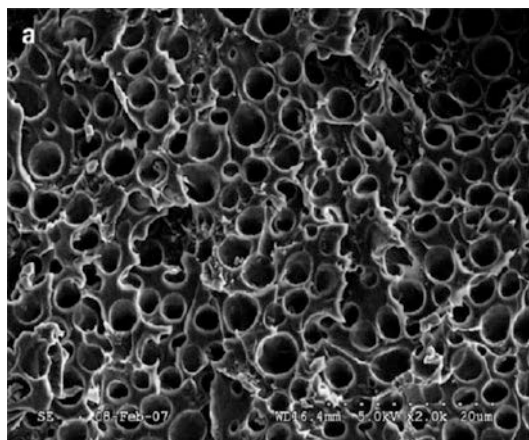


Fig. 26 SEM micrographs of fracture surface of (a) epoxy/20 phr CTBN (b) epoxy/3 phr clay (c) epoxy/20 phr CTBN/3 phr clay (Liu et al. 2004)

Fig. 27 Fracture surface images of hybrid epoxy–silica–rubber: rubber cavitation inducing massive matrix dilation (Liang and Pearson 2010)



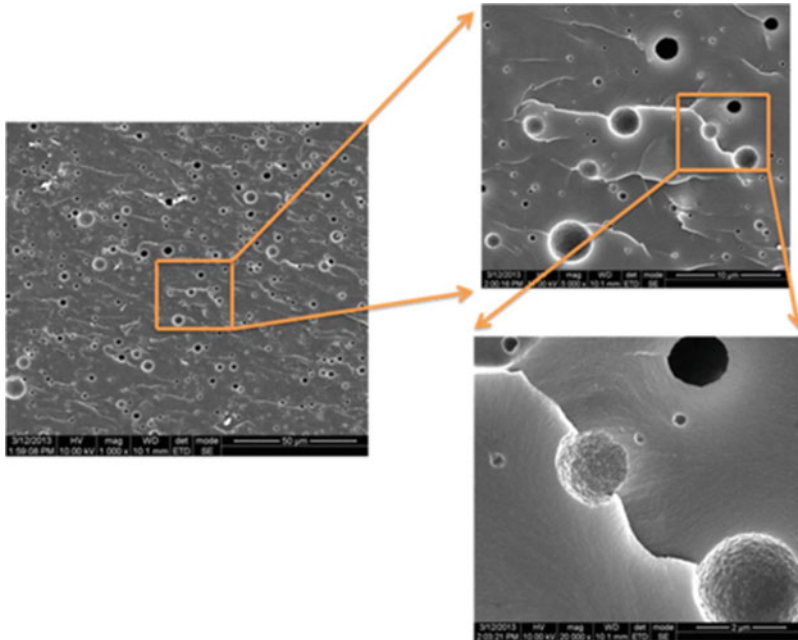


Fig. 28 FESEM images of fracture surface of epoxy/CTBN-modified POSS hybrid epoxy nanocomposite at different magnifications (Konnola et al. 2015)

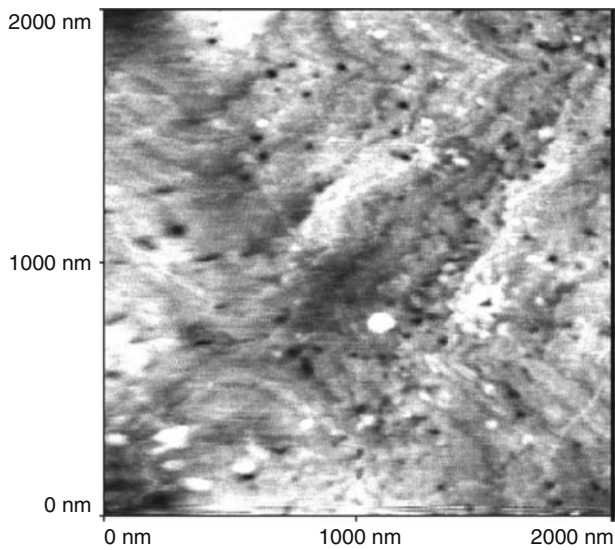


Fig. 29 2,000 nm scan of epoxy/CTBN blend showing the presence of nano-phase rubber particles (Russell and Chartoff 2005)

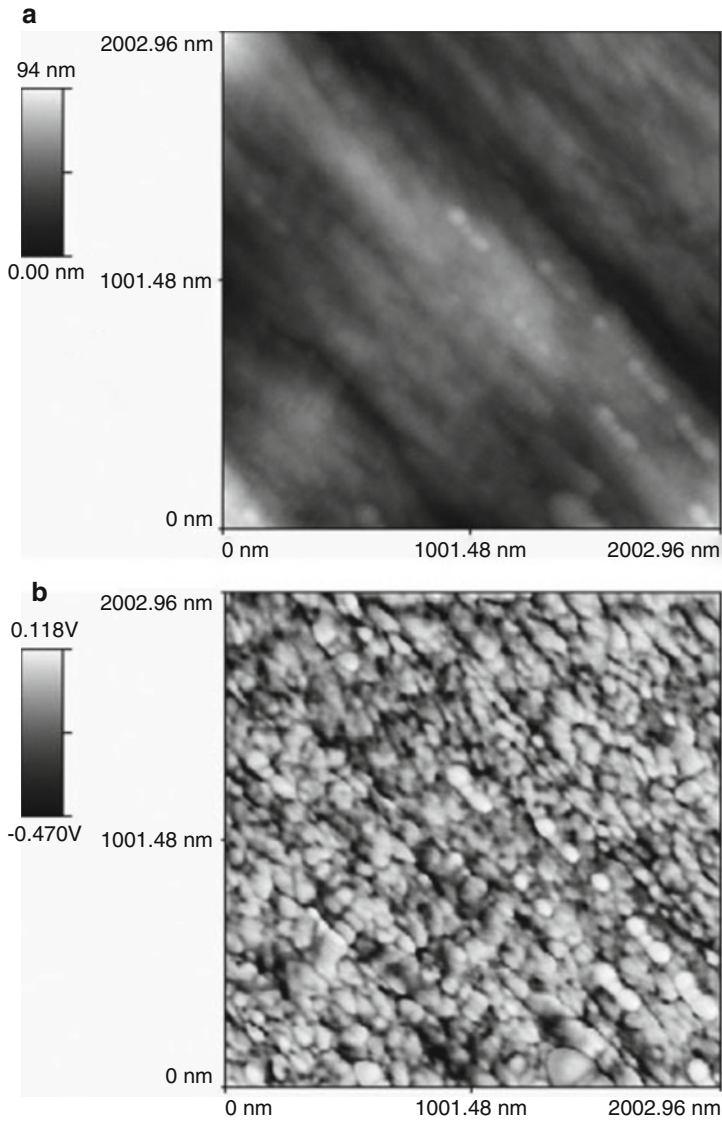


Fig. 30 AFM of the epoxy-NCOTPB network (a) topography and (b) phase contrast images (Soares et al. 2004)

These domains present a typical size of 80 and 65 nm for the longer and shorter axis, respectively.

The rubber particle size in preformed polysiloxane core-shell rubber (S-CSR)-modified epoxy was investigated using AFM technique (Chen et al. 2013). Moreover, the shell of the particle was detected as ring of lighter color surrounding the darker soft cores, and the phase image indicated that this shell area is harder

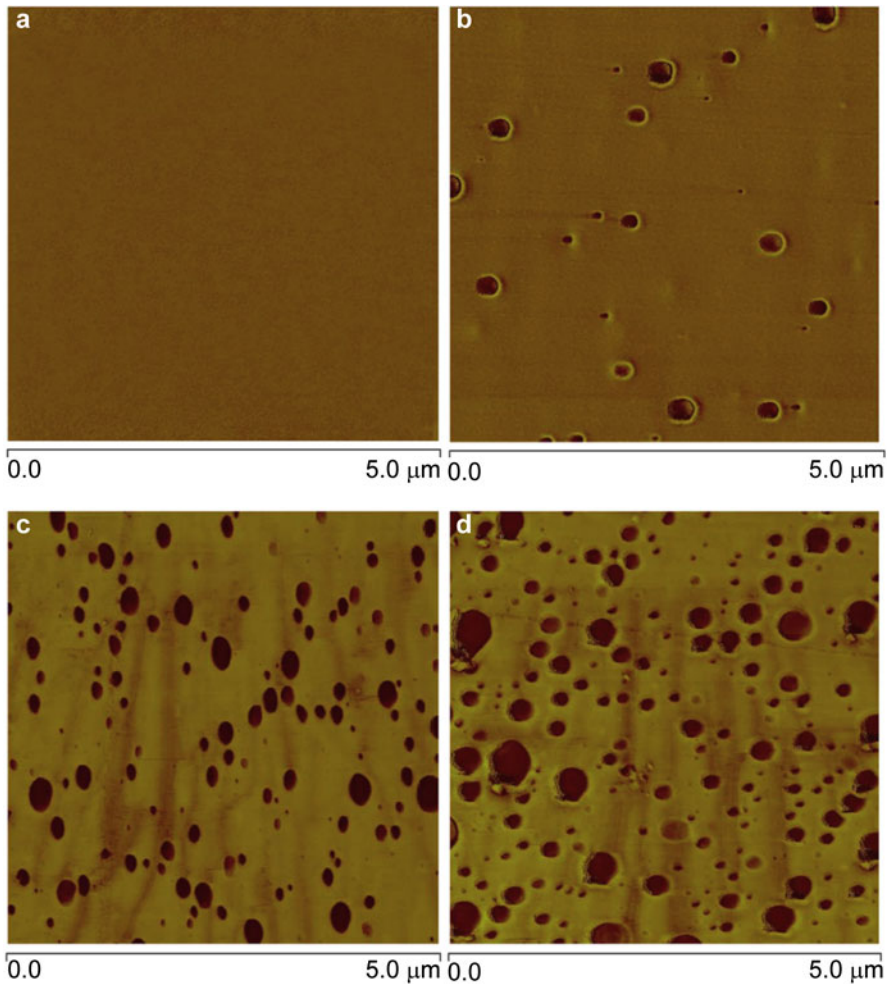


Fig. 31 AFM phase micrographs of the (a) unmodified epoxy polymer, and the epoxy polymers modified with (b) 2 wt.% (c) 10 wt.% and (d) 20 wt.% of S-CSR particles (Chen et al. 2013)

than the epoxy polymer (Fig. 31). The measured mean diameter of the core-shell rubber particles was $0.18 \mu\text{m}$, and the thickness of the shell was between 20 and 40 nm.

AFM can also be used to follow some hyperfine features observed in epoxy/rubber blends which are unable to do with SEM. AFM could effectively be used to observe occluded epoxy phase in micrometer-sized rubber particles (Chen et al. 1994; Bascom et al. 1981; Thomas et al. 2011) and interface regions (Shaffer et al. 1995) in epoxy/rubber blends, which are difficult to observe with SEM.

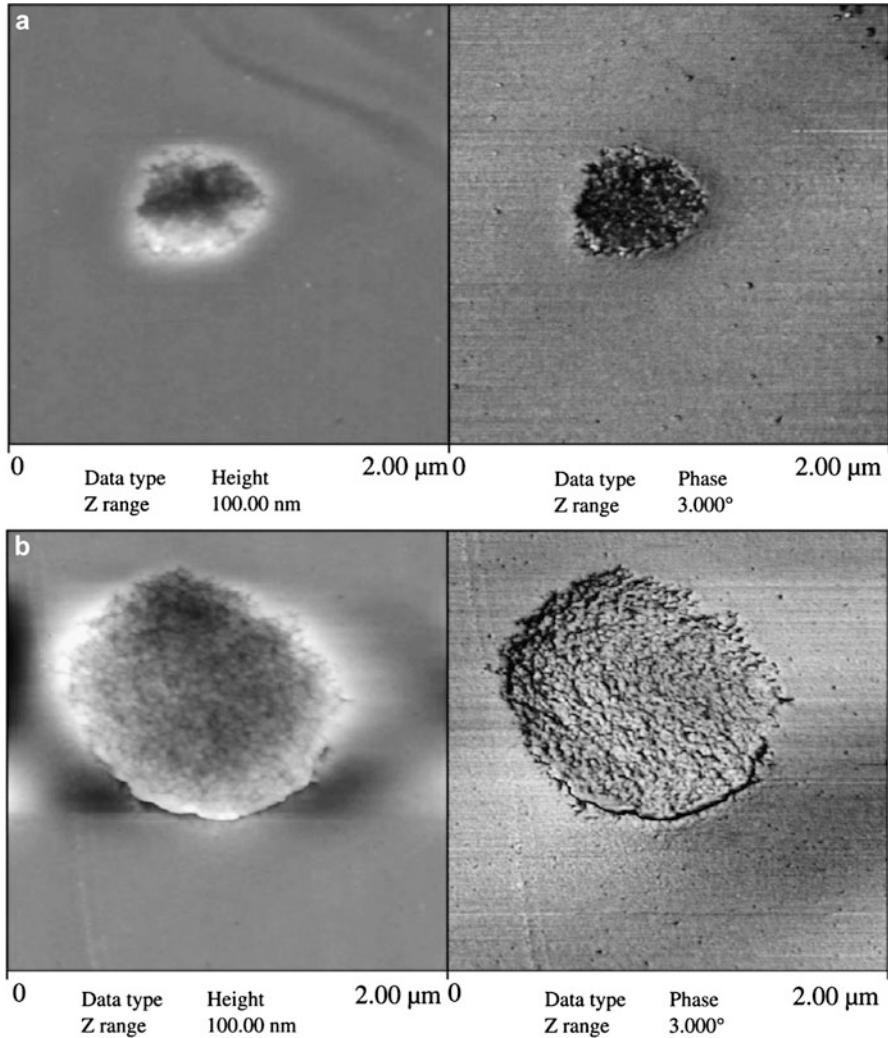


Fig. 32 AFM micrograph of (a) 5 phr CTBN/epoxy blend, (b) 20 phr CTBN-epoxy blend (Thomas et al. 2011)

Figure 32 shows the AFM images of epoxy toughened with 5 and 20 phr CTBN, where the inclusions of epoxy particles were noted inside the elastomer domains.

AFM was also found application in epoxy/rubber blend to detect the interface region (Fig. 33) and the characteristic features of the fracture surface such as growth of the rubber phase due to phase coalescence, fibrous structure of the matrix, cracks on the surface, etc. (Fig. 34).

Fig. 33 AFM image of a cavitated particle in the whitened zone of CTBN pre-reacted with diglycidyl ether of propylene glycol (*DGEP*)/epoxy. The positions where force distance measurements were taken have been labeled in the matrix (**A**), in the cavity (**B**), and in the interface region (**C**) (Shaffer et al. 1995)

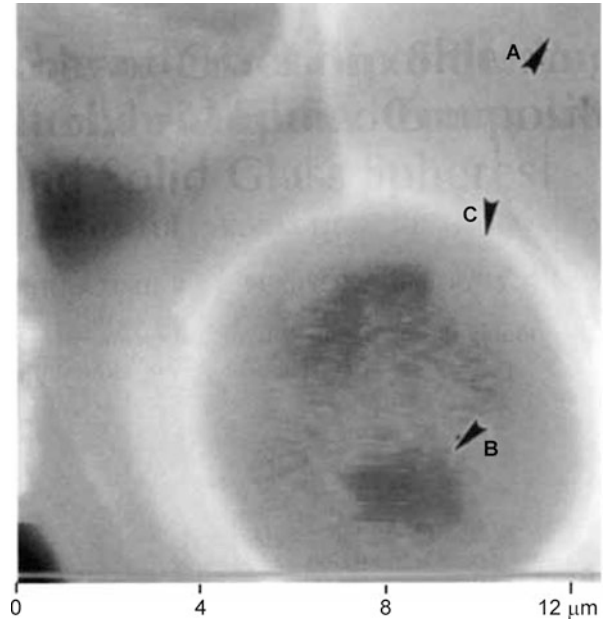
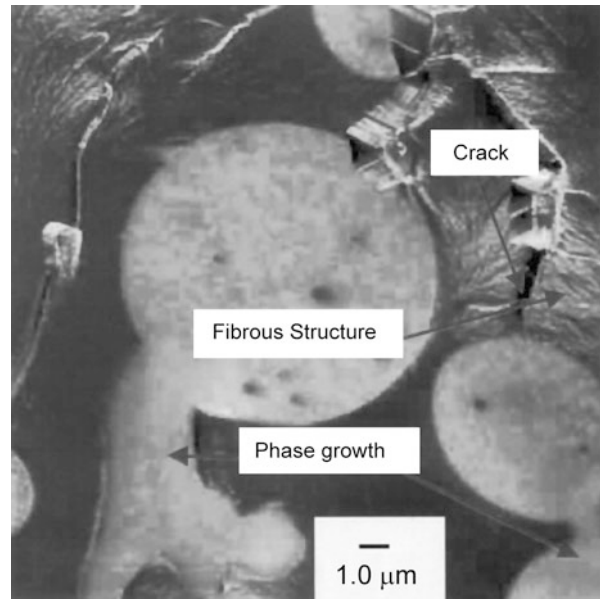


Fig. 34 AFM image of tensile fracture surface of epoxy cresol novolac resin (*ECN*) modified with 25 wt.% of carboxyl-terminated polybutadiene (*CTPB*) (Nigam et al. 2003)



Transmission Electron Microscopy (TEM)

With the advancement of nanotechnology, researchers have focused on the generation of new nanostructured epoxy/liquid rubber blends. Effective functionalization of liquid rubbers is required to tailor better compatibility between epoxy and rubber, and it is a requisite to achieve fine nanostructured epoxy/rubber blends. Soares and coworkers synthesized nanostructured epoxy/isocyanate-functionalized polybutadiene (PBNCO) blends (Barcia et al. 2003; Soares et al. 2011). The characterization of these nanosized rubber particle dispersed in epoxy was carried out using TEM in addition to AFM and a homogeneous distribution of the nanometer-scale rubber particles were detected (Fig. 35). The variation of shape and size of this dispersed rubber particle was well clear from the TEM images. While for blend containing 5 phr of PBNCO, the shape of the domains was not well defined with an average size of 5–10 nm; further increase in rubber content up to 20 phr resulted in more densely packed spherical rubber domains.

Epoxidized CTBN (ECTBN) rubber obtained by the epoxidation of CTBN using hydrogen peroxide and formic acid was found to be effective in producing nanostructured epoxy/rubber blend (Zhao et al. 2015). The effect of degree of epoxidation

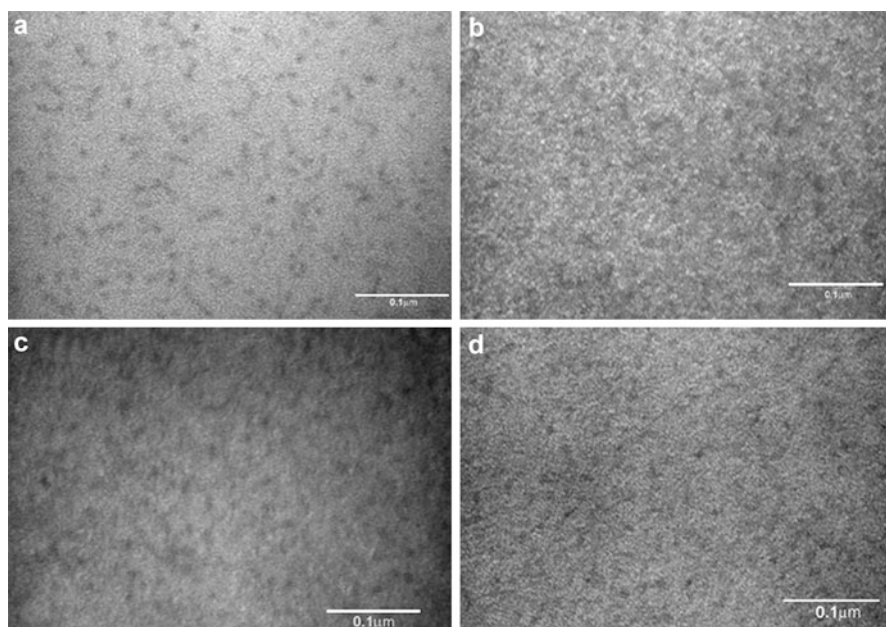


Fig. 35 TEM micrographs of modified epoxy network with (a) 5 phr, (b) 10 phr, (c) 15 phr and (d) 20 phr of PBNCO (each scale bar equals 100 nm) (Soares et al. 2011)

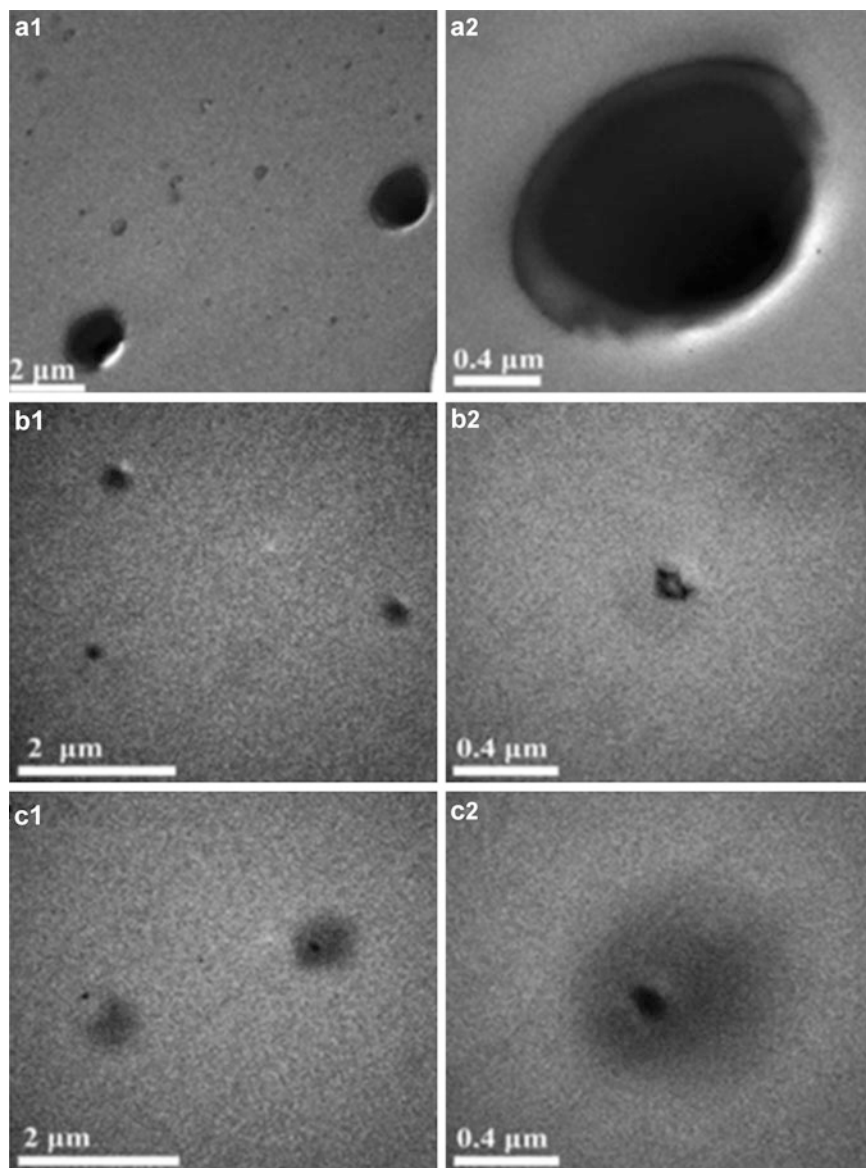


Fig. 36 TEM images of the epoxy blends containing 10 wt.% CTBN rubber epoxidized at different degrees: (a1) and (a2) $Ev = 0$ mol/100 g, (b1) and (b2) $Ev = 0.16$ mol/100 g, and (c1) and (c2) $Ev = 0.30$ mol/100 g; epoxidation degree is indicated by epoxide value (Ev) (Zhao et al. 2015)

of CTBN on the developed nanostructure morphology of epoxy/ECTBN blend was well investigated using TEM (Fig. 36). While the blend modified with CTBN showed micro-sized rubber particle and relatively clear the boundaries, the blends modified with ECTBN (epoxide value, $Ev = 0.16$ mol/100 g and 0.30 mol/100 g)

showed nanosized rubber particles with considerably blurred boundaries. This change in phase morphology could be due to the increase in degree of compatibility and reactivity between the rubber phase and epoxy resin upon epoxidation.

Another modifier derived from CTBN, which was able to form nanostructure in epoxy matrix was synthesized by Heng et al. (2015). They prepared poly(ethylene oxide)-block-carboxyl-terminated butadiene–acrylonitrile rubber diblock copolymer (PEG-*b*-CTBN) via the esterification reaction of hydroxy-terminated methoxypolyethylene glycols in the presence of CTBN with 4-dimethylaminopyridine as the catalyst. Using TEM micrographs of the blends, they confirmed the homogenous dispersion of spherical CTBN domains with an average size of about 10 nm in the continuous epoxy matrix.

The rubber particle size distribution and precipitated rubber volume fraction (V_p) was determined from TEM micrographs using quantitative methods (Yee and Pearson 1986; Chen and Jan 1995). Chen and Jan (1995) calculated the particle size distribution in different epoxy/hardener system modified with CTBN using an average of 20–30 micrographs from each system by applying the Schwartz–Saltykov quantitative method. The precipitated rubber volume fraction (V_p), the fraction of material enclosed within the boundaries of the rubber particles, including both the rubber itself and any resin trapped in the particles, was also calculated from the TEM micrographs by Guy's method. A very close value of V_p and volume fraction of the initial CTBN revealed that the phase separation between rubber and epoxy resin was complete.

Rubber nanoparticles were in situ synthesized in epoxy taking advantage of the reaction of oligomer diamine with epoxy. TEM was used to estimate the size and the dispersion state of in situ-formed rubber nanoparticles (Ma et al. 2008; Yu et al. 2008). The diameter of these particles measured from TEM image was 2–3 nm (Fig. 37).

Rubber particle size in two different liquid rubber-modified epoxies was identified using TEM images (Minfeng et al. 2008). From the TEM images of epoxy resin modified with carboxyl-randomized butadiene–acrylonitrile (CRBN) rubber and hydroxyl-terminated butadiene–acrylonitrile rubber (HTBN), it was confirmed that the rubber particle size of phase-separated CRBN particle (<200 nm) was much smaller than that of HTBN particles (Fig. 38). The observed particle size difference was explained due to the different reactivities of these two rubbers. CRBN could easily form chemical interaction with epoxy and then decrease the chance of agglomeration.

TEM images were used to compare the morphology including the dispersion state and size of submicron liquid rubber (LR) and preformed nanoscale-powered rubber (PR) in epoxy matrix (Fig. 39) (Guan et al. 2014). It was found that PR and LR particles in the epoxy matrix appear as dark and white in color, respectively, in the TEM images. Compared to PR particles (diameter of ~90 nm), the LR particles show a good dispersion in the epoxy at 9.2 wt.%. The LR particles exhibited a significant change in their size with the increase of rubber content (Fig. 39c). This could be due to the miscibility of LR in epoxy that resin would decrease the onset of gelation time at low rubber content which resisted further coalescence of particles to form smaller

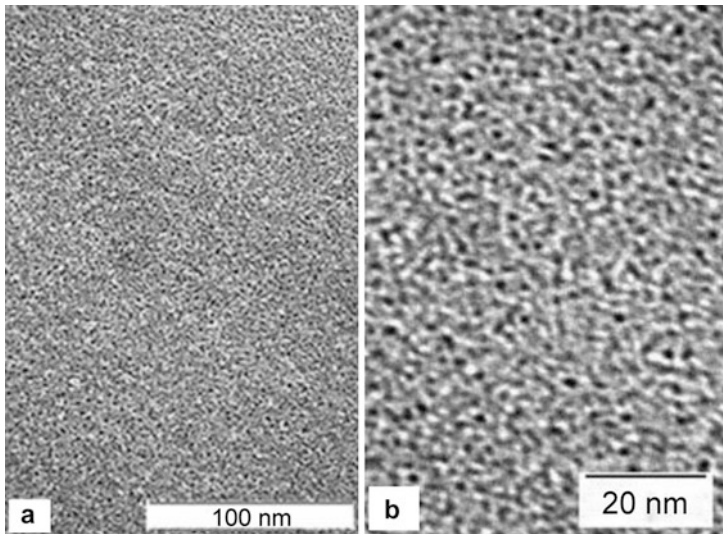


Fig. 37 TEM images of the epoxy/rubber nanocomposite containing 15 wt.% rubber: (a) at 230×10^3 magnification; (b) at 660×10^3 magnification (Ma et al. 2008)

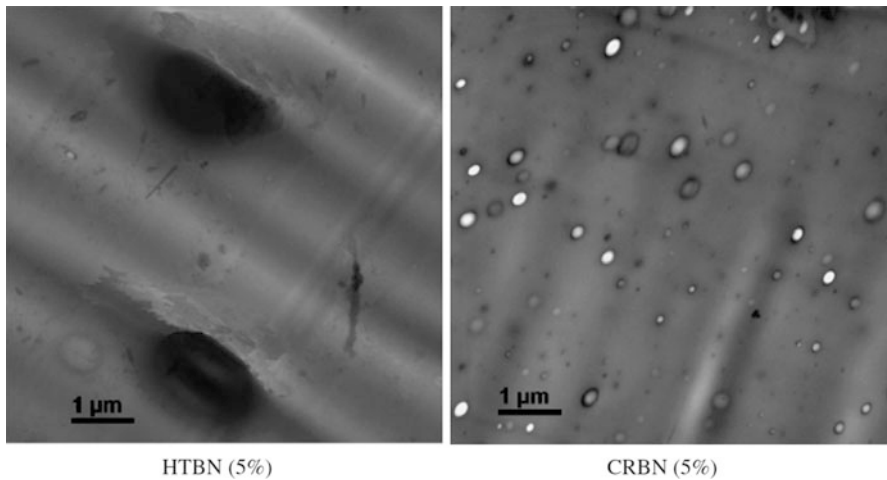


Fig. 38 TEM images of epoxy/HTBN and epoxy/CRBN blends (20,000 \times) (Minfeng et al. 2008)

phase-separated rubber particles. At high content of LR, the solubility parameters and surface tension of the rubbery phase should alter during the cure process, which could promote the phase separation of rubber from matrix to produce the large LR

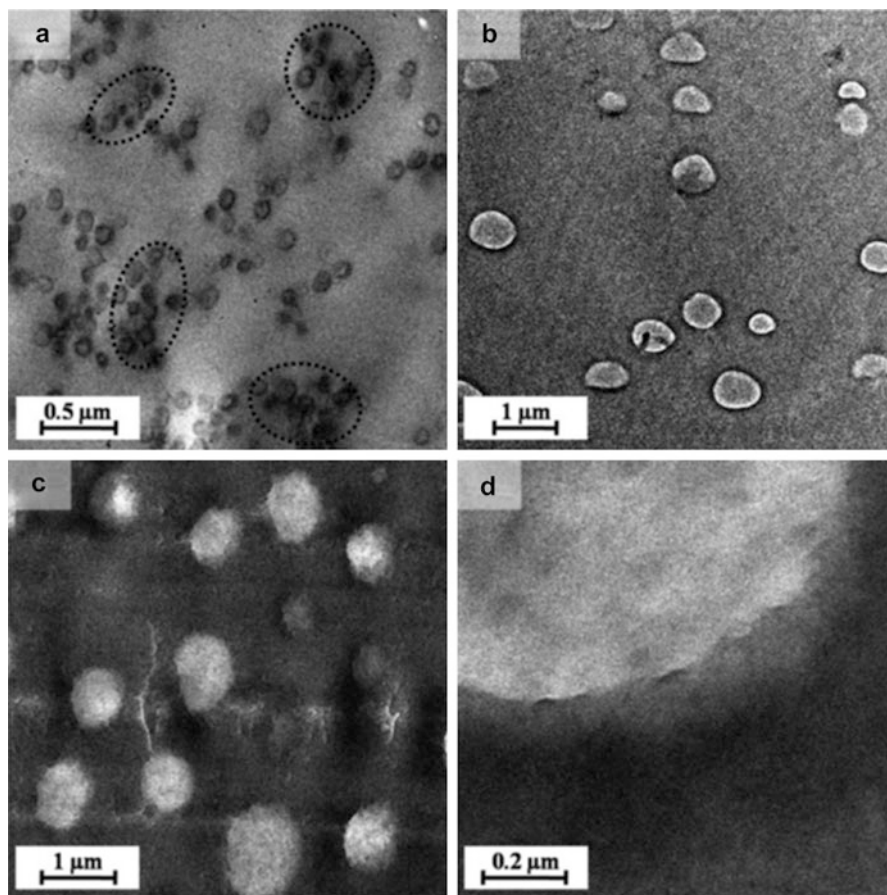


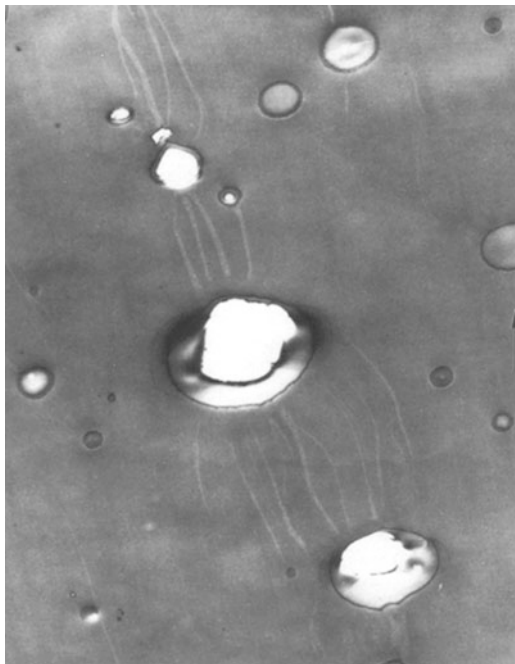
Fig. 39 TEM micrographs of epoxy composites containing: (a) 9.2 wt.% PR, (b) 9.2 wt.% LR, and (c, d) 14.8 wt.% LR (Guan et al. 2014)

particles. TEM image (Fig. 39d) also gave evidence of good interface between rubber and matrix in LR-modified epoxy.

TEM was also used to get idea about the fracture propagation in the damage surface in addition to the optical microscopic information. Although the formation of crazes in epoxy matrix is unlikely due to their high cross-link density, craze-like damage has been detected in transmission electron micrographs of subsurface of fatigue damaged epoxy/CTBN blend (Azimi et al. 1996) (Fig. 40).

The cavitation and shear yielding as major toughening Mechanisms operating in epoxy/rubber blends and the effect of the interfacial zone on these processes were studied by Chen and Jan (1991). The interface between the rubber particle and the

Fig. 40 Transmission electron micrograph revealing craze-like damage in the fatigue damage zone (Azimi et al. 1996)



epoxy matrix was modified by CTBN endcapped with various epoxies like rigid diglycidyl ether of bisphenol A (Epon 828), a short-chain flexible diglycidyl ether of propylene glycol (DER 736), and a long-chain flexible diglycidyl ether of propylene glycol (DER 732). In order to elucidate more clearly the effect of the modifiers, the same amount of modifier was directly added into epoxy resin instead of capping at the CTBN chain end. The TEM images were used to characterize the particle/matrix interface, and they observed that the width of the interfacial zone increased as the CTBN-endcapped epoxide changed from Epon 828, DER 736 to DER 732 (Fig. 41). The degree of cavitation was also found to increase as the width of the interfacial zone increased (Fig. 42). Moreover, the interface zone was not pronounced in blends where the modifier is directly added into epoxy resin.

Balakrishnan et al. (2005) reported a major morphological finding which is the reason for the higher fracture toughness shown by nanoclay-filled epoxy/acrylic rubber blend using TEM images. They found that the clay sheets tend to align around the walls of the rubber particle in the hybrid (Fig. 43). These clay platelets helped the rubber particles to withstand additional stretching forces before failure occurs at the epoxy matrix–rubber particle interface. These aligned clay particles can act as additional reinforcement to protect the interface from an external stretching force. They proposed a combination of mechanisms for the toughening effect in clay-filled epoxy/acrylic rubber blend including rubber particle cavitation, yielding, and plastic deformation of matrix initiated by rubber particles, crack diversion by clay platelets, and energy dissipation to create additional roughened area.

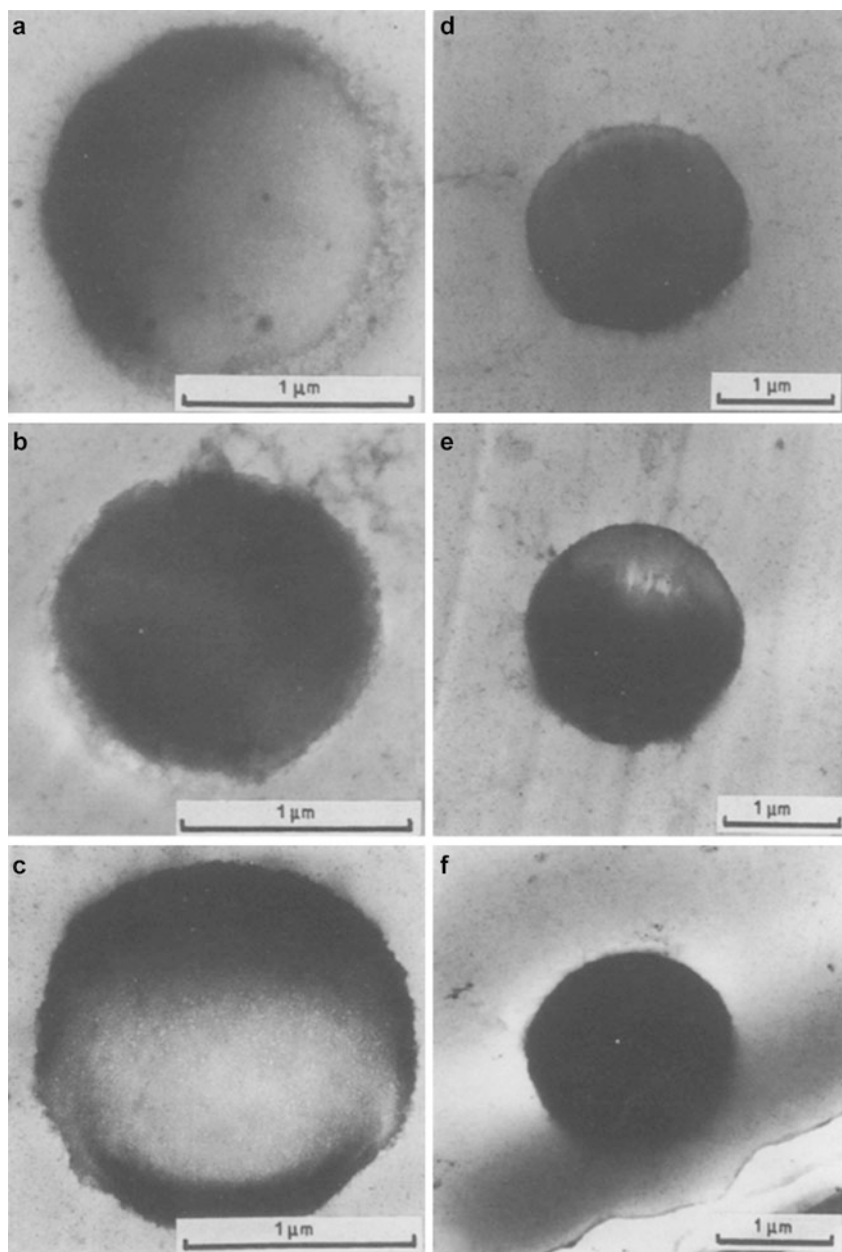


Fig. 41 Higher magnification TEM images of the microtomed sections of (a) epoxy/CTBN endcapped with DER732, (b) epoxy/CTBN endcapped with DER736, (c) epoxy/CTBN endcapped with Epon828, (d) epoxy matrix modified with DER732–CTBN, (e) epoxy matrix modified with DER736–CTBN, (f) epoxy matrix modified with Epon 828–CTBN (Chen and Jan 1991)

Fig. 42 Degree of cavitation on fracture surface of the toughened epoxy resins: (A) epoxy/CTBN endcapped with DER732, (B) epoxy/CTBN endcapped with DER736, (C) epoxy/CTBN endcapped with Epon828, (D) epoxy matrix modified with DER732-CTBN, (E) epoxy matrix modified with DER736-CTBN, (F) epoxy matrix modified with Epon 828-CTBN (Chen and Jan 1991)

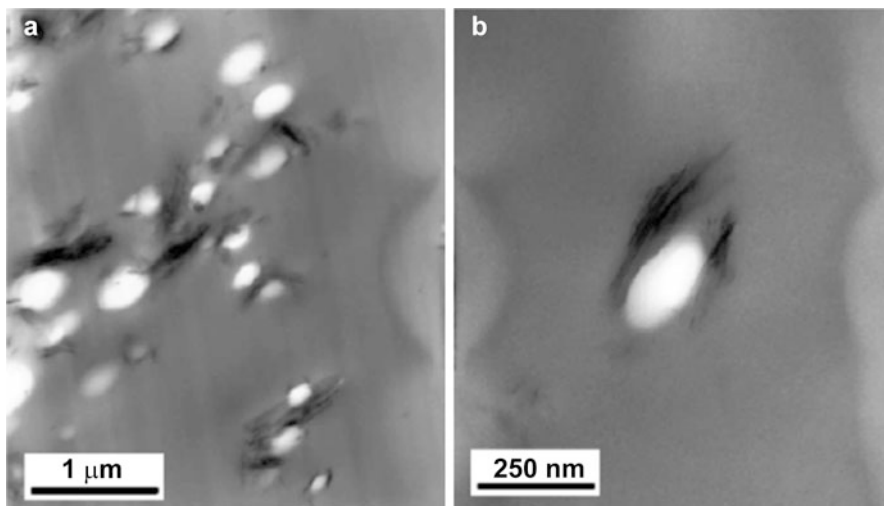
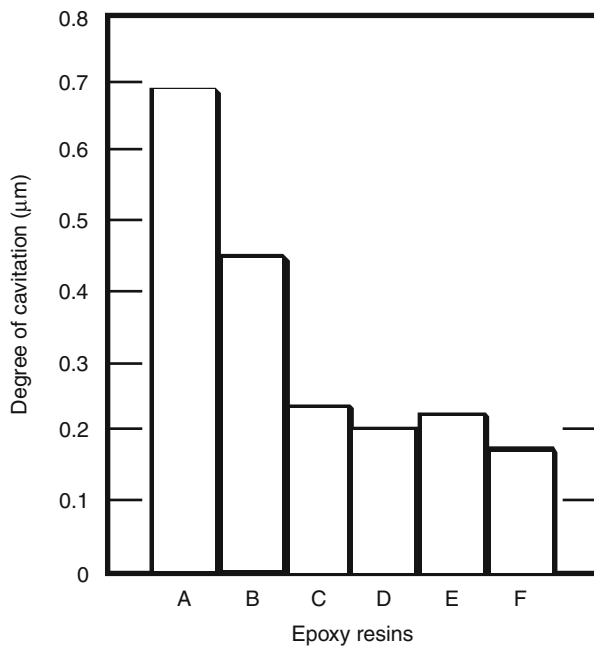


Fig. 43 Association of clay and rubber particles in hybrid epoxy system with 0.75% by mass nanoclay and acrylic rubber phr 16. TEM micrographs at (a) lower and (b) higher magnification (Balakrishnan et al. 2005)

Conclusions

In order to explore the process of phase separation and the final morphology in various epoxy/rubber blends, researchers have been effectively using microscopic techniques like OM, SEM, AFM, and TEM. Such investigations have been concisely presented in the current chapter. The existing literature on morphological studies of epoxy blends with liquid rubbers, preformed core-shell rubber particles, and in situ-formed rubber particles have been discussed. Moreover, the morphological studies on epoxy/rubber blends modified with nanofillers have also been included in this chapter.

The use of microscopic techniques allows one to correlate the mechanical performances of epoxy/rubber blends including their toughness. The supporting evidence in predicting the demixing mechanism in epoxy modified with various liquid rubbers could be drawn from optical microscopic images. OM has also been used to observe the phase behavior in nanofiller-modified epoxy/rubber blends. The transmission optical microscopy (TOM) has been found to be very effective in evaluating the fracture propagation in the damage surface. From TOM images, it has been possible to measure and compare the depth of fracture damage zone (FDZ) for epoxy and epoxy/rubber blends. It has been found that the size of the damage zone was proportional to the fracture energy of the blends. The difference in the size and shape of the plastic zone generated during fracture in epoxy/rubber blend induced by the nature of the interface has been identified using TOM. The various factors which affect the dynamics of phase separation and final morphology in epoxy/rubber blends have been well established using SEM. The features of fracture surfaces observed using SEM have been used to explore the toughening mechanism which operates in epoxy/rubber blends and nanofiller-modified epoxy/rubber blends. The nature of interface in epoxy/CTBN blend has been analyzed using AFM and TEM. While OM and SEM have been effectively worked out to explore the morphological features in microscale, AFM and TEM offered it in the nanometer scale. TEM and AFM could be effectively used to observe hyperfine features in epoxy/rubber blends. The use of these techniques together allows successful identification, and confirmation of both micro- and nanoscopic morphological features existing in epoxy/rubber blends.

References

- Azimi HR, Pearson RA, Hertzberg RW (1996) Fatigue of rubber-modified epoxies: effect of particle size and volume fraction. *J Mater Sci* 31:3777–3789
- Bagheri R, Pearson RA (1995) Interfacial studies in CTBN-modified epoxies. *J Appl Polym Sci* 58:427–437
- Bagheri R, Pearson RA (2000) Role of particle cavitation in rubber-toughened epoxies: II. Interparticle distance. *Polymer* 41:269–276

- Bagheri R, Marouf BT, Pearson RA (2009) Rubber-toughened epoxies: a critical review. *Polym Rev* 49:201–225
- Balakrishnan S, Start PR, Raghavan D, Hudson SD (2005) The influence of clay and elastomer concentration on the morphology and fracture energy of preformed acrylic rubber dispersed clay filled epoxy nanocomposites. *Polymer* 46:11255–11262
- Barcia FL, Amaral TP, Soares BG (2003) Synthesis and properties of epoxy resin modified with epoxy-terminated liquid polybutadiene. *Polymer* 44:5811–5819
- Bartlet P, Pascault JP, Sautereau H (1985) Relationships between structure and mechanical properties of rubber-modified epoxy networks cure with dicyanodiamide hardener. *J Appl Polym Sci* 30:2955–2966
- Bascom WD, Cottingham RL, Jones RL, Peyser P (1975) The fracture of epoxy- and elastomer-modified epoxy polymers in bulk and as adhesives. *J Appl Polym Sci* 19:2545–2562
- Bascom WD, Ting RY, Moulton RJ, Riew CK, Siebert AR (1981) The fracture of an epoxy polymer containing elastomeric modifiers. *J Mater Sci* 16:2657–2664
- Chen EK, Jan YH (1991) Toughening mechanism for a rubber-toughened epoxy resin with rubber/matrix interfacial modification. *J Mater Sci* 26:5848–5858
- Chen TK, Jan YH (1995) Effect of matrix ductility on the fracture behavior of rubber toughened epoxy resins. *Polym Eng Sci* 35:778–785
- Chen D, Pascault JP, Sautereau H (1994) Rubber-modified epoxies: IV. Role of chain ends on the morphologies and properties. *Polym Int* 33:263–271
- Chen J, Kinloch AJ, Sprenger S, Taylor AC (2013) The mechanical properties and toughening mechanisms of an epoxy polymer modified with polysiloxane-based core-shell particles. *Polymer* 54:4276–4289
- Guan L-Z, Gong L-X, Tang L-C, Wu L-B, Jiang J-X, Lai G-Q (2014) Mechanical properties and fracture behaviors of epoxy composites with phase-separation formed liquid rubber and preformed powered rubber nanoparticles: a comparative study. *Polym Compos.* doi:10.1002/pc.22995
- He J, Raghavan D, Hoffman D, Hunston D (1999) The influence of elastomer concentration on toughness in dispersions containing preformed acrylic elastomeric particles in an epoxy matrix. *Polymer* 40:1923–1933
- Heng Z, Chen Y, Zou H, Liang M (2015) Simultaneously enhanced tensile strength and fracture toughness of epoxy resins by a poly(ethylene oxide)-block-carboxyl terminated butadiene-acrylonitrile rubber dilock copolymer. *RSC Adv* 5:42362–42368
- Huang Y, Kinloch AJ (1992) The role of plastic void growth in the fracture of rubber-toughened epoxy polymers. *J Mater Sci Lett* 11:484–487
- Kim DS, Kim SC (1994) Rubber modified epoxy resin. II: phase separation behavior. *Polym Eng Sci* 34:1598–1604
- Kinloch AJ, Shaw SJ, Tod DA, Hunston DL (1983a) Deformation and fracture behaviour of a rubber-toughened epoxy: 1. Microstructure and fracture studies. *Polymer* 24:1341–1354
- Kinloch AJ, Shaw SJ, Hunston DL (1983b) Deformation and fracture behaviour of a rubber-toughened epoxy: 2. Failure criteria. *Polymer* 24:1355–1363
- Kinloch AJ, Lee SH, Taylor AC (2014) Improving the fracture toughness and the cyclic-fatigue resistance of epoxy-polymer blends. *Polymer* 55:6325–6334
- Konnola R, Parameswaranpillai J, Joseph K (2015) Mechanical, thermal, and viscoelastic response of novel in situ CTBN/POSS/epoxy hybrid composite system. *Polym Compos.* doi:10.1002/pc
- Kunz SC, Sayre JA, Assink RA (1982) Morphology and toughness characterization of epoxy resins modified with amine and carboxyl terminated rubbers. *Polymer* 23:1897–1906
- Lee HS, Kyu T (1990) Phase separation dynamics of rubber/epoxy mixtures. *Macromolecules* 23:459–464
- Liang YL, Pearson RA (2010) The toughening mechanism in Hybrid Epoxy-Silica-Rubber Nanocomposites (HESRNs). *Polymer* 51:4880–4890
- Liu W, Hoa SV, Pugh M (2004) Morphology and performance of epoxy nanocomposites modified with organoclay and rubber. *Polym Eng Sci* 44:1178–1186

- Ma J, Mo M-S, Du X-S, Dai S-R, Luck I (2008) Study of epoxy toughened by in situ formed rubber nanoparticles. *J Appl Polym Sci* 110:304–312
- Manziona LT, Gillham JK, McPherson CA (1981a) Rubber-modified epoxies. I. Transitions and morphology. *J Appl Polym Sci* 26:889–905
- Manziona LT, Gillham JK, McPherson CA (1981b) Rubber-modified epoxies. II. Morphology and mechanical properties. *J Appl Polym Sci* 26:907–919
- Mathew VS, George SC, Parameswaranpillai J, Thomas S (2014) Epoxidized natural rubber/epoxy blends: phase morphology and thermomechanical properties. *J Appl Polym Sci* 131:39906
- Minfeng Z, Xudong S, Huiquan X, Genzhong J, Xuewen J, Baoyi W, Chenze Q (2008) Investigation of free volume and the interfacial, and toughening behavior for epoxy resin/rubber composites by positron annihilation. *Radiat Phys Chem* 77:245–251
- Naè HN (1986) Phase separation in rubber-modified thermoset resins: optical microscopy and laser light scattering. *J Appl Polym Sci* 31:15–25
- Nigam V, Setua DK, Mathur GN (2003) Failure analysis of rubber toughened epoxy resin. *J Appl Polym Sci* 87:861–868
- Pearson RA, Yee AF (1986) Toughening mechanisms in elastomer-modified epoxies part 2 microscopy studies. *J Mater Sci* 21:2475–2488
- Pearson RA, Yee AF (1991) Influence of particle size and particle size distribution on toughening mechanisms in rubber-modified epoxies. *J Mater Sci* 26:3828–3844
- Quan D, Ivankovic A (2015) Effect of Core Shell Rubber (CSR) nano-particles on mechanical properties and fracture toughness of an epoxy polymer. *Polymer* 66:16–28
- Ratna D, Bantia AK (2000) Toughened epoxy adhesive modified with acrylate based liquid rubber. *Polym Int* 49:281–287
- Ratna D, Bantia AK (2007) Reactive acrylic liquid rubber with terminal and pendant carboxyl groups as a modifier for epoxy resin. *Polym Eng Sci* 47:26–33
- Ratna D, Simon GP (2010) Epoxy and hyperbranched polymer blends: morphology and free volume. *J Appl Polym Sci* 117:557–564
- Russell B, Chartoff R (2005) The influence of cure conditions on the morphology and phase distribution in a rubber-modified epoxy resin using scanning electron microscopy and atomic force microscopy. *Polymer* 46:785–798
- Shaffer OL, Bagheri R, Qian JY, Dimonie V, Pearson RA, El-aasser MS (1995) Characterization of the particle-matrix interface in rubber-modified epoxy by atomic force microscopy. *J Appl Polym Sci* 58:465–484
- Soares BG, Leyva ME, Moreira VX, Barcia FL, Khastgir D, Simão RA (2004) Morphology and dielectric properties of an epoxy network modified by end-functionalized liquid polybutadiene. *J Polym Sci B Polym Phys* 42:4053–4062
- Soares BG, Dahmouche K, Lima VD, Silva AA, Caplan SPC, Barcia FL (2011) Characterization of nanostructured epoxy networks modified with isocyanate-terminated liquid polybutadiene. *J Colloid Interface Sci* 358:338–346
- Sultan JN, McGarry FJ (1973) Effect of rubber particle size on deformation mechanisms in glassy epoxy. *Polym Eng Sci* 13:29–34
- Tang L-C, Wang X, Wan Y-J, Wu L-B, Jiang J-X, Lai G-Q (2013) Mechanical properties and fracture behaviors of epoxy composites with multi-scale rubber particles. *Mater Chem Phys* 141:333–342
- Thomas R, Abraham J, Thomas PS, Thomas S (2004) Influence of carboxyl-terminated (butadiene-co-acrylonitrile) loading on the mechanical and thermal properties of cured epoxy blends. *J Polym Sci B Polym Phys* 42:2531–2544
- Thomas R, Ronkay F, Czigany T, Cvelbac U, Mozetic M, Thomas S (2011) A probe on the failure mechanism in rubber-modified epoxy blends: morphological and acoustic emission analysis. *J Adhes Sci Technol* 25:1747–1765
- Tripathi G, Srivastava D (2007) Effect of carboxyl-terminated poly(butadiene-co-acrylonitrile) (CTBN) concentration on thermal and mechanical properties of binary blends of diglycidyl ether of bisphenol-a (DGEBA) epoxy resin. *Mater Sci Eng A* 443:262–269

- Verchere D, Pascault JP, Sautereau H, Moschiar SM, Riccardi CC, Williams RJJ (1991a) Rubber-modified epoxies. IV. Influence of morphology on mechanical properties. *J Appl Polym Sci* 43:293–304
- Verchere D, Pascault JP, Sautereau H, Moschiar SM, Riccardi CC, Williams RJJ (1991b) Rubber-modified epoxies. II. Influence of the cure schedule and rubber concentration on the generated morphology. *J Appl Polym Sci* 42:701–716
- Vijayan PP, Puglia D, Jyotishkumar P, Kenny JM, Thomas S (2012) Effect of nanoclay and carboxyl-terminated (butadiene-co-acrylonitrile) (CTBN) rubber on the reaction induced phase separation and cure kinetics of an epoxy/cyclic anhydride system. *J Mater Sci* 47:5241–5253
- Vijayan PP, Puglia D, Kenny JM, Thomas S (2013) Effect of organically modified nanoclay on the miscibility, rheology, morphology and physical properties of epoxy/carboxyl-terminated (butadiene-co-acrylonitrile) blend. *Soft Matter* 9:2899–2911
- Wise CW, Cook WD, Goodwin AA (2000) CTBN rubber phase precipitation in model epoxy resins. *Polymer* 41:4625–4633
- Xiao K, Ye L (2000) Rate-effect on fracture behavior of Core-Shell-Rubber (CSR)-modified epoxies. *Polym Eng Sci* 40:70–81
- Yamanaka K, Inoue T (1990) Phase separation mechanism of rubber-modified epoxy. *J Mater Sci* 25:241–245
- Yamanaka K, Takagi Y, Inoue T (1989) Reaction-induced phase separation in rubber-modified epoxy resins. *Polymer* 60:1839–1844
- Yee AF, Pearson RA (1986) Toughening mechanisms in elastomer-modified epoxies part 1 mechanical studies. *J Mater Sci* 21:2462–2474
- Yee AF, Li D, Li X (1993) The importance of constraint relief caused by rubber cavitation in the toughening of epoxy. *J Mater Sci* 28:6392–6398
- Yu S, Hu H, Ma J, Yin J (2008) Tribological properties of epoxy/rubber nanocomposites. *Tribol Int* 41:1205–1211
- Zhang J, Zhang H, Yang Y (1999) Polymerization-induced bimodal phase separation in a rubber-modified epoxy system. *J Appl Polym Sci* 72:59–67
- Zhao Y, Chen Z-K, Liu Y, Xiao H-M, Feng Q-P, Fu S-Y (2013) Simultaneously enhanced cryogenic tensile strength and fracture toughness of epoxy resins by carboxylic nitrile-butadiene nanorubber. *Compos Part A* 55:178–187
- Zhao K, Song X-X, Liang C-S, Wang J, Xu S-A (2015) Morphology and properties of nanostructured epoxy blends toughened with epoxidized carboxyl-terminated liquid rubber. *Iran Polym J* 24:425–435

Zhengguang Heng, Yang Chen, Huawei Zou, and Mei Liang

Abstract

Epoxy resin is a kind of widely used thermoset resins known for its excellent properties. While its inherent brittleness largely limited its application, the incorporation of rubber phases into epoxy resins is a classical method and could effectively make up the shortcomings. In order to acquire a deeper understanding of the mechanism of these properties, it is necessary for epoxy/rubber blends to be structurally well characterized. This chapter focuses on the practical aspects of using the five spectroscopic methods most often applied, Fourier transform infrared (FTIR) spectroscopy, nuclear magnetic resonance (NMR) spectroscopy, Raman spectroscopy, optical microscopy (OM), and X-ray scattering spectroscopy, in the structural investigation and microstructures of epoxy/rubber blends to study the driving forces producing miscibility in the blends. The application of other spectroscopic methods is also discussed. It should be mentioned that the study of driving forces producing miscibility in epoxy/rubber blends is based on the application of at least a few different types of spectroscopic methods during the same study.

Keywords

Spectroscopic • Epoxy • Rubber • Miscibility

Z. Heng • Y. Chen (✉) • H. Zou • M. Liang

State Key Laboratory of Polymer Materials Engineering, Polymer Research Institute of Sichuan University, Sichuan University, Chengdu, China

e-mail: hengzhengguang@163.com; cy3262276@163.com; hwzou@163.com; liangmeiww@163.com

Contents

Introduction	148
Spectroscopic Analysis of Epoxy/Rubber Blends	154
Fourier Transform Infrared (FTIR) Spectroscopy	154
Nuclear Magnetic Resonance (NMR) Spectroscopy	163
Raman Spectroscopy	168
Optical Microscopy (OM)	170
X-Ray Scattering	175
Other Spectroscopic Methods	179
Conclusions	179
References	180

Introduction

Epoxy resin (EP) is a vague term, which normally contains at least two epoxide groups known as the characteristic group. The epoxide group can also be referred to as a glycidyl, epoxy, or oxirane group. The term epoxy resin is applied to both prepolymers and cured resins. The invention of epoxy resins has experienced a long period of time, while its industrial application was the last sixty or seventy years. During the development, various epoxy resins have been invented. According to their chemical structure, epoxy resins can be divided into the following five categories: glycidyl ether resins, glycidyl ester resins, glycidyl amine resins, alicyclic epoxides, and aliphatic epoxides. Due to the raw materials readily available and at low cost, diglycidyl ether of bisphenol A (DGEBA)-based epoxy resin is the most important class in the application of epoxy; its structure is shown in Fig. 1. Among all the thermosetting resins, epoxy resins are unique due to several factors (Potter 1970), viz., minimum pressure needed for fabrication of products, shrinkage much lower and hence lower residual stress in the cured product, the use of a wide range of temperature by judicious selection of curing agent with good control over the degree of cross-linking, availability of the resin ranging from low viscous liquid to tack-free solid, etc. (Ratna and Banthia 2004). Since these unique characteristics and useful properties like good thermal and mechanical properties, high chemical and corrosion resistance, outstanding adhesion to various substrates, flexibility, low cure shrinkage, and good electrical properties, epoxy resin has become an essential class of thermosetting resins and widely utilized in engineering composites, coatings, structural adhesives, electronics, etc.

However, undesirable properties of EP are their inherently brittle and poor resistance to crack propagation, which adversely affects most physical and

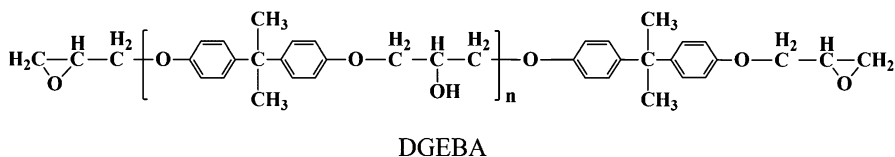
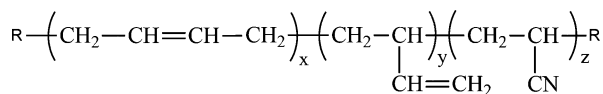


Fig. 1 The chemical structure of DGEBA

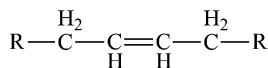
mechanical properties. Thereby, toughening epoxy resin has become a widespread concern subject all over the world. In light of these problems, a second phase (elastomer, particulate, thermoplastic, liquid crystal, etc.) was incorporated. Considering the effect and miscibility of epoxy and modifiers, the most successful was the incorporation of a second reactive elastomeric phase into the brittle epoxy matrix. The various types of elastomeric materials which have been studied with a view to rubber modification of epoxy resins are the following: reactive liquid rubbers, urethane rubber, polyacrylated elastomers, and silicone rubber.

Liquid rubbers with reactive groups in the terminal positions or pendant to the main chain are the most classical modifiers for toughening epoxy. Besides the most effective carboxyl group (Bucknall and Yoshii 1978), several functional groups including epoxy, phenol, vinyl, hydroxyl (Thomas et al. 2008), and amine have also been studied; two types of liquid rubber are shown in Fig. 2. In these cases, the rubbers are initially miscible with the matrix. When the reaction starts, the rubber first reacted with resin. With the curing reaction, the molecular weight of epoxy increases, and then reaction-induced phase separation occurs. Thus, the cured thermoset possesses a dispersed rubbery phase (Unnikrishnan and Thachil 2006). The methods of liquid rubber modifying epoxy can be divided into prereacted type and non-prereactive type, and the former effect is better. Three types of liquid polybutadiene, hydroxyl-terminated polybutadiene (HTPB), isocyanate end-capped HTPB (NCOTPB), and epoxide end-capped HTPB (CPBER), were used to modify epoxy by Barcia (et al. 2003). The study denotes that epoxy modified with HTPB and CPBER presents a heterogeneous system with a two-phase morphology, while NCOPBER (EP-NCOTPB-EP) shows transparent epoxy networks with no discernible phase-separated morphology. Besides, the diameters of rubber phase modified with CPBER are substantially smaller than that with HTPB. The different morphological characteristics observed in these modified systems were attributed to the different structures. Ramos et al. (2005) have modified epoxy resin by carboxyl-terminated butadiene-acrylonitrile copolymer (CTBN) and hydroxyl-terminated polybutadiene (HTPB). The results modified with CTBN showed dispersed phase size between 1 and 4 μm , while the HTPB-modified ER presented large difference in

Fig. 2 The chemical structure of liquid rubbers



Poly(butadiene-co-acrylonitrile)



Polybutadiene

R: The reactive functional groups

rubber particle size that ranges from 10 to 50 μm . Recently, in order to further increase the miscibility of liquid rubber and epoxy, block copolymers were used to modify epoxy resins. These block copolymers generally comprised by reactive liquid rubber and epoxy-miscible blocks (e.g., poly(ethylene oxide) (PEO) and poly(ϵ -caprolactone) (PCL)) (Clark et al. 1984; Luo et al. 1994; Guo and Groeninckx 2001; Zheng et al. 2003). It has been recognized that block copolymer could form nanostructures following either self-assembly (Hillmyer et al. 1997; Lipic et al. 1998) or reaction-induced microphase-separation (Grubbs et al. 2000; Mijovic et al. 2000) mechanism. Compared to epoxy modified with liquid rubber, rubber phase was homogeneously dispersed in the epoxy resin matrix at the nanometer scale because of the covalent bond between miscible blocks and rubber and the special interaction between miscible blocks and epoxy. Apart from the miscibility and effect that significantly increased, the amount of rubber becomes smaller achieving the same effects. The miscibility nanostructured blends of epoxy resin with poly(ϵ -caprolactone)-block-poly(*n*-butyl acrylate) diblock copolymer were studied by Xu (Xu and Zheng 2007). It is shown that all the subchains of the block copolymer were miscible with epoxy before curing; however, after curing only the PBA blocks were separated out, whereas the PCL blocks remained miscible with epoxy resin. Heng et al. (2015) prepared a poly(ethylene oxide)-block-carboxyl-terminated butadiene-acrylonitrile rubber diblock copolymer and used it to simultaneously enhance tensile strength and fracture toughness of epoxy resins.

Urethane rubber is a series of elastomeric material that contains many urethane groups in the main chain. Urethane polymers are traditionally and most commonly formed by reacting a di- or polyisocyanate with a polyol. Both the isocyanates and polyols used to make polyurethanes contain on average two or more functional groups per molecule. Due to the different type and ratio of raw material, various chemical structures of urethane rubber were prepared. According to the chemical structure of raw material, it can be divided into polyester urethane rubber and polyether urethane rubber. Urethane rubber has superior low-temperature elasticity; excellent tribological behavior; high temperature, oil, solvent, and ozone resistance; and thermal stability. Therefore, urethane-rubber-modified epoxy resins by the interpenetrating polymer networks (IPNs) have been rapidly developed. IPNs are a combination of two or more polymers in network form, held together by permanent entanglements with only occasional covalent bonds between different chains of the two or more types of polymers (Chen et al. 2011). IPNs can be prepared either simultaneously or sequentially; the two different processes of preparing IPNs are illustrated in Fig. 3. One of the polymers synthesized and/or cross-linked in the immediate presence of the others (Raymond and Bui 1998). In IPNs system, two or more networks are at least partially interlaced on a molecular scale and cannot be separated unless chemical bonds are broken. It is held together by permanent entanglement and shows excellent thermal stability and mechanical properties because of a synergistic effect induced by the forced compatibility of individual components (Chen et al. 2010). Frisch et al. first reported the simultaneous interpenetrating networks (SINs) composed of polyurethane (PU) and EP (Frisch et al. 1974a, Fig. 3a). Then graft IPNs were researched by Hsieh and Han (1990) and Raymond and Bui (1998). Graft IPNs occurred when the side

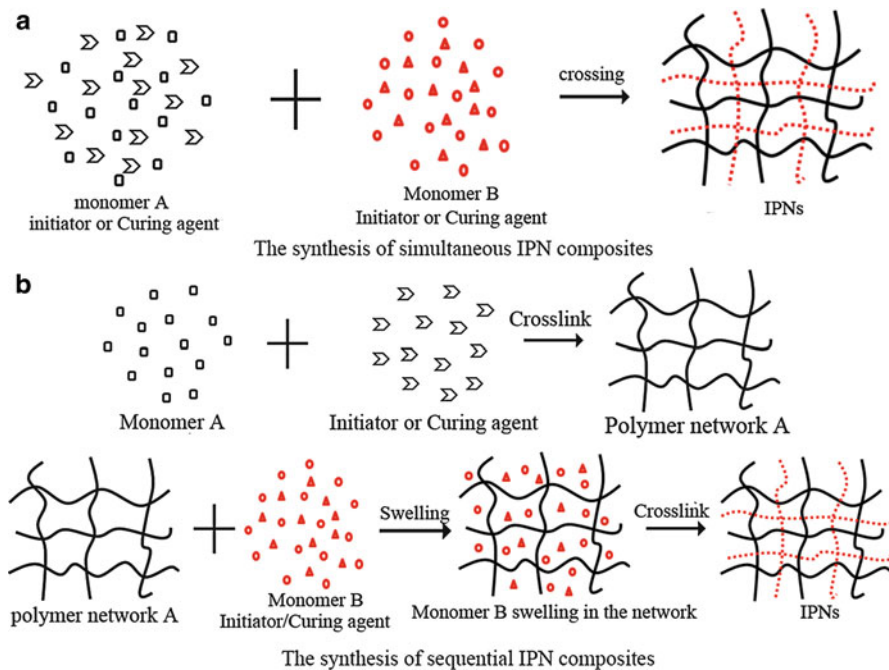


Fig. 3 The two different processes of preparing IPNs

chains of one polymer were connected to the main chain of another polymer in the IPNs. Mahesh et al. (2003) prepared graft IPNs of epoxy and polyurethane, which proceeded through the reaction between isocyanate group of polyurethane prepolymer and pendant hydroxyl group of the epoxy resin. Results showed that the system presented heterogeneous microstructure and the incorporation of polyurethane increased the mechanical strength and decreased the glass transition temperature, thermal stability, and heat distortion temperature, whereas the incorporation of bismaleimide having ester linkages into polyurethane-modified epoxy increased thermal stability and tensile and flexural properties and decreased the impact strength, the glass transition temperature, and heat distortion temperature. Influencing factors on the compatibility of IPNs had also been widely studied (Frisch et al. 1969, 1974a, b, 1977, 1982; Kim et al. 1975; Klempner et al. 1985; Wang et al. 1985; Werner 1989), such as the amount of soft segments of PU, the types of soft and hard segments of PU, the amount and types of chain extender and its pendant group, the types of epoxy, cure agents, etc.

Polyacrylate rubber is a general term for a type of specialty rubber, which may consist of one or more of the following monomers – ethyl acrylate, EA; butyl acrylate, BA; and methoxy ethyl acrylate, MEA – the structure of which are given as seen in Fig. 4. These are coupled with reactive groups, which may be epoxy or carboxyl groups or combinations thereof. The excellent heat, oxidation, ozone, and lubricating and transmission fluid resistance make it a significantly toughening effect on epoxy

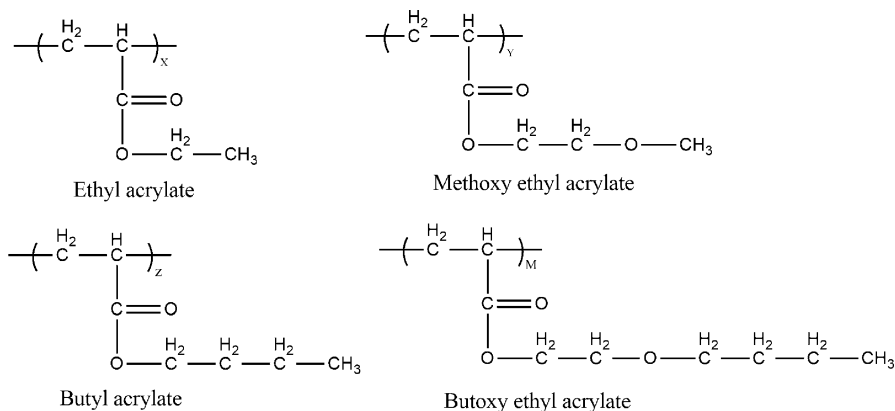
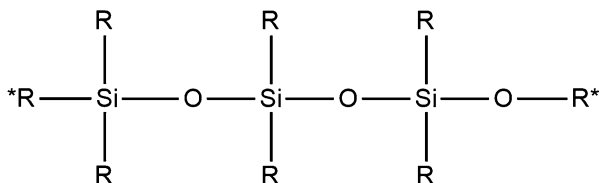


Fig. 4 Structure of the monomers of polyacrylate rubber

and become a worldwide hot topic. Polyacrylate-rubber-modified epoxy resins can be achieved by two methods, incorporating reactive groups on the acrylate copolymer to react with epoxy group or hydroxyl groups on epoxy resins and applying core-shell structure polyacrylate elastic particles (miscible blocks were incorporated and reacted with the functional groups on the surface of polyacrylate elastic particles) as toughening agent. For the former method, the molecular weight of modifier and the amount of reactive groups will affect the miscibility of modifier and epoxy. The more reactive groups and smaller molecular weight of modifier, the better miscibility of modifier and epoxy and the better effect achieved. For the latter method, the effect of the modification is related to the particle size, particle spacing, interface adhesion, etc. Wang et al. (1992a) have synthesized polyfunctional poly(*n*-butyl acrylates) (containing epoxy and carboxyl group) by photopolymerization and used it to toughen epoxy resin cured with diamino diphenyl methane (DDM). They found that there is an optimum functionality for maximum impact resistance in epoxy and carboxyl-functionalized and epoxy-functionalized liquid-rubber-modified systems. Lee and coworkers (1986) obtained similar results using *n*-butyl acrylate/acrylic acid copolymers. They reported that improvement of adhesion strength could be achieved by incorporating the nBA/AA copolymer in a DGEBA epoxy matrix and that an optimum functionality existed to achieve the highest interfacial adhesion.

Different from the previously mentioned elastomers, silicone rubber has an organic backbone made of silicone and oxygen atoms and belongs to a family compound known as silicones. Typical structure of silicone rubber is shown in Fig. 5. As a kind of specialty elastomer, more and more attentions have been focused on silicone rubber known for its retention of flexibility; resilience in a wide temperature range; superior ozone, weather, chemical, fuel, and oil resistance; excellent electrical insulation; and low surface energy. However, pure polydimethylsiloxane (PDMS) had very little use as a toughening agent because of the poor compatibility between soft segments of PDMS and polar hard segments in epoxy. The solubility parameter of PDMS is much lower than that of the epoxy resin. To improve the

Fig. 5 The structure of the monomers of silicone rubber



R: Ph, H, CH₃, OCH₃

R*: Reactive functional groups

compatibility of polysiloxanes with epoxy resins, various methods have been developed, including using silane coupling agents (Alagar et al. 2004; Prabu and Alagar 2005); introduction of functional groups, such as hydroxyl (Huang et al. 2001; Wu et al. 2002), amino (Shon and Kwon 2009), epoxy (Jang and Crivello 2003), and isocyanate (Shih et al. 1999) group; using polysiloxane-containing block copolymers (Gonzalez et al. 2004; Murias et al. 2012); and making use of sol-gel method to bridge the polysiloxane and the epoxy phases (Lin and Huang 1996). Hydroxyl-terminated silicone oligomer-bridged epoxy resins, which synthesized through the reaction between epoxy groups and hydroxyl groups on epoxy resins and hydroxyl groups on silicone oligomer, were studied by Chen (Chen et al. 2014). The diameter of the silicone phases considerably increased with the addition of modifiers. The toughness of the silicone-modified system increased considerably with a suitable diameter of silicone phases. Ren et al. (2014) synthesized a series of siloxane epoxy resins through reaction of poly(methylphenylsiloxane) with epoxy resin. The elongations at break improved markedly and the thermal stability was better than that of epoxy resin. The particle size of silicone had a significant effect on the mechanical properties of the modified epoxy resin.

It is well known that epoxy/rubber composites are heterogeneous systems, and their properties are mainly determined by the dispersed rubber phases. Thus, the study on the driving force for phase separation appears to be very essential. The driving force for phase separation is ascribed to the unfavorable entropic contribution to the mixing free energy due to the molecular weight of infinity for cross-linked components. Nonetheless, the miscibility of rubber/epoxy blends will also be changed by controlling the intermolecular specific interactions (e.g., hydrogen bonding) and the formation of covalent bond between rubbers and epoxy, which can be measured by highly sensitive optical techniques, such as infrared (IR), nuclear magnetic resonance (NMR), Raman and X-ray spectroscopies, optical microscopy (OM), small-angle light-scattering (SALS) technology, X-ray diffraction (XRD) technology, etc.

The present paper reviews the characterization of polymer blends by spectroscopy. As the most important and commonly used spectroscopic technologies in epoxy/rubber blends systems, infrared (IR), nuclear magnetic resonance (NMR), and Raman spectroscopies were introduced. And the driving forces producing

miscibility in epoxy/rubber blends, the reaction between epoxy and modifiers, and their chemical structures are discussed in detail.

Spectroscopic Analysis of Epoxy/Rubber Blends

Fourier Transform Infrared (FTIR) Spectroscopy

Infrared spectroscopy is certainly one of the most important and widely used analytical techniques available to scientists. Liquids, solutions, pastes, powders, films, fibers, and surfaces can all be examined with a judicious choice of sampling technique. Infrared spectroscopy, which allows to qualitatively and quantitatively synthesis samples, is a technique based on the vibrations of the atoms of a molecule. The infrared spectrum is commonly obtained by passing infrared electromagnetic radiation through a sample that possesses a permanent or induced dipole moment and determining what fraction of the incident radiation is absorbed at a particular energy (Stuart 2004). The energy of every peak appeared in the absorption spectrum corresponds to frequency of the vibration of a molecule part. An IR spectrometer usually records the energy of the radiation that is transmitted through a sample as a function of the wave number or frequency. Fourier transform infrared (FTIR) spectroscopy, which employs an interferometer and exploits the well-established mathematical process of Fourier transformation, has become the most widely utilized infrared spectrum. It has dramatically improved the quality of infrared spectra and minimized the time required to obtain data.

The basic components of an FTIR spectrometer are shown schematically in Fig. 6. The radiation emerging from the source is passed through an interferometer to the sample before reaching a detector. Upon amplification of the signal, in which high-frequency contributions have been eliminated by a filter, the data are converted to digital form by an analog-to-digital converter and transferred to the computer for Fourier transformation.

FTIR spectrum can be divided into three main regions: the near infrared ($13,000\text{--}4000\text{ cm}^{-1}$), the mid-infrared ($4000\text{--}400\text{ cm}^{-1}$), and the far infrared ($<400\text{ cm}^{-1}$). Although many infrared applications employ the mid-infrared region, the near- and far-infrared regions also provide important information about certain materials. Generally, there are less infrared bands in the $4000\text{--}1800\text{ cm}^{-1}$ region, while many bands are between 1800 and 400 cm^{-1} . Hence, the scale is sometimes changed so that the region between 4000 and 1800 cm^{-1} is contracted and the region between 1800 and 400 cm^{-1} is expanded to emphasize features of interest. The ordinate scale may be presented in % transmittance with 100% at the top of the spectrum. There is a choice of absorbance or transmittance as a measure of band intensity, and transmittance is traditionally used for spectral interpretation, while absorbance is used for quantitative work.

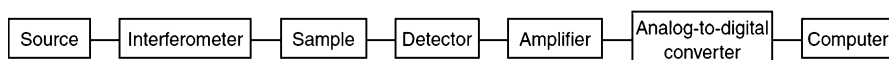


Fig. 6 The basic components of an FTIR spectrometer

Sample Preparation

The method of sample preparation is determined by the state of the sample. For the cured epoxy/rubber blends, the samples for FTIR analysis are prepared by grinding a small portion of the dry blended powders with powdered potassium bromide (KBr), then compressed to form pellets. For uncured blends, samples are spin coated onto a KBr disk directly or from a solution of the blends dissolved in an appropriate solvent (the concentration depends on the required film thickness). The thickness of the homogeneous film should be uniform and adjusted to avoid overabsorption in the range of interest. The solvent and water in samples also should be evaporated as much as possible to reduce the impact on the results. However, care must be taken as the heating of samples may cause degradation. Besides, films of the epoxy/rubber blends can also be used directly for FTIR studies. FTIR spectra are usually recorded in the mid-infrared (4000 cm^{-1} to 400 cm^{-1}) with a resolution of 4 cm^{-1} at room temperature.

Typical FTIR Spectra of Epoxy Resin and Rubber

With the development of epoxy/rubber system, different kinds of epoxy resins and rubbers have been synthesized. The description and interpretation of the infrared spectra of them have been published by many scientists (Bakar et al. 2008; Ismail et al. 2009). Here, some typical FTIR spectra are listed.

Figure 7 shows the typical FTIR spectra of diglycidyl ether of bisphenol A-based epoxy resin and HTPB, respectively (Thomas et al. 2012). The main peaks observed in pure epoxy resin occur at 913 and 826 cm^{-1} due to the oxirane group. The peaks

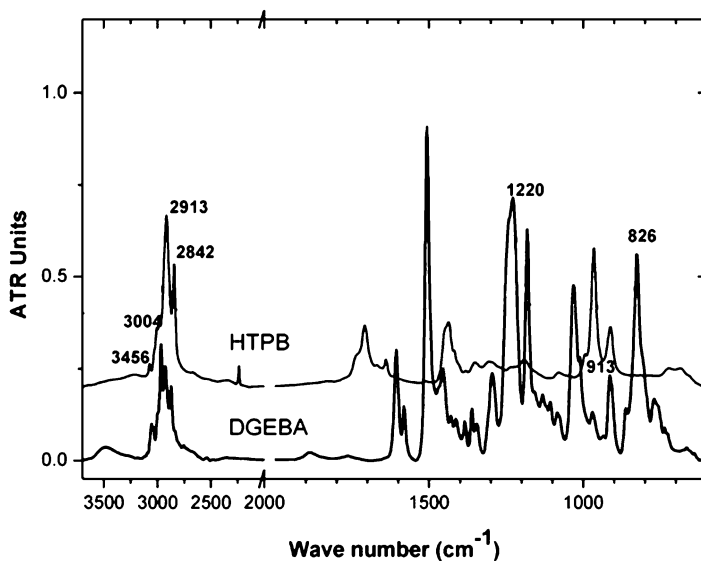


Fig. 7 The typical FTIR spectra of DGEBA and HTPB (Reprinted with permission from Industrial & Engineering Chemistry Research. (2012) 51, 12178–12191. Copyright 2012 American Chemical Society (Thomas et al. 2012))

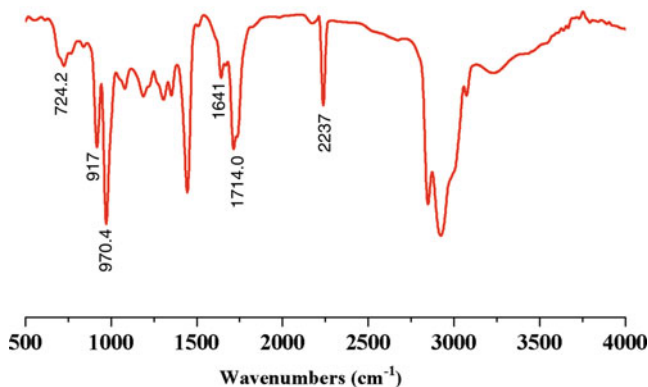


Fig. 8 The typical FTIR spectrum of CTBN (Reprinted with permission from RSC Advances. (2015) 5, 42362–42368. Copyright 2015 Royal Society of Chemistry (Heng et al. 2015))

at 1297–1184 and 1087 cm^{-1} were attributed to the asymmetrical and symmetrical stretching vibration of aryl alkyl ether (C–O–C), respectively. A peak near 1220 cm^{-1} was noted due to the stretching vibrations of C–O bond. 3056, 1582, 787, and 750 cm^{-1} were due to the stretching of aromatic rings. And the asymmetrical and symmetrical stretching vibrations of CH_2 , $(\text{CH}_3)_2\text{C}$, and CH_3 of quaternary carbon were also observed at 2872, 2929, 1381, and 2962 cm^{-1} (Ahmad et al. 2005).

The main absorption peaks of HTPB are the broad O–H band in the region of 3400–3500 cm^{-1} and band at 1640 cm^{-1} ascribed to C = C (double bond) and vinylene group. The absorption peaks near 2913 cm^{-1} and 2842 cm^{-1} are due to C–H stretching vibrations in CH_2 groups. The band at 3004 cm^{-1} is due to C–H stretching vibrations near C = C double bond.

The FTIR spectrum of CTBN was shown in Fig. 8 (Heng et al. 2015). The carbonyls (C = O) and $-\text{CH}=\text{CH}_2$ are characteristic of the stretching vibration at 1715 and 1641 cm^{-1} , respectively. The band at 2237 cm^{-1} is attributed to the stretching vibration of $-\text{CN}$ group in CTBN. The bands at 970 and 724 cm^{-1} are ascribed to the out-of-plane bending vibration = C–H bonds in trans-1,4 and cis-1,4+ moieties in CTBN, respectively. The weak absorption at 917 cm^{-1} is attributed to the out-of-plane bending vibration of 1,2-structures in the CTBN subchains.

FTIR Analysis of Epoxy/Rubber Blends

As an intuitive and simple method, FTIR has been widely used and reported in epoxy/rubber blends (Kar and Banthia 2005; He and Wang 2009). Through the analysis of FTIR, the compatibility and its influence factors of epoxy/rubber blends, the behavior of phase separation, chemical structure and reaction mechanism analysis, the real-time process of a reaction, the thermogravimetric process, etc., could be researched.

Chemical structure and reaction mechanism analysis are important applications of Fourier transform infrared spectroscopy. Two different types of epoxy-terminated polybutadiene were synthesized and used to modify epoxy resin by Barcia et al. (2002, 2003). The processes were shown in Fig. 9. In order to characterize

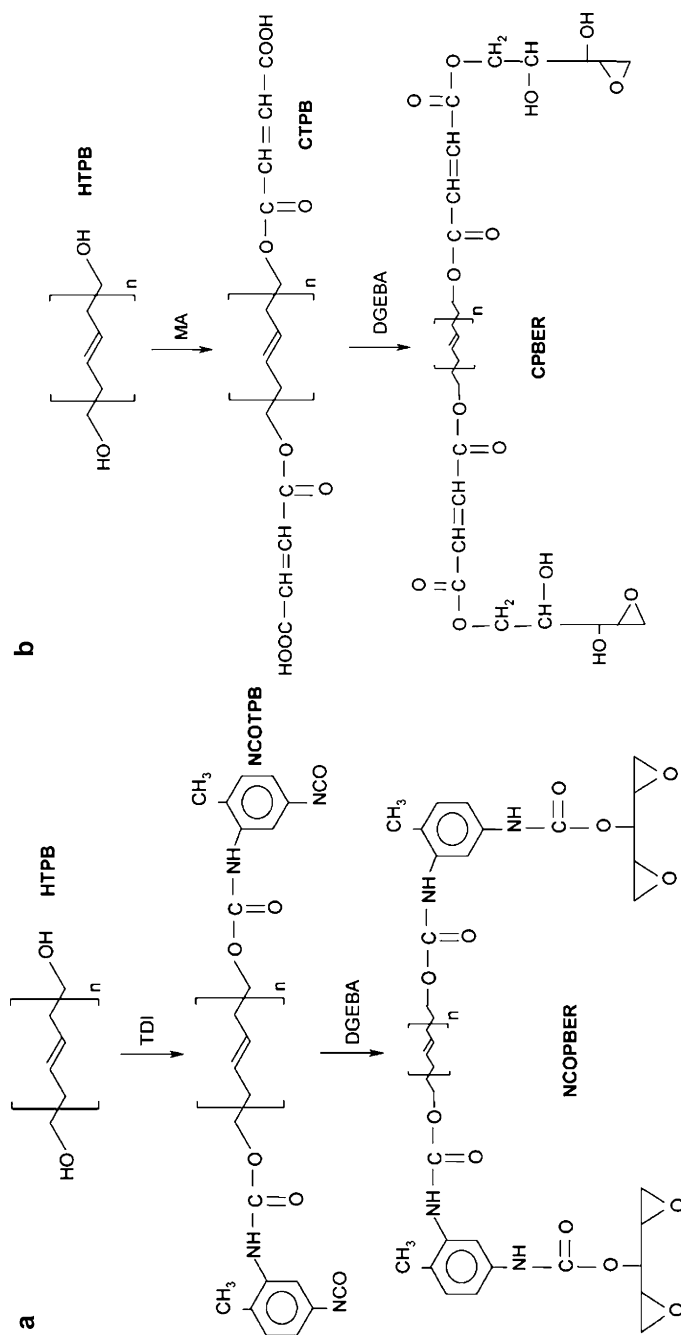


Fig. 9 The processes of preparing epoxy-terminated polybutadiene (HTPB carboxyl-terminated polybutadiene, NCOTPB isocyanate-terminated polybutadiene, NCOPBER epoxy-terminated polybutadiene-epoxy resin block copolymer obtained from NCOTPB, CTPB carboxyl-terminated polybutadiene, CPBER epoxy-terminated polybutadiene-epoxy resin block copolymer obtained from CTPB) (Reprinted with permission from Polymer. (2003) 44, 5811–5819. Copyright 2003 Elsevier (Barcia et al. 2003))

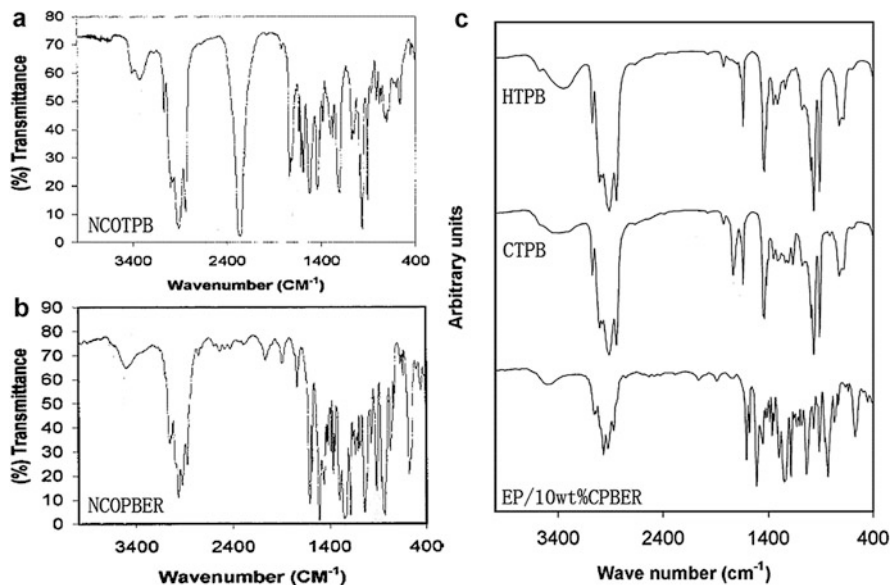


Fig. 10 FTIR spectroscopy of the products (Reprinted with permission from Polymer. (2003) 44, 5811–5819. Copyright 2003 Elsevier (Barcia et al. 2003), Reprinted with permission from Journal of Applied Polymer Science. (2002) 83, 838–849. Copyright 2002 John Wiley and Sons (Barcia et al. 2002))

the chemical structure and reaction mechanism, the products were measured by Fourier transform infrared (FTIR) spectroscopy, shown in Fig. 10.

In Fig. 10a, the disappearance of the peak at 3500 cm^{-1} (due to OH stretching vibrations) and the presence of absorptions at $3330\text{--}3057\text{ cm}^{-1}$ (characteristic of urethane groups), 2265 cm^{-1} (related to the isocyanate groups), and 1735 cm^{-1} (belonging to the carbonyl stretching of the urethane group) indicated the successful functionalization of HTPB with TDI and the OH groups of HTPB were completely reacted. For Fig. 10b, the absorption at 2265 cm^{-1} disappeared, while the peak of the oxirane ring appeared at 910 cm^{-1} , confirming successful synthesis of NCOPBER. An absorption at 1730 cm^{-1} , characteristic of carbonyl group of ester, is observed in the spectrum of CTPB, indicating the incorporation of maleic anhydride into the HTPB chain.

FTIR was also employed to study the real-time process of a reaction. Zeng et al. (2008) researched the different cure processes of epoxy modified by CTBN and amine-terminated butadiene-acrylonitrile copolymer (ATBN). The intensity of the epoxy absorption band was decreased after being cured, which means the reaction between epoxy and the modifiers occurred. The reaction was accelerated with the addition of both HTBN and CTBN (Fig. 11). The intensity of the epoxy absorption band decreased most quickly in the sample modified with CTBN. The high reactivity -COOH group of CTBN reacted much better than the -OH group of HTBN. For Fig. 11e, the absorption band at 1710 cm^{-1} could be attributed to -COOH group of

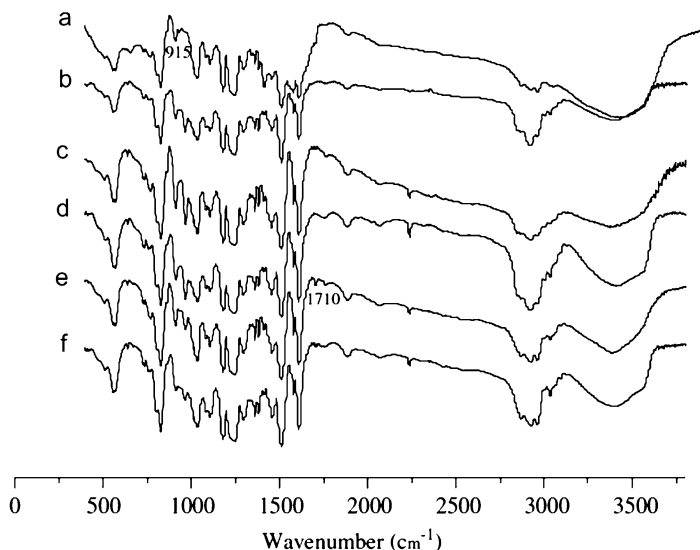


Fig. 11 FTIR spectra of the composites cured at 150 °C: (a) EP (0 min), (b) EP (1 h), (c) HTBN 95/5 (0 min), (d) EP/HTBN 95/5 (1 h), (e) EP/CTBN 95/5 (0 min), (f) EP/CTBN 95/5 (1 h) (Reprinted with permission from Radiation Physics and Chemistry. (2008) 77, 245–251. Copyright 2008 Elsevier (Minfeng et al. 2008))

CTBN. For Fig. 11f, the absorption band at such wave number could be attributed to the superposition of -COOH and the functional group ester formed during cure.

He et al. (2012) studied the effect of annealing on phase separation of epoxy/ATBN adhesive. Real-time Fourier transform infrared (FTIR) measurement was utilized to confirm the drive force of phase-separation behavior (Fig. 12). It shows that the annealing at 50 °C did not create any obvious spectrum change (Fig. 12a). This result means that the sample does not undergo a further cross-linking at this temperature. However, the annealing at 150 °C had generated apparent changes in the IR spectrum (Fig. 12b); significant changes of the spectrum in the region of 3100–3700 cm^{-1} with the annealing time were observed (Fig. 2e). The absorption in this region is related to the different existing condition of the hydroxyl (OH) groups. Usually free OH groups have a band at a high frequency around 3650 cm^{-1} , while OH groups in hydrogen bonds have a broad band at a lower frequency of 3200–3400 cm^{-1} . Figure 12 apparently showed that the ATBN cured epoxy contained large amount of OH groups which was produced from the reaction between the epoxy groups and the amine groups. Because of the relatively short length of the epoxy hard segments, OH group will mostly be located in the small region of hard domains, meaning a high OH concentration in this area. This feature will be beneficial for the formation of hydrogen bonding interaction between the hydroxyl groups. It explains a broad absorption band from 3200 to 3400 cm^{-1} in the IR spectrum of the RT-cured sample. However, when the sample was annealed at 150 °C, which was much higher than the glass transition temperature of the epoxy

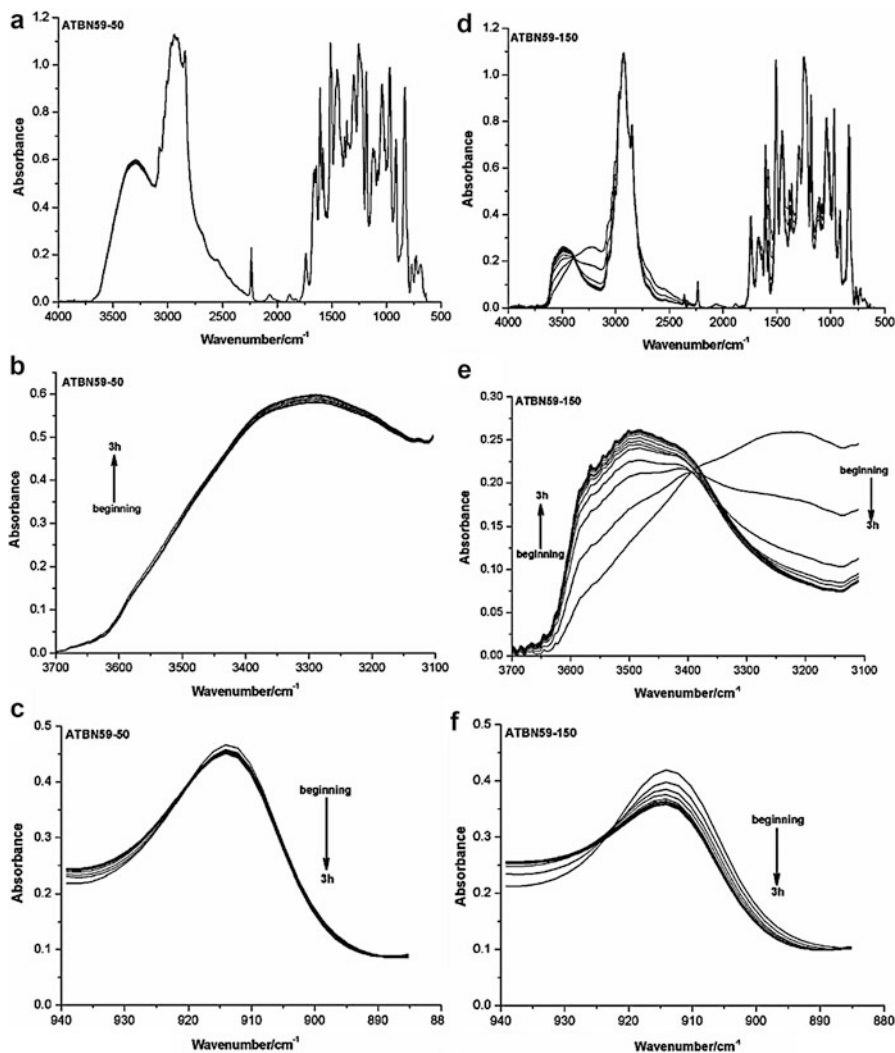


Fig. 12 Real-time FTIR spectra during the annealing process; full spectra (a), expanded region of 3100–3700 cm^{-1} (b) 880–940 cm^{-1} (c) of ATBN59-50, full spectra (d), 3100–3700 cm^{-1} (e) 880–940 cm^{-1} (f) of ATBN59-150 (Reprinted with permission from International Journal of Adhesion and Adhesives. (2012) 38, 11–16. Copyright 2012 Elsevier (He et al. 2008))

hard domain, the hard domain would be dissociated and the hard segments will mix with the soft segments of ATBN. This process would disperse the OH groups into the nonpolar matrix of the ATBN soft domain, preventing the OH groups from the formation of hydrogen bonds and resulting in a shift of the absorption to a higher frequency of $\sim 3500 \text{ cm}^{-1}$. This phenomenon in reverse proved the existence of the hard and soft domains once again in the RT-cured samples, and the improved mixing

of soft and hard segments in the 150 °C annealed samples. On the other hand, the annealing of the sample at 50 °C did not show this effect. This is because that the annealing temperature is much lower than the T_g of the hard domain (~95 °C). At this temperature, the hard domain will not dissociate. So the results' measurement indicated that this phenomenon was related to the disassociation of hydrogen bonding within the hard domain caused by the increased mixing of the hard segments into the soft domains by the high-temperature annealing.

Using FTIR Ismail et al. (2009) also tried to study the compatibilizing effect of epoxy resin on polypropylene/recycled acrylonitrile butadiene rubber blends (PP/NBRr). The results showed the OH stretching peak area in PP/NBRr-EP blends is larger than that in PP/NBRr blends and the peak of epoxy group appeared, which indicated the occurrence of reaction between epoxy and NBRr. At the same time, PP is more compatible with the epoxy resin because it contains a long nonpolar hydrocarbon chain. Therefore, the interfacial interaction between PP and NBR was improved by addition of epoxy resin into the PP/NBRr blends, and the compatibilizing effect of epoxy resin might be due to the chemical reaction between EP and NBRr and nonpolar physical interaction between EP and PP.

Combined with other tests, such as transmission electron microscopy (TEM), scanning electron microscope (SEM), and optical microscopy (OM), FTIR can be used to research the effect of types and reactivity of functional groups on the compatibility of epoxy/rubber blends. CTBN and HTBN were chosen to modify epoxy by Zeng et al. (2008). FTIR result showed both of CTBN and HTBN could be reacted with epoxy. The highly reactive -COOH group of CTBN reacted much better than the -OH group of HTBN. The micrograph synthesis showed that rubber particle size of EP/CTBN system is much smaller than that of EP/HTBN, indicating better interface adhesion and compatibility between the EP/CTBN blend. The different morphology observed in the two systems may be attributed to the different reactivities of these two rubbers: CTBN easily forms chemical interaction with EP and then decreases the chance of agglomeration, which was evidenced by FTIR. Polypropylene glycol/poly (ethylene glycol) copolymer (POPE) was functionalized with isocyanate groups by Soares et al. (2008) and polyether-based modifiers (with and without NCO groups) were used to improve the impact resistance of epoxy. The results showed POPE/EP blend presented two distinct phases while NCO-modified POPE/EP appeared visually transparent and homogeneous. This indicated that the preformed block copolymer was miscible with the epoxy matrix. Considering the result of FTIR, this behavior demonstrates that the isocyanate-functionalized polyether improved the interfacial adhesion and reduced the chance of phase separation even during the curing process.

The thermogravimetric process of epoxy/rubber can also be studied by FTIR (Grassie et al. 1979; Radhakrishnan 1999; Camino et al. 2001; Hamdani et al. 2009; Bao and Cai 2014). Chen et al. (2014) studied the TGA-FTIR spectra of the pyrolysis products of EG, epoxy resins with 40 wt% an epoxy-silicone copolymer with an epoxy value of 0.02–0.07 mol per 100 g and a siloxane content of 70%) (PSHG₄) and epoxy resins with 40 wt% Z-6018 (a mixture of phenyl, propyl silsesquioxanes (>60%) and a hydroxyl-terminated linear siloxane) (PSDG₄) at different times (Fig. 13). The synthesis of the pyrolysis products of EG showed

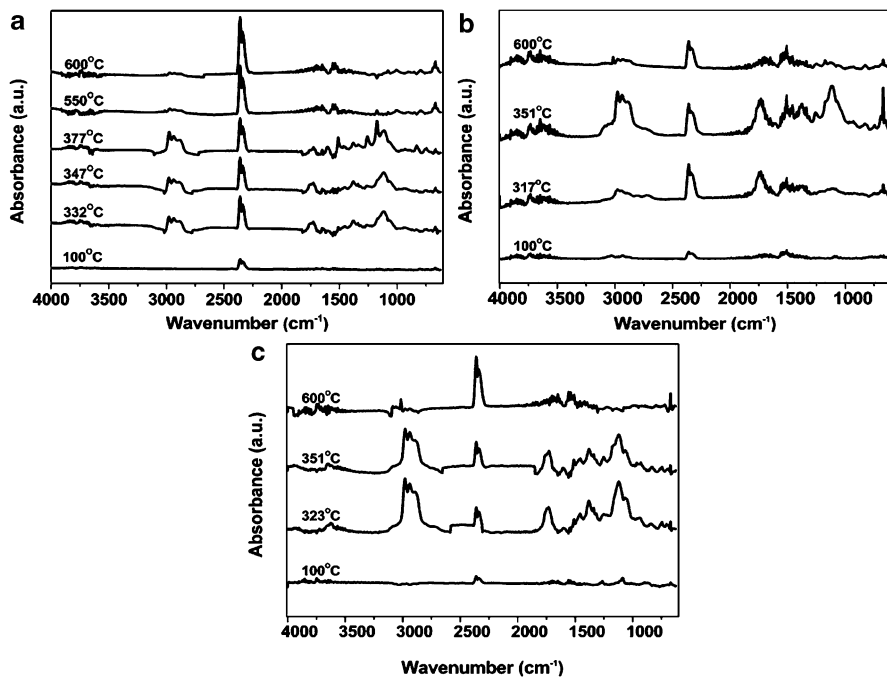


Fig. 13 FTIR spectra of volatile products recorded at the indicated temperatures for the decomposition of silicone-modified epoxy resins in a nitrogen atmosphere: (a) EG, (b) PSHG₄, (c) PSDG₄ (Reprinted with permission from RSC Advances. (2014) 4, 60685–60693. Copyright 2014 Royal Society of Chemistry (Chen et al. 2014))

water vapor was a predominant product. During the second step of thermal degradation, the characteristic peak of water still existed until 55 min (550 °C). The resultant water could be associated with the dehydration of the two hydroxy propyl groups of the phenoxy resin. The evolved gases also show bands at 2990–3020 cm⁻¹ and 1000–1300 cm⁻¹ which are related to the sp² and sp³ C–H stretching vibrations of para-disubstituted aromatic and aliphatic groups. The spectrum also revealed the presence of aldehyde-containing compounds by overlapping (C = O)–H stretches (around 2700 cm⁻¹ to 2900 cm⁻¹ and 1724 cm⁻¹) in the IR spectrum. The peaks that appeared at 3010 cm⁻¹ and 1316 cm⁻¹ are the characteristic peaks of CH₄. The spectrum showed the appearance of bands at 1608 cm⁻¹ at 340 °C and at 820 cm⁻¹, which could be attributed to the C = C stretching vibrations and the aromatic C–H stretching of para-disubstituted aromatic compounds, respectively. At 55 min (600 °C) the characteristic peaks of CO₂ and N–H appeared and the thermal degradation rates of these products were very low. As shown in Fig. 13b, c, the evolved gas analysis for PSHG₄ or PSDG₄ exhibited characteristic bands of compounds containing an –OH group (e.g., H₂O, phenol; 3500–3900 cm⁻¹), methyl-substituted compounds (CH₂/CH₃ stretching, 2890–3000 cm⁻¹), CO₂ (2330, 2360 cm⁻¹), compounds containing an aromatic ring (1320–1580 cm⁻¹,

823 cm^{-1}), hydrocarbons (C-H stretching at 1113 cm^{-1} , 1248 cm^{-1} , and 1172 cm^{-1}), and N-C (675 cm^{-1}). Consequently, it is noted that the main evolved gas products for EG were different from epoxy resins modified by SH023 or Z-6018. The main evolved gas products of EG were composed of small molecules, such as CO_2 . In another aspect, epoxy resins modified by SH023 or Z-6018 released mainly methyl-substituted, carbonyl, and aromatic gas products, which have higher molecular weights compared with that of the EG gas products.

Nuclear Magnetic Resonance (NMR) Spectroscopy

Nuclear magnetic resonance is one of the most powerful and flexible techniques with many applications (Abragam 1961; Rutledge 1997; Grant and Harris 2002). It can provide detailed structural information and physicochemical study of organic compounds, both small molecules and polymers, at atomic resolution. Information of chemical interest arises from the fact that nuclei of atoms in different chemical environments are also generally in quite different magnetic environments and come into resonance with a fixed frequency oscillator at different values of the applied magnetic field, thus giving access to details of the electronic structure of a molecule. In using NMR, it is possible not only to observe local nuclear interactions (e.g., dipole–dipole, chemical shift) to distinguish fine structural differences that elude these other measurements but also to study longer-range structure via spin diffusion, which allows the characterization of molecular homogeneity on a scale from the molecular level to a few hundred angstroms (Guo 1996).

An NMR spectrometer consists basically of a magnet, radio-frequency (RF) transmitter or oscillator, and a suitable RF detector. When a sample of a material comprised of atoms having nuclei with certain magnetic properties is placed in the magnet pole gap and subjected to the RF field of the oscillator, absorption of RF energy (resonance) occurs at particular combinations of the oscillator frequency and the magnetic field strength, and an RF signal is picked up by the detector. NMR uses the very weak interaction between a nucleus and the rest of the universe. The interaction between the magnetic moment of a nucleus and the RF field of an NMR receiver circuit is extremely weak. At first glance, this seems to be an enormous disadvantage as, for an equivalent sample mass, NMR has a much lower signal-to-noise ratio relative to many other spectroscopic techniques. However, the weak interaction also yields extremely high resolution. The weak interaction isolates the nucleus from external perturbation for long periods; relaxation times of the order of seconds are common and, conversely, line widths can be less than 1 Hz. Small changes to the environment at an NMR-active nucleus can be detected and identified. So it is obvious that NMR is a sensitive and effective method for deducing subtle details of molecular structure.

Sample Preparation

^1H -, ^{13}C -, and ^{29}Si -solution-state NMR techniques have been used to study epoxy/rubber blends. Solution-state NMR usually employs a 300–600 MHz NMR spectrometer. Several milligrams of pure sample is weighed and dissolved in 2 ml of deuterated

solvent (typically fully deuterated chloroform, acetone, benzene, or dichlorobenzene), then the solution is moved to high-precision glass sample tubes and sealed.

NMR Analysis of Epoxy/Rubber Blends

As mentioned above, NMR spectroscopy could afford more detailed information than FTIR spectrum. Apart from the qualitative analysis of chemical structure of epoxy/rubber blends, the stereoregularity and molecular weight can also be studied. Combining NMR and FTIR, more detail and comprehensive information of chemical structure and functional groups could be achieved, which is conducive to study the driving forces producing miscibility in epoxy/rubber blends. ^{13}C -NMR can directly achieve the information of functional groups without H atoms ($\text{C}=\text{O}$, $\text{C}=\text{C}=\text{C}$, $\text{N}=\text{C}=\text{O}$, etc.) and molecular skeleton which cannot be obtained from ^1H -NMR. Since the range of chemical shift is wider, the resolution capability is better than ^1H -NMR. Besides, ^{29}Si -NMR is usually used in epoxy/silicone rubber system.

From the chemical shift in the NMR spectroscopy, the chemical structure of epoxy/rubber blends can also be qualitatively analyzed. Diglycidyl ether of bisphenol A epoxy was modified with hydroxyl-terminated polydimethylsiloxane (HPDMS), through ring-opening addition polymerization reaction by Ahmad et al. (2005). The structural elucidation of the siloxane-modified epoxy resin was carried out by ^1H -NMR spectroscopic techniques with CDCl_3 as solvent (Fig. 14).

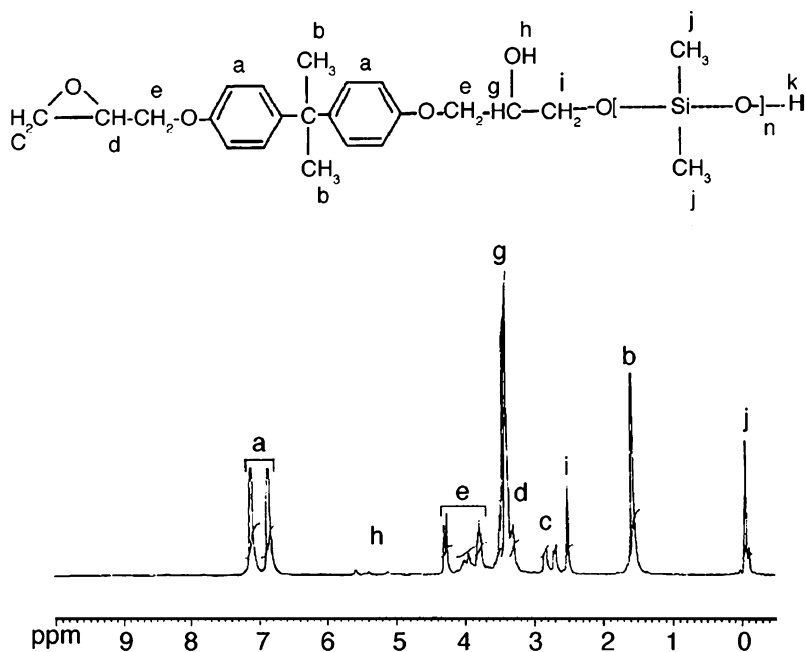
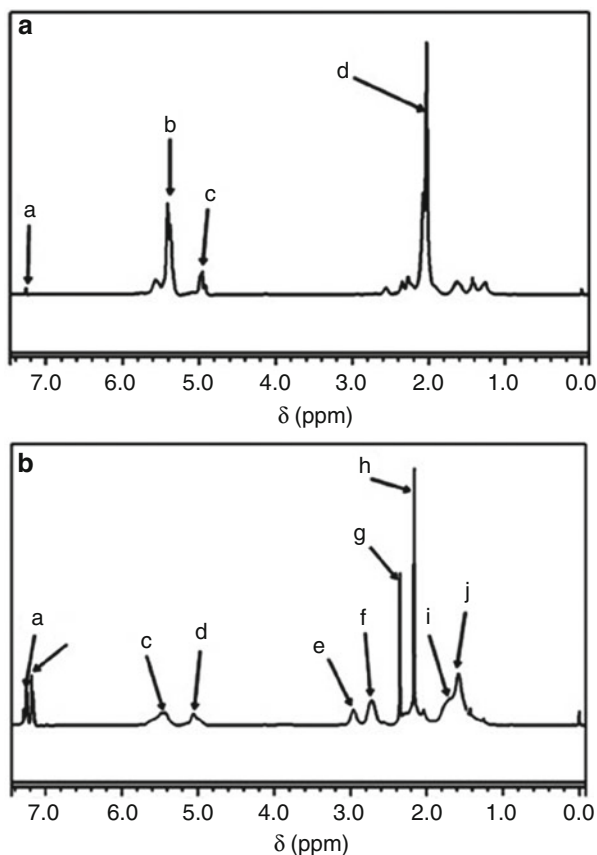


Fig. 14 ^1H NMR spectra of epoxy siloxane (Reprinted with permission from Progress in Organic Coatings. (2005) 54, 248–255. Copyright 2005 Elsevier (Ahmad et al. 2005))

Epoxy siloxane resin ($^1\text{H-NMR}$, CDCl_3) δ (ppm): 7.11–6.8 (aromatic ring protons), 5.58 (OH), 4.28–4.24 (CH-OH), 4.19 ($-\text{CH}_2\text{-O-Ar}$), 3.55–3.48 ($-\text{CH}_2\text{OH}$), 3.33–3.29 ($-\text{CH}$ oxirane), 2.8–2.69 ($-\text{CH}_2$ oxirane), 2.5 ($\text{CH}_2\text{-O-Si}$), 1.56 ($-\text{CH}_3$), and 0.064 ($-\text{CH}_3\text{-Si}$).

Researchers also tried to report the stereoregularity of the material in epoxy/rubber blend. Typical $^1\text{H-NMR}$ spectra of the CTBN and epoxidized CTBN (ECTBN) were reported by Zhao et al. (2015), shown in Fig. 15. The ^1H NMR spectrum of CTBN shows two signals at $\delta_b = 5.43$ ppm and $\delta_c = 4.98$ ppm, which are associated with the olefinic protons of the 1,4- and 1,2-butadiene units, respectively (Fig. 15a). Besides, the two signals (a and d) at $\delta_a = 7.26$ ppm and $\delta_d = 2.03$ ppm can be attributed to the protons attached to the deuterated chloroform and $-\text{H}_2\text{C}-$ groups for 1,4-butadiene units, respectively. The $^1\text{H-NMR}$ spectrum of ECTBN shows two new signals at $\delta_e = 2.96$ ppm and $\delta_f = 2.72$ ppm (Fig. 15b), which can be related with the protons attached to the cis- and trans-epoxy groups, respectively, thereby conforming the occurrence of CTBN epoxidation. In addition, three new signals at $\delta_h = 2.17$ ppm, $\delta_i = 1.70$ ppm, and $\delta_j = 1.58$ ppm correspond

Fig. 15 $^1\text{H-NMR}$ spectra of the CTBN (a) and ECTBN (b) (Reprinted with permission from Iranian Polymer Journal. (2015) 24, 425–435. Copyright 2015 Springer (Zhao et al. 2015))



to $-H_2C-$ groups for 1,4-epoxidized butadiene units and $-HC-$ aliphatic groups for epoxidized units, respectively. Besides, the new signals at $\delta_a = 7.25$ ppm, $\delta_b = 7.17$ ppm, and $\delta_g = 2.35$ ppm could be attributed to the protons attached to the residual toluene solvent after rotary evaporation.

Through the synthesis of the ratio of integration intensity in 1H -NMR spectroscopy of modifiers used in epoxy/rubber, the overall molecular weight of the modifier could also be estimated (Xu and Zheng 2007; Yang et al. 2009). PCL-b-PBN-b-PCL triblock copolymer was synthesized and used to toughen epoxy thermosets via the formation of nanostructures by Yang et al. (2009). The 1H -NMR spectrum of the copolymer is shown in Fig. 16. The resonances of protons from PCL and PBN blocks are indicated in this spectrum. In terms of the ratio of integration intensity of the terminal hydroxymethylene proton ($-CH_2-OH$, $\delta = 3.86$ ppm) to other methylene protons of PCL ($OCOCH_2CH_2CH_2CH_2CH_2$, $\delta = 1.35-1.41$ ppm; $OCOCH_2CH_2CH_2CH_2CH_2$, $\delta = 1.60-1.68$ ppm; $OCOCH_2(CH_2)_4$, $\delta = 2.28-2.38$ ppm; $OCO(CH_2)_4CH_2$, $\delta = 4.04-4.07$ ppm), the length of PCL can be calculated to be $M_n \approx 2600$. According to the length of PCL, the overall molecular weight of the triblock copolymer was estimated to be $M_n = 7700$, which is in a good agreement with the value predicted with the feed ratio.

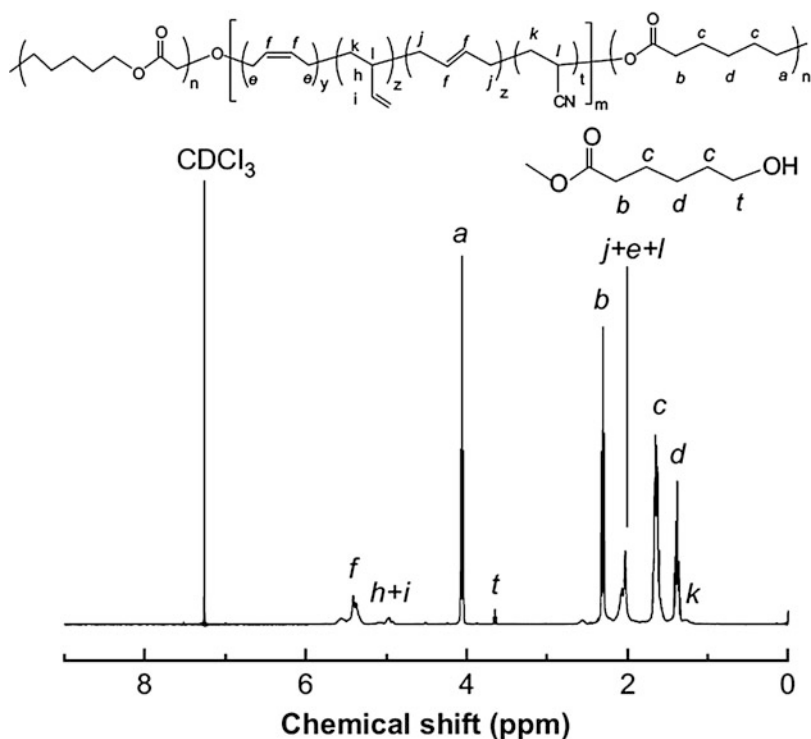


Fig. 16 1H -NMR spectrum of PCL-b-PBN-b-PCL triblock copolymer (Reprinted with permission from Polymer. (2009) 50, 4089–4100. Copyright 2009 Elsevier (Yang et al. 2009))

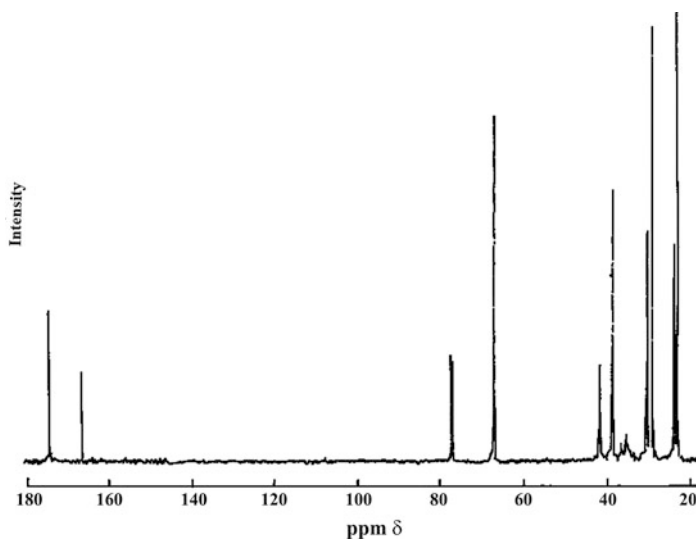


Fig. 17 ^{13}C -NMR spectrum of CTPEHA (Reprinted with permission from Journal of Applied Polymer Science. (2001) 80, 1792–1801. Copyright 2001 John Wiley & Sons, Inc. (Ratna et al. 2001))

Apart from ^1H -NMR, ^{13}C -NMR spectrum is always a most widely used nuclear magnetic resonance spectroscopy (Lin and Huang 1996; Ratna et al. 2001; Kumar et al. 2002; Bhuniya and Adhikari 2003; Ahmad et al. 2005; Park et al. 2005; Deng et al. 2012). Carboxyl-terminated poly(2-ethylhexyl acrylate) (CTPEHA) was synthesized by bulk polymerization in the form of liquid rubber and characterized by ^{13}C -NMR spectroscopic analysis (Ratna et al. 2001). The ^{13}C -NMR spectrum for CTPEHA is shown in Fig. 17. The NMR spectrum clearly shows two peaks for carboxyl and ester carbon. The peaks at 174–174.4 and 166 ppm can be attributed to the presence of the ester and carboxylic acid carbon, respectively. The higher intensity of the ester peak can be explained due to that the carboxyl groups are present only in the terminal position, whereas every repeat unit of the oligomer has an ester group. The peak at 77 ppm is due to the solvent CDCl_3 . The peaks at 41 and 36 ppm are due to the carbon atom attached to $-\text{O}$ and the $-\text{C}=\text{O}$ group, respectively. The rest of the peaks at 30–10 ppm are for aliphatic carbon atoms.

^{29}Si -NMR is usually applied in epoxy/silicone rubber system (Chiang and Ma 2002; Lee et al. 2006; Liu et al. 2010; Ma et al. 2010a, b). The microstructures of modified epoxy composite were studied by solid-state ^{29}S -NMR spectrum (Chiang and Ma 2002). Figure 18 displays the solid-state ^{29}Si -NMR spectrum of the epoxy nanocomposite. In condensed siloxane species for tetraethoxysilane (TEOS), silicon atoms through mono-, di-, tri-, and tetrasubstituted siloxane bonds are designated as Q^1 , Q^2 , Q^3 , and Q^4 , respectively. The chemical shifts of Q^2 , Q^3 , and Q^4 are -91 , -101 , and -109 ppm, respectively. For 3-isocyanatopropyltriethoxysilane and diethylphosphatoethyl-triethoxysilane, mono-, di-, tri-, and tetrasubstituted siloxane bonds are designated as T^1 , T^2 , T^3 , T^4 . The chemical shifts of T^2 and T^3 are -56 and

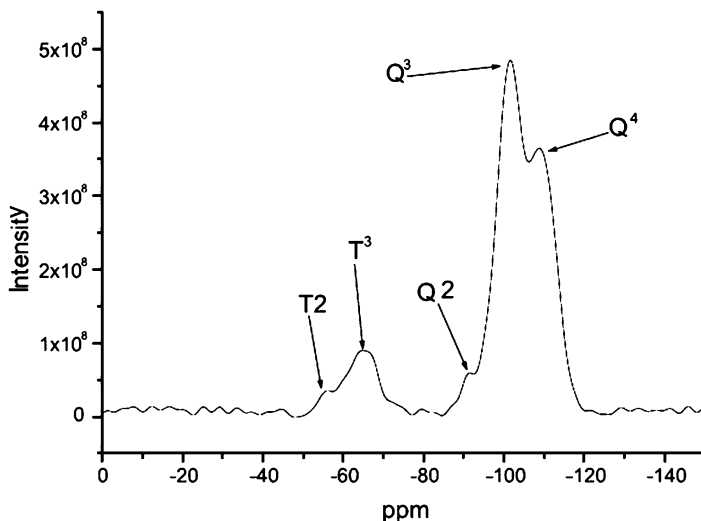


Fig. 18 Solid-state ^{29}Si -NMR spectrum of modified epoxy nanocomposite (Reprinted with permission from European Polymer Journal. (2002) 38, 2219–2224. Copyright 2002 Elsevier (Chiang et al. 2002))

–65 ppm, respectively, and conform to the literature values. Results revealed that Q^4 , Q^3 , and T^3 are the major microstructures forming the network structure.

Raman Spectroscopy

Raman effect, which was first discovered in 1927, is a light-scattering effect. In the Raman effect, incident light is elastically scattered from a sample and shifted in frequency by the energy of its characteristic molecular vibrations. The advent of laser light sources with monochromatic photons at high flux densities was a milestone in the history of Raman spectroscopy and resulted in dramatically improved scattering signals. Although both Raman spectroscopy and Fourier transform infrared spectroscopy are molecular vibrational spectroscopy, their principles are largely different. Fourier transform infrared spectroscopy is absorption spectra, while Raman spectroscopy is the scattering spectrum. Raman spectrometers are used to analyze light scattered by molecules.

When the sample was irradiated by an exciting monochromatic beam, part of the incident light will be scattered, and the energy of the molecules also will be changed (Fig. 19). In order to induce in the molecule a virtual energy state, the exciting monochromatic beam must be of high intensity (laser beam). Most of the molecules relax directly back to the E_0 state, whereby light of the same wavelength as the exciting light is emitted (Rayleigh scattering). Only a very small percentage of the excited molecules relax back to a vibrationally excited state; hence, the emitted

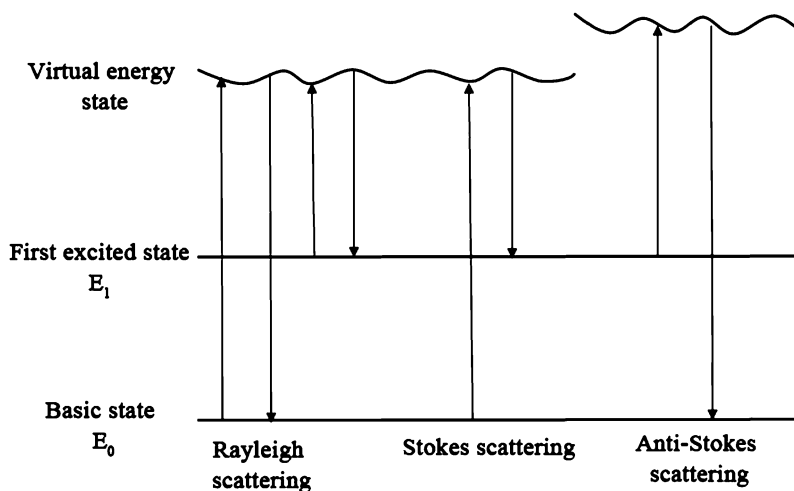


Fig. 19 Diagram of the energy state in Raman scattering

photons have smaller energy than the exciting photons (Stokes scattering). Molecules, which were originally in a vibrationally excited state, can after excitation relax to the ground state, emitting photons of higher energy than the exciting ones (anti-Stokes scattering). The latter two are collectively referred to as Raman scattering. Only Stokes scattering will be recorded in the experiments. Because the energy of Stokes scattering photons is smaller than incident light, the frequency will shift to lower wave number. In the Raman spectra, the variation of the wave number is the abscissa, and the ordinate is the strength of the Stokes scattering.

Because Raman scattering is always of very low intensity, its investigation requires high-quality instrumentation. A Raman spectrometer has to combine very good filter characteristics for eliminating Rayleigh and Tyndall scattering with high sensitivity for detecting very weak Raman bands. Currently, there are three types of Raman instruments available on the market: Raman grating spectrometer with single channel detector, FT-Raman spectrometer with NIR excitation, and Raman grating polychromator with multichannel detector. All three types of the instruments have particular advantages and disadvantages for a given analytical task.

As with optical spectroscopy, the Raman effect can be applied noninvasively under ambient conditions in almost every environment. Compared with infrared absorption spectroscopy, measuring a Raman spectrum does not require special sample preparation techniques and is especially suitable for aqueous solutions. Besides, the major advantage of Raman spectroscopy is the high spatial resolution that can be obtained, typically in the order of $1\ \mu\text{m}$ (compared to approximately $10\ \mu\text{m}$ in case of IR).

Sample Preparation

In the past few years, the range of excitation wavelengths has been extended to the near-infrared (NIR) region, in which background fluorescence is reduced and photo-

induced degradation from the sample is diminished. High-intensity NIR diode lasers are easily available, making this region attractive for compact, low-cost Raman instrumentation. In many cases, the sample does not need special treatment. Powders, blocks, tablets, or films can be directly used to measure. Liquid sample could first be mounted in a transparent container (e.g., tube without fluorescent).

Raman Analysis of Epoxy/Rubber Blends

Compared with FTIR spectrum, the relationship between frequency and functional groups is almost the same in Raman spectroscopy. The differences are that some spectral bands are observed both in Raman and FTIR spectrum with different intensity, while some are just in one spectrum. For example, the symmetrically substituted C = C and N = N bands could not be found in FTIR spectroscopy while observed in Raman. IR spectroscopy allows the study of the absolute and relative concentrations of epoxy groups in polymers. For epoxy polymer blends that contain other polymers with IR spectra absorption band at 915 cm^{-1} (characteristic vibration of the epoxy ring), the quantitative analysis of the epoxy group concentration using the intensity of these bands is quite difficult. As a consequence, Raman spectra are often used to follow the reaction of epoxides with carboxylic acids instead of IR. A number of bands in the Raman spectra were used for quantitative and qualitative analysis of the reaction, including kinetic measurements. The results obtained can be used for the analysis of epoxide reactions on a rubber surface and, moreover, in a rubber resin mixture and plastic constructions.

The effect of the epoxidation reaction on the microstructure of the epoxidized and hydroxyl-terminated polybutadiene resin (brand name Poly bd resin) chains was studied by Bussi and Ishida through FTIR spectroscopy, FT-Raman spectroscopy, and $^1\text{H-NMR}$ (Bussi and Ishida 1994). The results of FTIR and Raman showed that the internal oxirane exhibits two characteristic absorption frequencies in the region of $600\text{--}1200\text{ cm}^{-1}$, a broad, weak, symmetric in-plane ring deformation (I) at 816 cm^{-1} and a stronger antisymmetric mode (II) at 885 cm^{-1} . In general, (I) and (II) appear at lower frequency for an internal oxirane than for a terminal oxirane. The position of the lower frequency band was used to distinguish between monosubstituted (epoxidized vinyl unsaturation), disubstituted (epoxidized *cis*- or *trans*-unsaturation), and trisubstituted oxirane. Along with $^1\text{H-NMR}$, it is known that only *cis*- and *trans*-units undergo epoxidation, while vinyl units remain unaffected.

Optical Microscopy (OM)

OM is a technology that gets an image-magnified small specimen with visible light and using a system of lenses. It consists of transmission and reflection modes, and the former is only used to research transparent materials. Compared with transmission electron microscopy and scanning electronic microscopy, OM is a powerful tool for analyzing fracture surface morphology and toughening mechanisms of epoxy resin (EP)/rubber composites.

Sample Preparation

A petrographic polishing technique was employed to investigate damage zones around crack tips and the behavior of rubber particles in the damage zone. The details of this technique have been published by Holik et al. (1979). The technique is briefly explained as follows. A section in the vicinity of the damaged specimen is cut out using a low-speed diamond saw. The section taken from the damaged specimen is potted in a clear epoxy resin which cures at room temperature. The surface of this sample is ground and finely polished using alumina powder. Then, the surface of the polished sample is mounted onto a clean slide glass using clear epoxy resin adhesive. This sample is allowed to cure overnight at room temperature. Excess resin is removed using a diamond saw, and the sample is again ground and polished until the plane of interest is finally reached. To best observe dispersed particles in the matrix resin, the thin section should be 20–200 μm thick. The sample can be polished down to about 100 μm to measure the damage zones. A thinner sample is needed to observe the shapes of individual rubber particles.

Synthesis and Application of OM

OM is a very simple and facile approach to analyzing the microstructure, toughness mechanism (Liang and Pearson 2010; Le et al. 2010), and fracture behaviors (Chen and Lee 1995; Azimi et al. 1996; Klug and Seferis 1999; Ma et al. 2008) of EP/rubber composites; for example, the damage zone around crack tip and rubber particles near the damage zones of EP/CTBN composites (Lee et al. 2002), residual microstress between EP and rubber particles (Wang et al. 1992b), fracture mechanisms of epoxy-based ternary composites filled with rigid-soft particles (Tang et al. 2012), morphology of ternary blends of epoxy, poly(ether sulfone), and acrylonitrile butadiene rubber (Horiuchi et al. 1994), epoxy modified by CTBN (Chonkaew and Sombatsompop 2012), fracture surface of epoxy adhesive modified with acrylate-based liquid rubber (Ratna and Banthia 2000), silicone-modified epoxy (Sobhani et al. 2012), morphology of a three-component hybrid system with cubic silsesquioxane epoxy nanocomposites and core-shell rubber (CSR) particles (Choi et al. 2004).

The phase-separation process of a rubber-modified epoxy system during curing was studied by Chen (Chen and Lee 1995). The morphological changes were recorded in real time by means of optical microscopy. Optical micrographs show that a binary mixture of the epoxy oligomer and CTBN liquid rubber was heterogeneous at room temperature. The well-dispersed spherical CTBN domains gave the epoxy-CTBN systems (without dicyandiamide (DICY), the curing agent) a turbid or snowy appearance. When the temperature was elevated, e.g., to 80 °C, the mixture changed to a homogeneous system. When the homogeneous mixture was cooled down slowly, the clear solution became cloudy, at which point, depending on cooling rate, rubber particles formed. The rubber droplets appeared as tiny dots at the beginning, and then the diameter of the droplets grew gradually to around 10 μm . Owing to the low viscosity of DGEBA, some smaller spherical domains migrated into larger domains and coalesced.

Figure 20 shows representative optical micrographs observed at various stages for the curing B-8-2 (epoxy/DICY/CTBN = 100/4/2 phr) system at 150 °C.

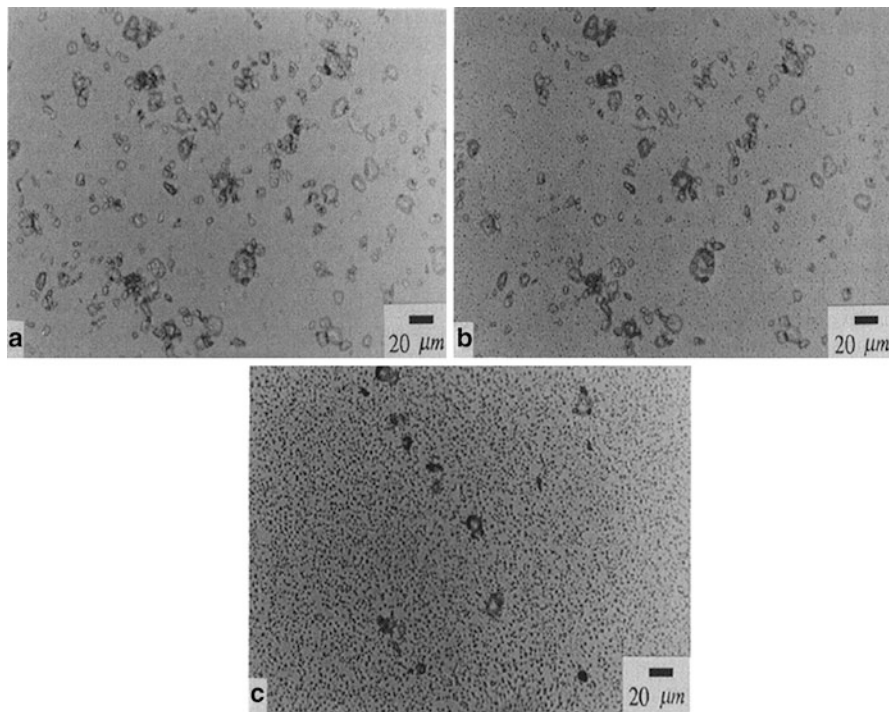


Fig. 20 Transmission light micrographs of B-8-2 sample cured at 150 °C. (a) 35 min, (b) 74 min, (c) 101 min (Reprinted with permission from Polymer. (1995) 36, 55–65. Copyright 1995 Elsevier (Chen et al. 1995))

Immediately after the temperature jumped from room temperature to the curing temperature, the epoxy/rubber mixture was homogeneous (Fig. 20a). The DICY powder (melt temperature 209–212 °C) was dispersed as islands in the epoxy/rubber mixture. At the early stage, the spherical CTBN domains dissolved, shrank, and disappeared. In the meantime, the DICY powder dissolved gradually as the cure continued. After a certain time elapsed, many tiny spots appeared, resulting in a fairly regular microscopic texture, i.e., phase separation (Fig. 20b). Then the image contrast of the texture became strong and the average diameter of the spots grew gradually with cure time (Fig. 20c). Finally, the diameter of the spherical second phase was fixed around 3 μm. The final morphology was arrested well before gelation.

Ratna and Banthia (2000) investigated the adhesive and mechanical properties of epoxy resins modified with carboxyl-terminated poly(2-ethylhexyl acrylate) (CTPEHA) liquid rubber. The adhesive and impact properties initially increased and reached a maximum with 10–15 phr of CTPEHA before decreasing. To correlate the molecular and morphological parameters with the fracture properties of the toughened networks, the microstructures of the fracture surfaces of various

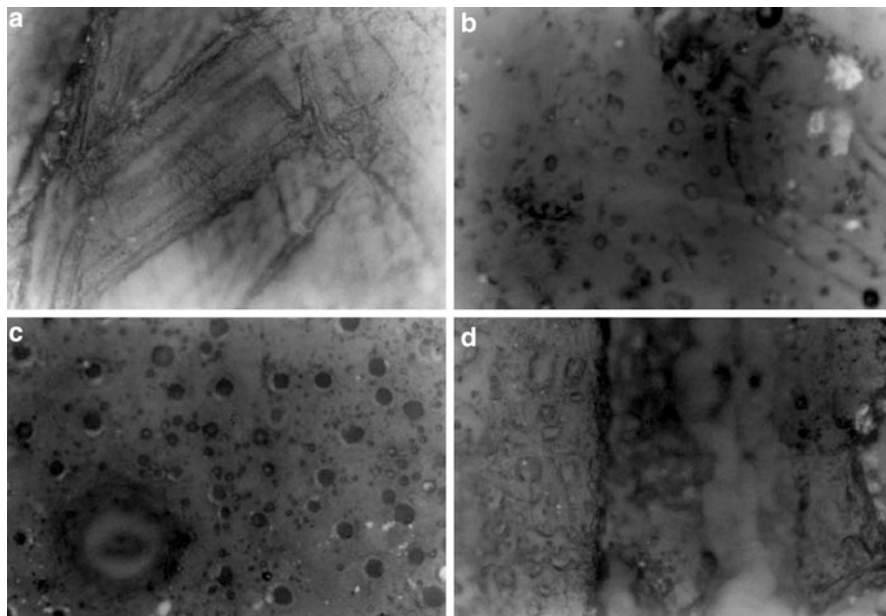


Fig. 21 Micrographs of the fracture surfaces of (a) unmodified epoxy, (b) 10 phr CTPEHA containing epoxy, (c) 20 phr CTPEHA containing epoxy, (d) 30 phr CTPEHA containing epoxy (Reprinted with permission from Polymer International. (2000) 49, 281–287. Copyright 2000 John Wiley and Sons (Ratna et al. 2000))

CTPEHA liquid-rubber-modified networks were analyzed by optical microscopy (OM). The micrographs for unmodified and modified networks are shown in Fig. 21. The fracture surface of the unmodified epoxy is homogeneous without any dispersed particles, whereas the fracture surfaces of modified networks consist of two distinct phases: globular particles are dispersed in a continuous epoxy matrix. The number of particles increases with an increase in the concentration of CTPEHA. The modified epoxy networks having 10 phr of liquid rubber contain rubber particles uniformly distributed throughout the matrix. The aggregation starts at higher concentration. This explains why the impact and adhesion properties attain a maximum value at about 10–15 phr and subsequently decrease.

Toughness mechanism of EPs modified by ATBN rubber and recycled tire particles was studied by Abadyan et al. (2012). When 7.5 phr small particles (ATBN) and 2.5 phr large particles (recycled tire) were incorporated, the fracture toughness (K_{IC}) measurement of the composites revealed synergistic toughening in the composites. Transmission optical micrographs (Fig. 22) showed different toughening mechanisms for the blends; fine ATBN particles increased the toughness by increasing the size of the damage zone and respective plastic deformation in the vicinity of the crack tip. However, in the case of hybrid resin, coarse recycled rubber particles acted as large stress concentrators and resulted in the branching of the

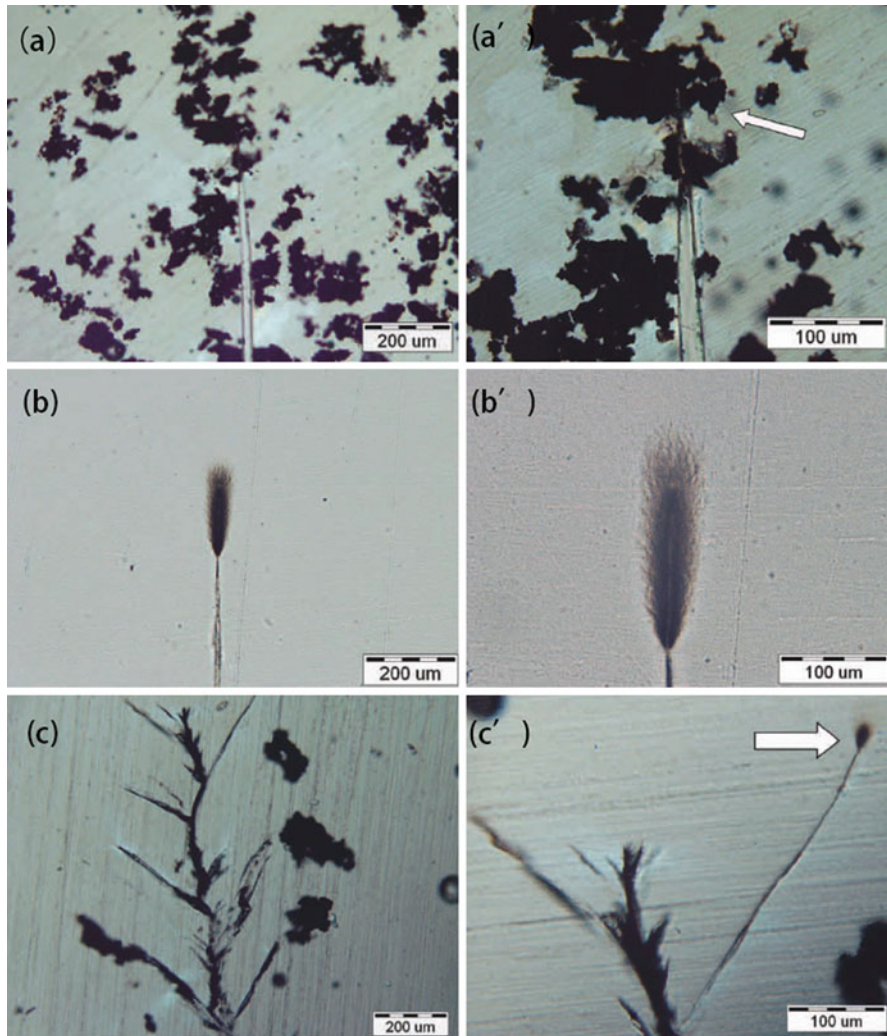


Fig. 22 TOM micrographs taken from the midplane of the crack-tip damage zones under bright-field conditions. On the left are (a) recycled-rubber-modified (T10), (b) ATBN-modified (A10), and (c) hybrid-modified (A*10) systems specimens, respectively. On the right are the corresponding crack wakes at higher magnifications. The crack-growth direction is from bottom to top. It shows that T10 system has no evidence of a process zone at the crack tip, A10 system is typical for rubber-toughened epoxies, where the cavitated particles induce massive shear deformation and A*10 specimen illustrates a highly branched damage zone, where the crack defects and branches toward the large rubber particles (Reprinted with permission from *Journal of Applied Polymer Science*. (2012) 125, 2467–2475. Copyright 2012 John Wiley and Sons (Abadyan et al. 2000))

original crack tip. Mode mixity at the branch tips led to synergistic K_{IC} in the hybrid system. The ductility of the matrix played an effective role in the nature of the crack-tip damage zone in the hybrid epoxies.

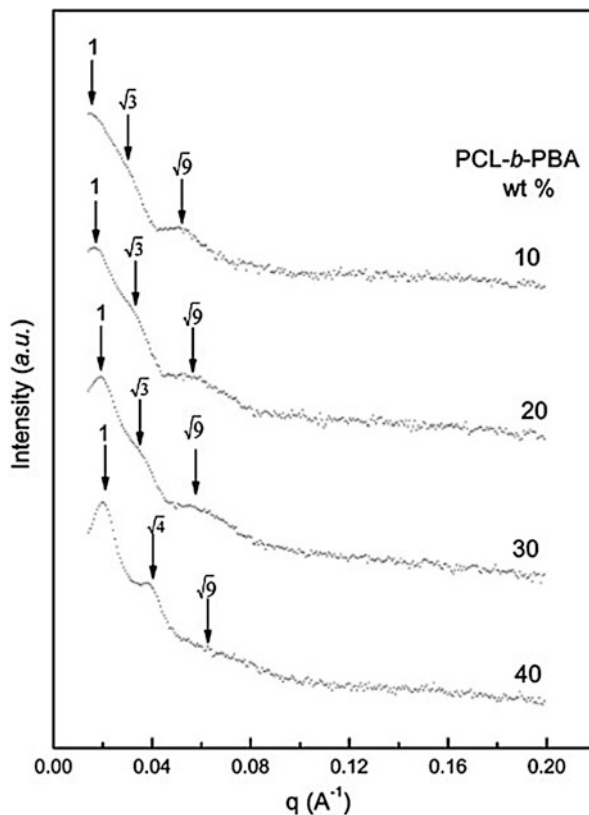
X-Ray Scattering

A very popular method of characterizing the polymer blends for their phase behavior is X-ray scattering. We know that blends may be made of a pair of polymers in which either one or both components are crystalline. The state of compatibility for such blends may be deduced by X-ray scattering studies. A survey of recent studies indicates that several binary blends of crystalline and amorphous polymers have been investigated using X-ray scattering techniques, both small-angle X-ray scattering (SAXS) and wide-angle X-ray scattering (WAXS).

Small-Angle X-Ray Scattering (SAXS)

Good examples of the application of SAXS are the analysis of the formation and changes of nanostructures in the epoxy/rubber (Grubbs et al. 2000; Hsu and Liang 2007; Xu and Zheng 2007; Yang et al. 2009). The nanostructures in epoxy/rubber thermosets were investigated by means of SAXS (Xu and Zheng 2007). The SAXS profiles of the thermosets containing 10, 20, 30, and 40 wt% of PCL-b-PBA diblock copolymer are shown in Fig. 23. It is seen that the well-defined scattering peaks were observed in all the cases, indicating that the thermosets containing PCL-b-PBA are

Fig. 23 SAXS profiles of the thermosets containing PCL-b-PBA diblock copolymer. Each profile has been shifted vertically for clarity (Reprinted with permission from *Macromolecules*. (2007) 40, 2548–2558. Copyright 2007 American Chemical Society (Xu et al. 2007))



microphase separated. In addition, it is noted that all the SAXS profiles possess the multiple scattering maxima as denoted with the arrows, indicating that the thermosets could possess long-range ordered microstructures. The positions of the scattering maxima remain essentially constant, apart from slight shifts to the higher q values with increasing the content of PCL-b-PBA. According to the position of the primary scattering peaks, the principal domain spacing d_m can be obtained to be 39.7, 36.9, 32.4, and 31.7 nm for the thermosets containing 10, 20, 30, and 40 wt% PCL-b-PBA diblock copolymer, respectively. It is noted that the average distance between neighboring domains decreased with increasing the content of the diblock copolymer. The slight shifts of the scattering maxima could be associated with local rearrangement leading to an enhancement of the long-range order. The scattering peaks of the thermosets situated at q values of 1, $\sqrt{3}$, and $\sqrt{9}$ relative to the first-order scattering peak positions (q_m) are discernible. It is plausible to propose that these are the lattice scattering peaks of spherical (or cylindrical) nanophases arranged in cubic lattices such as body-centered cubic (bcc), face-centered cubic (fcc), or simple cubic symmetries. In addition, hexagonally packed cylinder morphology is also possible.

The changes of the microstructures of epoxy/rubber blends before and after being cured have been studied by Grubbs et al. (2000). Neat B1x87 (symmetric poly(1,2-butadiene)-block-poly(epoxy-1,4-isoprene-*ran*-1,4-isoprene) copolymer, 87 represents the percentage of isoprene repeat units epoxidized) self-assembles into a lamellar (L) morphology with a principal spacing $d^* = 23.1$ nm at room temperature (Fig. 24). As diglycidyl ether of bisphenol A epoxy (BPA348) and 4,4'-

Fig. 24 SAXS patterns for uncured B1x87/BPA348/MDA blends: (a) B1x87, (b) 75 wt%, (c) 65 wt%, (d) 50 wt%, (e) 35 wt%, and (f) 15 wt% B1x87. Marked values indicate multiples of q^* . Unlabeled markers correspond to multiples above given pattern. Assigned microstructures: L lamellae, H hexagonal cylinders, S ordered spheres, M spherical micelles. Patterns are progressively shifted two decades vertically for clarity (Reprinted with permission from Macromolecules. (2000) 33, 9522–9534. Copyright 2000 American Chemical Society (Grubbs et al. 2000))

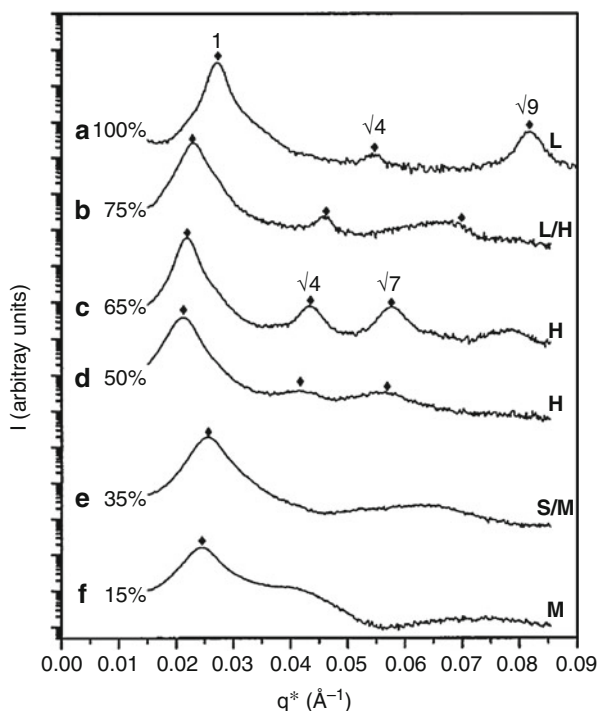
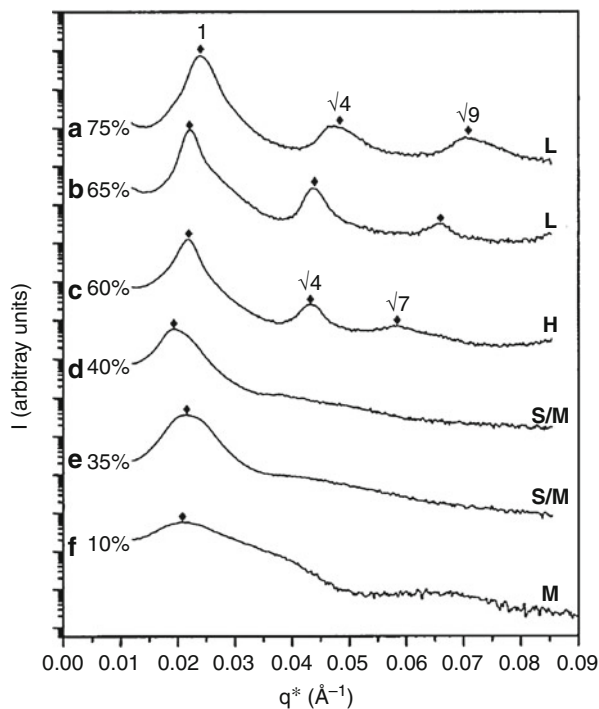


Fig. 25 SAXS patterns for cured **B1x87**/BPA348/MDA blends: (a) 75 wt%, (b) 65 wt%, (c) 60 wt%, (d) 40 wt%, (e) 35 wt%, and (f) 10 wt% **B1x87**. Microstructures are assigned as in Fig. 24. Patterns are progressively shifted two decades vertically for clarity (Reprinted with permission from *Macromolecules*. (2000) 33, 9522–9534. Copyright 2000 American Chemical Society (Grubbs et al. 2000))



methylenedianiline (MDA) selectively swell the PIOx (poly-(epoxy-1,4-isoprene-ran-1,4-isoprene)) block, interfacial curvature increases as cylindrical (H), spherical (S), and micellar (M) morphologies are expressed. The presence of local SAXS maxima at values of $\sqrt{4}q^*$ and $\sqrt{9}q^*$ points to the presence of lamellar morphologies at high copolymer concentrations (Fig. 24b). At concentrations between 40 and 70 wt%, scattering maxima at ratios of $q^*:\sqrt{4}q^*:\sqrt{7}q^*$ indicate self-assembly of the blends into hexagonal cylindrical morphologies (Fig. 24c, d). At lower concentrations, the breadth of the scattering maxima preclude differentiation between ordered spherical and spherical micellar arrangements, but it is clear from the length scales involved that the spheres are well dispersed in the epoxy matrix (Fig. 24e, f). After complete cure, the same range of morphologies is retained, yet, as was observed with symmetric copolymers, there is a shift toward morphologies with decreased interfacial curvature (Fig. 25). For example, at 65 wt% B1x87, the uncured blend self-assembles into a cylindrical morphology (Fig. 24c). After completion of the curing process, SAXS patterns for this blend exhibit maxima in the ratio $q^*:\sqrt{4}q^*:\sqrt{9}q^*$, consistent with the less-curved lamellar morphology (Fig. 25b).

Wide-Angle X-Ray Scattering (WAXS)

For wide-angle X-ray scattering, measurements are usually done in reflection mode. The intensity counts collected were corrected for polarization and absorption and in respect to air scatter. The corrected intensity was smoothed and plotted versus the

scattering angle (2θ). The position of the “peak maximum” was computed from the Bragg diffraction equation:

$$n\lambda = 2d\sin\theta \quad (1)$$

where n = order of reflection, λ = wavelength of radiation, d = interplanar distance, and θ = Bragg’s diffraction angle.

The average interchain separation $\langle R \rangle$ in Angstrom that gives rise to the strong maximum in the equatorial scan can be calculated from the following equation:

$$\langle R \rangle = 5/8 (\lambda/\sin\theta) \quad (2)$$

where θ = diffraction maximum angle.

The half-width $\langle HW \rangle$ of the WAXS amorphous maximum is the qualitative expression of the distribution of $\langle R \rangle$ and is calculated from the diffraction plot of scattering angle (2θ) versus intensity. Using the Bragg’s equation, the “ d ” spacings are determined for the strong maximum at half-height intensity. The half-width is the difference between these two calculated “ d ” spacings. An example of the calculation for $\langle R \rangle$ and $\langle HW \rangle$ for an amorphous system is shown in Fig. 26.

Wide-angle X-ray scattering is also a useful method in the study of epoxy/rubber (Nigam et al. 1998, 1999). WAXS has been applied to investigate the mechanism of toughening of epoxy cresol novolac resin (ECN) due to the addition of carboxyl-terminated polybutadiene (CTPB) liquid functional rubber (Nigam

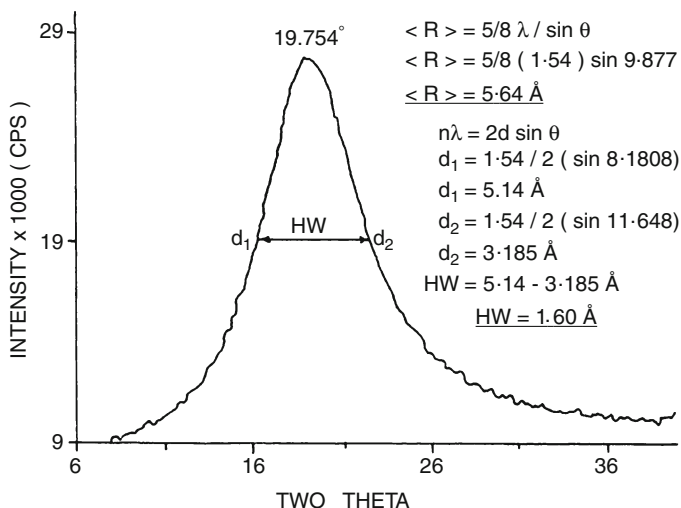


Fig. 26 Calculation of $\langle R \rangle$ and $\langle HW \rangle$ of an amorphous system (Reprinted with permission from Journal of Applied Polymer Science. (1998) 70, 537–543. Copyright 1998 John Wiley and Sons (Nigam et al. 1998))

et al. 1998). The WAXS studies of neat epoxy and the ECN–CTPB blends showed a steady increase of $\langle HW \rangle$ with increasing rubber concentration up to 15 wt%, beyond which $\langle HW \rangle$ increases abruptly. Interchain spacing $\langle R \rangle$ also shows a similar trend as the CTPB concentration in the blends is increased. From 5 to 15 wt% CTPB, the blends show a slow increase in $\langle R \rangle$, which is then followed by a sharp rise in the case of 25 wt% rubber. Nature of changes in the $\langle HW \rangle$ and $\langle R \rangle$ values thus signifies the development of a new molecular structure and stretching of the molecular chains further apart, resulting in an increase of interchain spacing. In the case of ECN–CTPB blends, miscibility values were obtained by calculating the crystallinity of the systems from WAXS profile data. The combination of X-ray and FTIR techniques has been demonstrated to be accurate and reliable methods for characterization of toughened epoxy as well as understanding the mechanism of toughening.

Other Spectroscopic Methods

Apart from the above test methods, some other spectroscopy was also used in epoxy/rubber blend. For example, Lee et al. (2010) used X-ray diffraction (XRD) to study the effect of incorporating CTBN into epoxy/clay. The interlayer distance of the CTBN-epoxy-clay system was larger than epoxy-clay blend. It seems to be due to the interaction between the –OH groups in the clay surface, which have hydrophilic properties, and the functional groups of CTBN. The nature of the developing morphology of modified epoxies was analyzed by small-angle laser light-scattering (SALLS) technique (Thomas et al. 2012). The SALLS technique is effectively employed to analyze the phase-separation nature of certain elastomer-modified epoxies, in which the elastomers are initially completely miscible and structure growth takes place during cure (Zhang et al. 1999). Small-angle light-scattering (SALS) technology is a powerful tool to analyze the reaction-induced phase-separation process during curing of EPs and their composites (Boisserie and Marchessault 1977; Kim and Kim 1990; Zhang et al. 1999; Hartwig et al. 2005; Lee et al. 2005; Peng et al. 2007).

Conclusions

Epoxy resin has been widely used in many applications such as composite materials, coatings, structural adhesives, and microelectronics due to its good mechanical properties, excellent chemical resistance, heat stability, excellent adhesion characteristics, and high electrical insulation. However, the major drawback of epoxy resin is the brittleness caused by its high degree of cross-linking. This inherent brittleness results in the poor impact strength of epoxy composites and the poor shear strength of epoxy-based adhesives. The incorporation of rubber phases into epoxy resins could effectively solve these problems, which enlarges their applications and favors the continuous development as a high-performance material with excellent potential

in various fields. In order to acquire a deeper understanding of the mechanism of these properties, it is necessary for epoxy/rubber blends to be structurally well characterized. This chapter focuses on the practical aspects of using the five spectroscopic methods most often applied – Fourier transform infrared (FTIR) spectroscopy, nuclear magnetic resonance (NMR) spectroscopy, Raman spectroscopy, optical microscopy (OM), and X-ray scattering spectroscopy – in the structural investigation and microstructures of epoxy/rubber blends to study the driving forces producing miscibility in the blends. The application of other spectroscopic methods is also discussed. This paper provides hands-on information about these valuable research tools, emphasizing practical aspects such as sample preparation or typical measurement conditions, their limitations and advantages, and interpretation of results. The usefulness of these methods in the driving force of miscibility, the compatibility of epoxy/rubber blends, chemical structure and reaction mechanism analysis, study of the real-time process of a reaction, thermogravimetric process, toughness mechanism, fracture behavior, microstructure, behavior of phase separation, etc., is discussed. It should also be mentioned that the study of driving forces producing miscibility in epoxy/rubber blends is based on the application of at least a few different types of spectroscopic methods during the same study.

References

- Abadyan M et al (2012) Fracture toughness of a hybrid-rubber-modified epoxy. I. Synergistic toughening. *J Appl Polym Sci* 125(3):2467–2475
- Abragam A (1961) The principles of nuclear magnetism. Oxford University Press, Oxford
- Ahmad S et al (2005) Synthesis, characterization and development of high performance siloxane-modified epoxy paints. *Prog Org Coat* 54(3):248–255
- Alagar M et al (2004) Modification of siliconized epoxy resin using multifunctional silanes. *Int J Polym Mater* 53(1):45–58
- Azimi H et al (1996) Fatigue of hybrid epoxy composites: epoxies containing rubber and hollow glass spheres. *Polym Eng Sci* 36(18):2352–2365
- Bakar M et al (2008) Mechanical and thermal properties of epoxy resin modified with polyurethane. *J Reinf Plast Compos* 28:953
- Bao X, Cai X (2014) Synergistic effect of methyl phenyl silicone resin and DOPO on the flame retardancy of epoxy resins. *J Therm Anal Calorim* 118(1):369–375
- Barcia FL et al (2002) Modification of epoxy resin by isocyanate-terminated polybutadiene. *J Appl Polym Sci* 83(4):838–849
- Barcia FL et al (2003) Synthesis and properties of epoxy resin modified with epoxy-terminated liquid polybutadiene. *Polymer* 44(19):5811–5819
- Bhuniya S, Adhikari B (2003) Toughening of epoxy resins by hydroxy-terminated, silicon-modified polyurethane oligomers. *J Appl Polym Sci* 90(6):1497–1506
- Boisserie C, Marchessault R (1977) Light scattering from epoxy-elastomer resins: a study of statistical methods in heterogeneity analysis. *J Polym Sci* 15(7):1211–1222
- Bucknall CB, Yoshii T (1978) Relationship between structure and mechanical properties in rubber-toughened epoxy resins. *Br Polym J* 10(1):53–59
- Bussi P, Ishida H (1994) Partially miscible blends of epoxy resin and epoxidized rubber: structural characterization of the epoxidized rubber and mechanical properties of the blends. *J Appl Polym Sci* 53(4):441–454

- Camino G et al (2001) Polydimethylsiloxane thermal degradation Part 1. Kinetic aspects. *Polymer* 42(6):2395–2402
- Chen J-P, Lee Y-D (1995) A real-time study of the phase-separation process during polymerization of rubber-modified epoxy. *Polymer* 36(1):55–65
- Chen S et al (2010) Dynamic mechanical properties of castor oil-based polyurethane/epoxy graft interpenetrating polymer network composites. *J Appl Polym Sci* 118(2):1144–1151
- Chen S et al (2011) Damping, thermal, and mechanical properties of montmorillonite modified castor oil-based polyurethane/epoxy graft IPN composites. *Mater Chem Phys* 130(1):680–684
- Chen Y et al (2014) The effect of epoxy–silicone copolymer content on the thermal and mechanical properties of cured epoxy resin modified with siloxane. *RSC Adv* 4(105):60685–60693
- Chiang C-L, Ma C-CM (2002) Synthesis, characterization and thermal properties of novel epoxy containing silicon and phosphorus nanocomposites by sol–gel method. *Eur Polym J* 38(11):2219–2224
- Choi J et al (2004) Toughening of cubic silsesquioxane epoxy nanocomposites using core-shell rubber particles: a three-component hybrid system. *Macromolecules* 37(9):3267–3276
- Chonkaew W, Sombatsomp N (2012) Mechanical and tribological properties of epoxy modified by liquid carboxyl terminated poly (butadiene-co-acrylonitrile) rubber. *J Appl Polym Sci* 125(1):361–369
- Clark JN et al (1984) Hydrogen bonding in epoxy resin/poly (ϵ -caprolactone) blends. *J Appl Polym Sci* 29(11):3381–3390
- Deng L et al (2012) Preparation, characterization, and flame retardancy of novel rosin-based siloxane epoxy resins. *Ind Eng Chem Res* 51(24):8178–8184
- Frisch HL et al (1969) A topologically interpenetrating elastomeric network. *J Polym Sci B* 7(11):775–779
- Frisch H et al (1974a) Glass transitions of topologically interpenetrating polymer networks. *Polym Eng Sci* 14(9):646–650
- Frisch KC et al (1974b) Stress–strain properties and thermal resistance of polyurethane–polyepoxide interpenetrating polymer networks. *J Appl Polym Sci* 18(3):689–698
- Frisch HL et al (1977) Barrier and surface properties of polyurethane–epoxy interpenetrating polymer networks. *Polym Sci Technol* 3:69
- Frisch KC et al (1982) Recent advances in interpenetrating polymer networks. *Polym Eng Sci* 22(17):1143–1152
- Gonzalez M et al (2004) Crosslinking of epoxy–polysiloxane system by reactive blending. *Polymer* 45(16):5533–5541
- Grant DM, Harris RK (2002) *Encyclopedia of nuclear magnetic resonance: advances in NMR*. Wiley, Chichester
- Grassie N et al (1979) The thermal degradation of polysiloxanes – II. Poly (methylphenylsiloxane). *Eur Polym J* 15(5):415–422
- Grubbs RB et al (2000) Reactive block copolymers for modification of thermosetting epoxy. *Macromolecules* 33(26):9522–9534
- Guo M (1996) Solid-state high-resolution NMR studies on the miscibility of polymer blends. *Trends Polym Sci* 4:238–244
- Guo Q, Groeninckx G (2001) Crystallization kinetics of poly (ϵ -caprolactone) in miscible thermosetting polymer blends of epoxy resin and poly (ϵ -caprolactone). *Polymer* 42(21):8647–8655
- Hamdani S et al (2009) Flame retardancy of silicone-based materials. *Polym Degrad Stab* 94(4):465–495
- Hartwig A, Sebald M, Pütz D et al (2005) Preparation, characterisation and properties of nanocomposites based on epoxy resins—an overview. In: *Macromolecular symposia*. WILEY - VCH Verlag 221(1):127–136
- He J, Wang J (2009) Preparation and characterization of epoxidate poly (1, 2-butadiene)–toughened diglycidyl ether bisphenol-A epoxy composites. *J Appl Polym Sci* 113(5):3165–3170

- He D et al (2012) Effect of annealing on phase separation and mechanical properties of epoxy/ATBN adhesive. *Int J Adhes Adhes* 38:11–16
- Heng Z et al (2015) Simultaneously enhanced tensile strength and fracture toughness of epoxy resins by a poly (ethylene oxide)-block-carboxyl terminated butadiene-acrylonitrile rubber dilock copolymer. *RSC Adv* 5(53):42362–42368
- Hillmyer MA et al (1997) Self-assembly and polymerization of epoxy resin-amphiphilic block copolymer nanocomposites. *J Am Chem Soc* 119(11):2749–2750
- Holik A et al (1979) Grinding and polishing techniques for thin sectioning of polymeric materials for transmission light microscopy. In: *Microstructural science*, vol 7. Elsevier, New York, pp 357–367
- Horiuchi S et al (1994) Fracture toughness and morphology study of ternary blends of epoxy, poly (ether sulfone) and acrylonitrile-butadiene rubber. *Polymer* 35(24):5283–5292
- Hsieh K, Han J (1990) Graft interpenetrating polymer networks of polyurethane and epoxy. I. mechanical behavior. *J Polym Sci B* 28(5):623–630
- Hsu YG, Liang CW (2007) Properties and behavior of CTBN-modified epoxy with IPN structure. *J Appl Polym Sci* 106(3):1576–1584
- Huang W et al (2001) Surface modification of epoxy resin by polyether–polydimethylsiloxanes–polyether triblock copolymers. *Polymer* 42(4):1763–1766
- Ismail H et al (2009) The compatibilizing effect of epoxy resin (EP) on polypropylene (PP)/recycled acrylonitrile butadiene rubber (NBRr) blends. *Polym Test* 28(4):363–370
- Jang M, Crivello JV (2003) Synthesis and cationic photopolymerization of epoxy-functional siloxane monomers and oligomers. *J Polym Sci A* 41(19):3056–3073
- Kar S, Banthia AK (2005) Synthesis and evaluation of liquid amine-terminated polybutadiene rubber and its role in epoxy toughening. *J Appl Polym Sci* 96(6):2446–2453
- Kim D, Kim SC (1990) Curing and phase separation behavior of amine terminated butadiene acrylonitrile copolymer (ATBN) modified epoxy. *Polym Adv Technol* 1(3–4):211–217
- Kim SC et al (1975) Polyurethane – polystyrene interpenetrating polymer networks. *Polym Eng Sci* 15(5):339–342
- Klempner D et al (1985) Two and three component interpenetrating polymer networks. *Polym Eng Sci* 25(8):488–493
- Klug JH, Seferis JC (1999) Phase separation influence on the performance of CTBN-toughened epoxy adhesives. *Polym Eng Sci* 39(10):1837
- Kumar AA et al (2002) Synthesis and characterization of siliconized epoxy-1, 3-bis (maleimido) benzene intercrosslinked matrix materials. *Polymer* 43(3):693–702
- Le Q-H et al (2010) Structure–property relations of 55nm particle-toughened epoxy. *Polymer* 51(21):4867–4879
- Lee YD et al (1986) Liquid-rubber-modified epoxy adhesives cured with dicyandiamide. I. Preparation and characterization. *J Appl Polym Sci* 32(8):6317–6327
- Lee D-B et al (2002) Damage zone around crack tip and fracture toughness of rubber-modified epoxy resin under mixed-mode conditions. *Eng Fract Mech* 69(12):1363–1375
- Lee J et al (2005) Reaction induced phase separation in mixtures of multifunctional polybutadiene and epoxy. *Polymer* 46(26):12511–12522
- Lee TM et al (2006) Syntheses of epoxy-bridged polyorganosiloxanes and the effects of terminated alkoxysilanes on cured thermal properties. *J Appl Polym Sci* 99(6):3491–3499
- Lee K-Y et al (2010) Thermal, tensile and morphological properties of gamma-ray irradiated epoxy-clay nanocomposites toughened with a liquid rubber. *Polym Test* 29(1):139–146
- Liang Y, Pearson R (2010) The toughening mechanism in hybrid epoxy-silica-rubber nanocomposites (HESRNs). *Polymer* 51(21):4880–4890
- Lin ST, Huang SK (1996) Synthesis and impact properties of siloxane–DGEBA epoxy copolymers. *J Polym Sci A* 34(10):1907–1922
- Lipic PM et al (1998) Nanostructured thermosets from self-assembled amphiphilic block copolymer/epoxy resin mixtures. *J Am Chem Soc* 120(35):8963–8970

- Liu W et al (2010) Morphologies and mechanical and thermal properties of highly epoxidized polysiloxane toughened epoxy resin composites. *Macromol Res* 18(9):853–861
- Luo X et al (1994) Miscibility of epoxy resins/poly (ethylene oxide) blends cured with phthalic anhydride. *Polymer* 35(12):2619–2623
- Ma J et al (2008) Study of epoxy toughened by in situ formed rubber nanoparticles. *J Appl Polym Sci* 110(1):304–312
- Ma S et al (2010a) Toughening of epoxy resin system using a novel dendritic polysiloxane. *Macromol Res* 18(4):392–398
- Ma S et al (2010b) Modification of epoxy resin with polyether-grafted-polysiloxane and epoxy-miscible polysiloxane particles. *Macromol Res* 18(1):22–28
- Mahesh K et al (2003) Mechanical, thermal and morphological behavior of bismaleimide modified polyurethane-epoxy IPN matrices. *Polym Adv Technol* 14(2):137–146
- Mijovic J et al (2000) Dynamics and morphology in nanostructured thermoset network/block copolymer blends during network formation. *Macromolecules* 33(14):5235–5244
- Murias P et al (2012) Epoxy resins modified with reactive low molecular weight siloxanes. *Eur Polym J* 48(4):769–773
- Nigam V et al (1998) Wide-angle X-ray scattering, Fourier transform infrared spectroscopy, and scanning electron microscopy studies on the influence of the addition of liquid functional rubber into epoxy thermoset. *J Appl Polym Sci* 70(3):537–543
- Nigam V et al (1999) Characterization of liquid carboxy terminated copolymer of butadiene acrylonitrile modified epoxy resin. *Polym Eng Sci* 39(8):1425–1432
- Park S-J et al (2005) Synthesis and characterization of a novel silicon-containing epoxy resin. *Macromol Res* 13(1):8–13
- Peng M et al (2007) Effect of an organoclay on the reaction-induced phase-separation kinetics and morphology of a poly (ether imide)/epoxy mixture. *J Appl Polym Sci* 104(2):1205–1214
- Potter W (1970) *Epoxide resins*. Springer, New York
- Prabu AA, Alagar M (2005) Thermal and morphological properties of silicone-polyurethane-epoxy intercrosslinked matrix materials. *J Macromol Sci A* 42(2):175–188
- Radhakrishnan T (1999) New method for evaluation of kinetic parameters and mechanism of degradation from pyrolysis–GC studies: thermal degradation of polydimethylsiloxanes. *J Appl Polym Sci* 73(3):441–450
- Ramos VD et al (2005) Modification of epoxy resin: a comparison of different types of elastomer. *Polym Test* 24(3):387–394
- Ratna D, Banthia AK (2000) Toughened epoxy adhesive modified with acrylate based liquid rubber. *Polym Int* 49(3):281–287
- Ratna D, Banthia AK (2004) Rubber toughened epoxy. *Macromol Res* 12(1):11–21
- Ratna D et al (2001) Acrylate-based liquid rubber as impact modifier for epoxy resin. *J Appl Polym Sci* 80(10):1792–1801
- Raymond MP, Bui V (1998) Epoxy/castor oil graft interpenetrating polymer networks. *J Appl Polym Sci* 70(9):1649–1659
- Ren Q et al (2014) The preparation and properties study of methoxy functionalized silicone-modified epoxy resins. *J Appl Polym Sci* 131(9):4583–4589
- Rutledge D (1997) *Encyclopedia of nuclear magnetic resonance*. Trends Anal Chem 7(16):XI–XII
- Shih WC et al (1999) Polydimethylsiloxane containing isocyanate group-modified epoxy resin: curing, characterization, and properties. *J Appl Polym Sci* 73(13):2739–2747
- Shon M, Kwon H (2009) Comparison of surface modification with amino terminated polydimethylsiloxane and amino branched polydimethylsiloxane on the corrosion protection of epoxy coating. *Corros Sci* 51(3):650–657
- Soares BG et al (2008) Toughening of an epoxy resin with an isocyanate-terminated polyether. *J Appl Polym Sci* 108(1):159–166
- Sobhani S et al (2012) Effect of molecular weight and content of PDMS on morphology and properties of silicone-modified epoxy resin. *J Appl Polym Sci* 123(1):162–178

- Stuart B (2004) *Infrared spectroscopy: fundamentals and applications*. Wiley, Chichester
- Tang L-C et al (2012) Fracture mechanisms of epoxy-based ternary composites filled with rigid-soft particles. *Compos Sci Technol* 72(5):558–565
- Thomas R et al (2008) Miscibility, morphology, thermal, and mechanical properties of a DGEBA based epoxy resin toughened with a liquid rubber. *Polymer* 49(1):278–294
- Thomas R et al (2012) In-situ cure and cure kinetic analysis of a liquid rubber modified epoxy resin. *Ind Eng Chem Res* 51(38):12178–12191
- Unnikrishnan K, Thachil ET (2006) Toughening of epoxy resins. *Des Monomers Polym* 9(2):129–152
- Wang CL et al (1985) Morphology of polyurethane–isocyanurate elastomers. *J Appl Polym Sci* 30(11):4337–4344
- Wang HB et al (1992a) Photosynthesis and application of polyfunctional poly (n-butyl acrylate) elastomers for use in epoxy resin toughening. *J Appl Polym Sci* 44(5):789–797
- Wang HB et al (1992b) A study of the residual microstress at the matrix interface in filled epoxy resins. *Polym Eng Sci* 32(10):678–685
- Werner TA (1989) Interpenetrating polymer network of blocked urethane prepolymer, polyol, epoxy resin and anhydride, U.S. Patent 4,923,934[P]. 1990-5-8
- Wu SY et al (2002) Polysiloxane modified epoxy networks. IV. Catalytic effect on fracture behaviors of jointed interpenetrating polymer networks. *J Appl Polym Sci* 84(13):2352–2357
- Xu Z, Zheng S (2007) Reaction-induced microphase separation in epoxy thermosets containing poly (ϵ -caprolactone)-block-poly (n-butyl acrylate) diblock copolymer. *Macromolecules* 40(7):2548–2558
- Yang X et al (2009) Morphology and mechanical properties of nanostructured blends of epoxy resin with poly (ϵ -caprolactone)-block-poly (butadiene-co-acrylonitrile)-block-poly (ϵ -caprolactone) triblock copolymer. *Polymer* 50(16):4089–4100
- Zeng M et al (2008) Investigation of free volume and the interfacial, and toughening behavior for epoxy resin/rubber composites by positron annihilation. *Radiat Phys Chem* 77(3):245–251
- Zhang J et al (1999) Polymerization-induced bimodal phase separation in a rubber-modified epoxy system. *J Appl Polym Sci* 72(1):59–67
- Zhao K et al (2015) Morphology and properties of nanostructured epoxy blends toughened with epoxidized carboxyl-terminated liquid rubber. *Iran Polym J* 24(5):425–435
- Zheng S et al (2003) Epoxy resin/poly (ϵ -caprolactone) blends cured with 2, 2-bis [4-(4-aminophenoxy) phenyl] propane. I. Miscibility and crystallization kinetics. *J Polym Sci B* 41(10):1085–1098

Padmanabhan Krishnan

Abstract

This chapter is an introduction to the rheology of epoxies and rubbers, their blends, classification, and types. Principles of rheology and polymer rheology are illustrated through conclusive plots and graphs. Rheology of rubbers, epoxies, and their blends are discussed with respect to their molecular structure, mobility, and conformational states. Rheology is explained with respect to the established viscoelasticity models for epoxies and their blends. A detailed account of rheometers and measurements is given. Miscibility, phase separation, and thermodynamics of epoxy-rubber systems form an integral part of this chapter. A correlation is drawn between rheology and shear behavior of these systems. Rheological insights on processing, manufacturing methods, curing reactions, and curing schedules are detailed for epoxy-rubber blend systems. Functional and product applications of rheology of epoxy/rubber blends are listed at the end.

Keywords

Epoxy-rubber blends • Rheology • Microrheology • Chemo-rheology • Viscoelastic models • Molecular deformation theories • Thermodynamics • Measurements • Phase separation • Shear rheotriology • Processing • Applications

Contents

Introduction	186
Epoxy Resins and Hardeners	188
Liquid and Particle Rubber Additives	189
Large Deformation and Flow	190
Theories of Large Deformation and Flow	191

P. Krishnan (✉)
VIT-University, Vellore, India
e-mail: padmanabhan.k@vit.ac.in

Viscoelastic Models for Epoxies and Epoxy Rubber Blends	194
Viscometers, Rheometers, and Measurements	196
Evolution of Epoxy-Rubber Phases	200
Thermodynamics of Epoxy-Rubber Blends	201
Feedback from Fracture Mechanisms in Processing	202
Applications of Epoxy-Rubber Blend Systems	207
Conclusions	207
Implications on Future Research	208
References	208

Introduction

Rheology is the science of deformation and flow of matter (Billmeyer 2015). Large deformation and flow kinetics dominate the shaping of the polymer in processing. The rheological behavior is related to the molecular orientations and mechanisms, which are as follows:

1. *Hookean elasticity*, where the stretching of the bonds and deformation of the bond angle of the polymers in question are restricted and the material behaves like a rigid body.
2. *Viscoelasticity*, where the polymer deformation is reversible but time dependent.
3. *Rubberlike elasticity*, where flow is restricted and small scale movement of chain segments is possible.
4. *Viscous flow*, large deformation of the polymer associated with irreversible molecular chain slippage.

These explanations for the mechanical properties of the amorphous polymers differ from those of crystalline and semicrystalline polymers which are not dealt with here due to our focus on rheology of epoxies and epoxy-rubber blends. A knowledge of rheology of epoxy-rubber blends is important for the processing methods like thermoforming, extrusion, and injection molding.

The phenomena of viscous flow can be understood as the relationship between the shear stress S and the rate of shear $\dot{\gamma}$ that govern the viscosity η (Bauer and Collins 1967) as follows:

$$S = \eta \dot{\gamma} \quad (1)$$

If viscosity is independent of the rate of shear, the liquid is said to be Newtonian or to exhibit ideal flow behavior. Shear thinning or pseudoplastic behavior is a reversible decrease in viscosity with increasing shear rate. Shear thinning is said to happen when long chains of the polymer are disturbed from their equilibrium conformation positions, causing elongation of chains in the direction of shear. The opposite of shear thinning is called shear thickening or dilatant behavior in which viscosity increases with increase in shear rate. This effect is not observed in

polymers. Figure 1 shows the relationship between viscosity and shear rate for different fluids.

Figure 2 shows the relationship between yield stress and shear rate in fluids. The two effects are time independent. The Newtonian behavior is characterized by a linear relationship between the yield stress and shear rate. Another deviation from the Newtonian flow is the result of a yield value, a critical stress only above which flow occurs. But the flow may be non-Newtonian or Newtonian. For polymers, it will be pseudoplastic like in thermoplastics or near Newtonian, like in epoxies and their blends. Bingham refers to an elastic-perfect plastic behavior, a situation beyond which the strain increases phenomenally with no further increase in stress. Plastics generally exhibit yielding beyond which the stress strain curve is nonlinear. Some of the polymers exhibit reversible time-dependent changes in viscosity when sheared at constant stress values. Viscosity decreases with time in a thixotropic fluid, and increases with time in a rheopectic fluid, under constant shear stress. Epoxies that cure under heat and pressure may exhibit a thixotropic behavior in the beginning and a rheopectic behavior just before gelation. Low molecular weight fluids exhibit a relationship between viscosity and temperature as follows:

$$\eta = A e^{E/RT} \tag{2}$$

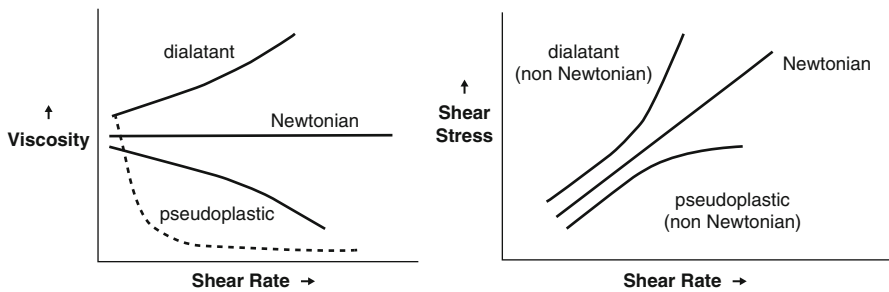
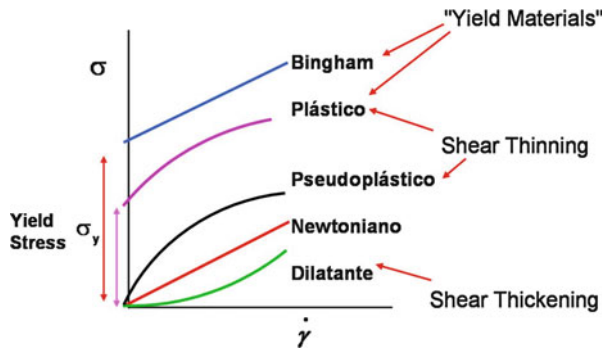


Fig. 1 Viscosity versus shear rate for fluids

Fig. 2 Rheology of fluids



Here, A and R are constants, E is the activation energy for viscous flow, and T is the absolute temperature. For a more illustrative discussion on the molecular theories of flow, the reader is referred to the work of Eyring (Glasstone et al. 1941).

Epoxy Resins and Hardeners

The chemical formulae of some of the popular epoxies and their hardeners are given below to appraise the reader about their functional groups, reactions, and their potential for blending with rubbers (Lee and Neville 1967).

Figures 3, 4, 5, 6, 7, and 8 provide the structures of epoxies and their hardeners used in synthesizing resins of good thermal stability and mechanical properties. As hardeners with higher functionality are used, the thermal stability of the resin thus synthesized also increases.

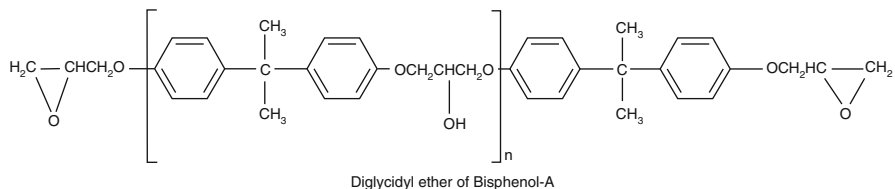


Fig. 3 Chemical structure of *DGEBA* epoxy resin

Fig. 4 Structure of diethylene triamine



Fig. 5 Chemical formula of triethylene tetramine

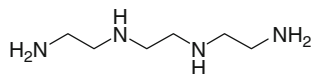
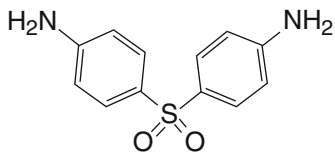


Fig. 6 Structure of diamino diphenyl sulphone



Liquid and Particle Rubber Additives

The chemical formulae of liquid and particle rubbers are given below. These are blended with epoxies for obtaining superior fracture toughness (Blow and Hepburn 1982).

Figures 9 and 10 detail the structures of various rubbers used in blending with epoxies. Figure 9 provides the details about the liquid rubbers whereas Fig. 10 that of solid rubbers that are mixed with the epoxies to obtain blends with good fracture toughness.

Fig. 7 Chemical structure of diamino diphenyl methane

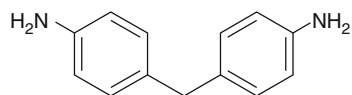
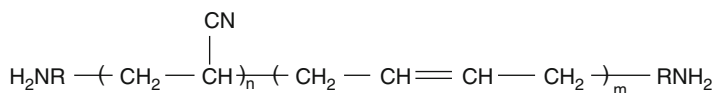
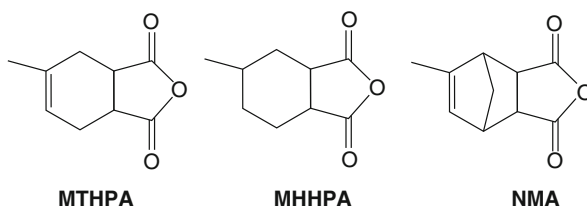
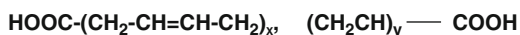


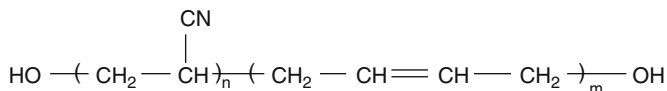
Fig. 8 Illustration of anhydride curing agents used for curing epoxies



Amino-terminated nitrile-butadiene rubber



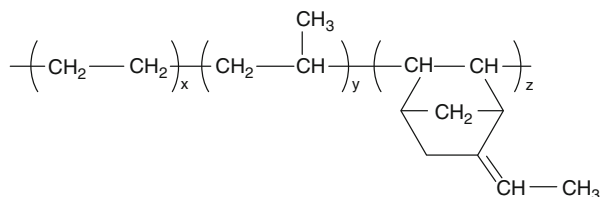
Carboxyl terminated nitrile butadiene rubber.



Hydroxyl Terminated Nitrile Butadiene Rubber

Fig. 9 Chemical formulae of ATBN, CTBN, and HTBN liquid rubbers

Fig. 10 Structure of EPDM rubber molecule



Large Deformation and Flow

The large deformation and flow of glassy amorphous polymers in general and epoxies in particular are further classified into the following:

1. Chemo-rheology, which is defined as the study of viscoelastic behavior of chemically reacting systems that cure under heat or pressure or both. This study covers knowledge of the changes in viscosity due to chemical reactions and processing conditions (chemo-viscosity) and characterization of growth of the infinite molecular network and gelation into a glassy state. The chemo-viscosity of thermosetting resins is affected by many variables like pressure, temperature, time, shear rate, and filler properties. The effect of cure on the chemo-viscosity are twofold; the viscosity initially decreases due to increased thermal effects and eventually increases due to formation of the cross-linked network via the curing reaction. This is seen schematically for the chemo-viscosity of an epoxy resin during curing in Fig. 11. Initially, during plasticization, the viscosity of the resin decreases due to shear heating and thermal effects (Stage I). As the temperature increases and time proceeds, the curing reaction begins and the decrease in viscosity due to heating is compensated by the increase in viscosity due to the gelation process from a fluidic state. At the point of minimum viscosity the epoxy is sprayed or applied to the mold (which is Stage II). Finally, the viscosity of the

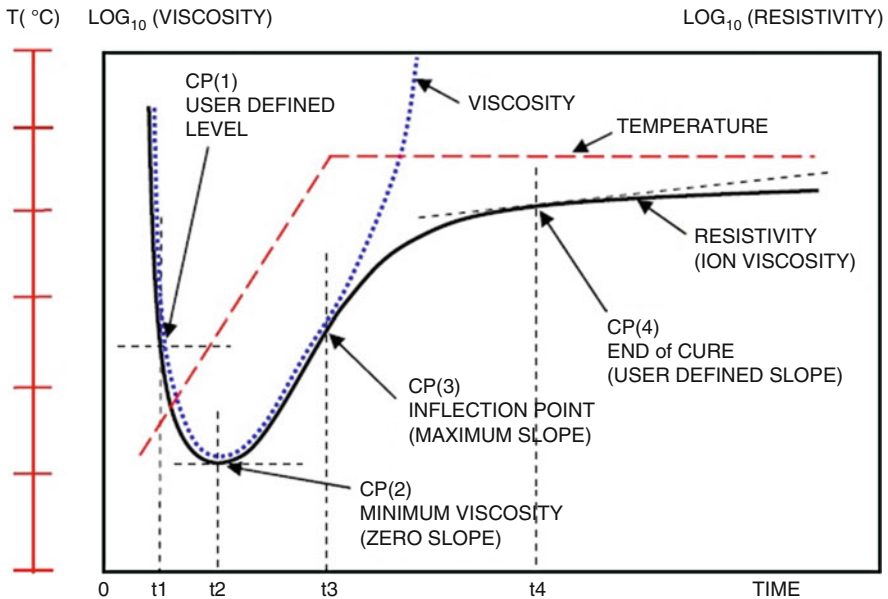


Fig. 11 Viscosity versus curing gel time and temperature in epoxies under curing

resin increases as the material is transformed into an infusible solid (which is Stage III). The gelation and cure effects on viscosity may be determined by the activation energies of the reaction and of viscous flow. The effects of temperature and time on the chemo-viscosity can also be described explicitly in terms of the extent of cure from knowledge of the kinetics of the cure and temperature. The determination of gel point and viscosity modeling has been dealt with by Ivankovic et al. in detail (Ivankovic 2003).

2. Microrheology, which is a technique used to measure the rheological properties of a medium, such as microviscosity, through the measurement of the path of a flow tracer (a micrometer-sized particle or a rubber particle). It relates microstructure of the polymer with its flow (Bucknall 1977). Microrheology is a rheology method that uses colloidal tracer particles, dispersed within a sample, as useful probes. Tracer rubber particles (with diameters ranging from 0.3 to 2.0 μm) may be naturally present in the system, as in suspensions and emulsions, or added to the medium intentionally. The motion of the tracer particles reflects the rheological properties of their local environment. In purely viscous samples, tracer particles freely diffuse through the whole sample. In cured or gelled samples their mobility is restricted.

Theories of Large Deformation and Flow

Flory (1953) has made significant contributions to the study of thermodynamics and the statistical thermodynamics of polymer solutions. The entropy, heat, and free energy of mixing can be calculated based on the Flory-Huggins Theory (Huggins 1958). In polymer systems, the activation energy for viscous flow is almost a constant for small or incremental ranges of temperature. For pure liquids, the change in the viscosity with temperature is associated with the concurrent change in volume. The WLF theory (Williams 1955) is based on the change of viscosity with respect to the free volume. The temperature dependence of fluid viscosity is expressed in terms of the glass transition temperature or T_g or another reference temperature and universal constants. The polymer fluid possesses a viscosity that is dependent on temperature and molecular weight in an independent manner; the WLF equation can be written for low shear rates as

$$\text{Log } \eta = 3.4 \log Z_w - \left\{ 17.44 (T - T_g) / 51.6 + T - T_g \right\} + k' \quad (3)$$

Where k' is a constant depending upon the type of the polymer. The equation holds good for a temperature range from T_g to about $T_g + 100$ K.

Here, $17.44 (T - T_g) / 51.6 + T - T_g$ is called the shift factor or a_T which is closely the relaxation time. Time and temperature affect the viscoelastic properties only through the shift factor. For glassy amorphous polymers the shift factor does not vary noticeably with the relaxation time. The molecular structure decides the dependence of the shift factor on the absolute temperature.

The WLF equation for log viscosity varies linearly above T_g

$$\text{Log } (\eta/\eta_g) = -a (T - T_g) / b + T - T_g. \quad (4)$$

Where “a” and “b” are numerical constants. Here η is the viscosity above the glass transition temperature and that of η_g , its value below the T_g .

For high molecular weight epoxies, Eq. 2 can be written by substituting η with the relaxation time τ (Aklonis and MacKnight 1983; Ferry 1970).

Here, $a_T = \tau/\tau_o = E/R (1/T - 1/T_o)$, where T is the given temperature and T_o is the reference temperature. Viscoelasticity or stress relaxation (could also mean creep here) is associated with a molecular relaxation process. When the relaxation time is shorter the material relaxes spontaneously. On the other hand, higher activation energy indicates that the shift factor varies to a greater extent with temperature (Woo 1993). Most polymeric materials exhibit a simple linear viscoelastic behavior. However, rubber toughened epoxies can be expected to exhibit nonlinear viscoelastic behavior especially under high stresses and high temperatures. The Schapery and Springer theories are normally applied to model the nonlinear time-temperature viscoelastic behavior of epoxy-rubber blend composites. However, under a dynamic shear deformation the epoxy rubber blends behave in a linear or near linear viscoelastic manner which is a rate-dependent phenomenon (Woo 1993). Generally, epoxies are more linear than their rubber blends.

Relaxation times are dependent on stress while that of retardation times on deformation. The following equation defines retardation times:

$$Y = Y_o e^{-t/\tau_r} \quad (5)$$

Where, Y is the deformation and Y_o its initial value. The symbols t and τ_r indicate time and retardation time. When stress is removed, the sample returns to its original shape along the exponential curve.

Epoxies are amorphous and highly cross-linked. They exhibit a mechanical behavior similar to that of glassy amorphous polymers up to the glass transition temperature, T_g . The deformation behavior and the time-temperature effects in epoxies and rubber modified epoxies have been studied earlier by many investigators (Kinloch 1983; Bucknall 1977; Marshall et al. 1970). Below the glass transition temperature, the following equations may be employed to calculate the shear moduli and shear stress:

$$\mu (T) = E (T) / 2(1 + \nu) \quad (6)$$

$$\tau (T) = \sigma_y(T) / \sqrt{3} \quad (7)$$

Argon's theory for glassy amorphous polymers (Argon 1973) predicts the relationship between the shear yield stress τ and shear modulus μ . It has been shown that

$$(\tau/\mu)^{5/6} = A-B (T/\mu) \quad (8)$$

Where T is the absolute temperature. The constants A and B are given by

$$A = [(0.77)/(1-\nu)]^{5/6} \quad (9)$$

$$B = A 16 (1-\nu) k \ln(\dot{\gamma}_o/\dot{\gamma}) / 3 \pi \omega^3 a^3 \quad (10)$$

Where ν is the Poisson ratio, ω the solid angle of rotation of the molecular segment between the initial and activated configuration, a the mean molecular radius, and k is the Boltzmann constant. $\dot{\gamma}$ is the shear strain rate, and $\dot{\gamma}_o$ is a preexponential frequency factor usually taken to be about 10^{13} s^{-1} . The mean molecular radius a of the epoxy molecule can then be calculated from Eq. 10. Argon's theory also gives the parameter to determine the critical separation at yield of a pair of kinks or wedge disclinations on the epoxy molecule. Argon's theory does not hold near and above the glass transition temperature as it is approached from a glassy state. On the other hand, Bowden's work (Bowden 1973) predicts the yield behavior of epoxies. Here, the critical step in the yield process is that of thermally activated nucleation under stress of small, disk-shaped, sheared regions in the polymer. The applicability of Bowden's theory is better than that of Argon's in the vicinity of the glass transition temperature or T_g . Kitagawa expanded and generalized Bowden's theory by showing that the relationship between τ and μ can be represented by a power law relation of the form

$$T_o \tau / T \tau_o = (T_o \mu / T \mu_o)^n \quad (11)$$

Where T_o is the reference temperature, and τ_o and μ_o are the shear yield stress and shear modulus, respectively, at T_o (Kitagawa 1977). He was rather partially successful in showing that the n exponent was independent of temperature and possessed a value of 1.63 for all glassy polymers. A more recent author (Padmanabhan 1996) has shown that the n exponent for epoxies is of the range 1.67–1.69 and the other parameters for epoxies are in the range shown in Table 1. The Z^* parameter or the wedge disclination parameter indicating the flexibility or rigidity of the epoxy molecules has been shown to be comparable to that of the glassy amorphous polymers like polycarbonates.

Robertson and Joynson (1966) developed a molecular theory of yield behavior of rigid polymers which is regarded as a slightly more elaborate version of the Eyring viscosity theory. It incorporates structural ideas rather than phenomenological

Table 1 Deformation data of various epoxies

Material	ν	A	B	a	Z^*
			(MPaK ⁻¹)	(Å)	(Å)
Formulation I	0.43	0.192	0.104	6.4	13.06
Formulation II	0.39	0.18	0.923	6.6	13.44
DGEBA + TETA ^a	0.35	0.12–0.17	0.25–0.28	4–4.4	8.25–9.03

^a Molecular radius

models. Conformational states are involved in the theory in relation to the energy states. In isotropic polymers, there is no preferred orientation of the structural elements which take part in the yield process. Robertson explained the rate dependence of yield stress in terms of an effective viscosity which is pressure, temperature, and shear stress dependent. This theory explains the yield behavior in relation to the low strain viscoelastic relaxation behavior. His theory can be applied to highly cross-linked epoxies with reasonable approximation as they are glassy amorphous polymers. This theory has also been reported by Ward (Ward 1971).

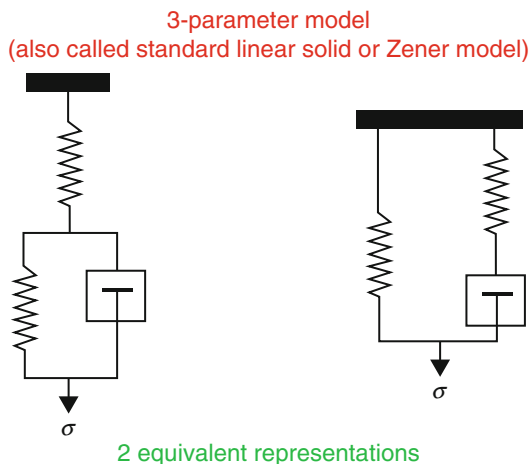
Viscoelastic Models for Epoxies and Epoxy Rubber Blends

Viscoelasticity of polymers is well documented in the book by Christensen (2010). The standard linear solid model combines aspects of the Maxwell and Kelvin–Voigt models to describe the overall behavior of a system under a given set of loading conditions. The behavior of a material applied to an instantaneous stress is shown as having an instant response. Instantaneous release of a stress also results in a discontinuous decrease in strain. The shape of the time-dependent strain curve characterizes the behavior of the model over time, depending upon how the model is loaded. Although this model can be used to accurately predict the general shape of the strain curve, as well as behavior for long time and instantaneous loads, the model lacks the ability to accurately model material systems numerically.

Though many rheological models based on the integral or the differential approach do exist, the Zener model is seen to explain creep and stress relaxation better than that of the Maxwell or Kelvin–Voigt model. The Zener model is shown in Fig. 12, which is a three-parameter model or a linear solid model.

Further, a **Burgers material** which is a viscoelastic material that obeys Eq. 12 consists of a Maxwell material and a Kelvin material in series. It is named after the

Fig. 12 Three-parameter viscoelastic model of epoxies and blends



Dutch physicist Johannes Martinus Burger. Given the four rheological constants, the Burgers model has the constitutive equation

$$\sigma + (\lambda_3 + \lambda_4)\dot{\sigma} + \lambda_3 \lambda_4 \ddot{\sigma} = (\eta_3 + \eta_4)\dot{\gamma} + (\eta_3 \lambda_4 + \eta_4 \lambda_3) \ddot{\gamma} \quad (12)$$

Where σ is the stress and γ is the rate of deformation. λ and η are constants, and the stress or rate derivatives are marked with a “.” or “..” above them.

The viscoelastic model for epoxies and rubber toughened epoxies obey a Zener three-parameter model, a Burgers model or a five-parameter model like the Mats Berg model which is a nonlinear five-parameter friction model. Epoxies are linear or near linear in their mechanical behavior and obey the Zener model. However, the rubber toughened epoxies generally do not exhibit this behavior as the rubber additions are anywhere between 1 Wt% and about 20 Wt% of the epoxy weight. Rubber additions are not made beyond this point as the matrix would then be all rubber with the epoxy appearing as a dispersed phase. The Burgers model or Mats Berg model would be a closer approximation for the mechanical behavior of rubber toughened epoxies provided the rubber additions are not marginal. Rubbers generally possess low T_g values and generally lower the T_g of the epoxy-rubber blends. But, the T_g of the rubber dispersions alone in the blend show an increase compared to their homogeneous values. However, the T_g of the epoxies in a rubber blend show a decrease. Figure 13 shows the glass transition versus chain segment movement for rigid polymers. This schematic diagram also explains the rubbery behavior of a rigid polymer above the T_g . As cured epoxies do not flow and melt above the T_g but turn rubbery and char later at higher temperatures, there is restriction on the mobility of the chain segments that are highly cross-linked. Figure 14 schematically shows the modulus loss of rigid polymers that are crystalline, highly cross-linked, or differing in molecular weight. Measuring modulus loss versus temperature provides an approximate range of T_g , which is often called as engineers T_g . Modulus loss for epoxies is not complete like in low molecular weight polymers but is rather slow after a drop near the engineers T_g . This is due to the rubbery behavior till thermal degradation leading to charring occurs.

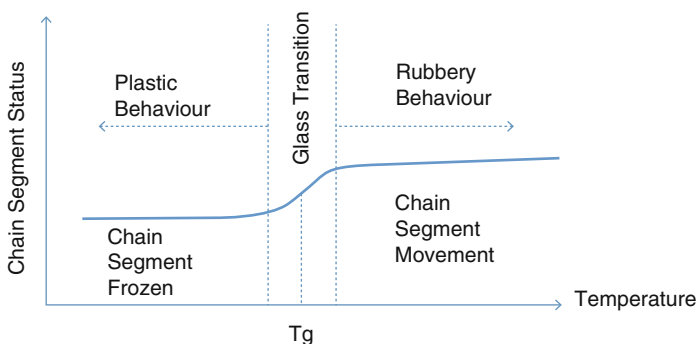
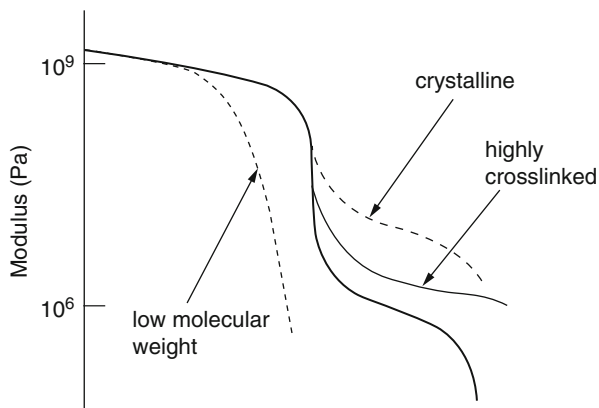


Fig. 13 Glass transition during viscoelastic transition

Fig. 14 Modulus versus temperature for highly cross-linked epoxies



Viscometers, Rheometers, and Measurements

Some of the basic laws on fluid flow are given here before a detailed understanding on rheometry is attempted. Darcy's law is a phenomenologically derived constitutive equation that describes the flow of a fluid through a porous medium. It also provides information on percolation, permeability, and Darcy's coefficient. Flow of epoxies and their blends through porous foams is best described through Darcy's law. One of the key definitions that the reader must understand before proceeding any further is the melt flow index. The melt flow index (MFI) is the measure of the ease of flow of a polymer melt. It is defined as the mass of polymer, in grams, flowing in 10 min through a capillary of a specific diameter and length by a pressure applied through a prescribed alternative gravimetric weight for alternative prescribed temperatures. Polymer processors correlate the value of MFI with the polymer grade that they have to choose for different processes, and usually this value is not accompanied by the units, because it is taken for granted to be grams per 10 min. Similarly, the test load conditions of MFI measurement is normally expressed in kilograms rather than any other units. The method is described in two similar standards (ASTM D1238 2013; ISO 1133 2005)

The methods used for measuring the viscosity of a polymer solution are:

1. Capillary pipette
2. Falling sphere
3. Capillary extrusion
4. Parallel plate
5. Falling coaxial cylinder
6. Stress relaxation
7. Rotating cylinder
8. Tensile creep

The important methods employ the capillary or rotational devices.

Viscosity varies with shear rate for broad and narrow distribution of molecular weights as shown in Fig. 15. An elementary capillary rheometer or extrusion plastometer is used to determine the flow rate of a polymer in terms of the melt index which is defined as the mass rate of the polymer through a specified capillary under controlled conditions of temperature and pressure. Figures 16, 17, and 18 illustrate the equipment used for determining the MFI and viscosity. Capillary rheometers are generally rugged and possess good precision, but their disadvantage

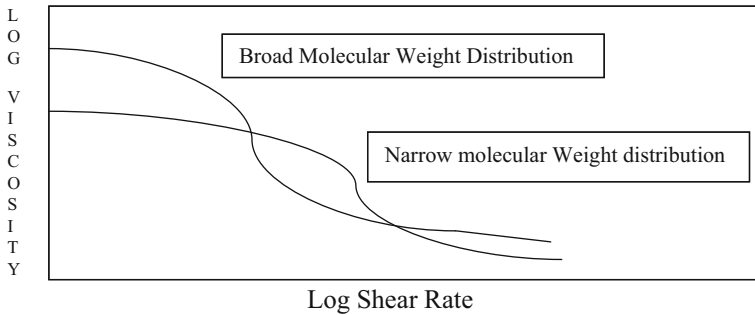


Fig. 15 Viscosity versus shear rate for two different molecular weight distributions

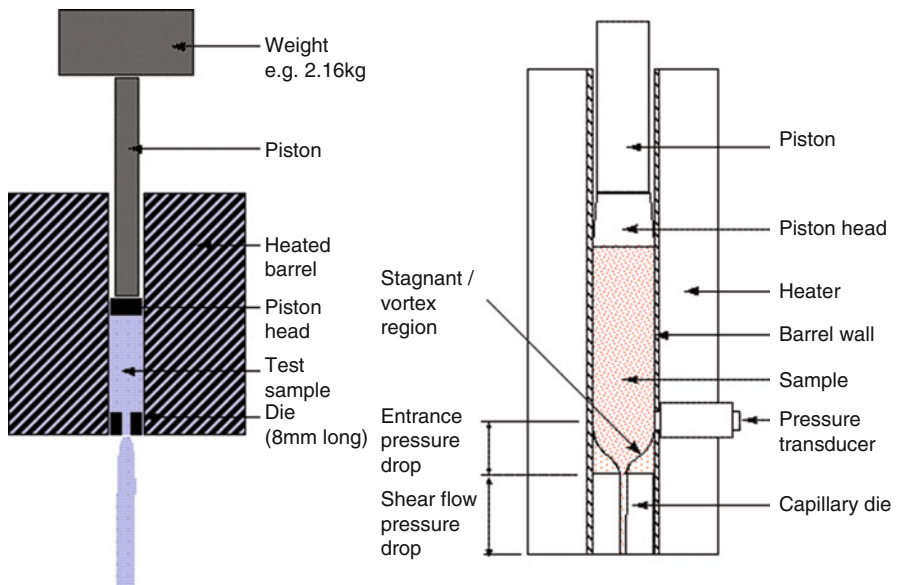


Fig. 16 Equipment for MFI and capillary rheometer

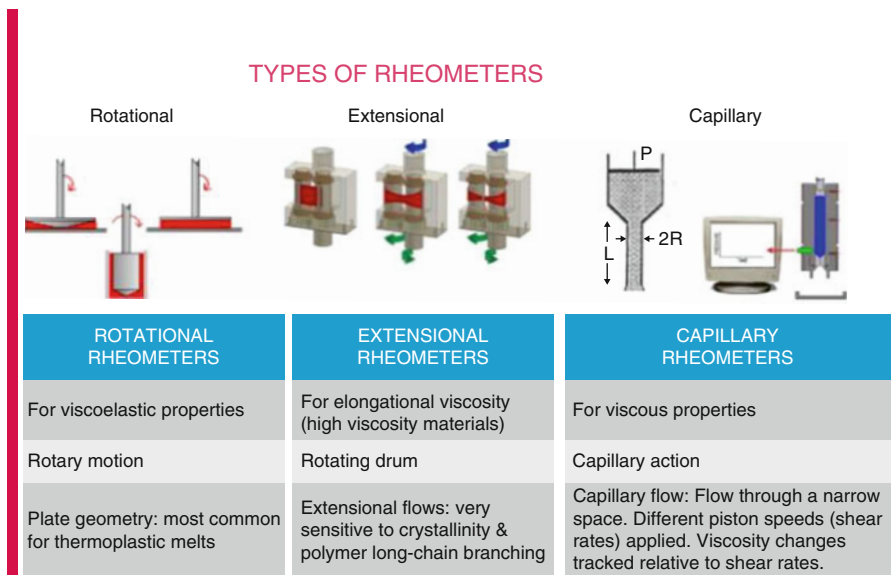


Fig. 17 Rheometer classifications

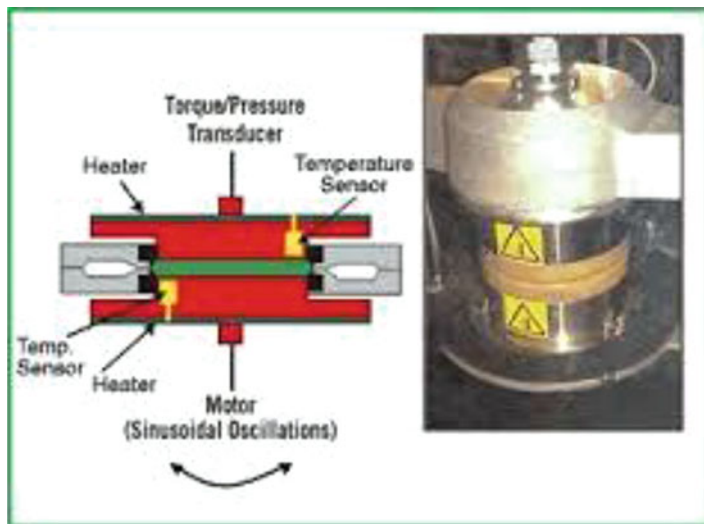


Fig. 18 Torque transducers for vulcanized and nonvulcanized rubbers

is that the shear stress in the capillary varies from zero at the center to a maximum near the walls of the tube. Rotational devices, on the other hand, are least precise at high shear stresses and rotational speeds, as heat develops due to dissipation of

energy. As a result, the specimen moves out of the region of high shear stress. This effect is called the *Weissenberg effect*. In the rubber industry, a rotational Mooney viscometer is used. The Brabender plastograph, a closer device is used to study the changes in the flow of rubber during mastication or milling. Figures 16, 17, and 18 illustrate the classification of rheometers used for polymers and blends and the rubber torque transducers used for most of the rubber materials.

A test method (ASTM D 4440 2015) outlines the use of dynamic mechanical instrumentation in determining and reporting the rheological properties of thermoplastic resins and other types of molten polymers. It may be used as a method for determining the complex viscosity and other significant viscoelastic characteristics of such materials as a function of frequency, strain amplitude, temperature, and time. Such properties may be influenced by fillers and other additives. It is noteworthy here that there is no specific standard for epoxies and their blends.

- ISO 1133: 2005 Plastics – Determination of the melt mass-flow rate (MFR) and the melt volume-flow rate (MVR) of thermoplastics
- ISO 11443: 2005 Plastics – Determination of the fluidity of plastics using capillary and slit-die rheometers
- ISO 20965: 2005 Plastics – Determination of the transient extensional viscosity of polymer melts [tensile drawing method]
- ISO 16790: 2004 Plastics – Determination of drawing characteristics of thermoplastics in the molten state [fiber-spinning method]
- ISO 17744: 2004 Plastics – PVT determination of specific volume as a function of temperature and pressure (PVT diagram) – Piston apparatus method

Following standards held by other TC61 rheology committees are:

- ISO 6721–10: 1999 Plastics – Determination of dynamic mechanical properties – Part 10: Complex shear viscosity using a parallel plate oscillatory rheometer
- ISO 11403–2 Plastics – Acquisition and presentation of comparable multipoint data – Part 2: Thermal and processing properties

Some investigators have successfully used a parallel plate rheometer with a diameter of 12.5 mm for the analysis of epoxy–rubber–DDM blend systems (George et al. 2014, 2015). A transducer measured the viscous response of the material under the form of a torque exerted by the fluid on the upper plate. A frequency of 1 Hz and 0.5% strain were used for the measurements. Freshly prepared samples (about 5–10 mg) were placed in the parallel plates, and the analysis was done isothermally at different temperatures (90, 110, and 130 °C). Nonisothermal analyses have also been carried out (Thomas 2014). Some investigators (Vlassopoulos et al. 1998) have successfully carried out multiple wave form dynamic rheology measurements for the epoxy-rubber blends and studied their curing kinetics.

Evolution of Epoxy-Rubber Phases

The evolution of a nanophase separation in epoxy-rubber blends during curing has been dealt in detail (Konnola et al. 2015a). There are various possible interactions in an epoxy-rubber blend or a nanocomposite (Gupta 2010). Four possible interactions have been suggested in a polymer blend or a nanocomposite. They are:

1. Polymer-polymer interaction
2. Polymer-solvent interaction
3. Polymer-particle interaction
4. Particle-particle interaction

A steric interaction occurs in a system due to the adsorption or grafting of polymers on particle surfaces, or vice versa. The strength of the interaction is a function of the mixing interaction and the volume exclusion term. The nature of the mixing interaction force depends on the nature of the continuous phase or the solvent. If the polymer is miscible in the solvent, then the interaction will lead to a negative free energy of mixing and, immiscibility of the polymer in the solvent is due to thermodynamic incompatibility (Gupta 2010). Figure 19a, b provide an insight into the liquid epoxy-rubber nanophase separation in a blend. A research article details the rheological aspects of epoxy-rubber blends and their nanocomposites (Frohlich 2003). Thirdly, the epoxy-solid rubber interactions between epoxy resins and ethylene-propylene-diene monomer (EPDM) rubbers have been exploited to a lesser extent as they have been understood to a lesser extent. Figure 20 shows one such rubber particle reinforcement of epoxies resulting in a tough matrix (Padmanabhan 2015). Here, the particles are mixed homogeneously along with the resin and the hardener and allowed to cure. The question of evolution and phase separation of the rubber particles does not arise at all, and the particle size can be chosen for the anticipated scale of fracture mechanisms for an optimized toughness value. Figure 21 illustrates the CTBN toughening of an epoxy matrix. The CTBN rubber particle size is known to show an increase in particle size with its molecular

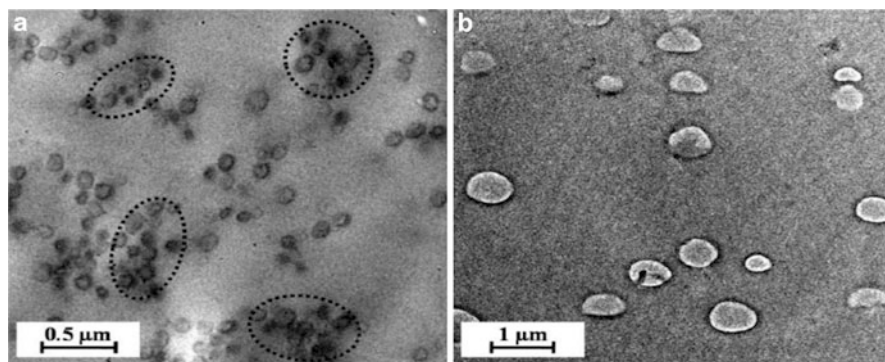
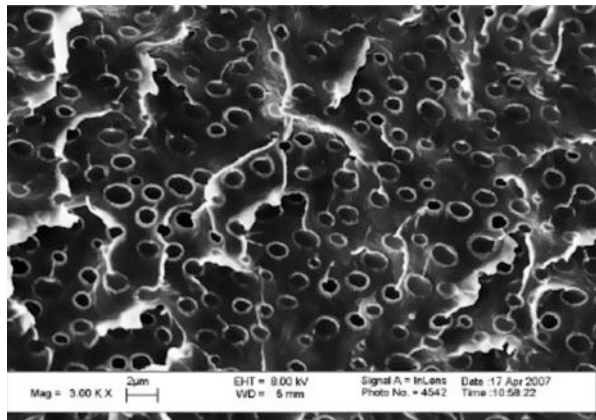


Fig. 19 Epoxy-liquid rubber phase separation during curing

Fig. 20 Epoxy-solid EPDM rubber blend showing a cracked rubber particle



Fig. 21 A micrograph CTBN liquid rubber toughened epoxy matrix (Mag 3000)



weight, as shown in Fig. 22. Curing of an epoxy and its accelerated curing due to the presence of CTBN rubber has been documented by a research group (Calabrese and Valenza 2003a).

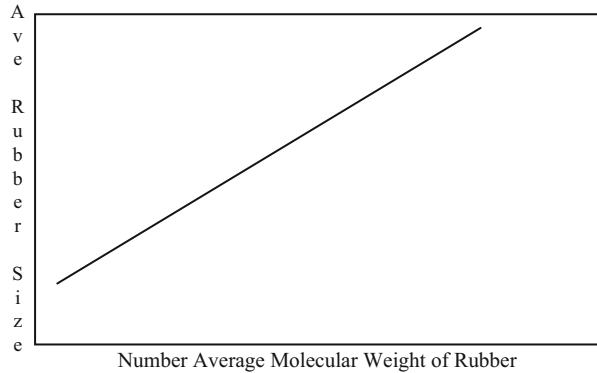
Thermodynamics of Epoxy-Rubber Blends

The enthalpy of mixing for an epoxy-liquid rubber is based on the measurements of cohesive energy density (CED) for liquids. The CED is the energy of vaporization of unit volume of the liquid, usually expressed in J/cm^3 .

$$\text{CED} = \delta^2 = \Delta H_{\text{vap}} - RT / V_{\text{liq}} \quad (13)$$

Where ΔH_{vap} is the enthalpy of vaporization, R is the universal gas constant, T the absolute temperature, and V_{liq} the molar volume of the liquid mixture. The quantity, δ ,

Fig. 22 A schematic of CTBN rubber particle size versus its molecular weight in a cured epoxy matrix blend



is called the solubility parameter whose units are $(\text{J}/\text{cm}^3)^{1/2}$. Here, de-mixing of liquids is attributed to the tendency of the molecules to attract their own species more strongly than a dissimilar species. The most important factor is the difference in solubility parameter between the rubber and the resin (Platzer 1970; White and Patel 1975; Rowe et al. 1970). When the difference is too small, the phase separation tends to be incomplete. However, if the difference is too large, the rubber will not disperse in the resin to form a homogeneous solution. The preferred difference is about $1 (\text{J}/\text{cm}^3)^{1/2}$. A rubber of adequate molecular weight of say over 3,500 will dissolve in the resin as the molecular weight is not too high and also go through a phase separation. Phase separation is necessary for the matrix to exhibit high fracture resistance. The molecular weight of the resin influences the phase separation to some extent.

In an epoxy-liquid rubber solution, the focus is on the equilibrium between two liquid phases, both of which contain an amorphous polymer (epoxy) and one or more solvents. When the temperature is raised due to the exothermic reaction and then lowered due to curing, the miscibility is reduced first and then phase separation occurs as the epoxy gels and cures into a solid structure. The maximum temperature for phase separation is designated as the upper critical solution temperature. The minimum temperature up to which phase separation occurs is designated as the lower critical solution temperature. Phase separation in epoxy rubber blend systems is discussed in details elsewhere (Konnola et al. 2015b). The condition for equilibrium between two phases in a binary polymer system is that the partial molar free energy of each component be equal in each phase. The critical concentration at which phase separation first appears is at a small volume fraction when the chain segment number is approximately 10^4 . The Flory-Huggins interaction parameter, χ_1 , exceeds $1/2$ for low molecular weights and is about $1/2$ for high molecular weights.

Feedback from Fracture Mechanisms in Processing

The addition of rubbers to epoxy matrices is about 45 years old as far as the recorded literature goes (McGarry 1970). The typical fracture energy of a brittle epoxy is

found to be approximately 100–200 J/m² compared with that required to break a covalent bond which is about 1 J/m². This suggests that a plastic zone exists at the crack tip, and viscoelastic processes contribute to the observed value. Thus only a proper understanding of the fracture and failure processes in these materials can lead to a better feedback on the development of tougher epoxies for utilization in applications (Bandhyopadhyay 1990). In glassy amorphous polymers there are two major energy absorbing processes: shear yielding and crazing. However, with rubber additions, the tensile yield strength decreases from about 70–100 MPa to 40–60 MPa. The elastic modulus also decreases from about 2–3 GPa by about 30%. These figures hold good for a CTBN liquid rubber additions of about 15 phr. The rubber particles can be seen under a scanning electron microscope (SEM) clearly by osmium staining the specimens for better clarity. The enhanced toughness in the epoxy-rubber blend is due to the dilational deformation of the rubber particles and the epoxy. The fracture tends to get brittle and does not provide any toughening at lower temperatures in the range of –20 °C. At room temperature, the crack tip plastic zone size has been proven to be about 25–75 μm. Such modified epoxy resins have been found to produce a fracture toughness value which is 10–30 times more than the unmodified epoxies (Garg and Mai 1988). The fracture toughness of a modified epoxy can go up to 6 kJ/m². The toughening mechanisms of a modified epoxy are:

- (i) Shear band formation near the rubber particle
- (ii) Fracture of rubber particles after cavitation
- (iii) Stretching, de-bonding, and tearing of rubber particles
- (iv) Trans-particle fracture
- (v) Crack deflection by hard rubber
- (vi) Voided cavitated rubber particles
- (vii) Crazing, a localized yielding process and fibrillation that lead to an interpenetrating local fracture
- (viii) Plastic zone at crack tip
- (ix) Diffuse shear yielding
- (x) Shear band craze interaction

Further, the deformation and fracture behavior of a rubber toughened epoxy has been well documented (Nicholson 1991; Kinloch 1983; Kinloch and Young 1983; Pearson and Yee 1986; Kinloch et al. 1983). Though crazing in epoxies is not as serious an issue as in thermoplastics like high impact polystyrene (HIPS), an interesting account of crazing is provided by an investigator (Bucknall 1977), and craze-like features in epoxies are briefly documented in another publication (Lilley and Holloway 1973). However, crazing in epoxy blends and nanocomposites of epoxy-rubber blends could be an interesting topic for research and development of strong and tough matrices for engineering applications. Figure 23 shows one such mechanism of reinforcement of epoxies by rubber particles.

Some of these fracture mechanisms are important in processing. They can occur during processing and have to be avoided through proper precautions. It is also seen that some of them do occur as a part of the processing process and cannot be

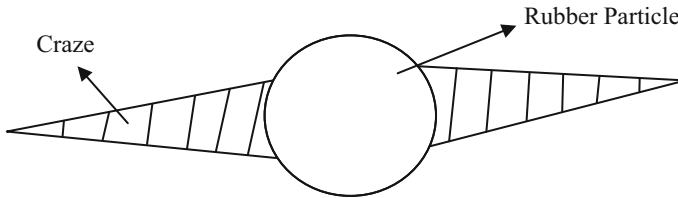


Fig. 23 Mechanism of reinforcement of epoxies by rubber particles

removed as they are a manifestation of the technique. Hence the post-yield viscoelastic behavior also gains significance.

Of the fracture mechanisms that we witnessed in the deformation of epoxies and blends, shear, shear banding, stretching, and tearing have to be considered with a special interest when the processing of epoxy-rubber blends have to be carried out with vacuum based, pressure based, and other techniques. As we gather that stretching and tearing of the rubber particles have to be avoided, shear and shear banding cannot be avoided. Shear that is inevitable can be understood from the point of view of transverse shear, shear near the walls, planar shear, and shear flow. For example, in compression molding which is a pressure-based technique, laminations and moldings depend on transverse shear which can be significant. This transverse shear across the laminations in a fiber-reinforced plastic containing a epoxy-rubber phase might result in considerable rubber particle fracture during the processing stage. Further the evolution of the rubber particles during curing under enormous pressure will not be as predicted under normal circumstances. However, the situation in an open contact molding provides for equilibrium evolution of the phase-separated blend. The vacuum-based techniques indirectly rely on pressure and so have to be studied with respect to the evolution under vacuum. The situation is considered very complex in injection and compression moldings where temperature, divergent and convergent shear flow, transverse flow, and rheotribology (www.tainstruments.com) play a significant role in the evolution of the phase-separated product. Tribology complements rheology, providing information on solid-solid interactions that adds an insight into the bulk fluid measurements of rheology. Tribology is especially concerned with quantifying the coefficient of friction as a function of sliding speed and load forces, under dry or lubricated conditions. This provides useful information about lubrication, wear, and tactility. Recent tribo-rheometry accessories rely on the control and measurement of angular velocity, forces, torque, and temperature of the rheometers. The system measures Stribeck curves, static friction, and coefficient of friction which are all useful for characterizing polymers. For the present application, the contact friction between the walls and the epoxy-rubber blend is a matter of interest for all the above said techniques. In fiber reinforced systems where the matrix is a rubber toughened epoxy, enough attention must be paid to rheotribology as the interfacial friction can

be a key governing factor requiring the correct lubricants or release agents at the mold walls.

The rheology of rubber epoxy blends is dealt with in detail by some investigators (Gabriel and Advani 2003) where the structure property correlation is illustrated in detail. The reader is also referred to the works of Agarwal (1989) on specialty polymers and polymer processing for a detailed treatise on processing of blends and the thermal aspects of rheology. It must be noted at this stage that investigations that report inspection of a sample after processing to check for possible fracture or damage are scanty compared to the reports that are published after mechanical testing. The later ones merely conclude that the fracture or damage is due to mechanical testing and not by processing parameters, which is incorrect. Investigations conducted carefully on this aspect will reveal the mechanisms that genuinely arise out of processing prior to testing. Figure 24 reveals the shear development in hot and cold runners during injection molding, where the central zone is considered low shear. Figure 25 shows the convergent and divergent flows during compression

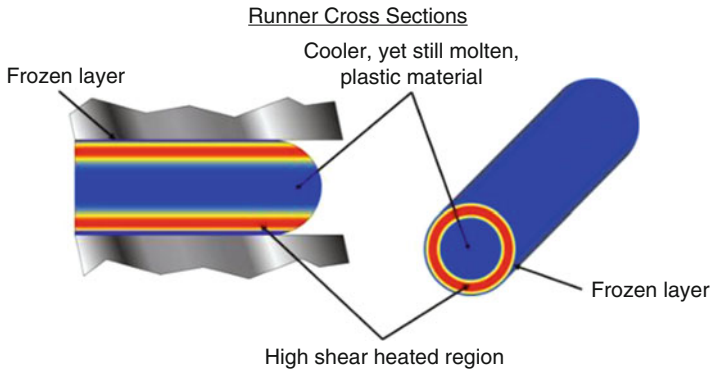
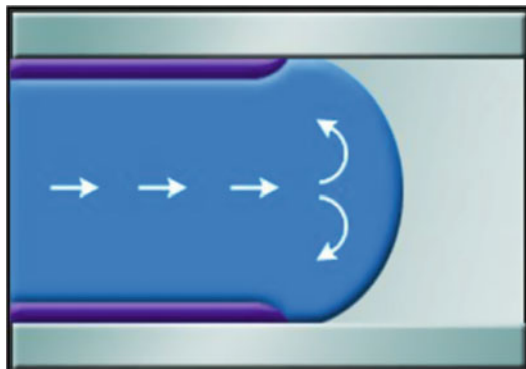


Fig. 24 Shear development and flow in injection molding

Fig. 25 Flow in compression molding, convergent, and divergent flow

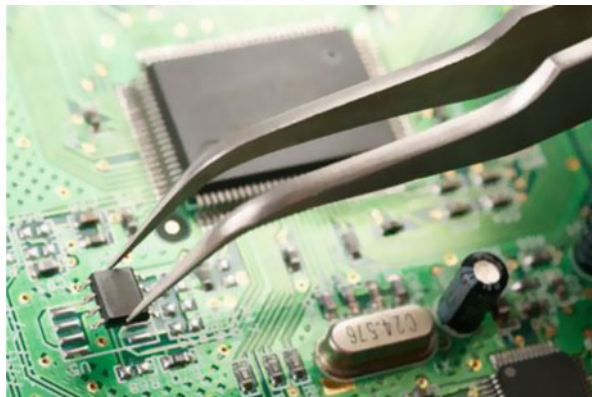


molding where the pressure developed in the blend can rise up to a few mega pascals. In compression molding, rheotribology and fracture mechanisms are expected to play a major role during processing, and a careful delineation of these is required before mechanical testing to eliminate the processing induced defects from those arising due to mechanical testing. Techniques that involve the use of moderate temperature and pressure, viz. vacuum bagging, contact molding, and vacuum infusion techniques are preferred while working with low and medium viscosity epoxy blends in order to mitigate the processing induced aberrations and avoid features like the rubber particle crushing. Pultrusion is also a favored technique, and reports of rheokinetic behavior analysis of pultrusion modeling of CTBN/epoxy blends are available (Calabrese and Valenza 2003b).

Microinjection molding of thermoplastics (www.Intechopen.com) is more than a decade old process. Microinjection molding using epoxy blends is off late gaining attention as miniaturization has reached a stage in the field of micromechanical, micro electro mechanical systems (MEMS), and electronic systems that demands better knowledge and implementation of microrheology. Mobile phone parts, microrobot parts, microgears in watches, neuro chips, microdevices for medical applications, and microelectronic circuits in general demand the use of parts fabricated through microinjection molding (www.Intechopen.com). The design of microchannels, microcavities, and the flow and cure simulation prior to manufacture have been dealt in details by some investigators. Many investigations exploiting this domain are awaited.

The prepreg manufacture of fiber-toughened epoxy matrix materials employs chemo-rheology extensively. Modified epoxy resin prepregs exhibit both viscous and elastic properties. During the curing process, their viscosity increases quickly in the gel region. The viscosity can be related to the degree of cure. Rheological equipment can be used to measure the epoxy-rubber blend properties effectively. The requirements for a rheological instrument to measure the rheological properties of the polymer successfully depend on the technique. The 50 mm parallel plates are beneficial for low viscosity, and the 25 mm parallel plates are good for high viscosity. This means that initially 50 mm parallel plates are used at the A-stage, and after B-staging or prepregging 25 mm plates are used for complete curing or C-staging studies. The viscosity of the polymer materials can be measured in the continuous rotation or oscillation mode. This ensures a good understanding of the rheological aspects when a prepreg is cured in an autoclave (Ciba Geigy 1983). Low viscosity epoxy systems are very popular in resin transfer molding (RTM) processes as the resin admixture is normally a one part system that is heated to lower the viscosity and cured after transfer into cavities. The RTM process is used extensively for the encapsulation purposes in nonhermetic and sometimes flexible electronic packaging (see Fig. 26) (Padmanabhan 2016). Here again, the process-induced inherent defects must be delineated from those arising out of mechanical and/or electrical testing alone, in order to understand the defects and eliminate or reduce them. Needless to say, some of the process-induced defects lead to a more serious defect upon testing. The fracture and failure progression studies thus gain significance.

Fig. 26 Encapsulations of ICs with epoxy blends



Applications of Epoxy-Rubber Blend Systems

Epoxy-rubber blends are used in functions that demand a very high fracture toughness with no deterrence to strength and stiffness even at elevated temperatures and hygrothermal environments. Tetra functional epoxy resin systems blended with silicone rubbers are an example of a good hygrothermal ceiling for novel applications. When used with high performance fibers like carbon (Padmanabhan and Kishore 1995), Kevlar (Padmanabhan 2012), or Zylon (Padmanabhan 2002), they find immense applications in laminated and sandwich aerostructures. High performance automobiles, electronic appliances, medical devices, MEMS devices, and mechanical equipment and devices require their parts to be made of epoxy-rubber blends for superior electrical insulation and mechanical properties like toughness and strength.

Conclusions

Rheology of epoxies and rubbers, their blends, classification, and types were introduced in this chapter. Principles of rheology and polymer rheology were illustrated through conclusive plots, graphs, and schematic sketches. Rheology of rubbers, epoxies, and their blends were discussed with respect to their molecular structure, mobility, and conformational states as proven by literature. Rheology was explained with respect to the established viscoelasticity models for epoxies and their blends. Linearity and nonlinearity due to rubber additions were illustrated. A detailed account of rheometers and measurements was given. Miscibility, phase separation, and thermodynamics of epoxy-rubber systems that form an integral part of this chapter were discussed in detail. A correlation was drawn between rheology and shear behavior of these systems. Rheological insights on processing, manufacturing methods, curing reactions, and curing schedules were provided for epoxy-rubber

blend systems. Functional and product applications of rheology of epoxy/rubber blends were listed at the end to kindle interest in the tertiary reader.

Implications on Future Research

Some of the unsolved problems like: (i) the effect of pressure on chemo-viscosity, (ii) system pressure and relevance to high pressure injection molding and transfer molding processes, (iii) flow behavior and correlation of molecular theories of high molecular weight polymer fluids, (iv) delineation of deformation mechanisms at the processing stage and testing stage, (v) issues in micromolding of epoxy rubber blends, (vi) issues in RTM of epoxy rubber blends, (vii) development of very high temperature moisture resistant HT epoxy-silicone rubber blends, (viii) exploitation of crazing in epoxy-rubber blends for development of high toughness systems, (ix) nano-rheological aspects of epoxy-rubber blends, and (x) influence of hygrothermal attack on epoxy-rubber blends, need attention. It is hoped that researchers who are more adept than this author would address these issues and lead to a complete understanding of the subject and its exploitation.

References

- Agarwal LS (1989) Specialty polymers and polymer processing, vol 7, Comprehensive polymer science. Pergamon, Oxford
- Aklonis JJ, MacKnight WJ (1983) Introduction to polymer viscoelasticity, 2nd edn. Wiley, New York
- Argon AS (1973) Polymeric materials – relationship between structure and mechanical behavior. *Phil Mag* 28:839
- ASTM D 4440 (2015), West Conshohocken, PA, USA
- ASTM D1238 (2013), West Conshohocken, PA, USA
- Bandhyopadhyay S (1990) Review of microscopic and macroscopic aspects of fracture of unmodified and modified epoxy resins. *Mater Sci Eng A* 125:157–184
- Bauer WH, Collins EA (1967) Thixotropy and dilatancy, chapter 8. In: Frederick RE (ed) *Rheology – theory and applications*, vol 4. Academic, New York
- Billmeyer FW (2015) *A text book of polymer science*. Wiley, New York
- Blow CM, Hepburn C (1982) *Rubber technology and manufacture*, 2nd edn. Butterworth Scientific, London
- Bowden PB (1973) *The physics of glassy polymers*. Wiley, New York, p 327
- Bucknall CB (1977) *Toughened plastics*. Applied Science Publishers, London
- Calabrese L, Valenza A (2003a) Effect of CTBN rubber inclusions on the curing kinetic of DGEBA–DGEBA epoxy resin. *Eur Polym J* 39(7):1355–1363
- Calabrese L, Valenza A (2003b) The effect of a liquid CTBN rubber modifier on the thermo-kinetic parameters of an epoxy resin during a pultrusion process. *Compos Sci Technol* 63(6):851–860
- Christensen RM (2010) *Theory of viscoelasticity – an introduction*, 2nd edn. Dover, New York
- Ciba-Geigy Information sheet No: FTA 46d, (1983) pp 1–15; FTA 49e (1984), Duxford, Cambridge
- Ferry JD (1970) *Viscoelastic properties of polymers*, 3rd edn. Wiley, New York
- Flory PJ (1953) *Principles of polymer chemistry*. Cornell University Press, Ithaca
- Frohlich J (2003) Toughened epoxy hybrid nano composites. *Macromolecules* 36:7205

- Gabriel OS, Advani SG (2003) Core-shell rubber/epoxy blends, rheology, advanced polymeric materials: structure property relationships. CRC Press, Boca Raton
- Garg AC, Mai YW (1988) Failure mechanisms in toughened epoxy resins – a review. *Compos Sci Technol* 31:179–223
- George SM, Puglia D, Kenny JM, Parameswaranpillai J, Thomas S (2014) Reaction-induced phase separation and thermomechanical properties in epoxidized styrene-block-butadiene-block-styrene triblock copolymer modified epoxy/DDM system. *Ind Eng Chem Res* 53:6941–6950
- George SM, Puglia D, Kenny JM, Parameswaranpillai J, Vijayan P, Pionteck J, Thomas S (2015) Volume shrinkage and rheological studies of epoxidised and unepoxidised poly(styrene-blockbutadiene-block-styrene) triblock copolymer modified epoxy resin-diamino diphenyl methane nanostructured blend systems. *Phys Chem Chem Phys* 17:12760
- Glasstone S, Laidler KJ, Eyring H (1941) The theory of rate processes. McGraw-Hill, New York
- Gupta RK (2010) Polymer nano composites handbook. CRC Press, Boca Raton
- Huggins ML (1958) Physical chemistry of high polymers. Wiley, New York
- ISO 1133 (2005) Determination of the melt mass-flow rate (MFR) and melt volume-flow rate (MVR) of thermoplastics – Part 1: standard method, International Standards Organization, Switzerland
- Ivankovic M (2003) Cure kinetics and chemo-rheology of epoxy/anhydride systems. *J Appl Poly Sci* 90:3012–3019
- Kinloch AJ (1983) Toughened multiphase thermosetting polymers. *Br Polym J* 15:83
- Kinloch AJ, Young RJ (1983) Fracture behavior of polymers. Applied Science Publishers, London/New York
- Kinloch AJ, Shaw SJ, Hunston DL (1983) Deformation and fracture behavior of a rubber-toughened epoxy: 2 failure criteria. *Polymer* 24(10):1355–1363
- Kitagawa M (1977) Power law relationship between yield stress and shear modulus for glassy polymers. *J Polym Sci Polym Phys Ed* 15:1601–1611
- Konnola R, Joji J, Parameswaranpillai J, Joseph K (2015a) Mechanical, thermal, and viscoelastic response of novel in situ CTBN/POSS/epoxy hybrid composite system. *RSC Adv* 5:61775
- Konnola R, Parameswaranpillai J, Joseph K (2015b) Structure and thermo-mechanical properties of CTBN-grafted-GO modified epoxy/DDS composites. *Polym Compos.* doi:10.1002/pc.23390
- Lee HL, Neville K (1967) Handbook of epoxy resins. McGraw-Hill/University of Michigan, Michigan
- Lilley J, Holloway DG (1973) Crazeing in epoxy resins, p 215
- Marshall GP, Culver LE, Williams JG (1970) *Proc R Soc A* 319:165
- McGarry FJ (1970) *Proc R Soc A* 319:59
- Nicholson JW (1991) The chemistry of polymers. Royal Society of Chemistry Paperbacks, Cambridge
- Padmanabhan K (1996) Time-temperature failure analysis of epoxies and unidirectional glass/epoxy composites in compression. *Compos: Part A* 27A:585–596
- Padmanabhan K (2002) Toyobo confidentiality report. www.toyobo.co.jp
- Padmanabhan K (2012) Mechanical behavior of Kevlar fibre/epoxy matrix composites. Lambert Academic Publishers, Germany
- Padmanabhan K (2015) 3rd Interim report, Project No: 1650, ARDB Structures Panel, India
- Padmanabhan K (2016) A multiphysics based finite element approach to evaluate the reliability of IC packages, chapter 2. In: Handbook of research on advanced computational techniques for simulation based engineering. IGI Global, Herche Ave
- Padmanabhan K, Kishore A (1995) Failure behavior of carbon fibre/epoxy composites in pin ended buckling and bending tests. *Composites* 26:201–206
- Pearson RA, Yee AF (1986) Toughening mechanisms in elastomer-modified epoxies, Part 2: microscopy studies. *J Mater Sci* 21:2475–2488
- Platzer N (1970) *Ind Eng Chem* 62:p6
- Robertson RE, Joynson CW (1966) *J Appl Phys* 37:3969
- Rowe EH, Siebert AR, Drake RS (1970) *Mod Plast* 49:110

- Thomas S (2014) Rheology of rubber toughened structural epoxy resin systems. Wiley, New York
- Vlassopoulos D, Chira I, Loppinet B, McGrail PT (1998) Gelation kinetics in elastomer/thermoset polymer blends. *Rheol Acta* 37(6):614
- Ward IM (1971) Review: the yield behavior of polymers. *J Mater Sci* 6:1397
- White JL, Patel RD (1975) *J Appl Poly Sci* 19:1775
- Williams ML, Landel RF, Ferry JD (1955) The temperature dependence of relaxation mechanisms in amorphous polymers and other glass-forming liquids. *J Am Chem Soc* 77(14):3701–3707
- Woo EM (1993) Time–temperature viscoelastic behavior of an interlaminar-toughened epoxy composite. *J Appl Polym Sci* 50(10):1683–1692
- www.intechopen.com
- www.tainstruments.com

Cure Kinetics of Epoxy/Rubber Polymer Blends

7

Debora Puglia and José Maria Kenny

Abstract

During the past decades, the toughening of epoxy resins has received increasing attention because many different applications demand epoxy materials with improved mechanical properties. Different approaches have been employed to toughen the epoxy system: agents as liquid rubbers, block copolymers, core–shell particles, glass beads, epoxidized thermoplastics, hyperbranched organic, and hybrid compounds and combinations of them have been considered as toughening agents for epoxy systems. The morphology of epoxy resins and, consequently, their mechanical properties strongly depend on the cure kinetics, and in the case of soluble liquid rubbers, phase separation takes place as the polymerization proceeds. Subsequently, the evolution of size and distribution of the rubber particles in the epoxy during the curing reaction represents a critical point for the success of the effect of rubber systems in terms of mechanical improvement of neat resin system. Therefore, different methods have been studied and developed to control the cure kinetic parameters of epoxy resins, in order to develop models and control their final morphology and properties. Among them, some of the most used are those based on chemical changes such as differential scanning calorimetry (DSC) and infrared (IR) spectroscopy methods, as well as those centered on bulk property changes such as rheological and pressure–volume–temperature (PVT) methods. In this chapter, these methods are discussed and the results obtained on toughening various types of epoxy systems are compared. Moreover, the studies are extended to nanostructured systems, where the presence of the nanofiller plays a crucial role in the evolution of the reaction kinetics.

Keywords

Rubber • Epoxy • DSC • Cure kinetics • Rheology

D. Puglia (✉) • J.M. Kenny

Civil and Environmental Engineering Department, Materials Engineering Center, UdR INSTM, University of Perugia, Terni, Italy

e-mail: debora.puglia@unipg.it; jose.kenny@unipg.it

Contents

Introduction	212
Cure Kinetics	216
Differential Scanning Calorimetry and Kinetic Analysis	218
Pressure–Volume–Temperature (PVT) Measurements and Real-Time FTIR Spectroscopy	224
Rheological Studies: Chemoreological Modeling of Cure Reaction	226
Conclusions	232
References	233

Introduction

High performance epoxy resin systems are becoming increasingly important as matrix materials for advanced composites used in aerospace, electronics, automotive, and other industries. Because of their excellent properties such as good mechanical behavior, very high adhesive properties, excellent chemical and solvent resistance, dimensional and thermal stability, and high electrical resistance epoxy thermosetting materials are widely used as adhesives, encapsulates, and matrices for composite materials (Fischer et al. 2011). However, the thermoset epoxies are generally brittle because of the highly cross-linked structure. While rigidity and strength are desired for many engineering applications, brittleness or lack of crack growth resistance eliminates wider usage of epoxies. Therefore, toughening of epoxies has become a necessity to ensure the feasibility of these materials for practical applications. In the application level, epoxy thermosets are usually modified, incorporating a rubber or a thermoplastic polymer in order to improve their toughness, strength, stiffness, or other properties of thermosetting systems (Ratna and Banthia 2004; Bagheri et al. 2009). Rubber modification has been found as a very successful approach to overcome the inherent brittleness of many engineering polymers (Wise et al. 2000; Ozturk et al. 2001).

Reactive liquid rubbers that are initially soluble in the base epoxy resin as well as rubbers that are initially immiscible in the resin are used as toughening agents (Ni and Zheng 2007; Williams et al. 1997). In the former case, phase separation of rubber takes place during cure, whereas in the latter case the rubber phase will be in the precipitated state. Nevertheless, this type of rubbers generates heterogeneity, and hence a very low content is enough for toughening. The former type of rubbers is considered as the best modifiers. On the other hand, rubbers with different functionalities, which permit to form covalent interactions at the epoxy interface, normally serve as the best tougheners. When low-modulus rubber particles are dispersed into the brittle resin matrix, the force that induces and propagates cracks is dissipated by the rubbery phase and prevents the catastrophic failure of the matrices. Major liquid rubbers used as tougheners are carboxyl-terminated butadiene-co-acrylonitrile (CTBN), hydroxyl-terminated polybutadiene (HTPB) liquid rubbers, epoxy-terminated liquid rubbers (ETLR), amine-terminated butadiene-acrylonitrile (ATBN) rubbers, and acrylic

elastomers (Visakh et al. 2013). Examples are reported for blending with a miscible high-performance thermoplastic (Jyotishkumar et al. 2011) and blending with liquid rubber or thermoplastic exhibiting initially low miscibility with the epoxy resins precursors, which then phase separates at some extent of cure leading to two-phase microstructure (Abdolreza and Siamak 2010; Francis et al. 2006) and dispersion of preformed rubbery particles in the mixed epoxy precursors, which remain phase separated after the curing process (Kong et al. 2008).

Within rubber-based modifiers, core-shell rubber particles represent another type of preformed thermoplastic particles with a glassy shell that can be designed to adhere better with resin and a rubbery core to improve toughness. Reactive core-shell-type hyperbranched block copolymers with onion-like molecular architecture were used as flexibilizers and toughening agents for thermosets. The system was reported to achieve good miscibility, low viscosity, and better interfacial adhesion (Frohlich et al. 2004). An important characteristic of core-shell particles as tougheners for epoxies is the role of the particle/epoxy interface (Qian et al. 1997). Discrete interface is generated between the particles and the matrix epoxy by the shell polymer of core-shell particles.

An important feature of using core/shell particles as toughening agents for epoxies is the role of the particle/epoxy interface. Compared to conventional CTBN-toughened system, in which rubber particles are directly surrounded by epoxy matrix, a discrete interface is introduced between the particles and the epoxy matrix by the shell polymer of core/shell particles. The architecture of this interface can be well controlled by varying the shell compositions and the thickness of core/shell particles by emulsion polymerization techniques, so that the role of particle/epoxy interface on toughening of epoxies can be investigated systematically, maintaining the rubbery core unchanged. The effect of shell composition of core/shell particles on toughening of epoxies has been studied by several investigators. However, the results are conflicting. Sue and co-workers (1993) found that introducing glycidyl methacrylate (GMA) into the shell of core/shell particles, which provided chemical bonds at the particle/epoxy interface, had no influence on the toughening, while incorporating AN into the shell improved the dispersibility of particles in the epoxy matrix and increases fracture toughness of the modified epoxies. Henton et al. (1988) concluded that the covalent bonding introduced at the rubber/epoxy interface was very crucial to the toughening.

The role of rubber/matrix interface on the fracture toughness of modified plastics is certainly a controversial issue. The rubber/matrix interface can be varied in terms of interfacial bonding force, thickness, flexibility, and composition. However, it is difficult to assess exactly how these changes in the rubber/matrix interface will effect the toughening mechanisms. The main toughening mechanisms operating in a rubber-toughened epoxy are internal cavitation of rubber particles and shear yielding in the matrix, which is believed to be promoted by the cavitation of the rubber particles. Obviously, this internal cavitation of rubber particles would require a minimum amount of interfacial adhesion between rubber particles and epoxy matrix. It was believed that the chemical bonding between rubber particles and epoxy matrix

is essential to the toughening of epoxies for a carboxyl-terminated butadiene-acrylonitrile (CTBN)-toughened epoxy system (Pearson and Yee 1986). However, it has been found that there is a competition between internal cavitation of rubber particles and debonding of the rubber particles from epoxy matrix. When the interfacial adhesion was sufficient, the rubber particles cavitated internally during the fracture; when the interracial bonding was poor, the rubber particles debonded interfacially from the matrix. Further investigation on the underlying mechanisms has shown that the degree of the internal cavitation of the rubber particles significantly increased as the rubber/epoxy interfacial zone changed from rigid and narrow to flexible and wide. The explanation for this phenomenon is that the size and deformability of the interfacial zone directly affected the triaxial tension around the rubber particles which induced the cavitation of the rubber particles.

Nanoparticulate composites have been also observed to be impact tougheners for epoxy matrices. They showed superior material properties than microscale fillers (Gleiter 2000) for toughening. Thermoplastics are also one of the best toughening agents for thermosetting polymers, particularly for epoxies, as they will not reduce the glass transition of the cured network. In addition, block copolymer-modified epoxy resins have generated significant interest because it was demonstrated that the combination could lead to nanostructured thermosets. Amphiphilic block copolymers self-assemble to form a variety of well-defined ordered and disordered microstructure morphologies such as spherical, cylindrical, lamellar, and gyroid phase (Vaia et al. 1999; Girard-Reydet et al. 2003). Studies show that introduction of block copolymers in epoxy resin can greatly improve mechanical and physical properties including tensile, flexural, impact, wear resistance, thermal resistance, and performance. The fracture toughness, modulus, and other thermomechanical properties of the nanostructured blends prepared using block copolymers are generally higher than that of pristine epoxy resin (Wu et al. 2005).

The addition of both a solid and a liquid rubber, as well as a liquid rubber and a thermoplastic, has been reported to give a major increase of the toughness of the material. Moreover, it is well known that the extent of toughening depends on the system morphology. Many papers have been published about the morphology occurring after curing in variously rubber-modified epoxy resins, and it is widely accepted that the enhanced toughness is mainly due to the formation of a two-phase system with rubbery particles precipitated into the matrix from an initially homogeneous solution (Pucciariello et al. 1991).

It is then clear how the curing phase in rubber-modified epoxy could present a determinant step in obtaining improved mechanical performance of different thermosetting systems. Differently from neat epoxy, the cure of an epoxy resin/curing agent/rubber formulation generally involves the sequential processes of phase separation, gelation, and vitrification. Phase separation of the rubber occurs because during the reaction the increase of the molecular weight of the epoxy-rich matrix lowers the compatibility between the rubber and the matrix itself (Klug and Seferis 1999). It has been established that phase separation stops at the gel point and no growth of the rubbery particles occurs during the subsequent cure. As gelation strongly depends on the cure temperature, the development of the morphology and

the growth of the rubbery particles strongly depend on the cure conditions (Ruseckaite et al. 1993). A variety of morphologies such as bicontinuous or inverted structures can be generated during the reaction-induced phase separation process. In the case of thermoplastic modifiers, the morphologies mainly depend on thermodynamic and kinetic factors, namely, the modifier concentration and its molar mass, the curing temperature and reaction rate, and the viscosity during the phase separation (Jose et al. 2008; Jyotishkumar et al. 2009, 2010).

In the case of liquid rubber, as the curing reaction proceeds, the molecular weight increases and the phase separation occurs at some stage, leading to the formation of a two-phase morphology (Bascom and Hunston 1989). Extensive studies (Romano et al. 1994) have shown that the phase separation process is a result of the decrease in configurational entropy due to the increase in molecular weight as epoxy cures. This changes the free energy of mixing leading to a decrease in solubility of the rubber that provides the driving force for phase separation. Various morphological parameters like particle size, particle size distribution, interparticle distance, and matrix to particle adhesion play an important role in toughening (Chen et al. 1993). These morphological parameters depend on chemistry, molecular weight, and concentration of the liquid rubber (Kim et al. 1995) as well as on the curing condition (Hsich 1990).

So, being epoxy of vital importance to many industries including aerospace technologies, automotive manufacturers, and many other specialized as well as nonspecialized applications, it has to be considered that a better understanding, design, and control of the processes used to formulate epoxy-modified systems became of crucial importance. Usually, these processes have been traditionally undertaken by trial and error methods due to the complexity of the reacting systems. However, advances in techniques have enabled a more scientific analysis of these systems and have led to a reduction in the design and raw material costs. The successful production of rubber-modified composites requires good knowledge of the kinetic and rheological properties of the specific systems, and the ability to predict and monitor the kinetic and viscosity changes during the reaction plays a key role in the development and the control of composite manufacturing (Lionetto and Maffezzoli 2013). It is clear that the chemical reaction dramatically affects the molecular structure of polymers. In addition, rheological properties of polymers depend on the molecular mobility, which is linked to the molecular structure. Indeed, the characteristics of the curing process and the final properties of rubber-modified epoxy-based composites are strongly dependent on the kinetic and chemorheological properties of the matrix (Palomo et al. 2013). Therefore, to analyze substantial relationships among the processing variables, resin structures, and properties, a comprehensive study of the evolution of resin cure and cross-linking should be always considered.

In the case of neat epoxies, during the initial stages of the cross-linking process, branched molecules of broadly distributed sizes and of various architectures are formed. Their average molecular weight increases as the cross-linking reaction progresses. The gel point determines the transition from liquid to solid and is defined by the instant at which the system reaches a critical extent of reaction for which

either the weight-average molecular weight diverges to infinity (infinite sample size) (Winter 1989; Winter and Chambon 1986) or a first macromolecular cluster extends across the entire sample (finite sample size). Beyond the gel point, the network stiffness continues to increase steadily with increasing cross-linking density until the system reaches completion of the chemical reaction. The epoxy prepolymer reacts further with a wide variety of primary or secondary amines to form a rigid polymer network (Rudin and Choi 2012). The conversion of an epoxy polymer to an interconnected network structure is formally similar to the vulcanization of rubber, but the process is termed curing in the epoxy system. It has been proved that the addition of rubbers to epoxy resins not only alter the final morphology and properties but also the curing kinetics (Thomas et al. 2007, 2012; Calabrese and Valenza 2003). Because phase separation of the elastomer currently takes place during curing after the rate of the reaction, the resultant heterogeneous morphology obtained after the reaction controls to an important extent the properties of the final product. It has been also shown that the rubber particle size in rubber-modified epoxy resins using a rubber butadiene-acrylonitrile copolymer with carboxyl or hydroxyl end groups influences the final toughness of the composite (Ramos et al. 2005; Tripathi and Srivastava 2009) due to the fact that, irrespective of the rubber end group, the curing kinetics of epoxy slows down due to dilution and viscosity effects, as determined from gelation time measurements (Romo-Urbe et al. 2014). So, according to these experimental results, it results deeply important to understand and model the curing reaction of epoxy systems in presence of a second rubber phase.

Cure Kinetics

Curing of epoxy resins is one of the most common procedures for preparing thermosetting materials, via polymerization addition, through the reaction of epoxy compounds containing two or more oxyrane groups in the molecule with polyfunctional amines, acid/anhydrides, polycarboxylic acids, or phenolic compounds as curing agents. During the curing process, various reactions take place, mainly glycidyl-primary amine and glycidyl-secondary amine, which give derivatives containing hydroxyl groups that further react with glycidyl groups to give ether links. At the beginning of the curing process, epoxy resin is generally a liquid of low viscosity; then viscosity rapidly increases in value with the advance of the curing reaction up to a very high value at the gel point, at which the resin is converted into rubbery three-dimensional network. Finally, it becomes a glassy material at the vitrification point, provided the cure temperature is lower than the glass transition temperature (T_g).

In the curing process, when rubber is initially added, it separates from the epoxy resin. The volume fraction, domain size, and concentration of particles of the phase-separated rubber are determined by the competing effects of nucleation (thermodynamic effects) and grow rates, on the one side, and the polymerization rate (kinetics), on the other (Williams et al. 1984; Vazquez et al. 1987; Wang and Zupko 1981). In general, phase separation occurs before gelation at early stage of conversion.

The inclusion of elastomers on epoxy resin results in a phase-separated network on curing (Kargarzadeh et al. 2015). However, there are several reports on DGEBA-based epoxy resin and elastomeric modified blends on immiscibility or miscibility depending on the structure of the curing agent. Curing reaction takes place between the epoxy and the curative, and hence the kinetics depends on the nature of the hardener employed. Thus, each system can be considered as a separate entity depending on the type of curative used. Many studies have been published on the cure kinetics of DGEBA-based epoxy resin with carboxyl-terminated liquid rubber (Morancho and Salla 1999; Tripathi and Srivastava 2007, 2008).

The most popular rubbery modifying agent is carboxyl-terminated butadiene-acrylonitrile random copolymer (CTBN) because of its miscibility with the epoxy hardener mixture during the initial polymerization period and also because the carboxyl functional groups in CTBN can react with the epoxide groups, thus achieving a high level of interfacial adhesion. The enhancement in toughness is achieved because the elastomeric phase precipitates at some stage of the curing process into particles of very small size (Akbari et al. 2013; Thomas et al. 2007; Russell and Chartoff 2005).

In many studies in which DGEBA was toughened with CTBN, the morphology study of the cured system revealed a two-phase region where the liquid rubber particles are distributed in the epoxy matrix, and a slight reduction in T_g on the addition of CTBN was observed. From the thermokinetic point of view, it has been observed that CTBN rubber-modified epoxy resins show a faster curing reaction and low gelation time.

Yamanaka et al. (1989) carried out detailed phase separation studies on the mixture of epoxy and CTBN, cured by using piperidine and Versamid 125 (Henkel-Hakusui Co.). They suggested that phase separation continued through spinodal decomposition (SD) induced by the increase in the molecular weight of epoxy, that structure fixation at the early stage of spinodal decomposition yielded the co-continuous two-phase structure, and that the formation of spherical domain structure was the result of the fixation of the phase separation structure at a late stage of spinodal decomposition by the formation of epoxy network. In another study, Chen and Lee (1995) observed that nucleation and growth (NG) mechanism dominates the phase separation process during the polymerization of CTBN-modified dicyandiamide-cured epoxy system. In this system, the spherical domain structure started as dispersed dots, then conjugated with gradually growing diameters. The fixation of the phase-separation structure is determined at an early stage of polymerization, and the domain size is dependent on the progress of reaction.

On the basis of these facts, it should be noted how the deep analysis of rubber/epoxy systems curing reaction is a need that has been solved by the research using many different methods to be considered for kinetic study. Kinetic results (that can be obtained by means of DSC method, dielectric analysis (DEA), IR spectroscopy, rheological, and PVT methods, as well as dynamic mechanical analysis (DMA)), combined with those obtained by characterization of the final resins, such as thermomechanical behavior, morphological, and electrical, among others, have been used to understand the existing correlation among their many different

properties and, on this basis, to be able to prepare these materials with better properties. DSC is a widely accepted tool for monitoring cure reaction since excellent results can be obtained with a small amount of sample in a relatively short time. Both isothermal and dynamic measurements were used to follow the cure reaction. DSC has two advantages: (i) it is the reaction rate method that permits to measure with great accuracy both the rate of reaction and degree of conversion, and (ii) the DSC cell may be considered as a mini reactor without temperature gradient. DSC kinetics provides variables required for solution of the heat/mass transfer equation, namely, heat flow and heat generation.

Therefore, an approach to obtain experimental data from DSC analysis to model the reaction kinetics of a rubber-modified epoxy resin is to relate the heat developed as a function of time to the evolution of the degree of reaction. Such a kind of approach is called a phenomenological approach; it uses the variation of some macroscopic properties in the reacting system as an indicator of the extent of the reaction. With this method, it is possible to obtain the evolution of the degree of cure from the measurement of the heat produced during the cure reaction and build a table of the degree of reaction as a function of time and temperature that can be used to produce the experimental data for the model. With such an approach, the degree of cure (α) can be equated to the ratio between the heat evolved during the cure process ($\Delta H(t)$) and the total heat of reaction (ΔH). The differential scanning calorimeter (DSC) is both the ideal tool to monitor these kinds of reactions and the most used one. The DSC provides the heat flow ($\partial H/\partial t$), or instantaneous heat, released or absorbed by the reactive system as a function of the absolute temperature or time. Dynamic and isothermal DSC analyses are widely used to obtain an indirect estimation of the degree of cure of a thermosetting system, assuming that the heat released during polymerization is always proportional to the consumption rate of reactive groups (which actually describes the extent of the reaction). Calorimetric data can therefore be used to both create and verify theoretical and empirical kinetic models and obviously to calculate kinetic parameters. A combination of the dynamic and isothermal tests makes possible to determine the variations of the degree of cure and the rate of cure as a function of time and/or temperature.

Differential Scanning Calorimetry and Kinetic Analysis

The study of curing kinetics by DSC is widespread in the literature. This well-established technique consists in applying isothermal step or linear temperature scan to a small sample (few milligrams) and to measure the temperature and the heat flux associated with a range of physical or chemical changes involving an exothermic or endothermic response. It is based on a differential measurement between a reference and the sample. The cross-linking being an exothermic physical phenomenon, the overall heat released during the reaction is used to monitor the evolution of the conversion degree. More precisely, it is assumed that the exothermic heat flux is proportional to the reaction rate. Both isothermal and dynamic temperature scans can be adopted to determine the kinetic parameters with DSC. Isothermal DSC is more

informative than dynamic DSC and leads to better interpretations. Since cure polymerization involves many reactions such as etherification, esterification, homopolymerization, etc., the isothermal mode is more effective than dynamic monitoring for detailed investigation.

For several decades, the empirical models proposed in the literature to describe experimental reaction rates of thermosetting resins (epoxy, polyester, etc.) were not substantially modified. They are also (fortunately) enough suitable for epoxy systems (under given conditions), which cross-link as the stepwise polymerization scheme. The mechanistic approach is much less used because it involves the determination of many kinetic parameters. Indeed, this type of model requires a detailed description of elementary reactions to describe the evolution of species concentration and thus the progress of cross-linking, which is also complex. The undeniable advantage of these models is the accuracy of prediction and interpretation. In contrast, a phenomenological model describes the kinetics from a macroscopic point of view, taking into account its main chemical and physical characteristics (effects of gelation, vitrification, etc.), thus reducing the parameters to be identified. They are thus widely preferred. In the following, we thus take part voluntarily to develop empirical models further at the expense of mechanistic models.

An optimal curing process depends on understanding the curing kinetics, the curing mechanism, and accurate modeling of the curing process. This modeling includes determination of the mechanism, or appropriate kinetic equation for an analyzed system, measurement of reaction order, and activation energy of the reaction. Many chemical reactions and physical state transformations (as the gelation or vitrification) occur during the cure process of the epoxy resin. Since the behavior of a thermosetting polymer is strongly affected by the curing process, poorly controlled cure can produce unwanted variations in the thermal and rheological properties of the system during the manufacturing processes of the final product. Therefore, an accurate model not only helps to monitor the evolution of the curing system (to plan and/or to control single processes), but it can also be used in material design to compare the behaviors of different formulations, obtained by mixing several resins, catalysts, additives, or fillers. The cure reaction in epoxy systems was monitored by several researchers using different techniques like Fourier transform infrared spectroscopy (FTIR), Raman spectroscopy, dielectric spectroscopy, rheometry, and differential scanning calorimetry (DSC).

DSC is a widely accepted tool for monitoring cure reaction since excellent results can be obtained with a small amount of sample in a relatively short time. DSC has two advantages: (1) it is the reaction rate method that permits to measure with great accuracy both the rate of reaction and degree of conversion, and (2) the DSC cell may be considered as a mini reactor without temperature gradient. DSC represents one of the most useful methods for studying the cure kinetics of epoxy resins and allows us to know the effect of additives, such as rubbers, since the kinetic analysis of DSC data allows for the reduction of a complex mechanism to an effective kinetic schema with basis on the reaction steps of major contribution to the overall process.

The phenomenological model for the reaction rate, $d\alpha/dt$, is usually described by the following equation:

$$\frac{d\alpha}{dt} = k(T)f(\alpha) \quad (1)$$

where $k(T)$ is the reaction rate constant and $f(\alpha)$ is a function of the conversion. Commonly, $k(T)$ is considered to depend only on temperature, T , as an Arrhenius-type expression, $k(T) = A \exp(-E_a/RT)$, and $f(\alpha)$ to depend only on conversion, $f(\alpha) = (1 - \alpha)^n$, and Eq. 1 can be written as

$$\frac{d\alpha}{dt} = A \exp\left[-\frac{E_a}{RT}\right] (1 - \alpha)^n \quad (2)$$

where A is the frequency factor, E_a is the activation energy, R is the universal gas constant, and n is the reaction order.

Researchers have early employed an n th-order kinetic model to describe the cure reaction of a thermoset resin (Turi 1981). But these models are valid for modeling reactions having a maximum rate at $t = 0$; hence, in order to predict autocatalysis of epoxy reaction by hydroxyl groups that shows a maximum reaction rate at $t > 0$, the model has to be generalized.

The autocatalytic kinetic model from Kamal has been developed for these types of reactions (Kamal 1974) by considering the reaction between the epoxy groups with all amines (primary and secondary) in addition to catalytic and autocatalytic effects. Accordingly, a general expression for the conversion rate is given by:

$$\frac{d\alpha}{dt} = (k_1 + k_2\alpha^m)(1 - \alpha)^n \quad (3)$$

where α is the conversion; k_1 and k_2 are the rate constants with two different activation energies and pre-exponential factors and represent the noncatalytic and the autocatalytic nature of the reaction, respectively; and m and n are variables (kinetic exponents) that determine the reaction order and can have different values, with $m+n$ being the overall reaction order. The kinetic constants, k_1 and k_2 , depend on the temperature according to an Arrhenius-type expression. Kamal's model considers only the chemical kinetics, whereas the influence of diffusion and the etherification reaction are not taken into account by this model.

Many useful methods have been proposed to estimate the cure rate of the epoxy system by DSC based on the assumption that the heat evolved during the cure reaction is proportional to the monomer conversion (Prime 1981). The Kissinger method, iso-conversional method, autocatalytic model, and fractional life method are well known, among others.

Kinetic parameters can be easily calculated by using nonisothermal conditions for curing epoxy resins. When the temperature varies with time at a constant heating rate, $\beta = dT/dt$, Eq. 1 is represented as follows:

$$\frac{d\alpha}{dt} = \left(\frac{A}{\beta}\right) \exp\left[-\frac{E_a}{RT}\right] f(\alpha) \quad (4)$$

Equations 2 and 4 allow the calculation of A , E_a , and $f(\alpha)$ for the overall process, but they do not allow for a possible change in the rate-limiting reaction. However, in the iso-conversional kinetic analysis, it is assumed that the reaction rate at constant conversion depends only on the temperature. Hence, the activation energy, E_a , can be obtained from the maximum reaction rate, where $d/dt(d\alpha/dt)$ is zero under a constant heating rate. On this basis, Kissinger derived a method for using experimental data obtained from DSC at different heating rates (Kissinger 1957; Ozawa 1970; Brown 1988):

$$\ln\left(\frac{q}{T_p^2}\right) = \ln\left[\frac{AR}{E_a} n(1-\alpha)^{n-1}\right] - \frac{E_a}{RT_p} \quad (5)$$

where q is the constant heating rate and T_p is the temperature corresponding to the maximum of the exothermic peak. Thus, by plotting $\ln(q/T_p^2)$ against $1/T_p$, the activation energy can be obtained from the slope, $m = (-E_a/R)$, without knowing the reaction order. In this equation, E_a is the effective activation energy at a given conversion, which is independent of α for a single-reaction step and varies with α for multistep processes. Only an overall activation energy can be obtained from the Kissinger method, whereas a more complete information of activation energy throughout the entire conversion can be calculated by the iso-conversional method developed by Flynn and Wall. This is the well-known Flynn–Wall–Ozawa method, expressed as follows:

$$\log(q) = \log\left[\frac{k_i E}{g(\alpha) R}\right] - 2.315 - \frac{0.457 E_a}{RT_p} \quad (6)$$

where $g(\alpha)$ is an integrated form given as $g(\alpha) = \int_0^\alpha d\alpha/f(\alpha) = K(T)t$. According to this method, a plot of $\log(q)$ against $1/T_m$ allows us to find the activation energy from the slope, $m = (-0.457 E_a/R)$, by fitting to a straight line without any assumption on conversion-dependent functions for different conversion levels. Both models give similar values of E_a , but slightly higher values for that Flynn–Wall–Ozawa model. In general, in the initial stage, E_a by both methods decreases with the increasing of conversion up to 30–40%, owing to the autocatalytic cure reaction resulting from the production of OH groups, and then increased after a minimum value owing to the increasing cross-link density in epoxy resins. The n-order model can be expressed in logarithmic form by fitting experimental data to a straight line:

$$\ln\left(\frac{d\alpha}{dt}\right) = \ln k + n \ln(1-\alpha) \quad (7)$$

In isothermal conditions, α and the conversion rate, $(d\alpha/dt)$, can be obtained from the change in the reaction heat measured by DSC, which has to be normalized with the total heat, as $\alpha(t) = \Delta H(t)/\Delta H_{total}$. So, by plotting $\ln(d\alpha/dt)$ versus $\ln(1-\alpha)$, a straight line is obtained. k can be calculated from the intercept, and n is the slope.

Then, taking natural logarithms, the Arrhenius' expression for k is $\ln k = \ln A - E_a/RT$, and A and E_a can be calculated for each temperature. As mentioned, the cure kinetics of epoxy resins generally obeys the catalytic model, and for many systems $n = m = 1$. In these cases, based on Eq. 3, the plot of $(d\alpha/dt)(1-\alpha)$ versus $\alpha(t)$ can be fitted to a straight line, from which k_1 and k_2 can be obtained. However, in general, $n \neq m \neq 1$, and fitting isothermal condition data to Eq. 3 is difficult because of the number of variables, including two different exponents n and m . Hence, other models have been proposed for evaluating the kinetic parameters, in which, nevertheless, n and m are not uncoupled. The method proposed by Kenny does not rely on combined order and involves taking the natural logarithm of both sides of Eq. 3, yielding (Kenny 1994):

$$\ln\left(\frac{d\alpha}{dt}\right) = \ln(k_1 + k_2\alpha^m) + n\ln(1-\alpha) \quad (8)$$

A plot of versus $\ln(1-\alpha)$ generates a straight line with slope n . Then, rearranging in another form gives:

$$\ln\left[\frac{d\alpha/dt}{(1-\alpha)^n}\right] = \ln k_2 + m\ln\alpha \quad (9)$$

Substituting n and k_1 , m can be calculated from the slope and k_2 from the intercept. In a different approach, Kim et al. (1998) used the well-known Avrami's equation by assuming that cross-linking process is a phenomenological analog to crystallization.

Looking back at the kinetics of rubber-modified epoxy, the general approach described above can be adapted and modified to find cure kinetic parameters of these specific systems, and many examples can be found to confirm that this approach can be considered correct even in the presence of a second rubber phase.

As an example, we report here the results of the work made by Vijayan et al. (2012), in which they studied the effects of carboxyl-terminated (butadiene-co-acrylonitrile) (CTBN) liquid rubber on the cure kinetics of diglycidyl ether of bisphenol-A (DGEBA)-based epoxy resin/nadic methyl anhydride (Fig. 1). The above curves illustrate that the rate of curing increases with increase in cure temperatures (Fig. 1a, b). The reaction rate increases with time at a particular temperature, and it occurs through a maximum after the start of the reaction, showing autocatalytic nature. The reaction mechanism remained the same even after the inclusion of the liquid rubber. The maximum peak value of the rate of the reaction is higher as the isothermal temperature is higher and shifts to shorter time with increase in isothermal temperature. Obeying an n th-order kinetics, the maximum cure reaction rate should be observed at $t = 0$. But the cure kinetics of neat as well as modified epoxies showed a maximum reaction rate at $t > 0$, negating the simple

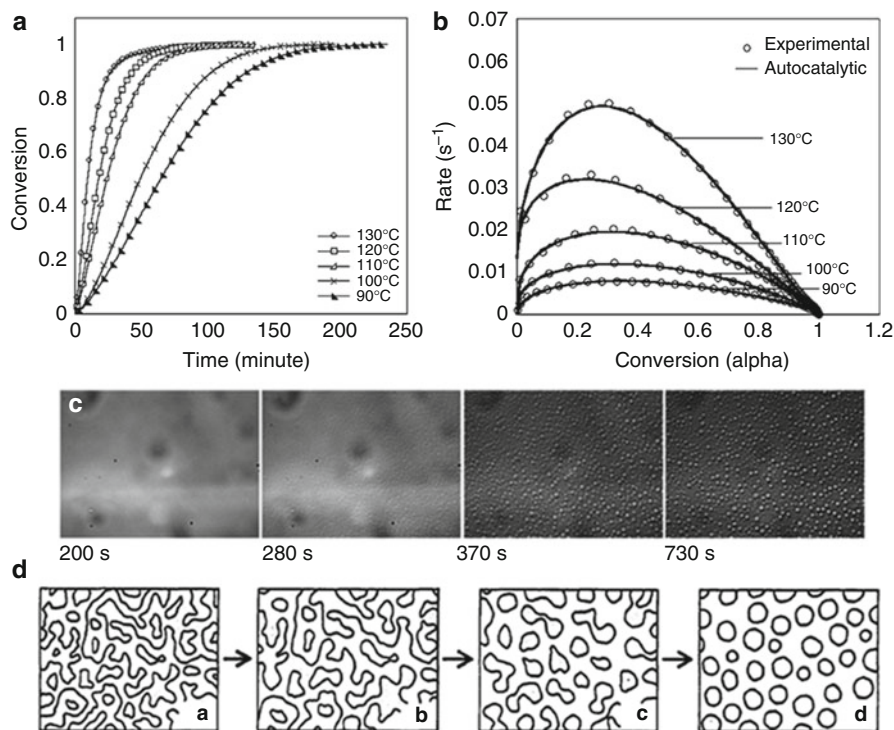


Fig. 1 (a) Conversion vs. time plots at different temperatures for epoxy/15 phr CTBN; (b) comparison of experimental data with model predictions: rate vs. conversion curve for epoxy/15 phr CTBN; (c) optical micrographs of phase separation in epoxy/15 phr CTBN at 130 °C ($200 \times 150 \mu\text{m}$); (d) schematic representation of phase separation (Vijayan et al. 2012; Yamanaka et al. 1989)

nth-order kinetics. It was also proved that the rate of conversion significantly increases with increase in temperature for neat as well as modified systems, showing the thermal effect of the cure reaction. A linear enhancement in the reaction rate with conversion was indicated for all modified systems during the initial stages of cure at all temperatures. However, a deviation in the rate of reaction from linearity was noticed as conversion proceeds (up to 60–80% of conversion, depending on the curing temperature). Deviations observed are attributed to the fact that the reaction becomes diffusion controlled at the onset of gelation (the diffusion-controlled model to be discussed next). There is a simultaneous increase in molecular weight and viscosity along with the development of the network structure. As a result, the rubber and epoxy become less compatible and a phase separation state is reached, whereby rubber-rich domains precipitate in the epoxy-rich matrix and the liquid rubber become phase separated (Fig. 1c, scheme in Fig. 1d). Thus ultimately, in the late stage of the curing process, the sample approaches a solid state. The movement of the reacting groups and the products is greatly diminished, and the rate of reaction, which was previously controlled by the chemical kinetics, now becomes diffusion

controlled. Thus, the curing slows down since further possible reaction is only due to diffusion. Higher rubber content inclusion may cause more dilution and thus flexibilize the matrix instead of enhancing the reaction rate.

The cure characteristics of epoxy/clay nanocomposites have been studied by many other researchers. Becker et al. (2003) studied the influence of organically modified clay on the cure behavior of three epoxy systems with different structures and functionalities. Nonisothermal DSC tests were employed by some researchers to study the cure kinetics of epoxy/amine system with organically modified clay (Ton-That et al. 2004; Torre et al. 2003). The cure reaction kinetics of epoxy resin with organically modified clay has been studied using isothermal DSC by Montserrat et al. (2008). In another study, the effect of organically modified clay on nonisothermal cure kinetics of brominated diglycidyl ether of bisphenol-A (BDGEBA)-based epoxy system with amine-functional aniline formaldehyde condensates (AFC) as curing agent was investigated (Saad et al. 2013). Many studies have been published on the cure kinetic studies of DGEBA-based epoxy resin with carboxyl-terminated liquid rubber. Wise et al. (2000) investigated the influence of CTBN on the cure reaction between diglycidyl ether of bisphenol-A (DGEBA) and diamino diphenyl methane (DDM) hardener. The cure kinetics of an epoxy resin matrix, based on diglycidyl ether of bisphenol-A and bisphenol-F (DGEBA–DGEBF), and methyl-tetrahydrophthalic anhydride (MTHPA) with CTBN were studied by Calabrese and Valenza (2003).

There are indeed several reports on DGEBA-based epoxy resin and elastomeric modified blends on immiscibility or miscibility depending on the structure of the curing agent. In the case of rubber-modified epoxy, George et al. (2012, 2014) reported the effect of epoxidized styrene-*b*-butadiene-*b*-styrene rubber, eSBS, of degree of epoxidation of 26, 39, and 47 mol%, on the DGEBA/diamino diphenyl methane (DDM) epoxy system. The maximum temperature of the exothermic peaks shifted to a higher temperature with the content of eSBS (47 mol%), due to plasticization effect and miscibility of this rubber in epoxy resins, as confirmed with DSC measurements. In this chapter, we reported the effect on cure kinetics of adding epoxidized triblock copolymer SBS (47 mol%) (0, 10, 20, and 30 wt%) in epoxy resin cured by DDM, and a delay in the cure kinetics occurred due to the addition of eSBS. Moreover, this effect was critical in determining a nanostructured morphology in epoxy systems containing different amounts of epoxidized triblock copolymer at the maximum degree of epoxidation (Fig. 2).

Pressure–Volume–Temperature (PVT) Measurements and Real-Time FTIR Spectroscopy

The analysis of curing reaction of epoxy resins can be carried out also by monitoring the variation in concentration of functional groups with FTIR spectroscopy by obtaining spectra at consecutive periods of time. As the degree of conversion increases, the intensity of the absorption bands of terminal groups decreases, that is, epoxy or amine bands, and new ones turn up because of the resulting hydroxyl

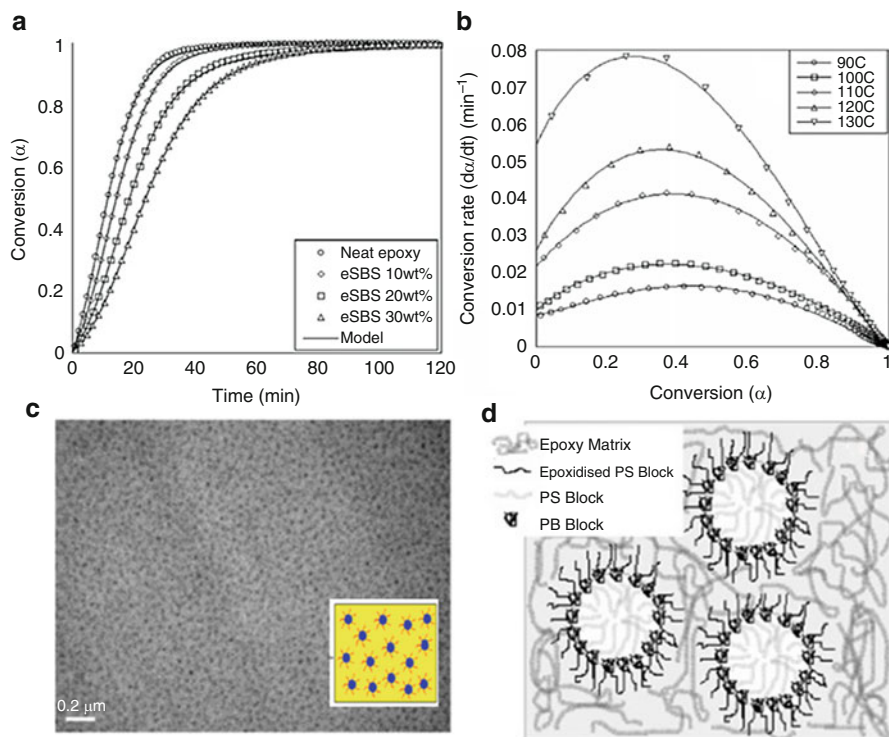


Fig. 2 (a) Conversion rate vs. conversion plots for DGEBA/eSBS (47 mol%)/DDM (10% wt.) blends (symbols denote experimental data and lines represent Kamal autocatalytic model fit); (b) conversion vs. time plot of DGEBA/eSBS (47 mol%)/DDM systems at 110 °C: experimental data (symbols) and calculated data (lines); (c) TEM image of epoxy/eSBS/DDM blend containing 10% wt. eSBS at 47% mol and (d) schematic representation (George et al. 2012, 2013)

and linear ether chemical functions. The region between 3,100 and 3,600 cm^{-1} , in which hydroxyl and amines have strong IR absorption, is generally very complex during the curing process. Hence, for quantitative analysis, the absorption band of epoxy groups in the range 900–920 cm^{-1} is used, instead of those of amine groups at 3,350 cm^{-1} , because they overlap with the hydroxyl band in this region of the spectrum. As an example, Vijayan et al. (2015) studied the role of carboxyl-terminated poly(butadiene-co-acrylonitrile) (CTBN) liquid rubber and reactive surfactant-modified nanoclay on the volume shrinkage during cure reaction and cure kinetics of epoxy/anhydride system in the presence of a catalyst, by using pressure–volume–temperature (PVT) measurements and real-time FTIR spectroscopic analysis. They found that dilution effect of CTBN and catalytic effect of clay modifier on the epoxy/anhydride reaction reflected in the volume shrinkage behavior of CTBN-modified epoxy/clay nanocomposites (epoxy/clay/CTBN hybrid) during cure. The consumption of epoxy band (913 cm^{-1}) during cure obtained from the real-time FTIR spectroscopic analysis was employed to compare

the effect of both CTBN and nanoclay on the cure kinetics. In epoxy/clay/CTBN hybrid, during the initial stage of cure, the catalytic activity of the clay modifier controls the cure rate, and at the final stage, the phase-separated CTBN obstruct the diffusion of reactive sites to slow down the conversion rate. The T_g obtained from DSC analysis of the cured samples confirmed the observed shrinkage and cure behavior.

The major conclusions from these studies are that in epoxy/CTBN blend, CTBN could not alter the cross-link density of epoxy/anhydride network, and CTBN had only a dilution effect on the volume shrinkage during the cure reaction. Both in epoxy/clay nanocomposite and epoxy/clay/CTBN hybrid, the presence of nanoclay enhanced the rate of cure without changing the mechanism of cure reaction between epoxy and anhydride. In epoxy/clay/CTBN hybrid, at the beginning of the cure, the catalytic effect of nanoclay on the cure reaction dominates. However, in the late stage of cure, the phase-separated CTBN retards the rate of cure.

Rheological Studies: Chemoreological Modeling of Cure Reaction

Although calorimetry and IR spectroscopy have been widely used to follow the cross-linking process of the curing reaction (kinetics and mechanism), they do not give direct information on the changes in bulk properties during the cure process of the curing systems. Therefore, other methods consisting of monitoring physical behavior, such as rheological tests, viscometry, densitometry, refractive index, and so on, have been used to follow the curing process.

One of the possible approaches to be used for the measurement of rheological properties for a reacting system is the monitoring of viscosity by using chemorheological approaches during the progression of reaction (Dealy and Wissburn 1990). Chemorheology is a necessary method to study the processing behavior of materials undergoing cross-linking reactions at which a transition from the liquid to solid phase takes place (Ivankovic et al. 2003), defined as the gel point (Heise and Martin 1990; Heseckamp et al. 1998). Rheological properties like viscoelastic moduli can be directly correlated to the evolving molecular structure and therefore the mechanical properties of a thermosetting system during cure. Consequently, rheometry can be potentially used as a technique to monitor the total curing process of thermosets.

The cure kinetic models are then used in parallel with chemorheological model in the flow simulation to predict the interrelated cure and flow properties. Chemorheology is the study of the deformation properties of reactive polymer systems. The chemorheology of thermoset polymers (a subset of reactive polymers) is often difficult to characterize as there are complex effects of temperature on the material. For example, at lower temperatures, the viscosity is high due to lack of thermal mobility of chains, but as temperatures increase, the viscosity will drop due to this increase in thermal motion. However, eventually, the higher temperatures will increase the reaction and cure of the material and viscosity will increase again. However, chemorheology remains an essential tool for characterizing thermoset flow.

Table 1 Chemorheological models for thermoset polymer systems combining cure, shear, and filler effects (Halley 2012)

Model	Expression	System
Power law/WLF	$\eta = \eta_0 \exp \left[\frac{1}{f_{\frac{\alpha_g}{\alpha_g - \alpha}}(T - T_g)} \right] M_w$	Epoxy resin (epoxy novolac/silica filler) (Hale et al. 1989)
	$\begin{aligned} M_w &= f(\alpha) \\ T_g &= T_g(\alpha) \\ \eta_0 &= A\gamma^{n-1} \end{aligned}$	
Power law/WLF/conversion	$\eta = A_1 \gamma^{A_2} \left[\frac{\alpha_g}{\alpha_g - \alpha} \right]^{A_3 + A_4 \alpha} \exp \left[\frac{C_1(T - T_g)}{C_2 + T - T_g} \right]$	Epoxy resin (Castro and Macosko 1982)
WLF/Arrhenius	$\log \eta^* = \ln \eta^*(T, \omega) + k_\alpha \int \exp \frac{\Delta E_k}{RT} dt$	Filled epoxy resin (Pahl and Hesekamp 1993) assumes Cox–Merz rule is valid
	$\eta^*(T, \omega) = \frac{a_T(T)}{A_0 + A_1 [\ln a_T(T)]^{A_2}}$	
Power law/Arrhenius/molecular #1	$\eta = \mu \left(\frac{\gamma}{\gamma_0} \right)^{n-1} \exp[-b(T - T_0) + aP] M_w^m \frac{d\gamma}{dr}$	Epoxy resin (epoxy/diamine) (Riccardi and Vazquez 1989)
	$M_w = f(a)$	
Power law/Arrhenius/molecular #2	$\eta = A\gamma^B \exp\left(\frac{C}{T}\right) \left[\frac{\alpha_g}{\alpha_g - \alpha} \right]^{(D+E\alpha)}$	Epoxy resin (Castro and Macosko 1982; Nguyen 1993)
Carreau	$\frac{\eta - \eta_a}{\eta_0 - \eta_a} = \left[1 + \left(\frac{\eta_0 \dot{\gamma}}{\tau^*} \right)^2 \right]^{\frac{n-1}{2}}$	Epoxy resin (Peters et al. 1993)
	where $-\eta_0 = A \exp(E/T) \left(\frac{\alpha_g}{\alpha_g - \alpha} \right)^{(B+C\alpha)}$	
Moldflow	$\ln \eta = A_1 + A_2 \ln \gamma + A_3 T + A_4 \ln \gamma^2 + A_5 \ln(\gamma T) + A_6 T^2 + (A_7 + A_8 X) \ln \left(\frac{\alpha_g}{\alpha_g - \alpha} \right)$	Epoxy resin (Peters et al. 1993)

By combining the effect of cure and shear rate, a complete model for the chemoviscosity can be established. Examples of these combined models are shown in Table 1. The main forms of combined effect models consists of WLF, power law or Carreau shear effects, Arrhenius or WLF thermal effects, and molecular, conversion, or empirical cure effects.

The variation of the system viscosity during thermosetting cure takes place as a consequence of the physical and chemical phenomena that occurs during polymerization reactions. In the case of an isothermal cure, the molecular structural changes caused by cross-linking make the viscosity steadily increase until the cross-linked polymer molecules form an infinite network and gelation takes place.

Since the formed polymer network acquires elastic properties, which are in general not present in the low molecular weight linear or branched polymeric chains, the gelation causes the transformation of a viscous liquid into a rubbery state solid.

The gelation point is of fundamental importance for the processing of thermosetting-based composites and nanocomposites, as it represents the limit over which there will be no possibility of shaping. The shaping must be completed

before gelation, when the polymer is still able to flow and stresses can be easily relaxed. In the case of nonisothermal conditions, the viscosity is also influenced by temperature; in this case, two main driving forces will affect the viscosity variation: the temperature and the polymerization reaction. The variation of the viscosity will be inversely proportional to the variation of the system temperature and will be directly proportional to the variation of the degree of reaction. It should also be taken into account that all the polymerization reactions are exothermic, and therefore they necessarily produce an increase of the system temperature that could also be consistent, considering that polymers are very good thermal insulators. Therefore, in the case of nonisothermal polymerization, more than a single variable should be considered in order to completely describe the trend of the viscosity.

These concepts are valid for all thermosetting polymers, and a lot of work was done in the last 30 years to develop appropriate models that best describe the chemoviscosity of thermosets. An advance was made from the batch-specific viscosity versus time or temperature correlations to the models that evaluate the time-dependent chemoviscosity as a function of the cure cycle and the cure kinetics of the resin formulations (Mijovic and Lee 1989). An extensive overview of the chemorheology of thermosetting systems is reported by Halley and Mackay (1996). When dealing with rubber-modified thermosets and thermoset-based nanocomposites, the same considerations made for the reaction kinetics can be done for the chemoviscosity modeling; the presence of rubber and nanofillers in fact not only affects the rheological behavior in terms of constitutive equation (Cueto et al. 2010), but also it changes the evolution of the viscosity during the cross-linking reaction. This fact introduces further difficulties in the construction of a chemorheological model of a thermosetting-based nanocomposite resin, which should necessarily take into account other variables such as the presence of the rubber- and/or filler-type concentration. Such simple considerations are enough to state that the introduction of so many variables in a model, which has already its own degree of complexity, would make it too hard to use for practical applications (process simulations) and would also compromise its reliability since the number of model parameters would increase. Therefore, a better way to develop a specific chemorheological model is to use the same models developed for pure thermosetting resin and account the effect of the rubber and/or eventual filler in the variation of the model parameters with respect to the unfilled system. Such procedure, although contains some approximations, has been successfully applied for many thermosetting resins.

An important parameter determinable from viscosity measurements during isothermal cure is the gel time, which characterizes the gelation, an important step of the thermoset polymerization. It is used to determine the activation energy of the kinetics and defined as

$$t_{\text{gel}} = \frac{1}{k(T)} \int_0^{\alpha_{\text{gel}}} \frac{1}{g(\alpha)} d\alpha \quad (10)$$

where α_{gel} is the degree of cure at the gel time. It is considered as a constant, regardless of the temperature. Developing the expression of $k(T)$ and taking the logarithm on both sides of Eq. 10:

$$\ln(t_{gel}) = \ln \left[\frac{1}{A_0} \left(\int_0^{\alpha_{gel}} \frac{1}{g(\alpha)} d\alpha \right) \right] + \frac{E_a}{R} \frac{1}{T} \quad (11)$$

From Eq. 11, one can obviously determine the apparent activation energy from the slope of the curve $\ln(t_{gel})$ versus $1/T$. From the point of view of viscosity, the variation of viscosity can be empirically expressed in a simple general form before gelation as $\eta = \eta_0/(1-\alpha)$, where η_0 is the initial viscosity, which is a constant at isothermal cure conditions. For a dynamic cure process, it is postulated that η_0 has an Arrhenius form:

$$\eta_0 = A_\eta \exp\left(\frac{-E_\eta}{RT}\right) \quad (12)$$

where A_η is the Arrhenius pre-exponential viscosity and E_η the activation energy for viscosity. In order to establish a relationship between the viscosity and the degree of cure, one can start from the equation of the reaction rate. Considering an n th-order model, Eq. 12 is solved:

$$\frac{1}{1-\alpha} = \left(1 + (n-1) \int_0^t k dt \right)^{\frac{1}{(n-1)}}, k = A_k \exp\left(\frac{-E_k}{RT}\right) \quad (13)$$

Substituting equations and taking the logarithm on both sides, one gets

$$\ln \eta = \ln A_n + \frac{E_\eta}{RT} + \frac{1}{n-1} \ln \left(1 + (n-1) A_k \int_0^t e^{-\frac{E_k}{RT} dt} \right) \quad (14)$$

Equation 14 is an empirical five-parameter model for the n th-order model ($n \neq 1$). For the first reaction order with an isothermal cure process, it is easy to demonstrate that

$$\eta = \eta_0 \exp(kt) \ln \eta = \ln A_\eta + \frac{E_\eta}{RT} + t A_k e^{-\frac{E_k}{RT}} \quad (15)$$

where η_0 and k can be obtained from plot of $\ln \eta$ versus t at each temperature. The values of A_η , E_η , A_k , and E_k are determined by Eq. 15 and the expression of k , respectively.

As an example of the method, we reported the work of Vijanan P. et al. (2013), in which the authors studied the role of CTBN, and nanoclay on cure kinetics of epoxy/clay/CTBN hybrid system was investigated using rheology measurements. Epoxy-anhydride cure reaction in the presence of nanoclay, CTBN, and both together was followed by isothermal rheological analysis (Fig. 3). The complex viscosity plot for

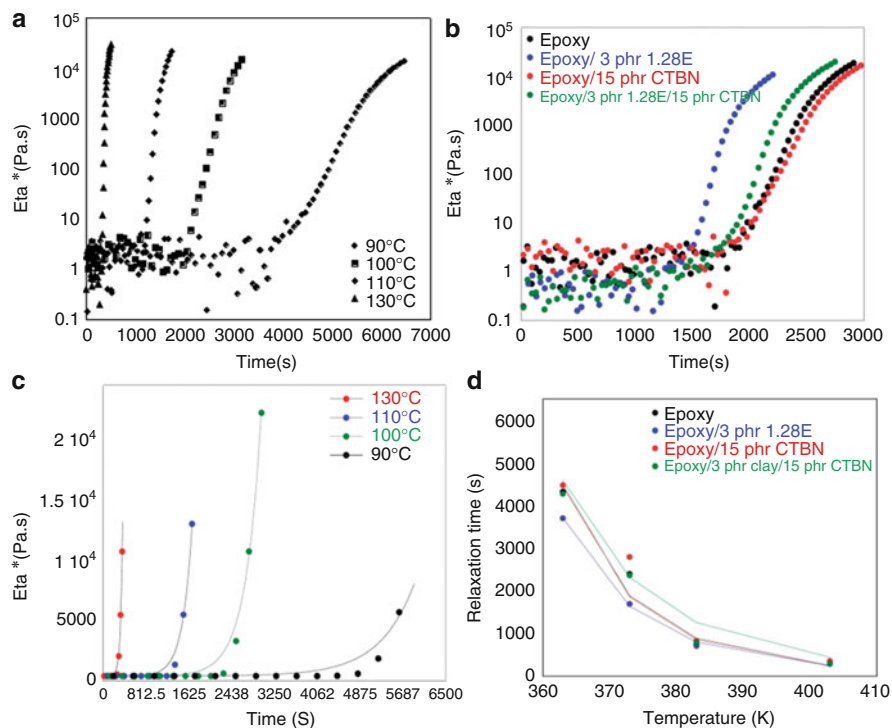


Fig. 3 (a) Complex viscosity vs. time plot for epoxy/15 phr CTBN at four different temperatures, (b) complex viscosity vs. time plot for neat epoxy and modified epoxy systems during the curing process at 100 °C; (c) exponential growth of viscosity of epoxy/3 phr I.28E/15 phr CTBN ternary nanocomposite at four different temperatures. *Symbols* correspond to the experimental data, and *lines* correspond to the simulation results; (d) plots of the relaxation time vs. temperature. The *points* correspond to experimental data and the *line* corresponds to results simulated by WLF equation (Vijanan et al. 2013)

different modified epoxy systems is given in Fig. 3a, b. The viscosity evolution processes are quite similar for all modified systems. It was found that the phase separation of CTBN from the epoxy matrix couldn't change the shape of the viscosity profile. The simple reaction-induced phase in epoxy/CTBN blend system could not be identified from the rheological profile, unlike the viscoelastic phase separation in thermoplastic modified epoxy matrix. Two structural transitions were observed in such systems. The first transition related to the structural change associated with phase separation process and the second one associated with the chemical gelation of thermosets. However, in epoxy/liquid rubber blends, only one transition was reported in rheological profile so far (Thomas et al. 2008). The phase separation of soft elastomeric particles is inept to make a significant viscosity fluctuation.

From the material processing point of view, the determination of individual and combined effect of rubber and nanoclay modifier on gelation time and vitrification

time were important. Gelation and vitrification times were measured at different curing temperatures for neat epoxy and modified epoxies. The miscibility of CTBN in epoxy monomer initially produces a dilution effect, which decreases the epoxy anhydride reactivity and hence increases the time of gelation. The phase separating CTBN particles also hinders the reaction significantly on vitrification period where the cure reaction is controlled by diffusion mechanism rather than kinetic effect. In epoxy/clay/CTBN ternary system, the catalytic effect of nanoclay (I.28E, Nanomer) and reduced miscibility of CTBN with epoxy in the presence of nanoclay causes a shorter gel time (prominent at lower temperatures) than the epoxy/CTBN binary blend.

Looking at rheological modeling of these systems, it has been observed that the growth of complex viscosity follows a Maxwell-type relaxation. The characterization time of the exponential growth of viscosity at different temperatures could be simulated by the equation:

$$\eta^*(t) = \eta_0^* + A_0 \exp(t/\tau_\eta) \quad (16)$$

where $\eta^*(t)$ is the complex viscosity of blend systems, A_0 is a parameter, and τ_η is the relaxation time of viscosity, which can be used to compare the growth rate of viscosity of different modified systems. Figure 3c shows exponential growth of viscosity of epoxy/3 phr I.28E/15 phr CTBN ternary system at four different temperatures along with the simulation results. Maxwell-type relaxation equation fits very well with the experimental viscosity evolution for neat and modified epoxy systems.

The relaxation time (Fig. 3d) was found to reduce with increase in temperature, which is characteristic of the thermally catalyzed reaction. The relaxation time obtained is lower for epoxy/clay nanocomposite and higher for epoxy/CTBN blend than neat epoxy at all temperatures. For epoxy/clay/CTBN ternary system, the relaxation time is lower than epoxy/CTBN blend and in some cases lower than neat epoxy especially at lower temperatures.

The relaxation time (τ_η) versus temperature (T) was simulated by the Williams–Landel–Ferry (WLF) equation. Assuming that $C_1 = 8.86$ K and $C_2 = 101.6$ K, the WLF equation can be written as

$$\tau_\eta = \tau_S \exp\{-\ln 10 \times 8.86 \times (T - T_S) / [101.6 + (T - T_S)]\} \quad (17)$$

As shown in Fig. 3d, the simulation results show a fine agreement with the experimental data, which implies that the relaxation time obeys the time-temperature superposition (TTS) principle and can be described by the WLF function.

In a similar study, George et al. (2015) focused on the importance of cure rheology on nanostructure formation, using rheometry. The reaction-induced phase separation of a polystyrene phase in the epoxy matrix was carefully explored through rheological measurements, and PVT measurements during curing were carried out to understand the volume shrinkage of the blend matrix, confirming that shrinkage behavior is related to the block copolymer phase separation process during cure.

In dynamic tests performed in the case of DGEBA blends with 10 wt% of eSBS epoxidized at different epoxidation degrees, the authors observed that, at the beginning of the test, the viscosity is found to increase with the increase in epoxidation degree. This is mainly due to the increase in compatibility of high molecular weight of epoxidized SBS in epoxy resin or due to some specific type of interaction (hydrogen bonding) between the epoxidized SBS and the epoxy resin. The main conclusions of this specific study were that:

- (i) The rheological studies showed a fluctuation in viscosity due to the nanophase separation of PS and unepoxidized PB domains in the continuous epoxy resin matrix.
- (ii) The gel time values are found to be increased with increase in modifier weight percentage and decreased with the isothermal curing temperature.
- (iii) The cure reaction is delayed by the addition of eSBS, being the delay in cure reaction due to the combined effects of plasticization and dilution and also due to the miscibility of epoxidized SBS in epoxy matrix.
- (iv) The miscibility of epoxidized SBS in epoxy resin and the viscosity were found to be increased with degree of epoxidation.

It has been demonstrated (Yingfeng 2014) that the rheological properties of polymer blends – and especially of thermosetting polymer blends – also share a close relationship to the morphology and reactions involved. Moreover, these properties can cause changes in shear or strain conditions that may lead to dramatic variations in the phase structure and other properties of polymer blends.

Conclusions

A deep understanding of curing mechanisms and cure kinetics is the key for obtaining an optimal cure, which allows one to model the reaction processes as accurately as possible. In this framework, the elaboration of an appropriate kinetic equation is of fundamental importance. As the behavior of a thermosetting polymer is strongly affected by the curing process, poorly controlled cure can produce unexpected variations in the thermal and rheological properties of the system during the manufacturing processes of the final product. Therefore, an accurate model not only allows us to monitor the evolution of the curing system (to plan and/or to control single processes), but it can also be used for the material design, to compare the behavior of different formulations. Although several studies have been carried out on the modeling of the kinetic behavior of thermosetting resins, a wide variety of resin formulations available implies a continuous study and introduces new experimental difficulties and complexities. Moreover, switching to rubber-modified system, even in presence of a nanofiller, introduces a further variable in the complexity of the modeling problem, as the effects of the rubber and the compatibilizer somehow affect the reaction kinetics. A better way to assure high-quality and low

manufacturing cost of the products is to create mathematical models of different processing stages.

References

- Abdolreza M, Siamak Z (2010) Epoxy/acrylonitrile-butadiene-styrene copolymer/clay ternary nanocomposite as impact toughened epoxy. *J Polym Res* 17:191–201
- Akbari R, Beheshty MH, Shervin M (2013) Toughening of dicyandiamide-cured DGEBA-based epoxy resins by CTBN liquid rubber Iran. *Polym J* 22:313–324
- Bagheri R, Marouf BT, Pearson RA (2009) Rubber-toughened epoxies: a critical review. *Polym Rev* 49(3):201–225
- Bascom WD, Hunston DL (1989) Rubber toughened plastics, vol 222, *Advances in Chemistry Series*. American Chemical Society, Washington, DC, p 193
- Becker O, Simon GP, Vaiuey RJ, Halley PJ (2003) Layered silicate nanocomposites based on various high-functionality epoxy resins: the influence of an organoclay on resin cure. *Polym Eng Sci* 2003(43):850
- Brown ME (1988) *Introduction to thermal analysis*. Chapman & Hall, London
- Calabrese L, Valenza A (2003) The effect of a liquid CTBN rubber modifier on the thermo-kinetic parameters of an epoxy resin during a pultrusion process. *Compos Sci Technol* 63(6):851–860
- Castro J, Macosko C (1982) Effects of cure, temperature and shear on rheology of epoxy systems *Polym Eng Sci* 28:250
- Chen JP, Lee YD (1995) A real time study of the phase-separation process during polymerization of rubber-modified epoxy. *Polymer* 36:55–65
- Chen D, Pascault JP, Sautereau H (1993) Rubber-modified epoxies. I. Influence of presence of a low level of rubber on the polymerization. *Polym Int* 32:361–367
- Cueto E, Monge R, Chinesta F, Poitou A, Alfaro I, Mackley MR (2010) Rheological modeling and forming process simulation of CNT nanocomposites. *Int J Mater Form* 3(2):1327–1338
- Dealy JM, Wissburn KF (1990) *Melt rheology and its role in plastic processing*. Van Nostrand Reinhold, New York, p 410
- Fischer F, Beier U, Wolff-Fabris F, Altstädt V (2011) Toughened high performance epoxy resin system for aerospace applications. *Sci Eng Compos Mat* 18(4):209–215
- Francis B, Rao VL, Jose S, Katherine BK, Ramaswamy R, Jose J, Thomas S (2006) Poly(ether ether ketone) with pendent methyl groups as a toughening agent for amine cured DGEBA epoxy resin *J. Mater Sci* 41:5467–5479
- Frohlich J, Kautz H, Thomann R, Frey H, Mulhaupt R (2004) Reactive core/shell type hyperbranched blockcopolyethers as new liquid rubbers for epoxy toughening. *Polymer* 45:2155–2164
- George SM, Puglia D, Kenny JM, Parameswaranpillai J, Thomas S (2012) Cure kinetics and thermal stability of micro and nanostructured thermosetting blends of epoxy resin and epoxidized styrene-block-butadiene-block-styrene triblock copolymer systems. *Polym Eng Sci* 52:2336–2347
- George SM, Puglia D, Kenny JM, Causin V, Parameswaranpillai J, Thomas J (2013) Morphological and mechanical characterization of nanostructured thermosets from epoxy and styrene- block- butadiene- block- styrene triblock copolymer. *Ind Eng Chem Res* 52(26):9121–9129
- George SM, Puglia D, Kenny JM, Parameswaranpillai J, Thomas S (2014) Reaction induced viscoelastic phase separation and thermo-mechanical properties in epoxidised styrene- block-butadiene- block- styrene triblock copolymer modified epoxy-DDM system. *Ind Eng Chem Res* 53(17):6941–6950
- George SM, Puglia D, Kenny JM, Parameswaranpillai J, Vijayan PP, Pionteck J, Thomas S (2015) Volume shrinkage and rheological studies of epoxidised and unepoxidised poly(styrene-block-

- butadiene-block-styrene) triblock copolymer modified epoxy resin-diamino diphenyl methane nanostructured blend systems. *Phys Chem Chem Phys* 17(19):12760–12770
- Girard-Reydet E, Pascault JP, Bonner A, Court F, Leibler L (2003) A new class of epoxy thermosets. *Macromol Symp* 198:309–322
- Gleiter H (2000) Nanostructured materials: basic concepts and microstructure. *Acta Mater* 48:1–29
- Hale A, Garcia M, Macosko C, Manzione L (1989) DSC and C13-NMR studies of the imidazole-accelerated reaction between epoxides and phenols society of plastics engineers annual proceedings ANTEC, p796
- Halley PJ (2012) Rheology of thermosets: the use of chemorheology to characterise and model thermoset flow behaviour. In: Guo Q (ed) *Thermosets structure, properties and applications*. Woodhead Publishing Limited, New Delhi, India
- Halley PJ, MacKay ME (1996) Chemorheology of thermosets – an overview. *Polym Eng Sci* 36:593–609
- Heise MS, Martin GC (1990) Gelation in thermosets formed by chain addition polymerization. *Polym Eng Sci* 30:83–89
- Henton DE, Pickelman DM, Arends CB, Meyer VE US Patent 4,778,851, 1988
- Hesekamp D, Broecker HC, Pahl MH (1998) Chemorheology of cross-linking polymers. *Chem Eng Technol* 21:149–153
- Hsieh HSY (1990) Thermodynamically reversible and irreversible control on morphology of multiphase systems. *J Mater Sci* 25:1568–1584
- Ivankovic M, Incarnato L, Kenny JM, Nicolais L (2003) Curing kinetics and chemorheology of epoxy/anhydride system. *J Appl Polym Sci* 90:3012–3019
- Jose J, Joseph K, Pionteck J, Thomas S (2008) PVT behavior of thermoplastic poly(styrene-co-acrylonitrile)-modified epoxy systems: relating polymerization-induced viscoelastic phase separation with the cure shrinkage performance. *J Phys Chem B* 112:14793
- Jyotishkumar P, Koetz J, Tiersch B, Strehmel V, Özdilek C, Moldenaers P, Hässler R, Thomas S (2009) Complex phase separation in poly(acrylonitrile-butadiene-styrene)-modified epoxy/4,4'-diaminodiphenyl sulfone blends: generation of new micro- and nanosubstructures. *J Phys Chem B* 113:5418–5430
- Jyotishkumar P, Özdilek C, Moldenaers P, Sinturel C, Janke A, Pionteck J, Thomas S (2010) Dynamics of phase separation in poly(acrylonitrile-butadiene-styrene)-modified epoxy/DDS system: kinetics and viscoelastic effects. *Phys Chem B* 114:13271–13281
- Jyotishkumar P, Pionteck J, Hasler R, George S, Cvelbar U, Thomas S (2011) Studies on stress relaxation and thermomechanical properties of poly(acrylonitrile-butadiene-styrene) modified epoxy – amine systems. *Ind Eng Chem Res* 50:4432–4440
- Kamal MR (1974) Thermoset characterization for moldability analysis. *Polym Eng Sci* 14:231–239
- Kargarzadeh H, Ahmad I, Abdullah I, Thomas R, Dufresne A, Thomas S, Hassan A (2015) Functionalized liquid natural rubber and liquid epoxidized natural rubber: a promising green toughening agent for polyester. *J Appl Polym Sci* 132:41292
- Kenny JM (1994) Determination of autocatalytic kinetic model parameters describing thermoset cure. *J Appl Polym Sci* 51:761–764
- Kim SC, Ko MB, Jo WK (1995) The effect of the viscosity of epoxy prepolymer on the generated morphology in rubber-toughened epoxy resin. *Polymer* 36:2189–2195
- Kim SW, Lu MG, Shim MJ (1998) The isothermal cure kinetic of epoxy/amine system analyzed by phase change theory. *Polymer* 30:90–94
- Kissinger HE (1957) Reaction kinetics in differential thermal analysis. *Anal Chem* 29:1702–1706
- Klug JH, Seferis JC (1999) Phase separation influence on the performance of CTBN-toughened epoxy adhesives. *Polym Eng Sci* 39:1837–1848
- Kong J, Tang Y, Zhang X, Gu J (2008) Synergic effect of acrylate liquid rubber and bisphenol A on toughness of epoxy resins. *Polym Bull* 60:229–236
- Lionetto L, Maffezzoli A (2013) Monitoring the cure state of thermosetting resins by ultrasound. *Materials* 6:3783–3804

- Mijovic J, Lee CH (1989) Modeling of chemorheology of thermoset cure by modified WLF equation. *J Appl Polym Sci* 37:889–900
- Montserrat S, Roman F, Hutchinson JM, Campos L (2008) Analysis of the cure of epoxy based layered silicate nanocomposites: reaction kinetics and nanostructure development. *J Appl Polym Sci* 108:923–938
- Morancho JM, Salla JM (1999) Relaxation in partially cured samples of an epoxy resin and of the same resin modified with a carboxyl-terminated rubber. *Polymer* 40(10):2821–2828
- Nguyen L (1993) Reactive flow simulation in transfer molding of ic packages Proceedings from the 43rd IEEE Electronic Component and Technology Conference. Buena Vista, FL, USA, 1
- Ni Y, Zheng S (2007) Nanostructured thermosets from epoxy resin and an organic-inorganic amphiphile. *Macromolecules* 40:7009–7018
- Ozawa T (1970) Kinetic analysis of derivative curves in thermal analysis. *J Therm Anal* 2:301–324
- Ozturk A, Kaynak C, Tincer T (2001) Effects of liquid rubber modification on the behaviour of epoxy resin European. *Polym J* 37(12):2353–2363
- Pahl M, Hesekamp D (1993) Modified cox merz rule *Appl Rheol*, 70–77
- Palomo B, Habas-Ulloa A, Pignolet P, Quentin N, Fellmann D, Habas JP (2013) Rheological and thermal study of the curing process of a cycloaliphatic epoxy resin: application to the optimization of the ultimate thermomechanical and electrical properties. *J Phys D: Appl Phys* 46:6
- Pearson RA, Yee AF (1986) Toughening mechanisms in elastomer-modified epoxies. *J Mater Sci* 21:2475–2488
- Peters G, Spoelstra A, Meuwissen M, Corbey R, Meijer H (1993) Rheology and rheomerty for highly filled reactive materials. In: Dijkstra J., Nieuwstadt FTM (eds) *Topics in Applied Mechanics*. The Netherlands: Kluwer Academic Publishers
- Prime RB (1981) In: Turi EA (ed) *Thermal characterization of polymeric materials*. Academic, New York, pp 435–569
- Pucciariello R, Villani V, Bianchi N, Braglia R (1991) Relationship between gelation and morphology of rubber-modified epoxy resins. *Polym Int* 26:69–73
- Qian JY, Pearson RA, Domonie VL, Shaffer OL, El-Aasser MS (1997) The role of dispersed phase morphology on toughening of epoxies. *Polymer* 38:21–30
- Ramos VD, da Costa HM, Soares VLP, Nascimento RSV (2005) Modification of epoxy resin: a comparison of different types of elastomer. *Polym Test Polym Test* 24(3):387–394
- Ratna D, Banthia AK (2004) Rubber toughened epoxy. *Macromol Res* 12(1):11–21
- Riccardi C, Vazquez A (1989) Tube flow of a particulate-filled thermosetting polymer *Polym Eng Sci* 29:120–126
- Romano AM, Garbassi F, Braglia R (1994) Rubber- and thermoplastic-toughened epoxy adhesive films. *J Appl Polym Sci* 52:1775–1783
- Romo-Urbe A, Arcos-Casarrubias JA, Flores A, Valerio-Cárdenas C, González AE (2014) Influence of rubber on the curing kinetics of DGEBA epoxy and the effect on the morphology and hardness of the composites. *Polym Bull* 71(5):1241–1262
- Rudin A, Choi P (2012) Introductory Concepts and Definitions, in *Elements of Polymer Science & Engineering (Third Edition)*, Ed. Rudin, Academic Press, Elsevier, 1–62
- Ruseckaite RA, Hu L, Riccardi CC, Williams RJ (1993) Castor-oil-modified epoxy resins as model systems of rubber-modified thermosets. 2: influence of cure conditions on morphologies generated. *Polym Int* 30:287–295
- Russell B, Chartoff R (2005) The influence of cure conditions on the morphology and phase distribution in a rubber-modified epoxy resin using scanning electron microscopy and atomic force microscopy. *Polymer* 46:785–798
- Saad GR, Naguib HF, Elmenyawy SA (2013) Effect of organically modified montmorillonite filler on the dynamic cure kinetics, thermal stability, and mechanical properties of brominated epoxy/aniline formaldehyde condensates system. *J Therm Anal Calorim* 111:1409–1417

- Sue HJ, Garcia-Meitin E, Pickelman MM, Yang PC (1993) In: Riew CK, Kinloeb AJ (Eds) "Toughened Plastics 1" ACS Series 233, Washington, DC., p 259
- Thomas R, Durix S, Sinturel C, Omonov T, Goossens S, Groeninckx G, Moldenaers P, Thomas S (2007) Cure kinetics, morphology and miscibility of modified DGEBA-based epoxy resin – effects of a liquid rubber inclusion. *Polymer* 48(6):1695–1710
- Thomas R, Yumei D, Yuelong H, Le Y, Moldenaers P, Weimin Y, Czizany T, Thomas S (2008) Miscibility, morphology, thermal, and mechanical properties of a DGEBA based epoxy resin toughened with a liquid rubber. *Polymer* 49:278–294
- Thomas R, Sinturel C, Pionteck J, Puliyalil H, Thomas S (2012) In-situ cure and cure kinetic analysis of a liquid rubber modified epoxy resin. *Ind Eng Chem Res* 51(38):12178–12191
- Ton-That MT, Ngo TD, Ding P, Fang G, Cole KC, Hoa SV (2004) Epoxy nanocomposites: analysis and kinetics of cure. *Polym Eng Sci* 44:1132–1141
- Torre L, Frulloni E, Kenny JM, Manfredi C, Camino G (2003) Processing and characterization of epoxy–anhydride-based intercalated nanocomposites. *J Appl Polym Sci* 90:2532–2539
- Tripathi G, Srivastava D (2007) Effect of carboxyl-terminated butadiene acrylonitrile copolymer concentration on mechanical and morphological features of binary blends of nonglycidyl-type epoxy resins. *Adv Polym Technol* 26(4):258–271
- Tripathi G, Srivastava D (2008) Studies on the physico-mechanical and thermal characteristics of blends of DGEBA epoxy, 3,4 epoxy cyclohexylmethyl, 3', 4'-epoxycyclohexane carboxylate and carboxyl terminated butadiene co-acrylonitrile (CTBN). *Mater Sci Eng A* 496:483–493
- Tripathi G, Srivastava D (2009) Toughened cycloaliphatic epoxy resin for demanding thermal applications and surface coatings. *J Appl Polym Sci* 114:2769–2776
- Turi EA (ed) (1981) Thermal characterization of polymeric materials. Academic, New York
- Vaia RA, Price G, Ruth PN, Nguyen HT, Lichtenhan JD (1999) Polymer/layered silicate nanocomposites as high performance ablative materials. *Appl Clay Sci* 15:67
- Vazquez A, Rojas AJ, Adabbo HE, Borrajo J, Williams RJJ (1987) Rubber-modified thermosets: prediction of the particle size distribution of dispersed domains. *Polymer* 28:1156–1164
- Vijayan PP, Puglia D, Jyotishkumar P, Kenny JM, Thomas S (2012) Effect of nanoclay and carboxyl-terminated (butadiene-co-acrylonitrile) (CTBN) rubber on the reaction induced phase separation and cure kinetics of an epoxy/cyclic anhydride system. *Mater Sci* 47:5241–5253. doi:10.1007/s10853-012-6409-z
- Vijayan PP, Puglia D, Kenny JM, Thomas S (2013) Effect of organically modified nanoclay on the miscibility, rheology, morphology and properties of epoxy/carboxyl-terminated (butadiene-co-acrylonitrile) blend. *Soft Matter* 9:2899–2911
- Vijayan PP, Pionteck J, Thomas S (2015) Volume shrinkage and cure kinetics in carboxyl-terminated poly(butadiene-co-acrylonitrile) (CTBN) modified epoxy/clay nanocomposites. *J Macromol Sci A: Pure Appl Chem* 52(5):2015. doi:10.1080/10601325.2015.1018805
- Visakh PM, Thomas S, Chandra AK, Mathew AP (2013) Advances in elastomers I: blends and interpenetrating networks, Advanced structured materials, Springer-Verlag Berlin Heidelberg
- Wang TT, Zupko HM (1981) Phase separation behavior of rubber-modified epoxies. *J Appl Polym Sci* 26:2391–2401
- Williams RJJ, Borrajo J, Adabbo HE, Rojas AJ (1984) In: Riewand CK, Gillham JK (eds) Rubber-modified thermosets resins, Advances in Chemistry Series 208. American Chemical Society, Washington, DC, p 195
- Williams RJJ, Rozenberg RA, Pascault JP (1997) Polymer analysis polymer physics, advances in polymer science. Springer, Berlin, pp 95–156
- Winter HH (1989) Gel point. In: Encyclopedia of polymer science and engineering, Supplement Volume, 2nd ed, John Wiley & Sons, Inc., New York, 349–351

- Winter HH, Chambon F (1986) Analysis of linear viscoelasticity of a crosslinking polymer at the gel point. *J Rheol* 30:367–382
- Wise CW, Cook WD, Goodwin AA (2000) CTBN rubber phase precipitation in model epoxy resins. *Polymer* 41(12):4625–4633
- Wu J, Thio YS, Bates FS (2005) Structure and properties of PBO–PEO diblock copolymer modified epoxy. *J Polym Sci B: Polym Phys* 43(15):1950–1965
- Yamanaka K, Takagi Y, Inoue T (1989) Reaction-induced phase separation in rubber-modified epoxy resins. *Polymer* 30(10):1839–1844
- Yingfeng Y (2014) Characterization of polymer blends: rheological studies. In: Thomas S, Grohens Y, Jyotishkumar P (eds) *Characterization of polymer blends miscibility, morphology and interfaces*. Wiley-VCH Verlag GmbH & Co. KGaA, Weinheim, Germany. pp 133–159

Dynamic Mechanical Thermal Analysis of Epoxy/Rubber Blends

8

Qinghua Zhang, Ren He, and Xiaoli Zhan

Abstract

For rubber-modified epoxy blends, dynamic mechanical thermal analysis (DMTA) was mainly used to investigate the influence of rubber content on the relaxation of modified epoxies. The storage modulus and glass transition temperature generally decrease as the rubber content increases in epoxy matrix. It is therefore DMTA that enables us to study the variations of these parameters of rubber-toughened epoxy blends. The combination uses of microscopic observations and DMTA help us to identify the phase structures of rubber in epoxy matrix. DMTA also provides supporting evidence to phase structures of rubber inclusions in epoxy matrix and an important reference for thermal stability of rubber-modified epoxy blends.

Keywords

Rubber • Epoxy • Blend • Dynamic mechanical thermal analysis (DMTA)

Contents

Introduction	240
Epoxy Blends Modified by ATBN Rubber	240
Epoxy Blends Modified by CTBN Rubber	241
Epoxy Blends Modified by Liquid Natural Rubber	243
Nanostructured Epoxy Rubber Blends	244
Conclusion	246
References	246

Q. Zhang (✉) • R. He • X. Zhan

College of Chemical and Biochemical Engineering, Zhejiang University, Hangzhou, China

e-mail: qhzhang@zju.edu.cn

© Springer International Publishing AG 2017

J. Parameswaranpillai et al. (eds.), *Handbook of Epoxy Blends*,

DOI 10.1007/978-3-319-40043-3_9

239

Introduction

In dynamic mechanical thermal analysis (DMTA), the rubber-modified epoxy blends reach the temperature or frequency range at which a chain movement occurs after undergoing a sinusoidal deformation; the energy dissipated increases up to a maximum. As the stress wave is delayed with respect to the strain, its decomposition leads to a component in phase and another one out of phase, related with two parts of the complex modulus (shear, bending, compression, or tensile modulus, depending on the test conditions), denoted as storage modulus (E') and loss modulus (E''), respectively. The loss tangent ($\tan \delta$) is the ratio of loss modulus to storage modulus. Generally, glass transition temperature (T_g) of rubber-modified epoxy blends can be determined from the peak of loss tangent versus temperature curve. The relationship between morphology and performance could be studied by the combination of microscopy observations and DMTA (Ratna and Banthia 2004). It is therefore dynamic mechanical thermal analysis that allows us to study the variations of these parameters of rubber-toughened epoxy blends, not only the glass transition temperature but also the local movements not detected by other techniques.

For rubber-modified epoxy blends, DMTA was mainly used to investigate the influence of rubber content on the relaxation of modified epoxies (Yang et al. 2015). The rubber relaxation was observed at lower temperature than T_g of the pure rubber, due to the interfacial stresses at the rubber particle/epoxy matrix interface resulting from the difference in thermal expansion coefficients between the two phases. The rubbery plateau region indicates that the shear modulus of the blends depends strongly on the volume fraction of the dispersed phase rather than the dissolved rubber in the continuous phase (Thomas et al. 2014).

Epoxy Blends Modified by ATBN Rubber

Numerous researchers have studied the rubber-modified epoxy blends by DMTA (Manziona et al. 1981). The relationship between phase separation and dynamic mechanical property of an amine-terminated butadiene acrylonitrile (ATBN) liquid-rubber-modified epoxy resin has been studied by Kim et al. (Kim and Kim 1994). The combination use of DMTA and scanning electron microscope (SEM) results demonstrated that the phase structures of the rubber state would influence the modulus and damping behavior of cured blends. The DMTA results of storage modulus and $\tan \delta$ vary with the variation in rubber content.

With the increase in the rubber ATBN amount, the modulus at room temperature of the epoxy decreased, while a significant drop of the modulus occurred when the amount of ATBN was 30 wt% where the phase inversion behavior took place. Correspondingly, the damping of the rubber phase increased and the glass transition temperature of epoxy-rich matrix phase shifted to lower temperature with the increase in rubber content due to the intermixed ATBN rubber in epoxy matrix.

The phase-inverted morphology of 30 wt% ATBN-modified epoxy blend could also result in a high $\tan \delta$ value at low temperature.

Epoxy Blends Modified by CTBN Rubber

Hsich et al. tailored the morphology and properties of carboxyl-terminated copolymer of butadiene acrylonitrile (CTBN)-modified epoxy alloy systems by the modification of phase separation kinetics with the help of phase diagrams consisting of bimodal and spinodal curves (Hsich 1990). Dynamic mechanical analysis suggested that this technique offers a means to shift the glass transition temperature of the rubber-rich phase drastically without reducing the glass transition temperature of the epoxy-rich phase significantly. Bucknall et al. prepared DGEBA-based epoxy resins toughened by CTBN (Bucknall and Yoshii 1978). The volume fraction of rubber phase could be measured by dynamic mechanical analysis, although T_g of the CTBN rubber coincided with β -relaxation of epoxy resin. It is therefore dynamic mechanical measurement that provides an alternative method for determining the degree of phase separation of epoxy blends. But the results are less reliable compared to microscopy.

Ratna studied phase separation behavior of carboxyl-terminated poly(2-ethyl hexyl acrylate) (CTPEHA) liquid rubber-modified epoxy mixtures using DMTA, as illustrated in Fig. 1 (Ratna 2001). The shift of relaxation peak toward slow temperature as a result of modification can be attributed to the presence of dissolved rubber. And the decreased peak value in the loss tangent versus temperature curves with the increasing content of CTPEHA in epoxy matrix indicates the presence of region of lower cross-link density.

Mathur et al. characterized CTBN rubber–epoxy blends by thermal analysis (see Fig. 2); the DMTA suggested a monotonic decrease in storage modulus (E') with the increase in rubber content of the blends (Nigam et al. 2001). The peak maximum of $\tan \delta$ showed shifts toward lower temperature which is due to compatibility and enhancement of rubber-matrix interaction. The results of DMA analysis signified that a 10 wt% rubber-filled epoxy composites can behave as a better damping material in dynamic applications compared to brittle neat epoxy.

Thomas et al. studied the effect of weight percent of CTBN on the viscoelastic performance of epoxy blends by DMA (Thomas et al. 2007). As shown in Fig. 3, the storage modulus of modified epoxy blends with lower content of CTBN was higher, while that of 20 wt% CTBN-modified blend was lower than that of neat epoxy. At a higher concentration (more than 15 wt%), the liquid rubber flexibilized the epoxy matrix and reduced the cross-linking density. The decrease in the storage modulus at high rubber content was attributed to the lowering of the cross-linking density and plasticization effect of the liquid rubber into the epoxy matrix. The addition of the liquid rubber led to the decrease in the T_g (Fig. 3) of the composite because of the

Fig. 1 $\tan \delta$ versus temperature plots of unmodified epoxy, 10 wt% and 20 wt% of CTPEHA modified epoxy

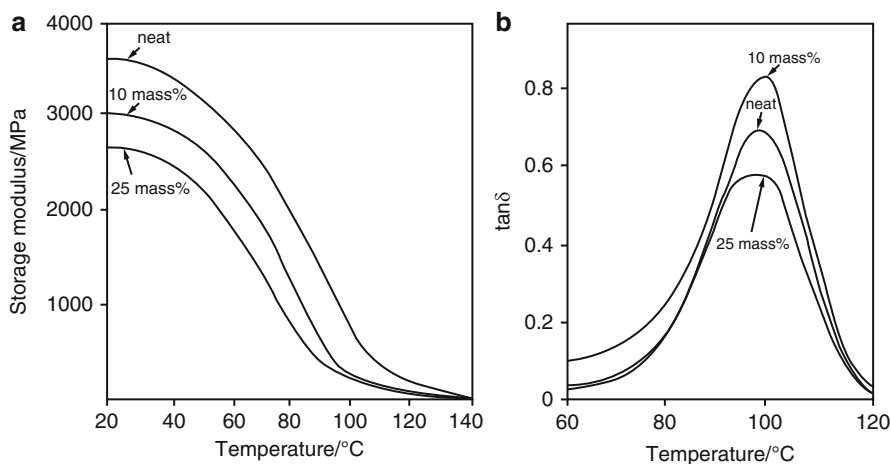
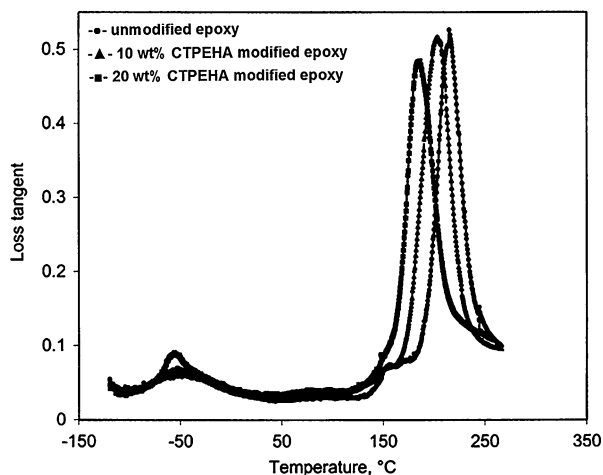


Fig. 2 DMTA results for CTBN rubber-modified epoxy cresol novolac resin, (a) storage modulus and (b) $\tan \delta$ values as a function of temperature

reduction in the cross-linking density and flexibilization of the epoxy matrix by dissolved liquid rubber. The shifted T_g s indicated that the phases are not pure. T_g of dispersed rubber phase in low temperature region shifted to a higher temperature because the modulus of rubber phase was increased by dissolved epoxy resin. The DGEBA-based epoxy resin modified by hydroxyl-terminated polybutadiene (HTPB) was also studied by Thomas et al. (2008). However, the tendency is not so clear due to the low solubility of rubber in epoxy matrix.

Cook et al. investigated the effect of rubber type on the morphologies of modified epoxy blends by comparing the height of rubber glass transition loss peak, which was generally considered as the proportion of rubber in the dispersed phase (Wise

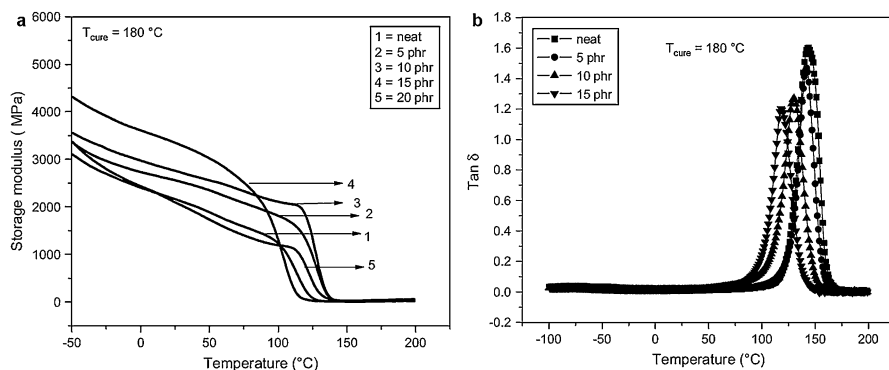


Fig. 3 (a) Storage modulus and (b) tan δ versus temperature of neat epoxy and CTBN-modified epoxy blends cured at 180 °C

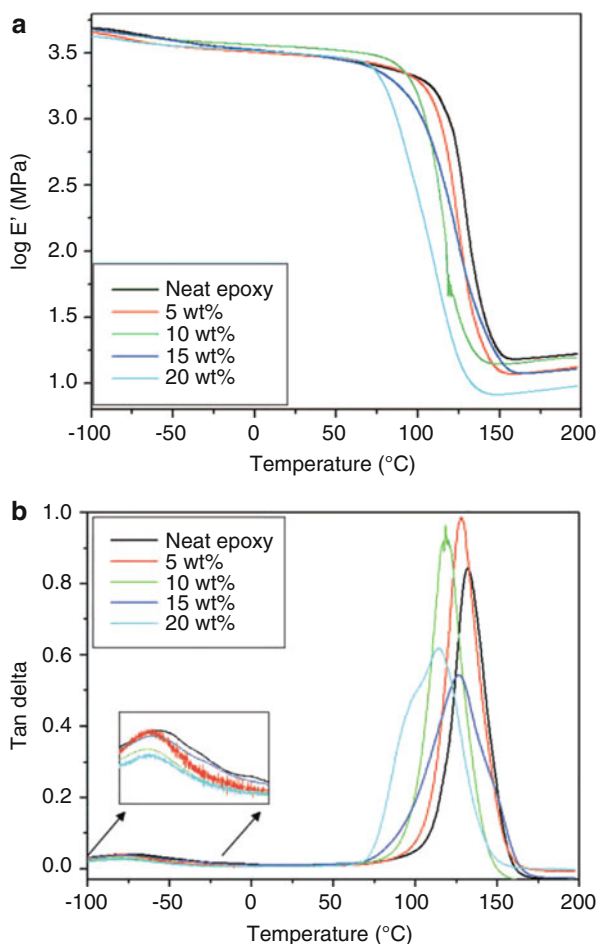
et al. 2000). The T_g of the epoxy matrix was slightly depressed for the CTBN-filled systems, probably due to the plasticizing action of small levels of rubber dissolved in the matrix. The glass transition temperature of the rubbery CTBN phase was also lower than the glass transition temperature of the neat CTBN. When α -relaxation of rubber phase was isolated with β -relaxation of epoxy resin, it was found that the height of resolved rubber tan δ peak was a linear function of CTBN loading. This study provides us an insight that the amount of rubber dissolved in cured epoxy matrix could be determined by DMTA.

The rubber structure has a profound impact on both morphology and viscoelastic properties of modified epoxy resins (Kishi et al. 2007a). Kishi et al. have studied the effect of acrylonitrile content on the damping and adhesive properties of CTBN-modified epoxy resins and found that the morphology changes from microphase separated to homogeneous morphology with the acrylonitrile content in CTBN, which results in broad glass transition temperature range and excellent energy absorbability as the bulk resin in a broad temperature range (Kishi et al. 2007b).

Epoxy Blends Modified by Liquid Natural Rubber

Thomas et al. modified diglycidyl ether of bisphenol A (DGEBA)-type epoxy resin with liquid natural rubber possessing hydroxyl functionality (HTLNR) (Susan et al. 2012). A sharp decrease in storage modulus was observed for all blends near the glass transition of the epoxy network, as illustrated in Fig. 4. The lower value of $\log E'$ in this region indicates that the cross-link density of the blends was lower. The decrease in T_g of epoxy-rich phase may be due to the dilution effect by the addition of HTLNR or due to the presence of miscible HTLNR in the epoxy phase and will result in an incomplete cross-linking. The tan δ peak height for 15 and 20 wt% HTLNR is lower than the other blends and neat cross-linked epoxy due to the formation of agglomerated sub-particles of epoxy phase in the HTLNR droplets,

Fig. 4 Variation of (a) $\log E'$ and (b) $\tan \delta$ with respect to temperature for HTLNR-modified epoxy



which may enhance the stiffness of the material. The increased peak area and peak width showed better miscibility at HTLNR loading.

Nanostructured Epoxy Rubber Blends

Nanostructures in epoxy composites confer many unique features (Ruiz-Pérez et al. 2008). Various reports have demonstrated that nano-inclusions well dispersed in matrix can significantly improve the modulus of polymers when compared to micro-sized particles. Soares et al. found that isocyanate-terminated liquid polybutadiene gave significant improvement in toughness and increased modulus and glass transition temperature (Soares et al. 2011). The interfacial adhesion was enhanced by covalent bonding between dispersed nanophase and epoxy matrix, imparted by the reaction between isocyanate groups in modifier and hydroxyl groups of epoxy resin.

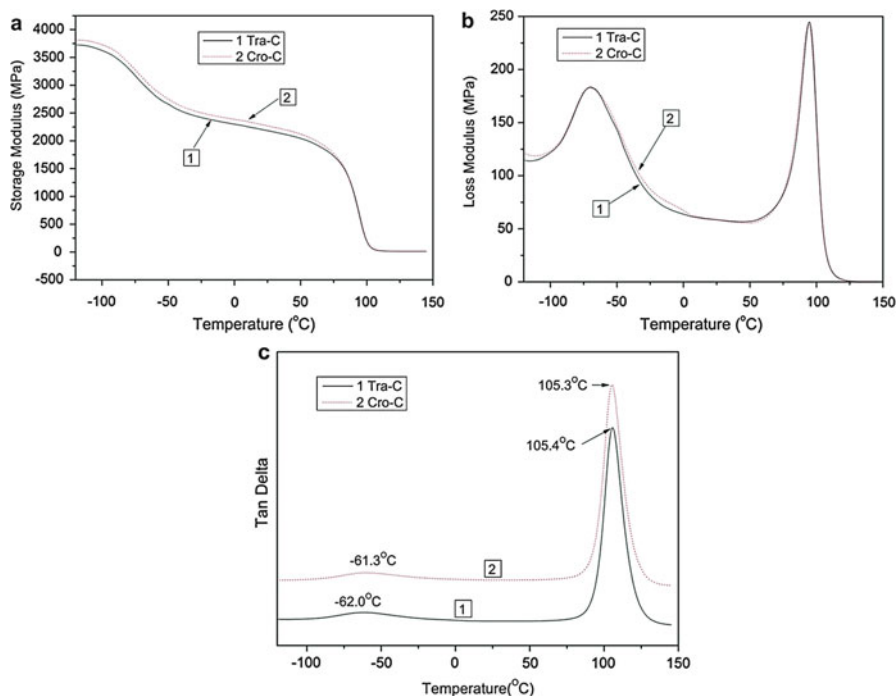


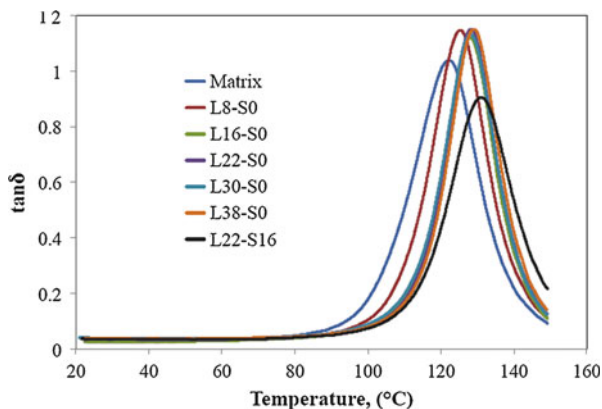
Fig. 5 DMA curves of the two epoxy blends toughened with liquid rubber. 1, The traditional blend; 2, the pre-cross-linked blend. (a) Storage modulus; (b) loss modulus; (c) $\tan \delta$

The relaxation of rubber phase could not be distinguished by DMA because it is probably overlapped with β -relaxation of epoxy resin.

Xu et al. prepared rubber-toughened epoxy blend by an in situ pre-cross-linking method, in which an initiator was added to the liquid rubber–epoxy mixture to initiate cross-linking reaction of liquid rubber, and then curing agent was added to form the thermoset (Fig. 5; Zhou et al. 2014). The dispersed particles are pure rubber phases in traditional CTBN/epoxy blend, whereas the rubber phase and the matrix form a local interpenetrating network in the pre-cross-linked CTBN/epoxy blend. The storage modulus of the pre-cross-linked blend is slightly higher than that of the traditional blend below the glass transition temperature. The impact strength, yield strength, and Young's modulus of the pre-cross-linked CTBN/epoxy blend were thus higher than traditional CTBN/epoxy blend. The glass transition temperatures of the blends prepared using traditional and pre-cross-linking processes are very close to each other.

The use of core–shell rubber instead of pure rubber is another strategy to maintain the T_g of blends (Naguib et al. 2013). Ivankovic et al. investigated DGEBA epoxy resin modified by core–shell rubber nanoparticles in two diameters, 300 nm (L) and 50 nm (S) (Quan and Ivankovic 2015). It was found that T_g increased as the volume fraction of core–shell rubber particles increased, as illustrated in Fig. 6. Here, the

Fig. 6 Tan δ versus temperature of core-shell rubber nanoparticle-modified epoxy blends. The numbers after L/S indicate the volume fraction percentage of core-shell rubber nanoparticles in different diameters



interfacial modification for core-shell rubber particles changed the polymer chain mobility of the blends and higher glass transition temperature. L22-S16 has a higher T_g than L38-S0 due to the reason that smaller particles have larger surface area and imposes more restriction on the mobility of polymer chain.

Conclusion

DMTA is one of the essential measurements for rubber-toughened epoxy blends to reveal the viscoelastic properties. It provides supporting evidence to study the phase structures of rubber inclusions in epoxy matrix. DMTA also provides an important reference for strength and thermal stability of rubber-modified epoxy blends.

References

- Bucknall CB, Yoshii T (1978) Relationship between structure and mechanical properties in rubber-toughened epoxy resins. *Br Polym J* 10:53–59
- Hsieh SY (1990) Morphology and properties control on rubber-epoxy alloy systems. *Polym Eng Sci* 30:493–510
- Kim DS, Kim SC (1994) Rubber-modified epoxy-resin. II: phase-separation behavior. *Polym Eng Sci* 34:1598–1604
- Kishi H, Nagao A, Kobayashi Y, Matsuda S, Asami T, Murakami A (2007a) Pre-reaction between CTBN/epoxy and the phase structures, damping properties and adhesive properties of the cured resins. *J Adh Soc Jpn* 43:50–57
- Kishi H, Nagao A, Kobayashi Y, Matsuda S, Asami T, Murakami A (2007b) Carboxyl-terminated butadiene acrylonitrile rubber/epoxy polymer alloys as damping adhesives and energy absorbable resins. *J Appl Polym Sci* 105:1817–1824
- Manzione LT, Gillham JK, McPherson CA (1981) Rubber-modified epoxies. II. Morphology and mechanical properties. *J Appl Polym Sci* 26:907–919
- Naguib M, Grassini S, Sangermano M (2013) Core/shell PBA/PMMA-PGMA nanoparticles to enhance the impact resistance of UV-cured epoxy systems. *Macromol Mater Eng* 298:106–112

- Nigam V, Setua DK, Mathur GN (2001) Characterization of rubber epoxy blends by thermal analysis. *J Therm Anal Calorim* 64:521–527
- Quan D, Ivankovic A (2015) Effect of core-shell rubber (CSR) nano-particles on mechanical properties and fracture toughness of an epoxy polymer. *Polymer* 66:16–28
- Ratna D (2001) Phase separation in liquid rubber modified epoxy mixture. Relationship between curing conditions, morphology and ultimate behavior. *Polymer* 42:4209–4218
- Ratna D, Banthia A (2004) Rubber toughened epoxy. *Macromol Res* 12:11–21
- Ruiz-Pérez L, Royston GJ, Fairclough JPA, Ryan AJ (2008) Toughening by nanostructure. *Polymer* 49:4475–4488
- Soares BG, Dahmouche K, Lima VD, Silva AA, Caplan SPC, Barcia FL (2011) Characterization of nanostructured epoxy networks modified with isocyanate-terminated liquid polybutadiene. *J Colloid Interf Sci* 358:338–346
- Susan MV, Jyotishkumar P, George SC, Preetha G, Laurent D, Marc SJ, Saikia PJ, Sabu T (2012) High performance HTLNr/epoxy blend—phase morphology and thermo-mechanical properties. *J Appl Polym Sci* 125:804–811
- Thomas R, Durix S, Sinturel C, Omonov T, Goossens S, Groeninckx G, Moldenaers P, Thomas S (2007) Cure kinetics, morphology and miscibility of modified DGEBA-based epoxy resin—Effects of a liquid rubber inclusion. *Polymer* 48:1695–1710
- Thomas R, Ding Y, He Y, Yang L, Moldenaers P, Yang W, Czigany T, Thomas S (2008) Miscibility, morphology, thermal, and mechanical properties of a DGEBA based epoxy resin toughened with a liquid rubber. *Polymer* 49:278–294
- Thomas S, Sinturel C, Thomas R (2014) 11. Viscoelastic measurements and properties of rubber-modified epoxies. Weinheim Germany: Wiley-VCH Verlag GmbH & Co. KGaA
- Wise CW, Cook WD, Goodwin AA (2000) CTBN rubber phase precipitation in model epoxy resins. *Polymer* 41:4625–4633
- Yang B, Wang W, Huang J (2015) Synergic effects of poly(vinyl butyral) on toughening epoxies by nanostructured rubbers. *Polymer* 77:129–142
- Zhou HS, Song XX, Xu SA (2014) Mechanical and thermal properties of novel rubber-toughened epoxy blend prepared by in situ precrosslinking. *J Appl Polym Sci* 131:547–557

Shoubing Chen, Tingmei Wang, and Qihua Wang

Abstract

The thermal properties of epoxy/rubber blends include glass transition, thermal conductivity, heat capacity, thermal expansion, and thermal stability and are systematically reviewed by a number of thermal analysis techniques including differential scanning calorimetry, thermogravimetric analysis, thermomechanical analysis, and dynamic mechanical analysis. The rubbers include usually used natural rubber, polybutadiene rubber, nitrile rubber, polyurethane rubber, silicon rubber, etc. Generally speaking, the addition of a rubber component to the epoxy resin will result in depression of glass transition temperature of it due to incomplete phase separation and incomplete curing reaction. It depends on the cross-linking density of the blends. The thermal conductivity of the blends is affected by the polar nature of rubber. The conductive rubber which is forming a continuous phase could enhance the thermal conductivity. Heat capacity of epoxy/rubber blends is affected not only by the polar nature of rubber but also the density of the formed blends. The thermal expansion behaviors are not only related to thermal and mechanical history but also depend on the network of modified epoxy resin. And further, the thermal stability of epoxy/rubber blends is mainly depending on the thermal stability of the rubber and the cross-linking density of the formed networks. The higher-heat-resistant rubber leads to higher thermal stability of epoxy/rubber blends.

Keywords

Epoxy/rubber blends • Thermal glass transition • Thermal conductivity • Thermal expansion • Thermal stability

S. Chen (✉) • T. Wang • Q. Wang
State Key Laboratory of Solid Lubrication, Lanzhou Institute of Chemical Physics, Chinese Academy of Sciences, Lanzhou, China
e-mail: chenshoubing@licp.cas.cn; tmwang@licp.cas.cn; wangtin3088@sina.com

Contents

Introduction	250
Thermal Properties of Epoxy/Rubber Blends	251
Glass Transition	251
Thermal Conductivity and Heat Capacity of Epoxy/Rubber Blends	262
Linear Thermal Expansion Behavior of Epoxy/Rubber Blends	263
Thermal Stability	267
Conclusions	274
References	275

Introduction

Thermal properties of polymer and polymer composites mainly include glass transition, thermal conductivity, heat capacity, thermal expansion, and thermal stability, which can be obtained by thermal analysis techniques (Raymond and Charles 1984). A number of thermal analysis techniques including differential scanning calorimetry (DSC), thermogravimetric analysis (TGA), thermomechanical analysis (TMA), and dynamic mechanical analysis (DMA) have been employed to detect the thermal properties of polymers and their composites. DSC is used to investigate physical transitions and chemical reactions. Properties such as the heat capacity, glass transition temperature, melting temperature, heat, and extent of reaction can be determined by it. In TGA, the change in mass of a sample is measured as a function of temperature or time. It can reflect the thermal stability of the samples. TMA measures the dimensional changes of a sample as it is heated. In the thermal expansion measurement, the probe exerts a low pressure on the surface of the sample. The samples are heated linearly over the temperature range of interest. The linear thermal expansion coefficient can be calculated directly from the measurement cure. In DMA, a mechanical modulus is determined as a function of temperature, frequency, and amplitude. By this means, relaxation behavior and phase transition in semicrystalline materials can be obtained (Bernhard 1990; Edith 1996).

Varieties of epoxy/rubber blends are widely applied in many different applications ranging from adhesives in civilian application to structural components in military and aerospace systems due to their outstanding versatility and performance (Nigam et al. 2001; Kothandaraman and Kulshreshtha 2003). In these applications, structural integrity and thermal stability of the polymer composites at elevated temperatures are of primary importance especially when the products undergo long-term serviceability in dynamic conditions. The thermal properties of epoxy/rubber blends are relevant to their mechanical properties, stability properties, and whether and how long they can be used in some specific circumstances. Therefore, to understand and study the thermal properties of epoxy/rubber blends are very important for their applications.

Thermal Properties of Epoxy/Rubber Blends

Glass Transition

The glass transition, T_g , is a phenomenon observed in amorphous polymers. It occurs at a fairly well-defined temperature when the bulk material ceases to be brittle and glassy in character and becomes less rigid and more rubbery. When a material is heated to this point and beyond, molecular rotation around single bond becomes significantly easier (Raymond and Charles 1984). Many physical properties change profoundly at the glass transition temperature, including coefficient of thermal expansion, heat capacity, mechanical damping, etc. Therefore, glass transition temperature of polymers is closely related to the properties and potential use of themselves.

Epoxy, as a cross-linked polymer when it cured, has a relative high T_g values. The degree of cross-linking can restrict chain mobility and thus increase the T_g values (Watanabe 1999; Petri 2005). Rubber is any type of elastomer which can undergo much more elastic deformation under stress than most materials and still return to its previous size without permanent deformation (Morton 1981; Smith et al. 1993). They have low T_g values. The T_g increases as the intermolecular forces in the polymer and the regularity or crystallinity of the polymer chain structure increase; when the epoxy blends with rubbers, the glass transition of the blends will change.

Glass Transition of Epoxy/Natural Rubber Blends

Hong et al. (2005) studied the glass transition temperature of epoxidized natural rubber (ENR, 25 mol.% epoxidation) modified epoxy systems by DSC. The results showed that the presence of ENR changes the viscosity/the flexibility (T_g) of the mixed resins (Table 1). When the ENR blended with epoxy, the T_g of the rubbery phase obtained which are 21 °C and 18 °C in the specimens R-5 and R-10 (the specimens R-5, R-10, and R-15 are prepared by the addition of 5, 10, and 15 parts of ENR in the basic formulation), respectively, are much greater than the T_g (−45 °C) of unreacted ENR. At the same time, the epoxy matrix in the R-5, R-10, and R-15 have T_g near 130 °C, 121 °C, and 117 °C, respectively, which are all lower than the T_g of the neat epoxy resin matrix (~134 °C). The presence of ENR in the epoxy matrix decreases the T_g of the epoxy phase, and the T_g decreases with the increasing ENR content (or with more dissolved ENR). Many equations have been proposed to calculate the T_g of miscible polymer blends, and all indicate an increase in miscible content of the low T_g constituent which could shift the T_g of miscible blend to a lower temperature and vice versa (Gordon and Taylor 1952).

ENRs (epoxy value: mg of potassium hydroxide/g of rubber is 16.23 mg/g) with different concentrations of up to 20 wt% were used as modifiers for epoxy resin and were also studied by Mathew et al. (2014). The glass transition properties of the blends were investigated by DMA. The T_g values of the fully cured epoxies were taken to be the temperatures at the maximum of the $\tan \delta$ peaks. The results showed the T_g of the epoxy resin decreased when it was blended with ENR and was more

Table 1 T_g ($^{\circ}\text{C}$) obtained from specimens cured at 170°C (Hong et al. 2005)

Specimen	T_g of rubber constituent	T_g of epoxy constituent			
		T_{gb}	T_{gf}	$T_{gbroadness}$	T_{gepoxy}
Reference	No.	126 (2.0)	140 (1.8)	14 (1.0)	134 (1.2)
R-5	21 (2.6)	119 (1.6)	139 (0.8)	20 (1.4)	130 (2.0)
R-10	18 (0.5)	110 (1.7)	131 (1.5)	21 (1.3)	121 (0.4)
R-15	23 (3.0)	106 (0.5)	129 (0.4)	23 (0.5)	117 (0.5)

T_{gb} : the beginning point of the glass transition region

T_{gf} : the end point of the glass transition region

$T_{gbroadness}$: the width of the glass transition region

significant for higher weight percentages of ENR. The different peak heights indicated that the damping properties of the toughened blends were different. The magnitude of $\tan \delta_{\max}$ was at a minimum for the blends because of an epoxy phase decrease in size with the addition of ENR and because the dimensions of the rubber-rich phase were larger at higher ENR concentrations.

Kumar and Kothandaraman (2008) investigated another kind of natural rubber with terminated carboxyl group (maleated depolymerized natural rubber (MDPR)) which blends with epoxy resin at three different ratios (the ratios of epoxy resin and rubber are 97/3, 98/2, and 99/1). With DSC analysis, the results showed that addition of MDPR to epoxy resin does not produce significant change in the T_g value of the neat epoxy resin. This could be attributed to the limited compatibility between the blend components and the very small amount of MDPR in the blends.

Glass Transition of Epoxy/Polybutadiene Rubber Blends

The glass transition of brittle epoxy resin modified by liquid rubber hydroxyl-terminated polybutadiene (HTPB) has been studied by DMA (Ozturk et al. 2001). HTPB, hardener, and epoxy were mixed directly; T_g of neat epoxy specimens decreased from 119°C to 117°C with 1% HTPB addition and further down to 114°C with 1.5% HTPB addition because of the toughening effect of HTPB.

Epoxy resin and varying content of HTPB (hydroxyl value $42.4 \text{ mg KOH g}^{-1}$, the HTPB content varied from 5 to 20 phr) which were cured using an anhydride hardener were studied by Thomas et al. (2008). The loss factor curve of neat epoxy resin shows a peak at around 142°C (Fig. 1). That is clearly related to the glass transition temperature of the epoxy resin. The presence of HTPB results only in a slight displacement of the transition peak; e.g., for 5 and 10 phr HTPB-modified epoxy networks, a shift to a lower region is observed by a shift of 1°C and 2°C , respectively. The authors attributed this to the lowering of cross-linking density in the modified samples. During the curing of epoxy resin, phase-separated rubber domains shall occupy the space in between the reaction sites, thereby impairing the cross-linking reaction at that particular site which can reduce the cross-linking density of cured systems. Thus, the glass transition temperature decreases by the incorporation of more rubber.

Zhang et al. (2010) investigated T_g of new elastomers based on a liquid amine-terminated polybutadiene (ATPB, an amine value of 62) and epoxy resin blends. The

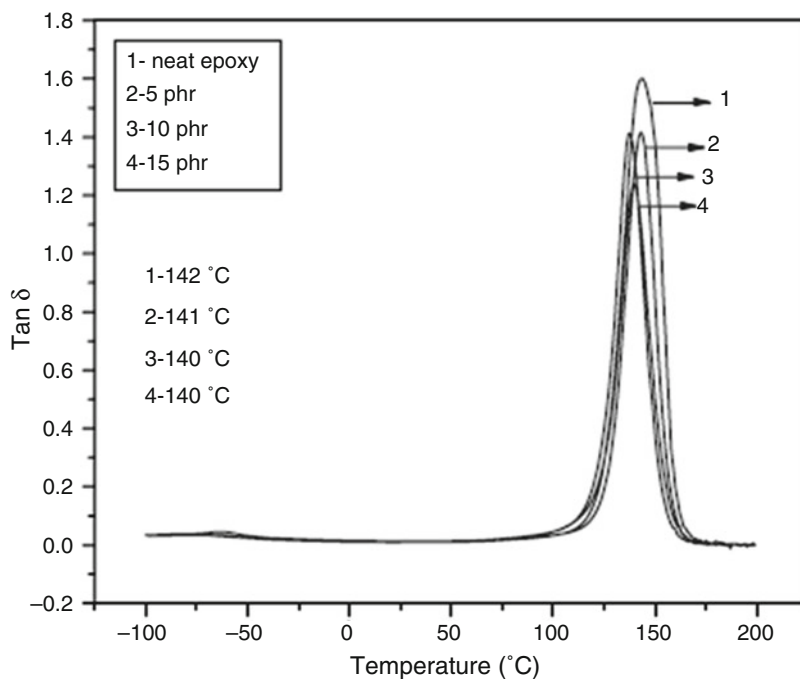


Fig. 1 Dynamic loss factor, $\tan \delta$ versus temperature of the neat and modified epoxies (Thomas et al. 2008) (Reprinted from Polymer, 49, Thomas R, Yumei D, Yuelong H, Le Y, Moldenaers P, Weimin Y, Czigany T, Thomas, S, Miscibility, morphology, thermal, and mechanical properties of a DGEBA based epoxy resin toughened with a liquid rubber, 278–294., Copyright (2008), with permission from Elsevier)

samples constitute ATP-1 (mole ratio of ATPB/triethylenetetramine (TETA)/m-xylylenediamine (MXDA)/epoxy resin is 11/0/0/10.4), ATP-2 (weight ratio of ATPB/TETA/MXDA/epoxy resin is 11/9/0/20.8), and ATP-3 (weight ratio of ATPB/TETA/MXDA/epoxy resin is 11/0/10/20.8). The study of cured ATP samples showed that the T_g of the soft segment appeared at -68 to -70 °C (Fig. 2). The value of the T_g in these elastomers was compared to a value of -70 °C for HTPB-based polyurethane, and its invariance with increasing epoxy resin content indicated that phase segregation was very nearly complete. Because amine and epoxy groups form amorphous hard regions, the driving force for phase segregation must have come from the extreme incompatibility of the polar hard segment and the nonpolar soft segment. In the high-temperature glass transition area, the T_g belongs to epoxy matrix part in the samples; the T_g increases as the cross-linking density increases (from 46.9 °C to 103.5 °C).

Glass Transition of Epoxy/Nitrile Rubber Blends

The T_g of a diglycidyl ether of bisphenol A-based epoxy resin, using an anhydride hardener (nadic methyl anhydride), at different weight contents (0 phr to 20 phr) of

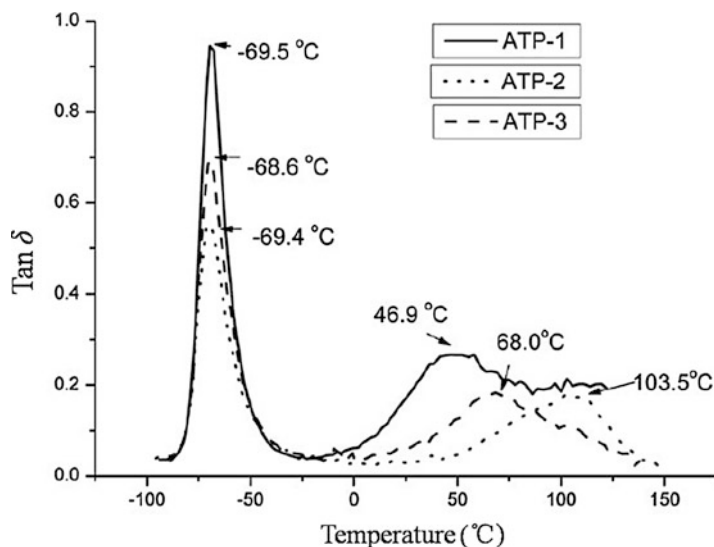


Fig. 2 Temperature dependence of $\tan \delta$ of the ATPB-based elastomers (Zhang et al. 2010)

carboxyl-terminated copolymer of butadiene and acrylonitrile liquid rubber (CTBN, Mn of 3500 g/mol, containing 18% acrylonitrile content and 3% carboxyl content) as modifier, was investigated using a DMA (Thomas et al. 2004, 2007). The T_g of the modified epoxy resin decreased with increase in cure temperature. Addition of the liquid rubber lowered the T_g of the epoxy/nitrile rubber network. This became prominent in the modification of the matrix with 15 and 20 phr of the elastomer. It is attributed to the flexibilization of the matrix. The shifted T_g s clearly indicate that the phases are not pure. The dissolved rubber plasticize the epoxy network. The T_g of the neat rubber in the low-temperature region was shifted to higher temperature upon the addition of the elastomer into epoxy resin. A higher shift was noted for 15 and 20 phr inclusion (Fig. 3). This was due to dissolved epoxy in the rubber-rich phase that increased the modulus of the rubbery phase. The inclusion of a large wt% of CTBN decreased the cross-linking density of the thermoset matrix.

Tripathi and Srivastava (2007, 2008) studied the blends of epoxy resin with varying weight ratios (0 phr–25 phr) and high carboxyl content of CTBN (Mn of 3500 g/mol, containing 27% acrylonitrile content and 32% carboxyl content). At high temperature, the T_g was observed as a large maximum in the loss modulus curve. The effect of the CTBN lowered the glass transition temperature of the cured epoxy resin/CTBN network (Fig. 4). It is observed that more and more inclusion of rubber shifted the T_g peak of epoxy resin/CTBN blends to lower temperature scale. This could be attributed to the inclusion of rubber into the epoxy network, which is forming homogeneous rubber-rich phase as reported earlier by Nigam et al. (2001).

In the case of epoxy/CTBN blends, the glass temperature transitions of the blends are significantly shifted to lower temperature which shows that the dissolved rubber plasticize the epoxy network and homogeneous rubber-rich phase formed in the

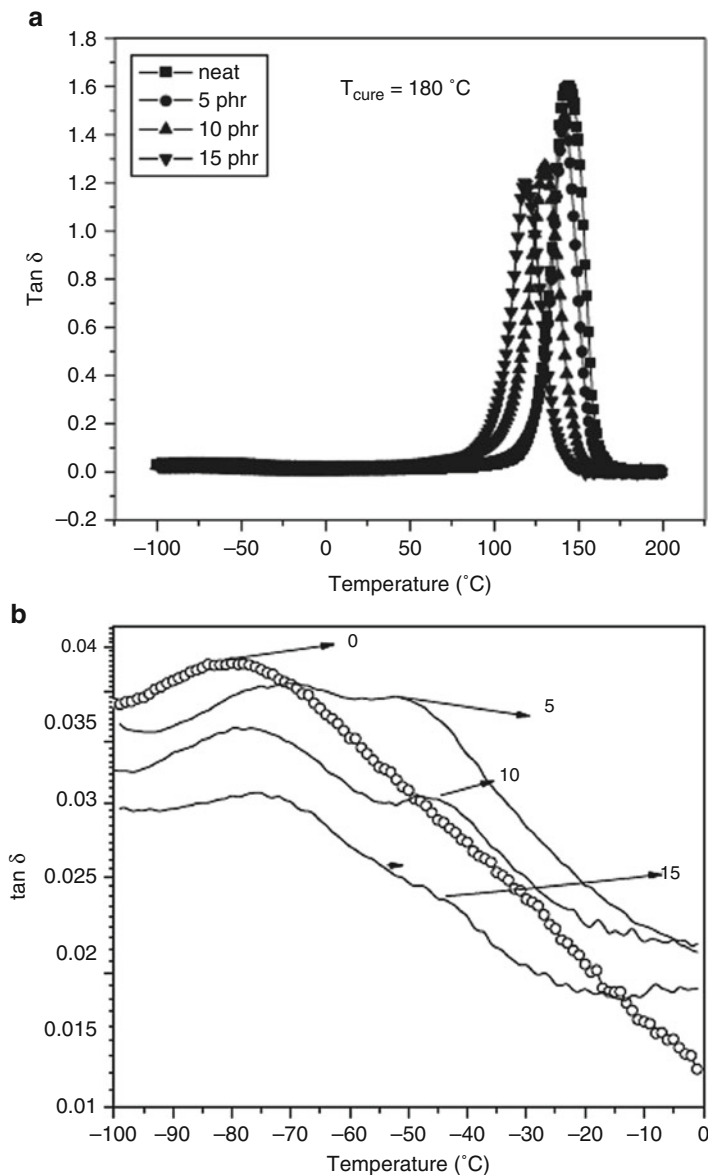


Fig. 3 (a) $\tan \delta$ versus temperature of the neat and modified epoxies at $T_{\text{cure}} 180^{\circ}\text{C}$. (b) Low-temperature region of the curves showed in (a) (Thomas et al. 2007) (Reprinted from Polymer, 48, Thomas R, Durix S, Sinturel C, Omonov T, Goossens S, Groeninckx G, Moldenaers P, Thomas S, Cure kinetics, morphology and miscibility of modified DGEBA-based epoxy resin - Effects of a liquid rubber inclusion, 1695–1710., Copyright (2007), with permission from Elsevier)

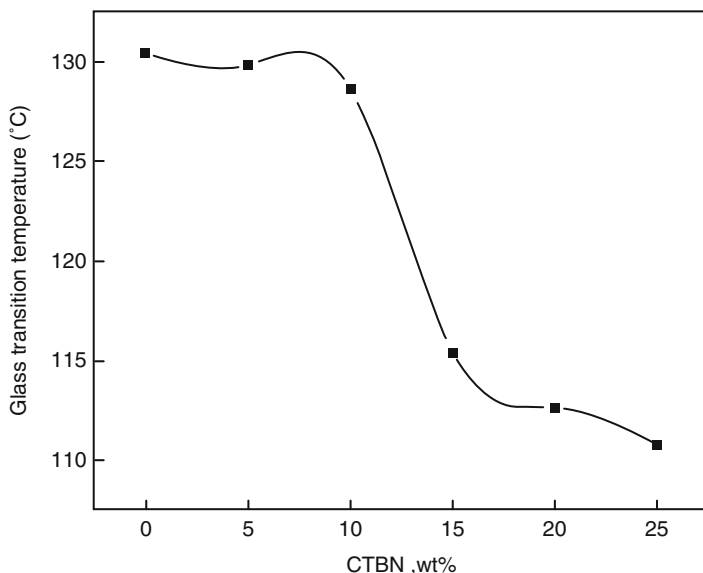


Fig. 4 Variation of glass transition temperature with CTBN concentration of prepared samples (Tripathi and Srivastava 2008) (Reprinted from Mater Sci Eng A-Struct Mater Prop Microstruct Process, 496, Tripathi G, Srivastava D, Studies on the physico-mechanical and thermal characteristics of blends of DGEBA epoxy, 3,4 epoxy cyclohexylmethyl, 3', 4'-epoxycyclohexane carboxylate and carboxyl terminated butadiene co-acrylonitrile (CTBN), 483–493., Copyright (2008), with permission from Elsevier)

blends. With different carboxyl content in CTBN, the T_g decreased as the carboxyl content increased. This can be explained by the solubility parameter concept. The solubility parameter of epoxy is $21.05 \text{ (J/cm}^3\text{)}^{0.5}$. As the carboxyl content increases in CTBN, the proximity of the solubility parameter becomes closer between CTBN and epoxy. It leads to better miscibility between CTBN and epoxy. And with the increase in the functionality of liquid rubber, the chemical interaction between the epoxy and rubber increases (terminate carboxyl reacts with epoxy group) which induces compatibility of the epoxy/rubber blends (Ratna and Simon 2001).

Glass Transition of Epoxy/Polyurethane Rubber Blends

Polyurethane (PU, synthesized by polyester diol and toluene diisocyanate) having different isocyanate index were used to modify epoxy resin by Bakar et al. (2009). With the addition of 15% of polyurethane, T_g of the epoxy and polyurethane blends decreases by more than 50 °C. The depression of T_g might be attributed to the additional free volume provided by the plasticizer facilitating segmental movements. The lowering of T_g is taken as a measure of plasticizer efficiency, which is more pronounced in polymers containing rigid chains. The similar results obtained by Tang et al. (2013) used a carboxyl-terminated polyether (polyol)-based polyurethane-modified epoxy resin. T_g values of the resins varied with the submicron PU weight content in the composite sample (Fig. 5). The presence of PU results in a

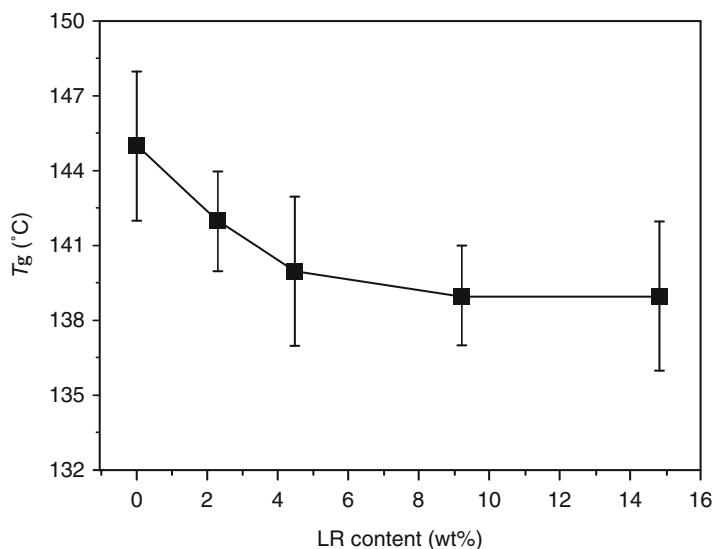


Fig. 5 Glass transition temperatures of neat epoxy and epoxy/PU binary composites (Tang et al. 2013) (Reprinted from Mater Chem Phys, 141, Tang LC, Wang X, Wan YJ, Wu LB, Jiang JX, Lai GQ, Cure kinetics, morphology and miscibility of modified DGEBA-based epoxy resin - Effects of a liquid rubber inclusion, 333–342., Copyright (2013), with permission from Elsevier)

slight displacement of the transition peak, e.g., a shift of 5 °C and 6 °C observed for 4.5 and 14.8 wt% PU-modified epoxy networks, respectively. The slight reduction in T_g is probably attributed to small amounts of liquid rubber, which possess a lower T_g , remaining in epoxy matrix after curing, and/or the decreased cross-linking density in the PU-modified epoxy composite samples.

Chen et al. (2010) investigated the glass transition properties of castor oil-based polyurethane (based on polymer triol) and epoxy resin (EP) composites with the polyurethane (PU) content from 5 wt% to 30 wt%. The results showed that there was only one T_g peak for all the composites and component ratio exerted much influence on the damping properties. In addition, the damping temperature range became wider, and the temperature for peak $\tan \delta$ became lower with the increase of PU content in the composites (Fig. 6). There are no separated T_g peaks corresponding to EP and PU rubber which existed in the DMA curves. It indicated that the EP and PU rubber forms a homogeneous network. That is to say the PU and EP were well compatible in the interpenetrating polymer networks (IPNs). The two possible reasons are as follows: on the one hand, there are interpenetration and entanglement between PU and EP in the IPNs; on the other hand, there is higher degree of hydrogen bonding and cross-linking in the composites, which could also improve the compatibility of the two polymers.

Jin et al. (2014) further studied a series of IPNs based on EP and PU prepolymer derived from soybean oil-based polyols (have more than three terminated -OH in one molecular of soybean oil-based polyols) with different mass ratios. T_g of the

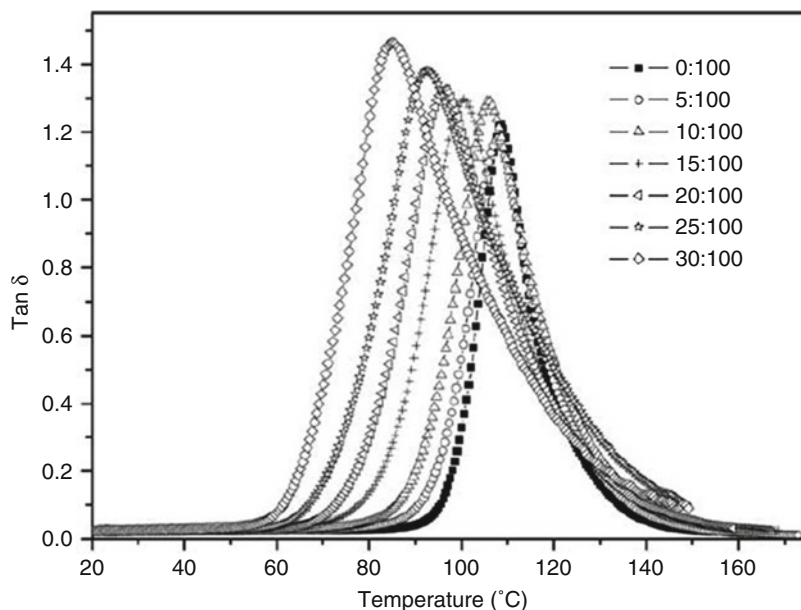


Fig. 6 DMA curves of CO-PU/EP IPNs with component ratios from 0:100–30:70 in steps of 5 wt.% at 10 Hz (Chen et al. 2010)

PU/EP IPNs was detected by DSC and DMA (Fig. 7). Only one T_g is observed for each soybean oil-based PU/EP IPN, which agrees well with the results of the other reports (Jia et al. 2006; Lin et al. 2007; Chen et al. 2010). It can be seen that the T_g of the pure EP is higher than that of the PU/EP IPN. Furthermore, the value of T_g of the soybean oil-based PU/EP IPN decreases clearly upon increasing the PU prepolymer contents. PU prepolymer reacts with the pendant hydroxyl group on the side chains of EP and exists with good compatibility in the PU/EP IPN structures on the molecular scale; thus, the low value of T_g and the soft properties of PU prepolymers affect the epoxy resin to a great extent to cause the decreased values of T_g . The T_g obtained from DMA had the same tendency as obtained from DSC.

Tang et al. (2014) used hyperbranched polyurethane (HBPU) as modifier of epoxy resin. The $\tan \delta$ curves of modified thermosets showed a single peak (Fig. 8), which is similar to the neat epoxy thermoset, at the temperature range of -40 °C to 160 °C (the HBPU-G3 used was characterized by DSC with a T_g of 3.7 °C). The appearance of one $\tan \delta$ peak indicates the good compatibility between HBPU and EP resins. These facts evidenced that there was no phase separation and that homogenous blends were formed. On the one hand, the HBPU has good compatibility with epoxy; on the other hand, the HBPU molecules can be incorporated into epoxy networks by covalent bond (Tang et al. 2014). In this study, by the addition of 5 wt% HBPU, slight increase in T_g was observed. At 10 and 15 wt% HBPU, the T_g decreased by 2 °C and 7 °C, respectively. The T_g slightly increased at low HBPU content (5 wt%) but decreased at higher HBPU content (10 and 15 wt%)

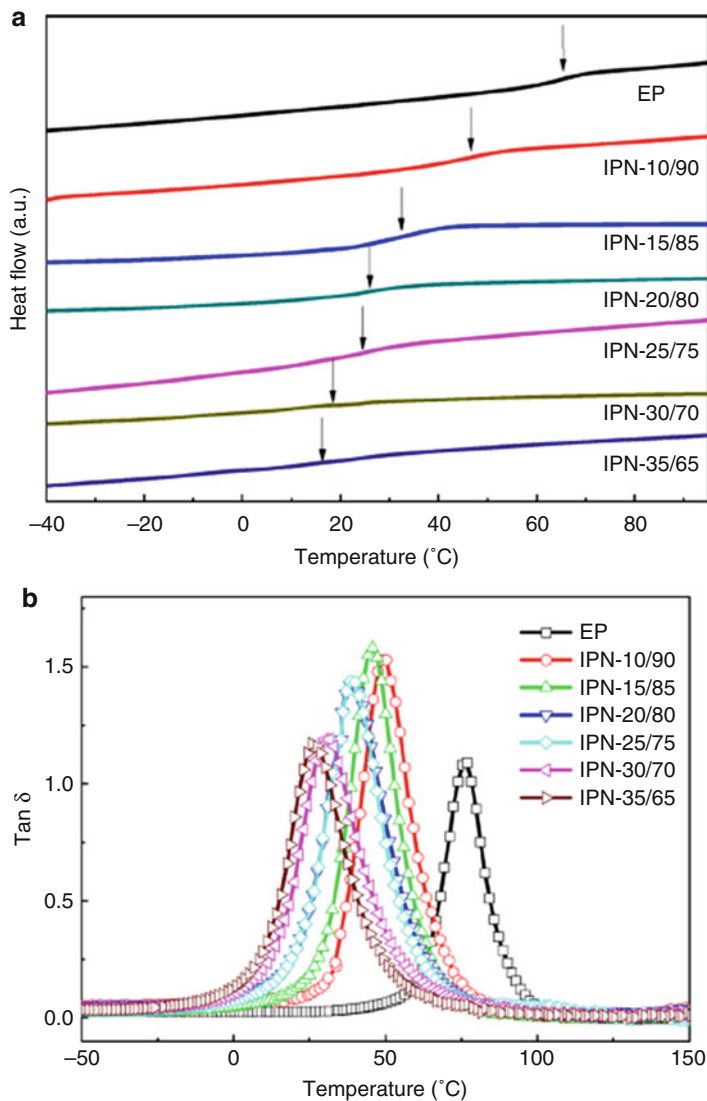


Fig. 7 DSC curves (a) and temperature dependence of $\tan \delta$ (b) of soybean oil-based PU/EP IPNs (Jin et al. 2014)

which could be attributed to two factors: on the one hand, the chemical incorporation of the HBPU into the epoxy networks would result in a higher cross-linking density which would lead to a shift in T_g to higher temperature (when the HBPU content is 5 wt%); on the other hand, the T_g of HBPU is low, and the HTPB could plasticize the epoxy network which would lead to a shift in T_g to lower temperature (when the HBPU content is 10 and 15 wt%).

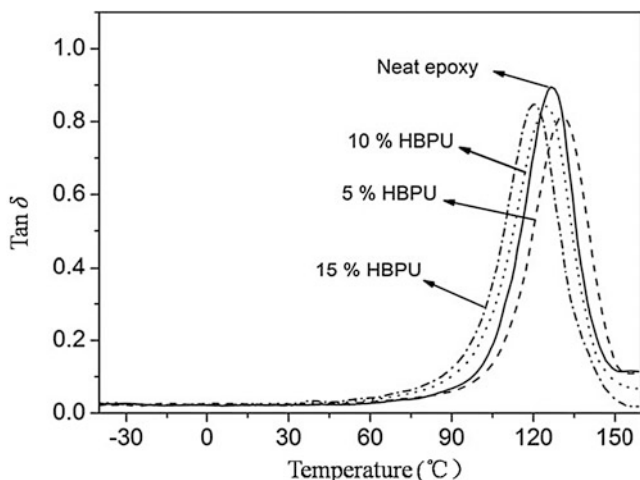


Fig. 8 Tan δ of cured neat and modified epoxies as a function of temperature (Tang et al. 2014)

Glass Transition of Epoxy/Silicon Rubber Blends

An epoxy-terminated organosilicon polymer (ETOP, with epoxide value of 0.02) was used as modifier to blend with bisphenol A-type epoxy resins cured with p-phenylenediamine (Zheng et al. 1995). The glass transition properties of the blends were detected by DSC and DMA. In DSC analysis, the cured products possess two T_g s, which were ascribed to T_g s of both the epoxy-rich and ETOP-rich phases (Table 2). In these cured blends, particularly at higher ETOP content (>10 wt%), the two T_g s corresponded to the ETOP- and EP-rich components, respectively, which are indicative of a heterogeneous morphology. While ETOP was blended into the systems, the epoxide groups in the ETOP molecules also participate in the cross-linking reaction and form a co-cured polymeric product. The T_g of the EP phase has a dramatic increase as a function of ETOP concentration. The T_g increased from 94 °C to 153 °C. T_g of cured EP is 94 °C, while blending with ETOP and curing under standard schedule, the T_g of cured epoxy matrices increased to 153 °C for EP/ETOP 30/70 blends. The increase in T_g may arise from the occurrence of reaction between resin and ETOP forming a copolymer. ETOP is a copolymer terminated with epoxide groups. The epoxide value is the reflection of reaction ability of ETOP. It can participate in the curing reaction of epoxy resins. The higher epoxide value of ETOP will increase the higher cross-linking density in the epoxy/ETOP blends. These epoxide groups will extend into the matrices and take part in the cross-linking reaction of epoxy matrices and elevate the cross-linking density, i.e., increase T_g of the matrix, particularly at a higher ETOP content in the blends. The T_g obtained from DMA had the same tendency as obtained from DSC (Fig. 9).

Ma et al. (2010; Liu et al. 2010) investigated a dendritic epoxidized polysiloxane (DPSO) blended with epoxy resin. The DSC results showed the T_g s of epoxy resins were slightly increased by introducing silicon compounds either (Fig. 10). This result can be explained that when DPSOs were incorporated into epoxy resin, they

Table 2 Glass transition temperature of epoxy resin/ETOP blends (Zheng et al. 1995)

Content of ETOP in wt.%	T_g (ETOP, °C)	T_g (epoxy, °C)
100	13	–
90	15	149
70	15	141
50	15	137
30	15	153
10	–	90
0	–	94

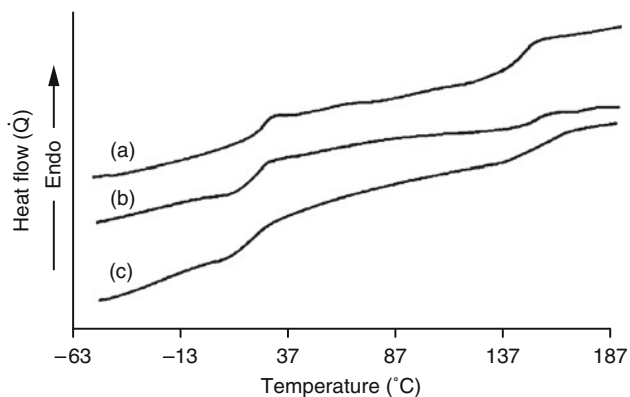


Fig. 9 DSC curves of cured DGEBA/ETOP blends (w/w): (a) 50/50 (b) 30/70 (c) 10/90 (Zheng et al. 1995)

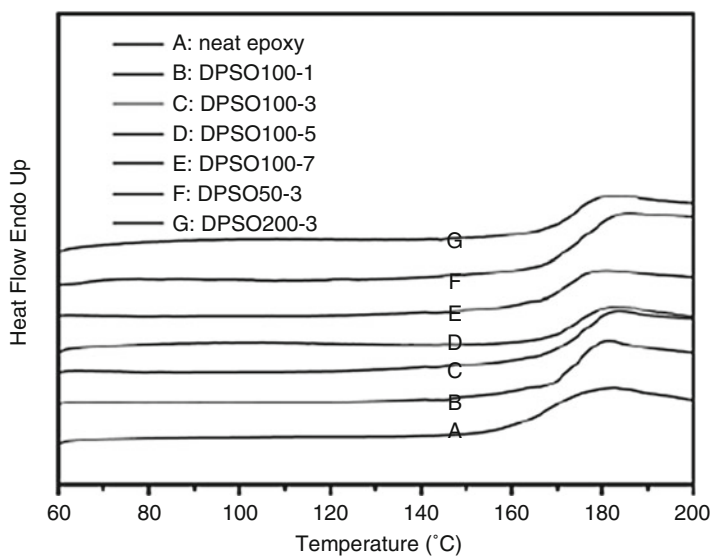


Fig. 10 DSC curves of the cured epoxy resin/DPSO blends (Ma et al. 2010)

could react with the curing agent and epoxy resin by their epoxide groups and Si-OH and enter into the cross-link network, which could function as the cross-link sites in some extent and lead to higher cross-linking density and consequently higher T_g . On the one hand, with the increase of the DPSO content in epoxy resin, more epoxide groups and Si-OH react at the curing process and increase the cross-linking density and increase the T_g s; on the other hand, the flexibility and the aggregation of DPSO would make the cross-linking density of the epoxy resin decrease, and consequently the T_g of epoxy/DPSO blends decreases. These two competing effects lead to finally T_g s of epoxy/DPSO blends.

Brief Summary

Glass transitions of epoxy resin and various rubber blends are reviewed. From the research, the free volume of the blends is the main effect for the glass transition temperature. When the rubber is added into the epoxy resin, it may act as a plasticizer facilitating segmental movements and lowering of cross-linking density of the networks which add additional free volume. Thus, the addition of the rubber lowered the T_g of the epoxy and rubber network, and the T_g decreases as the content of rubber increases. However, in some special conditions, the addition of some rubber into epoxy resin could increase the value of T_g . Because the reaction between resin and epoxidized silicon rubber could be form a copolymer. The epoxide groups of rubber will extend into the matrices and take part in the cross-linking reaction of epoxy matrices. The cross-linking density increases and thus the T_g increases. The two influencing factors are competitive. One of them will play a decisive role for glass transition property in epoxy/rubber blends.

Thermal Conductivity and Heat Capacity of Epoxy/Rubber Blends

Thermal conduction is the transfer of internal energy by microscopic diffusion and collisions of particles or quasiparticles within a body or between contiguous bodies. The microscopically diffusing and colliding objects include molecules, atoms, electrons, and phonons. The heat flow Q from any point in a solid is related to the temperature gradient dt/dx through the thermal conductivity κ as follows:

$$Q = -\kappa(dt/dx) \quad (1)$$

The transmission of heat is favored by the presence of ordered crystalline lattices and covalently bonded atoms. Thus, most polymeric materials have low κ values (Raymond and Charles 1984; Yang 2004).

Heat capacity is a measurable physical quantity equal to the ratio of the heat added to (or removed from) an object to the resulting temperature change, and specific heat capacity (C_p) is the heat capacity per unit mass of a material. C_p is related to the motion of vibration and rotation which thermally excited within the sample. Polymers typically have relatively (compared with metals) large specific heats (Raymond and Charles 1984). The κ is related to C_p :

$$\kappa = dC_p\rho \quad (2)$$

In the Eq. 2, d is the thermal diffusivity and ρ is the density of the material.

For blends of epoxy and rubbers, thermophysical properties such as thermal conductivity and heat capacity are important when used as heat-dissipating materials (e.g., encapsulants for electrical and electronic components) and heat-insulating materials (e.g., the aircraft shell).

Thomas et al. (2010) studied the thermophysical properties, such as thermal conductivity and diffusivity of epoxy resin blend systems with the incorporation of two largely used liquid rubbers (CTBN/HTPB) (Bussi and Ishida 1994; Tripathi and Srivastava 2009; Boudenne et al. 2006). The thermal conductivity was measured for both neat and modified epoxy blends with various volume contents of CTBN and HTPB shown in Fig. 11 by a periodical method. It showed a small increase of thermal conductivity as a function of the volume fraction of CTBN and HTPB. For the epoxy/HTPB, the ratio between the thermal conductivity of the HTPB rubber ($\kappa = 0.22 \text{ Wm}^{-1}\text{K}^{-1}$) and pure matrix ($\kappa = 0.147 \text{ Wm}^{-1}\text{K}^{-1}$) is lower than 1.5. The increase in thermal conductivity of blends as a function of the volume fraction of rubber can be attributed to the partial replacement of the matrix resin by the more conductive (polar) liquid rubbers that favor the energy (heat) dissipation mechanism. In the case of CTBN-modified epoxy blends, the thermal conductivity values show significant increase from 25 vol.% of rubber inclusion where the rubber phase has a tendency toward forming a continuous phase because of the polar character of the liquid rubber, which enable to enhance the conductivity nature.

As described in Eq. 2, the computation of C_p values requires the knowledge of sample densities. For epoxy resin and rubber blends, the density of the blends remained almost the same (Thomas et al. 2010). The specific heat values from Eq. 2 and the specific heat measured using DSC for epoxy and CTBN (and HTPB) blends had a good agreement at lower concentration of both liquid rubbers, while a slight deviation is observed at higher concentration. Therefore, the two methods can get the C_p of both the liquid rubber (CTBN and HTPB)-modified epoxies (Figs. 12 and 13). The C_p of epoxy and CTBN (and HTPB) blends remained almost the same as a function of the volume fraction of CTBN and HTPB.

For the CTBN- and HTPB-modified epoxy resin, the thermal conductivity properties are affected by the polar nature of rubber. The more conductive rubber and the conductive rubber forming a continuous phase could enhance the thermal conductivity property of the blends. However, the C_p of CTBN- or HTPB-modified epoxy resin is not only affected by the polar nature of rubber but also the density of the formed blends.

Linear Thermal Expansion Behavior of Epoxy/Rubber Blends

The coefficient of linear thermal expansion (CTE) is a material property that is indicative of the extent to which a material expands upon heating. For epoxy resin,

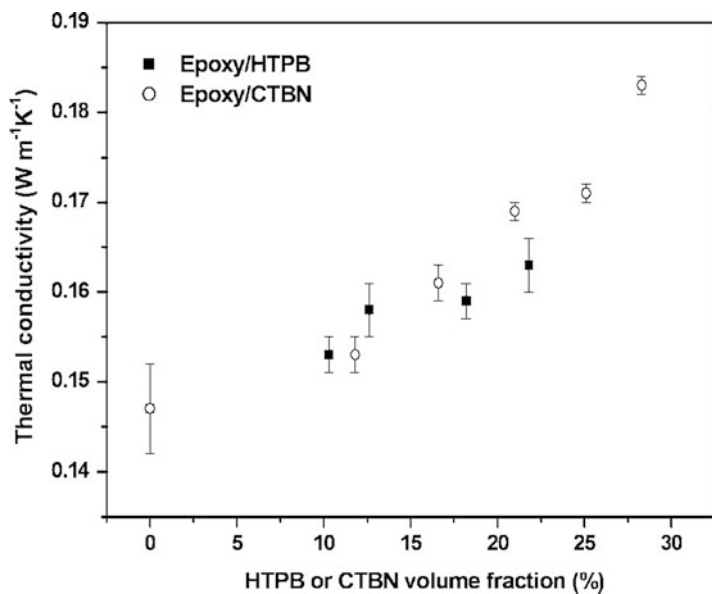


Fig. 11 Thermal conductivity of blends as a function of CTBN and HTPB volume fraction (Thomas et al. 2010)

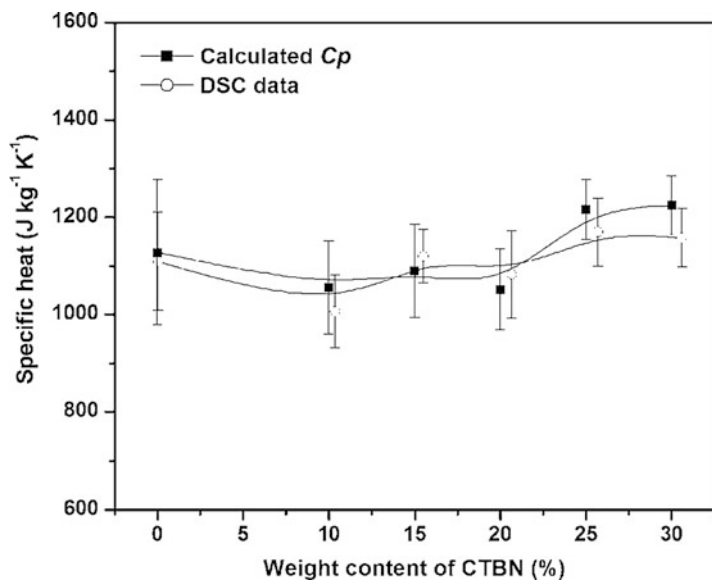


Fig. 12 Specific heat capacity of blends as a function of weight content of CTBN (Thomas et al. 2010)

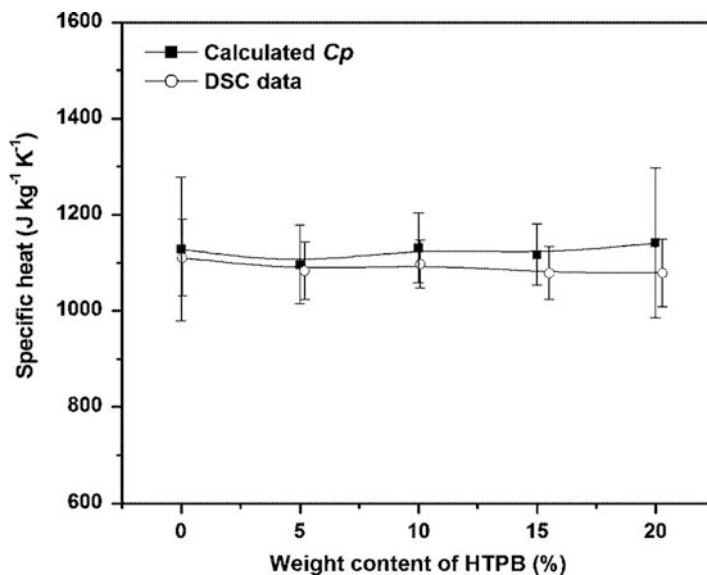


Fig. 13 Specific heat capacity versus weight content of HTPB (Thomas et al. 2010)

epoxy shrinkage may lead to the generation of excess internal stress while cooling during the processing cycle (Wang and Gillham 1993; Chen and Li 2001). This internal stress reduces adhesive strength and may even cause cracks in the casting material. The research to reduce this effect is needed for the application of epoxy composites.

Thermal expansion behavior of strained and unstrained epoxy networks based on diglycidyl ether of bisphenol A cured with diamino diphenyl sulfone and modified with poly(acrylonitrile-butadiene-styrene) (ABS) were studied by Jyotishkumar et al. (2011). In the thermal expansion study (Fig. 14), with an increase in sample temperature, the change in dimension also increases above the T_g of the ABS; the change in dimension increases quickly. TMA runs on strained samples show “bumps” in the TMA scans, which can be explained by the release of excess internal stress when approaching the glass transition during the TMA (heating) run. The presence of internal stress affects the dimensional stability of the blends at high temperatures (above the ABS T_g). The internal stress can be removed by two-step curing.

Li et al. (1997) investigated thermal expansion behavior of blends of epoxy resin with two kinds of polysiloxane with low molecular weight, ATPS (aminopropyl-dimethyl-terminated polysiloxane) and PTPS (phenyl-terminated polysiloxane). For the quenched blends of epoxy resin with polysiloxane rubber, the linear dimension drop Δl decreases with the addition of polysiloxane (Table 3). Especially, it decreases much more with the ATPS content. So this indicates that the introduction of polysiloxane, particularly a reactive one such as ATPS, improves the

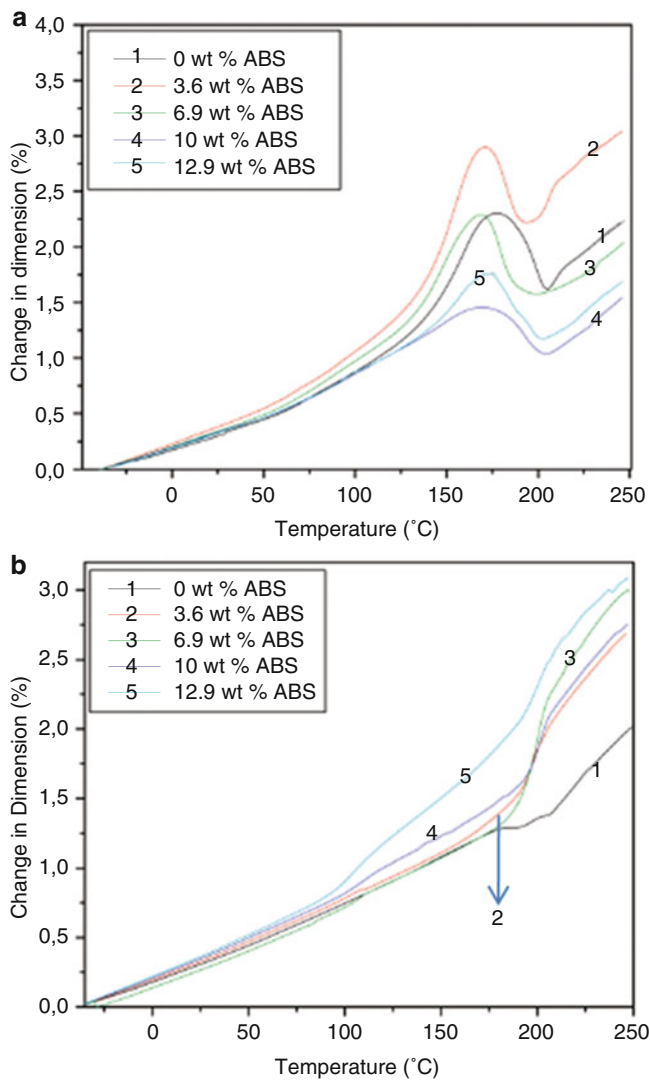


Fig. 14 TMA profiles for different cross-linked DGEBA/ABS blends; (a) cured and annealed in one step; (b) cured and annealed in two steps (Reprinted with permission from (Jyotishkumar et al. 2011). Copyright (2011) American Chemical Society)

Table 3 Thermal expansion behavior of quenched samples and strained samples (Li et al. 1997)

	EP 100%	EP/PTPS(90/10)	EP/PTPS/ATPS(90/5/5)	EP/ATPS(90/10)
Δl (μm) ^a	17.6	10.5	8.8	3.0
Quenched				
Strained	5.8	5.0	4.5	3.4

^aLinear dimension drop per millimeter height

capability of chain motion and leads to less frozen-in free volume. Therefore, the sample can be in a state closer to the equilibrium state. For the strained sample, the linear dimension drop Δl with different polysiloxane modifiers is similar with that of the quenched samples. From the research, the addition of polysiloxane rubber can decrease the thermal expansion of the blends. The thermal expansion behaviors are not only related to thermal and mechanical history but are also dependent on the network of modified epoxy resin.

Thermal Stability

Thermal stability can be said as the thermal protection of polymeric materials which lead to deterioration of properties. Thermal degradation of polymers typically begins around 100 °C (Pandey et al. 2005), and the rate of degradation increases as the temperature increases. Degradation generally shows a somewhat smooth downward slope when weight retention is plotted as a function of temperature after inception of degradation. The study of thermal stability of epoxy/rubber blends is an extremely important area from the scientific and industrial point of view which ensures them to be used in high-temperature applications.

Thermal Stability of Epoxy/Natural Rubber

Chuayjuljit et al. (2006) investigated the thermal stability of epoxy resin blended with natural rubber (NR) and epoxidized natural rubbers (ENRs) contained epoxide groups 25, 40, 50, 60, 70, and 80 mol%. The amounts of ENRs in the blends were 2, 5, 7, and 10 parts per hundred (phr) of epoxy resin. The onset of the decomposition of the blended resins was measured by TGA under nitrogen atmosphere (Table 4). The onset of the decomposition of the blended resins was unchanged compared with that of epoxy resin.

Mathew et al. (2014) prepared an ENR with epoxy value 16.23 mg/g (mg of KOH/g of rubber). Thermal stability of ENR and blends of ENRs with epoxy were studied by TGA in an N₂ atmosphere. The results showed that there were two stages of degradation for ENR: the first stage was between 220 °C and 350 °C, and the second stage was between 500 °C and 630 °C. The temperature of maximum degradation (T_{max} was taken as the maximum in the derivative thermogravimetry (DTG) curve) of the first stage occurred at 420 °C, and that of the second stage was 578 °C. As the actual decomposition began at elevated temperatures, the weight loss occurred at a faster rate. The main degradation step corresponded to the breaking down of the polymer chains into volatile fragments. For the TGA of neat epoxy and ENR/epoxy blends, a single-stage thermal decomposition was evident in the TGA. The average weight loss of around 1–2% up to 250 °C was due to the release of moisture. On the other hand, the weight loss before 300 °C was related to the decomposition of the polymer. The anhydride-cured epoxy exhibited a T_{max} around 419 °C and varied in the range of 416–419 °C in the case of the DGEBA/ENR blends with around a 50% mass loss. Beyond the main degradation stage, all of the volatile materials were driven off from the sample, and this resulted in the residual char. The

Table 4 Onset thermal decomposition temperature (Chuayjuljit et al. 2006)

	Onset thermal decomposition temperature (°C)				
	0 phr	2 phr	5 phr	7 phr	10 phr
Epoxy resin	353.0				
Epoxy/NR		353.0	355.0	353.6	354.4
Epoxy/ENR25		351.3	353.3	354.3	360.7
Epoxy/ENR40		353.9	351.4	352.9	351.5
Epoxy/ENR50		350.7	351.4	353.0	363.8
Epoxy/ENR60		353.6	352.8	355.4	353.3
Epoxy/ENR70		353.2	353.6	359.4	356.2
Epoxy/ENR80		352.2	353.8	355.3	355.4

residual percentage of the blends was not as good as that of the neat epoxy because of the presence of the less thermally stable rubber phase.

Thermal Stability of Epoxy/Polybutadiene Rubber Blends

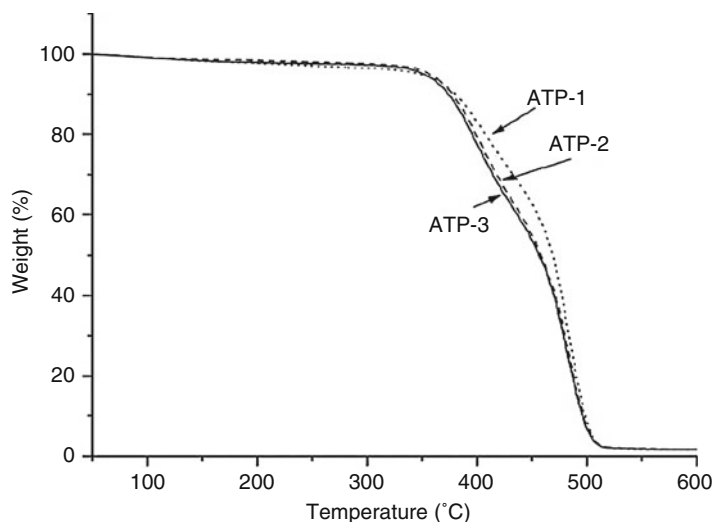
Zhang et al. (2010) investigated thermal stability of liquid amine-terminated polybutadiene (ATPB, an amine value of 62) modified with different amounts of epoxy resin (ATP-1: 17%, ATP-2 and ATP-3: 30%) based on DGEBA and varying hardners by TGA in N₂ atmosphere. Three-step degradation was observed in all of the thermogravimetric curves of the three ATPB-based elastomers. The elastomers were stable up to 340 °C and remained almost intact in the first step. The quantity of gaseous components, mainly water and trapped solvent, released in this step was relatively small. In the first step, the weight loss was less than 3%. The decomposition of step two corresponded to the amine-epoxy bond breaking, and step three was the polybutadiene decomposition. Almost complete decomposition was observed at about 500 °C. For the elastomers based on polybutadiene and epoxy resin, they exhibited a much better thermal stability with a 5% weight loss at a temperature of around 350 °C (Table 5). The derivative weight curves shown in Fig. 15 in TGA of the blends showed two main peaks in the temperature ranges of 350–430 and 430–500 °C in all curves which corresponded to the second- and third-stage decomposition of the elastomer in the TGA curves. A bigger exothermic peak existed in ATP-2 and ATP-3 curve, which validated that conclusion that the decomposition of the amine-epoxy bond occurred between 350 °C and 430 °C, and step three was the polybutadiene decomposition.

Thermal Stability of Epoxy/Nitrile Rubber Blends

Thermal stability of liquid CTBN rubber-modified epoxy resin blends was carried out by TGA. In the research of Tripathi and Srivastava (2009), the data on $T_{initial}$, peak derivative temperature (T_{max}), T_{final} , the temperature at which the material degraded 50% ($T_{1/2}$) as well as char yield at 600 °C (which compared the relative thermal stability of the cured blend samples) derived from different ratios of CTBN-modified epoxy resin (EP 100% denoted as EP₀₁₀₀, EP 95% denoted as EP₀₁₀₅, EP 90% denoted as EP₀₁₁₀, and EP 85% denoted as EP₀₁₁₅) traces are given in Table 6. The clear-cut single-step mass loss in TGA trace of unmodified and CTBN-modified systems and the shoulders observed in derivative thermogravimetry (DTG) traces of

Table 5 Weight-loss data of the ATPB-based elastomers (Zhang et al. 2010)

Specimen	ATP-1	ATP-2	ATP-3
Temperature at 5% weight loss (°C)	348	351	356
Temperature at 10% weight loss (°C)	380	373	377
Temperature at 20% weight loss (°C)	407	395	398

**Fig. 15** TGA curves of the ATPB-based elastomers (Zhang et al. 2010)**Table 6** Data obtained from TGA traces of prepared blends (Tripathi and Srivastava 2009)

SL no.	Sample code	$T_{initial}$ (°C)	T_{max} (°C)	T_{final} (°C)	$T_{1/2}$ (°C)	Mass loss (%)	Char yield (%)
1.	EP ₀₁₀₀	290	370	420	400	80.2	19.8
2.	EP ₀₁₀₅	347	405	516	412	78.3	21.7
3.	EP ₀₁₁₀	350	406	535	418	74.6	25.4
4.	EP ₀₁₁₅	356	417	481	420	86.4	13.6

these blend samples indicated a single-step decomposition behavior (Fig. 16). With the initial addition of 5 wt% CTBN in EP, the blend showed an abrupt increase in $T_{initial}$. The addition of increased rubber content, i.e., up to 15 wt% in unmodified blends, showed the enhancement in the thermal stability of the blends. The increase in thermal stability of the blend systems with increasing rubber content might be attributed to the fact that the rubber started functioning as a thermal stabilizer with increasing temperature and resulted in an increase in the thermal stability of EP-CTBN blends (Tripathi and Srivastava 2009).

Also, in the study of Nigam et al. (2001), the addition of the liquid rubber with higher thermal stability increased the thermal stability of blends compared to neat resin. The

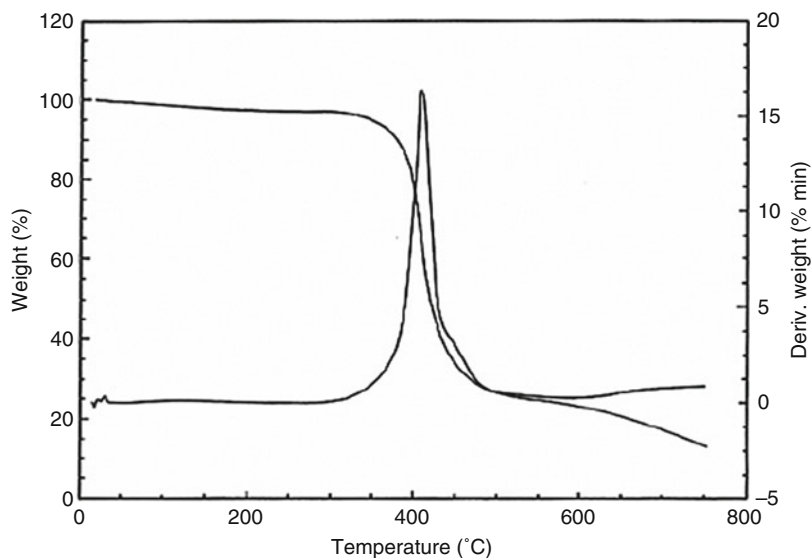


Fig. 16 TGA scan of blend sample, EP₀₁₁₀ (Tripathi and Srivastava 2009)

thermal stability of epoxy resin can be enhanced by increasing rubber concentration in the blends which also proved by Chen et al. (2011a) and Vijayan et al. (2013).

A study about the effect of NBR (Nitrile-Butadiene Rubber, in powdered form) concentration on the thermal behavior of epoxy resin is conducted by Dehaghi et al. (2013). The NBR is solved in an aromatic hydrocarbon solvent and is added to epoxy resin. The epoxy/rubber blends containing various amounts of rubber concentrations (0 phr, 5 phr, and 10 phr) were prepared. Under nitrogen atmosphere, TGA and DTG curves of composites showed a decrease in initial decomposition temperature of epoxy networks followed by incorporation of rubber into the resin system (Fig. 17). The composites exhibited substantial decrease especially in initial decomposition temperature and the maximum decomposition temperature, and only a slight increase in the final decomposition temperature was recorded followed by rubber incorporation to the system. T_{final} (the temperature at final mass loss) of higher value is probably due to the decomposition of the physically cross-linking moiety of elastomer particles with epoxy resin matrix (Table 7). The temperature at which 50 wt% mass loss occurred ($T_{1/2}$) for the samples containing 5 and 10 wt% of rubber content was also lower than that of the corresponding unmodified epoxy resin. It suggests that the presence of rubber could result in lower thermal stability than neat epoxy material in spite of more toughening behavior observation.

Thermal Stability of Epoxy/Polyurethane Rubber Blends

Wang et al. (2011) studied thermal degradation properties of a linear PU based on poly(tetramethylene glycol) (PTMG), PU 30%-PU/EP IPN, PU 50%-PU/EP IPN, and EP by TGA (Fig. 18). It can be seen that the thermal stability of PU/EP IPN was

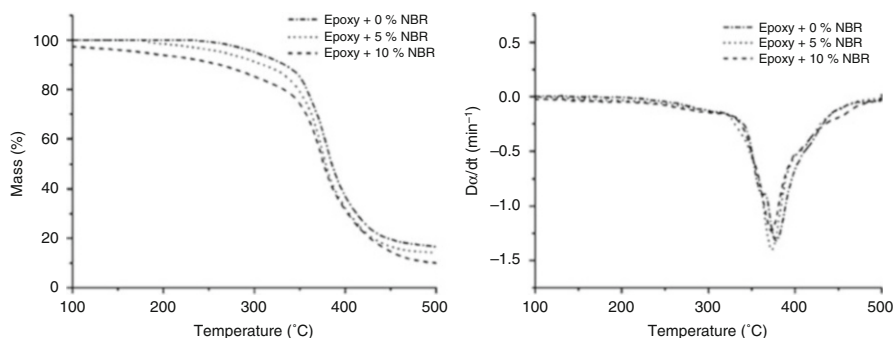


Fig. 17 Mass% (TGA) and DTG curves versus temperature for neat epoxy and compounds at the rate of $20\text{ }^{\circ}\text{C min}^{-1}$ (Dehaghi et al. 2013)

Table 7 Thermal properties of modified and unmodified epoxy resins obtained from TGA and DTG curves (Dehaghi et al. 2013)

Sample/phr	$T_{initial}/^{\circ}\text{C}$	$T_{1/2}/^{\circ}\text{C}$	$T_{max}/^{\circ}\text{C}$	$T_{final}/^{\circ}\text{C}$
0	185	370	385	480
5	175	360	377	490
10	170	350	370	498

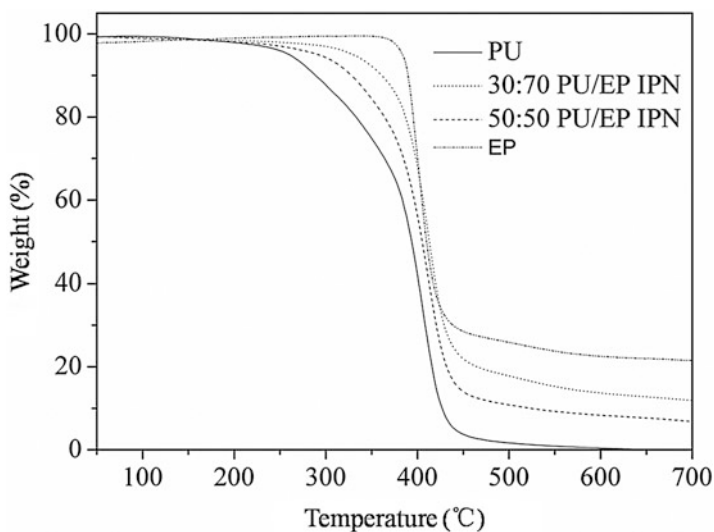


Fig. 18 TGA thermograms of pure PU based on PTMG, 30:70 PU/EP IPN, 50:50 PU/EP IPN ($R = 2$), and EP (derived from Wang et al. 2011)

much higher than that of pure PU, which can be ascribed to the good thermal stability of epoxy resin and the formation of PU/EP IPNs (the polyurethane prepolymer grafting into the -OH group of epoxy formed the graft IPN) (Raymond and Bui 1998; Chiou et al. 2006). However, the thermal stability of PU/EP composites is lower than cross-linked pure EP.

Gui et al. (2014) investigated the thermal stability of a liquid crystalline polyurethane-imide (PUI, synthesized from polyethyleneglycol, toluene diisocyanate, and pyromellitic dianhydride)-modified EP. The result suggests that the thermal decomposition temperature of PUI/EP-cured samples with different content of PUI has no obvious decline compared to epoxy resin. It can be contributed to imide bond in PUI, which is difficult to decompose at high temperature (Jiang et al. 2001) because of good heat resistance of PUI although the addition of PUI in epoxy leads to the decrease of cross-linking density of the composites.

Tang et al. (2014) used a hyperbranched polyurethane (HBPU) as modifier of EP and studied their thermal stability. The DTG (Fig. 19) curves for all thermosets investigated were single peak, indicating that a homogenous structure of the matrix was formed without apparent differences in thermal stability. The peak observed in DTG curves corresponds to the degradation of the thermosets, and it remains similar for all the samples. The initial decomposition temperature decreased with increasing the content of HBPU. However, the decrease was not significant because the interpenetrating networks formed in EP/HBPU blends. The interpenetrating networks increased the cross-linking density which can make the thermal stability higher than HBPU itself.

Thermal Stability of Epoxy and Silicon Rubber Blends

Ma et al. (2010) also investigated thermal stability increase of DGEBA epoxy resin modified with 1 to 7 phr of the high dendritic polysiloxane (DPSO100) by TGA in air and nitrogen atmosphere. The initial degradation temperature for 5% weight loss (T_d 5%), the temperature for 50% weight loss (T_d 50%), and the residual weight percent at 800 °C (R800) under nitrogen atmosphere increase with the increase of the DPSO100 content in epoxy resin which is shown in Table 8. And in air, the values of the T_d 5% and T_d 50% and R800 for the modified system are much higher than the neat epoxy resin. These indicate that the thermal stability improves as siloxane components are incorporated into the cured networks (Hou et al. 2000). This increasing thermal stability may be due to the high thermal stability of the silicon compound and the protecting effect of the silica layer formed during the decomposition process, where silica greatly restrained the oxidation weight loss of the polymeric materials, and resulted in high residual weight for the polymers at 800 °C (Ahmad et al. 2006). Nevertheless, the decomposition behavior of cured samples in air (Figs. 20 and 21) follows the two-step decomposition mechanism, which is different from that in N₂, and the T_d 5% and T_d 50% of epoxy resin do not increase exactly upon the addition of increasing amounts of DPSO100, which may be due to the complex decomposition behavior of cured samples under air atmosphere.

Moreover, Chen et al. (2011b) used a hydroxyl-terminated polydimethylsiloxane (HTPDMS) blended with PU and EP. The thermal stability from TGA showed that

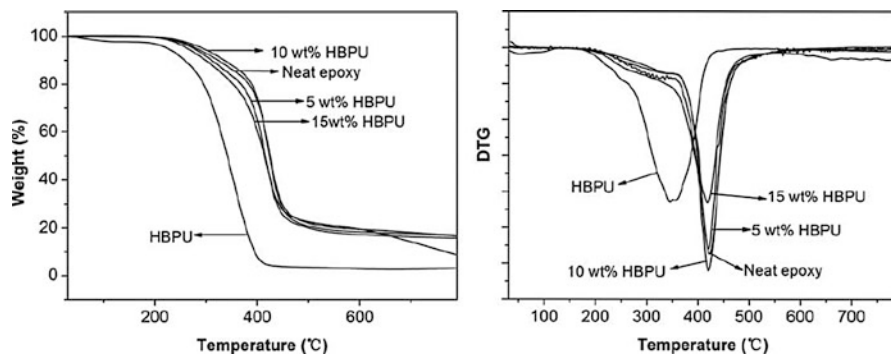


Fig. 19 TGA and DTG curves of the neat epoxy, HBPU, and HBPU/epoxy thermostets with different HBPU contents (Tang et al. 2014)

Table 8 Degradation behavior data of the cured epoxy resins containing DPSO at various ratios (Ma et al. 2010)

Sample	Under nitrogen			Under air		
	T_d 5%/°C	T_d 50%/°C	R800/%	T_d 5%/°C	T_d 50%/°C	R800/%
Neat epoxy	389.06	429.86	18.308	341.95	447.10	0.012
DPSO100-1	390.45	431.50	19.048	393.93	440.19	0.245
DPSO100-3	391.65	434.62	20.751	378.18	448.52	1.086
DPSO100-5	395.50	438.42	22.758	380.39	462.10	1.719
DPSO100-7	395.45	447.90	23.736	355.61	485.48	1.908

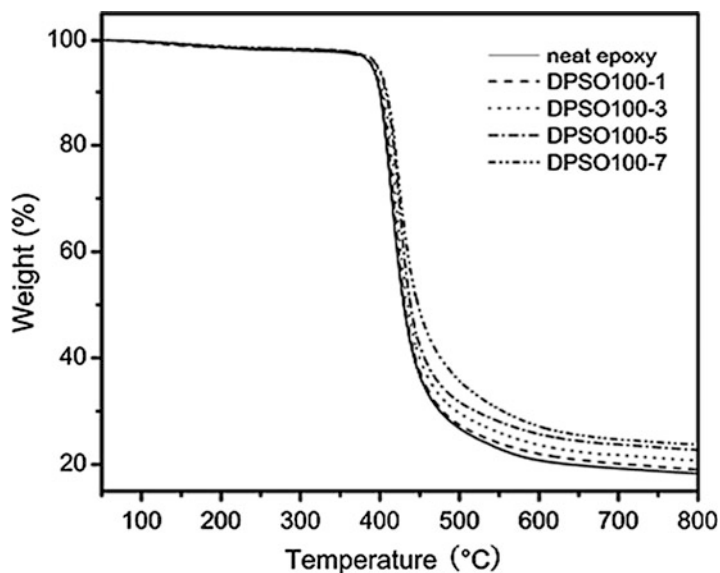


Fig. 20 TGA curves of DPSO-modified epoxy resins in N_2 (Ma et al. 2010)

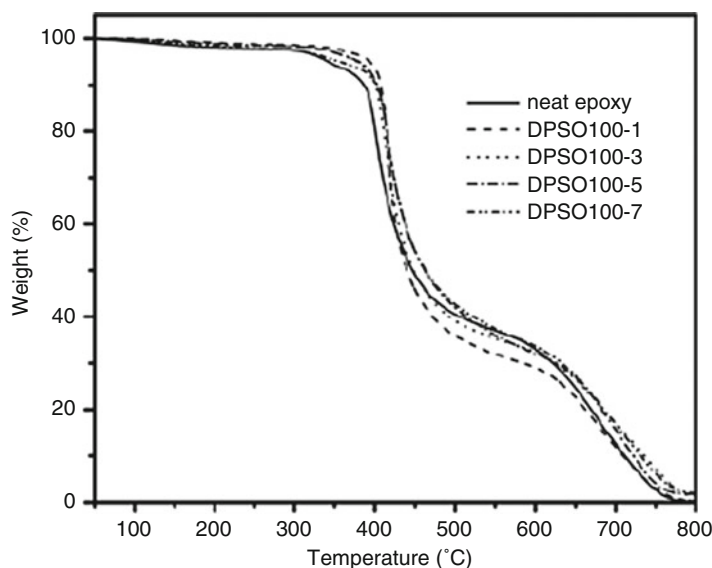


Fig. 21 TGA curves of DPSO-modified epoxy resins in air (Ma et al. 2010)

their thermal stability was further improved by the addition of HTPDMS into the composites, and the higher the HTPDMS content, the larger the thermal stability improvement. As the energy of the siloxane bond is significantly greater than those of C-C and C-O bonds (Kumar and Narayanan 2002), the inorganic nature of -Si-O-Si- structure in HTPDMS might prevent the composites from decomposition under heating process. Thus, the thermal stability was improved.

Brief Summary

The thermal stability of epoxy/rubber blends is mainly depending on the thermal stability of the rubber and the cross-linking density of the formed networks. The good heat resistance of rubbers plays a decisive role of thermal stability in the epoxy/rubber blends. And the cross-linking density formed between epoxy resin and rubber also impacts the thermal stability in the epoxy/rubber blends.

Conclusions

Thermal properties of epoxy/rubber blends including glass transition, thermal conductivity, heat capacity, thermal expansion, and thermal stability are systematically reviewed.

Generally speaking, addition of a rubber component to the epoxy resin will result in depression of T_g due to incomplete phase separation and incomplete curing reaction. When the rubber is added into epoxy resin, it may act as a plasticizer facilitating segmental movements and lowering of cross-linking density of the

networks. Addition of the rubber lowered the T_g of the epoxy and rubber network, and T_g decreases as the content of rubber increases. However, in some special conditions, addition of some rubber into epoxy resin could increase the value of T_g , because the reaction between resins may elevate the cross-linking density. Further, the rubber-modified epoxy resin showed one T_g or two T_g depending on the compatibility between the specific rubber and epoxy resins.

For the CTBN- and HTPB-modified epoxy resin in this chapter, the thermal conductivity properties are affected by the polar nature of rubber. More conductive rubber and conductive rubber forming a continuous phase could enhance the thermal conductivity property of the blends. However, the C_p of CTBN- or HTPB-modified epoxy resin is not only affected by the polar nature of rubber but also the density of the formed blends.

For the thermal expansion behaviors, they are not only related to thermal and mechanical history but are also dependent on the network of modified epoxy resin.

The thermal stability of epoxy/rubber blends is mainly depending on the thermal stability of the rubber and the cross-linking density of the formed networks. For most of the rubbers, the good heat resistance of themselves plays a decisive role. The higher-heat-resistant rubber leads to higher thermal stability of epoxy/rubber blends.

References

- Ahmad S, Ashraf SM, Sharmin E, Mohomad A, Alam M (2006) Synthesis, formulation, and characterization of siloxane-modified epoxy-based anticorrosive paints. *J Appl Polym Sci* 100:4981–4991
- Bakar M, Duk R, Przybyłek M, Kostrzewa M (2009) Mechanical and thermal properties of epoxy resin modified with polyurethane. *J Reinf Plast Compos* 28:2107–2118
- Bernhard W (1990) *Thermal analysis*. Academic, San Diego
- Boudenne A, Ibos L, Candau Y (2006) Analysis of uncertainties in thermophysical parameters of materials obtained from a periodic method. *Meas Sci Technol* 17:1870–1876
- Bussi P, Ishida H (1994) Partially miscible blends of epoxy-resin and epoxidized rubber-structural characterization of the epoxidized rubber and mechanical-properties of the blends. *J Appl Polym Sci* 53:441–454
- Chen X, Li S (2001) Further study of sub- T_g heat flow transition of a cured epoxy resin. *Macromol Rapid Commun* 22:349–352
- Chen S, Wang Q, Pei X, Wang T (2010) Dynamic mechanical properties of castor oil-based polyurethane/epoxy graft interpenetrating polymer network composites. *J Appl Polym Sci* 118:1144–1151
- Chen WS, Chang YL, Hsiang HI, Hsu FC, Shen YH, Yen FS (2011a) Mechanical and dielectric properties of NiZn ferrite powders-CTBN modified epoxy resin coatings. *Polym Plast Technol Eng* 50:568–572
- Chen S, Wang Q, Wang T (2011b) Physical properties of a high molecular weight hydroxyl-terminated polydimethylsiloxane modified castor oil based polyurethane/epoxy interpenetrating polymer network composites. *Appl Phys A: Mater Sci Process* 103:1047–1052
- Chiou WC, Yang DY, Han JL, Lee SN (2006) Synthesis and characterization of composites of polyaniline and polyurethane-modified epoxy. *Polym Int* 55:1222–1229
- Chauyuljit S, Soatthyanon N, Potiyaraj P (2006) Polymer blends of epoxy resin and epoxidized natural rubber. *J Appl Polym Sci* 102:452–459

- Dehaghi HAA, Mazinani S, Zaarei D, Kalae M, Jabari H, Sedaghat N (2013) Thermal and morphological characteristics of solution blended epoxy/NBR compound. *J Therm Anal Calorim* 114:185–194
- Edith T (1996) *Thermal characterization of polymeric materials*, 2nd edn. Wiley, New York
- Gordon M, Taylor JS (1952) Ideal copolymers and the 2nd-order transitions of synthetic rubbers. 1. Noncryst copolymer 2:493–500
- Gui D, Gao X, Hao J, Liu J (2014) Preparation and characterization of liquid crystalline polyurethane-imide modified epoxy resin composites. *Polym Eng Sci* 54:1704–1711
- Hong SG, Chan CK, Chuang CC, Keong CW, Hsueh YP (2005) The curing behavior and adhesion strength of the epoxidized natural rubber modified epoxy/dicyandiamide system. *J Polym Res* 12:295–303
- Hou SS, Chung YP, Chan CK, Kuo PL (2000) Function and performance of silicone copolymer Part IV Curing behavior and characterization of epoxy-siloxane copolymers blended with diglycidyl ether of bisphenol-A. *Polymer* 41:3263–3272
- Jia Q, Zheng M, Chen H, Shen R (2006) Morphologies and properties of polyurethane/epoxy resin interpenetrating network nanocomposites modified with organoclay. *Mater Lett* 60:1306–1309
- Jiang BB, Hao JJ, Wang WY, Jiang LX, Cai XX (2001) Synthesis and thermal properties of poly (urethane-imide). *J Appl Polym Sci* 81:773–781
- Jin H, Zhang Y, Wang C, Sun Y, Yuan Z, Pan Y, Xie H, Cheng R (2014) Thermal, mechanical, and morphological properties of soybean oil-based polyurethane/epoxy resin interpenetrating polymer networks (IPNs). *J Therm Anal Calorim* 117:773–781
- Jyotishkumar P, Pionteck J, Hassler R, George SM, Cvelbar U, Thomas S (2011) Studies on stress relaxation and thermomechanical properties of poly(acrylonitrile-butadiene-styrene) modified epoxy-amine systems. *Ind Eng Chem Res* 50:4432–4440
- Kothandaraman B, Kulshreshtha AK (2003) *Handbook of polymer blends and composites*. In: Vasile C, Kulshreshtha AK (eds) *Rubber toughened epoxies/thermosets*, 1st edn. Rapra Technology Limited, Shrewsbury, pp 441–459
- Kumar KD, Kothandaraman B (2008) Modification of (DGEBA) epoxy resin with maleated depolymerised natural rubber. *Express Polym Lett* 2:302–311
- Kumar SA, Narayanan T (2002) Thermal properties of siliconized epoxy interpenetrating coatings. *Prog Org Coat* 45:323–330
- Li S, Shen J, Chen X, Chen R, Luo X (1997) Studies on relaxation and thermal expansion behavior of polysiloxane-modified epoxy resin. *J Macromol Sci, Part B* 36:357–366
- Lin SP, Han JL, Yeh JT, Chang FC, Hsieh KH (2007) Composites of UHMWPE fiber reinforced PU/epoxy grafted interpenetrating polymer networks. *Eur Polym J* 43:996–1008
- Liu W, Ma S, Wang Z, Hu C, Tang C (2010) Morphologies and mechanical and thermal properties of highly epoxidized polysiloxane toughened epoxy resin composites. *Macromol Res* 18:853–861
- Ma S, Liu W, Hu C, Wang Z, Tang C (2010) Toughening of epoxy resin system using a novel dendritic polysiloxane. *Macromol Res* 18:392–398
- Mathew VS, George SC, Parameswaranpillai J, Thomas S (2014) Epoxidized natural rubber/epoxy blends: phase morphology and thermomechanical properties. *J Appl Polym Sci* 131. doi:10.1002/APP.39906
- Morton M (1981) History of synthetic rubber. *J Macromol Sci-Chem* 15:1289–1302
- Nigam V, Setua DK, Mathur GN (2001) Characterization of rubber epoxy blends by thermal analysis. *J Therm Anal Calorim* 6:521–527
- Ozturk A, Kaynak C, Tincer T (2001) Effects of liquid rubber modification on the behaviour of epoxy resin. *Eur Polym J* 37:2353–2363
- Pandey JK, Reddy KR, Kumar AP, Singh RP (2005) An overview on the degradability of polymer nanocomposites. *Polym Degrad Stab* 88:234–250
- Petri EM (2005) *Epoxy adhesive formulations*. McGRAW-HILL, New York

- Ratna D, Simon GP (2001) Mechanical characterization and morphology of carboxyl randomized poly(2-ethyl hexyl acrylate) liquid rubber toughened epoxy resins. *Polymer* 42:7739–7747
- Raymond MP, Bui VT (1998) Epoxy/castor oil graft interpenetrating polymer networks. *J Appl Polym Sci* 70:1649–1659
- Raymond S, Charles C (1984) *Structure–property relationships in polymers*. Springer, New York
- Smith CG, Smith PB, Pasztor AJ, McKelvy ML, Meunier DM, Froelicher SW, Ellaboudy ES (1993) Analysis of synthetic polymers and rubbers. *Anal Chem* 65:217–243
- Tang LC, Wang X, Wan YJ, Wu LB, Jiang JX, Lai GQ (2013) Mechanical properties and fracture behaviors of epoxy composites with multi-scale rubber particles. *Mater Chem Phys* 141:333–342
- Tang B, Liu X, Zhao X, Zhang J (2014) Highly efficient in situ toughening of epoxy thermosets with reactive hyperbranched polyurethane. *J Appl Polym Sci* 131. doi:10.1002/APP.40614
- Thomas R, Abraham J, Thomas S, Thomas S (2004) Influence of carboxyl-terminated (butadiene-co-acrylonitrile) loading on the mechanical and thermal properties of cured epoxy blends. *J Polym Sci Part B-Polym Phys* 42:2531–2544
- Thomas R, Durix S, Sinturel C, Omonov T, Goossens S, Groeninckx G, Moldenaers P, Thomas S (2007) Cure kinetics, morphology and miscibility of modified DGEBA-based epoxy resin - Effects of a liquid rubber inclusion. *Polymer* 48:1695–1710
- Thomas R, Yumei D, Yuelong H, Le Y, Moldenaers P, Weimin Y, Czigan T, Thomas S (2008) Miscibility, morphology, thermal, and mechanical properties of a DGEBA based epoxy resin toughened with a liquid rubber. *Polymer* 49:278–294
- Thomas R, Boudenne A, Ibos L, Candau Y, Thomas S (2010) Thermophysical properties of CTBN and HTPB liquid rubber modified epoxy blends. *J Appl Polym Sci* 116:3232–3241
- Tripathi G, Srivastava D (2007) Effect of carboxyl-terminated poly (butadiene-co-acrylonitrile) (CTBN) concentration on thermal and mechanical properties of binary blends of diglycidyl ether of bisphenol-A (DGEBA) epoxy resin. *Mater Sci Eng A-Struct Mater Prop Microstruct Process* 443:262–269
- Tripathi G, Srivastava D (2008) Studies on the physico-mechanical and thermal characteristics of blends of DGEBA epoxy, 3,4 epoxy cyclohexylmethyl, 3', 4'-epoxycyclohexane carboxylate and carboxyl terminated butadiene co-acrylonitrile (CTBN). *Mater Sci Eng A-Struct Mater Prop Microstruct Process* 496:483–493
- Tripathi G, Srivastava D (2009) Studies on blends of cycloaliphatic epoxy resin with varying concentrations of carboxyl terminated butadiene acrylonitrile copolymer I: thermal and morphological properties. *Bull Mater Sci* 32:199–204
- Vijayan PP, Puglia D, Maria HJ, Kenny JM, Thomas S (2013) Clay nanostructure and its localisation in an epoxy/liquid rubber blend. *Rsc Adv* 3:24634–24643
- Wang XR, Gillham JK (1993) Physical aging in the glassy state of a thermosetting system vs extent of cure. *J Appl Polym Sci* 47:447–460
- Wang Q, Chen S, Wang T, Zhang X (2011) Damping, thermal, and mechanical properties of polyurethane based on poly(tetramethylene glycol)/epoxy interpenetrating polymer networks: effects of composition and isocyanate index. *Appl Phys A: Mater Sci Process* 104: 375–382
- Watanabe H (1999) Viscoelasticity and dynamics of entangled polymers. *Prog Polym Sci* 24:1253–1403
- Yang JH (2004) Theory of thermal conductivity. In: Tritt TM (ed) *Thermal conductivity: theory, properties, and applications*, 1st edn. Kluwer Academic, New York, pp 1–17
- Zhang X, Ji S, Quan Y, Chen Q, Chang P (2010) Structure, mechanical properties, and gas permeability of elastomers based on polybutadiene and epoxy resin. *J Appl Polym Sci* 117:2366–2372
- Zheng SX, Wang HQ, Dai QH, Luo XL, Ma DH, Wang K (1995) Morphology and structure of organosilicon polymer-modified epoxy-resins. *Macromol Chem Phys* 196:269–278

Hanieh Kargarzadeh, Ishak Ahmad, and Ibrahim Abdullah

Abstract

Highly cross-linked epoxies that are susceptible to brittle failure can be effectively toughened by blending them with various types of rubber. Initially, a small amount of a miscible liquid rubber is incorporated into the matrix of the curing agent-incorporated epoxy resin, and then the whole mass is subjected to curing. The phase separation depends upon the formulation, processing, and curing conditions. The improvement in fracture toughness occurs due to the dissipation of mechanical energy by cavitation of the rubber particles, followed by shear yielding of the matrix. A few factors such as the size of the rubber particles, curing agent, cross-linking density, etc. play an important role in succeeding or failing to improve the toughness. This chapter provides an overview of the toughening mechanism of rubber-modified epoxies. The effects of a few major factors (i.e., the size of the rubber particles, curing agent, curing time and temperature, etc.) on the mechanical properties of rubber-modified blends were studied. The effect of the varieties of synthetic and natural liquid rubber on the impact, flexural, and tensile properties of the epoxy blend is compared and studied.

Keywords

Carboxyl-terminated poly(butadiene-co-acrylonitrile) (CTBN) • Differential scanning calorimetry (DSC) • Epoxy–liquid rubber blends • Cross-linking density • Curing agent • Curing times and temperatures • Fracture and impact test • Glass transition, matrix and rubbery phase • Interfacial adhesion • Liquid natural rubber, LNR • Liquid epoxidized natural rubber, LENR • Rubber concentration,

H. Kargarzadeh (✉) • I. Ahmad • I. Abdullah

Faculty of Science and Technology, School of Chemical Sciences and Food Technology, Polymer Research Center (PORCE), Universiti Kebangsaan Malaysia (UKM), Bangi, Selangor, Malaysia
e-mail: hanieh.kargar@gmail.com

particles size, and distribution • Tensile properties • Test temperature and rate • Toughening mechanism • Volume fraction

Contents

Introduction	280
Toughening Mechanism of Rubber–Epoxy Blends	282
Factors Affecting the Toughness of Rubber–Epoxy Blends	284
Rubber Concentration, Particles Size, and Distribution	284
Interfacial Adhesion	286
Curing Time and Temperature	286
Test Temperature and Rate	289
Cross-Linking Density	291
Glass Transition of the Matrix and Rubbery Phase	291
Curing Agent	292
Volume Fraction	294
Fracture and Impact Test	294
Synthetic Liquid Rubber-Modified Epoxy	295
Natural Liquid Rubber-Modified Epoxy	301
Tensile Properties	306
Synthetic Liquid Rubber-Modified Epoxy	306
Natural Liquid Rubber-Modified Epoxy	309
Summary	310
References	312

Introduction

Epoxy resins with desirable physical and mechanical properties, thermal stability, chemical resistance, and processability are attractive thermoset components that are widely applied in aerospace applications, electrical and electronic devices, automobiles, ships, and so on. However, their inherent brittleness, low fracture resistance, poor impact strength, and high notch sensitivity limit their application. It is therefore desirable to enhance toughness without adversely affecting the useful properties of the polymer, such as its thermomechanical properties and modulus.

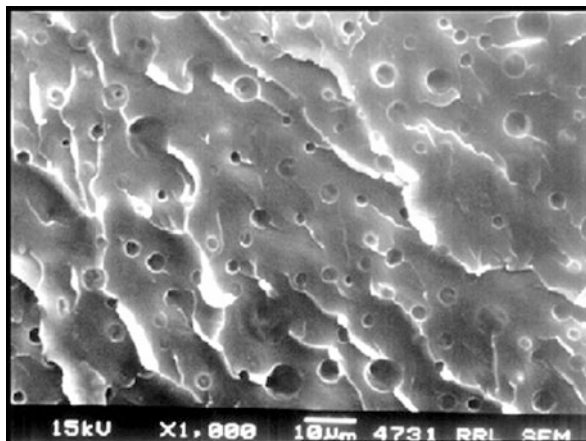
Many methods have been proposed for modifying epoxy resins to improve their toughness: (i) chemical modification of a given rigid thermoset backbone to a more flexible backbone structure or (ii) increasing the thermoset molecular flexibility by lowering the cross-link density of the cured resin via the use of low-functionality curing agents and the incorporation of a dispersed toughening phase (rubbery and/or thermoplastic) in the thermosetting matrix (Kargarzadeh et al. 2014).

Among these approaches, toughening via incorporation of a suitable rubbery phase in the resin has been shown to be the most effective method (Verchere et al. 1990; Sultan and McGarry 1973). The rubbery phase can be added as either core–shell rubber particles or initially miscible reactive rubber particles. Emulsion polymerization is the route taken for the preparation of core–shell rubber particles, which exhibit a rubbery core and an outer shell of glassy polymer. The rubbery core is generally based on polybutadiene. The outer glassy shell prevents coalescence of the rubbery particles during synthesis and

improves the interface with the matrix. The shell is usually based on styrene/acrylonitrile copolymers. However, core-shell toughening does not bring about good dispersion (Kim and Datta 2013). This is why the most widely used method for rubber toughening is the addition of initially miscible rubber particles into the thermosetting matrix. In this method, the rubber is added to the uncured epoxy resin; during the polymerization (curing) reaction, the rubber-modified epoxy exhibits a two-phase microstructure consisting of relatively small rubbery particles dispersed in an epoxy matrix. The multiphase structure of a rubber-modified epoxy is seen clearly in the scanning electron microscopy (SEM) micrograph of the fractured surface of a specimen (Fig. 1).

Studies (Verchere et al. 1990, 1991; Moschiar et al. 1991) have shown that the phase-separation process is a result of the decrease in configurational entropy due to the increase in molecular weight as the epoxy cures. As a consequence, the free energy of mixing changes, leading to a decrease in the solubility of the rubber. This then is the driving force for phase separation. Thus, the functionality of the matrix monomers, which control the development of the network and the cross-link density of the epoxy matrix, has an effect on the phase-separation process. The particle size and concentration of the precipitated rubber also depends on the curing process and the interaction between the rubber and the epoxy resin. These microstructures result in a material possessing higher toughness than the unmodified epoxy, with only a minimal reduction in other important properties such as modulus and glass transition temperature (T_g). For effective toughening, the rubber phase needs to be chemically bonded to the epoxy matrix because a weak interaction between the matrix and the rubber particles may cause debonding of the particles, leading to failure of the toughened system (Thomas et al. 2014). Because the mechanical properties of the epoxy blend are directly affected by the rubber, the mechanical properties of rubber-epoxy blends in synthetic and natural liquid rubber-epoxy systems, particularly the impact, fractural, and tensile properties, will be discussed in this chapter. In addition, the toughening mechanism and some factors affecting the toughening properties of rubber-epoxy blends will be studied.

Fig. 1 SEM micrograph of 10 wt% hydroxylated liquid natural rubber (HLNR)-modified epoxy resin (Reproduced from Mathew et al. (2010), with permission from Springer)



Toughening Mechanism of Rubber–Epoxy Blends

Toughness is the property of resisting fracture by absorbing and dissipating energy during deformation prior to ultimate fracture. Toughness is a very important property in applications where the material encounters a lot of mechanical shock and vibration. Many theories have been proposed to explain the toughening effect of rubber particles on brittle epoxy matrices.

The basic mechanism available for the energy absorption of a rubber-toughened epoxy network under load is rubber cavitation, followed by shear yielding. In rubber-modified plastics under triaxial tensile stress, voids can be initiated inside the rubber particles. Once the rubber particles are cavitated, the hydrostatic tension in the material is relieved, with the stress state in the thin ligaments of the matrix between the voids being converted from a triaxial to a more uniaxial tensile stress state. This new stress state is favorable for the initiation of shear bands. In other words, the role of rubber particles is to cavitate internally, thereby relieving the hydrostatic tension and initiating the ductile shear yielding mechanism (Ratna 2005).

In the mechanism of shear yielding, shear bands or deformation zones are initiated by interaction between the stress field ahead of the crack and the rubber particles, leading to stress concentration in the surrounding matrix. The improvement of toughness is proportional to the number of such particles; a higher number of particles contribute to the creation of more deformation zones before fracture occurs. Small micrometer-size rubber particles are quite effective in promoting extended shear yielding of the brittle epoxy matrix. The matrix undergoes plastic deformation (Kim and Datta 2013). This type of plastic deformation is supported by the fact that at the crack tip – where the hydrostatic tensile component is large and the magnitude of the concentrated hydrostatic stress in the vicinity of the rubber particles is insufficient to promote shear yielding – rubber particles elongate to the same extent as the matrix, as evidenced by microscopic studies, compared with undeformed spherical rubber particles. The internal cavitation of the rubber particles relieves the plain strain constraint by effectively reducing the bulk modulus. The magnitude of the concentrated deviatoric stress is then sufficient for shear yielding. The voids left behind by the cavitated rubber particles act as further stress concentrators (Kim and Datta 2013; Ratna 2005). Figure 2 shows a schematic of the shear yielding mechanism.

It has been reported (Li et al. 1994) that when rubber cavitation is suppressed by superimposed hydrostatic pressure, the fracture toughness of rubber-modified epoxy is no higher than that of the unmodified epoxy. This implies that the stress concentration by rubber particles alone will not necessarily induce massive shear yielding and increase the fracture toughness. Hence, rubber cavitation is very important to the toughening of rubber-modified epoxies (Fig. 3a); without cavitation, these rubber particles will still cause a stress concentration, but they will not be effective in toughening.

In addition to shear yielding, some other toughening mechanisms such as microcracking, crack deflection, crack bifurcation, crack pinning, crack bridging, or multilevel fracture paths (enlargement of fracture surface area) can also be operative (Kargarzadeh et al. 2014).

Fig. 2 Schematic diagram of shear yielding mechanism

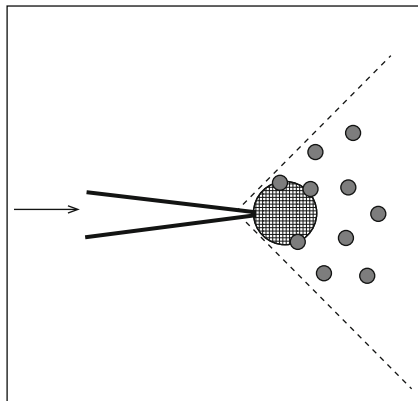
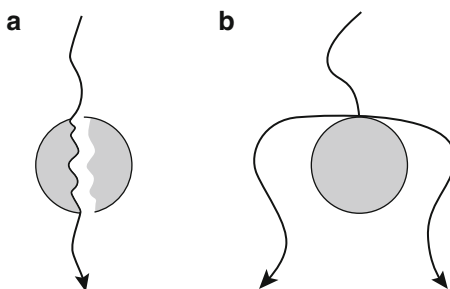


Fig. 3 Different crack paths in (a) cavitation and (b) crack deflection processes

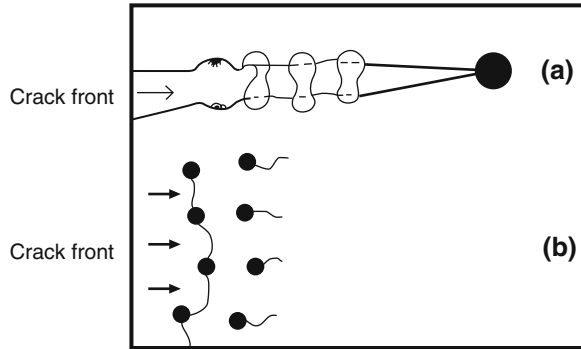


In order to deflect cracks, the rubber phase needs to produce a sufficiently large stress field in front of the growing crack (Fig. 3b). This stress field can alter the crack growth direction, allowing bifurcation and deflection mechanisms to take place in the matrix. Because such a deviation would result in increased surface area and reduce the opening of the crack either way, the energy required to propagate such a crack increases. Rubber particle (or hole) size also plays an important role in deflecting the crack. Larger particles can deflect the crack path more easily than smaller ones (Fig. 3b) (Arends 1996; Pearson and Yee 1993).

Crack bifurcation is a clear-cut and well-defined effect in which the main crack divides or branches, such that a test sample separates into three or more parts. However, the mechanism involved in macroscopic bifurcation closely resembles that which occurs at an earlier stage of fracture; it is thus convenient to use the expression “microbifurcation” for these effects (Hull 1996).

The particle-bridging mechanism is a straightforward phenomenon based on the principle of energy dissipation during stretching and bridging of the crack surfaces by rubber particles (Kunz-Douglass et al. 1980; Pascault 2002). When the crack advances in the rubber-modified epoxy system, it has a tendency to grow preferentially in the more brittle epoxy matrix phase, in effect growing around the rubber particles in the initial stage of crack growth. Subsequent to this, when the crack

Fig. 4 (a) Crack-bridging mechanism by particles behind the crack tip and (b) crack-pinning mechanism



begins to open up, the rubber particles start to span between the two separating crack planes. These rubber particles are extremely ductile, and they strain harden rapidly. As a result, the fracture energy required for crack growth is somewhat increased (Fig. 4a). In other words, the brittle thermoset matrix is toughened. The bridging particles should have the capacity to stretch between the two crack planes, and so they must exhibit ductility. The size of the particle also has to be much larger than that of the crack tip radius for it to function as an effective bridge. Finally, the interfacial adhesion between the particle and the matrix needs to be stronger than the cohesive strength of the particle itself. If all these requirements are satisfied, then the particle-bridging mechanism will be effective (Kim and Datta 2013). However, these mechanisms are less effective than the shear yielding mechanism and are relatively low in energy absorption capacity.

The crack-pinning mechanism, first described by Lange (1970), is very often mentioned with polymers filled with rigid particles, but it can also be considered to play a minor role in the case of soft rubber particles. As shown in Fig. 4b, the propagating crack front is slowed down, and it has to bend when meeting a line of particles. The fracture surface is thereby increased, and the fracture energy is distributed over a wider area. Upon breakaway of the crack front, the separated crack fronts unite again. Because of slight differences in the heights of the single crack fronts, small ridges are often formed behind the particles. These ridges are often referred to as “tails,” which can easily be detected by observation of the crack surface (Pascault 2002).

Factors Affecting the Toughness of Rubber–Epoxy Blends

Rubber Concentration, Particles Size, and Distribution

It has been established that the use of phase-separated, well-dispersed elastomers with a suitable particle size allows the inclusion of a large volume of the matrix in the process of plastic deformation, resulting in the absorption of a significant amount of

energy, and the impact energy of the rubber–epoxy blend increases with increasing rubber content. The enhancement is due to the dissipation of mechanical energy by the rubber particles by various mechanisms, as discussed previously. However, beyond an optimum rubber concentration, the impact energy decreases due to rubber agglomeration and phase inversion. Generally, the optimum rubber concentration is found to be 5–25 wt%.

Rubber particle size is another parameter that influences the fracture toughness of rubber–epoxy blends. The optimum particle size for toughening an epoxy matrix depends on the properties of the epoxy, primarily on its inherent fracture mechanism, but it is commonly within the range of 0.1–5 μm . Large rubber particles over 5 μm are often too large to interact with the stress field at the crack tip, and thus they are only able to act as bridging particles, which provides only a modest increase in fracture energy. On the other hand, rubber particles less than 0.1 μm in size are too small to cavitate effectively and thus do not take part in the toughening process because they need higher stress to cavitate. Without the cavitation of the rubber particles, subsequent matrix shear banding in the presence of a triaxial stress field at the crack tip is very unlikely (Walker and Collyer 1994; Gaymans and Dijkstra 1990; Oshinski et al. 1992, 1996). Immiscibility and phase separation also appear to be very important because rubber dissolved in the matrix acts merely as a plasticizer, which reduces the glass transition temperature and hence seriously affects the stiffness; however, it has only a limited influence on toughness. Moreover, a more homogenous rubber particle distribution provides higher fracture toughness (Kargarzadeh et al. 2015). However, no synergistic effects have been reported for rubber–epoxy blends containing small and large particles (Pearson and Yee 1991).

Thomas et al. (2004) reported toughening an epoxy blend using carboxyl-terminated poly(butadiene-*co*-acrylonitrile) (CTBN). They found that the size of the precipitated rubber particles increased with increasing rubber content. Table 1 represents the average diameters of the precipitated rubber domains, their distribution, and their polydispersity indices (D_w/D_n). Both the number and area average domain diameter were found to increase with increasing amounts of CTBN in the composition as well. The increase in the domain size of the dispersed CTBN phase was associated with the re-agglomeration or coalescence of the dispersed rubber particles, which was more prominent at higher concentrations of the dispersed CTBN phase. They have observed that the mechanical properties like tensile and flexural showed reduction, whereas impact strength and critical stress intensity factor both increased with higher concentration of liquid rubber. However, good results were obtained at a critical concentration of 15 wt%.

Mathew et al. (2010) studied the modification of epoxy using a liquid natural rubber possessing hydroxyl functionality (HLNR). It can be seen from Table 2 that the number, area, volume, and weight average domain diameters of HLNR increased as the amount of rubber increased. The critical rubber particle size that gave the highest toughness was found to be 6 μm , with a rubber composition of 15 wt%.

Table 1 Number, area, weight, and volume average diameters of domains dispersed in an epoxy matrix (Reproduced from Thomas et al. (2004), with permission from Elsevier)

CTBN content (phr)	D_n^a	D_a^b	D_w^c	D_v^d	PDI ^e
5	0.81	0.83	0.87	1.31	1.06
10	0.82	0.87	0.92	1.32	1.11
15	0.86	0.89	0.94	1.33	1.09
20	0.88	0.92	0.97	1.35	1.10
25	1.01	1.07	1.14	1.37	1.12
35	1.02	1.08	1.16	1.46	1.13

^aNumber average domain diameter in μm

^bArea average domain diameter in μm

^cWeight average domain diameter in μm

^dVolume average domain diameter in μm

^ePolydispersity indices

Table 2 Domain sizes of HLNR particles in an epoxy blend (Reproduced from Mathew et al. (2010), with permission from Springer)

HLNR content (wt%)	D_n	D_a	D_w	D_v	PDI
5	1.00	1.08	1.17	1.42	1.15
10	2.77	3.12	3.52	5.05	1.27
15	6.05	7.02	8.14	12.00	1.34
20	9.17	10.93	13.04	16.40	1.42

Interfacial Adhesion

Matrix–rubber particle adhesion is an important parameter for rubber toughening. For effective rubber toughening, the rubber particles must be well bonded to the epoxy matrix. Strong interfacial chemical bonds are usually present, of course, when a reactive rubber is used. Poor intrinsic adhesion across the particle–matrix interface causes premature particle debonding, leading to the catastrophic failure of the materials. Most of the studies reported in the literature have been concerned with reactive group-terminated rubber as a toughening agent for epoxies, which results in dispersed rubbery particles having interfacial chemical bonds as a consequence of chemical reactivity. It has been observed that further increases in the functionality of rubber improved the toughness. The toughening effect decreased beyond the optimum value (2.3–3 eq./mole) of functionality due to the formation of a single-phase morphology (Ratna 2005; Kar and Banthina 2006).

Curing Time and Temperature

Curing times and temperatures are important parameters affecting the phase-separation phenomena of rubber in an epoxy matrix. Generally, the compatibility of rubber and epoxy increases as the temperature increases. As mentioned

previously, the initial miscibility and compatibility of rubber and epoxy helps to create a homogenous distribution of small rubber particles during phase separation and cross-linking, which improve the fracture toughness of the epoxy blend.

Epoxy curing generally shows complex kinetics. Autocatalysis is the reason for the initial fast reaction rate. However, due to the onset of gelation, the reaction rate decreases in the next stage, and cross-linking leads to an increase in the T_g of the curing matrix. If the curing temperature (T_{cure}) is well above T_g , the kinetics of the reaction between the epoxy and the hardener is chemically controlled. The resin passes from a flexible rubbery state to a rigid glassy one when T_g approaches T_{cure} . The reaction rate at this stage decreases, becoming diffusion controlled. Verification is finally achieved and the reaction stops. The curing reaction takes place between the epoxy and the curing agent, and hence the kinetics depends on the nature of the hardener employed. Thus, each system can be considered as a separate entity depending on the type of curative used (Thomas et al. 2007).

Differential scanning calorimetry (DSC) is a widely employed technique for studying the curing of epoxy resins (Roşu et al. 2002; Lee et al. 2000; Sbirrazzuoli et al. 2003). The main advantages of using DSC include its reaction rate method of measurement, in which the rate of reaction and degree of conversion can be estimated with great accuracy. Also, DSC cells may be considered minireactors without a temperature gradient. Investigating kinetics using DSC offers variables such as heat flow and heat generation, which are required for solving heat/mass transfer equations. Because cure polymerization involves many reactions, such as etherification, esterification, homopolymerization, etc., the isothermal mode is more effective than dynamic monitoring for the detailed investigation. Moreover, the method is more informative and leads to better interpretation.

Thomas et al. (2007) investigated the cure kinetics of a DGEBA-based epoxy resin with CTBN using an anhydride as the curing agent. They reported that the addition of CTBN did not change the curing mechanism. However, at a particular cure time and temperature (150 °C), the conversion decreased with increasing rubber content, which is mainly attributed to physical changes such as the dilution effect. The viscosity increased as a result of the liquid rubber addition or the reduction in the density of the reactive groups. It was also reported that upon lowering the temperature, the rate and extent of the reaction decreased. The extent of the reaction decreased after attaining the gelation point due to the phase separation of the rubber from the epoxy matrix. In addition, the rate of curing increased with increasing curing temperature. The reaction rate increased as a function of time at a particular temperature, and it occurred upon reaching a maximum value after the start of the reaction, showing an autocatalytic nature.

It was found that the number, weight, and volume averages of the dispersed domains decreased with increasing temperature. As T_{cure} decreased, the particle size increased. At high temperature, the rate of the epoxy curing reaction was high. The onset of gelation was attained at a shorter time, which resulted in a lower degree of coalescence of particles and ultimately in the phase separation of smaller particles. This phenomenon led to higher fracture resistance of the epoxy blend. However, other factors such as the increase in the viscosity of the system, the difference in the

Table 3 Dispersed particle size and polydispersity of modified epoxies cured at different temperatures (Reproduced from Thomas et al. (2007), with permission from Springer)

CTBN content (phr)	Curing temperature (°C)							
	140				150			
	D_n	D_v	D_w	PDI	D_n	D_v	D_w	PDI
5	0.89	1.31	0.90	1.01	0.81	1.28	0.87	1.06
10	0.86	1.42	0.93	1.08	0.82	1.39	0.92	1.11
15	0.87	1.53	0.97	1.11	0.86	1.46	0.94	1.09
20	0.91	1.65	1.05	1.15	0.88	1.55	0.97	1.10

solubility parameters, and the surface tension of the rubbery phase during the curing process all contributed to the formation of particles. The volume average domain size increased with increasing CTBN content at a particular temperature, as discussed previously (Table 3).

Ben Saleh et al. (2009) studied the effects of CTBN on the reactivity of an epoxy blend system. They also concluded that in the epoxy–CTBN system, the gel time and cure time increase with increasing rubber content. The reason could be due to the fact that CTBN molecules reduce the reaction and movement of reactive molecules, which leads to a delay in the gel time and cure time. The gel and cure temperature values for all of the rubber-modified epoxy samples were higher than those of the unmodified epoxy. Table 4 represents the reactivity values of the epoxy as a function of CTBN content. The optimum rubber concentration for toughening of epoxy was found between 5 and 10 phr with the particle size in the range of 0.64–0.85 μm .

Chikhi et al. (2002) reported that unlike the effect of CTBN on the epoxy resin, amine-terminated butadiene–acrylonitrile (ATBN) reduced all reactivity characteristics of the epoxy resin, such as gel time, temperature, and cure time. They claimed that such behavior can be explained by the fact that during the reaction of ATBN with the epoxy resin, some of the exothermic energy released during epoxy cross-linking might have been consumed by ATBN, resulting in a decrease in gel, temperature, and cure times (as a result of a more rapid reaction). In addition, they have reported that the tensile strength and modulus reduced with increasing ATBN content. However, a threefold increase in Izod impact strength was observed by adding 12.5 phr ATBN compared to the unfilled epoxy.

He et al. (2012) reported that the tensile strength increased while elongation at break decreased with increasing curing time. Table 5 represents the tensile strength and elongation at break values of an ATBN/epoxy blend at different curing times.

Figure 5 shows the tensile properties of an ATBN/epoxy blend cured at room temperature and 150 °C tested at temperatures between –60 °C and 60 °C. The results showed that the tensile strength increased as the testing temperature decreased and that the elongation at break was well maintained until –40 °C. According to the testing results, the elongation at break before and after annealing was maintained at a level above 30% at –40 °C, indicating that the epoxy could be used at temperatures down to –40 °C with excellent toughness (He et al. 2012).

Table 4 The effects of the CTBN content on the reactivity of the epoxy (Ben Saleh et al. 2009)

CTBN content (phr)	Gel time (min)	Gel temp. (°C)	Cure time (min)	Cure temp. (°C)
0	4.0	81	6.0	115
5	4.4	87	7.0	145
10	4.5	92	8.0	142
15	5.1	96	8.0	136
20	6.0	90	9.0	128

Table 5 Tensile properties of ATBN-modified epoxy at different curing times (Reproduced from He et al. (2012), with permission from Elsevier)

Curing time (days)	Tensile strength (MPa)	Breaking elongation (%)
1	5.4 ± 0.4	193 ± 6.0
3	9.4 ± 0.5	138 ± 5.0
5	12.5 ± 0.3	96 ± 5.0
7	13.1 ± 0.2	61 ± 4.0
8	13.7 ± 0.4	53 ± 3.0
15	13.9 ± 0.3	50 ± 5.0

He et al. 2012 concluded that the tested epoxy/ATBN systems exhibited excellent toughness and good mechanical modulus and adhesive strength in the temperature range from $-40\text{ }^{\circ}\text{C}$ to $50\text{ }^{\circ}\text{C}$. The room temperature-cured samples displayed good mechanical modulus at temperatures up to $75\text{ }^{\circ}\text{C}$. However, annealing the sample at $150\text{ }^{\circ}\text{C}$, which is much higher than T_g of the hard domains, significantly degraded these properties between $50\text{ }^{\circ}\text{C}$ and $75\text{ }^{\circ}\text{C}$. The excellent mechanical properties of the RT-cured sample were associated with the phase-separated morphology, where the hard epoxy domains were dispersed in the soft ATBN matrix and acted as cross-linking spots, as well as rigid fillers to enhance the strength. High-level phase separation was observed in the RT-cured sample with a low ATBN content, whereas the sample with a high ATBN content exhibited reduced phase separation. On the other hand, high-temperature ($150\text{ }^{\circ}\text{C}$) annealing of the sample promoted further migration of unreacted epoxy groups into the ATBN matrix to enhance the cross-linking and to increase the mixing of the two components.

Test Temperature and Rate

The test temperature and test rate are two of the factors that affect the mechanical properties of modified thermosets. It has been reported that in the case of uniaxial compressive yield stress of epoxy-modified CTBN, the higher the test temperature, the lower the yield stress, the greater the plastic strain capability of the epoxy, and the easier the generation of plastic deformation. These phenomena are reflected in the increase of the fracture energy with increasing test temperature (Chan et al. 1984).

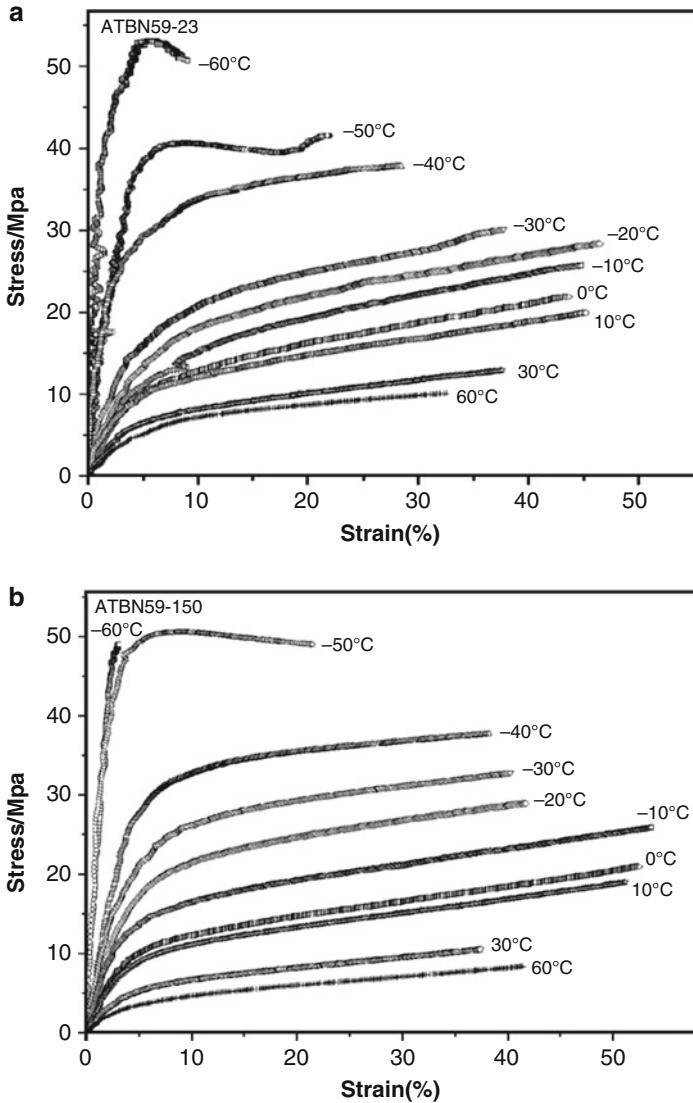


Fig. 5 Stress–strain curves of (a) ATBN59-23 (blend contains 59 wt% ATBN cured at 23 °C) and (b) ATBN59-150 (blend contains 59 wt% ATBN cured at 150 °C) at different temperatures (Reproduced from He et al. (2012), with permission from Elsevier)

Hunston et al. (1984) and Kinloch and Hunston (1987) found that rate and temperature effects were interrelated by constructing a master curve of G_{Ic} versus the reduced time of test, t_f/a_T , below the T_g of the epoxy matrix (t_f is the time to failure and a_T is the time–temperature shift factor). The values of a_T were ascertained experimentally by superimposing yield, stress relaxation, and dynamic mechanical

relaxation data. Thus, the effects of rate and temperature on the value of G_{Ic} may be simply combined, which not only enables objective comparison of different polymers by using an intrinsic reference point, it also permits the value of G_{Ic} to be predicted for any given test rate–temperature combination.

Abadyan et al. (2012) reported that for the epoxy-modified ATBN blend, an increase in the loading rate for the tensile test led to an increase in the modulus and a decrease in the elongation at break. Moreover, the dramatic influence of the loading rate on the fracture strength was observed, whereas the fracture strength did not have significant dependence on the loading rate in the modified blend.

Cross-Linking Density

One of the important behaviors that influence the mechanical properties of thermosets is cross-linking. The molecular weight, M_c , between cross-links in the thermoset matrix is known as the cross-link density. Investigation of a series of epoxy–CTBN polymers with different epoxy equivalent weights cured with the same curing agent showed that an increase in M_c produced a small increase in the fracture energy, G_{Ic} , for the unmodified polymers and a drastic increase in G_{Ic} for the rubber-toughened polymers. These results are ascribed to an increase in the inherent ductility of the matrix as M_c increases. Greater ductility leads to greater plastic energy dissipation and an increase in G_{Ic} . A greater effect is observed for the rubber-toughened polymer because the rubbery particles initiate a larger number of energy-dissipating shear zones (Pearson and Yee 1983).

Finch et al. (1987) confirmed the increase in ductility as M_c increases and the resulting increase in G_{Ic} that may be attained. In their study, the molecular weight was varied between cross-links in the epoxy matrix of an epoxy–CTBN system that was cured with piperidine by changing the cure time and temperature. No significant change in the microstructure of the dispersed rubbery particles in the modified materials by the different curing conditions was found. Plane-strain compression tests on the unmodified polymers clearly revealed that, although the modulus and yield stress were not greatly affected, the maximum plastic strain capability of the matrix dramatically increased as M_c increased.

Glass Transition of the Matrix and Rubbery Phase

The glass transition temperature, T_g , of the matrix phase is obviously affected by M_c . In other words, T_g is a qualitative measure of the cross-link density, i.e., the higher the cross-link density (M_c is reduced), the greater the glass transition temperature (Yee and Pearson 1984). In fact, the fracture toughness of neat epoxies decreases as the cross-link density increases. High cross-link densities have been cited as the reason for the lack of toughness in some elastomer-modified epoxies (sultan et al. 1971).

The value of T_g is influenced by other parameters, such as the degree of interchain attraction. Low interchain attractive forces, which may increase matrix ductility, often lead to low T_g values. Thus, increased ductility and toughness are frequently achieved only at the expense of elevated-temperature properties (Kar and Banthina 2006). As a corollary to this argument, thermosetting polymers that are extremely tightly cross-linked and possess high interchain attractive forces (and hence have high T_g values) are difficult to toughen to a high absolute level (Kinloch 1989).

Thomas et al. (2008) reported that the addition of hydroxyl-terminated polybutadiene (HTBP) in epoxy reduced the cross-linking density and T_g . They claimed that during the curing of the epoxy resin, phase-separated rubber domains occupied the space in between the reaction sites, thereby impairing the cross-linking reaction at those particular sites. Moreover, the molecular weight between cross-links increased with the addition of rubber to the epoxy resin, which decreased the cross-linking. Thus, the overall cross-linking density changed by the incorporation of more rubber. The fracture toughness value for this system was found to increase and attained a maximum for 10 phr rubber inclusion. However, the tensile strength, tensile modulus, and flexural properties decreased by addition of HTBP and reduction of cross-linking density. More details on the calculation of cross-linking density and its effect on the properties of the epoxy blend can be found in Thomas et al. (2008) and Yee and Pearson (1984).

On the other hand, the rubber particles need not be truly rubbery for a modified thermoset to be appreciably tougher than the unmodified materials. It has been reported that modified epoxy is significantly tougher, even when the test temperature is below T_g of the rubbery phase (i.e., below approximately $-55\text{ }^\circ\text{C}$). Nevertheless, the most substantial increases in G_{Ic} are observed at temperatures above T_g of the rubbery phase. Basically, the very low ratio of shear to bulk modulus of rubbery particles (i.e., when $T_{\text{test}} > T_g$ of the rubbery phase) means that the particles cannot only act as very effective stress initiators for shear yielding in the matrix, they can also bear their share of triaxial tensile stress along the crack front. Second, the high shear capability of rubber particles means that they can deform and accommodate the shear strains imposed by the shear bands that they initiate. Third, under certain test conditions, rubber particles may undergo cavitation and relieve the triaxial nature of the stress acting near the crack tip, hence enabling even further shear yielding in the matrix (Kinloch 1989).

Curing Agent

Chemical interactions between the epoxy and rubber particles are very important in terms of improving the mechanical properties of the epoxy. Meeks (1974) reported that the toughness enhancement obtained by elastomeric modification of epoxy resins is dependent on the structure of the curing agent. This dependence may actually reflect varying degrees of cross-link density. The higher the cross-linking density, the lower the toughening properties. Many types of curing agents have been used for curing epoxy such as amines, anhydrides, thiols, etc. Amine-curing agents

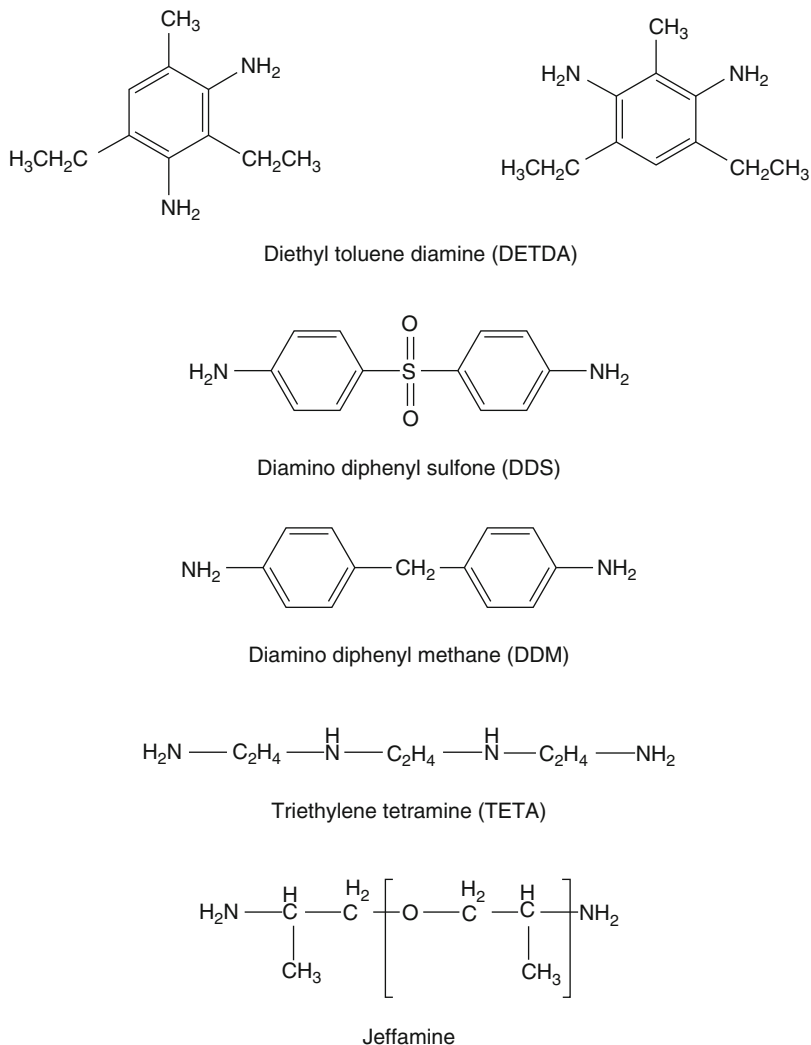


Fig. 6 Chemical structures of commonly used amine-curing agents

are the most widely used because of the better understanding/control of epoxy-amine reactions. Figure 6 presents the chemical structures of some commonly used curing agents.

Arias et al. (2003) modified epoxy with 15 wt% CTBN cured with piperidine and 4,4'-diamino-3,3'-dimethyl-dicyclohexylmethane (3DCM). They found from SEM micrographs that the average size of rubber particles in the epoxy-3DCM was 0.17 μm , which is smaller than the average size of rubber particles for the epoxy-piperidine (0.77 μm). In addition, they reported that epoxy-3DCM exhibited a higher T_g and yield stress than the epoxy-piperidine. The cross-linking density was

also higher, and the molar mass between cross-links was lower in the case of epoxy–piperidine than in the case of epoxy–3DCM. However, the critical stress intensity factor, K_{IC} , exhibited an inverse correlation with the yield stress value. The authors reported that all these effects were due to the different chemical structures of the curing agents, which provide different deformation behaviors.

Volume Fraction

The toughness of the modified epoxy generally increases as the volume fraction, v_f , of the dispersed rubbery phase increases, but the modulus and yield strength will usually decrease slightly. A linear relation between G_{Ic} and v_f for different epoxy resin hardener systems using CTAB has been reported by Bucknall and Yoshii (1978). However, Kunz et al. (1982) found that a v_f about 0.1 had been achieved in the epoxy–CTBN and epoxy–ATBN system and further increase in v_f resulted in only minor increase in the value of G_{Ic} . The work by Kinloch and Hunston (1987) has assisted in explaining these conflicting observations. They have used time–temperature superpositioning to separate the effect of changing v_f and the properties of the matrix. In this case, G_{Ic} was plotted against v_f at two different values of t_f/a_T . In the case of unimodal distribution of rubbery particles with a low value of t_f/a_T (i.e., a low test temperature), the relation between G_{Ic} and v_f was such that G_{Ic} increased only very slowly with increasing v_f and then reached a plateau value. At a higher value of t_f/a_T (i.e., a high test temperature), the relation was approximately linear, and the rate of increase of G_{Ic} as a function of v_f was far greater than that observed at the low value of t_f/a_T . These results demonstrate that when the epoxy matrix is more ductile, it can respond more readily to the presence of the rubbery particles. Therefore, there is no unique relationship between toughness and the volume fraction of rubbery particles. The maximum value of v_f that can be achieved via the in situ phase-separation technique is approximately 0.2–0.3. Attempts to produce higher values result in phase inversion and a loss of mechanical strength.

Fracture and Impact Test

The most frequent basis for assessment of toughening is the fracture test and impact test, which are determined with Izod or Charpy standardized tests. Fracture toughness is one of the most important properties of a material, and it is used to design materials for dynamic applications. Fracture toughness describes the resistance of a material with a crack to fracture. Because it is almost impossible to fabricate a material for practical purposes without cracks/defects, fracture toughness analysis is extremely important for design applications. The critical stress intensity factor, K_{Ic} (known as fracture toughness) and impact energy, G_{Ic} , are determined using ASTM D5045-99. The tests are carried out using an Instron machine using a flexure or tensile mode. An initial crack is machined into a rectangular specimen with a

thickness greater than 3.2 mm, and tapping on a fresh razor blade placed in the notch generates a natural crack.

Impact tests are used for quick assessment of the behavior of a material under dynamic loading conditions. The impact tests are used to determine the behavior of a material subjected to shock loading in bending, tension, and torsion. Mostly, the Charpy and Izod impact and occasionally tensile impact tests are used. These Izod/Charpy tests are widely applied in various industries due to the ease of sample preparation and the possibility of generating comparative data very quickly. Both tests are done as per ASTM D256. In the Charpy test, the specimen is supported as a simple beam, whereas in the Izod test, it is supported as a cantilever. The apparatus consists of a pendulum hammer swinging at a notched sample. The energy transferred to the material can be inferred by comparing the difference in height of the hammer before and after the fracture. Depending on the instrument, the impact energy (J/m) or the load history during the impact event can be recorded. The test can be carried out using different combinations of impactor mass and incident impact velocity to generate data on damage tolerance as functions of impact parameters, which are helpful for designing composite materials for a particular application.

Synthetic Liquid Rubber-Modified Epoxy

A wide range of synthetic liquid rubber materials have been proposed and used to modify epoxy resin, such as hydroxyl-terminated butadiene (HTPB) (Thomas et al. 2008), carboxyl-terminated butadiene–acrylonitrile (CTBN) (Thomas et al. 2004), vinyl-terminated poly(butadiene-co-acrylonitrile) (VTBN) (Auad et al. 2001; Robinette et al. 2004), epoxy-terminated rubber (ETBN) (Robinette et al. 2004), and epoxidized hydroxyl-terminated butadiene (EHTPB) (Latha et al. 1994). However, in this chapter, a few of the most commonly used synthetic liquid rubbers have been selected to explain the effects of rubber on the mechanical properties of epoxy.

Carboxyl-terminated butadiene–acrylonitrile (CTBN) is one of the most widely used liquid rubber materials for modifying epoxy resin (Calabrese and Valenza 2003; Chonkaew et al. 2013; Dadfar and Ghadami 2013). The flexural properties of the epoxy–CTBN system were studied by Tripathi and Srivastava (2008), and the results are shown in Fig. 7a. The rubber content was varied from 5 to 25 wt%. It can be seen that the flexural strength and modulus of the CTBN–epoxy networks are lower than those of the unmodified epoxy, except at 5 wt% of rubber content. The decrease in modulus is attributed to the presence of low-modulus rubber particles in the epoxy matrix. The reduction in flexural strength is due to the presence of some amount of rubber that remains dissolved in the epoxy matrix. A more significant reduction was observed for CTBN-modified epoxy containing 15 and 20 wt% CTBN. This shows the plasticizing effect of the dissolved rubber, which is also reflected in the significant increase in flexural strain. The rubber that is incorporated into the resin matrix is responsible for the reduction in flexural strength of the modified samples.

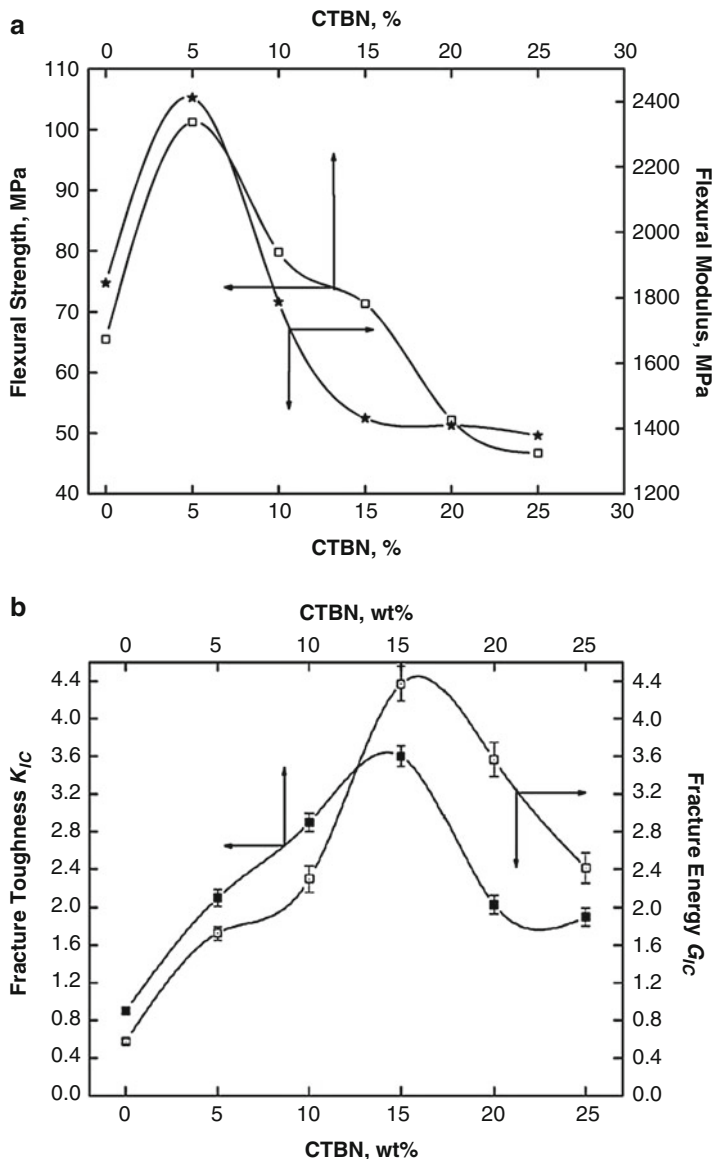


Fig. 7 Variation of (a) flexural strength and modulus and (b) fracture energy and toughness with varying concentrations of CTBN (Reproduced from Tripathi and Srivastava (2008), with permission from Elsevier)

The data on plane-strain fracture toughness (K_{IC}) revealed that the CTBN-modified epoxy gave values of K_{IC} that were greater than that of the unmodified epoxy (Fig. 7b). It was also revealed that K_{IC} increased with the addition of CTBN

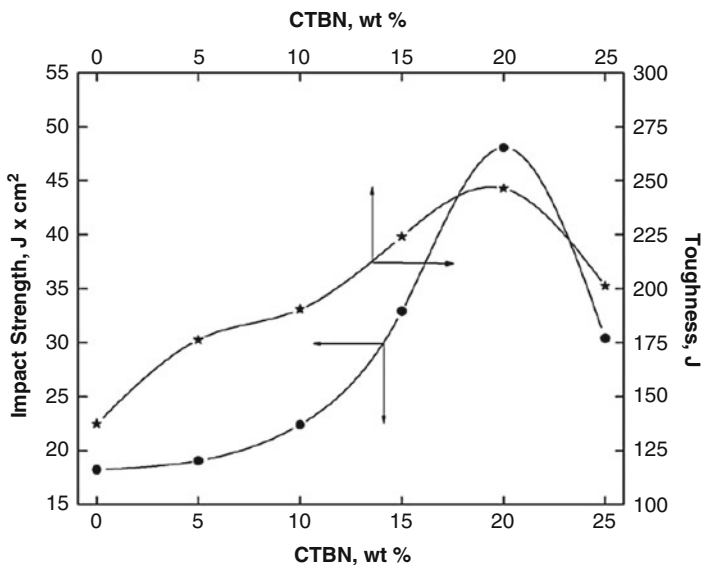


Fig. 8 Evaluation of impact strength and toughness with varying CTBN content (Reproduced from Tripathi and Srivastava (2008), with permission from Elsevier)

up to 15 wt%. Beyond 15 wt%, a decrease in K_{IC} was observed. The increase in K_{IC} is attributed to the percolation of rubber particles around the polymer chains of the matrix resin. This ultimately enhanced the stress dissipation between the phase components during growth of the fracture. Intimate contact between the phases also enhanced the stored energy density and correspondingly the failure properties (Tripathi and Srivastava 2008). Similar results were reported for an epoxy–CTBN blend studied by Dadfar and Ghadami (2013).

Figure 8 depicts the variation of impact strength as a function of CTBN concentration. The results indicate that cured materials containing 10 and 20 wt% CTBN showed the best balance of properties. The impact behavior of the cured material could be explained on the basis of the two-phase nature of the system. The rubber particles are considered to bridge the crack as it propagates through the material, thus preventing the crack from growing to a catastrophic size. The increase in toughness is due to the amount of elastic energy stored in the rubber particles during stretching. Thus, the deformation of the rubber particles in the matrix seems to be responsible for the enhanced stress transfer and hence improved impact resistance. It was also evidenced that the principle function of the rubber particles was to produce sufficient triaxial tension in the matrix so as to increase the local free volume, which enabled extensive shear yielding of the matrix. Thus, crack building of rubber particles along with shear yielding was the main toughening mechanism leading to enhanced impact behavior (Tripathi and Srivastava 2008).

Another synthetic rubber used to modify epoxy is ATBN. Chikhi et al. (2002) reported that the Izod impact strengths of notched and unnotched epoxy and

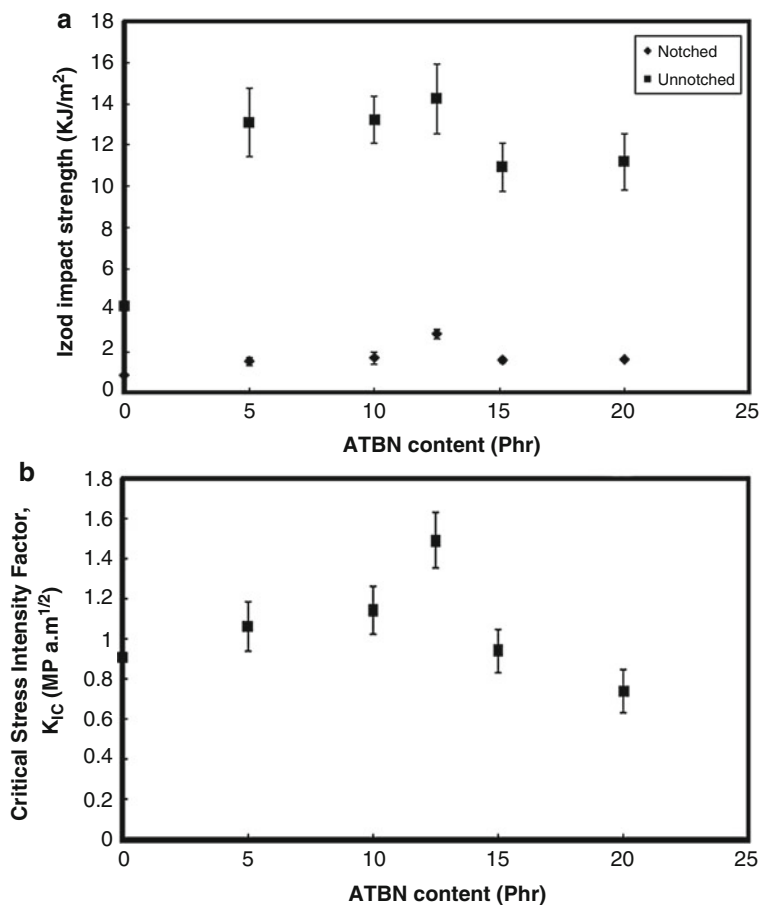


Fig. 9 Evaluation of (a) Izod impact strength and (b) critical stress intensity factor (K_{1c}) with varying ATBN content (Reproduced from Chikhi et al. (2002), with permission from Elsevier)

ATBN-modified epoxy specimens exhibited a bell-shaped curve with a maximum (threefold increase) at 12.5 phr ATBN content (Fig. 9a). They found that notched samples showed lower values than the unnotched ones because notches act as stress concentrators, resulting in a decrease in the impact strength. The energy required to initiate a crack is emphasized in unnotched specimens, and this energy is added onto the energy required to propagate the crack. The enhanced impact strength of both types of specimens was due to the good adhesion between ATBN and the epoxy resin via chemical reactions, as well as the small particle size of ATBN, factors that are known to improve impact properties. Furthermore, interfacial adhesion is known to improve the stress transfer, whereas the presence of a much tougher phase finely dispersed in a continuous matrix can increase the strength of the overall composition by means of

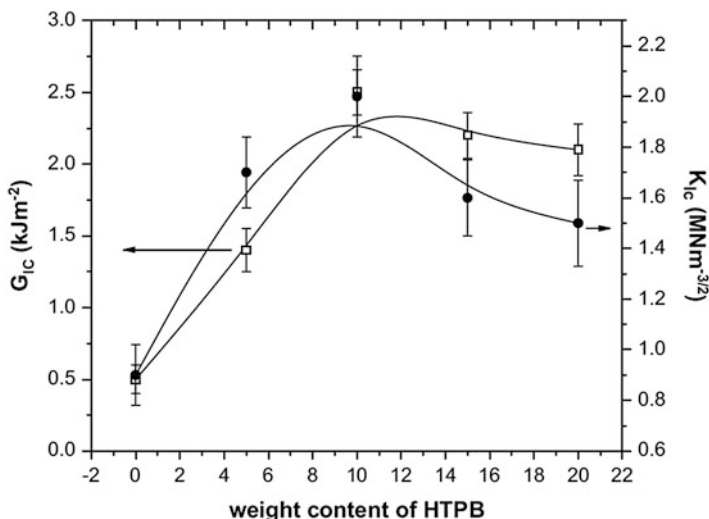


Fig. 10 Evaluation of fracture toughness (K_{IC}) and fracture energy (G_{IC}) as a function of HTPB content (Reproduced from Thomas et al. (2008), with permission from Elsevier)

damping the stress at the point of impact and at the crack tip, hence reducing the stress concentration (Chikhi et al. 2002).

A bell-shaped trend was also observed for κ_{IC} , as shown in Fig. 9b. The addition of 12.5 phr of ATBN led to a 1.5-fold maximum increase in κ_{IC} , followed by a decrease. The most probable reason for the improved toughness when the epoxy resin possesses a multiphase microstructure of dispersed rubber particles arises from the greater extent of energy-dissipation deformation occurring in the material near the crack tip (Chikhi et al. 2002).

Thomas et al. (2008) modified epoxy with hydroxyl-terminated polybutadiene (HTPB). The values of fracture toughness (critical stress intensity factor, κ_{IC}) and fracture energy (critical strain energy release rate, G_{IC}) as a function of HTPB weight percentage are furnished in Fig. 10. The authors reported that the addition of rubber increased κ_{IC} and G_{IC} up to an optimum HTPB content of 10 phr and that no further increase was found upon further loading of rubber. These results were due to the larger size of rubber particles at higher concentrations. As mentioned previously, large particles obtained at a high rubber content would deteriorate the impact toughness as this would result in high stress intensities around the agglomerated rubber particles.

The results of the Izod impact strength of neat and HTPB-modified epoxy are depicted in Fig. 11a. It is observed that the impact strength reached a maximum value (47% increase) at 10 phr of rubber content. The enhancement was due to the effective stress concentration behavior of the phase-separated rubber-rich particles, which amplified the plastic deformation of a highly brittle matrix to a certain extent. The decrease in the impact strength after an optimum level of 10 phr rubber inclusion

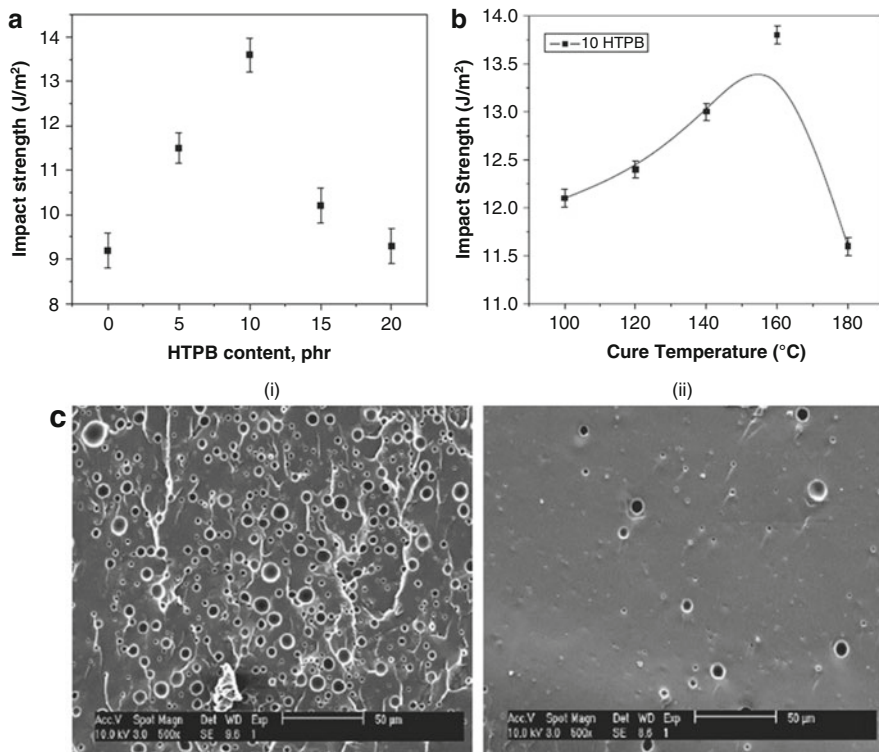


Fig. 11 Impact strength of (a) neat and HTPB-modified epoxy and (b) 10 phr HTPB-modified epoxy cured at different temperatures. (c) SEM micrograph of modified epoxy at (i) 160 and (ii) 200 °C (Reproduced from Thomas et al. (2008), with permission from Elsevier)

is attributed to the increased aggregation of rubber particles with increasing rubber concentration. Large rubber domains act as deflection sites and lead to catastrophic failure of the matrix.

Thomas et al. (2008) also investigated the relation between the curing temperature and impact strength of a modified sample containing 10 wt% HTPB. They found that the impact strength of the HTPB-modified epoxy increased slowly and attained a maximum at 160 °C, leveling off at 200 °C (Fig. 11b). The reason for this behavior was explained via the morphological study of modified epoxy cured at 160 at 200 °C, shown in Fig. 11c (i) and (ii), respectively. A well-defined domain distribution of particles is clearly observed in the micrograph of the blend cured at 160 °C. However, in the blend of the same composition cured at 200 °C, domain distribution is not uniformly defined. This was attributed to the fact that phase separation started well before gelation, and because high temperature leads to fast curing, particle growth was reduced due to restrictions caused by diffusion in the epoxy matrix. The modified epoxy thus showed an almost single-phase morphology on the fracture surface, which resulted in poor impact performance.

Table 6 Fracture toughness of epoxy and ETPB-modified epoxy blends (Reproduced from Yahyaie et al. (2013), with permission from Elsevier)

Rubber content (wt%)	K_{Ic} (MPa m ^{1/2})	G_{Ic} (J/m ²)
0	0.65 ± 10%	84 ± 3
5	0.66 ± 10%	421 ± 31
7.5	1.80 ± 10%	793 ± 54
10	1.45 ± 10%	361 ± 28

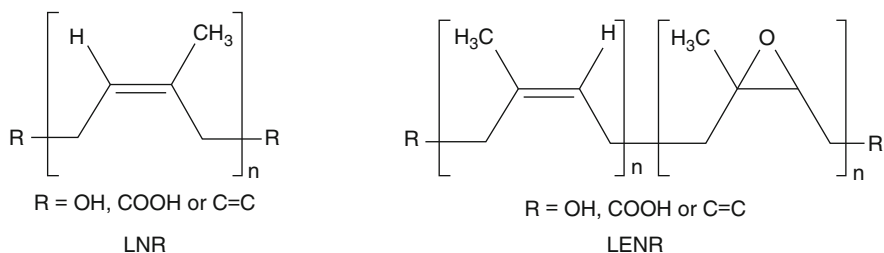


Fig. 12 Chemical structure of LNR and LENR

Recently, Yahyaie et al. (2013) synthesized epoxy-terminated polybutadiene (ETPB) and utilized it as an impact modifier for an epoxy system. They reported that maximum impact was achieved with 7.5 wt% ETPB content. The mean values of K_{Ic} and G_{Ic} for the neat and ETPB-modified epoxy are shown in Table 6.

Similar to previous researchers, Yahyaie et al. claimed that the reduction of K_{Ic} and G_{Ic} was due to the fact that the high rubber content resulted in a flexible sample and changed the morphology from a distinctive particulate rubber phase to a semicontinuous morphology. The main toughening mechanism reported for the ETPB/epoxy system was cavitation of rubber particles because of triaxial tension ahead of the crack tip, which reveals the stress concentration associated with cavitating particles to activate shear yielding in the matrix.

Natural Liquid Rubber-Modified Epoxy

Recently, utilization of natural liquid rubber as an impact modifier has generated significant interest due to its renewability, low cost, environmental friendliness, non-toxicity, and ease of processing (Kargarzadeh et al. 2015). Figure 12 shows the chemical structure of liquid natural rubber (LNR) and liquid epoxidized natural rubber (LENR) produced via photochemical degradation.

Ben Saleh et al. (2014) modified epoxy with LNR ($M_n = 16 \times 10^3$) prepared by the depolymerization of deproteinized natural rubber latex. A trend similar to that of other rubber-modified epoxy systems was found for the fracture toughness (K_{Ic}) of neat epoxy and the LNR-modified epoxy blend. Figure 13 shows the relationship between the LNR content and K_{Ic} and the effect of different testing speeds on the K_{Ic} of the epoxies. It can be seen that the K_{Ic} of the LNR-modified epoxies is higher than that of the unmodified epoxy. The improvement in the fracture toughness is

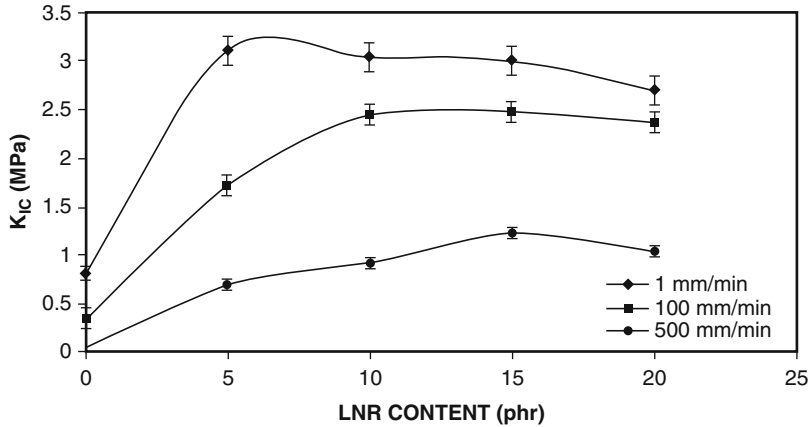


Fig. 13 Effects of LNR content and testing speed on the fracture toughness of neat and modified epoxies (Ben Saleh et al. 2014)

Table 7 Effect of LNR content on the flexural properties of neat and modified epoxies (Ben Saleh et al. 2014)

LNR (phr)	Flexural strength (MPa)	Flexural modulus (GPa)
0	93.13 ± 4.50	3.05 ± 0.25
5	67.50 ± 5.00	2.21 ± 0.22
10	65.50 ± 4.50	2.20 ± 0.23
15	47.37 ± 4.30	1.47 ± 0.20
20	55.48 ± 6.40	1.86 ± 0.33

attributed to the incorporation of LNR, which increased the fracture resistance of the matrix by enabling plastic deformation to occur in the matrix. In all cases, the K_{IC} values increased with increasing LNR content. Hence, the increase in toughness due to the increase in LNR content can be explained in terms of dissolved rubber. This effect makes the matrix more ductile and increases its toughness. At low testing speeds, i.e., 1 mm/min, a maximum value of K_{IC} was observed at 5 phr LNR. In this case, the rubber particles would have had more time to relax, and thus a small amount of LNR (5 phr) would be enough to significantly improve the fracture toughness. However, the fracture toughness attained a maximum value at 15 phr LNR at a testing speed of 500 mm/min. In all cases, the K_{IC} values decreased with increasing testing speed, and thus the effect of using different testing speeds on the K_{IC} of epoxies was reported.

The flexural strengths and moduli of LNR-modified epoxies were also found to be lower than those of the unmodified epoxy (Table 7). As discussed previously, the decrease of modulus was attributed to the presence of low-modulus rubber particles in the epoxy matrix. The reduction in strength was due to the presence of rubber particles, some of which were chemically bonded to the epoxy network. A more

significant reduction in the properties was observed at 15 and 20 phr LNR due to the plasticizing effect of the dissolved rubber (Ben Saleh et al. 2014).

In another work reported by Abu Bakar et al. (2011), LENR was used as a toughening agent in the preparation of an epoxy blend. The results from the flexural test with only 5.5 phr LENR content showed that the flexural strength and flexural modulus were reduced for the epoxy blend. However, the impact strength of the epoxy blend increased by 75% with the addition of only 5.5 phr rubber content.

A comparative study on the effects of LNR and LENR on the impact properties of epoxy was reported by Tan et al. (2013). The results of flexural tests showed that the bending modulus increased slightly up to 5 wt% LNR and then decreased with increasing rubber content. Meanwhile, the bending strength increased with 3 wt% LNR and then decreased with increasing rubber content (Fig. 14). The decrease in the bending modulus showed that the LNR-modified system became more ductile. In the case of LENR-modified epoxies, both the bending strength and bending modulus increased with 3 wt% rubber content and then leveled off with increasing LENR content.

The enhanced impact strength and modulus in both the LNR and LENR epoxy systems is unique behavior that other rubber-modified epoxy systems did not show. In fact, when stress is applied to a sample, the rubber particles existing in the matrix bear the stress that is applied. The addition of rubber to the epoxy resin in the system increases the toughness of the epoxy network. The increase in the main-chain mobility caused by chain extension might be one of the reasons for the improvement of the mechanical properties. In the case of LENR-modified epoxies, the oxirane groups from LENR participated in the reaction during the curing process. The interaction between the curing agent, epoxy resin, and LENR is one of the reasons for the improvement of the mechanical properties. Thus, mixed with the epoxy matrix, the interaction between the LENR and the epoxy contributed to the improvement of the bending properties. However, it was also noted that the bending properties decreased as the LENR content increased. Epoxidized natural rubber (ENR) undergoes strain crystallization because of the elastomeric properties, and hence the modulus of the sample is increased. Thus, when LENR was added to the epoxy system, entanglement between the epoxy resin and the ENR increased. This enhanced the bending strength of the toughened epoxy system because it could bear the stress that was added to the sample. At the same time, the epoxy system has the ability to transfer the stress applied very well, thus improving the bending strength (Tan et al. 2013).

Overall, LENR as a toughening agent shows better results as compared to the LNR-toughened epoxy. The reduction of impact strength and modulus at higher rubber contents for both systems is due to the agglomeration of rubber particles with increasing liquid rubber content. This agglomeration contributes to the formation of defects and initiates the failure of the samples.

The results of the Izod impact test for notched LNR/LENR-modified epoxy specimens showed that the impact strength of the epoxy increased with addition of rubber for both systems (Fig. 15). For the LNR-modified epoxy, 5 wt% LNR-modified epoxy achieved the optimum results. For the LENR series, when

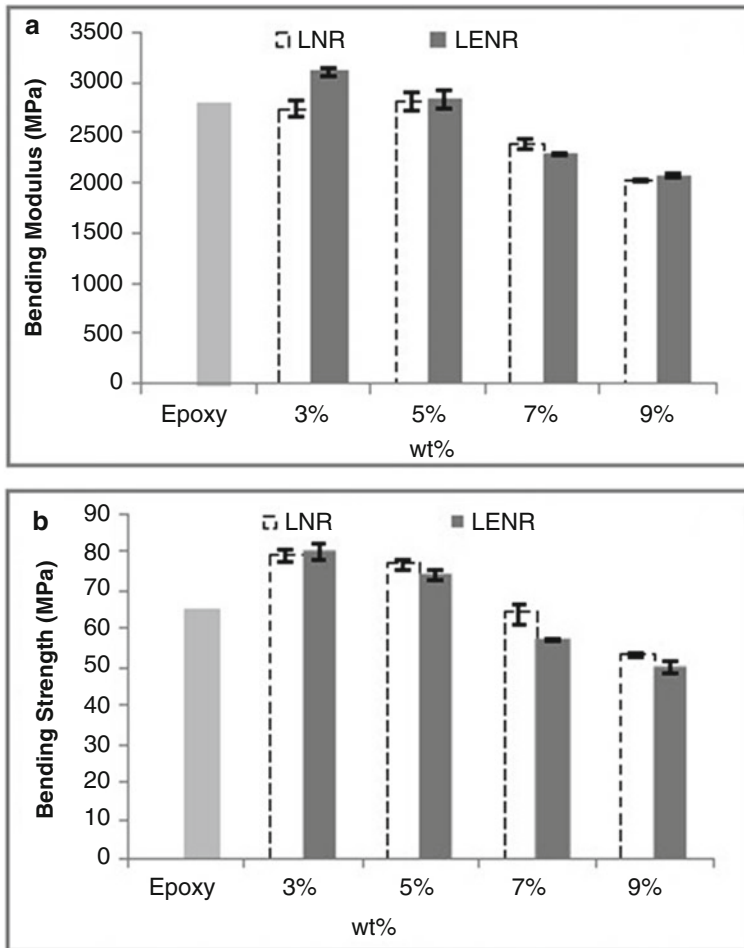


Fig. 14 (a) Bending modulus and (b) bending strength of neat and LNR/LENR-modified epoxies (Tan et al. 2013)

3 wt% LENR was added to the epoxy resin, it showed optimum results. However, the impact strength decreased gradually as the LENR content increased. The comparison between the two types of liquid rubber as toughening agents to the epoxy system shows that the LNR-toughened epoxy possessed lower impact performance than the LENR-toughened epoxy. This is due to the lower compatibility between the rubber particles in the LNR-toughened epoxy matrix, which is attributed to the aggregation of the rubber particles. LENR had better compatibility with the epoxy matrix due to the presence of oxirane groups, which possessed a good reaction with the epoxy. The improvement of the impact strength can be thus be correlated with the toughness enhancement.

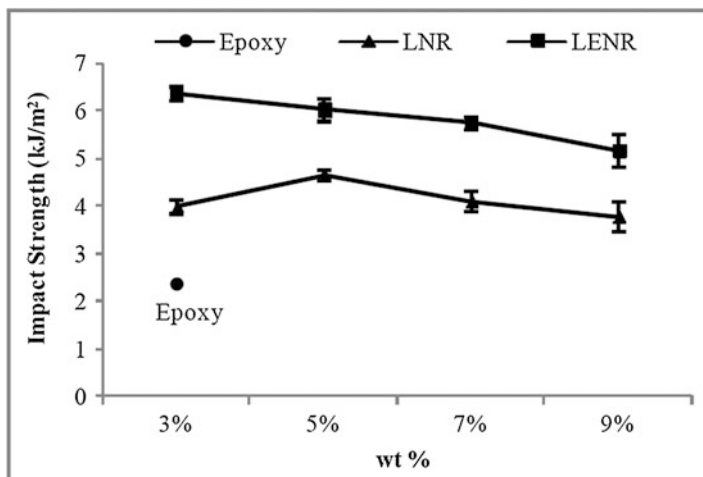


Fig. 15 Evaluation of Izod impact strength of neat and modified epoxies with LNR and LENR (Tan et al. 2013)

Mathew et al. (2012) modified epoxy resin with LNR possessing hydroxyl functionality (HTLNR). The epoxy monomer was cured using nadic methyl anhydride as a hardener in the presence of *N,N*-dimethylbenzylamine as an accelerator. The fracture toughness was found to increase with increasing rubber content, as shown in Fig. 16. A maximum 100% increase was observed for the 20 wt% HTLNR-modified epoxy, which was due to cavitation and shear deformation of the rubber particles.

They also reported that the impact properties were enhanced for the modified epoxy samples with an increase in HTLNR concentration up to 15 wt%, followed by a decrease. The maximum impact strength of 19.215 kJ/m² was obtained at 15 wt% HTLNR using an unnotched sample (Fig. 17a), which is approximately 100% higher than the maximum impact strength of the neat epoxy. Similarly, the work done by Ratna (2001) using carboxyl-terminated poly(2-ethyl hexyl acrylate) rubber (CTPEHA) to modify an epoxy matrix showed 60% improvement in impact properties.

The variations of the impact strength of the unnotched and notched samples are plotted as a function of rubber content in Fig. 17a, b. The unnotched samples were found to have higher impact strength than the notched ones because some energy is required to initiate a crack and continue crack propagation. With increasing rubber concentration, the impact strength was found to increase. The improvement in impact strength as a function of composition indicates that morphology plays an important role in the toughening of cross-linked epoxy systems (Mathew et al. 2012).

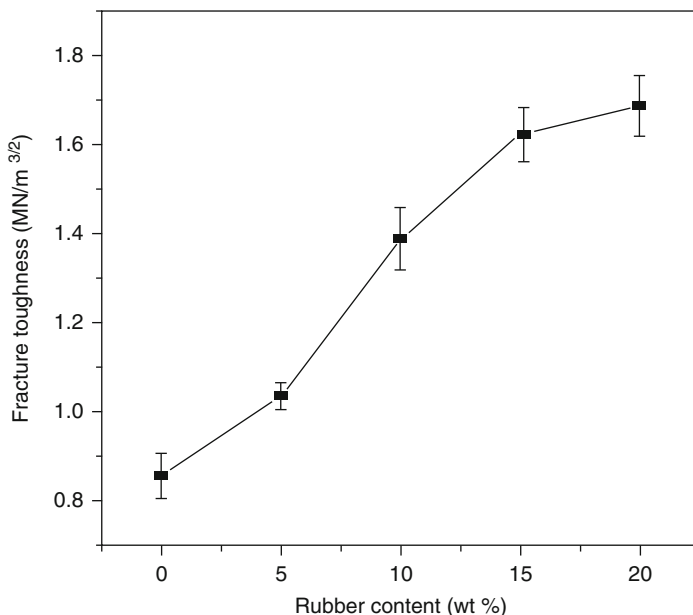


Fig. 16 Variation of fracture toughness with rubber content (Reproduced from Mathew et al. (2012). Copyright 2011 Wiley Periodicals, Inc.)

Tensile Properties

Rubber is generally well known to affect the tensile properties of epoxy matrices depending on its compatibility with the epoxy matrix, the surface area of contact, the particle size, shape, and content, etc., as mentioned previously. Tensile testing, also known as pull testing or tension testing, is a standard test (ASTM D-638) in which a sample is placed in grips and subjected to controlled tension until it fails. This provides valuable information about the material, including ultimate tensile strength, yield strength, elongation, and Young's modulus. As mentioned previously, the rate of pulling and the rate of material expansion response will influence the results. The following case studies show the effect of different types of synthetic and natural liquid rubber on the tensile properties of epoxy blends.

Synthetic Liquid Rubber-Modified Epoxy

Chikhi et al. (2002) reported that epoxy modified with 12.5 and 15 phr ATBN exhibited ductile deformation with the appearance of an upper yield stress. They claimed that the lower yield stress value observed indicates that shear yielding might be the prevailing mechanism of deformation in such a system. Table 8 shows the

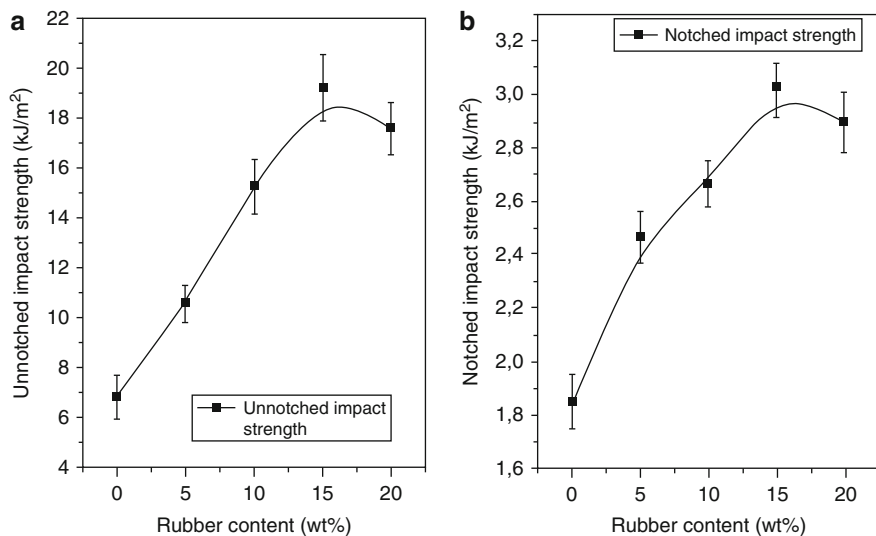


Fig. 17 Variation of impact strength as a function of rubber content in (a) unnotched and (b) notched samples (Reproduced from Mathew et al. (2012), with permission from John Wiley and Sons)

Table 8 Effect of ATBN content on the tensile properties of epoxy resin (Reproduced from Chikhi et al. (2002) with permission from Elsevier)

ATBN (phr)	Modulus (GPa)	Stress at yield (MPa)	Strain at yield (%)	Stress at break (MPa)	Strain at break (%)
0	1.8	—	—	34.4	3.5
5	1.7	31.7	3	31.3	3.6
10	1.7	29.8	3.8	28	6
12.5	1.6	29.5	4	26	6.7
15	1.3	24.1	4	21	8.8
20	1.4	25.9	3.8	24.6	7.3

tensile properties of the epoxy resin and its related modified blend. It can be seen that the tensile modulus and tensile strength gradually decreased with increasing ATBN content, which is due to the effect of the soft segment structure of ATBN. Tensile strain at break shows a drastic increase of approximately 2.5% for the sample with 15 phr ATBN, indicating good compatibility and adhesion via the chemical reaction between ATBN and the epoxy.

Similar behavior of the tensile properties was reported for CTBN–epoxy systems by Dadfar and Ghadami (2013) and Thomas et al. (2004). A gradual decrease in the tensile strength and Young's modulus was noted as the concentration of CTBN increased. They also claimed that the reduction was due to the fact that the strength and modulus of rubber were much lower than those of the epoxy matrix. In addition, low-modulus rubber particles acted as stress concentrators and thus decreasing the

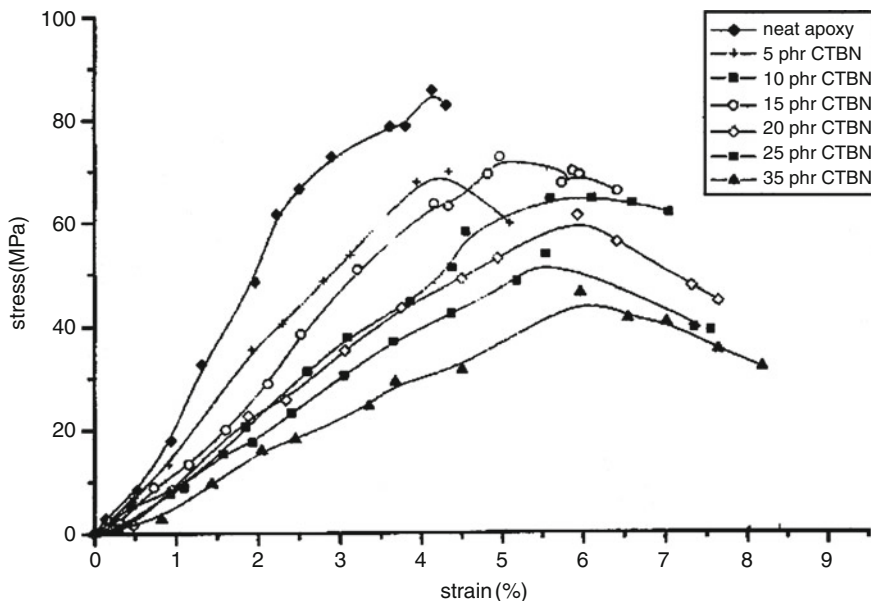


Fig. 18 Stress–strain curves of neat and CTBN modified epoxies (Reproduced from Thomas et al. 2004 with permission from Elsevier.)

Table 9 Tensile properties of unmodified and CTBN-modified epoxy (Reproduced from Dadfar and Ghadami (2013), with permission from Elsevier)

CTBN concentration (phr)	Tensile strength (MPa)	Young's modulus (MPa)
0	71	2980
5	65	2680
10	58	2350
15	53	2050

tensile strength. Figure 18 and Table 9 show the stress–strain curve and values of the CTBN–epoxy system reported by Thomas et al. (2004) and Dadfar and Ghadami (2013), respectively.

The effect of HTPB on the tensile properties of epoxy was reported by Zhou and Cai (2011). It can be seen from Table 10 that the tensile strength has been achieved with addition of 5–10 phr of HTPB when compared to the pure epoxy. The tensile modulus of epoxy decreased with the addition of HTPB. Meanwhile, elongation at break increased significantly, indicating that the ductility of the blend increased. In addition to the previous reason for the reduction of tensile modulus, the lower stiffness of the modified epoxy was also attributed to the decrease in the cross-linking density of the epoxy network because the modifier occupied the reaction centers during modification (Thomas et al. 2008). Furthermore, the reduction of

Table 10 Tensile properties of neat and HTPB-modified epoxy (Reproduced from Zhou and Cai (2011), with permission from John Wiley and Sons)

HTPB concentration (phr)	Tensile strength (MPa)	Tensile modulus (GPa)	Elongation at break (%)
0	65.20 ± 3.20	2.98 ± 0.26	2.40 ± 0.21
5	73.12 ± 3.60	2.95 ± 0.21	5.46 ± 0.32
10	67.31 ± 4.10	2.83 ± 0.23	7.75 ± 0.43
20	60.23 ± 3.40	2.41 ± 0.18	8.42 ± 0.46
30	52.36 ± 2.90	1.91 ± 0.13	8.71 ± 0.52

Table 11 Tensile properties of neat and LNR-modified epoxy (Reproduced from Ben Saleh et al. (2014), with permission from Elsevier)

LNR (phr)	Tensile strength (MPa)	Strain at break (MPa)	Young's modulus (GPa)
0	41.0 ± 1.7	5.1 ± 0.9	1.56 ± 0.13
5	35.6 ± 0.7	5.8 ± 0.8	1.46 ± 0.70
10	28.2 ± 1.2	6.0 ± 0.4	1.20 ± 0.05
15	22.4 ± 0.9	6.0 ± 0.8	1.08 ± 0.08
20	19.4 ± 0.8	7.9 ± 0.8	0.88 ± 0.12

modulus could be due to the increase in the relative amount of dissolved rubber as HTPB content increases. The rubber particles also may act as plasticizer with an increase of free volume, which conducts to decrease of epoxy resin stiffness (Zhou and Cai 2011).

Natural Liquid Rubber-Modified Epoxy

Table 11 shows the effect of LNR content on the tensile properties of the epoxy. Similar to the other rubber–epoxy systems, the tensile strengths and elastic moduli of the LNR-modified epoxies are lower than those of the unmodified epoxy. As discussed previously, the decrease of elastic modulus is attributed to the presence of low-modulus rubber particles in the epoxy matrix. The reduction in strength is due to the presence of rubber, some of which is chemically bonded to the epoxy network. A more significant reduction in the properties is observed at 15 and 20 phr LNR, indicating the plasticizing effect of the dissolved rubber (Ben Saleh et al. 2014). The area under the strain–stress curve, which is an indication of epoxy toughening properties, increased with increasing LNR content (Fig. 19).

Interestingly the tensile strength and modulus of the LNR/epoxy system reported by Seng et al. (2011) increased slightly with the addition of 3 phr LNR content. They claimed that the slight increase in tensile strength and Young's modulus may have been caused by entanglement between the epoxy and LNR. The obvious increase in failure strain was due to the diffusion of some LNR into the epoxy (Table 12).

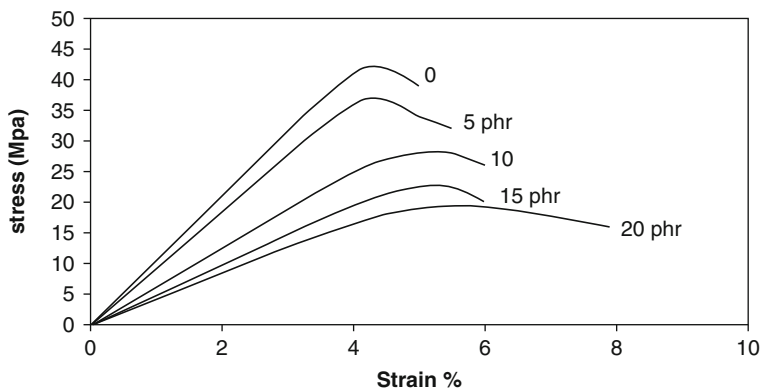


Fig. 19 Stress–strain curves of epoxy and its modified blend (Reproduced from Ben Saleh et al. (2014), with permission from Elsevier)

Table 12 Tensile properties of epoxy with different LNR loadings (Seng et al. 2011)

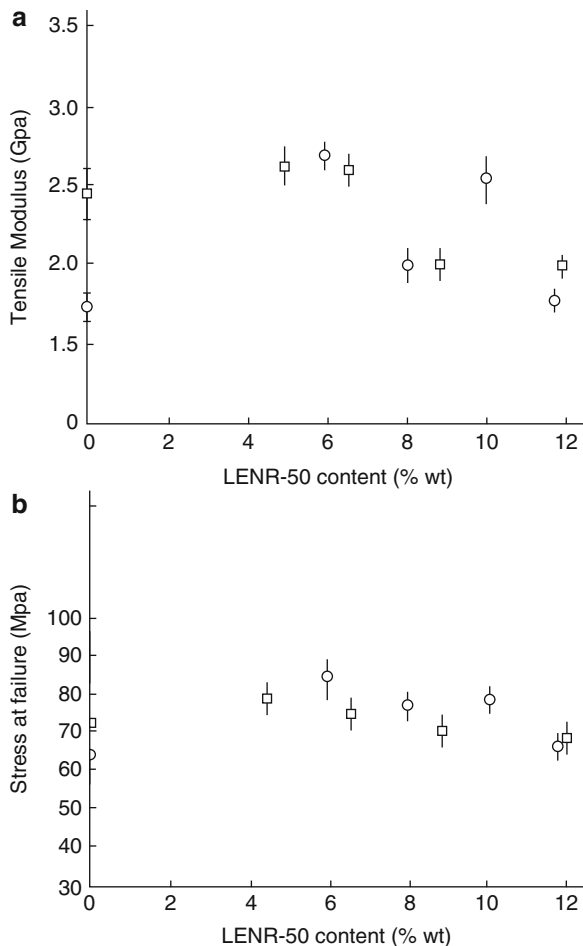
LNR (phr)	Tensile strength (MPa)	Failure strain (%)	Young's modulus (MPa)
0	48.9	2.7	2414
3	53.87	4.9	2463
5	48.54	6.2	2433
7	42.07	9.1	2370
9	29.69	7.1	2279

Two sets (A and B) of epoxy resin formulations with different glycidyl ether/reactive hydrogen molar ratios were modified with LENR by Cizravi and Subramaniam (1999). The tensile modulus and strength of the modified epoxies are presented in Fig. 20. It can be seen that both the tensile modulus and stress at failure increased slightly with the addition of 5.9 wt% and 4.5 wt% LENR for sets A and B, respectively, due to the good compatibility and probable chemical interaction between LENR and the epoxy.

Summary

Epoxy materials can be toughened successfully by blending them with proper synthetic or natural liquid rubber in small amounts. The phase separation of rubber during the curing process is an important phenomenon that depends on processing and curing conditions. There are several factors that affect the toughness of the final blend, such as morphology, rubber particle size, rubber composition, curing

Fig. 20 (a) Tensile moduli and (b) stress at failure of LENR-modified epoxy matrices. The *open circles* (○) indicate the set A formulation, and the *open squares* (□) indicate the set B formulation (Reproduced from Cizravi and Subramaniam (1999), with permission from John Wiley and Sons)



agent, etc. It is very difficult to study the effect of individual parameters because they are interdependent, although general aspects can be concluded. The major toughening mechanism of rubber-modified epoxies is cavitation of the rubber particles, followed by shear yielding. Some other toughening mechanisms such as microcracking, crack deflection, crack bifurcation, crack pinning, and crack bridging or multilevel fracture paths can also be operative. The presence of rubber particles improves the fracture toughness of the modified epoxy, whereas the tensile strength and tensile modulus decrease. Interestingly, the modification of epoxy with natural liquid rubber not only improves the impact properties but also increases the tensile strength slightly. The addition of an optimum amount of liquid rubber into the epoxy resin prior to curing provides a blend with desirable mechanical properties.

References

- Abadyan M, Kouchakzadeh MA, Bagheri R (2012) Fracture toughness of a hybrid rubber modified epoxy. II. Effect of loading rate. *J Appl Polym Sci* 125:2476–2483
- Abu Bakar MA, Ahmad HS, Kuntjoro W (2011) Effects of LENR addition on mechanical properties of kenaf fiber-reinforced epoxy composites. *Int J Plast Technol* 15:33–42
- Arends CB (ed) (1996) *Polymer toughening*. Marcel Dekker, New York
- Arias ML, Frontini PM, Williams RJJ (2003) Analysis of the damage zone around the crack tip for two rubber-modified epoxy matrices exhibiting different toughenability. *Polymer* 44:1537–1546
- Auad ML, Frontini PM, Borrajo J, Aranguren MI (2001) Liquid rubber modified vinyl ester resins: fracture and mechanical behavior. *Polymer* 42:3723–3730
- Ben Saleh AB, Mohd Ishak ZA, Hashim AS, Kamil WA (2009) Compatibility, mechanical, thermal, and morphological properties of epoxy resin modified with carbonyl-terminated butadiene acrylonitrile copolymer liquid rubber. *J Phys Sci* 20:1–12
- Ben Saleh AB, Mohd Ishak ZA, Hashim AS, Kamil WA, Ishiaku US (2014) Synthesis and characterization of liquid natural rubber as impact modifier for epoxy resin. *Phys Procedia* 55:129–137
- Bucknall CB, Yoshii T (1978) Relationship between structure and mechanical properties in rubber-toughened epoxy resins. *Br Polym J* 10:53–59
- Calabrese L, Valenza A (2003) Effect of CTBN rubber inclusions on the curing kinetic of DGEBA-DGEBF epoxy resin. *Eur Polym J* 39:1355–1363
- Chan LC, Gillham JK, Kinloch AJ, Shaw SJ (1984) Rubber-modified epoxies. In: Riew CK, Gillham JK (eds) *Rubber-modified thermoset resins*. American Chemical Society, Washington, DC, pp 235–260
- Chikhi N, Fellahi S, Bakar M (2002) Modification of epoxy resin using reactive liquid (ATBN) rubber. *Eur Polym J* 38:251–264
- Chonkaew W, Sombatsompop N, Brostow W (2013) High impact strength and low wear of epoxy modified by a combination of liquid carboxyl-terminated poly(butadiene-co-acrylonitrile) rubber and organoclay. *Eur Polym J* 49:1461–1470
- Cizravi JC, Subramaniam K (1999) Thermal and mechanical properties of epoxidized natural rubber-modified epoxy matrices. *Polym Int* 48:889–895
- Dadfar MR, Ghadami F (2013) Effect of rubber modification on fracture toughness properties of glass-reinforced hot-cured epoxy composites. *Mater Des* 47:16–20
- Finch CA, Hashemi S, Kinloch AJ (1987) Effect of segmental molecular mass between cross-links of matrix phase on the toughness of rubber-modified epoxies. *Polym Commun* 28:322
- Gaymans RJ, Dijkstra K (1990) Percolation model for brittle tough transition in nylon rubber blends-comments. Elsevier, Oxford
- He D, Ding X, Chang P, Chen Q (2012) Effect of annealing on phase separation and mechanical properties of epoxy/ATBN adhesive. *Int J Adhes Adhes* 38:11–16
- Hull D (1996) Influence of stress intensity and crack speed on fracture surface topography: mirror to mist to macroscopic bifurcation. *J Mater Sci* 31:4483–4492
- Hunston DL, Kinloch AJ, Shaw SJ, Wang SS (1984) Characterization of the fracture behavior of adhesive joints. In: Mittal KL (ed) *Adhesive joints: formation, characteristic, and testing*. Plenum, New York, pp 789–808
- Kar S, Banthina AK (2006) Recent trend in developing reactive liquid oligomers for toughening of epoxy rubber. In: Bregg RK (ed) *Frontal polymer research*. Nova, New York, pp 1–63
- Kargarzadeh H, Ahmad I, Abdullah I (2014) Liquid rubbers as toughening agents. In: Thomas S, Sinturel C, Thomas R (eds) *Micro- and nanostructured epoxy/rubber blends*. Wiley-VCH Verlag GmbH & Co., Germany, pp 31–52
- Kargarzadeh H, Ahmad I, Abdullah I, Thomas R, Dufresne A, Thomas S, Hassan A (2015) Functionalized liquid natural rubber and liquid epoxidized natural rubber: a promising green toughening agent for polyester. *J Appl Polym Sci*. 132, doi: 10.1002/APP.41292

- Kim JK, Datta S (2013) Rubber-thermoset blends: micro and nanostructured. In: Visakh PM, Thomas S, Chandra AK, Mathew AP (eds) *Advances in elastomers I*. Springer, Berlin/Heidelberg, pp 229–262
- Kinloch AJ (1989) Relationship between the microstructure and fracture behavior of rubber-toughened thermosetting polymers. In: Riew CK (ed) *Rubber-toughened plastics*. American Chemical Society, Washington, DC, pp 67–91
- Kinloch AJ, Hunston DL (1987) Effect of volume fraction of dispersed rubbery phase on the toughness of rubber-toughened epoxy polymers. *J Mater Sci Lett* 6:137–139
- Kunz SC, Sayre JA, Assink RA (1982) Morphology and toughness characterization of epoxy resins modified with amine and carboxyl terminated rubbers. *Polymer* 23:1897–1906
- Kunz-Douglass S, Beaumont PWR, Ashby MF (1980) A model for the toughness of epoxy–rubber particulate composites. *J Mater Sci* 15:1109–1123
- Lange FF (1970) The interaction of a crack front with a second phase dispersion. *Philos Mag* 22:983–992
- Latha PB, Adhinarayanan K, Ramaswamy R (1994) Epoxidized hydroxy-terminated polybutadiene – synthesis, characterization and toughening studies. *Int J Adhes Adhes* 14:57–61
- Lee JY, Choi HK, Shim MJ, Kim SW (2000) Kinetic studies of an epoxy cure reaction by isothermal DSC analysis. *Thermochim Acta* 343:111–117
- Li D, Yee AF, Chen IW (1994) Fracture behaviour of unmodified and rubber modified epoxies under hydrostatic pressure. *J Mater Sci* 29:2205–2215
- Mathew VS, Sinturel C, George SC, Thomas S (2010) Epoxy resin/liquid natural rubber system: secondary phase separation and its impact on mechanical properties. *J Mater Sci* 45:1769–1781
- Mathew VS, Jyotishkumar P, George SC, Gopalakrishnan P, Delbreilh L, Saiter JM, Saikia PJ, Thomas S (2012) High-performance HTLNR/epoxy blend – phase morphology and thermo-mechanical properties. *J Appl Polym Sci* 125:804–811
- Meeks C (1974) Fracture and mechanical properties of epoxy resins and rubber-modified epoxy resins. *Polymer* 15:675–681
- Moschiar SM, Riccardi CC, Williams RJJ, Verchere D, Sautereau H, Pascault JP (1991) Rubber-modified epoxies. III. Analysis of experimental trends through a phase-separation model. *J Appl Polym Sci* 42:717
- Oshinski AJ, Keskkula H, Paul DR (1992) Rubber toughening of polyamides with functionalized block copolymers: 1. Nylon-6. *Polymer* 33:268–283
- Oshinski AJ, Keskkula H, Paul DR (1996) The role of matrix molecular weight in rubber-toughened nylon 6 blends: 3. Ductile–brittle transition temperature. *Polymer* 37:4919–4928
- Pascault JP (2002) Yielding and fracture of toughened networks. In: Pascault JP, Sautereau H, Verdu J, Williams RJJ (eds) *Thermosetting polymers*. Marcel Dekker Incorporated, New York, pp 389–408
- Pearson RA, Yee AF (1983) The effect of cross-link density on the toughening mechanism of elastomer-modified epoxies. NASA. Langley Research Center Tough Composite Mater. 173–194. <http://ntrs.nasa.gov/search.jsp?R=19850004643>
- Pearson RA, Yee AF (1991) Influence of particle size and particle size distribution on toughening mechanisms in rubber-modified epoxies. *J Mater Sci* 26:3828–3844
- Pearson RA, Yee AF (1993) Toughening mechanisms in thermoplastic-modified epoxies: 1. Modification using poly(phenylene oxide). *Polymer* 34:3658–3670
- Ratna D (2001) Phase separation in liquid rubber modified epoxy mixture. Relationship between curing conditions, morphology and ultimate behavior. *Polymer* 42:4209–4218
- Ratna D (2005) *Epoxy composites: impact resistance and flame retardancy*, vol 16. Smithers Rapra Publishing, Shawbury, United Kingdom, pp 1–120
- Robinette EJ, Ziaee S, Palmese GR (2004) Toughening of vinyl ester resin using butadiene-acrylonitrile rubber modifiers. *Polymer* 45:6143–6154
- Roşu D, Caşcaval CN, Mustafa F, Ciobanu C (2002) Cure kinetics of epoxy resins studied by non-isothermal DSC data. *Thermochim Acta* 3(83):119–127

- Sbirrazzuoli N, Vyazovkin S, Mititelu A, Sladic C, Vincent L (2003) A study of epoxy-amine cure kinetics by combining isoconversional analysis with temperature-modulated DSC and dynamic rheometry. *Macromol Chem Phys* 204:1815–1821
- Seng YL, Ahmad SH, Rasid R, Noum SY, Hock YC, Tarawneh MA (2011) Effect of liquid natural rubber (LNR) on the mechanical properties of LNR-toughened epoxy composite. *Sains Malays* 40:679–683
- Sultan JN, McGarry FJ (1973) Effect of rubber particle size on deformation mechanisms in glassy epoxy. *Polym Eng Sci* 13:29–34
- Sultan JN, Laible RC, McGarry FJ (1971) Microstructure of two-phase polymers. *Appl Polym Symp* 16:127–136
- Tan SK, Ahmad S, Chia CH, Mamun A, Heim HP (2013) A comparison study of liquid natural rubber (LNR) and liquid epoxidized natural rubber (LENR) as toughening agent for epoxy. *Am J Mater Sci* 3:55–61
- Thomas R, Abraham J, Thomas PS, Thomas S (2004) Influence of carboxyl-terminated (butadiene-co-acrylonitrile) loading on the mechanical and thermal properties of cured epoxy blends. *J Polym Sci* 42:2531–2544
- Thomas R, Yumei D, He YL, Yang L, Moldenaers P, Yang WM, Czigan T, Thomas S (2007) Cure kinetics, morphology and miscibility of modified DGEBA-based epoxy resin-effect of liquid rubber inclusion. *Polymer* 48:1695–1710
- Thomas R, Yumei D, Yuelong H, Le Y, Moldenaers P, Weimin Y, Czigan T, Thomas S (2008) Miscibility, morphology, thermal, and mechanical properties of a DGEBA-based epoxy resin toughened with a liquid rubber. *Polymer* 49:278–294
- Thomas R, Ahmad I, Ahmad S, Koshy S (2014) Blends and IPNs of natural rubber with thermo-setting polymers. In: Thomas S, Chan CH, Pothan L, Rajisha KR, Maria Hanna J (eds) *Natural rubber materials*. Royal Society of Chemistry, Cambridge, pp 336–348
- Tripathi G, Srivastava D (2008) Studies on the physico-mechanical and thermal characteristics of blend of DGEBA epoxy, 3,4 epoxy cyclohexylmethyl, 3',4'-epoxycyclohexane carboxylate and carboxyl-terminated butadiene co-acrylonitrile (CTBN). *Mater Sci Eng* 496:483–493
- Verchere D, Sautereau H, Pascault JP, Moschiar SM, Riccardi CC, Williams RJJ (1990) Rubber-modified epoxies. I. Influence of carboxyl-terminated butadiene-acrylonitrile random copolymers (CTBN) on the polymerization and phase separation processes. *Appl Polym Sci* 41:467
- Verchere D, Pascault JP, Sautereau H, Moschiar SM, Riccardi CC, Williams RJJ (1991) Rubber-modified epoxies. II. Influence of the cure schedule and rubber concentration on the generated morphology. *J Appl Polym Sci* 42:701
- Walker I, Collyer AA (1994) Rubber toughening mechanisms in polymeric materials. In: Collyer AA (ed) *Rubber toughened engineering plastics*. Springer, Netherlands, pp 29–56
- Yahyaie H, Ebrahimi M, Vakili Tahami H, Mafi ER (2013) Toughening mechanisms of rubber modified thin film epoxy resins. *Prog Org Coat* 76:286–292
- Yee AF, Pearson RA (1984) *Toughening mechanism in elastomer-modified epoxy resin-Part 2*. Schenectady, New York
- Zhou W, Cai J (2011) Mechanical and dielectrical properties of epoxy resin modified using reactive liquid rubber (HTPB). *J Appl Polym Sci* 124:4346–4351

Padmanabhan Krishnan

Abstract

The water and solvent sorption behavior of epoxy/rubber polymer blends of various structures are discussed in this chapter. The sorption phenomena are explained in these blends with respect to the surrounding temperature, relative humidity, and moisture concentration profiles based on parameters like diffusion, part and laminate thickness, weight gain due to absorption over time, and saturation equilibration. A reasonable correlation is attempted through Fickian and non-Fickian absorption models for epoxies, rubbers, their blends, and the observed properties. A brief note is presented on the viscoelastic models of environmentally affected blends. The observed changes in the physical, chemical, mechanical, and electrical properties of the blends are documented. Here again, distinction is made between the sorption characteristics of solid rubber/epoxy and liquid rubber/epoxy blends. The hygrothermal performance of fiber composites fabricated with epoxy/rubber blends as the matrix materials is also discussed and presented along with their applications. Limitations, implications, and suggestions for future work have been included at the end of the chapter.

Keywords

Epoxy/rubber blends • Moisture uptake • Solvent sorption • Osmosis • Diffusion • Concentration profile • Absorption models • Hygrothermal conditioning • Property degradation

Contents

Introduction	316
Hygrothermal Effect on Structure	318
Design Criteria and Hygrothermal Influence	321

P. Krishnan (✉)
VIT-University, Vellore, India
e-mail: padmanabhan.k@vit.ac.in

Hygrothermal Conditioning and Evaluation	321
Theories and Laws of Sorption	323
Diffusion Models and Mechanisms	327
Performance and Function After Hygrothermal Attack	331
Summary and Conclusions	333
Implications and Suggestions for Further Work	334
References	335

Introduction

The epoxy resins and their hardeners are mixed together to cure in to a highly cross linked and chemically resistant thermosetting plastic solids (Lee and Neville 1967). Their functionality and the presence of initiators, other catalysts, and diluents determine their hardness, strength, stiffness, and above all their toughness, i.e., resistance to crack initiation and propagation. Epoxy matrices are basically brittle in nature, higher the functionality more the brittleness. Hence, tetrafunctional epoxy resins cured with anhydrides or tetramines are more brittle than their difunctional counterparts. This general drawback of epoxy systems is often countered by blending them with tougher materials like liquid rubber, thermoplastics, solid rubbers, and particulate fillers (Garg and Mai 1988).

In order to retard matrix cracking of epoxy systems in various service applications, liquid rubbers are often added up to 15 phr (parts per hundred resin) in the mixtures of epoxies and catalysts and homogenized thoroughly before phase separation occurs (Gabriel and Advani 2003). Solid rubber particles are also added instead of liquid rubbers if a tighter control over rubber particle size distribution and the fracture properties is required (Padmanabhan 2015). EPDM (Ethylene Propylene Diene Monomer) rubbers are also used as solid particulates to impart toughness in epoxy systems as their atmospheric and weathering resistance is also excellent (Blow and Hepburn 1982). This enables the use of such rubber toughened epoxies for long-term service life-oriented applications where mechanical property degradation over the life span is comparatively within the acceptable limits.

Epoxies or “Epi oxygen” positioned DGEBA (Diglycidyl Ether of BisPhenol A) can be cured in many ways in to solid networked polymers. They can be anhydride cured giving rise to copolymers, catalytically cured using BF_3 amine complexes leading to ring opening polymerization of the terminal epoxide groups or amine cured that generates hydroxyl groups. Here, the BF_3 amine group cured molecules are terminal in polymerization and have very low moisture concentrations at equilibrium. In the case of amine cured epoxies, the hydroxyl groups act as polar centers for hydrogen bonding with molecules of absorbed moisture. Depending on the type of the amine group, i.e., whether it is primary, secondary, or tertiary, variations in moisture concentrations and deviations from Fickian diffusion behavior can occur (Pritchard 1999). To appraise the young reader on what it means, we transport ourselves to 1855, when physiologist Adolf Fick first reported (Fick 1855a) his now-well-known laws governing the transport of matter through matter by diffusive

means. Fick was inspired by the earlier experiments of Thomas Graham, which were rather incomplete as no laws could be deduced from his work. The Fick's law is very much analogous to the relationships discovered by other eminent scientists. Darcy's law on hydraulic flow, Ohm's law on charge transport, and Fourier's Law on heat transport were the other laws that were laid down around the same epoch that dwelt on some form of transport or the other.

Depending upon their functionality, viscosity, wettability, moisture, and fluid uptake susceptibilities, epoxy systems are used in mechanical, aerospace, consumer, civil and electronic applications as adhesives, sealants, laminating resins, fillers, matrix materials, encapsulants, and boards.

The types and varieties in rubber utilized for blending with other plastics are large (Blow and Hepburn 1982). Though latex natural rubber and synthetic rubbers like SBR (Styrene Butadiene Rubber), Butyl, Nitrile, Stereoregular polymer rubbers, Ethylene propylene rubbers, Fluorocarbon rubbers, Silicone rubbers, Nylon rubbers, Chloroprene rubber, (ABS) Acrylonitrile Butadiene Styrene rubbers, Polyurethane rubbers, Neoprene, Isoprene, and vulcanized rubbers are currently in the market, only a handful of them are blended along with epoxies for obtaining the required properties and service life.

Rubbers require certain traits to be compatible with epoxies. Liquid rubbers go through a phase separation and cannot be added more than say about 15 phr in an epoxy/hardener system as then they would be the majority matrix materials causing deterrence in strength and stiffness. Open ended molecular systems with ionic, polar, and unsaturated liquid structures are mandatory for blending with epoxies in order to have good bonding but are moisture prone as they are open ended and susceptible to hydrogen and hydroxyl bond formations. Among rubbers, fluorocarbon rubbers, ABS rubbers, EPDM rubbers, and nitrile rubbers with high acrylonitrile content are fairly moisture and oil resistant. Epoxies are normally blended with carboxyl terminated, hydroxyl terminated, or amine terminated butadiene rubbers as it is believed that termination provides fewer avenues for moisture and fluid ingress. The CTBN (Carboxyl Terminated Butadiene Rubber) blended epoxies are very popular with those in the carbon fiber prepreg or the preimpregnated fiber/epoxy manufacturing trade as the epoxy-rubber blend provides for high fracture toughness even under conditions of hygrothermal attack – meaning combined attack of moisture and temperature (Thomas 2014). The isobutylene-isoprene rubbers have moderate to high moisture resistance and can be blended with epoxies.

Commercially many epoxy and modified epoxy systems are available for composite applications. (www.Cytec.com; www.hexcel.com; Ciba-Geigy Datasheet 1983, 1984). As some of the rubber modified epoxies are more susceptible to moisture absorption than the epoxies themselves, it becomes important to measure their moisture saturation equilibrium to evaluate their impact on the mechanical properties. Table 1 provides basic information about the moisture content at saturation for epoxies and modified epoxies (Lee 1989). Some of the rubber toughened epoxies are also listed for their moisture susceptibility. It is to be understood that a long-term moisture saturation of 1–3 wt% is considered good, a range between 3.1

Table 1 Moisture absorption at saturation for epoxies and modified epoxies

Material supplier	Designation	Polymer type	Moisture absorption at saturation (Wt%)
Shell	9101	Epoxy	2
Union Carbide	4901A (MDA)	Epoxy	7.2
Hercules	2220-1	Toughened epoxy	3.8
Hercules	2220-3	Toughened epoxy	4
Am. Cyanamid	907	Multiphase epoxy	5.1
Fibredux	914	Rubber toughened epoxy	7
Hexcel	F155	Rubber toughened epoxy (250 °F)	9.4

and 7.5 wt% is considered average, and anything beyond 7.5 wt% is not acceptable in sensitive industries like aerospace.

Hygrothermal Effect on Structure

Polymers are prone to absorb moisture over time and become swollen and plasticised that deter their mechanical and electrical function. As water is electrically and thermally conducting, these properties change with time once a polymer is put into service. For a detailed data and understanding of the moisture, oil, acid, alcohol, and alkali attack including the weathering behavior of polymers and elastomers, the reader is directed to the works of Billmeyer (2015). To know the influence of hygrothermal attack on the mechanical, chemical, and bio-medical properties of polymeric composites a thorough knowledge of equilibration saturation conditioning and diffusion kinetics is required (Padmanabhan 2006, 2009). Another investigation explains the influence of marine environment on the durability of plastics and reinforced plastics (Pritchard 1999). As the temperature of moisture conditioning increases up to 100 °C the moisture concentration at equilibrium also increases as due to swelling and micro-cracking moisture uptake shows a rise in the concentration level. Void content, resin type, temperature, stress levels, presence of flaws, cracks, and spiking have a pronounced effect on moisture absorption and fluid uptake by polymers (Mallick 1994). Adamson has proved a strange but noticeable reverse thermal effect in the moisture absorption characteristics of cast epoxy systems where the susceptibility increased with a sudden drop in the temperature (Adamson 1983).

Hydrolysis of cured epoxies is discussed in detail by Powers (2009). However, the chemistry of water reaction with cured epoxy blends has not been well

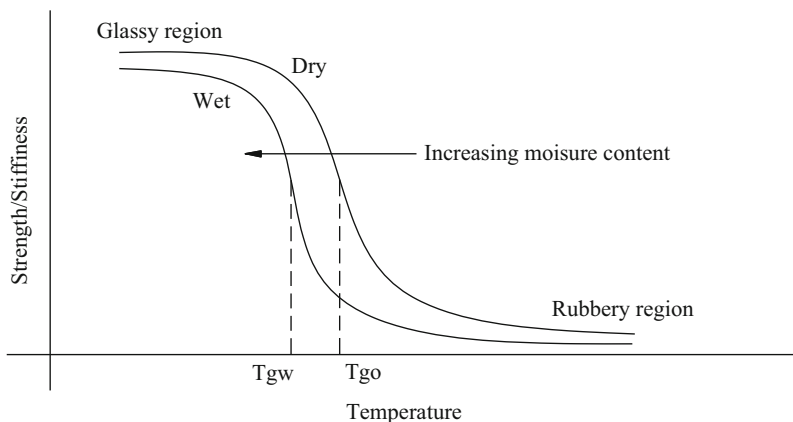


Fig. 1 A schematic illustration of Wet T_g forming with moisture content

investigated. The “epi” oxygen at the center of CH_2 and CH bonds that lead to the epoxy signature nomenclature open up and form hydroxyl bonds due to the reaction with moisture or water. Certain other organic compounds are also capable of hydrolyzing epoxies and their blends.

As the epoxies possess higher T_g (Glass Transition Temperatures) than the rubbers in their blends, the T_g of the blends are in between that of the rubber and the epoxy. To make things worse, the wet T_g of the blends after moisture saturation equilibrium is attained gets lowered from the dry initial T_g due to plasticization and nonlinear viscoelasticity setting in (Gibson 1994; Chamis and Sinclair 1982; Padmanabhan 2016). The relationship between dry T_g and wet T_g of plastics in general is illustrated schematically for moisture saturation conditions, in Fig. 1.

The hydrothermal degradation of the modified epoxy strength or stiffness can be estimated by using an empirical Eq. 1a, b (Gibson 1994) that is

$$F_m = \frac{P}{P_0} = \left[\frac{T_{gw} - T}{T_{go} - T_o} \right]^{1/2} \quad (1a)$$

and

$$T_{gw} = (0.005M_r^2 - 0.1M_r + 1.0)T_{go} \quad (1b)$$

Where,

F_m = Mechanical property retention ratio,

P = Strength or stiffness after hydrothermal degradation,

P_0 = Reference strength or stiffness before degradation,

T = Temperature at which P is to be predicted ($^{\circ}\text{C}$),

T_{go} = Glass transition temp. for reference dry condition,

T_{gw} = Glass transition temperature for reference wet condition at moisture content corresponding to property P ,

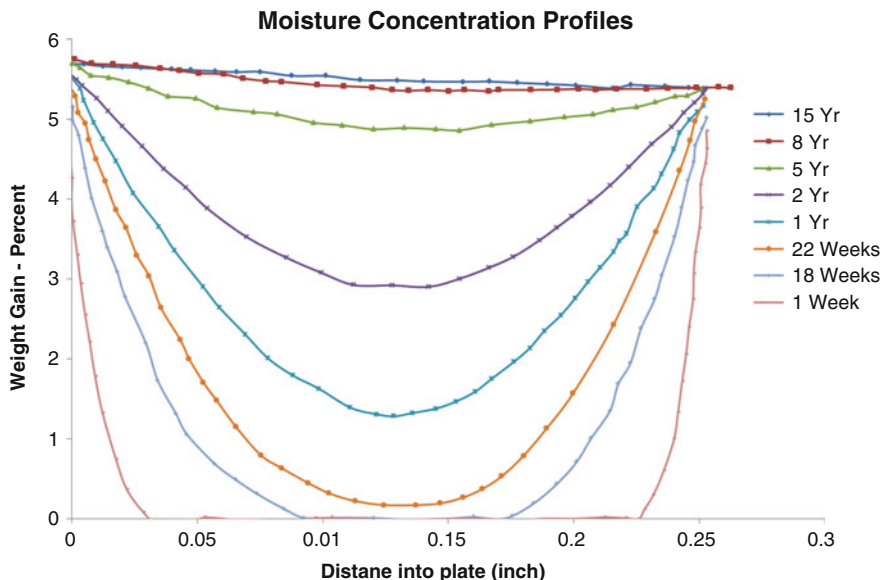


Fig. 2 Time variable moisture concentration profiles across the thickness of a typical epoxy resin plate at 100 °F and 100% RH

T_o = Test temp. at which P_o was measured (25 °C),

M_r = Weight percent of moisture at equilibrium.

Figure 1 depicts lowering of the T_g in wet conditions and that of the mechanical properties attained after equilibration due to moisture or fluid ingress. It must be stated that generally accelerated or humidity chamber conditioning at room or an elevated temperature is carried out between 50% and 100% RH (Relative Humidity) conditions. Many recommended combinations of temperature and RH are practiced for understanding the influence of hygrothermal attack on epoxies, modified epoxies, and composites (ASTM 5229M 1998). Many investigators have estimated the moisture concentration profiles across part or specimen thicknesses for thin and thick sections based on parameters like diffusivity, moisture concentration, diffusion coefficient, concentration gradient, time, and temperature. Figure 2 depicts one such investigation where the weight gain due to absorption over time is illustrated for conditioning at a fixed temperature and RH from few days to years for an epoxy resin specimen with a fixed thickness.

In amorphous materials like epoxy-rubber blends, diffusion is characterized by migration of molecules themselves. The structure is characterized by very strong covalent primary bonds which hold the molecules together and by much weaker secondary bonds between the molecules. Diffusion here is analogous to interstitial diffusion. If the polymer is bulky and heavily networked as in the present case, motion becomes difficult; polymer diffusion rate measurements are often used to relate to molecular weight determination as there is a relationship between diffusion

and molecular weight of a polymer. It is interesting to note that the evolution of the size of a rubber particle vs. its molecular weight has a direct influence on the diffusion of water through the bulk of it when present as a phase in epoxies. As the rubber particle size grows in evolution its molecular weight increases and the susceptibility to moisture diffusion decreases. On the other hand, the susceptibility of solid rubber additions, like EPDM, is directly related to their structure and has no bearing on the evolution of a phase from a liquid state in an epoxy blend that is in a state of curing (Padmanabhan 2015).

Design Criteria and Hygrothermal Influence

For a detailed understanding of the hygrothermal influence on the epoxies, epoxy–rubber blends, and their composites the reader is referred to the works of Joseph R. Soderquist. Much of the work is available in the form of reports on aircraft composite structures as the hygrothermal influence, and its effect on the function of FRP structures is a decisive factor in the qualification of aerospace polymer composites (Soderquist 1998; MILHDBK-17 and MIL-HDBK- 17B 2002). Parida et al. have investigated the airworthiness considerations in the type certification of FRP (Fiber Reinforced Plastics) composites for civil aircraft development with special relevance to mechanical property degradation after hygrothermal conditioning up to saturation (Parida et al. 1996). It is noteworthy that only the mechanical property evaluated after degradation due to hygrothermal saturation needs be considered as design criteria. The statistical A-basis and B-basis criteria for reliability in the strength and stiffness data have also been addressed. An A-basis design allowable of a component has at least a 99% probability of survival with a confidence level of 95%. But a B-basis design allowable of a component possesses only a 90 plus% probability of survival with a confidence level of 95% (Mallick 1994). It is seen that a statistical approach is adopted for polymeric and polymer composite materials to qualify them for critical applications as their mechanical property variability is higher than metallic materials. Figure 3 gives the moisture weight gain for a neat epoxy resin as a function of time for different humidity conditions. When many such samples are conditioned and tested later for mechanical properties, one could generate the required statistical reliability data.

Hygrothermal Conditioning and Evaluation

Natural aging of epoxy-rubber blends depends on the humidity and temperature conditions of the real environment. This means a local fluctuation of the daily temperature and humidity changes over a period of time that are required for saturation conditioning of the part or component. Random changes in temperature and relative humidity also cause absorption and desorption on a random scale by and from the blend. Natural aging is associated with weathering, discoloration, and degradation of the material which depend upon the randomness of the weather

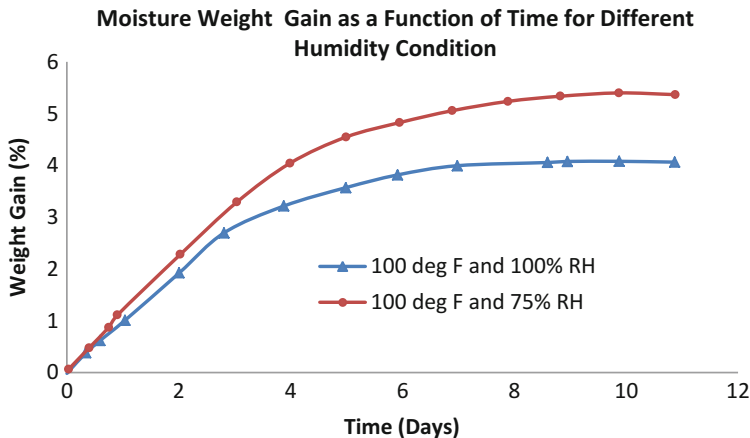


Fig. 3 Moisture weight gain for a typical neat epoxy resin as a function of time for different humidity conditions

conditions and the material response to it. Natural rubbers in general become brittle with moisture attack and harden in an epoxy blend. So they tend to embrittle the structure which is undesirable. The reactions responsible for this are condensation reaction and hygrothermal curing. Hence, the addition of natural rubbers to epoxies is never carried out as the synthetic rubbers enhance the toughness even under the influence of moisture or fluid uptake.

Artificial aging on the other hand is carried out in a humidity or environmental chamber under set conditions of relative humidity and temperature. The conditions vary from a cold-dry to a hot-wet setting. Some of the interesting standard practices for plastics and reinforced plastics are listed here (ASTM D 570 1995; ASTM D 618 1996; ASTM D 696 1991; ASTM D 756 1993; ASTM D 5229/D 5229M 1998). It must be emphasized here that none of the above standards refer to epoxy-rubber blends in particular. Some of them, like the D 5229 M, are considered more applicable. Humidity chambers normally possess temperature ranges of $-60\text{ }^{\circ}\text{C}$ to $100\text{ }^{\circ}\text{C}$ and relative humidity ranges from 0% to 100% RH. Depending on local, national, or international geographic needs, the temperature and the RH settings are fixed anywhere between $25\text{ }^{\circ}\text{C}/50\%$ RH for a dry room temperature environment to a $70\text{ }^{\circ}\text{C}/100\%$ RH hot-wet environment. The artificial weather conditions can also be replicated over weeks or months of conditioning with due changes for summer, fall, winter, and spring or a single phase conditioning that spans over the required time can also be deployed. Needless to say, some of the artificial and accelerated conditioning procedures provide us with the worst case influence and performance. They are normally used by standards that are meant to test and qualify a part or a component for performance in a rigorous environment, like the MIL-HDBK standards. Here again, not all the standards recommend conditioning up to moisture saturation equilibrium (which means that under conditions of a set temperature and relative humidity, the part or the component can no longer allow moisture or fluid

ingress after a given time). The swelling, change in the coefficient of thermal expansion (CTE), and weight gain due to sorption of an epoxy-rubber blend vary depending on a 24 h conditioning or a saturation conditioning. Here again, the time taken for postsaturation conditioning must also be taken into account for performance evaluation as it affects degradation.

Long-term and short-term exposures to moisture and fluids under set conditions of temperature are recommended depending upon the application. The deficiencies of short-term conditioning and evaluation procedures recommended for a part that otherwise functions in a super saturated critical environment are critical and lead to a premature and terminal behavior. For example, a polymer device meant to survive in a human body must go through the rigors of saturation and postsaturation conditioning and ensuing tests to qualify it for further use. Short-term accelerated conditioning would suffice for a third or second stage booster rocket part or component that is made of a polymer or its blend. Epoxy-rubber blends require long-term conditioning and evaluation when used in electronic packaging applications but need only a short-term conditioning and evaluation when used in a gasket application for a one time operation.

To illustrate the importance of natural or long-term aging over artificial or accelerated aging the reader is directed to Fig. 4 that explains this phenomenon through an analogy. A chicken egg is incubated for 21 days which yields a chicken, but cooking an omelet, boiling an egg, or toasting a bull's eye amounts to various schedules of accelerated aging as these three products are obtained in less than ten minutes. Figure 4 illustrates only the irreversible component of accelerated aging. Long-term aging and natural aging are understandably irreversible. Short-term attacks need not be.

Table 2 provides the algorithm for moisture conditioning of the epoxy-rubber specimens up to saturation and the method to prepare the specimens for subsequent mechanical testing in tension, compression, flexure, impact, fatigue, and creep. The results of the mechanical testing assist in the evaluation of degradation or improvement in the respective properties after conditioning.

Theories and Laws of Sorption

The phenomenon of moisture and fluid ingress or uptake is most often governed by a thermodynamic driving force, osmosis, reverse osmosis, or diffusion. Diffusion is known as transport of matter through matter, assisted by concentration gradient and temperature (Chiang et al. 1997) Thus, according to Arrhenius relationship,

$$D = D_0 \exp(-E_a/RT) \quad (2)$$

Where D = Diffusivity, D_0 = material constant, E_a = Activation energy for diffusion, R = Universal gas constant, and T = Absolute Temperature.

In polymeric materials $\log D$ versus $1/T$ falls on a straight line, which means that this law is obeyed. In polymeric materials moisture has been shown to cause

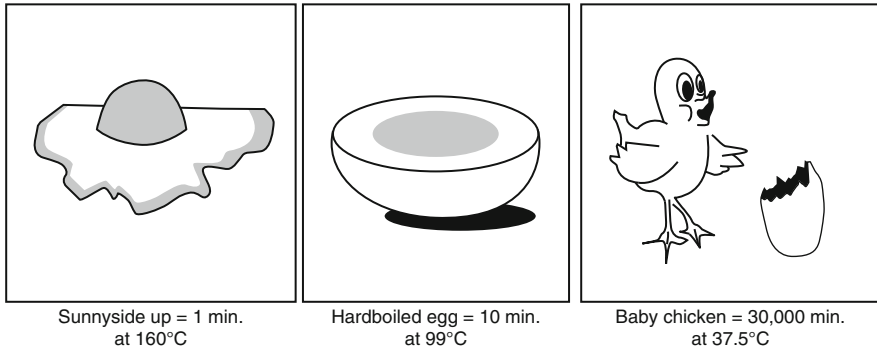
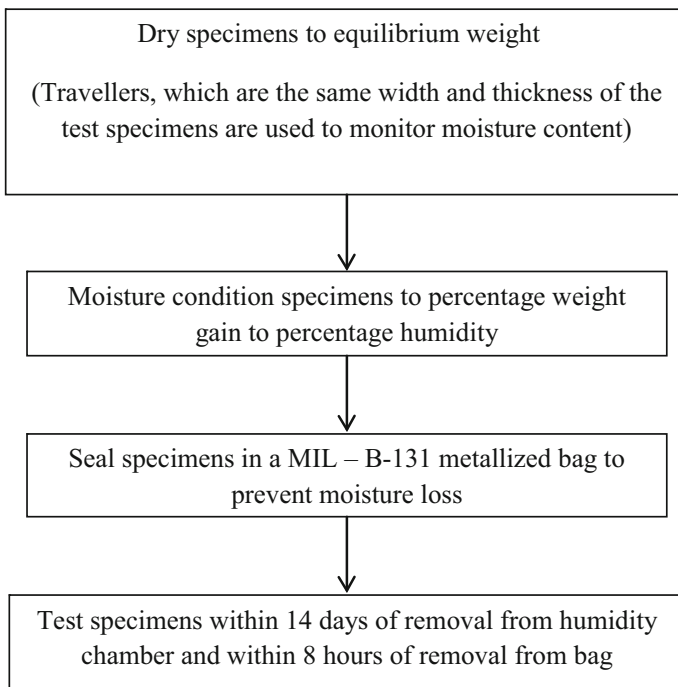


Fig. 4 Accelerated aging through an analogy

Table 2 Algorithm for saturation conditioning and testing procedure

Procedure for environmental conditioning of test specimens



hygroscopic expansions or contractions analogous to thermal strains. Moisture induced strains in isotropic materials like epoxy-rubber blends can be expressed as a function of βc , where β is the coefficient of hygroscopic expansion and c is the moisture concentration.

Diffusion can be termed Fickian or Non-Fickian. Fick's first law (Fick 1855) in one dimension states that the particle flux J (number per unit area per unit time) in a steady state is proportional to the concentration gradient dC/dx . The proportionality constant D is called diffusion coefficient and is written in m^2/s . It is a strong function of temperature and composition and only in some limiting cases can it be taken to be independent of concentration.

$$J = - D \cdot dC/dx \quad (3)$$

The spatial and time distribution of concentration varies from source to source, like a point source, semi-infinite source, line source, thin film source, or a spherical source.

Fick's second law (Fick 1855) describes the accrual or depletion of concentration, C , over time when steady state conditions are not achieved and is obtained from the spatial derivative of the flux:

$$\frac{\partial C}{\partial t} = - \frac{\partial J}{\partial x} = D \cdot [(\partial^2 C)/(\partial x^2)] \quad (4)$$

Fick's laws are mass transport analogues to heat transfer laws by Fourier and the mathematical solutions are similar. In continuum diffusion, Fick's second law can be used to determine the spatial concentration distribution. The value of D can vary significantly in epoxy-rubber blends as liquid rubbers, solid rubbers, natural, and silicone rubbers are blended with many types of epoxies. The atomistic and molecular mechanisms of diffusion determine the D parameter significantly (Crank 1975). As epoxy-rubber blends are molecular in structure, we will not digress into the atomistic processes of diffusion that are inherent in only alloys and binary inter-metallics.

Random walk diffusion where an atom or a molecule jumps from one location to the other with an equal probability in the presence of a concentration gradient, obeys Fick's first law. The frequency with which the atom or the molecule jumps depends on factors like the energy for migration, enthalpy of migration, temperature, and the availability of jump sites. The availability of intermolecular distances in epoxies and rubbers, cracks, flaws, microcracks, voids, cells, and blowholes is synonymous with the availability of lattice defect concentration in crystalline solids. These provide the jump sites or sites where moisture concentrates down through diffusion. Water or solvent molecules tend to diffuse through the epoxy-rubber blends into such trap sites and achieve saturation depending upon the driving force.

Diffusion is also a thermally activated process as described earlier in reference to the Arrhenius relationship (Shewmon 1989). Here, the driving force for water diffusion or solute/ion diffusion is small compared to the thermal energy kT and can be electrical or chemical potential. It is to be emphasized that the activation energy term, E_a , contains other energy terms such as the defect formation or association energy in addition to the migration enthalpy caused by the thermal activation.

The diffusion coefficient is often associated with impurity diffusion, chemical diffusion, or solute diffusion, interstitial diffusion, defect diffusion, boundary diffusion at the interfaces between the epoxy and the rubber phases separated due to curing, ambipolar diffusion, and interdiffusion. The ambipolar diffusion coefficient is restricted to ionic solids and is somewhat relevant to salt or marine water ingress into plastics and reinforced plastics. One more quantity of interest is the mobility of water or solvent molecules that is related to diffusivity through the Einstein-Nernst equation.

$$D_i = kT B_i \quad (5)$$

Here, D_i = Diffusivity, k = Boltzmann's constant, T = Absolute Temperature, and B_i is the absolute mobility that is defined as velocity/force due to the gradient in the driving force. Though the Einstein-Nernst equation is atomistic, it can be applied to chemical and electrical mobility correlations for solute diffusion like salt from marine water, or solution diffusion in general, causing a change in electrical conductivity provided a gradient is detected. The influence of electrochemical potentials in conducting epoxy-rubber-complex blends is a less investigated topic and many investigations are awaited.

Chemical diffusion is characterized by Hartley-Kirkendall effects. In case of interdiffusion, the interdiffusion coefficient is a single coefficient D which is written as

$$D = X_B D_A + X_A D_B \quad (6)$$

Where X_B and X_A are the mole fractions of species A and B. D_A is the diffusion coefficient of B in pure A and D_B , vice versa (Brophy et al. 1980). Interdiffusion in the case of solvents, impure water, and epoxy-rubber blends is a less researched topic. Though basic literature is available in the interdiffusion of marine water and epoxies, much needs to be done in the area of chemical diffusion in epoxy blends.

In general, there are three types of diffusion in our system of interest. Surface diffusion spreads through cracks, notches, and the likes; interface boundary (IB) diffusion between two phases, viz., epoxy and rubber; and volume diffusion of solvents, solutions, and solutes through the mass of epoxy-rubber blends. Their relative intensities and amounts are in the following order:

$$E_a(\text{Vol}) > E_a(\text{IB}) > E_a(\text{Surf}), \quad (7a)$$

$$D(\text{Surf}) > D(\text{IB}) > D(\text{Vol}), \text{ and} \quad (7b)$$

$$D_o(\text{Vol}) > D_o(\text{IB}) > D_o(\text{Surf}) \quad (7c)$$

As D and D_o appear on either side of the Arrhenius equation, the trends in diffusion coefficients, D , are reverse. Volume diffusion is severely affected by the presence of blow holes, cracks, microcracks, cells, and other flaws. It is also affected by the intermolecular distance between the epoxy molecules and rubber molecules.

In short, vacancy and interstitial diffusion are the major mechanisms in volume diffusion of water or solvents into these blends. Diffusion can be studied at the interfaces with the help of markers. The migration of the markers is indicative of diffusion over a volume. An incremental addition of radio isotopes assists in the process of diffusion measurements through detection of their migration through diffusion.

Diffusion through a surface area is one dimensional. So, one-dimensional Fourier and Fick's equations can be employed. In one-dimensional diffusion, temperature will approach equilibrium about a few tens of times faster than the moisture concentration. This is called the Lewis number which is a function of density, thermal conductivity, and specific heat capacity at constant pressure and diffusivity (Soderquist 1998). The reader is referred to Fig. 2 where diffusion across a thick cast epoxy resin plate is illustrated. It is noted that the temperature equilibrium is reached much earlier than the moisture equilibrium. Higher ambient temperatures accelerate the process.

Fourier's three-dimensional transient heat conduction equation can be written as

$$\rho C_p \frac{\partial T}{\partial t} = \frac{\partial}{\partial x} \left(K_x \frac{\partial T}{\partial x} \right) + \frac{\partial}{\partial y} \left(K_y \frac{\partial T}{\partial y} \right) + \frac{\partial}{\partial z} \left(K_z \frac{\partial T}{\partial z} \right). \quad (8)$$

where ρ is the density, C_p is the specific heat capacity at constant pressure, and K is the thermal conductivity. T and t are temperature and time, respectively. The symbols x , y , and z denote the spatial directions.

Fick's three-dimensional mass transfer equation (diffusion) can be represented as

$$\frac{\partial C}{\partial t} = \frac{\partial}{\partial x} \left(D_x \frac{\partial C}{\partial x} \right) + \frac{\partial}{\partial y} \left(D_y \frac{\partial C}{\partial y} \right) + \frac{\partial}{\partial z} \left(D_z \frac{\partial C}{\partial z} \right) \quad (9)$$

This equation represents the bulk diffusion in a solid. Bulk diffusion in epoxy-rubber blends can be mathematically expressed by the above equation where the moisture concentration varies spatially and along the time scale as $C(x, t)$. It is to be noted that time is a kinetic variable unlike temperature which is a thermodynamic variable. D_x , D_y , and D_z are the diffusion coefficients along the x , y , and z direction, respectively.

Diffusion Models and Mechanisms

Diffusion models are essentially twofold; single phase and two phase absorption models are fitted to epoxies and their blends (Bonniau and Bunsell 1984). Single phase water absorption is noticed when diamine hardeners are used to cure epoxies. On the other hand, a two phase absorption is noticed when the same epoxy resin is cured with a dicyandiamide hardener. For an easy understanding the single and the two phase models are illustrated in Figs. 5 and 6.

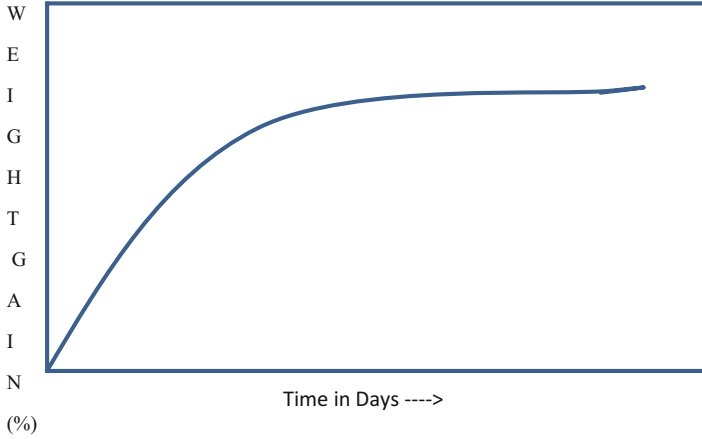


Fig. 5 A schematic diagram of a single phase absorption model

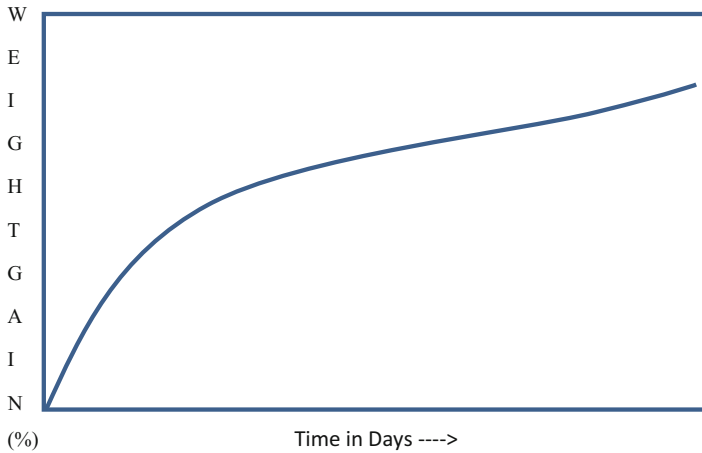


Fig. 6 A schematic diagram of a dual phase absorption model

In single phase diffusion the weight gain due to absorption can be expressed in terms of two parameters, the diffusivity D and the weight gain at saturation $M_m\%$. In a two phase model, the weight gain $M\%$ as a function of time t is written in terms of four parameters, the diffusivity D , weight gain at saturation $M_m\%$, the probability a of a molecule of water passing from a combined state (with the matrix) to the free phase (not combined with the matrix) and the probability β of a molecule of water passing from the free to the combined phase. This two phase model is also called Langmuir model, named after the researcher who coined it first. These theories and models are based on Fick's laws of diffusion. However, the deviation of Langmuir model from Fick's laws is noticeable in many systems and more so in thin slabs and

laminates. Membranes follow the Langmuir model as two phase absorption models are obeyed by them. Here, the combined state signifies a condition when no further diffusion takes place. Needless to say, the concerned epoxy-rubber blends also exhibit a single or a two phase absorption model depending upon the hardeners and the rubber structures used.

Cross-linked epoxy resins are effective semipermeable membranes. Water molecules can permeate through epoxy resin, but permeation of larger molecules or inorganic ions is inhibited. Hence, the larger polar ions and molecules act as inclusions and osmotic centers, providing a thermodynamic driving force for diffusion of moisture into the blend. Sometimes, blisters are formed due to plasticization, softening, and the osmotic pressure generated. Van't Hoff's relation gives the osmotic pressure, π , as

$$\pi = R.T.c \quad (10)$$

where, R is the gas constant, T is the absolute temperature, and c is the molal concentration of the solute (Van't Hoff 1874).

Fluid ingress is also low into epoxy rubber blends when the salt content is high at lower temperatures. Though insoluble solute inclusions act as osmotic pressure centers, their concentration inhibits moisture uptake beyond a certain level. Soluble salts have an effect on the fluid concentration in the absorbed state and are expected to have a lesser effect. This shows why marine water attack has anomalous effects depending on geography. This also explains why blisters form on epoxy blends with a higher probability in hotter climates where salinity of water is low causing high fluid ingress. Dead Sea near the Mediterranean region is a high saline sea, whereas certain other seas are closer to fresh water ecosystems. Marine structures made of FRPs have a higher life expectancy, provided their affinity with the solutes is understood, ratified correctly, and the anomalous effects well quantified. Boats and Yachts fabricated with epoxy-rubber blend composites and gel coats respond differently in different geographies, and their materials selection, maintenance, and repair schedules have to be adaptive. The reader is now clear as to why bigger FRP ships that are international have not found their way in to mass acceptance, as finding a single material system, fabrication process, maintenance schedule, and repair procedure is like taking up census work in the pacific ocean. Though the experience with smaller FRP ships like HMS Sandown and HMS Wilton have been acceptable locally, it remains to be seen whether a truly intercontinental large ship can survive its expected lifetime without any serious durability issues. It appears that other candidate materials might prove superior to epoxy-rubber blends in this regard.

Fouling and bio-fouling have an impact on the water sorption of structures in marine and fresh water ecosystems. Fouling by marine or fresh water organisms have an adverse impact on the service life of FRP structures if their outgassing or flatulence due to the life processes tend to degrade the FRP surfaces or coatings through biochemical processes and open up the surfaces to severe fluid ingress. Such a bio-hygrothermal attack severely degrades the structural integrity and the durability of marine and fresh water structures (Pritchard 1999). Certain hydrogen and

hydrocarbon producing bacteria affect the adhesive bonding of FRP boat structures making it easier for water sorption to occur between layers and cause degradation of mechanical properties.

In essence, we have covered the isothermal and nonisothermal Fickian and non-Fickian diffusion of moisture and fluids into polymers in general and epoxy-rubber blends in particular. It must be emphasized that non-Fickian diffusion occurs only due to

- The matrix containing voids
- The matrix itself exhibiting a non-Fickian two phase absorption
- Cracks, delaminations, and other damage sites in the matrix
- Moisture propagating along the weak interfaces
- Thinner Langmuir sections existing in an epoxy-rubber part
- Certain highly absorbing epoxy–natural rubber thin sections

Desorption from epoxy-rubber blends occurs due to a change in the ambience that reverses the concentration gradient and thermal spiking in a dry ambient condition after absorption. Reverse osmosis which aids desorption through a semi-permeable epoxy-rubber membrane can occur due to osmotic pressures developed due to solute and solvent ingress. Here, only pure water permeates through the micropores, leaving the ions and heavier salts trapped in the system. Microfiltration which allows particles of 50–100 nm size to permeate through along with water has led to later innovations in ultrafiltration and nano-filtration methods that allow particles of only 5–10 nm and 1–2 nm, respectively, thanks to the development of nano-dispersed epoxy-rubber blends (Thomas 2014; George et al. 2014; Jyotishkumar et al. 2011). For water potability, RO based ultrafiltration would suffice due to the necessity to have mineral water but the applications of nano-phase membranes in producing nano-filtered water lie in the industrial sector where deionized water is required for semiconductor polishing, ion exchange, and high purity applications. Desalination plants have increasingly adopted the nano-phase technology to provide clean water to the society. This has been achieved due to the hygrothermal studies and the desorption studies on polymers carried out by hundreds of investigators. However, these studies are on other polymers and not on epoxy-rubber blends. The author looks forward to the use of epoxy-rubber wastes in landfills that lead to purification of water through permeation and collection as a first step in producing cheap and safe potable water that also addresses the environmental issues.

Viscoelasticity models for epoxy-rubber systems after hygrothermal conditioning are not too different from the nonlinear 3 parameter Martinus Burger model and the 5 parameter friction model of Mat Berg that also is nonlinear. The linear 3 parameter Zener model is rarely acceptable to epoxies here as rubber additions and further plasticization due to hygrothermal attack up to saturation renders them nonlinear. There is no literature available on the influence of hygrothermal conditioning on WLF equations, relaxation times, and retardation times of epoxy-rubber blends.

A Fickian model for diffusion of moisture in permeable fiber polymer composites is discussed by Rao et al. (1984). Springer has contributed significantly to the

understanding of epoxy based composites and their environmental degradation (Springer 1980, 1984, 1988). However, moisture or fluid ingress in epoxy-rubber blends and their composites is a rarely researched topic as seen from the publications that have been documented. Some of the interesting investigations are available as publications with a limited understanding.

Performance and Function After Hygrothermal Attack

A recent investigation describes the effect of hot-wet conditioning and low temperatures on reliability, esp. fatigue of epoxy based composites (Bhanage and Padmanabhan 2016). Another investigation details the effect of hygrothermal conditioning on the mechanical properties of epoxy based composite laminates. Diffusion has been dealt with in greater details (Deepa et al. 2016). Clint and Wicks have discussed the adhesion of contaminants under water on polymer surfaces that are driven by the surface energies (Clint and Wicks 2001). This paper is important from the marine standpoint as it describes the ease at which contamination occurs on epoxy surfaces. Anticorrosive siliconized epoxy coatings have been developed by a team (Gupta and Bajpai 2011). Preparation of blends of epoxidized novolac resin and carboxylic terminated polybutadiene (CTPB) liquid rubber and evaluation of their physico-chemical characteristics has been discussed in detail (Tiwari et al. 2010). Perhaps, some of the solitary but interesting investigations on the effect of moisture on the properties of epoxy-rubber blends come from two investigators (Lin and Yeh 2002). These moisture absorbing materials act as sensors and switches in electrical and electronic applications as conductivity changes due to moisture absorption can be measured (Adhikari and Majumdar 2004). This exhaustive review article details the use of moisture absorbing polymers as moisture sensors with excellent applications. Rare cases of matrix stiffening due to moisture ingress and saturation conditioning are also reported. The changes brought forth by varying humidity, temperature, or thickness of an epoxy based fiber composite is well illustrated in Figs. 7, 8, and 9. It is clear from the illustrations that both Fickian and non-Fickian diffusion and absorption behavior are exhibited by these composites as humidity, temperature, or thickness are varied over a time period.

Thus, it can also be argued that Fickian or non-Fickian diffusion is also extrinsic as well as geometry oriented and need not depend only on the structure of epoxies, epoxy blends, or their composites. The three figures have been included as a case study to emphasize the importance of the time factor as what would look like non-Fickian could become Fickian due to a dwelling or leveling effect at longer time periods approximating with that of the single phase models.

Or it would simply stay non-Fickian and obey a double phase absorption model over a set period of time. This brings out the conditional and vital importance of long-term aging and natural long-term aging of these materials and the evaluation for durability thereafter. The conditioning and evaluation studies could also be simultaneous, if long term. Water and fluid uptake studies should be commensurate with the real time and real environment applications. To reinstate the facts, submersible FRP

Fig. 7 Moisture absorption of a typical HTS carbon/epoxy laminate at different RH values

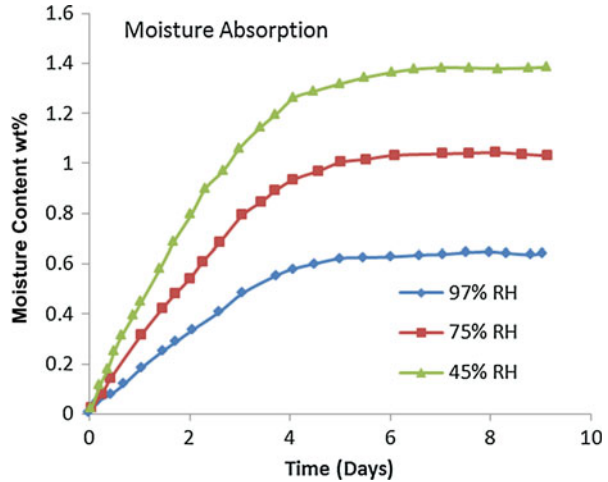
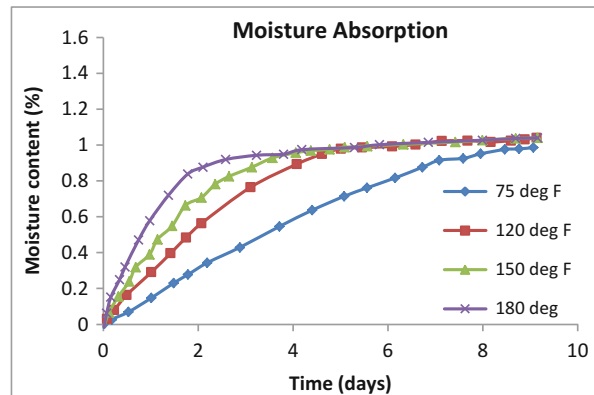


Fig. 8 Moisture absorption of the same laminate at different temperatures



storage tanks in petrol stations are to be evaluated for their long-term durability through rigorous conditioning and evaluation tests whereas that of one stop processes in external medical devices be taken through an accelerated process for qualification for the purpose, as the same material/device cannot be used again due to concerns for hygiene. It is important to add that epoxy-rubber blends are never used for internal bio-medical applications due to toxicity and lack of bio-compatibility and their long-term conditioning do not find any applications here.

Figure 10 illustrates the shrinking operational limit of an epoxy-blend composite due to wet conditioning. Increasing moisture content reduces the operational limits, the thermal ceiling or the MOT (Maximum Operating Temperature), and the failure strain of the composite. Though schematic, the figure is an indication of the degradation in mechanical properties over time when the material is exposed to hygrothermal attack.

Fig. 9 Moisture absorption of the same composite at different thicknesses

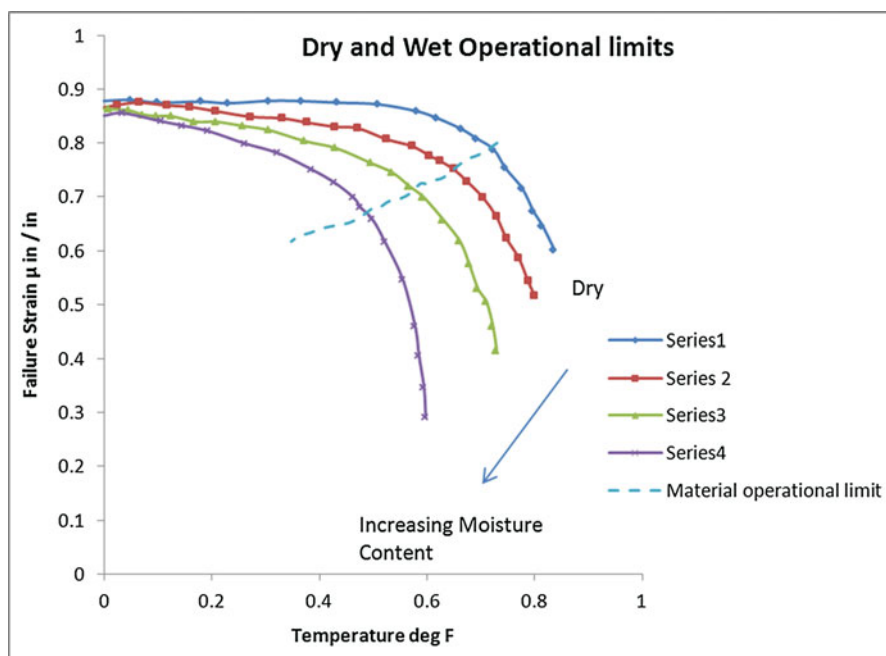
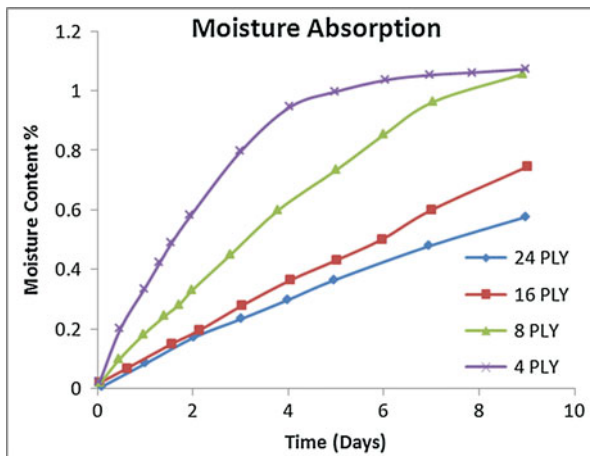


Fig. 10 A schematic illustration of dry and wet operational limits

Summary and Conclusions

The water, solute, and solvent sorption behavior of epoxy/rubber polymer blends of various structures are discussed in this chapter in a detailed but lucid manner keeping the graduate student in mind. The moisture affinities of epoxies, rubbers, and their

blends are quantified to enable materials selection. The sorption phenomena are explained in these blends with respect to the surrounding temperature, relative humidity, moisture concentration profiles based on parameters like diffusion, part and laminate thickness, weight gain due to absorption over time, and saturation equilibration. The statistical design criteria to be adopted after hygrothermal conditioning is listed. Short term and long-term conditioning, natural and artificial aging, the influence of structure, and the observed mechanisms of sorption have been illustrated. Here again, distinction is made between the sorption characteristics of solid rubber/epoxy and liquid rubber/epoxy blends. A summary of the types of diffusion encountered is clearly spelt out with mathematical foundations. A reasonable correlation is attempted through Fickian and non-Fickian absorption models for epoxies, rubbers, their blends, and the observed properties that lead to novel applications. A brief account of the viscoelastic models for the saturation conditioned epoxy-rubber blends is provided. The observed changes in the physical, chemical, mechanical, and electrical properties of the blends are documented. The hygrothermal performances of fiber composites fabricated with epoxy/rubber blends as the matrix materials are also discussed and presented along with their applications. The present state of available literature, implications from availability, and futuristic directions to take are detailed as suggestions for further work at the end.

Implications and Suggestions for Further Work

After a careful perusal and documentation of the available literature, the following topics are suggested as potential themes that researchers could take up as a dissertation, thesis, or funded project work. It is a matter of concern that the ratio of investigations that deal with the dry properties to those which deal with the wet properties for the same systems is alarmingly high. It is imperative that once epoxy-rubber blends are used, their moisture susceptibility and the long-term durability assume significance. Unfortunately, this knowledge gap has assumed gross proportions and the author considers it his prime duty to bring the dearth of literature on this front to the attention of potential case workers and suggest a few problems that are sensitive, considered mandatory, and would lead to further development. Some of the interesting problems could be:

1. Synthesis and development of high temperature epoxy systems with hydrophobic silicone and RTV rubber blends through microstructural modification for extra toughness, strength, and durability.
2. Intelligent use of hygrothermal attack that can be used to modify the chemistry and curing of epoxy systems that would cure in the presence of moisture at elevated temperatures.
3. Nano phase rubber-epoxy networks could be developed for improved hygrothermal resistance.
4. Advanced self-healing interpenetrating polymer networks (IPNs) of rubbers and epoxies that find wide structural applications could be developed.

5. Epoxy-rubber systems that find applications as moisture switches and sensors in electronics and electrical systems could be developed.
6. High temperature epoxy-rubber systems with low moisture absorption can be developed for high voltage insulation applications.
7. Electrochemical aspects of diffusion and mobility that could be evaluated for conducting epoxy-rubber complexes.
8. Moisture resistant high temperature epoxy-rubber blends are potential candidates as sealants, gaskets, O-rings, and pressure sensitive adhesives. These can be synthesized.
9. Chemical diffusion between rigid polymers and solvents/solution is a less investigated topic. This can be taken up.
10. Fickian and non-Fickian diffusion in epoxy-rubber adhesives and film adhesives is structure and dimension dependent. An understanding of the models and the mechanisms is required.
11. Nanoblend epoxy-rubber and nano-porous membranes can be developed for reverse osmosis and solvent purification.
12. Epoxy-rubber wastes can be used in landfill dumps for ground water purification and use.
13. Synthesis and characterization of other hydrophobic rubbers and blending with epoxies that find moisture resistant applications.
14. Studying the influence of hygrothermal conditioning on time-temperature superpositions, WLF equations, relaxation times, and retardation times of epoxy-rubber blends.

The list is unending and exhaustive and the author is hopeful that many able investigators would fill the knowledge gap in future.

References

- Adamson MJ (1983) A conceptual model of the thermal spike mechanism in graphite – epoxy laminates. Long term behaviour of composites, ASTM STP 813, ASTM, Philadelphia, p 179
- Adhikari B, Majumdar S (2004) Polymers in sensor applications. *Prog Polym Sci* 29:699–766
- ASTM D 5229/D 5229M (1998) Moisture absorption properties and equilibrium conditioning of polymer matrix composite materials
- ASTM D 570 (1995) STP for water absorption of plastics
- ASTM D 618 (1996) SP for conditioning plastics for testing
- ASTM D 696 (1991) STP for coefficient of linear thermal expansion of plastics between $-30\text{ }^{\circ}\text{C}$ and $30\text{ }^{\circ}\text{C}$
- ASTM D 756 (1993) SP for determination of weight and shape changes of plastics under accelerated service conditions
- Bhanage A, Padmanabhan K (2016) Fatigue and crashworthiness of automobile materials after DBTT and hygrothermal conditioning. In: Proceedings of the ISET 2016 ICDMM, 19–20 Feb, Pune
- Billmeyer FW (2015) A text book of polymer science. Wiley, New York
- Blow CM, Hepburn C (1982) Rubber technology and manufacture, 2nd edn. Butterworth Scientific, London

- Bonnaïu P, Bunsell AR (1984) A comparative study of water absorption theories applied to glass epoxy composites in Springer GS, Chapter 18. In: Environmental effects on composite materials, vol 2. Technomic Publishers, Lancaster, Pennsylvania
- Brophy JH, Rose RM, Wulff J (1980) Thermodynamics of structure, vol 2, Structure and properties of materials. Wiley Eastern Publications, New York
- Chamis CC, Sinclair JH (1982) Durability/life of fibre composites in hygrothermomechanical environments, ASTM STP 787, ASTM, Philadelphia, PA, pp 498–512
- Chiang YM, Birnie DP III, Kingery WD (1997) Physical ceramics. Wiley, New York
- Ciba-Geigy Information sheet No: FTA 46d, May (1983) pp 1–15
- Ciba-Geigy Information sheet No: FTA 49e August (1984). Duxford, Cambridge
- Clint JH, Wicks AC (2001) Adhesion under water: surface energy considerations. *Int J Adhes Adhes* 21:267–273
- Crank J (1975) Mathematics of diffusion. Oxford University Press, New York
- Deepa A, Padmanabhan K, Raghunadh G (2016) Effect of hygrothermal loading on laminate composites. In: Proceedings of the 2nd international conference on Design, analysis, manufacturing and simulation, (ICDAMS-2016), 7–8 Apr, Chennai
- Fick A (1855a) *Ann. der Physik* (in German) 94:59. doi:10.1002/andp.18551700105
- Fick A (1855a) Diffusion in solids. *Philos Mag* 10:30
- Fick A (1855c) On liquid diffusion. *Poggendorffs Ann* 94:59. Reprinted in *J Membr Sci* 100:33–38
- Gabriel OS, Advani SG (2003) Core-shell rubber/epoxy blends, rheology. In: Advanced polymeric materials, Structure property relationships. CRC Press, Boca Raton
- Garg AC, Mai YW (1988) Failure mechanisms in toughened epoxy resins. A review. *Compos Sci Technol* 31:179–223
- George SM, Puglia D, Kenny JM, Parameswaranpillai J, Thomas S (2014) Reaction-induced phase separation and thermomechanical properties in epoxidized styrene-block-butadiene-block-styrene triblock copolymer modified epoxy/DDM system. *Ind Eng Chem Res* 53:6941–6950
- Gibson RF (1994) Principles of composite material mechanics. McGraw Hill International Editions, New York
- Gupta P, Bajpai M (2011) Development of siliconized epoxy resins and their application as anticorrosive coatings. *Adv Chem Eng Sci* 1:133–139
- Jyotishkumar P, Pionteck J, Haßler R, George SM, Cvelbar U, Thomas S (2011) Studies on stress relaxation and thermomechanical properties of poly(acrylonitrile-butadiene-styrene) modified epoxy-amine systems. *Ind Eng Chem Res* 50:4432
- Lee SM (1989) Reference book for composites technology, vol 2. Technomic, Lancaster, p 61
- Lee HL, Neville K (1967) Handbook of epoxy resins. McGraw-Hill, University of Michigan, New York
- Lin KF, Yeh RJ (2002) Moisture absorption behavior of rubber-modified epoxy resins. *J Appl Polym Sci* 86:3718–3724
- Mallick PK (1994) Fibre reinforced composites, 2nd edn. Marcel and Dekker, New York
- MILHDBK Standards (2002) MIL-HDBK-17-1, Philadelphia, PA, Version: F, Date: Jun-17, (Vol 1–5)
- Padmanabhan K (2006) ‘The need to revise standards on dental restoratives’. A commentary. *Curr Sci* 91(4):418
- Padmanabhan K (2009) Comments on standards on restoratives. *Indian J Dent Res* 20(4):514
- Padmanabhan K (2015) 3rd Interim report, Project No: 1650, ARDB Structures Panel
- Padmanabhan K (2016) A multiphysics based finite element approach to evaluate the reliability of IC packages, Chapter 2. In: Handbook of Research on Advanced computational techniques for simulation based Engineering, IGI Global
- Parida BK, Rao RMVGK, Padmanabhan K (1996) Airworthiness considerations in certification of Frp composite materials for civil aircraft development. In: Proceedings of third jointnational aerospace laboratories Chinese Aircraft Establishment Work Shop on composites, 22–24 Apr, Bangalore, p 9

- Powers DA (2009) Interaction of water with epoxy, SANDIA REPORT, SAND2009-4405, Unlimited Release
- Pritchard G (1999) Reinforced plastics durability. CRC Press/Woodhead Publishing, Cambridge, UK
- Rao RMVGK, Chanda M, Balasubramanian N (1984) A fickian diffusion model for permeable fibre polymer composites, Chapter 16. In: Springer GS (ed) Environmental effects on composite materials, vol 2. Technomic Publishing, Westport
- Shewmon P (1989) Diffusion in solids. TMS, Warrendale
- Soderquist J (1998) Design/certification considerations in composite aircraft structure. Federal Aviation Administration, Springfield, Virginia, Apr 1998
- Springer GS (1980) Environmental effects on composite materials, vol 1. Technomic Publishing, Westport
- Springer GS (1984) Environmental effects on composite materials, vol 2. Technomic Publishing, Westport
- Springer GS (1988) Environmental effects on composite materials, vol 3. Technomic Publishing, Westport
- Thomas S (2014) Rheology of rubber toughened structural epoxy resin systems. Wiley-VCH, New York
- Tiwari AK, Kumar H, Bajpai R, Tripathi SK (2010) Preparation of blends of epoxidised novolac resin and carboxylic terminated polybutadiene (CTPB) liquid rubber and evaluation of their physico-chemical characteristics. *J Chem Pharm Res* 2(3):172–178
- Van Hoff JH (1874) Sur les formules de structure dans l'espace. *Arch Neerl Sci Exactes Nat* 9:445–454

Ternary System of Epoxy/Rubber Blend Clay Nanocomposite 12

Nor Yuliana Yuhana

Abstract

This chapter will be devoted to the study of ternary systems containing synthetic rubber or natural rubber in the epoxy system in the presence of nanoclay. Curing behavior, morphology, and properties of ternary systems containing epoxy, PMMA grafted natural rubber, and nanoclay were elaborated. Two types of nanoclay used in this coverage were natural montmorillonite (Cloisite Na) and organic chemically modified montmorillonite (Cloisite 30B). The amount of nanoclay used were 2,5, and 7 phr, while the amount of rubber was fixed at 5 phr. Poly(etheramine) was used as the curing agent, and the effect of the equivalent and higher molar ratio, 1.05, of amine-epoxy were also studied. The materials prepared were cured unmodified epoxy, cured toughened epoxy, cured unmodified epoxy/clay nanocomposites, and cured toughened epoxy/clay nanocomposites. Some experimental results related to transmission electron microscopy (TEM), scanning electron microscopy (SEM), X-ray diffraction (XRD), Fourier-Transformed infrared analysis (FTIR), differential scanning calorimetry (DSC), thermal gravimetric analysis (TGA), and impact tests were discussed.

Keywords

Epoxy • Rubber • Nanocomposite

Contents

Introduction	340
Polymer Nanocomposites	342
Modification of Epoxies	343
Rubber-Toughened Epoxy	343

N.Y. Yuhana (✉)

Department of Chemical and Process Engineering, Universiti Kebangsaan Malaysia, Bangi, Selangor, Malaysia

e-mail: yuliana@ukm.edu.my; noryuliana@gmail.com

Phase Separation in Epoxy/Rubber Blend	346
Epoxy/Clay Nanocomposite	350
Rubber-Toughened Epoxy/Clay Nanocomposite	353
Curing Reaction Behavior of the Ternary System	354
The Effect of Above-Stoichiometric Concentration of Curing Agent, Rubber, and Clay on Curing Behavior of Epoxy	355
Morphology of Ternary System	356
Glass Transition Temperatures of Ternary System	359
Impact Strength of Ternary System	362
Conclusions	365
References	365

Introduction

Rubber modification is the common way to toughen epoxy. The amount of rubber required is usually limited to concentrations of about 10 wt.% to ensure that the rubber remains as the dispersed phase. The presence of soluble rubber in the epoxy matrix can plasticize the polymer network, hence decreases the glass transition temperature and modulus. Rubber particles with diameter of 40 nm or less are considered as soluble rubber (Russell and Chartoff 2005).

Meanwhile, polymeric nanocomposites have shown a drastic alternative to the conventional filled polymers or polymer blends. The use of nanoparticles depends on the chosen application. For flame retardancy, an addition of layered silicates is workable. For health care uses, such as biozidic polymers, silver and titanium oxide nanoparticles are used. Electrical conductivity can be accomplished by incorporating nano silver or carbon nanotubes (Kny 2007).

Efforts on polymer- clay nanocomposite research, within the last 10 years, have revealed a doubling of the tensile modulus and strength without sacrificing impact resistance for numerous thermoplastic (nylon and thermoplastic olefin) and thermoset (urethane, siloxane, and epoxy) resins through the addition of as little as 2 vol.% layered silicate (Zander 2008).

Nanoclays were the start of polymer nanocomposite filler in the 1990s when Toyota for the first time utilized Nylon6 nanoclay nanocomposites to produce timing belt covers. Other automotive applications appeared rapidly, e.g., by Mitsubishi (Nylon 6 nanoclay engine covers) and by partners of General Motors/Basell/Southern Clay Products/Blackhawk in clay polyolefin nanocomposite materials for step assists in the GMC-Safari and Chevrolet Astro van. The most encouraging and already widely used applications are in food and beverage packaging, barrier liners in storage tanks, and fuel lines in aerospace system, in which polymer clay nanocomposite is used for barrier properties improvement (Koo 2006).

Epoxy/clay nanocomposites exhibit improved thermal, barrier, and mechanical properties (Becker and Simon 2005). The nanoclay may be added to the epoxy resin for high barrier application (Barbee et al. 2002), for aircraft (Garesche et al. 1995), marine

application, printed circuits (Lin et al. 2007; Ma et al. 2007), sealant (Pinnavaia and Lan 1998; Knoll and Mueller 2005), coating for steel structures (Mathivanan and Radhakrishna 1998; Knoll and Mueller 2005), building materials (Killilea et al. 2007), corrosion resistant pipes (Gersifi et al. 2006), consolidants or protectives material for the architectural heritage (Cardiano et al. 2005), liquid crystal displays, organic light emitting devices, electronic paper (Kim et al. 2007), and wind turbine (Lau 2008). Also it has a potential as a composite material for a Moon base (Kondyurina et al. 2006).

The brittleness of epoxy resins can be improved by the introduction of a second rubbery component such as carboxyl-terminated butadiene-acrylonitrile (CTBN) (Ramos et al. 2005; McEwan et al. 1999; Russell and Chartoff 2005), carboxyl-randomized butadiene-acrylonitrile (CRBN) (Zeng et al. 2007; Minfeng et al. 2008), HTPB (Thomas et al. 2008; Ramos et al. 2005), hydroxyl-terminated butadiene-acrylonitrile rubber (HTBN) (Minfeng et al. 2008) and nano rubber (Yu et al. 2008), and PMMA grafted natural rubber (Zainol et al. 2006; Rezaifard et al. 1994). However, the modification by addition of low glass transition temperature (T_g) materials results in a significant decrease of glass transition temperature of the system (Ratna 2001; Thomas et al. 2007; Zainol et al. 2006) and low barrier towards water (McEwan et al. 1999). These could limit its utilization for example in the aerospace, marine application, coating, and IC packaging material.

The moisture diffusion and barrier characteristics of epoxy-based nanocomposites containing organoclay studies showed a systematic decrease with increasing clay content (Kim et al. 2005), and Kinloch et al. concluded that intercalated structure of clay can improve the T_g (Kinloch and Taylor 2003). Also, Kormmann et al. (2001) and Yasmin et al. (2003a, b) found that the flexural modulus increases with small amounts of nanoclay added.

In polymer nanocomposites, a small amount of silicate nanoparticles (less than 5 wt.%) is commonly used. Some researchers observed the catalytic behavior of organically modified clay (Lan et al. 1996; Juwono and Edward 2006; Chen and He 2004; Weibing et al. 2003; Chen et al. 2003). The study on the influence of the stoichiometric epoxy/curing agent ratio on clay dispersion was done by Chin et al. (2001). They observed that addition of high amount of curing agent will lead to intercalated structure of clay in epoxy.

There are also work attempts to modify epoxy-rubber blend by adding the tertiary component such as nanoclay to improve the thermal, barrier, and mechanical properties of the system (Yuhana et al. 2012a; Khairulazfar et al. 2015; Khairulazfar and Yuhana 2016). The factors such as the clay loading, clay surface modification, and concentration of curing agent will result in different morphologies and properties of rubber-toughened epoxy/layered silicate nanocomposite.

The excess of polyetheramine was expected to fill the nanoclay gallery, acting as silicate surfactant in which the formation of primary or secondary ammonium cation (amine salt) may interact well with MMT negative charged surface, hence assist the silicate separation. The intragallery reaction rate may also increase with the slightly higher concentration of curing agent.

Polymer Nanocomposites

Polymer nanocomposites are a class of reinforced polymers that incorporate small amounts of nanosized particles that result in an enhancement of barrier properties, fire resistance, and strength. These improved properties have led to their increased value in panels, barrier, and coating materials in automobiles, as well as packaging. The reinforcement of polymers is becoming an attractive means of improving the properties and stability of polymers. Because of their nanometer-size features, nanocomposites possess unique properties typically not shared by more conventional composites. There are factors that affect the polymer nanocomposite properties such as synthesis methods, morphology of polymer nanocomposites, reaction chemistry, type of nanoparticles and its treatment, and polymer matrix characteristics (Koo 2006). These lead to quite complex analysis to fully understand the property improvement for polymer nanocomposite.

The most commonly reported nanoparticles in the literature are montmorillonite, carbon nanofibers, Polyhedral oligomeric silsesquioxane (POSS[®]), carbon nanotubes, nanosilica, and others.

Nanoclay is the most widely investigated nanoparticle in polymer nanocomposite area. The most common nanoclay used is montmorillonite, and naturally, it is hydrophilic material. This makes them poorly suited to mixing and interacting with most polymer matrices. Under the proper conditions, the gallery spaces can be filled with monomer, oligomer, or polymer. Three types of microstructures can be obtained, namely immiscible, intercalated, and exfoliated systems. In the exfoliated system, single sheets of montmorillonite are dispersed in the polymer matrix. The system is intercalated when one or a few polymer chains are intercalated between montmorillonite sheets. In order to facilitate the dispersion of the layers in a polymer matrix, the organically modified clay is used, and it is available in the market. The earliest generation of MMT organoclays used ammonium surfactants. Other types of surfactants, which are also being studied, are based on stibonium, imidazolium, and phosphonium (Calderon, Lennox, and Kamal). The method of mixing and preparing the nanocomposites samples was reviewed by Wang et al. (2006).

A small amount of silicate nanoparticles, which is less than 5 wt.%, is commonly used in polymer nanocomposites. The interesting feature of the layered silicates is their high aspect ratio. The impermeable clay layers mandate tortuous pathways for a permeant to transverse the nanocomposite. The enhanced barrier characteristics, chemical resistance, reduced solvent uptake, and flame retardance of polymer-silicate nanocomposite all benefit from the hindered diffusion pathways through nanocomposites.

Some of the common thermoplastic and thermoset that used nanoclay to improve the neat polymer properties are summarized in Table 1 and Table 2.

In this study, we focus on epoxy modification by using rubber and nanoparticles. The literature reviews on rubber-toughened epoxy and epoxy/clay nanocomposite are discussed next.

Table 1 Thermoplastic-based nanocomposite

Thermoplastic polymer	Filler	Improved properties	References
Poly(lactic acid) Starch	Cloisite 30B	Water vapor permeability Higher glass transition temperature and higher tensile strength	(Koh et al. 2008); (Tang et al. 2008)
Polyamide	Cloisite 30B	Thermal stability and mechanical properties	(Wang et al. 2004)
Polyethylene	Cloisite 20A	Barrier properties	(Hong and Rhim 2012)
Polyurethane	Triethanolamine treated MMT	Higher decomposition temperature	(Rehab and Salahuddin 2005)
Poly (methylmethacrylate)	Zwitterionic treated MMT	Higher glass transition temperature	(Meneghetti et al. 2004)
Poly(vinyl alcohol) (PVA)	Cloisite Na	Improved barrier properties	(Gaume et al. 2012)

Table 2 Thermoset-based nanocomposites examples

Thermoset based	Filler	Improved properties	Reference
Epoxy	Alkylphosphonium modified MMT Cloisite 30B Aminopropyltrimethoxysilane treated MMT	Anticorrosive Gas barrier, mechanical strength, thermal stability Adhesive strength and thermal stability Mechanical and thermal stability.	(Bagherzadeh and Mahdavi 2007, Dai et al. 2008) (Das and Karak 2010) (Phonthammachai et al. 2011)
Silicone	Gelmax 400	Mechanical properties	(Kaneko et al. 2010)
Polyaniline	Ammonium peroxydisulfate treated MMT	Corrosion resistance	(Hosseini et al. 2011, Akbarinezhad et al. 2011)
Phenolic	Dimethylsulfoxide treated kaolinite	Thermal stability and ablation performance	(Bahramian et al. 2008)
Polyimide	Dodecylamine-treated MMT	Thermal stability and tensile modulus	(Gintert et al. 2007)

Modification of Epoxies

Rubber-Toughened Epoxy

Natural rubber is known for the very good tensile strength, high resilience, excellent flexibility, and resistance to impact and tear. However, due to its unsaturated chain structure and nonpolarity, there are some disadvantages, in which it is less resistant

to oxidation, ozone, weathering, and a wide range of chemicals and solvents (Budiman 2002). Natural rubber used as toughening agent for epoxy were PMMA grafted natural rubber (Rezaifard et al. 1994, Yuhana et al. 2012a,2012b) and epoxidized natural rubber (Hong and Chan 2004).

Synthetic functionalized rubbers were also used to toughen epoxy such as acrylonitrile/butadiene/methacrylic acid rubber (Dispenza et al. 2001), amine-terminated butadiene–acrylonitrile rubber (Zhang et al. 2014), and core-shell rubber particle, namely, poly(butadiene-co-styrene) core/carboxy-functionalized poly(methyl methacrylate-co-styrene) shell (Becu et al. 1997).

The review on phase separation of rubber in epoxy was done by Ratna and Banthia (2004). Francis et al. (2006) described morphology of polymer blend as dispersed, co-continuous, or phase inverted morphologies. They stated that entropic and enthalpic contribution can contribute to the phase separation of the initial miscible homogeneous mixture Hong and Chan (2004) found that the reaction exotherm can be changed by the presence of epoxidized natural rubber because of the participation of the rubber in the curing reaction system. Ratna (2001) observed that the addition of CTPEHA liquid rubber causes a delay in polymerization of the epoxy matrix. The delay can be attributed to the chain extension during prereaction and viscosity effect.

Earlier studies have shown that the morphological parameters depend on several factors such as the chemistry, molecular weight, concentration of the liquid rubber, and the curing conditions (Ratna 2001). Thomas et al. (2008) described the variation of rubber particle sizes at difference epoxy cross-link density levels. Phase separation can occur according to two mechanisms: (i) spinodal decomposition and (ii) nucleation and growth. Kwon (Kwon 1998) studied and described the kinetics of phase separation of rubber particles. Yamanaka et al. (1989) concluded that the morphology of cured epoxy-rubber blends appear in three types of two-phase structure, namely, uniform spherical domain structure, bimodal spherical domain structure, and co-continuous structure, depending on several factors such as type of curing agent and the curing temperature. They also suggested that the two-phase morphology can be controlled by studying the phase separation and chemical reaction. The size of rubbery particles produced via reaction-induced phase separation is usually about 0.5–5 μm in diameter with a volume fraction of 5–20% (Kinloch et al. 2006; Kinloch 2003). Zainolet et al. (2006), using SEM, observed that the average rubber particle size obtained at low content of PMMA grafted natural rubber (1–5 phr) was between 0.4 and 0.8 μm . Kunz (Kunz and Beaumont 1981) mentioned that cavities surrounding rubber particles are an indication of interracial failure due to thermal contraction of the rubber. Thomas et al. (2007) observed that the size of the phase-separated rubber increased by increasing concentration of rubber and decreased with rise in curing temperature.

The main problems with the epoxy-rubber blend are the low glass transition temperature (Zainol et al. 2006) and low barrier properties (McEwan et al. 1999). According to McEwan et al. (1999), the highly polar group attached to rubber (e.g., acrylonitrile group in CTBN) could bind water very well.

The presence of dissolved rubber in epoxy can result in the depression of epoxy T_g (Ratna 2001; Thomas et al. 2007). This may be attributed to the good compatibility between rubber and epoxy that would cause rubber to remain in epoxy matrix and plasticize the system. The increase in T_g may be explained by phase separation of dissolved rubber (Lee et al. 1989; Balakrishnan et al. 2005). Arias et al. (2003) suggested that if the decrease in T_g was not significant, this would indicate that an almost complete phase separation of the liquid rubber in epoxy was achieved. The rubber-modified epoxies showed a significant decrease in the yield stress with respect to the values obtained for the neat epoxy matrices. This results from the stress concentration effect produced by the dispersed particles. The decrease of T_g should also contribute to the observed decrease in the yield stress. The elastic modulus in the glassy state decreases by increasing the volume fraction of the soft rubber particles. Ratna (2001) mentioned that the decrease in modulus can be attributed to the presence of low modulus rubber particles into the epoxy matrix, and the reduction in flexural strength is due to the presence of some amount of rubber. The reduction in T_g could indicate the dissolved rubbers in the epoxy matrix. The increase in the water uptake by increasing CTBN content reflects the ability of the highly polar acrylonitrile group to bind water (McEwan et al. 1999). When rubber is exposed to a gas, it is expected that solution forms at the rubber surface and the dissolved gas molecules diffuse into the interior. The gas molecules migrate from “holes” (free volume) to “holes” (free volume) (Zhang and Cloud 2006).

Choi et al. (2004) suggested that shear yielding and rubber particles pull-out are the sources of toughening. Optimum impact performance was achieved for the epoxy-rubber blend, which contains both phase-separated rubber as well as dissolved rubber (Ratna 2001). Also the impact strength of the modified networks was found to be dependent on cure temperature. Rubber particle cavitation and shear yielding of the matrix are found to be the main toughening mechanisms (Yang et al. 2015).

The reaction between epoxide group and polyetheramine as curing agent is exothermic, as can be observed in DSC thermograms in Fig. 1. The cure properties analysis on epoxy and epoxy-5 phr PMMA grafted natural rubber (MG30) blend is given in Table 3. Epoxy 1 and Epoxy 5MG30 1 were cured equivalent amine-epoxy molar ratio. While, Epoxy 2 and Epoxy 5MG30 2 were cured at higher molar ratio, 1.05, of amine-epoxy.

The addition of above-stoichiometric concentration of curing agent and rubber contributed to lower T_o , and it is about 5 °C earlier. The addition of rubber, with stoichiometric concentration of curing agent, increased ΔH_r by 30 J/g. The ester group of PMMA may react with amine to form amide, and it is exothermic reaction. The presence of rubber in the excess of curing agent, however, resulted in a decrease in ΔH_r by about 70 J/g. This may be due to the restricted heat release in high viscosity mixture.

The T_p may indicate the temperature at the maximum of polymerization rate. It was observed that the presence of MG30 rubber and excess curing agent could shift the T_p to lower temperature. These can suggest the growing reactive nature of the mixtures, in the presence of excess curing agent, and rubber.

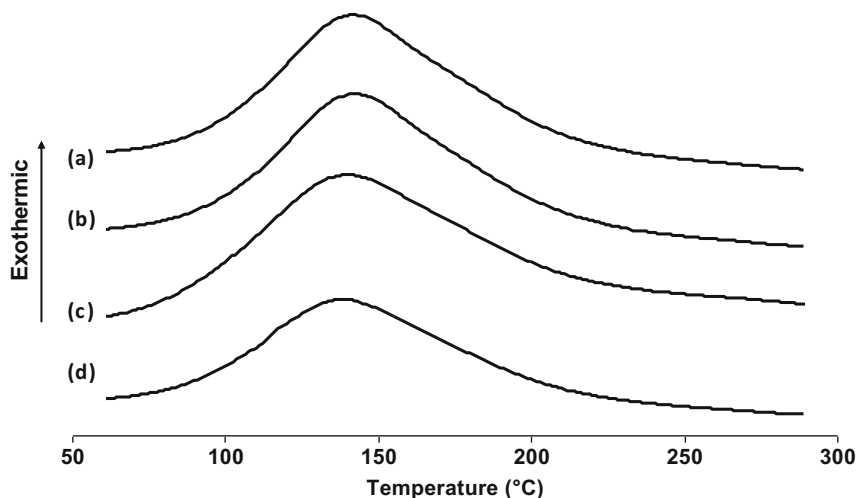


Fig. 1 DSC analysis on (a) Epoxy 1, (b) Epoxy 2, (c) Ep5MG301, (d) Ep5MG30 2

Table 3 Cure properties epoxy and epoxy-rubber blend

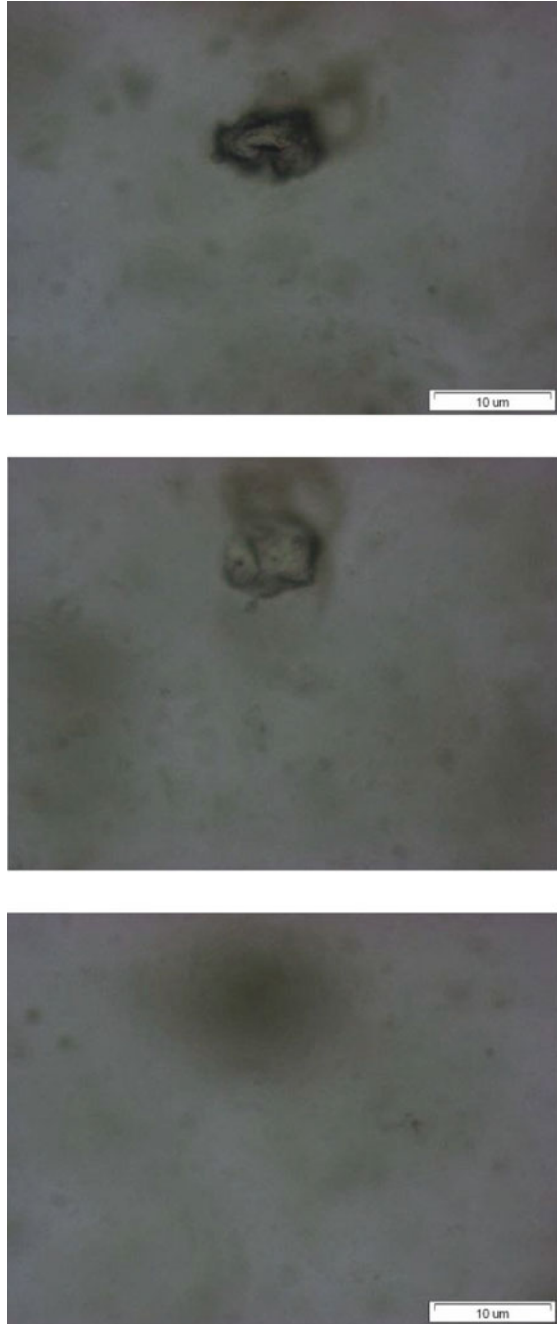
Graph	Liquid sample	Heat of reaction, ΔH_r (J/g)	Onset temperature of reaction, T_o ($^{\circ}\text{C}$)	Extrapolated peak temperature, T_p ($^{\circ}\text{C}$)
(a)	Epoxy 1	432	37	140
(b)	Epoxy 2	421	32	143
(c)	Ep5MG301	460	32	137
(d)	Ep5MG302	392	32	132

Phase Separation in Epoxy/Rubber Blend

The optical microscopy can be used to observe phase separation of rubber in epoxy. Our works exposed that natural rubber phase separated in epoxy in the presence of curing agent. The dissociation of rubber phase can be observed to occur when curing agent is added to the epoxy/rubber blend mixtures. Fig. 2 shows a rubber particle dissociates into smaller particles in nearly 3 mins. It is suggested that this is due to spinodal decomposition. The process is spontaneous to form interconnected particles from the parent phase.

Static light scattering is a classical tool for studying phase separation in general. The unpolarized or linearly polarized scattering geometries have been used in many cases (Baeke et al. 1997). Inoue has used light scattering to probe the evolution of the morphology (Inoue 1995). Jianwen Zhang studied the phase separation process using a time-resolved small-angle light scattering (TRSALS) for a rubber-modified epoxy system, consisting of diglycidyl ether of bisphenol-A (DGEBA), and a

Fig. 2 The optical microscope images showing phase separation of rubber phase in mixtures of epoxy and polyetheramine curing agent (Yuhana et al. 2012a)



hydroxyl-terminated butadiene–acrylonitrile random copolymer (HTBN), in the presence of tetrahydro- phthalic anhydride as the curing agent (Zhang et al. 1998). He used qualitative and quantitative approach to analyze. At higher curing temperatures, double-peak structures were observed from the matrix. The behavior was explained qualitatively by the competition between phase separation and polymerization, and the nucleation growth coupled with spinodal decomposition (NGCSD). He observed that spinodal decomposition is a fast process.

For the cured epoxy/rubber blend samples, TEM and SEM analysis can be used to study detailed morphology of the hard samples. Figure 3a, b show the TEM images of PMMA grafted natural rubber particles in epoxy-rubber blend cure by stoichiometric and excess concentration of curing agent, respectively.

The co-continuous phase, as shown in Fig. 3a, consists of agglomerates of small rubber particles. It appears that rubber particles, about 20 μm in diameter, dissociate into smaller particles. It is suggested that this is attributed to spinodal decomposition. This is a spontaneous process to form interconnected particles from the parent phase, which is thermodynamically in an unstable state. Also, there are occlusions of epoxy within the rubber particles (Yuhana et al. 2012a). Fig. 3b shows smaller dispersed rubber particles surrounding a 3 μm -diameter rubber particle, in the epoxy-rubber blend, cured above-stoichiometric concentration of curing agent. This could be the image of spinodal decomposition or nucleation growth process.

In the excess of polyetheramine, the chemical reaction occurring near the surface of rubber particles may be very vigorous, hence lead to dissociation of rubber particles. This image proved that the concentration of curing agent used will affect the size of rubber inside the epoxy matrix.

The reaction-induced phase separation is polymerization of a monomer, and the polymer being formed is incompatible with one or more of the other components in the system (Alfarraj and Nauman 2008). The phase separation of thermoplastic particle in epoxy composites ternary was studied by Olmos and González-Benito (2007). The detailed TEM studies for room temperature cured systems were discussed elsewhere (Yuhana et al. 2012a).

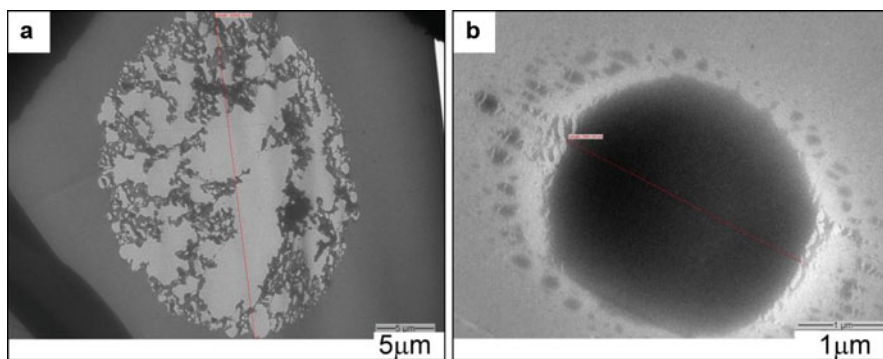


Fig. 3 TEM images of rubber particles in epoxy-rubber blend cure by (a) stoichiometric and (b) excess concentration of curing agent, respectively

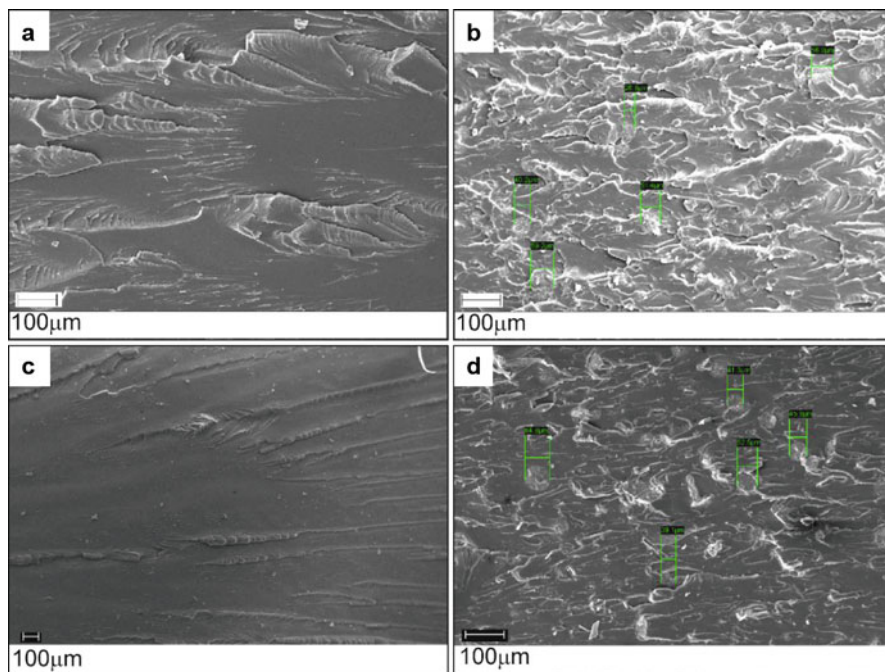


Fig. 4 SEM images of neat epoxy and epoxy-rubber blend system, cured by stoichiometric concentration (a, b) and above-stoichiometric concentration of curing agent (c, d)

The SEM images of fracture surface of neat epoxies and epoxy-PMMA grafted natural rubber blend systems cured by stoichiometric and above-stoichiometric concentration are shown in Fig. 4.

The fracture surface of the unmodified epoxies has a few river lines, as can be seen in Fig. 4a, c. According to the summary made by Huang et al. (1993), based on reports of other researchers, the main deformation micro-mechanism in the fracture is very localized shear yielding in the crack-tip region. Epoxy cured by excess curing agent seems to be very brittle, since fewer and smoother river lines can be seen.

Fig. 4b, d show that the size of rubber particles varied from approximately 30–50 µm. Crack propagation was observed passing through the epoxy matrix and rubber particles. It seems that the rubber particles' sizes were not influenced by the concentration of curing agent used.

Fig. 5 shows the impact strength of neat epoxies and epoxy-rubber blends. The impact strength of neat epoxy is about 600 kJ/m². Unexpectedly, the rubber-toughened epoxy possesses slightly lower impact strength. This can be due to weak interfacial interaction between rubber particles and epoxy matrix, as forces were applied. It was observed that the use of excess concentration of curing agent does not affect the impact strength of neat epoxy. However, the strength was improved by about 9% for rubber-toughened epoxy. This can be due to the ability of rubber phase to absorb crack energy, as can be observed in Fig. 4b, d.

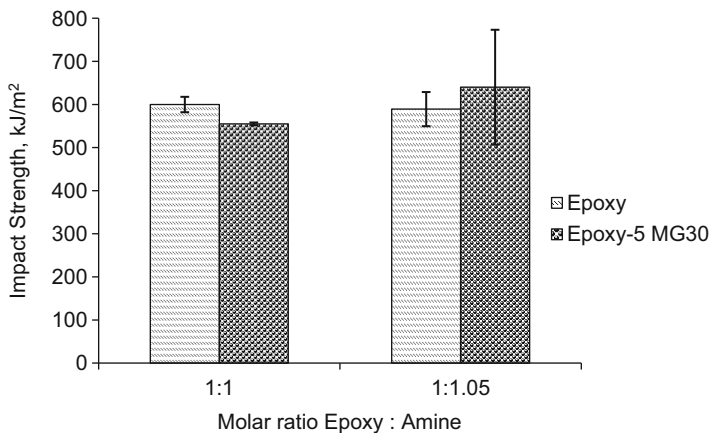


Fig. 5 The impact strength of neat epoxies and epoxy-rubber blends

Epoxy/Clay Nanocomposite

The use of nanoparticle to toughen epoxy was discussed by Zander (2008). The incorporation of nanometer-sized fillers (e.g., silicate, carbon or metal oxide nanoparticles) in polymer matrices to improve thermal, mechanical, barrier, electrical, and optical properties has gained interest recently. Many researchers have used nanoparticles, namely, montmorillonite and carbon nanotube (Villoria and Miravete 2007; Vaia 2002; Kny 2007; Becker and Simon 2005; Abdalla et al. 2008)). Other particles have been studied such as the layered double hydroxides (LDHs) clay (Tseng et al. 2007), nanosilica (Lu et al. 2004; Fujiwara et al. 2004), and nano-building blocks such as silsesquioxane (Choi et al. 2004).

The self-polymerization of epoxy in organic modified montmorillonite was studied by Lan et al. (1996). Harsch et al. (2007) used dynamic measurements to predict the total heat of reaction of the epoxy resin, and he managed to demonstrate the inhibition and acceleration effects of additives and fillers on the kinetics.

Chen and He (2004) found that the increasing cure temperature accelerated the cross-linking reactions for either nanocomposites or pure epoxy system. Meanwhile, the addition of organically modified montmorillonite reduces the gel time, cures time, and increases the rate of cure. Juwono and Edward (2006) in their literature review mentioned that most of researchers observed only one exothermal peak by DSC, and the addition of organo silicates shifts the exothermal peak to lower temperature. This suggests that the surface of the modified clay plays a significant role in the homopolymerization.

Liu et al. (2006) found that organoclay can hinder the curing behavior of epoxy-phenol blends, by hydrogen in the organoclay reacting with the catalyst. Bajaj et al. (1990) found that the hydroxyl group on untreated mica surface can act as catalyst for the curing of epoxy and amine. There were studies by previous researchers on the possible chemical reactions between the epoxide group and organoclay.

Lan et al. (Tie et al. 1995) concluded that acidic onium ions catalyze self-polymerization of DGEBA at increased temperatures.

However, Lu et al. (1999) found that the cure reaction can be accelerated in presence of fillers, but it can be retarded at low temperatures because of vitrification process.

Kornmann et al. (2001) concluded that the nanocomposite is termed intercalated, when the d_{001} basal is obtained. The exfoliated structure is where the d_{001} cannot be detected by XRD, and the increase in spacing between layers is known as increase in degree of exfoliation. The stronger peak suggests that an ordered intercalated nanocomposite was formed (Yasmin et al. 2003b).

The clay dispersion could be improved by improving the mixing method. Becker and Simon (2005), based on their work and that of other researchers, concluded that the interlayer spacing could be affected by shear mixing forces during cure. Mixing before curing process and the use of solvents as processing aids were observed to have little influence on the morphology of nanocomposite. Lan et al. (Tie et al. 1995) demonstrated that the exfoliation of the clay is dependent on the reactivity of the epoxy system and rate of intercalation of epoxy and curing agent. The rate of intercalation corresponds to the diffusion rate of the organic molecules between the clay layers. Definitely, if this rate is too slow, the polymerization rate outside the layers will be faster than the polymerization rate between the layers and only intercalated nanocomposites will form.

Interlayer expansion owing to the intercalation of epoxy resin and curing agent inside the clay galleries was described by Chen et al. (2002). Also, they studied the evolution of rheological parameters as a function of cure time. They found that the interlayer expansion increased with duration of the isothermal cure reaction. Kong and Park (2003) described the exfoliation process as a function of conversion. Jiankun et al. (2001) explained that interlayer expansion occurs when the exothermal curing heat of cure of the epoxy resin in the gallery exceeds the endothermic heat to increase the interlayer spacing.

Nigam et al. (2004) observed that the organoclay was found to be intercalated easily; however, the untreated montmorillonite clay could not be intercalated during the mixing or through the curing process. By using organoclay, the hydrophilic clay was converted to hydrophobic, in which the inorganic cations (Na^+) were replaced by the organic ones. The epoxy chains hence could be absorbed in the intragallery spaces and pushed the nanoclay layers apart during polymerization process.

Park and Jana (2003) concluded that the elastic force exerted by cross-linked epoxy molecules within the clay galleries could influence the exfoliation of layered silicates. The extra shear force due to high viscosity mixture may cause better exfoliation of clay platelets in polymer matrix (Fornes et al. 2001). According to Kornmann et al. (2001), the exfoliation of clay could be controlled by type of curing agent and curing conditions. Juwono (Juwono and Edward 2006) found that organoclays formed a mixed structure of exfoliated and intercalated structures by using TEM.

On increasing clay loading, the problems arised would be the formation of voids which may be attributed to the incomplete degassing before casting and the trapped

air during pouring of highly viscous mixture onto the mold (Yasmin et al. 2003b). Cracks that initiated from these voids could cause the specimen to fail at relatively low strain. Ramakrishna and Rai (2006) suggested that minimizing the presence of voids and bubbles will lead to an increase in both strength and modulus of composite material.

It is often stated that the layered silicate can increase the glass transition temperature (T_g) by restricting the epoxy chain mobility. This can also reduce the T_g , owing to the presence of hydroxyl group in unmodified mica and acidic onium ion in organically modified silicate where both could act as catalyst for epoxy homopolymerization (Becker et al. 2003; Froehlich et al. 2004). If this happens, the unreacted curing agent will plasticize the matrix. Kinloch et al. (Kinloch and Taylor 2003) concluded that intercalated structure of silicate could improve the T_g . Becker found that increasing organoclay concentration steadily decreased T_g (Becker et al. 2003). The presence of fillers in epoxy could reduce the cross-link density, hence the T_g . Also, the increase of free volume in epoxy may be the other possible reason (Lu et al. 1999).

The improvement in thermal stability of nanocomposites is often mentioned to be due to the torturous path for volatile decomposition products. The thermal stability of epoxy increased with the contents of inorganic components, because of the char yield increases (Chiang et al. 2007). The char layer could protect unburned structure materials during fire. The decrease in thermal stability may be attributed to the catalytic activity of organoclay on epoxy decomposition (Camino et al. 2005). Fujiwara mentioned that the high thermal could be due to the interaction of hydroxyl groups of DGEBA with silica (Fujiwara et al. 2004).

(Chin et al. 2001, 2007) found that the onset of mass loss started at a lower temperature could be attributed to the presence of low molecular weight volatile compounds that are easily removed from the polymer matrix. These species may be related to the accelerator and/or to the differences in curing agent formulation. The improvement in thermal stability of nanocomposites is often stated to be due to the torturous path for volatile decomposition products. According to Chena et al. (Chena et al. 2006), they suggested that the presence of inorganic nanofiller can produce more thermally stable material, as the filler particle reduces chemical bond movements of the organic component.

Also, it is often stated that the layered silicate can reduce the water absorption and permeability of epoxy by increasing layered silicate content (Hu and Kim 2005). The reduction is mainly due to the very large aspect ratio of the clay platelets which increased the effective penetration path for water molecules. Cui et al. (2009) mentioned that the microscopic free volume plays an important role in determining macroscopic barrier properties. Lekatou et al. (1997) suggested rapid preferential water transport through low resistance pathways, which may refer to interface between filler and matrix and low cross-link density region.

The flexural modulus is generally improved by incorporation of layered silicate, due to shear deformation and stress transfer to the layered particles. The decrease in flexural strength and failure strain, however, could be attributable to an

inhomogeneous and reduced network density in the presence of fillers. According to Kornmann et al. (2001) and Yasmin et al. (2003a, b), the flexural modulus increases with small amounts of silicate added. The better clay dispersion will result in larger stiffness improvement. Liu and Wu (2001) found that the decreased modulus could be attributed to the presence of unexfoliated aggregates. However, Kaynak et al. (2009) indicated that exfoliated particles may not necessarily provide the best stiffening effect.

As Sapuan et al. (2003) have shown, the increase in filler content results in the increase in flexural stress flexural modulus of elasticity. This increase is due to the relationship between the interface of fillers and matrix in which the fillers strengthen the composite materials. However, the strain decreases following a quadratic form with the increase in the filler content owing to the fact that the materials have become harder with the increase in filler content. It was also found that the elastic modulus of epoxy/silica nanocomposite was increased, as filler content increases. This may be attributed to the absence of silica aggregates in the nanocomposites samples (Bondioli et al. 2005).

Rubber-Toughened Epoxy/Clay Nanocomposite

The incorporation of dispersed rubbery particles in a layered silicate/epoxy nanocomposite has received significant attention (Becker and Simon 2005; Liu et al. 2004; Froehlich et al. 2004; Balakrishnan and Raghavan 2004; Balakrishnan et al. 2005; Ratna et al. 2003). Even though the research on the epoxy/layered silicate nanocomposite could be considered new, the effect of the addition of the rubbery material in epoxy is an interesting topic to be explored.

Morphological studies of the microstructure and nanostructure of the ternary system represent a challenge, because of the complexity of multicomponent systems. Balakrishnan et al. (Balakrishnan and Raghavan 2004) carried out extensive work on the morphology of elastomer acrylic toughened epoxy silicate nanocomposites. They found that the clay aggregates are well dispersed and are fewer in the epoxy matrix than in the epoxy nanocomposite. The clay layers tended to align around the walls of the rubber particle. Thus, they suggested that this might help the particles to withstand additional stretching forces before failure could occur at the interface of epoxy matrix-rubber particle system. It was also proposed that the aligned clay particles acted as additional reinforcement to protect the interface from the external stretching force, thus promoting cavitation.

Ratna et al. (2003) conducted TEM analysis on epoxy nanocomposites based on a combination of epoxy resin, hyperbranched epoxy (HBP), and a layered silicate. They observed distinct regions of silicate aggregates and HBP phase-separated regions. No silicate particles were observed in the HBP phase. It has been described that, while good intercalation was obtained in nanocomposites of layered silicate and epoxy, the interlayer spacing of silicates was reduced in the ternary system involving CTBN toughened epoxy layered silicate nanocomposites (Becker and Simon 2005).

The rubber, which was soluble in epoxy, could not intercalate the layered silicates as well as the epoxy resin did.

Balakrishnan et al. (2005), in their study of the morphology of preformed acrylic rubber dispersed silicate filled epoxy nanocomposites, also found that the clay particles were located along the boundaries of rubber particles, but no further explanation was given.

Froehlich et al. (2004) indicated that the phase separation of larger rubber particles assist the separation of silicate layers by diffusing into the silicate galleries. However, they did not produce evidence of this process.

According to Liu et al. (Lu et al. 2004), most of the organoclay in rubber-toughened epoxy-clay nanocomposite was exfoliated. The rubber phase could not be determined from the SEM image, on increasing the clay loading, although from DMA results showed the presence of two-phase system of this hybrid nanocomposite. They, however, did not discuss the reasons of the problem.

It was found that the flexural strength and modulus of rubber-toughened epoxy silicate nanocomposites were higher, compared to the unmodified epoxy (Balakrishnan et al. 2005). Furthermore, the addition of organoclay into rubber-modified epoxies increases the T_g (Liu et al. 2004). Also, the impact strength of ternary nanocomposite is better when filler dispersion is good (Ramakrishna and Rai 2006).

Epoxy resins are used as adhesive, coating, and composite matrices in the building, structural, and transportation industries. Hence, it is expected that rubber-toughened epoxy/clay nanocomposite material has great potential to be used for high barrier application, coating for marine industries and steel structures, building materials, corrosion resistant pipes, consolidants or protectives material for the architectural heritage and wind turbine, as well as printed circuits board.

Curing Reaction Behavior of the Ternary System

The endothermic peak can be observed in Fig. 6 resulted when heating of liquid mixture containing epoxy, silicate (Cloisite Na or Cloisite 30B), and PMMA grafted natural rubber. The endothermic peak could refer the melting point of PMMA.

In the absence of silicate, the endothermic peak is at 135 °C, as shown in Fig. 6a. But the peak is shifted to higher temperature, 172 °C in the presence of Cloisite Na, as illustrated in Fig. 6b. The peak shifting may be attributed to the ability of dispersed Cloisite Na to resist heat transfer in the mixture.

In contrast, it is obvious that Cloisite 30B addition shifts the endothermic peak to a lower temperature, 101 °C, as shown in Fig. 6c. The explanation for this is the possibility of ammonium ion salt to interact with epoxy and catalyze the decomposition process. This will ease the melting process of PMMA, and subsequently the decomposition process starts at 250 °C.

These findings indicate that the Cloisite 30B plays a catalytic role while the Cloisite Na plays an incatalytic role.

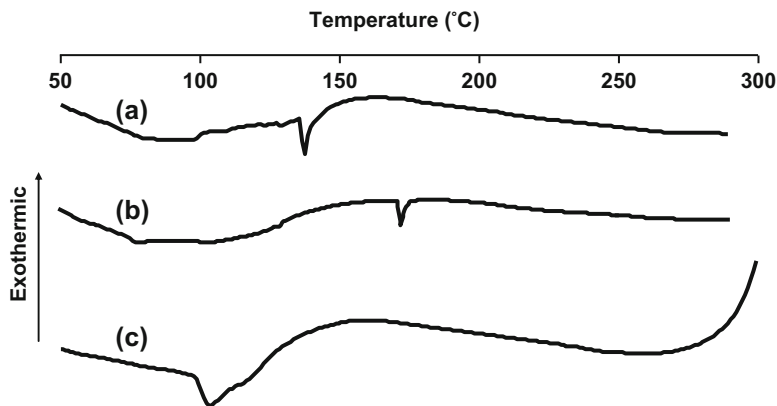


Fig. 6 DSC analysis on (a) Epoxy-5MG30 (b) Epoxy-5MG30-5 Cloisite Na (c) Epoxy-5MG30-5 Cloisite 30B

The Effect of Above-Stoichiometric Concentration of Curing Agent, Rubber, and Clay on Curing Behavior of Epoxy

The reaction between epoxide group and polyetheramine as curing agent is exothermic, as can be observed in DSC thermograms in Fig. 7. The DSC analysis was performed for neat epoxy and epoxy-rubber blend system cured by stoichiometric concentration (Epoxy 1 and Epoxy -5MG30 1) and above-stoichiometric concentration of curing agent (Epoxy 2 and Epoxy-5MG30 2). The cure properties analysis on epoxy and epoxy-rubber blend is given in Table 4.

The addition of above-stoichiometric concentration of curing agent and rubber contributed to lower T_o , and it is about 5 °C earlier. The addition of rubber, with stoichiometric concentration of curing agent, increased ΔH_r by 30 J/g. The ester group of PMMA may react with amine to form amide, and it is exothermic reaction. The presence of rubber in the excess of curing agent, however, resulted in a decrease in ΔH_r by about 70 J/g. This may be due to the restricted heat release in high viscosity mixture.

The T_p may indicate the temperature at the maximum of polymerization rate. It was observed that the presence of MG30 rubber and excess curing agent could shift the T_p to lower temperature. These can suggest the growing reactive nature of the mixtures, in the presence of excess curing agent, and rubber.

Fig. 8 shows the DSC thermograms of exothermic reaction between epoxide group and polyetheramine as curing agent, in the presence of nanoclay and rubber. The cure properties analysis on epoxy ternary systems is given in Table 5.

It was observed that the ΔH_r for epoxy containing 5 phrCloisite Na 2 was unaffected significantly. The ΔH_r was greatly reduced by the presence of Cloisite 30B. May be, some amount of heat is consumed for the reaction between the organic modifier of clay and the epoxy. The same results were observed by

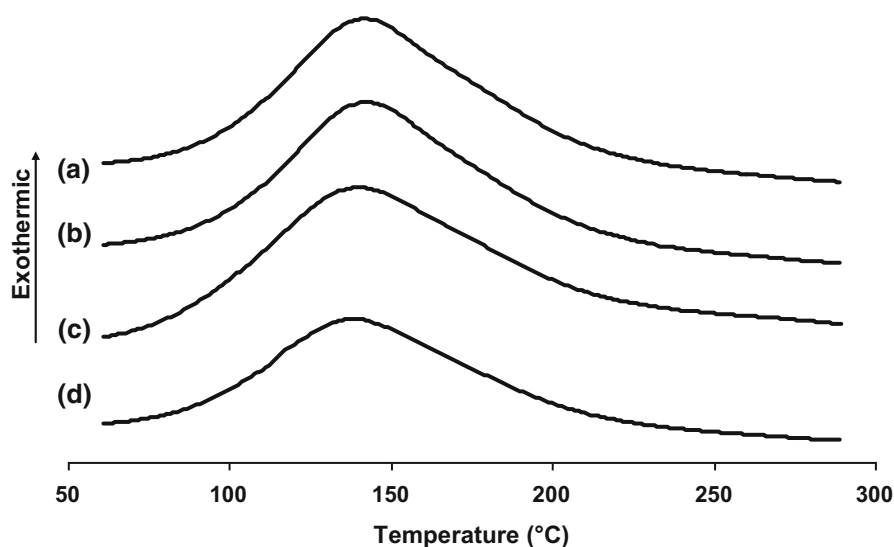


Fig. 7 DSC analysis on (a) Epoxy 1, (b) Epoxy 2, (c) Ep5MG301, (d) Ep5MG302

Table 4 Cure properties of epoxy and epoxy-rubber blend

Graph	Liquid sample	Heat of reaction, ΔH_r (J/g)	Onset temperature of reaction, T_o ($^{\circ}\text{C}$)	Extrapolated peak temperature, T_p ($^{\circ}\text{C}$)
(a)	Epoxy 1	432	37	140
(b)	Epoxy 2	421	32	143
(c)	Ep5MG301	460	32	137
(d)	Ep5MG302	392	32	132

Harsch et al. (2007). He mentioned that the possibility of fillers are acting as inhibitors for the reaction between epoxy and curing agent by adsorbing the reactants at their surfaces and thus affecting the stoichiometry. The solvent evaporation may also consume the curing exotherm (Hong and Wu 1998).

The higher T_o for all binary and ternary nanocomposite systems, compared to neat epoxy and epoxy-rubber blend, suggested that the fillers acted as inhibitors for the curing process.

Morphology of Ternary System

Fig. 9(a–f) represents the image of fractured surface of ternary systems of epoxy-Cloisite Na 1, epoxy-Cloisite Na 2, and epoxy-Cloisite 30B, respectively, at 2 and 5 phr clay loadings. It seems that at higher clay loadings, the rubber particles were not clearly observed especially for epoxy-Cloisite 30B systems. The difference in rubber

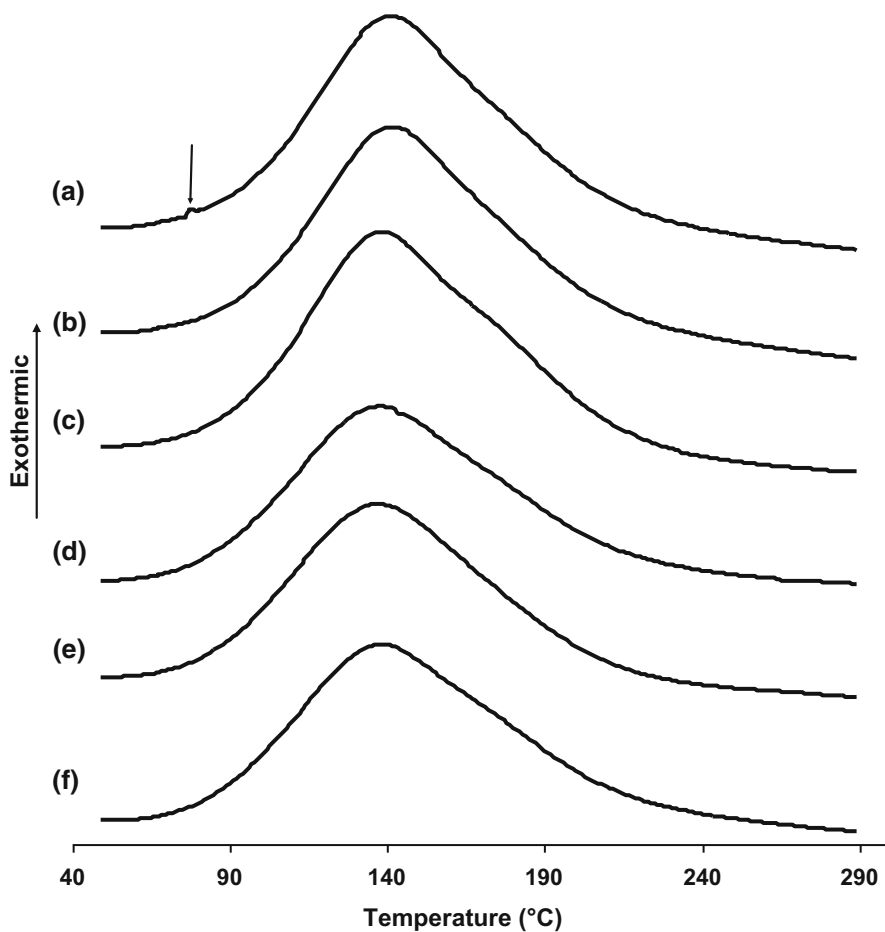


Fig. 8 DSC analysis on (a) Ep5Na1, (b) Ep5Na2, (c) Ep530B, (d) Ep5MG305Na1, (e) Ep5MG305Na2, (f) Ep5MG30530B

Table 5 Cure properties of binary and ternary systems

Graph	Liquid sample	Heat of reaction, ΔH_r (J/g)	Onset temperature of reaction, T_o ($^{\circ}\text{C}$)	Extrapolated peak temperature, T_p ($^{\circ}\text{C}$)
(a)	Ep5Na 1	420	57	139
(b)	Ep5Na 2	434	43	139
(c)	Ep530B	382	40	135
(d)	Ep5MG305Na1	364	65	135
(e)	Ep5MG305Na2	368	40	135
(f)	Ep5MG30530B	380	52	135

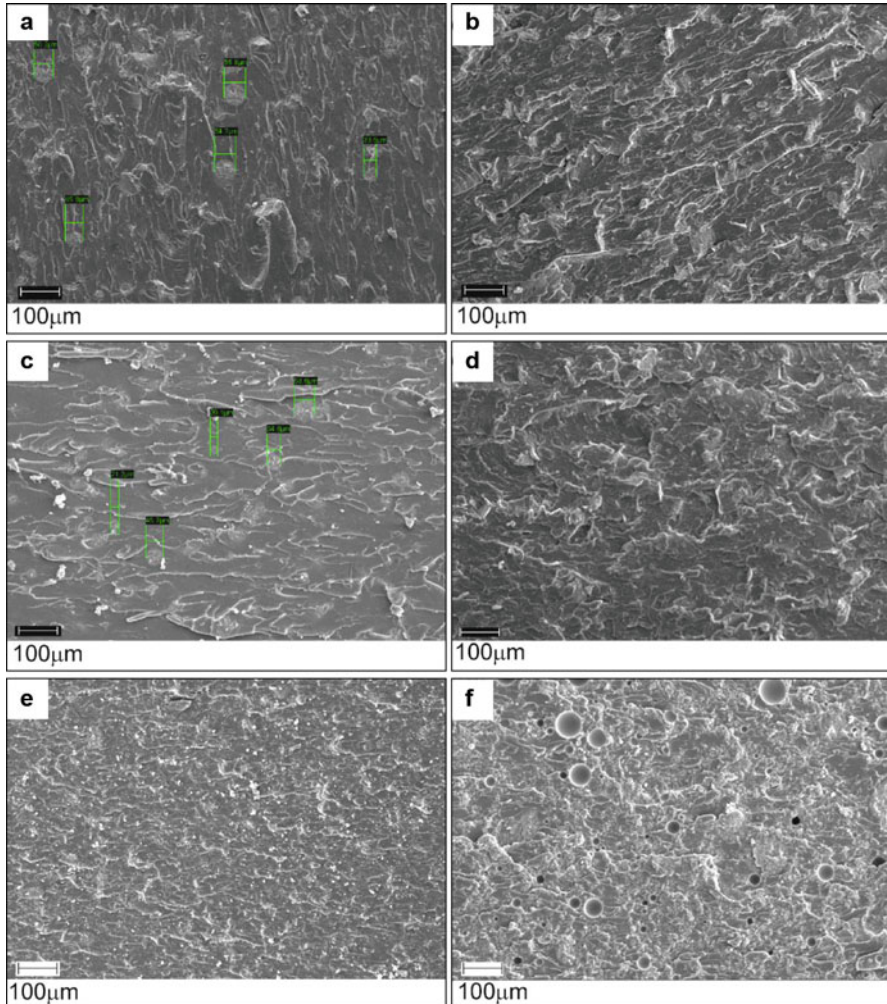


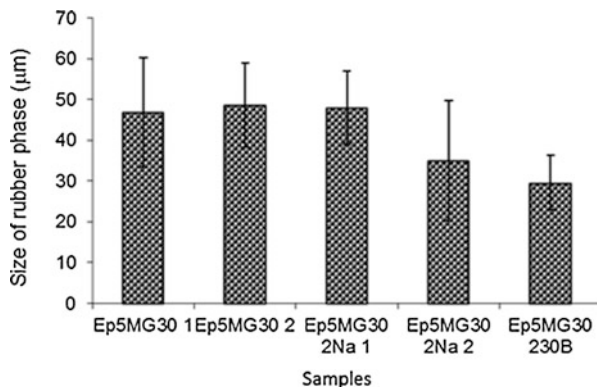
Fig. 9 SEM images of rubber-toughened epoxy nanocomposite systems, containing 2 and 5 phr (a,b) Cloisite Na 1, (c,d) Cloisite Na 2, and (e,f) Cloisite 30B

particle sizes in epoxy-Cloisite Na1, epoxy-Cloisite Na2, and epoxy-Cloisite 30B systems may be attributed to the difference in chemical reaction inducing phase separation process.

The presence of voids in rubber-toughened epoxy containing 5 phr Cloisite 30B, as in Fig. 9f, could indicate the improper degassing problem, due to high viscosity mixture during mixing.

Fig. 10 summarizes the sizes of rubber particles in blend and ternary systems containing 5 phr MG30 rubber and 2 phr nanoclay. At higher clay content, the SEM image of rubbers cannot be observed clearly.

Fig. 10 Sizes of rubber particles determined from SEM images



The presence of organoclay and excess of curing agent reduced the size of rubber particles from about 50 – 30 μm. The results of higher value of ΔH_f and lower T_g for Cloisite Na 2 and Cloisite 30B systems, as given in Table 5, suggest that they are more reactive systems. The reactive mixtures could assist the spinodal decomposition process, hence small rubber particles are formed.

Fig. 11(a,f) demonstrates the TEM images of ternary systems containing 5 phr PMMA grafted natural rubber and 5 phr layered silicate (Cloisite Na or Cloisite 30B) in epoxy, namely (a,b) Ep5MG30 5Na 1, (c,d) Ep5MG30 5Na 2, and (e,f) Ep5MG30530B

Fig. 11a demonstrates rubber particles in between intercalated clays of Cloisite Na. It seems that clays are not adsorbed on rubber surface. Similar observation can be seen for the one cured by excess concentration of curing agent, as illustrated in Fig. 11(c,d). The highly intercalated clay structure can be observed, for Cloisite Na system, in Fig. 11(b,d)

The good interaction between Cloisite 30B clays and rubber particles can be seen in Fig. 11(e,f). The TEM images showed that the organoclay dispersed well in the ternary nanocomposite system.

At higher clay amount the rubber particles could be reduced in sizes. The high amount of clay could act as “nano impeller” during the mixing process, hence they can break and tear the soft rubber particles.

The following images in Fig. 12 show the possible morphology of ternary nanocomposite system achieved, by using excess curing agent and organoclay. It can be concluded that the morphology of nanocomposites could be tailored by using chemically treated clay and concentration variation of curing agent.

Glass Transition Temperatures of Ternary System

The thermograms of DSC for four cured samples of epoxy, rubber-toughened epoxy, epoxy/Cloisite 30B nanocomposite, and rubber-toughened epoxy-Cloisite

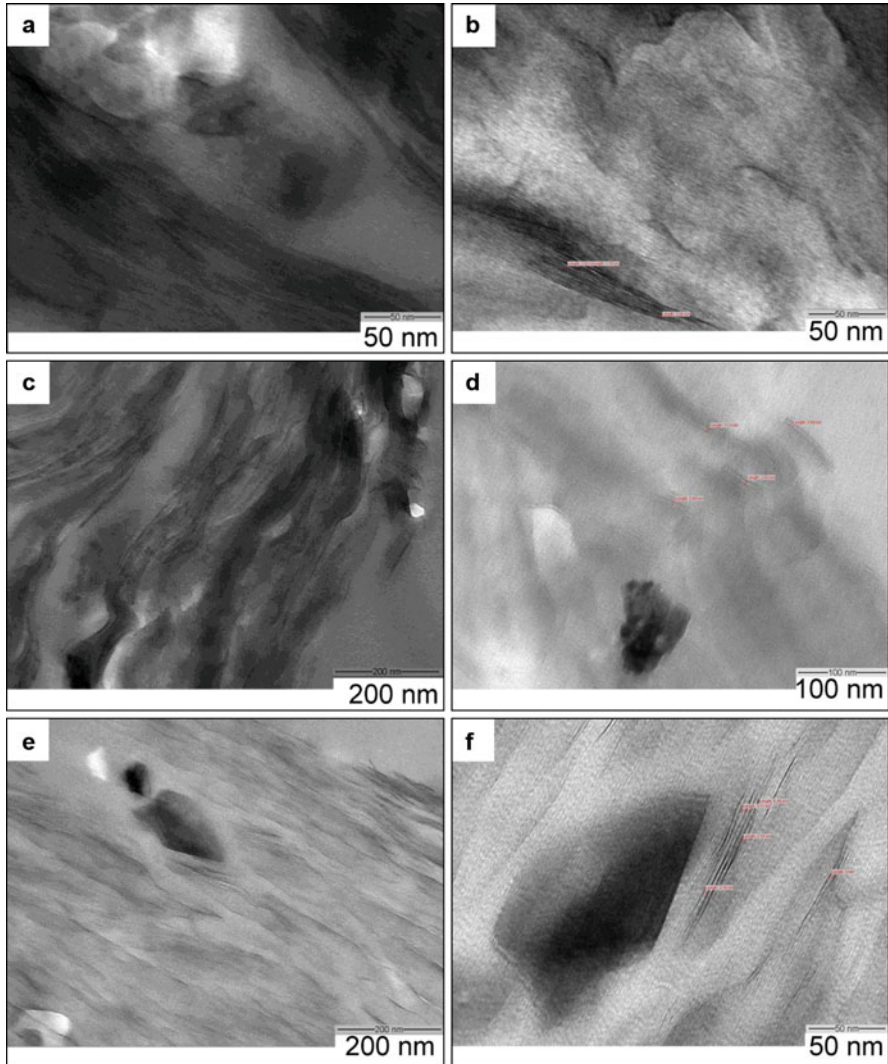


Fig. 11 The TEM images of ternary nanocomposites (a,b) Ep5Na1, (c,d) Ep5Na2, and (e,f) Ep530B

30B /nanocomposite are shown in Fig. 13. The onset of glass transition (T_g) and the inflection slope (m_g) for all cured samples are summarized in Fig. 14.

The use of above-stoichiometric concentration of curing agent was found to reduce the glass transition temperature of neat epoxy from 95 °C to 86 °C. The presence of unreacted epoxide may act as plasticizer, as proven by FTIR analysis. Addition of 5 phr rubber reduced slightly the T_g to 92 °C. The insignificant changes can be due to nearly completed phase separation occurrence. However, the

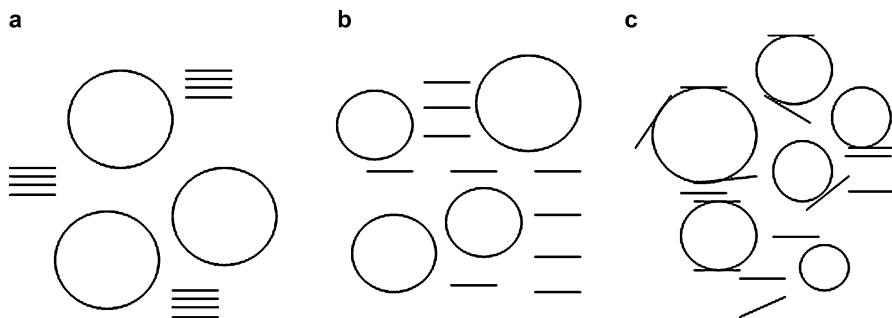


Fig. 12 The schematic diagram of morphology of rubber-toughened epoxy-clay nanocomposites containing (a) Cloisite Na, (b) Cloisite Na cured by above-stoichiometric concentration of curing agent, (c) Cloisite 30B

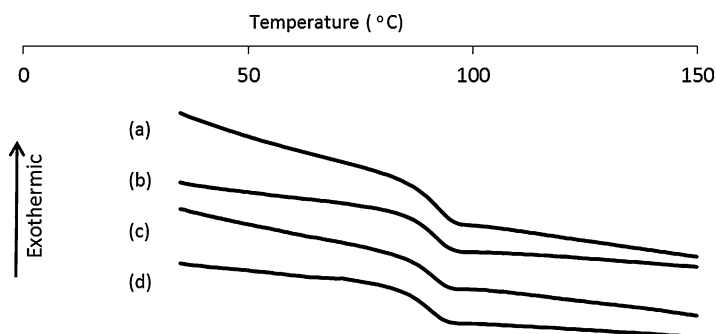


Fig. 13 DSC thermograms for cured (a) Epoxy 1, (b) Epoxy-5MG30 1, (c) Ep-5 30B, and (d) Ep-5MG30-530B

epoxy-rubber blend cured by above-stoichiometric concentration of curing agent has lower T_g , which is about 86 °C. Again, the presence of unreacted epoxide in the samples, as proven by FTIR results, can act as plasticizer, upon heating.

The use of 2–7 phr nanoclay in epoxy was found to decrease the T_g . The significant reduction could be observed for nanocomposite system cured by above-stoichiometric concentration of curing agent, followed by organoclay system. The presence of amine salts, as proven by FTIR analysis, can act as plasticizer, upon heating process. The utilization of 5 phr unmodified clay in ternary systems cured by stoichiometric concentration of curing agent, however, can maintain the T_g at about 92 °C. This may indicate the nearly complete phase separation of rubber phase. T_g values could be increased by several factors such as the presence of bulky side groups, polar groups, and double bonds in the backbone. The small amount of branching and lower molecular weight of epoxies tend to decrease the glass transition temperatures (Callister 2007). The presence of hydroxyl group in unmodified mica and acidic onium ion in organically modified silicate could act as catalyst for epoxy homopolymerization (Becker et al. 2003; Froehlich et al. 2004). If this happens, the unreacted curing agent will plasticize the

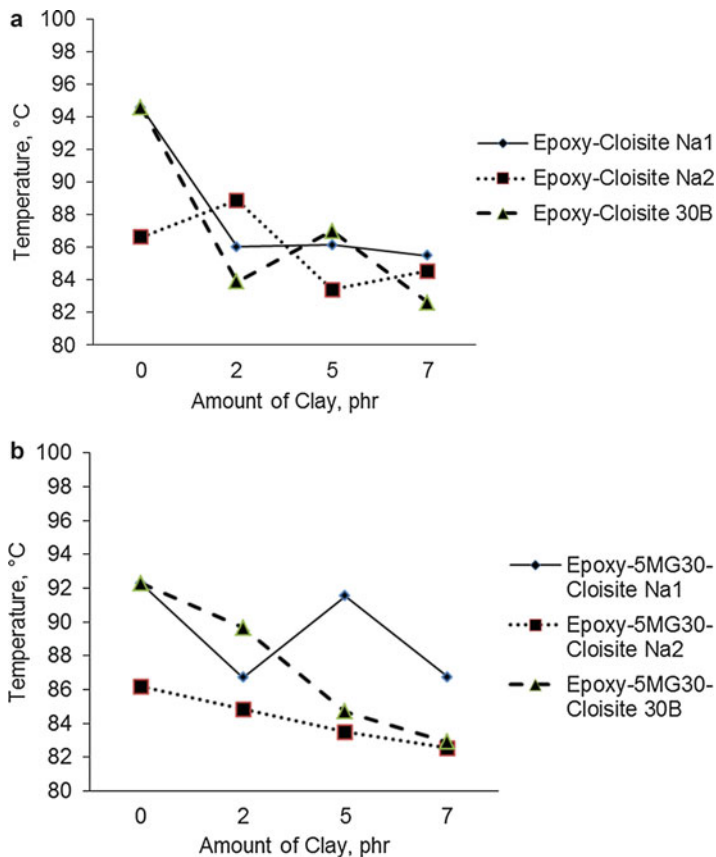


Fig. 14 The onset of glass transition temperatures of (a) neat epoxies and binary (b) epoxy-rubber blend and ternary nanocomposites

matrix. Becker et al. (2003) found that increasing organoclay concentration steadily decreased T_g . The presence of fillers in epoxy could reduce the cross-link density, hence the T_g . According to Fujiwara (Fujiwara et al. 2004), hydroxyl groups between bisphenol-A units are important because of the interaction with the silica particles, which restricts the free movement of the epoxy resin part.

Impact Strength of Ternary System

The impact strength of binary and ternary nanocomposites containing natural montmorillonite is shown in Fig. 15.

The use of nanoclay in epoxy reduced the impact strength greatly as clay content increased. This may be due to rigidity and agglomeration of Cloisite Na in the cured

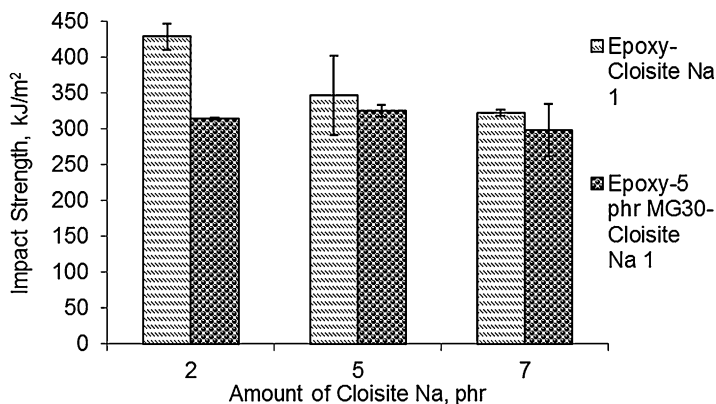


Fig. 15 The impact strength of epoxy-Cloisite Na 1 nanocomposite and rubber-toughened epoxy-Cloisite Na nanocomposite

samples as can be seen in SEM images Fig. 9(a,b). These agglomerates act as stress concentration points or crack initiation sites (Isik et al. 2003).

The presence of 5 phr MG30 rubber does not improve the impact strength of epoxy-Cloisite Na nanocomposite. The clay and rubber phase are separated quite distantly, especially at low silicate content.

In the presence of 5 phr Cloisite Na, rubber phase tend to show the ability to improve the impact strength. This may be due to the increased amount of clay near the rubber phase that tends to form barrier for crack propagation to pass through the rubber particles. The clay can reduce the intensity of crack propagation, hence rubber phase would have the potential to absorb the crack and eventually stop the crack propagation process.

In the presence of higher amount of nanoclay, the agglomeration would be a problem, hence reduces the ability of rubber to improve the impact strength of composites.

Fig. 16 shows the impact strength of binary and ternary nanocomposites containing natural montmorillonite cured by above-stoichiometric concentration of curing agent. The similar trends were observed, as Cloisite Na 1 system, suggested that the use of excess concentration of curing agent does not affect the impact strength significantly.

Fig. 17 shows the impact strength of binary and ternary nanocomposites containing organoclay cured stoichiometric concentration of curing agent.

The epoxy nanocomposites contained organoclay has about 50% lower impact strength of the neat epoxies. Although the exfoliated clay may exist, other problems such as voids in samples could be problematic. The SEM image, Fig. 9f, proves the existence of voids in samples. At low content of Cloisite 30B, the presence of rubber phase tends to improve the impact strength of ternary system, as less silicate surrounds the rubber phase. The clay aggregates could reduce the crack intensity

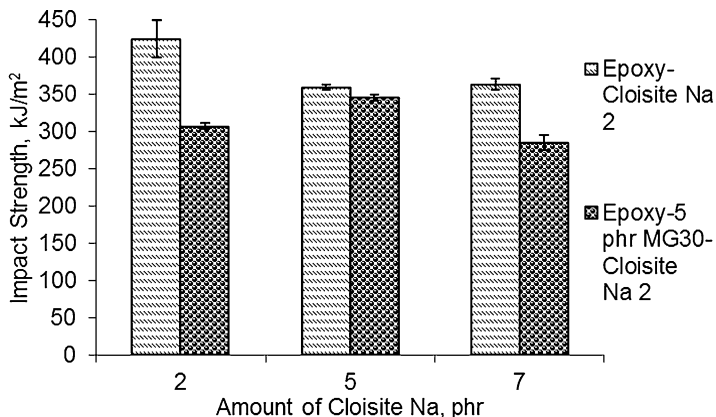


Fig. 16 The impact strength of epoxy-Cloisite Na 2 nanocomposite and rubber-toughened epoxy-Cloisite Na nanocomposite, cured by above-stoichiometric concentration of curing agent

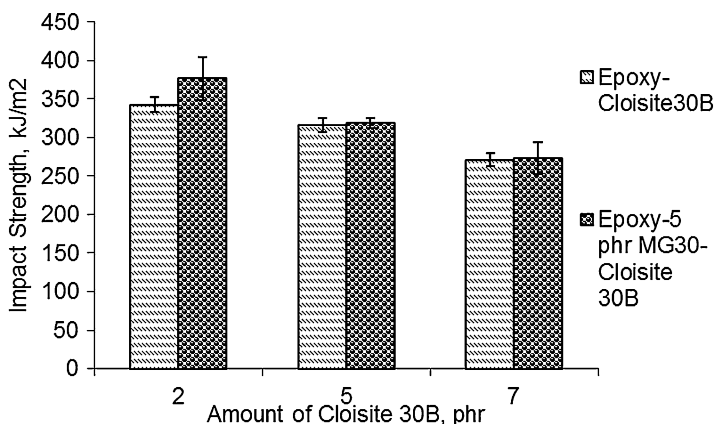


Fig. 17 The impact strength of epoxy-Cloisite 30B nanocomposites and rubber-toughened epoxy-Cloisite 30B nanocomposites

before reaching rubber phase and being absorbed and eventually stop the crack propagation.

In general, the addition of clay reduces the impact strength of nanocomposites. The clay particles tend to agglomerate at high clay content and act as stress concentrators. In samples with both clay and rubber, the impact strength tends to show some improvement in the material containing 2–5 wt.% nanoclay and 5 phr rubber in comparison to the impact strength of epoxy/clay nanocomposites.

Conclusions

The use of PMMA grafted natural rubber in combination with natural montmorillonite as plastic fillers could be further explored. The improvement in preparation techniques and processing parameters must be carefully studied, in order to get excellent properties of ternary nanocomposite material. The use of curing agent as dispersing agent could also be further investigated.

References

- Abdalla M, Dean D, Robinson P, Nyairo E (2008) Cure behavior of epoxy/MWCNT nanocomposites: the effect of nanotube surface modification. *Polymer* 49(15):3310–3317
- Akbarinezhad E, Ebrahimi M, Sharif F (2011) Synthesis of exfoliated polyaniline–clay nanocomposite in supercritical CO₂. *J Supercrit Fluids* 59(0):124–130. doi:10.1016/j.supflu.2011.08.010
- Alfarraj AA, Bruce Nauman E (2008) Reactive phase separation: prediction of an occlusion morphology. *Polymer* 49(1):339–344
- Arias ML, Frontini PM, Williams RJJ (2003) Analysis of the damage zone around the crack tip for two rubber-modified epoxy matrices exhibiting different toughenability. *Polymer* 44(5):1537–1546
- Baek L, Thioudelet P, Keates P, Navard P (1997) A depolarized light scattering study of the phase separation process in an epoxy–elastomer blend. *Polymer* 38(21):5283–5287. doi:10.1016/S0032-3861(97)00073-6
- Bagherzadeh MR, Mahdavi F (2007) Preparation of epoxy–clay nanocomposite and investigation on its anti-corrosive behavior in epoxy coating. *Prog Org Coat* 60(2):117–120. doi:10.1016/j.porgcoat.2007.07.011
- Bahramian AR, Kokabi M, Famili MHN, Beheshty MH (2008) High temperature ablation of kaolinite layered silicate/phenolic resin/asbestos cloth nanocomposite. *J Hazard Mater* 150(1):136–145. doi:10.1016/j.jhazmat.2007.04.104
- Bajaj P, Jha NK, Ananda Kumar R (1990) Effect of mica on the curing behaviour of an amine-cured epoxy system: differential scanning calorimetric studies. *J Appl Polym Sci* 40:203–212
- Balakrishnan S, Start PR, Raghavan D, Hudson SD (2005) The influence of clay and elastomer concentration on the morphology and fracture energy of preformed acrylic rubber dispersed clay filled epoxy nanocomposites. *Polymer* 46(25):11255–11262
- Balakrishnan S, Raghavan D (2004) Acrylic, elastomeric, particle-dispersed epoxy-clay hybrid nanocomposites: mechanical properties. *Macromol Rapid Commun* 25(3):481–485
- Barbee Robert Boyde, Jr James Christopher Matayabas, Jr Jack Wesley Trexler, Rodney Layne Piner, John Walker Gilmer, Gary Wayne Connell, Jeffrey Todd Owens, and Sam Richard Turner (2002) Nanocomposites for high barrier applications. In <http://www.freepatentsonline.com>, edited by US Patent, Eastman Chemical Company
- Becker O, Simon GP, Varley RJ, Halley PJ (2003) Layered silicate nanocomposites based on various high-functionality epoxy resins: the influence of an organoclay on resin cure. *Polym Eng Sci* 43(4):850–862
- Becker O, Simon GP (2005) Epoxy layered silicate nanocomposite. *Adv Polym Sci* 179:29–82
- Becu L, Maazouz A, Sautereau H, Gerard JF (1997) Fracture behavior of epoxy polymers modified with core-shell rubber particles. *J Appl Polym Sci* 65(12):2419–2431
- Bondioli F, Cannillo V, Fabbri E, Messori M (2005) Epoxy-silica nanocomposites: preparation, experimental characterization, and modeling. *J Appl Polym Sci* 97:2382–2386
- Budiman AFS (2002) Exciting times ahead for NR. Newsletter of the rubber foundation information center for natural rubber

- Calderon JU, Lennox B, Kamal MR (2007) Thermally stable phosphonium-montmorillonite organoclays. *Appl Clay Sci* 40(1):90–98
- Callister William D (2007) Material science and engineering: an introduction, 7th edn. Wiley (Asia) Pte Ltd
- Camino G, Tartaglione G, Frache A, Manferti C, Costa G (2005) Thermal and combustion behaviour of layered silicate–epoxy nanocomposites. *Polym Degrad Stab* 90(2):354–362
- Cardiano P, Ponterio RC, Sergi S, Lo Schiavo S, Piraino P (2005) Epoxy-silica polymers as stone conservation materials. *Polymer* 46(6):1857–1864
- Chen DZ, He PS, Pan LJ (2003) Cure kinetics of epoxy-based nanocomposites analyzed by Avrami theory of phase change. *Polym Test* 22(6):689–697
- Chen D, He P (2004) Monitoring the curing process of epoxy resin nanocomposites based on organo-montmorillonite – a new application of resin curemeter. *Compos Sci Technol* 64(16):2501–2507
- Chen J-S, Poliks MD, Ober CK, Zhang Y, Wiesner U, Giannelis E (2002) Study of interlayer expansion mechanism and thermal-mechanical properties of surface-initiated epoxy nanocomposites. *Polymer* 43(18):4895–4904
- Chena M-H, Chenc C-R, Hsuc S-H, Sunc S-P, Suc W-F (2006) Low shrinkage light curable nanocomposite for dental restorative material. *Dent Mater* 22:138–145
- Chiang C-L, Chang R-C, Chi Y-C (2007) Thermal stability and degradation kinetics of novel organic/inorganic epoxy hybrid containing nitrogen/silicon/phosphorus by sol–gel method. *Thermochim Acta* 453:97–104
- Chin I-J, Thum-Albrecht T, Kim H-C, Russell TP, Wang J (2001) On exfoliation of montmorillonite in epoxy. *Polymer* 42:5947–5952
- Chin Joannie, Don Hunston, and Aaron Forster (2007) Thermo-viscoelastic analysis of ambient cure epoxy adhesives used in construction applications. Polymeric Materials Group, Materials and Construction Research Division, National Institute of Standards and Technology
- Choi J, Yee AF, Laine RM (2004) Toughening of cubic silsesquioxane epoxy nanocomposites using core-shell rubber particles: a three-component hybrid system. *Macromolecules* 37(9):3267–3276
- Cui L, Yeh J-T, KeWang F-CT, Fu Q (2009) Relation of free volume and barrier properties in the miscible blends of poly(vinyl alcohol) and nylon 6-clay nanocomposites film. *J Membr Sci* 327:226–233
- Dai C-F, Li P-R, Yeh J-M (2008) Comparative studies for the effect of intercalating agent on the physical properties of epoxy resin-clay based nanocomposite materials. *Eur Polym J* 44(8):2439–2447. doi:10.1016/j.eurpolymj.2008.06.015
- Das G, Karak N (2010) Thermostable and flame retardant Mesua ferrea L. seed oil based non-halogenated epoxy resin/clay nanocomposites. *Prog Org Coat* 69(4):495–503. doi:10.1016/j.porgcoat.2010.09.004
- Dispenza C, Spadaro G, Carter JT, McGrail PT (2001) Reactive blending of functionalized acrylic rubbers and epoxy resins. *Polym Eng Sci* 41(9):1486–1496
- Fecht H-J, Werner M (eds) (2004) The Nano-micro interface: bridging the micro and nano worlds. Wiley-VCH Verlag GmbH, Weinheim
- Fornes TD, Yoon PJ, Keskkula H, Paul DR (2001) Nylon 6 nanocomposites: the effect of matrix molecular weight. *Polymer* 42(25):9929–9940
- Francis B, Lakshmana Rao V, Poel GV, Posada F, Gabriel G, Ramaswamy R, Thomas S (2006) Cure kinetics, morphological and dynamic mechanical analysis of diglycidyl ether of bisphenol-A epoxy resin modified with hydroxyl terminated poly(ether ether ketone) containing pendent tertiary butyl groups. *Polymer* 47(15):5411–5419
- Froehlich J, Thomann R, Gryshchuk O, Karger-Kocsis J, Muelhaupt R (2004) High-performance epoxy hybrid nanocomposites containing organophilic layered silicates and compatibilized liquid rubber. *J Appl Polym Sci* 92(5):3088–3096
- Fujiwara M, Kojima K, Tanakaa Y, Nomura R (2004) A simple preparation method of epoxy resin/silica nanocomposite for Tg loss material. *J Mater Chem* 14:1195–1202

- Garesche CarlE, Gerandus HJJ Roebroeks, Buwe V W Greidanus, Rob CV Oost, and Jan W Gunnink (1995) Spliced laminate for aircraft fuselage. In <http://www.freepatentsonline.com>, edited by US Patent, Structural Laminates Company, New Kensington, PA
- Gaume J, Taviot-Gueho C, Cros S, Rivaton A, Thérias S, Gardette J-L (2012) Optimization of PVA clay nanocomposite for ultra-barrier multilayer encapsulation of organic solar cells. *Sol Energy Mater Sol Cells* 99(0):240–249. doi:10.1016/j.solmat.2011.12.005
- Gersifi KE, Durand G, Tersac G (2006) Solvolysis of bisphenol A diglycidyl ether/anhydride model networks. *Polym Degrad Stab* 91(4):690–702
- Gintert MJ, Jana SC, Miller SG (2007) A novel strategy for nanoclay exfoliation in thermoset polyimide nanocomposite systems. *Polymer* 48(14):4166–4173. doi:10.1016/j.polymer.2007.05.053
- Harsch M, Karger-Kocsis J, Holst M (2007) Influence of fillers and additives on the cure kinetics of an epoxy/anhydride resin. *Eur Polym J* 43(4):1168–1178
- Hong S-I, Rhim J-W (2012) Preparation and properties of melt-intercalated linear low density polyethylene/clay nanocomposite films prepared by blow extrusion. *LWT Food Sci Technol* 48(1):43–51. doi:10.1016/j.lwt.2012.03.009
- Hong S-G, Chan C-K (2004) The curing behaviors of the epoxy/dicyanamide system modified with epoxidized natural rubber. *Thermochim Acta* 417(1):99–106
- Hong S-G, Wu C-S (1998) DSC and FTIR analysis of the curing behaviors of epoxy/DICY/solvent open systems. *Thermochim Acta* 316(2):167–175
- Hosseini MG, Jafari M, Najjar R (2011) Effect of polyaniline–montmorillonite nanocomposite powders addition on corrosion performance of epoxy coatings on Al 5000. *Surf Coat Technol* 206(2–3):280–286. doi:10.1016/j.surfcoat.2011.07.012
- Hu C, Kim J-K (2005) Epoxy-organoclay nanocomposites: morphology, moisture absorption behavior and thermo-mechanical properties. *Commun Int* 12(3–4):271–289
- Huang Y, Kinloch AJ, Bertsch RJ, Siebert AR (1993) Particle-matrix interfacial bonding: effect of fracture properties of rubber-modified epoxy polymers. In: Keith Riew C, Kinloch AJ (eds) *Toughened plastics*, vol 1. American Chemical Society, Washington DC, pp. 189–210
- Inoue T (1995) Reaction-induced phase decomposition in polymer blends. *Prog Polym Sci* 20(1):119–153. doi:10.1016/0079-6700(94)00032-W
- Isik I, Yilmazer U, Bayram G (2003) Impact modified epoxy/montmorillonite nanocomposites: synthesis and characterization. *Polity* 44(20):6371–6377. doi:10.1016/s0032-3861(03)00634-7
- Jiankun L, Yucai K, Zongneng Q, Xiao-Su Y (2001) Study on intercalation and exfoliation behaviour of organoclay in epoxy resins. *J Polym Sci B Polym Phys* 39(1):115
- Juwono A, Edward G (2006) A study of clay-epoxy nanocomposites consisting of unmodified clay and organo clay. *Makara, Sains*, pp. 6–12
- Kaneko MLQA, Romero RB, do Carmo Gonçalves M, Yoshida IVP (2010) High molar mass silicone rubber reinforced with montmorillonite clay masterbatches: morphology and mechanical properties. *Eur Polym J* 46(5):881–890. doi:10.1016/j.eurpolymj.2010.02.007
- Kaynak C, Ipek Nakas G, Isitman NA (2009) Mechanical properties, flammability and char morphology of epoxy resin/montmorillonite nanocomposites. *Appl Clay Sci* 46(3):319–324
- Khairulazfar M, Yuhana NY (2016) Curing kinetics, thermal and mechanical properties of epoxy layered silicate nanocomposite toughened with modified natural rubber. *J of Rubber Res* 19(1):1–18
- Khairulazfar M, Yuhana NY, Dzuhri S (2015) Curing kinetics and mechanical study of epoxy / clay nanocomposites. *Polym Res J* 9(4):475–489
- Killilea T Howard, Kevin W Evanson, Wylie H Wetzel, Archie W Garner, Glen Otto Vetter, John W Mittelsteadt, Stephen M Carlson, and Larry B Brandenburger (2007) Coating system for cement composite articles. In <http://www.freepatentsonline.com>, edited by United States Patent Application Publication, Valspar Sourcing, Inc
- Kim D-R, Kim G-C, and Park S-H (2007) Plastic substrate having multilayer structure and method for preparing the same. In <http://www.freepatentsonline.com>, edited by US Patent Application Publication

- Kim J-K, Hu C, Woo RSC, Sham M-L (2005) Moisture barrier characteristics of organoclay–epoxy nanocomposites. *Compos Sci Technol* 65(5):805–813
- Kinloch AJ (2003) Toughening epoxy adhesives to meet today's challenges. *MRS Bull* 28 (6):445–448
- Kinloch A J, R D Mohammed, A C Taylor, C Eger, S Sprenger, D Egan, and [Erratum to document cited in CA143:478605]. *J* (2006), CODEN: JMTSAS ISSN:0022–2461. CAN 144:413470 AN 2006:199197 CAPLUS (2006) The effect of silica nano particles and rubber particles on the toughness of multiphase thermosetting epoxy polymers. *J Mater Sci* 41(4):1293
- Kinloch AJ, Taylor AC (2003) Mechanical and fracture properties of epoxy/inorganic micro- and nano-composites. *J Mater Sci Lett* 22(20):1439–1441
- Knoll R, Mueller C (2005) Containers having improved barrier and mechanical properties. In <http://www.freepatentsonline.com>, edited by US Patent, Pechiney Emballage Flexible Europe
- Kny E (2007) Full proposal for a new COST action: polymer nanocomposites with novel functional and structural properties. Austrian Research Centers GmbH – ARC Technology Transfer
- Koh HC, Park JS, Jeong MA, Hwang HY, Hong YT, Ha SY, Nam SY (2008) Preparation and gas permeation properties of biodegradable polymer/layered silicate nanocomposite membranes. *Desalination* 233(1–3):201–209. doi:10.1016/j.desal.2007.09.043
- Kondyurina I, Kondyurin A, Lauke B, Figiel L, Vogel R, Reuter U (2006) Polymerisation of composite materials in space environment for development of a Moon base. *Adv Space Res* 37 (1):109–115
- Kong D, Park CE (2003) Real time exfoliation behavior of clay layers in epoxy-clay nanocomposite. *Chem Mater* 15(2):419–424
- Koo JH (2006) In: McCombs KP (ed) *Polymer nanocomposites: processing, characterization and application*. McGraw Hill, New York
- Kornmann X, Lindberg H, Berglund LA (2001) Synthesis of epoxy–clay nanocomposites. Influence of the nature of the curing agent on structure. *Polymer* 42(10):4493–4499
- Kunz SC, Beaumont PWR (1981) Low-temperature behavior of epoxy-rubber particulate composites. *J Mater Sci* 16(11):3141–3152
- Kwon Ojin (1998) Morphology development and fracture properties of toughened epoxy thermosets. Dissertation, Chemistry, Virginia Tech
- Lan T, Kaviratna PD, Pinnavaia TJ (1996) Epoxy self-polymerization in smectite clays. *J Phys Chem Solids* 57(6–8):1005–1010
- Lau D (2008) Application of epoxy composite. Pusanika, Universiti Kebangsaan Malaysia, 29 April
- Lee WH, Hodd KA, Wright WW (1989) In: Keith Riew C (ed) *Rubber-toughened plastics, Advances in chemistry series*. American Chemical Society, Washington, DC
- Lekatou A, Faidi SE, Ghidaoui D, Lyon SB, Newman RC (1997) Effect of water and its activity on transport properties of glass/epoxy particulate composites. *Compos A: Appl Sci Manuf* 28 (3):223–236
- Lin P-Y, Rajendran GP, and Zahr GE (2007) Printed circuits prepared from filled epoxy compositions. In <http://www.freepatentsonline.com>, edited by United States Patent Application Publication
- Liu D, Zixing S, Masashi M, Jie Y (2006) DSC investigation of the hindered effect on curing behavior for epoxy–phenol/MMT nanocomposites based on the acidic octadecylamine modifier. *Polym* 47(8):2918–2927
- Liu W, Hoa SV, Pugh M (2004) Morphology and performance of epoxy nanocomposites modified with organoclay and rubber. *Polym Eng Sci* 44(6):1178–1186
- Liu X, Wu Q (2001) PP/clay nanocomposites prepared by grafting-melt intercalation. *Polymer* 42 (25):10013–10019
- Lu J, Zhang MQ, Rong MZ, Yu SL, Wetzel B, Friedrich K (2004) Thermal stability of frictional surface layer and wear debris of epoxy nanocomposites in relation to the mechanism of tribological performance improvement. *J Mater Sci* 39:3817–3820
- Lu M, Shim M, Kim S (1999) Effect of filler on cure behavior of an epoxy system: cure modeling. *Polym Eng Sci* 39(2)

- Ma X, Jansen KMB, Ernst LJ, van Driel WD, van der Sluis O, Zhang GQ (2007) Characterization of moisture properties of polymers for IC packaging. *Microelectron Reliab* 47 (9–11):1685–1689
- Mathivanan L, Radhakrishna S (1998) Protection of steel structures in industries with epoxy-silicone based coatings. *Anti-Corros Methods Mater* 45(5):301–305
- McEwan I, Pethrick RA, Shaw SJ (1999) Water absorption in a rubber-modified epoxy resin; carboxy terminated butadiene acrylonitrile-amine cured epoxy resin system. *Polymer* 40 (15):4213–4222
- Meneghetti P, Qutubuddin S, Webber A (2004) Synthesis of polymer gel electrolyte with high molecular weight poly(methyl methacrylate)-clay nanocomposite. *Electrochim Acta* 49 (27):4923–4931. doi:10.1016/j.electacta.2004.06.023
- Minfeng Z, Xudong S, Huiquan X, Genzhong J, Xuwen J, Wang B, Chenze Q (2008) Investigation of free volume and the interfacial, and toughening behavior for epoxy resin/rubber composites by positron annihilation. *Radiat Phys Chem* 77(3):245–251
- Nigam V, Setua DK, Mathur GN, Kar KK (2004) Epoxy-montmorillonite clay nanocomposites: synthesis and characterization. *J Appl Polym Sci* 93:2201–2210
- Olmos D, González-Benito J (2007) Visualization of the morphology at the interphase of glass fibre reinforced epoxy-thermoplastic polymer composites. *Eur Polym J* 43(4):1487–1500
- Park JH, Jana SC (2003) Mechanism of exfoliation of nanoclay particles in Epoxy-Clay nanocomposites. *Macromolecules* 36:2758–2768
- Phonthammachai N, Li X, Wong S, Chia H, Tjiu WW, He C (2011) Fabrication of CFRP from high performance clay/epoxy nanocomposite: Preparation conditions, thermal-mechanical properties and interlaminar fracture characteristics. *Compos A: Appl Sci Manuf* 42(8):881–887. doi:10.1016/j.compositesa.2011.02.014
- Pinnavaia Thomas J, and Tie Lan (1998) Sealant method of epoxy resin-clay composites. In <http://www.freepatentsonline.com>, edited by United States Patent, Board of Trustees operating Michigan State University
- Ramakrishna HV, Rai SK (2006) Utilization of granite powder as a filler for polybutylene terephthalate toughened epoxy resin. *J Miner Mater Charact Eng* 5(1):1–19
- Ramos VD, da Costa HM, Soares VLP, Nascimento RSV (2005) Modification of epoxy resin: a comparison of different types of elastomer. *Polym Test* 24(3):387–394
- Ratna D (2001) Phase separation in liquid rubber modified epoxy mixture. Relationship between curing conditions, morphology and ultimate behavior. *Polymer* 42(9):4209–4218
- Ratna D, Banthia AK (2004) Rubber toughened epoxy. *Macromol Res* 12(1):11–21
- Ratna D, Becker O, Krishnamurthy R, Varley RJ, Simon GP (2003) Nanocomposites based on a combination of epoxy resin, hyperbranched epoxy and a layered silicate. *Polymer* 44 (24):7449–7457
- Rehab A, Salahuddin N (2005) Nanocomposite materials based on polyurethane intercalated into montmorillonite clay. *Mater Sci Eng A* 399(1–2):368–376. doi:10.1016/j.msea.2005.04.019
- Rezaifard AH, Hodd KA, Tod DA, Barton JM (1994) Toughening epoxy resins with poly (methyl methacrylate)-grafter-natural rubber, and its use in adhesive formulations. *Int J Adhes Adhes* 14 (2):153–159
- Russell B, Chartoff R (2005) The influence of cure conditions on the morphology and phase distribution in a rubber-modified epoxy resin using scanning electron microscopy and atomic force microscopy. *Polymer* 46(3):785–798
- Sapuan SM, Harimi M, Maleque MA (2003) Mechanical properties of epoxy/cocunut shell filler particle composites. *The Arab J Sci Eng* 28(2B):172–181
- Tang X, Alavi S, Herald TJ (2008) Effects of plasticizers on the structure and properties of starch-clay nanocomposite films. *Carbohydr Polym* 74(3):552–558. doi:10.1016/j.carbpol.2008.04.022
- Thomas R, Durix S, Sinturel C, Omonov T, Goossens S, Groeninckx G, Moldenaers P, Thomas S (2007) Cure kinetics, morphology and miscibility of modified DGEBA-based epoxy resin – Effects of a liquid rubber inclusion. *Polymer* 48(6):1695–1710

- Thomas R, Yumei D, Yuelong H, Yang L, Moldenaers P, Yang W, Czigany T, Thomas S (2008) Miscibility, morphology, thermal, and mechanical properties of a DGEBA based epoxy resin toughened with a liquid rubber. *Polymer* 49(1):278–294
- Tie L, Kaviratna PD, Pinnavaia TJ (1995) Mechanism of clay tactoid exfoliation in epoxy clay nanocomposites. *Chem Mater* 7(11):2144–2150
- Tseng C-H, Hsueh H-B, Chen C-Y (2007) Effect of reactive layered double hydroxides on the thermal and mechanical properties of LDHs/epoxy nanocomposites. *Compos Sci Technol* 67 (11–12):2350–2362
- Vaia ADR (2002) Polymer nanocomposites open a new dimension for plastics and composites. *The AMPTIAC Newsletter* 6:17–24
- de Villoria RG, Miravete A (2007) Mechanical model to evaluate the effect of the dispersion in nanocomposites. *Acta Mater* 55(9):3025–3031
- Wang H, Hoa SV, Wood-Adams PM (2006) New method for the synthesis of clay/epoxy nanocomposites. *J Appl Polym Sci* 100:4286–4296
- Wang Y-C, Fan S-C, Lee K-R, Li C-L, Huang S-H, Tsai H-A, Lai J-Y (2004) Polyamide/SDS–clay hybrid nanocomposite membrane application to water–ethanol mixture pervaporation separation. *J Membr Sci* 239(2):219–226. doi:10.1016/j.memsci.2004.03.037
- Weibing X, Pingsheng H, Dazhu C (2003) Cure behavior of epoxy resin/montmorillonite/imidazole nanocomposite by dynamic torsional vibration method. *Eur Polym J* 39(3):617–625
- Yamanaka K, Takagi Y, Inoue T (1989) Reaction-induced phase separation in rubber-modified epoxy resins. *Polymer* 30(10):1839–1844
- Yang B, Wang W, Huang J (2015) Synergic effects of poly(vinyl butyral) on toughening epoxies by nanostructured rubbers. *Polymer* 77:129–142. doi:10.1016/j.polymer.2015.09.027
- Yasmin A, Abot JL, Daniel IM (2003a) Processing of clay/epoxy nanocomposites by shear mixing. *Scr Mater* 49:81–86
- Yasmin A, Abot JL, Daniel IM (2003b) Processing of clay/epoxy nanocomposites with a three-roll mill machine. *Mater Res Soc Symp Proc* 740:13.7.1–13.7.6
- Yu S, Hu H, Ma J, Yin J (2008) Tribological properties of epoxy/rubber nanocomposites. *Tribol Int* 41(12):1205–1211
- Yuhana N Y, S Ahmad, M R Kamal, S C Jana, and A R Shamsul Bahri (2012a) Morphology study on room – temperature cured PMMA – grafted natural rubber – toughened epoxy/layered silicate nanocomposite. *J Nanomater* 2012:14. Article ID 760401. <http://dx.doi.org/10.1155/2012/760401>
- Yuhana NY, Ahmad S, Kamal MR, Jana SC, Shamsul Bahri AR (2012b) Thermal and flexural properties of room – temperature cured PMMA – grafted natural rubber – Toughened epoxy/layered silicate nanocomposite. *Int J Nano and Biomater* 5(1):45–58 2014
- Zainol I, Ahmad MI, Zakaria FA, Ramli A, Marzuki HFA, Aziz AA (2006) Modification of epoxy resin using liquid natural rubber. *Mater Sci Forum* 517:272–274
- Zander NE (2008) Epoxy nano-reinforced composite systems. Dynamic Science, Inc, Black Canyon/Highway Phoenix
- Zeng M, Sun X, Yao X, Ji G, Chen N, Wang B, Qi C (2007) Effects of SiO₂ nanoparticles on the performance of carboxyl-randomized liquid butadiene-acrylonitrile rubber modified epoxy nanocomposites. *J Appl Polym Sci* 106(2):1347–1352
- Zhang Haibing, and Andy Cloud (2006) The permeability characteristics of silicone rubber. Paper read at 2006 SAMPE fall technical conference, “Global advances in materials and process engineering”, proceedings, coatings and sealants section, Dallas
- Zhang J, Zhang H, Yang Y (1998) Polymerization-induced bimodal phase separation in a rubber-modified epoxy system. *J Appl Polym Sci* 72:59–67
- Zhang J, Wang Y, Wang X, Ding G, Pan Y, Xie H, Chen Q, Cheng R (2014) Effects of amino-functionalized carbon nanotubes on the properties of amine-terminated butadiene–acrylonitrile rubber-toughened epoxy resins. *J Appl Polym Sci* 131(13):40472

B. Kothandaraman

Abstract

The Chapter highlights the importance of epoxy based particulate composites with special reference to rubber modified epoxy resins. A brief account on modeling of toughened epoxies is given. Thereafter, mechanical properties of particulate composites based on epoxies are discussed followed by mathematical modeling approaches towards them. The combined effects of particulate fillers with rubbery additives(both CTBN and other rubbery modifiers) on epoxies are then discussed. Finally, the effect of nanoparticles as fillers, in addition to rubbery additives are also reviewed, followed by present and potential applications of such materials.

Keywords

Atomic-force microscopy (AFM) • Coalescence • Einstein's equation • Epoxy-based particulate composites • Silicone modifiers and core-shell rubber particles • Finite element modeling • Fracture toughness • Glycidoxypopyl triethoxy silane (GPTS) • Halpin and Tsai model • Heat distortion temperature (HDT) • Mooney's equation • Nanocomposites • Rubber-modified epoxies • Sol-gel process • Neilson's equation • Particulate composites • Fracture toughness • Rubber-modified epoxy resin • Theories of strength • Polydimethyl siloxane • Positron annihilation lifetime studies (PALS) • 2-D models • Mechanical properties • Nanoparticles • Volume fraction • Rubber-poly butadiene blend • Stress distribution • Trifluoropropyl siloxane (TFP) • von Mises stresses • Young's modulus

Contents

Introduction	372
Preparation of Epoxy-Based Particulate Composites	373
Epoxy-Based Particulate Composites	374

B. Kothandaraman (✉)

Madras Institute of Technology, Anna University, Chennai, Tamil Nadu, India

e-mail: bkraman@mitindia.edu

Rubber-Modified Epoxies	374
Particulate Composites	375
Modeling of a Rubber-Modified Epoxy Resin	375
Mechanical Properties of Particulate Composites	378
Modeling of Mechanical Properties of Particulate Composites	378
A Review on Particulate Composites	381
Toughening of Epoxy Using Particles in Addition to Rubbers	382
Distribution of the Particulates in an Epoxy-Rubber Blend	382
Nature of the Interface Between Filler Particle and Epoxy Resin	385
Use of Silicone Modifiers and Core-Shell Rubber Particles in Epoxy Based Particulate Composites	387
Toughening of Epoxy Rubber-Modified Epoxy Resins by Nanoparticles	390
Nanocomposites Based on Rubber Modified Epoxies	391
Nanocomposites by Sol–Gel Process	392
Applications of Particulate Composites	395
Conclusions	396
References	396

Introduction

Particulate composite is a composite material which consists of tiny particles of one or more materials embedded in a polymer. The polymer may be a thermoplastic or a thermoset. The particulates can be very small particles ($<0.25\ \mu\text{m}$), chopped fibers (such as glass), platelets, hollow or solid glass spheres, silica, alumina, etc. New materials especially those in nanoscale, such as bucky balls, carbon nanotubes, nano-inorganic particles like titania or silica, and nanoclay have also entered this field and are being eagerly researched for their potential to greatly improve mechanical, electrical, surface, flame retardant, and barrier properties of polymers. Though these new materials are likely to be added only in small quantities to the base resin, their mixing procedures with resin and product manufacturing techniques will be similar to those used for making the other particulate composites.

Particulate composites is a less popular area of research when compared with fiber-reinforced composites. The main reason for this is the fact that the reinforcement by particulate material is mostly isotropic. Particulate reinforcements lead to lower levels of reinforcements in mechanical properties, compared with fiber reinforcements. However, they too play an important role in engineering.

The advantages of particulate composites are: (i) products can be fabricated easily by a simple casting process, unlike fiber composites where many of the layup techniques are time consuming, (ii) tooling which may be needed for product manufacture may be simpler, compared with those for fiber composites, (iii) fewer precautions are required in this case for realizing the full strength of the finished product while in case of fiber composites, extra care is required to tailor the properties in specific directions, (iv) high levels of performances are not expected from particulate composite products except for those reinforced by nanoparticles and short fibers, and (v) reinforcement is isotropic.

Generally, properties like modulus, hardness, creep resistance, compressive modulus, and load bearing properties can be improved by particulate reinforcement. Shrinkage on cure too can be reduced by particulate reinforcement. Further, there may be improvements in processing behavior of the resin by way of lesser cure exotherm (the filler particles may act as a heat sink during cure).

However, major challenges are to be faced, to get defect free castings – the chief one being agglomeration of the filler particles, leading to less-than-expected levels of mechanical properties. To a good extent, the use of coupling agents can reduce these difficulties.

The effect of fillers on the properties of epoxy resins has been described in *Handbook of Epoxy Resins* by I.Skiest (1990, Table 6, p. 356). The table summarizes the effect of various fillers commonly used on epoxies. The important points from this table are:

- (i) Calcium carbonate, calcium silicate, aluminum powder and copper powder are used for improving thermal conductivity. These fillers may also improve heat distortion temperature (HDT), machinability, and dielectric constant while they deteriorate impact and tensile strengths.
- (ii) For machinability, aluminum, SiC, flint, and MoS₂ are used as fillers. They too improve thermal conductivity and HDT while they may reduce impact strength.
- (iii) Short glass fibers may improve mechanical strength, thermal conductivity, HDT, and dielectric constant while they may reduce machinability.
- (iv) Mica and silica may improve thermal conductivity, dielectric constant, and HDT while decreasing machinability, mechanical strength, and abrasion resistance.
- (v) Colloidal silica and bentonite clay improve thixotropic response while deteriorating abrasion resistance.

All of these fillers reduce peak exothermal temperature during cure by acting as heat sinks.

Preparation of Epoxy-Based Particulate Composites

Large scale production of particulate composites is often associated with polyester resins, with the famous examples being SMC and DMC molded products. Initially, the compound containing the resin, curatives, and the filler is to be prepared, which is to be followed by an appropriate molding technique. For composites based on other resins, procedures similar to those of the production of SMC or DMC may be adopted.

For preparing the compounds, equipment like a simple mechanical stirrer may be used, for low quantities. Many improvements in achieving higher shear rates, etc. have been done in this field. A common equipment which is used may be the sigma mixer. Another equipment is a high speed mixer, containing rotors fitted with a powerful motor.

In case of nanocomposites with layered particles like nanoclay, there is a need for high shear which alone cause intercalation and exfoliation, necessary for achieving the best performance. This is possible only with sonicators. Sonicators are used mainly when the resin is in solution state or the resin has a low viscosity. In high speed mixers, while preparing nanocomposites, there is a chance of the nanoclay losing its aspect ratio due to particle breakage during mixing.

To prepare a nanocomposite based on epoxy resin, without the use of any major equipment, the sol–gel process can be very useful. Here, the filler (silica, titania, etc.) can be generated in situ, by hydrolysis and condensation of alkoxides (e.g., tetra ethoxy silane-TEOS) with water. This is a case of hydrolytic sol–gel process. Nowadays, nonhydrolytic sol–gel process is also being studied with a lot of interest. Since, the filler is prepared in situ, it is expected that the lowest particle size of the filler can be produced in the polymer matrix – further, agglomeration of these particles too are expected to be reduced to a minimum.

Epoxy-Based Particulate Composites

Among particles used for modifying epoxy resins, a broad classification can be done, viz, rigid particles and rubbery particles.

A liquid rubber without any reactive end group can be merely blended with epoxy resin. When the resin cures, the rubber phase precipitates as small particles. This can improve strain-to-failure values but reduce modulus severely, e.g., liquid nitrile rubber. For toughening epoxies, specially engineered liquid rubbers (i.e., those containing reactive end groups, e.g., COOH in case of CTBN-carboxyl terminated acrylonitrile butadiene copolymer) are the most studied toughening modifiers for epoxy resin. This has been reviewed extensively in a number of books, e.g., Riew C.K. (1989).

Rubber-Modified Epoxies

Rubber-modified epoxies are not classified as particulate composites but rather as reactively blended polymer blends. Hence, this topic is discussed only for some aspects of modeling of their mechanical properties.

The main reason for blending an epoxy resin with rubbery particles is impact modification or improvement in strain-to-failure values. The COOH group in CTBN enables it to attach to epoxy group. The recommended stoichiometry for preparing this blend ensures that the CTBN chain is attached to epoxy resin molecule on both the ends. This increases the molecular weight between cross links besides leading to a block copolymer type morphology, with the rubber, i.e., CTBN phase in between two hard (epoxy) phases. During the cure of the resin, the rubber phase-separates to micron-sized particles (often 0.5–20 μm diameter). Due to the chemical bonding between the rubber, a load applied on the cured resin will cause shear yielding of the resin instead of allowing any crack to propagate.

Particulate Composites

There are a number of reviews covering the modeling of particulate composites based on epoxies. One of them is by Fu et al. (2008). Stiffness of a particulate composite can be improved by particulate fillers. This happens because of the relatively higher modulus of the particulate fillers which to some extent gets transmitted to the polymer. For transmission of strength, stress transfer from the filler to the polymer should be effective. This requires good bonding between the filler particle and the matrix (resin).

Fu et al. (2008) reviewed the effect of fillers on mechanical properties of composites. They compared various models used for predicting the mechanical properties.

Rigid particles like surface-treated alumina and functionalized engineering plastics like poly imides, poly esters, PEEK, poly sulphone, etc. too have been tried as possible tougheners for epoxies. Further, the use of core-shell particles with the core, being elastomeric and shell being polar and rigid and vice versa, too have been well explored. A recent article (Sprenger 2013) has also explored the use of a core shell particle with a very thin shell (nanometer level) of silicone on a rigid particle.

A recent development is the use of nanoparticles to toughen epoxies. Nanoparticles on their own and also in conjunction with rubbers are tried as possible tougheners for epoxies and the latter approach has been reported to be successful for toughening epoxies. A few examples of work done on this are by Kinloch et al. (2003, 2005) and Sprenger (2013).

Modeling of a Rubber-Modified Epoxy Resin

Modeling a rubber-modified thermosets for predicting the mechanical properties is a very complicated process because of nonlinear elasticity of rubbers. Studies by a few authors have enabled us attain a better understanding of the mechanical behavior of such materials under stress. The work by Guild and Kinloch (1995) in this area is discussed below.

When a two phase material is subjected to a load, different types of stress concentrations occur in the stress field. In rubber-modified epoxies, the two dominant strain energy dissipation mechanisms are epoxy matrix shear banding and rubber particle cavitation. Shear banding is associated with concentration of von Mises (deviatorial) stresses while particle cavitation is associated with hydrostatic (dilatational) tensile stress on the rubbery particle. By mapping these two, one can analyze the stress-strain behavior of such materials.

The initial modeling involved 2-D models. These models were able to predict the mechanical properties as a function of the inter (rubber) particle spacing. Other analyses which were used were axis-symmetrical analysis and spatial statistical technique. All these assumed elastic behavior of the matrix(epoxy) and the rubber. 2D modeling could not predict cavitation and debonding of the particles. Many of these analyses could not incorporate high Poisson's ratio values in their programs

(this is important because rubbers have a high Poisson's ratio values). Hence, finite element analysis along with analytical models has to be used for this purpose.

The authors used the idea of analyzing a representative cell of the material. The underlying assumption behind this study was: interactions of neighboring particles on the given particle are not directional but can be visualized as an average arising from all the neighboring particles (in view of the low volume fraction of the rubbery particles). Thus, the material as a whole can be divided into cells each containing a rubber sphere surrounded by a matrix of the epoxy polymer. The boundary of the cell can be considered as the surrounding matrix, which is closest to the rubber particle. The various toughening mechanisms like shear yielding, cavitation, etc. occur in a triaxial stress field ahead of the crack. The simplest triaxial stress which can be applied is a hydrostatic stress. This stress field can be applied without knowledge about the material properties. For an accurate modeling of the material, stresses applied are assumed to be of a low value, i.e., in the range of 60–100 MPa. Volume fraction of the rubber is often taken at around 20% (as commonly done in practice). Application of a triaxial stress should cause the spherical cell to deform to an elliptical one.

The real difficulty in this study is: how to assign the value of modulus for the rubber? Here, the rubber particle is formed in situ and hence it will not be possible to measure the modulus of the rubber particle. Hence, indirect measurements (through simulation of the in situ formation of the rubber particle) were done to determine the modulus of the rubber. It will be reasonable to assume the Young's modulus (E) value for a rubber to be in the range of 1–10 MPa. The Poisson's ratio value can be taken to be very close to 0.5 in this study.

The relationship between bulk modulus K and Young's modulus E for many solids is given by:

$$K = E/3(1 - 2\mu) \text{ where } \mu \text{ is the Poisson's ratio}$$

This equation implies that above μ value of 0.499, for a given value of E, bulk modulus K became very sensitive to even very little changes in μ values. (Please note that at $\mu = 0.5$, K will become infinity.)

Based on the above equation, for a rubber, at $E = 1$ MPa and a μ value of 0.4992 gives K value of about 2 GPa which is a reasonable value for bulk modulus of the rubber phase.

Application of this model, with an applied E (Young's modulus) value of 1 GPa, μ (Poisson's ratio) of 0.4999, and a pure hydrostatic tension of 100 MPa, gave the following results:

Stress Distribution

- (i) The von Mises stresses were maximum (35 MPa) at the resin-rubber interface.
- (ii) Tangential stress was maximum at the interface, at 118 MPa.
- (iii) Radial stresses were at 80 MPa at the interface and increased gradually to about 100 MPa (the given hydrostatic stress value) at the annulus of the element (far from the interface).

Effect of the Volume Fraction of the Rubber

Application of a hydrostatic stress will lead only to volumetric strains and hence bulk modulus will be the relevant parameter under this condition. Application of this model on a rubber-modified epoxy, at $\mu = 0.49$, the bulk modulus was relatively lower and dependent on the volume fraction (v_f) of the rubber while at $\mu = 0.49992$, bulk modulus of the toughened epoxy was deduced to be high and independent of its volume fraction. Further, the bulk modulus was also found to be nearly equal to what would have been the value had the rubber particle been replaced by a void. The hydrostatic stress in the rubber particle was about 40 times higher at $\mu = 0.4999$ compared with the one at 0.490. In both cases, the hydrostatic stress was independent of the volume fraction of the rubber. The von Mises and direct stresses too were found to be independent of volume fraction of the rubber at $\mu = 0.49$ while they increased with volume fraction at $\mu = 0.49992$. These results too were nearly identical if the rubber particles were to be replaced by voids. These results may be described as due to changes in stress concentrations arising out of the difference in properties between a rubber particle and the epoxy annulus. Hence, increasing the μ value of the rubber decreases the difference, which should lead to lower stress concentrations.

Mechanical Properties

As already explained (section “[Modelling of a Rubber-Modified Epoxy Resin](#)”), the bulk modulus of the modified epoxy increased rapidly when μ increased from 0.4992 to 0.4999. The hydrostatic stress in the rubber sphere was predicted to increase with bulk modulus (K) of the rubber, though the rate of increase may be lower at higher K values. If K for both the resin and the rubber were equal, the rubber particle may behave like an isotropic sphere and the stress state will be purely hydrostatic. At this point, the maximum von Mises stress is predicted to reach zero and with a further increase in μ is predicted to increase thereafter.

From these studies, it is apparent that K and μ can be deduced as a function of volume fraction of the rubber. For v_f of 20%, decrease in K value of the material can be predicted to be by around 10–15%. Experimental results show such a trend.

From these studies, another prediction which emerges is: a rubber with a relatively low value of K and μ should lead to low hydrostatic stresses in the rubber but high von Mises stresses in the epoxy. This should in turn promote shear yielding in preference over cavitation or debonding of the rubber particle. If the K value is high, particle cavitation should predominate over shear yielding. Further, cavitation will lead to void formation and if the rubber has a high value of K , the void will be expected to increase the von Mises stresses in the epoxy phase. The review by Guild and Kinloch (1995) mentions that these have been observed in an experiment done on polycarbonate matrix filled with preformed rubber particles.

However, it must be remembered that Poisson's ratio value of the rubber is not easy to predict as the rubber particles also trap epoxy phase inside them. Hence, in some studies, cavitation has been found to precede shear yielding in a few toughened epoxies.

These in turn predict that voids (holes) formed by cavitation of the rubber particles should further help in increasing toughness. This means that small, well-dispersed holes can help in improving toughness. However, in practice, it is not easy to introduce small-sized uniformly distributed holes in an epoxy matrix. Further, the holes can reduce properties like water resistance and increase permeability to gases, etc. which are undesirable effects.

Mechanical Properties of Particulate Composites

The effects of particulates on the properties of the epoxies are reviewed by Fu et al. (2008). This is summarized in this section below.

Mechanical properties generally depend on: (i) particle size, (ii) particle filler interactions, and (iii) extent of filler loading in the composite. Generally, smaller particles are known to reinforce better. This is due to greater surface area available for interaction with the matrix. For example, the review mentions that in a study on epoxy compounds filled by alumina trihydrate, particle size (from 2 to 12 μm diameter) had little effect on modulus of the composite. Filler loading was reported to have increased modulus – nearly doubled when filler loading was increased from nearly 10% (volume fraction) to 40 vol.% while particle size did not show much change. There seems to be a critical particle size above which it does not affect composite modulus while below it may affect composite modulus drastically.

Modeling of Mechanical Properties of Particulate Composites

Modulus is often independent of particle-filler interactions – this has been explained as due to the fact modulus is measured at low deformations, a condition in which not much dilatation of the resin-filler interface can occur. An example for this was given by studies on glass bead filled epoxies. In one study, even a little coating of mold release agent on the glass spheres did not cause a drastic reduction in composite modulus.

The extent of increase in composite modulus due to filler loading may be explained through a number of models. Some of these are mentioned below.

Einstein's equation is the most basic equation which describes the variation of modulus of a composite with filler content.

$$E_c/E_m = 1 + 2.5 V_p \quad (1)$$

Where E_c is the modulus of the composite and E_m is the modulus of the matrix (i.e., the resin)

V_p is the volume fraction of the filler particles

A number of improvements were made on this equation.

Examples:

According to Guth's theory of Filler reinforcement:

$$E_c/E_m = 1 + 2.5 V_p + 14.1 V_p^2 \quad (2)$$

Here, the second term in the right-hand side indicates the effect of the individual particle while the third term covers particle-filler interaction.

According to Halpin and Tsai model:

$$E_c/E_m = 1 + A_1 B_1 V_p / 1 - B_1 V_p \quad (3)$$

here, A_1 is a constant which depends on particle size and Poisson's ratio while B_1 is another constant which depends on modulus of particle and matrix.

According to Neilson's equation:

$$E_c/E_m = \frac{1 + A_1 B_1 V_p}{1 - \Psi B_1 V_p} \quad (4)$$

where Ψ is a coefficient which depends on packing fraction of the particles.

Mooney made another variation for Einstein's coefficient and his equation is as follows:

$$E_c/E_m = \exp \frac{2.5 V_p}{1 - s V_p} \quad (5)$$

where s is a crowding factor for the particles which is related to the volume of the particles occupied to that of its own true volume.

For nonspherical particles, the Mooney's equation gets modified further.

$$E_c/E_m = \exp \frac{2.5 V_p + 0.407 (p - 1)^{1.508}}{1 - s V_p} \quad (6)$$

with $1 \leq P \leq 15$ where P is the aspect ratio of the particles.

Further, a few more models for describing composite modulus have been proposed.

Theories of Strength

If bonding between resin and fillers is negligible, a simple equation can predict the tensile strength of a composite:

$$\sigma_c = \sigma_m (1 - a v_p^b) \quad (7)$$

where σ_c and σ_m are tensile strengths of the composite and matrix respectively V_p is the volume fraction of the filler, a and b are coefficients.

Nicholais and Nicodemo derived the following equation for predicting strength:

$$\sigma_c = \sigma_m(1 - 1.21V_p^{2/3}) \quad (8)$$

assuming negligible adhesion between resin and the filler.

Jancar modified this equation as follows:

$$\sigma_c = \sigma_m(1 - 1.21V_p^{2/3})S_r \quad (9)$$

where S_r is a strength reduction factor varying between 0.2 (high volume fraction) and 1.0 for low volume fraction.

Leidner and Woodhams considered friction between resin and the filler and residual pressure and derived the following equation:

$$\sigma_c = 0.83pf V_p + k\sigma_m(1 - V_p) \quad (10)$$

in which, the first term on the right-hand side covered friction component while the second one, the pressure component.

If adhesion between the filler and resin is good, the Leidner and Woodhams equation can be modified as:

$$\sigma_c = 0.83pf V_p + k\sigma_m(1 - V_p) + \sigma_a H(1 - V_p) \quad (11)$$

where σ_a is the adhesion strength and H is a constant.

For very strong adhesion strength between the resin and the filler, Pukanszky gave an empirical equation:

$$\sigma_c = \frac{1 - V_p}{1 + 2.5V_p} \sigma_m \exp(BV_p) \quad (12)$$

where B is an empirical constant which depends on particle surface area, particle density, and interfacial bonding energy. For poor bonding, the particles will not carry load and hence $B = 0$.

For correlating tensile strength of the composite with particle diameter, two equations were proposed:

$$\sigma_c = \sigma_m(1 - V_p) - k(V_p)d_p \quad (13)$$

for poor interfacial bonding while for good adhesion between filler and the resin,

$$\sigma_c = \sigma_m + k_p(V_p)d_p^{-1/2} \quad (14)$$

where K and K_p are constants and d_p is the particle diameter.

Another model covered all aspects of strength-particle size, its distribution, and its adhesion to the matrix besides matrix degradation. However, this model was mentioned as difficult to use due to complicated calculations. Further, its suitability to nanocomposites is also doubtful.

Fracture Toughness

Fracture toughness depends on initial crack length besides other strength parameters like critical stress for crack growth. Expressions for stress intensity factor (K_{Ic}) and critical strain energy release rate (G_c) can easily be done for homogenous materials. For particulate composites, if the dimensions of the heterogeneity are small compared with the specimen dimensions, it will be easy to predict the values of these parameters. In that case,

$$G_c = K_{Ic} E$$

where E is the effective modulus of the composite.

It can be shown that toughness depends on particle size, loading, and interfacial adhesion. In ductile matrices, lack of interfacial adhesion causes decrease of toughness with filler loading while this may not be true for thermoset matrices.

A Review on Particulate Composites

A review article by Fu et al. (2008) gives a few examples of the effect of particle diameter on the toughness of particulate composites. (i) Studies by Nakamura and Yamaguchi (1991) showed that fracture toughness (both G_c and K_{Ic}) improved with particle diameter (the filler being angular shaped natural silica); the increase is less steep at particle diameter of above 40 μm . The filler contents in these studies were 55 and 64 wt%. (ii) In a work by Radford (1971), on modifying epoxy properties by alumina particles, it was reported that the toughness was maximum when filler content was about 22 vol.%. (iii) Regarding the effect of fiber-resin interactions, stronger interactions need not improve toughness in thermoset particulate composites in contrast with thermoplastic composites. This may be due to different toughening mechanisms operating in these cases. In thermosets, failure may occur by matrix failure or filler particle breakage. In both cases, filler-matrix adhesion becomes irrelevant. (iv) In case of impact toughness, alumina particles (particle size = 13 nm) at about 1 vol.% improved the Charpy impact strength of epoxy composites (by about 50%).

The mechanisms for toughening by particles are: (i) crack pinning or crack tip bowing, (ii) crack tip blunting, (iii) particle-matrix interface debonding, (iv) diffused matrix shear yielding, (v) microcracking, (vi) crack deflection by hard particles, (vii) microshear banding, and (viii) breakage of particles. More than one of these too can occur in some cases, with synergy between them. Crack pinning mechanism is more commonly used to explain the toughness of particulate composites. As per this

mechanism, larger particles should pin the crack over more load and hence improve toughness. Further, crack pinning can occur only if resin–particle bonding is strong.

Toughening of Epoxy Using Particles in Addition to Rubbers

A few articles have described attempts to toughen epoxies using micro- and nanoparticles *in addition to rubbers*. The main reason for this is: rubber toughening is often accompanied by loss in modulus. This necessitates some compensatory action by way of addition of rigid particles. Rubber toughening of epoxies has been/is being researched for the past three decades. The question is: can there be synergy between rubber toughening and rigid particle toughening in composites containing a rubber along with rigid particles? This question assumes more importance in view of the advent of nanoparticles as possible tougheners for epoxies.

One of the well-quoted articles in this area is by Takahashi et al. (1989) which covered work on epoxies modified by silicone polymers (especially amine terminated poly dimethyl siloxane) filled with silica for electronic applications. They reported a few distinct advantages in using silicone instead of CTBN for toughening epoxy particulate composites (with silica filler) for electronics applications. This aspect will be discussed later in this chapter.

Distribution of the Particulates in an Epoxy-Rubber Blend

Uneven distribution of the filler particles between the constituent polymers of any polymer blend can affect the properties of the composites. This has been studied in great depth in rubber–rubber blends. A classic case is the distribution of carbon black between natural rubber and polybutadiene rubber in a typical tire tread compound. For nearly 40 years, many papers have been published in this field and are still being published. A question arises: Is it really necessary to have equal distribution of the carbon black in the natural rubber and polybutadiene phases? It is easy to argue that it is not so because natural rubber has a tendency to crystallize on stretching and hence is a stiffer rubber, while polybutadiene is a much softer rubber and hence more carbon black in the polybutadiene phase should equalize the modulus of the two phases and hence this should lead to better mechanical properties. This supposition is found to be partially true and hence mixing procedures in the rubber industry are tuned to get this effect.

In case of natural rubber–polybutadiene blend, natural rubber has higher stiffness **and also higher raw polymer viscosity** compared with polybutadiene. In case of epoxy–CTBN blend, the epoxy is a stiffer phase compared with CTBN **but at the same time**, less viscous than the CTBN resin (this is because the molecular weight of CTBN is at least 2–3 times higher than that of the epoxy resin). In such a situation, will the filler particles be located preferentially in the CTBN phase or the epoxy phase? Viscosity considerations should favor the particles to be located in the epoxy phase predominantly while modulus considerations should favor the particles to

prefer the CTBN phase. Before gelation and vitrification of the resin, the particles can move easily in the epoxy (the less viscous) phase. In most of the cases, CTBN content is less than 20% of the total resin content. Hence, we should not expect the filler particles to prefer the CTBN phase.

There are a few publications on this aspect.

A few of them indicate that filler particles tend to migrate towards the epoxy phase during the cure. Some authors observe that they may settle in the rubber phase, but, near their boundaries. Lee et al. (2009a) observed that in epoxy-nanoclay-CTBN composites, intercalation by CTBN of the clay before mixing it with epoxy gives better mechanical properties. It is difficult to imagine CTBN (usually with a higher molecular weight and hence of higher viscosity than the epoxy) getting into the clay galleries. However, according to Vijayan et al. (2013), CTBN has a number of chains with low molecular weights which may be responsible for the easy exfoliation of clay, contrary to our expectations. They observed that clay platelets tended to concentrate near the rubber–epoxy interface which can prevent the coalescence of the rubber particles (since they become stiffer due to the clay platelets). This may occur before gelation. Actually, the CTBN phase becomes smaller in diameter, in presence of nanoclay, compared with the unfilled epoxy–CTBN blend. The TEM photograph showing this is presented below.

Coalescence of rubber particles may be prevented by the clay particles. The decrease in particle size of the rubbery phase may also be due to the increase in rate of epoxy amine reaction due to the presence of CTBN (Fig. 1).

According to Liu et al. (2004), the CTBN phase becomes larger in diameter when clay content was 3%. At 6% the dispersed phase was not visible. The diameter of the

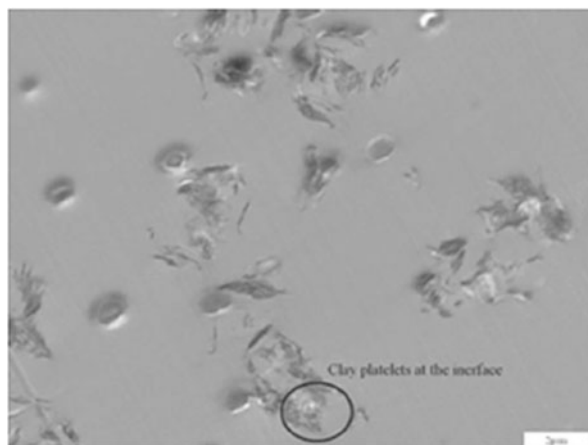


Fig. 1 Clay platelets near the epoxy-CTBN interphase (From Vijayan et al. 2013) (With permission of Springer, Journal of Materials Science, Effect of nanoclay and carboxyl-terminated (butadiene-co-acrylonitrile) (CTBN) rubber on the reaction induced phase separation and cure kinetics of an epoxy/cyclic anhydride system, 47, 2012, pp 5241–5253, P. Poornima Vijayan, Debora Puglia, P. Jyotishkumar, Jose M. Kenny, Sabu Thomas. © Springer Science+Business Media, LLC 2012)

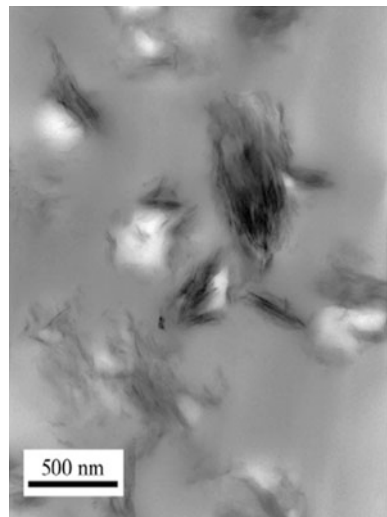
dispersed phase (CTBN) was found to be higher when nanoclay content was 3% (compared with the unfilled, CTBN modified resin). Perhaps, at higher filler (nanoclay) loadings, the diameter of the dispersed phase increases so much they eventually merge, leading to loss of distinctiveness of the rubbery phase in the SEM images. This study too indicates speeding up of the epoxy cure by the CTBN and further, an increase in T_g when the nanoclay was added to the CTBN modified epoxy. It must be remembered that in the unmodified resin, the nanoclay caused a slight decrease in T_g (due to a slight decrease in extent of cure by the nanoclay). Their studies indicate that modification by nanoclay combined with CTBN increases toughness to a greater level compared with toughening by the rubber or clay alone.

Balakrishnan et al. (2005), too, observed that the clay platelets concentrated around the rubber phase – near the wall of the rubber particle – in this study, the rubber was an acrylic rubber. The rubber phase adsorbs the clay particles when the clay content in the composite was up to 3% by weight, but at higher clay content the particles were seen in the epoxy phase because at some clay content, the rubber phase got saturated by clay and any further addition of clay causes it to concentrate in the epoxy phase too. A similar effect was seen when the rubber concentration was decreased with clay content held constant (Fig. 2).

One possible benefit of this study can be this: while modification by a rubber is the best way for toughening epoxy resin, this is accompanied by a considerable loss of stiffness. This can be offset to some extent by adding a rigid particle in addition to a rubber, to toughen epoxy resin.

A good number of recent studies indicate that a combination of nanoparticles and rubber can toughen epoxy composite to a better level when compared with rubber or rigid particles alone. Some of them seem to indicate that nanoparticles may prefer the

Fig. 2 Clay platelets found near rubber-resin interface (From Balakrishnan et al. 2005)



rubber phase. It must be remembered that in these studies, the nanoparticle content in the resin may be lower (often below 5%) than the rubber content (often 10–20%).

Nature of the Interface Between Filler Particle and Epoxy Resin

This aspect is covered in a work done by Tognana et al. (2013). They measured the size of the free volume hole at the interphase (between the resin and the filler) using free volume measurements (positron annihilation lifetime spectroscopy) and also atomic-force measurements. The matrix immediately around the filler particle has properties markedly different from the bulk of the resin. Such interphases can form during curing process. A few studies have measured the interphase region besides the residual stresses in the resin due to the filler inclusion. It is possible to relate the size of the interphase with free volume. A relationship was proposed for relating the free volume and the average radial stress in the matrix. It predicted that the free volume will decrease with filler content up to 15% and beyond it, it will increase. Experimental results show such a trend. The contribution of the interphase to nanohole free volume is considerable at higher filler contents, while it becomes negligible at lower filler contents. Thus, the thermal mismatch between resin and filler becomes the dominating factor at lower filler contents. Further, DSC studies used in this work also help us to infer the presence of an interphase between the filler and the matrix. The work did not explain the exact chemical nature of the interphase.

Figure below shows the interphase and topographic mapping of an epoxy-filler system (by atomic-force microscopy (AFM) measurements). In the top left AFM image, the dark colored phase is the filler particle while the region (light yellow) around the particle is the interface detected by AFM (from Tognana et al. 2013) (Fig. 3).

A number of articles have explored the possible uses of free volume measurements using positron annihilation lifetime studies (PALS) to explain mechanical properties of polymer blends and composites (e.g., Altaweel et al. 2009, 2011). If the compatibility between the constituent polymer of a blend or between the polymer and the filler is poor, larger free volume holes will be formed between the phases (polymer–polymer or polymer–filler particle). At this condition, the positron will take longer time to get annihilated by an electron with which it may collide. This time can be correlated with free volume radius which in turn can be converted to volume.

Factors like cross-linking, crystallization, or other attractive forces between the constituent polymers (or between polymer and filler), etc., reduce the free volume content (which may be expressed as a product of volume of the free volume hole and the number density of the free volume holes) and hence the impinging positron has lesser time (in pico- to nanoseconds range) to get annihilated as they can collide with an electron. Thus, on blending a polymer with another or filler, if free volume content decreases, it may indicate better compatibility – this can improve modulus, while showing lesser thermal expansion coefficient (and sometimes, a small but measurable increase in T_g too). The two papers by Altaweel et al. explain the

correlation of free volume parameters with mechanical properties, for epoxy-based particulate composites containing fly ash or cenospheres (hollow glass spheres) and a modifying additive, the silicone polymer containing amino groups.

Residual stresses occur in the polymer–filler interfaces because of thermal mismatch between the filler particle and resin during the cooling of the resin after curing. This is mainly due to the differences in thermal expansion coefficient between the resin and the filler.

To counter the problem of thermal mismatch between the filler and the resin resulting from the differences in their thermal expansion coefficients, a study explored the use of negative thermal expansion filler (zirconium tungstate) and compared it with silica for possible use in particulate composites. Finite element modeling was done on a composite of epoxy with zirconium tungstate and compared with epoxy silica composites. This work suggests that it may be possible to use a less stiff filler to get a composite with low negative thermal expansion coefficient (Miller

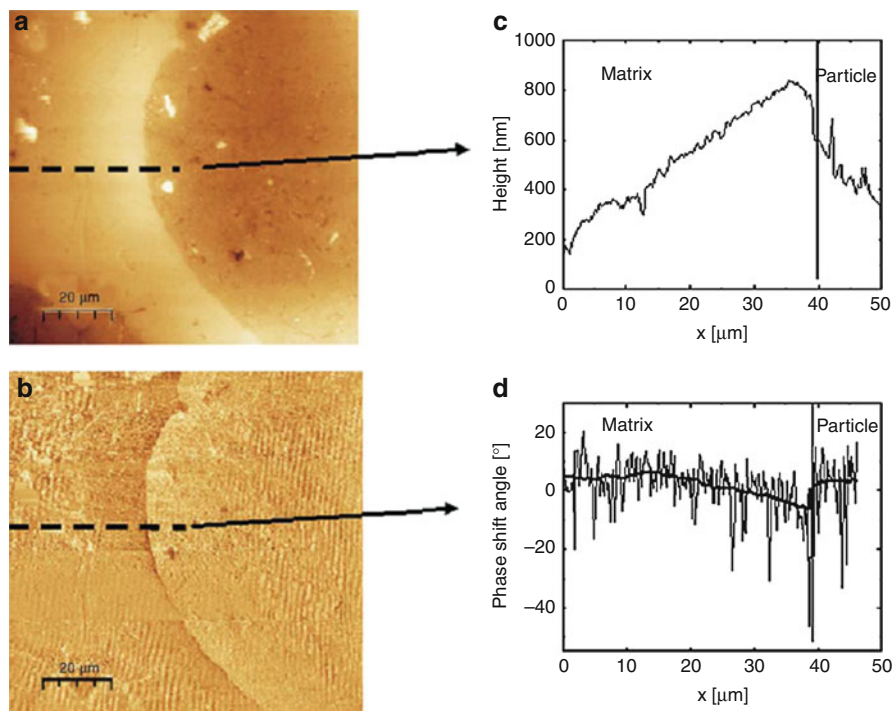


Fig. 3 AFM images of epoxy filled with alumina (30%) which shows the interphase with topographic mapping (From Tognana et al. 2013). (a) AFM–topographic mapping, (b) phase shift around an aluminum particle, (c) profile height, and (d) plot showing phase shift angle versus displacement x , corresponding to the displacement along x axis-dashed line in (c). The solid line in (d) is obtained by smoothing the experimental data

et al. 2010). If the composite is free to expand thermally, adhesion between the polymer and filler becomes important while if the composite is highly constrained, adhesion becomes less important.

These concepts are important while designing microchip assemblies. Less thermal mismatch between the silicon chip and the printed circuit board can lead to circuits with longer life or to function at higher operating temperature.

Use of Silicone Modifiers and Core-Shell Rubber Particles in Epoxy Based Particulate Composites

CTBN is the most studied rubbery modifier for epoxies. It has a few disadvantages: (i) it has many double bonds in the butadiene units – this can impair the weather resistance of the composites and (ii) its glass transition temperature is around $-55\text{ }^{\circ}\text{C}$ – this can prevent the composite from getting the best performance at low temperatures. Polydimethyl siloxane with reactive end groups can be made to combine with epoxy resin and modify its properties. Silicones have lower Tg compared with CTBN and, hence, may lead to better low temperature performance of the epoxy-based composites. Silicones do not have double bonds and hence will not deteriorate its weather resistance.

Takahashi et al. (1989), through their work, showed that addition of an amine terminated silicone polymer of a low molecular weight caused reduced flexural modulus and thermal expansion coefficient (and hence less stressed circuits) in epoxy compounds for use in electronics (e.g., ICs-integrated circuits). The requirements of such a material are: lower modulus and lower thermal expansion coefficient. Attempts to reduce thermal expansion coefficient of epoxy (by adding fillers) will normally lead to increase in modulus too. The studies show that by modifying epoxy with an amine terminated silicone polymer caused a reduction in modulus and thermal expansion coefficient while at the same time increased flexural strength. The authors explained this as due to the silicone acting as an additional coupling agent which could avoid the tendency to reduce strength. Similar studies in the same article also showed that CTBN, the commonly used toughener for epoxy, caused an increase in thermal expansion coefficient, while reducing the modulus. A few more authors have confirmed these findings e.g., Shieh et al. (1997).

The exact nature of the changes in interactions between the filler and the epoxy caused by the silicone is not yet known.

Our studies (Altaweel et al. 2009, 2011) have given evidence for improved interaction between epoxy and fillers related to silica (fly ash and solid glass spheres) caused by modification of epoxy by silicone by free volume measurements (Fig. 4).

The basic idea behind the use of free volume studies is: if silicone can cause better polymer–fly ash interactions, the free volume content should decrease in the composite. In these cases, we do observe this. The same trend is not seen in the neat resin. In the neat resin, presence of the rubbery modifier (ACS-amine containing silicone) caused an increase in the free volume due to limited compatibility

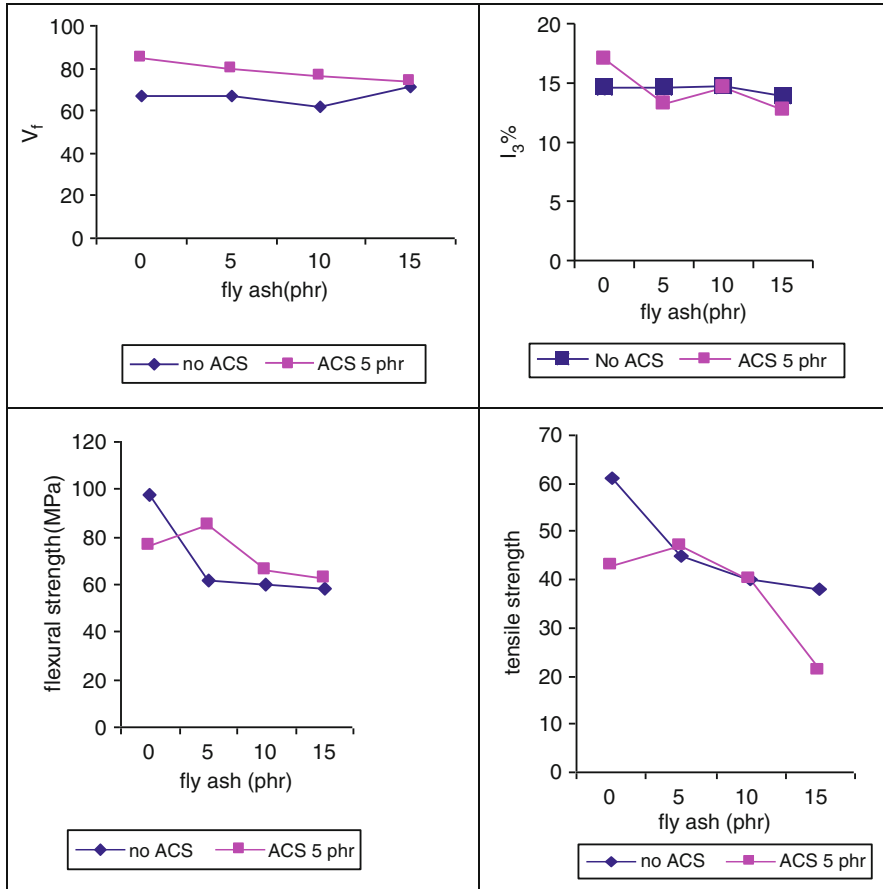


Fig. 4 (a) Variation of size of the free volume hole with fly ash content. (b) Variation of the relative density of the free volume hole with fly ash content. (c) Variation of flexural strength with fly ash content. (d) Variation of tensile strength with fly ash content (Adapted from figures from Altaweel et al. 2009)

between the resin and the silicone. Hence, the rubbery additive reduces tensile and flexural strength and moduli in the neat resin. However, this trend is not seen in silicone modified epoxies with silica as fillers here, actually, a slight increase in tensile and flexural strength is seen in the particulate composite. Further, silicone polymer has been reported to have reduced thermal expansion coefficient (in silica filled epoxies); this, coupled with a reduction in stiffness leads to reducing the stresses in encapsulations – a factor which has led to increased interest in exploring the use of silicone as a toughener for epoxies, for use in electronics (Takahashi et al. (1989); Shieh et al. (1997)).

The toughening of epoxy casting materials by silicone gel was studied by Shimzu et al. (1994). In this work, epoxy resin was toughened using silicone gel (which is a

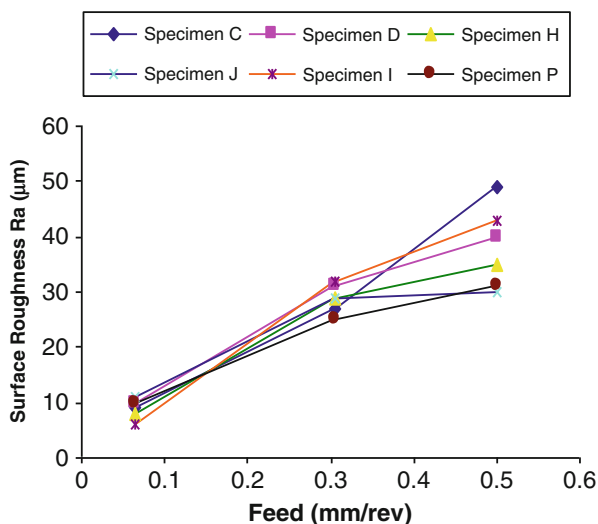
slightly cross-linked PDMS) with various particle sizes (up to 30 phr loading). In addition, silica flour (up to 400 phr) was used as a filler. The flexural strength of the unfilled resins decreased with silicone gel content but in presence of the filler the fall was moderated. The drop in flexural strength was negligible up to 10 phr of silicone gel. The flexural modulus decreased with the silicone content both in the filled and in the unfilled castings. Fracture toughness (K_{1C}) showed remarkable increase in presence of the gel – both in the filled and unfilled resins. The best toughening was seen with the silicone gel particle size at about around $0.3 \mu\text{m}$. SEM fractographs showed silicone particle detachments, which indicates that even though the adhesion of the silicone phase with the epoxy matrix was not good, toughening was considerable.

Elangovan (2013) studied the effect of amine containing silicone (ACS-poly dimethyl siloxane co aminopropyl methyl siloxane with a molecular weight of 5000 and with about 7–8 amine groups per silicone chain) on epoxy castings with aluminum (Al) and/or solid glass spheres (Sp G) as fillers. The studies were done for evaluating the changes in machinability of the composites so that they may be considered for tooling materials for making temporary molds for injection molding. The presence of silicone in these castings improves machinability by reducing the cutting force and also giving surfaces of smoother finishes, in the silicone containing castings (Fig. 5).

The improvement may be due to some migration of silicone chains to the air interface which in turn may give a lubricating effect for the cutting tool. SEM studies also seem to indicate that, in castings containing both aluminum and solid glass spheres, the solid glass spheres retain their identities while the aluminum phase is not so easily seen. This may indicate agglomeration of aluminum particles.

In another work, Eiss and Czichos (1986) have observed that wear rates were reduced by blending of silicones to epoxies. They blended PDMS copolymerized

Fig. 5 Surface roughness of various epoxy castings containing a silicone modifier (ACS), aluminum, and solid glass spheres (Sp G) (From Elangovan 2013) (Note: H contains the rubber modifier (ACS) while C and D do not contain the rubber modifier)



with methyl trifluoropropyl siloxane (TFP) for improving compatibility between PDMS and epoxy. The highest wear resistance was noted in the blend containing 10–15% silicone where 20% of the silicone was TFP. The proportion of silicone at the surface was found to be higher than at the bulk. Further, the wear seemed to start by removal of the silicone domains (especially those with larger diameters) and then spread to the epoxy phase. The silicone phase caused a reduction in modulus and this reduced the stress on the material. In compositions where silicone domains were too small and were closely spaced, wear was too rapid as the thin epoxy phases between the silicone domains were not able to resist the stress and hence higher wear rates.

Lee et al. (2009b) studied sol–gel process to prepare a nanocomposite containing a cycloaliphatic epoxy resin modified by HTPDMS and GPTS (a precursor for POSS besides a chain stopper for the epoxy polymerization). This system was cured by cationic polymerization using aluminum acetylacetonate [$\text{Al}(\text{acac})_3$]. These materials were studied for possible use as LED materials. The silica domains formed by hydrolysis of the GPTS had a particle of around 200 nm. Increased amounts of HTPDMS did not cause the transmissibility of UV light to decrease, indicating good compatibility between the epoxy and the silicone. The silica precursor was added in two different concentrations – at 5 and 10% by weight. Up to 10% silica precursor contents in the reaction mixture, the silica domain formations did not reduce the transmissibility of the UV light, indicating their usability for the stated application.

Marouf et al (2009) studied the combined effect of a core shell rubber (butadiene-styrene core with methyl methacrylate shell) and organo-modified clay for toughening epoxies. This paper also reviewed the models used to predict the mechanical properties of rubber and particle modified epoxy systems. Under the experimental conditions used by them for mixing the rubber and the clay particles, they could observe intercalation to a good extent. The rubber particles were observed to form clusters in the epoxy matrix. This study indicates that a combination of core shell rubber particles with organoclay did not increase the compressive yield stress and fracture toughness of the resin compared with rubber alone or clay alone. The formation of the clusters by the rubber particles may be a possible reason for lack of synergy between rubber and nanoclay in the epoxy studied by them. Clay layers could have acted as stress concentrators. More importantly, competition between various micromechanisms might be the cause of lack of synergy between rubber modification and toughening by nanoclay particles. However, a strong possibility of lack of synergy due to nanoclay platelets preventing rubber particle cavitation is suspected, as per this work

Toughening of Epoxy Rubber-Modified Epoxy Resins by Nanoparticles

In a study by Bray et al. (2013), a model based on FEA was proposed and experimental studies to verify the predictions based on this model were done. The system studied was a piperidine-cured epoxy resin and the filler was nanosilica with three different particle sizes – 23, 74, and 170 nm.

The mechanisms observed were shear banding and particle debonding, followed by plastic void growth after debonding from the matrix. In these studies, it was predicted that only about 14.3% of the nanoparticles were debonded while for each debonded nanoparticle, its immediate neighboring silica particles were shielded from debonding. The model was able to predict the individual contributions of shear banding and plastic void growth after particle detachment. The model predicted that all these three class of particles (based on particle sizes) could be expected to enhance toughness to equal degree – experimental studies show a similar trend, approximately. A salient feature of this paper was: normally failure mechanisms and the number of particles of the dispersed phase (silica nanoparticles in this case) are determined by performing SEM of the fractured surfaces (i.e., **after** fracture occurred) while in this case, the FEA modeling was done **before** fracture was done, to calculate the number of particles.

Robinette et al. (2007) evaluated two grades of RTM grade epoxy resins which were compounded with silica nanoparticles (which were actually dispersed in bisphenol-F) for toughening. The grades contained some elastomer, though the nature and the actual proportions of the elastomeric modifier are unknown, as these resins are proprietary in nature. This study indicated that in one of the grades, better synergy between the nanoparticles and the rubber was observed. The TEM analysis on the fractured surfaces indicated that the silica particles migrated more to the epoxy phase and no silica particle was seen in the elastomer phase. For comparison, the authors made a CTBN-modified epoxy composites and studied their fracture surfaces. They showed that addition of silica nanoparticles caused phase separation of a greater number of CTBN domains but with smaller domain sizes (compared with the unfilled blend). This may indicate that the silica nanoparticles acted as a nucleation site for the CTBN to phase-separate inside the matrix. This gave much better synergy in toughening between silica nanoparticles and elastomer, compared with the commercial resins.

Konnola et al. (2015) studied preparation of epoxy-CTBN-POSS hybrid (i.e., toughening both by rubber and POSS) systems and found that a combination of CTBN and POSS toughens DGEBA epoxy (DDS cured) but to a lesser extent than POSS itself. The POSS used was an octa-functional one. FESEM of the fractured surfaces show that in the hybrid composite, the cross-link density near the rubber phase might have increased, leading to poorer toughening ability. The rubber phase showed rough surface and reduced domain size after the addition of POSS – this might be attributed to higher cross-link density near the CTBN phase caused by the octa-functional POSS. Further, here too, it is inferred that nucleation of the CTBN phase by the POSS particle might have occurred.

Nanocomposites Based on Rubber Modified Epoxies

A few articles have dealt with this subject. Sprenger (2013) reviewed the effect of surface modified nanosilica as a filler for epoxies. Various rubbers were used for

modification of epoxy in this study. He notes that: (i) Loss of modulus by a core-shell rubber modifier (styrene-butadiene type) was compensated by adding a nanosilica, but synergy between the rubber and nanosilica was not seen. (ii) Toughness values were higher when rubber (of CTBN type) and nanosilica were combined. However, there was a lowering of T_g and modulus. (iii) Increase in toughness was more prominent when the curative was anhydride rather than amine. The article, further, speculates the reason for the synergy when CTBN was used, as follows: in the presence of nanosilica particles, the number of epoxy chains not participating in the phase separation (of the rubber phase) increases – this may lead to a more ductile matrix, leading to synergy between CTBN and nanosilica. No evidence was seen, for the nanosilica particles preferentially migrating to the CTBN phase, in this study.

Wang et al. (2012), in their work, studied the effect of carboxy functionalized multi-walled carbon nanotubes (MWCNT) on mechanical properties of CTBN-modified epoxies. They report an improvement of tensile and flexural strength by about 20% by addition of 0.5 wt% of MWCNT. At this concentration, the CNTs distributed themselves well in the epoxy matrix while at higher loadings, they tended to agglomerate.

Nanocomposites by Sol–Gel Process

In sol–gel process, the nanoparticles grow in size slowly in presence of the polymerization mixture. Sol–gel process is highly advantageous for coatings due to issues involving removal of the aqueous media from the system.

In sol–gel process, the particle size and the nature of the silica particle produced may depend on the pH and the molar ratio of water:TEOS (called R value). Higher R values are expected to give smaller silica nanoparticles but new difficulties may arise in removing the excess water from the system. Acidic pH often gives smaller particles and also speeds up the hydrolysis and condensation while alkaline pH may be slow and give a more open structure (long chain silica).

Further, the properties depend on whether the sol–gel process occurs concurrently with epoxy curing or before curing. Ideally we should expect better results if the sol–gel process is completed before adding the mixture to the epoxy. Our studies (Meenakshi 2014) indicate that better mechanical properties result when the sol–gel process occurs in presence of the epoxy resin (curing done after the sol–gel process is completed). This may be due to incompatibility between the sol–gel mixture after hydrolysis with the epoxy resin.

Flexural strength shows increase by about 40% after the sol–gel process when R value is between 6 and 8 (Fig. 6a). At higher R values, difficulties in removing the excess water is seen which leads to agglomeration of the silica agglomerates. The silica particle size is around 100–200 nm (Fig. 6b).

Presence of amine-containing silicone modifier (ethoxy terminated poly dimethyl siloxane-coaminopropyl methyl siloxane with a molecular weight of 5000) helps in improving the properties further (Fig. 6c).

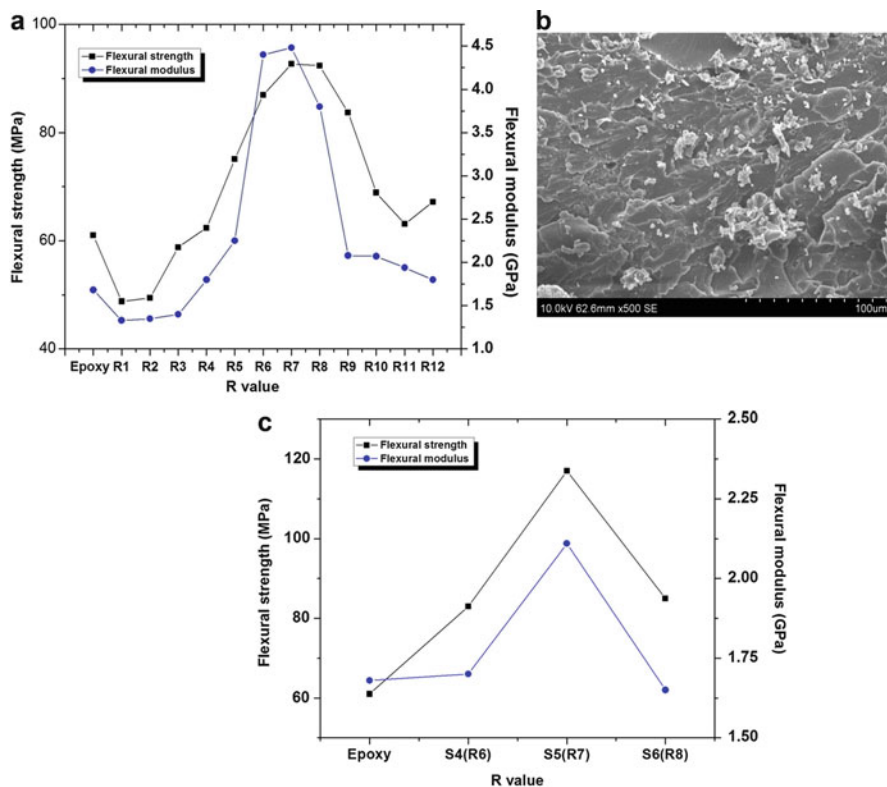


Fig. 6 (a) Variation of flexural strength and modulus with R value (sol–gel in neutral medium) (fig 3.18, p 106, From Meenakshi 2015). (b) SEM of fractured specimen for sol–gel process on epoxy resin, done at R value of 6 (fig 3.21, p110, From Meenakshi 2015). (c) Variation of mechanical properties by sol–gel process on silicone modified epoxy (fig 3.37, page 130, Meenakshi 2015)

Matejka et al. (1998) studied nanocomposite formation on epoxies cured by polyetheramine (which should lead to rubber epoxy network) by sol–gel process. He compared the particle distribution of the nanosilica generated by two processes: (i) sol–gel process and curing occurring simultaneously and (ii) sol–gel process after curing. He found finer silica distribution was seen when sol–gel process was done after the curing of the epoxy.

Sol–gel process was done on a cycloaliphatic epoxy resin along with UV curing. An easy method for preparing nanocomposite was described by Malucelli et al. (2009). The base resin, diluent (hexane diol diglycidyl ether-HDGE) and coupling agent – cum-chain stopper – glycidoxypropyl triethoxy silane(GPTS) were mixed and cured to give a film. Hydrolysis–condensation of the TEOS incorporated into the epoxy was done by exposing the film to humidity. This gave very hard films with nanosilica incorporation upto 60%. However, the resulting films were too brittle. Hence, another study (Kothandaraman et al. 2014) was done on sol–gel process after curing of the epoxy by swelling the cured in Tetra Methoxy

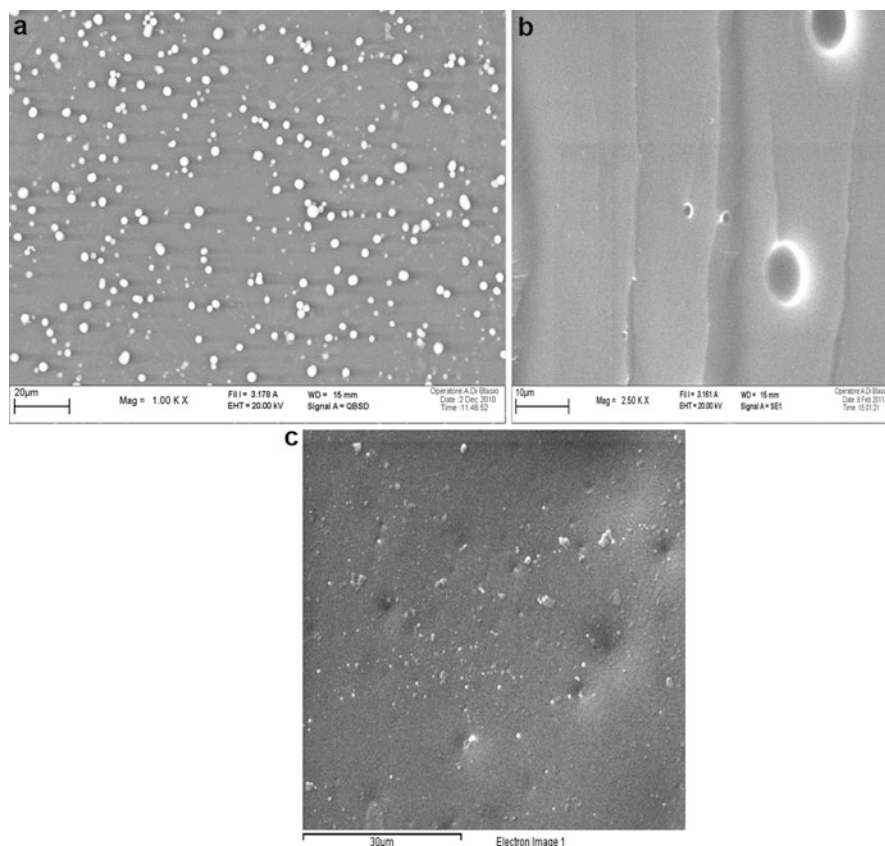


Fig. 7 (a) SEM of surface of UV cured, epoxy resin (not modified by a rubbery modifier) subjected to sol–gel process – cross section showed negligible amount of the silica phase. (b) SEM of cross section of a UV cured, silicone modified epoxy film subjected to sol–gel process. (c) SEM of surface of a UV cured, silicone modified epoxy film subjected to sol–gel process (Adopted from Kothandaraman et al. (2014))

Silane (TMOS) at 80 °C. To increase the TMOS intake, the epoxy was modified by glycidoxy terminated poly dimethyl siloxane. This also made the film more flexible. On exposing the swollen film to humid air at 80°C, most of the silica was found to be located in the PDMS phase (Fig. 7b – in the dispersed phase in the form of white bands around them) and the film became stiffer but with a surface similar to that of a ceramic. SEM showed that silica is more in the PDMS phase and that too at its interface with the epoxy (Fig. 7b). It is to be noted that, in the epoxy not modified by the PDMS, the surface showed silica domains (Fig. 7a) but not in the bulk. After completion of the hydrolysis–condensation, the PDMS phase was found to be eroded and its edges were enriched in silica (this caused an increase in the Tg of the PDMS phase – from somewhere near –100°C to +50°C). Further, the silica formed was seen more on the surface of the film rather than the bulk of the film,

as submicron-sized domains (Fig. 7c). However, the films developed porosity too. Such a procedure can lead to self-organized nanostructures, giving polymeric films with an inorganic rich surface – for better flame retardancy, scratch resistance, and modified electrical properties.

A similar observation was made by De Luca et al. (2009), when they compounded epoxidized SBR with aminosilane (APTS) and TEOS and water to conduct the curing and sol–gel process simultaneously. They found that films formed from compositions with excess TEOS showed more ceramic characteristics and not rubbery ones.

Applications of Particulate Composites

A few uses of particulate composites may be:

- (i) Appliances, toys, electrical products, computer housings, cell phone casings, office furniture, helmets, etc. are made from particulate reinforced plastics.
- (ii) Glass reinforced plastics in the form of SMC and DMC mouldings are used in many automotive applications including body panels, bumpers, dashboards, and intake manifolds.
- (iii) Friction composites like clutch facings, brake linings, and brake shoes can be considered as particulate composites as they may contain short fibers like those of asbestos and aramid pulp.
- (iv) In electronics, particulate composites may be used for encapsulating circuits, printed circuit boards, etc.
- (v) In manufacturing engineering, particulate composites may be used for making prototypes and tooling material for making sample products (Freeman Manufacturing and Supply Company 2016).

Epoxies were studied for structural applications where absorption of ultrasonic waves was necessary (Gabriel and Petrie 2000). Rigid particles were needed for structural integrity while rubbery additive was for sound absorption property. For this, toughened epoxies filled by solid glass spheres were tried. DoE was used to develop experimental regime to investigate the impact of density, T_g, and volume fraction of the rubber on absorption of sound. Maximum absorption was found to occur in materials with higher loading of the low T_g polymer (here it was various types of room temperature vulcanizable silicones).

Nanocomposites with nanoclay as the filler may be useful in developing products with altered barrier properties or flame retardant properties. Nanocomposites based on silica filler may be useful in preparing materials with better flame retardance or superior scratch resistance or altered electrical or optical properties (e.g., wave guides). Sol–gel process has also been tried to prepare nanocomposites containing silver for altered conductivity, antibacterial surface, etc.

The major applications of polymeric nanocomposites will be in the area of electrical and electronics engineering. Insulation breakdown strength was reported

to have been improved drastically (by about 25%) by addition of a small amount of nanotitanium dioxide to epoxy resin. Further, deterioration of dielectric endurance after exposure to electric fields was found to be much lesser for nanocomposites compared with composites with micron-sized fillers (Nelson and Hu 2005).

Further, a set of properties which is difficult to achieve is: high thermal conductivity but with low electrical conductivity. This can be achieved by nanocomposites, according to a few authors. This can lead to insulators which will be lighter in weight and avoid the use of cooling systems (thus saving energies in transformers, etc.) (European Commission (2013))

Conclusions

Particulate composites based on thermosets are an important class of materials in engineering and find extensive uses as replacement of metals, for applications involving light weight, corrosion resistance, etc. This chapter mentioned the importance of this subject followed by methods to manufacture such materials.

This chapter also reviewed modeling of rubber-modified epoxy resin followed by its implications on the mechanical properties of such materials. Further, modeling of mechanical properties of particulate composites was reviewed. The effect of adding nanoparticles to rubber-modified epoxy was discussed. This chapter also touched upon the use of silicone modifiers for epoxy and their possible advantages over CTBN as a modifier for epoxy resin and its composites.

References

- Altaweel AMAM, Ranganathaiah C, Kothandaraman B (2009) Mechanical properties of modified epoxies as related to free volume parameters. *J Adhes* 85:200–215
- Altaweel AMAM, Ranganathaiah C, Kothandaraman B, Raj JM, Chandrashekar MN (2011) Characterisation of ACS modified epoxy resin composites with fly ash and cenospheres as fillers-mechanical and microstructural properties. *Polym Compos* 32(1):139–146
- Balakrishnan S, Start PR, Raghavan D, Hudson SD (2005) The influence of clay and elastomer concentration on the morphology and fracture energy of preformed acrylic rubber dispersed clay filled epoxy nanocomposites. *Polymer* 46:11255–11262
- Bray DJ, Dittanet P, Guild FJ, Kinloch AJ, Masania K, Pearson RA (2013) The modeling of the toughening of epoxy polymers via silica nanoparticles-the effects of volume fraction and particle size. *Polymer* 54:7022–7032
- De Luca MA, Jacobi MM, Orlandini LF (2009) Synthesis and characterization of elastomeric composites from epoxidised styrene butadiene rubber, 3 aminopropyl triethoxysilane and tetraethoxysilane. *J Sol-Gel Sci Technol* 49:150–158
- Eiss NS, Czichos H (1986) Tribological studies on rubber-modified epoxies: influence of material properties and operating conditions. *Wear* 111:346–361
- Elangovan K (2013) In studies on epoxy and modified epoxy particulate composite, Ph.D Thesis, Anna University, Chennai, Chapter 4, p93
- European Commission (2013) ANASTASIA (Advanced Nanostructured Tapes for Electrotechnical High Power Insulating Applications) Project report summary, Project ref 228581, p 1

- Epoxy Castings Catalogue (2016) Liquid Tooling Materials-selection guide, vol 24. Freeman Manufacturing and Supply Company, Avon, p 32.
- Fu S-Y, Feng X-Q, Lauke B, Mai Y-W (2008) Effects of particle size, particle/matrix interface adhesion and particle loading on mechanical properties of particulate-polymer composites. *Compos Part B* 39:933–961
- Gabriel K, Petrie S (2000) Ultrasonic absorption in rubber filled epoxies. In: ANTEC Proceedings, SPE, vol 3, 1488–1493
- Guild FJ, Kinloch AJ (1995) Modelling the properties of rubber modified epoxy polymers. *J Mater Sci* 30:1689–1697
- Kinloch AJ, Mohammed RD, Taylor AC, Egar C, Sprenger S, Egan D (2003) Toughening structural adhesives via nano and micro phase inclusions. *J Adhes* 79:867–873
- Kinloch AJ, Mohammed RD, Taylor AC, Egar C, Sprenger S, Egan D (2005) The effect of silica nanoparticles and rubber particles on the toughness of multiphase thermosetting polymers. *J Mater Sci Lett* 1:2461–2465
- Konnola R, Parameswaranpillai J, Joseph K (2015) Mechanical, thermal and viscoelastic response of novel insitu CTBN/POSS/epoxy hybrid composite system. *Polym Compos*. doi:10.1002/PC.23390
- Kothandaraman B, Malucelli G, Camino G (2014) Preparation of a nanocomposite by swelling of a UV cured cycloaliphatic epoxy film in a silica precursor. *Inter J Plast Technol* 18(2):173–182
- Lee H-B, Kim H-G, Yoon K-B, Lee D-H, Min K-E (2009a) Preparation and Properties of a CTBN toughened epoxy/montmorillonite nanocomposite. *J Appl Polym Sci* 113:685–692
- Lee SS, Song GS, Lee DW, Kim HM, Kang KH, Lee DS (2009b) Preparation and properties of epoxy resin/silicone hybrids for electronics applications. In: 11th Proceedings electronics packaging technology conference. pp 348–351, IEEE
- Liu W, Hoa SV, Pugh M (2004) Morphology and performance of epoxy nanocomposites modified with organoclay and rubber. *Polym Eng Sci* 44(6):1178–1186
- Malucelli G, Amerio E, Minelli M, De Angelis MG (2009) Epoxy-siloxane hybrid coatings by a dual curing process. *Adv Polym Technol* 28(2):77–85
- Marouf BT, Pearson RA, Bagheri R (2009) Anomalous fracture behaviour in an epoxy based hybrid composite. *Mater Sci Eng A* 515:49–58
- Matejka L, Dusek K, Plestil L, Kriz J, Lednický F (1998) Formation and structure of epoxy-silica hybrids. *Polymer* 40:171–181
- Meenakshi D (2014) In studies on In-situ generation of nanosilica network in polymer matrix by sol-gel process, Ph.D Thesis, Anna University, Chennai, Chapter 3, pp 106, 110, 130
- Miller W, Smith CW, Dooling P, Burgess AN, Evans KE (2010) Reduced thermal stress in composites via negative thermal expansion particulate fillers. *Compos Sci Technol* 70:318–327
- Nakamura Y, Yamaguchi M (1991) Effect of particle size on fracture toughness of epoxy filled with angular shaped silica. *Polymer* 32:2221–2229
- Nelson JK, Hu Y (2005) Nanocomposite dielectrics – properties and implications. *J Phys D Appl Phys* 38:213–222
- Radford KC (1971) The mechanical properties of an epoxy resin with a second phase dispersion. *J Mater Sci* 6:1286–1291
- Riew CK (ed) (1989) Rubber toughened plastics, vol 222. American Chemical Society (ACS), Washington, DC
- Robinette J, Bujanda A, DeSchepper D, Dibelka J, Costanzo P, Jensen R, McKnight S (2007) Nanosilica modification of elastomer-modified VARTM epoxy resins for improved resin and composite toughness in ARL-TR-4084
- Shieh J-Y, Ho T-S, Wang C-S (1997) Synthesis and modification of a trifunctional epoxy resin with amino terminated poly(dimethyl siloxane)s for semiconductor encapsulation. *Angew Makromol Chem* 245(1):125–137
- Shimzu T, Kamino M, Miyagawa M, Nishiwaki N, Kida S (1994) Deformation, proceedings of conference on yield and fracture of polymers, Cambridge, pp P76/1-P76/4

- Skiest I (1990) Handbook of epoxy resins. Table 6. van Nostrand Reinhold, New York, p 356
- Sprenger S (2013) Epoxy resins modified with elastomers and surface modified silica nanoparticles. *Polymer* 54:4790–4797
- Takahashi T, Nakajima N, Saito N (1989) Morphology and mechanical properties of rubber modified epoxy systems. In: Riew CK (ed) Rubber toughened plastics, vol 222. American Chemical Society (ACS), Washington, DC, pp 243–261
- Tognana S, Salgueiro W, Somoza A, Marzocca AJ (2013) Influence of the filler content on the free nanohole volume in epoxy-based composites. *Exp Polym Lett* 7(2):120–133
- Vijayan P, Puglia D, Kenny JM, Thomas S (2013) Effect of organically modified nanoclay on miscibility, rheology, morphology and properties of epoxy/CTBN blend. *Soft Matter* 9:2899–2911
- Wang YT, Wang CS, Yin HY, Wang LL, Xie HF, Cheng R (2012) CTBN toughened epoxy/carboxyl modified CNT nanocomposites-thermal and mechanical properties. *Exp Polym Lett* 6(9):719–728

B. T. Marouf and R. Bagheri

Abstract

Epoxy resins have been used in a very wide range of industrial applications for more than half a century. Paints, adhesives, coatings, and matrix material for many different kinds of composites are the main applications of epoxy resins. Excellent adhesion properties along with high mechanical strength and thermal stability are the major attractions of this family of engineering materials. However, epoxy resins suffer from the inherent brittleness which can potentially limit their applications. Among different approaches which have been employed to reduce this deficiency, rubber toughening has been practiced the most. Different types of rubber modifiers which are blended with epoxy resins for this purpose include reactive oligomers, preformed rubber particles, and di- or tri-block copolymers. This chapter tries to give a general overview of the whole concept of rubber-toughened epoxies to the reader. Delivering a more realistic sense of industrial applications of epoxy/rubber and epoxy/copolymer blends by means of practical examples is done in this chapter as well. The goal is that the reader can benefit from this chapter in expectations from epoxy blends in practice. Engineers interested in epoxy resins may find insights in this chapter for their developing industrial/research plans.

Keywords

Epoxy • Rubber • Block copolymer • Nano/micro modifier • Application

B.T. Marouf (✉)

Department of Materials Science and Engineering, Faculty of Engineering, Urmia University, Urmia, Iran

e-mail: b.marouf@urmia.ac.ir

R. Bagheri

Polymeric Materials Research Group, Department of Materials Science and Engineering, Sharif University of Technology, Tehran, Iran

e-mail: rezabagh@sharif.edu

Contents

Introduction	400
Rubber Toughening of Epoxies	401
Types of Rubber Modifiers Used in Epoxy Blends	402
Reactive Oligomers	403
Preformed Particles	404
Block Copolymers (BCPs)	405
Industrial Applications of Epoxy/Rubber Blends	406
Coatings	406
Composites	411
Adhesives	414
Conclusion	422
References	422

Introduction

Epoxy resins have been in the market since mid-twentieth century and used in many applications as paints, adhesives, coatings, and matrix material in different types of composites (Marouf et al. 2016; Bagheri et al. 2009). Figure 1 illustrates distribution of epoxy resin markets around the globe in 2009. The total consumption of epoxy resins in these markets was around 1.8 million tons in 2009 (provided by PlasticsEurope's PC/PBA-group on www.bisphenol-a-europe.org) and is estimated to go beyond 3 million tons by 2017 (reported by Global Industry Analyst Inc. on www.prweb.com). Such a wide range of industrial applications is due to the attracting engineering properties of epoxy polymers including good thermal stability and creep resistance, relatively high elastic modulus, and excellent adhesion properties (Kinloch et al. 2014). The wide range of chemistry of epoxy resins along with the large number of cross-linking materials have enabled people in academia and industry to synthesize huge number of epoxies for so many different applications.

Epoxy resins are low molecular weight prepolymers or higher molecular weight polymers having at least two epoxide groups, each containing two carbon atoms single bonded to an oxygen atom (Pulgisi and Chaudhari 1988). There are two families of epoxies, namely, glycidyls and cycloaliphatics. The first group is made by a reaction with epichlorohydrin, while the latter are produced by peroxidizing olefins. Epoxidized phenols, or phenol glycidyl ethers, are the most commercially important resins (Pulgisi and Chaudhari 1988), in particular, epoxidized bisphenol A, known as diglycidyl ether of bisphenol A (DGEBA), which provides an excellent balance of physical, chemical, and electrical properties (May 1988). Curing agents normally used are aromatic and aliphatic amines or anhydrides (May 1988).

Despite attracting engineering properties of epoxy resins named above, they suffer from severe brittleness which limits their application in many industries. It is noteworthy that epoxy polymers are just slightly tougher than inorganic glasses. This is why toughening of epoxies has been the subject of many research activities over the past few decades (Bray et al. 2013). Among different approaches

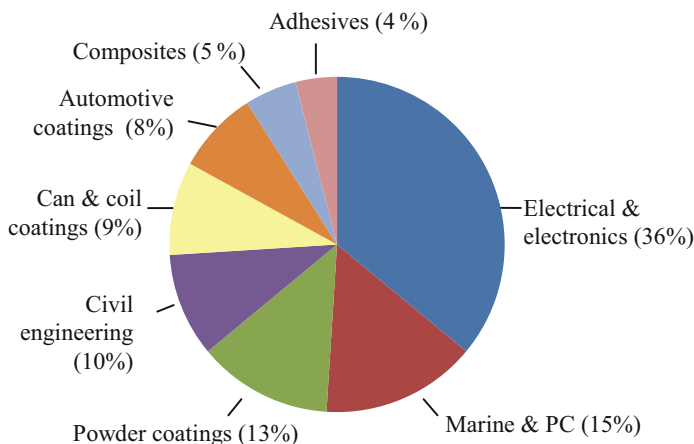


Fig. 1 Distribution of global epoxy market in 2009 (Data are obtained from PlasticsEurope's PC/PBA-group available on www.bisphenol-a-europe.org/en_GB/what-is-bisphenol-a/epoxy-resins)

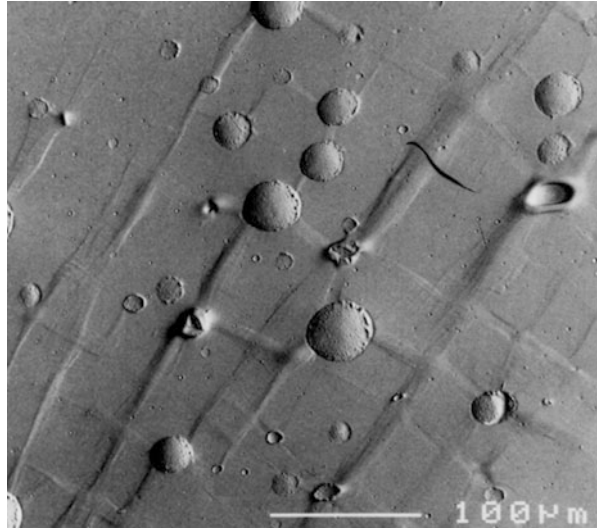
incorporated to overcome this problem, rubber toughening has been the most practiced solution for a wide range of epoxies. This technique is based on the incorporation of rubbery second phase particles in the epoxy matrix, i.e., making a blend of epoxy and rubber. Addition of rubber particles to epoxy resins may increase the fracture toughness of the brittle matrix by several orders of magnitude. This technique, however, has some trade-offs including reduced yield strength and stiffness (Bagheri et al. 2009). Use of proper rubber modifier can lessen this problem. In addition, if necessary, fillers or reinforcements are incorporated into the blend as well to compensate this deficiency.

Epoxy/rubber blends, also called rubber-toughened epoxies, were introduced by Sultan and his coworkers in the early 1970s (Yee and Pearson 1986a). Since then, huge number of studies have been focused on this subject (Liang and Pearson 2010; Chen et al. 2013). The following section provides an overview of the progress made in this field with emphasis on the mechanism of toughening in these two-phase materials. Types of the rubbers used in epoxy blends will be introduced in section “Types of Rubber Modifiers Used in Epoxy Blends” of this chapter. Industrial applications of rubber-modified epoxies are explored in section “Industrial Applications of Epoxy/Rubber Blends.”

Rubber Toughening of Epoxies

The inherent brittleness of epoxies is due to their limited ability to absorb energy prior to fracture. Early studies conducted in the 1970s and 1980s attributed the toughness improvement in modified epoxies to the tearing energy of the second phase rubber particles (Kunz-Douglass et al. 1980). This hypothesis, however, was

Fig. 2 Shear bands initiating from second phase rubber particles in an epoxy/rubber blend loaded in compression. Rubber particles in the blend have a wide range of particle sizes from 1 to more than 30 μm (Image courtesy of Reza Bagheri and Raymond A. Pearson)



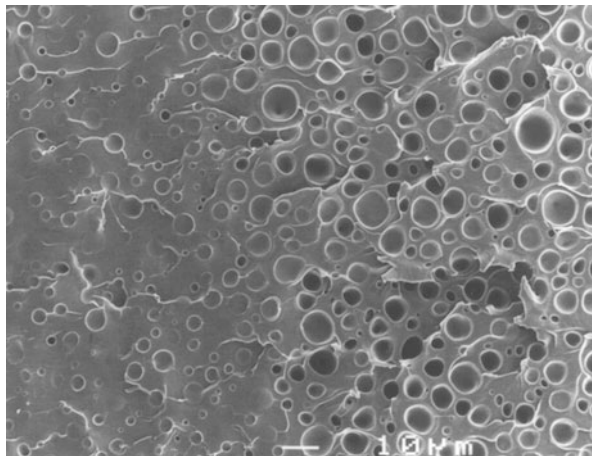
refuted by the original works of Meeks (1974) and Kinloch et al. (1987) who highlighted the role of molecular structure of the epoxy resins on their toughness improvement. The decisive study conducted by Pearson and Yee (1989) showed clearly that by increasing the molecular weight between the cross-linking tie points, the ductility and, thus, the toughenability of the epoxy resin increase.

Considering the key role of the ductility of epoxy resins in their potential to be toughened by second rubbery phase particles, one can figure out the role of rubber particles as initiation sites for plastic deformation. Figure 2 illustrates shear bands formation and propagation from rubber particles in an epoxy matrix. This fact that the major contribution in toughening of epoxy/rubber blends is due to heterogeneous shear banding of the matrix has been accepted by researchers (Bagheri et al. 2009). However, some investigators believe that the effect of rubber particles on toughness improvement of epoxies is not limited to promoting localized shear banding of the matrix through concentrating stress. They have argued that plastic void growth of the matrix which occurs after cavitation of the rubber particles under triaxial loading conditions at the crack tip also contributes in toughening (Kinloch et al. 2014). Figure 3 illustrates cavitation of rubber particles followed by plastic dilation of the matrix in an epoxy/rubber blend.

Types of Rubber Modifiers Used in Epoxy Blends

This section goes through the evolution of the technologies incorporated over the past four decades in epoxy/rubber blends. The emphasis is on introducing types of rubbers and associated approaches while highlighting advantages and disadvantages of each technology for better implementation in different applications.

Fig. 3 Fracture surface of an epoxy/rubber blend showing rubber particles before cavitation (on the *left* side) and after cavitation and subsequent plastic dilation of the matrix (on the *right* side) (Image courtesy of Reza Bagheri and Raymond A. Pearson)



Reactive Oligomers

As mentioned earlier, rubber modification of epoxies was first introduced in the early 1970s (Yee and Pearson 1986a). The technology was soon commercialized based on the use of reactive oligomers. In brief, the reactive oligomer is dissolved in the epoxy prepolymer first. Introduction of the curing agent to the blend results in polymerization and rising of the molecular weight of the oligomer molecules, i.e., rubber chains. As the cross-linking process continues, the rubbery phase precipitates out. The volume fraction and size of the rubber domains depend on the compatibility between the two phases and the gelation kinetics of the epoxy-hardener pair. This means that high degree of compatibility and rapid kinetics of gelation promote extra-fine morphology and may even suppress precipitation of the rubbery phase (Yee and Pearson 1986b). In the case of incomplete phase separation of the elastomeric phase, the remained rubber molecules in the matrix act as plasticizer and reduce glass transition temperature of the epoxy resin. They also increase the linear thermal coefficient of expansion of the matrix. Such a phenomenon is not favored in rubber-toughened epoxies and eliminates industrial application of the material.

At the other extreme, very low compatibility and slow-curing kinetics facilitate enlargement of particles which in turn, harms mechanical properties and in particular fracture toughness. Such a dependency of the blend morphology to the materials and processing conditions is not acceptable in applications where reproducibility of the properties is crucial. Therefore, although reactive oligomers are relatively easy to work with and often result in well-dispersed rubber particles, use of this type of modifiers is not the desired choice for some applications.

Butadiene-acrylonitrile base rubbers have been the principal reactive oligomer used for toughening of epoxies (Bagheri et al. 2009). In order to have better control on the size and dispersion of the second phase particles and also to control the adhesion of rubber particles to the matrix, end-capping butadiene-acrylonitrile

rubber with different groups has been practiced (Yee and Pearson 1986b). Carboxyl-terminated butadiene-acrylonitrile (CTBN) rubbers with different acrylonitrile content have been used extensively for this purpose (Yee and Pearson 1986b). Similar elastomers used include ATBN (amino-terminated), ETBN (epoxy-terminated), and VTBN (vinyl-terminated) (Chikhi et al. 2002).

Preformed Particles

As mentioned, desired morphology may not be obtained when using reactive oligomers for toughening of epoxy resins. Therefore, use of preformed rubber particles which yields a given particle size could be an alternative approach. First attempts for incorporation of preformed rubber particles for toughening of epoxies were reported in the early 1990s, i.e., almost two decades after introduction of reactive oligomers (Pearson and Yee 1991). The modifier used was a kind of core-shell rubber (CSR) particles made via emulsion polymerization technique. The structure of these kinds of particles includes a rubbery core covered with a thin layer of a glassy shell. Typical core materials in this type of modifiers include butadiene based, acrylate based, and polysiloxane rubbers (Kinloch et al. 2014). The glassy shell is chosen to be compatible with epoxy matrix. Use of poly(methyl methacrylate) (PMMA) is very common as the glassy shell in these types of modifiers (Kinloch et al. 2014). Contrary to the phase-separating particles, core-shell rubber modifiers synthesized by emulsion polymerization have controlled size in the range of submicron down to a few-ten nanometers.

In such a structured particle, the rubbery core is responsible for concentrating the stress and triggers plastic deformation in the neighboring matrix. This is the same function that earlier version of rubber modifiers did. The thin glassy shell in this type of modifiers has two functions. The first one is acting as a solid barrier preventing the rubber particles from sticking together when particles are dried after polymerization. This allows handling of the preformed rubber powder in the room ambient conditions. The second benefit of the glassy shell is that its chemistry can be tailored based on the polymer matrix without altering the rubbery core. Doing this, one can control the compatibility of the particles with the matrix and, thus, can affect dispersion of the particles and their adhesion to the matrix independently from the chemistry of the rubbery core. This class of modifiers was further developed into the form of multilayer core-shell particles where the rubbery interlayer is surrounded by a glassy seed and an outer glassy shell (Lovell et al. 1993). It has been claimed that the multilayer modifiers toughen plastics similar to that simple core-shell particles do while they lessen the drawback of the rubber modification in reducing strength and stiffness of the blend (Lovell et al. 1993).

Preformed rubber particles used for toughening of epoxies are not limited to core-shell type modifiers. There have been efforts in synthesizing preformed cross-linked epoxy rubbers (Jansen et al. 1999). In this particular study, droplets containing rubbery epoxy chains were cured in an aqueous media and dried to a

preformed powder. The submicron-sized particles were then blended with an epoxy resin. The results demonstrated the superiority of the synthesized particles in toughening of epoxy compared to a conventional reactive oligomer (Jansen et al. 1999). Use of ground-recycled rubber particles has been examined by researchers as well (Karger-Kocsis et al. 2012). These preformed rubber particles do not improve fracture toughness of epoxy resins as much as reactive oligomers or core-shell particles do since they are normally too big with irregular shapes (Bagheri et al. 1997). Interestingly, simultaneous use of these types of rubbers with conventional modifiers has shown to be an effective approach for obtaining synergistically high fracture toughness values (Bagheri et al. 1997).

Block Copolymers (BCPs)

A new approach for toughening of epoxy resins based on incorporation of self-assembling copolymers was introduced early in the twenty-first century (Grubbs et al. 2000). The technique is based on making a blend of epoxy resin and a block copolymer (BCP) where the copolymer self-assembles to a hierarchical substructure during the cross-linking process. Different substructures in such a blend have been reported by researchers including spherical and wormlike micelles as well as vesicles (Ruzette and Leibler 2005). Both di-block and tri-block copolymers have been incorporated. Based on the molecular structure of the copolymer, substructures formed can be ordered or disordered and may be as fine as a few nanometers (Wu et al. 2005). Many different types of chemistries are found in the literature including poly(ethylene oxide-*b*-ethylene propylene) (PEO-PEP) (Dean et al. 2001, 2003), poly(butylene oxide-*b*-ethylene oxide) (PBO-PEO) (Wu et al. 2005), poly(ethylene-*alt*-propylene)-*b*-poly(ethylene oxide) (PEP-PEO) (Liu et al. 2008), poly(ethylene oxide)-*b*-poly(ethylene-*alt*-propylene) (OP) (Thompson et al. 2009), etc.

Lorena et al. reviewed a large number of studies on epoxy/block copolymer blends (Lorena et al. 2008). These researchers addressed significant improvements in fracture toughness of epoxy resins by incorporation of block copolymers. Although many of the addressed studies have tried to propose mechanism(s) involved in fracture toughness improvement in associated blends, there is no conclusive finding in this regard. Liu et al. claimed a combination of several toughening mechanisms in epoxy/copolymer blends including voiding or interfacial debonding, shear yielding of the matrix, crack tip blunting, crack bridging, and viscoelastic energy dissipation (Liu et al. 2010). However, a recently published investigation by Perez et al. highlighted micelle properties along with the cross-link density of the matrix as the key parameters in toughening of epoxy/copolymer blends (Declet-Perez et al. 2015). These researchers believed that cavitation of the rubbery core of the micelles followed by shear deformation of the epoxy matrix was responsible for the significant improvement of fracture toughness observed in their study (Declet-Perez et al. 2015). In conclusion, it seems the general knowledge on epoxy/block copolymers has not reached to its maturity level yet. This arises from the complexities associated with the chemistry and morphological aspects of these

blends which makes their characterization rather difficult. It is expected that investigators continue heavy research on epoxy/copolymer blends in the coming years.

Industrial Applications of Epoxy/Rubber Blends

As mentioned in the previous sections, the inherent brittleness of epoxy resins is a major obstacle against their industrial growth and that rubber modification is an established practice to overcome this deficiency (Marouf et al. 2016; Bagheri et al. 2009). A linear raise in K_{IC} and G_{IC} up to a certain level of rubber content, 10–20 wt.%, has been reported in the literature by incorporating reactive oligomers or CSR particles (Bagheri et al. 2009; Marouf et al. 2009; Yee and Pearson 1986a; Bucknall and Yoshii 1978; Bascom et al. 1975). Excellent mechanical properties combined with the lightweight makes rubber-modified epoxies or their hybrids an excellent choice for applications where combination of toughness, stiffness, and strength is required. Based on the current status of the global market, customers of epoxy resins and their rubber-modified blends can be divided into three main categories including coatings, composites, and adhesives. This section aims to address the current and potential markets of epoxy/rubber and epoxy/copolymer blends in different *structural* and *nonstructural* applications. It is unattainable to provide a full description of all present and prospective demands of epoxy blends. Therefore, the following tries to present some of the more established applications of the current market along with selected prospective examples. Subsections “Coatings,” “Composites,” and “Adhesives” are dedicated to the market of epoxy blends in coating, composite, and adhesive industries, respectively. Incorporation of liquid rubbers, preformed CSR particles, and block copolymers into epoxy blends is found in the examples provided in the following subsections.

Coatings

The global market of epoxies is expected to reach US\$ 10.55 billion by 2020 from US\$ 6.64 billion in 2013. The key factor stimulating this remarkable growth is the rising demand for paints and coatings in industrial applications (Transparency Market Research 2015). Depending upon the application requirements, modified coatings such as epoxy/rubber blends or epoxy/copolymer blends may need to be employed as the advanced coating. Epoxy coatings are divided into five categories (Plastics Europe’s PC/BPA Group 2011):

- Automotive coatings: automotives/buses/railcars waterborne primers
- Can coatings: food/drink cans and trays, caps and closures, drum and pails, general line cans, and collapsible tubes of toothpaste and cream

- Coil coatings: construction panels; mobile homes and caravans; cookers; heater, ventilators, and air conditionings; office furniture; and household appliances (fridges and freezers, dishwashers, washing machines, dryers)
- Marine and protective coatings: water and gas pipelines, water ballast tanks, storage tanks and sea containers, cargo tank lining, underwater ship hulls, offshore oil-drilling platforms, supporting steel structures, steel bridges, power plant scrubbers, electric motors, engines, and machinery
- Powder coatings: pipelines, automotive parts, construction panels, rebars, engine blocks, radiators, steel furniture/racks/frames/beds, and office furniture and gardening tools

To achieve sustainable environment, the pipeline industry has attempted to increase security of energy and water supply systems with enhancement of meeting the requirements of pipeline protection market (Humphreys 2011). The pipeline coating market was valued around 5 and 6.5 billion euros in 2009 and 2013, respectively (Humphreys 2011). Rubber-modified epoxies are excellent candidates when more flexible and damage-resistant coatings are required (Mallozzi et al. 2014; Pham et al. 2007). Gas, oil, and water pipelines and their related joints, fittings, and components such as valves, pumps, tapping saddles, manifolds, pipe hangers, ladders, rebar, mesh, cable and wire rope, I-beams, column coils, anchor plates, chairs, etc., need to have long-standing corrosion resistance with least amount of monitoring and repair (Mallozzi et al. 2014; Kehr 2012). Fusion-bonded epoxy powder coatings, first introduced by 3M in 1960, and liquid coatings have been applied as two more accepted methods for corrosion protection of buried pipelines (Kehr 2012). Most of the pipeline coatings are used in gas and oil pipelines while the water distribution systems have little share (Humphreys 2011). These protective coatings are expected to be in service for rather long life of 20–30 years. Apart from excellent anticorrosion and high chemical resistance, the pipeline coating has outstanding flexibility, high crack, and impact resistance and excellent adhesion to the substrate as well as high abrasion resistance to fulfill the shipping, handling, installation, and extreme operation requirements (Kehr 2012; Pham et al. 2007).

Conventionally, either increasing thickness of the coating or incorporating filler into the epoxy material has been considered to increase the damage resistance of the coating (Pham et al. 2007). Furthermore, addition of fillers reduces the cost of formulation. While these techniques are successful in betterment of some required properties, both decrease the flexibility of the protective coating unfavorably (Mallozzi et al. 2014). Other negative points of filler incorporation especially micro-fillers include decrease in impact strength and tensile strength and loss of transparency of the coating which is required in some applications.

Rubber modification is the alternative strategy to respond this demand. Given the benefits of rubber modification, this toughening technology has been employed for obtaining high impact coatings as tough primer in car's painting. This is done despite the reduction of elastic modulus and lowering of glass transition

Table 1 List of some commercial epoxy/CTBN adducts, epoxy/core-shell rubber particle pre-dispersions, and epoxy/block copolymer blends

Product (manufacturer)	Formulation	Applications
Araldite [®] LT 1522 (Huntsman)	Solid epoxy/CTBN blend	Adhesives, prepregs, molding compounds, powder coatings
FORTEGRA [™] 201 (Dow Chemical)	Epoxy/40 wt.% CTBN blend	To increase peel strength and fracture toughness
FORTEGRA [™] 301 (Dow Chemical)	Epoxy/15 wt.% CSR pre-dispersion	To remarkably increase lap shear strength, fracture toughness, and durability with minimal effects on modulus and T _g
FORTEGRA [™] 353 (Dow Chemical)	Liquid epoxy/25 wt.% CSR nanoparticles (190 nm) pre-dispersion	
FORTEGRA [™] 102 (Dow Chemical)	Liquid epoxy/50 wt.% BCP blend, suitable for amine, anhydride, DICY, phenolic curing agents	Adhesives, civil engineering, composites, marine, protective coatings, photocure coatings, potting, and encapsulation
FORTEGRA [™] 104 (Dow Chemical)	Solid epoxy/12 wt.% BCP	Decorative and functional coatings, powder coatings
Kane [™] Ace MX (Kaneca)	Epoxy/CSR nanoparticles pre-dispersion	Suitable for low-high cross-linked epoxies

CTBN Carboxyl-terminated butadiene nitrile, CSR Core-shell rubber, BCP block copolymer, DICY dicyandiamide

temperature by incorporation of rubber modifiers in epoxy resins, especially when using liquid rubbers such as ATBN, CTBN, etc. (Bagheri et al. 2009; Kozii and Rozenberg 1992; Yee and Pearson 1986a).

Difficulty in dispersion and possible increase in viscosity can be the adverse effects of introducing preformed rubber modifiers into the epoxy resins for coating of pipelines (Pham et al. 2007). Preformed core-shell rubber particles could be useful if a mixture of pre-dispersed core-shell nanoparticles in epoxy is selected as the coating material. Table 1 presents a list of epoxy/CSR pre-dispersions commercially available in the market. In this regard and along with other toughening advances, Dow Chemical has introduced its new product with the trade name of FORTEGRA[™] 301 which is a blend of epoxy with pre-dispersed core-shell rubber particles. FORTEGRA[™] 301 contains 15 wt.% CSR particles (Xie et al. 2011). Adding this CSR pre-dispersion to a dicyandiamide (DICY)-cured epoxy for fusion bonded epoxy (FBE) coating purposes has improved flexibility and adhesion of the CSR-modified FBE coating to the steel substrate at -32 °C with no detrimental effect on T_g. Not only this enhancement proposes a longer service life for FBE coatings at extreme conditions but also is beneficial in reducing the maintenance cost of gas and oil pipelines (Xie et al. 2011). Considering the use of DICY in the above coating formulation, it would be helpful to mention that dicyandiamide is a

latent-curing agent with high melting point (207–210 °C), long pot life (24 h), and relatively high curing temperature (160–180 °C). Given that DICY generates large quantity of heat during curing, it can be only used in thin film applications in adhesives, coatings, and paints, laminates/prepregs, and one-part adhesives (Three Bond Technical News 1990).

FORTEGRA™ 353 is another pre-dispersed core-shell rubber particle in a liquid epoxy resin from Dow Chemical. This 190 nm pre-dispersed CSR product is commercially available as 25 wt.% master batch with epoxy equivalent weight (EEW) of 240 and average CSR particle size of 190 nm. Kaneca also has uniformly pre-dispersed CSR nanoparticles/epoxy products under the trade name of Kane™ Ace MX. Kane™ Ace MX is manipulated for a range of low to high cross-linked density epoxy systems (Miyatake 2013).

Furthermore, Dow has introduced a block copolymer-toughened epoxy formulation cured with DICY. This tailored blend contains small amount of self-nanostructuring block copolymers (8 wt.%). The block copolymer nanoparticle-epoxy coating presents significantly improved flexibility and impact resistance with no change in viscosity and T_g (Pham et al. 2007). More recently, 3M introduced an FBE coating modified with a combination of tri-block copolymers and a filler to accommodate all specific requirements of the application simultaneously (Mallozzi et al. 2014).

Barrier coatings fabricated with high aspect ratio exfoliated nanoclay and carbon nanotubes (CNTs) in epoxies can be used effectively against corrosion caused by moisture/gas diffusion in cases like underground sewer pipes or steel infrastructures (Lu and Mai 2005). To improve flexibility and adhesion of these coatings, a proper combination of nanofiller and rubber nano-modifier (perhaps in the form of CSR or block copolymer) is suitable.

EPOKUKDO KR-693 is an example of a micron-sized acrylic core-shell modified epoxy recommended for uniform powder coatings with good chemical resistance, anticorrosive properties, anti-chip resistance, and good mechanical properties (enhanced impact strength, strength at break, shear strength, and flexibility with no decrease in elastic modulus and thermal stability) in a wide range of temperatures. The particle size of the core-shell particles incorporated into the epoxy resin in this material is in the order of 0.5 μm (www.kukdo.com).

Reactive liquid rubber modifiers have found a well-established market in floor coatings. For instance, a CTBN-modified epoxy with the trade name EPOKUKDO KR-170 is commercially available for floor coating, waterproof coating, and flexible coating on various substrates (www.kukdo.com). Due to its excellent flexibility, T-peeling adhesive strength and toughness in a wide range of temperatures, good water resistance, and excellent oil-base resistance, the product has found significant number of applications (www.kukdo.com).

Bagheri et al. investigated the feasibility of using surface-treated recycled rubber particles for toughening of epoxy polymers (Bagheri et al. 1997). The recycled rubber particles were obtained through grinding of scrap tires. The findings revealed that while the recycled rubber particles improve fracture resistance of the epoxy resin by less than 20%, the CTBN rubber enhances the fracture toughness

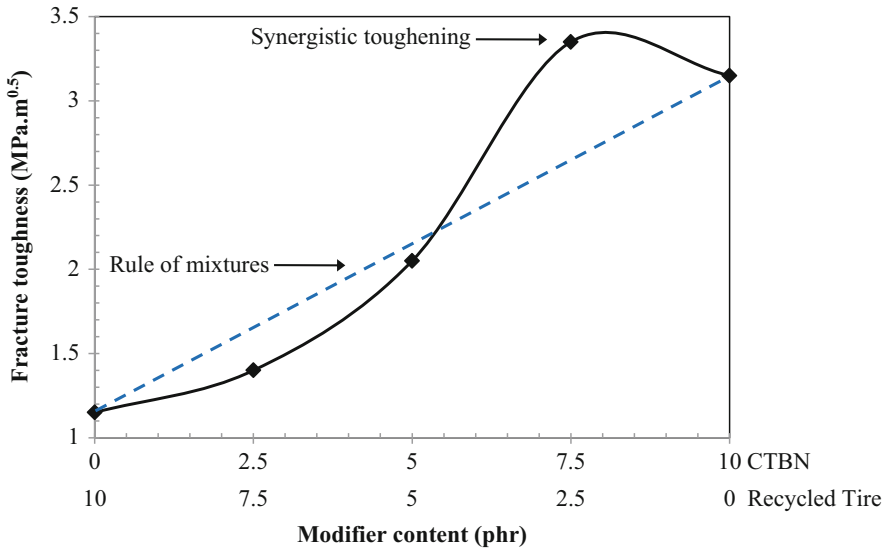


Fig. 4 Variation of fracture toughness versus modifier composition. A combination of CTBN and recycled tire was used as toughening agent for a toughenable epoxy (Data are obtained with permission from Bagheri et al. (1997), John Wiley & Sons)

to more than 200%. The reason for this significant difference in crack growth resistance lies in different toughening mechanisms, i.e., crack deflection and microcracking with recycled rubber particles versus particle cavitation and massive shear yielding of the matrix with CTBN. The results also indicated synergistic toughening when 2.5 phr recycled rubbers and 7.5 phr CTBN were added into the epoxy resin (Fig. 4). The mechanism responsible for the unexpectedly high fracture toughness in this blend was plastic zone branching caused by interaction of the stress field of recycled particles with that of the crack tip. Please note that the stress field associated with recycled rubber particles enhances cavitation of neighboring CTBN domains and stretches the shear deformation from the crack tip toward the large particles. Plastic zone branching mechanism enlarges the effective damage zone size and further enhances the crack growth resistance. Their study introduced a new approach for rubber toughening of engineering plastics by blending traditional modifiers and surface-treated recycled particles. In addition to cost savings, this approach resulted in improved mechanical properties such as higher fracture toughness (Bagheri et al. 1997). These kinds of recycled rubber-modified epoxies have found demanding markets in floor coatings in industrial environments and playgrounds (Al-Aqeeli 2015). In general, epoxy/rubber (reactive oligomers, preformed rubbers) blends can be tailored for floor coatings in industrial/public buildings, chemical plants, food industry, pharmaceutical companies, and hospitals. Furthermore, the rubber-modified epoxies can also be used as sound and vibration dampers.

Formulations based on rubber-toughened epoxies are also available commercially for acid-base resistant anticorrosive paints. Having good physical and mechanical properties and excellent protection against strong acids and alkali, atmosphere aging, and ozone fit has made these rubber-modified epoxies excellent candidates for outdoor chemical equipment, steel frames, and structures as well as cement walls (www.hiseamarine.com).

Modified epoxies offer good oil resistance, water resistance, oil and water alternation corrosion resistance, abrasion resistance, good adhesion and film firm for primers in marine applications, mainly used as anticorrosion of shipping boat deck, and freeboard inside (www.hiseamarine.com).

And finally as another example, silicon-based rubber modifiers not only increase fracture toughness with retained physical properties of epoxy polymers but also improve water repellency. This kind of rubber modifiers provides superior thermal stability and oxidation resistance, partial ionic nature, and low surface energy with low toxicity suitable for coating applications (Gupta and Bajpai 2011).

Composites

Fiber-reinforced epoxy composites have been widely used in (Plastics Europe's PC/BPA Group 2011):

- Aircraft/aerospace
- Wind turbine blades
- Chemical: storage tanks, containers, gas bottles and scrubbers, pipes, valves, and fittings
- Construction/buildings: pultruded rods/bars/shafts/beams/gratings, bridge decks, etc.
- Electrical and electronics: potting and encapsulation parts such as transformers, inductors, and printed circuit boards
- Ground/rail/marine transportation: automotive components such as body panels, cabin, spoiler, leaf springs, and drive shafts; railcars; and boats and yachts
- Sport goods: badminton/squash/tennis rackets; hockey sticks and golf clubs; ski poles and snowboards; surfboards, boats, and canoes; hang gliders; helmets; and lightweight bicycles

With respect to the growing demand for achieving higher performance and more reliable fiber-reinforced composites, epoxy matrices need to be modified. Considering the superior beneficial effect of rubber modifiers, highly toughened epoxy matrices for composites (used in green energy, aerospace, transportation, construction, electronics and electrical applications, and sport goods) can be formulated using reactive oligomers, preformed particles, and block copolymers depending on the specific requirements. Micro- or nano-sized rubber modifiers may be desired to be employed. Chemistry and properties of the epoxy resin, curing agent, and block

copolymer accompanied with the curing cycle determine morphology of the block copolymer modifier after curing of the blend.

Rubber modification has found great interest in passive safety applications such as helmets, knee pads, etc., which need high fracture toughness and impact resistance (Utracki 2010).

The use of uniformly pre-dispersed CSR particles is on the rise in fiber-reinforced epoxy composites manufactured through filament winding, RTM/infusion, and prepreg processes. Modification of epoxies with CSR particles improves crack growth resistance not only in service conditions but also in manufacturing processes such as drilling, cutting, etc. (Kunal and Sprenger 2014; Miyatake 2013). Taking advantages of toughening with CSR nanoparticles alone or simultaneously with nanofillers such as silica nanoparticles has been tried by automotive industry where both high performance and ultrafast manufacturing process are important (Kunal and Sprenger 2014).

Nowadays, energy and environmental concerns are the two crucial issues human beings encounter. Thus, transition from nonrenewable energy sources such as natural gas, coal, and petroleum to renewable energy resources such as wind and solar is vital for a sustainable future. The market of clean technologies is forecast to reach US\$ 2 trillion by 2020. The contribution of wind energy in the US power supply is predicted to increase 20% by 2030 (Loos et al. 2012a, b). To achieve this megatrend, wind turbines (wind turbine blades) need to be made bigger because the energy supply increases proportionally with the square of the rotor radius (Loos et al. 2012a, b). Current maximum length of turbine blades is 180 m, and it is designed to increase to 300 m to provide the projected energy demand within the next 5 years. The growing trend of larger turbine blades raises the challenge of need to high performance materials with long lifetime, i.e., high specific strength, high specific stiffness, high fracture toughness, and long fatigue life. Wind turbine blades are made of fiber-reinforced polymer composites, and with rapid growing of this green energy industry, wind turbines are established as one of the largest consumption markets for composites in the world as it is expected to reach US\$ 3.2 million in 2018 globally. Glass fiber/polyester and glass fiber/epoxy have been used in earlier generation of wind turbines with shorter blades, while carbon fiber/epoxy composites and carbon fiber/glass fiber/epoxy hybrid composites have found a dominating place in the later generations with larger turbine blades to overcome inherent limitations of glass fiber and polyester. In service, turbine blades undergo severe stresses due to rotation, movement, wind, and other environmental factors such as temperature, moisture, dust and solid particles suspended in air, bird strikes and lightning strikes, etc. Therefore, stringent requirements are applied in designing wind turbine components. For example, the Germanischer Lloyd guideline (GL) calls for 20-year lifetime with full loading of 3000 h/year for certification of a turbine blade (Jacob et al. 2007). In 50% of cases, either fatigue failure or catastrophic fast fracture causes failure of installed wind turbines. Cracking and delamination can cause failure of the structure. Cost of failure is surprisingly exorbitant. To avoid costly downtime, it is vital to improve fatigue resistance of blade materials. Therefore, much research has been focused on increasing lifetime

of wind turbine blades (Chen and Pearson 2014; Kinloch et al. 2014; Loos et al. 2012a, b; Turakhia et al. 2009; Jacob et al. 2007).

As mentioned in section “Introduction,” rubber modifiers are well-known toughening agents for polymers, especially epoxy resins (Bagheri et al. 2009; Marouf et al. 2009; Jansen et al. 1999; Kim and Ma 1996). These kinds of modifiers are used in the forms of reactive oligomers (e.g., carboxyl-terminated butadiene-acrylonitrile (CTBN), amine-terminated butadiene-acrylonitrile (ATBN), etc.) (Garg and Mai 1988; Sultan and McGarry 1973), preformed particles (Chen et al. 2013; Lovell et al. 1993, and block copolymers (Kishi et al. 2011; Liu et al. 2010; Hydro and Pearson 2007; Oldak et al. 2007; Ruzette and Leibler 2005; Rebizant et al. 2004; Ritzenthaler et al. 2002).

Considering the importance of wind energy market, major companies such as Dow Chemical and Arkema Inc. in partnership with universities have focused extensive investigations on understanding the effect of block copolymers on mechanical and physical behavior of epoxy resins (Kishi et al. 2015; Chen and Pearson 2014; Chong and Taylor 2013; Turakhia et al. 2009; Barsotti et al. 2008; Jacob et al. 2007). The toughening effect of the state-of-the-art nano-sized block copolymers in comparison with conventional micron-sized CTBN for a DICY-cured epoxy is reported in Table 2. As seen, at the same level of loading, di-block and tri-blocks offered more toughening effect compared to CTBN microparticles (Barsotti et al. 2010).

Apart from the great interests in producing longer-lasting wind turbine blades, there is a real need for faster manufacturing processes. To achieve this, vacuum-assisted resin transfer molding (VARTM) has been considered remarkably for wind blades (Jacob et al. 2007). Di-block copolymers are proposed for wind turbine blade composites for infusion applications by Arkema. Dissolution of block copolymer modifiers in epoxy resin eases processing, and self-assembly of block copolymer nanostructures provides an opportunity for fabrication of composites with small inter-fiber spacing using infusion process. Low viscosity is critical for infusion. Study of the influence of block copolymers on rheological behavior of an epoxy resin showed less increase in viscosity when a di-block copolymer incorporated into the epoxy (viscosity = 14.0 Pa.S) in comparison to introduction of a tri-block copolymer (viscosity = 28.6 Pa.S) (Barsotti et al. 2010) (Table 2). Limited increase in viscosity by incorporation of di-block copolymer was due to its low molecular

Table 2 Properties of a DICY-cured epoxy incorporated with different rubber modifiers

Formulation	K_{IC} (MPa.m ^{0.5})	G_{IC} (KJ.m ⁻²)	Viscosity (Pa.S at 40 °C)	T_g (°C)
0% modifier	0.88	–	–	148.1
10 wt.% Di-BCP	1.86	1.87	14.0	128.4
10 wt.% Tri-BCP	1.82	1.55	28.6	135.4
10 wt.% CTBN	1.62	–	–	129.2

The reported values are obtained with permission from Barsotti et al. 2010.

Table 3 Effect of di-block copolymer nanostructures on fatigue life of an epoxy

Stress level (MPa)	Number of cycles (thousands)	
	Reference	3 wt.% di-BCP
300	675	938
350	119	335
430	72	119

The reported values are obtained with permission from Barsotti et al. 2010.

weight as opposed to rather high molecular weight of the tri-block modifier (Chen and Pearson 2014; Thio et al. 2006).

Table 3 presents effect of di-block copolymer nanostructure modification on fatigue behavior of a DICY-cured epoxy at different stress levels. Interestingly, incorporation of only 3 wt.% di-block copolymer into the epoxy enhanced its fatigue life at all three stress levels studied. The improvements in K_{IC} , G_{IC} , and fatigue life of the epoxy/di-block copolymer blends propose epoxy/di-block copolymer blends as promising materials to be used as toughened matrices in fiber-reinforced composites.

It has been shown that incorporation of small amounts of nanofillers into epoxy resins increases strength, stiffness, and fracture toughness. Epoxies filled with combination of rubber modifiers and nanofillers, such as silica, CNT, halloysite, clay, or graphene are nanocomposites with a good balance of stiffness and toughness. Such a hybrid nanocomposites, then, can be used as a modified matrix in carbon fiber or glass fiber-reinforced laminates (Loos et al. 2012a; Marouf and Bagheri 2010; Njuguna et al. 2007), thereby increasing the interlaminar shear strength and toughness. This approach has found potential markets in manufacturing of wind turbine blades, aircraft structures, deepwater-drilling composite risers, hydrogen and helium storage tanks, etc. The objective has been come to reality by means of epoxy resin master batches containing different types of nanofillers, e.g., silica nanoparticles, core-shell rubber nanoparticles, block copolymer nanostructures, CNTs, and nanoclay. The usage of composites in air transport has been dramatically increasing, e.g., growing from 10% to more than 50% in the last decade. This means that the market of epoxy composites in aviation is experiencing a sharp growth. Therefore, the need for improving performance of epoxy-based composites is more important than before. Multicomponent epoxy composites consisting of carbon or glass fiber reinforcements embedded in epoxy resins modified with core-shell or block copolymer rubbers and nanofillers such as silica nanoparticles, CNTs, clay, or graphene are most promising materials for responding to this market demand.

Adhesives

Providing excellent corrosion and chemical resistance, thermal resistance, heat distortion temperature (HDT), low shrinkage, high dimensional stability, strength,

Table 4 Some rubber-modified epoxy adhesives commercially available in the market

Product (manufacturer)	Characteristics and applications
(Intertronics)	Two- part black rubber-modified epoxy adhesive, bonding dissimilar materials with different thermal expansion coefficient (metals, rubbers, GRP, wood, glass, ABS, PVC, PC, and PMMA) to provide a tough and resilient joint for <i>electronics and electrical applications, automotive, and specialist vehicles</i>
ALIPOX (Evonik)	Reactive liquid rubber-modified epoxy adhesive, improved impact resistance in a wide range of temperatures, enhanced adhesion to minerals, metals, and oil-treated steel substrates
ALIDUR (Evonik)	100 nm–3 μ m silicon core-shell toughened epoxy adhesive, RT curing systems, very fast-curing adhesives, heat curing adhesives, UV curing adhesives, enhanced impact resistance, low viscosity, <i>electronics and electrical applications</i>
Loctite [®] Super Glue ULTRA Gel Control [™] (Henkel)	Rubber-toughened instant adhesive; resistance to impact, shock, vibration, moisture, and temperature extremes; ideal for bonds subject to daily use and harsh conditions; outdoor safe; transparent
7823G (3M)	One-component rubber-modified epoxy paste adhesive

GRP Glass-reinforced plastic, ABS acrylonitrile butadiene styrene, PVC polyvinyl chloride, PC polycarbonate, RT room temperature, CSR Core-shell rubber, UV Ultraviolet

elastic modulus, and adhesion to various materials and the possibility of obtaining wide range of properties have made epoxy polymers unrivaled for adhesive applications, either as one-component or two-component materials (Dunn 2003). The opportunity of manipulating a wide range of attributes is tuned with epoxy and hardener chemistry, epoxy molecular weight, curing condition, and additive/modifier properties. The main disadvantage of epoxy adhesives is their inherent brittleness, i.e., low fracture toughness and interfacial fracture energy as a consequence of amorphous and cross-linked nature of the cured epoxy (Ratna and Banthia 2004; He et al. 1999). To overcome this critical drawback, rubber-modified epoxy adhesives have been developed (Kinloch et al. 2007). Table 4 presents a list of some commercially available rubber-toughened epoxy adhesives.

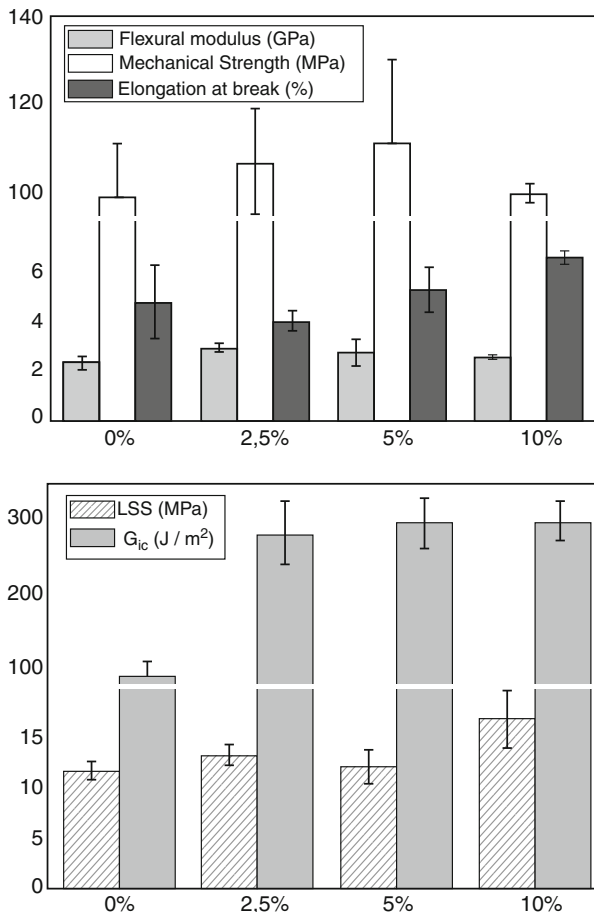
Various leading worldwide adhesive manufacturing companies such as 3M, Henkel AG & Co. KGaA, Huntsman, Evonik Hanse, Illinois Tool Works (ITW), etc., produce rubber-toughened epoxy adhesives designed for a wide range of applications from low viscosity liquids to solid pastes and films. As an example, Loctite[®] Super Glue ULTRA Gel Control[™] is a rubber-modified epoxy formulation from Henkel. This product is ideal for instant adhesive applications with high impact resistance, shock resistance, and vibration resistance at extreme temperatures and severe conditions. This rubber-toughened adhesive is also moisture resistant and outdoor safe with reasonable gelation time to align pieces (www.henkel.com).

Liquid rubber modification of epoxies has been widely used in structural adhesives such as automotive, railway, truck, aerospace, and electrical applications (Sprenger et al. 2009; Kinloch 2003), and functionalization of reactive oligomers is a key factor for toughness improvement. CTBN, a very common type of reactive liquid rubbers, is suitable for toughening of single-part heat curing epoxy adhesives, while ATBN is utilized in two-part epoxy adhesives. In two-component adhesive systems, the epoxy resin and curing agent are kept separated. When using CTBN as the modifier in single-part adhesives, carboxyl functional groups at both ends of butadiene nitrile rubber molecular chain react with the excess epoxy portion and produce a so-called adduct. In two-component adhesives, ATBN modifiers are employed as part of the formulation in the hardener component. Incorporation of both CTBN and ATBN rubbers has positive effect on lap shear strength of the respective adhesive. Furthermore, two times increases in toughness and improvement in wedge impact resistance and roller peel property of the ATBN-modified adhesive have been reported in the literature (Sprenger et al. 2003, 2004, 2006, 2009). Disadvantage of rubber modification using reactive oligomers is their detrimental effect on elastic modulus and T_g of the cured epoxy (Bagheri et al. 2009; Kozii and Rozenberg 1992; Yee and Pearson 1986a). A linear decrease in elastic modulus and yield strength by the addition of rubber particles, up to about 20%, has been reported for some epoxy resins (Kozii and Rozenberg 1992; Yee and Pearson 1986a). The lower modulus and glass transition temperature of liquid rubber-modified epoxy adhesives, as mentioned earlier, are due to the plasticizing effect of remained flexible rubber chains in the epoxy matrix (Bagheri et al. 2009).

Contrary to the reactive oligomers, preformed rubber modifiers improve fracture toughness not at the expense of lowering thermo-mechanical properties (Bagheri et al. 2009). Furthermore, epoxies modified with CSR particles are easier to process compared to their counterpart where liquid oligomers are employed since introduction of CSR particles into the epoxy resins causes less viscosity build up, i.e., a drawback of rubber modification of epoxies. Besides the above advantages, the particle size and volume fraction of the preformed particles are well controlled when CSR is added instead of reactive oligomers (Bagheri et al. 2009). Thus, core-shell rubber-modified epoxy adhesives have found a dominant market for *structural* applications regardless of the higher cost of CSRs compared to reactive oligomers (Sprenger et al. 2009; Kinloch 2003). Preformed rubber particles are suitable modifiers for fast-curing adhesives, while reactive oligomers are not recommended for toughening of snap cure adhesives (Sprenger et al. 2009).

Nanorubber-toughened adhesives are epoxy resins modified by block copolymers and have formed a new class of *tough* adhesives which provide desired mechanical properties along with improved crack growth resistance. The state-of-the-art nanostructured block copolymers are especially suitable for toughening of thin adhesive bond lines. Poly(methyl methacrylate)-block-poly(butyl acrylate)-block-poly(methyl methacrylate) (PMMA-block-PBuA-block-PMMA: MAM) is a tri-block copolymer recommended for toughening of epoxy-based adhesives when low polarity curing agents such as polyetheramines and methyl

Fig. 5 Mechanical properties of an epoxy-based adhesive modified with polystyrene-block-polybutadiene-block-poly(methyl methacrylate) (SBM) block copolymers (Copyright © 2012, Prolongo SG, et al., J Mater Sci Eng)



diethanolamine (*N*-methyl-diethanolamine) abbreviated as M-DEA are employed, while dimethylacrylamide (DMA)-functionalized MAM is designed for modification of adhesives hardened with more polar curing agents such as DICY and diaminodiphenyl sulfone (DDS) (Barsotti et al. 2008).

Epoxy adhesives have good compatibility with fiber-reinforced epoxy-based composites and have been greatly considered for replacement of mechanical joints. Employing epoxy-based adhesives for joining fiber-reinforced epoxy composites is significantly appealing for high performance applications with large, intricate, and lightweight structures such as wind turbine, aerospace, and automotive industry. Figure 5 illustrates the effect of styrene-butadiene-methyl methacrylate (SBM)-modification on lap shear strength (LSS), fracture energy (G_{IC}), modulus, strength, and elongation of an epoxy-based adhesive. As shown in this figure, SBM-modification increases shear lap strength, G_{IC} , strength, and elongation at break with no elastic modulus decrease (Prolongo 2012a, b). Thus,

SBM-modification of epoxy-based adhesives can be used for joining carbon-reinforced epoxy laminates.

Adhesives also have structural applications in wind energy industry. The components of a rotor blade are bonded together using adhesive joints. Highlighted by Dow Chemical, crack resistance, fatigue life, and longevity are the most important demands of the wind turbine application to be addressed.

Concerning the wind energy requirements, toughening efficiency of epoxy/block copolymer blends for high performance adhesive purposes has been examined. The results showed that the fracture toughness of an intermediate T_g epoxy/DICY epoxy ($0.88 \text{ MPa}\cdot\text{m}^{0.5}$) increased to $1.82 \text{ MPa}\cdot\text{m}^{0.5}$ when 10 wt.% BCP was incorporated into the epoxy, while the fracture toughness of 10 wt.% CTBN/epoxy blend was measured $1.62 \text{ MPa}\cdot\text{m}^{0.5}$. The outcomes indicated more beneficial effect of nano-sized block copolymer modification on the fracture behavior of epoxy/DICY system than that of the micron-sized CTBN modification. That is at the same loading of rubber modifier, block copolymers yield higher fracture toughness than that CTBN does. In practice, for obtaining a given level of toughness, lower content of BCP nanostructures is needed compared to CTBN micron-domains. Thus, less negative effect of rubber modification on glass transition is observed when block copolymers are incorporated. Furthermore, it seems that tri-block copolymers are preferred for toughening of wind energy adhesives, while di-block copolymers give the impression to be more promising for composite-related applications (Barsotti et al. 2010; Table 2). Formation of rubber nanostructures through self-assembling of block copolymers is significantly beneficial for toughening of thin adhesive bond lines (Barsotti et al. 2010).

In a project entitled “Developing Water Loss Prevention” guided by Vienna Water, the influence of epoxy modification on physical and mechanical properties of an epoxy resin for sealing purposes was studied (Schoberleitner et al. 2013). The aim of the project was to develop an adhesive compound for repairing leaky lead joint sockets of 150-year-old Vienna’s water supplying system. Different modifiers investigated in this study included ATBN liquid rubber, ethylene propylene diene monomer (EPDM) rubber powder, and two kinds of epoxidized flexibilizers. The results revealed that incorporation of ATBN-modified epoxy sealant was the most effective strategy in increasing flexibility for socket rehabilitation of gray cast iron pipes compared to either EPDM modification or use of epoxidized modifiers (Schoberleitner et al. 2013).

Rubber-toughened epoxy adhesives have opened up a well-established market in automobile joints because of their high impact resistance under high strain rates of loading (Lataillade et al. 1994; Kinloch 2003). Dicyandiamide is used as a latent hardener for formulation of one-part epoxy adhesives given that DICY is insoluble in epoxy at room temperature and needs to be heated to become soluble and active. These one-part epoxy/DICY adhesives are suitable for hem-flange bonding in automobiles (Dunn 2003). One-component CTBN-modified epoxy adhesives have been typically used in automotive industry for bonding of different parts, such as aluminum-aluminum bonding. These rubber-modified adhesives provide higher lap shear strength ($LSS = 17 \text{ MPa}$) than the unmodified epoxy adhesive ($LSS = 11 \text{ MPa}$) (Sprenger et al. 2009; Kinloch 2003).

Use of two toughening agents simultaneously is a common practice to further improve adhesive performance in automotive industry. With the growing demands for super-tough adhesives, recently, hybrid modification of one-component and two-component epoxy adhesives using a combination of micron-sized rubber modifier and silica nanoparticles has been studied in adhesively bonded joints under impact loadings in automotive and aerospace applications (Sprenger et al. 2009). Adhesive performance for Al-Al, composite-composite, and metal-composite bonding was explored. In this particular study, the one-component epoxy/DICY adhesive was modified with CTBN adducts, while ATBN was incorporated in the two-component epoxy adhesive. The ATBN reactive oligomers were premixed with a mixture of a polyamidoamine, an amine-terminated polyether polyol and isophorone diamine. Simultaneous existence of CTBN micro-domains and silica nanoparticles resulted in more enhancements in adhesive properties of composite-composite bonding and metal-composite bonding ($LSS_{CTBN/nanosilica\ hybrid} = 20.5\text{ MPa}$; $LSS_{CTBN} = 17\text{ MPa}$; $LSS_{unmodified\ adhesive} = 11\text{ MPa}$) (Sprenger et al. 2009). Synergistic toughening effect of ATBN/silica nanoparticle hybrid was also observed by addition of only 2.5–5 wt.% silica nanoparticles. Using small amount of silica nanoparticles did not alter the cost of manufacturing significantly (Sprenger et al. 2009). Evaluation of the fatigue behavior of these kinds of *super-tough* hybrid adhesives is an important task to be addressed.

Epoxy adhesives are widely used in electrical and electronics applications as well. Cycloaliphatic epoxy resins not only have high strength and modulus with good thermal stability at high temperatures and chemical resistance but also have superior electrical properties and good processability. Combination of these high quality properties of cycloaliphatic epoxies with toughening effect of rubber modifiers has opened up a good market for rubber-toughened epoxies as adhesives and encapsulants in electronics (Tripathi and Srivastava 2009). Anhydride curing agents offer superior electrical properties at high temperatures; however they tend to cure slowly (Dunn 2003).

It is shown that incorporation of acrylate rubber modifiers into epoxy formulation for electronic packaging results in extension of the semiconductor device life since the rubber modification significantly reduces shrinking stresses when epoxy is getting cured and greatly enhances the thermal shock resistance of the adhesive (Ho and Wang 1994).

The recent development in printed circuit boards and microelectronic packaging has migrated toward lead-free solders (Wang et al. 2008). This movement requires flexible copper clad laminates (FCCLs) with higher thermal resistance. Employing epoxy adhesives with improved thermal resistance extends the stability limit of the FCCLs to higher temperatures. In printed circuit boards, copper foil is bonded to the polyimide film, and laminates are joined together using epoxy-based adhesives. The required thermal stability of adhesive has been achieved through incorporation of superior rigid chains such as bismaleimide (BMI) into epoxy resin with the expense of negative impact on the adhesive strength and crack propagation resistance. To overcome this brittleness drawback, modification of the adhesive using CTBN-reactive rubbers was studied. The results showed improvement in toughness, peel

strength, and shear strength by toughening of the high thermal resistant epoxy adhesive with CTBN (Wang et al. 2008).

In the process of attaining required resistance to crack growth in laminates, Dow Chemical has launched a toughening technology for laminates used in printed circuit boards and packaging. This toughening technology is based on a blend of pre-dispersed CSR particles in epoxy and has been marketed under the trade name of FORTEGRA™ 353. This preformed rubber/epoxy pre-dispersion, FORTEGRATM 353 as described in Table 1, can remarkably increase lap shear strength, fracture toughness, and durability with minimal negative effect on thermomechanical properties. Use of this pre-dispersed CSR-modified epoxy in the manufacturing of electrical laminates improves toughness and thermal resistance of the products to withstand stresses applied through drilling and high-temperature soldering in the assembling process.

Silicone rubbers are suitable tougheners for electrical and electronic applications as UV curing adhesives and heat curing and room temperature curing adhesives, especially very fast-curing systems. As listed in Table 4, ALIDUR is a trade name for a series of toughened epoxy adhesives containing silicone rubber in the form of 100 nm–3 µm CSR particles. This CSR-toughened epoxy formulation can be cured quickly at room temperature (Evonik Adhesive Applications 2008).

Rubber-toughened epoxies can be also utilized as adhesive in bonding and sealing medical devices such as pacemakers and filter components (Fakhar et al. 2012). Bonding of end-caps to the main tube of blood filters is an example of medical application for epoxy adhesives. Epoxies are thermal resistant, and thus epoxy-based adhesives are suitable for applications which need sterilization before usage. Rubber modification of medical-grade epoxies helps improvement of the adhesive lap shear strength and bonding strength to provide a suitable bonding and avoid any chance of leakage or disconnection.

Biocompatible epoxy-based composite adhesives have been used in dental restorations (Thompson et al. 2013; Vitale et al. 2014; Bowen 1982). The restorative material requires satisfactorily high strength and wear resistance and chemical erosion resistance, plus low coefficient of thermal conductivity and expansion to assure tooth functions during the patient life span. Besides the mentioned properties, toughness and fatigue resistance are important parameters in selecting a reliable dental filling material as well as transparency and easiness of the material to manipulate and shape. A common dental filling material is a highly filled silica/epoxy (40–90 wt.% surface-modified fillers) (Vitale et al. 2014). Recently, a group of researchers studied the effects of block copolymer-grafted silica nanoparticles on mechanical behavior of an epoxy (Gao et al. 2012). The block copolymer grafted to the nanoparticles consisted a rubbery inner block of poly(hexyl methacrylate) (PHMA) and an epoxy-compatible block of poly(glycidyl methacrylate) (PGMA). The results revealed 60% increase in tensile ductility, 300% enhancement in fracture toughness, and improved fatigue resistance without scarifying Young's modulus when only 2 wt.% of block copolymer-grafted silica nanoparticles was incorporated into an epoxy resin. The toughening effect was mainly attributed to

plastic void growth and formation of shear bands in the epoxy matrix (Gao et al. 2012). These findings can be extended to dental-epoxy-based materials. The quality and properties of the interface between the restorative material and tooth play an important role in performance and lifetime of the filled tooth.

Aramid fiber-reinforced aluminum laminates (ARALL), glass laminate aluminum reinforced epoxy (GLARE), and carbon fiber-reinforced metal are among highly applicable materials in the aerospace industry. These materials consist of a number of thin metallic layers bonded together with fiber-reinforced epoxy adhesives. It is essential that these materials have high impact resistance (Marouf et al. 2004, 2008; Vaziri et al. 1996). Marouf et al. (2008) studied the impact resistance of adhesively bonded aluminum laminates as a function of the interfacial fracture energy of the adhesive. They were able to alter the interfacial fracture energy by means of different modifiers, i.e., core-shell rubber particles and micron-sized SiC particles, added into an epoxy-based adhesive. Their results showed that introduction of preformed rubber modifier increases interfacial fracture energy while addition of SiC particles reduces this parameter. They attributed this observation to the effect of modifier on the rigidity of the adhesive. In other words, they believed that incorporation of the rubber modifier in the adhesive reduces its rigidity and increases the interfacial fracture energy of the laminate. Their impact resistance study revealed that improving the interfacial fracture energy of the laminate by help of rubber modifier can raise the impact strength of the laminate. However, as they showed, too strong interface suppresses interfacial delamination prior to fracture of the laminate which reduces the performance of the aluminum laminate against impact loading. Therefore, these researchers claimed an optimum interfacial adhesion for obtaining high impact strength of the laminate (Marouf et al. 2008).

In another study, Forte et al. (2000) also observed a decrease in interfacial fracture energy of their laminates when they incorporated rigid glass beads in their epoxy adhesive. These researchers reported a linear dependence of interfacial fracture energy to the ratio of adhesive modulus to adhesive impact resistance. These two studies illustrate the possibility of controlling the interfacial fracture energy in laminates by help of additives incorporated in the adhesive formulation and that the interfacial fracture energy can significantly affect the impact strength of the laminate. Therefore, proper use of rubber modifiers is crucial in controlling the impact strength of laminates bonded by epoxy-based adhesives.

To summarize this section, epoxies modified with reactive oligomers, preformed core-shell rubber particles, and block copolymers either in nanoscale or micron-scale can be used separately or conjointly as very high performance structural adhesives in electronics and electrical applications, aeronautics/aircraft, automobiles, wind turbines, solar cell panels, constructions/buildings, marine vehicles/boats, railway, sport goods, etc. These tough adhesives can join dissimilar materials such as honeycombs, sandwich panels, composite laminates/prepregs, thin sheet materials, metals, plastics, rubbers, ceramics, and minerals with a balance of toughness, stiffness, and low weight.

Conclusion

This chapter tries to give a general overview of the whole concept of rubber-toughened epoxies to the reader and to deliver a more realistic sense of industrial applications of epoxy/rubber and epoxy/copolymer blends by means of practical examples. The current and potential market for the state-of-the-art toughened epoxy blends includes advanced coatings, matrix for composites, and structural adhesives employed in green energy (wind and solar), aeronautics, transportation (automotive, railway, and marine), and sport industry.

References

- Al-Aqeeli N (2015) Fabrication and assessment of crumb-rubber-modified coatings with anticorrosive properties. *Materials* 8:181–192
- Bagheri R, Williams MA, Pearson RA (1997) Use of surface modified recycled rubber particles for toughening of epoxy polymers. *Polym Eng Sci* 37:245–251
- Bagheri R, Marouf BT, Pearson RA (2009) Rubber-toughened epoxies: a critical review. *Polym Rev* 49:201–225
- Barsotti R, Fine T, Inoubli R, Gerard P, Schmidt S, Macy N, Magnet S, Navarro C (2008) Nanostrength[®] block copolymers for epoxy toughening. The meeting of the thermoset resin formulators association, Chicago, 15–16 Sept
- Barsotti RJ, Alu A, Bentzel G, Allen P, Macy N, Schmidt S, Wells MO (2010) Nanostrength[®] block copolymers for wind energy. 2010 Wind Turbine Blade Workshop, Sandia National Labs, 20 July
- Bascom WD, Cottingham RL, Jones RL, Peyser P (1975) The fracture of epoxy- and elastomers modified epoxy polymers in bulk and as adhesives. *J Appl Polym Sci* 19:2545–2562
- Bowen RL (1982) Composite and sealant resins – past, present, and future. *Pediatr Dent* 4:10–15
- Bray DJ, Dittanet P, Guild FJ, Kinloch AJ, Masania K, Pearson RA, Taylor AC (2013) The modelling of the toughening of epoxy polymers via silica nanoparticles: the effects of volume fraction and particle size. *Polymer* 54:7022–7032
- Bucknall CB, Yoshii T (1978) Relationship between structure and mechanical properties in rubber toughened epoxy resins. *Br Polym J* 10:53–59
- Chen Y, Pearson RA (2014) On the use of self-assembling block copolymers to toughen a model epoxy. The 2014 annual meeting of the Adhesion Society, San Diego, p 3
- Chen J, Kinloch AJ, Sprenger S, Taylor AC (2013) The mechanical properties and toughening mechanisms of an epoxy polymer modified with polysiloxane-based core-shell particles. *Polymer* 54:4276–4289
- Chikhi N, Fellahi S, Bakar M (2002) Modification of epoxy resin using reactive liquid (ETBN) rubber. *Eur Polym J* 38:251–264
- Chong HM, Taylor AC (2013) The microstructure and fracture performance of styrene-butadiene-methylmethacrylate block copolymer-modified epoxy polymers. *J Mater Sci* 48:6762–6777
- Dean JM, Lipic PM, Grubbs RB, Cook RF, Bates FS (2001) Micellar structure and mechanical properties of block copolymer-modified epoxies. *J Polym Sci Pol Phys* 39:2996–3010
- Dean JM, Grubbs RB, Saad W, Cook RF, Bates FS (2003) Mechanical properties of block copolymer vesicle and micelle modified epoxies. *J Polym Sci Pol Phys* 41:2444–2456
- Declet-Perez C, Francis LF, Bates FS (2015) Deformation process in block copolymer toughened epoxies. *Macromolecules* 48:3672–3684
- Dunn DJ (2003) Adhesives and sealants: technology, applications and markets. *Rapra Technology, Shrewsbury*, pp 27–30

- Evonik (2008) Adhesive applications: product portfolio, May
- Fakhar A, Aabedaaan M, Keivani M, Langari M (2012) Use of reactive oligomer to improve fracture resistance of epoxy used in medical applications and GRP pipelines. *World Appl Sci J* 20:259–263
- Forte MS, Whitney JM, Schoeppner GA (2000) The influence of adhesive reinforcement on the mode-I fracture toughness of a bonded joint. *Comp Sci Technol* 60:2389–2405
- Gao J, Li J, Benicewicz BC, Zhao S, Hillborg H, Schadler LS (2012) The mechanical properties of epoxy composites filled with rubbery copolymer grafted SiO₂. *Polymers* 4:187–210
- Garg AC, Mai Y-W (1988) Failure mechanisms in toughened epoxy resins – a review. *Compos Sci Technol* 31:179–223
- Grubbs RB, Dean JM, Broz ME, Bates FS (2000) Reactive block copolymers for modification of thermosetting epoxy. *Macromolecules* 33:9522–9534
- Gupta P, Bajpai M (2011) Development of siliconized epoxy resins and their applications as anticorrosive coatings. *Adv Chem Eng Sci* 2:1333–139
- He J, Raghavan D, Hoffman D, Hunston D (1999) The influence of elastomer concentration on toughness in dispersions containing acrylic elastomeric particles in an epoxy matrix. *Polymer* 40:1923–1933
- Ho TH, Wang CS (1994) Dispersed acrylate rubber-modified epoxy resins for electronic encapsulation. *J Polym Res* 1:103–108
- Humphreys S (2011) Impact, weight and anti-corrosion coatings for pipelines. Applied Market Information, UK (available on <https://www.amiplastics.com/pressreleases/newsitem.aspx?item=1000140>)
- Hydro RM, Pearson RA (2007) Epoxies toughened with triblock copolymers. *J Polym Sci Part B Polym Phys* 45:1470–1481
- Jacob GC, Hoevel B, Pham HQ, Dettlof ML, Verghese NE, Turakhia RH, Hunter G (2007) Technical advances in epoxy technology for wind turbine blade composite fabrication. SAMPE, Baltimore, 15 pp
- Jansen BJP, Tamminga KY, Meijer HEH, Lemstra PJ (1999) Preparation of thermoset rubbery epoxy particles as novel toughening modifiers for glassy epoxy resins. *Polymer* 40:5601–5607
- Karger-Kocsis J, Meszaros L, Barany T (2012) Ground tyre rubber (GTR) in thermoplastics, thermosets and rubbers. *J Mater Sci* 48:1–38
- Kehr JA (2012) How fusion-bonded epoxies protect pipeline: single- and double-layer systems. Protecting and maintaining transmission pipeline. Technology Publishing, Pittsburgh, pp 13–22
- Kim HS, Ma P (1996) Correlation between stress-whitening and fracture toughness in rubber-modified epoxies. *J Appl Polym Sci* 61:659–662
- Kinloch AJ (2003) Toughening epoxy adhesives to meet today's challenges. *MRS Bull* 28 445–448
- Kinloch AJ, Finch CA, Hashemi S (1987) Effect of segmental molecular mass between cross-links of the matrix phase on the toughness of rubber-modified epoxies. *Polym Commun* 28:322–325
- Kinloch AJ, Korenberg CF, Tan KT, Watts JF (2007) Crack growth in structural adhesive joints in aqueous environments. *J Mater Sci* 42:6353–6370
- Kinloch AJ, Lee SH, Taylor AC (2014) Improving the fracture toughness and cyclic-fatigue resistance of epoxy-polymer blends. *Polymer* 55:6325–6334
- Kishi H, Kunimitsu Y, Imade J, Oshita S, Morishita Y, Asada M (2011) Nano-phase structures and mechanical properties of epoxy/acryl triblock copolymer alloys. *Polymer* 52:760–768
- Kishi H, Kunimitsu Y, Nakashima Y, Abe T, Imade J, Oshita S, Morishita Y, Asada M (2015) Control of nanostructures generated in epoxy matrices blended with PMMA-b-PnBA-b-PMMA triblock copolymers. *Express Polym Lett* 9:23–35
- Kozii VV, Rozenberg BA (1992) Mechanisms of energy dissipation in elastomer-modified thermosetting polymer matrices and composites based on such polymers. *Polym Sci* 34:919–951

- Kunal K, Sprenger S (2014) optimized epoxy resins for automotive composites: tough, stiff and fatigue resistant. Automotive, composites conference and exhibition, Society of Plastic Engineers (SPE) 9–11 Sept, 5 pp
- Kunz-Douglass S, Beamont PWR, Ashby MF (1980) A model for toughness of epoxy-rubber particulate composites. *J Mater Sci* 15:1109–1123
- Lataillade J, Grapotte D, Cayssisals F (1994) The impact resistance of CTBN-modified epoxy adhesive joints. *J Phys IV C8:771–776*
- Liang YL, Pearson RA (2010) The toughening mechanism in hybrid epoxy-silica-rubber nanocomposites. *Polymer* 51:4880–4890
- Liu J, Sue HJ, Thompson ZJ, Bates FS, Dettloff M, Jacob G, Verghese N, Pham H (2008) Nanocavitation in self-assembled amphiphilic block copolymer-modified epoxy. *Macromolecules* 41:7616–7624
- Liu J, Thompson ZJ, Sue HJ, Bates FS, Hillmyer MA, Dettloff MV, Jacob G, Verghese N, Pham H (2010) Toughening of epoxies with block copolymer micelles of wormlike morphology. *Macromolecules* 43:7238–7243
- Loos MR, Yang J, Feke DL, Manas-Zloczower I (2012a) Effect of block-copolymer dispersants on properties of carbon nanotube/epoxy systems. *Comp Sci Technol* 72:482–488
- Loos M, Yang J, Feke D, Manas-Zloczower I (2012b) Carbon nanotube-reinforced epoxy composites for wind turbine blades. Society of Plastics Engineers (SPE), *Plastics Research Online* 10.1002/spepro.004276: 3 pp
- Lorena RP, Royston GJ, Fairclough PA, Ryan AJ (2008) Toughening by nanostructures. *Polymer* 49:4475–4488
- Lovell PA, McDonald J, Saunders DEJ, Young RJ (1993) Studies of rubber-toughened poly (methyl methacrylate): 1. Preparation and thermal properties of blends of poly(methyl methacrylate) with multiple-layer toughening particles. *Polymer* 34:61–69
- Lu C, Mai Y-W (2005) Influence of the aspect ratio on barrier properties of polymer-clay nanocomposites. *Phys Rev Lett* 95:088303
- Mallozzi ML, Attaguiile SM, Baratto DJ (2014) Damage resistant epoxy compounds. Patent No # CA2630583 C
- Marouf BT, Bagheri R (2010) Physical properties and applications of clay nanofiller/epoxy nanocomposites. In: Tjong SC, Mai Y-W (eds) *Physical properties and applications of polymer nanocomposites*. Woodhead, Cambridge, UK, pp 743–772
- Marouf BT, Bagheri R, Mahmudi R (2004) Effects of number of layers and adhesive ductility on impact behavior of laminates. *Mater Lett* 58:2721–2724
- Marouf BT, Bagheri R, Mahmudi R (2008) Role of interfacial fracture energy and laminate architecture on impact performance of aluminum laminates. *Compos Part A* 39:1685–1693
- Marouf BT, Pearson RA, Bagheri R (2009) Anomalous fracture behavior in an epoxy-based hybrid composite. *Mater Sci Eng A* 515:49–58
- Marouf BT, Mai Y-W, Bagheri R, Pearson RA (2016) Toughening of epoxy nanocomposites: nano and hybrid effects. *Polym Rev* Published online 8 January
- May CA (1988) *Introduction to epoxy resins, chemistry and technology*. Marcel Dekker, New York, pp 1–6
- Meeks AC (1974) Fracture and mechanical properties of epoxy resin and rubber-modified epoxies. *Polymer* 15:675–681
- Miyatake N (2013) New advances in core-shell rubber toughening for epoxy resins. *JEC Comps Mag*, March (issue 79): p85
- Njuguna J, Pielichowski K, Alcock JR (2007) Epoxy-based fibre reinforced nanocomposites. *Adv Eng Mater* 9:835–847
- Oldak RK, Hydro RM, Pearson RA (2007) On the use of triblock copolymers as toughening agents for epoxies. Adhesion Society, Tampa, 3 pp
- Pearson RA, Yee AF (1989) Toughening mechanisms in elastomer modified epoxies: the effect of cross-link density. *J Mater Sci* 24:2571–2580

- Pearson RA, Yee AF (1991) Influence of particle size and particle size distribution on toughening mechanisms in rubber-modified epoxies. *J Mater Sci* 26:3828–3844
- Pham H, Aguirre F, Dettloff M, Verghese N (2007) Development of novel toughening technology for fusion-bonded-epoxy (FBE) powder coatings. *Paint Coat Ind Mag*, October: 4 pp
- Plastics Europe's PC/BPA Group (2011) Application of bisphenol A, 34 pp (Available on www.bisphenol-a-europe.org/uploads/EN_BPA%20applications%20.pdf)
- Plastics Europe's PC/BPA Group, Bisphenol A epoxy resins (Available on http://www.bisphenol-a-europe.org/en_GB/what-is-bisphenol-a/epoxy-resins)
- Prolongo SG, Gude MR, Ureña A (2012a) Adhesive strength and toughness improvement of epoxy resin modified with polystyrene-*b*-polybutadiene-*b*-poly(methyl methacrylate) block copolymer. *J Mater Sci Eng* 1:109. doi:10.4172/2169-0022.1000109
- Prolongo SG, Vadillo V, Gude MR, Sánchez L, Ureña A (2012b) Nanostructured epoxy adhesive modified with self-assembling block copolymers for joining fiber carbon epoxy composites. In: 15th European conference on composite materials (ECCM15), Venice, 24–28 June
- Pulgisi JS, Chaudhari MA (1988) Epoxies, engineering plastics. ASM International, Metals Park, pp 240–245
- Ratna D, Banthia AK (2004) Rubber toughened epoxy. *Macromol Res* 12:11–21
- Rebizant V, Venet AS, Tournilhac F, Girard-Reydet E, Navarro C, Pascault JP, Leibler L (2004) Chemistry and mechanical properties of epoxy-based thermosets reinforced by reactive and nonreactive SBMX block copolymers. *Macromolecules* 37:8017–8027
- Ritzenthaler S, Court F, David L, Girard-Reydet E, Leibler L, Pascault JP (2002) ABC triblock copolymers/epoxy – diamine blends. 1. Keys to achieve nanostructured thermosets. *Macromolecules* 35:6245–6254
- Ruzette AV, Leibler L (2005) Block copolymers in tomorrow's plastics. *Nat Mater* 4:19–31
- Schoberleitner C, Archodoulaki VC, Koch T, Lüftl S, Werderitsch M, Kuschnig G (2013) Developing a sealing material: effect of epoxy modification on specific physical and mechanical properties. *Materials* 6:5490–5501
- Sprenger S, Eger C, Kinloch AJ, Lee JH, Taylor AC, Egan D (2003) Toughening structural adhesives via nano- and micro-phase inclusions. *J Adhes* 79:867–873
- Sprenger S, Eger C, Kinloch AJ, Lee JH, Taylor AC, Egan D (2004) Nanomodified ambient temperature curing epoxy adhesives. *Adhäsion Kleben Dichten* 3:17–21
- Sprenger S, Kinloch AJ, Taylor AC, Lee JH, Mohammed RD, Egan D (2006) Improving structural epoxy adhesives with SiO₂ nanoparticles. The 29th annual meeting of the Adhesion Society, Jacksonville, 19–22 Feb, 232–234
- Sprenger S, Kinloch AJ, Taylor AC (2009) Making industrial adhesives tougher. *Eur Coatings J* 3:9 pp
- Sultan JN, McGarry FJ (1973) Effect of rubber particle size on deformation mechanisms in glassy epoxy. *Polym Eng Sci* 13:29–34
- Thio YS, Wu J, Bates FS (2006) Epoxy toughening using low molecular weight poly(hexylene oxide)-poly(ethylene oxide) di-block copolymers. *Macromolecules* 39:7187–7189
- Thompson ZJ, Hillmyer MA, Liu J, Sue HJ, Dettloff MV, Bates FS (2009) Block copolymer toughened epoxy: role of cross-link density. *Macromolecules* 42:2333–2335
- Thompson VP, Watson TF, Marshall GW, Blackman BRK, Stansbury JW, Schadler LS, Pearson RA, Libanori R (2013) Outside-the-(cavity-prep)-box thinking. *Adv Dent Res* 25:24–32
- Three Bond Technical News (1990) Curing agents for epoxy resins. 20 Dec, 10 pp
- Transparency Market Research (2015) Epoxy resins market for paints & coatings, wind energy, composites, construction, electrical & electronics, adhesives and other applications – Global industry analysis, size, share, growth, trends and forecast 2014–2020, 28 Jan
- Tripathi G, Srivastava D (2009) Studies on blends of cycloaliphatic epoxy resin with varying concentrations of carboxyl terminated butadiene acrylonitrile copolymer I: thermal and morphological properties. *Bull Mater Sci* 32:199–204

- Turakhia R, Pham H, Jacob G, Hunter G, Hoevel B (2009) Advances in epoxy technology for windmill blade composite fabrication. Thermoset Resin Formulators Association (TRFA), Pittsburgh
- Utracki LA (2010) Rigid ballistic composites. NRC Publications Archive, Canada: 78 pp
- Vaziri R, Quan X, Olson MD (1996) Impact analysis of laminated composite plates and shells by super finite elements. *Int J Impact Eng* 18:765–782
- Vitale A, Sangermano M, Bongiovanni R, Burtscher P, Moszner N (2014) Visible light curable restorative composites for dental applications based on epoxy monomer. *Materials* 7:554–562
- Wang H, Xu Y, Liu Y (2008) Novel modified epoxy adhesive for FCCL with high thermal resistance. IPC Printed Circuits Expo, APEX and the Designers Summit, Las Vegas, 1–3 Apr
- Wu J, Thio YS, Bates FS (2005) Structure and properties of PBO-PEO diblock copolymer modified epoxy. *J Polym Sci Pol Phys* 43:1950–1965
- www.henkel.com
- www.kukdo.com
- www.prweb.com/releases/epoxy_resins/paints_coatings_laminates/prweb8343600.htm
- www.hiseamarine.com/fnrh-610-rubber-modified-acid-base-resistant-anticorrosive-paint-4374.html, “Rubber-modified acid-base resistant anti-corrosive paint”
- www.hiseamarine.com/popular-type-modified-epoxy-anticorrosive-paint-2534.html, “Popular type modified epoxy anticorrosive paint”
- Xie R, Theophanous T, Aguirre F, Verghese N, Valette L, Pham H (2011) Advanced epoxy resins with enhanced toughness for demanding applications. TRFA 2011 annual meeting, Ontario, 11–13 Sept
- Yee AF, Pearson RA (1986a) Toughening mechanisms in elastomer-modified epoxies: mechanical studies. *J Mater Sci* 21:2462–2474
- Yee AF, Pearson RA (1986b) Toughening mechanisms in elastomer-modified epoxies: microscopy studies. *J Mater Sci* 21:2475–2488

Part II

Epoxy/Thermoplastic Blends

Jinyan Wang, Rui Liu, and Xigao Jian

Abstract

The incorporation of thermoplastics in epoxy matrices is considered to be a highly effective method to improve some mechanical properties of epoxy resins, especially the fracture toughness. In this chapter, a comprehensive review of the development in thermoplastic/epoxy blends is provided. Also the effects of the addition of different thermoplastics such as polysulfone (PSF), poly(ether sulfone) (PES), poly(ether imide) (PEI), and poly(phthalazinone ether)s on fracture toughness, modulus, and strength of the epoxy resins have been reviewed. Then, the reaction-induced phase separation and the influence factors of toughening effect such as content of additives, molecular weight and end groups, etc., are also summarized. In addition, the toughening mechanisms of thermoplastics/epoxy blends are described generally.

Keywords

Epoxy resin • Fracture toughness • Reaction-induced phase separation • Concentration of thermoplastic • End groups • Molecular weight • Toughening mechanisms

J. Wang (✉) • X. Jian (✉)

State Key Laboratory of Fine Chemicals, Dalian University of Technology, Dalian, China

Department of Polymer Science and Materials, Dalian University of Technology, Dalian, China

e-mail: wangjinyan@dlut.edu.cn; jian4616@dlut.edu.cn

R. Liu (✉)

State Key Laboratory of Fine Chemicals, Department of Polymer Science and Materials, Dalian University of Technology, Dalian, China

e-mail: raultracy@163.com

Contents

Introduction	430
Different Epoxy/Engineering Thermoplastic Blends	431
Poly(ether sulfone) (PES)	431
Poly(ether imide) (PEI)	435
Polysulfone (PSF)	436
Poly(phthalazinone ether)s	439
Other Thermoplastics	440
Reaction-Induced Phase Separation	440
Influence Factors of Phase Morphology and Toughening Effect	447
Content of Thermoplastics	447
End Groups of Thermoplastics	448
Molecular Weight of Thermoplastics	449
Toughening Mechanisms of Thermoplastic/Epoxy Blends	451
Conclusions	454
References	456

Introduction

Epoxy resins, containing two or more epoxy groups in their molecular backbone, have become a category of momentous thermosetting resin. As we all have known, the uncured epoxy resins have little useful value. They have to react with suitable curing agent, such as amines and anhydrides, to form the three-dimensional cross-linked structures to give them excellent mechanical properties and thermal stability. Their inherent high adhesion strength and good processability also broaden their applications in the fields of adhesive, coating, electronic encapsulation material, and the matrix for advanced fiber-reinforced plastics (FRP). Unfortunately, the high-cross-linking-density epoxies display inherently brittle material with poor crack resistance and low fracture toughness at room temperature. To overcome these drawbacks, many methods have been developed to successfully enhance the fracture toughness of epoxies. In general, the dominant strategy adopted to toughening the epoxy resins is the addition of a second microphase into epoxy system. These second microphase will precipitate into the epoxy network during curing. Thus the forming of multiphase morphology is able to initiate a variety of toughening mechanisms during crack growth. The frequently used additives include rubbers, inorganic nanoparticles, liquid crystal polymers (LCP), and thermoplastics. Among these methods, many additives can be effective as toughening additives for epoxy resins, but their drawbacks such as reduction in overall resin modulus and reduction in epoxy end-use temperature limit their application in aerospace (Wu et al. 2013; Frigione et al. 1995). In addition, for highly cross-linked epoxy resins (trifunctional and tetrafunctional) commonly used in aerospace composites, some additives like rubbers are ineffective toughening additives due to a decreasing capability of the highly cross-linked resins to be plastically deformed (Siddhamalli 2000). So high-performance engineering thermoplastics have been selected as eligible modifiers for epoxy resins. Engineering thermoplastic modification of epoxy resins, studied since the early 1980s, has been considered as an effective way to improve toughness of

epoxy resins without significant decreases in desirable properties such as high stiffness and strength (which always occurred for epoxy/rubber system), good thermal stability, chemical and creep resistance, and good process ability. In common, these additives toughen epoxy resins and involve polysulfone (PSF), poly(ether sulfone) (PES), poly(ether imide) (PEI), polyamides (PA), poly(ether ether ketone) (PEEK), poly(phthalazinone ether)s, etc. There are a number of reviews on thermoplastic/epoxy blends (Hodgkin et al. 1998; Frigione et al. 1995) from the different viewpoint. The present review, served for *Handbook of Epoxy Blends*, is intended to provide an approximate outline of the science and technology of epoxy/thermoplastic blends and hope to complement the previous reviews by summarizing some recent reports. The paper focused upon the different thermoplastics and their chemical requirements, such as thermoplastic end groups, followed by content of additives and molecular weight of the polymers, modulus, and strength of the epoxy resins. The toughening mechanisms of thermoplastics/epoxy blends are just described generally.

Different Epoxy/Engineering Thermoplastic Blends

Toughening epoxy resins by blending with various engineering thermoplastics has been concentrated to develop and then widely applied in industry. In epoxy/engineering thermoplastic blends, three kinds of epoxy resins have been mainly studied. They are the diglycidyl ether of bisphenol A (DGEBA), tetraglycidyl diamino diphenyl methane (TGDDM) (the most commonly used in aerospace), and triglycidyl p-aminophenol (TGAP). Diamino hardener is always selected in epoxy/engineering thermoplastic blends, including diamino diphenyl sulfone (DDS), which is the most common hardener, especially in aerospace, and displays the slow reaction with epoxy in the result of easy control and excellent thermal stability and high glass transition temperature for the resulting cured specimens. Figure 1 shows the chemical structure of the main epoxy resins listed above. Other types of hardeners reported included diaminodiphenylmethane (DDM), m-phenylenediamine (MPDA), and dicyandiamide (DICY). There are a few dianhydride hardeners reported.

Typical engineering thermoplastics that are concentrated to study are polyetherimide (PEI, invented by General Electric and now marketed by SABIC), polyethersulfone (PES, sold by Victrex now), and bisphenol A polyethersulfone (PSF, Union Carbide), and novel poly(aryl ether)s containing phthalazinone moieties are also introduced into this system, and some progress improvements will be discussed in the coming sections. The chemical structures of the thermoplastic abovementioned are shown in Fig. 2.

Poly(ether sulfone) (PES)

Poly(ether sulfone) resins with a glass transition temperature about 220 °C are stable at higher temperatures (>200 °C) in the air and possess excellent mechanical properties.

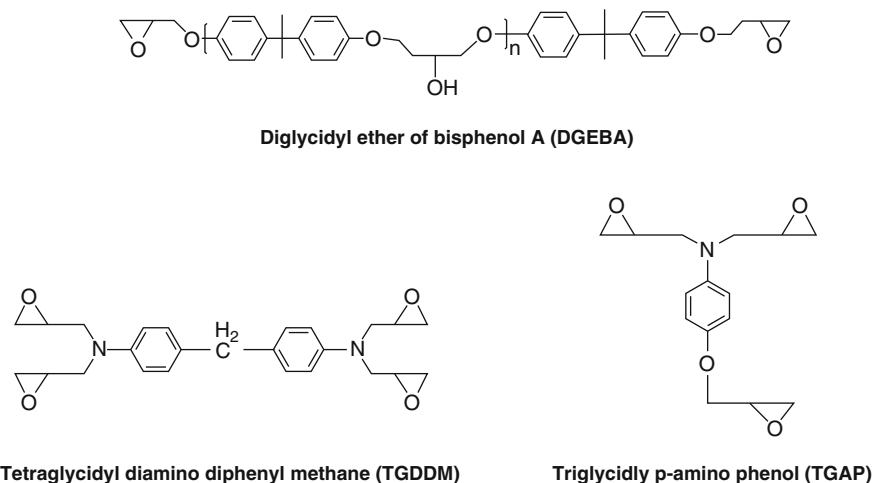


Fig. 1 The chemical structure of the most used epoxy resins in epoxy/ thermoplastic system

Bucknall and Partridge (1983) first used a low molecular weight commercial PES to modify the trifunctional and tetrafunctional epoxy resins using diamino diphenyl sulfone (DDS) or dicyandiamide (DICY) as the hardener. The results showed that the variety of morphologies was obtained in mixtures of PES with different hardeners and epoxy resins, but modulus and fracture toughness showed little dependence upon composition. Then Raghava studied the miscibility and fracture toughness of a tetrafunctional epoxy resin (Ciba-Geigy: MY-720) with 15-phr PES (Victrex 100P, a low molecular weight and hydroxyl-terminated polyethersulfone) cured with aromatic anhydrides (Raghava 1987). They found that the fracture toughness values of this system were similar with the neat epoxy resin in the low temperature ($-80\text{ }^{\circ}\text{C}$). Their K_{IC} and G_{IC} values were increased above $50\text{ }^{\circ}\text{C}$ with the increase of the test temperature, due to the presence of large plastic deformation during fracture, evidenced by the scanning electron microscopy (SEM) photograph of their fracture. Next year, Raghava varied the molecular weights of PES to toughen a tetrafunctional epoxy resin cured with aromatic anhydrides. He concluded that particle/matrix separation was very important to toughness enhancement, and the presence of in situ developed or externally added inclusions, soft or hard, in a hard matrix may be a minimum condition for the toughening of a brittle material, but it is not a sufficient condition (Raghava 1988). Fernández et al. (2004) investigated the influence of PES as a modifying agent of a tetrafunctional epoxy matrix (TGDDM) cured with 4,4',-diaminodiphenylmethane (DDM) on the mechanical behavior. No evidence of phase separation was observed by using dynamic mechanical analysis (DMA) and SEM. Their atomic force microscope (AFM) pictures showed a morphological change, which is difficult to clarify, after PES addition. The morphology obtained

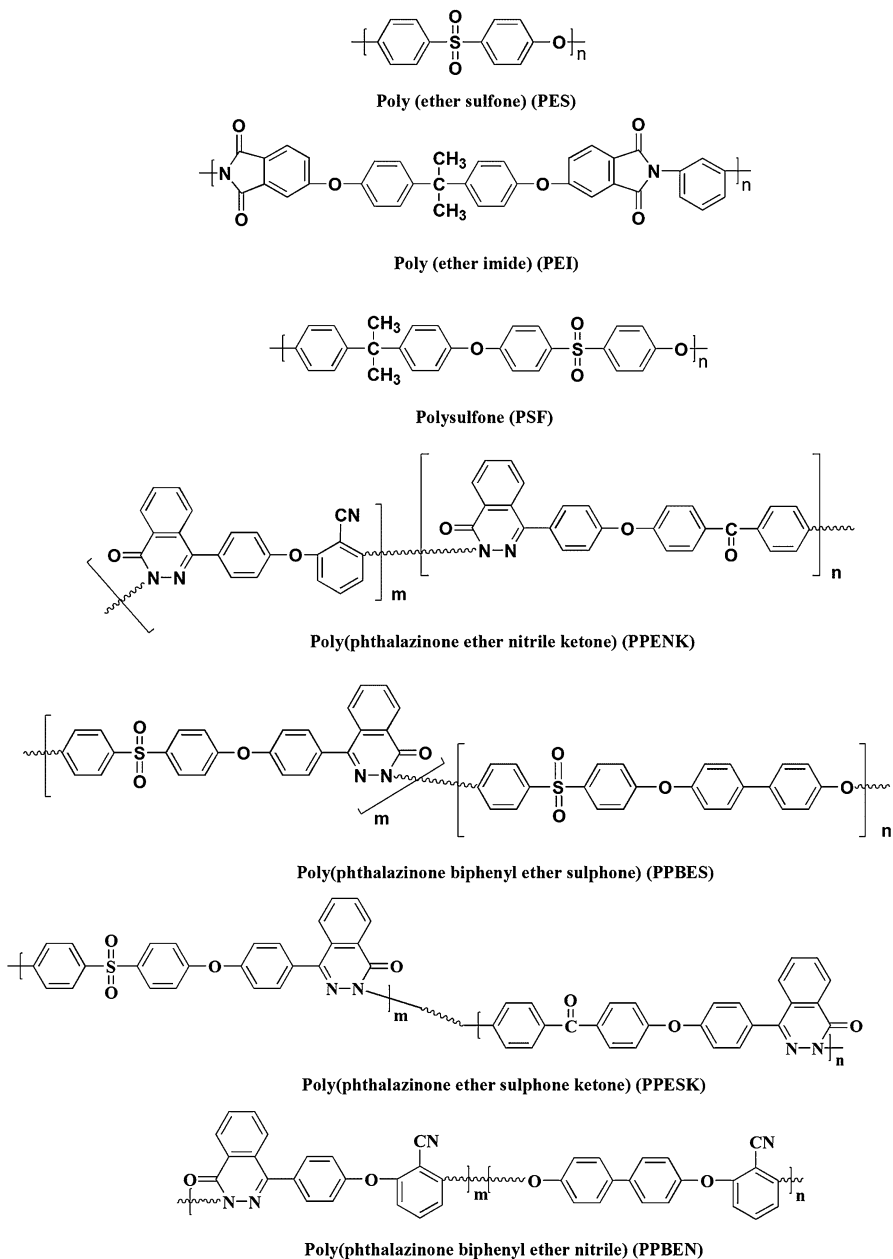


Fig. 2 The chemical structures of thermoplastics in epoxy/thermoplastic system

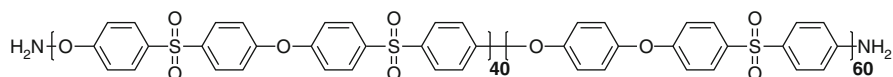


Fig. 3 The structure of PES copolymer (Reproduced with permission from I. Blanco et al. (2006). Copyright (2006), Wiley)

was possibly related to phase separation. It seemed that a phase separation progress stayed at nanoscale. The K_{IC} and G_{IC} values for this PES-modified epoxy resin were no significant improvement at all ranges of composition investigated since the phase separation at the nanoscale level was not able to stabilize the fracture process. In 1992, MacKinnon et al. (1992) achieved a marked improvement in the fracture toughness for PES/TGDDM system using diamino diphenyl sulfone (DDS) as the hardener, coincident with the occurrence of a co-continuous phase.

In the recent decades, more modified PES/epoxy blends are established. Mimura et al. (2000) added PES to a biphenyl-type epoxy resin (YX4000; Yuka-Shell Epoxy Co.) cured with phenol novolac-type resin (PSM4261; Gunei Chem. Ind. Co.). They found that the dispersion state of the PES in the epoxy resin was controlled by changing the molding temperature, and the value of the fracture toughness was in turn controlled by the particle size of thermoplastic in the epoxy matrix. When containing 10 wt% PES, the fracture toughness increased about 60% more than that of the unmodified epoxy resin, which is attributed to the formation of the semi-interpenetrating polymer networks (semi-IPNs) composed of the epoxy network and linear PES. When 20 wt% PES was added, the PES formed continuous phase morphology, a significant increase in toughness was obtained, and the value of the cured resin containing 20 wt% PES was about 1.9 times greater than that of the unmodified resin. This result was similar with MacKinnon et al. (1992).

Blanco et al. (2003) synthesized a novel PES copolymer ($M_n = 12,000$, molecular structure shown as Fig. 3) with reactive amine as terminal groups to modify diglycidyl ether of bisphenol S (DGEBS) hardened with DDS. Transmission electron microscope (TEM) and dynamic mechanical analysis (DMA) showed the presence of a single-phase morphology that can be attributed to the formation of a full-IPN network. The formation of the full-IPN structure makes it possible to homogeneously blend the epoxy matrix and the thermoplastics or to uniformly disperse the thermoplastic in the epoxy matrix at a microscopic level. The full-IPN network shows combined properties of the two polymers because of the composite structure at the molecular level. K_{IC} and G_{IC} values confirmed the remarkable effect of an amine-ended copolymer to increase the fracture toughness of inherently brittle epoxy resin. When 30 wt% PES copolymer was added, the K_{IC} value of epoxy blend was about $1.34 \text{ MPa} \cdot \text{m}^{0.5}$. This K_{IC} value was in the same order as that for a commercially toughened epoxy resin used as a matrix in aerospace composites (Cycrom 977-2, produced by Cytec Engineered Materials, $K_{IC} = 1.30 \text{ MPa} \cdot \text{m}^{0.5}$).

Then Blanco et al. (2006) used the same PES copolymer to modify a new epoxy novolac resin based on dicyclopentadiene (Tactix556) hardened with DDS. The resulting blends also presented single phase morphology, speculating the formation

of a full-IPN network due to the reaction of amine end group with epoxy resin. The fracture toughness of modified epoxy resin was also improved. Moreover, compared with the actual matrices for aerospace composites, this epoxy system showed that the water uptake values were minimized. The T_g value of modified epoxy resin was higher than 180 °C, so this modified epoxy resin was suitable as a matrix for advanced fiber-reinforced polymers.

Zhang et al. (2009) investigated the effect of heating rate on the cure behavior and monitored phase separation of PES-modified epoxy systems. They used PES-modified multifunctional epoxies, TGDDM, and TGAP, hardened by DDS. And they found that heating rate had a significant influence on the cure kinetics and phase structures of epoxy blend. Greater heating rate causes higher epoxy conversion. The domain size of the microphases formed from phase separation increased with the increase of heating rate. As heating rate increased from 1.5 °C/min to 10 °C/min, the diameter of the microphases increased from 9.67 μm to 11.41 μm. A more complete phase separation was achieved by fast-heated PES-modified epoxy blends. This discovery is helpful to the controlling of phase morphology, but whether it is suitable for all the epoxy/thermoplastic system is yet to be proved.

Poly(ether imide) (PEI)

Poly(ether imide) resin is a kind of high-performance engineering thermoplastics with a high glass transition temperature (about 215 °C). An early toughening study that used commercial polyetherimide (PEI) was reported by Bucknall and Gilbert (1989). They found that PEI/epoxy system displayed similar morphologic structure, but better fracture toughness values than PES/epoxy system. It is mainly because of the good adhesion between the epoxy matrix and thermoplastic particles. Then PEI was widely investigated as a toughening additive.

Su and Woo (1995) investigated the cure kinetics and morphology of a PEI/TGDDM/DDS system. They found an autocatalytic mechanism for amine-cured epoxy-PEI blends over a range of compositions. And the morphology of the epoxy blends changed from a continuous epoxy/discrete PEI pattern at low PEI contents (10 phr or lower) to an intertwined continuous PEI/epoxy strand pattern at a PEI content of 40 phr or higher.

Jang and Shin (1995) mixed PEI with EPON HPT 1071, which was cured by an amine curing agent (EPON HPT 1061 M). Open tension tests showed an increase in fracture toughness with PEI content, from 0.61 GPa · m^{0.5} in the pristine resin to 1.32 GPa · m^{0.5} at 15 wt% PEI. Similar results were obtained for the flexural properties of the epoxy resin. In order to improve the fracture toughness of epoxy resins, increasing the interfacial adhesion strength between the dispersed PEI phase and tetrafunctional epoxy resin was necessary. When hydrolyzed PEI was introduced into the tetrafunctional epoxy resin, an IPN structure was formed with forming the chemical bonds that existed at the interface between the hydrolyzed PEI and epoxy resin in the result of the better interfacial strength. Fracture stress could be transferred to the hydrolyzed PEI dispersed phase more effectively than to the

unmodified PEI dispersed phase through the chemical bonds formed. At a concentration of 5 wt% PEI, hydrolyzed PEI/epoxy resin had 40% more fracture toughness than the unhydrolyzed PEI/epoxy resin.

Giannotti et al. (2005) modified DGEBA/DDS and DGEBA/MCDEA systems simultaneously by two immiscible thermoplastic polymers, polysulfone (PSF) and poly(ether imide) (PEI). They found that when samples contain 10 and 15 wt% PEI, then a small part of PEI (about 25%) was replaced by PSF, and drastic changes in morphology, leading to co-continuity between the phases, occurred together with fracture (critical stress intensity factor, K_{IC}) improvements (up to 40%) compared to the systems modified only with PEI. In this way, without adding high quantities of thermoplastics, by varying PSF/PEI ratio, appropriate morphology changes can be induced, epoxy resin with better fracture properties can be obtained, keeping formulations viscosity constant.

Zhang and Xie (2011) prepared PEI/silica nanocomposites by sol-gel process to modify a DGEBA/DDS system. The results showed that using PEI/silica composites as the modifier of epoxy resin could lead to the improvement of the impact strength and storage modulus. The addition of the silica particles resulted in an interesting morphology transformation as the increase of silica particle content. It is important that the nanoparticles forced the phase separation and morphology evolution process to end in the earlier stage (shown as Fig. 4), illustrating that the introduction of nanoparticles into the system was a feasible method to achieve the morphology control purpose. In addition, in the range of their study, the higher the silica concentration in ER/PEI/silica composite, the greater the impact strength is. The impact strength increased from 8.7 KJ/m² for the unmodified epoxy to 20.4 KJ/m² of ER/PEI/silica (100/30/2.25). The combined toughening from both thermoplastic and particles here resulted in a telling reinforcement to this system.

Polysulfone (PSF)

Hedrick et al. (1985) used a functionally terminated PSF in toughening the DGEBA/DDS network. Considerable improvements in the fracture toughness of the network were obtained with the addition of 15 wt% PSF. A two-phase morphology could be seen with a relatively homogeneous distribution of PSF particles in the epoxy matrix.

Fu and Sun (1989) investigated the mechanical properties of DGEBA/PSF blends with piperidine curing agent. They found that the addition of 15 wt% PSF led to 110% increase in K_{IC} without sacrificing the epoxy stiffness and strength. In this case, the phase inversion occurred. And the particle bridging combined with shear banding was the main toughening mechanism. Huang et al. (1997) reported a similar result. They investigated the influence of PSF content on the mechanical properties of PSF-modified DGEBA/DDM networks. With the addition of 15 wt% PSF, K_{IC} increased 20% than neat epoxy resin. In addition, both tensile modulus and strength of the blends slightly improved compared to those of neat epoxy.

A classical DGEBA was modified by an amorphous PSF and cured by DDM. I. Martinez et al. (2000) studied the influence of a precure temperature for a prefixed

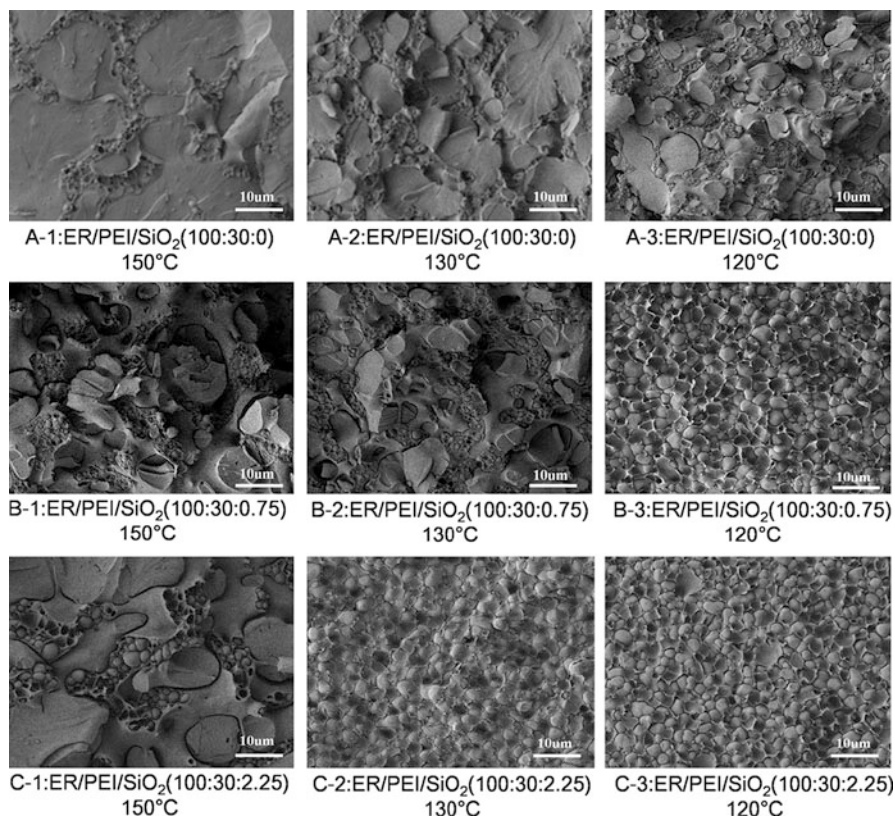


Fig. 4 SEM images of the fracture surface of (a) ER/PEI/SiO₂(100:30:0), (b) ER/PEI/SiO₂(100:30:0.75), and (c) ER/PEI/SiO₂(100:30:2.25) composites cured at 150 °C, 130 °C, and 120 °C, respectively (Reprinted with permission from Zhang and Xie (2011). Copyright (2011), Elsevier)

amount of modifier in the generated morphologies. Figure 5 has shown the SEM micrographs of mixtures containing 15 wt% PSF pre-cured at different temperatures. As shown in Fig. 5a, no phase separation insights were detected for the sample pre-cured at 60 °C possibly because vitrification of the polymerizing resin mixed with the thermoplastic occurred before chemical gelation at this pre-curing temperature, therefore increasing the solution viscosity and thereafter the high polymerization rate in the post-curing stage arrested demixing. As shown in Fig. 5b–d, PSF formed small spherical particles to disperse into the epoxy matrix indicating that phase separation possibly occurred via a binodal mechanism. The fracture toughness of 15 wt% PSF-modified epoxy resin pre-cured at different temperatures was investigated. The lower G_{IC} for the mixture was pre-cured at 60 °C, in which no phase separation occurred. Then they also investigated the influence of PSF content in the final properties of a DGEBA/DDM stoichiometric epoxy matrix modified with PSF. Fracture toughness measurement showed that thermoplastic addition only led to a

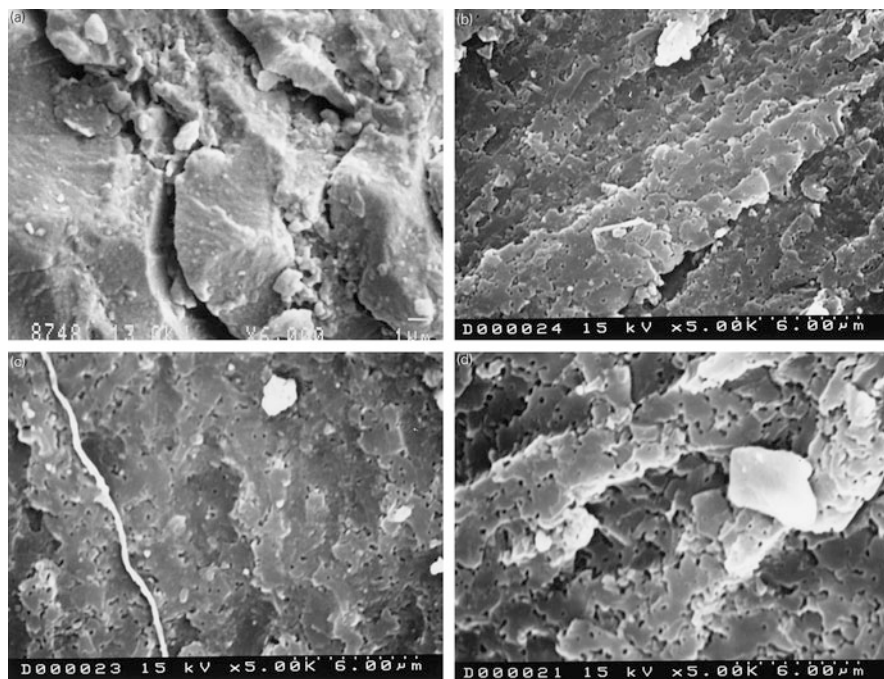


Fig. 5 SEM micrographs for mixtures containing 15 wt% PSF precured at several temperatures: (a) 60, (b) 100, (c) 120, and (d) 160 °C (Reprinted with permission from Martinez et al. (2000). Copyright (2000), Elsevier)

small improvement in fracture properties as K_{IC} and G_{IC} at low PSF contents, but the increase in G_{IC} was around fivefold for percentages higher than 15 wt% PSU (from 0.18 KJ/m² for the neat epoxy resin to 1.0 KJ/m²) because of the near bicontinuous morphology shown by these mixtures. These results indicated that phase separation was a boundary condition for toughness improvement in modifier-containing thermosetting mixtures.

Varley et al. (2001) used PSF to modified TGAP/DDS system. They prepared two kinds of PSF-modified epoxy via two different methods, which will be referred to as “prereacted” and “non-prereacted.” The non-prereacted samples were prepared by mixing the PSF with the TGAP together on a rotary evaporator under vacuum at 130 °C, until the PSF was completely dissolved and free of bubbles. The “prereacted” samples were prepared by placing a methanolic solution of tetramethylammonium hydroxide (TMAH) in a round-bottomed flask with the PSF and TGAP, which were both dissolved in a minimum quantity of dichloromethane. The solution was then mixed on the rotary evaporator under vacuum and heated to 130 °C for 30 min to allow reaction between the TGAP and PSF to occur, as well as to completely remove the dichloromethane. Then the temperature was increased to 165 °C for a further 20 min in order to decompose any remaining TMAH. They investigated the cure reaction of both samples by near infrared spectroscopy. They

found that during curing of the non-prereacted samples, all of the reaction occurred via epoxide/amine addition reactions, while during post-cure at 205 °C for 2 h, most of the reaction took place via etherification. For the prereacted samples, the amount of etherification that occurred increased with increasing PSF content during curing reaction. The toughness of the system was also investigated. They found that the toughness of PSF-modified epoxy was dependent upon morphology, with relatively small increases in toughness observed when the morphology remained dispersed particulate or co-continuous in nature. A much larger increase in toughness was found when the morphology became phase inverted for the 20 wt% PSF sample, and the K_{IC} value increased from 0.8 MPa · m^{0.5} for the unmodified epoxy to 1.4 MPa · m^{0.5}. However, the prereacted samples failed to improve the toughness of the systems, indicating that etherification was not beneficial to improving mechanical properties. The modulus was found to be relatively unaffected regardless of whether the samples were prereacted or non-prereacted.

The rheological behavior of the PSF-modified epoxy during the reaction-induced phase separation was investigated by Zhang et al. (2014). This research is helpful to control the phase morphology in the processing.

Poly(phthalazinone ether)s

Poly(phthalazinone ether)s, a kind of novel high-performance thermoplastic, are developed successfully in recent years. Their wholly aromatic twisted noncoplanar structure endows them with excellent comprehensive properties, such as outstanding thermal properties, excellent mechanical properties, good solubility, etc. Their T_g values in the range of 220–305 °C with different molecular structure. Poly(phthalazinone ether)s are expected to become a new kind of epoxy modifier.

Xu et al. (2008) prepared a series of blends by adding a novel thermoplastic poly(phthalazinone ether sulfone ketone) (PPESK) in varying proportions to DGEBA cured with DDS. They found that all the blends exhibited heterogeneity and their morphologies were dependent on the content of PPESK. Addition of the PPESK resulted in great enhancement of glass transition temperatures (T_g) both in the epoxy-rich phase and in the PPESK-rich phase by reason of the special structure of PPESK. There was moderate increase in the fracture toughness as estimated by impact strength. Fracture mechanisms, such as crack deflection and branches, ductile microcracks, ductile tearing of the thermoplastic, and local plastic deformation of the matrix, were responsible for the increase in the fracture toughness of the blends. Another study by the same authors (Xu et al. 2011) employed the copoly(phthalazinone ether sulfone) (PPBES) to toughen a DGEBA/DDS system. The results showed that the microstructure changed from sea-island to phase-inverted structure with the various concentrations of PPBES. PPBES could enhance the glass transition temperature (T_g) of the DGEBA epoxy resin and retain its thermal stability. The fracture toughness, expressed as notched impact strength, increased with the addition of PPBES and made the maximum value with 15-phr PPBES. It is worth noting that a complete phase-inverted structure was observed in this proportion

(15-phr PPBES). In common, this phase structure occurred with higher thermoplastic levels (>20%).

In addition, Liu et al. (2015, 2016) used two other novel poly(phthalazinone ether)s, poly(phthalazinone ether nitrile ketone) (PPENK) and copoly(phthalazinone ether nitrile) (PPBEN), to toughen a TGDDM/DDS system, respectively. In the PPENK-modified epoxy system, they found that a large number of physical cross-links formed by intermolecular and intramolecular hydrogen bonding indeed existed in the PPENK/epoxy blends by differential scanning calorimetry (DSC), FT-IR, and dynamic mechanical analysis (DMA). The formation of these hydrogen bonds enhanced the miscibility of the blends, so that any phase separation had not been detected by DMA and SEM. These physical interactions could maintain the T_g and stiffness of the blends. Compared with the neat epoxy resin, the critical stress intensity factor values reached the maximum at 10-phr PPENK, as well as the impact strength, although there was no phase separation. Mainly because of a semi-IPN with molecular-level entanglement of segments was formed. In the PPBEN-modified epoxy system, the results showed that the curing mechanism of the blend system was not affected. The blends with 15% PPBEN content showed the best toughening property, possibly due to its special sea-island structure, in which some small epoxy particles were embedded in the thermoplastic-rich phase. Increasing proportion (104%) of impact strength for the blends was obtained.

Other Thermoplastics

Some other thermoplastics such as aromatic polyesters (Iijima et al. 1995), polycarbonate (PC) (Rong and Zeng 1996), poly(phenylene oxide) (PPO) (Larrañaga et al. 2007), and polystyrene (PS) (Johnsen et al. 2005) have also been used for toughening epoxy. Herein we didn't describe them in detail.

Reaction-Induced Phase Separation

Because of the application need, toughness was the first focusing point for the epoxy resins. However, it is well known that the toughness of the epoxy blend is to a large extent determined by the final phase morphology. So it is necessary to understand the mechanism of reaction-induced phase separation.

In common, the thermoplastic/epoxy blend is homogeneous before curing. During curing, the molar mass of epoxy resin increases leading to the immiscible thermoplastic with epoxy cross-linked net. Then a liquid-liquid phase separation occurs up to the gel point (Bonnet et al. 1999). This kind of phase separation is known as reaction-induced phase separation (Inoue 1995). Different from classic thermal-induced phase decomposition, reaction-induced phase separation in epoxy/thermoplastic blends is usually caused by the molecular weight increase of epoxy during curing. Due to molecular weight increase of epoxy resin, epoxy and

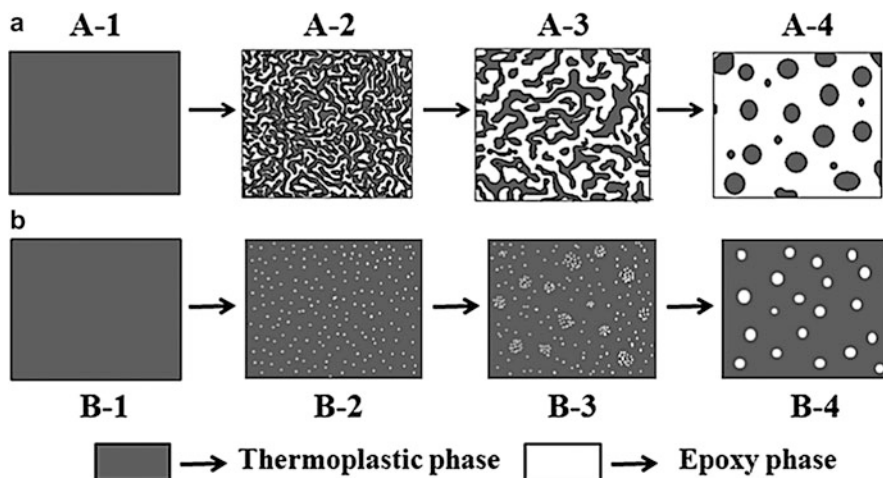


Fig. 6 The simulated process of (a) spinodal decomposition (SD) and (b) the nucleus growth (NG) mechanism in an epoxy/thermoplastic polymer binary system (Reprinted with permission from Yu and Wu (2014). Copyright (2014), Royal Society of Chemistry)

thermoplastic become immiscible, which makes them thermodynamically incompatible and causes phase separation.

The reaction-induced phase separation can occur via two mechanisms: spinodal decomposition (SD) or nucleus growth (NG). Figure 5 shows the simulated process of SD and NG mechanism. Cahn (1965) introduced the spinodal decomposition mechanism in detail. Spinodal decomposition occurs at a range of metastability, so it is more prevalent and preferred. A particular striking feature of this mechanism is the connectivity of the two phases which is expected when the volume fraction of the minor phase exceeds about 15%. As shown in Fig. 6, initially, the blend is homogeneous, and there is a single phase (A-1). Then with the process of curing reaction, the thermoplastic begins to separate out. A tangly co-continuous structure is presented (A-2). Subsequently, the epoxy regions grow and connect with each other (coarsening), leading to the destruction of the continuous thermoplastic phase (A-3). The epoxy resin becomes a continuous phase with the thermoplastic particles, irregular or regular in shape, forming the island structure (A-4). Nucleation and growth are expected to occur in the unstable region (Girard-Reydet et al. 1998). In the NG mechanism, the mixture is also homogeneous at first (B-1). As the molar mass of epoxy resin increases, thermoplastic will separate out in the shape of small round particles with the epoxy phase as the continuous phase (B-2), and then the small thermoplastic particles aggregate into bigger ones (B-3). Finally, the binary system also exhibits an island structure, in which the round thermoplastic particles are regularly distributed in the epoxy continuous phase (B-4) (Yu and Wu 2014). In common, the NG mode is not expected to take place in any case, mainly because of the fact that nucleation is recognized to be a very slow process.

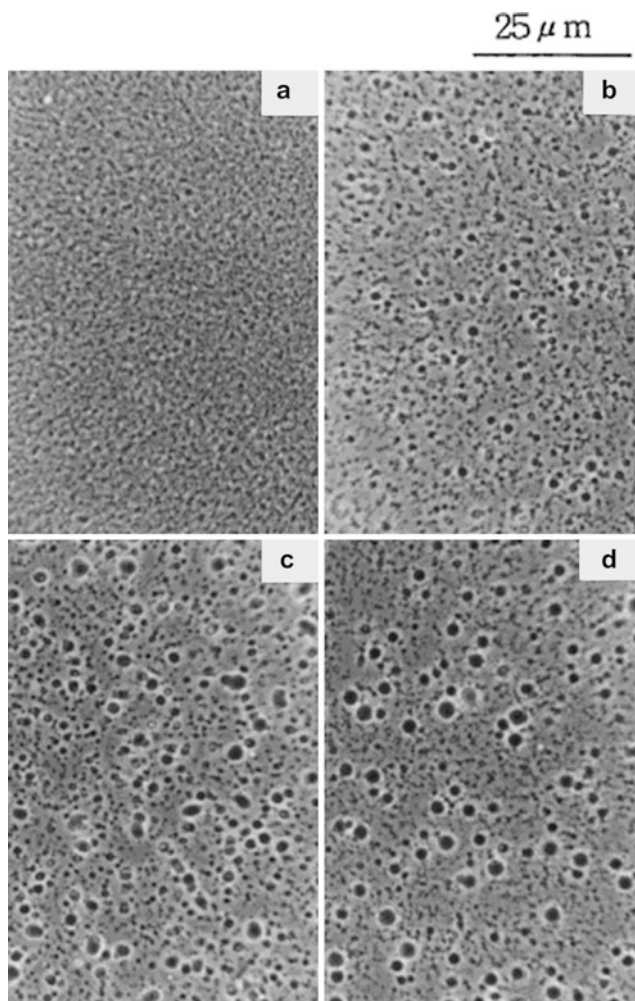


Fig. 7 Morphological development of EP/PSF (95/5 wt%) during cure at 220 °C. Scale bar: 25 μm ; (a) 13 min, (b) 15 min, (c) 17 min, (d) 20 min (Reprinted with permission from T. S. Yoon et al. (1997). Copyright (1997), Wiley)

The beginning of the phase separation process can be observed by light scattering (LS) or small-angle X-ray scattering (SAXS). And the final phase morphology can be investigated by scanning electron microscopy (SEM), transmission electron microscope (TEM), and atomic force microscope (AFM). Thus, many studies of phase morphology about thermoplastic/epoxy blends have been reported.

Yoon et al. (1997) investigated reaction-induced phase separation of a TGDDM/PSF system. The TGDDM/PSF blend without the curing agent exhibited a lower critical solution temperature (LCST)-type phase behavior (LCST = 241 °C). At the early stage of curing, the blend was homogeneous at the cure temperature. As the cure

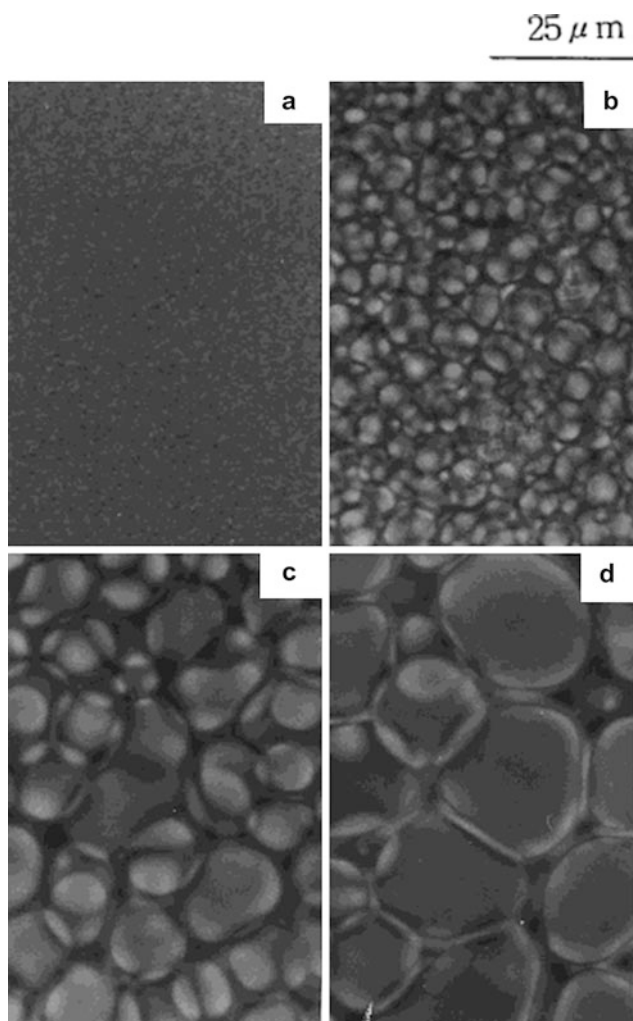


Fig. 8 Morphological development of EP/PSF (80/20 wt%) during cure at 220 °C. Scale bar: 25 μm; (a) 15 min, (b) 20 min, (c) 23 min, (d) 25 min (Reprinted with permission from T. S. Yoon et al. (1997). Copyright (1997), Wiley)

reaction proceeded, the blend was thrust into a two-phase regime by the LCST depression caused by the increase in a molecular weight of the epoxy-rich phase, and the phase separation took place via a spinodal decomposition (SD) or nucleation and growth (NG) mode, depending on the blend composition and the cure temperature. When cured isothermally at 220 °C, the blend exhibited a sea-island morphology formed via the NG mode below 5 wt% PSF content (shown as Fig. 7), and as can be seen in Fig. 7, the phase separation started at 13 min via the nucleation and growth (NG) mode. The spherical domains of PSF dispersed in

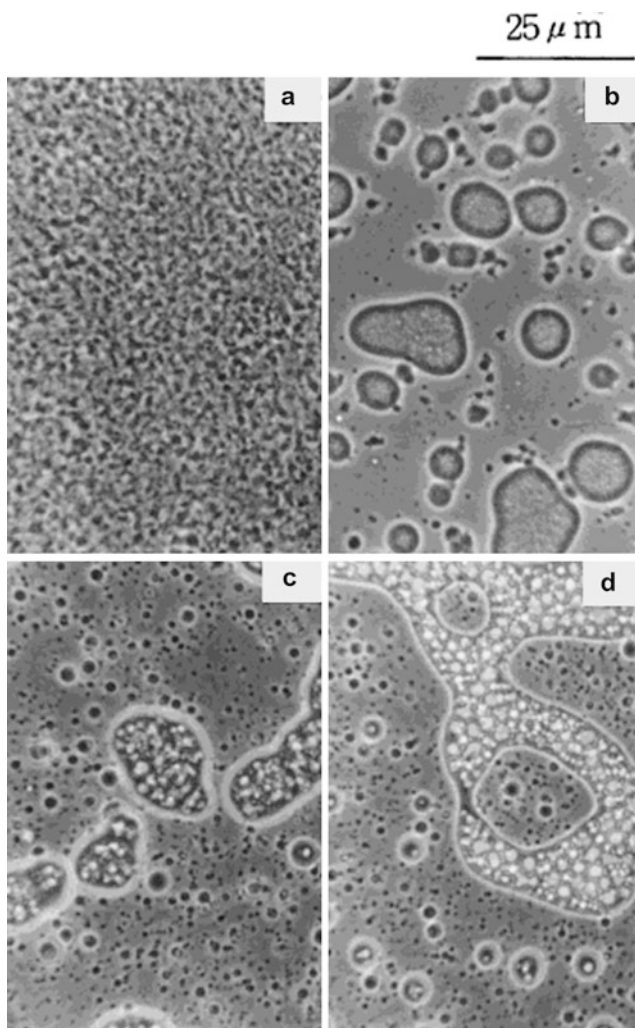
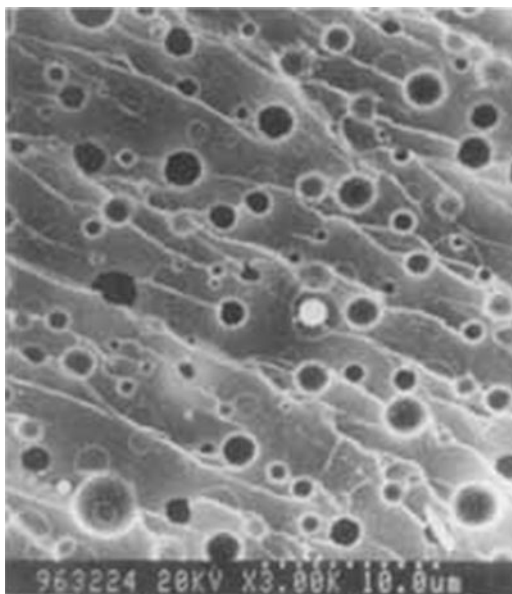


Fig. 9 Morphological development of EP/PSF (90/10 wt%) during cure at 220 °C. Scale bar: 25 μm ; (a) 13 min, (b) 15 min, (c) 17 min, (d) 20 min (Reprinted with permission from T. S. Yoon et al. (1997). Copyright (1997), Wiley)

the epoxy matrix were shown. With curing, the dispersed PSF domains grew in size without changing their loci. Finally, the structure was fixed by gelation or vitrification of the epoxy-rich phase at the late stage of curing. As shown in Fig. 8, phase separation started via the SD mode when the PSF content was above 20 wt%. Epoxy-rich globules with a uniform diameter of a few micrometers were dispersed in a PSF matrix. At the intermediate composition range (10, 15 wt% of PSF content), combining morphology with both sea-island and co-continuous structure was observed (shown as Fig. 9). On the other hand, by lowering the cure

Fig. 10 SEM of PEI (0.39)-modified epoxy resin with 20 wt% PEI (Reproduced with permission from Y. F. Yu et al. (1998). Copyright (1998), Taylor & Francis)



temperature and/or increasing the content of PSF component, a two-phase structure with a shorter periodic distance was obtained.

Kim et al. (1995) reported the structure development via reaction-induced phase separation in epoxy/PES blends. They stated that the NG mode was not expected to take place in any case, mainly because of the fact that nucleation was recognized to be a very slow process and the sea-island morphology as well as co-continuous morphology was developed by only the SD mode during cure. They explained that the structure development via the SD or NG mode during cure was governed by two competitive progresses of the phase separation and the chemical reaction.

Yu et al. (1998) investigated the effects of molecular weight on the phase separation of PEI-modified TGDDM/DDS systems. They used four kinds of PEI with different inherent viscosity (0.39, 0.58, 0.61, 0.67 g/dL, respectively). They found that different molecular weight PEI-modified systems may not have the same phase separation process. As shown in Fig. 10, the fracture surface of the PEI (0.39)-modified system showed a continuous epoxy matrix with regularly dispersed PEI domains. While the morphology of the PEI (0.58, 0.61, 0.67)-modified systems were similar, all showed the “sandwich” morphology, in which there were regions of phase inversion and continuous epoxy structure (shown in Fig. 11). Then they observed the phase separation process during curing reaction by time-resolved light scattering (TRLS). The system with PEI (0.39) had the longest induced period (20 min), while the other three systems were shorter than 10 min. Because the higher molecular weight PEI had a larger interaction parameter χ with epoxy resin, which caused the phase separation of systems with higher molecular

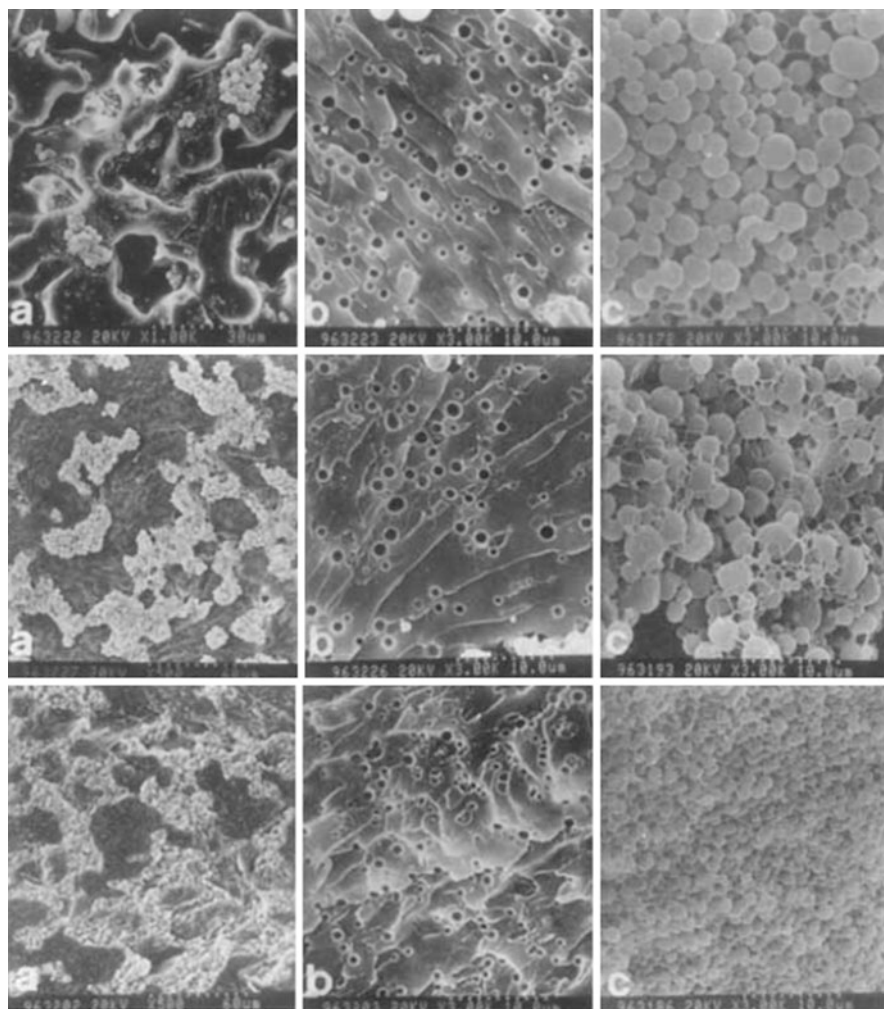


Fig. 11 SEM of PEI (0.58, 0.61, 0.67)-modified epoxy resin with 20 wt% PEI; (a) “sandwich” morphology; (b) continuous epoxy region, etched in CH_2Cl_2 ; (c) continuous PEI region, etched in CH_2Cl_2 (up: 0.58; mid: 0.61; low: 0.67) (Reproduced with permission from Y. F. Yu et al. (1998). Copyright (1998), Taylor & Francis)

weight PEI to occur at an earlier stage. At the later stage of curing the viscosity of epoxy-rich phase also increased which hinders further phase separation. So the morphology was determined chiefly at the early stage. For the epoxy-rich spheres in the PEI-rich matrix (shown in Fig. 11c), the higher the molecular weight of PEI, the smaller the epoxy spheres. This was because higher molecular weight PEI-rich phase tended to be more viscous which suppressed the phase separation at an earlier stage.

Influence Factors of Phase Morphology and Toughening Effect

It has been showed that many factors correlated with thermoplastic, such as their concentration, molecular weight, and end groups of thermoplastic, play the key role to influence properties of the cured thermoplastic/epoxy blends. Many studies showed that a co-continuous morphology with higher thermoplastic levels (>20%) is required to achieve optimum mechanical properties. The influence factors are introduced in detail as follows.

Content of Thermoplastics

The concentration of component has a primary effect on morphology for multicomponent mixture. So the content of thermoplastic has a direct effect on the toughness of the blend. Gilbert and Bucknall (1991) found that, in TGDDM/PEI cured by DDS, the toughening effect was clearly dependent on the concentration of PES. A significant improvement of 218% in fracture toughness was found for the blends with 30 wt% PEI. In this case, the phase inversion occurred, epoxy-rich domain particles dispersing in ductile PEI forming the matrix. The major toughening mechanism was particle bridging. Murakami et al. (1992) investigated the fracture behavior of a DICY-epoxy system varying the content of PEI. When the PEI content was less than 10 wt%, no clear fracture toughness was observed. However, in the PEI content of 20 wt% or greater modified systems, the fracture toughness increases markedly. When the PEI content was higher than 20 wt%, the phase inversion also occurred.

Hourston and Lane (1992) used PEI to modified TGAP/DDS system. They prepared a series of blends in varying PEI proportions (0 ~ 40 wt%). All the samples showed two-phase morphology, and their morphology altered considerably with thermoplastic content. Phase inversion occurred when the PEI content was about 15 wt% or greater. The addition of 10 wt% PEI has led to no improvement in fracture properties, increasing the PEI content to 15 wt% which resulted in a significant increase in toughness, and the G_{IC} value increased from 0.23 KJ/m² for unmodified epoxy to 1.13 KJ/m² for 15 wt% PEI-modified epoxy.

MacKinnon et al. (1992) used PES to modified TGAP/DDS system and investigated the effect of variation of the PES content on the properties of blends. An increase in the PES content in the blends has led to an increase in fracture toughness. The fracture toughness (K_{IC} and G_{IC}) showed little variation with lower PES content ($x < 15$ wt%). However, when PES became the continuous phase (>20 wt%), marked improvements in the fracture toughness were observed. When content of PES reached 35 wt%, the K_{IC} value was from around 0.6 MN · m^{-3/2} for the unmodified epoxy to around 2.0 MN · m^{-3/2}. This illustrates that the phase structure has a pronounced effect on the mechanical properties of epoxy/thermoplastic blends.

Brooker et al. (2010) also used PEI to toughen a mixed epoxy resin (a mix of a diglycidyl ether of bisphenol F (DGEF) and TGAP), which hardened by a 4,4'-methylenebis-(3-chloro 2,6-diethylaniline) (MCDEA, an amine hardener), by using a poly(ether sulfone) copolymer. They investigated the effect on the

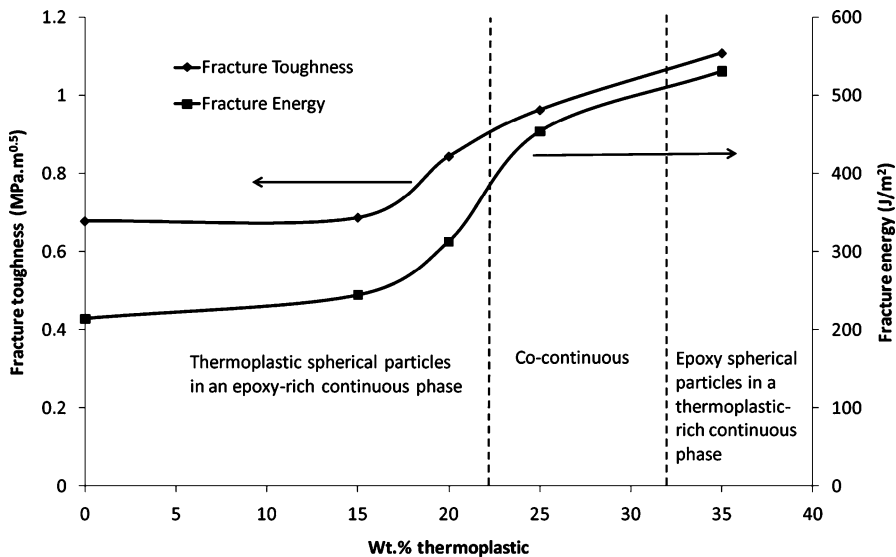


Fig. 12 Fracture toughness and fracture energy as a function of the weight percentage of added thermoplastic toughener (Reprinted with permission from R. D. Brooker et al. (2010). Copyright (2010), Taylor & Francis)

morphology, fracture performances, and tensile properties of an epoxy polymer when modified with various percentages of a thermoplastic-polymeric toughener. They found that the different contents of the thermoplastic toughener gave rise to a range of morphologies from spherical particulate, through co-continuous, to phase inverted. And both the fracture toughness and the fracture energy increased with an increasing percentage of the thermoplastic toughener. The increase in toughness was a steady progressive rise as a function of the added content of the thermoplastic toughener (shown as Fig. 12), i.e., There was no sudden increase in the fracture properties which coincided with a change in morphology. When the concentration of thermoplastic was increased to 35 wt%, the morphology was found to become a phase-inverted type, which the epoxy polymer forming well-dispersed phase-separated particles within a thermoplastic-rich continuous-phase). And the fracture toughness increased from $0.68 \text{ MPa} \cdot \text{m}^{0.5}$ for the unmodified epoxy to $1.11 \text{ MPa} \cdot \text{m}^{0.5}$, and the fracture energy rose from 215 to 530 J/m^2 .

End Groups of Thermoplastics

In order to achieve good interfacial binding, Hedrick et al. (1985) first used a functionally terminated PSF to toughen the epoxy resin. They believed that the functional end groups were advantageous for improving toughness. Then, Yoon et al. (1995) employed an amino phenyl-terminated PES (reactive) and a t-butyl-

terminated PES (nonreactive) to toughen a DGEBA/DDS system, respectively. They reported that very significantly improved fracture toughness was obtained with reactive PES toughening without loss of chemical resistance and the fracture toughness increased from $0.6 \text{ MPa} \cdot \text{m}^{0.5}$ for the unmodified epoxy to $2.2 \text{ MPa} \cdot \text{m}^{0.5}$ at 30 wt% of reactive PES, while nonreactive PES was able to improve the fracture toughness only if a double phase-separated co-continuous morphology was developed. Otherwise, a very low fracture toughness was achieved because of poor adhesion between the physically blended phases. The maximum K_{IC} fracture toughness of nonreactive PES-modified epoxy was around $1.8 \text{ MPa} \cdot \text{m}^{0.5}$ at 25 wt% of nonreactive PES. From the SEM micrographs, they considered that the major toughening mechanism in the reactive PES-toughened epoxy resins was ductile fracture of PES phase, which was enhanced by good adhesion possibly via chemical bonding.

Some studies had come to the opposite conclusion. Iijima et al. (1992) synthesized an epoxy-terminated PES (reactive), compared with a chloro-terminated PES (nonreactive), to toughen a DGEBA/DDS system. They found that chloro-terminated PES was an effective modifier than epoxy-terminated PES. Chen et al. (1995) synthesized a nitrated PEI to study the effect of interfacial strength for a TGAP/DDS system. They compared the toughness of nitrated and un-nitrated PEI at varying thermoplastic concentrations. The nitrated PEI was more compatible with the epoxy resin leading to no multiphase structure in this system, and consequently the toughening effect was reduced. It seems like introducing the reactive end groups on the thermoplastic indeed serves to increase the miscibility between the thermoplastic and epoxy resin. However, the reported findings about the effect of reactive end groups on fracture properties of epoxy resin system are contradictory. Maybe it is mainly depended on the different epoxy/thermoplastic system.

Molecular Weight of Thermoplastics

Molecular weight of the thermoplastics is an important factor to influence the toughening effect. Many researchers showed that increasing the molecular weight of the thermoplastic results in an increase in the toughness of the epoxy blend. Grishchuk et al. (2012) modified a tetrafunctional epoxy resin with PES of different molecular weight curing with anhydride hardener. With an addition of 10 wt% PES, the final morphology of EP/PES depended on the molecular weight of PES. As shown in Fig. 13, low ($M_n = 8800$) and medium ($M_n = 12,500$) molecular weight PES formed submicron scale spherical droplets, whereas high molecular weight PES ($M_n = 16,800$) was present in micron scale inclusions of complex (sea-island) structure. With the increasing molecular weight of PES, the fracture mechanical properties, especially the fracture energy, were increased. The G_{IC} value increased from 151 J/m^2 for neat epoxy resin to 369 J/m^2 for the 10 wt% high molecular weight PES-modified epoxy.

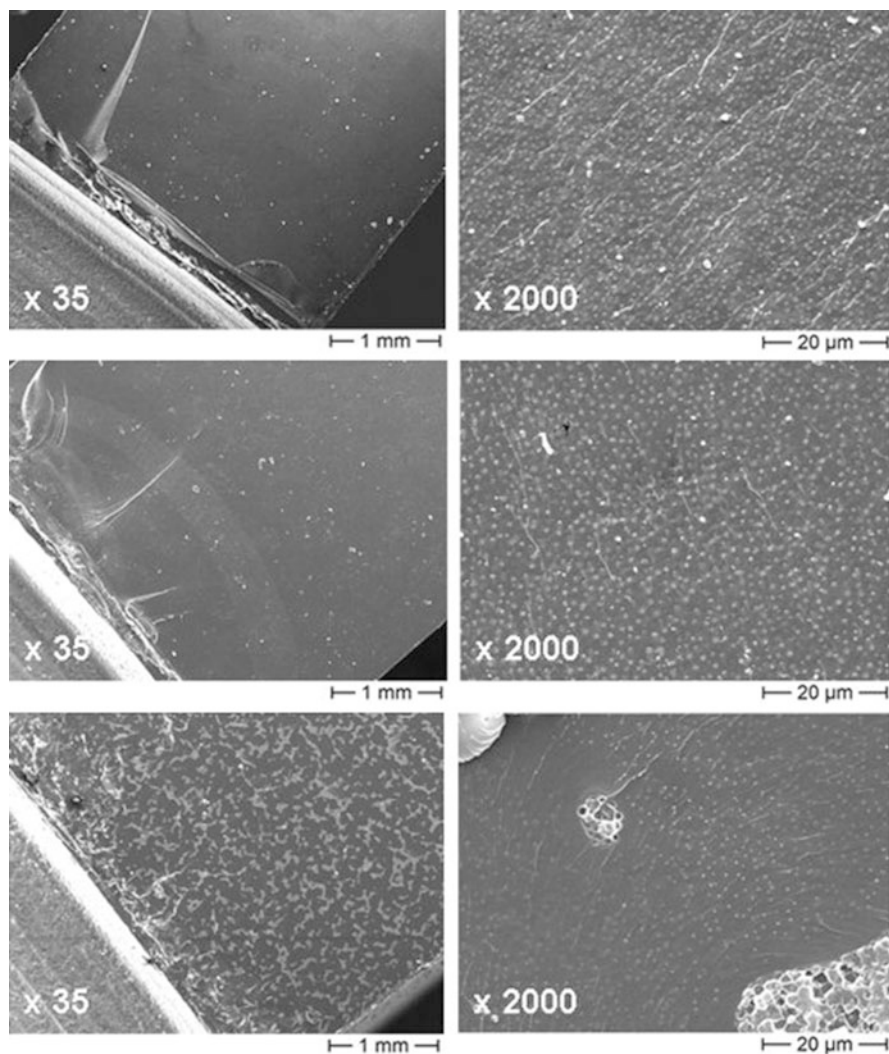
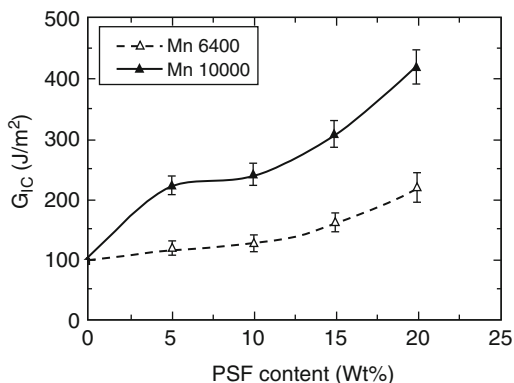


Fig. 13 SEM pictures at different magnifications taken from the fracture surface of blends with 10 wt% different molecular weight PES (up, low molecular weight; mid, medium molecular weight; low, high molecular weight) (Reproduced with permission from S. Grishchuk et al. (2012). Copyright (2012), Wiley)

Min et al. (1993) investigated the microstructure and fracture properties of DGEBA/DDS system as a function of the molecular weight of phenolic hydroxyl-terminated PSF, the designed toughening agent. In their experimental regions (0 ~ 20 wt% PSF concentration), the transition of the microstructure from pure epoxy to particulate and then from particulate to phase-inverted structures was observed, respectively, regardless of whether the PSF was low molecular weight or high molecular weight. The fracture toughness of a low molecular weight

Fig. 14 Plot of mode I critical strain energy release rate against PSF content for DGEBA/DDS systems modified with Mn = 6400 and 10,000 PSF (Reproduced with permission from B. G. Min et al. (1993). Copyright (1993), Wiley)



(Mn = 6400) functional PSF-modified system did not vary noticeably with the variation in phenolic hydroxyl-terminated PSF concentration. Even at 20 wt%, the maximum fracture toughness of the low molecular weight phenolic hydroxyl-terminated PSF-modified system is lower than the fracture toughness of the 5 wt% high molecular weight (Mn = 10,000) PSF-modified system (shown as Fig. 14). Meanwhile, the fracture toughness of the high molecular weight PSF-modified system increased rapidly with increasing concentration. These concurrent transitions in the microstructure and fracture toughness with increasing concentration of PSF suggested that the microstructure strongly influences the fracture toughness and, presumably, the phase-inverted structure is the optimum structure for achieving high fracture toughness.

Hedrick et al. (1985) and Fu and Sun (1989) also obtained a similar conclusion by using PSF and PES. The practical difficulty of high molecular weight thermoplastic is the dramatically increased viscosity of the blend, which limits the molecular weights of thermoplastic additives used in advanced composites. Thus the molecular weight of thermoplastic should be determined by processing of composite. These toughening systems usually cannot be selected in resin transfer molding where good resin flow is essential.

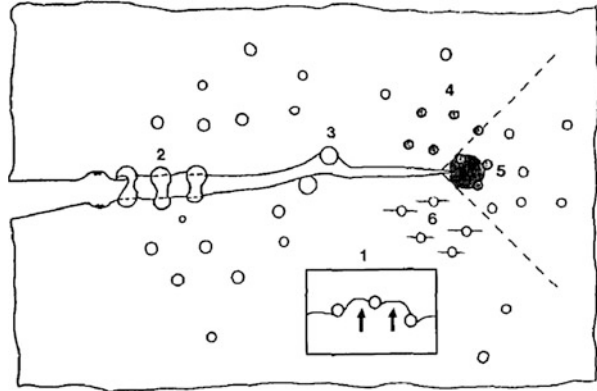
Toughening Mechanisms of Thermoplastic/Epoxy Blends

The fracture and toughening mechanisms of epoxy/thermoplastic blends are not perfectly clear yet, even though this system has been significantly developed in the past years. Herein we just listed the typical toughening mechanisms.

Several mechanisms of the toughening of epoxy systems by rigid thermoplastic particles have been proposed by Pearson and Yee (1993), namely, particle bridging, crack pinning, crack path deflection, particle-yielding-induced shear banding, particle yielding, and microcracking, as depicted in Fig. 15.

The particle-bridging mechanism was developed from rubber-modified polymers. It could conceivably be a more dominant mechanism when rigid thermoplastic particles are used, since they are much more rigid and much stronger than elastomeric particles.

Fig. 15 Schematic diagram of toughening mechanisms proposed for thermoplastic-modified epoxies: (1) crack pinning, (2) particle bridging, (3) crack path deflection, (4) particle yielding, (5) particle-yielding-induced shear banding, and (6) microcracking (Reprinted from Pearson and Yee (1993). Copyright (1993), Elsevier)



In the particle-bridging mechanism, the proposed role of the rigid plastic particles is to distance two crack surfaces and apply surface tractions that efficiently alleviate the stress applied at the crack tip. An alternative explanation for this toughening via crack bridging takes into account the energy consumed when the crack deforms and tears the rigid plastic particles. Cardwell and Yee (1998) investigated the toughening mechanism of two epoxy matrices containing varying concentrations of preformed polyamide-12 particles. They observed that these particles toughened the epoxies through a crack-bridging mechanism involving large plastic deformation of the second phase.

In the crack-pinning mechanism, the proposed role of the rigid thermoplastic particles is to behave as impenetrable objects that cause the crack to bow out, which consumes extra energy. Indeed, the difference in toughness between the brittle epoxy and the ductile thermoplastic phase is large enough to consider these particles as relatively impenetrable, while in the crack path deflection, the thermoplastic causes the crack to deviate from its original direction; hence, the surface area of the crack is increased resulting in increasing energy to propagate such crack.

In the particle-yielding-induced shear-banding mechanism, the rigid plastic particles would yield, which lowers their modulus to that of a rubber; such a modulus mismatch would produce a significant stress concentration, which initiates shear banding in the matrix.

Mimura et al. (2000) investigated the fracture mechanism of PES-modified epoxy resins using an optical microscope. The results of the phase-separated resins with bright light were shown in Fig. 16. In the unmodified resin, it was observed that the pre-crack was extended straightly and that the crack branching did not occur. However, in the 10 wt% PES-modified resin that formed a particulate morphology, the occurrence of crack branching was observed at the crack tip region. In the cured resin modified with 20 wt% PES, which had a co-continuous phase morphology, it was observed that the crack branching spread extensively and reached the region remote from the pre-crack. Accordingly, it may be concluded that the increase in fracture toughness of the particulate resins is due to the depression of the crack growth with the formation of branches. Moreover, the crack cannot avoid progressing through the

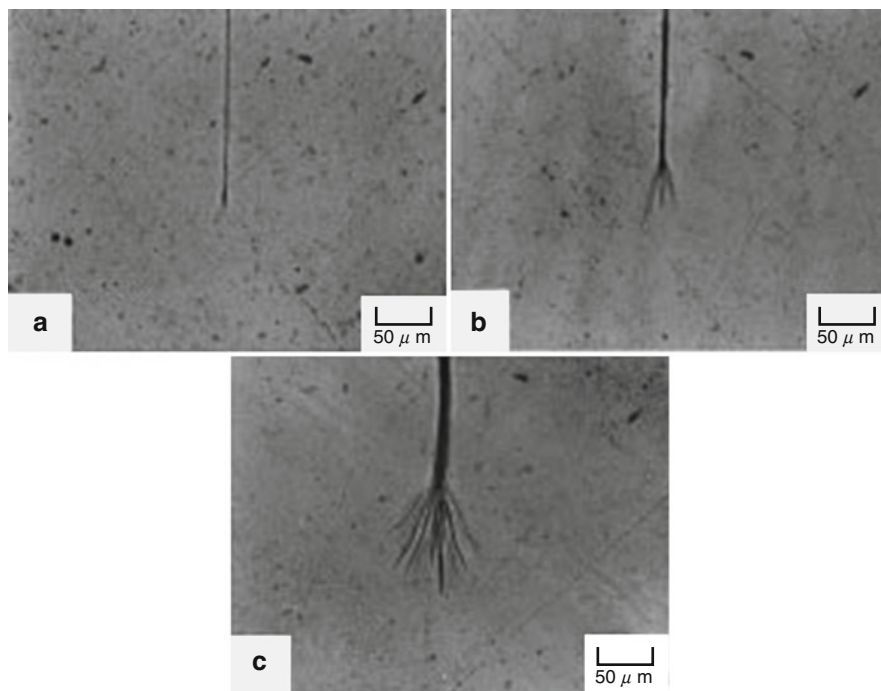


Fig. 16 Optical micrographs of sub-fracture surfaces in PES-modified epoxy resins taken under bright light; molding temperature – 180 °C: (a) unmodified resin, (b) PES content 10 wt%, (c) PES content 20 wt% (Reprinted with permission from Mimura et al. (2000). Copyright (2000), Elsevier)

tough PES phase once PES forms a continuous phase, which causes the drastic increase in the toughness of the resin with a co-continuous phase morphology.

As shown in Fig. 16, the homogeneous phase resins were observed under crossed polarized light. A bright region observed under crossed polarized light represents the region where a shear deformation of the matrix occurred. A very bright region around the crack tip was seen in the resin with 10 wt% PES. Consequently, it was confirmed that in this resin the shear deformation of the matrix occurred, resulting in the drastic improvement in toughness with lower PES content. However, the shear deformation region of the resin with 20 wt% PES was smaller than that of the resin with 10 wt% PES, which leads to the small increase in toughness. Thus, they observed in detail with TEM (shown as Fig. 17), in order to reveal the reason why the fracture toughness of the modified resins with the homogeneous morphology decreased at high PES content. In the observation of the resin containing 10 wt% PES (Fig. 18b), PES formed very fine domains with diameters ranging 50–80 nm in the epoxy matrix. For the resin containing 20 wt% PES (Fig. 18c), it was observed that the obvious PES microdomains disappeared and that more microscopic PES was dispersed on the whole epoxy matrix. This difference in the microstructure of the resins with the homogeneous morphology seems to represent as the gap in the

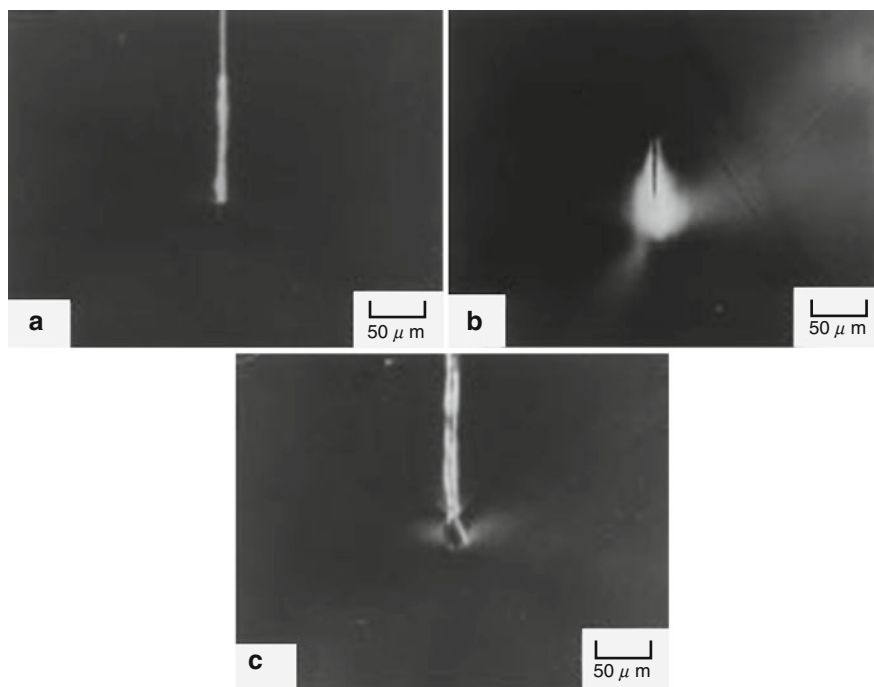


Fig. 17 Optical micrographs of sub-fracture surfaces in PES-modified epoxy resins taken under crossed polarized light; molding temperature – 140 °C: (a) unmodified resin, (b) PES content 10 wt%, (c) PES content 20 wt% (Reprinted with permission from Mimura et al. (2000). Copyright (2000), Elsevier)

toughness. For the resin containing 10 wt% PES, these PES microdomains seem to be adhered to the epoxy matrix because the PES chains are entangled in the epoxy networks by the formation of semi-IPN structure. It can be concluded that the drastic improvement in toughness attributes to the presence of strongly adhering PES microdomains in the epoxy matrix, which induced the shear deformation of the epoxy matrix. For the resin containing 20 wt% PES, however, these PES microdomains disappeared. Therefore, the decrease in the improvement effect of the fracture toughness seems to be responsible for the disappearance of the obvious PES microdomains, which was caused by further inhibition of the phase separation for the enormously high viscosity of the modified resin. In consequence, if the phase morphology was different, the fracture mechanism is also not the same.

Conclusions

It has been proved that thermoplastic-toughening epoxy resins can possess the desirable toughness enhancement and slight decrease or increase of mechanical strengths and thermal stability, extremely depending on the chemical structure of

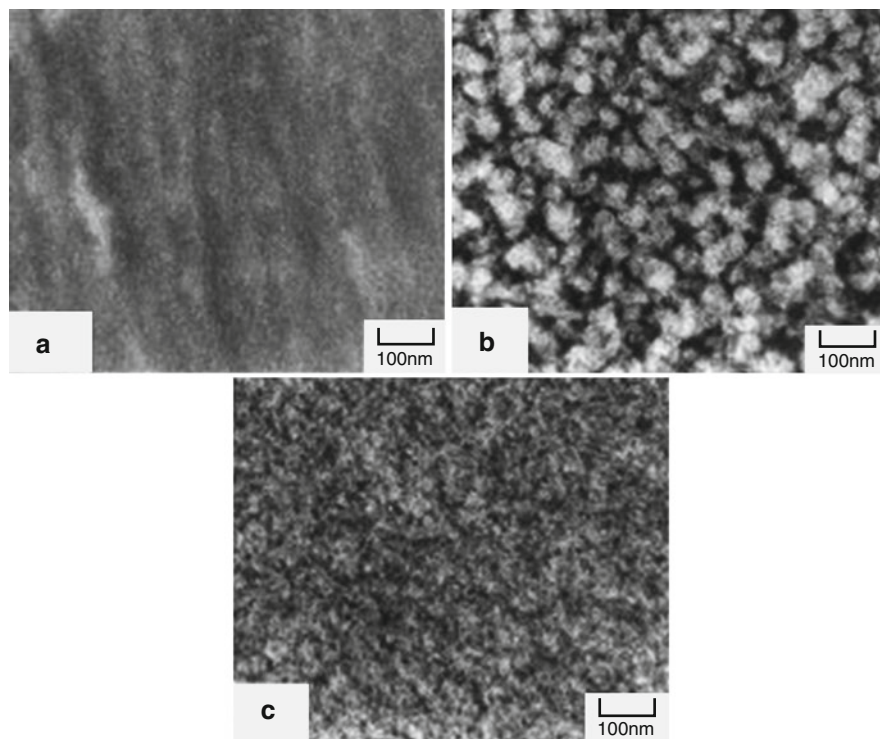


Fig. 18 Transmission electron micrographs of the modified resins with homogeneous morphology: (a) unmodified resin, (b) PES content 10 wt%, (c) PES content 20 wt% (Reprinted with permission from Mimura et al. (2000). Copyright (2000), Elsevier)

thermoplastic. To achieve good properties of epoxy/thermoplastic blends, high-performance engineering thermoplastic having high T_g s and excellent mechanical properties should be used, and they should be soluble in raw epoxy resin. The reaction-induced separation will occur during curing. The end groups of thermoplastic can help the compatibility of thermoplastic with epoxy, but their precise importance about toughness is unclear and appears to depend upon the thermoplastic used. The best toughness will be obtained through attainment of a co-continuous or phase-inverted morphology when more content of thermoplastic is in the blend. Increasing thermoplastic molecular weight is beneficial to increase the toughness of the blend, but the resulting increasing viscosity will be constraint in some composite process. The commercialized and novel high-performance toughening thermoplastic additives have been available. Epoxy toughened by thermoplastic has been used in application such as aerospace composites. However, the criteria for this system are still ambiguous. The predominant criteria for achieving optimum toughness enhancement in the toughening of resin are still under research.

References

- Blanco I, Cicala G, Lo Faro C, Recca A (2003) Development of a toughened DGEBS/DDS system toward improved thermal and mechanical properties by the addition of a tetrafunctional epoxy resin and a novel thermoplastic. *J Appl Polym Sci* 89:268–273
- Blanco I, Cicala G, Costa M, Recca A (2006) Development of an epoxy system characterized by low water absorption and high thermomechanical performances. *J Appl Polym Sci* 100:4880–4887
- Bonnet A, Pascault JP, Sautereau H, Taha M (1999) Epoxy-diamine thermoset/thermoplastic blends. 1. rates of reactions before and after phase separation. *Macromolecules* 32:8517–8523
- Brooker RD, Kinloch AJ, Taylor AC (2010) The morphology and fracture properties of thermoplastic-toughened epoxy polymers. *J Adhes* 86(7):726–741
- Bucknall CB, Gilbert AH (1989) Toughening tetrafunctional epoxy resins using polyetherimide. *Polymer* 30:213–217
- Bucknall CB, Partridge IK (1983) Phase separation in epoxy resins containing polyethersulfone. *Polymer* 24:639–644
- Cahn JW (1965) Phase separation by spinodal decomposition in isotropic systems. *J Chem Phys* 42(1):93–99
- Cardwell BJ, Yee AF (1998) Toughening of epoxies through thermoplastic crack bridging. *J Mater Sci* 33:5473–5484
- Chen MC, Hourston DJ, Schafer FU, Huckerby TN (1995) Miscibility and fracture behaviour of epoxy resin-nitrated polyetherimide blends. *Polymer* 36:3287–3293
- Fernández B, Arbelaiz A, Diaz E, Mondragon I (2004) Influence of polyethersulfone modification of a tetrafunctional epoxy matrix on the fracture behavior of composite laminates based on woven carbon fibers. *Polym Compos* 25(5):480–488
- Frigione ME, Mascia L, Acierno D (1995) Oligomeric and polymeric modifiers for toughening of epoxy resins. *Eur Polym J* 31(11):1021–1029
- Fu Z, Sun Y (1989) Epoxy resin toughened by thermoplastics. *Chin J Polym Sci* 7:367–378
- Giannotti MI, Bernal CR, Oyanguren PA, Galante MJ (2005) Morphology and fracture properties relationship of epoxy-diamine systems simultaneously modified with polysulfone and poly(ether imide). *Polym Eng Sci* 45:1312–1318
- Gilbert AH, Bucknall CB (1991) Epoxy-resin toughened with thermoplastic. *Macromol Symp* 45:289–298
- Girard-Reydet E, Sautereau H, Pascault JP, Keates P, Navard P, Thollet G, Vigier G (1998) Reaction-induced phase separation mechanisms in modified thermosets. *Polymer* 39(11):2269–2280
- Grishchuk S, Gryshchuk O, Weber M, Karger-Kocsis J (2012) Structure and toughness of polyethersulfone (PESU)-modified anhydride-cured tetrafunctional epoxy resin: effect of PESU molecular mass. *J Appl Polym Sci* 123:1193–1200
- Hedrick JL, Yilgor I, Wilkes GL, McGrath JE (1985) Chemical modification of matrix resin networks with engineering thermoplastics. *Polym Bull* 13:201–208
- Hodgkin JH, Simon GP, Varley RJ (1998) Thermoplastic toughening of epoxy resins: a critical review. *Polym Adv Technol* 9:3–10
- Hourston DJ, Lane JM (1992) The toughening of epoxy resins with thermoplastics: 1. Trifunctional epoxy resin-polyetherimide blends. *Polymer* 33(7):1379–1383
- Huang P, Zheng S, Huang J, Guo Q, Zhu W (1997) Miscibility and mechanical properties of epoxy resin/polysulfone blends. *Polymer* 38:5565–5574
- Iijima T, Hiraoka H, Tomoi M (1992) Preparation of epoxy-terminated Poly(aryl ether sulfone)s and their use as modifiers for epoxy resins. *J Appl Polym Sci* 45:709–721
- Iijima T, Arai N, Fukuda W, Tomoi M (1995) Toughening of aromatic diamine-cured epoxy resin by poly(ethylene phthalate)s and the related copolyesters. *Eur Polym J* 31(3):275–284
- Inoue T (1995) Reaction-induced phase decomposition in polymer blends. *Prog Polym Sci* 20:119–153

- Jang J, Shin S (1995) Toughness improvement of tetrafunctional epoxy resin by using hydrolysed poly(ether imide). *Polymer* 36(6):1199–1207
- Johnsen BB, Kinloch AJ, Taylor AC (2005) Toughness of syndiotactic polystyrene/epoxy polymer blends: microstructure and toughening mechanisms. *Polymer* 46:7352–7369
- Kim BS, Chiba T, Inoue T (1995) Morphology development via reaction-induced phase separation in epoxy/poly(ether sulfone) blends: morphology control using poly(ether sulfone) with functional end-groups. *Polymer* 36(1):43–47
- Larrañaga M, Mondragon I, Riccardi CC (2007) Miscibility and mechanical properties of an amine-cured epoxy resin blended with poly(ethylene oxide). *Polym Int* 56:426–433
- Liu R, Wang J, Li J, Jian X (2015) An investigation of epoxy/thermoplastic blends based on addition of a novel copoly(aryl ether nitrile) containing phthalazinone and biphenyl moieties. *Polym Int* 64(12):1786–1793
- Liu R, Wang J, He Q, Zong L, Jian X (2016) Interaction and properties of epoxy-amine system modified with poly(phthalazinone ether nitrile ketone). *J Appl Polym Sci* 133(10):2301–2309
- Mackinnon AJ, Jenkins SD, McGrail PT, Pethrick RA (1992) A dielectric, mechanical, rheological, and electron microscopy study of cure and properties of a thermoplastic-modified epoxy resin. *Macromolecules* 25:3492–3499
- Martinez I, Martin MD, Eceiza A, Oyanguren P, Mondragon I (2000) Phase separation in polysulfone-modified epoxy mixtures. Relationships between curing conditions, morphology and ultimate behavior. *Polymer* 41:1027–1035
- Mimura K, Ito H, Fujioka H (2000) Improvement of thermal and mechanical properties by control of morphologies in PES-modified epoxy resins. *Polymer* 41:4451–4459
- Min BG, Hodchin JH, Stachurski ZH (1993) Reaction mechanisms, microstructure, and fracture properties of thermoplastic polysulfone-modified epoxy resin. *J Appl Polym Sci* 50:1065–1073
- Murakami A, Saunders D, Ooishi K, Yoshiki T, Saitoo M, Watanabe O, Takezawa M (1992) Fracture behaviour of thermoplastic modified epoxy resins. *J Adhes* 39:221–242
- Pearson RA, Yee AF (1993) Toughening mechanisms in thermoplastic-modified epoxies: 1. Modification using poly(phenylene oxide). *Polymer* 34(17):3658–3670
- Raghava RS (1987) Role of matrix-particle interface adhesion on fracture toughness of dual phase epoxy-polyethersulfone blend. *J Polym Sci Part B: Polym Phys* 25:1017–1031
- Raghava RS (1988) Development and characterization of thermosetting thermoplastic polymer blends for applications in damage-tolerant composites. *J Polym Sci Part B: Polym Phys* 26:65–81
- Rong M, Zeng H (1996) Polycarbonate/epoxy semi-interpenetrating polymer network: 1. Preparation, interaction and curing behavior. *Polymer* 37:2525–2531
- Siddhamalli SK (2000) Phase-separation behavior in poly(ether imide)-modified epoxy blends. *Polym-Plast Technol* 39:699–710
- Su CC, Woo EM (1995) Cure kinetics and morphology of amine cured tetraglycidyl-4,4'-diaminodiphenylmethane epoxy blends with poly(ether imide). *Polymer* 36:2883–2894
- Varley RJ, Hodgkina JH, Simon GP (2001) Toughening of a trifunctional epoxy system Part VI. Structure property relationships of the thermoplastic toughened system. *Polymer* 42:3847–3858
- Wu S, Guo Q, Kraska M, Stvhn B, Mai Y-W (2013) Toughening epoxy thermosets with block ionomers: the role of phase domain size. *Macromolecules* 46:8190–8202
- Xu Y, Liao G, Gu T, Zheng L, Jian X (2008) Mechanical and morphological properties of epoxy resins modified by poly(phthalazinone ether sulfone ketone). *J Appl Polym Sci* 110:2253–2260
- Xu Y, Liao G, Gu T, Zhou H, Jian X (2011) Preparation, morphology and thermo-mechanical properties of epoxy resins modified by co-poly(phthalazinone ether sulfone). *High Perform Polym* 23(3):248–254
- Yoon TH, Priddy DB, Lyle GD, McGrath JE (1995) Mechanical and morphological investigations of reactive polysulfone toughened epoxy networks. *Macromol Symp* 98:673–686
- Yoon TS, Kim BS, Lee DS (1997) Structure development via reaction-induced phase separation in tetrafunctional epoxy/polysulfone blends. *J Appl Polym Sci* 66:2233–2242

- Yu G, Wu P (2014) Effect of chemically modified graphene oxide on the phase separation behaviour and properties of an epoxy/polyetherimide binary system. *Polym Chem* 5:96–104
- Yu YF, Cui J, Chen WJ, Li SJ (1998) Studies on the phase separation of polyetherimide modified tetrafunctional epoxy resin. II. Effects of the molecular weight. *J Macromol Sci Part A* 35:121–135
- Zhang J, Xie X (2011) Influence of addition of silica particles on reaction-induced phase separation and properties of epoxy/PEI blends. *Compos: Part B* 42:2163–2169
- Zhang J, Guo Q, Bronwyn LF (2009) Study on thermoplastic-modified multifunctional epoxies: influence of heating rate on cure behaviour and phase separation. *Compos Sci Technol* 69:1172–1179
- Zhang Y, Chen F, Liu W, Zhao S, Liu X, Dong X, Han CC (2014) Rheological behavior of the epoxy/thermoplastic blends during the reaction induced phase separation. *Polymer* 55:4983–4989

Xiaole Cheng and Jeffrey S. Wiggins

Abstract

Epoxy/thermoplastic blends have received a high degree of attention owing to the fracture toughness improving without significantly compromising the thermal and mechanical properties. These materials are mostly prepared by mixing thermoplastic with epoxy monomers and curatives, and then undergoing a reaction-induced phase separation mechanism to form the final products. The mixing processes are very critical for forming the blends with the optimal properties and processabilities. A poor mixing can lead to localized property variation and deteriorate the morphological and mechanical properties of the final cured blends. Due to the importance of the mixing process, methods used for fabrication of epoxy/thermoplastic blends are described in detail in this chapter. Some novel techniques suitable for specific epoxy/thermoplastic blends are also discussed.

Keywords

Epoxy/thermoplastic • Blends • Mixing • Phase separation

Contents

Introduction	460
Mechanical Methods	462
Batch Mixers	463
Continuous Mixers	469
Continuous Polymerization Reactor	476
Nonmechanical Methods	479
Solvent Casting	479
Resonant Acoustic Mixer	480

X. Cheng (✉) • J.S. Wiggins

School of Polymers and High Performance Materials, Polymer Science and Engineering,
University of Southern Mississippi, Hattiesburg, MS, USA

e-mail: xiaole.cheng@eagles.usm.edu; jeffrey.wiggins@usm.edu

In Situ Polymerization	480
In Situ Dissolution	482
Conclusion	483
References	484

Introduction

Epoxy resins are increasingly being used as coatings, adhesives, and resin matrices for composite materials such as advanced carbon-fiber-reinforced polymer composites. As the network forms during cure, the chemical, morphological, and rheological environments change substantially and the system transits from liquid to gel and to vitrified states. The versatile chemistries and the availability of commercial epoxies and curatives allow designing glassy resin networks with a broad range of properties. In general, glassy epoxy resins are known for their excellent mechanical properties, thermal stability, solvent resistance, manufacturability, and low shrinkage (May 1988). The factor that governs most of these characteristics is the order of the chemical cross-link density, as it ultimately determines the network architecture. However, those highly cross-linked structures of glassy epoxy networks result in inherent brittleness which limits their applications. Therefore, efforts to increase the toughness of glassy epoxy networks continue to be an important area of polymer scientific research.

Rubber elastomers such as carboxyl-terminated butadiene-acrylonitrile rubbers (CTBN) (Arias et al. 2003; Sultan and McGarry 1973) and amine-terminated butadiene-acrylonitrile rubbers (ATBN) (Butta et al. 1986) have traditionally been used as rubber tougheners to improve epoxy toughness. However, rubber tougheners are known to reduce the thermal and mechanical properties of glassy epoxy networks, which is undesirable for advanced application such as aerospace composite materials (Kim and Char 2000; Park and Kim 2001). More recently, linear high-molecular-weight thermoplastics have been used as the tougheners for epoxies with an advantage for preservation of thermal and mechanical properties. The first two toughening studies using thermoplastic additives were reported by Bucknall and Partridge (1983a, b). Commercial polyethersulfone (PES, Victrex 100P) was used in their studies to toughen epoxy resins, and effective enhancement was obtained when thermoplastic phase separated from epoxy matrix combined with good interfacial adhesion. Since then, various types of high-performance linear thermoplastics including polysulfone (PSF) (Kim et al. 1995), polyetherimide (PEI) (Hourston and Lane 1992), polyetherketone (PEK) (Bennett et al. 1991), etc. have been intensively explored in literatures. The selection of the optimum thermoplastic depends on its compatibility, heat resistance, and thermal stability.

Epoxy/thermoplastic blends generally formulated by mixing of a thermoplastic polymer with epoxy monomers and curatives and subsequently curing the mixtures that may undergo the following three possibilities: (a) Thermoplastic is fully

miscible in epoxies before curing. Once cure reaction is initiated by heat or UV light, the increased molecular weight of epoxies reduces the miscibility between thermoplastic and epoxy matrix. At a certain extent of cure, system can cross the thermodynamic phase boundaries and enter the unstable region, resulting in a transition from homogeneously miscible state into phase-separated state to give heterogeneous structures such as droplet-dispersed morphology, co-continuous morphology, and phase-inverted morphology. This phase-separating process induced by cure reaction of epoxy thermosets is called cure-reaction-induced phase separation (CRIPS). (b) The initial homogeneous mixture of thermoplastic and epoxy remains miscible during cure process and shows no indication of phase separation after cured. This is most likely due to the chain-extended chemical reaction between thermoplastic reactive chain ends and epoxide groups. The chain-extended thermoplastic is more soluble than thermoplastic itself and suppresses the degree of demixing during cure, resulting a microscale homogenous morphology. The CRIPS can still occur but the domain size was found to be smaller than expected, often in the order of tens of nanometer. In this case, commonly used techniques such as scanning electron microscopy, optical microscopy, and rheological analysis are not able to produce a recognizable feature of phase separation. Epoxy/polycarbonate transesterification (Di Liello et al. 1994) and epoxy/phenolic-terminated PES chain-extended reaction (Blanco et al. 2006) are the best examples. (c) Thermoplastic is immiscible in epoxy matrix before cure and remains heterogeneous during cure, such as polyacrylonitrile (PAN) (Zhang et al. 2012) and poly(vinylidene fluoride) (PVDF) (Kim and Robertson 1992).

Most epoxy/thermoplastic blends of practical interest are prepared through CRIPS mechanism. CRIPS is a promising technique to control the morphologies of epoxy/thermoplastic blends within the range of nanoscale to microscale with tunable thermal and mechanical properties. Phase separation is a kinetic process and can be distinguished into two types of kinetic mechanism: spinodal decomposition (SD) and nucleation and growth (NG). For SD mechanism, a new phase is spontaneously generated from the parent phase at a thermodynamically unstable state. The new phase and parent phase form an interconnected co-continuous structure and can continue growing until they reach their equilibrium states. If the viscosity of the system were sufficiently low, density differences of both phases may lead to dynamic asymmetry between the two components and cause the phase transition from a co-continuous structure to spheres structure with a lower interfacial energy. SD occurs when the system enters the spinodal region of the phase diagram. A fast transition such as quench is typically required to allow the system moving from the stable region through the metastable region and into the unstable spinodal region. For NG mechanism, a series of new nuclei is generated from the parent phase so that the parent phase reduces its composition with a decreased free energy. Once the nuclei are formed, they can grow spherically and may coalesce with each other. In order for nuclei formation, it is required that the system maintain at the metastable state and composition fluctuations is large enough. NG differs from SD in that phase separation only occurs at nucleation sites instead of

throughout the parent phase. However, both mechanisms may give the same phase-separated morphology at the end of phase separation if matrix viscosity is sufficiently low.

Since phase separation is a kinetic process and highly viscosity-dependent, the increased molecular weight and viscosity of epoxy matrices upon cure reaction could reduce the phase separation rate and completely suppress when system is vitrified. As a consequence, the final cured morphology of epoxy/thermoplastic binary system is affected by the competition between phase separation kinetics and cure reaction rate. Knowledge of phase separation mechanism and cross-linked reaction kinetics comprise the basis of morphology design for thermoplastic/thermoset systems. Numerous studies, including some reviews (Inoue 1995; Williams et al. 1997), have been devoted to investigate the morphologies of epoxy/thermoplastic blends from different points of view. It has been known that the morphologies can be modified in multiple ways including changing thermoplastic weight fraction and molecular weight (Yu et al. 2008), altering thermoplastic end-group functionality (Ma et al. 2009), and varying epoxy cure chemistry such as cure rate, cure temperature, epoxy-amine stoichiometric ratio, and cure agents (Girard-Reydet et al. 1997; Mimura et al. 2000). General trends have been found that decreasing miscibility of thermoplastic in epoxy before curing or reducing cure rate of epoxy cross-linking chemical reaction could facilitate phase separation process.

The mixing processes of epoxy/thermoplastic blends are not well discussed in literatures, yet they are very critical for forming the blends with optimal properties and processabilities. An efficient modification of epoxy resin by thermoplastic polymers usually prefers to form a homogenous blend before cure and phase separate after cure. A poor mixing and heterogeneous dispersion of thermoplastic polymers in epoxies can lead to localized matrix property variation and deteriorate morphological and mechanical properties of the final cured blends. Due to the importance of mixing, this chapter will be focused on the preparation techniques for epoxy/thermoplastic blends which are divided into two major parts: mechanical methods and nonmechanical methods.

Mechanical Methods

The mechanical mixers used for blending epoxy and thermoplastic are either batch or continuous types. In batch mixers, all components are added into the mixer vessel together or in a predefined sequence and mixed until a homogenous solution is achieved. On the other hand, in continuous mixers, components are continuously fed into the mixer according to the formulation. The mixing takes place during the material transport from the feeding port to the discharge nozzle. While batch mixers are generally based upon relatively low-temperature mixing over long periods of time, continuous mixers are designed for higher-temperature mixing over short periods of time. Residence time distribution in a continuous mixer is typically in the range of 1–5 min. The selection of batch or continuous mixers depends on several

factors such as material physical states, mixing quality and efficiency, handling equipment, energy consumption, and labor cost.

Batch Mixers

Batch mixers are the oldest type of mixers developed for polymer processing and still widely used in polymer society. A typical batch mixer consists of a tank with an agitator and integral heating/cooling system. They have versatile designs and can be modified to suit different polymer applications since the processing conditions can be varied during mixing, additives can be added at a flexible time sequence, and mixing temperature and time can be accurately controlled. Furthermore, they are available in a broad range of sizes from less than 1 L to more than 15,000 L that can be easily accommodated to laboratory-scale trials or industrial-scale production.

There is no standard engineering classification for batch mixer equipment. Different types of mixers may fulfill the same mixing task. Based on their application purposes, batch mixers can be divided into two broad categories: solid mixers and liquid mixers. They can also be classified according to their shear forces: high-shear mixers, medium-shear mixers, and low-shear mixers. Details about different types of batch mixers and their mixing mechanisms have been well discussed and published by J. L. White (White and Bumm 2011), Z. Tadmor (Tadmor and Gogos 2006), and L. A. Utracki (Utracki and Wilkie 2002). This section will be primarily focused on the introduction of batch mixers used for epoxy/thermoplastic blends and their mixing mechanism.

Low-Shear Liquid Batch Mixer

Epoxy/thermoplastic blends have been predominantly prepared using low-shear liquid batch mixers. In a typical batch mixing process, epoxy/thermoplastic blends are prepared in two steps. Epoxies are firstly heated at elevated temperature (usually above 120 °C) to mix with thermoplastics. Thermoplastics in powder form are preferred to facilitate thermoplastic dispersion and solubilization in epoxy resins. Once homogeneous mixing is reached, batch mixer temperature is adjusted and curatives are added with continuing mixing. Degassing is required for both steps to eliminate air bubbles trapped during mixing. Any trapped air will cause negative impacts on material properties. Once curatives are dissolved, the resulted epoxy/thermoplastic curable mixtures may be partially cured in the batch mixer for a period of time and quenched to maintain a target cure conversion for further processing or discharged immediately from the batch mixer with minimal extent of cure, molded to certain shapes, and then fully cured in programmable ovens to form the final products. The choice of cure profile depends on the epoxy curative chemistry.

Myers Engineering Mixer VL550/500A (Fig. 1) is a batch mixer designed specifically for producing epoxy matrix polymers. The system is a dual motor tri-shaft high-viscosity mixer equipped with a hot oil temperature control system and pneumatic ram discharge press. In addition, the system is equipped with a full

Fig. 1 Myers tri-shaft VL550/500A batch mixer (Courtesy: Myers Mixers, LLC)



vacuum assembly to remove reaction solvents, degas during mixing, and assure solubilized gasses are minimized in the matrix materials. Dispersive and distributive mixing are accomplished using the tri-shaft dual motor advanced mixing system which simultaneously incorporates various blade configurations: a flat-bar/low-profile sweep blade with risers and wipers which sweeps the base and sides of the mixer, a distributive mixing gate blade with action which keeps the reaction regulated throughout the mixture assuring homogenous distribution, and a Myers dispersion blade is ultimately responsible for shear motions that reduce aggregate size and distribute particles evenly throughout the matrix. Low-shear liquid batch mixers operating with multiple blades are versatile, making them ideal for handling epoxy liquids over a broad range of viscosities. They are typically capable of processing resin viscosities from water-like to around 50,000 centipoises.

Incorporation of a significant amount of thermoplastic into epoxies inevitably raises the matrix viscosity, especially when thermoplastic with high-molecular weight is used. The highly viscous matrix is not efficient for handling by batch mixers and becomes extremely difficult to mix with curatives. As a consequence, the nonuniform dispersion of curatives may disrupt the local resin stoichiometry and affect the way that a cross-link network forms and other desirable properties of final cured blends. Although elevating temperature of batch mixers can reduce the

epoxy/thermoplastic blend viscosity, it is impractical to control epoxy cure conversion and prevent runaway reaction due to the substantial heat released by exothermal cure at elevated temperature.

In order to solve this problem and prepare epoxy/thermoplastic blends with relatively high-loading thermoplastic (*ca.* 20–30 wt.%), diluents, both reactive as well as nonreactive, are often incorporated into epoxy resins prior to adding curatives to reduce epoxy/thermoplastic mixture viscosity and enhance its processability. Commonly used diluents include monofunctional epoxies such as butyl glycidyl ether, octylene oxide, and phenyl glycidyl ether and multifunctional epoxies such as diglycidyl ether bisphenol F (DGEFBF) and triglycidyl para-aminophenol (TGAP). Addition of those diluents can significantly reduce resin viscosities, further increase the shelf and pot life and wetting ability, and enable to add a higher amount of thermoplastic. For example, low viscous TGAP (around 700 centipoises at 25 °C) is often used in aerospace tetraglycidyl 4, 4'-diaminodiphenylmethane (TGDDM) (around 5,000 centipoises at 25 °C) with thermoplastic content of up to 30 wt.% to enhance fiber impregnation and control prepreg tack (Zhang et al. 2009). However, it needs to be noticed that diluents adversely affect the cross-link density, thermal stability, and chemical resistance of cured epoxies.

Epoxy/thermoplastic blends with thermoplastic concentration of more than 30 wt.% are difficult to prepare using traditional batch mixer approach even with the aid of dilutes. Above this concentration, thermoplastic-dispersed phase starts to collapse and form a continuous phase where epoxies disperse as droplets. The continuous thermoplastic matrix becomes too viscous to flow in batch mixers and reduces the mixing efficiency. Furthermore, the resulted mixtures are too viscous for many commercially used shaping processes such as prepreg filming and vacuum-assisted resin transfer molding process. Shifting to a different style of batch mixer is recommended in this case.

Internal Mixer

Internal mixers are very efficient batch mixers designed for materials with medium- and high-viscosity with continuous improvement of mixer design and mixing efficiency since the 1930s, internal mixers have been exceedingly used in the rubber and thermoplastic industries. It is a melt mixing process which employs high temperature and intense shear force to obtain homogenous mixing of polymeric materials. As recognized, internal mixer is a versatile and cost-saving process which is capable of producing a variety of thermoplastic polymers and composites in large volume scales.

The internal mixer typically consists of two rotors enclosed in a heating chamber and a drive unit. The two rotors in the mixer serve as its heart for mixing. They may be tangential or intermeshing and with different directions of rotation (counterrotating and corotating) (Moribe 2012). The design of the rotors has a significant influence on its mixing performance. A tangential rotor provides a short mixing time because the clearance between the two rotors is large and the intake is generally fast. However, because the mixing is performed between the rotor and the

chamber wall, there is difficulty in distribution and cooling. On the contrary, an intermeshing rotor typically requires a long mixing time since the rotor clearance is small. Due to the mixing that occurs not only between the rotor and the chamber wall but also between the two rotors, it has excellent distribution and cooling performance which is particularly suitable for temperature-sensitive compounds.

Mixing temperature of an internal mixer is dependent on the transfer of heat from chamber surfaces to the polymer matrix and often the limiting factor of mixing performance. The mix chamber is only heated from the outside and the rotors transfer the heat away from the molten polymers, causing temperature drop across the chamber. In order to minimize the temperature variation, the mixing chamber, rotors, and discharge door are all temperature controlled with steam or circulating water.

Filling factor should also be taken into consideration during internal mixing. It defines the proportion of the mixing chamber volume occupied by the finished mixture which can be calculated from the weights and densities of the materials to be mixed. Filling factors in the range of 0.65–0.85 are generally preferred to achieve good level of mixing. Very low filling factors are obviously uneconomic, and excessively high filling factors result in material remaining in the stagnant region of the chamber and not taking part into the mixing process.

Figure 2 presents the example of a laboratory-scaled internal mixer head with non-intermeshing counterrotating mixing rotors produced by C.W. Brabender Instruments, Inc., one of the leading companies for the development of internal mixers. The mixer requires a small amount of raw materials, short residence time, little effort and operational expense, and is often used for the evaluation of compounds on a small scale. It is a three-piece design with a capacity of

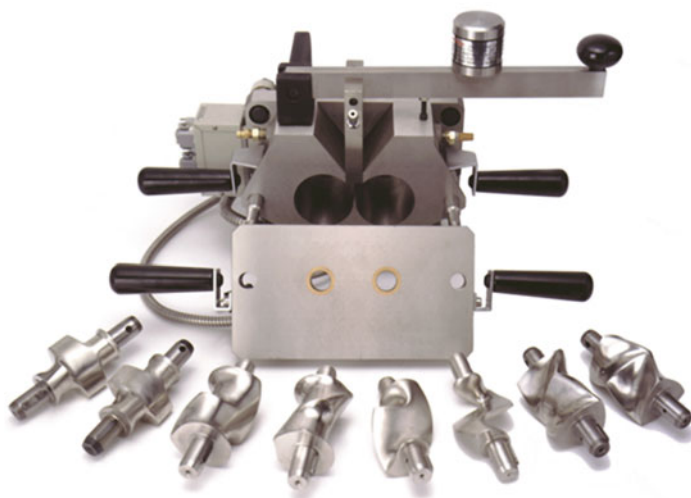


Fig. 2 C.W. Brabender Prep-Mixer internal mixer head with blades: roller, Banbury, cam, and sigma (from left to right) (Courtesy: C.W. Brabender[®] Instruments, Inc.)

350–420 ml depending on mixer blade configurations. The blade configurations are varied including roller, Banbury, cam, and sigma to achieve optimum shape for mixing. The selection of blade shapes is typically dependent on the materials to be mixed, and different blades may fulfill the same mixing task. Recently, Salahudeen et al. (2011) systematically evaluated the distributive mixing performance of various blade configurations of the internal mixer using simulation and verified by tracer experiment. The overall efficiency of distributive mixing in the roller type of mixer was found to be substantially better than cam and Banbury types of mixers due to better length of stretching and reorientation.

Internal mixers are able to handle materials with a very broad viscosity range and therefore particularly useful for preparing epoxy/thermoplastic blends with higher thermoplastic content (above 30 wt.%). The material adding sequence is different from liquid batch mixer. As a general guide, thermoplastic is firstly melted in the chamber and mixed with epoxies. The mixing temperature is set at the thermoplastic-melting temperature to allow it to be quickly converted to melting state in which it will accept liquid additives. After adequate mixing is achieved, the cure agents are added through the feeding port of chamber for further mixing. Since the cure reaction takes place immediately during the continuation of the mixing process, the mixing time for cure agents must be carefully controlled to prevent system gelation and vitrification especially when stoichiometric amounts of cure agents are used. For example, Y. Ishii (Ishii and Ryan 2000) described a process wherein epoxy and thermoplastic poly (phenylene ether) (PPE) blends were prepared in a Brabender kneader at 185 °C by kneading for about one hour. The mixture was cooled to 150 °C and a stoichiometric mass of curatives was added using a syringe. After mixing for another 2 min, the mixture was quickly removed from the kneader and stored in a freezer.

One of the requirements for epoxy/thermoplastic blend preparation using internal mixers is that the used thermoplastic should have a relatively low melting temperature such as poly (methyl methacrylate), polypropylene, polyethylene, etc. For those high-performance thermoplastics such as PES, PEI, PEEK, etc. with much higher melting temperatures (above 250 °C), the required melt mixing temperature is too high to mix with epoxies and cure agents due to the difficulties in controlling the following cure reaction and preventing side reactions. If gelation or cross-link of epoxy matrix occurs during mixing, the torque increases dramatically which may cause potential damages to the rotors and leave the produced mixtures very difficult to clean after mixing.

Rheo Mixing (RMX)

Another interesting method for preparing epoxy/thermoplastic blends with high thermoplastic concentration is to use Rheo mixing (RMX) device which is recently designed by Muller et al. (Bouquey et al. 2011). Unlike the traditional batch mixers in which shear flows are predominant for mixing, RMX relies on the elongational flows to enhance the efficiency of mixing. As schematically represented in Fig. 3, RMX consists of several major components: two cylindrical chambers with two reciprocally moving pistons to alternately push the materials from one chamber to the other, the central channel connecting the cylindrical chambers, a mixing

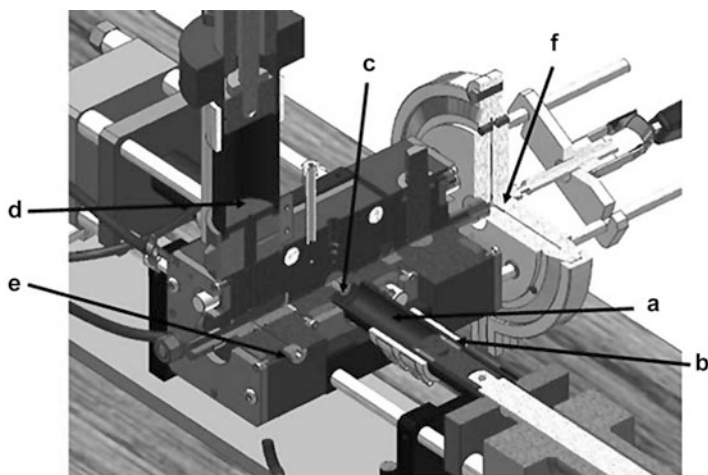


Fig. 3 Three-dimensional view of the RMX device: (a) chamber, (b) piston with seal, (c) mixing element, (d) feeding unit for melt, (e) feeding channel for liquids, and (f) mold (Reproduced with permission from John Wiley and Sons)

element with modulated geometry and L/D ratio, feeding units which allow the melting of polymer pellets and liquids entering the central channel, and an outlet port of the mixed materials. The volume of materials inside the mixer can be adjusted by the initial positions of the pistons with a maximum mixing volume of $10\text{--}100\text{ cm}^3$. When the materials are forced to pass through the narrow mixing elements, the high shear stress generated by convergent and divergent elongation flows induces the breakup of the agglomerates and results in a strong dispersive mixing. The outlet port of RMX device can be directly connected to a mold. As a result, no additional step (e.g., reheating, placing it into a mold, and molding) is required to mold specimens of specified shapes after mixing.

Chandran et al. (2015) was firstly reported using RMX device to prepare epoxy/thermoplastic blends and demonstrated its capability to address the difficulty for mixing high loadings of thermoplastic in conventional batch mixers. In his study, diglycidyl ether bisphenol A (DGEBA)/poly(trimethylene terephthalate) (PTT) blends with PTT content of up to 30 wt.% were mixed in RMX at $245\text{ }^\circ\text{C}$ for 10 min. A stoichiometric amount of 4, 4'-diaminodiphenylsulfone (44DDS) was then introduced and mixed for another 10 min at the same temperature. The mixture was directly transferred to a preheated mold at $220\text{ }^\circ\text{C}$ and cured for 4 h. The DGEBA/PTT blends prepared by RMX device exhibited significantly improved properties. The cured samples were optically transparent and no phase separation was observed by TEM. The author claimed molecular level dispersion of thermoplastic in epoxy matrix was achieved because of the excellent dispersive mixing of RMX device. The convergent and divergent field near the mixing element induced the breakup of the initially formed PPT-rich phases and pinned further phase separation. In addition, the blends prepared by RMX device showed a lower glass transition temperature and much

higher elastic modulus as compared to the conventional batch mixing samples. Surprisingly no transporting issue was mentioned about mixing DGEBA/PTT/44DDS blends at 245 °C for 10 min in RMX whereas the system can be vitrified in less than 5 min in conventional batch reactors. This is likely caused by the inefficiently distributive mixing of RMX device which is being investigated and not reported yet.

Continuous Mixers

Despite being widely used for epoxy/thermoplastic blends, batch mixer approaches are still facing several challenges in industry. Firstly, the batch mixing process is energy intensive. Epoxides, thermoplastics, and curatives are mixed and reacted in the batch mixers which may exceed 1,000 L volume through slow heating. Once homogeneously dispersed, the mixtures are discharged from the batch mixers and stored at low temperature for indefinite periods of time to retard cure and preserve processability. Subsequently, the curable epoxy/thermoplastic mixtures are removed from cold storage, heated above their glass transition temperatures, converted into different shapes, and fully cured in ovens. The total energy consumption throughout this entire process is substantial. Furthermore, products prepared by batch mixers often suffer batch-to-batch variations. This behavior counts for the inherent inconsistencies in quality and leads to variation in the final cured blend structures and properties. Therefore, there is an increasing demand from manufacturers to reduce the energy consumption required to produce epoxy/thermoplastic blends and to minimize batch-to-batch variation in quality.

Continuous mixers carry material as a flowing stream where components are fed into the mixer, mixed, and discharged continuously. They typically consist of several feeding systems for handling materials with different physical states, one or more rotating screws that are capable of transporting and mixing, and a discharge end (die). Continuous mixers are operated under steady-state conditions. The power consumption is usually lower than in batch operations. Although continuous mixers require high capital investment, they are easy to automate and robotize, have high output, and can be run with a statistical quality loop control (Moad 1999). Due to these advantages of continuous mixers over batch mixers, more and more attention has been drawn into preparation of epoxy/thermoplastic blends using continuous mixers.

Extruder

Extruder is one of the most commonly used continuous mixers for polymer processing. It has drawn much attention in both academia and industry since the 1960s as it is a continuous and economic method for industrial scale manufacturing. Literature reviews about twin-screw extruder mixing process have been published by Brown and Orlando (1988) and Xanthos (1992).

The primary advantage of extruders compared to other mixers, such as batch mixers, is the capability of transporting materials over a broad range of viscosities. Additionally, the absence of solvent combined with simultaneous transport of

low-molecular-weight monomers and high-molecular-weight polymers improves energy consumption making the mixer environmentally favorable. Extruders also provide controlled shear energy, excellent heat transfer, precision feeding, mixing, devolatilization, and insensitivity to viscosity changes. They can divide into three categories according to their number of screw shafts including single-screw extruder, twin-screw extruder, and multiple-screw extruder.

Single-screw extruder is a simple and economic continuous mixer type. The main sections of the extruder include the barrels, a single screw that fits inside the barrel, a motor-drive unit, a control system for the barrel temperature and screw speed, and a die to discharge the molten materials. A hopper is attached to the barrel at upstream of the extruder and the materials are fed into the barrel either by gravity feeding or starve feeding using screw flights. Once materials are fed into the barrel, they are compressed and transported by drag flow, which generated from the contact between materials, barrels, and the moving screws. The screw within the barrel can be divided into three zones: solids conveying, melting, and metering zone. The solid-conveying zone begins at the feed port and extends to a point where the solid starts to melt. The screw design in this zone is characterized by screw elements with deeper flight between the root and the tip of the screw. The melting zone follows the solid-conveying zone and is used to compress the solid materials. Within this zone the screw channel depth decreases and the solids coexist with its melt. The metering zone begins at the point where all the solids are melted and it extends to the discharge of the extruder. It acts as a pump, transferring and homogenizing the molten materials and building up the pressure to force the material through the die. When mixing is important, dispersing screw elements with narrow slits can be incorporated in the metering zone to promote dispersion. To enter the slit, the materials are exposed to an increased shear force caused by the elongational flow. But compared to other mixers especially twin-screw extruder, the mixing efficiency provided by single-screw extruder is still very limited.

There are many types of twin-screw extruders. The main geometrical features that distinguish them are the sense of rotation and the degree of intermeshing. Twin-screw extruders with screws that rotate in the same direction are called corotating extruders. When the screws rotate in the opposite direction, it is called counterrotating extruder. The degree of intermeshing can vary from fully intermeshing, partially intermeshing, to non-intermeshing.

Among all types of extruders, fully intermeshing corotating twin-screw extruders offer the highest level of mixing, dispersion, and shear control, making them the primary technology used as continuous mixers (Rauwendaal 1981, 1998). Figure 4 shows a typical twin-screw extruder based on ZSK 26MC Compounder with $L/D = 40$. The processing section is the core technology of twin-screw extruders. Barrels along the extruder are the points where various liquids, solid reactants, catalysts, modifiers, vacuums, etc. are introduced. Each barrel is equipped with independent temperature control by adjusting heating and cooling. Mixer shafts and screw elements are precisely fit within the series of barrels. It offers a broad array of screw element configurations that provides necessary transport, mixing, and shear abilities. Modular screws are designed by placing

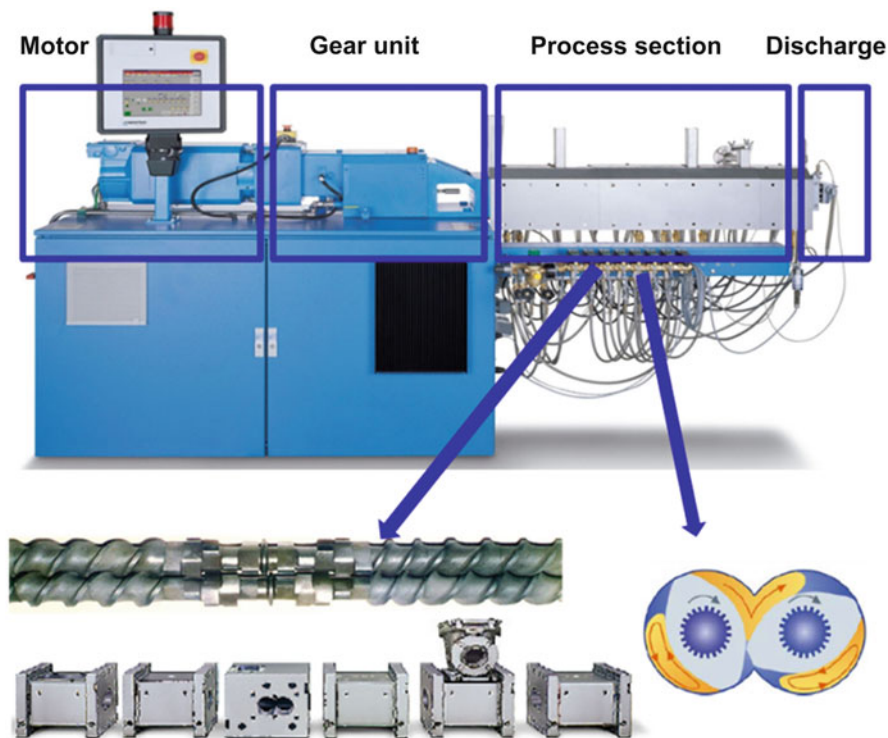


Fig. 4 Corotating intermeshing twin-screw extruder based on ZSK 26MC Compounder (Courtesy: Coperion, Inc.)

appropriate screw elements in their proper positions according to the type of action favorable to accomplish specific reactions or activities within specified regions of the mixers.

Typically, three types of screw elements are used including conveying elements, kneading elements, and reversing elements. Examples of modular screw elements used for intermeshing corotating twin-screw extruders are illustrated in Fig. 5. Classical conveying elements are used to convey materials away from feed opening or discharge processed materials at the end of the extruder. They also serve as drivers to provide forwarding pressure that supplies material to kneading and mixing elements. Conveying elements can have various flights with different pitches. Single-flight elements have a deep channel and are useful when good conveying is required. Double-flight screws have a medium channel depth and moderate conveying ability. Triple-flight elements have shallow channels and low conveying capability. They are useful when considerable shear is necessary. The double-flight elements are most commonly used in reactive extrusion, as they have the largest reactive volume combined with the minimum shear work input. Kneading blocks are the dominant elements in determining the mixing efficiency and the degree of fill as well as residence time distribution. They are usually used

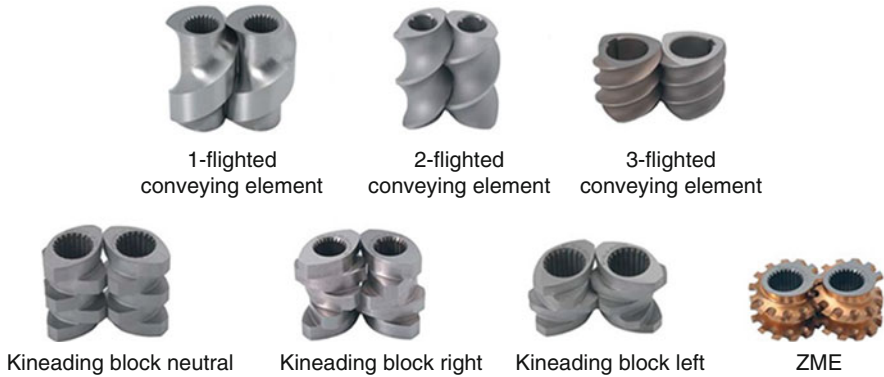


Fig. 5 Screw elements for corotating twin-screw extruder

when materials have to be sheared and dispersively mixed. Kneading blocks are staggered at an angle, which is called advance angle. These advance angles determine the conveying ability of the elements ranging from forwarding (right) to neutral to reversing (left). Neutral elements push material neither forward nor backward. Reverse kneading blocks have a retaining character and are usually utilized when large mechanical stress needs to be built up. Mixing elements (ZME) meet the challenge of conveying and mixing simultaneously. They provide more space for distributive mixing without or nearly no loss in forwarding properties.

During continuous processing, mixing mechanism is generally categorized into dispersive mixing and distributive mixing. For dispersive mixing, a critical stress is applied to the dispersant through laminar shear stress generated along the screw elements which overcomes cohesive forces of particulates so phase sizes are reduced. High shear rates are a requirement for successful dispersive mixing. In contrast, distributive mixing is more effectively carried out by shear stress that generates large strains as there is no critical stress threshold. Distributive mixing is facilitated by splitting and reorienting the flow streams. Figure 6 illustrates the dispersive and distributive mixing in a particle/liquid system. When considering screw element geometries, wide kneading blocks with reverse pitch facilitate dispersive mixing while narrower kneading blocks with forward pitch, gear, and tooth elements provide distributive mixing.

The advantages of twin-screw extruders are related to the fact that some thermoplastic polymers are difficult to mix with epoxies and curatives using the traditional batch mixers in view of their high melting temperature and high loading level. The short mixing time, reduced mixing volume, and broad viscosity range of twin-screw extruder make it ideal for melt mixing thermoplastic with epoxy resins at elevated temperatures.

Continuous preparation of thermoplastic epoxies based on twin-screw extruders can be preceded with two approaches: (a) thermoplastic and epoxies are extruded at the melting temperature of thermoplastic without curatives followed by quickly

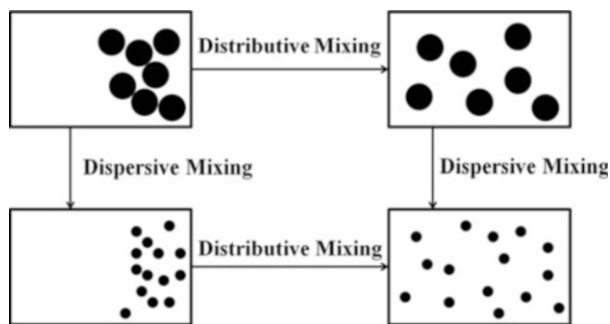


Fig. 6 Schematic dispersive mixing and distributive mixing mechanism

mixing with curatives to ensure no cross-link reaction occurs and (b) thermoplastic, epoxies, and curatives are slurry mixed in one step at temperature below the cure temperature of the system. Both methods require carefully controlling the mixing temperature, mixing time, and curing kinetics to minimize the cure reaction during the continuous mixer process in order to avoid chemical cross-link reaction and prevent potential damage to the screw elements.

For the first approach, S. Izawa (Izawa and Toyama 1973) described a continuous process to prepare glass-fiber-reinforced polyphenylene ether (PPE)/epoxy resin blends using corotating intermeshing twin-screw extruder. Uncured epoxy resins were added in an amount of 45 wt.% or less of the total weight to improve the molding processability of PPE without losing the advantage of glass-fiber reinforcement. For example, PPE (90 parts) and solid epoxy resin (10 parts) having an average molecular weight of 8,000 g/mol (trademark: Dow D.E.R. 669) were mixed at barrel temperatures of 310 °C. The resinous composition was then mixed with glass fibers by being fed at the vent of extruder whereby the barrel temperature was adjusted to 330 °C. The produced glass-fiber-reinforced PPE/uncured epoxy blends were shaped by injection molding with no cure agents. F. Constantin et al. (2003) prepared poly (hydroxyl-amino ether) (PHAE)/diglycidyl ether of bisphenol A (DGEBA) blends in a corotating twin-screw extruder. Thermoplastic PHAE was grounded into fine powder to increase surface contact area with DGEBA. The initial epoxy monomer and PHAE (up to 70 wt.%) were extruded using a classical thermoplastic/liquid twin screw profile, and the extrudates were quenched in water and dried. Subsequently a curing agent was added to the blends and mixed for 1 min at 135 °C using an internal mixer. In both examples, since curatives are either not used or added after mixing thermoplastic with epoxies, it is not a real sense of continuous mixing method for preparing epoxy thermosets/thermoplastic blends.

The continuous mixer method was further developed by E. A. van den Berg (Berg et al. 1997). He proposed a simple but promising one-step preparation of PPE/epoxy resin blends with curatives using a modified twin-screw extrusion device, as shown in Fig. 7. PPE and epoxies were added through the feed port of the extruder. The barrel temperatures and the screw design were modulated in such

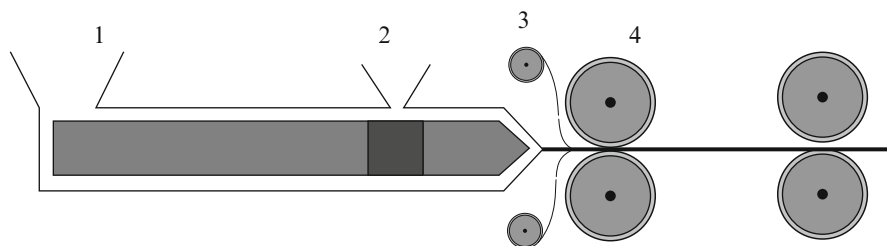


Fig. 7 One-step methods for preparing PPE/epoxy resin blends using twin-screw extruder: (1) main feeders, (2) side feeder, (3) rolls, (4) nip rolls

way that PPE and epoxy resin were melted and mixed in the upstream portion of the extruder. Then at the downstream barrels, the molten blends were further mixed with a suitable curative by adding the curative through a side stuffer. Mixing elements such as kneading blocks, turbine mixing elements, and gear mixing elements are preferably used to facilitate the homogenous mixing of curatives. Adding the curing agent in the downstream barrel zone of the extruder shortly before the molten blends exiting the extruder is important to minimize the cure reaction and prevent the cross-link. The blends comprising PPE, epoxy, and curatives were then pumped through a pelletizing die to a water bath and pelletizer, or through a sheet die to nip roll pairs for sheet/film extrusion, or through a sheet die, then combined with carbon fiber or glass fiber in nip roll pairs or double belt lamination device for fiber reinforced composite manufacture.

The second approach for preparing epoxy/thermoplastic blends using continuous mixer is to slurry mix the thermoplastic, epoxies, and curatives at a temperature below the cure temperature of the system. In this case, a miscible thermoplastic and curatives are mixed in liquid epoxies to form solid discontinuous phase with a particle size less than $20\ \mu\text{m}$ (Repecka 1988). During the mixing process, only a very small amount of thermoplastic and curatives were dissolved without causing significant changes in the matrix viscosity. Those well-dispersed thermoplastic and curative particles can further dissolve in the liquid epoxy monomers at elevated temperatures and undergo reaction-induced phase separation to form the final blends. Thermoplastics such as the polyimides, polyetherimides (PEI), polysulfones (PSF), polyethersulfones (PES), and polyetheretherketones (PEEK) with glass transition temperatures greater than $150\ ^\circ\text{C}$ are ideal candidates for this method due to their excellent compatibility with epoxies. This method is particularly useful for prepregs and film adhesive applications where tack and drape are the primary concerns of resin properties at their intended operating temperature.

The University of Southern Mississippi (Mississippi, USA) recently developed a method to prepare heat-curable PEEK-reinforced epoxy blends using twin-screw extruder (Kingsley et al. 2012). ZSK 26 MC Compounder ($L/D = 40$) equipped with a liquid resin feeding system, a solid curative feeder, and a PEEK feeder was used as shown in Fig. 8. Epoxies, curatives, and PEEK were slurry mixed at the barrel temperatures below $100\ ^\circ\text{C}$ to ensure no cure reaction occurs during

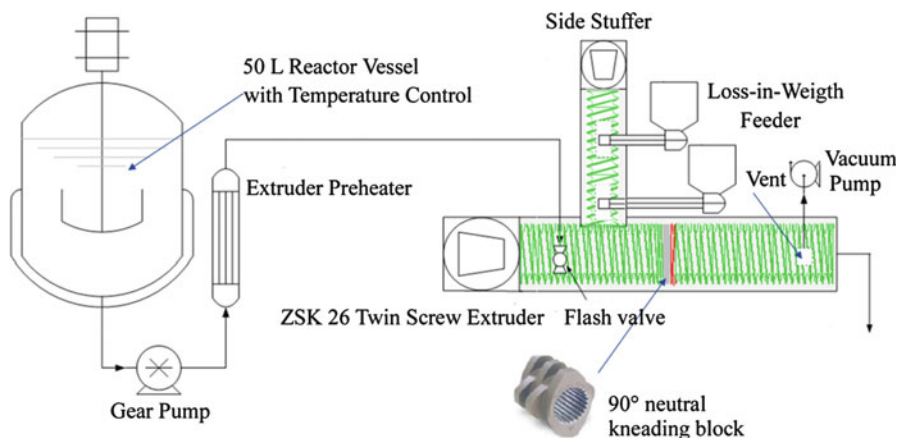


Fig. 8 Twin-screw extruder preparation of heat-curable PEEK-reinforced epoxy blends using slurry mixing

continuous mixing. The slurry products are solid-like materials at room temperature and can be compression molded and cured into the final shape at elevated temperature.

Three-Roller Mills

Three-roller mills, commonly known as calendaring mills, are another ideal continuous mixer for blending high viscous materials such as epoxies. It employs both shear flow and extensional flow created by rotating rollers with different speeds to mix, disperse, and homogenize viscous matrices with additives or particles. In addition, it is a solvent-free process which is environmentally favorable. Theoretically three-roller mills are capable of handling materials with viscosity ranging from 200 to 2,000,000 centipoises. It can be easily combined with other resin processes such as filming to create a continuous production.

The basic design of three-roller mills consists of three counterrotating cylindrical rollers that are adjacent to each other with a circulating oil temperature control system (Fig. 9). The first and third roller, called the feeding and apron rollers, rotate in the same direction while the center roller rotates in the opposite direction. The three-roller mills offer different rotating speeds which are varied by drive units. The speed ratio for the three rollers (known as friction ratio) is usually about 1:3:9.

In a typical mixing cycle, the materials to be mixed are either pre-blended or fed directly into the hopper. After being pre-dispersed in the first gap between the feeding roller and central roller, materials are transported into the second gap by the central roller. In the second gap, the material is subjected to even higher shear force due to the higher speed of apron roller and dispersed into desired dispersing level. The resulted materials are then discharged and collected for further processing. This milling cycle can be repeated several times until uniform mixing is achieved.

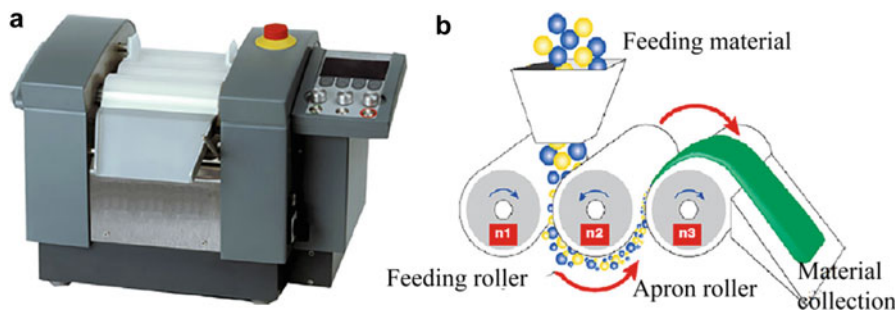


Fig. 9 (a) EXAKT three-roll mills and (b) corresponding schematic showing the general configuration and its working mechanism (Courtesy: EXAKT Technologies, Inc.)

Friction, speed ratio, sizes, and gap of the rollers impact the dispersion and intensity of mixing.

Application of three-roller mills has been primarily focused on dispersing inorganic particles in epoxy matrices. It has been proved to be a highly efficient dispersion method for nanoparticles containing fiber-like fillers such as glass fiber, carbon nanotubes, carbon fiber, etc. (Chang et al. 2009; Gojny et al. 2004). Because of the strong shear force between the three rollers, particles can achieve a high degree of intercalation/exfoliation within a short period of time. Another major advantage of using this method is the gap between rollers can be mechanically adjusted within micro length so that the particle sizes are controllable to obtain a narrow size distribution of nanoparticles.

Literatures about mixing epoxies with thermoplastic using three-roller mills are in fact limited. One of the possible reasons is that the three-roll millers that are currently being used are designed with limited heating capability (up to 60 °C for EXAKT). The feeding materials should be in viscous state when mixing with other materials. Thus this mixing technique may not be applied for mixing thermoplastic which typically has much higher melting temperature. However, owing to the broad viscosity processing window of three-roll mixers, it can be used for dispersing curative into the pre-dissolved epoxies/thermoplastic mixtures without the need of elevated temperature. Choe et al. (2003) prepared polyamide copolymer and polyetherimide-modified DGEBA blends by mixing a stoichiometrically balanced amount of curing agent with pre-dissolved DGEBA/thermoplastic mixture in a three-roll mill. Curable mixtures were obtained after mixing for 1 h at room temperature. This approach is very promising for room temperature curing epoxy systems for which elevated temperature mixing is not practical.

Continuous Polymerization Reactor

The term “continuous polymerization reactor” is used to describe a polymer process that involves chemical reactions. It is a continuous, flexible process offering the

technical and economic advantages compared to other reactors such as batch reactors. Corotating twin-screw extruder is an excellent chemical reactor and can be used to efficiently control polymerization reactions. Through simultaneously applying kneading, shearing, pressuring, and heating, continuous reaction results in highly homogenous mixing products with low reaction duration and high consistency, which are the major manufacturing cost-saving factors. Examples for twin-screw extruders being used as chemical reactors include grafting reactions (Cai et al. 2008), post-reaction processes including bulk polymer reactions (Finnigan et al. 2004), reactive compatibilization of particulates and reinforcements (Shokoohi et al. 2011), and reactive blending (Oyama 2009).

While batch reactors are generally based upon relatively low-temperature reactions over long periods of time, continuous reactors are designed for higher-temperature reactions over short periods of time. Reaction time of continuous reactor is described as residence time. It is controlled through screw configuration, screw speed, feeding rate, and reactor length and typically in the range of 1–10 min. Since residence time is short, reaction quantities are small and heat-transfer efficiencies are high; continuous reactors based on twin-screw extruders are preferred to conduct at elevated temperature. Catalyst and intensive mixing, as well as pressure, are often used to accelerate the reaction rates.

Within numerous applications for polymer reactions, continuous reactors have been mainly used for high-molecular-weight thermoplastic matrices. They are nontraditional for conducting cure reaction when preparing cured glassy epoxies. As the gelation occurs and the network forms during cure, the system transits from liquid to gel and to vitrified states which will result in conveying issues in continuous reactor. This is the major reason that curatives are added after mixing thermoplastics and epoxies with reduced mixing time or slurry mixed with epoxies in twin-screw extruders as discussed in the previous section.

For certain applications such as aerospace prepreg, partially reacted epoxy oligomers, also called B-stage epoxy prepolymers, are required for the purpose of controlled flow and self-adhesion. This brings the possibility of using continuous reactor to prepare partially cured epoxy prepolymers. Traditionally the epoxy prepolymers are prepared using liquid batch mixers. Epoxies are firstly mixed with additives such as thermoplastic tougheners and curatives at elevated temperature. After mixed, cure reaction continues at appropriate temperature over long periods of time to advance to a prescribed molecular weight with desired viscosity. The produced epoxy prepolymers are discharged from the batch mixers and stored at low temperature for indefinite periods of time to retard cure and preserve viscosity.

Attempts to conduct epoxy prepolymer reaction in continuous reactors are rare. Previous research reported by Titier (Titier et al. 1995, 1996) described a continuous reactor method using corotating twin-screw extruder to synthesize epoxy-amine multiacrylate prepolymers. The system is based on a competitive reaction of a difunctional amine with a difunctional epoxy, DGEBA, acting as a chain extender and a mono-epoxide acrylate, acting as a chain termination agent, avoiding the gelation of the system and introducing double bonds in the epoxy oligomer formed.

The formed epoxy-amine multiacrylate prepolymers can further lead to cross-linked networks via double-bond polymerizations.

Very recently, X. Cheng (Cheng and Wiggins 2014) designed a continuous reactor to prepare thermoplastic-modified epoxy prepolymer blends with a thermoplastic content of up to 20 wt.% of total mass weight. Thermo Prism 16 mm corotating twin-screw extruder ($L/D = 25$) was used in his study. The reactor consists of a feed zone, five electrically heated and liquid-cooled zones, and an electrically heated die zone. The screw configuration shown in Fig. 10 was designed to balance shear mixing and residence time with a combination of various conveying, kneading, and reversing elements. Thermoplastic PES and a stoichiometric amount of 44DDS was fully dissolved in TGDDM after the continuous reaction process at the barrel temperatures of 180–220 °C. The produced prepolymers were optically transparent. In addition, concurrent epoxy-amine chain extension reaction advanced the TGDDM prepolymer to targeted molecular weights and viscosities. The level of cure was kinetically controlled by adjusting barrel temperatures and residence times of the continuous reactor. Gelation and cross-link were eliminated through a systematic analysis of epoxy cure reaction kinetics, processing conditions, and continuous reactor design. The produced epoxy prepolymers can be directly used for prepreg filming operations.

Compared to the batch reactor, the continuous reactor efficiency in mixing and dissolution is attributed to the high shear, excellent heat transfer, and small reaction volume. Although temperature can be increased to accelerate thermoplastic mixing in a batch reactor, it is impractical to control curative dissolution and reaction conversion at high temperatures considering the large volume of batch reactor. Small reaction volumes and excellent heat transfer in continuous reactors allow to prepare epoxy prepolymers at elevated temperature within reduced reaction time. But the challenge for avoiding gelation remains a critical problem. It was found that 220 °C was the maximum processing temperature for TGDDM/44DDS system using continuous reactor method.

The advancement of continuous reactors in this field is very promising and will lead to new avenues for mixing and blending a broad array of co-reactants, thermoplastics, nanoparticles with epoxy matrices due to better control over rheology, shear states, and reactor design advantages.

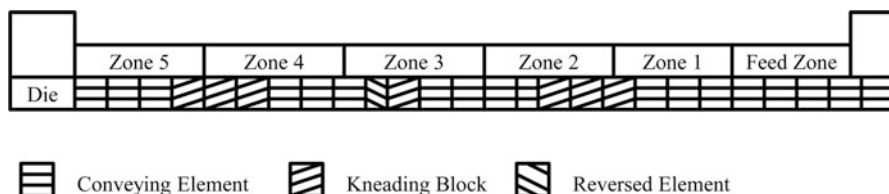


Fig. 10 Screw configuration of the continuous polymerization reactor for epoxy/thermoplastic prepolymer blends (Reproduced with permission from John Wiley and Sons)

Nonmechanical Methods

There are many nonmechanical methods used for material mixing while not all of them are designed for epoxy/thermoplastic blending. One of the examples is the sonication which is known for effective nanoparticle dispersion. It applies ultrasound energy through ultrasonic batch or ultrasonic probe to agitate particles in solution or polymer melt and result in the separation of individualized nanoparticles from the bundles. However, it is too powerful to blend epoxy and thermoplastic due to the degradation and therefore is out of the scope in this chapter.

Solvent Casting

Solvent casting has been the main technique to fabricate thin-layered polymer films since the early nineteenth century. It consists of dissolution of the ingredients in a volatile solvent and then evaporation of the solvent through suitable drying devices. Compared to melt mixing process, solvent casting exhibits higher mixing quality, thinner film, lack of residual stresses, and higher purity and clarity (Ricklin 1983). In addition, the solution or polymer film is exposed to relatively low thermal or mechanical stress throughout the entire production process. As a result, degradation or side reactions are insignificant.

There are numerous literatures concerned with the mixing of epoxy and thermoplastics using solvent-casting techniques (Bucknall et al. 1994; Mustata and Bicu 2006; Hourston et al. 1997). In a typical process, the epoxy resins and curatives are dissolved in a solvent such as dichloromethane with low boiling temperature of 39.6 °C. Thermoplastics are then added to the resin/curative solution under stirring. After homogeneously mixed, the solution is heated to the boiling temperature of solvent to remove most of the solvent and then poured into a preheated mold set at a temperature with a reasonable viscosity for casting. The residual solvent is further removed by degassing under vacuum. The solvent-free mixture is fully cured into final products at elevated temperature. The unique advantage of solvent casting for preparing epoxy/thermoplastic blends is to produce an epoxy solution with greatly reduced viscosity which aids thermoplastic mixing and improves the resin processability.

Although adding the thermoplastic to epoxy resins is made easier by the use of a solvent, it does cause problems. The evaporation and degassing of the solvent prior to the use of the resin is time consuming. Furthermore, solvent is hard to be fully removed from the mixture. Any residual solvent acts as a plasticizer for the polymer and has noticeable effects on the modulus of the final resin matrix. Last but not least, extensive use in solvent makes the process less commercially attractive and less environmentally friendly. As a consequence, solvent-casting method is often limited in laboratory-scale experiments instead of industrial scale manufacturing.

Resonant Acoustic Mixer

Resonant acoustic mixer (RAM) is a relatively new non-contact mixing approach to disperse and distribute materials within a broad range of viscosities. It relies upon the application of low-frequency and high-intensity acoustic field throughout the entire mixing vessel to facilitate fast mixing. This differs from traditional mixers such as batch mixers or continuous mixers where the mixing only occurs at the localized region near the tips of mixing blades. Figure 11 shows the laboratory-scale resonant acoustic mixer and its schematic mixing mechanism. The mixer device includes three major components: the mixing vessel, the plate, and the spring-mass system which is composed of multiple springs and masses. During its operation, the springs and masses move simultaneously by applying an external force and initiate oscillation of the system. At a particular oscillating frequency, the inertia force of the masses is offset by the stored force in the springs, allowing transferring of the mechanical energy created by the mixer to the materials in the vessel via the propagation of acoustic pressure wave. This in turn causes the micro-mixing cells throughout the vessel with a mixing cell length around 50 μm as indicated in Fig. 11. The particular oscillating frequency is adjusted according to the properties of the materials to be mixed and normally set at 60 Hz. The only controllable parameter of the RAM mixer is the mixing intensity which determines the amplitude of the mechanical oscillation.

There has been no peer-reviewed publications about the application of RAM technology. According to the limited information provided by the Resodyn Acoustic Mixers, Inc., RAM mixer is capable of mixing various types of materials, which include liquid-liquid, liquid-solid, gas-liquid, and solid-solid systems with viscosities ranging from 100 to 100,000,000 centipoises. The temperature increase during mixing caused by the acoustic resonance is insignificant. Vacuum can be applied to eliminate the bubbles being trapped during mixing. RAM mixer also tends to be cost and time saving through the substantial reduction in mixing times and the elimination of time and costs associated with cleanup. All these characteristics of RAM mixer are of extreme interest for a broad range of industries that involves material mixing, in particular for mixing epoxy/thermoplastic blends. It has the potential to be used for scale-up manufacturing. More and more attention is expected to be devoted to this interesting technology.

In Situ Polymerization

Approaches for preparing epoxy/thermoplastic blends described so far have been primarily focused on homogeneously dissolving thermoplastic polymers into epoxy resins with or without the aid of solvent. This is a semi-interpenetrating polymer network (semi-IPN) technique that blends two polymers by entangling the molecular chain of thermoplastic polymers to an epoxy network without chemical bonding between them. The formation of the semi-IPN structure allows to homogeneously blend the epoxy matrix and thermoplastic polymer in a molecular level or to microscopically disperse the thermoplastic in epoxy matrix. However, all of

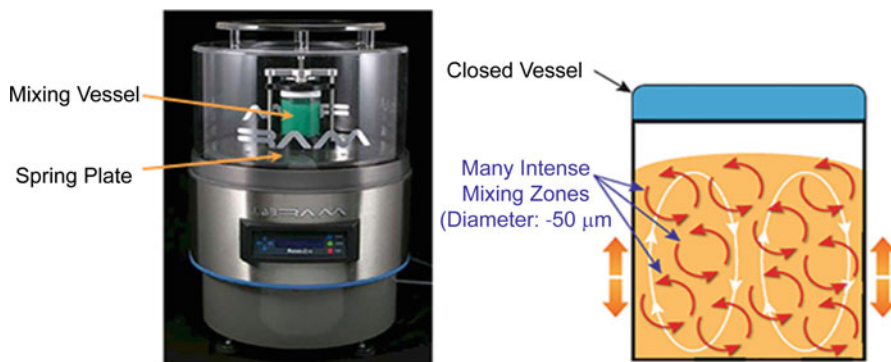


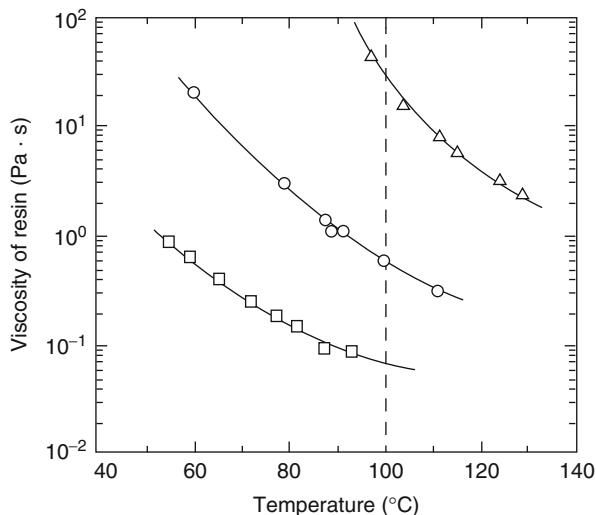
Fig. 11 Laboratory-scale resonant acoustic mixer and schematic showing the resonant acoustic mixing process (Courtesy: Resodyn Acoustic Mixers, Inc.)

those approaches face the same problem: the increased viscosity caused by incorporation of thermoplastic reduces epoxy resin processing window, especially when epoxies are used for applications such as wet-lay-up laminating process and resin infusion process. The resin viscosities for those processes need to be sufficiently low to provide controlled resin flow and self-adhesion and is typically in the range between 1,000 and 10,000 centipoises.

Recently, attempt was made to address this problem by using in situ polymerization technique. The in situ polymerization method is very similar to the simultaneous interoperating polymer network technique (SIPN) except one of the polymer architectures is not a cross-linking network. The thermoplastic monomers, polymerization activators, and curatives are firstly mixed with the epoxy monomers. The polymerization reactions of thermoplastics and cure reactions of epoxies are carried out simultaneously but by noninterfering reactions. Thermoplastic polymer is formed during the cure process of the epoxy resin by radical polymerization. K. Mimura (Mimura et al. 2001) prepared epoxy/thermoplastic blends using the in situ polymerization method. Thermoplastic polymer was prepared by homogeneously dissolved *N*-phenylmaleimide (PMI), benzyl methacrylate (BzMA), and styrene (St) monomers in DGEBA resin and phenol curatives at their cure temperature of 100 °C. As soon as the accelerator 1-isobutyl-2-methylimidazol (IBMI) and initiator 2, 5-dimethyl-2, 5-bis (benzoyl peroxy) hexane were added and dissolved, the mixture was rapidly poured into glass molds and fully cured in the oven. During cure process, thermoplastic polymers were quickly formed through radical polymerization of PMI/BzMA/St monomers and separated from epoxy matrix via reaction-induced phase separation.

Since the thermoplastic was formed during the cure process of epoxy resin, it avoids any increase in viscosity at the time of mixing and molding. Figure 12 shows the viscosities of the neat resin composed of epoxy and phenol curative, the resin containing PMI/BzMA/St monomers, and the resin modified with a thermoplastic polymer which had been previously polymerized with approximately the same molecular weight as the one obtained by the in situ polymerization. The viscosity

Fig. 12 Effect of addition of vinyl monomers or thermoplastic polymer on the viscosity of epoxy resins before curing. ○ unmodified resin. □ resin containing vinyl monomers (PMI/BzMA/St = 5/5/3 in molar ratio; content: 23.6 wt.%); Δ resin modified with the thermoplastic polymer 23.6 wt.% (Reproduced with permission from Elsevier)



of the neat resin composed only of the epoxy and the curatives was 550 centipoises at 100 °C. When thermoplastic polymer was added to the resin using conventional mixing method, the viscosity became very high and was about 28,000 centipoises. In contrast, when the monomers were added, the viscosity of resin containing these monomers was only 65 centipoises at 100 °C, decreasing to about one-eighth of the neat resin and several orders of magnitude lower than the one containing thermoplastic polymer prepared by conventional technique.

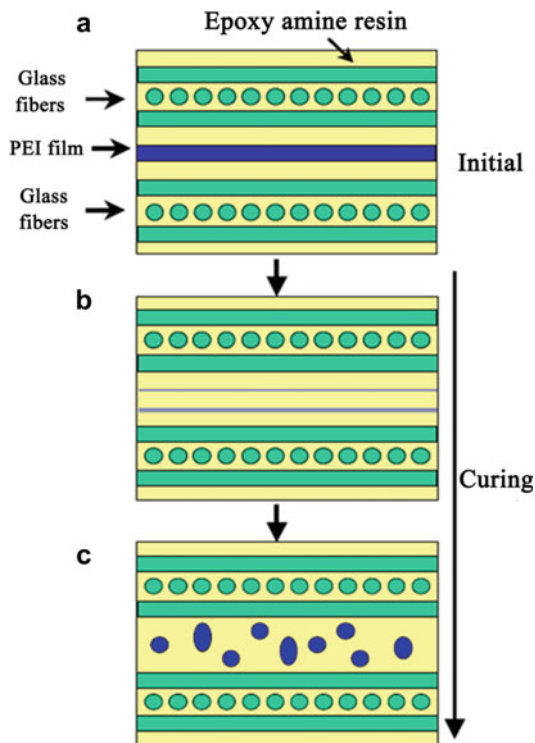
In situ polymerization method, however, has a certain limitation. During thermoplastic polymerization, the growth of thermoplastic molecular weights can be hindered by the increased viscosity of epoxy matrix upon cure and completely suppressed when system is vitrified. As a result fast-cured epoxy systems are impractical to use considering its short gelation and vitrification time.

In Situ Dissolution

In order to overcome viscosity increase in the traditional thermoplastic-toughening strategy used for prepreg-based composite, a novel in situ dissolution method is recently proposed by M. Naffakh et al. (2006). In this method, polyetherimide (PEI) thin films were firstly prepared using solvent casting. Alternative layers of glass fibers and thermoplastic PEI films were then put into a mold. The epoxy reactive mixture was injected into the heated mold using resin transfer molding process (RTM) to form the prepreg structure.

During the cure process, several physic-chemical events take place in a sequential way including epoxy impregnation, in situ dissolution of the thermoplastic film, epoxy cure reaction, and subsequent phase separation as schematically illustrated in Fig. 13. The important factors allowing these event sequences are the cure reaction

Fig. 13 RTM processing based on the in situ dissolution of epoxy/PEI blends: (a) insertion of a PEI film in between fiber plies, (b) dissolution of the PEI film and polymerization processes, and (c) generation of a PEI-dispersed phase from a reaction-induced phase separation and final curing of the epoxy matrix (Reproduced with permission from Elsevier)



kinetics of epoxy, initial solubility of thermoplastics, evolution of rheology, and the onset of reaction-induced phase separation. The PEI thermoplastic films need to be readily dissolved by the reactive resin at the early stage of cure where no phase separation occurs. Studies of dissolution time versus film thickness have proved that thermoplastic film with a thickness below $20\ \mu\text{m}$ is necessary to ensure thermoplastic layers readily dissolving into the resin matrices (Cicala et al. 2009). Subsequently, the reaction-induced phase separation is initiated by epoxy cure reaction and yields an epoxy/thermoplastic thin layer in the interply regions with desired phase-separated morphology to prevent crack prorogation. The formed epoxy/thermoplastic thin layer, so-called interleaf, can lead to similar morphology and mechanical properties compared to the system prepared via the traditional method. In addition, the viscosity increase caused by adding thermoplastic is appropriately addressed without changing any of the processing aspects of the RTM method.

Conclusion

In this chapter, an overview about the techniques used for preparation of epoxy/thermoplastic blends was provided. As discussed, the majority of epoxy/thermoplastics blends are mechanically mixed in batch mixers and continuous mixers.

The selection of batch or continuous mixers depends on material physical states, mixing quality and efficiency, handling equipment, energy consumption, and labor cost.

It is understood that mixing thermoplastic with epoxy resins inevitably increased resin viscosity. Liquid low-shear batch mixers are preferred to use when preparing epoxy/thermoplastic blends with a relatively low thermoplastic content. For the blends with a high amount of thermoplastic, especially when thermoplastics form a continuous matrix phase, highly viscous mixers such as internal mixers or twin-screw extruders are often used. In addition, compared to batch mixers, continuous mixers based on twin-screw extruders offer more modularity to handle different types of components and chemistries. Because of this unique advantage, they can be used as continuous reactors to produce curable epoxy/thermoplastic blends in a one-step approach.

Nonmechanical methods are also an important routine to prepare epoxy/thermoplastic blends. Solvent casting is a simple and effective method for mixing thermoplastic with epoxy but is often limited in laboratory-scale experiments due to cost, safety, and environment reasons. Some other novel techniques such as RAM technology, in situ polymerization, and in situ dissolution are very attractive since the processing issues caused by adding thermoplastic are appropriately addressed without significantly changing the manufacturing methods. However, it must be stressed that each method mentioned here has a strict requirement for chemistry and compatibility of selected epoxy and thermoplastic.

References

- Arias ML, Frontini PM, Williams RJJ (2003) Analysis of the damage zone around the crack tip for two rubber-modified epoxy matrices exhibiting different toughenability. *Polymer* 44:1537–1546
- Bennett GS, Farris RJ, Thompson SA (1991) Amine-terminated poly(aryl ether ketone)-epoxy/amine resin systems as tough high performance materials. *Polymer* 32:1633–1641
- Berg EA et al (1997) Melt-mixing thermoplastic and epoxy resin above T_g or T_m of thermoplastic with curing agent. US 6,197,898
- Blanco I, Cicala G, Costa M, Recca AJ (2006) Development of an epoxy system characterized by low water absorption and high thermomechanical performances. *Appl Polym Sci* 100:4880–4887
- Bouquey M, Loux C, Muller R, Bouchet G (2011) Morphological study of two-phase polymer blends during compounding in a novel compounder on the basis of elongational flows. *J Appl Polym Sci* 119:482–490
- Brown SB, Orlando CM (1988) *Encyclopedia of polymer science and engineering*. Wiley, New York
- Bucknall CB, Partridge IK (1983a) Addition of polyethersulfone to epoxy resins. *Br Polym J* 15:71–75
- Bucknall CB, Partridge IK (1983b) Phase separation in epoxy resins containing polyethersulphone. *Polymer* 24:639–644
- Bucknall CB, Gomez CM, Quintard I (1994) Phase separation from solutions of poly(ether sulphone) in epoxy resins. *Polymer* 35:353–359

- Butta E, Levita G, Marchetti A, Lazeri A (1986) Morphology and mechanical properties of amine-terminated butadiene-acrylonitrile/epoxy blends. *Polym Eng Sci* 26:63–73
- Cai C, Shi Q, Li L, Zhu L, Yin J (2008) Grafting acrylic acid onto polypropylene by reactive extrusion with pre-irradiated PP as initiator. *Radiat Phys Chem* 77:370–372
- Chandran CS, Muller R, Bouquey M, Serra C, Thomas S (2015) Effect of blend ratio and elongation on the morphology and properties of epoxy resin- poly(trimethylene terephthalate) blends. *Polym Eng Sci* 55:1679–1688
- Chang L, Friedrich K, Ye L, Toro P (2009) Evaluation and visualization of the percolating networks in multi-wall carbon nanotube/epoxy composites. *J Mater Sci* 44:4003–4012
- Cheng X, Wiggins JS (2014) Continuous reactor preparation of thermoplastic modified epoxy-amine prepolymers. *Polym Int* 63:1777–1784
- Choe Y, Kim M, Kim W (2003) In situ detection of the onset of phase separation and gelation in epoxy/anhydride/thermoplastic blends. *Macromol Res* 11:267–272
- Cicala G, Recca G, Ziegmann G, Niemeyer S (2009) Development of thermoplastic interleaf films which build up a controlled morphology for toughening of rtm resins. In: 17th international conference on composite materials, Edinburgh, pp 51–57
- Constantin F, Fenouillot F, Guillaume JL, Koeing R, Pascault JP (2003) Blends of a new thermoplastic in a thermoset epoxy matrix. *Macromol Symp* 198:335–344
- Di Liello V, Martuscelli E, Musto P, Ragosta G, Scarinzi GJ (1994) Toughening of highly crosslinked epoxy resins by reactive blending with bisphenol A polycarbonate. II. Yield and fracture behavior. *J Appl Polym Sci* 32:409–419
- Finnigan B, Martin D, Halley P, Truss R, Campbell K (2004) Morphology and properties of thermoplastic polyurethane nanocomposites incorporating hydrophilic layered silicates. *Polymer* 45:2249–2260
- Girard-Reydet E, Vicard V, Pascault JP, Sautereau HJ (1997) Polyetherimide-modified epoxy networks: influence of cure conditions on morphology and mechanical properties. *J Appl Polym Sci* 65:2433–2445
- Gojny FH, Wichmann MHG, Köpke U, Fiedler B, Schulte K (2004) Carbon nanotube-reinforced epoxy-composites: enhanced stiffness and fracture toughness at low nanotube content. *Compos Sci Technol* 64:2363–2371
- Hourston DJ, Lane JM (1992) The toughening of epoxy resins with thermoplastics: 1. Trifunctional epoxy resin-polyetherimide blends. *Polymer* 33:1379–1383
- Hourston DJ, Lane JM, Zhang HX (1997) Toughening of epoxy resins with thermoplastics: 3. An investigation into the effects of composition on the properties of epoxy resin blends. *Polym Int* 42:349–355
- Inoue T (1995) Reaction-induced phase decomposition in polymer blends. *Prog Polym Sci* 20:119–153
- Ishii Y, Ryan AJ (2000) Processing of poly(2,6-dimethyl-1,4-phenylene ether) with epoxy resin. 1. Reaction-induced phase separation. *Macromolecules* 33:158–166
- Izawa S, Toyama K (1973) Glass fiber reinforced thermoplastic resinous composition. US 3,763,088
- Kim HC, Char KH (2000) Effect of phase separation on rheological properties during the isothermal curing of epoxy toughened with thermoplastic polymer. *Ind Eng Chem Res* 39:955–959
- Kim JK, Robertson RE (1992) Toughening of thermoset polymers by rigid crystalline particles. *J Mater Sci* 27:161–174
- Kim BS, Chiba T, Inoue T (1995) Morphology development via reaction-induced phase separation in epoxy/poly(ether sulfone) blends: morphology control using poly(ether sulfone) with functional end-groups. *Polymer* 1:43–47
- Kingsley D, Cheng X, Yang J, Wiggins JS (2012) Continuous polymer reactor design for prepreg epoxy matrix prepolymers. In: International SAMPE technical conference, Charleston
- Ma Z, Stanford JL, Dutta BK (2009) Reaction kinetics of epoxy resin modified with reactive and nonreactive thermoplastic copolymers. *J Appl Polym Sci* 112:2391–2400

- May C (1988) *Epoxy resins: chemistry and technology*. Marcel Dekker, New York
- Mimura K, Ito H, Fujioka H (2000) Improvement of thermal and mechanical properties by control of morphologies in PES-modified epoxy resins. *Polymer* 41:4451–4459
- Mimura K, Ito H, Fujioka H (2001) Toughening of epoxy resin modified with in-situ polymerized thermoplastic polymers. *Polymer* 42:9223–9233
- Moad G (1999) The synthesis of polyolefin graft copolymers by reactive extrusion. *Prog Polym Sci* 24:81–142
- Moribe T (2012) Advanced intermeshing mixers for energy saving and reduction of environmental impact. *Mitsubishi Heavy Ind Technol Rev* 49:38–43
- Mustata F, Bicu I (2006) Synthesis, characterization, and properties of multifunctional epoxy maleimide resins. *Macromol Mater Eng* 29:732–741
- Naffakh M, Dumon M, Gerard JF (2006) Study of a reactive epoxy–amine resin enabling in-situ dissolution of thermoplastic films during resin transfer moulding for toughening composites. *Compos Sci Technol* 66:1376–1384
- Oyama HT (2009) Super-tough poly(lactic acid) materials: reactive blending with ethylene copolymer. *Polymer* 50:747–751
- Park SJ, Kim HC (2001) Thermal stability and toughening of epoxy resin with polysulfone resin. *J Polym Sci B Polym Phys* 39:121–128
- Rauwendaal C (1981) Analysis and experimental evaluation of twin screw extruders. *Polym Eng Sci* 21:1092–1100
- Rauwendaal C (1998) *Polymer mixing, a self-study guide*. Carl Hanser Verlag, Munich
- Repecka LN (1988) Slurry-mixed heat-curable resin systems having superior tack and drape. US 5,747,615
- Ricklin S (1983) Solvent cast films. *Plast Eng* 39:29–33
- Salahudeen SA, Elleithy RH, Alothman O, Alzahrani SM (2011) Comparative study of internal batch mixer such as cam, banbury and roller: numerical simulation and experimental verification. *Chem Eng Sci* 66:2502–2511
- Shokoohi S, Arefazer A, Naderi G (2011) Compatibilized polypropylene/ethylene–propylene–diene–monomer/polyamide6 ternary blends: effect of twin screw extruder processing parameters. *Mater Des* 32:1697–1703
- Sultan JN, McGarry FJ (1973) Effect of rubber particle size on deformation mechanisms in glassy epoxy. *Polym Eng Sci* 13:29–34
- Tadmor Z, Gogos CG (2006) *Principles of polymer processing*. Wiley, New York
- Titier C, Pascault JP, Taha M, Rozenberg BJ (1995) Epoxy-amine multimethacrylic prepolymers, kinetic and structural studies. *J Polym Sci A* 33:175–184
- Titier C, Pascault JP, Taha M (1996) Synthesis of epoxy–amine multiacrylic prepolymers by reactive extrusion. *J Polym Sci A* 59:415–422
- Utracki LA, Wilkie C (2002) *Polymer blends handbook*. Springer, New York
- White JL, Bumm SH (2011) *Encyclopedia of polymer blends, volume 2, processing*. Wiley, New York
- Williams RJJ, Rozenberg BA, Pascault JP (1997) Reaction-induced phase separation in modified thermosetting polymers. *Adv Polym Sci* 128:95–156
- Xanthos M (1992) *Reactive extrusion: principles and practice*. Hanser, Munich
- Yu Y, Wang M, Foix D, Li S (2008) Rheological study of epoxy systems blended with poly(ether sulfone) of different molecular weights. *Ind Eng Chem Res* 47:9361–9369
- Zhang J, Guo Q, Fox BL (2009) Study on thermoplastic-modified multifunctional epoxies: influence of heating rate on cure behavior and phase separation. *Compos Sci Technol* 69:1172–1179
- Zhang J, Yang T, Lin T, Wang CH (2012) Phase morphology of nanofibre interlayers: critical factor for toughening carbon/epoxy composites. *Compos Sci Technol* 72:256–262

Miscibility, Phase Separation, and Mechanism of Phase Separation in Epoxy/Thermoplastic Blends

17

Fenghua Chen, Yan Zhang, Tongchen Sun, and Charles C. Han

Abstract

Reaction-induced phase separation in the epoxy/thermoplastic (TP) blends has received considerable interests since the early 1980s. Phase separation studies mostly focused on the miscibility, phase separation mechanism, and morphology formation in the various epoxy/TP systems and processing conditions. This is peculiarly important, since there are still some disagreements on the mechanisms when the traditional understandings of phase separation kinetics are used to explain the phase evolution and unique nodular structure in the present reactive systems. In the existing published work, sea-island, bicontinuous, and nodular structures were mostly reported. It seems that majority of the morphology formation analysis can reach some kind of agreement; however, questions have been raised again and again whenever consistent morphology and performance relationship cannot be obtained or reached. In this chapter, some of the

F. Chen

Laboratory of Advanced Polymer Materials, Institute of Chemistry, Chinese Academy of Sciences, Beijing, China

e-mail: fhchen@iccas.ac.cn

Y. Zhang

College of Engineering, and National Engineering and Technology Research Center of Wood-based Resources Comprehensive Utilization, Zhejiang Agriculture and Forestry University, Hangzhou, China

T. Sun

Aerospace Special Materials and Processing Technology Institute, Beijing, China

C.C. Han (✉)

Beijing National Laboratory for Molecular Sciences, State Key Laboratory of Polymer Physics and Chemistry, Joint Laboratory of Polymer Science and Materials, Institute of Chemistry, Chinese Academy of Sciences, Beijing, China

Institute for Advanced Study, Shenzhen University, Guangdong, China

e-mail: c.c.han@iccas.ac.cn

previous reports were briefly reviewed and a more complete three-dimensional view of the phase structure evolution, including the combined in situ optical microscope and light scattering observation and comprehensive information on *xy* plane and *z* directions of the whole sample, was introduced. The significant difference between molecule mobility and dynamics of the epoxy oligomers and TP polymer chains was noticeable. Consequently, dynamically asymmetric phase separation was found useful for the discussion of phase separation kinetics of the epoxy/TP systems, which made the nodular structure formation and volume fraction of the TP-rich phase understandable. Layered structure and gradient morphology ubiquitously formed during the cross-linking reaction of many thermoset/thermoplastic systems, which was considered useful for interlamellar toughening or inter-parts adhesion applications.

Keywords

Dynamically asymmetric phase separation • Layered structure • Volume shrinking • Bicontinuous • Fractured surface • Light scattering

Contents

Introduction	488
DGEBA/DDS/PSF System	495
Curing Reaction	495
Phase Separation Process and Volume-Shrinking Phenomena	496
Phase Separation Mechanism	505
DGEBA/DDS/FPI System	507
Ubiquitous Nature of the Layered Structure Formation	513
Influences of the Molecular Weight and T_g of the TP	514
Curing Agent Variations	517
Conclusions	518
References	518

Introduction

In the 1980s, Bucknall CB et al. used a polyethersulfone to modify the tetraglycidyl diamminodiphenyl methane (TGDDM) epoxy (Bucknall and Partridge 1983), in order to overcome the shortcomings caused by the rubber modifier. From then on, many thermoplastic (TP) species, including polystyrene (PS), poly(methyl methacrylate) (PMMA), poly(2,6-dimethyl-1,4-phenylene ether) (PPE), polyether ether ketone (PEEK), polyetherimide (PEI), polysulfone (PSF), polyethersulfone (PES), etc., have been introduced into the epoxy composites. In the epoxy/rubber blends, sea-island morphology generally formed and toughness was successfully enhanced based on the cavitation of rubber-rich particles (Yee et al. 2000). In the epoxy/thermoplastic blends, sea-island and the inverted structures, i.e., nodular structure, were normally observed at the relatively low and high TP concentrations (if soluble). In between, bicontinuous structure was

expected, while dual morphology (continuous epoxy-rich matrix and TP-rich separate phase, including smaller epoxy-rich domains inside) (Park and Kim 1996) was also obtained. The bicontinuous and nodular structures were considered to obtain excellent toughness for the epoxy/TP composites (Williams et al. 1997; Kinloch et al. 1994). However, the mechanical properties were not enhanced as much as expected (Hourston and Lane 1992; Cicala 2014). This was a puzzling problem when the academic knowledge was utilized to the industrial applications. In another sense, because of the featured characteristics also different from that of rubber blends, TP-rich domains may be glassy during phase separation in the epoxy/TP blends, as might play a key role for the morphology manipulation, and the mechanism of this kinetics was still an open question.

During the cross-linking process of the epoxy/TP composites, the TP is firstly required to be initially miscible with the epoxy monomers, in order for fine dispersion. Miscibility of the polymer blends was usually measured by the phase contrast microscope, scattering methods (Han and Akcasu 2011), differential scanning calorimeter (DSC), and dynamic mechanical analysis (DMA) techniques. Computational and modeling methods were also used to predict the compatibility between the various components (Lee 1999). In the epoxy/thermoplastic blends, compatibility between the components was changed with the cross-linking reaction of epoxy monomers into oligomers or even larger polymers. As predicted in the Flory-Huggins (FH) lattice model, the molecular weight increase of epoxy will reduce the mixing free energy. And phase separation occurs at a certain conversion range, which is dependent on the interaction parameter between the components of the specific systems. In order to understand the competition and synergistic effect between the reaction and phase separation, a kind of time-temperature-transformation cure diagram was proposed and organized (Enns and Gillham 1983, Simon and Gillham 1992). In the epoxy/TP blends, phase separation generally occurred after reaction started for a while, developed along with the reaction and slowed down and almost finished before gelation and/or vitrification of epoxy.

Williams et al. used an almost monodisperse PS to study the applicability of the FH model for modified thermosetting polymers (Zucchi et al. 2004). Considering the interaction parameter dependent on temperature and composition but independent of the molar mass, the FH model was confirmed versatile enough to fit the cloud-point curve (CPC) for the primary epoxy/PS solutions. According to the different miscibility of PS and PMMA in the epoxy matrix, these two thermoplastics can be successively segregated out from the matrix with the epoxy conversion increasing, and encapsulated PS/PMMA core-shell particles were formed (Galante et al. 2001). Considering the concentration dependence of the interaction parameter as predicted by Koningsveld (Solc and Koningsveld 1995; Ishii et al. 2003), the FH lattice theory successfully computed the binodal, spinodal, and critical points, which showed good agreement with experimental data of the epoxy/PS, epoxy/PES, and epoxy/PEI systems (Figueroa et al. 2008). However, polydispersity of the transient polymerization products was a common feature of the industrial epoxy systems, where both the entropic contribution to the free energy of mixing and the variation of interaction parameter with conversion should be considered during the

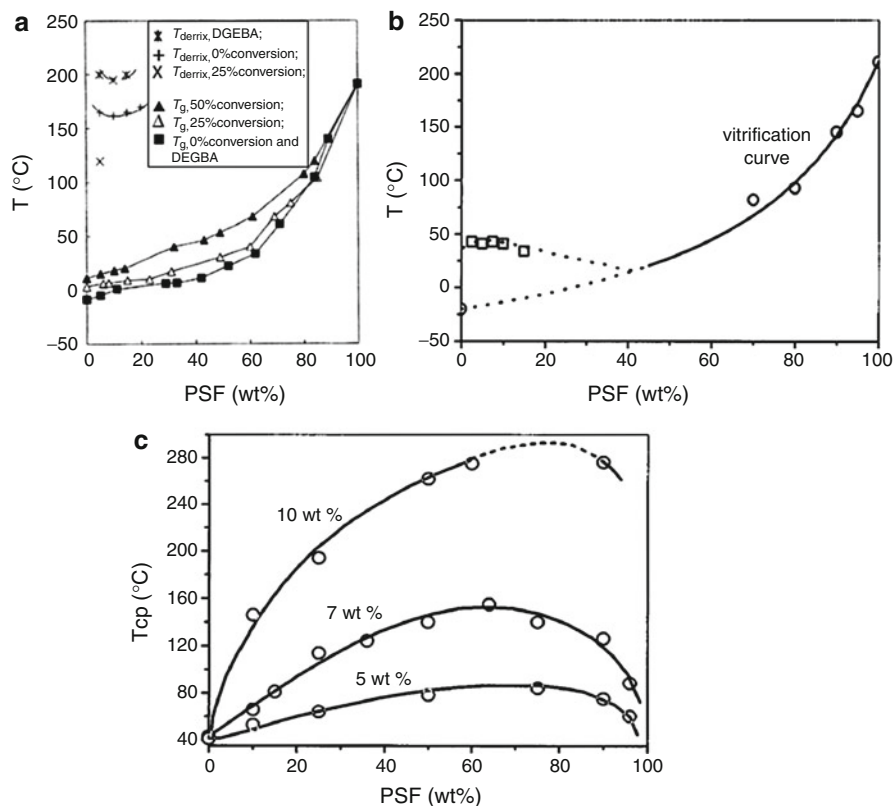


Fig. 1 (a) Phase diagram of PSF in mixture of DGEBA/modified amine adducts. The *upper first curve* shows that of DGEBA/PSF (Reprinted from ref. de Graaf et al. 1995, with kind permission by Prof. Martin Möller). (b) Cloud-point curve (CPC) and vitrification curve in epoxy/PEI blends. (c) Cloud-point temperature (T_{cp}) of epoxy/PSF/PEI blends, containing 5, 7, and 10 wt.% total thermoplastics ((b) and (c) are reprinted from ref. Giannotti et al. 2004, with kind permission from Prof. Patricia Oyanguren and John Wiley and Sons)

CPC analysis (Williams et al. 1997). It has been reported that the epoxy/PEI systems typically showed upper critical solution temperature (UCST) behaviors (Girard-Reydet et al. 1998; Giannotti et al. 2004), while lower critical solution temperature (LCST) was reported for the epoxy/PSF system (de Graaf et al. 1995; Yoon et al. 1997; Giannotti et al. 2003). However, the UCST temperature of epoxy/PEI system was increased with the PSF addition, where no specific physicochemical interactions existed between PSF and PEI (Giannotti et al. 2004). As shown in Fig. 1, LCST of DGEBA/PSF was about 197 $^{\circ}\text{C}$; UCST of epoxy/PEI was around 40 $^{\circ}\text{C}$ (note: in the work of ref. Girard-Reydet et al. 1998, UCST of DGEBA/DDS/PEI was a little higher than 60 $^{\circ}\text{C}$), while in the system of epoxy/PSF/PEI, cloud-point temperature was greatly increased with PSF addition. In these studies, the asymmetrical shape of phase diagram was commonly agreed due to the low

molecular weight (MW) of epoxy monomers (similar as the solvent) and high MW of the TP polymer (similar as the solute).

With the reaction proceeding, molecular weight of epoxy kept increasing. The TP was firstly miscible with and then segregated from epoxy after the induction time. Academic studies on such a reaction-induced phase separation (RIPS) (Inoue 1995) in the epoxy/TP blends included the phase separation mechanism, morphology, performance, and relationship between these aspects, which are consistent and can be correlated with known polymer physics. Pascault et al. studied the in situ RIPS of epoxy/PEI blends through the small-angle X-ray scattering and light scattering techniques (Girard-Reydet et al. 1998). Depending on the initial PEI concentration, different phase decomposition processes were observed. At PEI loadings close to the critical composition, the system was directly quenched to the unstable region and phase separation generally proceeded through the spinodal decomposition (SD) mechanism. Meanwhile nucleation and growth (NG) mechanism dominated the segregation process, when PEI loadings were much higher than the critical composition. In the epoxy/PES blend, Inoue T investigated the phase evolution and speculated the SD mechanism correlation with the interconnected globule formation at the relatively high PES loadings (Inoue 1995). Interestingly, experimental studies on epoxy/PEI at various epoxy conversions showed bimodal-type CPCs (Park and Kim 1996). Sea-island structure was speculated to form through NG at low PEI concentrations, while SD was ascribed as the mechanism for dual morphology and nodular structure obtained at the middle and high PEI concentrations. Phase diagram and light transmitting and scattering studies on the in situ evolving phase patterns were studied in these work. While phase separation mechanism seems not agreeing on the bicontinuous, dual, and nodular structure formation, it seems that the agreement and sometimes the disagreement may be caused by the variation or powerlessness of the simple phase diagram and traditional simple understanding of these separation kinetics, and more complicate combination between the thermodynamics and kinetics should be considered in the reactive systems.

In the nonreactive blend system, one can judge whether NG or SD mechanism works mainly according to the phase diagram and equilibrium coexistence curve predictions. For the reactive systems, the equilibrium phase diagram keeps on changing with the reaction proceeding. Phase diagram of epoxy monomer/TP binary or quasi-binary system may be obtained as the typical case. However, once reaction starts, critical point, including the corresponding temperature and concentration, starts to shift with the epoxy molecule size increasing. In the case when refractive index (RI) contrast between the phase domains allows for light scattering detection at the early stage of phase separation, mechanism can be temporally followed and discussed as NG or SD through light scattering measurements. However, different mechanisms were analyzed and discussed for the similar nodular structure formation in various systems (Xie and Yang 2001). The concepts of “phase inversion” and secondary phase separation were used as explanation for the morphology evolution, especially for the bicontinuous structure development and dual morphology formation. Phase inversion was also used to describe the morphology formed at the high TP concentrations, where nodular, interconnected

globule and spongelike or inverted structure were literally different but similarly explained in these reports. However, the use of 'phase inversion' concept diverged from its initial definition for phase evolution discussion by Tanaka (Tanaka 2000). For the secondary phase separation, it maybe corresponds to the appearance of another phase in the already existed phase domains (Clarke et al. 1996). The corresponding bimodal coexistence curves at different conversions were considered to quasi-thermodynamically cause this phenomenon (Park and Kim 1996). Kinetic studies on the interfacial quench and hydrodynamic effect (Tang et al. 2004) were also considered for the secondary phase separation analysis, which was similar as the double phase separation in the blended oligomers of ϵ -caprolactone and styrene (Tanaka 1994).

According to previous reports, it showed that TP loadings and curing temperature, i.e., volume fraction and quench depth, were the key factors to construct the final morphology, whereas phase separation process study was more straightforwardly used to understand morphology transformation and relationship between initial phase domains and the final structure. The in situ light transmission, light scattering, and small-angle X-ray scattering techniques have been extensively useful for such investigations. Besides, analysis based on the characteristic features of the components was necessary in the explanation of the phase separation mechanism (Jyotishkumar et al. 2013; Zhang et al. 2011). Li et al. investigated the viscoelastic phase separation (VPS) in various epoxy/TP blends and noticed the cage effect of the slow PES or PEI component during the reaction-induced phase separation process. Because of the slow molecule chain relaxation of the TP, bicontinuous morphology can be formed when the TP loadings were relative low. This phenomenon was closely related to the dynamic asymmetry, which can be caused by the large difference in molecule size and chain length and different T_g values of the components (Gan et al. 2003; Yu et al. 2004).

Viscoelastic phase separation was systematically studied in various polymer solutions, polymer blends, and colloidal systems (Tanaka 1993, 2000). The moving droplet phase (MDP) and phase inversion phenomena are typical examples of VPS, as shown in the PS/diethyl malonate (DEM) solutions at low and critical PS concentrations, respectively. The MDP showed much smaller growth rate than the usual case dominated by the Brownian coagulation mechanism. MDP formation was also observed in the reaction-induced phase separation of the 4-chlorostyrene/silicone oil blends (Wang et al. 2005). Because of the elastic gel ball-like behavior, the moving droplets arranged into a regular array like a crystal. The so-called phase inversion was defined as a process, where the DEM solvent phase firstly appeared at the early stage but transformed to become the matrix at the late stage, while the PS slow component phase appeared through phase inversion. The transient PS-rich network retained under the bulk stress of its elastomer nature. This phase was elongated and broke under the shear stress and force balance conditions. The phase inversion process is a unique feature of the viscoelastic phase separation. The viscoelasticity effect on phase separation has been noticed during the dynamics study in the entangled polymer solutions, where dynamic coupling between the stress and diffusion was analyzed (de Gennes 1976). After that, the two-fluid model

was introduced (Doi and Onuki 1992) and modified to describe the viscoelastic model (Tanaka 2000):

$$\frac{\partial \phi}{\partial t} = -\nabla \cdot (\phi v) - \nabla \cdot [\phi(1 - \phi)(v_1 - v_2)] \quad (1)$$

with the volume-average velocity v being

$$v = \phi v_1 + (1 - \phi)v_2 \quad (2)$$

v_1 and v_2 are the average velocities of components 1 and 2, respectively.

$$\nabla \cdot v = 0 \quad (3)$$

$$v_1 - v_2 = -\frac{1 - \phi}{\zeta} \left[\nabla \cdot \Pi - \nabla \cdot \sigma^{(1)} + \frac{\phi}{1 - \phi} \nabla \cdot \sigma^{(2)} \right] \quad (4)$$

where ζ is the friction constant and Π is the osmotic stress tensor.

$$\rho \frac{\partial v}{\partial t} \cong -\nabla \cdot \Pi + \nabla p + \nabla \cdot \sigma^{(1)} + \nabla \cdot \sigma^{(2)} \quad (5)$$

Here, ρ is the density, p is a part of the pressure, and σ is the total stress tensor and composed of the shear stress σ^S and bulk stress σ^B as $\sigma = \sigma^S + \sigma^B$. σ^j follows the upper-convective Maxwell-type equation:

$$\frac{\partial \sigma^j}{\partial t} + (v \cdot \nabla) \sigma^j = D \cdot \sigma^j + \sigma^j \cdot D^T - \frac{\sigma^j}{\tau_j(\phi)} + G_j(\phi)(D + D^T) \quad (6)$$

$$D = \nabla v_r \quad (7)$$

For the shear and bulk relaxation modulus,

$$G_j(\phi, t) = G_j(\phi) \exp[-t/\tau_j(\phi)] \quad (8)$$

Here, τ_j is the stress relaxation time, $j = S$ is for shear or B for bulk, and $G_j(\phi(\mathbf{r}))$ is the local elastic plateau modulus at \mathbf{r} (after coarse-graining).

$$\sigma^S = \sigma^S - \frac{1}{d} \text{Tr}(\sigma^S) I \quad (9)$$

$$\sigma^B = \frac{1}{d} \text{Tr}(\sigma^B) I \quad (10)$$

The above equations were derived solely on the basis of the two-fluid model, without assumption about any specific system, and they should be general for all dynamic asymmetry analysis. The basic concept is that molecule mobility depends on the chain relaxation and thus different velocities are caused by the different

molecule size or chain dynamic relaxation times. For the reaction-induced phase separation of the epoxy/TP system, this dynamic asymmetry is dependent on the curing time, with which the mobility and friction constant continuously changed. Phase separation is induced after the reaction starts for a while, when the system is featured with the small epoxy molecules and large-sized TP polymers. It indicates that only the slow TP component can support the elastic stress at this stage. Velocity of epoxy prepolymers is fairly high, and hydrodynamic flow must occur. The epoxy molecular weight gradually increases with the reaction proceeding; however, this MW cannot be very high till the gelation, and the dynamic asymmetry always exists during the phase separation process. For the micrometer or submicron wavelength fluctuation occurrence at the early stage of phase separation, i.e., bicontinuous phase domains formation in the VPS, the strong dynamic asymmetry and hydrodynamic flow will inevitably influence the phase evolution and morphology construction.

In the early literatures, phase separation competition with reaction and gelation was mostly considered, where the probable completeness of phase separation before gelation was discussed. In recent years, VPS was introduced for the discussion in the epoxy/TP systems; interesting cage effect of the slow TP component was observed and interpreted. Phase evolution at the critical concentrations and nodular structure formation at the relative high (but much lower than the usual symmetric systems) TP loadings were more apprehensible than before. However, the discussion on morphology formation did not reach an agreement. The structure-performance relationship was left as an open question. In the epoxy/rubber blends, rubber modifier usually shows low T_g ; the dynamic relaxation of long rubber molecule chains can follow or be faster than phase separation rate. That is why sea-island structures were mostly observed and the structure-correlated performance was successfully established in the epoxy/rubber systems (Williams et al. 1997; Zhang et al. 2014a). If one wants to construct nodular structure in the epoxy/rubber, low curing temperature is needed so that viscoelastic nature of rubber can be expressed (Inoue 1995). While in the epoxy/TP systems, several distinct factors should be considered. On the one hand, molecule size of epoxy continuously increases and phase diagram accordingly shifts, which makes the thermodynamic driving force the crucial factor for phase separation, varying during the evolution. On the other hand, high glass transition temperature (T_g) and MW of TP should be carefully considered. Besides the gelation and vitrification of epoxy reaction, physical gelation and/or vitrification of TP also exist in the reaction and phase separation of epoxy/TP system (Jyotishkumar et al. 2013). TP polymer chains need much time to relax while the epoxy monomers and prepolymers show good fluidity. In this sense, dynamic asymmetry and hydrodynamic flow will inevitably become important during the phase separation process. Meanwhile, it is still a challenge for the systematic structure-performance analysis in these epoxy/TP blends. When observations on the cross section covered the whole sample (Hourston and Lane 1992; Giannotti et al. 2005), including the edge information, bubbles, and/or impurities, complementary information were obtained and all-around analysis can be made, which may then give a clue for all of the inconsistencies previously

reported. In this chapter, phase separation study in the epoxy/polysulfone and epoxy/polyimide systems was introduced. Several other examples were also briefly described for a systematic understanding on the phase separation mechanism.

DGEBA/DDS/PSF System

Taking the blending of epoxy (bisphenol A diglycidyl ether (DGEBA), with epoxide equivalent weight of 189), polysulfone (PSF, $M_n = 38,000$ g/mol, $T_g = 183$ °C), and curing agent 4,4'-diaminodiphenyl sulfone (DDS) as the example, the reaction between DGEBA and DDS was in complicate multisteps: reaction between primary amine and epoxide group produced secondary amine, while reaction rate of secondary amine with epoxide group was greatly influenced by curing temperature and conversion degree (Tanaka and Mika 1973; Min et al. 1993). Molecular weight of the epoxy oligomers gradually increased and semi-binary system was assumed for the discussion. The correlation between curing reaction, phase separation evolution, and mechanism was considered and revealed (Zhang et al. 2011).

Curing Reaction

To study the curing reaction of the reactive blend, DSC measurement was utilized and reaction mechanism was found unchanged with the addition of PSF. Conversion value decreased as PSF fraction was increased, implying the depression effect of PSF on the curing reaction. Dilution of the functional groups was considered as the main reason for this influence. Although the low molecular weight and low T_g ensured a good fluidity of epoxy at the early stage of reaction, the PSF molecules decreased the concentration of DGEBA and DDS and thus decreased the transport efficiency of the epoxy molecules and possibly the chemical reaction rate (Bonnet et al. 1999a, b). Meanwhile, the slow molecule chain relaxation of the PSF may also contribute to the retardation of the reaction. Because of the high T_g , the PSF chains should have a much slower dynamic relaxation in both diffusion process and stress relaxation. With PSF content increasing, viscosity of the whole system was increased, and the actual reaction rate decreased more. The former dilution effect was a static average effect, while the latter was a dynamic transportation process and may be correlated with the morphology.

According to Eq. 11, conversion at the various curing times (α_t) was about 41% and 59% after the sample was cured at 130 °C for about 200 and 300 min, respectively (Fig. 2):

$$\alpha_t = \frac{H_0 - H_r}{H_0} \quad (11)$$

where H_0 is the total area of the exotherm and H_r is the residual heat.

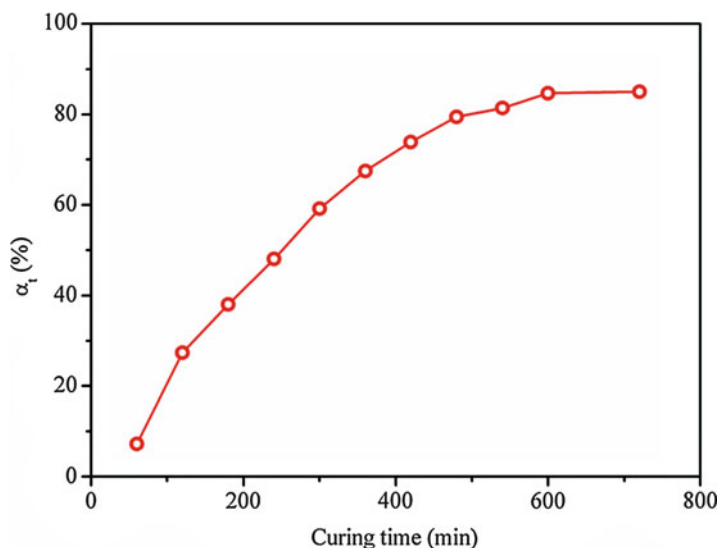


Fig. 2 Conversion (α_t) at various curing time for $w = 0.15$ cured at 130°C . The open symbols are related to the experimental data points and *solid lines* are only to guide the eyes

According to the gelation theory deduced by Flory (Flory 1953), gelation in this system would occur at the epoxy conversion $\alpha_t = 0.65$. Also molecular weight of epoxy gradually increased as the curing reaction progressed and could not be very high before gelation occurred. During this period, the reaction was controlled by the reaction kinetics but not by the monomer diffusion process. As the molecular weight of epoxy was increasing with the curing reaction, phase separation could also start to happen and the phase separation time was around 200 min or earlier, as shown below, which meant that phase separation for this blend can complete before gelation and the slow dynamic of PSF became very important during the phase separation process.

Phase Separation Process and Volume-Shrinking Phenomena

Several typical concentrations, at weight fraction of PSF $w = 0.10$, 0.15 , and 0.20 , were chosen for the phase separation study. The time-resolved light scattering (TRLS) technique is effectively used to follow the onset and development of phase separation process. Typical scattering patterns, $I(q)$, of phase separation information were obtained after a certain induction time. The TRLS curves of $w = 0.10$ and 0.20 were similar in shape, while that of $w = 0.15$ was different. As shown in Fig. 2, for the sample at $w = 0.10$, phase separation occurred at $t = 170$ min, with the maximum scattering intensity (I_m) locating at peak scattering wave number $q_m = 3.8 \mu\text{m}^{-1}$, while for $w = 0.20$, it occurred at about $t = 210$ min and $q_m = 3.5 \mu\text{m}^{-1}$. Then in both cases, q_m and I_m gradually changed in a similar

way: q_m moved slowly toward the smaller wave number and simultaneously I_m became stronger and stronger, which showed the coarsening process of the phase-separated domains. In the late period, q_m changed very slowly, while I_m began to decrease slightly, which was probably caused by RI matching between the phase domains. This was reasonable since RI of epoxy was increasing as the MW of epoxy increased, approaching the RI of PSF. Finally, q_m and I_m did not change any more due to gelation or vitrification of the system. Variation of q_m at different times was summarized in one plot, q_m vs. t , shown in the right lower part of Fig. 3a, c. In this asymmetrical system, self-similarity was absent and conventional analysis of q_m variations based on the scaling law (such as $q_m = t^{-\alpha}$ (Hashimoto et al. 1986)) was not applicable. Evolution behavior of q_m was found to be a Maxwell-type relaxation mode and showed an exponential decay function (Gan et al. 2003).

$$q_m = q_0 + A_0 \exp[-(t - t_0)/\tau] \quad (12)$$

where A_0 is the magnifier, t_0 is the onset time of phase separation, and τ is the relaxation time of the phase separation. At $t = \infty$, $q_m = q_0$, q_0 corresponds to the dimension of the final structure at gelation or vitrification. Good fitting of this empirical equation to the experimental data and the inherent characteristics of the present system showed the viscoelastic effect (dynamic asymmetry) dominated the phase separation process. When PSF content increased, the system would be more viscous, so the relaxation of polymer chains became slower and the relaxation time τ became longer.

For the sample at $w = 0.15$, the TRLS patterns were relative complicate and the Maxwell-type viscoelastic relaxation model $q_m \sim t$ relationship was not applicable any more, as shown in Fig. 3b. Phase separation occurred at $t = 227$ min with the scattering peak q_m at around $1.6 \mu\text{m}^{-1}$. When phase separation has begun, I_m increased slowly with time, while the change of corresponding q_m was not obvious at this time range. Subsequently, I_m became stronger and stronger with q_m gradually decreasing, which illustrated the development of phase separation and coarsening of phase structures. However, at $t = 241$ min, another scattering peak was observed at smaller wave number $0.42 \mu\text{m}^{-1}$. Then the intensities, I_m , of the two peaks slowly decreased and their q_m were also decreasing with time increasing, corresponding to the RI-approaching phenomenon. However, from $t = 355$ min on, the two scattering peaks seemed to have merged into one peak, with the location and intensity almost fixed in the following process. Since $q \sim 2\pi/L$, where L denotes the dimension of structures, evolution of the scattering peaks indicated that larger domains were formed after the phase separation developed for a certain time. The large domains coexisted with the smaller domains (the initial one) for a while. Then the two size scale domains merged together or one of them disappeared. Finally, only the domains in one size scale can be detected. This phenomenon seems puzzling at this point, but after more detailed phase contrast optical microscope (PCOM) observation and scanning electron microscope (SEM) studies on the cross section of the sample are carried out, physics of this phase separation mechanism can be explained and understood.

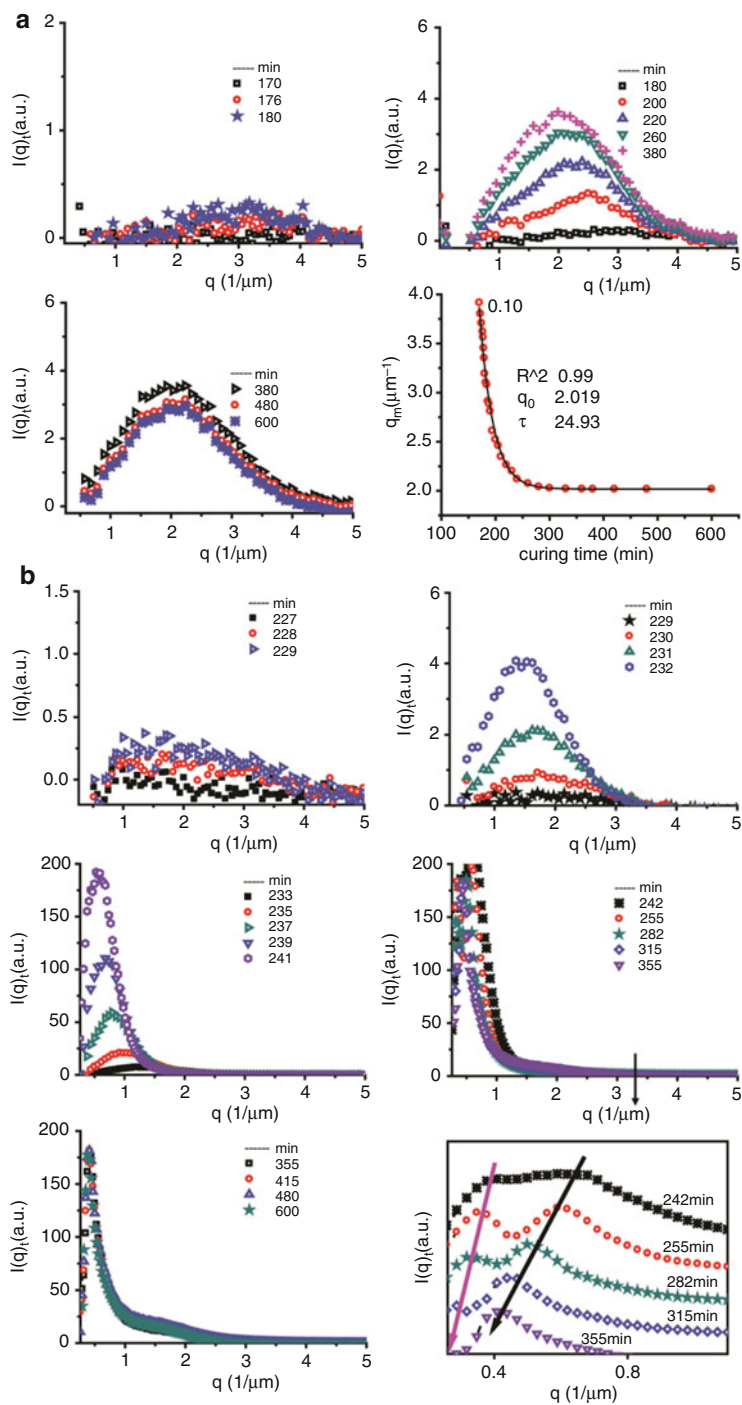


Fig. 3 (continued)

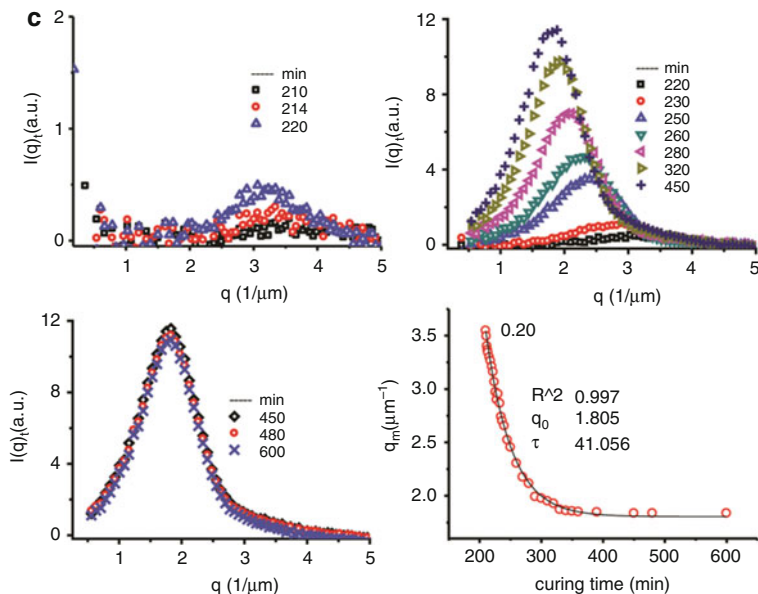


Fig. 3 Variation of light scattering pattern and the corresponding q_m versus time plots for the samples $w = 0.10$ (a), 0.15 (b), and 0.20 (c) cured at $130\text{ }^\circ\text{C}$ (*au* arbitrary unit for scattering intensity). The *right* last pattern of (b) is the magnification of the scattering peaks at the corresponding times, where each curve is vertically shifted for apparent comparison. In the *right lower* pattern of (a) and (c), the *circled points* and the *real line* correspond to the experimental data and the result simulated by $q_m = q_0 + A_0 \exp[-(t - t_0)/\tau]$, respectively (Reprinted from ref. Zhang et al. 2010, 2011, with kind permission from Elsevier (Copyright 2010, for 2b) and American Chemical Society (Copyright 2011 for 2a and 2c))

PCOM observation focused on the middle depth of the sample was presented in Fig. 4. After the sample $w = 0.15$ was placed at $130\text{ }^\circ\text{C}$ for about 170 min, phase separation was observed. With reaction and phase separation continuing, phase structures grew in size slowly. The morphological structure was gradually discerned as bicontinuous and further coarsened. From $t = 205$ min on, many large domains quickly formed, continuously grew in size (up to $20\text{--}30\text{ }\mu\text{m}$), coalesced, and converged into channels, corresponding to the double-peak phenomenon as illustrated in Fig. 3b. However, at about 320 min, the large domains left from the visual field. After $t = 360$ min, when gelation of the epoxy curing reaction has occurred, the morphological structure was fixed completely.

Here it should be noted that the onset time of phase separation obtained from TRLS and PCOM measurement was reasonably different, considering the experimental uncertainties and resolution differences. Meanwhile development of the morphologies obtained was relatively consistent. Time intervals for the morphology development were consistent in these two methods. After phase separation was observed for $w = 0.15$, it developed in the usual phase-separated structures firstly.

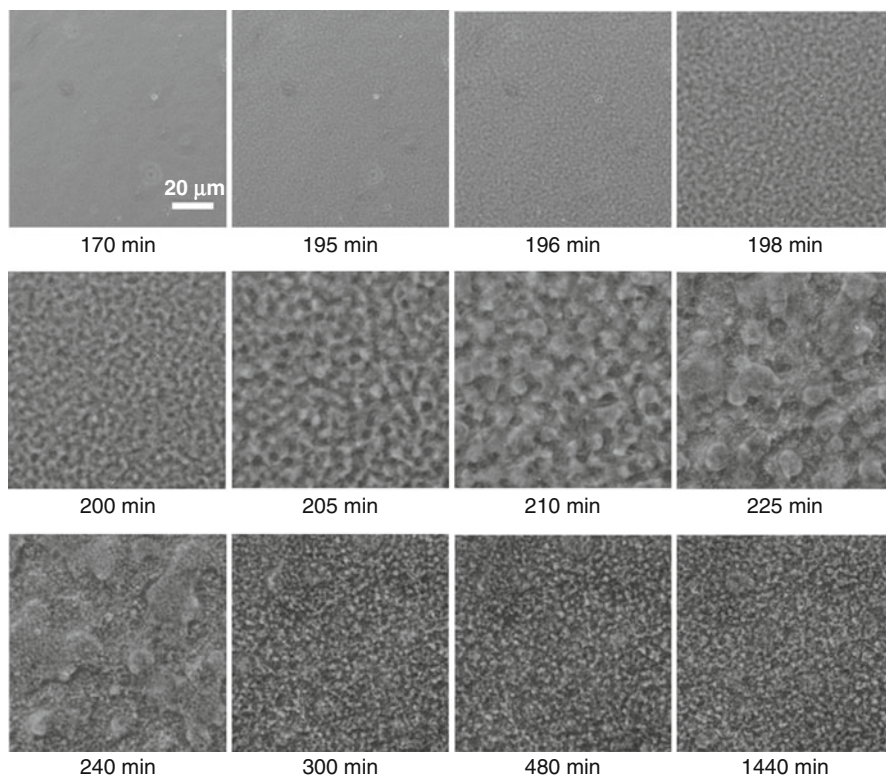
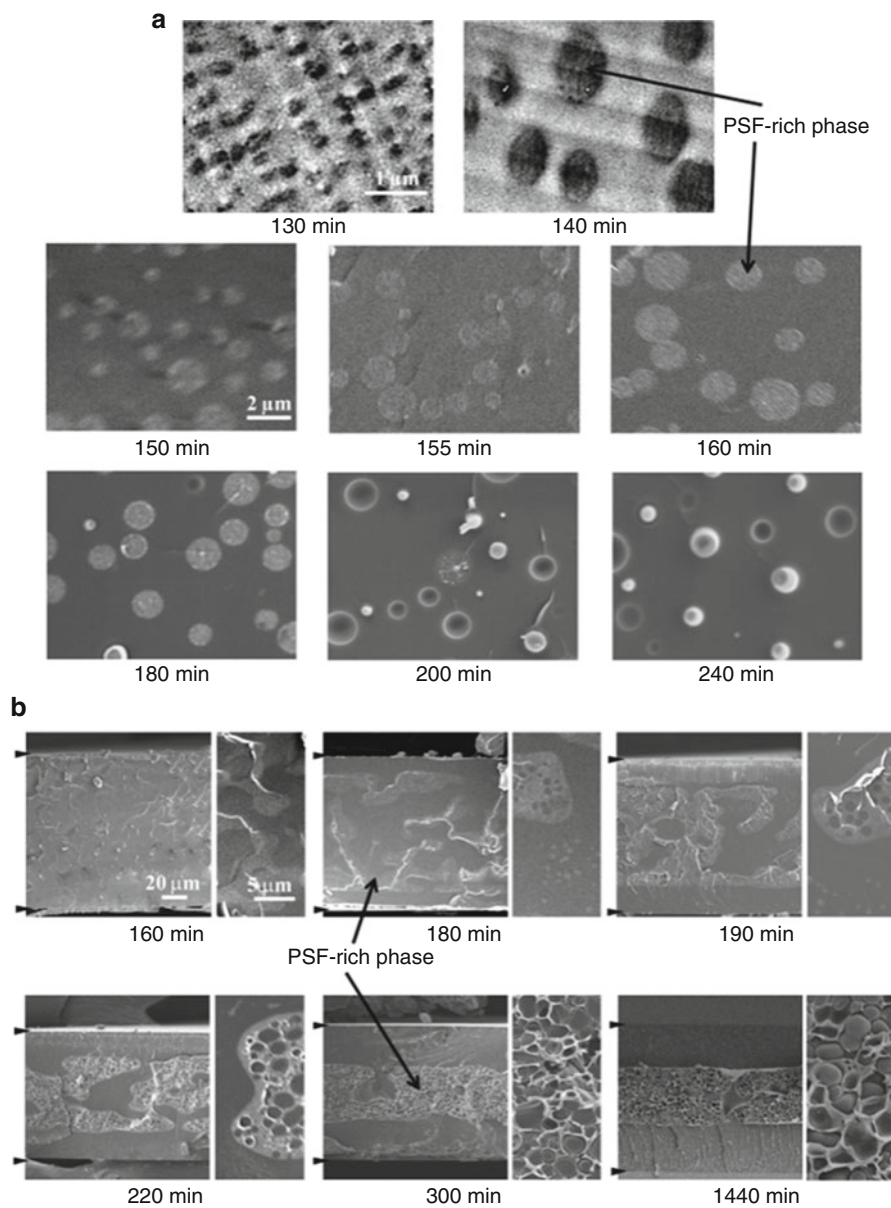


Fig. 4 PCOM images of sample $w = 0.15$ cured at $130\text{ }^{\circ}\text{C}$, with observation focusing on the middle depth (Reprinted from ref. Zhang et al. 2010, with kind permission from Elsevier, Copyright (2010))

The bicontinuous structure coarsened for about 20 min (~ 14 min for TRLS and ~ 26 min for PCOM) and then rapid coalescence occurred to form large domains. The large domains, even up to $20\text{--}30\text{ }\mu\text{m}$ size, coexisted with the small domains, around several microns, in the following long period (~ 127 min for TRLS and more than 130 min for PCOM observation). Then the large domains disappeared from the PCOM observation of the middle part, as corresponded to the disappearance of the smaller scattering peak in the TRLS measurement.

In order to understand the distinct phase separation evolution of the three samples, it is necessary to study the information in z direction, which is normal to the xy plane observed in PCOM, and complementary data will be obtained for the analysis. In this sense, the SEM information of the samples cured at different time intervals was critically important. The puzzling question on the large domain development in PCOM observation will be answered in the fractured surface images as shown in Fig. 5b. For the sample $w = 0.15$, at the beginning of phase separation, homogeneous structure formed in the whole sample film and the bicontinuous structure was discerned clearer and clearer. In the following process,

**Fig. 5** (continued)

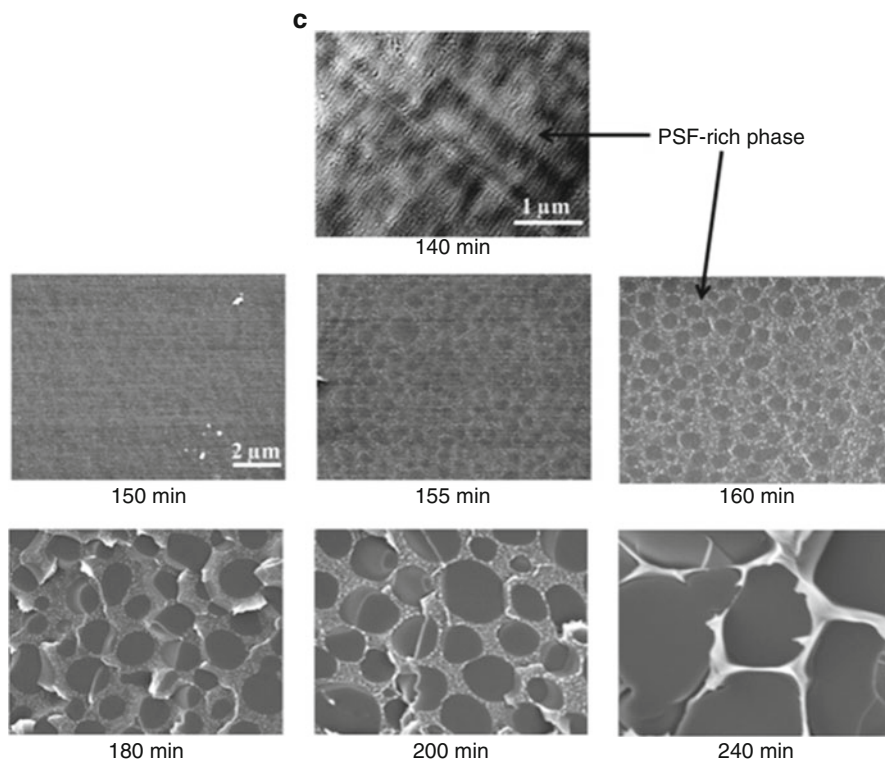


Fig. 5 Electron micrographs of the fractured surfaces for the sample $w = 0.10$ (a), 0.15 (b), and 0.20 (c). Pictures in the first row of pattern (a) and (c) are the TEM micrographs, while the others are SEM images. Pictures on the *right* in each panel of (b) are higher magnifications for the middle part of the sample. PSF-rich phase is indicated by the *solid line* with *arrow* to guide eyes (Reprinted from ref. Zhang et al. 2010 and 2011, with kind permission from Elsevier (Copyright 2010, for 4b) and American Chemical Society (Copyright 2011 for 4a and 4c))

both PSF- and epoxy-rich phases were more and more concentrated. About 20 min later, it was surprise to observe a three-layered structure on the fractured surface. The upper and lower layers were mainly epoxy-rich and relatively thin. The middle layer was constructed with bicontinuous phase structure, where some large epoxy-rich domains (tens of microns) were remarkably residing in between the PSF-rich continuous phase and small epoxy-rich dots (several microns or smaller) existed inside of the PSF-rich domains. The PSF-rich phase was more and more aggregated, moving to the center part of the film. Volume fraction of the PSF-rich phase was decreasing, and the kinetic process is described as “volume shrinking” (Tanaka 2000). The large epoxy-rich domains gradually reduced their volume fraction in the middle part, while thickness of the outer layers was spontaneously increasing in the following more than 100 min. Before gelation of the epoxy resin occurred, the continuous PSF-rich phase continued to shrink and the epoxy-rich phase could

gradually flow to the outer layer. Finally, three parallel layers were formed in the sample film. Images at $t = 300$ and 1440 min were very similar, which means that the phase separation was almost complete before the gel point at about $t = 360$ min. If the large epoxy-rich domains did not flow out before the gelation occurred, they could be trapped in the middle layer, contributing to the remaining bicontinuous structure.

As shown in the TRLS description at lower and higher concentrations, viscoelastic phase separation was dominant in these blends. The transmission electron microscope (TEM) and SEM images in Fig. 5a, c at different curing intervals also supported this speculation. At the early stage of phase separation, uniformly distributed spherical PSF-rich particles were observed with the average diameter of 200 nm. These particles grew in size slowly. About 30 min later, the PSF-rich particles would not grow but shrink instead. Volume fraction of the PSF-rich phase kept decreasing with time and the contrast and interface between PSF- and epoxy-rich phases became more and more pronounced. The epoxy gradually transferred from the PSF-rich phase to the epoxy-rich matrix and each phase was more and more concentrated. From $t = 200$ min on, the PSF-rich particles were rigid enough to maintain their shape during the fracture process. The particle size changed very slowly in the subsequent process. Similar phenomenon of volume shrinking was observed for the sample at $w = 0.20$. The epoxy-rich phase was quickly found to be droplets after the phase separation was observed, while PSF-rich phase kept continuous. With the phase separation continuing, epoxy-rich droplets gradually grew in size, while the PSF-rich phase decreased its volume fraction and became a network. During this period, with the shrinking of the slow dynamic PSF-rich phase, epoxy-rich phase diffused out and caused the PSF-rich network walls to become thinner and thinner. At a certain time, percolation of the epoxy-rich phase happened under the stress field of the network and the epoxy-rich droplets can be interconnected. If morphology at short curing time is frozen, partially interconnected epoxy-rich particles may be observed. For even longer time, the nodular structure, i.e., interconnected irregular epoxy-rich globules, will form and morphology of the whole specimen will be fixed.

The dynamic asymmetry effect was considered to work at curing temperatures lower than the T_g of PSF 183 °C, while this effect also existed when the curing temperature became higher as long as the dynamic asymmetry was maintained (through the molecular weight). This was confirmed in Fig. 6, with the detailed structure varied. The higher the curing temperature was, the faster the epoxy molecular weight increased and mixing entropy decreased, and the less time for the occurrence of phase separation was available. When the sample was cured at $T_{\text{cure}} = 130$ °C, phase separation was observed by PCOM at $t_{\text{ps}} = 170$ min, while at $T_{\text{cure}} = 180$ and 200 °C, $t_{\text{ps}} = 20$ and 12 min, respectively. The bicontinuous structure might coarsen to be spongelike with PSF-rich network and interconnected epoxy-rich globules at higher curing temperatures. It should be attributed by the enhanced PSF-rich phase disentanglement, relaxation, and large epoxy-rich domains' rapid flow out. At higher curing temperatures, decreased PSF-rich particles, thinning middle layer, and enlarged epoxy-rich interconnected particles were resulted at

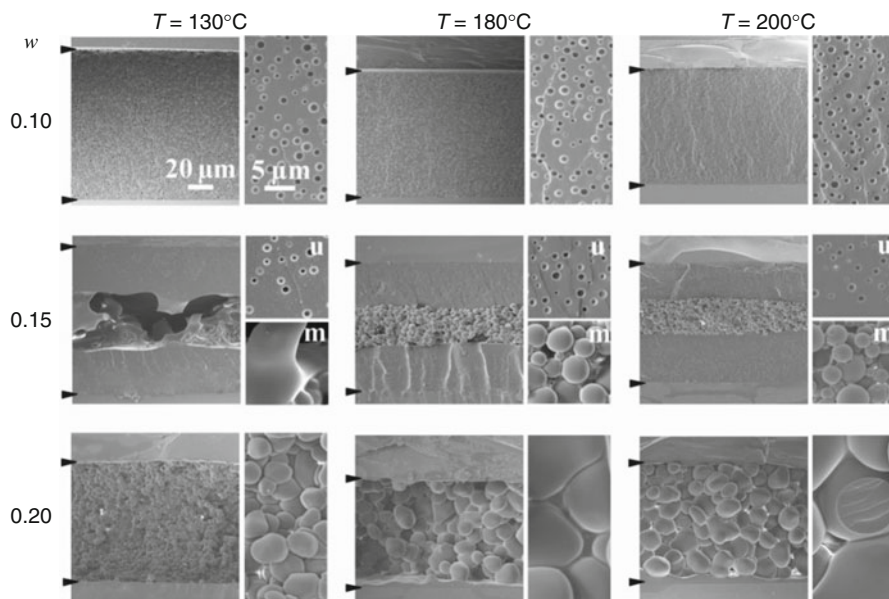


Fig. 6 SEM micrographs of fractured surfaces of epoxy/PSF samples, cured at various temperatures for 1440 min. *Right side* pictures in each panel are at the higher magnifications. For $w = 0.15$, the upper (*u*) and middle (*m*) parts are shown. Voids correspond to the PSF-rich domains (Reprinted from ref. Zhang et al. 2011, with kind permission from American Chemical Society, Copyright (2011))

lower, middle, and higher PSF loadings, respectively. Generally in this system, molecule chain relaxation was greatly enhanced for the PSF, hydrodynamic flow of the fast epoxy component was promoted, and phase separation proceeded further during the competition with curing reaction at higher temperatures.

The various composition ranges and their corresponding morphologies were summarized in Fig. 7. In the same composition range, similar morphological structures always formed at the experimental curing temperatures, no matter which were lower or a little higher than the $T_{g,PSF}$. That is to say, sea-island structure (I) and nodular structure (III) were obtained at low and high PSF weight fractions, respectively; three-layered structure (II) formed at the middle concentrations. It suggested that PSF-rich phase always behaved as a slow dynamic component at the various temperatures. When the curing temperature was increased, mobility of PSF was enhanced, which made the disentanglement of the PSF chains easier and phase segregate more easily. Therefore, periodical distance of final structures for both $w = 0.10$ and 0.20 increased, while the relative thickness of middle layer for $w = 0.15$ decreased with temperature increasing. And more complicate layered structure formed at higher temperatures for $w = 0.15$, since some parts of the PSF-rich network could be broken and most of the large continuous epoxy-rich phase could flow out under the stress field of the deformed PSF-rich network.

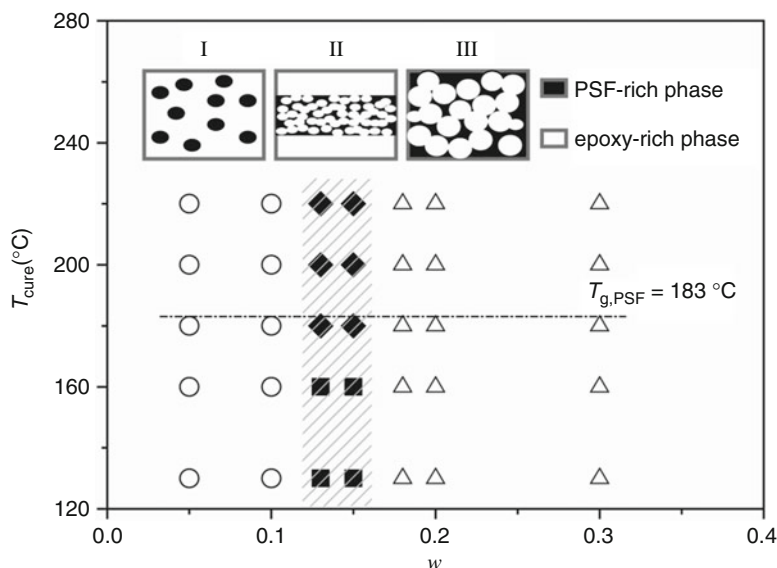


Fig. 7 The curing temperature (T_{cure}) and PSF weigh fraction (w) regions, where various morphological structures are observed: *I*, sea-island structure (\circ); *II*, three-layered structure (\blacksquare), three-layered coexisting with sea-island structure (\blacklozenge); *III*, nodular structure (\triangle). The *dashed line*, corresponding to the $T_{g,\text{PSF}}$, was only to guide the eyes. The *shadowed area* shows the region where three layers can be observed. Model morphologies are mapped correspondingly in the *top* of the Figure (Reprinted from ref. Zhang et al. 2011, with kind permission from American Chemical Society, Copyright (2011))

Phase Separation Mechanism

In this system, viscoelastic properties between the components were quite different, especially at the beginning of phase separation. The PSF has a high molecular weight and high glass transition temperature, while both molecular weight and glass transition temperature of epoxy were very low at the early stage of phase separation. With reaction and phase separation continuing, PSF- and epoxy-rich phases were both moving toward their more concentrated coexisting compositions. When the curing temperature (T_{cure}) is lower than $T_{g,\text{PSF}}$, PSF-rich phase would behave like glassy solid; at $T_{\text{cure}} > T_{g,\text{PSF}}$, PSF-rich phase would behave like a polymeric elastomer. At the same time, molecular weight of epoxy gradually increased, which could not be very high before gelation occurred. Compared with the PSF-rich phase, the epoxy-rich phase has a faster dynamics before it is gelled. Therefore, with various amounts of PSF added, dynamic asymmetry was always observed to dominate the phase separation process. On the one aspect, characteristic length which can be detected at the early phase separation stage was much larger than that in the dynamically symmetric phase separation. On the other aspect, this mechanism was characterized by the volume fraction change of the PSF-rich phase and was realized by the volume-shrinking process of the PSF-rich domains.

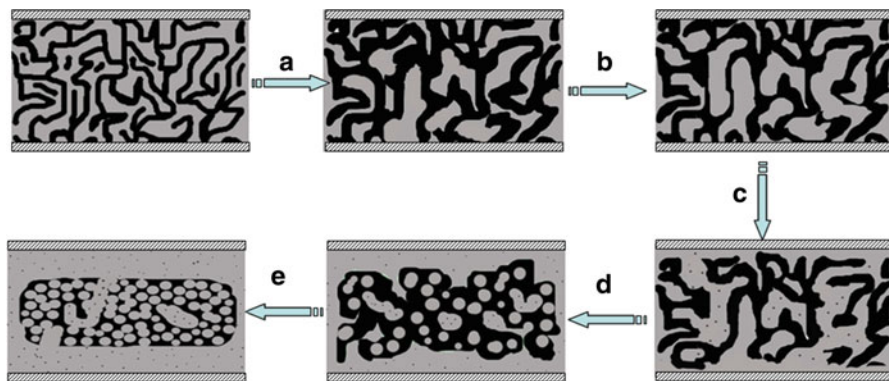


Fig. 8 Schematic model of the three-layered structure formation process. Epoxy-rich phase, ■ (gray); PSF-rich phase, ■ (dark). (a) Bicontinuous structure growing in size, (b) PSF-rich domains shrinking (becoming thinner and thinner), (c) epoxy-rich phase converging as channels, (d) large epoxy-rich domains flowing out, and (e) PSF-rich domains shrinking further toward the center (Reprinted from ref. Zhang et al. 2010, with kind permission from Elsevier, Copyright (2010))

After phase separation was observed, it developed in the normal (symmetric system) way firstly, although the time period could be very short. With phase separation proceeding, PSF concentration increased and thus its viscoelasticity also increased in the PSF-rich domains. Dynamic asymmetry began to control the phase separation dynamics and accordingly the growth of normal composition fluctuation was suppressed. Instead of continuous growing in size, the slow dynamic PSF-rich domains began to shrink and the fast dynamic epoxy-rich phase gradually diffused out. Volume shrinking of the PSF-rich domain continued until the phase separation was pinned. Finally, due to the gelation or vitrification of the system, the sea-island and nodular structures were obtained at low and high PSF concentrations, in the absence of the hydrodynamic flow regime as the usual viscoelastic phase separation. For the middle PSF concentration, the continuous PSF-rich phase kept shrinking, while collapse of the continuous epoxy-rich domains was realized and three-layered structure formed finally. The morphology variation could be illustrated in the cartoon shown in Fig. 8 (Zhang et al. 2010, 2014b). The bicontinuous structure initially formed and coarsened (Stage a–b). With decrease of the volume fraction, PSF-rich phase became thinning and shrinking. Due to the large molecular weight entangled polymer chain and elasticity of the network, the PSF-rich domains started to shrink inward. The low viscous epoxy-rich domains simultaneously flew under the negative driving force of Gibbs free energy and hydrodynamic flow driving force of the PSF-rich network shrinkage (Stage b–c). Relaxation of physically entangled PSF-rich network may also happen and cause some fractures in the network, which promoted the collapse and flow of the epoxy-rich domain (Stage c–e). This process continued until gelation of the epoxy component. And three-layered structure was finally pinned in this composite.

Since the PSF-rich phase always showed slower dynamical behaviors compared with the fast dynamics of epoxy-rich phase, the influence of dynamic asymmetry on

phase separation and final morphologies was always significant and the overall structures formed at any w were qualitatively similar and did not drastically change at different curing temperatures. However, for very low concentration (like $w = 0.10$), a tight entanglement network cannot be formed and the asymmetric phase separation behavior was less obvious. Also at any even higher temperatures, the fast extended curing reaction will make all behaviors similar to that of decreasing concentration of PSF.

DGEBA/DDS/FPI System

Polyimide is one kind of high-performance thermoplastics, with extremely high glass transition temperatures, and is expected to enhance the toughening property of the epoxy/TP blends. The fluorine polyimide (FPI) here was a product of the 2,2-bis(3,4-dicarboxyphenyl) hexafluoropropane dianhydride (6FDA) and 4,4'-methylenedianiline (MDA). M_n of the FPI was 2×10^4 g/mol and $T_g \sim 270$ °C. As in the phase separation mechanism discussed above, stronger dynamic asymmetry was expected for the epoxy/FPI system. Interestingly, the layered structure was observed in a wider concentration range of $0.14 \leq w \leq 0.21$, as shown in Fig. 9. At lower FPI concentration, e.g., $w = 0.10$, the FPI-rich phase formed discrete spherical domains, i.e., particles, with a relatively narrow size

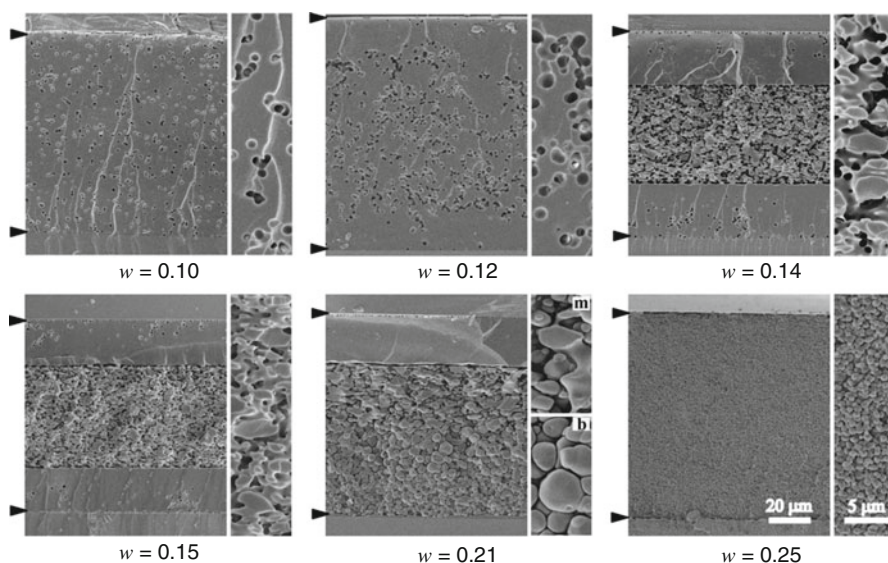


Fig. 9 SEM images of fractured surfaces of epoxy/FPI blends with different FPI weight fractions w . All samples were cured at 130 °C for 1440 min. For $w = 0.21$, the middle (m) and the bottom (b) parts are specially shown. THF etching removes the PI-rich domains, corresponding to the voids in the pictures (Reprinted from ref. Chen et al. 2008b, with kind permission from American Chemical Society, Copyright (2008))

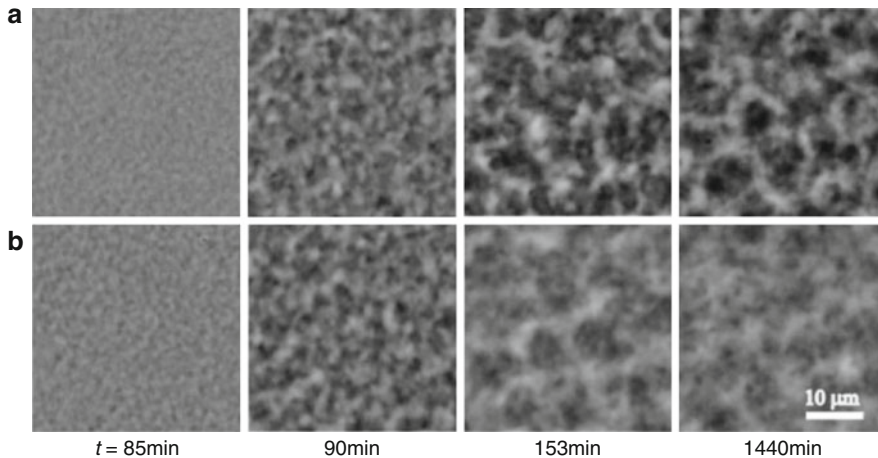


Fig. 10 PCOM in situ observation during epoxy/FPI $w = 0.15$ curing at $130\text{ }^{\circ}\text{C}$, (a) focusing on the middle depth and (b) lower part focusing on a point close to the *bottom* (Reprinted from ref. Chen et al. 2008a, with kind permission from John Wiley and Sons, Copyright (2008))

distribution. At higher concentrations, e.g., $w = 0.25$, FPI-rich phase formed continuous domains extending over the whole film thickness, and the epoxy-rich phase presented as the nodular structure (Chen et al. 2008a).

The layered structure was effectively observed by the SEM study on the fractured surface, as shown in the above context. If we want to in situ observe the phase evolution, confocal light scattering microscopy, PCOM observation on different focus depth, and TRLS techniques were extremely useful. No fluorescence signal could be detected in this system, and the latter two methods were used here. Phase separation was induced after the sample was cured for a certain period. Although it is difficult to distinguish the detailed structure, images at the middle and lower part showed similar patterns in the early period, as shown in Fig. 10. Phase structure gradually coarsened with the reaction proceeding. However, image at the lower part quickly became blurred, while the image at the middle depth remained relatively sharp and clear. The refractive index (RI)-matching between the two demixing phases, which was caused by the RI increase with reaction of epoxy, was also illustrated in the PCOM observation, as was not the main discussion here. Finally, the bicontinuous structure in the middle depth and blurred image at the lower part were fixed in the completely cured sample.

According to the TRLS results in Fig. 11, the scattering vector q_m , corresponding to the maximum intensity I_m , did not change in the early several minutes after the weak scattering pattern was detected, or the change was not observed due to the low scattered light intensity. Although contrast of the scattering pattern was relatively weak in Fig. 11a, characteristic phenomenon of spinodal decomposition could be found after the circular average integration. Time dependence of light scattering profiles, $I(q)_t$, showed that bicontinuous structure formed at the beginning of phase

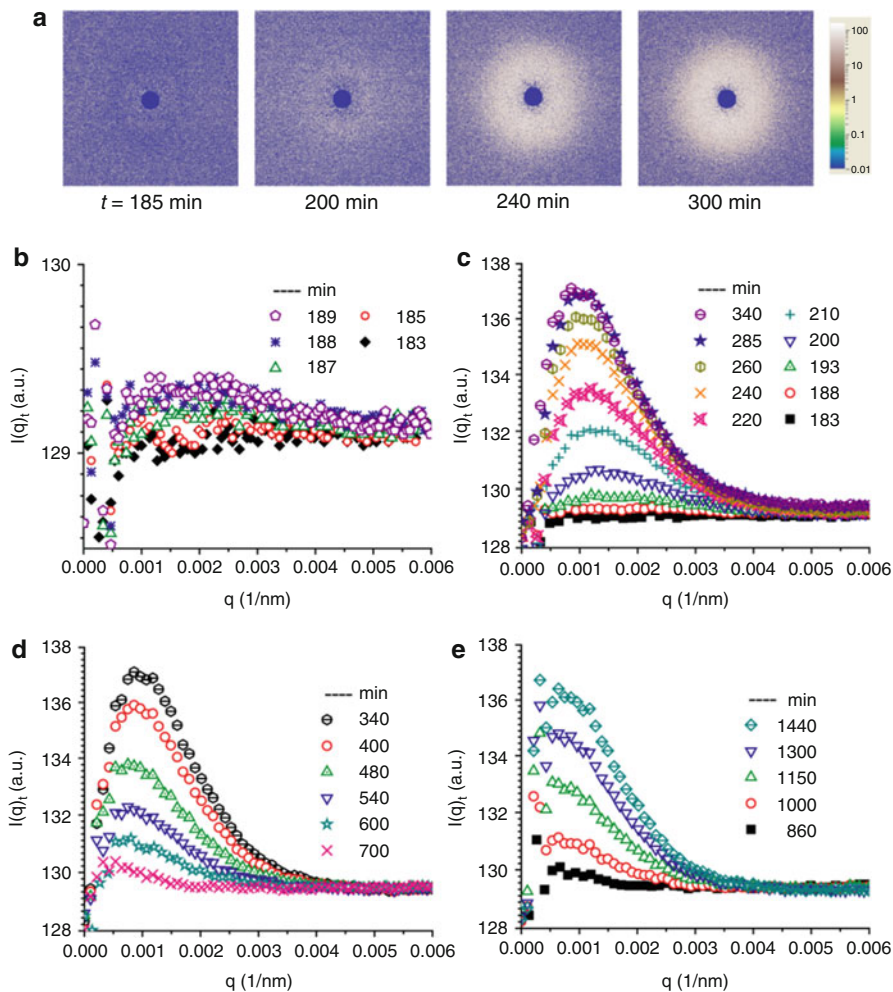


Fig. 11 Time-resolved light scattering pattern (a) and circular averaged intensity profiles (b–e) of the sample $w = 0.15$ cured at $115\text{ }^{\circ}\text{C}$ (au arbitrary unit) (Reprinted from ref. Chen et al. 2008b, with kind permission from American Chemical Society, Copyright (2008))

separation (Fig. 11b). Afterward, the scattering intensity became stronger; correspondingly, I_m gradually increased and q_m gradually decreased for about 1 h. Afterward, the scattering peak got broader than before and became a shoulder-like pattern with the I_m increasing and q_m decreasing (Fig. 11c). This phenomenon continued for tens of minutes and then I_m was observed to decrease with the q_m decreasing (Fig. 11d), which corresponded to the refractive index crossover of the two phase-separated phases. The TRLS pattern evolution here seemed different with that of epoxy/PSF system. The shoulder peak occurred long after the onset of phase separation, while double-peak evolution of epoxy/PSF was synchronized

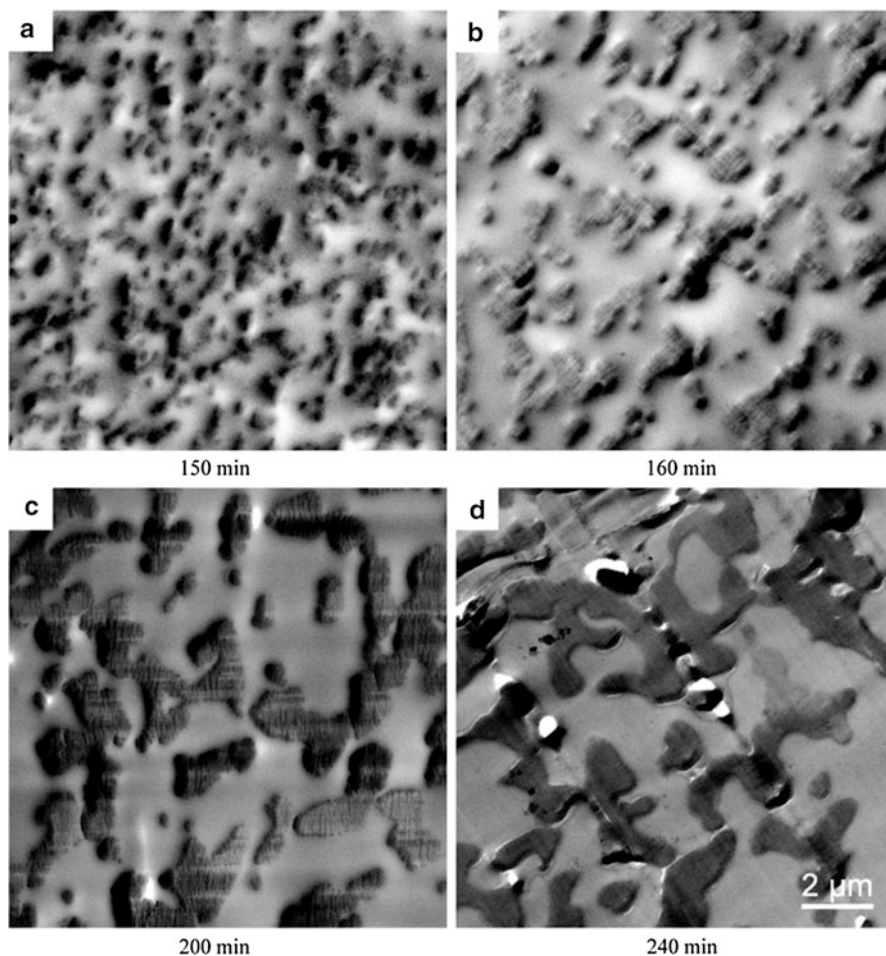


Fig. 12 Transmission electron micrographs of microtomed films of sample $w = 0.15$ cured at $115\text{ }^{\circ}\text{C}$ for short times (Reprinted from ref. Chen et al. 2008b, with kind permission from American Chemical Society, Copyright (2008))

with the large epoxy-rich domain and layer structure formation, as shown in Fig. 3 of this chapter. However, this is reasonably correlated with the features of the two systems, since the dynamic asymmetry was much stronger in the epoxy/FPI system. After the bicontinuous structure was initially formed, the coalescence and flowing out of epoxy-rich was retarded and need much longer time to complete, which continued for a long period after the layered structure was formed.

Domain size and development of the phase structure could be observed through TEM, with results shown in Fig. 12. The central part of the microtomed film was observed. At $t = 150\text{ min}$, small FPI-rich domains (black) formed. Connection between the domains was discerned. The domain size was growing with the

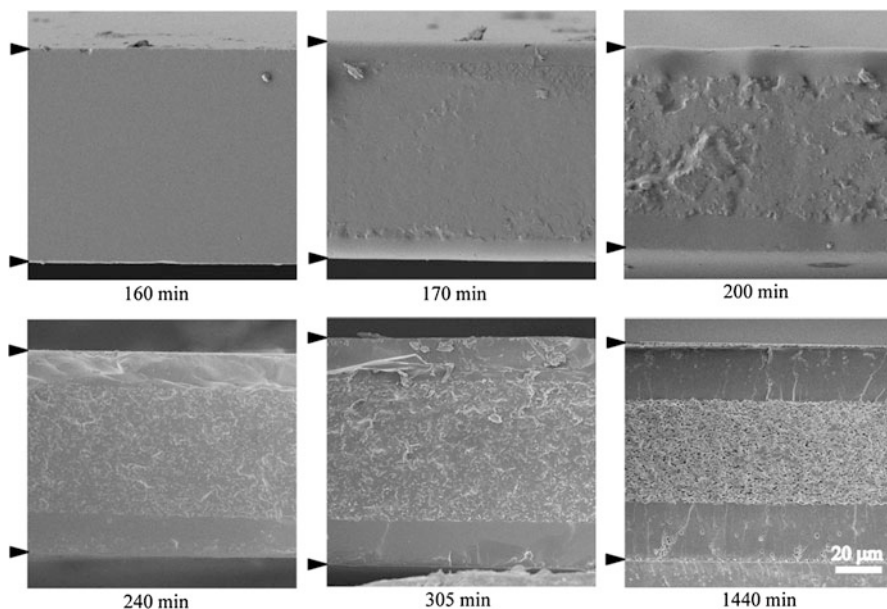


Fig. 13 Sample $w = 0.15$ being cured at $115\text{ }^{\circ}\text{C}$ for different times: scanning electron micrographs of the fractured cross-sectional surfaces (Reprinted from ref. Chen et al. 2008b, with kind permission from American Chemical Society, Copyright (2008))

proceeding of reaction and phase separation. At $t = 240$ min, size of the FPI-rich domains was much larger than that of the initial ones, and bicontinuous phase-separated structure was clearly recognizable. The domain scales and coarsening process were consistent with the TRLS results. Information on z direction was intuitively shown from the SEM images in Fig. 13. After the samples were cured for different times, layered structure quickly occurred after phase separation was observed. Boundaries between the layers became clear and sharp quickly; phase-separated domains gradually became clear in the middle layer and no phase-separated domains were observed on the outside. A classical bicontinuous structure formed in the middle layer and only a very small amount of PI-rich particles existed in the outer epoxy-rich layers.

Since the layered structure information was not commonly reported in the previous studies (Hourston and Lane 1992; Giannotti et al. 2005), it was necessary to check the various sample environment for the morphology formation. Considering the inhomogeneity of the initial sample (Giannotti et al. 2005), different mixing methods such as the solution mixing at room temperature or melt mixing at high temperatures were also tried. The initially homogeneous samples could be obtained and layered structure was generally formed at the certain conditions. Surface energy or interface interaction was considered and studied as the possible cause for the depletion layer formation. In this case, hydrophilic and hydrophobic glasses and a certain polyimide film were used as the substrates, with the result shown in Fig. 14

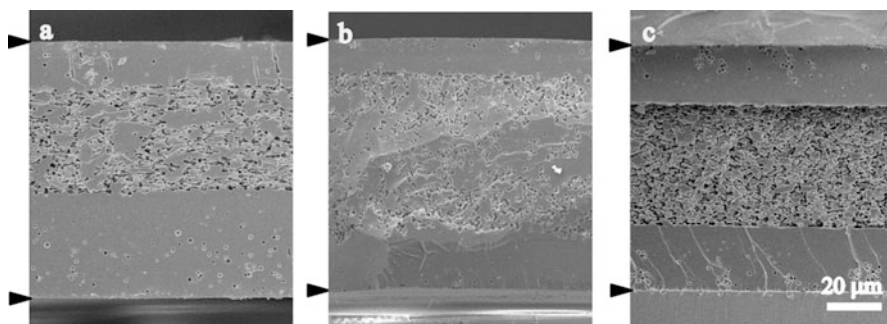


Fig. 14 SEM micrographs of fractured and etched surfaces of sample $w = 0.15$ cured at $130\text{ }^{\circ}\text{C}$ for 1440 min. The samples were cured between various substrates: hydrophobic glasses (a), polyimide film (b). (c) Shows the result with hydrophilic glasses as substrates and also with the sample held vertically during the curing process (Reprinted from ref. Chen et al. 2008b, with kind permission from American Chemical Society, Copyright (2008))

(Chen et al. 2008b). Driving force for the FPI exfoliation from the substrate should be effectively reduced through this method. Although slightly different bicontinuous structures were resulted, the layered structure was generally obtained. It also should be noted that the dewetting force can only work in the distance of nanometers and several microns at most, as may work during the onset of depletion but will not drive for the thick outer layer formation without the volume shrinking of FPI-rich phase. It indicated that the outer epoxy-rich layers were not caused by the phase separation induced by the surface wetting layers. When the sample was positioned with surface normal to the horizontal during the curing process, the layered structure also formed, resembling that observed in Fig. 8. It confirmed that gravity effect should be excluded as the possible cause for this morphology formation as well. The three-layered structure was observed at the experimental temperatures $\leq 200\text{ }^{\circ}\text{C}$ for $w = 0.15$. Thickness of the middle layer decreased with the increase of temperature. However, bicontinuous phase domains of the middle layer were always recognizable.

Phase diagram and its shift with reaction were illustrated in Fig. 15. In the initially homogeneous sample, the epoxy monomer worked as the solvent of FPI. The initial coexistence curve was quite asymmetrical, with the critical concentration w_c located at a low FPI concentration. After reaction started, molecular weight of epoxy gradually increased, and the coexistence curve simultaneously shifted, with the critical temperature T_{crit} moving to higher temperature and w_c shifting to higher w . The coexistence curve became less asymmetrical with reaction proceeding. Assuming Φ_0 being the initially homogeneous sample, its coexistent concentrations varied from A, B to C, D and E, and F at the various reaction and phase separation period, respectively. Because of the asymmetrical phase diagram, there existed a relationship $\text{AO/OB} > \text{CO/OD} \gg \text{EO/OF}$. Volume fraction of the FPI-rich phase will decrease after the initial increase at the onset of phase separation. When FPI located near to the critical concentration, bicontinuous structure

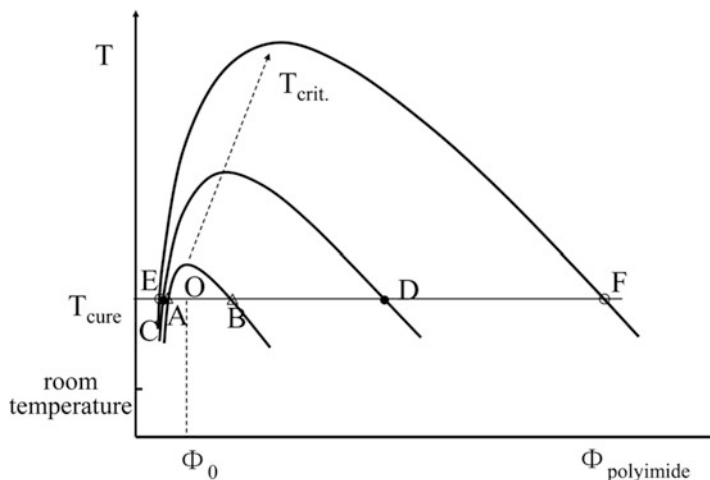


Fig. 15 Schematic description of the shift of phase diagram in the system of DGEBA/DDS/6FDA-MDA during curing reaction (Reprinted from ref. Chen et al. 2008b, with kind permission from American Chemical Society, Copyright (2008))

firstly formed and developed. Because of the elasticity of the slow and entangled FPI-rich network and the fluidity of the fast epoxy-rich continuous domains, the FPI-rich phase shrank to its centroid to lower the volume fraction, and simultaneously the epoxy-rich phase was driven to flow out. The interesting three-layered structure was formed. At other concentration ranges, dynamic asymmetry also dominated the phase separation process. Sea-island and nodular structure formed without the significant hydrodynamic flow effect.

Ubiquitous Nature of the Layered Structure Formation

Here we will take these interesting morphologies as a sign for the viscoelastic phase separation in the epoxy/TP system. In the unreactive system, where the disentanglement of the slow component could complete, phase inversion will occur. While in the reactive system, the instantaneous domains may be fixed by the sudden increase of viscosity through linear polymerization or cross-link network formation of polycondensation reaction. That is to say, salami pattern of PSF- and FPI-rich domains may form at the high curing temperatures, with sufficient disentanglement of the TP chains (Chen et al. 2008b). More importantly, the dynamic asymmetry always dominated the phase separation evolution, especially at the early period. When TP in the epoxy/TP is also reactive, e.g., high MW TP with functional groups or reactive prepolymers of TP used instead of the nonreactive TP as previously discussed, phase separation will proceed in a more complicate way. In the former case, i.e., epoxy/reactive high MW TP blends, phase behavior was quite similar with our discussion, depending on the compatibility between the components

(Hodgkin et al. 1998; Yoon et al. 1995). In the latter case when reactive prepolymer of TP was used, phase behavior and the morphology formation greatly depended on the competition between the two kinds of reactions, since both epoxy and the TP components were reactive during the curing process (Gaw and Kakimoto 1999). If the TP with low glass transition temperature or small molecule chain (but long enough for entanglement) was utilized, the above mentioned phenomenon may also be observed at appropriate situations (Zhang et al. 2012; Kimoto and Mizutani 1997).

Influences of the Molecular Weight and T_g of the TP

The low T_g amorphous polymer, poly(vinyl acetate) (PVAc, $M_n = 24,000$ g/mol, $T_g = 40$ °C), was used to blend with epoxy. Sea-island and nodular structures were obtained at the low and high PVAc concentrations. While at the middle concentration $w = 0.20$, dual morphology containing complex microstructures was obtained, as shown in Fig. 16. Although some part of the sample film was irregularly occupied with skinning-like epoxy-rich matrix, most of the sample was composed of large

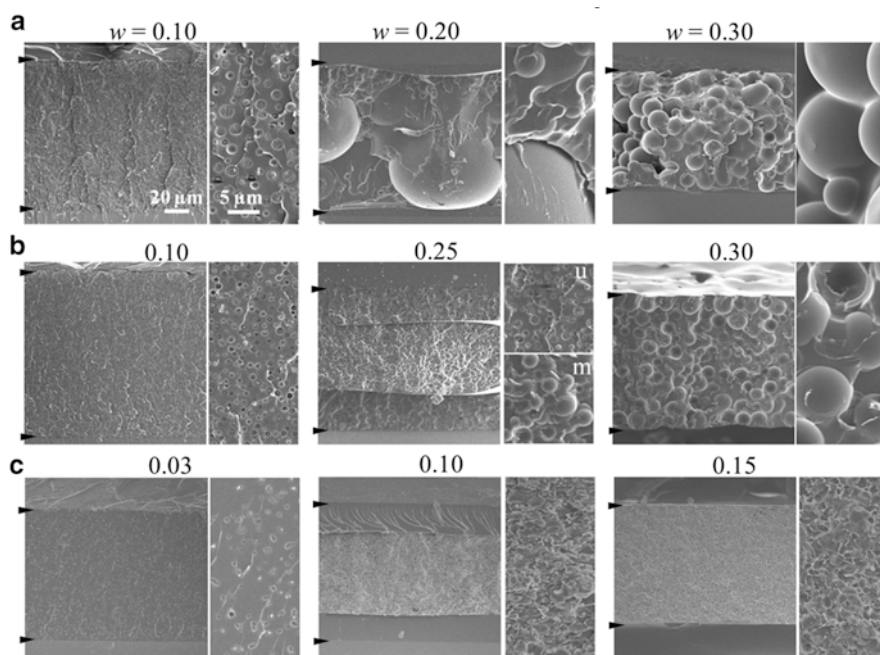


Fig. 16 SEM micrographs of fractured surfaces (normal to the film sample surface) of various epoxy/thermoplastic blends with different compositions w , cured at 130 °C for 1440 min: (a) epoxy/PVAc, (b) epoxy/LPMMA, (c) epoxy/HPMMA. The location of the glass slide surfaces was indicated by arrows. Right pictures in each panel are at higher magnifications. (*u*) and (*m*) represent the upper and middle parts (Reprinted from ref. Zhang et al. 2012, with kind permission from Elsevier, Copyright (2012))

(tens of microns) and small (several microns) epoxy-rich particles with PVAc-rich continuous phase running through these domains. This structure was developed from the bicontinuous structure and resulted by the sufficient PVAc chain relaxation at the relatively high curing temperature (90 °C higher than the T_g of PVAc).

Besides the influence of T_g , molecular weight of the TP was considered to be another important factor affecting the morphological structure formation. Thus poly (methyl methacrylate)s with high and low molecular weight were used, with HPMMA, $M_n = 168,000$ g/mol, $T_g = 120$ °C and LPMMA, $M_n = 10,000$ g/mol, $T_g = 91$ °C. The sea-island, three-layered, and nodular structures were obtained. The layered structure extended through the whole sample of epoxy/HPMMA at $w = 0.10$, except for the edge and bubble locations, where core (outer epoxy-rich layer)-shell (coexistence of epoxy- and TP-rich domains) could be described as a whole, as was commonly observed for the layered structure formation in epoxy/PSF and epoxy/FPI systems previously discussed. For the epoxy/LPMMA blend, small epoxy-rich particles were embedded inside the LPMMA-rich continuous phase, which was different from the bicontinuous structure of epoxy/PSF formed at 130 °C but was similar as that formed at 180 °C and more higher temperatures. The structures of epoxy/HPMMA were more compact than those of epoxy/LPMMA blend. In other words, the HPMMA- and epoxy-rich particles in the corresponding sea-island and nodular structures, respectively, were smaller than those formed in the epoxy/LPMMA blends. For the three-layered structure formed at middle concentrations, bicontinuous structure was observed in the middle layer, with much larger middle layer thickness. Meanwhile, the compositions w , where three-layered and nodular structure could be observed, moved to smaller weight fractions. All these phenomena implied that, when the molecular weight of the TP increased, three-layered structure was easier to be formed. The higher the molecular weight of the TP was, the lower the concentration with broader concentration range for the three-layered structure formation was, and the more continuous epoxy-rich domains were located in the middle layer.

Isothermally cure the DGEBA/DDS for certain time intervals, then measure the transient samples through DSC, and T_g of epoxy at various curing stages was obtained as shown in Fig. 17. As expected, the T_g values were very low before gelation, $T_g \sim 70$ °C at about 300 min. This contributed to the understanding of the dynamic asymmetry, especially when the high T_g thermoplastics were used in the epoxy/TP systems.

As discussed above, each of the three morphological types can be obtained at the corresponding TP concentrations: dual- or three-layered structure was observed in the middle w range, sea-island structure at lower w , and nodular structure at higher w . Here, we summarized the middle composition w ranges (obtained from the SEM observations) of the various epoxy/TP blends in Fig. 18. The value $\Delta T = T_{\text{cure}} - T_g$, where T_{cure} is the curing temperature and T_g is the glass transition temperature of TP, denoted the mobility of the TP polymer chains. When the T_{cure} was much higher than T_g , the relaxation of the TP chains can be fast, which may be even close to that of the epoxy oligomer chains at the time of phase separation, e.g., the case of epoxy/PVAc. The entangled TP-rich network can be relaxed before the dynamic

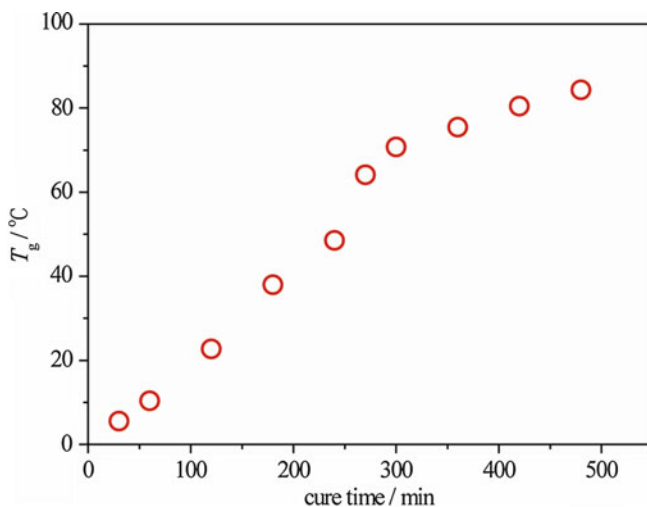


Fig. 17 Glass transition temperatures (T_g) of the DGEBA/DDS mixtures cured at 130 °C for different time (Reprinted from ref. Zhang et al. 2012, with kind permission from Elsevier, Copyright (2012))

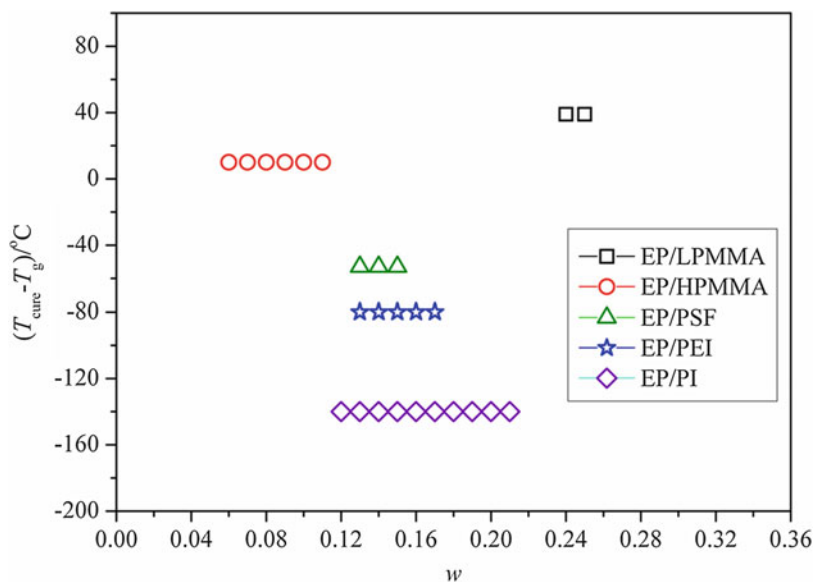


Fig. 18 The corresponding TP weight fraction w ranges for the layered structure formation in the epoxy/TP blends cured at $T_{\text{cure}} = 130$ °C (Reprinted from ref. Zhang et al. 2012, with kind permission from Elsevier, Copyright (2012))

asymmetry was established. Thus the three-layered structure cannot be formed. When T_{cure} was around or lower than T_g , motions of the TP chains were depressed and the TP component showed slow dynamic characteristics. Then the three-layered structure can be formed. In the case of epoxy/LPMMA blend, three-layered structure was observed in a rather narrow w range of 0.24–0.25, while for the case of epoxy/PSF, epoxy/PEI, and epoxy/FPI blends, the middle w ranges were somewhat wider, being 0.13–0.15, 0.13–0.17, and 0.12–0.21, respectively. Moreover, when the molecular weight of the TP increased, the middle w range was even wider and moved to the lower TP contents, e.g., $w = 0.05$ –0.11 for the epoxy/HPMMA blend. It meant that the higher the T_g or higher MW of TP was, the wider the middle w range and the lower the threshold composition became for the layered structure formation.

Curing Agent Variations

Curing agent is a crucial component for the epoxy curing. The curing procedure was normally determined according to the manufacture procedures of the curing agent species used. Amines, anhydrides, phenols, carboxylic acids, and alcohols are commonly used as the curing agents. The specific choice of curing agent mainly depends on application requirements, curing temperature and time, curing procedure, etc. Aromatic amines are mostly used for wide applications. Using different curing agent species, chemical reaction and structure of the product are basically changed (Kimoto and Mizutani 1997; Chen et al. 2012). In this sense, interaction force and compatibility between the components varied. With the same DGEBA and PES used, macroscopic phase domains may form when DDM (4,4'-diaminodiphenylmethane) was used for curing. A kind of complex morphology, with large PES domains containing a high proportion of resin sub-inclusions, was obtained in the blends of about 15 wt.% of PES. However, no phase separation was detected through the existing optical or electrical microscopy techniques at any stage of curing when DDS was used as the curing agent, although initially homogeneous sample was also prepared (Bucknall et al. 1994). Similarly for the DGEBA/PSF blends, when DDS was used for the curing, various morphologies were found with different PSF loadings (Zhang et al. 2010, 2014b), while only one phase was detected through electron microscopes and typical characteristics of brittle fracture was observed from the mechanic cracks when DDM was used instead (Huang et al. 1997). It is meaningful to discuss the curing agent's influence on phase separation when different amount of curing agent was used (Bauchiere et al. 2000), since compatibility between the components was not changed but the composition was changed. However, the increased curing agent loadings promoted reaction and phase separation simultaneously, and morphology type was not varied distinctly. There were also explorations with mixtures of curing agents in the DGEBA/PMMA blends. DDM and *p*-toluidine were employed for the curing, so that various physical appearance (phase separated or not) could be obtained at various agent ratios based on the ideal thermodynamic change driving kinetic feature variations (Blanco et al. 2009).

Conclusions

For the epoxy resins, toughness was the first focusing point because of the application need. In this sense, morphology study has been widely reported. However, without systematic study on phase evolution and the analysis on phase separation mechanism, it was difficult to control the morphology organization and understand the structure-performance relationship. Phase separation can be investigated through the combination of in situ PCOM and TRLS and the ex situ SEM and TEM techniques. Besides evolution on xy plane, information on z direction was important complementary information for the phase separation mechanism analysis. Typically three kinds of morphology can be obtained: sea-island and nodular structures formed at low and high TP concentrations, while a whole core-shell structure formed at the middle TP concentrations. The shell was epoxy-rich, with few TP-rich particles random distribution, and was the outer layer locally observed. Bicontinuous domains formed the core (locally middle layer in thin film sample). The bicontinuous structure can develop to be dual with the TP-rich continuous phase transforming to be disperse, when the TP entanglement can relax further.

Dynamically asymmetric phase separation was interpreted as the mechanism for the above morphological formation. TP usually has high glass transition temperature, which is much higher than that of epoxy during the phase separation process. The different chain mobility between the components caused the remarkable dynamic asymmetry in the epoxy/TP system. Miscibility determines the thermodynamics of the system, while dynamic asymmetry dominates the phase separation process. Miscibility may greatly change when any special component was introduced. This is understandable in the reactive system, since chemical structure of the product may be changed and the compatibility change will follow. If one wants to obtain an ideal morphology, e.g., bicontinuous structure, phase separation process should be followed and characteristics of the components should be considered. The asymmetrical phase separation procedure in curing may also be used to produce gradient layers for interlamellar toughening or inter-parts adhesion applications.

References

- Bauchiere D, Halary JL, Monnerie L, Schirrer R (2000) Relationships between thermally induced residual stresses and architecture of epoxy-amine model networks. *J Appl Polym Sci* 75:638–650
- Blanco M, López M, Fernández R, Martín L, Riccardi CC, Mondragon I (2009) Thermoplastic-modified epoxy resins cured with different functionalities amine mixtures. Kinetics and miscibility study. *J Therm Anal Calorim* 97:969–978
- Bonnet A, Pascault JP, Sautereau H, Taha M, Camberlin Y (1999a) Epoxy-diamine thermoset/thermoplastic blends. 1. Rates of reactions before and after phase separation. *Macromolecules* 32:8517–8523
- Bonnet A, Pascault JP, Sautereau H, Camberlin Y (1999b) Epoxy-diamine thermoset/thermoplastic blends. 2. Rheological behavior before and after phase separation. *Macromolecules* 32:8524–8530

- Bucknall CB, Partridge IK (1983) Phase-separation in epoxy-resins containing polyethersulfone. *Polymer* 24:639–644
- Bucknall CB, Gomez CM, Quintard I (1994) Phase separation from solutions of poly(ether sulfone) in epoxy resins. *Polymer* 35:353–359
- Chen F, Wang X, Zhao X, Liu J, Yang S, Han CC (2008a) Spontaneous three-layer formation in the curing of polyimide/epoxy blends. *Macromol Rapid Commun* 29:74–79
- Chen F, Sun T, Hong S, Meng K, Han CC (2008b) Layered structure formation in the reaction-induced phase separation of epoxy/polyimide blends. *Macromolecules* 41:7469–7477
- Chen F, Zhang Y, Shi W, Yang S, Zhao X, Han CC (2012) Curing agent influence on the layered-structure formation in the epoxy/polysulfone blends. *Acta Polym Sin* 6:673–678
- Cicala G (2014) Comparison of epoxy/rubber blends with other toughening strategies: thermo-plastic and hyperbranched modifiers. In: Thomas S, Sinturel C, Thomas R (eds) *Micro- and nanostructured epoxy/rubber blends*. Wiley, Weinheim, pp 363–390
- Clarke N, McLeish TCB, Jenkins SD (1996) Phase behavior of linear/branched polymer blends. *Macromolecules* 28:4650–4659
- de Gennes PG (1976) Dynamics of entangled polymer solutions. *Macromolecules* 9:587–593, 594–598
- de Graaf LA, Hempenius MA, Möller M (1995) Demixing behaviour as a tool to control the morphology of thermoplast modified epoxy resins. *Polym Prep* 36:787–788
- Doi M, Onuki A (1992) Dynamic coupling between stress and composition in polymer-solutions and blends. *J Phys* 2:1631–1656
- Enns JB, Gillham JK (1983) Time-temperature-transformation (TTT) cure diagram: modeling the cure behavior of thermosets. *J Appl Polym Sci* 28:2567–2591
- Figueruelo JE, Gomez CM, Monzo IS, Abad C, Campos A (2008) Thermodynamic study on phase equilibrium of epoxy resin/thermoplastic blends. *J Chem Thermodyn* 40:677–687
- Flory PJ (1953) *Principles of polymer chemistry*. Cornell University Press, New York
- Galante MJ, Borrajo J, Williams RJJ, Girard-Reydet E, Pascault JP (2001) Double phase separation induced by polymerization in ternary blends of epoxies with polystyrene and poly(methyl methacrylate). *Macromolecules* 34:2686–2694
- Gan WJ, Yu YF, Wang MH, Tao QS, Li SJ (2003) Viscoelastic effects on the phase separation in thermoplastics-modified epoxy resin. *Macromolecules* 36:7746–7751
- Gaw KO, Kakimoto M (1999) Polyimide-epoxy composites. *Adv Polym Sci* 140:107–136
- Giannotti MI, Solsona MS, Galante MJ, Oyanguren PA (2003) Morphology control in polysulfone-modified epoxy resins by demixing behavior. *J Appl Polym Sci* 89:405–412
- Giannotti MI, Foresti ML, Mondragon I, Galante MJ, Oyanguren PA (2004) Reaction-induced phase separation in epoxy/polysulfone/poly(ether imide) systems. I. Phase diagrams. *J Polym Sci Part B: Polym Phys* 42:3953–3963
- Giannotti MI, Mondragon I, Galante MJ, Oyanguren PA (2005) Morphology profiles obtained by reaction-induced phase separation in epoxy/polysulfone/poly(ether imide) systems. *Polym Int* 54:897–903
- Girard-Reydet E, Sautereau H, Pascault JP, Keates P, Navard P, Thollet G, Vigier G (1998) Reaction-induced phase separation mechanisms in modified thermosets. *Polymer* 39:2269–2280
- Han CC, Akcasu AZ (2011) *Scattering and dynamics of polymers: seeking order in disordered systems*. Wiley, Singapore
- Hashimoto T, Itakura M, Shimidzu (1986) Late stage spinodal decomposition of a binary polymer mixture. II. Scaling analyses on $Q_m(\tau)$ and $I_m(\tau)$. *J Chem Phys* 85:6773–6786
- Hodgkin JH, Simon JP, Varley RJ (1998) Thermoplastic toughening of epoxy resins: a critical review. *Polym Adv Tech* 9:3–10
- Hourston DJ, Lane JM (1992) The toughening of epoxy resins with thermoplastics: 1. Trifunctional epoxy resin-polyetherimide blends. *Polymer* 33:1379–1383
- Huang P, Zheng S, Huang J, Guo Q, Zhu W (1997) Miscibility and mechanical properties of epoxy resin/polysulfone blends. *Polymer* 38:5565–5571

- Inoue T (1995) Reaction-induced phase separation in polymer blends. *Prog Polym Sci* 20:119–153
- Ishii Y, Ryan AJ, Clarke N (2003) Phase diagram prediction for a blend of Poly(2,6-dimethyl-1,4-phenylene ether) (PPE)/epoxy resin during reaction induced phase separation. *Polymer* 44:3641–3647
- Jyotishkumar P, Paula M, Thomas S (2013) Rheological study of the SAN modified epoxy–DDM system: relationship between viscosity and viscoelastic phase separation. *RSC Adv* 3:23967–23971
- Kimoto M, Mizutani K (1997) Blends of thermoplastic polyimide with epoxy resin part II mechanical studies. *J Mater Sci* 32:2479–2483
- Kinloch AJ, Yuen ML, Jenkins SD (1994) Thermoplastic-toughened epoxy polymers. *J Mater Sci* 29:3781–3790
- Lee JC (1999) Polymerization-induced phase separation. *Phys Rev E* 60:1930–1935
- Min BG, Stachurski ZH, Hodgkin JH, Heath GR (1993) Quantitative analysis of the cure reaction of DGEBA/DDS epoxy resins without and with thermoplastic polysulfone modifier using near infra-red spectroscopy. *Polymer* 34:3620–3627
- Park JW, Kim SC (1996) Phase separation during synthesis of polyetherimide/epoxy semi-IPNs. *Polym Adv Tech* 7:209–220
- Simon SL, Gillham JK (1992) Reaction kinetics and TTT cure diagrams for off-stoichiometric ratios of a high- T_g epoxy/amine system. *J Appl Polym Sci* 46:1245–1270
- Solc K, Koningsveld R (1995) Liquid-liquid phase separation in multicomponent polymer systems. XXVI. Blends of two polydisperse polymers. *Collect Czech Chem Commun* 60:1689–1718
- Tanaka H (1993) Unusual phase separation in a polymer solution caused by asymmetric molecular dynamics. *Phys Rev Lett* 71:3158–3161
- Tanaka H (1994) Double phase separation in a confined, symmetric binary mixture: interface quench effect unique to bicontinuous phase separation. *Phys Rev Lett* 72:3690–3693
- Tanaka H (2000) Viscoelastic phase separation. *J Phys Condens Matter* 12:R207–R264
- Tanaka Y, Mika TF (1973) Epoxide-curing reactions. In: May CA, Tanaka Y (eds) *Epoxy resins chemistry and technology*. Marcel Dekker, New York, pp 135–238
- Tang X, Zhang L, Wang M, Gan W, Li S (2004) Hydrodynamic effect on secondary phase separation in an epoxy resin modified with polyethersulfone. *Macromol Rapid Commun* 25:1419–1424
- Wang X, Okada M, Matsushita Y, Furukawa H, Han CC (2005) Crystal-like array formation in phase separation induced by radical polymerization. *Macromolecules* 38:7127–7133
- Williams RJJ, Rozenberg BA, Pascault JP (1997) Reaction-induced phase separation in modified thermosetting polymers. *Adv Polym Sci* 128:95–156
- Xie XM, Yang H (2001) Phase structure control of epoxy/polysulfone blends-effects of molecular weight of epoxy resins. *Mater Des* 22:7–9
- Yee AF, Du J, Thouless MD (2000) Toughening of epoxies. In: Paul DR, Bucknall CB (eds) *Polymer blends, vol 2, Performance*. Wiley, New York, pp 225–267
- Yoon TH, Priddy DB, Lyle GD, Mcgrath JE (1995) Mechanical and morphological investigations of reactive polysulfone toughened epoxy networks. *Macromol Symp* 98:673–686
- Yoon T, Kim BS, Lee DS (1997) Structure development via reaction-induced phase separation in tetrafunctional epoxy/polysulfone blends. *J Appl Polym Sci* 66:2233–2242
- Yu YF, Wang MH, Gan WJ, Tao QS, Li SJ (2004) Polymerization-induced viscoelastic phase separation in polyethersulfone-modified epoxy systems. *J Phys Chem B* 108:6208–6215
- Zhang Y, Chen F, Shi W, Liang Y, Han CC (2010) Layered structure formation in the reaction-induced phase separation of epoxy/polysulfone blends. *Polymer* 51:6030–6036
- Zhang Y, Shi W, Chen F, Han CC (2011) Dynamically asymmetric phase separation and morphological structure formation in the epoxy/polysulfone blends. *Macromolecules* 44:7465–7472
- Zhang Y, Chen F, Li Z, Han CC (2012) Ubiquitous nature of the three-layered structure formation in the asymmetric phase separation of the epoxy/thermoplastic blends. *Polymer* 53:588–594

-
- Zhang D, Zhang J, Zhang A (2014a) Morphology analysis by microscopy techniques and light scattering. In: Thomas S, Sinturel C, Thomas R (eds) *Micro- and nanostructured epoxy/rubber blends*. Wiley-VCH, Weinheim, pp 147–178
- Zhang Y, Chen F, Liu W, Zhao S, Liu X, Dong X, Han CC (2014b) Rheological behavior of the epoxy/thermoplastic blends during the reaction induced phase separation. *Polymer* 55:4983–4989
- Zucchi IA, Galante MJ, Borrajo J, Williams RJJ (2004) A model system for the thermodynamic analysis of reaction-induced phase separation: solutions of polystyrene in bifunctional epoxy/amine monomers. *Macromol Rapid Commun* 205:676–683

Yingfeng Yu, Gebin Shen, and Zhuoyu Liu

Abstract

The morphology of the blends has great impact on the thermal mechanical properties of multicomponent materials. For epoxy modified with thermoplastic resins, both thermodynamic and kinetic factors may affect the evolution and final phase structure of the blends. The chemical structure, end groups, side groups, molecular weight, and distribution of thermoplastics may influence the compatibility and interfacial conditions of blends, while the curing conditions and difference in the mobility of components have fundamental effects on the viscoelastic phase-separation process of these kinds of blends. Various techniques, such as optical microscopy (OM), scanning electron microscopy (SEM), transmission electron microscope (TEM), atomic force microscope (AFM), and light scattering (LS), have been employed in the morphology study of materials.

Keywords

Epoxy resins • Epoxy/thermoplastic blends • Morphology • Phase separation • Polymerization-induced phase separation. *See* polymerization-induced phase separation • Viscoelastic effect • Viscoelastic phase separation • Light scattering • Curing agent • Linear block copolymers • Molecular weight • Physical and chemical properties • Precure temperature • Reactive end group • SEM • Thermoplastics concentration • Spinodal decomposition (SD)

Y. Yu (✉) • G. Shen • Z. Liu

State Key Laboratory of Molecular Engineering of Polymers, Collaborative Innovation Center of Polymers and Polymer Composite Materials, Department of Macromolecular Science, Fudan

University, Shanghai, China

e-mail: yfyu@fudan.edu.cn

Contents

Introduction	524
General Introduction of Polymerization-Induced Phase Separation	525
Morphology Development Studied by Light Scattering and SEM	526
The Effect of Thermoplastics Concentration on the Morphology	528
The Effect of Molecular Weight of Thermoplastics on the Morphology	530
Effect of Reactive End Groups on the Morphology and Interfaces	532
The Effect of Precure Temperature on Morphologies of Epoxy/PEI Blends	534
The Effect of Linear Block Copolymers on Microphase Morphological Structure	537
The Effect of Curing Agent on Phase Separation Behavior	539
Viscoelastic Phase Separation	540
Polymerization-Induced Viscoelastic Phase Separation	541
Enhanced Viscoelastic Effect	550
Conclusions	554
References	554

Introduction

Epoxy resins are materials that are used in a wide variety of applications in the automotive, electronics, construction, and aerospace industries primarily because of their excellent mechanical properties, thermal stability, solvent resistance, and ease of processing. Unfortunately, owing to the high cross-link density of epoxy resin, they are inherently brittle materials. This lack of toughness is a major reason in preventing their further application to extreme conditions. Thus, the challenge to toughen them has been a field of intense research for many years (Hodgkin et al. 1998).

Thermoplastic toughening of epoxy resins has been actively studied since the early 1980s with considerable progress in property improvement and understanding of mechanisms. The main advantage in using thermoplastics to toughen epoxy resins is that their incorporation need not result in significant decreases in desirable properties such as modulus and yield strengths as is generally the case when rubbers are used as toughening agents. While the predominant criteria for achieving optimum toughness enhancement in the thermoplastic toughening of epoxy resin are still under research, there are a few factors that have been discussed in sufficient detail. For instance, the importance of morphology to the properties of epoxy–thermoplastic blends has received much attention in the literature. And understanding the mechanism of phase separation in epoxy–thermoplastic blends is the key to control its morphology and resulting properties.

Phase separation is usually caused by immiscibility between polymer blends. Many combinations of dissimilar polymers have been found to follow phase diagrams, i.e., the polymers are miscible within limited temperature and composition ranges but are immiscible outside of these ranges. The study of spinodal decomposition induced by a temperature jump from a miscible region to an immiscible region was once an intensively studied field. In the late 1980s, Inoue proposed reaction-induced phase separation (Yamanaka et al. 1989). Contrary to the classic thermally induced spinodal decomposition, one can combine chemical reactions with spinodal

decomposition in an attempt to induce phase separation and obtain designed morphology. Researchers have used various kinds of epoxy–thermoplastic blends as model systems to study the influence of temperature, curing rate, end group, and molecular weight to polymerization-induced phase separation.

In the last few decades, Tanaka (1993, 1996, 1997) and Onuki et al. (Taniguchi and Onuki 1996; Onuki and Taniguchi 1997; Onuki et al. 1997) found a novel type of phase-separation behavior, the “viscoelastic phase separation,” which is composed of fast and slow dynamic components. Such “dynamic asymmetry” can be induced by either the large size difference or the difference in glass transition temperature (T_g) between the components of a mixture.

In thermosetting blends, Yu YF (Liu et al. 2010, 2012), Li SJ (Gan et al. 2003; Tang et al. 2004; Zhao et al. 2008), Thomas (Jose et al. 2008), and Groeninckx (Goossens et al. 2006) have confirmed and improved this theory. Recently, a noteworthy development is the enhanced viscoelastic effect induced by a third component such as mesoscopic fillers (Zhong et al. 2011; Zhang et al. 2014).

In this chapter an overview of phase separation and resulting morphology of epoxy–thermoplastic blends is presented, mainly employing the characterization of OM, SEM, TEM, and AFM. Other characterizing methods such as Time-Resolved Light-Scattering are also employed as supplements to explain the hydrodynamic evolution. Note that the intent of this chapter is to illustrate the application of visual methods to the characterization of morphology, while these methods are often not decisive in some studies.

General Introduction of Polymerization-Induced Phase Separation

Different from classic thermal-induced phase decomposition, polymerization-induced phase separation (polymerization-induced phase separation is more accurate than reaction-induced phase separation; thus it is used in the following sections instead of the latter term) in epoxy-thermoplastic blends is usually caused by the molecular weight increase of epoxy during curing. Before and in the early stage of curing, epoxy monomer or oligomer and thermoplastic are homogeneous blend. As the curing proceeds, epoxy and thermoplastic blend become immiscible due to molecular weight increase of epoxy resin. This thermodynamic incompatibility causes phase separation until the curing process ceases (Inoue 1995).

The physical and chemical properties are constantly changing during reaction-induced phase separation, so its quenching depth increases as curing proceeds. Unlike thermal-induced phase separation, the rate and depth of quenching have a huge impact on final phase structure. Although this complexity increases the difficulty of both thermodynamic and hydrodynamic researches on polymerization-induced phased separation, it also provides researchers with more means to control the morphologies of epoxy–thermoplastic blends.

In general, the morphologies of cured epoxy–thermoplastic blends depend on thermodynamic imputes and hydrodynamic restrain. Through regulating these two

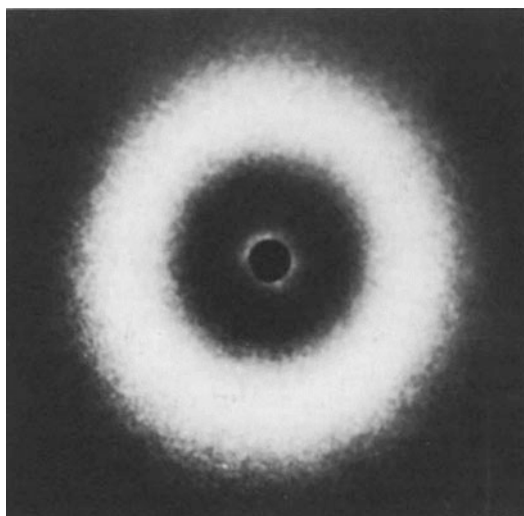
factors, researchers can obtain designed morphology and material properties. The following contents illustrate various studies concerning the influence of polymer blend composition, molecular weight, temperature, functional end groups, and block copolymer and curing rate on morphology in more detail.

Morphology Development Studied by Light Scattering and SEM

Light scattering can provide a statistical value of phase size during decomposition process. Inoue et al. had (Yamanaka and Inoue 1989) investigated the structure development of epoxy and poly(ether sulfone) (PES) blends during curing by light scattering and further verified the results by scanning electron microscopy.

An epoxy/PES mixture loaded with a curing agent DDM (diaminodiphenylmethane), e.g., Epikote 828/PES/DDM = 100/30/26, is a single-phase system at a curing temperature of 140 °C, and no appreciable light-scattering pattern is detected from the mixture during the early stages of curing. After curing for 6 min, a ring pattern due to light scattering caused by phase separation appeared as shown in Fig. 1. The ring pattern implies the development of a regularly phase-separated structure. It also indicates no preferred orientation of the structure in the plane parallel to the film surface. A typical example of the goniometer trace of scattered light is presented in Fig. 2. The ring pattern and the characteristic change in the scattering profile are hallmarks of spinodal decomposition. The increase in the periodic distance with curing time from Fig. 2 is shown by curve (d) in Fig. 3. Such variation is also shown for second formulation (epoxy/PES/DDM = 100/50/26) and various temperatures. All of these curves indicate that the periodic distance initially increases with time and then eventually levels off suggesting that further

Fig. 1 Light-scattering pattern reproduced from Inoue T (1995)



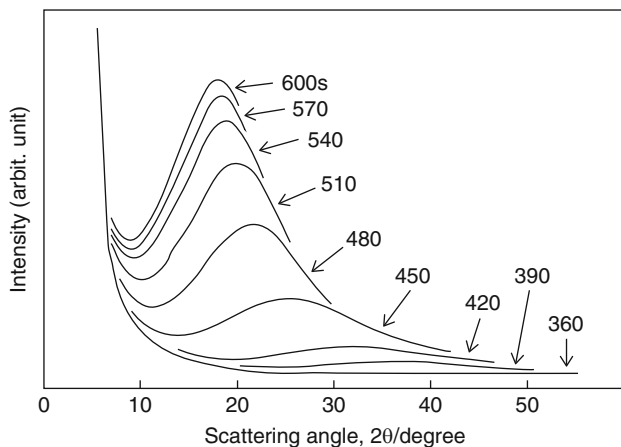
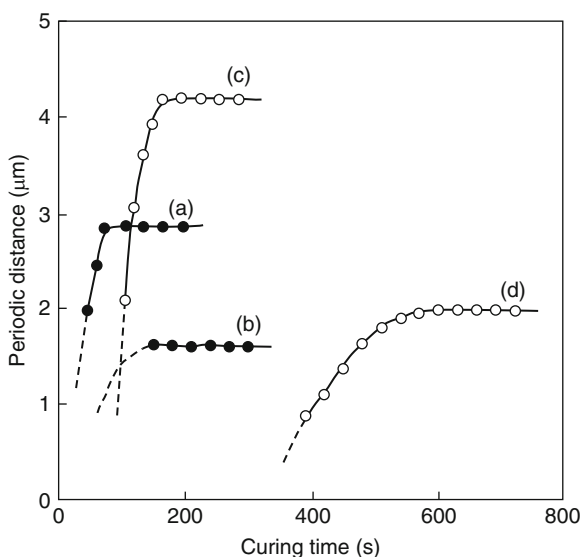


Fig. 2 Change in the light-scattering profile with curing: epoxy/PES/DDM = 100/30/26; curing temperature = 140 °C reproduced from Inoue T (1995)

Fig. 3 Variation of periodic distance with cure: (a) epoxy/PES/DDM = 100/50/26; curing temperature 200 °C and (b) 170 °C; (c) epoxy/PES/DDM = 100/30/26; curing temperature 170 °C and (d) 140 °C reproduced from Inoue T (1995)



structure development is suppressed by cross-linking or by vitrification of the PES-rich region due to the approach of the T_g curve.

The periodic distance obtained by light scattering was verified by scanning electron micrographs for the cured resins. The cured specimen was first fractured in liquid nitrogen and then immersed in methylene chloride at 24 °C for 12 h. The fractured-etched surface was observed under SEM. PES phase is assumed to be rinsed away by methylene chloride, and the remaining material is a cross-linked epoxy-rich phase. As shown in Fig. 4, fine globules of a few micrometers diameter

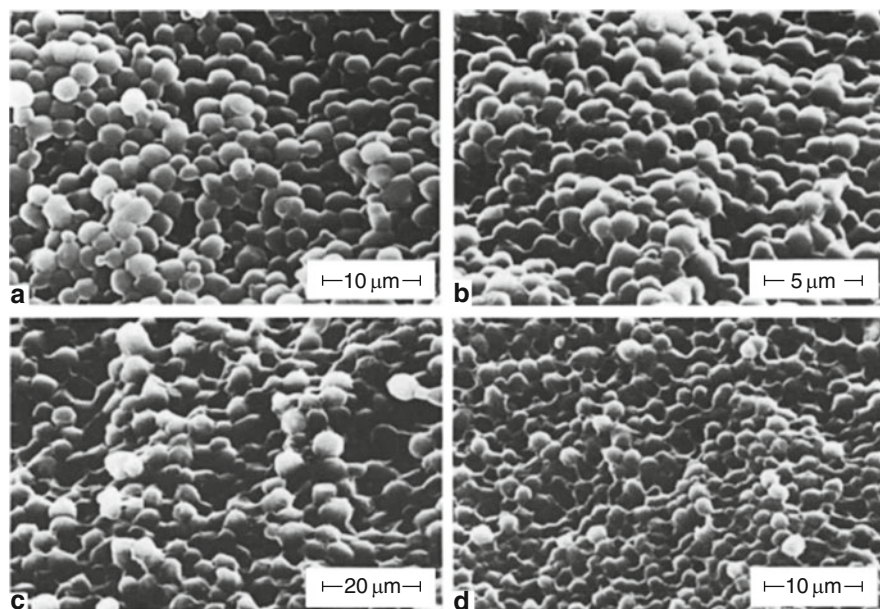


Fig. 4 SEM micrographs of cured resins. (a) PES 50 phr, 200 °C, 0.5 h; (b) PES 50 phr, 170 °C, 3 h; (c) PES 30 phr, 170 °C, 3 h; (d) PES 30 phr, 140 °C, 3 h reproduced from Inoue T (1995)

are seen and seem to be connected to each other. The connected-globule structure in SEM observation implies a two-phase morphology of interconnected spherical domains of an epoxy-rich phase dispersed regularly in a matrix of PES. The periodic distances between the globules in SEM exactly correspond to those obtained by light scattering.

A plausible scenario for the development of the connected-globule structure had been explained on the basis of traditional thermal-induced phase separation, which proposed that most process may follow spinodal decomposition.

The Effect of Thermoplastics Concentration on the Morphology

As it could be well anticipated from phase diagram that concentration of component has primary effect on morphology, various concentrations of thermoplastics have been studied for their effect on final structure. For example, Oyanguren et al. (1998) mixed PSu with DGEBA, which were cured by methyltetrahydrophthalic anhydride (MTHPA).

Figure 5 (Oyanguren et al. 1998) shows SEM micrographs of epoxy samples containing 5, 10, and 15 wt% PSu. At 5 wt% PSu, the formulation is located at the left of the critical point, and the dispersed phase consists of a random distribution of spheres rich in PSu. The average diameter $\bar{d} = 1.2 \mu\text{m}$ and the volume fraction of dispersed phase are close to 0.06. At 15 wt% PSu, the formulation is located at the

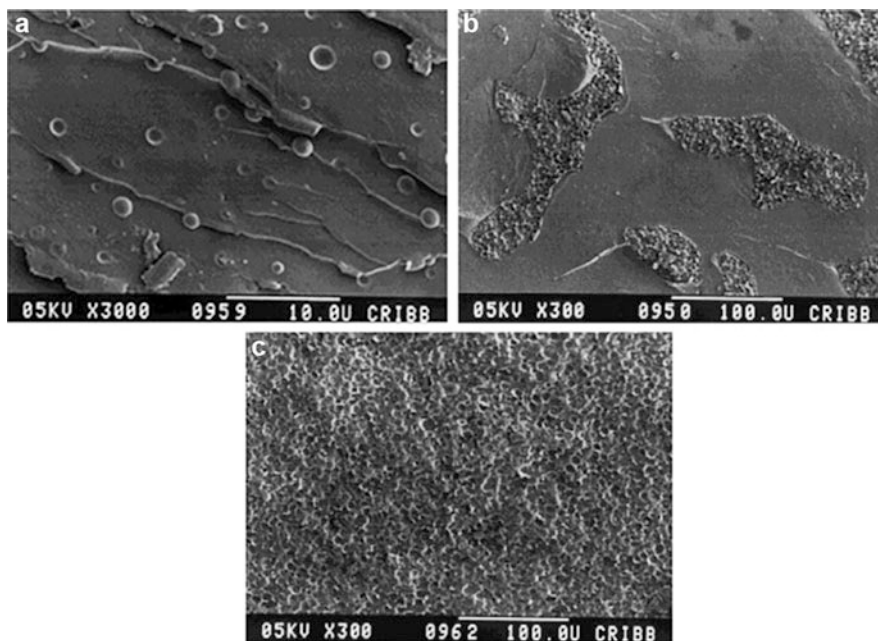


Fig. 5 SEM micrographs of samples containing different PSu amounts, precured at 80 °C and postcured at 200 °C; (a) 5 wt% PSu, (b) 10 wt% PSu, (c) 15 wt% PSu reproduced from Oyanguren et al. (1998)

right of the critical point, and a phase-inverted morphology is observed. Particles rich in the epoxy–anhydride copolymer ($\bar{d} = 9.2 \mu\text{m}$) are dispersed in a continuous matrix in PSu. At 10 wt% PSu, complex morphologies consisting of large domains (characteristic length in the order of 100 μm), exhibiting irregular shapes and dispersed in a continuous matrix, were found.

A secondary phase separation took place in both phases as shown in Fig. 6. The matrix (Fig. 6a) represents a continuous epoxy–anhydride phase with a random dispersion of PSu-rich particles ($\bar{d} = 1.1 \mu\text{m}$). Evidence of particle drawing by a crack bridging mechanism was observed. Magnified large domains are shown in Fig. 6b. A dispersion of particles rich in the epoxy–anhydride copolymer ($\bar{d} = 3.7 \mu\text{m}$) in a continuous PSu-rich matrix is observed.

Therefore, in the sample containing 10 wt% PSu, morphologies present in materials with 5 and 15 wt% PSu coexist in different regions (Fig. 6c shows a magnification of a sample with 15 wt% PSu). Epoxy–anhydride particles exhibit a poor adhesion with the PSu-rich matrix. Debonding of these particles is clearly observed in the SEM micrographs of fracture surfaces. However, an opposite situation occurs when the PSu particles are present in the epoxy matrix. Here the adhesion is good enough to promote particle drawing through crack bridging. Therefore, the same chemistry gives regions of poor and good adhesion between particles and matrix, depending on the nature of continuum and dispersed phases. A possible explanation

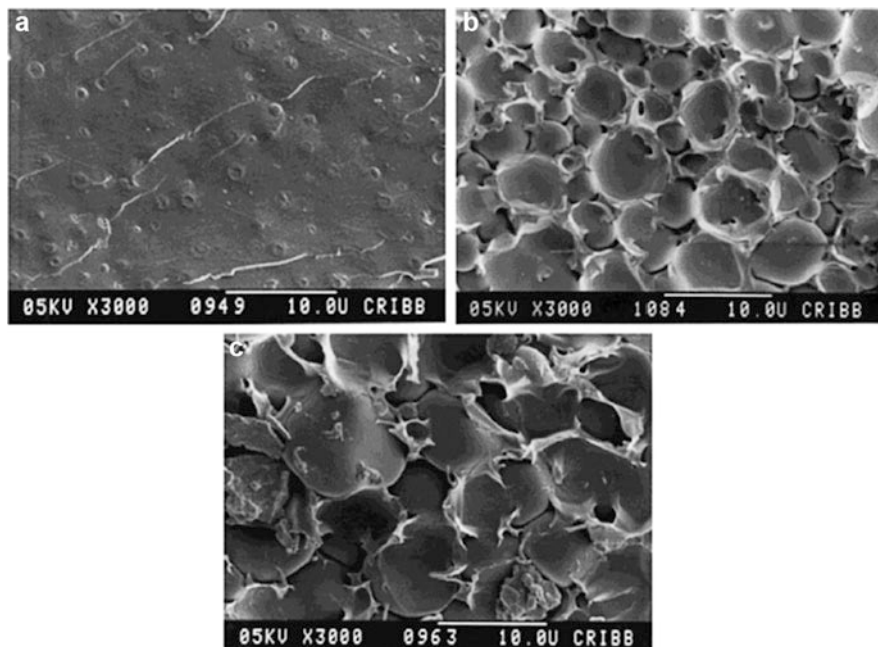


Fig. 6 SEM micrographs. (a) Amplification of the matrix for the sample containing 10 wt% PSu; (b) amplification of the irregular domains for the sample containing 10 wt% PSu; (c) amplification of the sample containing 15 wt% PSu reproduced from Oyanguren et al. (1998)

may be related to the different T_{gs} of these two phases. When cooling from the cure temperature, the PSu-rich phase will vitrify first. In the temperature range comprised between both T_{gs} , the contraction of the thermosetting polymer, still present in the rubbery state, will be higher than the PSu-rich phase. Poor adhesion may be thus caused when the thermosetting polymer constitutes the dispersed phase and good adhesion may be expected when it forms the continuous matrix.

The presence of a secondary phase separation as shown in Fig. 6b indicates that the process evolves out of equilibrium. This is a usual observation in modified thermosetting polymers, and it is the result of the high viscosities and correspondingly low diffusion coefficients in one or both primary phases.

The Effect of Molecular Weight of Thermoplastics on the Morphology

The polymer molecular weight is one of the most important factors influencing the thermodynamic and kinetic properties and thus the final morphology of materials. The effect of the molecular weight of thermoplastic on rheological behavior was extensively studied. It was shown that phase separation occurred first in a high molecular weight PEI-modified epoxy resin and that the time of the occurrence of phase separation increased as the inherent viscosity of PEI decreased (Cui et al. 1997). An

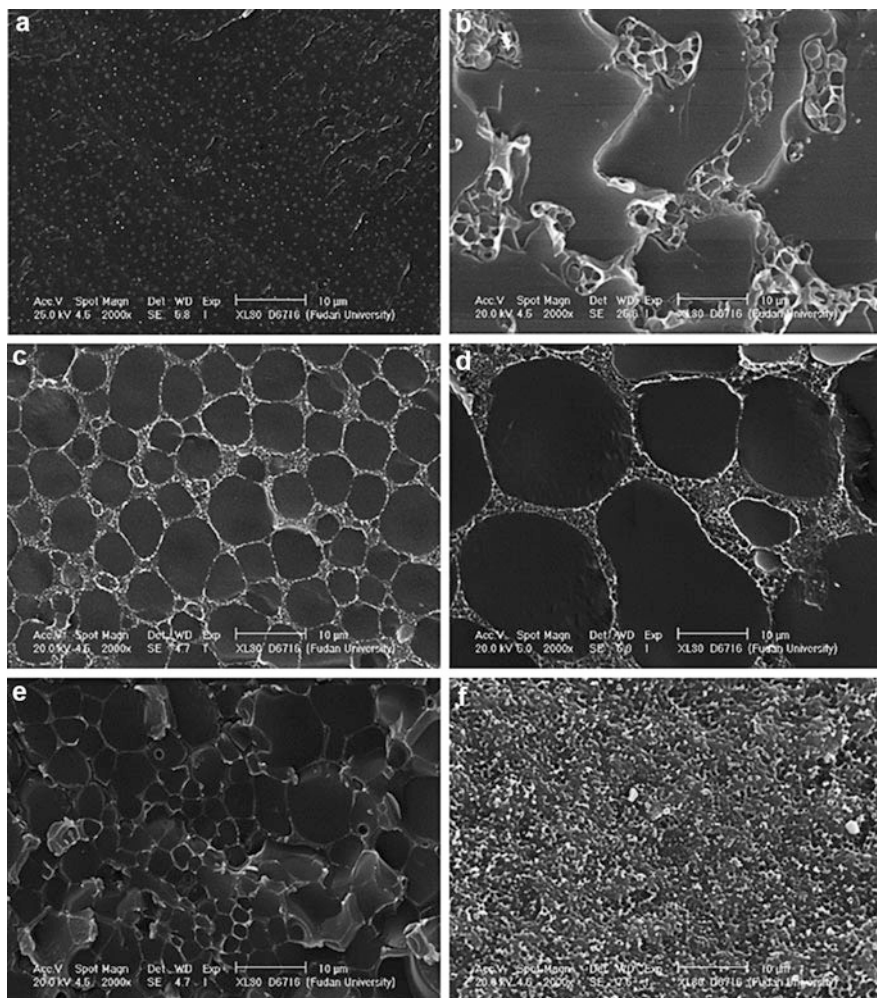


Fig. 7 Morphologies of the modified epoxy systems with different molecular weights and contents of PES after being cured at 150 °C for 5 h. (a) PES (0.22)-14%; (b) PES (0.36)-14%; (c) PES (0.53)-14%; (d) PES (0.22)-20%; (e) PES (0.36)-20%; (f) PES (0.53)-20% reproduced from Yu et al. (2008)

increase of the molecular weight of PEI raised the cure rate of the modified systems and changed the morphology from PEI-rich domain in the low molecular weight PEI-modified system to PEI-epoxy co-continuous phase structure in the high molecular weight systems (Yu et al. 1998).

Yu et al. (2008) conducted a study of epoxy systems blended with poly(ether sulfone) of different molecular weights. The fracture surfaces of the blends were examined by SEM. The morphology changed drastically depending on the PES content and molecular weight. Figure 7a–c shows the typical morphologies of blends

with different molecular weight PES (14 wt%), with inherent viscosity of 0.22, 0.36, and 0.53 dL/g. For low molecular weight PES, the blend PES (0.22)-14% showed spherical domains dispersed in the epoxy-rich matrix. In the case of intermediate molecular weight PES, the morphology of the blend PES (0.36)-14% was a bicontinuous phase structure. Small PES particles could be seen in the epoxy continuous phase; meanwhile, spherical particles of epoxy could also be found dispersed in the PES continuous phase. However, the size distribution of the epoxy particles in the PES continuous phase was not uniform, probably because of the high viscosity at the late stage of the curing reaction, which restricted the further development of the microstructure. Moreover, for high molecular weight PES, the blend PES (0.53)-14% appears more co-continuous in nature, rather than a phase-inverted structure. Meanwhile, the PES phase formed the matrix, and epoxy appeared as big, interconnected spherical domains.

Figure 7d–f shows the effects of molecular weight on the morphologies of blends with PES at 20 wt%. All three blends show a phase-inversion structure. PES (0.22)-20%, similar to PES (0.53)-14%, forms a spongelike (bicontinuous) phase structure, although large epoxy spheres were found in the PES-rich membrane-like structures. For PES (0.36)-20% and PES (0.53)-20%, totally phase-inverted structures were observed, and diameter of epoxy-rich globules decreased with the increased of PES molecular weight.

Effect of Reactive End Groups on the Morphology and Interfaces

The reactive end group of thermoplastics could improve the interactions between the two components and thus increase the phase interfacial conditions.

PESs with reactive end groups were blended with epoxy to investigate the influence of functional end groups to morphology of epoxy/DDS system (Kim et al. 1995). The chain ends of the active PES mostly consist of amine (PES-NH₂). A nonreactive PES with 100% Cl chain ends was also used as a control polymer (PES). PES was dissolved in a mixed solvent of methylene chloride/methanol (= 90/10 in volume ratio), and epoxy was added to the solution. The cured film was fractured at liquid-nitrogen temperature, and the fractured surface was observed by scanning electron microscopy (SEM). The fractured specimen was immersed in methylene chloride (preferential solvent for PES) at room temperature to remove PES. The fractured and etched surface was also observed by SEM. For TEM observation the film was cut into an ultrathin section of 70 nm thickness by ultramicrotome, and the ultrathin section was stained by OsO₄. OsO₄ is found to stain selectively cured epoxy resin.

Figure 8 shows spherical domains of epoxy resin dispersed quite regularly in nonreactive PES matrix as expected. In contrast, when reactive PES is used, one cannot see any clear morphology under SEM (Fig. 9a), and there is no change in the SEM micrograph with solvent etching (Fig. 9b). It may suggest that the PES has reacted with epoxy, and it is hard to rinse it away with the solvent.

The morphology is revealed under TEM as shown in Fig. 10a; the dark region stained by OsO₄ can be assigned to the cured epoxy phase. Figure 10a resembles the

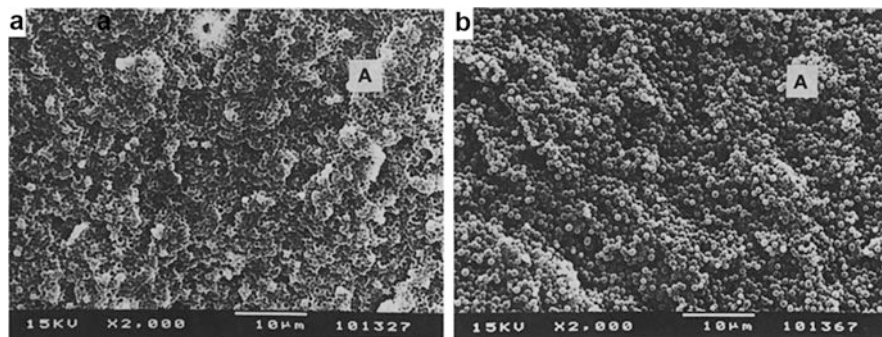


Fig. 8 SEM micrographs of epoxy/DDS/nonreactive PES = 47/23/30 cured at 180 °C for 3 h: (a) fractured; (b) fractured and etched reproduced from Yu et al. (2008)

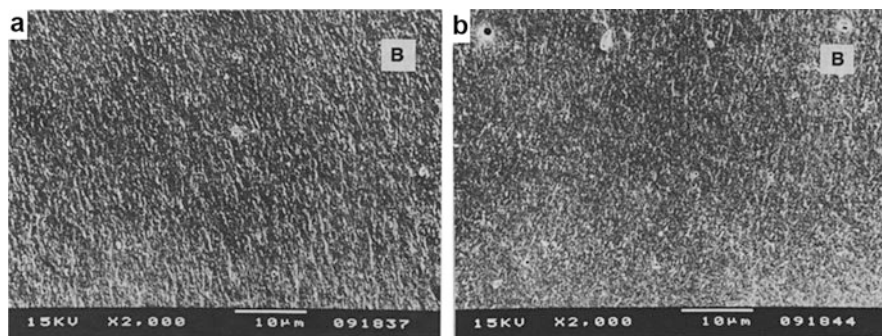


Fig. 9 SEM micrographs of epoxy/DDS/PES-NH₂ = 47/23/30 cured at 180 °C for 3 h: (a) fractured; (b) fractured and etched reproduced from Kim et al. (1995)

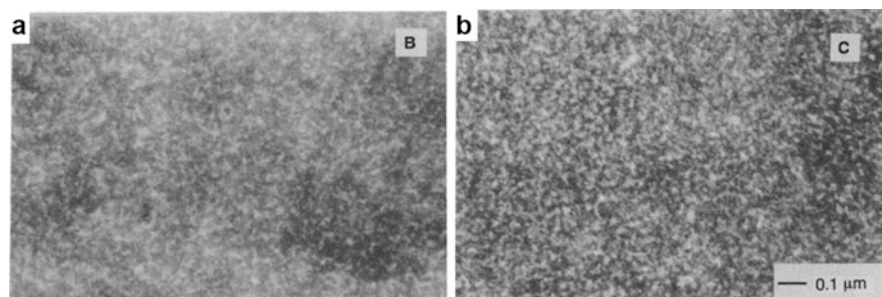


Fig. 10 TEM micrographs of epoxy/DDS/PES-NH₂ = 47/23/30: (a) cured at 180 °C for 3 h; (b) epoxy and PES-NH₂ pre-reacted at 180 °C for 3 h, DDS added at 145 °C, and then cured at 180 °C for 3 h reproduced from Kim et al. (1995)

morphology in Fig. 9. Note that the periodic distance is about 20 nm, suggesting the bicontinuous structure at the very early stage of SD is successfully fixed. Figure 10b is the TEM micrograph of the pre-reacted and then cured material, i.e., PES-NH₂ was reacted with epoxy at 180 °C for 3 h to provide PES endcapped with epoxy; and, after adding DDS at 145 °C, the system was cured at 180 °C for 3 h. One sees that the morphology is almost the same as that of one-step cure in Fig. 8a. It may imply that the reactivity of NH₂ chain ends is almost equal to that of amine groups of DDS, so that the similar situation can be provided for the in situ formation of block copolymer.

The Effect of Precure Temperature on Morphologies of Epoxy/PEI Blends

The precure temperature can effect morphologies of epoxy/PEI blends through influencing its phase-separation process. A classical diepoxy prepolymer diglycidyl ether of bisphenol A (DGEBA) was modified by an amorphous non-functionalized polyetherimide (PEI) and cured by 4,4'-methylenebis [3-chloro,2,6-diethylaniline] (MCDEA). After precure and postcure, the morphological micrographs of the samples were obtained using TEM.

Figure 11 (GirardReydet et al. 1997) shows the domain structures of 10P systems (10% by weight or 9.2% by volume) observed by TEM, depending on the precure temperature. The bright parts correspond to the epoxy-rich phase, and the dark parts correspond to the PEI-rich phase. It can be seen that, with 10 wt% of PEI, phase separation produced a dispersed PEI-rich phase in thermoplastic modifier in a continuous epoxy phase. A low precure temperature, 80 °C, leads to the formation of some very extensive non-spherical PEI domains, and the higher the precure temperature, the more spherical the PEI domains.

However, it has been shown that, at this modifier concentration, phase separation proceeded via the spinodal decomposition (SD) mechanism whatever the precure temperature. Due to the very low reactivity of the DGEBA–MCDEA system, SD under nonisoquench conditions was found to be very similar to the classical isoquench SD. Then, in the latest stage of demixing, the initial high degree of phase connectivity is gradually lost due to (a) the minimization of the interfacial area and (b) the redissolution of PEI insofar as the quench depth keeps on increasing. Nevertheless, the vitrification of the PEI-rich phase in high T_g thermoplastic affects the level of fragmentation of PEI domains. The higher precure temperature is, the later vitrification of the PEI phase occurs, and the further the phase-separation process goes. Therefore, when the precure temperature increases, the extent of phase separation increases and the extent of fragmentation/coalescence of PEI increases so that spherical particles are obtained for precure at 160 °C.

Figure 12 shows the domain structures of 20P systems (20% by weight or 18.6% by volume) observed by TEM. With 20 wt% of PEI, phase separation then leads to the formation of inverted structures (precure at 80 °C) or bicontinuous structures

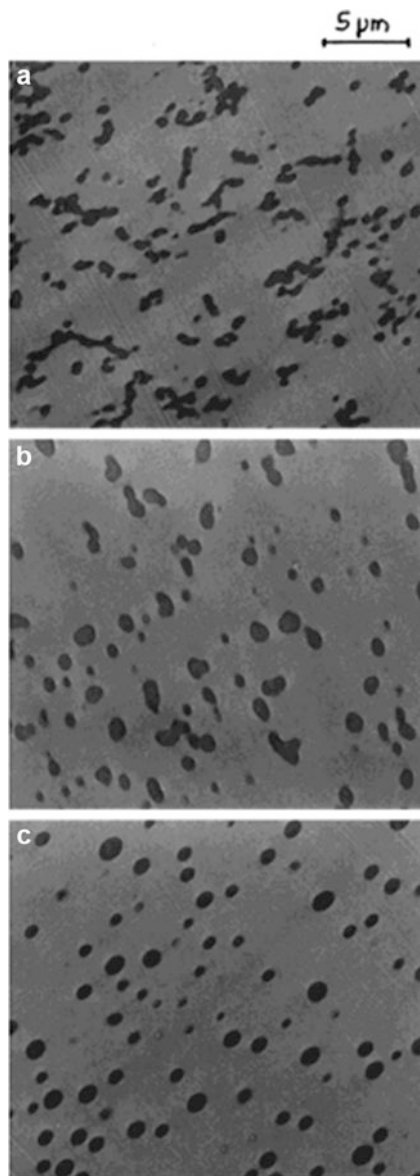


Fig. 11 Transmission electron micrographs of the 10P blends depending on the precure temperature: (a) 80 °C; (b) 135 °C; (c) 160 °C reproduced from Girardreydet et al. (1997)

(precure at 135 °C, 160 °C). In addition to the effect of the vitrification of the PEI phase, the much higher viscosity of 20P systems could also exacerbate differences in mobility depending on precure temperature. In particular, we observed at precure 80 °C first, the development of bicontinuous structures, thereafter, the interruption of

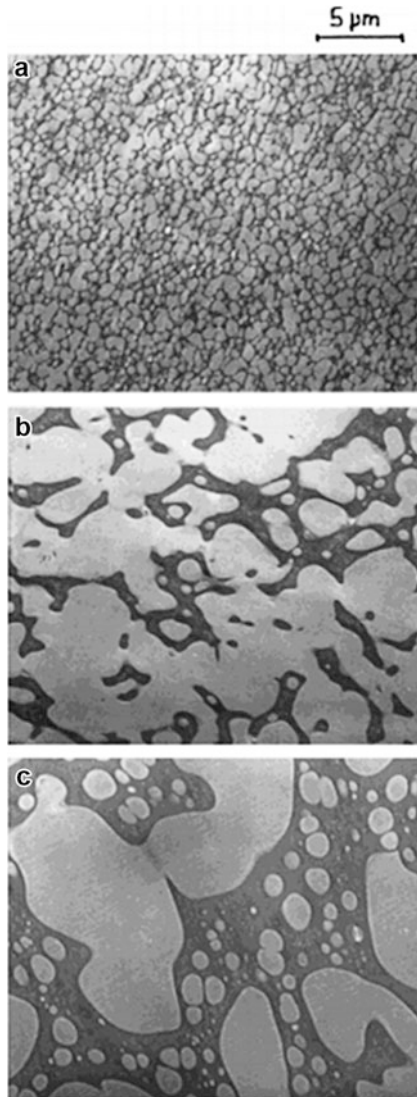


Fig. 12 Transmission electron micrographs of the 10P blends depending on the precure temperature: (a) 80 °C; (b) 135 °C; (c) 160 °C reproduced from Girardreydet et al. (1997)

the phase continuity leading to growing epoxy domains in a continuous PEI matrix. One can imagine their growth to go further at higher temperature so that the continuity of the PEI phase stops as well. It is worth noting the presence of a subinclusion in the PEI domains for precure at 135 °C and especially 160 °C, suggesting secondary phase separation has occurred.

The Effect of Linear Block Copolymers on Microphase Morphological Structure

In general, the polymerization-induced phase separation occurs on the macroscopic scale since some of these modifiers are homopolymers or random copolymers. If block copolymers are used with the presence of miscible blocks, the polymerization-induced phase separation could be confined to the nanometer scales and thus the nanostructures were obtained.

Polystyrene-block-poly(methyl methacrylate) (PS-*b*-PMMA) was blended with DGEBA to investigate the influence of block copolymers on the formation of nanostructures in epoxy thermosets (Fan and Zheng 2008). It has been known that PMMA blocks are miscible with epoxy after and before curing reaction, whereas the polymerization-induced microphase separation occurs in the thermosetting blends of epoxy resin and polystyrene. Three block copolymers with different topological structures (linear versus star-shaped) and sequential structures of blocks were used. All the blends of thermosets containing the diblock copolymers were prepared by curing at 150 °C for 2 h plus 180 °C for 2 h to access a complete curing reaction. Atomic force microscopy (AFM) is used to examine the disordered or ordered nanostructures formed via the polymerization-induced microphase separation.

The AFM micrographs of the thermosets containing 10, 20, 30, and 40 wt% of the linear PMMA-*b*-PS are presented in Fig. 13. Shown in the left-hand side of each micrograph is the topography image and in the right is the phase image. It is seen that the thermosetting blends containing the linear block copolymer less than 40 wt% exhibited nanostructured morphologies. In terms of the volume fraction of PS in the thermosets, it is plausible to propose that the continuous matrix is attributed to the cross-linked epoxy, which could be miscible with PMMA subchains of the diblock copolymer, while the light region is responsible for PS domains. For the thermoset containing 10 wt% *l*-PMMA-*b*-PS, the PS spherical nanoparticles with the size of 50–60 nm in diameter were homogeneously dispersed into the continuous epoxy matrix. With increasing the content of the block copolymer, some interconnected PS microdomains began to appear (Fig. 13c), and quantity of the PS microdomains was increased, whereas the size of the spherical particle remains almost invariant. It is interesting that corona-like microdomains with the size of 100 nm were observed for the thermoset containing 40 wt% *l*-PMMA-*b*-PS (Fig. 13d). It is seen that the spherical PS nanoparticles were surrounded by a layer with the thickness of 20 nm. It is proposed that the external layer of PS nanodomains is formed from the demixing of PMMA subchains induced by polymerization. Due to the steric hindrance, the PMMA chains at the intimate surface of PS nanodomains could not be well mixed with epoxy matrix.

The effect of star-shaped block copolymers on microphase separation was also discussed in this literature. Similar works have been done by Bates (Lipic et al. 1998; Grubbs et al. 2000) and Pascault (Maiez-Tribut et al. 2007; Ritzenthaler et al. 2003). Besides the factors that affect normal polymerization-induced phase separation, the

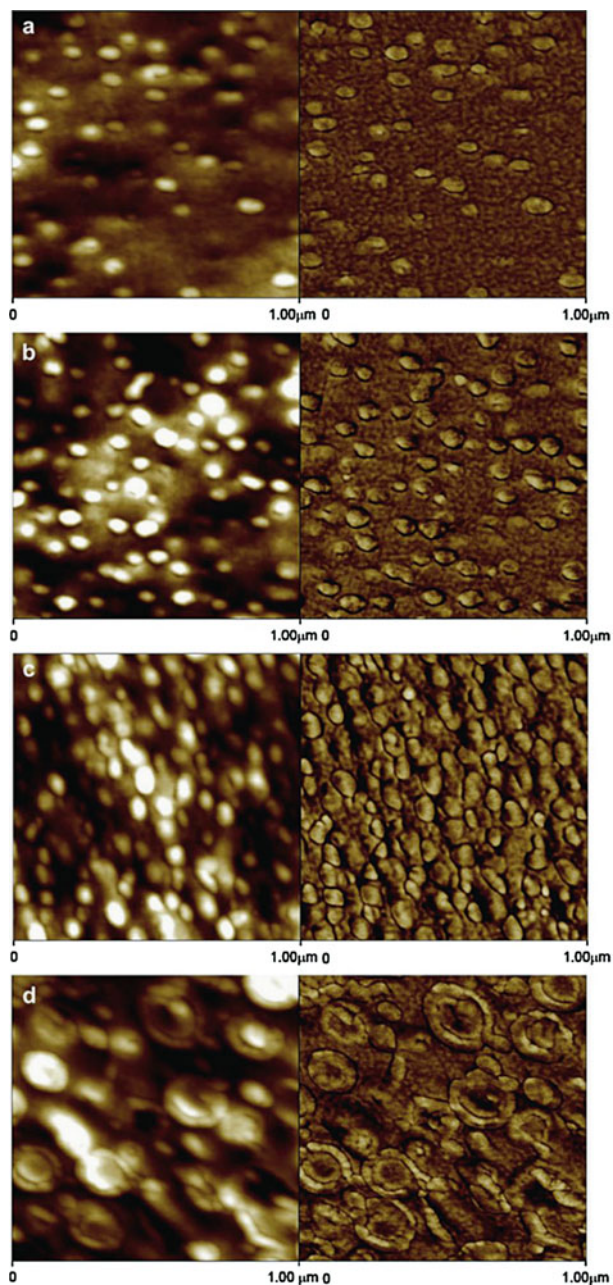


Fig. 13 AFM images of the thermosets containing (a) 10, (b) 20, (c) 30, and (d) 40 wt% of *l*-PMMA-*b*-PS diblock copolymer. *Left*: topography; *right*: phase contrast images Fan WC, reproduced from Zheng SX (2008)

molecular weight, ratio, and unique properties of each block have effects on microphase separation of epoxy/block copolymer blends as well.

The Effect of Curing Agent on Phase Separation Behavior

Curing agent accounts for a necessary part in an epoxy/cure agent/thermoplastic blend, and its types and concentration play a prominent role in phase-separation behavior through effecting solubility and cure rate.

In order to investigate the effect of different curing agents on phase separation and rheological behavior of a thermoplastic-modified epoxy system, two curing agents 3,3'-diaminodiphenylsulfone (3,3'DDS) and 4,4'-methylenebis(2,6-diethylaniline) (MDEA) were used to cure DGEBA and an amine-ended copolymer, 40:60 polyethersulfone:polyetherethersulfone (PES:PEES) (Blanco et al. 2004). In a complex viscosity profile for isothermal investigation at different temperatures for the epoxy resin cured with MDEA and 15% of PES:PEES, it shows a fluctuation that is presumably related to the separation of PES:PEES domains. However, in such a viscosity profile for the epoxy resin cured with 3,3'DDS and 15% of PES:PEES, no fluctuation was observed. There were only increasing values of viscosity with the reaction time caused by an increase in molecular weight of the epoxy matrix. The lack of fluctuation can be attributed to the absence of phase separation. In this case a homogenous interpenetrating network can be formed. No morphology was observed in SEM image, thus confirming the presence of a homogenous IPN.

The author argued that these different types of behavior could be related to the fact that for a PEI/DGEBA system, a DDS-based system presents an increased solubility compared to that of a MDEA-based system (Williams et al. 1997). Although no meaningful difference exists in reactivity between the two systems described in conversion versus time trace, the 3,3'DDS-based system is characterized by higher viscosity compared to that of MDEA system in rheological trace. The difference in solubility and viscosity plays against phase separation.

Besides the types of curing agent, its concentration could influence phase-separation behavior as well. By changing the amount of curing agent, the cure rate can be altered accordingly (Peng et al. 2000). The author found that the cure rate is higher in the blend with more cure agent. However, the occurrence time of the maximum rate is not consistent with the change of the amount of cure agent, which could be caused by different kinetic mechanisms.

It was found that different amount of curing agent caused very different final morphology by influencing cure rate, since morphology is determined by cure reaction and phase separation. If phase separation is faster than the cure reaction, phase decomposition may occur in the metastable region and the initial reduction of the length scale may be observed.

The author also observed that the change of the amount of cure agent only varies the cure rate but has no influence on the diffusion of the components.

Viscoelastic Phase Separation

In the early 1980s, de Gennes (1980) discussed the effect of viscoelastic on the early stage of phase separation when they considered the dynamics of the concentration fluctuations in binary polymer blends. Later, the two-fluid model was developed to describe the dynamic difference between two component mixtures. Then, Doi and Onuki (1992) have proposed a set of phenomenological hydrodynamic equations describing the coupling as a generalization of the earlier theories, the two-fluid model in polymer solutions and the Brochard theory for mutual diffusion in polymer blends. As applications of the present theory, they have successfully explained the coupling between stress and diffusion in polymer solutions and changing in the structure factor under shear flow. But the present theory assumed that the isotropic part of the network stress is zero, so it is only applicable to polymer solution system.

Tanaka (2000) reviewed the experiments and theories on phase separation and proposed a new model which is different from a solid model (model B) and a fluid model (model H), namely, “viscoelastic model.” This model is required to describe the phase-separation behavior of a dynamically asymmetric mixture, which is composed of fast and slow components. This viscoelastic model can explain (i) the moving droplet phase, (ii) transient gel, and (iii) phase-inversion phenomenon which existed in dynamic asymmetry mixtures. It is considered that viscoelastic effects play a dominant role in the dynamic asymmetry mixtures, which can be induced by either the large size difference or the difference in glass transition temperature between the components of a mixture.

Tanaka summarized the basic equations describing a viscoelastic model:

$$\begin{aligned} \frac{\partial \phi}{\partial t} &= -\nabla \cdot (\phi v) - \nabla \cdot [\phi(1 - \phi)(v_1 - v_2)] \\ v_1 - v_2 &= -\frac{1 - \phi}{\zeta} \left[\nabla \cdot \Pi - \nabla \cdot \sigma^{(1)} + \frac{\phi}{1 - \phi} \nabla \cdot \sigma^{(2)} \right] \\ \rho \frac{\partial V}{\partial t} &\cong -\nabla \cdot \Pi + \nabla \cdot p + \nabla \cdot \sigma^{(1)} + \nabla \cdot \sigma^{(2)} \end{aligned} \quad (1)$$

where Π is the osmotic tensor and v_1 and v_2 are the average velocities of components 1 and 2 at point r , respectively. The volume-average velocity v is given by

$$v = \phi v_1 + (1 - \phi)v_2 \quad (2)$$

Viscoelastic model can reduce to various models under certain assumptions. Solid and fluid models are special cases of viscoelastic model. For example, fluid phase separation described by model H, which is believed to be the usual case, can be viewed as a “special” case of viscoelastic phase separation. Generally, material is classified into the following three types: fluid, viscoelastic matter, and solid according to the internal rheological time τ_t and the observation time τ_o , as shown in Fig. 14. It was proposed that corresponding to this mechanical classification of material, descriptions of phase separation can be classified into the following three

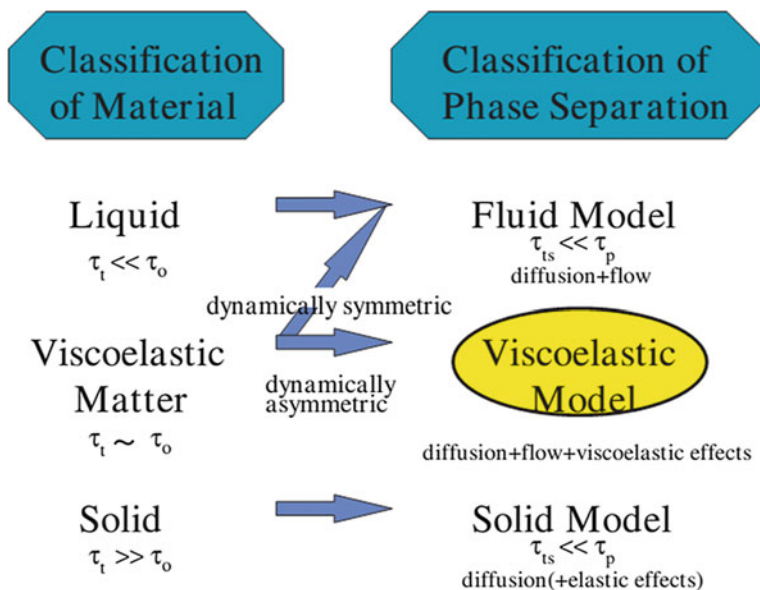


Fig. 14 Classification of material on the basis of rheological properties and the corresponding classification of descriptions of phase separation reproduced from Tanaka H (2000)

models: fluid, viscoelasticity, and solid models. In this case, the criteria are based on whether there are the velocity fields and dynamic asymmetry.

Tanaka primarily studied the phase separation in polymer solution and thermoplastic/thermoplastic blends. viscoelastic effect on the phase separation of thermoplastic–thermoset systems had not been noticed at that time. Hence, the viscoelastic phase separation on thermoplastic-modified thermoset blends will be discussed in detail in the next paragraph.

Polymerization-Induced Viscoelastic Phase Separation

Even though reaction-induced phase separation of thermoplastic-modified thermosetting blends has been intensively studied by many researchers, the morphologic evolution of these blends cannot be well explained using classic phase-separation theory. Yu and Li et al. (Gan et al. 2003; Tao et al. 2004; Wang et al. 2004; Yu et al. 2004; Liu et al. 2006; Zhan et al. 2006) introduced the concept of viscoelastic phase-separation theory into the thermosetting systems, while Jyotishkumar et al. (2009, 2010, 2011, 2012) undertook considerable research in this area. In the blend of epoxy resin modified with polyetherimide (PEI), PEI has a high T_g of 217 °C; however, epoxy resin has a low T_g of about -5 °C. The T_g of a fully cured epoxy resin with methyltetrahydrophthalic anhydride (MTHPA) as the hardener will be about 110 °C, which is much less than that of PEI. Thus, the dynamic asymmetry

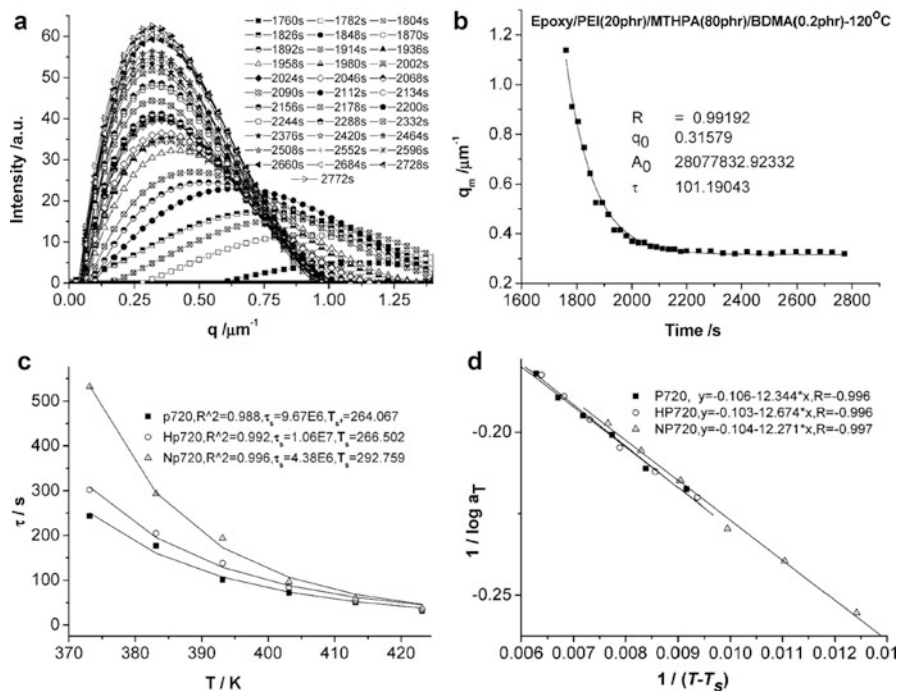


Fig. 15 Light-scattering results of viscoelastic phase separation of polyetherimide-modified epoxy-anhydride systems. (a) Intensity versus q_m at different times; (b) exponential decay of q_m versus time; (c) relaxation time of phase-separation plot of phase separation plotted by fitting WLF equation; (d) linear fitting of shift factor for systems with different amounts of accelerators reproduced from (Gan et al. 2003)

will accompany the entire phase separation due to the difference in the glass transition between the two components. And phase separation would be influenced by the viscoelastic behavior. The morphologies of the blends with the accelerator (benzyl dimethylamine) are of the co-continuous type, exhibiting irregular shapes. They are quite different from that without accelerator in which the morphology is spherical. Results of light-scattering studies revealed that the Williams-Landel-Ferry (WLF) equation was well used to describe the phase-separation behavior (as shown in Fig. 15). It demonstrated experimentally that the coarsening processes of epoxy droplets and the final morphologies obtained in these PEI-epoxy blends are affected by viscoelastic behavior (Gan et al. 2003).

Therefore, relaxation of the thermoplastic plays a very important role as long as the thermosetting phase has unblocked its chain mobility. The viscoelastic phase separation of a PES-modified epoxy system was examined by Yu et al. (2004). The morphologies of fractured surfaces of the two final cured compositions were observed by SEM. The blend PES-20% displays a phase-inversion structure, while the blend PES-14% showed bicontinuous morphologies. The morphologic evolution of the PES-14% blend cured at 120 °C was monitored by optical microscope as

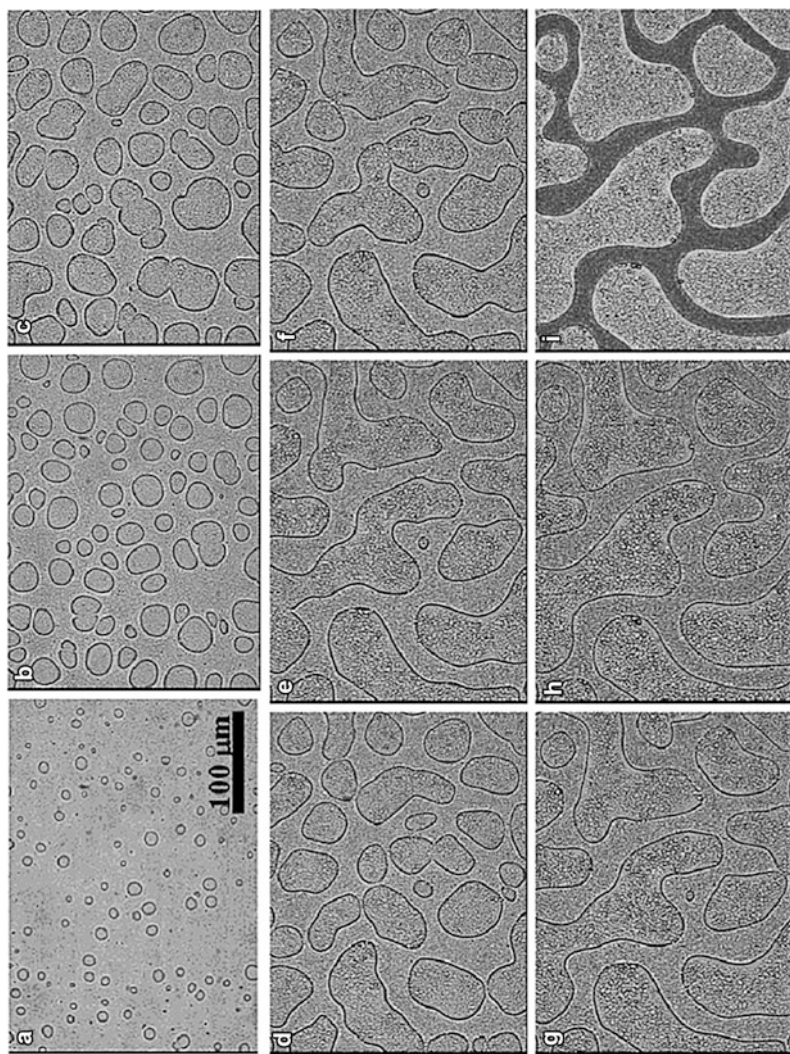


Fig. 16 Development of morphologies in a PES-14% blend cured at 120 °C, followed by optical microscopy: (a) 600 s, (b) 660 s, (c) 720 s, (d) 780 s, (e) 840 s, (f) 900 s, (g) 960 s, (h) 1,200 s, (i) 3,600 s reproduced from Yu et al. (2004)

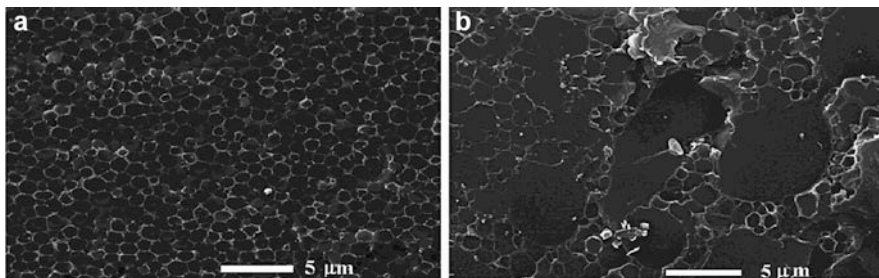


Fig. 17 SEM of PES-14% cured at 120 °C at different times: (a) 480 s and (b) 600 s reproduced from Yu et al. (2004)

shown in Fig. 16. The cloud-point time was about 9 min, and the first micrograph with enough contrast between phases was recorded 1 min after the beginning of phase separation. The fractured surface of another sample at the same conditions was also observed by SEM as shown in Fig. 17. A phase-inversion structure was observed by optical microscope and SEM in which the epoxy spheres are surrounded by the membrane-like PES-rich phase. As the polymerization proceeds, larger epoxy droplets appear, grow ever larger, connect to each other, and, finally, bicontinuous phase structure formed.

In the present dynamic asymmetry systems of PES and thermoset monomer/growing thermoset, in the middle and late stage of phase separation, the slower dynamic phase (PES-rich) becomes more and more viscoelastic with the escape of thermoset monomer (or low MW growing thermoset) from the PES-rich phase and eventually behaves as an elastic body. Meanwhile, the less viscoelastic phase (thermoset-rich phase) starts to coarsen with time, and the elastic force balance dominates the morphology instead of the interface tension, which leads to the anisotropic shape of the domain. This is in accord with the elastic regime ($\tau_d < \tau_{ts}$). As the rate of curing reaction is slow enough, the coarsening process proceeds further, and phase separation drops into the hydrodynamic regime ($\tau_d > \tau_{ts}$), where disentanglement of PES chains occurs in PES-14%. The anisotropic shape of the domain becomes spherical again with the lowest interfacial energy since the interface energy overcomes the elastic energy. While the coarsening of thermoset-rich particles made the thermoset-rich phase become a continuous structure, further phase separation or disentanglement of PES chains slowed down in the region of the PES-rich phase.

Correspondingly, in order to describe the characteristic of the evolution process of phase separation in the early age, imidazole as a fast curing agent was introduced into PEI-modified epoxy system (Wang et al. 2004). The morphologies of blends were shown in Fig. 18, at all curing temperature, PEI-5 has a homogenous structure. PEI-10 shows also a homogenous structure at 130 °C; however, it forms spongelike phase structure at lower curing temperature, in which uniform epoxy-rich globules with 0.2–0.5 mm diameter dispersed in the membrane-like PEI-rich phase. For PEI-18 and PEI-25, similar spongelike phase structures were also observed; the diameter of epoxy-rich globules decreases with the increase of PEI concentration. To understand

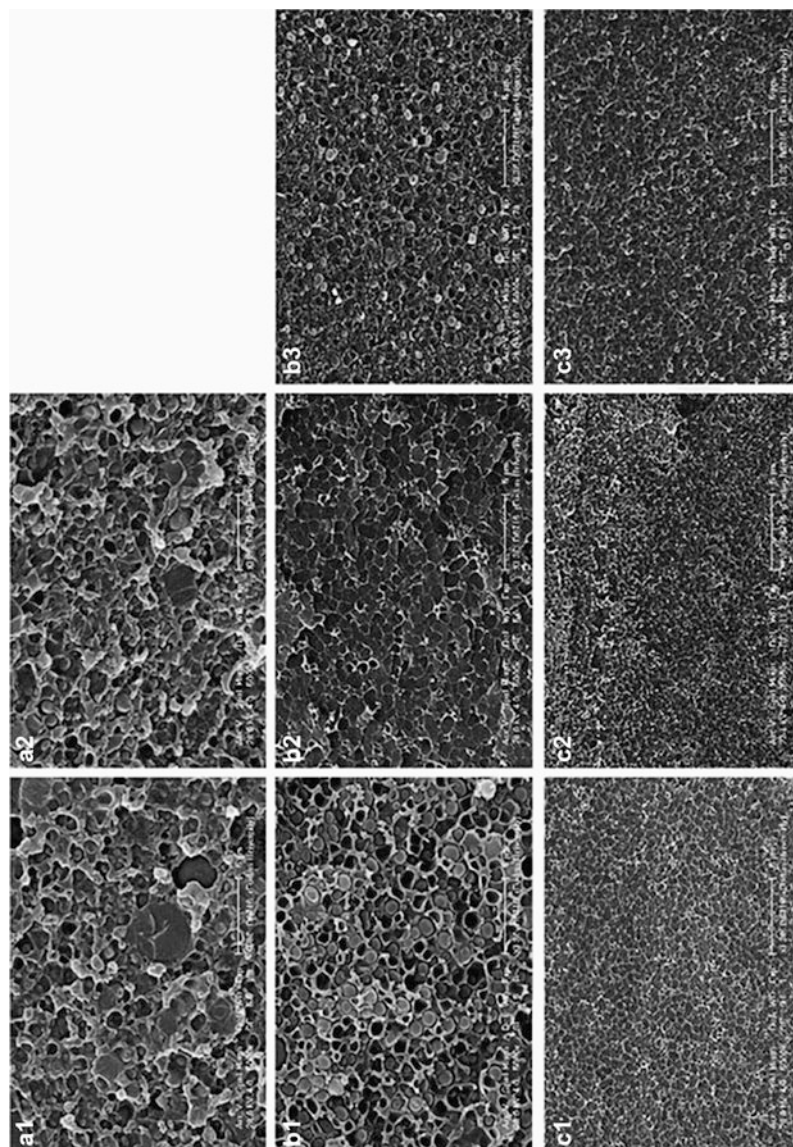


Fig. 18 SEM of blends after curing 2 h at different temperatures. (a1) PEI-10 110 °C, (a2) PEI-10 120 °C, (a3) PEI-10 130 °C, (b1) PEI-25 110 °C, (b2) PEI-25 120 °C, (b3) PEI-25 130 °C, (c1) PEI-18 110 °C, (c2) PEI-18 120 °C, (c3) PEI-18 130 °C reproduced from Wang et al. (2004)

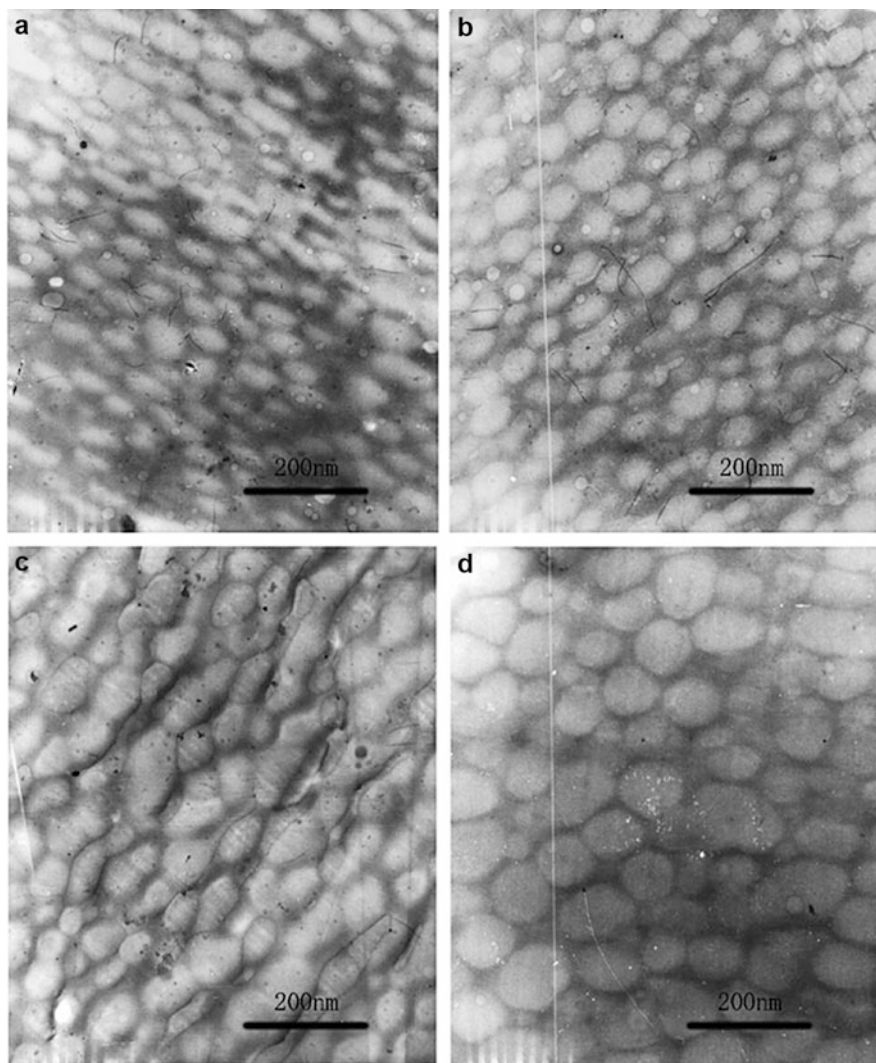


Fig. 19 TEM of PEI-18 cured at 110 °C at different times: (a) 15 min, (b) 20 min, (c) 30 min, (d) 40 min reproduced from Wang et al. (2004)

the early stage of phase-separation mechanism, SR-SAXS and TEM were used to study the early stage of phase separation in PEI-18 cured at 110 °C. The results of SR-SAXS implied a typical SD mechanism of phase separation. The TEM graphs of PEI-18 are shown in Fig. 19. As one can see, a spongelike phase structure formed from the very beginning of the phase separation, and the epoxy-rich particles grew from about 75 to 100 nm in diameter with time. The TEM results correspond well with the results of synchrotron radiation small angle X-ray scattering (SR-SAXS).

In these blends, the phase structure was first strongly affected by the dynamic asymmetry in early stage. Because the viscosity of the epoxy-rich medium is quite low whereas the PEI viscosity is too high to measure at experimental temperatures that are far below the glass transition temperature of PEI, strong dynamic asymmetry forms between PEI-rich and epoxy-rich. And then the phase structure was frozen by the gelation. Since PEI-5 has the fastest curing rate than other three modified systems, i.e., deeper quench depth and early gelation, phase separation was hindered and homogenous structure was achieved because of the diffusion of epoxy molecules being prevented by the network formation of epoxy matrix. For PEI-10 cured at 130 °C, the better solubility at high temperature and faster curing rate shortens the time available for phase separation; as a result, PEI molecules are frozen in the epoxy network. While the lower curing rate of PEI-18 and PEI-25 extends the phase-separation time but enhanced the characteristic relaxation time of chain disentanglement due to the increase of PEI volume fraction, as a result, spongelike phase structure is formed.

In a polyesterimide (PEI)-modified DGEBA-anhydride system, where the phase-separation process evolved much earlier than the gel time, by considering the viscoelastic relaxation of the phase-separation behavior, Yu et al. (2006) were the first to observe an exponential growth of complex viscosity during phase separation (Fig. 20):

$$\eta^*(t) = \eta_0^* + A_0 \exp(t/\tau_\square) \quad (3)$$

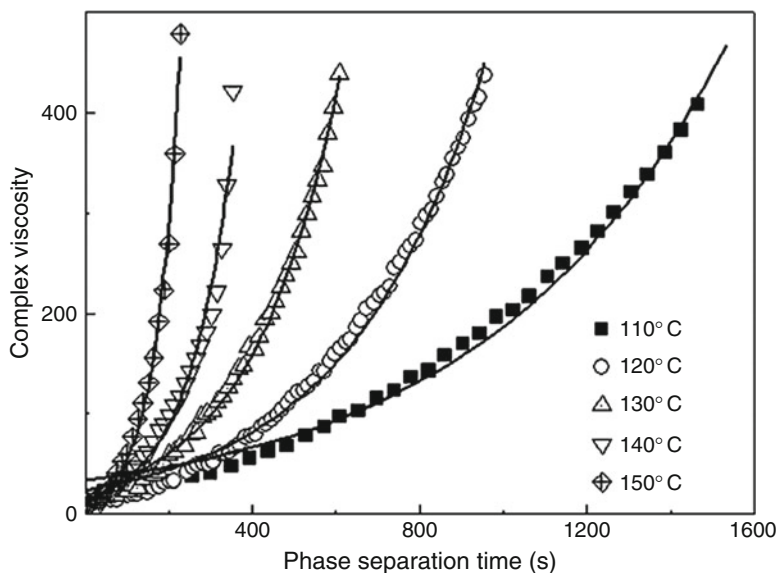


Fig. 20 Complex viscosity evolution during phase separation in PEI-20-cured at different temperatures. *Dot* corresponds to the experimental data, and line corresponds to exponentially growth simulation reproduced from Yu et al. (2006)

where A_0 is magnifier and τ is the relaxation time. Much like the relaxation time from light scattering of light intensity and q_m , the rheological results can also be well fitted to the WLF equation.

Recently, Thomas et al. (Jyotishkumar et al. 2011) found that this type of exponential growth of viscosity has connections with the thermoplastic content on the ABS-modified DGEBA/DDS system. In the blends with 3.6 and 6.9 wt%, ABS showed dispersed phase structure, suggesting a nucleation and growth (NG) mechanism by optical microscope. For 10 and 12.9 wt% ABS containing blends, very complex phase-separation process was observed as shown in Fig. 21. In the initial stage of phase separation, spherical ABS particles are dispersed in the continuous epoxy matrix typical for the NG mechanism (Fig. 22a), and then, co-continuous structure is formed from the SD mechanism (Fig. 22b). After a few seconds, the co-continuous structure gets ruptured; rapidly the ABS-rich phase becomes the continuous phase, and the epoxy-rich phase becomes the dispersed phase indicating a phase-inversion process which is typical for viscoelastic phase separation (Fig. 22c). This phenomenon is due to the high molecular weight of ABS compared to the epoxy resin. Within seconds, the epoxy-rich droplets grow very rapidly. This results in a co-continuous structure in which both the epoxy-rich and the ABS-rich phase are continuous (Fig. 22d). Finally the big elongated islands of the ABS phase dispersed in the epoxy matrix (Fig. 22f).

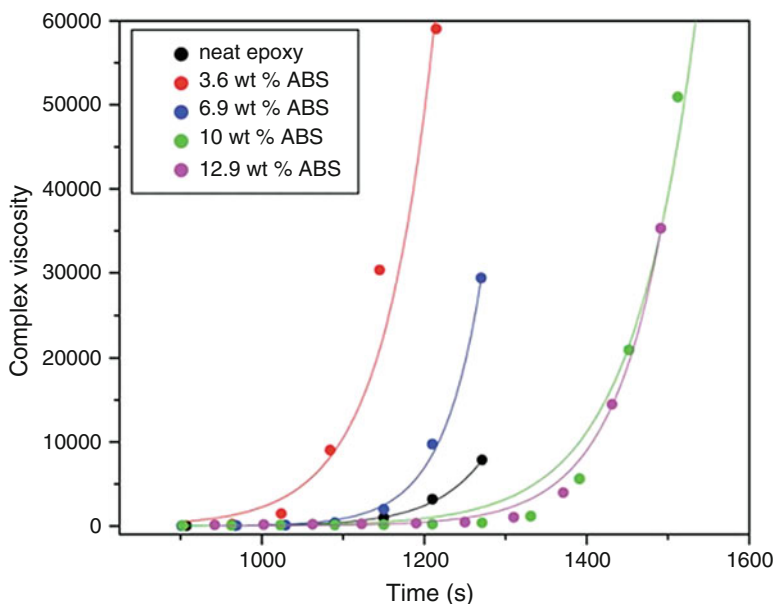


Fig. 21 Exponential growth behaviors of complex viscosity during curing in epoxy/ABS blends at 180 °C (dots correspond to the experiment data and solid lines correspond to exponential growth simulation) reproduced from Jyotishkumar et al. (2011)

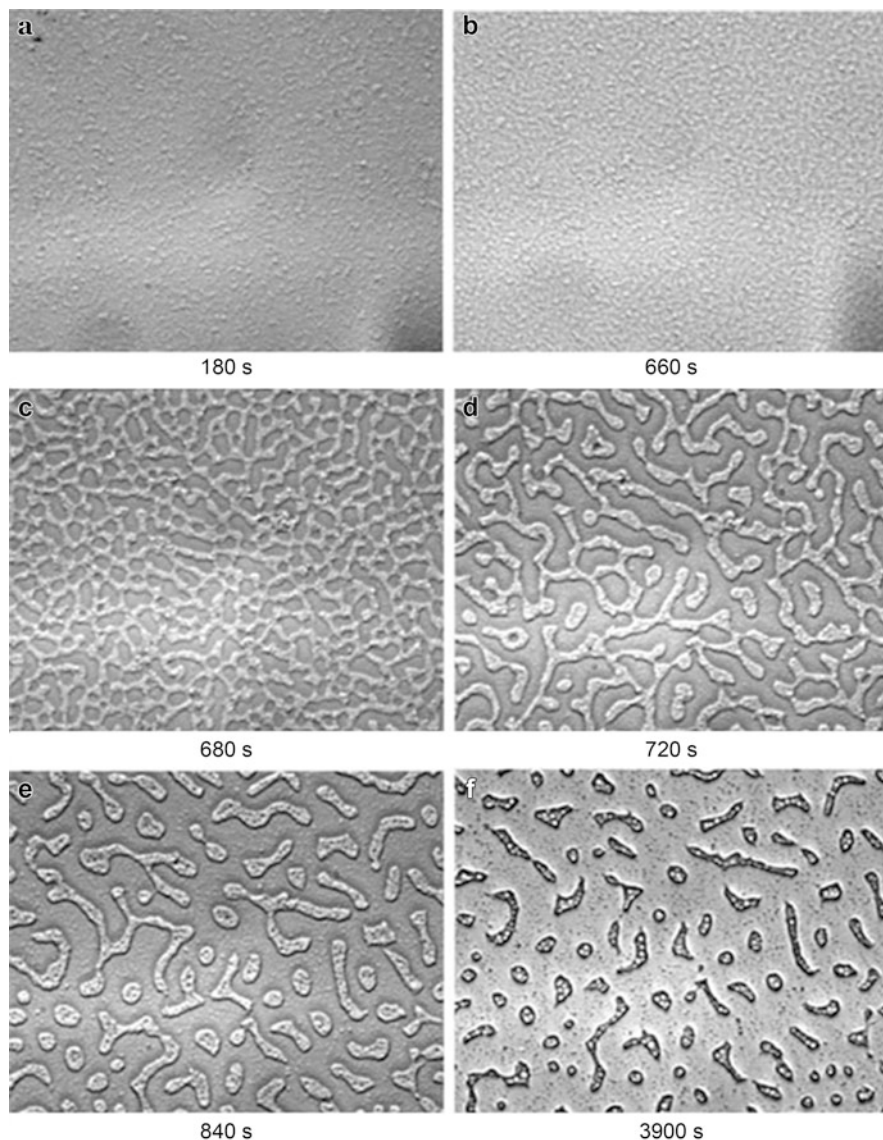


Fig. 22 Evolution of morphologies in 10 wt% ABS-modified epoxy blends at 180 °C ($800 \times 800 \text{ mm}^2$) reproduced from Jyotishkumar et al. (2011)

Gan et al. (2009) also examined the effect of the molecular weight of PEI on the viscoelastic phase separation of PEI/epoxy blends. The processes of phase separation at different temperatures for the blends with PEIs of different molecular weights were monitored by TRLS. It has been found that the phase separation of PEI/epoxy blends takes place via spinodal decomposition, which is initiated by the increasing

molecular weight of the thermoset epoxy resin and stopped by the very high viscosity of the blend before gelation. The lower the molecular weight is, the higher the conversion is for phase separation. Then, an increase in the PEI molecular weight leads to a decrease in the onset time of phase separation and cloud-point conversion.

Molecular weight also has dramatic effect on viscoelastic phase separation. On the basis of the theories of viscoelastic phase separation, increasing thermoplastics molecular weight will increase dynamic asymmetry between thermoplastics and the growing thermoset/thermoset monomer. As the initial morphology during phase separation tends to be the phase-inversion structure morphology in the dynamic asymmetry systems, quicker phase separation in high molecular weight thermoplastics systems would result in more elastic deformation of thermoplastics-rich phase, and thus thermoplastics continuous structures are easier to obtain for higher molecular weight thermoplastics systems at the same content because of the large difference between thermoplastics and slightly cured thermoset phases in both molecular weight and chain mobility. At the same time, the quicker phase separation and elastic deformation in the higher molecular weight thermoplastics systems would also result in a sharper increase of blend viscosity, which also comes from the sensitivity of higher molecular weight thermoplastics to solution concentration and the curing of epoxy.

Thermoplastic/thermosetting polymer blends, exhibiting both phase separation and crystallization, are of particular interest since their morphology and properties can be influenced by both processes. By choosing a thermoplastic component with melting and crystallization temperatures in the temperature range of the curing epoxy oligomers, phase separation can be influenced by the isothermal crystallization of the thermoplastic polymer and vice versa. The reaction-induced phase separation of DGEBA/DDS/POM blends was studied by Groeninckx et al. (Goossens et al. 2006). Blends with different amounts of POM at curing temperatures above (180 °C) and below (150 and 145 °C) the melting temperature of POM ($T_m = 168$ °C) were considered. For all these blends cured at 180 °C, a co-continuous structure was observed at the beginning of phase separation. The final blend morphologies of the different blend compositions after 4 h curing were different because of their position with respect to the critical point.

The phase-separation process for the 15 wt% POM blend is depicted in Fig. 23. The morphological changes can be also well described by viscoelastic phase separation.

Enhanced Viscoelastic Effect

In the researches of viscoelastic effect, ternary systems of blends containing fillers have also drawn much attention. Recent studies have shown that the dispersion of nanoscale fillers in polymer systems can change their mechanical, thermal, and electrical properties dramatically (Balazs et al. 2000, 2006; Allegra et al. 2008; Hooper and Schweizer 2006). Inspired by this notion, some researchers started to

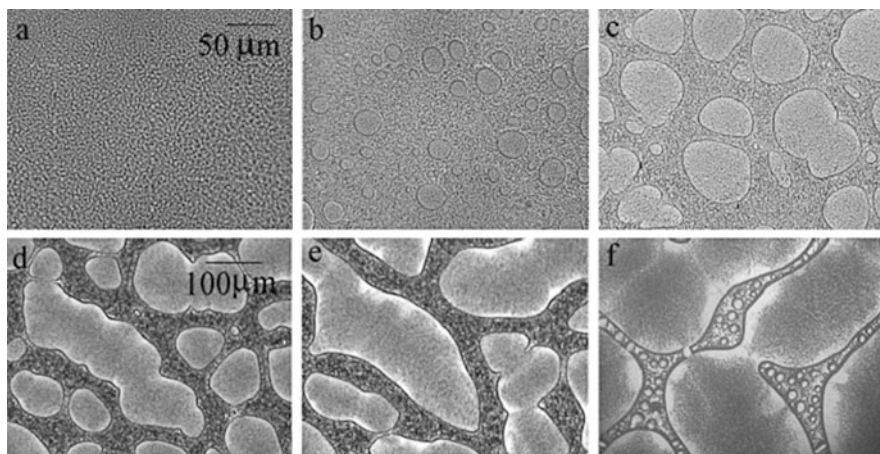


Fig. 23 OM pictures of a blend with 15 wt% POM cured with different time at 180 °C: (a) 10.7 min, (b) 11.25 min, (c) 11.75 min, (d) 12.5 min, (e) 13.5 min, (f) 60 min reproduced from Goossens et al. (2006)

investigate the effect of mesoscopic fillers on polymer blends, especially with dynamic asymmetry.

Several mesoscopic fillers were blended into epoxy/PES system, which was then cured by methyltetrahydrophthalic anhydride (MTHPA) (Zhong et al. 2011). OM experiments and TRLS were performed to monitor the curing process. Final cured films were observed by TEM.

As compared to Fig. 16 of a typical evolution process of the polymerization-induced viscoelastic phase separation in the thermoplastics–epoxy system observed by OM, Fig. 24 showed a dramatic change in morphology evolution when 2 wt% of surface-modified sepiolite is added to PES-modified epoxy system (sample PES13Sep2). At the early stage of the phase separation, a micro-bicontinuous phase structure is observed, which is the same as that seen in PES13 (without sepiolite). However, rather than coarsen rapidly, the PES13 and epoxy-rich phases in PES13Sep2 grow slowly till the chemical gelation of the epoxy. Bicontinuous networks with much smaller characteristic length scales are obtained at the end of phase separation. Quite different from the sample without sepiolite, there is no clear inverted phase structure, while the bicontinuous structure formed at the early stage coarsens slowly, and the network formed by the PES-rich phase relaxes tardily (Fig. 25).

TRLS is applied to trace the effect of meso-fillers on the phase-separation process. Figure 25 shows typical example of scattering profiles with time for the two systems. PES13Sep2 with meso-fillers has a much larger scattering vector q_m than that of the sample without fillers. This indicates that the sepiolite added has a refinement effect resulting in a much smaller characteristic length scale, which accords well with the results from OM.

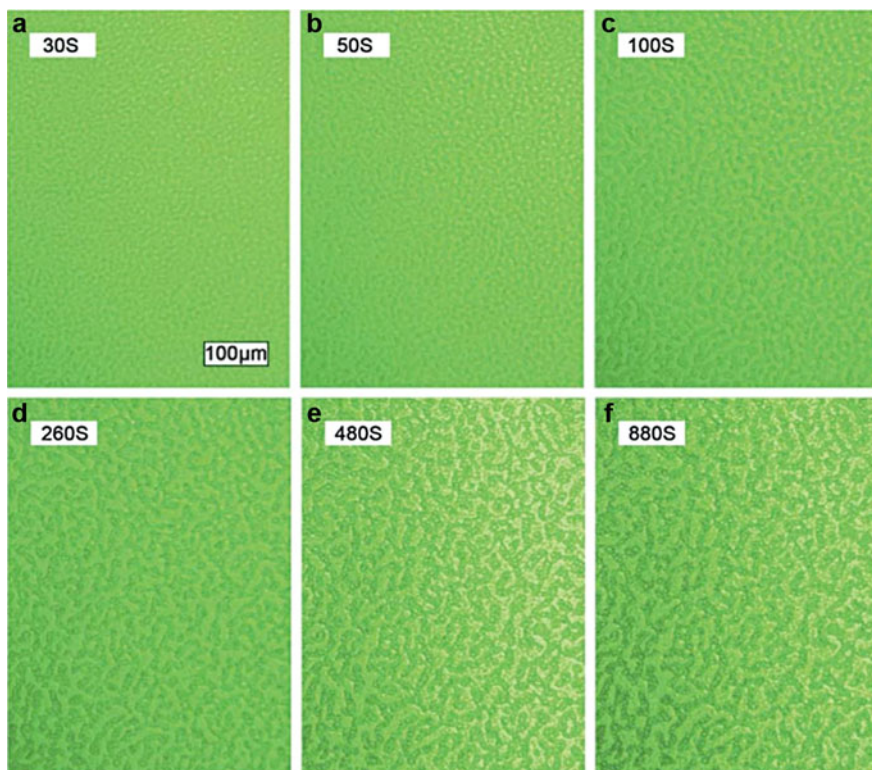


Fig. 24 Morphology evolution of PES13Sep2 with mesoscopic sepiolite at 120 °C reproduced from Zhong et al. (2011)

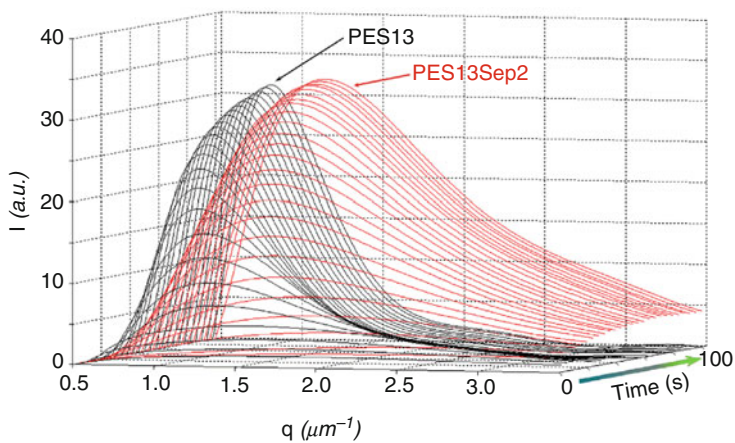


Fig. 25 TRLS profiles of PES13 and PES13Sep2 cured at 110 °C reproduced from Zhong et al. (2011)

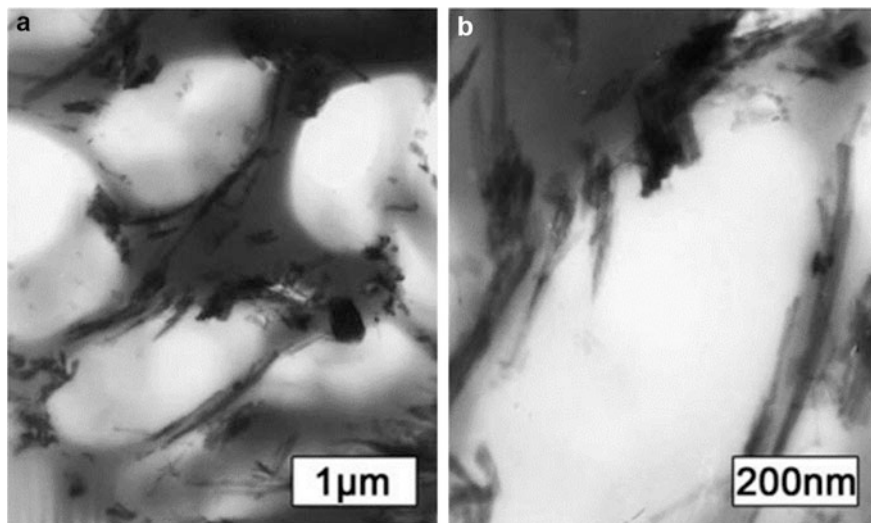


Fig. 26 TEM micrographs of the morphologies of PES13Sep2 cured at 120 °C reproduced from Zhong et al. (2011)

TEM was used to observe the location and dispersion conditions of sepiolite in sample PES13Sep2 after final curing at 120 °C. In Fig. 26, the bright regions correspond to the epoxy-rich phase, the gray regions to the PES-rich, and the dark regions to inorganic sepiolite. The TEM micrographs show that most of the sepiolite fillers are in the PES-rich phase, some also cross through the interface of the PES-rich and epoxy-rich, but few distribute in the epoxy-rich phases (bright area). It is noteworthy that most of the rodlike sepiolite particles with high aspect ratio are not randomly dispersed but oriented along the direction of the stress of the PES-rich phase.

It indicates that dynamic factors rather than thermodynamics factors should be used to explain the distribution of fillers in dynamic asymmetry systems. During the phase-separation process, sepiolite has the lowest mobility and is unable to be transported long distances due to its mesoscale size, and the movement of sepiolite is also restricted by the entanglement of sepiolite with long molecular chains; although epoxy precursors may have the chance to gather around the sepiolite particles due to thermodynamic affinity, the large stress of the PES-rich phase pushes the epoxy diffusing away. The main reason of selective distribution of sepiolite comes from the large dynamic difference between the immiscible components and asymmetric stress division during phase separation.

Other related researches show that, for blends near critical concentration, the introduction of fillers led to much finer phase structure with smaller characteristic length scale. At off-critical composition (i.e., blends with low concentration of slow dynamic component), the strong polymer chain entanglement resulted in enwrapped mesoscopic fillers within a slow dynamic phase (Liu et al. 2012). The effect of size

and content of mesoscopic fillers on viscoelastic phase separation was also investigated (Zhang et al. 2014).

Conclusions

In this chapter, the evolution of mechanism of phase separation of thermoplastic-modified epoxy blends was reviewed, and the techniques such as OM, SEM, and TEM play an important role in characterization of structure of blends and understanding the mechanism of phase separation. Moreover, the properties of polymer blends are mainly determined by the morphology on different length scales. To understand more about mechanism of phase separation helps us to design suitable polymer blends for particular application.

References

- Allegra G, Raos G, Vacatello M (2008) Theories and simulations of polymer-based nanocomposites: from chain statistics to reinforcement. *Prog Polym Sci* 33:683–731
- Balazs AC, Ginzburg VV, Qiu F, Peng GW, Jasnow D (2000) Multi-scale model for binary mixtures containing nanoscopic particles. *J Phys Chem B* 104:3411–3422
- Balazs AC, Emrick T, Russell TP (2006) Nanoparticle polymer composites: where two small worlds meet. *Science* 314:1107–1110
- Blanco I, Cicala G, Motta O, Recca A (2004) Influence of a selected hardener on the phase separation in epoxy/thermoplastic polymer blends. *J Appl Polym Sci* 94:361–371
- Cui J, Yu Y, Chen W, Li S (1997) Studies on the phase separation of polyetherimide-modified epoxy resin, 2. Effect of molecular weight of PEI on the structure formation. *Macromol Chem Phys* 198:3267–3276
- de Gennes PG (1980) Dynamics of fluctuations and spinodal decomposition in polymer blends. *J Chem Phys* 72:4756–4763
- Doi M, Onuki A (1992) Dynamic coupling between stress and composition in polymer solutions and blends. *J Phys II France* 2: 1631–1656
- Fan WC, Zheng SX (2008) Reaction-induced microphase separation in thermosetting blends of epoxy resin with poly(methyl methacrylate)-block-polystyrene block copolymers: effect of topologies of block copolymers on morphological structures. *Polymer* 49:3157–3167
- Gan W, Yu Y, Wang M, Tao Q, Li S (2003) Viscoelastic effects on the phase separation in thermoplastics-modified epoxy resin. *Macromolecules* 36:7746–7751
- Gan W, Xiong W, Yu Y, Li S (2009) Effects of the molecular weight of poly(ether imide) on the viscoelastic phase separation of poly(ether imide)/epoxy blends. *J Appl Polym Sci* 114:3158–3167
- Girardretydet E, Vicard V, Pascault JP, Sautereau H (1997) Polyetherimide-modified epoxy networks: influence of cure conditions on morphology and mechanical properties. *J Appl Polym Sci* 65:2433–2445
- Goossens S, Goderis B, Groeninckx G (2006) Reaction-induced phase separation in crystallizable micro- and nanostructured high melting thermoplastic/epoxy resin blends. *Macromolecules* 39:2953–2963
- Grubbs RB, Dean JM, Broz ME, Bates FS (2000) Reactive block copolymers for modification of thermosetting epoxy. *Macromolecules* 33:9522–9534
- Hodgkin JH, Simon GP, Varley RJ (1998) Thermoplastic toughening of epoxy resins: a critical review. *Polym Adv Technol* 9:3–10

- Hooper JB, Schweizer KS (2006) Theory of phase separation in polymer nanocomposites. *Macromolecules* 39:5133–5142
- Inoue T (1995) Reaction-induced phase decomposition in polymer blends. *Prog Polym Sci* 20:119–153
- Jose J, Joseph K, Pionteck J, Thomas S (2008) PVT behavior of thermoplastic poly(styrene-co-acrylonitrile)-modified epoxy systems: relating polymerization-induced viscoelastic phase separation with the cure shrinkage performance. *J Phys Chem B* 112:14793–14803
- Jyotishkumar P, Koetz J, Tiersch B, Strehmel V, Özdilek C, Moldenaers PH, Ssler R, Thomas S (2009) Complex phase separation in poly(acrylonitrile-butadiene-styrene)-modified epoxy/4,4'-diaminodiphenyl sulfone blends: generation of new micro- and nanosubstructures. *J Phys Chem B* 113:5418–5430
- Jyotishkumar P, Özdilek C, Moldenaers P, Sinturel C, Janke A, Pionteck J, Thomas S (2010) Dynamics of phase separation in poly(acrylonitrile-butadiene-styrene)-modified epoxy/DDS system: kinetics and viscoelastic effects. *J Phys Chem B* 114:13271–13281
- Jyotishkumar P, Pionteck J, Özdilek C, Moldenaers P, Cvelbar U, Mozetic M, Thomas S (2011) Rheology and pressure-volume-temperature behavior of the thermoplastic poly(acrylonitrile-butadiene-styrene)-modified epoxy-DDS system during reaction induced phase separation. *Soft Matter* 7:7248–7256
- Jyotishkumar P, Moldenaers P, George SM, Thomas S (2012) Viscoelastic effects in thermoplastic poly(styrene-acrylonitrile)-modified epoxy-DDM system during reaction induced phase separation. *Soft Matter* 8:7452
- Kim BS, Chiba T, Inoue T (1995) Morphology development via reaction-induced phase-separation in epoxy poly(ether sulfone) blends – morphology control using poly(ether sulfone) with functional end-groups. *Polymer* 36:43–47
- Lipic PM, Bates FS, Hillmyer MA (1998) Nanostructured thermosets from self-assembled amphiphilic block copolymer/epoxy resin mixtures. *J Am Chem Soc* 120:8963–8970
- Liu X, Yu Y, Li S (2006) Viscoelastic phase separation in polyethersulfone modified bismaleimide resin. *Eur Polym J* 42:835–842
- Liu Y, Zhong XH, Yu YF (2010) Gelation behavior of thermoplastic-modified epoxy systems during polymerization-induced phase separation. *Colloid Polym Sci* 288:1561–1570
- Liu Y, Zhong XH, Zhan GZ, Yu YF, Jin JY (2012) Effect of mesoscopic fillers on the polymerization induced viscoelastic phase separation at near- and off-critical compositions. *J Phys Chem B* 116:3671–3682
- Maiez-Tribut S, Pascault JP, Soule ER, Borrajo J, Williams RJJ (2007) Nanostructured epoxies based on the self-assembly of block copolymers: a new miscible block that can be tailored to different epoxy formulations. *Macromolecules* 40:1268–1273
- Onuki A, Taniguchi T (1997) Viscoelastic effects in early stage phase separation in polymeric systems. *J Chem Phys* 106:5761–5770
- Onuki A, Yamamoto R, Taniguchi T (1997) Phase separation in polymer solutions induced by shear. *J Phys II Fr* 7:295–304
- Oyanguren PA, Riccardi CC, Williams RJJ, Mondragon I (1998) Phase separation induced by a chain polymerization: polysulfone-modified epoxy/anhydride systems. *J Polym Sci B Polym Phys* 36:1349–1359
- Peng LQ, Cui J, Li SJ (2000) Studies on the phase separation of a polyetherimide-modified epoxy resin, 4(a) – kinetic effect on the phase separation mechanism of a blend at different cure rates. *Macromol Chem Phys* 201:699–704
- Ritzenthaler S, Court F, Girard-Reydet E, Leibler L, Pascault JP (2003) ABC triblock copolymers/epoxy-diamine blends. 2. Parameters controlling the morphologies and properties. *Macromolecules* 36:118–126
- Tanaka H (1993) Unusual phase separation in a polymer solution caused by asymmetric molecular dynamics. *Phys Rev Lett* 71:3158–3161
- Tanaka H (1996) Universality of viscoelastic phase separation in dynamically asymmetric fluid mixtures. *Phys Rev Lett* 76:787–790

- Tanaka H (1997) Viscoelastic model of phase separation. *Phys Rev E* 56:4451–4462
- Tanaka H (2000) Viscoelastic phase separation. *J Phys Condens Matter* 12:R207
- Tang XL, Zhang LX, Wang T, Yu YF, Gan WJ, Li SJ (2004) Hydrodynamic effect on secondary phase separation in an epoxy resin modified with polyethersulfone. *Macromol Rapid Commun* 25:1419–1424
- Taniguchi T, Onuki A (1996) Network domain structure in viscoelastic phase separation. *Phys Rev Lett* 77:4910–4913
- Tao Q, Gan W, Yu Y, Wang M, Tang X, Li S (2004) Viscoelastic effects on the phase separation in thermoplastics modified cyanate ester resin. *Polymer* 45:3505–3510
- Wang M, Yu Y, Wu X, Li S (2004) Polymerization induced phase separation in poly(ether imide)-modified epoxy resin cured with imidazole. *Polymer* 45:1253–1259
- Williams RJJ, Rozenberg BA, Pascault JP (1997) Reaction-induced phase separation in modified thermosetting polymers. *Polym Anal Pol Phys* 128:95–156
- Yamanaka K, Inoue T (1989) Structure development in epoxy-resin modified with poly(ether sulfone). *Polymer* 30:662–667
- Yamanaka K, Takagi Y, Inoue T (1989) Reaction-induced phase-separation in rubber-modified epoxy-resins. *Polymer* 30:1839–1884
- Yu YF, Cui J, Chen WJ, Li SJ (1998) Studies on the phase separation of polyetherimide modified tetrafunctional epoxy resin. II. Effects of the molecular weight. *J Macromol Sci A* 35:121–135
- Yu Y, Wang M, Gan W, Tao Q, Li S (2004) Polymerization-induced viscoelastic phase separation in polyethersulfone-modified epoxy systems. *J Phys Chem B* 108:6208–6215
- Yu Y, Wang M, Gan W, Li S (2006) Phase separation and rheological behavior in thermoplastic modified epoxy systems. *Colloid Polym Sci* 284:1185–1190
- Yu Y, Wang M, Foix D, Li S (2008) Rheological study of epoxy systems blended with poly(ether sulfone) of different molecular weights. *Ind Eng Chem Res* 47:9361–9369
- Zhan G, Yu Y, Tang X, Tao Q, Li S (2006) Further study of the viscoelastic phase separation of cyanate ester modified with poly(ether imide). *J Polym Sci B* 44:517–523
- Zhang J, Li T, Hu ZN, Wang HP, Yu YF (2014) Effect of size and content of mesoscopic fillers on the polymerization induced viscoelastic phase separation. *RSC Adv* 4:442–454
- Zhao L, Zhan GZ, Yu YF, Tang XL, Li SJ (2008) Influence of attapulgites on cure-reaction-induced phase separation in epoxy/poly(ether sulfone) blends. *J Appl Polym Sci* 108:953–959
- Zhong XH, Liu Y, Su HH, Zhan GZ, Yu YF, Gan WJ (2011) Enhanced viscoelastic effect of mesoscopic fillers in phase separation. *Soft Matter* 7:3642–3650

Anbazhagan Palanisamy and Nishar Hameed

Abstract

Light scattering is a popular in situ technique commonly used to study the morphology evolution in real time in heterogeneous systems. The immediate response and short sample preparation times are the distinct advantages of light scattering compared to electron microscopy to study the morphology evolution in polymer blends. The small-angle light scattering (SALS) technique is extensively used to study the reaction-induced phase separation in epoxy blends. Studies involving various epoxy/block copolymer and epoxy/thermoplastic blends were included in this chapter. During the epoxy curing process, the morphology change with respect to curing time and blend composition was followed via the change in scattering patterns using time-resolved light scattering technique (TRLS). The formation of secondary structures within the phase-separated primary domains and their mechanism of phase separation were also studied using light scattering technique. More importantly, in reactive blending, the light scattering technique will provide deeper understanding of the effect of polymer functionality and processing parameters on the phase-separated morphology. This chapter would give an overview of morphology evolution studied in various reactive epoxy blends using light scattering technique.

Keywords

Polymer blends • Light scattering • Time-resolved light scattering • Morphology • Thermoplastic • Block copolymer • Phase separation

A. Palanisamy (✉)

Institute for Frontier Materials, Deakin University, Geelong, Australia

e-mail: psabchem@gmail.com

N. Hameed (✉)

Carbon Nexus, Institute for Frontier Materials, Deakin University, Geelong, VIC, Australia

Factory of the Future, Swinburne University of Technology, Melbourne, VIC, Australia

e-mail: nishar.hameed@deakin.edu.au

Contents

Introduction	558
Epoxy/PES Blends	559
Epoxy/PSF blends	562
Epoxy/PS Blends	563
Epoxy/PEI Blends	566
Epoxy/SAN Blends	569
Epoxy/ABS Blends	570
Epoxy/PMMA Blends	572
Epoxy/PCL Blends	573
Epoxy/PBT Blends	574
Epoxy/Phenoxy Blends	574
Epoxy/Polycarbonate Blends	576
Epoxy/PS- <i>b</i> -PCL Blend	577
Conclusions	579
References	580

Introduction

Epoxy polymers were commercialized in the late 1940s, and since then, they have been used in a wide range of industrial applications such as adhesives, tooling compounds, encapsulating materials, molding powders, casting compounds, etc. because of their good mechanical properties, thermal stability, and outstanding corrosion resistance (Wright 1986). Even though epoxy materials have good mechanical properties such as rigidity and high strength, their brittleness eliminates wider usage. Hence, toughening agents such as rubber, thermoplastics, and block copolymers were used to improve the fracture toughness of the epoxies (Bagheri et al. 2009; Hodgkin et al. 1998; Ruiz-Pérez et al. 2008). However, thermoplastics and block copolymers have been considered advantageous compared to rubber toughening of epoxies, due to technical difficulties such as expulsion of dispersed molecules or particles from the epoxy network while curing (Ruzette and Leibler 2005). A variety of thermoplastic materials such as poly(ether imide)s, polycarbonates, poly(caprolactone)s, polysulfones, etc. can be found in recent literature that has been used to toughen and improve processability of epoxies via blending technique (Omriani and Shahhossieni 2013; Yongtao et al. 2016; Arinina et al. 2015). In case of thermoplastic-modified epoxy systems, due to variable interaction and solubility of thermoplastics with epoxy pre-polymers and cured resins, phase separation occurs between thermoplastic-rich phase and epoxy-rich phase during the curing reaction. Since the bulk properties such as mechanical and electrical properties of epoxy materials depend on the microphase-separated morphology to some extent, the basic understanding and study of phase separation mechanism and its control via blending techniques has gained enormous attention (Mohan 2013). Phase separation in blends can be followed by techniques such as light scattering, neutron scattering, ellipsometry, and rheology (Parameswaranpillai et al. 2013; Jyotishkumar et al. 2011). The morphologies as a result of phase separation can be studied by scanning electron microscopy (SEM), transmission

electron microscopy (TEM), atomic force microscopy (AFM), fluorescence microscopy, etc. In particular, application of light scattering technique to study phase separation mechanism in various epoxy/thermoplastic and epoxy/block copolymer blends has been discussed in this chapter.

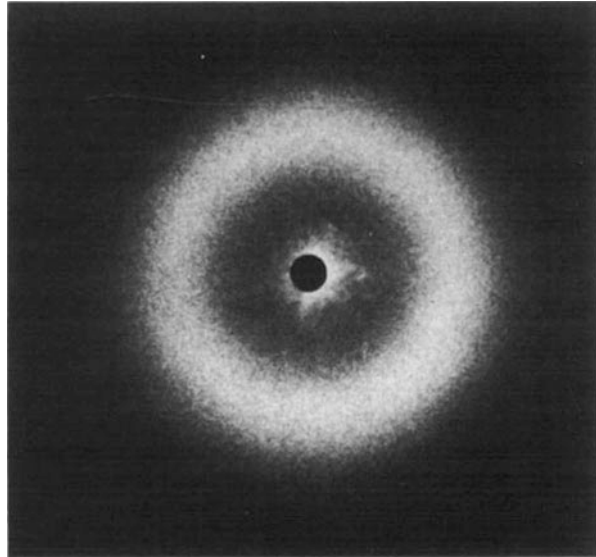
Small-angle light scattering (SALS) technique has been used since the 1980s to study phase separation in polymer blends due to its sensitivity to weak concentration fluctuations (Hashimoto et al. 1983; Tromp et al. 1995). Light scattering in polymers is an important phenomenon, especially in industrial polymers such as epoxy and epoxy blends, which have potential applications such as developing privacy windows, displays, thermal sensors, and smart optical materials (Mucha 2003). Polymers generally scatter light due to inhomogeneity in their composition. The scattering intensity is directly proportional to the difference in density or concentration within the material examined. In phase-separated polymer blends, the phases with different refractive indices give rise to specific light scattering profiles. Light scattering can also be conveniently used to follow dynamic phenomenon such as spinodal decomposition, coalescence, and crystallization and to study reactive processing in polymer blends. In time-resolved light scattering technique, the angular dependence of the scattering pattern is recorded in short time intervals to follow phase transition (Svoboda 2014). Here, the peak scattering vector that corresponds to the wavenumber of the concentration fluctuation is given by the equation $q_m = \frac{4\pi}{\lambda} \sin \frac{\Theta}{2}$, where λ and Θ are the wavelength of incident beam and the peak scattering angle, respectively. The reciprocal of the peak scattering vector (q_m) gives the periodic distance Λ_m ($\Lambda_m = \frac{2\pi}{q_m}$) of the dispersed particles or phases. The change in q_m and Λ_m is commonly used to follow the phase separation in blends combined with morphology data from electron microscopes. The movement of q_m values to the lower scattering angle denotes the phase separation; the smaller the characteristic scattering vector q_m , the larger the periodic distance Λ_m of the phase-separated structures.

In epoxy/thermoplastic blends, the multicomponent mixture is homogenous at the curing temperature which is lower than LCST (lower critical solution temperature). When curing proceeds, the phase separation occurs via depression in LCST due to increase in molecular weight of epoxy phase due to polymerization reaction. Various phase-separated structures such as spherical domains and interconnected globules were observed depending on the composition of the blend components (Inoue 1995). In this chapter, phase separation mechanism elucidated by light scattering technique in various epoxy/thermoplastic and epoxy/block copolymer blends was discussed.

Epoxy/PES Blends

In a tetrafunctional epoxy resin/poly(ether sulfone)/dicyandiamide blend (epoxy/PES/DICY), light scattering and scanning electron microscope (SEM) were used to follow phase separation during the curing reaction. The tetrafunctional epoxy resin used in this study was tetraglycidyl 4,4'-diaminodiphenylmethane (Kim et al. 1993).

Fig. 1 Light scattering pattern of spherical structures in epoxy/PES/DICY blend (Kim et al. 1993) (Reproduced with permission of Elsevier)



The blend was prepared at ratio epoxy/PES/DICY (100/25/5), cured at 190 °C, and light scattering profile was recorded at various time intervals to study onset and end of phase separation process. This thermoset/thermoplastic system exhibited an LCST behavior (LCST = 265 °C), single-phase below LCST temperature, in the initial stages of curing. During the curing process, phase separation started after an induction period and epoxy-rich region phase separated into spherical structures in the PES matrix. At the initial stages of curing, during the induction period, no light scattering was observed. After some cure time, appearance of a ringlike pattern of light scattering implies the formation of regularly phase-separated spherical structures (Fig. 1). As the curing proceeds, the ring pattern becomes brighter with a decrease in ring diameter. The corresponding scattering profile is shown in Fig. 2, where the peaks shifted toward lower scattering angle denote the growth of spherical structures via viscoelastic phase separation. Furthermore, the shift in scattering peaks level off, and further growth of structures was suppressed after gelation. The scattering profile is supported by the SEM images of cured resin showing the growth of dark spherical epoxy domain in the bright PES phase (Fig. 3).

Reaction-induced phase separation has been studied extensively to optimize the microstructures formed in epoxy composites (Oyanguren et al. 1996; Siddhamalli and Kyu 2000). In the same vein, a trifunctional epoxy/thermoplastic blend, triglycidyl *p*-aminophenol/PES/4,4'-diaminodiphenylsulfone system, was studied for the morphology change during the curing process (Kim et al. 1995a). Similar to the abovementioned tetrafunctional epoxy system, the phase separation occurred here via spinodal decomposition, and spherical domains of epoxy were observed in electron micrographs and light scattering experiments. However, the periodic distance of the domains in fully cured blends was larger due to rapid phase separation. To control the rate of spinodal decomposition, PES was functionalized with reactive

Fig. 2 Change in scattering profile of epoxy/PES/DICY blend at different cure times (cure times denoted as numbers in seconds). The decrease in scattering angle upon curing denotes the increase in periodic distance among the phase-separated structures (Kim et al. 1993) (Reproduced with permission of Elsevier)

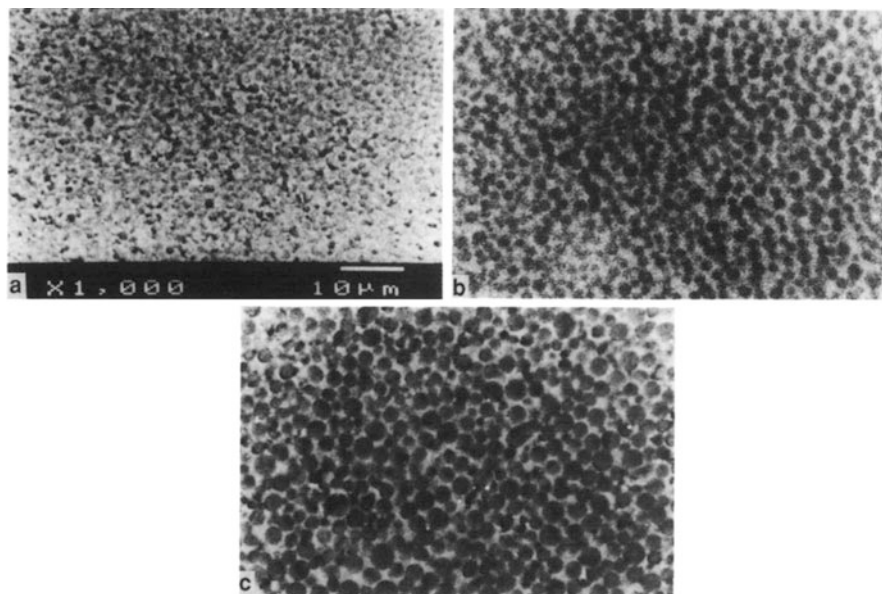
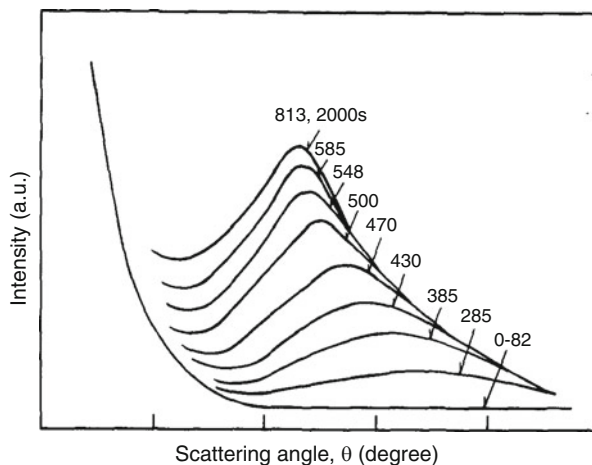


Fig. 3 SEM images of epoxy/PES/DICY blend showing the growth of phase-separated spherical structures at cure times (a) 2, (b) 6, and (c) 30 min (Kim et al. 1993) (Reproduced with permission of Elsevier)

chain end groups such as amine (NH_2) and hydroxyl (OH) groups and studied reaction-induced phase separation during curing process. Here, the periodic distance in spherical or bicontinuous structures was around 20 nm–1 μm , whereas in nonreactive system, the periodic distance was around 0.3–14 μm as estimated from light scattering experiments. The decrease in domain size in reactive system

was ascribed to the formation of epoxy-PES block copolymer that reduced the interfacial tension in those blends. Time-resolved light scattering has been used to follow the phase separation and structure evolution in epoxy blends. However, one should pay close attention to the change in refractive index of the phase-separated domains, as it may lead to wrong conclusions when refractive index of the phase-separated domains matches (Kim et al. 1995b).

Epoxy/PSF blends

Zhang et al. used time-resolved light scattering (TRLS) to investigate the reaction-induced phase evolution in diglycidyl ether of bisphenol A (DGEBA)/polysulfone (PSF) blends cured with 4,4'-diaminodiphenyl sulfone (DDS) (Zhang et al. 2010). Depending on the PSF content in the blends, PSF domains phase separated as dispersed particles and co-continuous structures in the epoxy matrix. At particular PSF content, a layered structure with three layers was observed, where outer layers composed of epoxy-rich phase and middle layer of both epoxy and PSF were continuous. TRLS was used here to study the formation of three-layered structures. Figure 4 represents the TRLS profiles of DGEBS/PSF blends cured at 130 °C.

The PSF and epoxy domains phase separated due to their difference in molecular weight caused by polymerization of epoxy polymer upon curing. The q value of the scattering peaks can be observed to decrease with curing time with increase in the peak intensity (Fig. 4a–e). This is due to coarsening of the epoxy domains upon curing. However, a second scattering peak at slightly lower q value was observed at time $t = 242$ min (Fig. 4f). As the curing proceeds, the second scattering peak showed a decrease in intensity and finally disappeared. The formation of second scattering peak was ascribed to the formation of large epoxy domains that coexisted with the smaller domains. Then the large domains flew out of the middle part and formed outer layers; thus the second scattering peak decreased in intensity and finally disappeared. This phenomenon supports the formation of three-layered structures and further confirmed via phase contrast optical microscopy and scanning electron microscopy studies.

Phase separation via spinodal decomposition (SD) and nucleation and growth mechanism (NG) was observed in DGEBA/PSF blends cured with hexahydrophthalic anhydride (HHPA) depending on the content of polysulfone (PSF) (Xu et al. 2007). At 15 wt% of PSF, first scattering peak was observed on the onset of phase separation, and a second scattering peak corresponding to the secondary phases inside both PSF- and epoxy-rich phases was also observed as shoulder peak (Fig. 5). Here, mechanism of phase separation was through SD. The spinodal lines moved continuously upward showing a UCST behavior (reaction-induced quenching is considered to be analogous to the transfer of one-phase region into two-phase region upon curing). At 25 wt% of PSF, the second scattering peak was ascribed to the “second order” of the main peak because no secondary structure was observed in the OM and TEM observation (Fig. 6). The scattering pattern was related to the coherent scattering of the droplet ensemble or by depletion zones around the droplets.

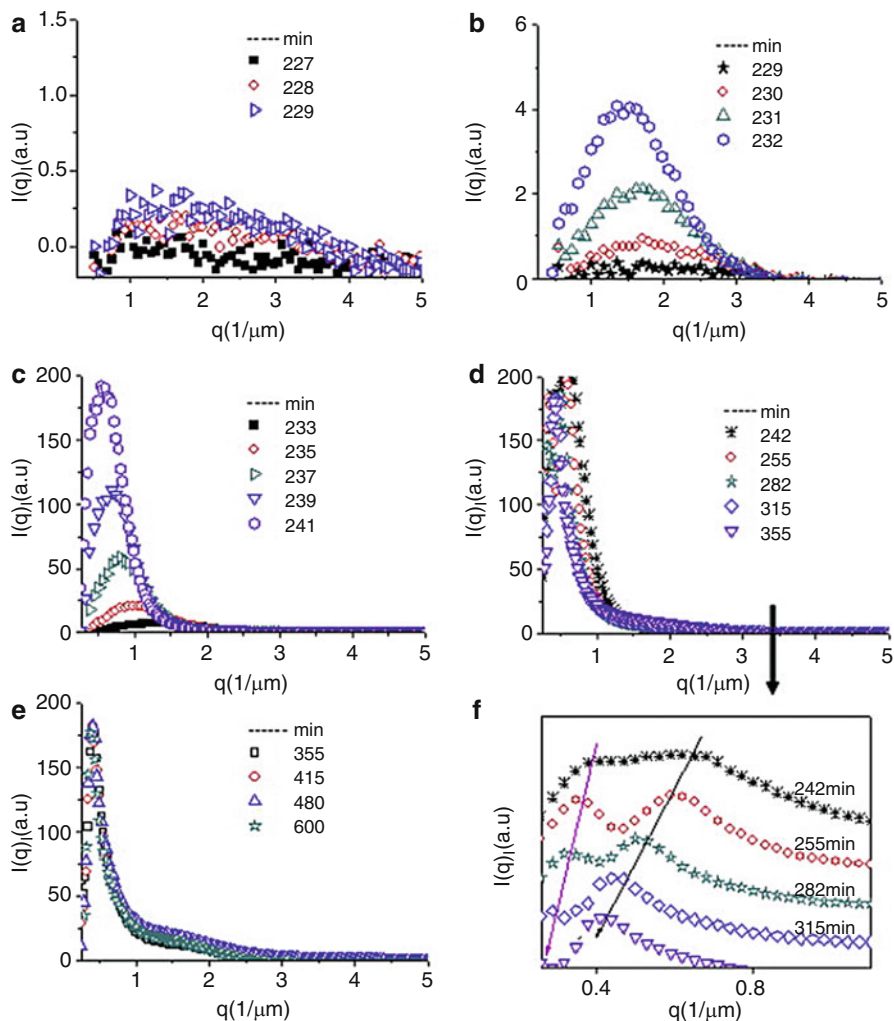


Fig. 4 Time-resolved light scattering profile of three-layered phase evolution in DGEBS/PSF blends upon isothermal curing (a–e). Pattern f is the magnification of pattern d showing the appearance of second scattering peak (Zhang et al. 2010) (Reproduced with permission of Elsevier)

Epoxy/PS Blends

The polystyrene (PS)-based block copolymers or homopolymers phase separate into domains of various morphologies in the epoxy matrix, and significant difference was observed in refractive index of polystyrene and epoxy phase. These blends can be made optically transparent by choosing suitable thermoplastic/thermoset

Fig. 5 SALS profile for DGEBA/PSF blends at 15 wt% of PSF cure at 80 °C, where phase separation was by spinodal decomposition mechanism (Xu et al. 2007) (Reproduced with permission of Taylor and Francis)

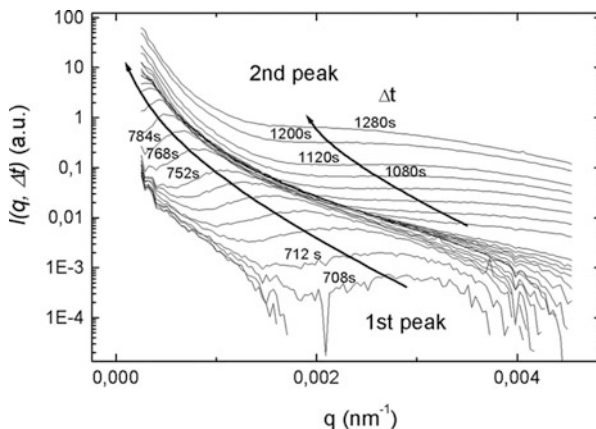
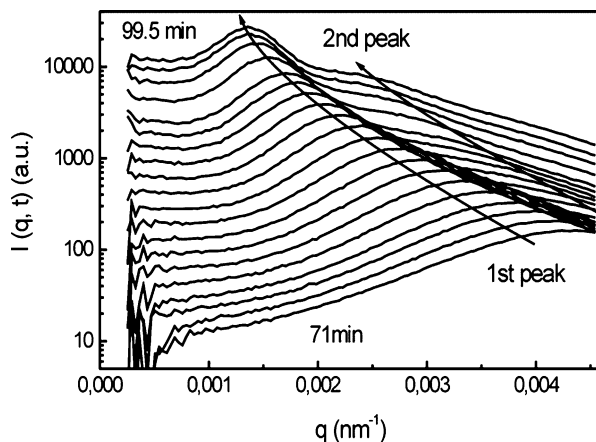


Fig. 6 SALS profile for DGEBA/PSF blends at 25 wt% of PSF cure at 80 °C, where phase separation was by nucleation and growth mechanism (Xu et al. 2007) (Reproduced with permission of Taylor & Francis)



components and by controlling the epoxy conversion or polymerization. In PS/diglycidyl ether of bisphenol A (DGEBA) blend, initiated by a tertiary amine benzyldimethylamine (BDMA), there was a mismatch in refractive index among the phase-separated domains at lower conversion of epoxy. However, at higher conversion of epoxy, the material transformed into transparent biphasic material (Hoppe et al. 2002). This transparent behavior at fully cured state was exploited to synthesize a thermally reversible light scattering (TRLS) film by incorporating *N*-4-ethoxybenzylidene-4'-*n*-butylaniline (EBBA) liquid crystal in these blends (Hoppe et al. 2004). Here, the liquid crystals are expected to be dispersed within the phase-separated PS domains. Transmission optical microscopy (TOM) was used to study the morphology of these blends, and Fig. 7 shows the phase-separated domains of PS in epoxy at

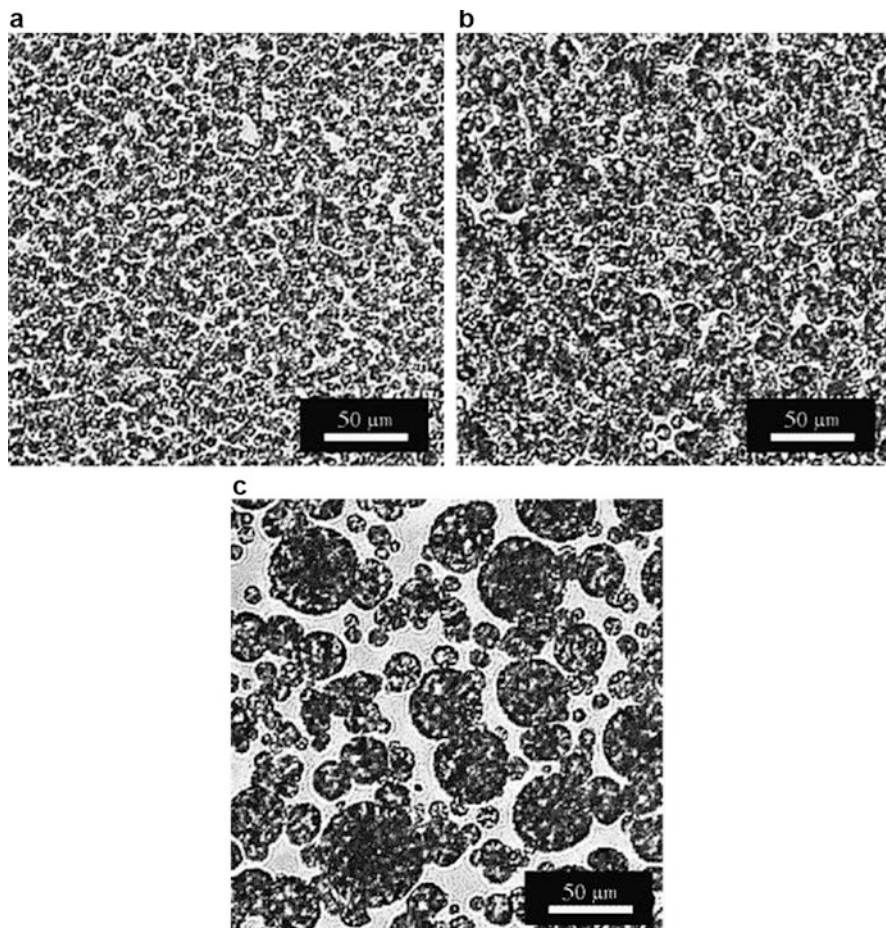


Fig. 7 TOM images of epoxy blends containing EBBA liquid crystal (50 wt%) and PS (a) 1 wt%, (b) 3 wt%, and (c) 5 wt% (Hoppe et al. 2004) (Reproduced with permission of American Chemical Society)

various compositions. The primary spherical PS domains in cured epoxy didn't show any variation upon changing the temperature between 20 °C and 80 °C. However, a thermally reversible phase separation of liquid crystal inside the PS domains was observed. At lower temperatures, the liquid crystals phase separates into nematic phase and dissolved again upon increasing the temperature (Fig. 8). Hence, by adjusting the concentration of liquid crystal, the temperature window in which phase separation occurs can be controlled. Additionally, the contrast between the light scattering centers can be controlled by tuning the composition of the blend and may generate novel temperature-sensitive materials.

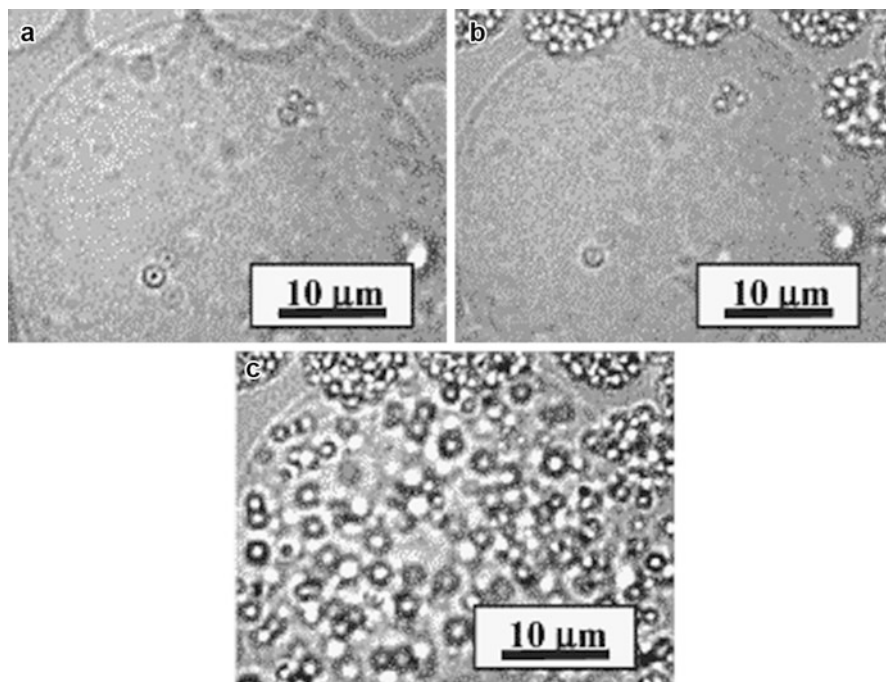


Fig. 8 TOM images of phase separation of nematic EBBA liquid crystal domains inside PS droplets at various temperatures. The epoxy film was prepared with 50 wt% EBBA and 5 wt% PS and subject to cooling at 1 °C/min from 80 °C: (a) at 80 °C, (b) 69.5 °C, and (c) 69 °C (Hoppe et al. 2004) (Reproduced with permission of American Chemical Society)

Epoxy/PEI Blends

Polyetherimide has been used as a toughening modifier in polyfunctional epoxy resins that were used for aerospace applications. Additionally, polyetherimides (Hourston et al. 1991) and polyetherketones (Augustine et al. 2014; Francis et al. 2006; Francis et al. 2007) have been known to improve toughness of epoxies without sacrificing thermal properties. Recently, time-resolved light scattering (TRLS) has been used to follow the phase separation during isothermal curing reaction in epoxy/polyetherimide/silica nanoparticle blends (Li et al. 2015). Due to specific interaction between silica nanoparticles and epoxy, the silica particles were distributed in epoxy-rich domains. Hence, these silica nanoparticles suppressed the coarsening of epoxy domains, which in turn improved the viscoelastic properties and decreased the phase separation temperatures. The TRLS was performed on both the neat epoxy/PEI and epoxy/PEI/SiO₂ blends during isothermal curing at 110 °C. Figure 9 shows the phase structure evolution with time in epoxy/PEI (100:25) blend cured at 110 °C. As curing proceeds, the q_m shifted to lower values with increase in the intensity, indicating the increase in size of the phase-separated domains. The intensity of the scattering

Fig. 9 Time-resolved light scattering profiles of epoxy/PEI (100:25) blend cured at 110 °C (Li et al. 2015) (Reproduced with permission of Royal Society of Chemistry)

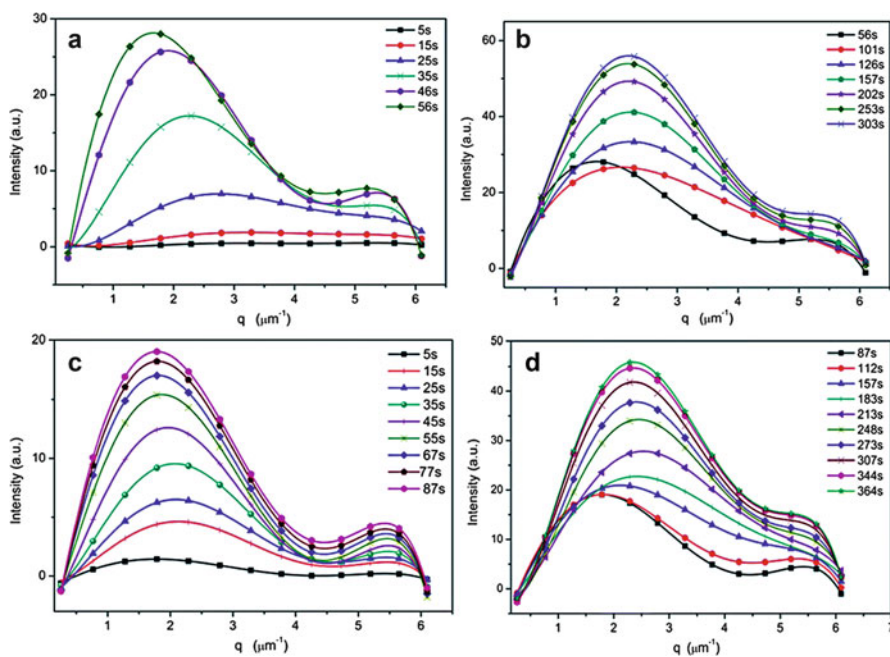
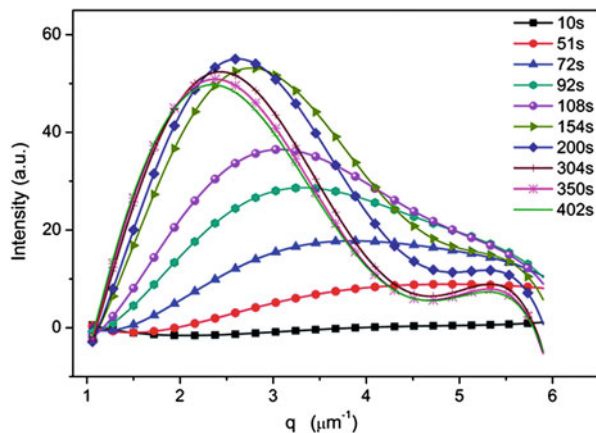


Fig. 10 Time-resolved light scattering profiles of epoxy/PEI (100:25) blends with silica nanoparticles (a and b) 1 wt% and (c and d) 2 wt% cured at 110 °C (Li et al. 2015) (Reproduced with permission of Royal Society of Chemistry)

peak increased first, then decreased, and becomes invariant, which was due to the decrease in refractive indices between the two phases as curing proceeds. In addition, the secondary scattering peaks were observed in later stages of curing due to secondary phase separation within the phase-separated epoxy and PEI domains. Figure 10 shows the phase structure evolution with time in epoxy/PEI/SiO₂ blends at different

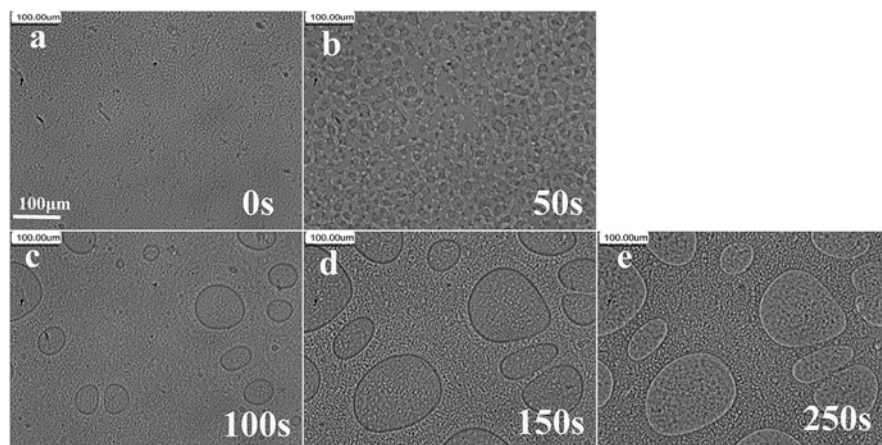
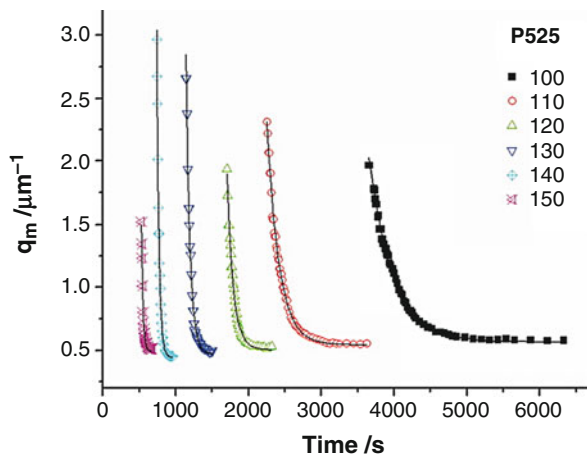


Fig. 11 Optical microscope images of epoxy/PEI/SiO₂ blend showing phase separation during the curing process at 110 °C (Li et al. 2015) (Reproduced with permission of Royal Society of Chemistry)

SiO₂ contents. Here, the light scattering profiles were similar to the neat epoxy blends without SiO₂ nanoparticles. However, the onset of secondary phase separation was earlier, and the average periodic distance between the phase-separated domains was smaller in the presence of SiO₂ particles. Also the increase in SiO₂ particle concentration displayed the same phenomenons mentioned above. The optical microscope images showing phase separation in epoxy/PEI/SiO₂ blend were shown in Fig. 11 to better understand the phase separation process.

In a similar study, PS-*b*-PCL block copolymer was added to epoxy/PEI blends, and reaction-induced phase evolution was studied using TRLS (Xia et al. 2014). Similar to the epoxy/PEI/SiO₂ blends, here the block copolymer resides in epoxy-rich phase and enhanced the viscoelastic properties of the system. In the epoxy domains, secondary phase separation was observed in the later stage of curing process as expected. Additionally, the presence of block copolymer in the epoxy phase plays an important role on the balance of the diffusion and geometrical growth of epoxy molecules. Figure 12 shows the change in q_m values with cure time at different cure temperatures of neat epoxy/PEI blends (Gan et al. 2009). Here, the PEI phase separated into irregular PEI-rich domains dispersed in a continuous epoxy phase. The decrease in q_m values observed from the light scattering profile denotes growth or increase in periodic distances of PEI domains during the curing reaction. The time-dependent version of q_m values was simulated according to a Maxwell-type viscoelastic relaxation equation (Gan et al. 2003; Yu et al. 2004). The change in q_m values corresponding to morphology evolution in these blends fits very well with this equation. It is obvious from Fig. 12 that the onset time of viscoelastic phase separation rapidly decreases with increase in the

Fig. 12 Change in q_m values with curing time at different curing temperatures for epoxy/PEI blend. The dots correspond to experimental data from light scattering profiles, and lines correspond to the results simulated by the Maxwell-type viscoelastic relaxation equation (Gan et al. 2009) (Reproduced with permission of John Wiley & Sons)



temperature in this epoxy/PEI system with PEI (P525) of certain molecular weight. In addition to curing temperature, the phase separation and morphology depend on the molecular weight of the thermoplastic modifier PEI as well. Additionally, in blends with spinodal decomposition, the phase separation and the final morphologies depend on kinetic factor and the viscoelastic effect associated with dynamic asymmetry due to difference in glass transition temperature between the blend components (Gan et al. 2003).

Epoxy/SAN Blends

Poly(styrene-co-acrylonitrile) (SAN) is one of the engineering thermoplastic polymers used to toughen brittle epoxy polymers via simple blending technique (Song et al. 2000; López et al. 2002). In one particular study, SAN was blended with diglycidyl ether of bisphenol A (DGEBA), cured with 4,4'-diaminodiphenylmethane (DDM), and the mechanism of phase separation was investigated using small-angle laser light scattering (SALLS) and optical microscopy (OM) (Jyotishkumar et al. 2012). The viscoelastic phase separation originating from dynamic asymmetry in relaxation and diffusion of polymer chains was studied in this thermoset/thermoplastic blend. Initially, SAN was miscible with the epoxy prepolymer, and the homogeneous SAN/epoxy system phase separated upon curing, which was due to the disparity in molecular weight among the blending components. The phase separation was monitored by SALLS, and the light scattering vector (q) was recorded at various time intervals. Figure 13 shows the light scattering profile for epoxy/SAN (12.9 wt%) blend cured at 130 °C. As the epoxy phase coarsens upon curing, the q value decreased with an increase in the intensity of scattering. This change in q value corresponds to the growth of epoxy droplets in SAN matrix.

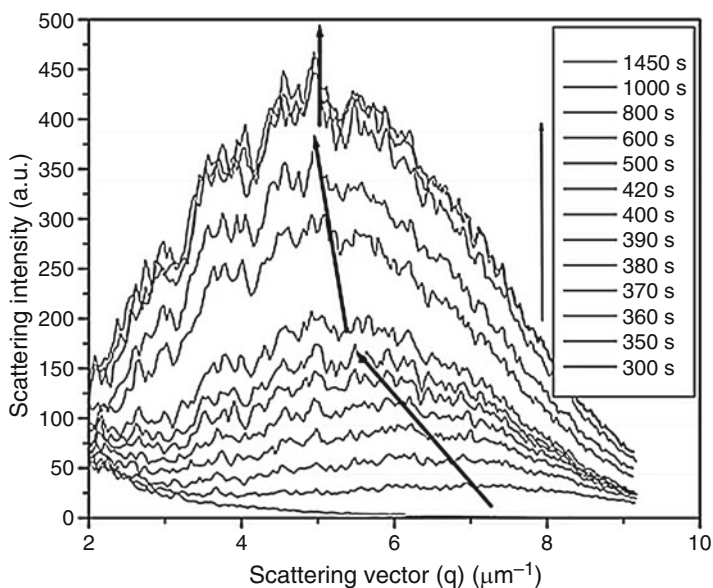


Fig. 13 SALS profile of epoxy/SAN blend at various cure times (Jyotishkumar et al. 2012) (Reproduced with permission of Royal Society of Chemistry)

Epoxy/ABS Blends

A time-resolved study of phase separation in epoxy/poly(acrylonitrile butadiene styrene) (ABS) blends cured with 4,4'-diaminodiphenylsulfone (DDS) was carried out by Jyotishkumar et al. (2009, 2010). The epoxy/ABS blends were prepared with 12.9 wt% of the ABS and cured at various temperatures, where phase-separated morphologies from initial simple droplets to final complex co-continuous morphology were observed from OM and AFM (Atomic Force Microscopy) analysis. The light scattering profile was recorded for the blends cured at 135, 150, 165, and 180 °C at appropriate time intervals. Figure 14a shows the scattering profiles for initial stages of curing at 135 °C. Here, the peaks at lower q values are ascribed to the insoluble SAN-grafted PB particles in the epoxy matrix. The scattering profiles of later stages of curing at 135 °C were shown in Fig. 14b. Here, the scattering peaks appeared first at the higher q values and moved toward lower q values with an increase in the intensity, which implies the phase separation occurring via viscoelastic phase separation and coarsening of epoxy phase upon curing. The second or later stage scattering peaks corresponding to the curing at 150 °C, 165 °C, and 180 °C were shown in Fig. 14c, d, and e, respectively. Here, irrespective of the curing temperatures, the shape of the scattering peaks remained unchanged. However, curing at 180 °C showed a rapid decrease in q values when compared to curing at lower temperatures. This phenomenon may be due to the rapid coarsening of epoxy

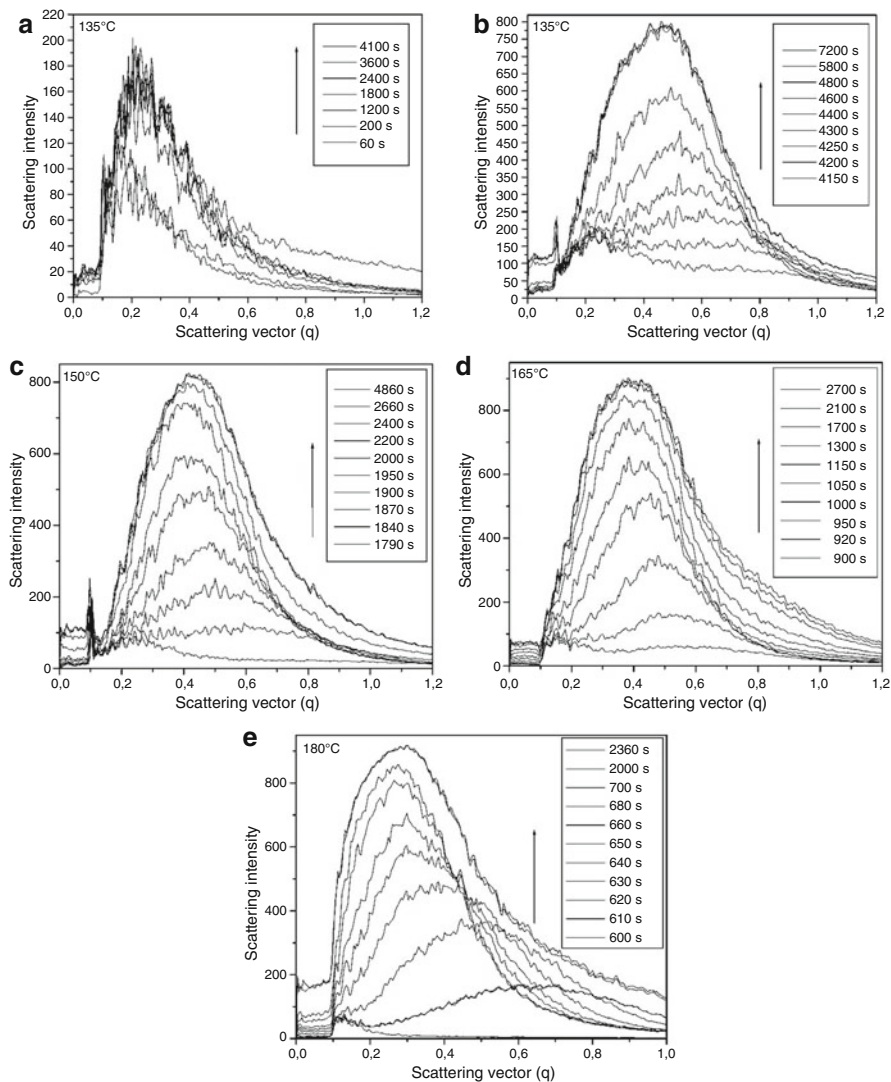


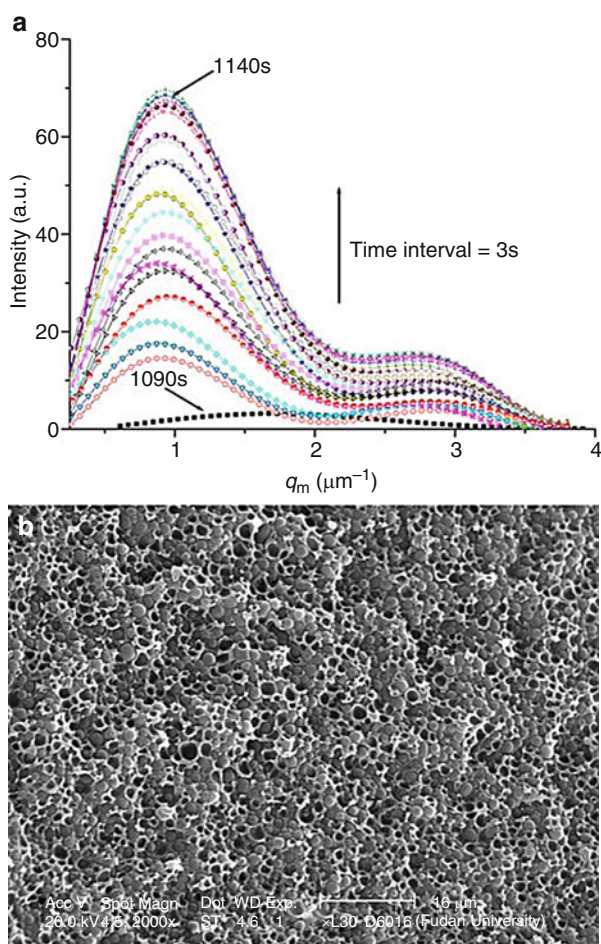
Fig. 14 SALLS profile of epoxy/ABS blends cured at 135 (a, b), 150 (c), 165 (d), and 180 °C (e) (Jyotishkumar et al. 2010) (Reproduced with permission of American Chemical Society)

phase at higher temperatures. In another study, the epoxidized polybutadiene-*b*-polystyrene (EBS) was blended with poly(phenylene oxide)/DGEBA, and reaction-induced phase separation behavior was studied using TRLS. The EBS had a restriction effect on the phase separation, and phase sizes of bicontinuous structures were diminished upon increasing the EBS content (Hu et al. 2009).

Epoxy/PMMA Blends

A low-molecular-weight DGEBA-type epoxy resin was blended with an acrylic thermoplastic polymer poly(methyl methacrylate) and cured using methyltetrahydrophthalic anhydride (MTHPA) curing agent. The phase separation process taking place during isothermal curing at 130 °C was studied in real time using time-resolved light scattering method (Liu et al. 2010). Here, the PMMA-rich phase with minor volume fraction formed a continuous phase, while the spherical epoxy domains dispersed uniformly in the PMMA matrix. No scattering was observed in early stages of curing and after the onset of phase separation, the scattering intensity increased (Fig. 15a). However, no change in q values during curing reaction indicates that the size of phase-separated domains remained same during curing process. Here, the chemical gelation of epoxy phase hindered further phase

Fig. 15 The TRLS profiles of phase separation (a) in epoxy/PMMA blend during isothermal curing and the corresponding SEM image (b) of phase-separated blend (Liu et al. 2010) (Reproduced with permission of Springer)



transformation of PMMA-rich phase from continuous to dispersed structures. Hence, the PMMA remained as continuous phase, with epoxy polymer phase separated into spherical domains as its molecular weight increased during curing. The corresponding SEM image of epoxy/PMMA blend is shown in Fig. 15b.

Epoxy/PCL Blends

Thermoplastic vulcanizates (TPVs) are blends containing thermoplastic matrix with cross-linked elastomer as dispersed phase that exhibit unique elastic and melt properties. Blends of poly(ϵ -caprolactone) (PCL) and epoxy based on poly(propylene oxide) (PPO) were used to prepare TPVs via reaction-induced phase separation (RIPS) (I'Abbe et al. 2008). Triethylene tetramine (TETA) was used as a curing agent. Time-resolved small-angle light scattering (SALS) and SEM were used to study the morphology development during the phase separation. In SEM observation, interconnected spherical PPO droplets (cross-linked epoxy-PPO) were observed in the continuous phase of PCL. Epoxy/PCL blend with 30 wt% of PCL was cured at 100 °C, and change in q values was measured from SALS on different cure times (Fig. 16). Until 4 min, no appreciable light scattering was observed; after

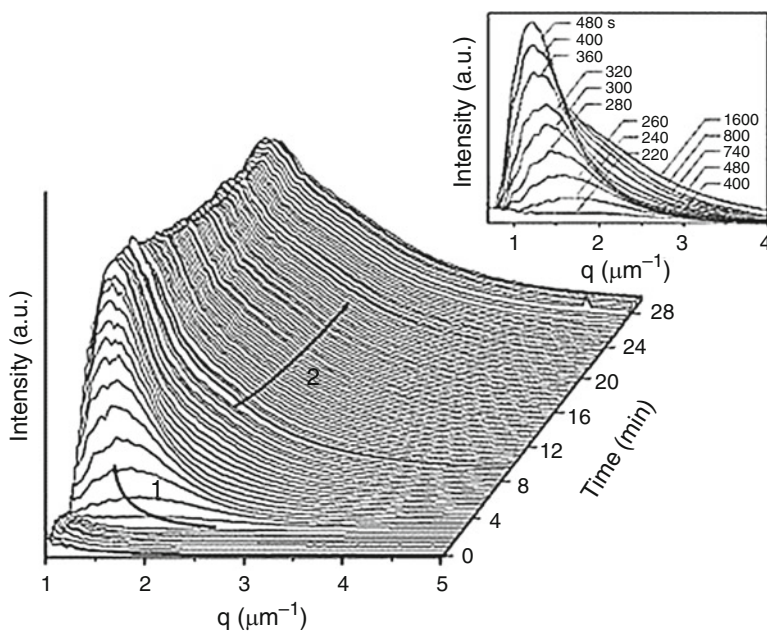


Fig. 16 Time-resolved evolution of SALS pattern in epoxy/PCL blend with 30 wt% of PCL cured at 100 °C (I'Abbe et al. 2008) (Reproduced with permission of Elsevier)

~4 min, scattering was observed with a shift of q values to lower numbers which implies coarsening of phase-separated structures. The scattering profile of this epoxy/thermoplastic blend indicates that the phase separation occurs via spinodal decomposition mechanism. Due to higher reaction rate in this blend, the earlier stages of spinodal decomposition characterized by increasing intensity at constant q value couldn't be captured.

Epoxy/PBT Blends

The processing characteristics of thermoplastics can be improved by solvents and additives such as epoxy resins. The main advantage of using epoxy is that it functions as reactive solvent in which thermoplastic can be dissolved and cured inside a mold at lower processing temperatures in absence of toxic solvents. Similarly, polybutylene terephthalate (PBT), a versatile semi-crystalline engineering thermoplastic, has been processed with epoxy resin as reactive solvent. DGEBA was cured with 4,4'-methylenebis(3-chloro-2, 6 diethyl aniline) (M-CDEA) curing agent at various PBT concentrations (Kulshreshtha et al. 2003). The rate of PBT crystallization and spherulitic morphology development at various compositions and cure temperatures were studied using SALS. Figure 17 shows the SALS pattern and the corresponding optical micrograph of PBT and PBT/epoxy-cured blends, isothermally crystallized at 50 °C. The four-lobe unusual type of scattering was observed for pure PBT and PBT/epoxy 90/10 composition. For blends with 20% or greater epoxy content, usual four-lobe scattering pattern was observed. For blends with comparatively higher epoxy content, 40% and 50%, the intensity of scattering pattern decreased due to the presence of glassy epoxy resin. This study was conducted to improve the understanding of crystallization of PBT in epoxy and also with an aim to improve processing characteristics of PBT.

Epoxy/Phenoxy Blends

The emergence of phase separation in DGEBA/phenoxy blends cured with diamino diphenyl sulfone (DDS) was studied using TRLS, OM, and SEM techniques (Siddhamalli and Kyu 2000). The solution cast films didn't show any phase separation in room temperature, and the film remained transparent. However, upon curing at 180 °C, scattering peaks appeared after certain induction time. As expected, the scattering peaks moved toward lower q_m values with increase in intensity, suggestive of coarsening of epoxy domains dispersed in phenoxy matrix (Fig. 18a). Here, at 10% phenoxy content, droplet morphology was observed; co-continuous or interconnected globular structures at 20% and phase inverter morphology for greater than 30% were observed. Figure 18b shows the time-dependent change in q_m values.

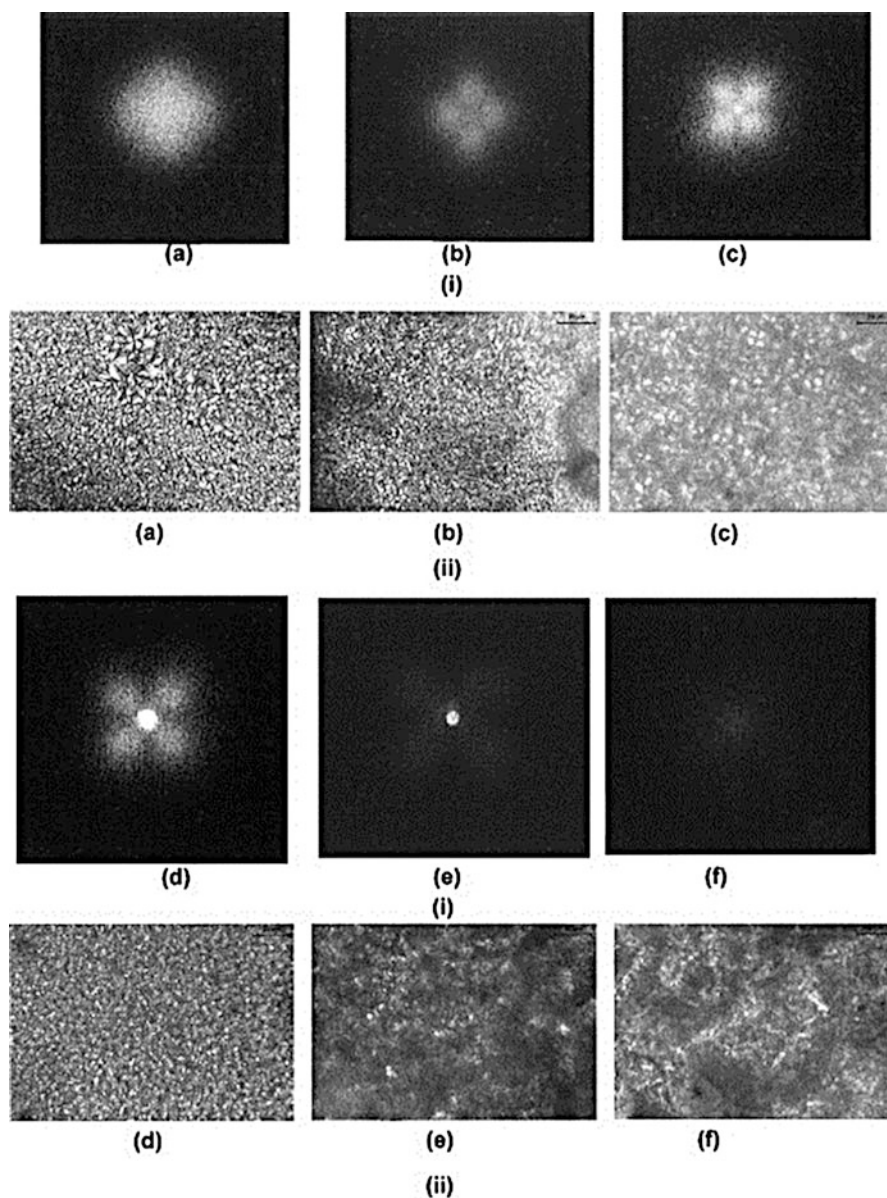


Fig. 17 SALS pattern (i) and corresponding optical micrographs (ii) of PBT/epoxy-cured blends of compositions (a) PBT, (b) 90/10, (c) 80/20, (d) 70/30, (e) 60/40, and (f) 50/50 (Kulshreshtha et al. 2003) (Reproduced with permission of Elsevier)

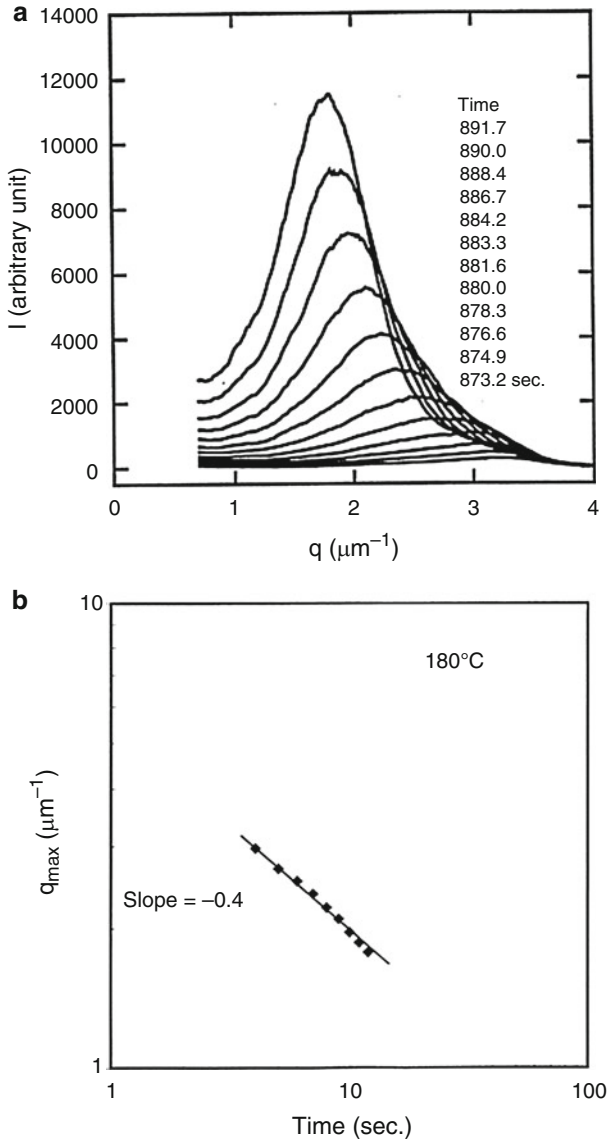


Fig. 18 TRLS profile of epoxy/phenoxy blend (70:30) cured at 180 °C (a), log q_m versus log t plot (b) (Siddhamalli and Kyu 2000) (Reproduced with permission of John Wiley & Sons)

Epoxy/Polycarbonate Blends

Epoxy blends containing polycarbonate were used to prepare super tough materials with improved fracture behavior (Sun et al. 2013; Wang et al. 2012). The reaction temperature and composition have greater influence on phase separation and

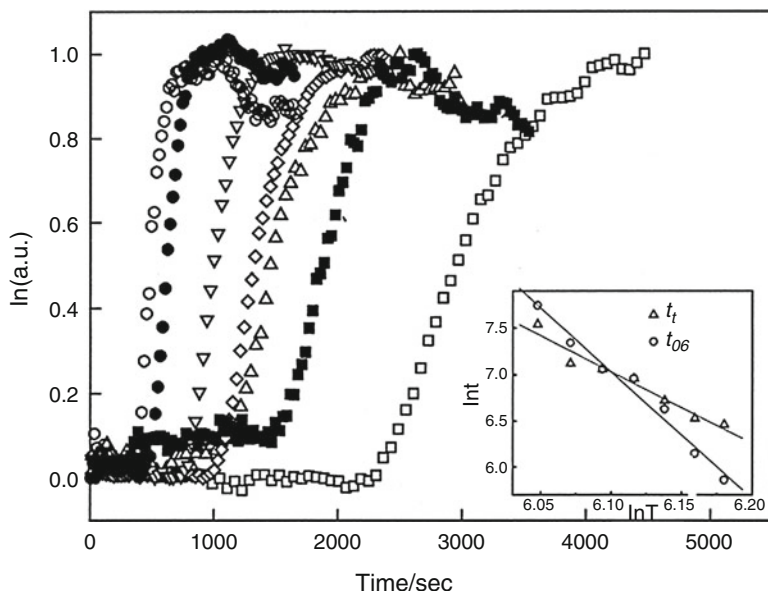


Fig. 19 Change in scattering intensity (I_n) with time in epoxy/PEI/PC (100/10/10) blends isothermally cured at various temperatures (\square) 150, (\bullet) 160, (\triangle) 170, (\diamond) 180, (∇) 190, (\circ) 200, and (\circ) 210 °C. The inset shows the temperature dependence of phase separation. The onset of phase separation (t_{os}) and time period of phase separation (t_i) decrease with increase in curing temperature (Zheng et al. 2002) (Reproduced with permission of John Wiley & Sons)

morphology development of blends in addition to the type of epoxy and thermoplastic components. Zheng et al. studied phase separation in ternary blends of DGEBA-type epoxy mixed with PEI and polycarbonate (PC) and cured with DDS (Zheng et al. 2002). Phase separation was through spinodal decomposition mechanism, and co-continuous morphology was confirmed by optical microscopy. The curing temperature and compositions were considered to be determining factors of domain size and phase separation behavior. Figure 19 shows the effect of temperature on phase separation kinetics. At higher temperatures, higher mobility in epoxy chains speeds up the curing reaction and hence the decrease in time period of phase separation (t_i). The onset of phase separation (t_{os}) was also found to be early at high-temperature curing. Additionally, phase separation was studied upon changing the PC content. Here, the t_{os} was found to appear earlier with increasing the PC content. The PC was found to have promoting effect on curing reaction by forming hydrogen bonding with epoxy or DDS, hence the earlier phase separation.

Epoxy/PS-*b*-PCL Blend

The influence of poly(styrene-*b*-caprolactone) (PS-*b*-PCL) block copolymer on the reaction-induced phase separation of epoxy/polyetherimide (PEI) blend was studied using various microscopic and light scattering techniques (Xia et al. 2014). The

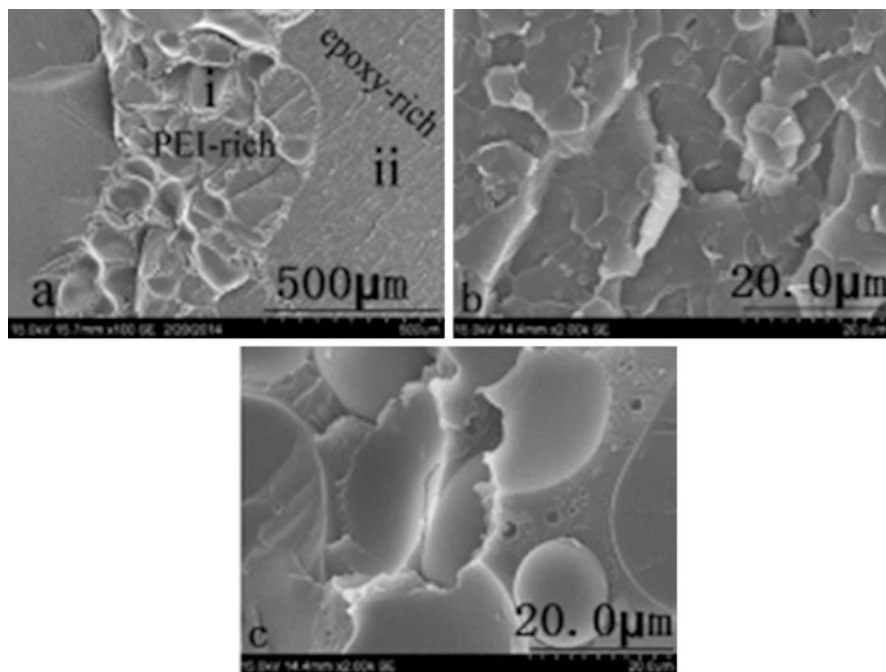


Fig. 20 SEM images of (a) epoxy/PEI/PS-*b*-PCL: 100/15/5 blend [*i*] PEI-rich phase, (*ii*) epoxy-rich phase], (b) magnification of epoxy-rich phase (a-*ii*), and (c) magnification of PEI-rich phase (a-*i*). The SEM images show dispersion of many PEI and epoxy droplets in epoxy-rich (b) and PEI-rich (c) phases, respectively (Xia et al. 2014) (Reproduced with permission of John Wiley & Sons)

block copolymer was added to the epoxy/PEI blend at different wt% (epoxy/PEI/PS-*b*-PCL: 100/15/2, 100/15/5, 100/20/2 and 100/20/5), and morphology evolution was studied with respect to curing time. The TRLS profiles of the blends without block copolymer showed a single peak shifting toward lower q_m value, indicating the growth of periodic structure size, and further confirm the droplet-matrix morphology (PEI droplets in continuous epoxy matrix). However, upon adding the block copolymer, a secondary phase separation within the PEI- and epoxy-rich domains was observed (Fig. 20). The TRLS profiles initially showed a decrease in q_m value upon curing, but after a certain time (50s in 100/20/2 and 150 s in 100/20/5), a secondary scattering peak was observed at higher scattering vector value (Fig. 21). The secondary peak was ascribed to the faster dynamic epoxy droplets retarded within the slower dynamic PEI-rich phase facilitated by the presence of block copolymer. At higher block copolymer content (100/20/5), this secondary phase separation was further slowed down, and the secondary peak appeared only after 150 s. Hence, the block copolymer slows down the diffusion of fast dynamic epoxy phase and drastically increases the relaxation time. A significant slowdown of phase separation in epoxy blends containing block copolymer suggests the role of viscoelastic effect in reaction-induced phase separation process.

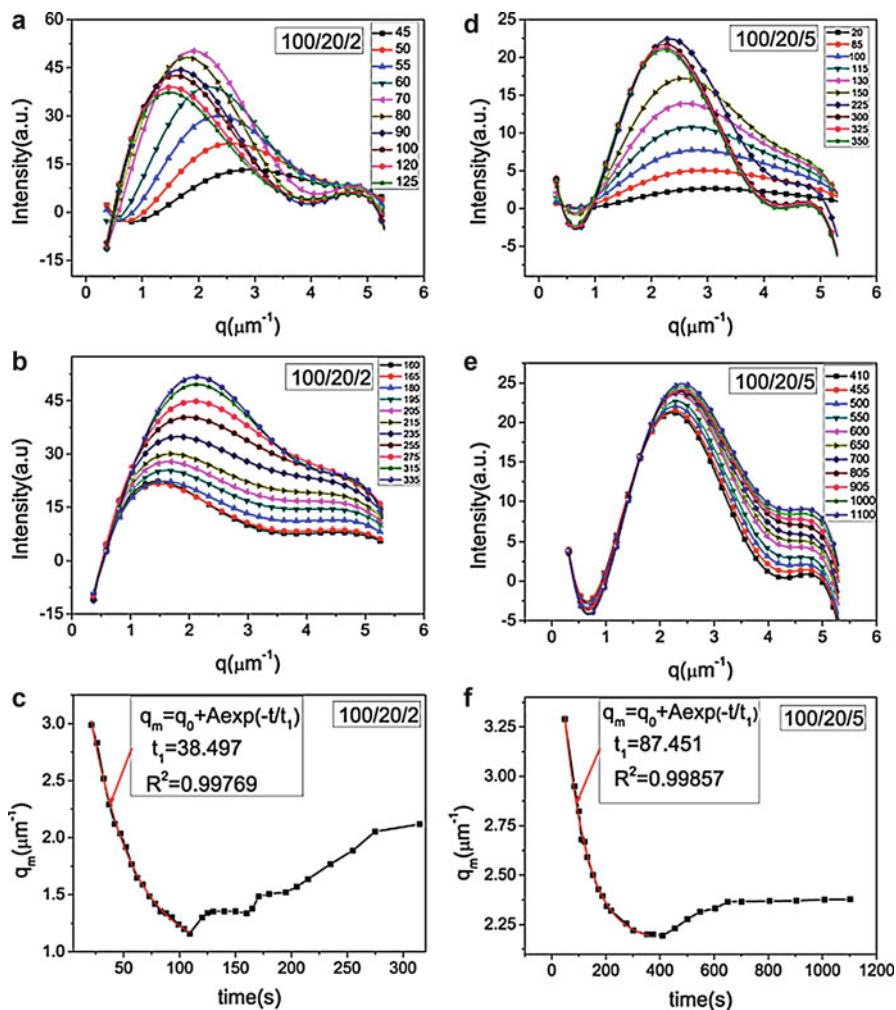


Fig. 21 TRLS profiles of epoxy/PEI/PS-*b*-PCL blends at different block copolymer contents 100/20/2 (a, b) and 100/20/5 (d, e) cured at 110 °C. The time-dependent q_m was fitted with a Maxwell-type relaxation equation for corresponding block copolymer contents (c, f) and shows a drastic increase in relaxation time with increasing the block copolymer content (Xia et al. 2014) (Reproduced with permission of John Wiley & Sons)

Conclusions

Thermoplastics and block copolymers are found to be the excellent candidate to toughen epoxy polymers, and also controlling phase separation is important to achieve necessary macroscopic properties in epoxy blends. Time-resolved light scattering was found to be a versatile technique to study dynamics of phase

separation during the curing reaction. In thermoset/thermoplastic or block copolymer blends, the epoxy-rich phase was found to coarsen upon curing due to increase in molecular weight upon polymerization. The scattering peaks were found to shift toward lower q values indicating the increase in size of phase-separated domains, which is the characteristic of spinodal decomposition. Depending on the composition in epoxy blends, various morphologies such as dispersed spherical domains, co-continuous structures, layered structures, and interconnected globules were elucidated from light scattering experiments. The real-time observation of concentration fluctuations within polymers by light scattering helps in following the dynamic processes like crystallization, coalescence, and phase separation. Hence, light scattering is used to study the coarsening kinetics in real time in epoxy/thermoplastic and epoxy/block copolymer blends during curing reaction.

References

- Arinina MP, Ilyin SO, Makarova VV, Gorbunova IY, Kerber ML, Kulichikhin VG (2015) Miscibility and rheological properties of epoxy resin blends with aromatic polyethers. *Poly Sci A* 57 (2):177–185. doi:10.1134/s0965545x15020017
- Augustine D, Vijayalakshmi KP, Sadhana R, Mathew D, Reghunadhan Nair CP (2014) Hydroxyl terminated PEEK-toughened epoxy–amino novolac phthalonitrile blends – synthesis, cure studies and adhesive properties. *Polymer* 55(23):6006–6016. doi:10.1016/j.polymer.2014.09.042
- Bagheri R, Marouf BT, Pearson RA (2009) Rubber-toughened epoxies: a critical review. *Polym Rev* 49(3):201–225. doi:10.1080/15583720903048227
- Francis B, Ramaswamy R, Lakshmana Rao V, Thomas S (2006) Toughening of diglycidyl ether of bisphenol-A epoxy resin using poly(ether ether ketone) with pendent tert-butyl groups. *Int J Poly Mater Poly Biomat* 55(9):681–702. doi:10.1080/00914030500323326
- Francis B, Thomas S, Sadhana R, Thuaud N, Ramaswamy R, Jose S, Rao VL (2007) Diglycidyl ether of bisphenol-A epoxy resin modified using poly(ether ether ketone) with pendent tert-butyl groups. *J Polym Sci B* 45(17):2481–2496. doi:10.1002/polb.21238
- Gan W, Yu Y, Wang M, Tao Q, Li S (2003) Viscoelastic effects on the phase separation in thermoplastics-modified epoxy resin. *Macromolecules* 36(20):7746–7751. doi:10.1021/ma034649a
- Gan W, Xiong W, Yu Y, Li S (2009) Effects of the molecular weight of poly(ether imide) on the viscoelastic phase separation of poly(ether imide)/epoxy blends. *J Appl Polym Sci* 114 (5):3158–3167. doi:10.1002/app.30897
- Hashimoto T, Kumaki J, Kawai H (1983) Time-resolved light scattering studies on kinetics of phase separation and phase dissolution of polymer blends. 1. Kinetics of phase separation of a binary mixture of polystyrene and poly(vinyl methyl ether). *Macromolecules* 16(4):641–648. doi:10.1021/ma00238a030
- Hodgkin JH, Simon GP, Varley RJ (1998) Thermoplastic toughening of epoxy resins: a critical review. *Polym Adv Technol* 9(1):3–10. doi:10.1002/(SICI)1099-1581(199801)9:1<3::AID-PAT727>3.0.CO;2-I
- Hoppe CE, Galante MJ, Oyanguren PA, Williams RJJ, Girard-Reydet E, Pascault JP (2002) Transparent multiphase polystyrene/epoxy blends. *Polym Eng Sci* 42(12):2361–2368. doi:10.1002/pen.11122
- Hoppe CE, Galante MJ, Oyanguren PA, Williams RJJ (2004) Thermally reversible light scattering films based on droplets of a liquid crystal (N-4-ethoxybenzylidene-4'-n-butylaniline)/

- polystyrene solution dispersed in an epoxy matrix. *Macromolecules* 37(14):5352–5357. doi:10.1021/ma0496955
- Hourston DJ, Lane JM, MacBeath NA (1991) Toughening of epoxy resins with thermoplastics. II. Tetrafunctional epoxy resin-polyetherimide blends. *Polym Int* 26(1):17–21
- Hu S, Zhao L, Zhan GZ, Tang XL, Li SJ (2009) Effect of epoxidized polybutadiene-*b*-polystyrene on the reaction induced phase separation behavior of poly(phenylene oxide) modified epoxy blends. *Acta Chim Sin* 67(15):1815–1821
- Inoue T (1995) Reaction-induced phase decomposition in polymer blends. *Prog Polym Sci* 20(1):119–153. doi:10.1016/0079-6700(94)00032-W
- Jyotishkumar P, Koetz J, Tiersch B, Strehmel V, Özdilek C, Moldenaers P, Hässler R, Thomas S (2009) Complex phase separation in poly(acrylonitrile – butadiene – styrene)-modified epoxy/4,4'-diaminodiphenyl sulfone blends: generation of new micro- and nanosubstructures. *J Phys Chem B* 113(16):5418–5430. doi:10.1021/jp8094566
- Jyotishkumar P, Özdilek C, Moldenaers P, Sinturel C, Janke A, Pionteck J, Thomas S (2010) Dynamics of phase separation in poly(acrylonitrile-butadiene-styrene)-modified epoxy/DDS system: kinetics and viscoelastic effects. *J Phys Chem B* 114(42):13271–13281. doi:10.1021/jp101661t
- Jyotishkumar P, Pionteck J, Ozdilek C, Moldenaers P, Cvelbar U, Mozetic M, Thomas S (2011) Rheology and pressure-volume-temperature behavior of the thermoplastic poly(acrylonitrile-butadiene-styrene)-modified epoxy-DDS system during reaction induced phase separation. *Soft Matter* 7(16):7248–7256. doi:10.1039/C1SM05718A
- Jyotishkumar P, Moldenaers P, George SM, Thomas S (2012) Viscoelastic effects in thermoplastic poly(styrene-acrylonitrile)-modified epoxy-DDM system during reaction induced phase separation. *Soft Matter* 8(28):7452–7462. doi:10.1039/C2SM07055C
- Kim BS, Chiba T, Inoue T (1993) A new time-temperature-transformation cure diagram for thermoset/thermoplastic blend: tetrafunctional epoxy/poly(ether sulfone). *Polymer* 34(13):2809–2815. doi:10.1016/0032-3861(93)90125-T
- Kim BS, Chiba T, Inoue T (1995a) Morphology development via reaction-induced phase separation in epoxy/poly(ether sulfone) blends: morphology control using poly(ether sulfone) with functional end-groups. *Polymer* 36(1):43–47. doi:10.1016/0032-3861(95)90673-P
- Kim BS, Chiba T, Inoue T (1995b) Phase separation and apparent phase dissolution during cure process of thermoset/thermoplastic blend. *Polymer* 36(1):67–71. doi:10.1016/0032-3861(95)90676-S
- Kulshreshtha B, Ghosh AK, Misra A (2003) Crystallization kinetics and morphological behavior of reactively processed PBT/epoxy blends. *Polymer* 44(16):4723–4734. doi:10.1016/S0032-3861(03)00347-1
- l'Abée R, Goossens H, van Duin M (2008) Thermoplastic vulcanizates obtained by reaction-induced phase separation: interplay between phase separation dynamics, final morphology and mechanical properties. *Polymer* 49(9):2288–2297. doi:10.1016/j.polymer.2008.03.030
- Li W, Xia Z, Li A, Ling Y, Wang B, Gan W (2015) Effect of SiO₂ nanoparticles on the reaction-induced phase separation in dynamically asymmetric epoxy/PEI blends. *RSC Adv* 5(11):8471–8478. doi:10.1039/C4RA12261E
- Liu Y, Zhong X, Yu Y (2010) Gelation behavior of thermoplastic-modified epoxy systems during polymerization-induced phase separation. *Colloid Polym Sci* 288(16):1561–1570. doi:10.1007/s00396-010-2288-5
- López J, Ramírez C, Abad MJ, Barral L, Cano J, Díez F (2002) Dynamic mechanical analysis of an epoxy/thermoplastic blend: polymerization-induced phase separation. *Polym Int* 51(10):1100–1106. doi:10.1002/pi.953
- Mohan P (2013) A critical review: the modification, properties, and applications of epoxy resins. *Polym-Plast Technol Eng* 52(2):107–125. doi:10.1080/03602559.2012.727057
- Mucha M (2003) Polymer as an important component of blends and composites with liquid crystals. *Prog Polym Sci* 28(5):837–873. doi:10.1016/S0079-6700(02)00117-X

- Omriani A, Shahhossieni F (2013) Preparation and characterization of a tertiary nanocomposite from polycarbonate and epoxy resin. *J Macromol Sci A* 50(7):747–756. doi:10.1080/10601325.2013.792644
- Oyanguren PA, Frontini PM, Williams RJJ, Vigier G, Pascault JP (1996) Reaction-induced phase separation in poly(butylene terephthalate)-epoxy systems: 2. Morphologies generated and resulting properties. *Polymer* 37(14):3087–3092. doi:10.1016/0032-3861(96)89408-0
- Parameswaranpillai J, Moldenaers P, Thomas S (2013) Rheological study of the SAN modified epoxy-DDM system: relationship between viscosity and viscoelastic phase separation. *RSC Adv* 3(46):23967–23971. doi:10.1039/C3RA43138J
- Ruiz-Pérez L, Royston GJ, Fairclough JPA, Ryan AJ (2008) Toughening by nanostructure. *Polymer* 49(21):4475–4488. doi:10.1016/j.polymer.2008.07.048
- Ruzette A-V, Leibler L (2005) Block copolymers in tomorrow's plastics. *Nat Mater* 4(1):19–31. doi:10.1038/nmat1295
- Siddhamalli SK, Kyu T (2000) Toughening of thermoset/thermoplastic composites via reaction-induced phase separation: epoxy/phenoxy blends. *J Appl Polym Sci* 77(6):1257–1268. doi:10.1002/1097-4628(20000808)77:6<1257::AID-APP10>3.0.CO;2-Z
- Song X, Zheng S, Huang J, Zhu P, Guo Q (2000) Miscibility, morphology and fracture toughness of tetrafunctional epoxy resin/poly (styrene-co-acrylonitrile) blends. *J Mater Sci* 35(22):5613–5619. doi:10.1023/a:1004824628535
- Sun S, Zhang F, Fu Y, Zhou C, Zhang H (2013) Properties of poly(butylene terephthalate)/bisphenol A polycarbonate blends toughening with epoxy-functionalized acrylonitrile-butadiene-styrene particles. *J Macromol Sci B* 52(6):861–872. doi:10.1080/00222348.2012.738156
- Svoboda P (2014) Characterization of phase behavior in polymer blends by light scattering. In: *Characterization of polymer blends*. Wiley-VCH Verlag GmbH, Weinheim, pp 159–208. doi:10.1002/9783527645602.ch05
- Tromp RH, Rennie AR, Jones RAL (1995) Kinetics of the simultaneous phase separation and gelation in solutions of dextran and gelatin. *Macromolecules* 28(12):4129–4138. doi:10.1021/ma00116a012
- Wang Q, Jiang Y, Li L, Wang P, Yang Q, Li G (2012) Mechanical properties, rheology, and crystallization of epoxy-resin-compatible polyamide 6/polycarbonate blends: effect of mixing sequences. *J Macromol Sci B* 51(1):96–108. doi:10.1080/00222348.2011.565273
- Wright WW (1986) In: K. Dusek (ed) *Epoxy resins and composites II*. *Advances in polymer science*, vol 75. Springer, Berlin/Heidelberg, xiii+180, price DM 118.00. ISBN 3-540-15825-1. *Br Polym J* 18(5):349–349. doi:10.1002/pi.4980180514
- Xia Z, Li W, Ding J, Li A, Gan W (2014) Effect of PS-b-PCL block copolymer on reaction-induced phase separation in epoxy/PEI blend. *J Polym Sci B* 52(21):1395–1402. doi:10.1002/polb.23575
- Xu J, Holst M, Rüllmann M, Wenzel M, Alig I (2007) Reaction-induced phase separation in a polysulfone-modified epoxy-anhydride thermoset. *J Macromol Sci B* 46(1):155–181. doi:10.1080/00222340601044342
- Yongtao Y, Jingjie W, Haibao L, Ben X, Yongqing F, Yanju L, Jinsong L (2016) Thermosetting epoxy resin/thermoplastic system with combined shape memory and self-healing properties. *Smart Mater Struct* 25(1):015021
- Yu Y, Wang M, Gan W, Tao Q, Li S (2004) Polymerization-induced viscoelastic phase separation in polyethersulfone-modified epoxy systems. *J Phys Chem B* 108(20):6208–6215. doi:10.1021/jp036628o
- Zhang Y, Chen F, Shi W, Liang Y, Han CC (2010) Layered structure formation in the reaction-induced phase separation of epoxy/polysulfone blends. *Polymer* 51(25):6030–6036. doi:10.1016/j.polymer.2010.10.027
- Zheng Q, Tan K, Peng M, Pan Y (2002) Study on the phase separation of thermoplastic-modified epoxy systems by time-resolved small-angle laser light scattering. *J Appl Polym Sci* 85(5):950–956. doi:10.1002/app.10405

Juan Carlos Cabanelas, Claire Antonelli, Verónica San Miguel, Berna Serrano, and Juan Baselga

Abstract

In this chapter, the main findings of spectroscopic analysis applied to epoxy/thermoplastic (TP) blends are presented. This includes vibrational spectroscopy (infrared and Raman), nuclear magnetic resonance spectroscopy, fluorescence spectroscopy, energy-dispersive X-ray spectroscopy, and dielectric relaxation spectroscopy. These techniques have been employed alone or combined to monitor polymerization processes, the glass transition, and structural relaxations, to study reaction-induced phase separation (RIPS), to obtain a complete chemical characterization of the different phases, or to analyze compositional gradients at the interphases. The study of the specific interactions between the epoxy components and the thermoplastic modifier allowed the interpretation of chain interdiffusion and miscibility data and helped to explain microstructure. Several examples are discussed.

Keywords

Epoxy resins • Epoxy/thermoplastic blends • Reaction-induced phase separation • Curing • Specific intermolecular interactions • Morphology • Phase composition • Chemical characterization • Diffusion • Water uptake • Structural relaxation • Spectroscopy techniques • Infrared spectroscopy • Raman spectroscopy • Nuclear magnetic resonance spectroscopy • X-ray spectroscopy • Fluorescence spectroscopy • Dielectric relaxation spectroscopy

J.C. Cabanelas (✉) • C. Antonelli • V. San Miguel • B. Serrano • J. Baselga
Department of Materials Science and Engineering and Chemical Engineering, Universidad Carlos III de Madrid, Leganes, Spain
e-mail: caba@ing.uc3m.es; vmiguel@ing.uc3m.es

Contents

Introduction	584
Spectroscopic Techniques Applied to Epoxy/Thermoplastic Blends	585
Vibrational Spectroscopy: Infrared and Raman	585
Nuclear Magnetic Resonance Spectroscopy	595
Fluorescence Spectroscopy	599
Energy Dispersive X-Ray Spectroscopy	604
Dielectric Relaxation Spectroscopy	605
Scattering and Other Techniques	606
Conclusions	608
References	609

Introduction

The development of multiphase materials in the last decades cannot be understood without considering the advances in resolution and versatility of spectroscopic techniques such as vibrational spectroscopy (infrared and Raman); UV–Vis absorption and emission, including photoluminescence spectroscopy; or scattering techniques, among others. This wide range of available techniques has enabled significant advances in the design and improvement of these materials, very often in conjunction with imaging techniques such as SEM, TEM, AFM, and confocal microscopy. The main uses of spectroscopic techniques in the field of polymeric materials are chemical and structural identification, monitoring reactive and diffusion processes, and analysis of intermolecular interactions (including hydrogen bonding). To the abovementioned applications, it must be added the monitoring of network formation with the elucidation of the most important physicochemical changes observed in thermoset polymers: gelation, vitrification, and phase separation.

With regard to thermoplastic-modified epoxy matrices, several processes of capital importance take place during curing, which greatly influence the final morphology and properties of the polymer blend. Mixtures of cured epoxy resins with thermoplastics are normally immiscible, with few exceptions, and therefore they show a wide range of heterogeneous morphologies. However, it is very common for the thermoplastic to be miscible or at least partially soluble in the reactive mixture of epoxy and hardener monomers. These homogeneous mixtures are deeply transformed during curing. The molecular weight of the thermosetting polymer increases because of network buildup, and therefore the entropy of mixing decreases, causing the system to become more incompatible, until reaction-induced phase separation (RIPS) occurs, via spinodal or nucleation and growth mechanisms. This phase separation typically appears before gelation, and morphology is always set before the vitrification of the thermoset network.

Many spectroscopic techniques are useful for the abovementioned purposes. The curing process can be followed very precisely by infrared spectroscopy, following the extinction of some band corresponding to a reactive group of the resin, to such an extent that this technique has replaced the previously used calorimetric experiments.

Other spectroscopic techniques such as nuclear magnetic resonance spectroscopy or dielectric relaxation have proven to be useful to study the network buildup. The study of the phases present in the cured material can be performed by infrared spectroscopy and Raman spectroscopy, nuclear magnetic resonance, fluorescence spectroscopy, X-ray spectroscopy, or dielectric spectroscopy. In addition to the phase composition, information about the miscibility of the components at the molecular level, cross-section compositional gradients, and specific interactions including hydrogen bonding are also obtained. The spectroscopic analysis of the interfacial structure enables to know the interpenetration of networks and the degree of cross-linking, the degree of interaction between polymers, and network relaxation dynamics at the interface chains, shedding light on the mechanisms that govern the miscibility of these systems. Other phenomena, closely related to the network structure and morphology, have also been studied. This is the case of diffusion, swelling, and water uptake.

In this chapter the use of spectroscopic techniques in the field of epoxy/thermoplastic blends is reviewed. Each technique or group of techniques is analyzed separately indicating its usefulness and the main information provided by them. Since there are a huge number of spectroscopic techniques, the selection made for this chapter has taken into account mainly their use in epoxy/thermoplastic blends. In some cases, as for the different scattering techniques (SAXS, TRLS), a brief description is presented here because of their relevance, but they are presented more exhaustively in another chapter. Unless absolutely necessary, this chapter is focused only on blends of epoxy resins with thermoplastics, ignoring the abundant recent literature on block copolymers mixtures, which is treated in another specific chapter. Finally, common accepted names have been used for both the thermoset precursors and the thermoplastic modifiers.

Spectroscopic Techniques Applied to Epoxy/Thermoplastic Blends

Vibrational Spectroscopy: Infrared and Raman

Vibrational spectroscopy includes two physically different spectroscopic techniques, infrared (IR) and Raman spectroscopy, which are at the same time fully complementary to provide complete information on the molecular structure. Each technique measures a kind of light–matter interactions, and, as a consequence, different types of molecular vibrations are detected (Smith and Dent 2004; Stuart 2004). IR spectroscopy is sensitive to any significant change in the dipole moment of a chemical group, while Raman spectroscopy is sensitive to a change in polarizability of a molecule. Thus, IR spectroscopy is adapted for heteronuclear vibrations and polar bonds (C–H, C = O) which generally are polymer side groups, whereas Raman spectroscopy is suitable for homonuclear molecular bonds, being able to distinguish C–C, C = C, and C \equiv C bonds, which are commonly part of polymer chain backbones. Hence, nonpolar bands will provide strong Raman bands and weak

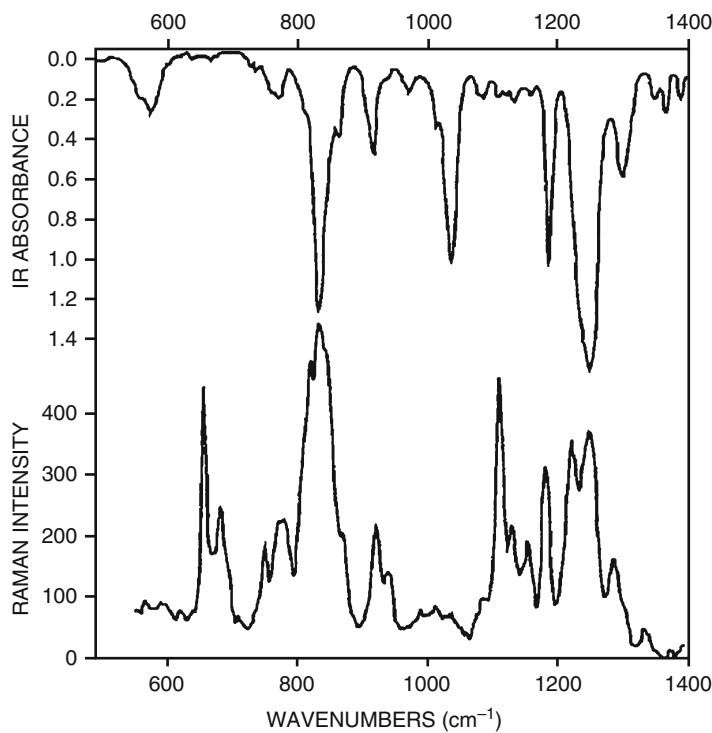


Fig. 1 Raman and mid-infrared spectra of the diglycidyl ether of bisphenol-A (*DGEBA*) (Reproduced with permission from Lyon et al. (1994))

IR bands, and on the contrary polar bonds will lead to intense peaks in IR and weak Raman bands. This complementarity can be easily observed from the Raman and mid-infrared spectra of diglycidyl ether of bisphenol-A (*DGEBA*) epoxy monomer shown in Fig. 1. The main characteristic bands of the epoxy monomer in near and mid-infrared are compiled in Table 1, as well as the most common Raman spectral bands relevant for this section. The distinction between near- and mid-infrared spectroscopy seems arbitrary, as they are essentially the same technique. Nevertheless, there is an important practical difference. The vibrational bands in the near infrared are overtones and combinatorial bands belonging mainly to C–H, N–H, and O–H bonds with very low molar absorptivity and relatively high detection limit. That means that the ability to identify chemical structures is quite low compared with midrange IR, but the penetration capacity of the IR beam in the samples is much higher, allowing more versatile studies even on millimeter-thick cured specimens. In epoxy/TP blends, this feature is very useful, since in many cases multicomponent blends present a surface morphology different from the bulk due to capillary phenomena, surface tension, or a different wettability on the curing mold.

Table 1 (a) Main characteristic bands of epoxy monomer in (a) near and mid-infrared; (b) Raman spectra. Extracted from references Gonzalez et al. (2012), Lyon et al. (1994), and Socrates (2004)

(a)	
Band (cm ⁻¹)	Assignment
Near IR	
7099	O–H overtone
6072	First overtone of terminal CH ₂ stretching mode
5988-5889	Overtones of -CH and -CH ₂ stretching
5244	Combination asymmetric stretching and bending of O–H
4623	Overtone of C–H stretching of the aromatic ring
4531	Combination band of the second overtone of the epoxy ring stretching with the fundamental C–H stretching
4066	Stretching C–H of aromatic ring
Mid-IR	
3500	O–H stretching
3057	Stretching of C–H of the oxirane ring
2965-2873	Stretching C–H of CH ₂ and CH aromatic and aliphatic
1608	Stretching C = C of aromatic rings
1509	Stretching C–C of aromatic
1036	Stretching C–O–C of ethers
915	Stretching C–O of oxirane group
831	Stretching C–O–C of oxirane group
772	Rocking CH ₂
(b)	
Band (cm ⁻¹)	Assignment
3070	Asymmetric stretching C–H of epoxide
3001	Symmetric stretching C–H of epoxide, C–H stretching of the aromatic ring
2940-2915	Asymmetric stretching C–H in CH ₂
1610	Stretching C = C of aromatic rings
1584	Stretching C–H of the aromatic ring
1460	Deformation –CH ₂
1366	Deformation –CH ₃
1258	Breathing of the epoxide ring
1188-1112	Deformation of aromatic C–H in plane
1026	Deformation of aromatic C–H in plane
907	Deformation of epoxy ring (asymmetric)
846	Deformation –CH ₂ of epoxy ring
790	Monosubstituted benzene
750	Deformation –CH ₂ skeletal
642	p-Sub benzene ring (monosubstituted benzene)

Both IR and Raman spectroscopy are widely used in polymer science providing valuable information which may have a quantitative or qualitative character (Everall et al. 2007; Koenig 1999). These techniques allow to identify polymer chemical structure and to study their characteristics such as molecular weight, conformations, orientation, or crystallinity and also the polymerization process, chemical transformations, and intermolecular interactions.

Infrared Spectroscopy

IR spectroscopy is commonly used and represents a powerful tool to study a wide variety of phenomena in polymer science. Nevertheless, in epoxy/thermoplastic polymer blends, most of the studies used IR spectroscopy to investigate essentially intermolecular interactions (prior and after curing) and the completion of the curing reaction. Both aspects are of the prime importance since they determine the thermal and mechanical properties of the blend. The IR study of intermolecular interactions between the different components of the blend gives information on their strength and on the miscibility state of the components and may shed light on the influence of sample preparation. Regarding the study of the epoxy network formation in the presence of thermoplastics, IR spectroscopy gives information about the final cross-linking density reached so that the thermal and mechanical behavior of such materials may be better understood.

For example, polycarbonate (PC)/epoxy blends have been extensively studied by IR spectroscopy due to numerous controversies about the possible side reactions that may occur between the epoxy monomer and the polycarbonate chains during the preparation of the blend in the absence of curing agent. Most of these research works (Abbate et al. 1994; Don and Bell 1996; Li et al. 1997) have focused their attention on the evolution and shifting of the carbonyl group peak of PC ($C=O$ at 1776 cm^{-1}), on the decrease of the stretching band belonging to ethers from the PC skeleton ($O-C-O$ at 1193 and 1163 cm^{-1}), and also on the eventual appearance of a broad absorption band centered around 3530 cm^{-1} coming from the generation of hydroxyl groups or on the potential diminution of the oxirane ring vibration band centered at 916 cm^{-1} . The changes observed for these absorption bands evidence strong molecular interactions between the carbonyl groups of PC and the proton donor groups of the epoxy monomers according to the sample preparation method. Nevertheless, it has been showed that if the mixing of both components is performed at high temperatures, chemical reactions such as transesterification may take place influencing the properties of the blend. Besides, more detailed IR investigations have allowed proposing complex reaction mechanisms for trans and cyclization reactions observed in PC/epoxy blends (Li et al. 1996a, b).

Intermolecular interactions of hydrogen bond type have been also observed by IR spectroscopy in a huge variety of epoxy blends. In poly(ethylene oxide) (PEO)/epoxy blends (Zhong and Guo 1998b), it is common to observe how the stretching region between 3000 and 3800 cm^{-1} of hydroxyl groups from the epoxy resin is modified when PEO is added. Generally, the pure resin shows a broad absorption band ($3420\text{--}3330\text{ cm}^{-1}$) with a slight shoulder at $3500\text{--}3560\text{ cm}^{-1}$. These bands are attributed to self-associated and free hydroxyl groups, respectively. In the absence of

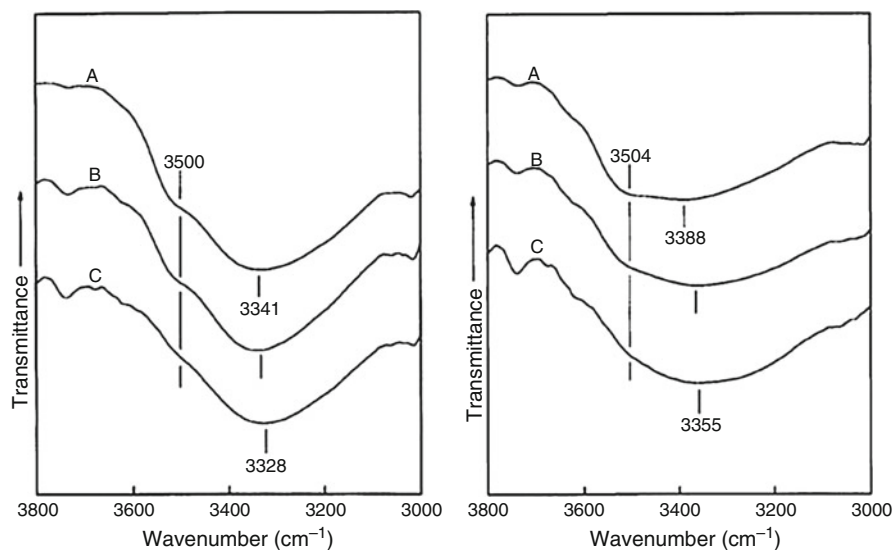


Fig. 2 FTIR spectra in the 3000–3800 cm^{-1} region of novolac epoxy resin/PEO blend at different ratios: 100/0 (A), 90/10 (B), and 70/30 (C) without curing agent (*left*) and with curing agent (*right*) (Reproduced with permission from Zhong and Guo (1998b))

curing agent, the addition of PEO causes a slight shifting to lower frequencies of the broad hydroxyl band, while the shoulder band remains unchanged (Fig. 2a). As the PEO content increases, the intensity ratio between the broad band and the shoulder increases illustrating a gradual increase of associated hydroxyl groups through the creation of hydrogen bonding interactions between the hydroxyl groups of the epoxy and the ether oxygens of PEO. As a consequence, PEO is completely miscible at the molecular level in the uncured resin. The frequency difference between both absorption bands (broad and shoulder) is a measure of the average strength of the intermolecular interactions (Purcell and Drago 1967). From the abovementioned observations, it can be deduced that hydrogen bonds between the resin and the PEO are stronger than the intra- or intermolecular hydrogen bonds present in the pure resin. When an amine curing agent is used, the global amount of hydroxyl groups increases due to the network formation, but similar observations may be made, namely, that the intensity ratio between the associated and the free hydroxyl bands increases with PEO content (Fig. 2b). This indicates that hydrogen bonding between the cured resin and the PEO remains in the cured blend although its strength is somewhat lower than in the corresponding uncured blend. However, the amount of hydrogen-bonded hydroxyl groups is much lower in the cured blend since the tridimensional network formed upon the amine addition hinders the necessary segmental motion for its formation.

The study of the spectral region corresponding to the hydroxyl groups stretching region between 3000 and 3800 cm^{-1} is also relevant for many other blends. For instance, a similar trend has been observed when poly(N-vinylpyrrolidone) (PNVP)

is the thermoplastic modifier, but in this case hydrogen bonding is formed between the carbonyl group of PNVP and the hydroxyl groups of the epoxy resin (Janarthanan and Thyagarajan 1992). As a consequence, a second band closer to the C = O stretching (1675 cm^{-1}) appears in the uncured blend which grows with the epoxy content. This vibration corresponds to the C = O involved in hydrogen bonding with the epoxy resin (1658 cm^{-1}) and becomes more intense than the non-bonded C = O for high content of epoxy providing, thus, quantitative and qualitative information on the miscibility of both components.

In poly(ϵ -caprolactone) (PCL) blends, hydrogen bonding between the carbonyl group and hydroxyls has been also detected by IR spectroscopy through the observation of the carbonyl and hydroxyls absorption bands (Zhong and Guo 1997). In these cases, the presence of hydrogen bonding manifests as a shift of the hydroxyl group self-associated band toward higher frequencies as the PCL content increases, showing that the hydrogen bonds between the hydroxyl group of the epoxy and the PCL carbonyl groups are less strong than between hydroxyl groups in the pure resin. Regarding the absorption band of carbonyl group, a similar trend than that observed for PNVP/epoxy blend is also followed confirming the complete miscibility between the epoxy resin and the PCL. Depending on the studied system, some variants may appear, as, for example, the apparition of an intermediate band (Ni and Zheng 2005), but, in any case, there is enough experimental evidence supporting hydrogen bonding between PCL and the epoxy matrices.

Similar behavior is observed in poly(methyl methacrylate) (PMMA) epoxy blends although they present different vibrations to observe possible interactions between components. In the spectral region $3000\text{--}3800\text{ cm}^{-1}$, it can be observed (Janarthanan and Thyagarajan 1992) that the self-associated hydroxyl group band from the pure resin is strongly shifted to a lower frequency (3440 cm^{-1}) in the presence of PMMA, whereas the free hydroxyl group band disappears. The formation of hydrogen bonding between the carbonyl group of PMMA and the hydroxyl groups of the epoxy weakens the self-association of OH and leads to the absence of free hydroxyl groups in the uncured blend. When the PMMA content increases, a second peak appears at around 3500 cm^{-1} , revealing hydrogen bonding between hydroxyl epoxy groups and the carbonyl of PMMA. At the same time, there is a global decrease in the broadness of the hydrogen-bonded hydroxyl band. The narrowing of the band is ascribed to a more uniform distribution in distances and geometries due to the presence of the PMMA chains. Indeed, in the pure resin this uniformity is avoided by the presence of the bulky benzene rings which, through its steric constraint, lead to a random distribution of hydrogen bonding. Regarding the carbonyl band of PMMA (C = O at 1725 cm^{-1}), a shift or an asymmetrical broadening on the lower frequency side is generally observed and confirms the hydrogen bonding between C = O and the hydroxyl groups of epoxy or epoxy-amine. Also, it is possible to observe a shift to higher frequency of the asymmetric and symmetric stretching modes of the N-H group when an amine is used as a curing agent for PMMA/epoxy blend (Gomez and Bucknall 1993). Such shifts illustrate hydrogen bonding between the carbonyl group of PMMA and the amine. But if the carbonyl peak remains unchanged, this behavior will certify a

limited solubility of PMMA, since these hydrogen bonding interactions will be weaker than the self-association of the hardener. Finally, in PMMA/epoxy blends, the intensity decrease of the O–CH₃ vibration (2850–2950 cm⁻¹) is generally associated to a transesterification reaction between PMMA and the epoxy monomer (Ritzenthaler et al. 2000).

The other important application of the IR spectroscopy on epoxy/thermoplastic polymer blends is the study of the completion of the curing reaction between the epoxy monomers and the hardener in the presence of a thermoplastic. Such studies may be qualitative or quantitative and can be followed in the mid- or in the near-infrared range, but all of them have in common the time evolution of the oxirane ring band whose intensity gradually decreases as the network is formed. The kinetic analysis of the time evolution of the peaks assigned to reactive groups can report on the catalytic nature of the curing reaction, on the contribution of secondary reactions to the curing process, and to explain the final properties of the material in terms of its structure. For example, in poly(ether ether ketone) (PEEK)/epoxy blend, it has been qualitatively observed (Zhong et al. 1998) that even a post-curing schedule does not allow the total disappearance of the epoxy absorption band in the mid-IR (916 cm⁻¹). This is due to the fact that the system has vitrified during the cure and a high-temperature post-curing is not able to complete the reaction due to the high viscosity of PEEK. As a consequence, the cure reaction is incomplete, and the glass transition temperatures of the blends diminish with the PEEK content due to the lower final cross-link density reached.

From the mid-IR spectra, it is also possible to qualitatively study the curing reaction of nylon, which owns amide groups, with DGEBA (Zhong and Guo 1998a). For the uncured blends, the characteristic absorption of the oxirane ring at 916 cm⁻¹, a sharp absorptive peak at 3304 cm⁻¹, and a shoulder peak at about 3480 cm⁻¹ corresponding to the stretching vibrations of the N–H and O–H groups, respectively, can be observed. After curing, the mid-IR spectra of the blends show the total disappearance of the oxirane vibration along with the diminution of the stretching vibration of the N–H group and the increase of the stretching vibration of the O–H group. This behavior, which is independent on the nylon content in the blend, illustrates the complete reaction of DGEBA through the nucleophilic attack on the oxirane ring by the amide nitrogen of nylon. In addition, a new absorption at 1726 cm⁻¹ appears after curing, and its intensity depends on the nylon content in the blend. This absorption peak corresponds with the carbonyl of an ester group generated by a secondary reaction between the carbonyl group of the nylon and the hydroxyl groups of the resin, liberating a secondary amine group which can react further with an oxirane group.

The epoxy and amine conversion as a function of the cure time may be also quantitatively determined from mid-IR, although this is sometimes difficult to accomplish due to the overlapping of absorption bands (Don and Bell 1998). Generally, the phenyl group absorption band at 1602 cm⁻¹ is used as a reference band, and the epoxy and amine conversions are, respectively, calculated from the epoxy ring band at 916 cm⁻¹ and the N–H bending mode at 1720 cm⁻¹ (Abbate et al. 1994; Kim et al. 1995).

The quantitative determination of the epoxy and amine conversion as a function of the cure time may be obtained easily from the spectral data in the near IR, if the thermoplastic infrared spectrum does not overlap with either the epoxy or the amine bands (Cabanelas et al. 2005a; Gonzalez et al. 2012; Kortaberria et al. 2004). Epoxy conversion, α , is determined monitoring the extinction of the oxirane ring vibration at 4530 cm^{-1} and using as a reference the combination band C–H stretching vibration of the benzene ring at 4622 cm^{-1} according to Eq. 1:

$$\alpha(t) = 1 - \frac{A_{4530}(t)/A_{4622}(t)}{A_{4530}(t=0)/A_{4622}(t=0)} \quad (1)$$

In the same way, the primary amine conversion, β , may be obtained from the N–H stretching and bending combination band centered at around 4935 cm^{-1} using the same C–H band as reference (Eq. 2):

$$\beta(t) = 1 - \frac{A_{4935}(t)/A_{4622}(t)}{A_{4935}(t=0)/A_{4622}(t=0)} \quad (2)$$

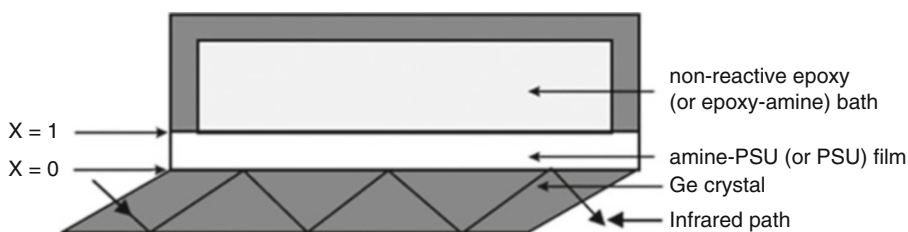
In both equations, A is the integrated absorbance of the band. From these conversions and through a mass balance, it is possible to calculate the concentration of epoxy and hydroxyl groups as well as of primary, secondary, and tertiary amine groups as a function of the cure time. This set of experimentally derived data may permit to elaborate kinetic models which are generally more complex than those proposed from calorimetric data, since these models take into account the simultaneous evaluation in the concentrations of all the species present in the reaction medium during the curing process (González et al. 2012).

Finally, it may be also mentioned the potential of Fourier transform infrared spectroscopy–attenuated total reflectance (FTIR–ATR) to study the swelling, diffusion, and transport phenomena in polymer matrices. For instance, this technique has been used to study the diffusion of epoxy monomers and diamine curing agents into polysulfone (PSU) (Immordino et al. 1998; Rajagopalan et al. 2000). With this purpose, the intensity changes of selected characteristic absorbance bands (Table 2) were monitored in real time according to the experimental device described in Fig. 3.

For a given temperature, the normalized absorbance intensity of each band is therefore obtained (Fig. 4), and its evolution with time is fitted to an appropriate diffusion equation to determine the diffusion coefficients. In Fig. 4, the initial increase of both peaks illustrates the diffusion of the epoxy molecule, but the subsequent decrease of the absorbance of the epoxide ring is not followed by any change in the aromatic ring band which remains stable. This evidences the reaction with the curing agent in the presence of the PSU to form an interpenetrating network at the interphase. According to this method, the diffusivity of the amine is an order of magnitude greater than the diffusivity of epoxy. Besides, since the small amine molecules swell the PSU, the diffusivity of the larger epoxy molecules in polysulfone is also enhanced.

Table 2 Epoxy, amine, and PSU characteristic bands monitored for diffusion coefficient determination

Component	Band (cm^{-1})	Chemical group	Depth of penetration (μm)	Chemical nature
Epoxy	915	Epoxide ring	0.54	Reactive
	1036	Aromatic deformation	0.48	Nonreactive
	1508	C–C skeletal stretching	0.33	Nonreactive
	1609	C–C skeletal stretching	0.31	Nonreactive
Amine	2916	Asymmetric cyclohexane ring stretch		Nonreactive
Polysulfone	1488	Aromatic skeletal stretching	0.34	Nonreactive

**Fig. 3** Experimental setup for diffusion–reaction studies. Configuration 1: single-component diffusion studies with Ge crystal coated with $3\ \mu\text{m}$ thick PSU – 61% amine film and epoxy bath. Configuration 2: two-component diffusion and reaction studies used crystals coated with 100% PSU and epoxy–amine bath (Reproduced with permission from Rajagopalan et al. (2000))

Raman Spectroscopy

Despite its advantages to examine aqueous solutions or samples without any preparation and the valuable information that Raman spectroscopy may provide in polymer science, its use is until now very limited in the study of epoxy/thermoplastic polymer blends. Nevertheless, a complete work has been reported for a copoly(ether sulfone)/epoxy blend (Van Overbeke et al. 2000, 2001a, b, 2003) which illustrates very well the potential of this technique to study such materials.

Raman spectroscopy has been firstly used with the aim to observe “in situ” the reaction between an amine-ended copoly(ether sulfone) thermoplastic and the growing epoxy network (van Overbeke et al. 2000). From the Raman spectra, a peak located near $996\ \text{cm}^{-1}$ is observed for the amine-ended copoly(ether sulfone) and its model compound, the bis(4-(3-aminophenoxy)phenyl)sulfone. This peak is assigned to the vibration of the aromatic ring carrying the amine group in the meta-position. Upon reaction with the epoxy groups, the peak vanishes, while two peaks progressively appear at lower wave numbers, 991 and $984\ \text{cm}^{-1}$. The same behavior was also observed for aniline, a monosubstituted aromatic compound, when reacted with epoxy monomers. Analysis of the Raman spectra of commercial aniline derivatives (N-ethylaniline and N,N-diethylaniline) allowed to assign the two new vibration bands to secondary ($991\ \text{cm}^{-1}$) and tertiary ($984\ \text{cm}^{-1}$) amine groups. Therefore, the

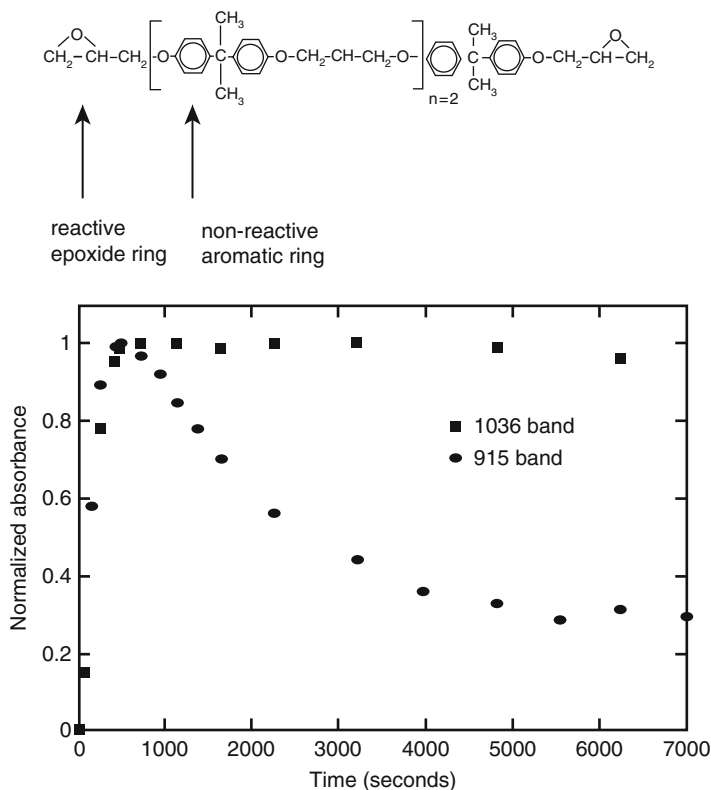


Fig. 4 Experimental evolution of the normalized absorbance of the reactive peak of the epoxide ring (915 cm^{-1}) together with the nonreacting aromatic peak (1036 cm^{-1}) for a two-component diffusion and reaction experiment (configuration 2 in Fig. 3) (Reproduced with permission from Rajagopalan et al. (2000))

reaction between the amine-ended thermoplastics and epoxy monomers may be at least qualitatively monitored through this method.

Regarding the blend of amine-ended copoly(ether sulfone) with epoxide, cured with 4,4'-diaminodiphenyl sulfone (DDS), the reaction of the chain ends cannot be monitored since a broad peak appears during the network formation overlapping with the band located at 996 cm^{-1} . The authors focused on the study of this reactive blend by examining the Raman spectra between 2714 cm^{-1} and 3414 cm^{-1} and also in the range which goes from 685 cm^{-1} to 1672 cm^{-1} (van Overbeke et al. 2001a). The first spectral region shows several vibrations of interest such as the aliphatic C-H scatter from 2800 to 3000 cm^{-1} , the aromatic ring signal between 3000 up to 3100 cm^{-1} , and two epoxide signals located at $3002\text{--}3005\text{ cm}^{-1}$ and $3050\text{--}3070\text{ cm}^{-1}$. A large band at $3330\text{--}3400\text{ cm}^{-1}$ is indicative of primary amine groups. For the second region, several vibrations allow to determine the epoxy conversion.

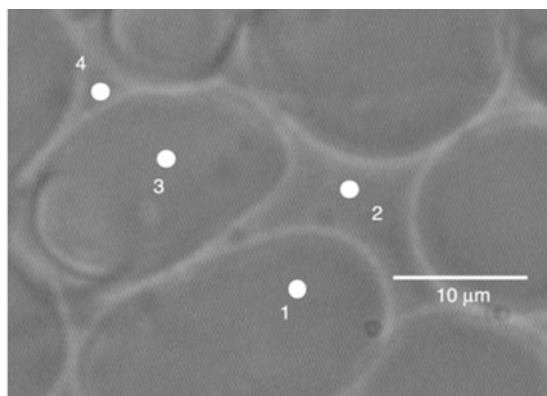
For both spectral regions, the curing of the epoxy with DDS was monitored from spectral data that would not be influenced by the future or further addition of the reactive copoly(ether sulfone) neither by moderate changes in DDS stoichiometry. Two different analyses were then applied. The first one followed the evolution of the peak area of the epoxide ring at 3005 cm^{-1} normalized by the six aliphatic peaks area ($2833\text{--}3005\text{ cm}^{-1}$), and the second one consisted of a multivariate analysis that considers simultaneously the intensity of Raman spectra for a large interval of wave numbers, and results were successfully calibrated with the epoxy conversion determined by differential scanning calorimetry (DSC). The methods were then applied to the blends, but obtaining only a qualitative estimation of the epoxy conversion due to some discrepancies coming from the analysis of Raman spectra signal which is slightly influenced by the thermoplastic presence. In addition, Raman spectroscopy has proven to be useful for determining the content of copoly(ether sulfone) in the epoxy blend (van Overbeke et al. 2001b).

Indeed, using a multivariate calibration, it is possible to correlate the Raman intensities with the thermoplastic content even if the curing agent and thermoplastic present many common vibration bands. For a similar epoxy blend (25% copoly(ether sulfone)) cured with methylene bis(2,6-diethylaniline) (MDEA), the system presents phase separation with a final coarse phase-inverted morphology (van Overbeke et al. 2003). Using micro-Raman spectroscopy and a multivariate calibration, the copoly(ether sulfone) content was determined in both phases as a function of cure time as it is illustrated in Fig. 5.

From the thermoplastic content distribution obtained at different sample locations at curing times, it was observed that each phase tends to expel the other component, but even at the longest studied cure time, about 50% of epoxy-curing agent species remained in the thermoplastic-rich phase, while 10% of copoly(ether sulfone) remained in the epoxy-rich phase. Concerning the epoxy conversion, it increases gradually with the cure time in the epoxy-rich phase, whereas, in the copoly(ether sulfone)-rich phase, the conversion decreases at the beginning of the phase separation process and it is stabilized at higher cure times. This illustrates experimentally the coexistence curves relating the evolution of the epoxy conversion with the copoly(ether sulfone) content during the phase separation phenomena and demonstrates that Raman spectroscopy may be a powerful tool to study epoxy blends.

Nuclear Magnetic Resonance Spectroscopy

Nowadays, high-resolution nuclear magnetic resonance (NMR) spectroscopy is a widely employed technique to investigate the specific intermolecular interactions (miscibility) and phase behavior of polymer blends. As blending influences the molecular dynamics of each individual component, characterization of the chain dynamics in polymeric blends is of significant interest. Solid-state NMR spectroscopy is frequently applied to characterize the phase behavior of polymer blends at the molecular level providing information on the microstructures of blends and on the dynamics of chain relaxation. Furthermore, solid-state NMR methods offer



Point	Copoly(ethersulfone) content (%)	Epoxy conversion (%)
1	16.0	75.8
2	41.7	57.4
3	18.2	67.4
4	46.0	62.5

Fig. 5 Image obtained with an optical microscope mounted on the Raman spectrometer for an epoxy–MDEA/copoly(ether sulfone) blend cured for 30 min at 160 °C and quenched. For each point (1–4), copoly(ether sulfone) content and epoxy conversions have been calculated from the Raman spectra analysis (Reproduced with permission from Van Overbeke et al. (2003))

powerful tools for understanding miscibility between polymers, with a specific ability to quantify the length scales of mixing below that accessible by other experimental tools and to detect the inter- and intramolecular interactions that are responsible for miscibility. Schaefer's group was the first to introduce the solid-state NMR technique to analyze the polymer blends (Schaefer et al. 1981). At present, the area of understanding miscible blend dynamics is of particular interest to many NMR-based investigations.

As previously reported, NMR spectroscopy was used to identify possible transesterification reactions in homogenous poly(ϵ -caprolactone)/epoxy blends during the hot melt process (Chen et al. 1999). Reaction was carried out between the hydroxyl groups of the epoxy monomer and the ester groups of the PCL. $^1\text{H-NMR}$ spectra showed the greater transesterification extent after increasing post-curing temperature in these systems. The effects of transesterification processes affect the thermal properties such as a broader glass transition temperature, and, in consequence, they could influence on the final application of the materials.

Polyaniline/epoxy (DGEBA) polymer blends were also characterized by $^1\text{H-NMR}$ and $^{13}\text{C-NMR}$ spectroscopies in order to determine the grafting section and identify the molecular structure of the systems (Teh et al. 2009). In this study, polyaniline was copolymerized with DGEBA. Anionic copolymerization was carried out grafting on polyaniline via ring opening polymerization of epoxide from DGEBA. The formation

of grafting occurred throughout and at chain end of polyaniline backbones which led to different levels of cross-linking of the polymer with the resin. Results of NMR analysis revealed that grafting took place together with the side reaction (cross-linking) and DGEBA homopolymerization. In terms of application, the grafted section on this system was important because it imparted conductive properties to the system in its solid form in order to produce a conductive resin material.

Polymers with enhanced thermal resistance, reduced dielectric constant, and flame-retardant properties have attracted a great interest of research for the last years. Incorporation of poly(alkyl-phenylene oxide) to DGEBA epoxy systems resulted in a significant increase in its glass transition temperature, thermal stability, and flame resistance (Su et al. 2010). The structures and properties of those blends were studied by nuclear magnetic resonance spectroscopy, differential scanning calorimetry (DSC), thermogravimetric analysis (TGA), and gel permeation chromatography (GPC). ^1H -NMR and ^{13}C -NMR analysis in deuterated chloroform was carried out in order to verify the chemical structure of those blends.

NMR spectroscopy can also monitor the progress of cure in epoxy/thermoplastic systems. Network formation of blends of amine/epoxy resin was followed by NMR in combination with other cure monitoring techniques: ultrasonic wave propagation and dielectric permittivity (Challis et al. 2003). In Fig. 6a, the scheme of the NMR test cell is shown. The mobility of magnetically active nuclei was analyzed, and the technique was found especially sensitive to spin relaxations of hydrogen nuclei bound at specific sites in the resin, hardener, and resin–hardener molecules. Therefore, the device could be used to follow the degree of polymerization as a function of time, since free induction decay (FID) measurements may take advantage of detecting the change from viscous liquid to cross-linked solid as the resin cures. Short-pulse radiation supplied to the sample led to radio frequency signal decay after the relaxation of excited nuclei. These signals were processed to extract the amplitude–time signal, that is, the free induction decay (FID). The NMR FID exponential amplitudes of both the liquid and solid fractions were plotted against the cure time (Fig. 6b) to follow the progress of cure. In the first stage of the cure process, in the liquid phase, there was a very little change in the NMR data, indicating no change in proton mobility. In the second stage, gelation, data showed a rapid reduction in the liquid curve and an increase in the solid curve, that is, the transition to the solid accelerates with a consequent reduction in proton mobility. Finally, at the third stage, post-gelation and vitrification, the NMR curves reached saturation values. The liquid signal fell close to zero, and the conversion from liquid to solid appeared to be complete which indicated that all the material was solid.

The ^{13}C chemical shifts and line shapes of the carbon resonance in cross-polarization/magic-angle spinning (CP–MAS) spectra identify the chemical environment of the carbon nucleus, and their changes usually reflect the intimacy of mixing between the blend components. The ^1H spin–lattice relaxation times in the laboratory (T_1^{H}) and rotating ($T_{1\rho}^{\text{H}}$) frames obtained from CP–MAS NMR can provide information regarding the domain size of polymer blends by measuring proton spin diffusion. It is possible to evaluate the scale of the miscibility of polymer

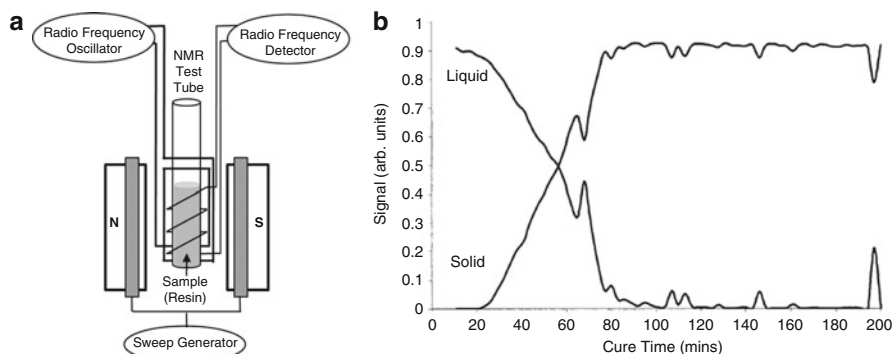


Fig. 6 (a) Scheme of the NMR test cell; (b) NMR solid and liquid signal amplitude measurements versus the cure time (Reproduced with permission from Challis et al. (2003))

blends according to the dynamic NMR relaxation measurement (McBrierty and Packer 1993).

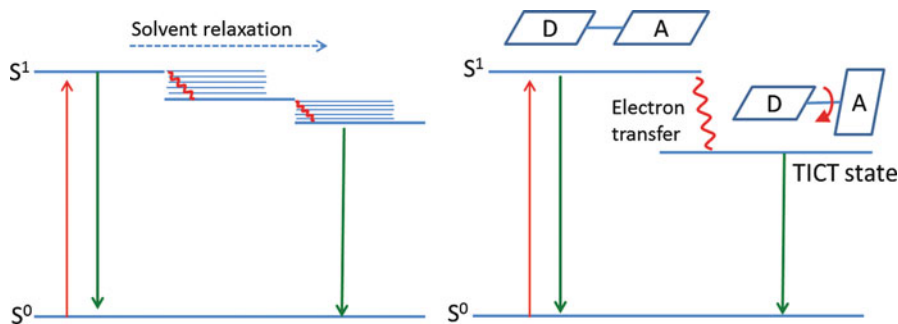
High-resolution solid-state ^{13}C cross-polarization/magic-angle spinning (CP-MAS) NMR spectroscopy was employed for the examination of the miscibility of the thermosetting blends composed of poly(ϵ -caprolactone)/epoxy resin at the molecular level (Zheng et al. 2003). Resonance of the carbons involved in the intermolecular hydrogen bonding interactions between the cross-linked epoxy resin and PCL presented significant changes in the line shapes and chemical shifts. The chemical shift of the carbonyl carbon resonance of PCL was shifted to a low field with increasing epoxy contents in the blends. This indicated that the magnetic shielding of the carbonyl carbon decreased due to specific intermolecular interactions between carbonyls of PCL and the pendant hydroxyls of epoxy. Moreover, the line width of spectra decreased with increasing PCL content in the blends. The narrower spectral lines were attributed to the ordered PCL chains in the crystalline region and the high mobility of the amorphous region with T_g s (i.e., 30/70 epoxy resin/PCL blend -39.2°C) lower than the experimental temperature (27°C), which could eliminate the anisotropy of the chemical shifts. The spectral changes due to blending suggested an intimate mixing of the polymer chains of the two components. This study demonstrated that the homogeneity of the thermosetting blends at the molecular level was quite dependent on the blend composition.

The compatibility and interaction behavior of a series of interpenetrating polymer networks (IPNs) based on unsaturated polyester/epoxy resin have been investigated by solid-state NMR spectroscopy, among other techniques (Shih and Jeng 2004). ^{13}C CP-MAS spectra revealed that the peaks of the IPNs were shifted downfield compared with pristine unsaturated polyester. These results suggested an intermolecular interaction, such as hydrogen bonding, between the epoxy and the thermoplastic components. Moreover, the carbonyl carbon resonance of polyester shifted continuously downfield with increasing epoxy content, revealing the gradual increase in hydrogen bonding. Therefore, an improved miscibility for IPN can be

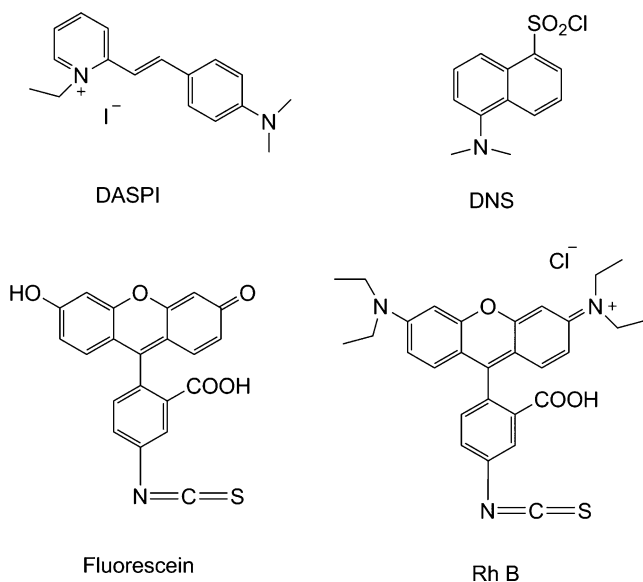
obtained for a composition with similar amounts of hydrogen donors in epoxy resin and carbonyl groups in unsaturated polyester. ^{13}C solid-state NMR technique has demonstrated to be useful in studying IPN systems effectively apart from investigating polymer blends.

Fluorescence Spectroscopy

Luminescence occurs when any substance shows light emission from excited electronic states. It can be presented as fluorescence or phosphorescence. The fluorescence phenomena are associated to electron promotion to a singlet excited state (paired spin with the ground state) with subsequent radiative decay to the ground state in a timescale up to tens of nanoseconds, whereas phosphorescence is associated with the promotion to a triplet state (opposite spin with the ground state) with much longer decay time. Fluorescence is by far the most commonly used in polymer science. This phenomenon is typical of aromatic molecules which present an electronic delocalized distribution through π orbitals and many times is presented as a broadband without vibrational structure. A sample of some fluorescent molecules, particularly those used in the works reported in this chapter, is presented in Scheme 2. Emission energy is always lower than excitation due to vibrational relaxation, and the difference between absorption and emission maximum intensity is called the Stokes shift. This shift allows collecting and evaluating easily the fluorescence emission of a fluorescent reporter in solid samples without the interference of the scatter of the excitation beam. But the most outstanding feature of the fluorescence of organic molecules is its dependence on the conditions of the chromophore environment. The energy emission in the radiative decay depends on the relative stabilization of the excited state, which in turn is a function of the dipolar coupling with the immediate environment of the chromophore, since the excited state usually has large charge separation and high dipolar moments (Lakowicz 1999). So there are solvatochromic chromophores whose emission spectrum varies greatly depending on the polarity of the environment. The greater the polarity, the better the dipolar coupling, and emission occurs from an excited relaxed state of low energy. But the radiative decay is also dependent on the rigidity of the environment, since a stiffer environment entails an increased relaxation time of the excited state. If the relaxation time is longer than the fluorescent lifetime in the excited state, decay does not take place from a relaxed state, and fluorescent emission will shift to the red (shorter wavelength; see Scheme 1, left). Both factors, polarity and rigidity, are changing during the formation of a thermoset polymer network and can be monitored accordingly. In fact, fluorescence spectroscopy has been used in polymer science to monitor polymerization processes, thermal relaxations, and morphology and phase distribution in polymer blends (Baselga et al. 2010; Bosch et al. 2005). Indeed, phase separation processes in epoxy-TP blends may cause an abrupt change in the environment of the fluorescent probe: thermoplastic- and thermoset-rich phases, which should be reflected in changes in fluorescence emission.



Scheme 1 Two of the relaxation mechanisms which contribute to a blue shift in the fluorescence emission. *Left*: upon excitation from ground state (S^0), dipolar coupling of the excited state (S^1) with the surrounding environment of the chromophore leads to a low-energy emission spectrum. The extent of relaxation depends on the solvent polarity and relaxation time. *Right*: twisted intramolecular charge transfer dynamics on TICT probes (see text). Fast electron transfer from donor (D) to acceptor (A) leads to a stabilized electronic transfer state with radiative decay. The probability of charge transfer is related to the polarity and free volume of the surrounding environment. Both mechanisms may occur simultaneously



Scheme 2 Chemical structure of fluorescence probes and labels reported in the text. DNS is a sulfonyl chloride derivative of dansyl, and regarding rhodamine B (Rh B) and fluorescein, the isocyanate derivatives are presented, but there are also available other reactive functionalities

Therefore, a gradual blue shift in the fluorescence spectra due to the emission from a less relaxed excited state is a common observation when the environment of any fluorophore becomes more rigid. An interesting experimental observation but of limited utility is the increase observed in fluorescence intensity when the

surrounding environment of the probe becomes more rigid. This fact may be explained, in brief, as being a consequence of the decrease in the mean fluorescence lifetime, which makes the non-radiative decays less effective.

Fluorescence of extrinsic molecular probes has demonstrated to be useful to monitor cross-linking in epoxy resins. For example, DGEBA/4,4'-diaminodiphenylmethane (DDM) curing was followed by using free volume-sensitive probes, such as p-N,N-dimethylamino-styryl-2-ethylpyridinium iodide (DASPI, Scheme 1) (Strehmel et al. 1999), which belongs to a family of fluorophores known as twisted intramolecular charge transfer (TICT) probes. DASPI forms an excited intramolecular charge transfer complex which is stabilized by a rotation through the single bonds between the alkene and the aromatic rings of the molecule, leading to a red-shifted emission of lower energy, as it is shown in Scheme 1, right. The TICT state is only reached if the molecular neighborhood allows rotation, as twisting needs a minimum reaction volume. Therefore, following the changes in emission spectrum of DASPI, it was possible to monitor cross-linking and also to detect the glass transition in the fully cured thermoset. In another interesting work (Hakala et al. 2000), the curing of an epoxy-anhydride system was analyzed with several extrinsic TICT probes. Fluorescence changes were analyzed by an intensity ratio method which eliminates the effect that other factors have in the intensity, such as lamp intensity, optical alignment, illuminated surface, or temperature. A linear correlation between the fluorescence intensity ratio and curing degree was found.

Several polymers have an intrinsic fluorescence emission due to their aromatic benzene ring backbone. This is the case of DGEBA, which shows an intrinsic luminescence when excited with UV radiation. The emission spectrum presents a maximum at about 300–340 nm depending on the solvent, but its quantum yield is very low. Some aromatic hardeners such as 4,4'-diaminodiphenyl sulfone (DDS) or 4,4'-diaminodiphenylmethane (DDM) also present intrinsic fluorescent emission in the range 400–480 nm. Its emission spectrum shows a red shift, and intensity increases with curing (Sales and Brunelli 2005). This is not only a consequence of a more rigid environment but also a result of the gradual conversion of primary to secondary and tertiary aromatic amines (Paik and Sung 1994). On the contrary, when cured with aliphatic amines, tertiary amine quenching of intrinsic epoxy fluorescence has been observed. The quenching of the fluorescence of organic molecules by aliphatic amine is well documented. The relative ability of amino groups to quench a fluorophore was estimated as 1:4:36 for the primary, secondary, and tertiary amines (Rigail-Cedeño and Sung 2005). Therefore, quenching may be used to monitor changes during curing since tertiary amine evolution can be monitored.

However, it is much more versatile the use of extrinsic chromophores, either free probes dissolved in the blend or covalently attached to any of the network-forming components as a label. There is a wide range of fluorescent probes available with excitation and emission wavelengths ranging from ultraviolet to 800 nm and with different responses to changes in polarity, temperature, or free volume. Extrinsic fluorescence spectroscopy has been used to characterize domain architecture in toughened epoxy networks, many times in conjunction with epifluorescence

microscopy or laser scanning confocal microscopy (LSCM). DGEBA was cured with Jeffamine (amine-ended poly(ethylene oxides)) modified with two fluorescent reporters, fluorescein and rhodamine B (Rh B) isocyanate derivatives, for a morphological characterization (Davis et al. 2013). The appropriate choice of the fluorescence probe allowed a better resolution between similar components with respect to SEM. 5-(Dimethylamino)naphthalene-1-sulfonyl chloride, known as dansyl chloride (DNS), has been used to monitor curing and phase separation in epoxy/PMMA blends (Olmos and Gonzalez-Benito 2006) and epoxy/PEO blends (Gonzalez-Benito and Esteban 2005). A typical red shift accompanied by an increase in fluorescence intensity with curing progress was observed, but the technique has shown also to be sensitive to reaction-induced phase separation (RIPS). Fluorescence spectrum was a balance of two effects, the chemical change derived from the reaction and the physical change due to increasing viscosity. On the epoxy/PEO blend, it has been possible to analyze the enhancement in the miscibility between the PEO and the epoxy network as the curing temperature is increased. The RIPS of DGEBA organic–inorganic hybrid thermosets blended with PMMA has been also studied (Cabanelas et al. 2005a). For studying the phase separation, PMMA was labeled with 9-vinylanthracene, and the reaction was also followed by FTNIR. Beyond the dilution effect, PMMA does not influence the curing kinetics, but it strongly affects the compatibility between the epoxy precursors.

It has been also analyzed by fluorescence the reactive compatibilization. A poly (aminopropyl methyl siloxane) (PAMS) was cured both with DGEBA (Cabanelas et al. 2005b) and 3,4-epoxycyclohexyl-3'4'-epoxycyclohexane (ECC) (Gonzalez et al. 2011), which is a typical cycloaliphatic epoxy resin for UV curing. Reaction was followed by NIR and by fluorescence labeling PAMS with rhodamine B sulfonyl chloride. In both epoxy resins, initially immiscible with PAMS, it has been possible to check the compatibilization with the silicone due to chemical reaction. With the help of LSCM imaging and analyzing the fluorescence intensity profiles through the interphase (Fig. 7), it has been possible to demonstrate the diffusion of the epoxy resin through the PAMS-rich domains with simultaneous chemical reaction. Results showed that as curing temperature increases, the material becomes more homogeneous with a narrower and diffuse interphase between both components.

The ability of fluorescent reporters to report on the cross-linking degree and the glass transition temperature on epoxy heterogeneous systems has been also demonstrated in nanocomposites. DNS has been attached to silica nanospheres through low-molecular-weight amino-ended PEO tethers and introduced in a DGEBA resin which was cured with MXDA (Antonelli et al. 2014, 2015). Fluorescence steady-state spectrum and also fluorescence lifetimes were recorded during curing and in fully cured samples. The DNS was able to report the local glass transition related with the interpenetration of PEO chains in the epoxy matrix and the thickness of the interphase. Concerning the curing process, fluorescence spectroscopy allowed determining heterogeneous curing, revealing that gelation and vitrification occur first on the silica surface due to silanol catalytic activity.

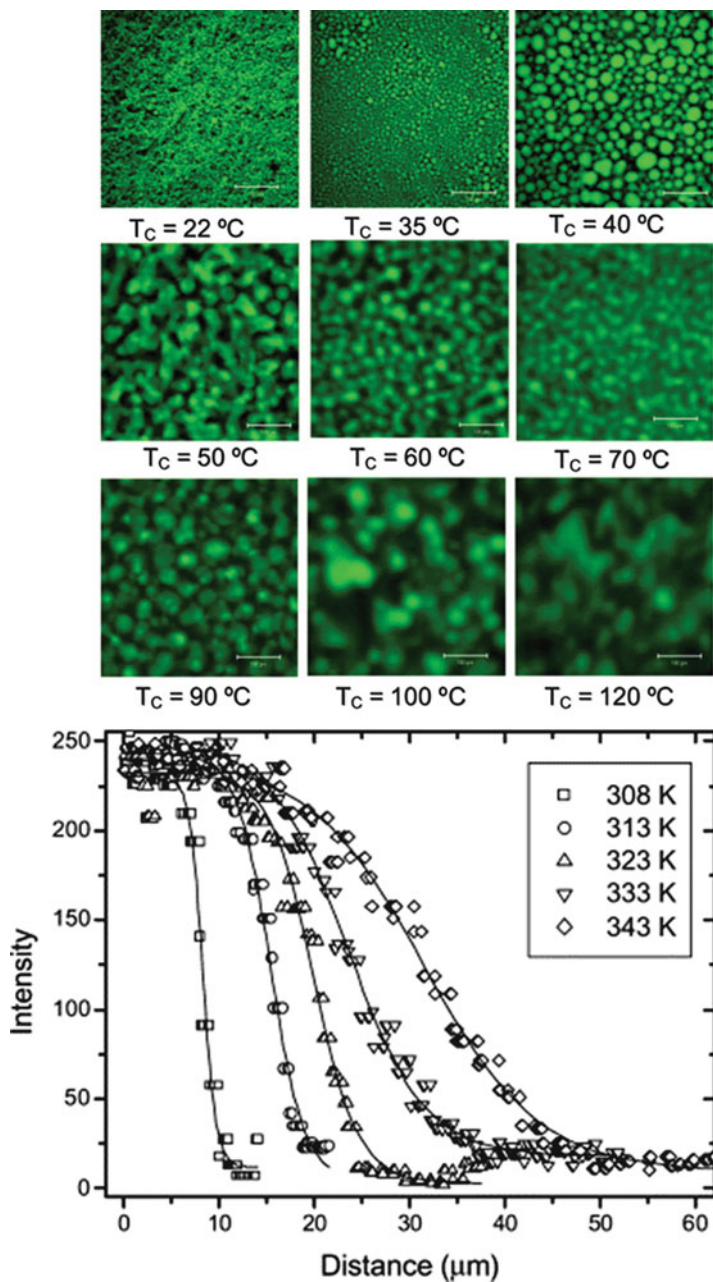


Fig. 7 LSCM images of DGEBA/PAMS cured at different temperatures (*up*) and fluorescence intensity profiles across the interphase (*down*), showing the progressive compatibilization. The scale bar corresponds to 100 μm (Reproduced with permission from Cabanelas et al. (2005b))

Energy Dispersive X-Ray Spectroscopy

Energy-dispersive X-ray spectroscopy or energy-dispersive X-ray (EDX) fluorescence technique allows qualitative and quantitative analysis of elements comprising a material by tracing the reemitted characteristic X-ray generated as a result of transitions between inner atomic electron energy levels of the specific elements contained in a sample.

EDX analysis has been used to evaluate cross-section composition and morphology of binary epoxy-fluorinated polymer blends (Penoff et al. 2007). Fluorine groups were introduced to improve chemical resistance and optical and electrical properties and to be evaluated as potential surface modifiers to prepare, for instance, water-repellent surfaces. The fluorinated thermoplastic (FT) was synthesized from a small amount of 3-(trifluoromethyl)aniline added to an excess of DGEBA. The slight excess of epoxy groups could promote chemical bonds with the growing epoxy-amine copolymer. Depth profiles in terms of the atomic ratio of F in FT-modified samples at different curing conditions were obtained from EDX measurements. The results confirmed that fluorinated polymer migrated toward the surface when curing in the presence of air and that FT distribution was practically independent of cure temperature.

EDX has been also employed to analyze morphologies of blends of epoxy and brominated phenoxy as the thermoplastic (Yokoyama et al. 2007). These blends are interesting as adhesives for flexible printed circuits (FPC). Required properties are high tensile strength and high T-peel adhesion strength without decreasing elongation, lap shear adhesion strength, and T_g to maintain the reliability of FPCs. Co-continuous phase structures allowed to reach the desired properties. Furthermore, the morphologies of the cured blends showed better impact properties than that of the neat cured system. In this way, a more uniform stress distribution in the material under load could be achieved by the strong interaction between the phases, which avoided premature failure due to localized stress concentration (Venderbosh et al. 1994). EDX measurements evidenced co-continuous structures consisting of rigid epoxy-rich phases and ductile brominated phenoxy-rich phases when content of thermoplastic was 30–40 wt%.

A practical approach to toughen epoxy resins is to use high-performance engineering thermoplastics with high glass transition temperature, high thermal stability, and toughness. The obtained morphology influences on the final properties of the materials: for instance, it is widely acknowledged that the effective improvement in toughness will be obtained with co-continuous phases or phase inversion structures; hence, the study of phase separation and morphology control is worthwhile. Poly(ether imide) (PEI)/silica nanocomposites, prepared by sol-gel process, have been used to modify the epoxy resin and to study the influence of the silica particles on phase separation during the curing process (Zhang and Xie 2011). Some compositions presented phase inversion structure containing an epoxy-rich dispersed phase within the thermoplastic-rich continuous phase. To analyze the distribution of silica particles, EDX measurements were carried out. And it was found (Fig. 8) that the mean content of silica in epoxy resin-rich phase was much higher than in PEI-rich

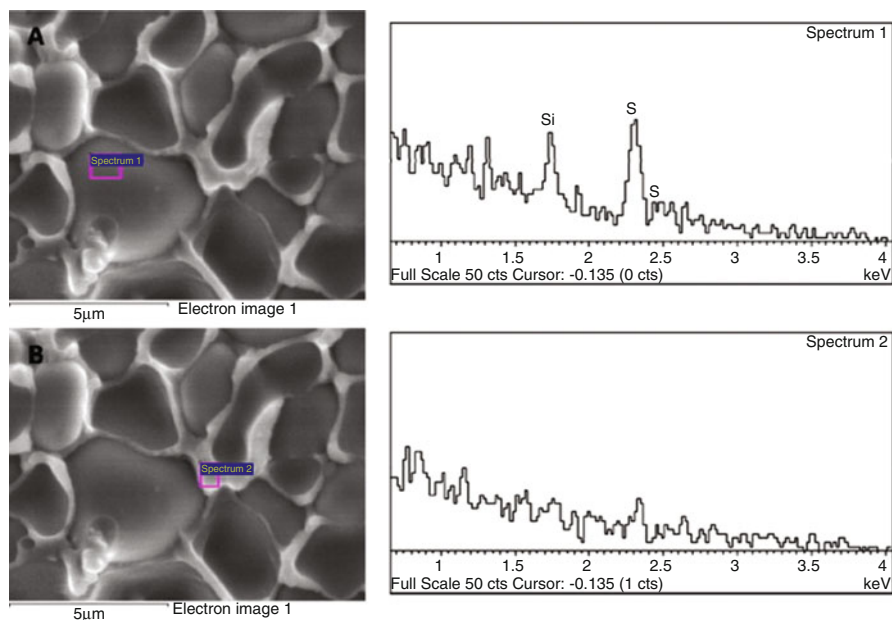


Fig. 8 EDX analysis of epoxy resin/PEI/SiO₂ (100:30:2.25) composite. (a) Epoxy resin-rich phase; (b) Poly(ether imide)-rich phase (Reproduced with permission from Zhang and Xie (2011))

phase. SEM-EDX results indicated that silica nanoparticles formed in the PEI gradually migrated and concentrated in the epoxy-rich region during the phase separation due to the better affinity between the nanoparticles and epoxy resin. Silica also accelerated the rate of curing reaction and therefore decreased the gelation time, so the particles forced an earlier phase separation. Therefore, the addition of the silica particles into the system has turned out to be a suitable method to control the morphology. Moreover, the use of PEI/silica as the modifier of epoxy resin also led to the improvement of the impact strength and storage modulus.

Dielectric Relaxation Spectroscopy

Dielectric spectroscopy analyzes the dielectric properties of a material as a function of frequency (and temperature), measuring the interaction of the electrical dipole of the sample (permittivity) with an external field. Dielectric relaxation studies (DRS) are of great relevance in polymer science. They have been used to study curing chemistry and kinetics, water absorption, aging, and interfacial phenomena (Petrick and Hayward 2002). When an alternating electric field is applied, the orientational distribution function of the molecular dipoles is perturbed, and dielectric relaxation occurs through reorientational motions in a broad frequency range. According to Eq. 3, the complex dielectric permittivity ϵ^* is the sum of the contributions of the real part, capacitance (ϵ'), and the imaginary part, conductance (ϵ''):

$$\epsilon^*(\omega) = \epsilon'(\omega) - i\epsilon''(\omega) \quad (3)$$

For a thermosetting polymer, ϵ' and ϵ'' can be measured during curing at frequencies between 1 and 10^5 Hz, but the analysis is quite complex because of the simultaneous changes in chemical composition, molecular size, and viscosity. Compared with DSC, dielectric relaxation is more sensitive to structural heterogeneities in polymer blends, due to the smaller probe length scales, providing information on phase interactions and miscibility. There have been published several studies about dielectric relaxation on epoxy polymers, but there are also some interesting works in epoxy/thermoplastic blends. For example, DRS was used to analyze molecular relaxations in epoxy/poly(ethylene oxide) (PEO) blends (Kalogeris et al. 2006), and a “plasticization” phenomenon on PEO addition was found, which reduces the number and/or strength of intermolecular interactions in the epoxy network. The formation of hydrogen bonds between hydroxyl epoxy groups and the ether group of PEO avoids the self-association of hydroxyls in pure epoxy resin. In another work, dielectric measurements on DGEBA/4,4'-methylene bis(3-chloro-2,6-diethylaniline) (MCDEA) modified with poly(2,6-dimethyl-1,4-phenylene ether) (PPE) were performed to monitor and characterize the phase separation process (Poncet et al. 1999; Bonnet et al. 2000). Dielectric properties monitored the buildup of the T_g in both the epoxy-rich phase and the PPE-rich phase after RIPS, the vitrification of both phases, including the thermoset occluded particles (secondary morphology) which appear inside the PPE-rich phase.

The aforementioned work of Kortaberria et al. (Kortaberria et al. 2004) about DGEBA/DDM modified with PMMA also made use of DRS in the frequency domain to analyze changes in molecular mobility in the reaction mixture. Figure 9 shows ϵ' and ϵ'' values as a function of curing time for different PMMA contents. The initial value of ϵ'' is higher in the unmodified matrix due to its lower viscosity. The peak in ϵ'' at higher curing times, which corresponds with the fall in ϵ' , is related with the α -relaxation process, which arises from the large-scale motions of dipoles associated to polymeric chains present in the mixture. This peak appears at longer times in epoxy/PMMA systems because the modifier delays the polymerization reaction. DRS results were in a very good agreement with NIR observations.

Scattering and Other Techniques

Positron annihilation lifetime spectroscopy (PALS) is a technique sensitive to voids and defects in materials and, hence, useful to characterize the size and content of free volume in polymers. It has been used to determine the water uptake in epoxy/PEI blends as a function of the thermoplastic content (Li et al. 2004). X-ray photoelectron spectroscopy (XPS) is a powerful surface technique that analyzes the elemental composition and chemical state of the surface of a material. It has been scarcely used in epoxy/thermoplastic blends. Examples are the blends of epoxy resin with poly(ϵ -caprolactone) (PCL) and poly(dimethyl siloxane) (PDMS) (Liu et al. 2008). PCL

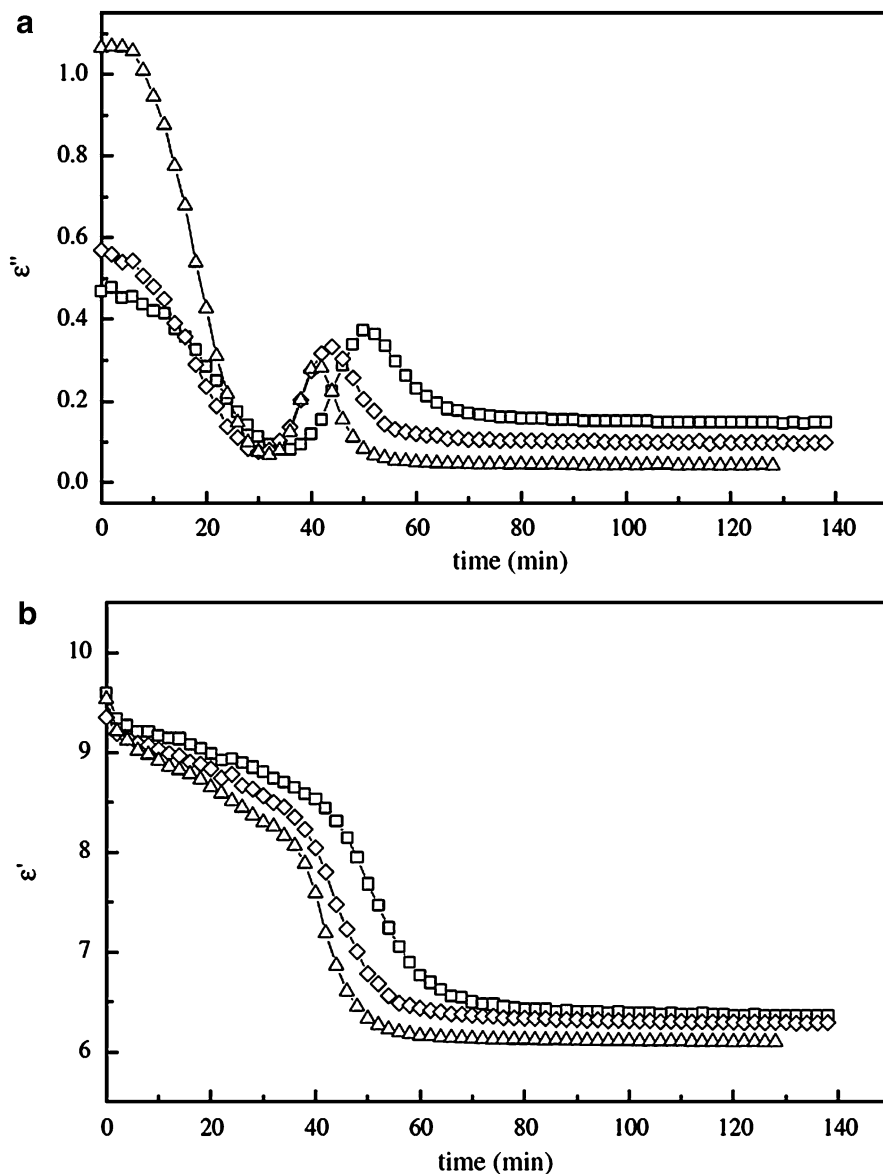


Fig. 9 (a) ϵ' and (b) ϵ'' vs. curing time for DGEBA/DDM cured without PMMA (*triangles*) and with 5% (*diamonds*) and 10% (*squares*) of PMMA modifier, at 10 kHz (Reproduced with permission from Kortaberria et al. (2004))

was added to increase the miscibility of PDMS on the epoxy resin. XPS was used to confirm the migration of the PDMS to the film surface, by analyzing the C_{1s} , O_{1s} , and Si_{2p} signals from the air surface area of the films. These results were in good agreement with contact angle measurements.

Scattering is also a mode of interaction of radiation with matter, comparable to the absorption and emission phenomena. Although there is a specific chapter in this book on light scattering, in this section a brief overview of the different scattering techniques applied to epoxy/thermoplastic blends will be presented. The use of the light scattering to determine the cloud point in mixtures, which corresponds to the phase separation process, is well known. The simplest method is to measure light transmission with a spectrophotometer, although the sensitivity to the incipient formation of phases is limited by the wavelength of the incident radiation. To determine the phase behavior at a very low length scale, the use of more sophisticated techniques such as small-angle X-ray scattering (SAXS) able to detect domains below 0.2 μm is necessary. This feature, which is very important in epoxy/copolymer blends, is also of great interest in blends with thermoplastics when a secondary morphology is suspected (Williams et al. 1997). Some examples are the use of SAXS to determine the incipient RIPS in blends of epoxy resin with poly(ether imide) (PEI) (Wang et al. 2004) and the semicrystalline morphology in epoxy/PEO blends (Guo et al. 2001a, b). Time-resolved light scattering (TRLS) has been used also to determine the RIPS and crystallization processes in epoxy/thermoplastic blends, for example, with poly(methylene oxide) (POM) (Goossens et al. 2006), PPE (Ishii and Ryan 2000), PSU (Zhang et al. 2011), or PEI (Gan et al. 2003). Another interesting technique is small-angle neutron scattering (SANS), which has been used to determine the interaction parameters in blends of epoxy/poly(aryl sulfone) (PAS) (Elliniadis et al. 1997). By using deuterated compounds, SANS may give information about heterogeneities down to a few nanometers and about the nature of the interface.

Finally, wide-angle X-ray diffraction (WAXD) is used mainly to evaluate crystalline structure, and therefore it has been useful to determine the thermoplastic crystallinity on blends of epoxy resins with PCL (Park and Jana 2003) or poly(butylene terephthalate) (PBT) (Zhang et al. 2008).

Conclusions

Spectroscopic techniques have proven to be good tools to study specific processes of epoxy/thermoplastic blends. Often coupled with scattering and imaging techniques, they have improved the understanding of the thermoplastic modifier influence on the curing process and allowed to analyze the reaction-induced phase separation process. The use of different techniques is quite unequal. Dielectric spectroscopy and infrared spectroscopy are widely used, and especially the latter is now a standard for measuring progress curing. However, spectroscopy allows also to know the specific interactions between components and to study local structural relaxations at a molecular scale. In this sense, several techniques are underused in thermoplastic epoxy/mixtures. The potential of Raman spectroscopy, nuclear magnetic resonance spectroscopy, and fluorescence spectroscopy to monitor, at a molecular level, diffusional processes and specific interactions between the thermoplastic chains and the

thermoset network has been well established, but these techniques remain with little use.

Some of the spectroscopic techniques have their equivalent microscopy technique (Raman, infrared, fluorescence) which allows making surface or volume mappings over heterogeneous epoxy/thermoplastic materials, allowing the simultaneous analysis of the morphology, chemical state, and composition of the segregated phases.

References

- Abbate M, Martuscelli E, Musto P, Ragosta G, Scarinzi G (1994) Toughening of a highly cross-linked epoxy resin by reactive blending with bisphenol A polycarbonate. I. FTIR spectroscopy. *J Polym Sci B: Polym Phys* 32:395–408
- Antonelli C, Serrano B, Baselga J, Cabanelas JC (2014) Fluorescence probes the early formation of network at the interface of epoxy-silica nanocomposite during curing. *Mater Lett* 137:460–463
- Antonelli C, Serrano B, Baselga J, Ozisik R, Cabanelas JC (2015) Interfacial characterization of epoxy/silica nanocomposites measured by fluorescence. *Eur Polym J* 62:31–42
- Baselga J, Piérola I, Serrano B, Pozuelo J, Cabanelas JC, Martín O (2010) Fluorescence of polymers at interfaces: polymerization, relaxations and imaging. In: Geddes JCD (ed) *Reviews in fluorescence*. Springer, New York, pp 311–347
- Bonnet A, Pascault JP, Sautereau H, Rogozinski J, Kranbuehl D (2000) Epoxy-diamine thermoset/thermoplastic blends: dielectric properties before, during, and after phase separation. *Macromolecules* 33:3833–3843
- Bosch P, Catalina F, Corrales T, Peinado C (2005) Fluorescent probes for sensing processes in polymers. *Chem Eur J* 11:4314–4325
- Cabanelas JC, Serrano B, Baselga J (2005a) Development of cocontinuous morphologies in initially heterogeneous thermosets blended with poly(methyl methacrylate). *Macromolecules* 38:961–970
- Cabanelas JC, Serrano B, Gonzalez M, Baselga J (2005b) Confocal microscopy study of phase morphology evolution in epoxy/polysiloxane blends. *Polymer* 46:6633–6639
- Challis RE, Unwin ME, Chadwick DL, Freemantle RJ, Partridge IK, Dare DJ, Karkanis PI (2003) Following network formation in an epoxy/amine system by ultrasound, dielectric, and nuclear magnetic resonance measurements: a comparative study. *J Appl Polym Sci* 88:1665–1675
- Chen JL, Huang HM, Li MS, Chang FC (1999) Transesterification in homogeneous poly(ϵ -caprolactone)-epoxy blends. *J Appl Polym Sci* 71:75–82
- Davis KB, Braasch DA, Pramanik M, Rawlins JW (2013) Use of fluorescent probes to determine molecular architecture in phase separating epoxy systems. *Ind Eng Chem Res* 53:228–234
- Don T, Bell JP (1996) Polycarbonate-modified epoxies. I. Studies on the reactions of epoxy resin/polycarbonate blends prior to cure. *J Polym Sci A Polym Chem* 34:2103–2116
- Don TM, Bell JP (1998) Fourier transform infrared analysis of polycarbonate/epoxy mixtures cured with an aromatic amine. *J Appl Polym Sci* 69:2395–2407
- Elliniadis S, Higgins JS, Clarke N, McLeish TCB, Choudhery RA, Jenkins SD (1997) Phase diagram prediction for thermoset/thermoplastic polymer blends. *Polymer* 38:4855–4862
- Everall NJ, Griffiths PR, Chalmers JM (2007) *Vibrational spectroscopy of polymers: principles and practice*. Wiley, Hoboken, p 586
- Gan W, Yu Y, Wang M, Tao Q, Li S (2003) Viscoelastic effect on the phase separation in thermoplastics-modified epoxy resin. *Macromolecules* 36:7746–7751
- Gomez CM, Bucknall CB (1993) Blends of poly(methyl methacrylate) with epoxy resin and an aliphatic amine hardener. *Polymer* 34:2111–2117
- Gonzalez J, Esteban I (2005) Morphologic and kinetic study of an epoxy-poly(ethylene oxide) system. The fluorescence to predict miscibility. *Colloid Polym Sci* 283:559–569

- Gonzalez M, Cabanelas JC, Pozuelo J, Baselga J (2011) Preparation of cycloaliphatic epoxy hybrids with non-conventional amine-curing agents. *J Therm Anal Calorim* 103:717–723
- González M, Cabanelas JC, Baselga J (2012) Applications of FTIR on epoxy resins – identification, monitoring the curing process, phase separation and water uptake, Chapter 13. In: Theophanides DT (ed) *Infrared spectroscopy-materials science, engineering and technology*. Intech, Rijeka (for Intech Open Europe) or Shanghai (for Intech Open China). (ISBN 978-953-51-0537-4)
- Goosens S, Goderis B, Groeninckx G (2006) Reaction-induced phase separation in crystallizable micro- and nanostructured high melting thermoplastic/epoxy resin blends. *Macromolecules* 39:2953–2963
- Guo Q, Harrats C, Groeninckx G, Koch MH (2001a) Miscibility, crystallization kinetics and real-time small-angle X-ray scattering investigation of the semicrystalline morphology in thermosetting polymer blends of epoxy resin and poly(ethylene oxide). *Polymer* 42:4127–4140
- Guo Q, Harrats C, Groeninckx G, Reynaers H, Koch MHJ (2001b) Miscibility, crystallization and real-time small-angle X-ray scattering investigation of the semicrystalline morphology in thermosetting polymer blends. *Polymer* 42:6031–6041
- Hakala K, Vatanparast R, Li S, Peinado C, Bosch P, Catalina F, Lemmetynen H (2000) Monitoring of curing process and shelf life of epoxy-anhydride system with TICT compounds by the fluorescence technique. *Macromolecules* 33:5954–5959
- Immordino KM, McKnight SH, Gillespie JW (1998) In-situ evaluation of the diffusion of epoxy and amine in thermoplastic polymers. *J Adhes* 65:115–129
- Ishii Y, Ryan AJ (2000) Processing of poly(2,6-dimethyl-1,4-phenylene ether) with epoxy resin. 1. Reaction-induced phase separation. *Macromolecules* 33:158–166
- Janarthanan V, Thyagarajan G (1992) Miscibility studies in blends of poly(*N*-vinyl pyrrolidone) and poly(methyl methacrylate) with epoxy resin: a comparison. *Polymer* 33:3593–3597
- Kalogeris IM, Dova AV, Christakis I, Pietkiewicz D, Brostow W (2006) Thermophysical properties and molecular relaxations in cured epoxy resin + PEO blends: observations on factors controlling miscibility. *Macromol Chem Phys* 207:879–892
- Kim BS, Chiba T, Inoue T (1995) Morphology development via reaction-induced phase separation in epoxy/poly(ether sulfone) blends: morphology control using poly(ether sulfone) with functional end-groups. *Polymer* 36:43–47
- Koenig JL (1999) *Spectroscopy of polymers*, 2nd edn. Elsevier, Oxford
- Kortaberria G, Arruti P, Gabilondo N, Mondragon I (2004) Curing of an epoxy resin modified with poly(methylmethacrylate) monitored by simultaneous dielectric/near infrared spectroscopies. *Eur Polym J* 40:129–136
- Lakowicz JR (1999) *Principles of fluorescence spectroscopy*, 2nd edn. Kluwer, New York
- Li M, Ma CM, Chen J, Lin M, Chang F (1996a) Epoxy – polycarbonate blends catalyzed by a tertiary amine. 1. Mechanism of transesterification and cyclization. *Macromolecules* 29:499–506
- Li MS, Su YF, Ma CCM, Chen JL, Lu MS, Chang FC (1996b) Transesterification and cyclization of polycarbonate-epoxy blends cured with anhydride. *Polymer* 37:3899–3905
- Li MS, Ma CCM, Lin ML, Chang FC (1997) Chemical reactions occurring during the preparation of polycarbonate-epoxy blends. *Polymer* 38:4903–4913
- Li L, Liu M, Li S (2004) Morphology effect on water sorption behavior in a thermoplastic modified epoxy resin system. *Polymer* 45:2837–2842
- Liu P, Song J, He L, Liang X, Ding H, Li Q (2008) Alkoxysilane functionalized polycaprolactone/polyloxane epoxy resin through sol-gel process. *Eur Polym J* 44:940–951
- Lyon RE, Chike KE, Angel SM (1994) In situ cure monitoring of epoxy resins using fiber-optic Raman spectroscopy. *J Appl Polym Sci* 53:1805
- McBrierty VJ, Packer KJ (1993) In: Davis EA, Ward IM (eds) *Nuclear magnetic resonance in solid polymers*. Cambridge University Press, Cambridge
- Ni Y, Zheng S (2005) Influence of intramolecular specific interactions on phase behavior of epoxy resin and poly(*ε*-caprolactone) blends cured with aromatic amines. *Polymer* 46:5828–5839

- Olmos D, González-Benito J (2006) Cure process and reaction-induced phase separation in a diepoxy-diamine/PMMA blend. Monitoring by steady-state fluorescence and FT-IR (near and medium range). *Colloid Polym Sci* 284:654–667
- Paik H-J, Sung N-H (1994) Fiber-optic intrinsic fluorescence for in-situ cure monitoring of amine cured epoxy and composites. *Polym Eng Sci* 34:1025–1032
- Park JH, Jana SC (2003) The relationship between nano- and micro-structures and mechanical properties in PMMA-epoxy-nanoclay composites. *Polymer* 44:2091–2100
- Penoff ME, Papagni G, Yañez MJ, Montemartini PE, Oyanguren PA (2007) Synthesis and characterization of an epoxy based thermoset containing a fluorinated thermoplastic. *J Polym Sci B: Polym Phys* 45:2781–2792
- Petrick RA, Hayward D (2002) Real time dielectric relaxation studies of dynamic polymeric systems. *Prog Polym Sci* 27:1983–2017
- Poncet S, Boiteux G, Pascault JP, Sautereau H, Seytre G, Rogozinski J, Kranbuehl D (1999) Monitoring phase separation and reaction advancement in situ in thermoplastic/epoxy blends. *Polymer* 40:6811–6820
- Purcell KF, Drago RS (1967) Theoretical aspects of the linear enthalpy wavenumber shift relation for hydrogen-bonded phenols. *J Am Chem Soc* 89:2874–2879
- Rajagopalan G, Immordino KM, Gillespie JW, McKnight SH (2000) Diffusion and reaction of epoxy and amine in polysulfone studied using Fourier transform infrared spectroscopy: experimental results. *Polymer* 41:2591–2602
- Rigail-Cedeño A, Sung CSP (2005) Fluorescence and IR characterization of epoxy cured with aliphatic amines. *Polymer* 46:9378–9384
- Ritzenthaler S, Girard-Reydet E, Pascault JP (2000) Influence of epoxy hardener on miscibility of blends of poly(methyl methacrylate) and epoxy networks. *Polymer* 41:6375–6386
- Sales RCM, Brunelli DD (2005) Luminescence spectroscopy applied to a study of the curing process of diglycidyl-ether of bisphenol-A(DGEBA). *Mater Res* 3:299–304
- Schaefer J, Sefcik MD, Stejskal EO, McKay RA (1981) Magic-angle carbon-13 nuclear magnetic resonance analysis of the interface between phases in a blend of polystyrene with a polystyrene-polybutadiene block copolymer. *Macromolecules* 14:188–192
- Shih YF, Jeng RJ (2004) IPNs based on unsaturated polyester/epoxy: IV. Investigation on hydrogen bonding, compatibility and interaction behavior. *Polym Int* 53:1892–1898
- Smith E, Dent G (2004) *Modern Raman spectroscopy – a practical approach*. Wiley, Chichester
- Socrates G (2004) *Infrared and Raman characteristic group frequencies: tables and charts*, 3rd edn. Wiley, Hoboken
- Strehmel B, Strehmel V, Younes MJ (1999) Fluorescence probes for investigation of epoxy systems and monitoring of crosslinking processes. *J Polym Sci B: Polym Phys* 37:1367–1386
- Stuart B (2004) *Infrared spectroscopy: fundamentals and applications*. Wiley, Chichester
- Su CT, Lin KY, Lee TJ, Liang M (2010) Preparation, characterization and curing properties of epoxy-terminated poly(alkyl-phenylene oxide)s. *Eur Polym J* 46:1488–1497
- Teh CH, Rozaidi R, Rusli D, Sahrim HA (2009) Synthesis and spectroscopic studies of DGEBA-grafted polyaniline. *Polym Plast Technol Eng* 48:17–24
- Van Overbeke E, Devaux J, Legras R, Carter JT, McGrail PT, Carlier V (2000) The use of Raman spectroscopy to study the reaction between an amine-terminated thermoplastic and epoxy resins. *Polymer* 41:8241–8245
- Van Overbeke E, Devaux J, Legras R, Carter JT, McGrail PT, Carlier V (2001a) Raman spectroscopy and DSC determination of conversion in DDS-cured epoxy resin: application to epoxy-copolyethersulfone blends. *Appl Spectrosc* 55:540–551
- Van Overbeke E, Devaux J, Legras R, Carter JT, McGrail PT, Carlier V (2001b) Raman spectroscopy determination of the thermoplastic content within epoxy resin-copolyethersulfone blends. *Appl Spectrosc* 55:1514–1522
- Van Overbeke E, Devaux J, Legras R, Carter JT, McGrail PT, Carlier V (2003) Phase separation in epoxy-copolyethersulphone blends: morphologies and local characterisation by micro-Raman spectroscopy. *Polymer* 44:4899–4908

- Venderbosch RW, Meijer HEH, Lemstra PJ (1994) Processing of intractable polymers using reactive solvents. 1. Poly(2,6-dimethyl-1,4-phenylene ether) epoxy-resin. *Polymer* 35:4349–4357
- Wang M, Yu Y, Wu X, Li S (2004) Polymerization induced phase separation in poly(ether-imide)-modified epoxy resin cured with imidazole. *Polymer* 45:1253–1259
- Williams RJJ, Rozenberg BA, Pascault JP (1997) Reaction-induced phase separation in modified thermosetting polymers. *Adv Polym Sci* 128:97–155
- Yokoyama N, Yasushi N, Kurata T, Sakai S, Takahashi S, Kasemura T (2007) Morphologies and properties of cured epoxy/brominated-phenoxy blends. *J Appl Polym Sci* 104:1702–1713
- Zhang J, Xie X (2011) Influence of addition of silica particles on reaction-induced phase separation and properties of epoxy/PEI blends. *Compos B: Eng* 42:2163–2169
- Zhang H, Sun S, Ren M, Chen Q, Song J, Zhang H, Mo Z (2008) Thermal and mechanical properties of poly(butylene terephthalate)/epoxy blends. *J Appl Polym Sci* 109:4082–4088
- Zhang Y, Shi W, Chen F, Han CC (2011) Dynamically asymmetric phase separation and morphological structure formation in the epoxy/polysulfone blends. *Macromolecules* 44:7465–7472
- Zheng S, Guo Q, Chan CM (2003) Epoxy resin/poly(*ε*-caprolactone) blends cured with 2,2-bis[4-(4-aminophenoxy)phenyl]propane. II. Studies by Fourier transform infrared and carbon-13 cross-polarization/magic-angle spinning nuclear magnetic resonance spectroscopy. *J Polym Sci B Polym Phys* 41:1099–1111
- Zhong Z, Guo O (1997) The miscibility and morphology of hexamine cross-linked novolac/poly(*ε*-caprolactone) blends. *Polymer* 38:279–286
- Zhong Z, Guo Q (1998a) Miscibility and cure kinetics of nylon/epoxy resin reactive blends. *Polymer* 39:3451–3458
- Zhong Z, Guo Q (1998b) Miscibility and morphology of thermosetting polymer blends of novolac resin with poly(ethylene oxide). *Polymer* 39:517–523
- Zhong Z, Zheng S, Huang J, Cheng X, Guo O, Wei J (1998) Phase behaviour and mechanical properties of epoxy resin containing phenolphthalein poly (ether ether ketone). *Polymer* 39:1075–1080

Leah M. Johnson and Nicolas D. Huffman

Abstract

Epoxy–thermosets hold value in many industrial applications, owing to their favorable characteristics including excellent adhesion, ease of processing, and thermal and chemical stability. Despite these benefits, the high cross-linking density of epoxy–thermosets also results in a brittleness that limits utility in many high-performance structures that are subject to high impact, such as aerospace and automotive applications. The inclusion of thermoplastics within the epoxy can improve toughness and impact resistance. Rheological analysis of epoxy–thermoplastic blends serves as a critical analytical technique for evaluating the viscoelastic properties during the pre-cure formulating stage and during the cure. Chemorheology is useful to characterize the distinct viscoelastic changes that occur during the cure of epoxy–thermoplastics, which involve phase separation, epoxy gelation, and vitrification. Through rheological modeling, the behavior during cure can be further evaluated to predict flow behavior and mechanisms of phase separation. Importantly, rheology meets the analytical demands in industrial applications, where details concerning preprocessing conditions, quality control, and cure cycle design are crucial.

Keywords

Chemorheology • Viscosity • Modulus • Viscoelastic phase separation • Gel Point • Williams–Landel–Ferry equation • Time–temperature superposition • Morphology

L.M. Johnson (✉) • N.D. Huffman (✉)

Advanced Materials and System Integration, Research Triangle Institute (RTI) International,
Research Triangle Park, NC, USA

e-mail: leahjohnson@rti.org; nhuffman@rti.org

© Springer International Publishing AG 2017

J. Parameswaranpillai et al. (eds.), *Handbook of Epoxy Blends*,

DOI 10.1007/978-3-319-40043-3_21

613

Contents

Introduction	614
Overview of Epoxy–Thermoplastic Blends	616
Chemical Constituents: Epoxy–Thermosets Used with Thermoplastics	616
Evolution of Morphology During the Cure of Epoxy–Thermoplastic Blends	616
Early Non-rheological Studies of Epoxy–Thermoplastic Blends	618
Overview of Rheology for Epoxy–Thermosets	618
Measurement Configurations and Techniques	619
Rheological Properties	620
Using Rheology to Monitor the Cure of Epoxy–Thermosets	622
Data Transformations	624
Instrumentation Configurations for Dynamic Measurements	625
Rheological Behavior of Epoxy–Thermoplastic Blends	625
Rheological Behavior Resultant of Phase Separation	626
Viscoelastic Phase Separation: Rheological Analysis	630
Modeling Viscoelastic Phase Separation	632
Rheological Analysis During Other Structural Arrangements: Gelation and Crystallization-Induced Phase Separation (CIPS)	635
Rheological Parameters for Industrial Applications: Assessment of Epoxy–Thermoplastic Blended Material	638
Industrial Applications	639
Viscosity During Formulation	639
Viscosity During Molding	641
Practical Considerations	643
Conclusions	643
References	645

Introduction

The value of epoxy–thermosets is evident from the widespread use of this material in high-performance industrial applications, such as aerospace structures, automotive manufacturing, and microelectronics. Epoxies exhibit beneficial properties including thermal stability, excellent adhesion, and mechanical strength. Despite these benefits, epoxy materials exhibit low toughness typical of thermoset resins and often require modification to compete with metals and thermoplastics. Thermoplastics are one type of material that have been investigated as toughening agents for epoxy material since the early 1980s (Bucknall and Partridge 1983). As compared to other toughening additives (e.g., rubbers), thermoplastic additives generally do not impair the mechanical properties of the epoxy material and preserve glass transition temperature (T_g) and modulus values. Inclusion of thermoplastics within an epoxy resin produces a multiphase morphology that resists crack propagation and toughens the polymer product. Thermoplastic modifiers commonly used as toughening agents in epoxy materials include Polyetherimide (PEI), poly(ethersulfone) (PES), polycarbonates, poly(phenylene oxide) (PPO), and polysulfones. In general, thermoplastic modifiers are added between 2 and 50 wt% to induce the necessary structural changes for the requisite toughening characteristics (Williams et al. 1997). Crucially, the additive must not impair the heat deflection temperature

(HDT), modulus, or strength of the epoxy–thermoset. The addition of thermoplastics to the epoxy resins may also participate in the polymerization reactions by contributing additional functional groups, as demonstrated with phenolic hydroxyl-terminated polysulfone in an Epon828/4,4'-diaminodiphenylsulfone (4,4'-DDS) system (Hedrick et al. 1985). Many sources exist that further detail neat epoxy–thermoset materials (Lee and Neville 1967; Pascault and Williams 2010) and thermoplastics as toughening agents for epoxy materials (Hedrick et al. 1993; Pearson 1993; Hodgkin et al. 1998; Unnikrishnan and Thachil 2006; Deng et al. 2015).

Over the last three decades, an enhanced understanding of epoxy–thermoplastic blends has transpired, based on information obtained from important characterization techniques. Various analytical techniques exist for characterizing epoxy–thermoplastic blends: thermal analysis (e.g., differential scanning calorimetry (DSC), thermogravimetric analysis (TGA)), mechanical analysis (dynamic mechanical analysis (DMA), tensile testing, Izod/Charpy testing, compression after impact (CAI)), and spectroscopic analysis (e.g., scanning electron microscopy (SEM), time-resolved light scattering (TRLS)). Each of these characterization techniques reveals distinct features of material properties, which when combined can provide a comprehensive profile of an epoxy–thermoplastic system. In particular, rheology is a valuable component in this toolbox of analytical techniques. The central purpose of many rheological studies is to correlate rheological properties with molecular properties of the viscoelastic material under investigation (Malkin and Isayev 2012). For epoxy–thermoplastic blends, rheological analysis provides insight into various aspects, such as the viscosity at the pre-cure processing stage and also viscosity changes resulting from molecular rearrangements during the cure. Advantageously, rheology enables evaluation of how variables (e.g., time, temperature, deformation rate, formulation) affect the rheological behavior, providing insight into mechanisms during morphological evolution of the material.

The goal of this chapter is to provide an overview of rheological characterization of epoxy–thermoplastic materials. To this end, this chapter will cover a subset of related matters to support a clear understanding of rheological analysis of these materials. The first section will provide a brief summary of epoxy–thermoplastics (e.g., chemical constituents, structural transformations) followed by a condensed overview of rheology in terms of epoxy–thermosets. An in-depth discussion of rheological trends for epoxy–thermoplastic materials will follow, providing details concerning cure profiles, viscoelastic phase separation, and rheological modeling approaches. The last section addresses the importance of rheological properties in utilizing epoxy–thermoplastics for industrial applications. Although individual epoxy–thermoplastic systems can each exhibit unique rheological behavior, certain generalized trends are summarized to aid in understanding rheological investigations. To date, the vast majority of information concerning the rheological characterization of epoxy–thermoplastics exists within journal literature, but relevant books and reviews are also cited throughout the chapter. The overarching aim is to provide deeper understanding of rheological analysis of epoxy–thermoplastic blends to support the continued advancements in this field.

Overview of Epoxy–Thermoplastic Blends

Chemical Constituents: Epoxy–Thermosets Used with Thermoplastics

The term “epoxy” encompasses broad connotations across disciplines: a monomer or prepolymer that contains at least two epoxide chemical groups (i.e., epoxy resin), the epoxide chemical functional group itself, an epoxy/curative mixture, or a polymer produced from epoxy resins. The meaning of this term “epoxy” is typically deciphered from context, but the end user must always verify the exact meaning of the term to support their needs and applications. Various types of epoxy resins exist, categorized according to the chemical structure of the resin backbone, including aliphatic, cycloaliphatic, or aromatic epoxy resins. The most common epoxy resins used in epoxy–thermoplastic blends are derived from bisphenol A (e.g., diglycidyl ether of bisphenol A (DGEBA)), which exhibit good mechanical and thermal properties at moderate cost. Although not widely reported in epoxy–thermoplastic systems, bisphenol F resins can provide lower viscosity, while the phenol formaldehyde resins that have higher functionality (i.e., novolac epoxy resins) can enhance the material properties at elevated temperatures. Similarly, epoxy resins based on dicyclopentadiene, as well as a host of trifunctional and tetrafunctional resins, are used to achieve material properties required to meet design requirements, for example, in aerospace applications.

The polymerization (i.e., curing) of an epoxy material may ensue via step-growth polymerization, where chemical constituents react in a stepwise manner to ultimately generate a high molecular weight polymer (Oadian 2004b). This step-growth polymerization occurs through reactions between the epoxide chemical group and a curative (e.g., compounds that contain nucleophiles such as primary amines or mercaptans). Common curatives include 4,4'-methylenebis(2,6-diethylaniline) (MDEA) and 4,4'-diaminodiphenylsulfone (4,4'-DDS), 1,4-bis(aminocyclohexyl) methane (PACM), and diethyltoluene diamine (DETDA). Alternatively, the generation of an epoxy material can occur via chain-growth polymerization, where a reactive site can undergo consecutive addition reactions to generate a high molecular weight polymer (Oadian 2004). Epoxy resins can proceed through various chain-growth routes that depend on the chemical constituents: cationic polymerization via aromatic salts of Lewis acids or boron trifluoride complexes and anionic polymerization via tertiary amine or imidazoles (Pascault and Williams 2010). Some common curatives, such as dicyandiamide and various anhydrides, cure in a complex manner which includes both step-growth and catalytic polymerization. For epoxy–thermoplastics, both chain-growth and step-growth mechanisms have been employed.

Evolution of Morphology During the Cure of Epoxy–Thermoplastic Blends

Depending on the formulation and experimental conditions, the final morphology of an epoxy–thermoplastic blend broadly falls into two categories: homogenous composition

and heterogeneous composition (Liu 2013). For a homogeneous composition, the epoxy resin and thermoplastic material remain well mixed throughout the polymerization of the thermoset, resulting in a final homogenous structure. This homogeneous morphology often comprises interpenetrating polymer networks (IPNs), where the thermoplastic and thermoset are interwoven without displaying distinguishable properties of phase separation. The attainment of a homogeneous structure greatly depends on the chosen formulation and processing conditions. Exemplary systems that have retained the homogenous characteristic post-cure include specific epoxy–thermoset formulations blended with polycarbonate (Abbate et al. 1994; Di Liello et al. 1994) and poly(ϵ -caprolactone) (Barone et al. 2006). From a practical standpoint, homogeneous epoxy–thermoplastic blends typically fail to achieve substantial improvements in the toughening of the epoxy, as explored in early studies involving the effects of phase separation (Bucknall and Partridge 1983; Raghava 1987, 1988).

The second category of final structural arrangement, the heterogeneous composition, results from the separation of the epoxy material from the thermoplastic. This separation could result from the immiscibility that initially exists between the thermoplastic and the epoxy resin starting material and remains throughout the cure, generating a heterogeneous cured material. Alternatively, a reaction-induced phase separation (RIPS) can also result in a final heterogeneous composition. An early comprehensive review by Williams et al. (1997) describes reaction-induced phase separation, wherein an initially homogeneous and miscible system undergoes phase separation during the cure. For epoxy-thermoplastic blends, the phase separation occurs during the polymerization of the epoxy resin, often occurring prior to the gelation, when low molecular weight epoxy chains begin to grow. Other factors must also be considered, such as the crystallization of the thermoplastic, which may affect the RIPS (Tercjak et al. 2005). An enhanced understanding of this mechanism involves viscoelastic phase separation, which considers viscoelastic differences between the components of the blended formulations.

The mechanism of phase separation is guided by both thermodynamic factors and kinetic aspects, which ultimately dictate the morphology of an epoxy–thermoplastic blend (Hedrick et al. 1993). By tuning these competing factors through experimental design, the control over morphological arrangements is possible. A variety of morphological patterns result from reaction-induced phase separation of epoxy–thermoplastic blends: epoxy continuous phase (i.e., phase dispersion, thermoplastic particle), bicontinuous phase (i.e., co-continuous phase), and phase inversion (i.e., phase inverted) (Fig. 1a). The epoxy continuous phase structure comprises thermoplastic particles within an epoxy-rich matrix (i.e., continuous phase), whereas the inverted structure comprises epoxy-based polymer particles within a thermoplastic matrix. The bicontinuous phase exists structurally intermediate, with irregular domains of both thermoplastic and epoxy (Yu et al. 2004). Many factors guide these structural arrangements, as reported in an early investigation by Bonnet et al., that showed that the quantity of PEI within the epoxy resin dictated the resultant morphology (Fig. 1b). Structures containing higher quantity of thermoplastic (e.g., bicontinuous or phase inversion) generally show exceptional improvements in fracture toughness and are often considered necessary to achieve toughening of the material.

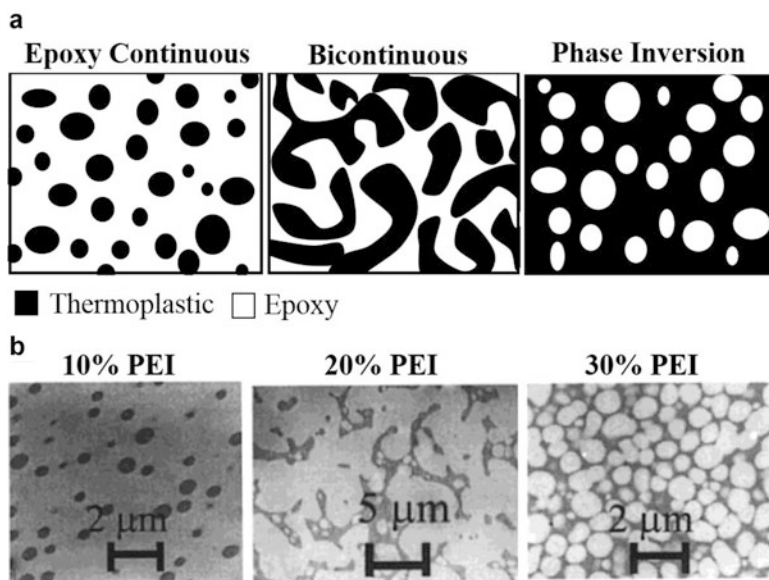


Fig. 1 (a) Schematic representing structures generated from phase separation between epoxy and thermoplastics. (b) TEM images from DGEBA/MCDEA cured in the presence of 10%, 20%, or 30% PEI (Reprinted with permission from *Macromolecules* (1999) 32, 8524–8530 (Bonnet et al. 1999) Copyright 1999 American Chemical Society)

Early Non-rheological Studies of Epoxy–Thermoplastic Blends

The inclusion of thermoplastics within epoxy–thermosets was first reported in 1983 by Bucknall and Raghava (1983; Raghava 1983). In general, early investigations of epoxy–thermoplastic blends did not extensively employ rheological characterization, but rather relied on alternative methods. Analytical tools, including SEM, dynamic mechanical spectroscopy (DMS), optical microscopy, DMA, TRLS, and DSC, can be used to assess structural changes occurring during the formation of epoxy–thermoplastic blends. For instance, Bucknall and Partridge utilized SEM and DMS to study phase separation within epoxy–thermosets prepared with trifunctional and tetrafunctional epoxy resin blended with PES. Nearly 16 years passed between the first reports in 1983 and the first detailed report assessing epoxy–thermosets with rheology by Bonnett et al. (1999). Thorough reviews exist that detail the earlier, non-rheological studies of epoxy–thermoplastic blends (Hedrick et al. 1993; Pearson 1993).

Overview of Rheology for Epoxy–Thermosets

Fundamentally, rheology focuses on properties of matter that govern its response to deformation and flow (i.e., rheological behavior) (Malkin and Isayev 2012b). At the vanguard of many rheological evaluations stands the objective to correlate

rheological properties with molecular properties of the material under investigation, such as chemical structure, molecular weight, quantity of components, reaction products, intermolecular interactions, and morphological evolution. Establishment of this relationship between rheological properties and molecular properties enables the user to predict how molecular changes affect material, ultimately enabling the tuning of the material to meet both research and industrial demands. For epoxy–thermosets within industrial settings, rheology is often used to evaluate processing parameters, design a cure cycle, and verify final product specifications. Rheology also reveals how variables such as time, temperature, formulation, and deformation rate affect the epoxy material properties, which is invaluable for many research and development goals. When evaluating blended polymers, such as epoxy–thermoplastics, behavioral complexities additional to neat epoxy resins are commonplace. Therefore, to support the subsequent description of more complex epoxy–thermoplastic blends, this section will review certain basic principles of rheology and how the technique is applied to analyze neat epoxy–thermoset materials. Further details concerning the rheology of thermosets can be found in other informative sources (Ryan 1984; Halley and Mackay 1996; Chartoff et al. 2008; Menard 2008; Mezger 2014).

Measurement Configurations and Techniques

Various testing configurations can be used for rheological characterization of epoxy materials, the choice of which depends on the information sought and the measurement constraints for a particular sample. Measurement techniques that apply a constant load to a sample and monitor the subsequent response after load removal over time include creep testing and recovery testing, which are useful in thermoset–thermoplastic blends (Menard 2008b). These constant load tests provide insight to molecular relaxations occurring within an epoxy material, providing valuable information for evaluating utilization of materials for long-term industrial and consumer applications. Another measurement technique involves dynamic testing, which measures the response (stress or strain) that results from an applied sinusoidal force (stress or strain) (Menard 2008b). Steady-shear measurements are typically utilized to characterize viscosity profiles of epoxy–thermosets prior to the gelation, whereas dynamic oscillatory measurements are utilized to monitor the epoxy–thermoset throughout the cure cycle. Dynamic measurement techniques include frequency studies, temperature–time studies, and dynamic stress–strain studies. Advantageously, dynamic measurements facilitate rapid accumulation of information and show widespread use for evaluating viscoelastic properties of epoxy materials.

Very importantly, any selected measurement technique must comply with appropriate testing parameters (e.g., shear rate, strain mode) to ensure measurement validity. Dynamic experiments must be performed within the linear viscoelastic range to guarantee that the behavior of the material is independent of the magnitude of the applied force. In this manner, the molecular structure of the epoxy material

remains intact, ensuring that the rheological measurements are representative of the material rather than a function of the measurement parameters.

Rheological Properties

A complete rheological description of epoxy–thermosets and epoxy–thermoplastic blends requires information about rheological properties (e.g., viscosity, storage modulus, loss modulus) and additional parameters, such as formulation, morphology changes, degree of cure, and state transitions (Yu 2014). For dynamic rheology, the response of a material resulting from the application of an oscillating force can be used to calculate viscosity, storage modulus (G'), loss modulus (G''), and phase angle (δ). From a qualitative standpoint, these measurements describe the viscoelastic behavior of an epoxy material, with G' describing the elastic qualities and G'' describing viscous qualities. The tangent of the phase angle ($\tan \delta$) is related to modulus and viscosity (Menard 2008):

$$\tan \delta = \frac{G''}{G'} = \frac{\eta'}{\eta''} \quad (1)$$

The $\tan \delta$ describes a material's ability to maintain or lose energy after applied deformation. The loss of energy may result from various possibilities such as heat loss or changes in molecular structure during a reaction.

One paramount rheological property for describing epoxy–thermosets is viscosity, which provides insight into various features, such as the workability during processing steps and material behavior resulting from different cure cycles, resin formulations, and additives. Changes in viscosity that result from chemical reactions, an occurrence referred to as chemoviscosity (Tajima and Crozier 1983, 1986; Yousefi et al. 1997), are imperative to understand the system and to apply this understanding to optimize processing parameters. Rheological evaluation of chemoviscosity profiles is affected by many variables, which include shear rate, pressure, time, temperature, and formulation (Ryan 1984). Chemoviscosity can also be affected by processing details, such as degree of solvent removal, extent of B-staging, moisture content, product outlife, or overly cold storage.

Dynamic shear measurements of epoxy–thermoplastics can provide the complex viscosity (η^*), which is a frequency-dependent parameter readily obtained from frequency scans. A function that separates an in-phase and out-of-phase factor can be used to define η^* :

$$\eta^* = \eta' - i\eta'' \quad (2)$$

where η' represents energy loss (i.e., viscous response) and η'' represents stored energy (i.e., elastic response). Complex viscosity affords details about the various processes that occur during the formation of an epoxy–thermoplastic material, such as changes occurring during the cure of the epoxy resin (i.e., chemoviscosity).

The relationship between complex viscosity (η^*) and complex shear modulus (G^*) follows:

$$|\eta^*| = |\eta'^2 + \eta''^2|^{1/2} = \frac{|G^*|}{\omega} \quad (3)$$

where,

$$\eta' = \frac{G''}{\omega} \quad (4)$$

$$\eta'' = \frac{G'}{\omega} \quad (5)$$

$$\eta^* = \frac{G^*}{i\omega} \quad (6)$$

and ω is the frequency. Complex viscosity comprises two modulus components (i.e., G' and G''), which provide information about different processes during the generation of epoxy material. For example, during the cure of an epoxy, the complex viscosity may initially decrease as the resin softens, which results in the dominance of the loss modulus (G'') component. As the epoxy resin polymerizes, the complex viscosity increases during the formation of a highly cross-linked network, which results in the higher contribution of the storage modulus (G') component.

The relationship between complex viscosity (η^*) at frequency (ω) and steady-shear viscosity (η) at shear rate ($\dot{\gamma}$) is explained by the Cox–Merz empirical rule (Cox and Merz 1958):

$$|\eta^*(\omega)| = \eta(\dot{\gamma})|_{\dot{\gamma}=\omega} \quad (7)$$

The steady-shear viscosity (η) is typically measured via isothermal steady-shear tests over time.

The viscosity of epoxy–thermosets changes extensively over the course of the polymerization reaction, often exhibiting an initial decrease from thermal influences and subsequently increasing rapidly during monomer-to-polymer conversion and cross-linking reactions. Viscosity profiles provide insight to structural evolutions that occur during the polymerization reactions of epoxy–thermosets. To capture this information, various models have been used to predict these viscosity changes over time. In one example, Roller reported an empirical model for expressing viscosity of an isothermal cure as a function of cure temperature (T) and time (t):

$$\ln \eta(t) = \ln \eta_\infty + \frac{\Delta E_\eta}{RT} + tk_\infty e^{\frac{\Delta E_k}{RT}} \quad (8)$$

where η is the viscosity at time (t) and temperature (T), η_∞ is the calculated viscosity at $T = \infty$, k_∞ is the kinetic analog of η_∞ , ΔE_η is Arrhenius activation energy for

viscosity, ΔE_k is the kinetic analog of ΔE_η , R is the universal gas constant, and T is absolute temperature. By applying a time–temperature integral to this viscosity model, the prediction of viscosity changes was extended to non-isothermal systems (Roller 1975, 1986; Yousefi et al. 1997):

$$\ln \eta(t, T) = \ln \eta_\infty + \frac{\Delta E_\eta}{RT} + \int_0^t k_\infty \exp\left(\frac{\Delta E_k}{RT}\right) dt \quad (9)$$

The activation energies, ΔE_η and ΔE_k , are calculated through plots of natural log of initial viscosity versus $1/T$ and plots of natural log of k versus $1/T$, respectively (Menard 2008). Although limitations in this model exist above the gel point, Roller's empirical model is useful for predicting the viscosity changes for epoxy systems when temperature is a function of time.

Using Rheology to Monitor the Cure of Epoxy–Thermosets

The rheological analysis of the viscoelastic behavior of reacting thermosets, referred to as chemorheology (Halley and Mackay 1996), captures information about chemoviscosity, modulus, and state transitions that occur during the polymerization of epoxy materials, including gel point and vitrification. The chemorheological profiles for a typical epoxy resin generally shows that $G' < G''$ during the early stages of the cure, indicating low conversion of monomer to polymer. As the epoxy polymerization proceeds, the epoxy chains lengthen resulting in a change in both G' and G'' until a crossover point is reached (where $G' = G''$). Typically, the phase angle (δ) is near to 90° early in the polymerization reaction (liquid-like) and approximately 45° at the gel point and proceeds to nearly 0° when the resin is fully cured. The viscosity profiles also reveal changes during the cure, as epoxy resins rapidly increase in viscosity during gelation.

As the epoxy material transitions from a low molecular weight resin to a highly cross-linked product, the system exhibits a gel point. The gel point refers to the time or temperature that results in full connectivity through a polymer sample. During the nonreversible passage through this gel point, the material transitions from a lower-viscosity liquid, which contains readily diffusible reactants, to a highly viscous (e.g., rubbery) sample, which can slow diffusion rates. Upon reaching the epoxy gel point, the overall system becomes spatially confined, which limits the mobility of the constituents of the system. Rheology is an effective tool for evaluating the gel point of epoxy resins. The approach for acquiring gel point values, however, differs according to selected rheological test. Some examples are provided here (Michon et al. 1993; Winter 1987; Halley and Mackay 1996):

- The crossover point of G' and G''
- Point where shear viscosity approaches infinity ($\eta \rightarrow \infty$)

- Point at which $\tan \delta$ is independent of frequency
- First time point at which no epoxy is transferred to an implement touched to the resin surface

All of these approaches for the measurement of gel point must be evaluated for appropriateness for individual epoxy formulations and instrumental setups. For example, the determination of gel point from where $\eta \rightarrow \infty$ exhibits limitations, including instrumentation constraints and the inability to differentiate between transformations, such as vitrification or phase separation. As with any rheological study, the instrumentation parameters must also satisfy the measurement needs, such as ensuring the choice of frequency allows adequate relaxation time for the material.

Importantly, the working life or “pot life” of an epoxy formulation is defined as the amount of time before polymerization has advanced too far to adequately perform its function. Pot life is usually reported as the time to reach a given viscosity at a specified temperature. The pot life is before the gel point, but the exact point will depend on the nature of the resin’s application. For example, a vacuum infusion resin should generally be under approximately 600 cps to adequately flow through a fiber reinforcement, while a lamination resin should be under approximately 10,000 cps to wet woven reinforcements without trapping gas bubbles. Furthermore, paste adhesives can bond well at viscosities over 100,000 cps. Since these materials are sometimes non-Newtonian, the viscosity should be measured at an appropriate shear rate for the given application.

An additional transition that may occur during the cure of an epoxy–thermoset is vitrification. Defined as a process that takes place when the glass transition temperature (T_g) rises to the isothermal temperature of cure (T_{cure}), vitrification generates a glassy material (Gillham 1986). The vitrification point can be measured from various criteria, such as the onset of time or frequency dependence in G' , the peak in $\tan \delta$, or the peak in G'' (Harran and Laudouard 1986; Serrano and Harran 1989; Lange 1999; Jyotishkumar et al. 2011). Importantly, as compared to gel point determinations, the rheological analysis of vitrification requires additional considerations, often owing to limitations in measuring large breadths of viscosity ranges in many instruments. Supplemental measurement techniques, such as DMA-dielectric analysis (DEA) or parallel conversion analysis via infrared spectroscopy, can be used to determine the vitrification point (Menard 2008).

In general, the cure temperature directs both the gel point and vitrification during the polymerization of epoxy materials. As detailed for a cycloaliphatic epoxy and anhydride formulation by Gillham et al. (1974) and reviewed by Yu (2014), three categories of isothermal behaviors exist, which involve the $T_{g\infty}$ (maximum glass transition temperature) and T_{gg} (glass transition temperature at the gel point):

- If $T_{\text{cure}} > T_{g\infty}$, then only gelation is detected.
- If $T_{g\infty} > T_{\text{cure}} > T_{gg}$, then vitrification and gelation are detected.
- If $T_{\text{cure}} < T_{gg}$, then only vitrification is detected.

For the last category ($T_{\text{cure}} < T_{\text{gg}}$), certain materials exhibit sufficient mobility within the vitrified state to enable gelation after vitrification (Lange et al. 2000). In practice, T_g is generally 20–30 °C above cure temperature, with $T_{g\infty}$ ultimately limited by chemical structure and cross-link density. It is commercially important to note that some epoxy formulations can reach a vitrified state with relatively low T_g prior to post bake that is too brittle to demold. In such applications, more expensive high-temperature-resistant molds are required. Other formulations develop strength more rapidly. These can be formed in low-temperature molds and then undergo a freestanding post bake without cracking, slumping, or deforming. Formulation to achieve a cure time that balances adequate time for fabrication with the cost of cure (autoclave time and availability, oven time, energy consumption, tool time, etc.) is usually accomplished through appropriate curative selection.

Data Transformations

When measuring the dependence of frequency on modulus in linear polymers, a useful method in rheological analysis is the time–temperature superposition (TTS) principle, which enables the prediction of viscoelastic behavior outside of frequencies tested experimentally (Dealy and Plazek 2009, Malkin and Isayev 2012). Advantageously, the TTS principle reduces the number of required experiments and permits data acquisition otherwise unattainable through experimental approaches (e.g., instrumental limitations). The TTS principle allows for the establishment of a master curve by employing temperature-dependent shift factors, ultimately detailing the viscoelastic behavior at a single reference temperature over a broad range of time or frequency (Dealy and Plazek 2009). The shift factor (a_T), as a function of temperature, enables shifting of the master curve to other temperatures of interest and can be determined by fitting experimental values to an appropriate model. One approach for fitting the shift factor uses the Arrhenius relationship:

$$\ln a_T = \frac{E (T_g - T)}{RT_g T} \quad (10)$$

where E is the activation energy of the relaxation process, T and T_g are absolute temperatures, and R is the universal gas constant. Another common function for fitting shift factors is described by the Williams–Landel–Ferry (WLF) empirical equation (Williams et al. 1955):

$$\log a_T = \frac{-C_1 (T - T_g)}{C_2 + (T - T_g)} \quad (11)$$

where T is the measurement temperature and C_1 and C_2 are empirical constants. Importantly, limitations exist and require consideration when applying the TTS principle to certain polymer systems, such as degrading polymers, as detailed by Chartoff and Menczel (Chartoff et al. 2008).

Instrumentation Configurations for Dynamic Measurements

Development of instrumentation and test methods for measuring rheological characteristics has progressed substantially in recent decades. The limited capabilities of early rheometers often thwarted a detailed understanding of rheological behavior of epoxy–thermoplastic material. The capacity to easily monitor rheological properties during the cure of a material expanded in the early 1990s with advancements in instrumentation. For example, early reports utilized a Strathclyde curometer instrument to monitor changes in viscosity during the cure of an epoxy resin blended with PES (MacKinnon et al. 1992) or modified PES (MacKinnon et al. 1993). Although not a widely used instrument, the Strathclyde curometer design was used more recently to study solvent effects during the cure of DGEBA resin (Le Craz and Pethrick 2011). Studies beginning in the late 1990s embarked upon more comprehensive rheology of epoxy–thermoplastic blends. During this time, researchers began evaluating how factors, such as cure temperature, chemical content, and concentrations, affected the phase separation of blended material.

As thoroughly reviewed by Menard (2008), two broad groups of instrument configurations exist, based on classification of applied force (stress or strain) to the sample: axial and torsional. In axial instrumentation configurations, a linear force is applied to the sample, whereas in torsional configurations, a twisting movement is applied to the sample. Although liquid or solid samples can be tested using either of these configurations, typically liquid samples are evaluated with torsional force and solid samples are evaluated via axial force. For torsional measurement conformations, various testing geometries exist: cone and plate, parallel plate, coaxial cylinders, and torsion bar. The vast majority of reports on epoxy–thermoplastic blends have employed torsional configurations for analysis, particularly the parallel plate configuration, which generated data concerning viscosity measurements and cure profiles. Disposable parallel plates are available for testing samples to full cure strength.

Rheological Behavior of Epoxy–Thermoplastic Blends

As compared to neat epoxy material, rheological studies of blended or filled epoxy materials often result in additional complexities during data analysis, which arise from structural transitions such as phase separation. Rheology proves a valuable technique for monitoring phase separation, owing to its ability to capture the viscoelastic changes in a material. Early rheological studies of epoxy–thermoplastic blends assumed a classical phase separation mechanism, which has advanced more recently to include the concept of viscoelastic phase separation. A goal for rheological studies is to correlate behaviors in the rheological profiles (e.g., complex viscosity, modulus) with changes in molecular arrangements (e.g., phase separation, gelation). Although each individual epoxy–thermoplastic formulation and accompanying processing parameters exhibit unique rheological behavior, certain generalized trends can be summarized to aid in understanding rheology for

epoxy–thermoplastic blends. The following section will describe rheological behavior resulting from phase separation, followed by a discussion of viscoelastic phase separation and the complementary modeling approaches. The last portion of this section will describe other rheological considerations of epoxy–thermoplastic blends.

Rheological Behavior Resultant of Phase Separation

Phase separation is the overwhelmingly prominent structural alteration that appears during the cure of epoxy–thermoplastic blends. The existence of a phase-separated morphology is crucial to attain the desired toughening characteristics of these materials. This structural transition appears as a distinct, and often unanticipated, fluctuation in the complex viscosity profiles (Bonnet et al. 1999; Kim and Char 2000; Yu et al. 2003; Blanco et al. 2004; Cicala et al. 2006, 2007). Such fluctuations were shown in a seminal study from Bonnet et al. (1999), which was the first to employ rheology during the isothermal cure of a thermoplastic–epoxy blend comprising the PEI thermoplastic, within an epoxy–amine resin DGEBA and 4,4'-methylenebis[3-chloro-2,6-diethylaniline] (MCDEA). The authors evaluated how the concentration of PEI thermoplastic affected the rheological performance during phase separation, showing a correlation between distinct morphological changes and the complex viscosity profiles. Specifically, the concentration ratio of PEI thermoplastic to the epoxy–thermoset directly influenced the final heterogeneous morphology resulting from phase separation.

The development of these heterogeneous structures was captured in complex viscosity profiles (Fig. 2), which depicts curves for three different formulations, each with varying content of PEI. Notably, the concentration of PEI affected the mechanism of phase separation, as shown by the unique fluctuations in complex viscosity. For example, formulations with lower thermoplastic content (i.e., 10 wt% of PEI) generated an epoxy continuous phase that showed a sharp decrease in complex viscosity during phase separation, resulting from the separation of the less viscous, low molecular weight epoxy resin from the thermoplastic. Intermediate PEI concentrations (i.e., 20 wt% of PEI) also resulted in a fluctuation in viscosity, owing to the formation and subsequent elimination of a bicontinuous structure. The highest PEI concentration evaluated in this study (i.e., 33 wt% of PEI) resulted in a thermoplastic-rich continuous phase (i.e., phase inversion) and gradually increased in viscosity after the phase separation.

The plot in Fig. 2 provides clear examples of distinct fluctuations in complex viscosity profiles that emerge during the cure of epoxy–thermoplastic blends. Contrary to neat epoxy materials, which generally show a continuous increase in viscosity during the cure, epoxy–thermoplastic blends often exhibit phase-change-dependent viscosity fluctuations. These fluctuations, as described here, refer to the abrupt bump occurring in the viscosity traces (e.g., immediately following t_{cp} in Fig. 2) that reveal structural rearrangements within the system during phase separation.

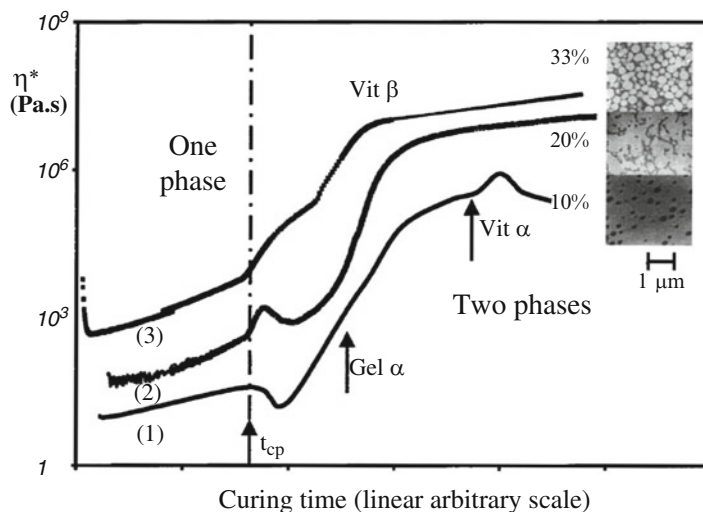


Fig. 2 Complex viscosity versus curing time for the DGEBA/MCDEA epoxy blended with PEI at three different concentrations: (1) 10 wt%, (2) 20 wt%, and (3) 33 wt%. The inset TEM images show the morphologies of the material post-cure (Reprinted with permission from *Macromolecules* (1999) 32, 8524–8530 (Bonnet et al. 1999) Copyright 1999 American Chemical Society)

The appearance of distinct fluctuations in viscosity profiles during the formation of epoxy–thermoplastic materials was also observed by Kim et al. (2000). Similar to the report by Bonnet et al., this study demonstrated a distinct fluctuation in complex viscosity ascribed to phase separation, as further verified using small-angle light scattering (SALS). The viscosity profile resulting from the isothermal cure of DGEBA and 4,4'-diaminodiphenylmethane (DDM) in combination with 20% PES was categorized into three distinct sections based on the morphological evolution (Fig. 3a). In the initial stage (I), a homogeneous mixture of epoxy and thermoplastic remains low in viscosity as the epoxy resin and curative are predominately unreacted. As the epoxy cure proceeds (II), the newly formed epoxy oligomer phase separates from the thermoplastic, which is higher in viscosity than the low molecular weight epoxy polymer, hence the slight drop in viscosity. During the final stage (III), the viscosity continues increasing as the epoxy ultimately generates a cross-linked polymer network. In this early report, Kim et al. also proposed a suspension model to describe the viscosity profiles of this system.

Various parameters influence the structures that evolve during the cure of epoxy–thermoplastic blends, including cure temperature, chemical composition, and the concentration of components (e.g., thermoplastic modifier). Specifically, the isothermal cure temperature of epoxy–thermoplastic blends affect the viscosity profiles (Kim and Char 2000; Luo et al. 2001; Blanco et al. 2004). As shown by Blanco et al. (2004), viscosity profiles during the polymerization of DGEBA with MDEA combined with 15 wt% of a copolymer thermoplastic (40:60 polyethersulfone/polyetherethersulfone (PES/PEES)) depend on the isothermal

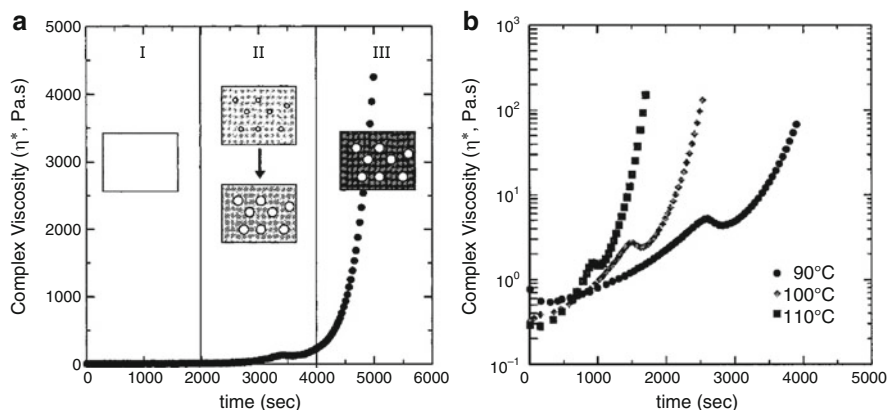


Fig. 3 (a) Complex viscosity versus curing time for the DGEBA/DDM epoxy blended with PES at 20 wt% during an isothermal cure at 90 °C. The insets pictorially describe the phases of cure. (b) Complex viscosity versus time for DGEBA/DDM epoxy blended with PES at 10 wt% and cured at different temperatures (Reprinted with permission from *Ind. Eng. Chem.* (2000) 39, 955–959. Copyright 2000 American Chemical Society (Kim and Char 2000))

cure temperature. An increase in isothermal cure temperature results in an increase in conversion rate, which more rapidly generates the conditions necessary for phase separation and the accompanying fluctuation in viscosity. This same trend was also shown by Kim et al. (2000) during the isothermal cure of DGEBA with DDM and 10% PES, wherein a higher isothermal cure temperature (e.g., 90 °C, 100 °C, 110 °C) accompanies an earlier fluctuation in complex viscosity (Fig 3b). In general, the increase in molecular weight of the epoxy resin drives the phase separation, a process that increases with faster epoxy polymerization rates resultant of an increase in temperature.

Another parameter that greatly influences phase separation is the chemical composition of the epoxy–thermoplastic blends, which affects solubility, viscosity, and chemical compatibility of the formulation (Blanco et al. 2003, 2004; Yu et al. 2003; Cicala et al. 2006, 2007). Because the chemical constituents contribute greatly to the structural evolution, conditions can be chosen to tune the final desired morphology. Blanco (Blanco et al. 2004) also demonstrated the importance of curative selection on the viscosity and morphology of epoxy–thermoplastic blends. The cure of DGEBA using either MDEA or 3,3'-DDS as the curatives, both epoxy systems in combination with 15 wt% of thermoplastic (PES/PEES at a 40:60 ratio), shows unique viscosity profiles during the cure. In the MDEA system, a signature fluctuation in viscosity occurred during the cure originating from phase separation. Conversely, the 3,3'-DDS formulation lacked this fluctuation and produced a homogenous system, likely comprising an interpenetrating network. The lack of phase separation in the 3,3'-DDS system was suggested to originate from the increased solubility of 3,3'-DDS in the thermoplastic and the increased viscosity of the blend prior to cure.

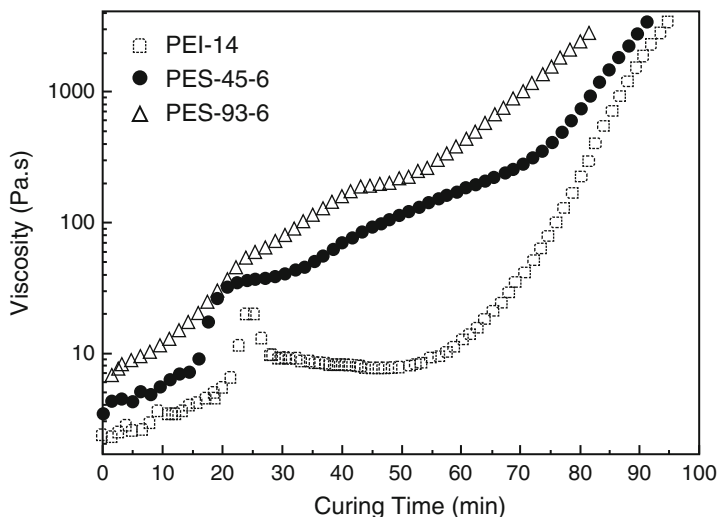


Fig. 4 Viscosity versus curing time for the DGEBA/4,4'-DDS epoxy blended with PEI (PEI-14), PEI with either a low molecular weight PES (PEI-45-6) or a high molecular weight PES (PEI-93-6) (Reprinted with permission from *Ind. Eng. Chem.* (2003) 42, 3250–3256. Copyright 2003 American Chemical Society (Yu et al. 2003))

In addition to the choice of the epoxy resin constituents, the choice of thermoplastic can also influence rheological behavior. For example, an early study by Yu (Yu et al. 2003) showed the importance of thermoplastic variety and molecular weight on the viscosity profiles. The authors showed that the quantity, type, and molecular weight of thermoplastic, either PEI or a hydroxyl-terminated PES, altered the complex viscosity profiles during the cure of epoxy resin comprising a low molecular weight DGEBA with 4,4'-DDS (Fig. 4). The incorporation of a high molecular weight PES into the DGEBA/4,4'-DDS/PEI formulation resulted in a thermoplastic continuous phase throughout the cure cycle. Conversely, other thermoplastics (i.e., lower molecular weight PES with PEI, PEI alone) within the same epoxy formulation resulted in more complex viscosity profiles, attributed to destruction of the thermoplastic continuous phase.

Similarity, Cicala et al. (2006) showed the importance of chemical groups and molecular weight of PES/PEES thermoplastic modifiers when added to DGEBA/MDEA epoxy resin. The viscosity traces drastically varied between two formulations that each contained amine-terminated PES/PEES copolymers of differing molecular weight, but otherwise identical formulation content. The study also examined PES/PEES with differing end groups (chlorine, amine, hydroxyl) in addition to differing molecular weights (between 5,000 and 12,000), showing that individual formulations can affect the time to reach phase separation in viscosity traces and the final morphology. The capability of tuning these chemistries unlocks a multitude of possible epoxy–thermoplastic materials exhibiting distinct mechanical and chemical characteristics. For example, the ability to include more than one

thermoplastic can result in unique morphologies. Using a Flory–Huggins model to understand rheological data, Galante et al. (2001) showed a unique double phase separation of the system comprising DGEBA/4,4'-DDS combined with two thermoplastics, poly(methyl methacrylate) (PMMA) and polystyrene (PS). Additionally, core–shell particle morphology (i.e., PS encapsulated by PMMA) was achieved and suggested to occur during the second phase separation.

The dilution effect is also significant for certain blended samples, as the thermoplastic can dilute the formulation, effectively reducing the rate of polymerization in an epoxy cure. In one example, the content of the thermoplastic, poly(2,5-dimethyl phenylene oxide), affected the gel point of DGEBA/MCDA systems (Rusli 2014). The authors showed that increasing the content of poly(2,5-dimethyl phenylene oxide) correspondingly increased the time to phase separation, the time to vitrification, and the gelation time, which was obtained from the $\tan \delta$. The concentration of thermoplastic affects the viscoelastic phase separation, and this concept of viscoelastic phase separation is described in more detail in the following section.

Overall, the early investigations of rheological behavior primarily focused on relating structural changes with phase separation mechanisms. Both the formulation and processing parameters of the epoxy–thermoplastic blends greatly affect the morphological evolution, as monitored through complex viscosity profiles or modulus profiles. Importantly, the shape of viscosity traces provides insight into the mechanism of phase separation, with the signature fluctuations (e.g., dip or peak) in viscosity typically associated with phase separation in these systems. In general, experimental conditions that favor a fast epoxy polymerization rate can also favor a faster time to reach phase separation. For example, higher temperatures increase the rate of cure, which initiate an earlier phase separation, as seen in the distinct fluctuation earlier in the viscosity profiles. The formulations (e.g., chemical structure, molecular weight, and quantity of thermoplastic) also contribute substantially to the mechanistic details of phase separation and final morphologies. Confirmation with alternative analytical techniques, such as light scattering and spectroscopy, can verify the phase separation behavior and final morphologies. The next section provides more details surrounding viscoelastic phase separation.

Viscoelastic Phase Separation: Rheological Analysis

An enriched description of phase separation in polymer systems, involving the concept of viscoelasticity, was first demonstrated experimentally by Tanaka (1993). Beyond the conventional solid or fluid models of phase separation, this new explanation, termed viscoelastic phase separation, incorporated the notion that the mechanical balance of thermodynamic and viscoelastic forces ultimately dictates the morphology of the material (Tanaka 2000, 2012; Tanaka and Araki 2006). The key to this theory involves the concept of “dynamic asymmetry” where the components of a system exhibit differences in dynamics (i.e., fast and slow components). As nicely reviewed in a report on dynamic critical phenomena by Hohenberg and Halperin, dynamic properties of a system involve components that rely on equations

of motion (e.g., transport coefficients, relaxation rates, multi-time correlation functions), as opposed to static properties of a system that rely on single-time equilibrium distribution (e.g., thermodynamic coefficients, single-time correlation functions, and the linear response to time-independent perturbations) (Hohenberg and Halperin 1977). The conventional explanation for binary phase separation has typically presumed identical symmetry between the two components of the system, termed “dynamic symmetry.” This description holds validity in many circumstances, such as mixture of liquid constituents that exhibit similarly fast dynamics.

As described thus far in this chapter, early rheological studies of epoxy–thermoplastic blends primarily considered conventional phase separation theories to explain the mechanisms for guiding final morphologies. More recently, studies have shown that epoxy–thermoplastic blends often display dynamic asymmetry behavior, with the epoxy resin and the thermoplastic each exhibiting distinct dynamic properties comprising either a fast component (e.g., viscous phase) or a slow component (e.g., elastic phase). For epoxy–thermoplastic systems, the rate of relaxation of the slower component, such as epoxy chain disentanglement, fails to match the rate of deformation of the phase separation, ultimately resulting in viscoelastic phase separation. The dynamic asymmetries typically arise from vast differences in glass transition temperatures or molecular weight between the epoxy and the thermoplastic, which leads to viscoelastic phase separation. The relationship between viscoelastic effects and phase separation of epoxy-thermoplastic material was first experimentally evaluated using a formulation comprising DGEBA and methyltetrahydrophthalic anhydride (MTHPA) blended with PEI (Gan et al. 2003). A clever approach to probe these viscoelastic mechanisms involved the use of an accelerator, benzyldimethylamine (BDMA), to control the epoxy curing rates and enable an enhanced understanding of evolving morphologies. Through TRLS, the authors described the occurrence of a spinodal decomposition mechanism and showed that differences in T_g between the epoxy and PEI guided morphological evolution. The WLF equation was used to adequately justify the temperature-dependent relaxation times during phase separation.

Yu and colleagues further investigated the viscoelastic phase separation in epoxy–thermoplastic blends continuously throughout the generation of the sample using rheological analysis, combined with TRLS and microscopy (Yu et al. 2004). This was one of the earliest reports using rheology to examine viscoelastic phase separation of epoxy–thermoplastics. Using a formulation comprising DGEBA/MTHPA blended with different concentrations of PES thermoplastic, the authors showed the importance of the concentration of thermoplastic on the complex viscosity profiles, in accordance to previous studies, as discussed above (Bonnet et al. 1999). Ultimately, formulations containing 20 wt% PES resulted in a phase inversion structure, and formulations containing 14 wt% PES resulted in a bicontinuous phase structure. In terms of the viscoelastic phase separation, the authors described an initial phase inverted morphology, which originates from large differences in molecular weight and chain mobility between PES and the low molecular weight epoxy. The viscoelastic enhancement of the PES domain occurs during the late stages of cure, when PES acts as an elastic moiety resulting from the

diffusion of the low molecular weight epoxy monomer out of the PES phase. The authors also described the relaxation time of phase separation by the WLF equation, which will be further discussed below.

The control of epoxy curing rate enables rapid securement of different morphologies, which facilitates a deeper understanding of viscoelastic phase separation. By employing an imidazole hardener (1-cyanoethyl-2-undecylimidazole trimellitate) for chain polymerization, Wang and colleagues rapidly cured a DGEBA resin blended with different concentrations of PEI, which immobilized the structure in the early stages of phase separation (Wang et al. 2004). Using both the Debye viscosity relationship and rheological data, the authors describe that the rapid increases in viscosity at 6–8% conversion accompany an increase in relaxation time of chain disentanglement and slow diffusion, which fixes the structures early in-phase separation process. Using this approach enabled verification of morphologies that contain a PEI-rich continuous phase (phase inverted structure) at low concentrations of PEI, resulting from the viscoelastic effect.

As previously discussed, many parameters influence morphologic evolutions during the cure of epoxy–thermoplastic blends, such as molecular weight (Yu et al. 2003). An explanation based on the concept of viscoelastic phase separation provides deeper insight into the influence of these parameters and the associated mechanisms. For instance, an inverse relationship exists between the simulated relaxation times and molecular weight of the PES thermoplastic when cured at identical temperatures, with a decrease in relaxation times accompanying an increase in PES molecular weight (Yu et al. 2008). An explanation of this relationship involves the concept of viscoelastic phase separation, wherein dynamic asymmetries within a system are more prevalent when using a higher molecular weight thermoplastic. At a higher molecular weight, the PES thermoplastic more rapidly separates from the epoxy and acts as an elastic body to promote PES continuous structures. A phase-inverted structure transpired when using a higher concentration of PES (20%).

Modeling Viscoelastic Phase Separation

The comparison between experimental results and simulations can provide valuable insight about viscoelastic behavior of polymeric systems. In particular, rheological models hold potential to provide a better understanding of viscoelastic phase separation during the preparation of epoxy–thermoplastic blends (Tribut et al. 2007, 2008). In one example, the growth rate of complex viscosity during the phase separation can be modeled with the single exponential equation (Eq. 12):

$$\eta^*(t) = \eta_0^* + A_0 \exp\left(\frac{t}{\tau_\eta}\right) \quad (12)$$

where $\eta^*(t)$ is the complex viscosity of the epoxy–thermoplastic blend, A_0 is the magnifier, and τ_η is the relaxation time of viscosity (a parameter useful when comparing the rate of viscosity growth between different systems) (Yu et al. 2006,

2008; Jyotishkumar et al. 2011; Parameswaranpillai et al. 2013). This relationship enables the determination of τ_{η} by simulation of complex viscosity data. Using this approach, Yu et al. first demonstrated the exponential growth of complex viscosity during phase separation of DGEBA cured with MTHPA and blended with approximately 20 wt% PEI, resulting in a phase-inverted morphology (Yu et al. 2006). By using a combination of rheometry, TRLS, and DSC analytical techniques, the authors showed that phase separation of this formulation occurred before gelation, but was hindered by vitrification of PEI. A good correlation existed between complex viscosity from experimental results and simulation of complex viscosity using Eq. 9, which was described by the WLF equation. The exponential growth of complex viscosity profiles was ascribed to viscoelastic flow characteristics of epoxy material from the PEI during the phase separation. Similar systems also followed an exponential growth in complex viscosity profiles during the early period of cure. For example, formulations comprising DGEBA/MTHPA blended with 20 wt% PES thermoplastics exhibit exponential growth of complex viscosities (Yu et al. 2008). As shown in Fig. 5, a good correlation existed between simulation results from Eq. 12 and experimental data acquired at different temperatures. These exponential growth profiles of viscosity were chiefly ascribed to diffusion of epoxy molecules from the PES phase during phase separation.

Additional understanding of viscoelastic behavior of epoxy–thermoplastic blends entails the simulation of relaxation times of viscosity growth versus temperature using the WLF equation, as provided by Eq. 13:

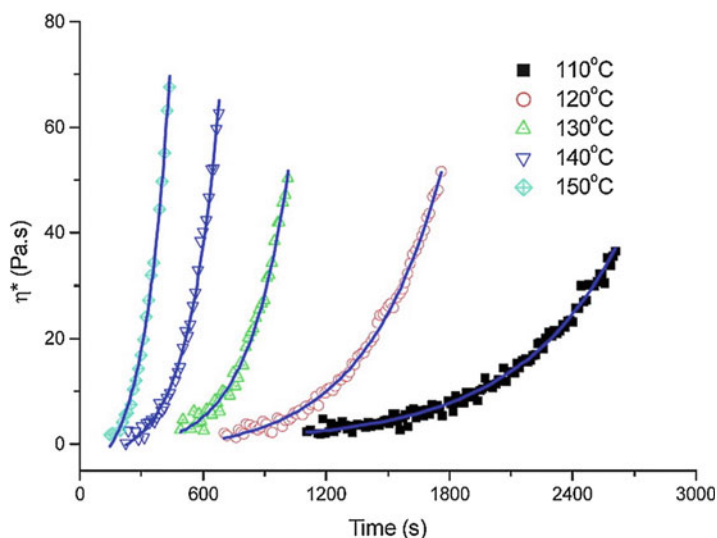


Fig. 5 Complex viscosity versus time for the DGEBA/MTHPA epoxy blended with 20 wt% PES and cured at different temperatures. The symbols show experimental data and the lines represent results acquired from simulations using Eq. 12 (Reprinted with permission from Ind. Eng. Chem. (2008) 47, 9361–9369. Copyright 2000 American Chemical Society (Yu et al. 2008))

$$\log \frac{\tau}{\tau_s} = \frac{-C_1 (T - T_s)}{C_2 + (T - T_s)} \quad (13)$$

where T_s and τ_s are the temperature and relaxation time at a selected reference temperature. If the empirical constants are chosen as $C_1 = 8.86$ K and $C_2 = 101.6$ K, then Eq. 13 can be rewritten as Eq. 14 (Williams et al. 1955):

$$\tau = \tau_s \exp \left[\frac{-\ln 10 \times 8.86 \times (T - T_s)}{(101.6 + (T - T_s))} \right] \quad (14)$$

Equation 14 can simulate the relationship between temperature and relaxation times of an epoxy–thermoplastic blend. The value of T_s is associated with a temperature enabling polymer flow, often regarded as 50 °C above T_g of the polymer (Gan et al. 2009). If a good correlation exists between the WLF simulation and experimental results of the epoxy–thermoplastic system, then this suggests the relaxation time obeys the TTS principle.

The use of WLF simulations to evaluate if relaxation times obey the TTS principle has been used in various circumstances (Yu et al. 2004, 2006, 2008; Gan et al. 2009; Jyotishkumar et al. 2010, 2011, 2012; Parameswaranpillai et al. 2013). In one interesting example, Parameswaranpillai et al. showed that the relaxation time of viscosity growth for epoxy (DGEBA/4,4'-diamino diphenyl methane (DDM)) modified with SAN obeyed the WLF equation for formulations containing different concentrations of SAN thermoplastic (Parameswaranpillai et al. 2013). The report showed that increasing the quantity of SAN thermoplastic consequently increases the relaxation time, which implies a decreased rate of viscoelastic phase separation. The elastic characteristics of the SAN thermoplastic, particularly at high concentrations, impede the diffusion and growth of the epoxy network, ultimately immobilizing the phase-inverted structure. The authors described the benefit of the TTS principle in calculating τ_s , owing to the difficulty in experimentally determining these values at lower temperatures, which hinders polymer chain movement of epoxy resins.

Another critical aspect of rheology is the effect of frequency or shear rate on rheological behavior. The requirement to understand the tolerance of shear rates in a system is crucial for translation of materials to real-world applications, as will be further discussed in the last section of this chapter. The frequency dependence of complex viscosity during phase separation can depend on the formulation of the epoxy–thermoplastic. For instance, Varley showed that using a lower amount of thermoplastic (10 wt% PEI, in combination with RTM6 resin) produced an epoxy continuous morphology (i.e., PEI particle), which exhibited quasi-Newtonian behavior during phase separation, where frequency did not substantially affect the viscosity (Varley 2007). Conversely, a higher concentration of thermoplastic (20 wt% PEI in combination with RTM6 resin) generated a phase-inverted or co-continuous structure, which showed a non-Newtonian behavior during phase separation, where frequency affected the viscosity. Yu and colleagues also showed that frequency affects the rheological behavior by using DGEBA/MTHPA blended with

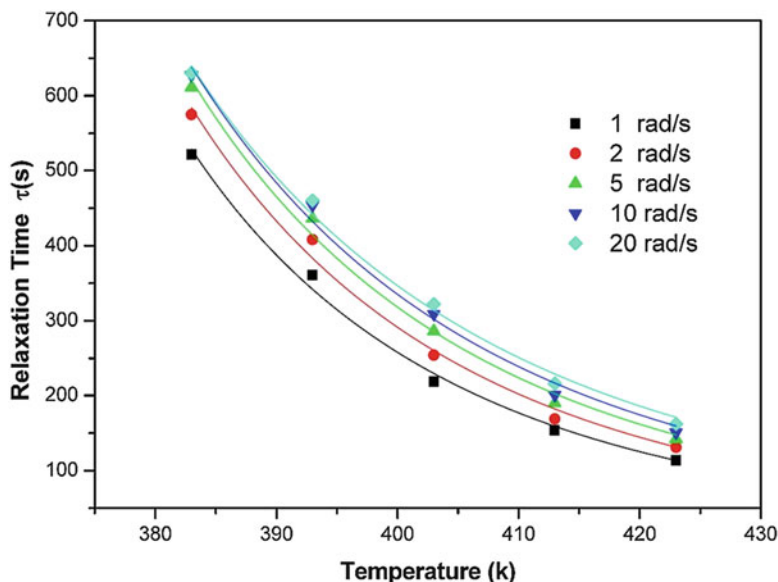


Fig. 6 Relaxation times versus temperature for DGEBA/MTHPA blended with 20 wt% PES at different frequencies. The symbols represent the experimental data, whereas the lines represent simulations using Eq. 14 (Reprinted with permission from *Ind. Eng. Chem.* (2008) 47, 9361–9369. Copyright 2000 American Chemical Society (Yu et al. 2008))

PES of different molecular weights (Fig. 6; Yu et al. 2008). The formulations comprising a thermoplastic-rich continuous phase (i.e., phase inverted at 20% PES) showed non-Newtonian behavior during the exponential growth of complex viscosity during isothermal cure at 120 °C. For all tested frequencies, the relaxation times (calculated from complex viscosity data) obeyed the WLF equation (Eq. 14).

Rheological Analysis During Other Structural Arrangements: Gelation and Crystallization-Induced Phase Separation (CIPS)

Rheological analysis of epoxy–thermoplastics requires considerations additional to phase separation. There exists a critical requirement to characterize and differentiate between multiple stages during production of the material, such as gelation of epoxy, vitrification (of both the thermoset and thermoplastic), and phase separation. Depending on the formulation and processing conditions, these material transitions can occur independently or concurrently. Careful assessment of rheological behavior is thus crucial to characterize these transitions, such as multiple crossover points of G' and G'' during the curing process. An example of double gelation occurred during the isothermal cure of DGEBA/MTHPA blended with PES, where the frequency independence of $\tan \delta$ occurred during two critical states (i.e., structural transitions or “gel points”), which was maintained at five different frequencies (Fig. 7; Gan

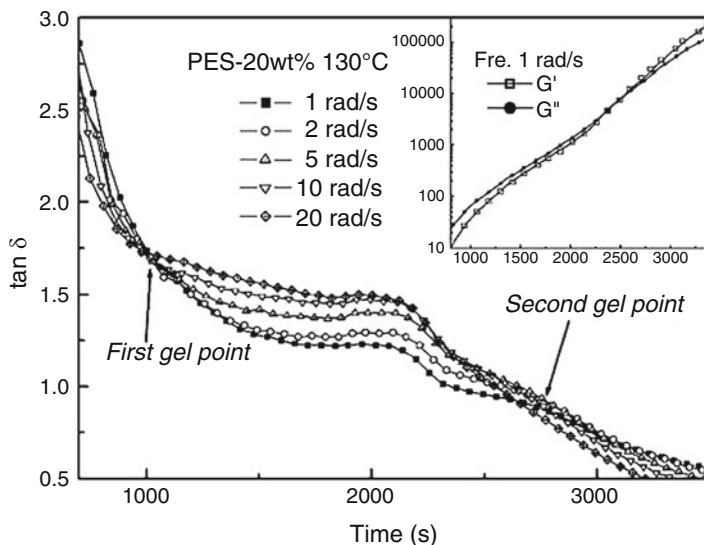


Fig. 7 Profiles of $\tan \delta$ versus time for DGEBA/MTHPA blended with PES cured at 130 °C (Reprinted with permission from *Colloid Polym. Sci.* (2007) 285, 1727–1731 (Gan et al. 2007))

et al. 2007). By using rheology, DSC and TRLS, the authors concluded that the first critical state represented phase separation, whereas the second critical state represented the gelation of the epoxy. Additionally, the growth rate of complex viscosity was exponential, suggested to result from viscoelastic flow of epoxy resin out of the thermoplastic phase.

In general, the analysis of $\tan \delta$ profiles can reveal multiple fluctuations originating from viscoelastic transitions occurring during the cure of an epoxy–thermoplastic blend. Prior to the gel point, the $\tan \delta$ values will often drop, owing to the generation of a thermoplastic-rich phase from viscoelastic phase separation. Depending on the formulation, this initial drop is followed by an increase in $\tan \delta$ value resulting from the less viscous epoxy that phase separated. Ultimately, the $\tan \delta$ values reach near zero from the gelation or vitrification of the epoxy–thermoset. For instance, this trend in $\tan \delta$ was explained and observed during the cure of a DGEBA/DDM blend during the viscoelastic phase separation of the thermoplastic poly(styrene-acrylonitrile) (SAN) (Jyotishkumar et al. 2012).

Importantly, the definition and determination of gel point requires detailed consideration in blended materials, owing to the distinct changes in morphology. Contingent on the formulation and processing conditions, epoxy gelation and phase separation can proceed independently or concomitantly. The initiation of phase separation can occur prior to epoxy gelation, where the two events remain distinct. Alternatively, the two processes can proceed concomitantly, whereupon rapid epoxy cure rates can fully halt phase separation or freeze phase separation at differing degrees. As discussed above, a variety of approaches exist to determine the

gel point, with method choice dependent on the system under investigation. The methodology for ascertaining the gel point becomes critical with dual-gel point systems.

In an insightful review on gelation behavior of blended materials, Yu et al. (2014) detailed the approach distinguishing between the physical changes (e.g., phase separation) and the chemical gelation of the epoxy–thermoset. Briefly, the critical gel theory (Winter and Chambon 1986) describes a power law relationship between gel point and stress relaxation of the network in Eq. 15:

$$G(t) = St^{-n} \quad (15)$$

where n is the relaxation exponent (i.e., viscoelastic parameter and $(0 < n < 1)$) and S is the gel strength (i.e., chain mobility parameter). Yu further described the frequency dependence of dynamic shear modulus in Eq. 16:

$$G'(\omega) = \frac{G''(\omega)}{\tan \frac{n\pi}{2}} \quad (16)$$

Equation 16 shows that utilization of the crossover between G' and G'' to determine gel point is valid if $n = 0.5$, which does not occur in many epoxy-cross-linked systems. Justification for using the time at which $\tan \delta$ is independent of frequency as the gel point involved the following relationship in Eq. 17:

$$\tan \delta = \frac{G''}{G'} = \tan \frac{n\pi}{2} \quad (17)$$

An additional transition that may occur during the cure of epoxy–thermoplastic blends is crystallization-induced phase separation (CIPS) ((Tercjak et al. 2005, 2006), which takes place when a chemical constituent (e.g., polymer) has sufficient structural regularity to crystallize and separate from the surrounding solution (Witte et al. 1996). The rheological differentiation between CIPS, RIPS, and gelation of the epoxy resin must be considered for many formulations. The existence of CIPS critically relies on the formulation and processing parameters, as demonstrated during the cure of DGEBA/MCDEA blended with a syndiotactic polystyrene (Tercjak et al. 2006). Using dynamic oscillatory shear measurements, the authors showed that the concentration of the polystyrene and isothermal curing temperature governed the rheological behavior. The characteristics of the complex viscosity profiles varied above and below a critical concentration of syndiotactic polystyrene (i.e., 7.5 wt%). Below 7.5 wt% of the thermoplastic, a rapid increase in viscosity resulted from crystallization of the polystyrene; above 7.5 wt% of thermoplastic, the viscosity profiles suggested a more complex behavior ultimately resulting in a co-continuous structure. The occurrence of CIPS was further evaluated via employing various isothermal curing temperatures, which resulted in an increase in η^* , G' , and G'' over time for the lowest tested temperature (210 °C), which the authors suggested stemming from CIPS.

In many occasions, the supplementation of rheological data with alternative analysis is necessary to fully understand transitions and behavior of the material. Because rheology is concerned with viscoelastic measurements, the combination of alternative analytical techniques is often necessary to elucidate mechanistic details. Although not detailed here, a multitude of examples exist that have used additional analysis to supplement rheological studies (Tercjak et al. 2005; Yu et al. 2006; Xu et al. 2007). In one example, using TRLS and DSC, Yu et al. (2006) determined the conversion and onset time for phase separation during the cure of DGEBA/MTHPA blended with 20 wt% PEI. The use of TRLS to measure the onset/offset of phase separation and the use of rheology to evaluate complex viscosity fluctuations enabled verification of phase separation prior to gelation. In other epoxy–thermoplastic formulations that exhibit both RIPS and CIPS, transmission optical microscopy can assist in distinguishing between these two modes of phase separation (Tercjak et al. 2005). The ability to differentiate between similar transitions often requires additional analysis to support these occurrences of the physical mechanisms.

Additionally, similar to neat resin systems, epoxy–thermoplastic blends often require a cure or secondary post-cure performed at temperatures above the T_g of the thermoplastic to ensure sufficient polymerization of the epoxy resin and fixation of the final morphology. For the blended systems, the secondary post-cure may coincide with a secondary phase separation, during which residual epoxy resin within the thermoplastic phase continues gelation (Girard-Reydet et al. 1998; Blanco et al. 2004).

Rheological Parameters for Industrial Applications: Assessment of Epoxy–Thermoplastic Blended Material

A thorough understanding of the chemical and physical properties of epoxy-based materials is required to operate in various industries, such as the electronic, automotive, and aerospace sectors. Rheology is an important tool to characterize the preparation of these polymers to ensure properties match the expected product design. The knowledge of chemoviscosity behavior enables the design of processing parameters and production cure cycles to ensure quality control over the design, manufacturing, and output of epoxy-based products. By performing a temperature scan, for example, the viscosity and modulus are obtained for each time point during the cure cycle, thereby offering invaluable insight when making decisions about processing requirements and appropriate times for molding. For instance, the prediction of chemoviscosity behavior of epoxy composites is mandatory to fabricate large laminated parts for aircraft, which must allow for release of trapped gas and fiber compaction during the cure cycle (Tajima and Crozier 1983).

A critical aspect in a product pipeline involves the translation of fundamental knowledge of a material into industrial product development, which will ultimately impact performance. In this section, these translational components are described by considering various rheological aspects in processing design and points to consider when using epoxy–thermoplastic blends for commercial applications. The goal of

this section is to complement the fundamental laboratory studies profiled in this chapter, thus far.

Industrial Applications

It is important to understand the markets in which thermoplastic-toughened epoxies offer a significant advantage over untoughened systems, alternate toughening systems, and alternate materials. The competitive advantage of thermoplastic-toughened epoxies (as well as core-shell-toughened epoxies) is in applications that require toughness combined with high glass transition temperatures (T_g). Many rubber-toughened systems will fall short in this regard. Alternate toughening regimes, such as particulate toughening systems, can maintain high T_g , but the higher density of the particles increases the overall weight of the system, which can be a significant disadvantage in aerospace, for example.

One significant application for thermoplastic-toughened epoxy is the advanced composite market in the aerospace sector. In such applications, the resin acts as a matrix to support a larger fraction of structural fiber, such as carbon fiber, fiberglass, or Kevlar[®]. Advanced composites hold considerable promise for reducing the weight of structures while significantly improving corrosion resistance. In addition, composites allow designers to change the stiffness of a structure to match load paths through their ability to produce anisotropic structures. Further, composites allow for reduced part counts and significant reductions in the number of fasteners required to produce a structure through adhesive bonding. As such, composite materials, with carbon fiber-reinforced plastic (CFRP) leading the way, are replacing traditional aerospace aluminums such as 7075 aluminum alloy and 2024 aluminum alloy. Early attempts at material swapping were very prone to impact damage and came to be regarded as “black aluminum” designs, as designers had treated CFRP if it were simply a different grade of aluminum with the usual toughness. Aerospace structures with these designs did not possess the toughness to withstand operational conditions such as hail strike or even the impact of the inevitable dropped tool. Consequently, certain parts were not changed to CFRP and those that were often were overbuilt to meet toughness requirements. This, of course, increased structure weight, negating some of the benefit of switching to CFRP in the first place. Resin formulators have realized that toughening the matrix resin allows the designers to use less material, ultimately recapturing some of the lost weight savings. Aerospace qualification is lengthy and expensive, so alternate market entry in sports equipment (bicycle rims subjected to braking heat) or motorsports (structures near the engine, exhaust system, or brakes) may be appealing.

Viscosity During Formulation

Consideration of viscosity profiles during formulation (i.e., here referring to preparing materials prior to fabrication) is imperative to ensure workability of blended

epoxy resins. The viscosity and flow an epoxy blend, dictates the uniformity and porosity of the final product, which makes rheological analysis of each processing stages very important. Typically, thermoplastics are incorporated into epoxy by melt blending of the two components at elevated temperature. Through melt blending, multiple benefits are realized: enhanced workability via the decrease in viscosity of both components, increase of the dissolution rate, and elimination of solvent by using neat materials. These characteristics are important in terms of cost and ease of processing for industrial applications. The melt blending process, however, is ultimately limited by the time and temperature at which the materials can be processed, as the epoxide holds a strong propensity to homopolymerize at elevated temperature (e.g., >150 °C), especially in the presence of hydroxyl functional groups or other catalytic moieties. If the thermoplastic exists in solid form, the rate of dissolution into epoxy resin can be improved by increasing the surface area of the thermoplastic powder. Although difficulties arise in forming a very fine powder due to the inherent toughness of thermoplastics, this can be overcome in some cases by applying high shear at cryogenic temperatures. An alternate method of producing epoxy–thermoplastic blends is to dissolve the thermoplastic into a solvent and subsequently mix the dissolved thermoplastic into the epoxy followed by degassing via vacuum to remove the solvent. In some situations, it may be possible to leave the solvent in the thermoplastic–epoxy solution for removal after application processes, such as structural fabric impregnation. Note that some thermoplastics are supplied as a pre-made solution.

Viscosity During Formulation of Prepreg Materials

Epoxy resin is often pre-impregnated into structural reinforcement fabrics, typically carbon fiber, glass fiber, or Kevlar[®], for future lamination into high-performance structures, such as elements for aerospace applications. These “prepregs” are most often infused with low-viscosity resin, acquired via solvent addition (~95% of the current market) or impregnation at elevated temperature (~5% of the current market). The low viscosity improves wetting of the fabric, as the neat resins are often too much viscous for rapid processing. After impregnation, the materials are passed through a series of doctor blades and rollers to achieve uniform resin content via in-line processes. Subsequently, the materials pass through a “drying tower” at elevated temperature, which serves to remove any solvent and “B-stage” or advance the degree of cure to the point that the resin cannot drip from the reinforcement (Dorworth et al. 2009). Of note, new types of prepreg have been developed for out-of-autoclave (OOA) or vacuum-bag-only (VBO) manufacture. These prepregs are purposely not fully impregnated, leaving a fraction of the fabric dry such that it can serve as a path for volatiles to be pulled from the lamination prior to heating/wetting/consolidation. Autoclave fabrication involves the lamination of many layers of prepreg onto a mold. These prepreg layers have a self-adhesive quality, which aids in accurate placement of the fibers. Importantly, this adhesion is strongly related to the initial viscosity of the resin and to its degree of advancement.

The viscosity of the formulations during preprocessing steps plays a critical role in industrial processes. The resultant prepreg must possess enough tack to adhere

built-up laminations, which often must remain adhered to vertical mold surfaces for up to several days prior to cure. If a resin cannot adhere to low surface energy mold surfaces due to excessive B-staging or continued cure resulting from excessive storage time, then the material has surpassed its “outlife” and cannot be used. Furthermore, if excessive cure advancement prevents the laminated layers from adhering to one another or impairs the resin’s ability to flow and release air bubbles during cure, the material is past its outlife. For these reasons, it is desirable to B-stage a material as minimally as practical. In other words, the chemoviscosity profile of a prepreg resin is important in the A-stage for controlling the wetting of reinforcement, in the B-stage for controlling tack and conformability, and in the C-stage for controlling the morphology and hence the toughness of the finished part.

Materials for the microelectronics industry are often supplied as “1 K” systems, which are premixed and vacuum degassed epoxies. These materials are supplied in syringes, which are typically stored at -20°C . This arrangement prevents a manufacturer from needing to mix resins, degas resins (to prevent bubbling), and load resins into syringes for automated dispense. 1 K epoxies most often use a latent curative to prevent cure until parts are cured in ovens. Latent curatives can either be materials of low reactivity or can be solids that do not diffuse into the epoxy until they melt. Viscosity profiles can vary greatly depending on application. For example, a capillary underfill needs to have low enough viscosity at cure temperatures to wick between a solder bumped die and the underlying printed circuit board. On the other end of the spectrum, a thermal interface material (TIM) can be as viscous at 125 Pa.s and still be able to be dispensed through an automated needle. In both of these cases, it is desirable to include as much thermally conductive filler as can be accommodated within viscosity limits.

Viscosity During Molding

To meet the demands of most high-performance industrial applications (e.g., aerospace, automotive, recreational), the inherent brittleness of neat epoxy materials must be improved. Translation of new toughened formulations, such as epoxy–thermoplastics, to industrial processes involving composite materials requires compatibility of the materials with established molding techniques. One of those techniques, vacuum-assisted resin transfer molding (VARTM), is broadly used for many processes. VARTM involves placing woven structural fiber preforms on a one-sided mold surface, covering the mold with a membrane to act as the second mold half, evacuating gasses within the mold cavity, and impregnating the preform with resin under the force of vacuum. These processes can produce very high-quality, low-void structures without the cost of autoclave processing. For a resin to work well in this application, the viscosity should be less than about 600cps (0.6 Pa*s). This viscosity usually requires the use of reactive diluents, which tend to reduce the cured properties of the composite.

In terms of epoxy–thermoplastic blends, the addition of thermoplastic to a VARTM resin would likely increase the viscosity to an impractical point. Given

this limitation, several potential solutions have been proposed. One of these solutions is the incorporation of thermoplastic sheets between layers of woven reinforcement, prior to a standard VARTM infusion-type fabrication. During the infusion, the thermoplastic sheets dissolve into the epoxy resin prior to phase separation. In a similar manner, thermoplastic filaments can be woven into reinforcements, which dissolve on infusion and then phase separate on cure (Composites 2003). An alternate method of applying thermoplastic toughening to VARTM would be to employ elevated temperature to decrease the impregnation viscosity of the resin in combination with very slow curatives to obtain reasonable infusion times.

The method of resin transfer molding (RTM) overcomes some of the issues with VARTM by injecting resin at high pressure into dry fabric reinforcements that are contained by a double sided mold. While injecting the resin at tens or hundreds of atmospheres would seem to be well suited to relatively high-viscosity thermoplastic-modified epoxies, the <5 min cure cycles often used in RTM applications would need consideration in terms of time required for phase separation. Formulations of the epoxy-thermoplastic blends may require adjustment to enable enough time for RIPS to occur.

Filament winding is used to produce parts by pulling fiber tows through a resin bath and winding them at specific angles onto a rotated mandrel to produce hollow parts. This is most applicable to tubular shapes such as storage tanks, drive shafts, and missile bodies. For use in filament winding, epoxy-thermoplastic-toughened resins must achieve relatively low viscosity of $< \sim 10 \text{ Pa}\cdot\text{s}$ (10,000 cps) to achieve wet out of the tows, which could be done by heating the resin bath. Filament winding is therefore amenable to thermoplastic toughening. An alternative fabrication method for structural parts is pultrusion, which pulls tows of reinforcing fiber through a vat of resin and then through a heated forming die that cures the composite before it emerges from the downstream end. This is a very low-cost, high-speed process; however, the rapid cure cycle may preclude phase separation in certain epoxy-thermoplastic systems.

Autoclave fabrication is accomplished by laminating many layers of resin-impregnated structural fabric (usually carbon fiber, glass fiber, or Kevlar[®]) onto a mold. These “prepreg” layers have a self-adhesive quality, which aids in accurate placement of the fibers. This adhesion is strongly related to the initial viscosity of the resin and to its degree of advancement. It is commonly tailored during lay-up by brief modification of temperature via heat guns or aerosol cans of freeze agent. Laminations are carefully placed to align fibers with load paths and to prevent warping of the composites due to cure shrinkage of the resin. Generally, five to ten plies are applied, followed by covering the laminated stack with a plastic membrane and pulling vacuum. These “debulk” steps serve to remove volatiles while flattening and aligning the fibers in the plane of the mold surface. Many lamination/debulk stages are performed over the course of laying up a large part. Finally, the laminate/mold is covered with plastic “bagging” and placed under vacuum in an autoclave. The autoclave is then pressurized to $\sim 3\text{--}7$ bar to further compress and align the laminate while also compressing any remaining gas pockets until they dissolve in the

resin, which eliminates voids. Heated cure is then affected, often using a staged series of isothermal cures to preclude the possibility of exotherm. Cycom[®] 977-2 prepreg is an example of a thermoplastic-toughened epoxy prepreg used in this manner. The rheology of the resin is of key importance here, since the resin must be fluid enough to allow for compaction of the plies during debulk steps and able to flow to form a monocoque structure on cure. Autoclave processing is the gold standard of composite fabrication, however it is quite costly.

Another method that requires viscosity considerations is out-of-autoclave (OOA) or vacuum-bag-only (VBO) processing, which is performed in a manner similar to autoclave fabrication, without the benefit (and cost) of the autoclave. OOA fabrication requires a specially produced type of prepreg in order to produce parts with reasonable void content (<2%). These prepreps are only partially impregnated, so the dry areas of the reinforcement fabric function as flow paths for air and volatiles when the laminate is placed under vacuum prior to cure. The B-staged resin viscosity must be high enough to prevent it from shutting off the flow paths and trapping gas. This requirement may be of interest with epoxy-thermoplastic systems that exhibit high viscosities. Lengthy debulk stages are often used to ensure that the degassing goes to completion prior to cure.

Practical Considerations

The ramp rate for curing epoxies within industrial settings often lacks the precision, uniformity, and temporal control afforded by modern laboratory instruments. Variations in mold thickness, uneven distribution of heat, and difficulties in uniformity resultant of curing parts large-scale products (e.g., range in tens of meters in length) cause this. Even small-scale laboratory molds have shown to experience a lag time (e.g., one hour) when placed in an oven, as determined from thermocouples positioned in the sample and in the oven cavity. For most aerospace applications, a cure rate range of 1–3 °C/min is recommended. Even at this slow rate, it is common to specify intermediate isothermal pauses to preclude exotherm. Due to these considerations, formulators must design thermoplastic-toughened epoxies to be relatively insensitive to cure ramp rate. Rheological profiles can serve as the benchmarks for these quality control efforts to ascertain the window of processing.

Conclusions

The favorable characteristics of epoxy-thermosets, including superior mechanical properties, facile processing, chemical resistance, and thermal stability, render these materials advantageous for many industrial applications. Investigations of thermoplastic toughening agents for epoxy materials has expanded over the last three decades, owing to the need for improved toughness and impact resistance in high-performance applications. Numerous analytical tools exist to characterize the properties of epoxy-thermoplastic blends (e.g., SEM, TRLS, DSC, DMA), with each

method contributing valuable insight into the fundamental and practical aspects of material properties. Because each of these analytical techniques reveals distinct aspects of material properties, a comprehensive characterization profile would encompass all of these tools to provide a multifaceted analysis of the material.

Rheology is a valuable tool for evaluating the material transitions occurring during preprocessing and cure of epoxy–thermoplastics. A prevalent goal in rheological analysis of epoxy–thermoplastics is the correlation of observed rheological measurements, such as viscosity and modulus, with molecular properties of the material, including chemical structure, molecular weight, quantity of components, reaction products, intermolecular interactions, and morphological evolution. This correlation enables the prediction of how molecular changes effect the material formulation, ultimately providing control over the design of material properties. Advantageously, rheology is often employed in industrial settings to evaluate processing parameters, design a cure cycle, and verify final product specifications and to analyze how parameters such as time, temperature, and formulation affect the material properties.

Chemorheology is useful to characterize the distinct viscoelastic changes that occur during the cure of epoxy–thermoplastics, which result from RIPS, epoxy gelation, and vitrification. A prominent structural change that transpires during the cure of many epoxy–thermoplastic blends is phase separation. Depending on the formulation (e.g., chemical structure, quantity of epoxy resin, curative, and thermoplastic) and experimental conditions (e.g., temperature, curative type), the final multiphase structure can assume various morphologies. The morphology resulting from phase separation substantially affects the toughening of the final product, with phase-inverted structures or bicontinuous structure exhibiting highly toughened characteristics. Early rheological studies of epoxy–thermoplastic blends assumed a classical phase separation mechanism, which has more recently progressed to include the factors of dynamic asymmetries during viscoelastic phase separation, where differences exist in T_g or molecular weight between the epoxy and the thermoplastic. Rheological models have been used to better understand viscoelastic phase separation during the preparation of epoxy–thermoplastic blends. Reports have shown good correlations between complex viscosity from experimental results and simulation of complex viscosity using empirical equations. The use of WLF simulations to evaluate if relaxation times obey the TTS principle has been used in various circumstances to further establish viscoelastic phase separation.

The complex viscosity profiles of epoxy–thermoplastics are greatly affected by the experimental conditions and formulations. Compared to neat epoxy materials, distinct fluctuations can occur during the phase separation, such as rapid viscosity drops during escape of low molecular weight epoxy oligomers from thermoplastics. Rheological behavior of epoxy–thermoplastics also requires considerations additional to phase separation, such as gelation of the epoxy resin and vitrification. These material transitions can occur independently or concurrently, and additional characterization techniques can help decipher between these transitions.

To date, rheological reports of epoxy–thermoplastic blends have described a narrow subset of epoxy resins (e.g., DGEBA) and thermoplastics (e.g., PEI, PES),

which opens opportunities for new explorations into alternative formulations. Because the chemical properties of the resin and the thermoplastic affect the final material properties, great potential exists to discover novel formulations with enhanced toughening properties. Rheological analysis will remain an important characterization tool during the development of new combinations of materials, including inclusion of nanomaterials, fibers, etc., to produce more complex ternary structures. Over the last three decades, great strides have been taken to improve the understanding of epoxy–thermoplastics, with characterization techniques serving as the tool to support these research advancements. In particular, innovations in instrument design of rheometers has enabled the generation of precise rheological behavior profiles in real-time to understanding the fundamental mechanistic details and characteristics of systems. The scientific community looks forward to future reports of new epoxy–thermoplastic blends, building the repertoire of toughened epoxy materials.

References

- Abbate M, Martuscelli E, Musto P, Ragosta G, Scarinzi G (1994) Toughening of a highly cross-linked epoxy resin by reactive blending with bisphenol A polycarbonate. I. FTIR spectroscopy. *J Polym Sci B* 32(3):395–408
- Barone L, Carciotto S, Cicala G, Recca A (2006) Thermomechanical properties of epoxy/poly (ϵ -caprolactone) blends. *Polym Eng Sci* 46(11):1576–1582
- Blanco I, Cicala G, Faro CL, Recca A (2003) Development of a toughened DGEBS/DDS system toward improved thermal and mechanical properties by the addition of a tetrafunctional epoxy resin and a novel thermoplastic. *J Appl Polym Sci* 89(1):268–273
- Blanco I, Cicala G, Motta O, Recca A (2004) Influence of a selected hardener on the phase separation in epoxy/thermoplastic polymer blends. *J Appl Polym Sci* 94(1):361–371
- Bonnet A, Pascault JP, Sautereau H, Camberlin Y (1999) Epoxy – diamine thermoset/thermoplastic blends. 2. Rheological behavior before and after phase separation. *Macromolecules* 32 (25):8524–8530
- Bucknall CB, Partridge IK (1983) Phase separation in epoxy resins containing polyethersulphone. *Polymer* 24(5):639–644
- Chartoff RP, Menczel JD, Dillman SH (2008) Dynamic mechanical analysis (DMA). In: *Thermal analysis of polymers*. Wiley, pp 387–495
- Cicala G, La Spina R, Recca A, Sturiale S (2006) Influence of copolymer's end groups and molecular weights on the rheological and thermomechanical properties of blends of novel thermoplastic copolymers and epoxy resins. *J Appl Polym Sci* 101(1):250–257
- Cicala G, Mamo A, Recca G, Restuccia CL (2007) Study on epoxy/thermoplastic blends based on the addition of a novel aromatic block copolymer. *Polym Eng Sci* 47(12):2027–2033
- Composites H-P (2003) Airbus A340 carbon composite spoiler made with RTM. *Composites World*, Gardner Business Media
- Cox WP, Merz EH (1958) Correlation of dynamic and steady flow viscosities. *J Polym Sci* 28 (118):619–622
- Dealy J, Plazek D (2009) Time-temperature superposition—a users guide. *Rheol Bull* 78(2):16–31
- Deng S, Djukic L, Paton R, Ye L (2015) Thermoplastic–epoxy interactions and their potential applications in joining composite structures – a review. *Compos A: Appl Sci Manuf* 68:121–132
- Di Liello V, Martuscelli E, Musto P, Ragosta G, Scarinzi G (1994) Toughening of highly crosslinked epoxy resins by reactive blending with bisphenol A polycarbonate. II. Yield and fracture behavior. *J Polym Sci B* 32(3):409–419

- Dorworth LC, Gardiner GL, Mellema GM (2009) Essentials of advanced composite fabrication and repair. Aviation Supplies & Academic, Newcastle/Washington, DC
- Galante MJ, Borrajo J, Williams RJJ, Girard-Reydet E, Pascault JP (2001) Double phase separation induced by polymerization in ternary blends of epoxies with polystyrene and poly(methyl methacrylate). *Macromolecules* 34(8):2686–2694
- Gan W, Yu Y, Wang M, Tao Q, Li S (2003) Viscoelastic effects on the phase separation in thermoplastics-modified epoxy resin. *Macromolecules* 36(20):7746–7751
- Gan W, Zhan G, Wang M, Yu Y, Xu Y, Li S (2007) Rheological behaviors and structural transitions in a polyethersulfone-modified epoxy system during phase separation. *Colloid Polym Sci* 285 (15):1727–1731
- Gan W, Xiong W, Yu Y, Li S (2009) Effects of the molecular weight of poly(ether imide) on the viscoelastic phase separation of poly(ether imide)/epoxy blends. *J Appl Polym Sci* 114 (5):3158–3167
- Gillham JK (1986) Formation and properties of thermosetting and high Tg polymeric materials. *Polym Eng Sci* 26(20):1429–1433
- Gillham JK, Benci JA, Noshay A (1974) Isothermal transitions of a thermosetting system. *J Appl Polym Sci* 18(4):951–961
- Girard-Reydet E, Sautereau H, Pascault JP, Keates P, Navard P, Thollet G, Vigier G (1998) Reaction-induced phase separation mechanisms in modified thermosets. *Polymer* 39 (11):2269–2279
- Halley PJ, Mackay ME (1996) Chemorheology of thermosets – an overview. *Polym Eng Sci* 36 (5):593–609
- Harran D, Laudouard A (1986) Rheological study of the isothermal reticulation of an epoxy resin. *J Appl Polym Sci* 32(7):6043–6062
- Hedrick JL, Yilgör I, Wilkes GL, McGrath JE (1985) Chemical modification of matrix resin networks with engineering thermoplastics. *Polym Bull* 13(3):201–208
- Hedrick JC, Patel NM, McGrath JE (1993) Toughening of epoxy resin networks with functionalized engineering thermoplastics. *Toughened plastics I. Am Chem Soc* 233:293–304
- Hodgkin JH, Simon GP, Varley RJ (1998) Thermoplastic toughening of epoxy resins: a critical review. *Polym Adv Technol* 9(1):3–10
- Hohenberg PC, Halperin BI (1977) Theory of dynamic critical phenomena. *Rev Mod Phys* 49 (3):435–479
- Jyotishkumar P, Özdilek C, Moldenaers P, Sinturel C, Janke A, Pionteck J, Thomas S (2010) Dynamics of phase separation in poly(acrylonitrile-butadiene-styrene)-modified epoxy/DDS system: kinetics and viscoelastic effects. *J Phys Chem B* 114(42):13271–13281
- Jyotishkumar P, Pionteck J, Özdilek C, Moldenaers P, Cvelbar U, Mozetic M, Thomas S (2011) Rheology and pressure-volume-temperature behavior of the thermoplastic poly(acrylonitrile-butadiene-styrene)-modified epoxy-DDS system during reaction induced phase separation. *Soft Matter* 7(16):7248–7256
- Jyotishkumar P, Moldenaers P, George SM, Thomas S (2012) Viscoelastic effects in thermoplastic poly(styrene-acrylonitrile)-modified epoxy-DDM system during reaction induced phase separation. *Soft Matter* 8(28):7452–7462
- Kim H, Char K (2000) Effect of phase separation on rheological properties during the isothermal curing of epoxy toughened with thermoplastic polymer. *Ind Eng Chem Res* 39(4):955–959
- Lange J (1999) Viscoelastic properties and transitions during thermal and UV cure of a methacrylate resin. *Polym Eng Sci* 39(9):1651–1660
- Lange J, Altmann N, Kelly CT, Halley PJ (2000) Understanding vitrification during cure of epoxy resins using dynamic scanning calorimetry and rheological techniques. *Polymer* 41 (15):5949–5955
- Le Cruz S, Pethrick RA (2011) Solvent effects on cure 1-Benzyl alcohol on epoxy cure. *Int J Polym Mater* 60(7):441–455
- Lee H, Neville K (1967) Handbook of epoxy resins. McGraw-Hill, New York
- Liu Y (2013) Polymerization-induced phase separation and resulting thermomechanical properties of thermosetting/reactive nonlinear polymer blends: a review. *J Appl Polym Sci* 127(5):3279–3292

- Luo Y, Li H, Li S (2001) Studies on phase separation of polyesterimide-modified epoxy resin. II. Effect of curing temperature on phase separation and adhesive property. *J Macromol Sci A* 38 (10):1019–1031
- MacKinnon AJ, Jenkins SD, McGrail PT, Pethrick RA (1992) A dielectric, mechanical, rheological and electron microscopy study of cure and properties of a thermoplastic-modified epoxy resin. *Macromolecules* 25(13):3492–3499
- MacKinnon AJ, Jenkins SD, McGrail PT, Pethrick RA (1993) Dielectric, mechanical and rheological studies of phase separation and cure of a thermoplastic modified epoxy resin: incorporation of reactively terminated polysulfones. *Polymer* 34(15):3252–3263
- Malkin AY, Isayev AI (2012a) 2 – Viscoelasticity. In: Malkin AY, Isayev AI (eds) *Rheology concepts, methods, and applications*, 2nd edn. Elsevier, Oxford, pp 43–126
- Malkin AY, Isayev AI (2012b) Introduction. *Rheology: subject and goals*. In: Malkin AY, Isayev AI (eds) *Rheology concepts, methods, and applications*, 2nd edn. Elsevier, Oxford, pp 1–8
- Menard KP (2008a) Dynamic testing and instrumentation. In: *Dynamic mechanical analysis*. CRC Press, Boca Raton, pp 71–93
- Menard KP (2008b) An introduction to dynamic mechanical analysis. In: *Dynamic mechanical analysis*. CRC Press, Boca Raton, pp 1–13
- Menard KP (2008c) Rheology basic. In: *Dynamic mechanical analysis: a practical introduction*. CRC Press, Boca Raton, pp 37–56
- Menard KP (2008d) Time and temperature scans part II. In: *Dynamic mechanical analysis: a practical introduction*. CRC Press, Boca Raton, pp 123–143
- Mezger TG (2014) *The rheology handbook*. Vincentz Network, Hanover
- Michon C, Cuvelier G, Launay B (1993) Concentration dependence of the critical viscoelastic properties of gelatin at the gel point. *Rheol Acta* 32(1):94–103
- Odian G (2004a) Radical chain polymerization. In: *Principles of polymerization*. Wiley, Hoboken, pp 198–349
- Odian G (2004b) Step polymerization. In: *Principles of polymerization*. Wiley, Hoboken, pp 39–197
- Parameswaranpillai J, Moldenaers P, Thomas S (2013) Rheological study of the SAN modified epoxy-DDM system: relationship between viscosity and viscoelastic phase separation. *RSC Adv* 3(46):23967–23971
- Pascault J-P, Williams RJJ (2010) General concepts about epoxy polymers. In: *Epoxy Polymers*. Wiley-VCH Verlag GmbH & Co. KGaA, Weinheim, pp 1–12
- Pearson RA (1993) Toughening epoxies using rigid thermoplastic particles. *Toughened plastics I*. *Am Chem Soc* 233:405–425
- Raghava RS (1983) 28th National SAMPE Symposium, Corvino
- Raghava RS (1987) Role of matrix-particle interface adhesion on fracture toughness of dual phase epoxy-polyethersulfone blend. *J Polym Sci B* 25(5):1017–1031
- Raghava RS (1988) Development and characterization of thermosetting-thermoplastic polymer blends for applications in damage-tolerant composites. *J Polym Sci B* 26(1):65–81
- Roller MB (1975) Characterization of the time-temperature-viscosity behavior of curing B-staged epoxy resin. *Polym Eng Sci* 15(6):406–414
- Roller MB (1986) Rheology of curing thermosets: a review. *Polym Eng Sci* 26(6):432–440
- Rusli A, Cook WD, Schiller TL (2014) Blends of epoxy resins and polyphenylene oxide as processing aids and toughening agents 2: curing kinetics, rheology, structure and properties. *Polym Int* 63(8):1414–1426
- Ryan ME (1984) Rheological and heat-transfer considerations for the processing of reactive systems. *Polym Eng Sci* 24(9):698–706
- Serrano D, Harran D (1989) On the increase of viscoelastic modulus with advancement of reaction of an epoxy resin. *Polym Eng Sci* 29(8):531–537
- Tajima YA, Crozier D (1983) Thermokinetic modeling of an epoxy resin I. Chemoviscosity. *Polym Eng Sci* 23(4):186–190
- Tajima YA, Crozier DG (1986) Chemorheology of an amine-cured epoxy resin. *Polym Eng Sci* 26 (6):427–431

- Tanaka H (1993) Unusual phase separation in a polymer solution caused by asymmetric molecular dynamics. *Phys Rev Lett* 71(19):3158–3161
- Tanaka H (2000) Viscoelastic phase separation. *J Phys Condens Matter* 12(15):R207
- Tanaka H (2012) Viscoelastic phase separation in soft matter and foods. *Faraday Discuss* 158:371–406
- Tanaka H, Araki T (2006) Viscoelastic phase separation in soft matter: numerical-simulation study on its physical mechanism. *Chem Eng Sci* 61(7):2108–2141
- Tercjak A, Remiro PM, Mondragon I (2005) Phase separation and rheological behavior during curing of an epoxy resin modified with syndiotactic polystyrene. *Polym Eng Sci* 45(3):303–313
- Tercjak A, Serrano E, Remiro PM, Mondragon I (2006) Viscoelastic behavior of thermosetting epoxy mixtures modified with syndiotactic polystyrene during network formation. *J Appl Polym Sci* 100(3):2348–2355
- Thermal solutions: determination of the linear viscoelastic region of a polymer using a strain sweep on the DMA 2980. TA Instruments. T. Instruments. TS-61: TS-61
- Tribut L, Fenouillot F, Carrot C, Pascault JP (2007) Rheological behavior of thermoset/thermoplastic blends during isothermal curing: experiments and modeling. *Polymer* 48(22):6639–6647
- Tribut L, Carrot C, Fenouillot F, Pascault JP (2008) A phenomenological modification of rheological models for concentrated two-phase systems: application to a thermoplastic/thermoset blend. *Rheol Acta* 47(4):459–468
- Unnikrishnan KP, Thachil ET (2006) Toughening of epoxy resins. *Des Monomers Polym* 9(2):129–152
- van de Witte P, Dijkstra PJ, van den Berg JWA, Feijen J (1996) Phase separation processes in polymer solutions in relation to membrane formation. *J Membr Sci* 117(1–2):1–31
- Varley RJ (2007) Reaction kinetics and phase transformations during cure of a thermoplastic-modified epoxy thermoset. *Macromol Mater Eng* 292(1):46–61
- Wang M, Yu Y, Wu X, Li S (2004) Polymerization induced phase separation in poly(ether imide)-modified epoxy resin cured with imidazole. *Polymer* 45(4):1253–1259
- Williams ML, Landel RF, Ferry JD (1955) The temperature dependence of relaxation mechanisms in amorphous polymers and other glass-forming liquids. *J Am Chem Soc* 77(14):3701–3707
- Williams RJ, Rozenberg B, Pascault J-P (1997) Reaction-induced phase separation in modified thermosetting polymers. In: *Polymer analysis polymer physics*, vol 128. Springer, Berlin/Heidelberg, pp 95–156
- Winter HH (1987) Can the gel point of a cross-linking polymer be detected by the $G' - G''$ crossover? *Polym Eng Sci* 27(22):1698–1702
- Winter HH, Chambon F (1986) Analysis of linear viscoelasticity of a crosslinking polymer at the gel point. *J Rheol* 30(2):367–382
- Xu J, Holst M, Rüllmann M, Wenzel M, Alig I (2007) Reaction induced phase separation in a polysulfone modified epoxy anhydride thermoset. *J Macromol Sci Part B* 46(1):155–181
- Yousefi A, Lafleur PG, Gauvin R (1997) Kinetic studies of thermoset cure reactions: a review. *Polym Compos* 18(2):157–168
- Yu Y (2014) Characterization of polymer blends: rheological studies. In: *Characterization of polymer blends*. Wiley, Wiley-VCH Verlag GmbH & Co. KGaA, pp 133–158
- Yu Y, Zhang Z, Gan W, Wang M, Li S (2003) Effect of polyethersulfone on the mechanical and rheological properties of polyetherimide-modified epoxy systems. *Ind Eng Chem Res* 42(14):3250–3256
- Yu Y, Wang M, Gan W, Tao Q, Li S (2004) Polymerization-induced viscoelastic phase separation in polyethersulfone-modified epoxy systems. *J Phys Chem B* 108(20):6208–6215
- Yu Y, Wang M, Gan W, Li S (2006) Phase separation and rheological behavior in thermoplastic modified epoxy systems. *Colloid Polym Sci* 284(10):1185–1190
- Yu Y, Wang M, Foix D, Li S (2008) Rheological study of epoxy systems blended with poly(ether sulfone) of different molecular weights. *Ind Eng Chem Res* 47(23):9361–9369

Bejoy Francis

Abstract

Thermoplastic toughening of epoxy resins had aroused considerable interest in the past few decades. Functionalized as well as nonfunctionalized thermoplastics have been extensively used to toughen epoxy resins. The ultimate properties of the blends are strongly dependent on the cure conditions employed. Investigation of the cure kinetics is therefore very important in predicting the ultimate properties. Kinetic analysis gives information regarding the extent of cure, curing mechanism, activation energy, etc. Techniques such as differential scanning calorimetry, Fourier transform infrared spectroscopy, dielectric relaxation spectroscopy, etc. are useful tools for kinetic analysis. Various models have been developed for the evaluation of cure kinetics. This chapter summarizes the various aspects of the kinetics of epoxy resin/thermoplastic blends.

Keywords

Cycloaliphatic amine-cured resins • Differential scanning calorimetry • Epoxy resin/thermoplastic blends • Dynamic kinetic analysis • Isothermal kinetic analysis • Epoxy resins • Curing • Etherification • Flynn–Wall–Ozawa method • Hardeners • Isothermal kinetic model • Kamal model • Kinetic analysis • Kinetic modeling • Kissinger method • Polyoxypropylene diamine (POPDA) • Reaction-induced phase separation • Transamidation reaction • Vitrified state

B. Francis (✉)

Department of Chemistry, St. Berchmans College, Changanassery, Kottayam, Kerala, India

e-mail: bejoy@sbcollege.ac.in

Contents

Introduction	650
Curing of Epoxy Resins	650
Kinetic Modeling	655
Kamal Model (Isothermal Kinetic Model)	655
Kissinger Method (Dynamic Kinetic Model)	656
Flynn–Wall–Ozawa Method (Dynamic Kinetic Model)	657
Kinetic Analysis	657
Kinetic Analysis Using DSC	658
Epoxy Resin/Thermoplastic Blends	659
Dynamic Kinetic Analysis	660
Isothermal Kinetic Analysis	662
Conclusions	669
References	670

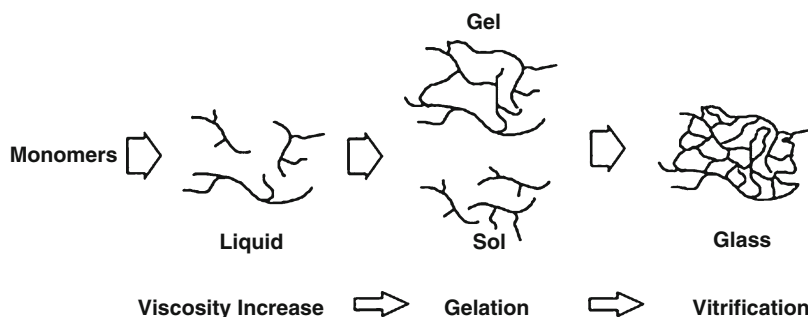
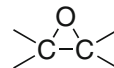
Introduction

Epoxy resins were made available commercially in 1946. Since then, their technology has grown to such an extent that they were accepted as workhorse raw material among the various thermosetting resins. Epoxy resin technology is extensively used in a variety of applications ranging from coatings to military and aerospace applications due to their extraordinary mechanical properties and good handling characteristics (May 1988). Adhesion to a variety of substrates, low cure shrinkage, processing flexibility, etc. are a few important properties of epoxy resins to mention (Skiest 1978; Pascault and Williams 2010). Epoxy resins are now available in various physical forms. The diglycidyl ether of bisphenol A (DGEBA) is the widely used resin among the different types of epoxy resins commercialized. Epoxy phenol novolac (EPN) and epoxy cresol novolac (ECN) resins are also commercially important aromatic glycidyl ether resins. The physical state of the resins changed as the functionality changed. Multifunctional epoxy resins are either highly viscous or low melting solids. Such resins are mainly used in high-performance materials. Multifunctional glycidyl amino resins like triglycidyl-p-aminophenol (TGAP) and tetraglycidyl-4,4'-diaminodiphenylmethane (TGDDM) are used for such applications.

Curing of Epoxy Resins

Epoxy resins are characterized by a three-membered ring known as epoxy, epoxide, oxirane, or ethoxylene group, consisting of an oxygen atom attached to two interconnected carbon atoms as shown in Fig. 1.

The strained three-membered ring structure makes epoxy resin reactive. Hence it is attacked by nucleophilic and electrophilic reagents. The ultimate properties of epoxy resin are achieved by converting them to insoluble and infusible network. This is achieved by reaction with various chemical compounds known as curing

Fig. 1 Epoxy group**Fig. 2** Schematic representation of the physical changes occurring during the curing of epoxy resin

agents or hardeners. A large number of compounds with active hydrogen atoms are capable of reacting with epoxy resin. Amines, phenols, alcohols, thiols, carboxylic acids, acid anhydrides, etc. are potential coreactive cross-linking agents for epoxy resin. However the choice depends on the availability, processability, handling characteristics, and final properties of the cured resin. For industrial application, the final performance and processing aids determine the selection of curing agent (Young and Chuang 1995; Holmberg and Berglung 1997; Abraham and Mc Ilhagger 1998; Pascault et al. 2002).

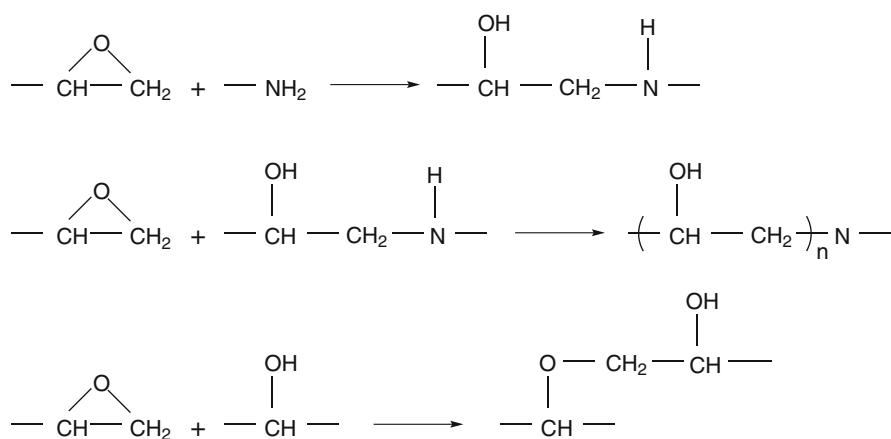
The ultimate properties can be tailored as per user requirement by judicious selection of the resin and curing agent. The functionality of the reactants controls the network formation and cross-link density. The network structure, curing degree, curing time, and cure temperatures determine the physical properties of the cured epoxy resins (Montserrat and Málek 1993; Caçcaval et al. 1997; Jagadeesh et al. 2000; Roşu et al. 2001). The epoxy resin and curing agent forms linear chains in the early stages of curing. As the reaction proceeds further, branches will form and finally it emerges as a highly cross-linked structure. During curing, the molecular weight of epoxy resin increases rapidly and becomes linked together into networks of infinite molecular weight.

Many physical changes occur during curing of epoxy resins. Usually the processing of epoxy resin is done in the liquid state. If the resin is in the solid state, it is melted and processed. The low viscosity liquid first forms a sol. As cross-linking reaction proceeds, it becomes a gel, and further cross-linking leads to a highly cross-linked structure called glassy state or vitrified state. The curing reaction is accompanied by a gradual increase in the viscosity of the epoxy resin-curing agent mixture. Once the system gels, the curing reaction becomes slow due to the increase in viscosity. A schematic representation of the physical changes during curing reaction of epoxy resin is given in Fig. 2. The handling, processing, and development of ultimate properties are dependent on gelation and vitrification.

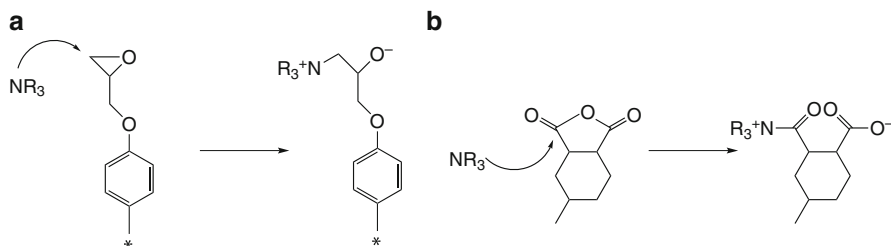
Although a large number of compounds are reactive toward epoxy group, amines and anhydrides are the most commonly used curing agents. A range of aromatic and aliphatic amines were used for curing epoxy resins. The ultimate properties of the resin depend on the nature of the amine used. Aliphatic amine offers ambient cure temperature and low viscosity. The cured resins have good physical properties and excellent chemical and solvent resistance. They retain their properties up to 100 °C for extended periods. These properties are controlled by the mixing ratio. However the toughness of the cured resin is low. Cycloaliphatic amine-cured resins have better toughness than aliphatic amine-cured resins. The reactivity of cycloaliphatic amine toward epoxy is less compared to acyclic aliphatic amines. Hence these systems have longer pot life. Aromatic amines are less reactive than aliphatic and cycloaliphatic amines due to the delocalization of electrons. Hence these systems have long pot lives and need elevated temperature for curing. But they have better chemical and thermal resistance than aliphatic and cycloaliphatic amine-cured resins. Also they retain their properties at temperatures as high as 150 °C for longer times. Another important class of curing agents is acid anhydride. They usually require catalyst and post curing for optimum performance. Other characteristics of anhydride curing are low viscosity, low exothermic heat of reaction, and long pot life. They extend excellent mechanical and electrical properties too.

The reaction of epoxide with amine involves several reactions like addition of amine to epoxide, homopolymerization of epoxy by etherification or ionic polymerization, cyclisation, and various side transformations and degradation reactions. In most cases, the addition of amine is the predominating reaction. The reaction between epoxy resin and an amine-curing agent is given in Scheme 1.

Reaction of primary amine with epoxy yields a secondary amine and secondary hydroxyl group. The secondary amine in turn reacts with an epoxy to give a tertiary amine and two secondary hydroxyl groups. The last step is the etherification;



Scheme 1 Reaction between amine-curing agent and epoxy resin



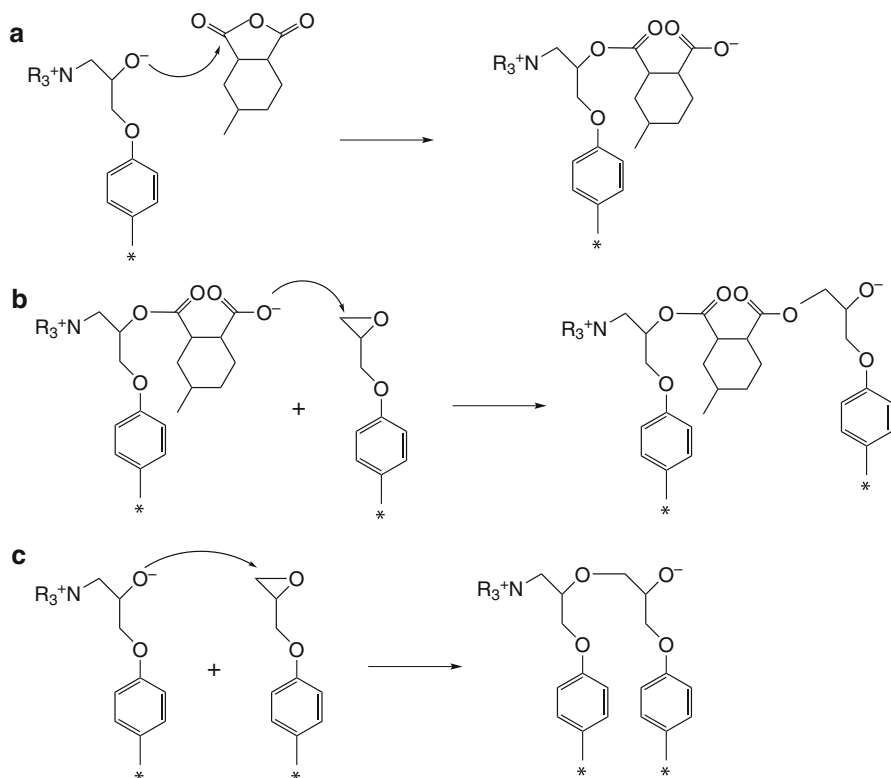
Scheme 2 Initiation step of the curing of epoxy-anhydride formulations with tertiary amines by nucleophilic attack (a) to an oxirane ring and (b) to a cyclic anhydride

however, the tendency of the etherification reaction depends on the curing temperature, basicity of the diamine, and the initial epoxy/amine ratio (Lunak and Dusek 1975; Riccardi and Williams 1986).

The reactivity of amine toward epoxy curing changed with the structure and other groups on the amine. Experiments using size exclusion chromatography and viscosity measurements on the reactivity of amine toward DGEBA epoxy resin revealed that DDM was the most reactive. The reactivity decreased in the order DDM > BAPP > BAPS > 3,3'-DDS > 4,4'-DDS, where DDM, BAPP, BAPS, 3,3'-DDS, and 4,4'-DDS represent 4,4'-diaminodiphenylmethane, 2,2'-bis[4-(4-aminophenoxy)phenyl]propane, bis[4-(4-aminophenoxy)phenyl]sulfone, 3,3'-diaminodiphenylsulfone, and 4,4'-diaminodiphenylsulfone, respectively. Basicity of the amines was the controlling factor. In DDS, sulfone group, being an electron withdrawing group, decreased the basicity of the diamine. 4,4'-DDS is least reactive because the electron transfer from -NH_2 to -SO_2 is the easiest for *para* substitution. BAPP and BAPS are more reactive than DDS and less reactive than DDM due to the action of phenoxy group (Grillet et al. 1989). The reactivity of amine decreased in the order DDM > MDEA > DDS > MCDEA for DGEBA epoxy resin (Reydet et al. 1995). MDA, MDEA, and MCDEA exhibited same secondary to primary amine reactivity ratio of 0.65, but DDS exhibited a different value (0.45). The lower value is due to the lower number of stable conformations afforded by -SO_2 group in comparison to -CH_2 group. MDEA and MCDEA represent 4,4'-methylenebis(2,6-diethylaniline) and 4,4'-methylenebis(3-chloro-2,6-diethylaniline), respectively.

The anhydride curing of epoxy resin is rather complex due to the large number of competitive reactions involved in the curing reaction. The reactions become more complicated in the presence of accelerators, which is often necessary when anhydrides are used as the curing agent. Many reaction schemes have been proposed in the presence and absence of accelerators (Dusek et al. 1982; Khanna and Chanda 1993, 1996; Teil et al. 2004; Fernandez-Francos et al. 2014). Two possible initiation steps are there as shown in Scheme 2. The tertiary amine can nucleophilically attack the epoxy ring or the anhydride.

It is believed that Scheme 2a, the reaction of alkoxide ion with anhydride to form carboxylate anion, takes place. The anion then reacts with epoxy group to give another alkoxide ion (Scheme 3a, b). In the presence of excess epoxy groups, the



Scheme 3 Propagation of the reaction by (a) nucleophilic attack of the alkoxide anion to an anhydride, (b) followed by nucleophilic attack of the carboxylate anion to an epoxy group, or (c) nucleophilic attack of the alkoxide anion to an epoxy group

alkoxide anion can add to another epoxy group (Scheme 3c). Presence of excess epoxy is necessary because the formation of resonance-stabilized carboxylate anion is highly favorable.

In an alternative scheme, the epoxy group reacts directly with the epoxy group in the propagation step. Finally the initiator is regenerated by unimolecular elimination of the carboxyl-amine ion pair followed by a proton transfer (Mauri et al. 1997).

The hydroxyl group can react with anhydrides either in the presence or absence of a catalyst-like tertiary amine giving rise to a carboxylic ester. The carboxylic acids can then react with epoxy groups to give rise to β -hydroxy esters in the presence of catalysts (Trappe et al. 1991; Blank et al. 2002; Rocks et al. 2004; Foix et al. 2009). When tertiary amines are used as catalysts, the mechanism involved the formation of a carboxylate anion (Blank et al. 2002). In addition to the above mechanisms, other reactions like transesterification can occur in the presence of carboxylic acids (Matějka et al. 1985). From the above schemes, it is clear that the anhydride curing of epoxy resin is quite complicated.

Kinetic Modeling

Two types of equations are used for kinetic modeling; one is based on the reaction pathway and the other is the phenomenological kinetic equations (Pascault et al. 2002). The model proposed by Horie et al. (1970) and simplified by Kamal and Sourour is the most widely used phenomenological kinetic equation (Kamal and Sourour 1973; Sourour and Kamal 1976). The Kissinger and Flynn–Wall–Ozawa models are also used in the kinetic analysis of epoxy curing.

Kamal Model (Isothermal Kinetic Model)

This model is simple to use and does not need prior knowledge of the reaction mechanism. It has been used widely in various thermosetting systems for resin transfer molding (RTM), filament winding, resin injection molding (RIM), micro-wave curing, etc. (Karkanias et al. 1996; Halley and Mackay 1996; Bonnaud et al. 2000; Um et al. 2002; Naffakh et al. 2005). The model assumes that the epoxy–amine reaction is catalyzed by the hydroxyl groups formed during curing and those existing in the resin or by acidic impurities present in the system. Also the degree of reactivity of primary and secondary amine hydrogens toward epoxy group is the same. The kinetic equation is

$$\frac{d\alpha}{dt} = (k_1 + k_2\alpha^m)(1 - \alpha)^n \quad (1)$$

where k_1 is the rate constant for the reaction catalyzed by groups initially present in the resin, k_2 is the rate constant for the reaction catalyzed by hydroxyl groups formed during the reaction, and $m + n$ gives the overall order of the reaction.

In a modified version of the Kamal equation, it was assumed that the curing reaction followed second-order process. But as cure reaction proceeds, the glass transition temperature T_g of the system approaches the curing temperature T_{cure} . In addition, the viscosity of the system will also increase. When T_g approaches T_{cure} , the reaction becomes diffusion controlled, and the reaction rate becomes zero before complete reaction. So the final conversion is dependent on the cure temperature. The effect of cure temperature is incorporated in the models replacing the term $1 - \alpha$ with $\alpha_{\text{max}} - \alpha$, where α_{max} represents the final conversion reached at the investigated temperature (Musto et al. 1999).

The equation becomes

$$\frac{d\alpha}{dt} = (k_1 + k_2\alpha^m)(\alpha_{\text{max}} - \alpha)^n \quad (2)$$

Plot of $\frac{d\alpha}{dt} / (\alpha_{\text{max}} - \alpha)$ versus α gives a straight line with intercept k_1 and slope k_2 . These constants follow the Arrhenius relationship with cure temperature.

$$k_i = A_i e^{-E_i/RT} \quad (3)$$

$$i = 1, 2$$

In these models, the kinetic parameters were determined using least squares method without any constraints. Toward the end of the curing reaction, the reaction becomes diffusion controlled. In order to incorporate diffusion control, a semi-empirical equation was used. When degree of cure reaches critical value α_c , diffusion becomes the dominant phenomenon, and rate constant k_d is given by

$$k_d = k_c e^{-C(\alpha - \alpha_c)} \quad (4)$$

where k_c is the rate constant for chemical kinetics and C is the diffusion coefficient.

According to this equation, diffusion control begins when α becomes equal to α_c . But in actual conditions, the onset of diffusion control is a gradual process, and there is a certain curing stage where both chemical and diffusion factors are controlling the reaction.

The overall effective rate constant k_e is given by

$$\frac{1}{k_e} = \frac{1}{k_d} + \frac{1}{k_c} \quad (5)$$

The diffusion factor $f(\alpha)$ is given by

$$f(\alpha) = \frac{k_e}{k_c} = \frac{1}{1 + \exp[C(\alpha - \alpha_c)]} \quad (6)$$

The diffusion factor is the ratio of the experimental reaction rate to the reaction rate predicted by Kamal model. When α is much smaller than critical value ($\alpha \ll \alpha_c$), $f(\alpha)$ approximates unity, and the reaction is kinetically controlled, and diffusion effect is negligible. As α approaches α_c , $f(\alpha)$ begins to decrease and approaches zero as the reaction effectively stops. The effective reaction rate at any conversion is equal to the chemical reaction rate multiplied by $f(\alpha)$. The values of α_c and C are determined by the nonlinear regression analysis to $f(\alpha)$ versus α plot.

Kissinger Method (Dynamic Kinetic Model)

In the Kissinger method, the activation energy is obtained from the maximum reaction rate where $\frac{d}{dt}(d\alpha/dt)$ is zero under a constant heating rate condition.

$$\frac{d \left[\ln \left(q/T_p^2 \right) \right]}{d(1/T_p)} = -\frac{E}{R} \quad (7)$$

where T_p is the maximum rate temperature, q is the constant heating rate, E is the activation energy, and R is the gas constant. A plot of $\ln(q/T_p^2)$ versus $1/T_p$ gives the activation energy without a specific assumption on the conversion-dependent function.

Flynn–Wall–Ozawa Method (Dynamic Kinetic Model)

In this method, it is assumed that the extent reaction is proportional to the heat generated during the reaction. The reaction rate is expressed as

$$\frac{d\alpha}{dt} = k(T)f(\alpha) \quad (8)$$

where t is the time, $k(T)$ is the Arrhenius rate constant, and $f(\alpha)$ is a function that depends on the reaction mechanism. The integrated form of the above equation is

$$g(\alpha) = \int_0^{\alpha} \frac{d\alpha}{f(\alpha)} = k(T)t \quad (9)$$

where $g(\alpha)$ is the integrated form of the conversion dependent function.

Flynn–Wall–Ozawa modified the equation for $g(\alpha)$ as

$$\log(q) = \log \left[\frac{AE}{g(\alpha)R} \right] - 2.315 - \frac{0.457E}{RT} \quad (10)$$

where A is a pre-exponential factor, q is the heating rate, R is the universal gas constant, and T is the temperature.

The activation energy (E) at different conversion can be calculated using this equation. The activation energy can be calculated from the slope $\frac{0.457E}{RT}$, obtained from a plot of $\log(q)$ versus $1/T$. It is also assumed that the degree of conversion is independent of heating rate once exothermic peak is reached (Salla and Ramis 1996).

Kinetic Analysis

Analytical techniques such as differential scanning calorimetry (DSC) (Montserrat and Martin 2002; Ivankovic et al. 2003; Swier et al. 2004), thermal scanning rheometry (Laza et al. 1999), dielectric spectroscopy (Levita et al. 1996), Raman spectroscopy (Overbeke et al. 2001), and Fourier transform infrared spectroscopy (FTIR) (George et al. 1991; Varley et al. 1995; Mijović et al. 1996) have been used to monitor the curing reaction of epoxy resins. Extensive kinetic analysis of the curing reaction revealed that the epoxy-amine curing reaction followed an autocatalytic mechanism (Vyazovkin and

Sbirrazzuoli 1996; Shen et al. 2001; Zvetkov 2001). The curing kinetics was influenced by the changes in the chemical structure of curing agents (Kim and Lee 2002).

Kinetic Analysis Using DSC

DSC is a convenient and simple-to-use tool for monitoring cure reaction since precise results were obtained with a small amount of sample in a relatively short time span. The basic assumption is that the heat evolution recorded by DSC is proportional to the extent of consumption of the functional groups, such as the epoxide groups in the epoxy resin or amine groups in the curing agent. DSC has two advantages: (i) it is the reaction rate method that permits to measure with great accuracy both the rate of reaction and degree of conversion, and (ii) the DSC cell may be considered as a mini-reactor without temperature gradient. Both isothermal and dynamic measurements can be used to follow the cure reaction. The dynamic measurements are fast compared to isothermal measurements. DSC kinetics provides heat flow and heat generation data required for the solution of the heat/mass transfer equation. The basic assumption for the application of DSC technique to the cure of the epoxy resin is that the rate of reaction is proportional to the measured heat flow (ϕ).

$$\text{Rate of reaction, } \frac{d\alpha}{dt} = \frac{\phi}{\Delta H} \quad (11)$$

where ΔH is the enthalpy of curing reaction.

The curing involves several reactions including primary and secondary amine attack on epoxy group, homopolymerization, etherification, and degradation (Schiraldi and Baldini 1983). This makes the analysis of polymerization kinetics from dynamic DSC measurements difficult. But in isothermal mode, the overall process can be analyzed, and more information regarding the kinetics can be obtained (Sourour and Kamal 1976). The isothermal measurements provide more reliable heat of reaction and kinetic parameters (Salla and Ramis 1996; Gonis et al. 1999).

The important parameters required for kinetic analysis are the total heat of the reaction ΔH_{tot} and the fractional conversion α at time t . The ΔH_{tot} can be obtained from dynamic and isothermal methods in the following ways. (i) ΔH_{tot} was taken as the average of the enthalpy values obtained from the calorimetric measurements at different heating rates in dynamic mode. (ii) The sample is analyzed isothermally at a particular temperature, and after the measurement, the same sample was analyzed in dynamic mode for examining the completeness of the curing reaction. The sum of the heat of reaction obtained from isothermal measurement and the subsequent dynamic mode is taken as ΔH_{tot} .

In order to calculate the conversion (α) at time t , the heat of reaction at time t (ΔH_t) is required. The isothermal scan of the sample was done and the curve was integrated at different times. From the area of the curve at a particular time, the heat of reaction at that time interval can be calculated. In another approach, the sample

was cured isothermally and the curing reaction was quenched at different time intervals. The dynamic DSC scan of the quenched samples gave the residual heat of reaction. The difference between the total heat of reaction and the residual heat will give the value of ΔH_{tot} . From these values, the conversion α at time t is calculated using the equation

$$\alpha = \frac{\Delta H_t}{\Delta H_{tot}} \quad (12)$$

Epoxy Resin/Thermoplastic Blends

Blending two or more polymers is an easy and cost-effective way of developing materials with desirable properties. The ultimate properties of the blends can be manipulated according to end use by the proper selection of component polymers. As mentioned in the introduction, the properties of epoxy resin are attributed to their high cross-link density. Because of high cross-link density, these materials have very low resistance to crack initiation and propagation. Therefore it is very important to increase the toughness of these materials without causing major losses in other desirable properties. Of all the methods that have been considered and adopted in an attempt to alleviate the brittle characteristics of epoxy resin, elastomeric and thermoplastic (TP) modifications were found to be most successful. The frequently used thermoplastics are polysulfone (Andrés et al. 1998; Mimura et al. 2000), polyether imide (PEI) (Reydet et al. 1997; Bonnet et al. 2001), polyether ether ketone (Pasquale et al. 1997; Francis et al. 2005, 2006a, b, 2007), polycarbonate (PC) (Liello et al. 1994), polyethylene terephthalate (Ochi et al. 1989, 1994), etc.

The addition of a thermoplastic modifier generates further complexities in the already complicated system. The following events could happen upon adding a thermoplastic to the epoxy resin:

- Increase in the viscosity of the system
- Interaction of the functional groups on thermoplastic with epoxy resin
- Reaction-induced phase separation (RIPS) upon curing
- Entrapment of some thermoplastic in epoxy phase and vice versa

Other factors such as gelation, vitrification, and change from chemical kinetic to diffusion control with the advancement of curing also influence the processing and ultimate properties of the blend.

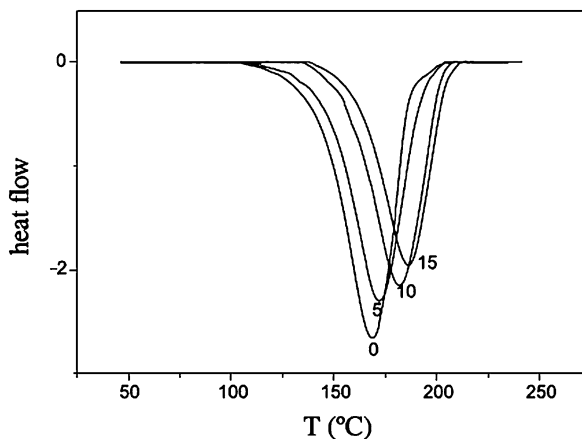
The cured epoxy resin/thermoplastic blends as well as the epoxy resin result from the irreversible reaction of the reactive species in the formulation. This means that the properties once fixed cannot be altered at a later stage. Thus there is an intimate relationship between the ultimate properties, structure, and reaction kinetics. Kinetic parameters provide significant information about the final structure of the network, properties, and material processability. Hence the kinetic studies of epoxy resin/thermoplastic blends are extremely important.

Dynamic Kinetic Analysis

Extensive research has been done on the kinetics of thermoplastic-toughened epoxy resin. The presence of thermoplastic did not alter the autocatalytic mechanism observed in epoxy resin curing (Barral et al. 2000a; Francis et al. 2003, 2006c; Naffakh et al. 2005; Cabezudo et al. 2006; Prolongo et al. 2007; Lopez et al. 2009; Jyotishkumar et al. 2010, 2012; Jyotishkumar and Thomas 2011; Xu et al. 2012). But the extent of cure, maximum rate of the reaction, conversion at maximum rate, activation energy, etc., are affected by the curing conditions and the amount of thermoplastic present in the blends. The kinetic parameters are also influenced by the thermoplastic used to toughen epoxy resin. Figure 3 represents the heat flow versus temperature curves for a thermoplastic-toughened epoxy resin. The exothermic peak temperature (T_p) shifted to higher values in the blends. The increased shift in T_p is due to the decrease in the polymerization rate due to a dilution effect where the presence of thermoplastic reduces the concentration of reactive groups, thus decreasing the cure rate (Rusli et al. 2014). The decrease in reaction rate can also be due to the decrease in the amount of catalytic group. For example, in nadic methyl anhydride (NMA)-cured tetrafunctional epoxy resin, benzyl dimethylaniline (BDMA) was used as the catalyst. But the carboxyl end group in perfluoroether oligomer used as modifier reacted with the catalyst to form quaternary ammonium salt decreasing the amount of catalyst which in turn reduced the final conversion (Musto et al. 2001).

Shoulder peaks are not generally expected in the thermograms. Cyanate ester-cured DGEBA epoxy resin modified with phenolphthalein poly(ether ketone) (PEK-C) presents a different behavior. It is observed from the dynamic scan of the blends in Fig. 4 that the initial temperature (T_i) and T_p decreased with increase in PEK-C content. A shoulder peak was also observed in the dynamic scan. These changes from the expected behavior are due to the fast curing rate of the epoxy resin

Fig. 3 Dynamic thermograms for neat and epoxy matrices with several contents of polyethersulfone (Reprinted from Eur Polym J (2001) 37:1863 with permission from Elsevier)



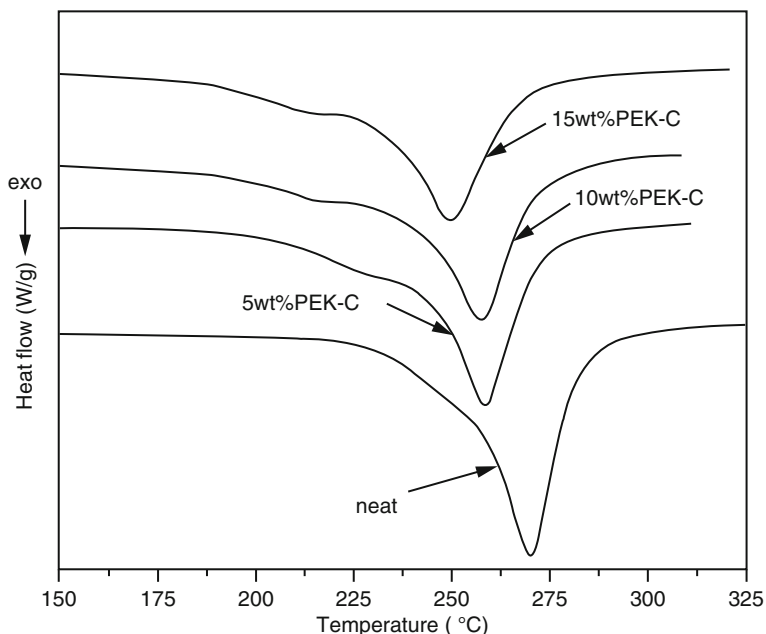


Fig. 4 Dynamic DSC thermograms of epoxy/PEK-C blends at a heating rate of 10 °C/min (Reprinted from *J App Polym Sci* (2009) 111:2590 with permission from Wiley)

as a result of the accelerated trimerization reaction of cyanate monomers by the phenolic end groups on PEK-C (Li et al. 2009).

Two distinct peaks are explicit in the dynamic DSC thermograms (Fig. 5) of a bisphenol A polycarbonate-modified DGEBA epoxy resin (Lin et al. 1997) cured with diamines. An aliphatic amine-curing agent, polyoxypropylene diamine (POPDA), with different molecular weights was used to cure the blends. The major peak was due to the heat generated by the normal curing reaction between POPDA and epoxide, and the second peak was due to the substitution reactions between N-aliphatic aromatic carbamate and urea with hydroxyl group of the epoxy.

When a thermoplastic is added to an epoxy resin, it will increase the viscosity of the system. Also the long polymer chains prevent the diffusion of epoxy and reactive group on the curing agent toward each other. In addition, the concentration of reactive species decreased with blending. As a result of the combined effects mentioned above, the heat of polymerization obtained from the dynamic scans decreased with the addition of thermoplastics. The decrease became more pronounced with the thermoplastic content in the blends (Barral et al. 1999; Fernandez et al. 2001; Lopez et al. 2001; Benito and Esteban 2005; Mounif et al. 2009). However the decrease in ΔH_{tot} for polycarbonate (PC)-modified epoxy is due to the following reason: transamidation reaction between amine and carbonate which proceeds at a high rate at room temperature; the exotherm of this reaction being not included in these thermograms, the amine groups participating in the transamidation

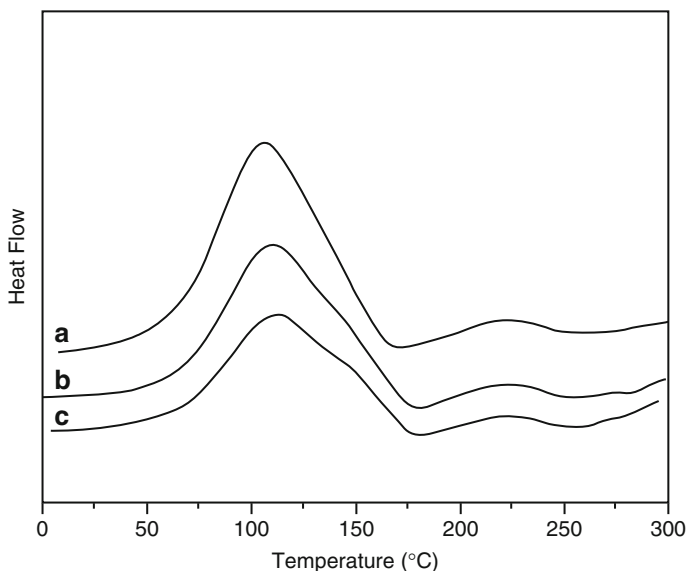


Fig. 5 Dynamic DSC runs in the temperature range between 30 °C and 300 °C (Reprinted from *J Polym Sci Part B Polym Phys* (1997) 35:2169 with permission from Wiley)

reaction does not react with oxirane, causing nonstoichiometry between oxirane and amine, and the heat of substitution reactions may be substantially lower than that of the normal curing reaction. The transamidation reaction produced phenolic hydroxyl groups which can catalyze epoxy–amine reaction. But the transamidation reaction and presence of PC dilute the system and decrease the value of the pre-exponential factor A (Lin et al. 1997). When amino-PC was used as the modifier, the amino group reacted with epoxy resin causing an increase in ΔH_{tot} and decrease in activation energy (Hao et al. 2001). When multiepoxy-terminated poly (2,6-dimethyl-1,4-phenylene oxide) was used to modify epoxy resin, ΔH_{tot} increased because of the reaction of terminal epoxy groups with the curing agent (Wang et al. 2014). The activation energy tends to increase with increase in thermoplastic in the blends. The kinetic analysis of the curing reaction in SAN/DGEBA/DDS system was performed using Kissinger and Flynn–Wall–Ozawa methods. Both the methods gave similar kinetic parameters. In this system, the activation energy showed little variation with increase in SAN in the blends (Lopez et al. 2001).

Isothermal Kinetic Analysis

The isothermal measurements of the blends and neat resin were carried out at different temperatures. The fractional conversion and rate of reaction were calculated from the heat flow against time curves. The rate of reaction, final conversion, position of peak in the isothermal curve, and area changed with isothermal cure temperature. Conventionally the isothermal curve broadened, and peak in the

isothermal curve shifted to higher cure time indicating reduced curing rate (Jenninger et al. 2000; Martinez et al. 2000; Barral et al. 2000b). But an increase in cure temperature increased the rate, final conversion, and conversion at which vitrification occurred (Fernandez et al. 2001; Zhang et al. 2009). In most of the blends, the reaction rate increased first and then decreased as the reaction progressed. This is typical of autocatalytic reactions. A representative example is DDS-cured TGDDM epoxy resin modified with polystyrene-co-acrylonitrile (SAN). The maximum conversion and rate of conversion decreased with the addition of SAN to epoxy resin. The values decreased further as more and more SAN is added to epoxy resin (Barral et al. 1999; Lopez et al. 2001).

There are exceptions to the expected behavior. In poly(2,6-dimethyl-1,4-phenylene oxide) (PPO)-modified cyanate ester cured epoxy resin, PPO acted as a catalyst in the curing reaction resulting in a higher curing rate for the blend than neat resin in the beginning, but later the reaction rate decreased (Wu et al. 2000; Wu 2006). Due to the presence of epoxy groups, the multi-epoxy-terminated PPO increased rate of reaction than the neat resin in the early stages of curing (Wang et al. 2014). In another work, the rate of reaction increased as a result of phase separation in syndiotactic polystyrene (sPS)-modified DGEBA epoxy resin. In amine-cured system, phase separation resulted in DGEBA/MCDEA-rich phase containing some sPS and an sPS-rich phase with some dissolved DGEBA and MCDEA. In the epoxy-rich phase, the dilution and viscosity effects are negligible resulting in a faster reaction rate (Salmon et al. 2005). The presence of hydroxyl groups increased the curing rates of the blends than the neat resin in DDS-cured TGDDM/phenoxy and DGEBA/polyvinyl phenol blends (Hsieh et al. 1998; Su et al. 2005). The final cure conversion of 10 wt% PEI was found to be higher than that of neat resin until a cure temperature of 160 °C (Varley 2007; Su and Woo 1995) in an amine-cured tetrafunctional epoxy resin (Table 1). The deviation is due to the plasticization of the epoxy phase by PEI which enhanced the mobility of the epoxy network and also due to an uneven distribution of epoxide and amino species in the thermoplastic phase after RIPS.

The kinetics of the curing reactions was modeled, employing various equations described earlier. In some cases, other models were also used. Comparison of the experimental and theoretical values showed that the rate of reaction deviated from the experimental values toward the end of the reaction or at higher conversions in general. The blends showed deviation from autocatalytic behavior with increase in thermoplastic content and lowering of curing temperature and at higher conversions (Varley et al. 2000; Man et al. 2009). Toward the end of curing reaction, the viscosity of the system will increase as a result of gelation. As a consequence, the chemically controlled reaction became diffusion controlled. The increase in viscosity of the system will hinder the curing reaction, reduce the final conversion, and prevent the system from reaching full conversion. The models agreed with the experimental data with the introduction of a diffusion factor during the later stages of cure.

Reaction-induced phase separation is typical of blends of epoxy resin. Depending on the composition of the blends, dispersed or co-continuous morphology will be developed. Hence the rate of curing reaction is dependent on the phase separation

Table 1 Effect of cure temperature on the final conversion (Reprinted from *Macromol Mater Eng* (2007) 292:46 with permission from Wiley)

Cure temperature (°C)	Final conversion		
	Neat resin	10 wt% PEI	20 wt% PEI
110	0.61	0.66	0.59
120	0.65	0.73	0.96
130	0.68	0.77	0.70
140	0.73	0.80	0.65
150	0.8	0.85	0.79
160	0.88	0.87	0.85
170	0.91	0.89	0.87
180	0.97	0.96	0.89

process. As a consequence of RIPS, the curing agent and epoxy resin will be distributed in the separated phases causing a decrease in the final epoxy conversion. The MCDEA-cured DGEBA epoxy resin modified with PEI shows an interesting phenomenon. The blends showed two-phase morphology. The reaction rate at a higher PEI concentration (30 wt%) showed an increase after RIPS, whereas no sudden change was observed at 10 wt% loading of PEI. The increase in rate after phase separation results in an epoxy-amine rich phase with a faster reaction rate. In the same epoxy resin-curing agent system modified with polystyrene, the increase in rate is more pronounced due to faster phase separation (Fig. 6). In this case, the lower viscosity of the system at the initial stages of phase separation plays an important role (Bonnet et al. 1999).

The reduced reaction rate against conversion plots for phenolic-terminated PSF-modified DDS-cured TGAP is shown in Fig. 7. The parabolic shape of the curve implied a complex diffusion-controlled reaction mechanism due to higher viscosity and reduction in reactive group density (Varley et al. 2000). This phenomenon is more pronounced at higher polysulfone content (30% and 50%) and lower cure temperature (120 °C).

The activation energy of the blends calculated using the kinetic models increased with increase in thermoplastic content (Park 2009). This is because the thermoplastics hindered the curing reaction. The values of reaction orders m and n are indicators of the curing reaction. For example, in NMA-cured DGEBA epoxy resin, the value of n varied from 1.6 to 4 with increase in cure temperature and PEI content. This showed that the reaction is hindered. The value of m near 1 was similar in all cases indicating an autocatalytic mechanism (Kim et al. 2002). In the above system, the activation energy was calculated according to Arrhenius kinetics as follows:

$$r = \frac{d\alpha}{dt} = kf(\alpha) \quad (13)$$

where r is the rate of reaction, k is the apparent reaction rate coefficient, and $f(\alpha)$ is some functional dependence of rate on conversion, $\alpha(t)$. Assuming that k takes the form of an Arrhenius rate equation,

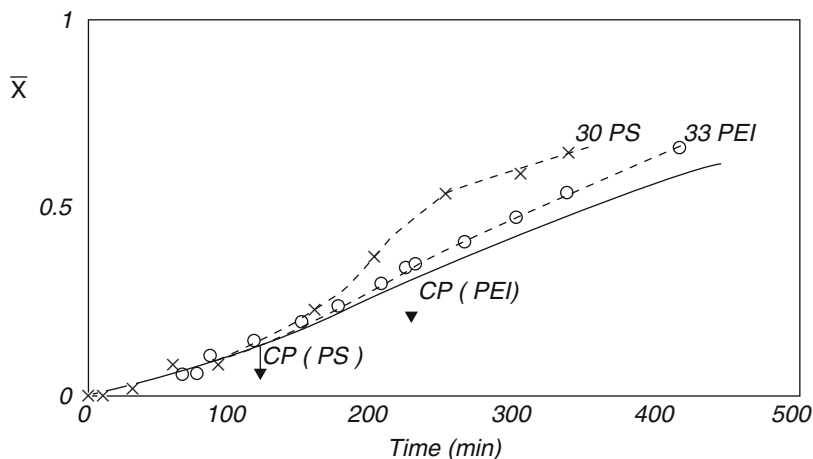


Fig. 6 Influence of the type of thermoplastic on the epoxy-amine reaction of the DGEBA–MCDEA system; experimental points for PS (×) and PEI (○) (Reprinted from *Macromolecules* (1999) 32:8517 with permission from American Chemical Society)

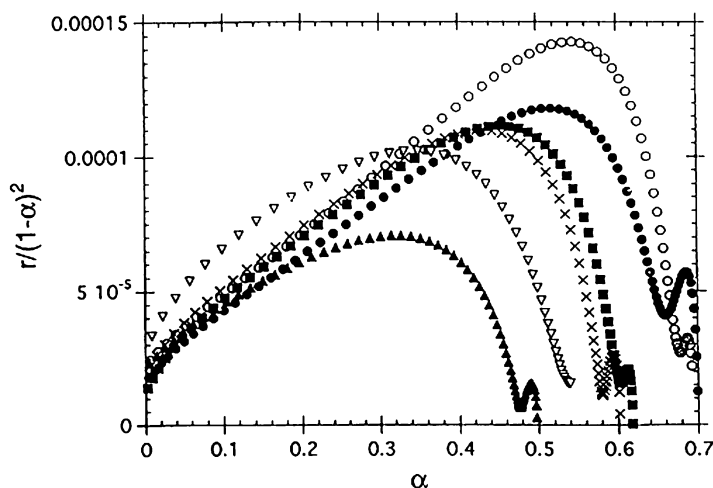


Fig. 7 Plot of the reduced rate, for $n = 2$ and $m = 1$; versus fractional cure conversion for (○) neat resin, (●) 10, (■) 15, (×) 20, (▽) 30, and (▲) 50% PSF samples during cure at 120 °C (Reprinted from *Polymer* (2000) 41:3425 with permission from Elsevier)

$$k = A \exp\left(\frac{-E_a}{RT}\right) \quad (14)$$

where A is the pre-exponential factor, E_a is the apparent activation energy, and R is the real gas constant, then

$$\ln r = \ln A - \frac{E_a}{RT} + \ln f(\alpha) \quad (15)$$

By plotting $\ln r$ versus $1/T$, this equation can be used to calculate the activation energy barrier to reaction at each level of conversion without having to know accurately the function $f(\alpha)$.

The activation energy profile of a phenolic hydroxyl-terminated, polysulfone-modified TGAP cured with an amine using the above method is shown in Fig. 8. The activation energy showed large values at higher polysulfone content and at higher conversions. This shows that the curing reaction became difficult as the reaction progressed (Varley et al. 2000).

A slightly different activation energy evolution is shown in Fig. 9. The activation energy initially decreased due to the formation of hydroxyl groups which catalyzed the curing reaction, and at a later stage, it increased due to increased system viscosity. The reduction in activation energy is more for amine-terminated polyethersulfone:polyether ether sulfone copolymer (PES:PEES) than chlorine terminal PES:PEES copolymer since the amine groups reacted with epoxy resin producing more numbers of catalyzing hydroxyl groups (Man et al. 2009).

Similar activation energy profile was observed in epoxy cresol novolac resin blended with PPO, epoxide-terminated PPO with epichlorohydrin (EPPO), and multipoxy-terminated, low-molecular-weight poly(phenylene oxide) (PPOE) cured with DDS (Wang et al. 2014). The lowest activation energy was observed in PPOE system due to the presence of epoxy groups and highest in PPO-modified

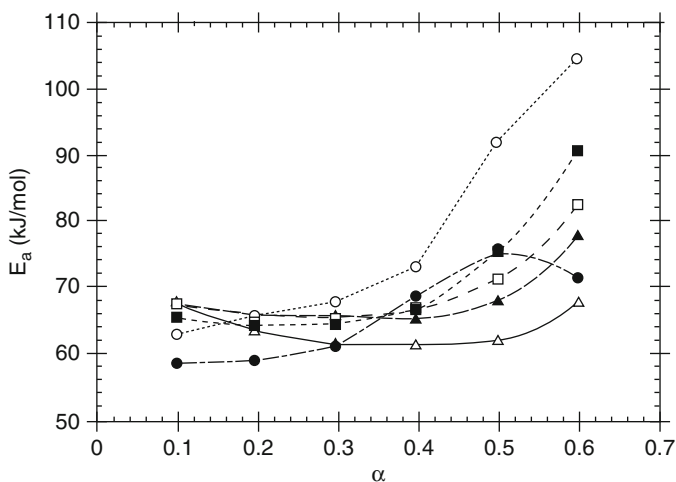


Fig. 8 Plot of activation energy versus fractional cure conversion for (Δ) neat resin, (\blacktriangle) 10, (\square) 15, (\blacksquare) 20, (\circ) 30, and (\bullet) 50% PSF samples during cure at 120 °C (Reprinted from Polymer (2000) 41:3425 with permission from Elsevier)

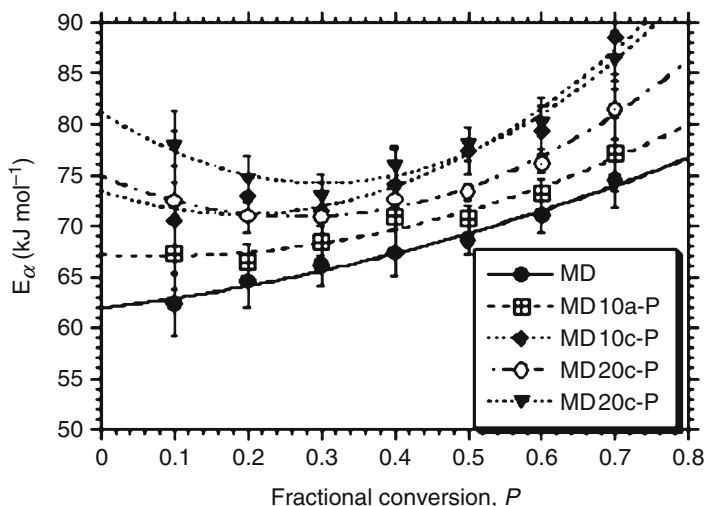


Fig. 9 The evolution of activation energy versus fractional conversion for the unmodified and modified epoxy resin system; MD10a-P and 20a-P – 10 wt% and 20 wt% amine terminal PES: PEES, MD10c-P and 20c-P – 10 wt% and 20 wt% chlorine terminal PES:PEES (Reprinted from *J App Polym Sci* (2009) 112:2391 with permission from Wiley)

system which does not contain epoxy groups. In general, the modifiers acted as catalyst at lower concentration, and at higher compositions they obstructed the curing reaction (Fig. 10).

The introduction of amine functionality on PEI altered the reaction rate versus time plot of an NMA-cured DGEBA epoxy resin (Kim et al. 2003). The plots of amino-PEI (DNCA) and PEI (DNCP) systems are shown in Fig. 11. Two peaks were observed in the DNCA system, whereas only one peak which is expected to be observed for usual thermoplastic modified epoxy resin is shown by DNCP system. The first peak in the DNCA system is attributed to the reaction between amine-terminated polyetherimide (ATPEI) with hardener/DGEBA and the second peak due to autocatalytic reaction of catalyst with hardener/DGEBA.

A modified equation was used to predict the kinetics in this case:

$$-r = \frac{d\alpha}{dt} = \sum r_i = (-r_1) + (-r_2) \quad (16)$$

where $-r_i$ is the total reaction rate and $-r_1$ and $-r_2$ are the partial reaction rates. Each reaction model can be assumed to the autocatalytic mechanism, so $-r_1$ and $-r_2$ can be written as follows:

$$-r_1 = (k_{11} + k_{12}\alpha^{m_1})(1 - \alpha)^n \quad (17)$$

$$-r_2 = (k_{21} + k_{22}\alpha^{m_2})(1 - \alpha)^n \quad (18)$$

Fig. 10 Activation energy in the non-isothermal curing processes of EPN/PPO, EPN/EPPO, and EPN/PPOE blends with different compositions (Reprinted from Polym Eng Sci (2014) 54:2595 with permission from Wiley)

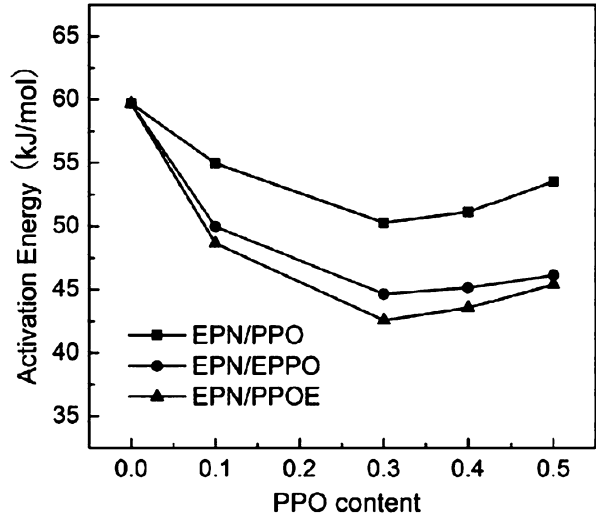
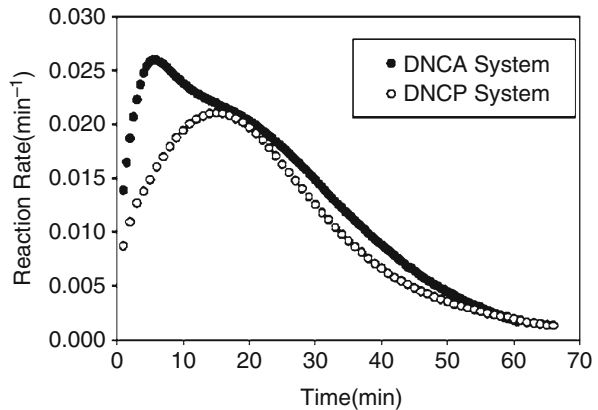


Fig. 11 Reaction rate versus time curves for the DNCP and DNCA systems at 120 °C (Reprinted from Polym Bull (2003) 51:167 with permission from Springer)



Equation 16 can be rewritten by combining the diffusion control factor, $f(\alpha)$, as follows:

$$\begin{aligned}
 -r &= \frac{d\alpha}{dt} = (k_{\alpha} + k_{12}\alpha^{m_1} + k_{22}\alpha^{m_2})(1 - \alpha)^n f(\alpha) \\
 -r &= \frac{(k_{\alpha} + k_{12}\alpha^{m_1} + k_{22}\alpha^{m_2})(1 - \alpha)^n}{1 + \exp[C(\alpha - \alpha_c)]} \tag{19}
 \end{aligned}$$

where $k_{\alpha} = k_{11} + k_{21}$.

The modified equation fits well with the experimental values as shown in the Fig. 12.

Fig. 12 Reaction rate versus degree of conversion plot for the cure process of DNCA system, experimental data (symbols) and calculated data (lines) at 140 °C (Reprinted from Polym Bull (2003) 51:167 with permission from Springer)

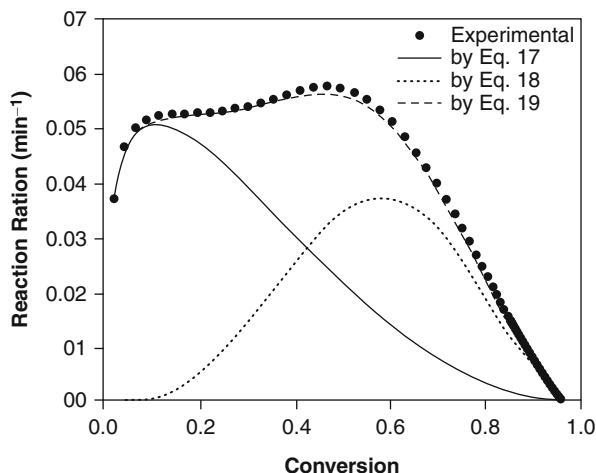


Table 2 Kinetic constants of autocatalysis models on the DNCA system (Reprinted from Polym Bull (2003) 51:167 with permission from Springer)

T (°C)	m_1	m_2	n	k_{12} (min ⁻¹)	k_{22} (min ⁻¹)
120	0.3707	3.7839	2.9677	0.0524	0.8226
130	0.3108	3.5216	2.4297	0.0889	1.2367
140	0.2735	3.0913	2.1893	0.1160	1.9263

The kinetic parameters calculated are shown in Table 2.

The values of m_1 , m_2 , and n are controlled, respectively, by the reactions of ATPEI with hardener/epoxy, catalyst with hardener/epoxy, and epoxy with hardener. The autocatalytic reaction of ATPEI was predominant in the early stages of cure due to the high activation energy of the anhydride-cured system. So m_1 was low value in the initial stages, and at the later stages, m_2 was high. The critical conversion α_c was also larger than unmodified and PEI-modified systems.

DDS-cured TGDDM/PC blends were completely miscible due to the interaction of PC with epoxy resin. As described earlier, the rate of cure reaction was higher for the blends than the neat resin. In contrary to the usual autocatalytic mechanism, the blends exhibited an n th-order reaction mechanism with n varying from 1.2 to 1.5. The model and experimental data were in good agreement till vitrification (Su et al. 1995).

Conclusions

Extensive studies have been done on the cure kinetics of thermoplastic-toughened epoxy resin. DSC is a convenient and easy-to-use technique to monitor the progress of the curing reaction. The dynamic and isothermal DSC thermograms were smooth except where there are specific interactions or side reactions. The modification with

thermoplastics did not alter the autocatalytic mechanism in general. But they influenced the final conversion and kinetic parameters due to the interaction with epoxy resin or curing agent, dilution effect, viscosity effects, and RIPS. The final conversion and the reaction rate decreased in most of the cases. The reaction rate increased in systems where the functional groups on the thermoplastic catalyzed the curing reaction. The activation energy of the epoxy-curing agent reactions also decreased in such cases. Various kinetic models were employed, and the experimental values agreed with theoretical values up to critical conversion. After critical conversion, viscosity effects dominated. After the introduction of the diffusion factor, the kinetic models agreed well with the experimental values.

References

- Abraham D, Mc Ilhagger R (1998) Investigations into various methods of liquid injection to achieve mouldings with minimum void contents and full wet out. *Compos Part A* 29:533–539
- Andrés MA, Garmendia J, Valea A, Eceiza A, Mondragon I (1998) Fracture toughness of epoxy resins modified with polyethersulfone: influence of stoichiometry on the morphology of the mixtures. *J Appl Poly Sci* 69:183–191
- Barral L, Cano J, Lopez J, Lopez-Bueno I, Nogueira P, Ramirez C, Torres A, Abad MJ (1999) Cure kinetics of amine cured tetrafunctional epoxy blends with poly(styrene-co-acrylonitrile). *J Therm Ana Calor* 56:1033–1040
- Barral L, Cano J, López J, López-Bueno I, Nogueira P, Abad MJ, Ramírez C (2000a) Blends of an epoxy/cycloaliphatic amine resin with poly(ether imide). *Polymer* 41:2657–2666
- Barral L, Cano J, López J, López-Bueno I, Nogueira P, Torres A, Ramírez C, Abad MJ (2000b) Cure kinetics of amine-cured diglycidyl ether of bisphenol: a epoxy blended with poly(ether imide). *Thermochim Acta* 344:127–136
- Benito JG, Esteban I (2005) Morphologic and kinetic study of an epoxy-poly(ethyleneoxide) system. The fluorescence to predict miscibility. *Colloid Polym Sci* 283:559–569
- Blank WJ, He ZA, Picci M (2002) Catalysis of the epoxy-carboxyl reaction. *J Coat Technol* 74:33–41
- Bonnaud L, Pascault JP, Sautereau H (2000) Kinetic of a thermoplastic-modified epoxy-aromatic diamine formulation: modeling and influence of a trifunctional epoxy prepolymer. *Eur Polym J* 36:1313–1321
- Bonnet A, Pascault JP, Sautereau H, Taha M, Camberlin Y (1999) Epoxy-diamine thermoset/thermoplastic blends. 1. Rates of reactions before and after phase separation. *Macromolecules* 32:8517–8523
- Bonnet A, Lestriez B, Pascault JP, Sautereau H (2001) Intractable high-Tg thermoplastics processed with epoxy resin: interfacial adhesion and mechanical properties of the cured blends. *J Polym Sci Part B Polym Phys* 39:363–373
- Cabezudo MS, Prolongo MG, Salom C, Masegosa RM (2006) Cure kinetics of epoxy resin and thermoplastic polymer. *J Therm Anal Calor* 86:699–705
- Çaçcaval CN, Roşu D, Stoleriu A (1997) Curing of some epoxy-acrylate glycidyl ethers based on para-alkyl substituted phenols. *Polym Degrad Stab* 55:281–285
- Dušek K, Luňák S, Matějka L (1982) Gelation in the curing of epoxy resins with anhydrides. *Polym Bull* 7:145–152
- Fernandez B, Corcuera MA, Marieta C, Mondragon I (2001) Rheokinetic variations during curing of a tetrafunctional epoxy resin modified with two thermoplastics. *Eur Polym J* 37:1863–1869

- Fernandez-Francos X, Ramis X, Serra A (2014) From curing kinetics to network structure: a novel approach to the modeling of the network buildup of epoxy–anhydride thermosets. *J Polym Sci Part A Polym Chem* 52:61–75
- Foix D, Yu Y, Serra A, Ramis X, Salla JM (2009) Study on the chemical modification of epoxy/anhydride thermosets using a hydroxyl terminated hyperbranched polymer. *Eur Polym J* 45:1454–1466
- Francis B, Poel GV, Posada F, Groeninckx G, Rao VL, Ramaswamy R, Thomas S (2003) Cure kinetics and morphology of blends of epoxy resin with poly (ether ether ketone) containing pendant tertiary butyl groups. *Polymer* 44:3687–3699
- Francis B, Thomas S, Jose J, Ramaswamy R, Rao VL (2005) Hydroxyl terminated poly(ether ether ketone) with pendent methyl group toughened epoxy resin: miscibility, morphology and mechanical properties. *Polymer* 46:12372–12385
- Francis B, Rao VL, Jose S, Catherine BK, Ramaswamy R, Jose J, Thomas S (2006a) Poly(ether ether ketone) with pendent methyl groups as a toughening agent for amine cured DGEBA epoxy resin. *J Mater Sci* 41:5467–5479
- Francis B, Thomas S, Asari GV, Ramaswamy R, Jose S, Rao VL (2006b) Synthesis of hydroxyl-terminated poly(ether ether ketone) with pendent tert-butyl groups and its use as a toughener for epoxy resins. *J Polym Sci Part B Polym Phys* 44:541–556
- Francis B, Rao VL, Poel GV, Posada F, Groeninckx G, Ramaswamy R, Thomas S (2006c) Cure kinetics, morphological and dynamic mechanical analysis of diglycidyl ether of bisphenol-A epoxy resin modified with hydroxyl terminated poly(ether ether ketone) containing pendent tertiary butyl groups. *Polymer* 47:5411–5419
- Francis B, Thomas S, Sadhana R, Thuaud N, Ramaswamy R, Jose S, Rao VL (2007) Diglycidyl ether of bisphenol-A epoxy resin modified using poly(ether ether ketone) with pendent tert-butyl groups. *J Polym Sci Part B Polym Phys* 45:2481–2496
- George GA, Clarke PC, John NS, Friend G (1991) Real-time monitoring of the cure reaction of a TGDDM/DDA epoxy resin using fiber optic FT-IR. *J Appl Polym Sci* 42:643–657
- Gonis J, Simon GP, Cook WD (1999) Cure properties of epoxies with varying chain length as studied by DSC. *J Appl Polym Sci* 72:1479–1488
- Grillet AC, Galy J, Pascault JP, Bardin I (1989) Effects of the structure of the aromatic curing agent on the cure kinetics of epoxy networks. *Polymer* 30:2094–2103
- Halley PJ, Mackay ME (1996) Chemorheology of thermosets—an overview. *Polym Eng Sci* 36:593–609
- Hao D, Tang X, Wang X LY (2001) Effect of amino-polycarbonate on the curing kinetics and morphology of epoxy resin. *J Appl Polym Sci* 82:833–838
- Holmberg JA, Berglung LA (1997) Manufacturing and performance of RTM U-beams. *Compos Part A* 28:513–521
- Horie K, Hiura H, Sawada M, Mita I, Kambe H (1970) Calorimetric investigation of polymerization reactions. III. Curing reaction of epoxides with amines. *J Polym Sci A* 8:1357–1372
- Hsieh HK, Su CC, Woo EM (1998) Cure kinetics and inter-domain etherification in an amine-cured phenoxy/epoxy system. *Polymer* 39:2175–2183
- Ivankovic M, Incarnato L, Kenny JM, Nicolais L (2003) Curing kinetics and chemorheology of epoxy/anhydride system. *J Appl Polym Sci* 90:3012–3019
- Jagadeesh KS, Rao JG, Shashikiran K, Suvarna S, Ambekar SY, Saletori M, Biswas C, Rajanna AV (2000) Cure kinetics of multifunctional epoxies with 2,2'-dichloro-4,4'-diaminodiphenylmethane as hardener. *J Appl Polym Sci* 77:2097–2103
- Jenninger W, Schawe JEK, Alig I (2000) Calorimetric studies of isothermal curing of phase separating epoxy networks. *Polymer* 41:1577–1588
- Jyotishkumar P, Thomas S (2011) Cure kinetics of poly(acrylonitrile-butadiene-styrene) modified epoxy–amine system. *J Macromol Sci Part A Pure Appl Chem* 48:751–756
- Jyotishkumar P, Ozdilek C, Moldenaers P, Sinturel C, Janke A, Pionteck J, Thomas S (2010) Dynamics of phase separation in poly(acrylonitrile-butadiene-styrene)-modified epoxy/dds system: kinetics and viscoelastic effects. *J Phys Chem B* 114:13271–13281

- Jyotishkumar P, Pionteck J, Häubler L, Adam G, Thomas S (2012) Poly(acrylonitrile-butadiene-styrene) modified epoxy-amine systems analyzed by FTIR and modulated DSC. *J Macromol Sci Part B Phys* 51:1425–1436
- Kamal MR, Sourour S (1973) Kinetics and thermal characterization of thermoset cure. *Polym Eng Sci* 13:59–64
- Karkanas PI, Partridge IK, Attwood D (1996) Modelling the cure of a commercial epoxy resin for applications in resin transfer moulding. *Polym Int* 41:183–191
- Khanna U, Chanda M (1993) Kinetics of anhydride curing of isophthalic diglycidyl ester using differential scanning calorimetry. *J Appl Polym Sci* 49:319–329
- Khanna U, Chanda M (1996) Monte Carlo simulation of network formation based on structural fragments in epoxy-anhydride systems. *Polymer* 37:2831–2844
- Kim WG, Lee JY (2002) Contributions of the network structure to the cure kinetics of epoxy resin systems according to the change of hardeners. *Polymer* 43:5713–5722
- Kim M, Kim W, Choe Y, Park JM, Park IS (2002) Characterization of cure reactions of anhydride/epoxy/polyetherimide blends. *Polym Int* 51:1353–1360
- Kim M, Kim W, Choe Y, Ahn B, Kim D, Park JM (2003) Modeling of multi-autocatalytic cure reactions of an epoxy/amine terminated polyetherimide/NMA system. *Polym Bull* 51:167–174
- Laza JM, Julian CA, Larrauri E, Rodriguez M, Leon LM (1999) Thermal scanning rheometer analysis of curing kinetic of an epoxy resin: 2. An amine as curing agent. *Polymer* 40:35–45
- Levita G, Livi A, Roollo PA, Culicchi C (1996) Dielectric monitoring of epoxy cure. *J Polym Sci Part B Polym Phys* 34:2731–2737
- Li J, Chen P, Ma Z, Ma K, Wang B (2009) Reaction kinetics and thermal properties of cyanate ester-cured epoxy resin with phenolphthalein poly(ether ketone). *J Appl Polym Sci* 111:2590–2596
- Liello VD, Martuscelli E, Musto P, Ragosta G, Scarinzi G (1994) Toughening of highly crosslinked epoxy resins by reactive blending with bisphenol A polycarbonate. II. Yield and fracture behavior. *J Polym Sci Part B Polym Phys* 32:409–419
- Lin ML, Chang K, Chang FC, Li MS, Ma CCM (1997) The epoxy-polycarbonate blends cured with aliphatic amine – I. Mechanism and kinetics. *J Polym Sci B Polym Phys* 35:2169–2181
- Lopez J, Lopez-Bueno I, Nogueira P, Ramirez C, Abad MJ, Barral L, Cano J (2001) Effect of poly(styrene-co-acrylonitrile) on the curing of an epoxy/amine resin. *Polymer* 42:1669–1677
- López J, Rico M, Montero B, Díez J, Ramírez C (2009) Polymer blends based on an epoxy-amine thermoset and a thermoplastic. Effect of thermoplastic on cure reaction and thermal stability of the system. *J Therm Anal Calor* 95:369–376
- Luňák S, Dušek K (1975) Curing of epoxy resins II. Curing of bisphenol A diglycidyl ether with diamines. *J Polym Sci Polym Symp* 53:45–55
- Man Z, Stanford JL, Dutta BK (2009) Reaction kinetics of epoxy resin modified with reactive and nonreactive thermoplastic copolymers. *J Appl Polym Sci* 112:2391–2400
- Martínez I, Martín MD, Eceiza A, Oyanguren P, Mondragon I (2000) Phase separation in polysulfone-modified epoxy mixtures. Relationships between curing conditions, morphology and ultimate behavior. *Polymer* 41:1027–1035
- Matějka L, Pokorný S, Dušek K (1985) Acid curing of epoxy resins. A comparison between the polymerization of diepoxide-diacid and monoepoxide-cyclic anhydride systems. *Die Makromol Chem* 186:2025–2036
- Mauri AN, Galego N, Riccardi CC, Williams RJJ (1997) Kinetic model for gelation in the diepoxide-cyclic anhydride copolymerization initiated by tertiary amines. *Macromolecules* 30:1616–1620
- May CA (1988) *Epoxy resins: chemistry and technology*, 2nd edn. Marcel Dekker, New York
- Mijović J, Andjelić S, Kenny JM (1996) In situ real-time monitoring of epoxy/amine kinetics by remote near infrared spectroscopy. *Polym Adv Technol* 7:1–16
- Mimura K, Ito H, Fujioka H (2000) Improvement of thermal and mechanical properties by control of morphologies in PES-modified epoxy resins. *Polymer* 41:4451–4459
- Montserrat S, Málek J (1993) A kinetic analysis of the curing reaction of an epoxy resin. *Thermochim Acta* 228:47–60

- Montserrat S, Martin JG (2002) Non-isothermal curing of a diepoxide-cycloaliphatic diamine system by temperature modulated differential scanning calorimetry. *Thermochim Acta* 388:343–354
- Mounif E, Liang GG, Cook WD, Bellengera V, Tcharkhatchia A (2009) Poly(methylmethacrylate)-modified epoxy/amine system for reactive rotational moulding: crosslinking kinetics and rheological properties. *Polym Int* 58:954–961
- Musto P, Martuscelli E, Ragosta G, Russo P, Villano P (1999) Tetrafunctional epoxy resins: modeling the curing kinetics based on FTIR spectroscopy data. *J Appl Polym Sci* 74:532–540
- Musto P, Martuscelli E, Ragosta G, Mascia L (2001) Cure kinetics and ultimate properties of a tetrafunctional epoxy resin toughened by a perfluoro-ether oligomer. *Polymer* 42:5189–5198
- Naffakh M, Dumon M, Dupuy J, Gerard JF (2005) Cure kinetics of an epoxy/liquid aromatic diamine modified with poly(ether imide). *J Appl Polym Sci* 96:660–672
- Ochi M, Chiba T, Takiuchi H, Tazhizumi M, Shimbo M (1989) Effect of the introduction of methoxy branches on low-temperature relaxations and fracture toughness of epoxide resins. *Polymer* 30:1079–1084
- Ochi M, Ikegami K, Ueda S, Kotora K (1994) Effect of the low-temperature relaxation on toughness of cured epoxy resins. *J Appl Polym Sci* 54:1893–1898
- Overbeke EV, Devaux J, Legras R, Carter JT, Mc Grail PT, Carlier V (2001) Raman spectroscopy and DSC determination of conversion in DDS-cured epoxy resin: application to epoxy-copolyethersulfone blends. *Appl Spectro* 55:540–551
- Park SJ (2009) Studies on cure behaviors, dielectric characteristics and mechanical properties of DGEBA/poly(ethylene terephthalate) blends. *Macromol Res* 17:585–590
- Pascault JP, Williams RJJ (2010) *Epoxy polymers: new materials and innovations*. Wiley-VCH, Weinheim
- Pascault JP, Sautereau H, Verdu J, Williams RJJ (2002) *Thermosetting polymers*, *Plastics engineering series*. Marcel Dekker, New York
- Pasquale GD, Motta O, Recca A, Carter JT, McGrail PT, Acierno D (1997) New high-performance thermoplastic toughened epoxy thermosets. *Polymer* 38:4345–4348
- Prolongo MG, Arribas C, Salom C, Masegosa RM (2007) Phase separation, cure kinetics, and morphology of epoxy/poly(vinyl acetate) blends. *J Appl Polym Sci* 103:1507–1516
- Reydet EG, Riccardi CC, Sautereau H, Pascault JP (1995) Epoxy-aromatic diamine kinetics. Part 1. Modeling and influence of the diamine structure. *Macromolecules* 28:7599–7607
- Reydet EG, Vicard V, Pascault JP, Sautereau H (1997) Polyetherimide-modified epoxy networks: influence of cure conditions on morphology and mechanical properties. *J Appl Polym Sci* 65:2433–2445
- Riccardi CC, Williams RJJ (1986) A kinetic scheme for an amine-epoxy reaction with simultaneous etherification. *J Appl Polym Sci* 32:3445–3456
- Rocks J, Rintoul L, Vohwinkel F, George G (2004) The kinetics and mechanism of cure of an amino-glycidyl epoxy resin by a co-anhydride as studied by FT-Raman spectroscopy. *Polymer* 45:6799–6811
- Roşu D, Mustăţ F, Caşcaval CN (2001) Investigation of the curing reactions of some multifunctional epoxy resins using differential scanning calorimetry. *Thermochim Acta* 370:105–110
- Rusli A, Cook WD, Schiller TL (2014) Blends of epoxy resins and polyphenylene oxide as processing aids and toughening agents 2: curing kinetics, rheology, structure and properties. *Polym Int* 63:1414–1426
- Salla JM, Ramis X (1996) Comparative study of the cure kinetics of an unsaturated polyester resin using different procedures. *Polym Eng Sci* 36:835–851
- Salmon N, Carlier V, Schut J, Remiro PM, Mondragon I (2005) Curing behaviour of syndiotactic polystyrene-epoxy blends: 1. Kinetics of curing and phase separation process. *Polym Int* 54:667–672
- Schiraldi A, Baldini P (1983) Epoxy polymers. *J Thermal Anal* 28:295–301

- Shen S, Li Y, Gao J, Sun H (2001) Curing kinetics and mechanism of bisphenol S epoxy resin with 4,4'-diaminodiphenyl ether or phthalic anhydride. *Int J Chem Kine* 33:558–563
- Skiest I (1978) *Handbook of adhesives*, 2nd edn. VNR Company, New York
- Sourour S, Kamal MR (1976) Differential scanning calorimetry of epoxy cure: isothermal cure kinetics. *Thermochim Acta* 14:41–59
- Su CC, Woo EM (1995) Cure kinetics and morphology of amine-cured tetraglycidyl-4,4'-diaminodiphenylmethane epoxy blends with poly (etherimide). *Polymer* 36:2883–2894
- Su CC, Kuo JF, Woo EM (1995) Miscibility and cure kinetics studies on blends of bisphenol-A polycarbonate and tetraglycidyl-4,4'-diaminodiphenylmethane epoxy cured with an amine. *J Polym Sci B Polym Phys* 33:2235–2244
- Su CC, Woo EM, Huang YP (2005) Curing kinetics and reaction-induced homogeneity in networks of poly(4-vinyl phenol) and diglycidylether epoxide cured with amine. *Polym Eng Sci* 45:1–10
- Swier S, Assche GV, Mele BV (2004) Reaction kinetics modeling and thermal properties of epoxy-amines as measured by modulated-temperature DSC. II. Network-forming DGEBA + MDA. *J Appl Polym Sci* 91:2814–2833
- Teil H, Page SA, Michaud V, Manson JAE (2004) TTT-cure diagram of an anhydride-cured epoxy system including gelation, vitrification, curing kinetics model and monitoring of the glass transition temperature. *J Appl Polym Sci* 93:1774–1787
- Trappe V, Burchard W, Steinmann B (1991) Anhydride-cured epoxies via chain reaction. 1. The phenyl glycidyl ether/phthalic acid anhydride system. *Macromolecules* 24:4738–4744
- Um MK, Daniel IM, Hwang BS (2002) A study of cure kinetics by the use of dynamic differential scanning calorimetry. *Compos Sci Technol* 62:29–40
- Varley RJ (2007) Reaction kinetics and phase transformations during cure of a thermoplastic-modified epoxy thermoset. *Macromol Mater Eng* 292:46–61
- Varley RJ, Heath GR, Hawthorne DG, Hodgkin JH, Simon GP (1995) Toughening of a trifunctional epoxy system: 1. Near infra-red spectroscopy study of homopolymer cure. *Polymer* 36:1347–1355
- Varley RJ, Hodgkin JH, Hawthorne DG, Simon GP, McCulloch D (2000) Toughening of a trifunctional epoxy system part III. Kinetic and morphological study of the thermoplastic modified cure process. *Polymer* 41:3425–3436
- Vyazovkin S, Sbirrazzuoli N (1996) Mechanism and kinetics of epoxy – amine cure studied by differential scanning calorimetry. *Macromolecules* 29:1867–1873
- Wang H, Mo J, Shentu B, Weng Z (2014) Preparation, curing properties, and phase morphology of epoxy-novolac resin/multi-epoxy-terminated low-molecular-weight poly(phenylene oxide) blend. *Polym Eng Sci* 54:2595–2604
- Wu SJ (2006) Cure reaction and phase separation behavior of cyanate ester-cured epoxy/polyphenylene oxide blends. *J Appl Polym Sci* 102:1139–1145
- Wu SJ, Lin TK, Shyu SS (2000) Cure behavior, morphology, and mechanical properties of the melt blends of epoxy with polyphenylene oxide. *J Appl Polym Sci* 75:26–34
- Xu Y, Zhou S, Liao G, Jian X (2012) Curing kinetics of DGEBA epoxy resin modified by poly (phthalazinone ether ketone) (PPEK). *Polym Plast Technol Eng* 51:128–133
- Young W, Chuang M (1995) Fabrication of T-shaped structural composite through resin transfer molding. *J Comp Mater* 29:2192–2214
- Zhang J, Guo Q, Fox BL (2009) Study on thermoplastic-modified multifunctional epoxies: influence of heating rate on cure behaviour and phase separation. *Comp Sci Technol* 69:1172–1179
- Zvetkov VL (2001) Comparative DSC kinetics of the reaction of DGEBA with aromatic diamines.: I. Non-isothermal kinetic study of the reaction of DGEBA with m-phenylene diamine. *Polymer* 42:6687–6697

Angel Romo-Uribe

Abstract

Epoxy/thermoplastic blends have been primarily developed to meet requirements in high-performance applications rendering toughness to the epoxy resins without sacrificing thermal resistance and mechanical performance. Engineering thermoplastics are the natural choice having high glass transition temperature, high thermal degradation temperatures, and impact resistance. The challenge is to understand and control phase separation in these systems and determine the correlation with mechanical properties. This chapter presents the application of dynamic mechanical thermal analysis (DMTA) as a suitable analytical tool to investigate the mechanical behavior and energy dissipation of epoxy resins modified with thermoplastics and aspects and consequences of miscibility, partial miscibility, or phase separation between thermoplastic domains and epoxy matrix. The type of thermoplastics utilized (amorphous vs. semicrystalline) and the influence of curing agents and curing temperature on the phase separation dynamics and nanophase of epoxy thermosets are discussed. Finally, application of DMTA to design and characterize the performance of a new generation of smart epoxy/thermoplastic blends with self-healing and shape memory properties is also discussed.

Keywords

Compatibility • Viscoelastic properties • Phase structure • Toughness • Glass transition temperature

A. Romo-Uribe (✉)

Advanced Science and Technology, Johnson & Johnson Vision Care, Inc., Jacksonville, FL, USA
e-mail: aromouri@its.jnj.com

Contents

Introduction	676
Background	676
Influence of Glass Transition Temperature T_g	678
High-Performance Thermoplastic/Epoxy Blends	681
PES/Epoxy Blends	681
PES-PEES/Epoxy Blends	684
Polyether Ketone-Based/Epoxy Blends	685
Engineering Thermoplastic/Epoxy Blends	688
Smart Thermoplastic/Epoxy Blends	693
Thermoplastic/Epoxy Blends with Shape Memory Behavior	694
Self-Healing Thermoplastic/Epoxy Blends	696
Conclusions	698
Glossary of Terms	700
References	702

Introduction

Background

Epoxy resins are used in industry as protective coatings and for structural applications, such as advanced laminates and composites, tooling, molding, casting, encapsulating, electronic packaging, coatings, bonding, and adhesives. Epoxy resins are having high chemical and corrosion resistance and exhibit good mechanical and thermal properties, outstanding adhesion to various substrates, low shrinkage upon cure, good electrical insulating properties, and the ability to be processed under a variety of conditions. These properties make epoxy resins very versatile and suitable for applications in demanding environments like corrosion-resistant coatings or in high-performance applications like those encountered in the automotive, aerospace, and electronics industry. For reviews on the chemistry and applications of epoxy resins, the reader is referred to May (1988) and Ellis (1993). Whereas high-performance properties of epoxy resins remain highly important for commercial and defense applications, new developments include smart epoxy/thermoplastic blends, which comprise shape memory behavior (Xie and Rousseau 2009) and self-healing behavior (Luo et al. 2009).

The ability of the epoxy ring to react with a variety of substrates gives the epoxy resins versatility. However, the rather high mechanical modulus achievable with a highly cross-linked state makes epoxy resins usually brittle and low impact resistant. As a result, a great deal of research has been focused on the improvement of toughness (McGarry 1996; Meister 2000; Robeson 2007; Parameswaranpillai et al. 2015).

There are a variety of approaches to induce impact resistance to epoxy resins which are discussed in this series (Parameswaranpillai et al. 2015), and the approaches include (i) thermoplastic polymer dissolved (or dispersed as particles) in liquid uncured epoxy, (ii) monomers of thermoplastic polymers mixed with liquid uncured epoxy, (iii) reactive liquid rubber mixed with liquid uncured epoxy, and

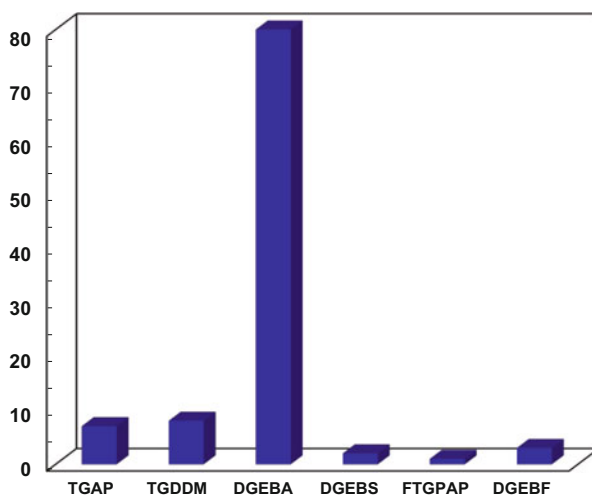
(iv) rubber nanoparticles mixed with liquid uncured epoxy (McGarry 1996; Dusek 1986; Howell 2000; Huang et al. 2005; Robeson 2007; Hedrick et al. 2009; Parameswaranpillai et al. 2015).

The addition of elastomers to epoxy resins was pioneered by McGarry at MIT (Sultan and McGarry 1973; McGarry and Rosner 1993; McGarry 1996). This approach is discussed in detail in this series; it suffices to say that rubbers alter not only the final morphology and physical properties but also the curing kinetics. Furthermore, toughness can be increased but at the expense of compromising the composite's performance as there can be significant reduction of glass transition temperature, T_g , and mechanical modulus. Furthermore, epoxies modified with butadiene-based rubbers are also susceptible to thermal and oxidative degradation and also lose mechanical properties when exposed to high temperatures or moisture for long periods (Howell 2000).

Thermoplastics, and in particular high-performance thermoplastics, are a suitable approach to induce toughness to epoxy resins without reducing T_g while maintaining or even increasing mechanical modulus. High-performance thermoplastics would be the natural choice having high glass transition temperature, high thermal degradation temperatures, and impact resistance. Therefore, epoxy/thermoplastic blends appear suitable for high-temperature/high-modulus applications rendering toughness to the epoxy resins without sacrificing thermal resistance and mechanical performance.

However, fairly few epoxy/thermoplastic blends have been investigated as both phases have to be miscible in a common solvent, or able to mix prior to curing the epoxy phase (for instance, micrometer-sized polymer powders dispersed in the epoxy liquid), or melt mixing but without triggering the curing of the epoxy phase. The difficulty is to a great extent due to high-performance thermoplastics being inherently resistant to chemicals and temperature. Figure 1 prepared by the author from data mining of the open literature in leading publishing houses (Elsevier,

Fig. 1 Frequency of epoxy resins commonly utilized for blending with thermoplastics (Source: Elsevier, Springer, Wiley, Google Scholar)



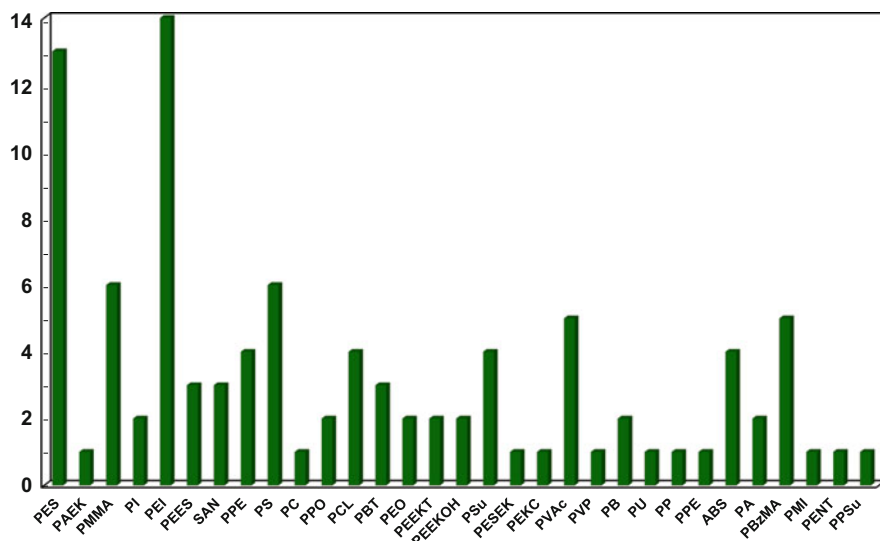


Fig. 2 Frequency of utilized thermoplastics in blends with epoxy resins (Source: Elsevier, Springer, Wiley, Google Scholar)

Springer, Wiley, and the like) (i.e., patents are not included) shows the different types of epoxy resins blended with thermoplastics. There is a glossary of acronyms for epoxy resins, thermoplastics, and hardeners at the end of this chapter. It is not presumed that the list is exhaustive; however, it can be seen that an overwhelming body of research has been focused on diglycidyl ether of bisphenol A (DGEBA). The timeframe corresponds from 1983, with the pioneering work of Bucknall (Bucknall and Partridge 1983) on blends of epoxy and polyether sulfone (PES), to the present time.

On the other hand, Fig. 2 shows the frequency plot of thermoplastics utilized for blending with epoxy resins. It can be seen that most research has been carried out on blends with PES and polyetherimide (PEI). This is due to these blends being suitable for aerospace and defense applications as PES and PEI exhibit T_g of approximately 210 °C and 221 °C, respectively (Bucknall and Partridge 1983; Bucknall and Gilbert 1989).

Influence of Glass Transition Temperature T_g

The T_g of the chosen epoxy resin is also considered for blending and this is tuned by the hardener utilized for curing. Figure 3 summarizes the hardeners predominantly utilized in epoxy/thermoplastic blends. For instance, DGEBA cured with 4,4'-diaminodiphenyl sulfone (DDS) exhibits a T_g of ca. 225 °C (Francis et al. 2007), whereas the T_g of DGEBA cured with 1,2-diaminocyclohexane (DCH) is ca. 103 °C (Romo-Urbe et al. 2014).

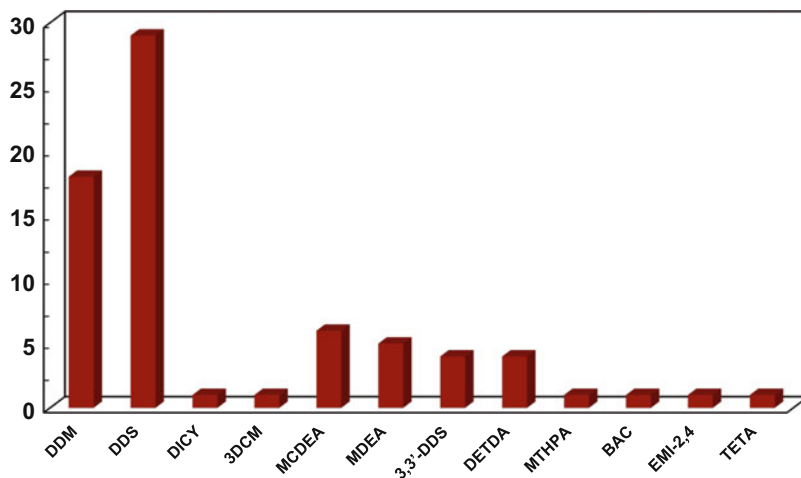


Fig. 3 Type of curing agent utilized in epoxy/thermoplastic blends (Source: Elsevier, Springer, Wiley, Google Scholar)

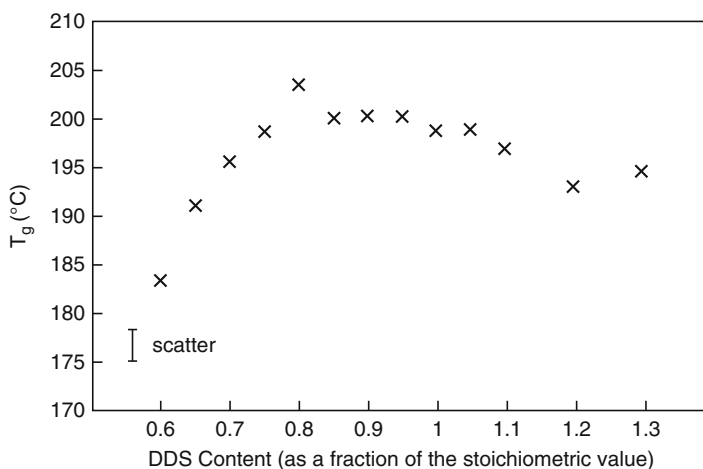


Fig. 4 Variation of the glass transition temperature T_g of an epoxy network with concentration of DDS (Akay and Cracknell 1994)

The significant difference in T_g values for the same epoxy resin is due to the degree of cross-linking attained with each hardener. Varying the concentration of hardener for a given epoxy resin also tunes the T_g of the cured epoxy. Figure 4 shows a plot of T_g of an epoxy resin as a function of hardener concentration, DDS. The higher the degree of cross-linking, the higher the T_g and mechanical modulus with the penalty of decreasing the impact resistance. It will be shown in the following

Table 1 Glass transition temperature T_g of thermoplastics utilized for blending with epoxy resins

Thermoplastic	T_g (°C)	References
PES	210	Bucknall and Partridge (1983)
PMMA	110	Gómez and Bucknall (1993)
PI	220	Bonnet et al. (2001)
PEI	221	Bucknall and Gilbert (1989)
SAN	105	López et al. (2002)
PPE	215	Bonnet et al. (2001)
HBP	35	Blanco et al. (2006)
PCL	-66	Vanden Poel et al. (2005)
PBT	58	Aróstegui and Nazábal (2004)
PEEK-T	134	Francis et al. (2007)
PEEKOH	162	Francis et al. (2005)
PSu	183	Zhang et al. (2011)
PESEK	192	Francis et al. (2006)
PEK-C	228	Qipeng et al. (1991)
PVAc	44	Prolongo et al. (2010)
PVP	181	Remiro et al. (1999)
PB	-88	Jyotishkumar et al. (2009)
PU	-57	Kishi et al. (2004)
ABS	105	Jyotishkumar et al. (2009)
PA6	25–28	Vyas and Iroh (2013)
PBzMA	80	Prolongo et al. (2010)
PENT	151	Saxena et al. (2006)
PPSu	208	Cedeño and Vázquez-Torres (2005)

sections the utility of dynamic mechanical thermal analysis (DMTA) in the elucidation of elastic and viscous moduli performance as a function of temperature and the influence of degree of cross-linking on the dynamic moduli.

As stated above, the choice of a suitable thermoplastic for blending with epoxy resins is largely based on its T_g . Table 1 summarizes the T_g values of some thermoplastics used for blending with epoxy resins. It will be shown in the following sections that thermoplastics with high T_g increase the toughness of the epoxy without reducing the thermal properties and dynamic moduli of the epoxy matrix (Bucknall and Partridge 1983). On the other hand, thermoplastics with relatively low T_g , like some engineering and common thermoplastics, significantly depress the T_g and dynamic moduli of the blend (Vyas and Iroh 2013).

The case of PCL is quite interesting, as it has very low T_g (~ -66 °C) (Vanden Poel et al. 2005), so mechanical properties are not expected to improve. However, PCL/epoxy blends have given rise to smart shape memory epoxy blends (Luo and Mather 2010; Lützen et al. 2012; Torbati et al. 2014). Additionally, recent investigations have demonstrated self-healing behavior in thermoplastic epoxy blends (Luo et al. 2009; Jones et al. 2015). These properties provide more flexibility in design and open up opportunities in multi-shape coatings, adhesives, and films.

This chapter reviews the dynamic mechanical properties of thermoplastic epoxy blends. It will be shown that dynamic mechanical thermal analysis (DMTA) is a unique analytical tool to determine the extent of phase separation, mechanical behavior, and degree of interaction between both phases and the influence of crystallinity. Furthermore, DMTA is ideal to assess the suitability of a given blend to produce smart materials exhibiting shape memory or self-healing behavior. The following section discusses the application of DMTA to the investigation of epoxy resins blended with high-performance and engineering polymers.

High-Performance Thermoplastic/Epoxy Blends

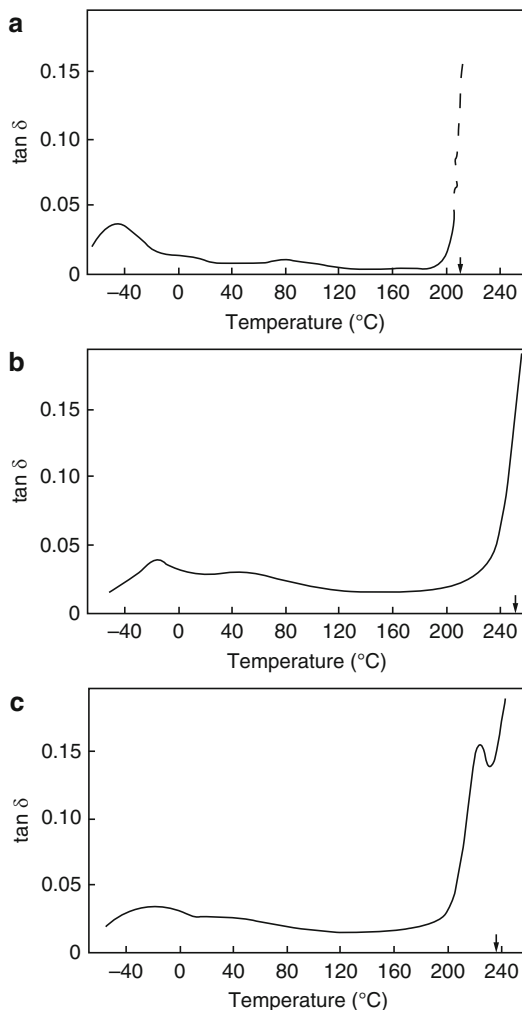
As stated above, these sorts of blends are suitable for high-performance applications (e.g., aerospace) due to the high glass transition temperature, T_g , of the thermoplastic. Some of these thermoplastics comprise polyether sulfone (PES) (Bucknall and Partridge 1983), polyetherimide (PEI) (Bucknall and Gilbert 1989), PI (Bonnet et al. 2001), hydroxyl- and tert-butyl-terminated polyether-ether ketone (PEEK) (Francis et al. 2005, 2007), and polyphenylsulfone (PPSu) (Cedeño and Vázquez-Torres 2005).

PES/Epoxy Blends

Bucknall and coworkers pioneered research on thermoplastics/epoxy blends, focusing on the high-performance PES Victrex 100-P (ICI) and two experimental epoxy resins named epoxy III and epoxy IV (Bucknall and Partridge 1983, 1984, 1986). The authors applied DMTA to investigate dynamic tensile properties and mechanical damping $\tan \delta (=E''/E')$ of the blends. Figure 5 shows plots of $\tan \delta$ of (a) neat PES, (b) cured epoxy, and (c) PES/epoxy blend with 25 phr (parts per hundred) PES. Figure 5a, b show the beginning of maximum damping associated to maximum energy dissipation per cycle of oscillation. These maxima are associated with the α -relaxation of each individual specimen, and this relaxation is identified as the T_g of the specimens. These results show that PES has a T_g of approximately 210 °C, whereas the T_g of the epoxy resin is about 250 °C. The relatively low values of $\tan \delta$ for both specimens which indicate high rigidity, i.e., very low energy dissipation per cycle of oscillation, are also noticed. The low $\tan \delta$ values of PES are associated to the stiffness of the polymeric chain.

Figure 5c shows the DMTA heating scan of the blend, which now exhibits two peaks, and these two peaks are associated to the T_g of PES and the epoxy resin, i.e., there is a phase-separated morphology in the blend. The authors pointed out to the usefulness of DMTA to discern phase separation in these blends. The results, however, showed that, as the PES and the two epoxy resins had comparable moduli, it was not entirely unexpected that the presence of a separate PES-rich, cross-linked phase had relatively little effect on the modulus of the blend. The authors also reported that the effect of the PES-rich phase upon fracture behavior was to produce

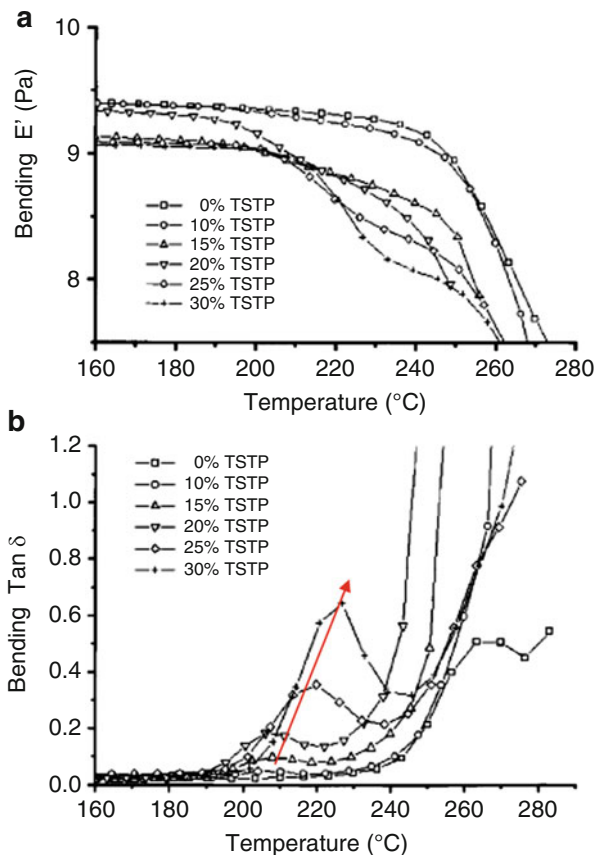
Fig. 5 Dynamic mechanical spectra of (a) neat PES, (b) 100 epoxy III 30 DDS, and (c) 100 epoxy III 30 DDS and 25 PES blend (Adapted from Bucknall and Partridge 1983)



deviation of the crack front around a nodular morphology, in a very similar way to elastomeric inclusions in samples fractured at low temperatures. Finally, Bucknall and Partridge (1983) concluded that the blend morphology had little influence if any on the mechanical performance of the blends.

Pethrick et al. (1996) reported on the dynamic mechanical properties and water absorption of a PES Victrex 5003P ($M_n = 24,000$ g/mol) blended with an amine-cured epoxy, triglycidylaminophenol (MY0510), using DDS as curing agent. PES was added up to 30 wt.% into the epoxy resin and the DMTA spectra for neat resin and blends are shown in Fig. 6. The $\tan \delta$ plots shown in Fig. 6b show that the neat epoxy exhibits a $T_g \sim 265$ $^{\circ}\text{C}$. Addition of 10% PES shows a lower temperature maximum in $\tan \delta$ at about 205 $^{\circ}\text{C}$ associated to PES, denoting a phase-separated

Fig. 6 Dynamic mechanical spectra of epoxy/PES blends varying the concentration of PES up to 30 wt.%. (a) Elastic tensile modulus E' , (b) mechanical damping $\tan \delta$ (Reprinted with permission from Pethrick RA, Hollins EA, McEwan I, MacKinnon JA, Hayward D, Cannon LA (1996) *Macromolecules* 29:5208-5214. Copyright 1996 American Chemical Society)



morphology in the blend. Note that, by increasing the concentration of PES, the lower temperature maximum shifted to higher temperatures and $\tan \delta$ increased in magnitude, as indicated by the arrow. The increase in glass transition temperature of PES phase suggests a degree of interpenetration between phases or an induced fractionation phenomenon where low molar mass PES was dissolved in the epoxy rich phase (Prolongo et al. 2010). The increase in magnitude of $\tan \delta$ indicates higher dissipation of energy in the blend as concentration of PES increased and suggests an increase of toughness in the blend. The elastic tensile modulus plots shown in Fig. 6a show that the modulus is relatively independent of PES concentration over a temperature range up to the glass transition of the thermoplastic. Above the glass transition, the elastic modulus behavior is tuned by the concentration of PES. Pethrick et al. (1996) showed that increasing the amount of thermoplastic in the epoxy system had the effect of reducing the amount of water sorption in the system indicating that the water is only present in the epoxy phase.

Akay and Cracknell (1994) investigated epoxy/PES blends using PES Victrex 5003P and mixing two epoxy resins, triglycidylaminophenol (MY0510) and a

phenol-formaldehyde novolac epoxy (DEN431); DDS was the curing agent. These authors reported increased toughness and ductility; at 20–40% concentration of PES, the impact strength increased over an order of magnitude, and the ultimate tensile strength (UTS) nearly increased twofold. The glass transition temperatures of the blends gradually decreased as concentration of PES increased, a behavior also reported by Pethrick et al. (1996). Akay and Cracknell (1994) associated the increase in toughness to spinodal/co-continuous morphologies.

The phase separation phenomenon between PES and the epoxy resin during curing gives rise to a number of morphologies in the blend (Yamanaka and Inoue 1989; Kim et al. 1993, 1995; Andres et al. 1998; Oyanguren et al. 1999; Kim and Char 2000). The phase separation eventually impacts the rheology, curing behavior, thermal properties, and mechanical performance of the blends (Mimura et al. 2000; Yu et al. 2003; Liu et al. 2010; Mackinnon et al. 1995). DMTA is quite effective to assess the influence of the thermoplastic phase on the final mechanical properties.

PES-PEES/Epoxy Blends

In order to improve the miscibility between PES and the epoxy resin, Blanco et al. (2003a, b, 2004) prepared a copolymer of 40:60 polyethersulfone-polyetherethersulfone (PES-PEES) ($M_n = 9,000$ g/mol) functionalized with amine end groups. Investigation using DGEBA epoxy and different curing agents, DDS and MDEA, showed quite distinct results (Blanco et al. 2004). Figure 7a, b shows plots of dynamic storage modulus as a function of temperature using MDEA and DDS, respectively, and increasing the concentration of PES-PEES up to 30%. Interestingly, the blend cured with MDEA exhibits phase separation (Fig. 7a), with a deleterious effect on the mechanical modulus. This viscoelastic behavior is not desirable as far as structural applications are concerned. However, the buildup of three elastic plateaus, which is more evident at 30 wt% concentration of PES-PEES, is noted. The first decay of storage modulus corresponds to the T_g of the epoxy rich phase, and the second decay corresponds to the T_g of the thermoplastic-rich phase. It will be shown in section “[Smart Thermoplastic/Epoxy Blends](#)” that this viscoelastic spectrum is quite suitable for shape memory behavior.

On the other hand, the blends cured with DDS exhibit a single phase which suggests the existence of an interpenetrating network (IPN) (Fig. 7b). The latter exhibits better mechanical properties. The difference in morphology was mainly attributed to different viscosity and solubility effects of the curing agents, MDEA versus DDS. These types of studies show the importance of the choice of curing agent on the phase separation behavior of epoxy/thermoplastic blends.

An investigation on DGEBS/PES-PEES blends adding a second tetrafunctional epoxy, TGDDM, to the mixture and curing with DDS showed the existence of an IPN, improvement in impact resistance, and the gradual increase of glass transition temperature, thus widening the range of the working temperature (Blanco et al. 2003a, b).

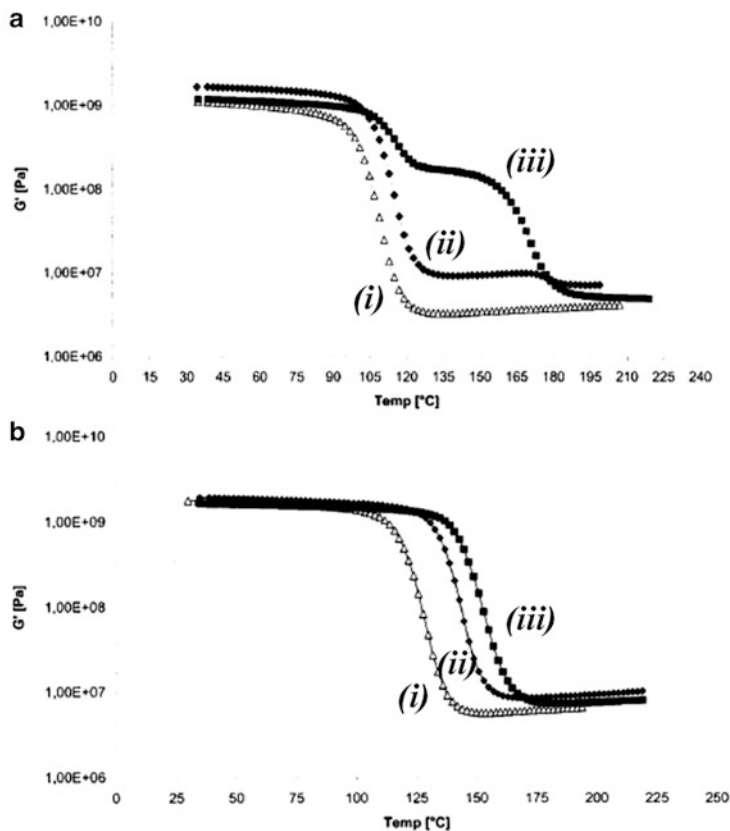


Fig. 7 Dynamic storage modulus as a function of temperature for DGEBA/PES-PEES blends cured with (a) MDEA and (b) DDS. The concentration PES-PEES is (i) 0, (ii) 15, and (iii) 30 wt.% (Adapted from Blanco et al. 2004)

Polyether Ketone-Based/Epoxy Blends

Poly(ether ether ketone) (PEEK) is a semicrystalline high-performance thermoplastic exhibiting high tensile modulus, thermo-oxidative stability, and high T_g (~143 °C) and melting transition temperature T_m (~343 °C) (Velisarís and Seferis 1986). PEEK is immiscible in epoxy resins limiting its application as reinforcer. However, reduction or disruption of crystallinity by chemical modification to produce amorphous PEEK enables miscibility with epoxy resins.

Zhong et al. (1998) modified PEEK with phenolphthalein (PEK-C) to obtain miscibility with bisphenol A-type epoxy resins; the blends were cured with DDM. The results showed incomplete curing reaction due to the high viscosity of PEK-C, and post-thermal treatment at elevated temperatures did not influence the degree of curing due to vitrification of the blends. Increasing the concentration of PEK-C leads to a slight reduction of the flexural modulus as well as reduction of the fracture

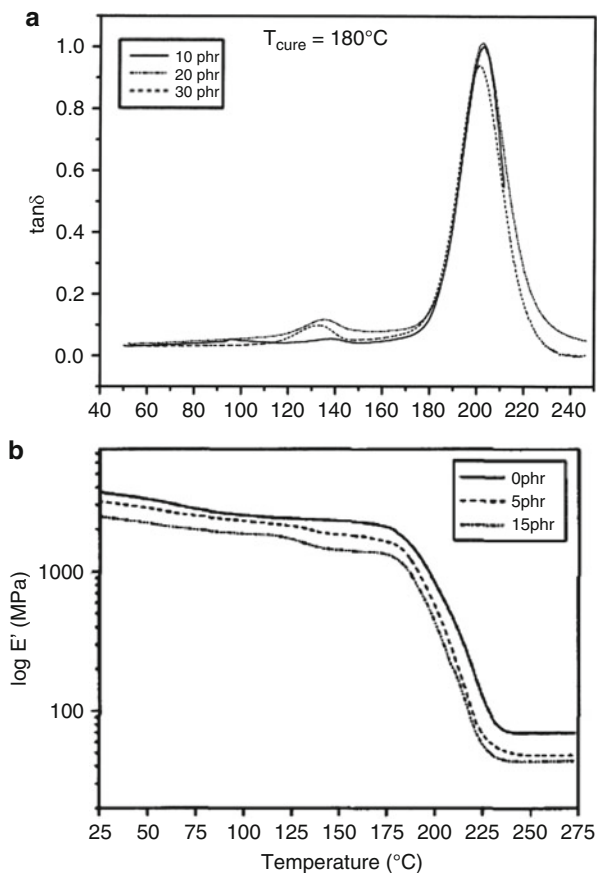
toughness factor which the authors ascribed to a reduced cross-link density in the blends. Although reduction in cross-link density generally increases the toughness and elongation at break, Zhong et al. (1998) reported slight reduction in elongation at break and brittle fracture behavior of DGEBA-PEK-C blends. On the other hand, Bennet et al. (1991) reported miscibility with TGDDM epoxy and considerable increase of fracture toughness (~350%) with no reduction of modulus when using amine-terminated PEEK oligomers based on tert-butyl hydroquinone and methyl hydroquinone. The greatest resistance to fracture was attained around 30% concentration, when PEK-C formed a continuous phase in the blend. Song et al. (2001) also studied blends of PEK-C and TGDDM and confirmed miscibility of the components. However, these authors also reported incomplete curing reaction, presumably due to the high viscosity of PEK-C. The smaller cross-link density resulted in lower tensile properties and reduced fracture toughness.

Francis et al. (2003, 2007) investigated the thermomechanical properties of blends of poly(ether ether ketone) with pendent tert-butyl groups (PEEKT) with DGEBA utilizing DDS. In the unreacted state, the mixtures were homogeneous; however, curing produced phase separation, i.e., $\tan \delta$ exhibited two well-separated maxima (Fig. 8a). The higher temperature peak associated to the epoxy T_g remained unchanged regardless of PEEKT concentration. On the other hand, the lower temperature peak associated to PEEKT T_g had small variations in the range of 130–140 °C. The authors reported considerable increase of impact resistance, relative to the neat epoxy, with relatively small changes of tensile strength and without influencing the thermal stability.

Note that the storage modulus was slightly reduced upon addition of PEEKT; however, it remained above 1 GPa up to the onset for glass transition (~175 °C), showing that PEEKT did not compromise the mechanical properties of the blend. Furthermore, the rubber-like moduli of the blends are smaller than the neat epoxy, thus indicating a reduction of cross-link density in the blends.

Francis et al. (2005) also investigated blends of hydroxyl-modified PEEK (PEEKTOH) and DGEBA epoxy, cured with DDS. PEEKTOH was dissolved in the epoxy resin by stirring at 120 °C, and the catalyst was added to promote the reaction between the hydroxyl group of PEEK and the epoxy ring. Contrary to PEEKT/epoxy blends, these blends did not exhibit a phase-separated morphology when analyzed by DMTA, i.e., $\tan \delta$ exhibited only one peak associated to the epoxy T_g . The T_g of the blends was slightly decreased with the addition of PEEKTOH probably due to interactions between the epoxy resin and PEEKTOH. Phase separation was established by scanning electron microscopy (SEM), and unlike classical polymer blends, the domain size was decreased when increasing the concentration of PEEKTOH. Moreover, the tensile storage modulus showed little variation, relative to the neat epoxy, and the modulus remained above 1 GPa up to about 175 °C. These blends also exhibited smaller cross-link density (extracted from the rubber plateau modulus) and fracture toughness more than double at only 15 phr concentration of PEEKTOH.

Fig. 8 Dynamic mechanical properties as a function of temperature of DGEBA/PEEKT blends cured with DDS. **(a)** Mechanical damping $\tan \delta$ (Francis et al. 2003); **(b)** tensile storage modulus E' (Francis et al. 2007)



The blend preparation and curing profile play a major role in the resultant morphology and thermomechanical properties of PEEKTOH/DGEBA blends. Contrary to Francis et al. (2005, 2006a) reported phase-separated morphologies when dissolving PEEKTOH in the DGEBA epoxy resin at 180 $^{\circ}\text{C}$, using DDS as curing agent.

The epoxy resin DGEBA was also blended with poly(ether sulfone ether ketone) (PESEK) using DDS as curing agent (Francis et al. 2006b). The authors reported a homogeneous morphology, i.e., $\tan \delta$ exhibited only one peak, which was confirmed by SEM analysis. The homogeneity of the blends was attributed to the similarity in chemical structure of the modifier and the cured epoxy network and due to the H-bonding interactions between the blend components. The storage moduli of the epoxy/PESEK were reduced relative to the neat epoxy, and the cross-link density of the blends was found to decrease with increase in PESEK concentration.

Engineering Thermoplastic/Epoxy Blends

Engineering polymers comprise a set of thermomechanical properties, thermal and chemical resistance, and barrier properties against oxygen, which enable a variety of applications ranging from structural to biomedical and food packaging. Examples include polyoxymethylene (POM), polyamides (PA, also known as nylon), polyesters (e.g., polyethylene terephthalate (PET) and polybutylene terephthalate (PBT)), and polycarbonate (PC).

Research on blends of engineering thermoplastics with epoxy resins is less frequent as miscibility is still the main hurdle and the resultant thermomechanical properties are relatively poor as compared to those obtained by blending high-performance thermoplastics with epoxy resins. The thermomechanical properties are seriously compromised due to the relatively low T_g of these thermoplastics. For instance, Vyas and Iroh (2013) reported blends of PA6 with DGEBA, where T_g of PA6 was 25 °C. Figure 9 shows dynamic mechanical properties of these blends. It can be seen that the glass transition is significantly decreased at only 5% concentration of PA6, shifting some 30 °C, from 70 °C (neat epoxy) to 40 °C. At 30% concentration of PA6, the blend exhibits a T_g around room temperature. Thus, although the storage modulus is relatively unchanged at low temperatures, the working range of temperatures is seriously compromised by the addition of a low T_g thermoplastic. It is noted that in the rubber-like regime the moduli of the blends are higher than the neat epoxy. This is due to the crystallization of PA6 during curing leading to the formation of crystalline regions in the amorphous matrix. The crystals act as nanoreinforcers in the rubber-like regime.

Another approach in thermoplastic/epoxy blends is utilizing the epoxy as a *compatibilizer* agent in order to increase the toughness of the thermoplastic. This approach was used by Arostegui and Nazabal (2004) when toughening PBT. Blends of PBT and PEO were prepared adding epoxy up to 2 wt.%. The epoxy resin acted as the compatibilizer agent because under melt conditions the end groups of PBT would be able to react with the oxirane groups of the epoxy. DMTA results showed a phase-separated morphology, i.e., $\tan \delta$ exhibited two peaks associated to the glass transitions of PBT and PEO. Nevertheless, the results showed that the impact strength of the 80:20 PBT-PEO blend increased threefold at only 1 wt.% concentration of epoxy. Further aspects of crystallization kinetics and reactive extrusion of PBT/epoxy blends have been reported by Kulshreshtha et al. (2003) and Hert (1992), respectively.

Blends of poly(benzyl methacrylate) (PBzMA) with DGEBA and cured with DDM were studied by Prolongo et al. (2010), increasing concentration of PBzMA up to 25 wt.%. PBzMA is an amorphous thermoplastic with $T_g \sim 65$ °C as measured by DSC (note that Prolongo et al. (2010) reported $T_g \sim 80$ °C as measured by DMTA at 1 Hz and this value was utilized for their discussion of results). PBzMA is easily soluble in common solvents; therefore, solution mixing with the epoxy resin is straightforward. The blends exhibited phase separation at all concentrations of PBzMA, as shown by DMTA analysis; mechanical damping $\tan \delta$ plots are shown in Fig. 10. Figure 10a shows that, at low concentrations of PBzMA, the T_g of

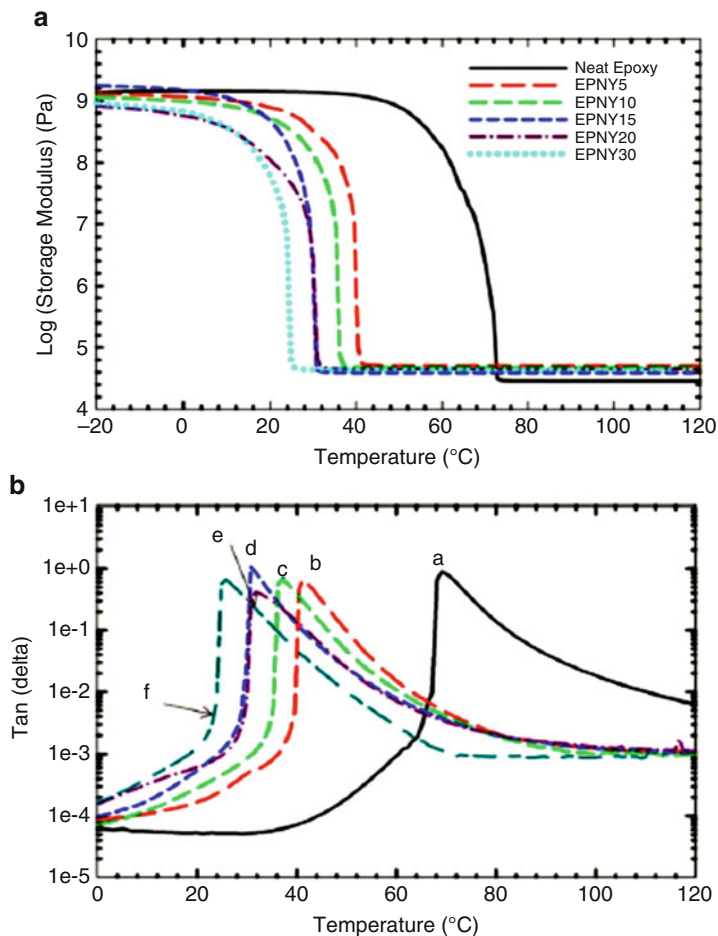
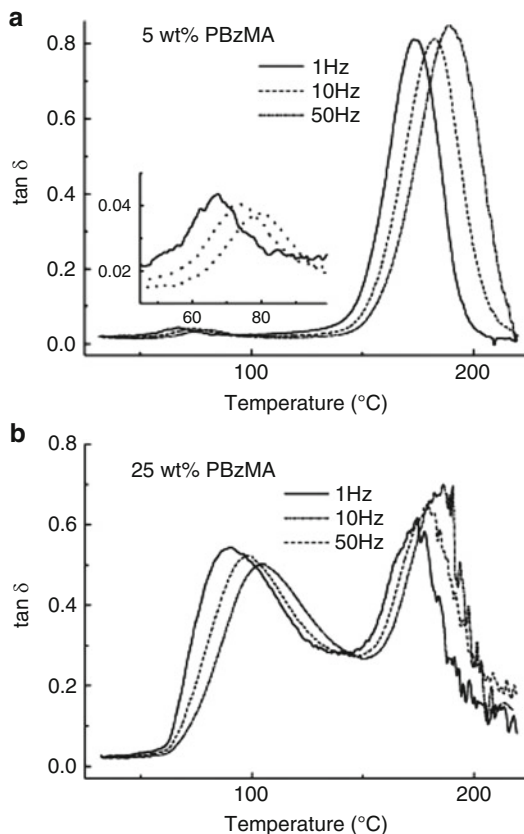


Fig. 9 Dynamic mechanical properties as a function of temperature and concentration of PA6 of DGEBA/PA6 blends. (a) Storage modulus; (b) mechanical damping $\tan \delta$ (Vyas and Iroh 2013)

PBzMA phase was slightly reduced to 68 °C (the temperature of $\tan \delta$ peak at 1 Hz). This reduction of T_g was ascribed to the plasticization by residual epoxy oligomers trapped in the PBzMA phase, in a manner similar to poly methyl-methacrylate (PMMA)/epoxy blends (Mondragon et al. 1998). Interestingly, at high concentration of PBzMA, the T_g of this phase became higher than the neat PBzMA (Fig. 10b) due to induced fractionation phenomena. That is, low molar mass PBzMA remained dissolved in the epoxy rich phase. Furthermore, at higher concentrations of PBzMA, the morphology was phase inverted, and the dissipation of energy per cycle of oscillation was comparable for the PBzMA and epoxy phases (Fig. 10b). Thus, variations of T_g and $\tan \delta$ appeared to be correlated with the morphology attained in the blend.

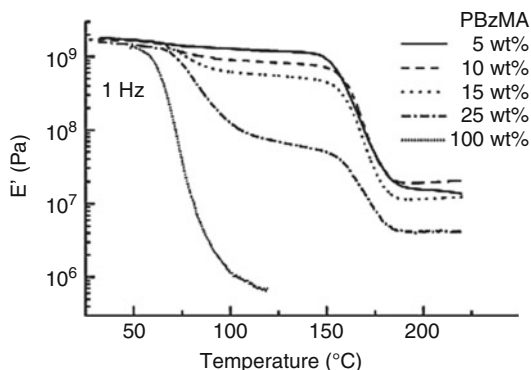
Fig. 10 Mechanical damping $\tan \delta$ as a function of temperature, frequency of oscillation, and concentration of PBzMA of DGEBA/PBzMA blends. (a) 5 wt.% PBzMA; (b) 25 wt.% PBzMA (Adapted from Prolongo et al. 2010)



Plot of dynamic storage modulus as a function of temperature for PBzMA/epoxy blends is shown in Fig. 11. Note that the moduli of the blends are similar to the neat epoxy at low temperatures (~ 2 GPa). As in other thermoplastics, the T_g and concentration of PBzMA greatly influence the mechanical performance of the blend. Whereas the blend with 5% PBzMA exhibited excellent mechanical performance up to ca. 150 °C, increasing the concentration of PBzMA gradually reduced the storage modulus above T_g of the PBzMA phase. The viscoelastic spectrum of the 25% PBzMA/epoxy blend is quite interesting as it shows three plateaus: (a) at $T < 75$ °C, there is a low-temperature glassy regime of PBzMA and epoxy phases; (b) at $75 < T < 150$ °C, there is a plateau due to the glassy state of the poly-rich phase; (c) at $T > 150$ °C, there is the rubber-like plateau due to the cross-linked network. It is the view of this author that the 25% PBzMA/epoxy blend would exhibit shape memory behavior, in fact triple-shape memory behavior. Shape memory behavior in thermoplastic/epoxy blends will be discussed in the following section.

Determination of the *peak factor* Γ , defined as the width at half maximum height of $\tan \delta$ peak divided by its height, is a useful method to qualitatively assess the

Fig. 11 Mechanical storage modulus as a function of temperature and concentration of PBzMA of DGEBA/PBzMA blends (Adapted from Prolongo et al. 2010)



homogeneity of the phases. Prolongo et al. (2010) reported that neat PBzMA had a $T_g = 12^\circ\text{C}$, whereas blends containing 5–17% PBzMA had T_g varying from 23°C to 37°C , indicating greater heterogeneity of the phase. These results support the hypothesis that some epoxy molecules remained mixed with the PBzMA phase in the blends. Analysis of the peak factor for the epoxy peak showed negligible variations, $T_g = 32^\circ\text{C}$ for the neat epoxy, and T_g varied from 25°C to 32°C for the epoxy phase.

The activation energy for the glass rubber relaxation is another important property that can be determined by DMTA by carrying out temperature frequency scans and using the Arrhenius equation

$$\ln f = \ln A - E_a / (RT_{\max}) \quad (1)$$

where T_{\max} is the temperature at the maximum $\tan \delta$ at the frequency f , A is the pre-exponential factor, E_a is the apparent activation energy for the glass rubber relaxation, and R is the universal gas constant. Thus, plots of $\ln f$ versus $1/T_{\max}$ produce straight lines, and the slope equals E_a/R . The activation energy is a quantitative measure to assess molecular mobility, i.e., it characterizes the sensitivity of a relaxation process to temperature, which depends on the types of motions concerned. Prolongo et al. (2010) reported E_a values for PBzMA/epoxy blends; the E_a for PBzMA phase was significantly smaller than E_a for the epoxy phase. This was associated to the higher molecular flexibility of PBzMA compared with the highly cross-linked epoxy network.

Mimura et al. (2001) investigated blends of PBzMA/epoxy based copolymers prepared in situ, i.e., by reacting the monomers during the epoxy curing process. Depending on the copolymer composition, this method produced a semi-interpenetrating network, and the SEM results showed the formation of a homogeneous phase, which was consistent with a single $\tan \delta$ peak observed by DMTA. The epoxy/thermoplastic blend displayed an increase of glass transition (up to $\sim 10^\circ\text{C}$) and twofold increase of fracture toughness.

Blends of poly(styrene-*co*-acrylonitrile) (SAN) with epoxy have also been studied by Song et al. (2000), Lopez et al. (2002), and José et al. (2008). The curing kinetics of SAN/TGDDM epoxy cured with DDS was characterized by DMTA (Lopez et al. 2002). These authors established that gelation and vitrification are controlling factors of phase separation which occur during curing. Jose et al. (2008) reported that SAN/epoxy blends exhibited phase-separated morphologies. DMTA analysis showed that there was an increase in the height of the α -relaxation peak of SAN with increase of SAN concentration. These authors ascribed this increase to the shift in primary morphology from a particulate to phase inversion. Independent morphology analysis corroborated the DMTA results.

The thermomechanical properties and morphology of poly(acrylonitrile-butadiene-styrene) (ABS)/epoxy blends have been reported by Jyotishkumar et al. (2009), whereas the thermal decomposition and mechanical properties were reported by Abad et al. (2001). Jyotishkumar et al. (2009) used DGEBA epoxy and DDS as curing agent. ABS is an interesting thermoplastic with a phase-separated morphology of its own and T_g ca. -88 °C (butadiene phase) and 105 °C (styrene phase). The rather low-temperature T_g of the butadiene phase would play a limited role, if any, in the mechanical performance of blends at higher temperatures. Neat DGEBA cured with DDS exhibits a $T_g \sim 216$ °C.

DMTA scans of ABS blended with DGEBA and cured with DDS are shown in Fig. 12a, b. The plots of $\tan \delta$ (Fig. 12a) evidence a phase-separated morphology with a high-temperature peak associated to the epoxy phase and a low-temperature peak associated to the ABS phase. Increasing the concentration of ABS produced a slight shift to lower temperatures of the epoxy peak and a slight temperature increase of the ABS peak, denoting some degree of interaction between these phases.

Figure 12b shows the storage modulus as a function of temperature of the neat epoxy and thermoplastic and their blends. It can be seen that the storage modulus of ABS decays rapidly after the onset of glass transition, c.a. 100 °C. On the other hand, the storage modulus of the cured epoxy remained relatively constant up to ca. 200 °C, just below its glass transition. Noteworthy, the storage moduli of all blends are higher than the neat epoxy up to the glass transition temperature of the ABS phase, i.e., the ABS phase acted as reinforcer of the epoxy resin. The mechanical performance is strongly influenced by the concentration of ABS. At low concentrations of ABS (5 and 10 phr), the storage moduli of the blends remained higher than that of the neat epoxy, after the glass transition of the ABS phase, and this trend continued even in the rubber-like regime ($T > 225$ °C). On the other hand, for the blends with higher concentrations of ABS (15 and 20 phr), the storage moduli of the blends decayed below that of the neat epoxy at the onset of glass transition of ABS. Interestingly, the storage moduli of these blends were smaller than the neat epoxy even in the rubber-like regime. Jyotishkumar et al. (2009) concluded that the higher values of the storage modulus suggest better load-bearing capacity of the blends. Moreover, these authors suggest that higher values of the storage modulus in the rubber-like regime are an indication that the blends have better interaction between the phases. Lower values of the storage modulus suggest smaller cross-link density probably due to ABS disrupting/interpenetrating to some extent the epoxy phase.

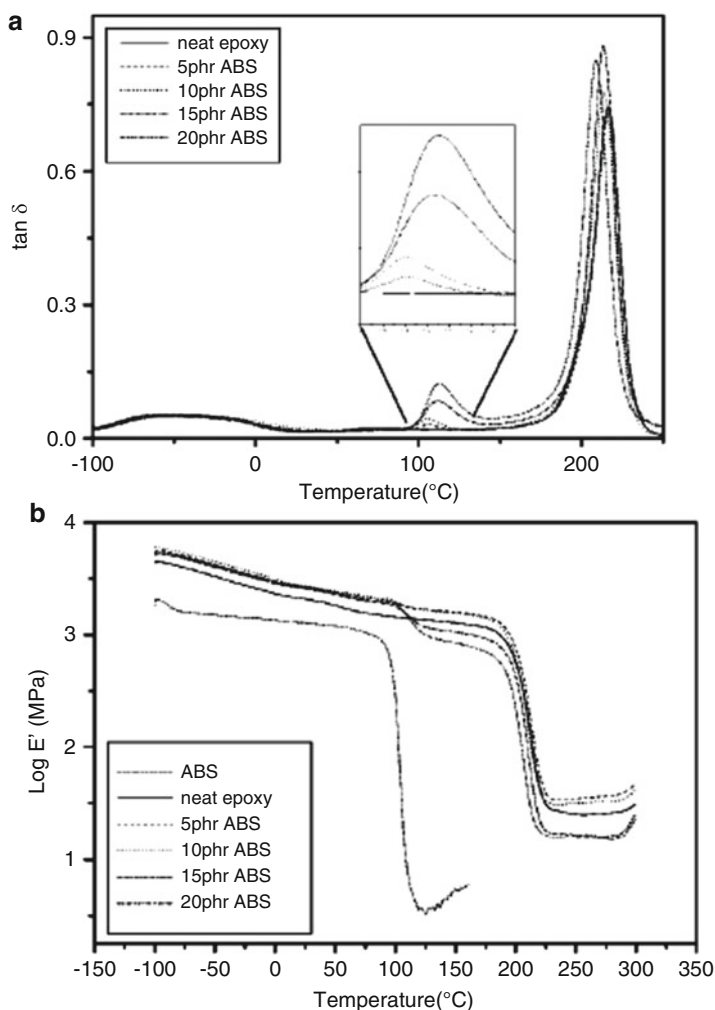


Fig. 12 Dynamic mechanical properties as a function of temperature of ABS/epoxy blends. **a** Mechanical damping $\tan \delta$; **b** storage modulus (Reprinted with permission from Jyotishkumar P, Koetz J, Tiersch B, Strehmel V, Özdilek C, Moldenaers P, Hässler R, Thomas S (2009) *J Phys Chem B* 113:5418–5430. Copyright 2009 American Chemical Society)

Smart Thermoplastic/Epoxy Blends

In the above sections, the body of research focused on enhancing the fracture toughness of epoxy resins by blending with high-performance and engineering thermoplastics and with the aim of not compromising the original mechanical and thermal properties of the epoxy phase has been described. New materials

innovations have been in the direction of producing smart materials by taking advantage of quite dissimilar thermal transitions and mechanical modulus of both components. Moreover, aspects like crystallinity in the thermoplastic or epoxy are also advantageous as crystallinity can be fine-tuned by thermal treatments and this can influence mechanical performance. Recent developments in shape memory and self-healing thermoplastic/epoxy blends are discussed.

Thermoplastic/Epoxy Blends with Shape Memory Behavior

Shape memory polymers (SMPs) are a class of smart materials that respond dynamically to external stimuli like heat, electric field, magnetic field, infrared radiation, and UV radiation. Because SMPs can store a temporal shape and return to their original (permanent) shape simply by applying the proper stimulus, these materials have acquired application relevance in a variety of technological fields ranging from medical to aeronautics. A shape memory phenomenon is not an intrinsic property of polymers. Under the appropriate thermomechanical conditions, these polymeric materials will exhibit more or less temporal shape stability – so-called shape “fixing” – and shape recovery to the permanent shape (Mather et al. 2009).

There is now much research on designing polymeric materials with shape memory properties including molecular networks (Bellin et al. 2006; Liu et al. 2002; Chung et al. 2008), nanostructured molecular networks (Alvarado-Tenorio et al. 2011, 2015), epoxy systems (Xie and Rousseau 2009), hyperbranched polymers/epoxy blends (Santiago et al. 2015), and thermoplastic/epoxy blends (Luo and Mather 2010; Torbati et al. 2014).

Design of thermoplastic/epoxy blends with shape memory behavior consists of choosing components with well-separated thermal transition temperatures (which act as triggers for shape fixing and shape recovery) and quite distinct elastic modulus plateaus. This mechanical behavior appeared as a drawback for structural applications, as described in the previous sections, but it is advantageous in the design of shape memory behavior. DMTA is an ideal tool to predict shape memory properties and provides information for designing thermomechanical programs for shape fixing and recovery. The thermally activated shape memory behavior is illustrated in Fig. 13.

Luo and Mather (2010) utilized DMTA to design a thermoplastic/epoxy blend with triple-shape memory behavior. Triple-shape memory polymers are capable of fixing *two* temporary shapes and recovering sequentially from one temporary shape to the other and eventually to the permanent shape upon heating. A triple-shape memory polymer needs two separate shape-fixing mechanisms distinguished by separated thermal transitions in the application temperature range, leading to a cascade of three elastic modulus plateaus of decreasing magnitude with increasing temperature. These authors blended electrospun PCL microfibers ($M_w = 65,000$ g/mol) with the shape memory epoxy formulation based on DGEBA, neopentyl glycol diglycidyl ether (NGDE), and poly(propylene glycol) bis(2-amino propyl) ether (Xie and Rousseau 2009). The large interfacial area intrinsic with this percolating

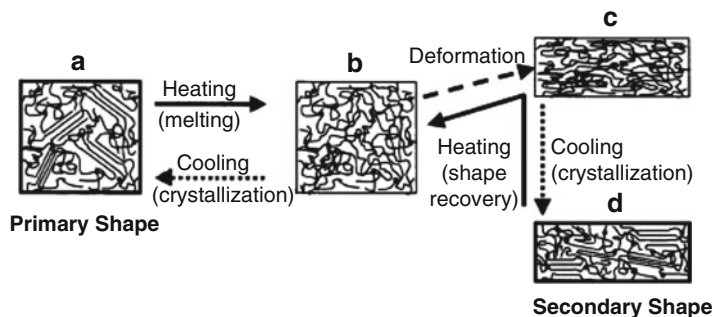


Fig. 13 Schematic depiction of the microstructural transformations during a shape memory cycle of a chemically cross-linked semicrystalline polymeric network (Reprinted with permission from Liu C, Chun SB, Mather PT, Zheng L, Haley EH, Coughlin EB (2002) *Macromolecules* 35: 9868-9874. Copyright 2002 American Chemical Society)

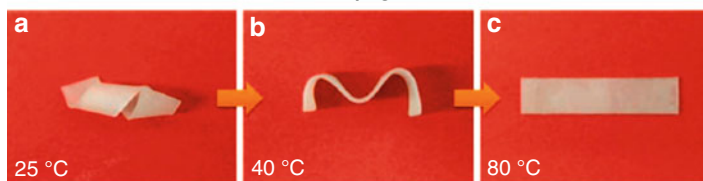
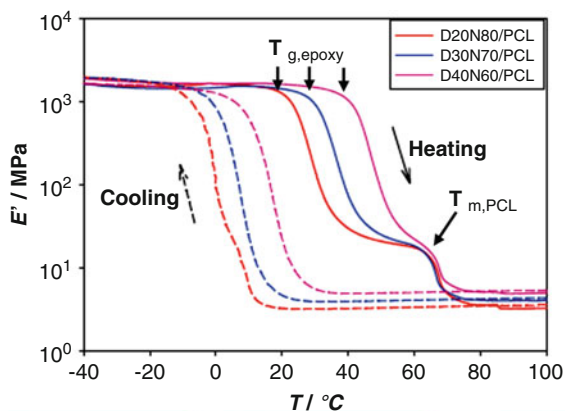


Fig. 14 Tensile storage modulus as a function of temperature during heating and cooling of epoxy/PCL blends. Varying the epoxy formulation enables fine-tuning of its T_g . Three elastic plateaus are identified promoting triple-shape memory behavior. Photographs show the triple-shape memory behavior of D30N70/PCL (Adapted from Luo and Mather 2010)

nonwoven fiber/matrix morphology greatly facilitated load transfer and load distribution and led to enhanced shape fixing. The T_g of the epoxy was tuned by controlling the ratio DGEBA/NGDE, and the viscoelastic spectra and shape memory behavior of these blends are shown in Fig. 14.

The DMTA spectra of Fig. 14 show that the T_m of PCL is not affected by the concentration of epoxy which suggests no interaction between the phases and enables better control of shape fixing and recovery. Luo and Mather (2010) pointed out that the semicrystalline nature of the thermoplastic component imposes restrictions to promote triple-shape memory behavior due to its tendency to crystallize under specific conditions. The crystallization of the thermoplastic was monitored using DMTA and enabled to identify 40 °C as the optimum temperature for thermomechanical programming.

Tobarti et al. (2014) also reported triple-shape memory behavior in thermoplastic/epoxy blends. These authors investigated blends of amorphous and semicrystalline epoxy formulations with electrospun PCL. Although the behavior of these epoxy formulations was quite distinct (the semicrystalline epoxy behaved elastomeric, whereas the amorphous epoxy was quite stiff), the blends exhibited distinct transition temperatures and elastic moduli, enabling shape memory behavior. The shape memory cycles as determined by DMTA assessed the excellent shape fixing and recovery displayed by these blends.

Tobarti et al. (2014) showed that these systems were able to fix two separate deformations, one based on PCL crystallization and a second one by crystallization or vitrification of the epoxy phase.

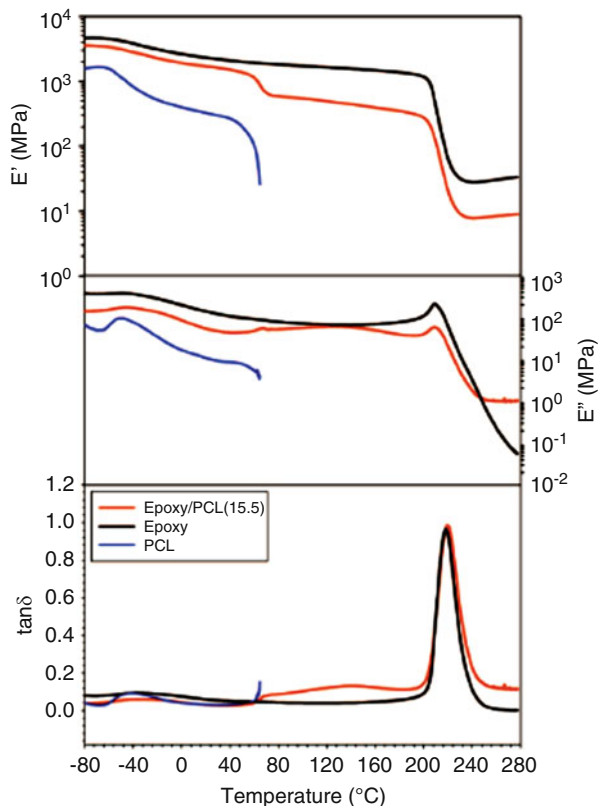
Self-Healing Thermoplastic/Epoxy Blends

Self-healing is a process inspired by biological organism where specific mechanisms can be triggered to automatically repair damage. This property is quite attractive as it would enable mending fractures in structures without the need of dismounting parts with the consequence of cost and downtime. Fracture-initiated chemical reaction has been utilized where hollow microspheres or fibers are loaded with different reactive species.

However, Luo et al. (2009) reported a different route using a thermoplastic/epoxy blend and taking advantage of the low melting transition temperature of the thermoplastic relative to the glass transition temperature of the cured epoxy. This means that heating the blend above the T_m of the thermoplastic phase, but still below the T_g of the epoxy phase, would promote flow of the thermoplastic phase, thus filling voids/fractured regions in the blend, i.e., a healing process.

Luo et al. (2009) blended PCL with DGEBA and cured using DDS. The PCL had relatively high molecular weight ($M_n = 42,500$ g/mol and $M_w = 65,000$ g/mol), and the epoxy and PCL were melt mixed at 120 °C, DDS was added at 140 °C, and the mixture was cured for 3 h at 180 °C. Figure 15 shows dynamic mechanical properties of a PCL/epoxy blend and the neat epoxy and neat PCL. The blend consists of a mass ratio $m_{\text{DGEBA}}/m_{\text{PCL}} = 80:20$ and was denoted epoxy/PCL(15.5). Note that the T_m of PCL is ca. 59 °C and the T_g of the cured epoxy is 203 °C. Therefore, there is an ample range of temperatures where PCL is molten without affecting the epoxy phase. These authors identified the $m_{\text{DGEBA}}/m_{\text{PCL}} = 80:20$ as the optimum

Fig. 15 Dynamic mechanical properties as a function of temperature of DGEBA/PCL 80:20 blends compared with neat epoxy and neat PCL (Reprinted with permission from Luo X, Ou R, Eberly DE, Singhal A, Vyratyaporn W, Mather PT (2009) ACS Appl Mater Interfaces 1: 612-620. Copyright 2009 American Chemical Society)



concentration of PCL for the self-healing effect, and this composition corresponded to an inverted morphology, where PCL forms a percolating continuous phase highly interpenetrated with the epoxy phase, as shown in Fig. 16. Figure 17 illustrates the healing process of heating the blend at 190 °C ($<T_g$ of the epoxy phase) for 8 min. The authors demonstrated that the healed specimen had similar or even better mechanical performance than the virgin specimen.

Another approach was reported by Luo and Mather (2013) where the T_m of the thermoplastic phase is now greater than the T_g of the epoxy phase and taking advantage of an epoxy formulation with shape memory behavior, thus producing a shape memory-assisted self-healing (SMASH) coating. The thermoplastic was PCL ($T_m = 60$ °C) and it was first electrospun as nonwoven mats consisting of micro- and nanoscale-diameter fibers in order to maximize the interfacial area and provide a more sustained healing agent. The epoxy formulation with shape memory behavior consisted of an equimolar mixture of DGEBA, neopentyl glycol diglycidyl ether (NGDE), and poly(propylene glycol) bis(2-amino propyl) ether (Xie and Rosseau 2009). Self-healing is initiated by heating the damaged coating to a temperature

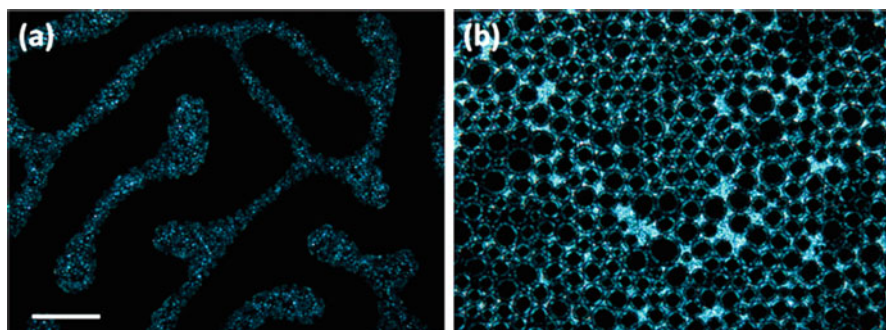


Fig. 16 Polarized optical micrographs of DGEBA:PCL blends with composition **a** 85:15 and **b** 80:20, exhibiting a bi-continuous and phase-inverted morphologies, respectively (Reprinted with permission from Luo X, Ou R, Eberly DE, Singhal A, Vyratyaporn W, Mather PT (2009) ACS Appl Mater Interfaces 1: 612-620. Copyright 2009 American Chemical Society)

higher than T_m of the fibers as well as the T_g of the shape memory epoxy. The following events take place simultaneously: (1) shape recovery of the epoxy matrix that releases the stored strain energy in the plastic zone and brings crack surfaces into spatial proximity and (2) melting and flow of the thermoplastic to heal the crack. The SMASH process is illustrated in Fig. 18.

It is anticipated that these simple approaches of smart epoxy-based materials design relying on quite dissimilar thermal transitions and mechanical moduli (as determined by DMTA) between the thermoplastic-rich phase and the epoxy-rich phase would be applicable to other thermoplastic/epoxy blends opening up opportunities for a new generation of reinforced self-healing coatings and films.

Conclusions

Epoxy/thermoplastic blends are very versatile materials where materials design must balance the properties between the thermoplastic phase and the epoxy phase. This implies the selection of the epoxy resin and curing agent to modulate the glass transition temperature and cross-link density. Then, the thermoplastic must be selected with the appropriate glass transition temperature and perhaps added functionality (e.g., amine or hydroxyl end groups) to favor compatibility/interaction with the epoxy matrix. Phase separation upon curing is a critical factor driving the epoxy/thermoplastic physical properties, and DMTA has proved a key analytical technique to assess the phase separation *and* its influence on mechanical properties and thermal transitions.

In reviewing the literature, it can be seen that structural applications of epoxy/thermoplastic blends rely on achieving high-performance properties where the thermoplastic-rich phase will contribute to increase fracture toughness but without being penalized by the loss of modulus and thermal stability. This goal has been largely accomplished by using high-performance thermoplastics.

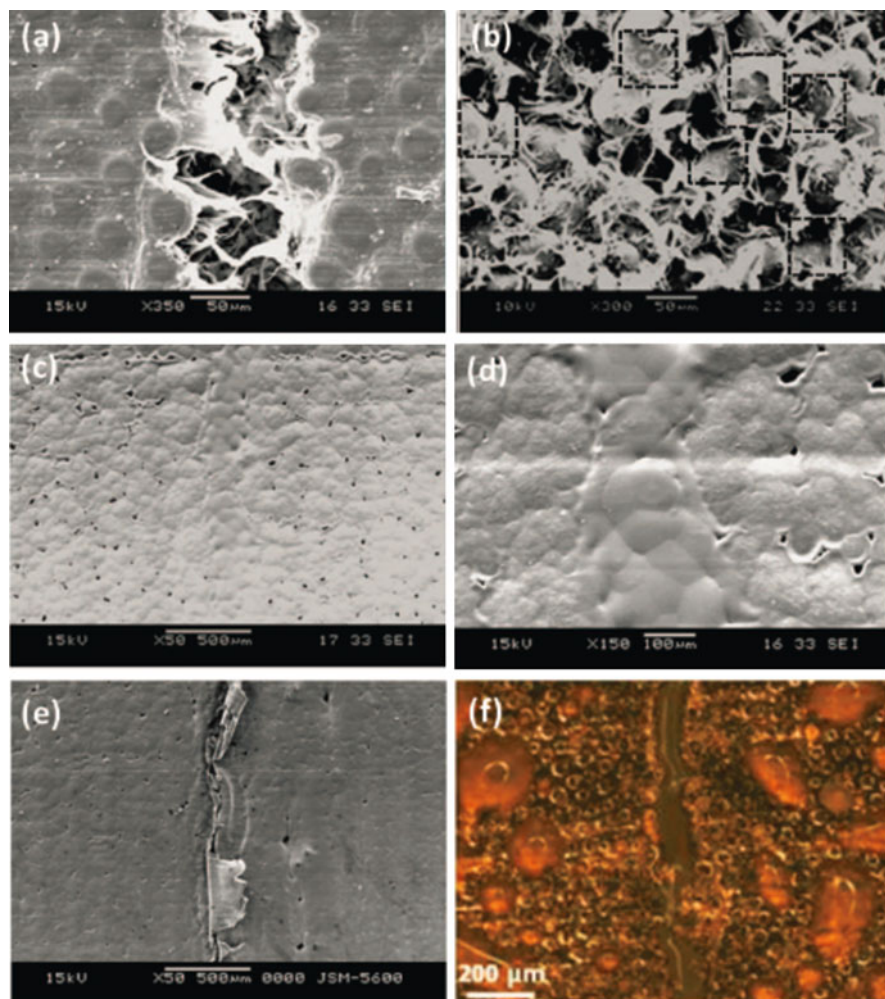


Fig. 17 Visualization of the fracture healing process in DGEBA/PCL 80:20 blend. SEM micrographs of **a** crack of fractured specimen, **b** the fractured surface, **c**, **d** the cracked surface after thermal mending, **e** the crack of a previously mended sample. **f** Stereoptical micrograph taken during the thermal healing process (Reprinted with permission from Luo X, Ou R, Eberly DE, Singhal A, Vyratyaporn W, Mather PT (2009) ACS Appl Mater Interfaces 1: 612-620. Copyright 2009 American Chemical Society)

In using engineering thermoplastics, with moderate to low glass transition temperatures, it has been seen that T_g defines the upper working limit as the mechanical modulus of the blend decays drastically above the T_g of the thermoplastic phase. The decay in modulus can be mitigated when an interpenetrated network is achieved between the blend components.

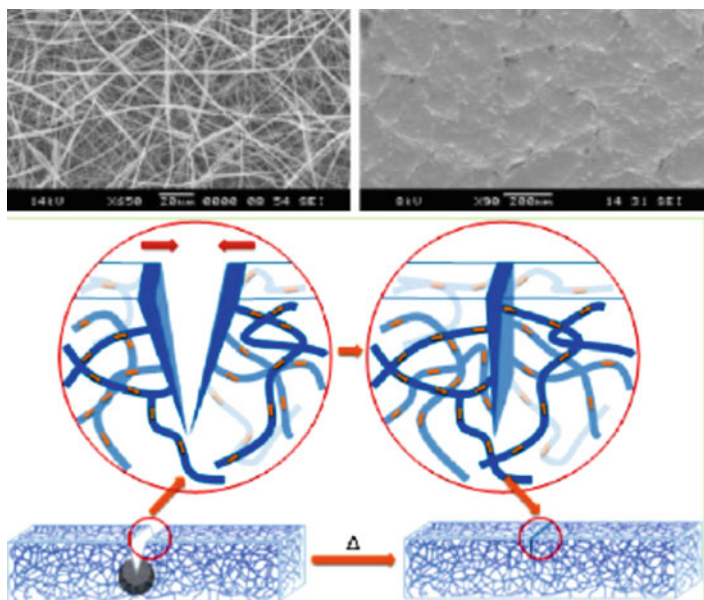


Fig. 18 SEM micrographs of electrospun nonwoven PCL microfibers and PCL/epoxy coating. Scheme illustrates the SMASH process (Reprinted with permission from Luo X, and Mather PT (2013) ACS Macro Lett 2: 152-156. Copyright 2013 American Chemical Society)

A different, and quite effective, approach in epoxy/thermoplastic blends has been to utilize the epoxy phase at low concentrations. Phase separation promotes the formation of epoxy domains which act as reinforcers of the thermoplastic.

Finally, it is striking that the dissimilarities between thermal transitions and mechanical modulus which have been traditionally considered a major hurdle have recently proved to be advantageous when designing smart epoxy/thermoplastic blends. Indeed, recent innovations have shown that temperature-activated shape memory and self-healing behavior rely on well-separated transition temperatures and quite different elastic plateau modulus. It has been shown that DMTA is a critical tool to assess the potential for smart behavior and define thermomechanical programming for optimum performance. In light of these findings, it is anticipated that previously studied epoxy/thermoplastic blends which went unnoticed as smart materials would be revised and more research would be fueled with the goal of identifying novel properties on epoxy/thermoplastic blends.

Glossary of Terms

Epoxy Resins

DGEBA Diglycidyl ether of bisphenol A

DGEBF Diglycidyl ether of bisphenol F

DGEBS Diglycidyl ether of bisphenol S
FTGPAP Triglycidylparaaminophenol
TGAP Triglycidyl p-aminophenol
TGDDM Tetraglycidyl 4,4'-diaminediphenylmethane

Hardeners

BAC 1,3-Bisaminomethylcyclohexane
DDM 4,4'-Diaminodiphenylmethane
DDS 4,4'-Diaminodiphenylsulfone
DETDA 3,5-Diethyltoluene-2,4-diamine or 3,5-diethyltoluene-2,6-diamine
DICY Dicyandiamide
EMI-2,4 2-Ethylene-4-methane-imidazole
MCDEA 4,4'-Methylene bis[3-chloro-2,6-diethylaniline]
MDEA 4,4'-Methylenebis(2,6-diethylaniline)
MTHPA Methyltetrahydrophthalic anhydride
TETA Triethylenetetramine
3DCM 4,4'-Diamino-3,3'-dimethydicyclohexylmethane
3,3'-DDS 3,3'-Diaminodiphenylsulfone

Thermoplastics

ABS Acrylonitrile-butadiene-styrene
ATPDMS Diaminopropyl-terminated polydimethylsiloxane
HBP Hydroxy-functionalized hyperbranched polymer
HTPDMS Dihydroxypropyl-terminated PDMS
PA Polyamide
PAEK Poly(aryl ether ketone)
PB Poly(butadiene)
PBT Poly(butylene terephthalate)
PBzMA Poly(benzyl methacrylate)
PC Polycarbonate
PCL Poly(ϵ -caprolactone)
PDMS Polydimethylsiloxane
PEEKOH Hydroxyl-terminated poly(ether ether ketone) based on tert-butyl hydroquinone
PEEKT Poly(ether ether ketone) based on tertiary butyl hydroquinone
PEES Polyetherethersulfone
PEI Polyetherimide
PEK-C Phenolphthalein poly(ether ether ketone)
PENT Poly(cyanoarylene ether)
PEO Poly(ethylene octene)

PES Poly(ether sulfone)
PESEK Poly(ether sulfone ether ketone)
PI Polyimide
PMI Poly(phenylmaleimide)
PMMA Poly(methyl-methacrylate)
PP Poly(propylene)
PPE Poly(phenylene ether)
PPE Poly(2,6-dimethyl-1,4-phenylene ether)
PPO Poly(2,6-dimethyl-1,4-phenylene oxide or poly(propylene oxide))
PPSu Poly(phenyl sulfone)
PS Poly(styrene)
PSu Polysulfone
PU Poly(urethane)
PVAc Poly(vinyl acetate)
PVP Poly(N-vinyl pyrrolidone)
RTPSA Amine-terminated polysulfones
SAN Poly(styrene-co-acrylonitrile)

References

- Abad MJ, Barral L, Cano J, López J, Nogueira P, Ramírez C, Torres A (2001) Thermal decomposition behavior and the mechanical properties of an epoxy/cycloaliphatic amine resin with ABS. *Eur Polym J* 37:1613–1623
- Akay M, Cracknell JG (1994) Epoxy resin-polyethersulphone blends. *J Appl Polym Sci* 52:663–685
- Alvarado-Tenorio B, Romo-Uribe A, Mather PT (2011) Microstructure and phase behavior of POSS/PCL shape memory nanocomposites. *Macromolecules* 44:5682–5692
- Alvarado-Tenorio B, Romo-Uribe A, Mather PT (2015) Nanoscale order and crystallization in POSS/PCL shape memory molecular networks. *Macromolecules* 48:5770–5779
- Andrés MA, Garmendia J, Velea A, Eceiza A, Mondragon I (1998) Fracture toughness of epoxy resins modified with polyethersulfone: influence of stoichiometry on the morphology of the mixtures. *J Appl Polym Sci* 69:183–191
- Aróstegui A, Nazábal J (2004) Compatibilization of a poly(butylene terephthalate)/poly(ethylene octene) copolymer blends with different amounts of an epoxy resin. *J Appl Polym Sci* 91:260–269
- Bellin I, Kelch S, Robert L, Lendlein A (2006) Polymeric triple-shape materials. *Proc Natl Acad Sci U S A* 103:18043–18047
- Bennett GS, Farris RJ, Thompson SA (1991) Amine-terminated poly(aryI ether ketone)-epoxy/amine resin systems as tough high performance materials. *Polymer* 32:1633–1641
- Blanco I, Cicala G, Lo Faro C, Recca A (2003a) Improvement of thermomechanical properties of a DGEBS/DDS system blended with a novel thermoplastic copolymer by realization of a semi-IPN network. *J Appl Polym Sci* 88:3021–3025
- Blanco I, Cicala G, Lo Faro C, Recca A (2003b) Development of a toughened DGEBS/DDS system toward improved thermal and mechanical properties by the addition of a tetrafunctional epoxy resin and a novel thermoplastic. *J Appl Polym Sci* 89:268–273
- Blanco I, Cicala G, Motta O, Recca A (2004) Influence of a selected hardener on the phase separation in epoxy/thermoplastic polymer blends. *J Appl Polym Sci* 94:361–371

- Blanco I, Cicala G, Lo Faro C, Motta O, Recca G (2006) Thermomechanical and morphological properties of epoxy resins modified with functionalized hyperbranched polyester. *Polym Eng Sci* 46:1502–1511
- Bonnet A, Lestriez B, Pascualt JP, Sautereau H (2001) Intractable high-T_g thermoplastics processed with epoxy resin: interfacial adhesion and mechanical properties of the cured blends. *J Polym Sci Part B Polym Phys* 39:363–373
- Bucknall CB, Gilbert AH (1989) Toughening tetrafunctional epoxy resins. *Polymer* 30:213–217
- Bucknall CB, Partridge IK (1983) Phase separation in epoxy resins containing polyethersulphone. *Polymer* 24:639–644
- Bucknall CB, Partridge IK (1984) Effects of morphology in the epoxy/PES matrix on the fatigue behaviour of uniaxial CFRP. *Composites* 15:129–133
- Bucknall CB, Partridge IK (1986) Phase separation in crosslinked resins containing polymeric modifiers. *Polym Eng Sci* 26:54–62
- Cardwell BJ, Yee AF (1998) Toughening of epoxies through thermoplastic crack bridging. *J Mater Sci* 33:5473–5484
- Cedeño AJ, Vazquez-Torres H (2005) Kinetic study of the effect of poly(phenylsulfone) on the curing of an epoxy/amine resin by conventional and by temperature modulated differential scanning calorimetry. *Polym Int* 54:1141–1152
- Chung T, Romo-Urbe A, Mather PT (2008) Two-way reversible shape memory in a semicrystalline network. *Macromolecules* 41:184–192
- Dusek K (1986) Epoxy resins and composites IV. Springer, Berlin, pp 173–202
- Ellis B (1993) Chemistry and technology of epoxy resins. Springer, Dordrecht
- Francis B, Poel GV, Posada F, Groeninckx G, Rao VL, Ramaswamy R, Thomas S (2003) Cure kinetics and morphology of blends of epoxy resin with poly (ether ether ketone) containing pendant tertiary butyl groups. *Polymer* 44:3687–3699
- Francis B, Rao VL, Ramaswamy JS, Thomas S, Raju KVS (2005) Morphology, viscoelastic properties, and mechanical behavior of epoxy resin modified with hydroxyl-terminated poly(ether ether ketone) oligomer with pendent tert-butyl groups. *Polym Eng Sci* 45:1645–1654
- Francis B, Rao VL, Poel GV, Posada F, Groeninckx G, Ramaswamy R, Thomas S (2006a) Cure kinetics, morphological and dynamic mechanical analysis of diglycidyl ether of bisphenol-A epoxy resin modified with hydroxyl terminated poly(ether ether ketone) containing pendent tertiary butyl groups. *Polymer* 47:5411–5419
- Francis B, Thomas S, Thomas SP, Ramaswamy R, Lakshmana Rao VL (2006b) Diglycidyl ether of bisphenol-A epoxy resin polyethersulfone/polyether sulfone ether ketone blends: phase morphology, fracture toughness and thermo-mechanical properties. *Colloid Polym Sci* 285:83–93
- Francis B, Thomas S, Sadhana R, Thuaud N, Ramaswamy R, Jose S, Rao VL (2007) Diglycidyl ether of bisphenol-a epoxy resin modified using poly(ether ether ketone) with pendent tert-butyl groups. *J Polym Sci Part B: Polym Phys* 45:2481–2496
- Gomez CM, Bucknallt CB (1993) Blends of poly(methyl methacrylate) with epoxy resin and an aliphatic amine hardener. *Polymer* 34:2111–2117
- Hedrick JC, Patel NM, McGrath JE (2009) Toughening of epoxy resin networks with functionalized engineering thermoplastics. *Adv Chem* 233:293–304
- Hert M (1992) Tough thermoplastic polyesters by reactive extrusion with epoxy-containing copolymers. *Macromol Mater Sci* 196:89–99
- Howell BF (2000) In: Meister JJ (ed) Polymer modification. Principles, techniques and applications. Marcel Dekker, New York, pp 479–573
- Huang F, Liu Y, Zhang X, Gao J, Song Z, Tang B, Wei G, Qiao J (2005) Interface and properties of epoxy resin modified by elastomeric nano-particles. *Sci Chin Ser B Chem* 48:148–155
- Jiang X, Huang H, Zhang Y, Zhang Y (2004a) Dynamically cured polypropylene/epoxy blends. *J Appl Polym Sci* 92:1437–1448
- Jiang X, Zhang Y, Zhang Y (2004b) Study of dynamically cured PP/MAH-g-EPDM/epoxy blends. *Polym Test* 23:259–266

- Jones AR, Watkins CA, White SR, Sottos NR (2015) Self-healing thermoplastic-toughened epoxy. *Polymer* 74:254–261
- Jose J, Joseph K, Pionteck J, Thomas S (2008) *PVT* behavior of thermoplastic poly(styrene-co-acrylonitrile)-modified epoxy systems: relating polymerization-induced viscoelastic phase separation with the cure shrinkage performance. *J Phys Chem B* 112:14793–14803
- Jyotishkumar P, Koetz J, Tiersch B, Strehmel V, Özdilek C, Moldenaers P, Hässler R, Thomas S (2009) Complex phase separation in poly(acrylonitrile-butadiene-styrene)-modified epoxy/4,4'-diaminodiphenyl sulfone blends: generation of new micro- and nanosubstructures. *J Phys Chem B* 113:5418–5430
- Kim H, Char K (2000) Effect of phase separation on rheological properties during the isothermal curing of epoxy toughened with thermoplastic polymer. *Ind Eng Chem Res* 39:955–959
- Kim BS, Chiba T, Inoue T (1993) A new time-temperature-transformation cure diagram for thermoset/thermoplastic blend: tetrafunctional epoxy/poly(ether sulfone). *Polymer* 34:2809–2815
- Kim BS, Chiba T, Inoue T (1995) Phase separation and apparent phase dissolution during cure process of thermoset/thermoplastic blend. *Polymer* 36:67–71
- Kishi H, Kuwata M, Matsuda S, Asami T, Murakami A (2004) Damping properties of thermoplastic-elastomer interleaved carbon fiber reinforced epoxy composites. *Comp Sci Tech* 64:2517–2523
- Kulshreshtha B, Ghosh AK, Misra A (2003) Crystallization kinetics and morphological behavior of reactively processed PBT/epoxy blends. *Polymer* 44:4723–4734
- Liu C, Chun SB, Mather PT, Zheng L, Haley EH, Coughlin EB (2002) Chemically cross-linked polycyclooctene: synthesis, characterization and shape memory behavior. *Macromolecules* 35:9868–9874
- Liu Y, Zhong X, Yu Y (2010) Gelation behavior of thermoplastic-modified epoxy systems during polymerization-induced phase separation. *Colloid Polym Sci* 288:1561–1570
- López J, Ramírez C, Abad MJ, Barral L, Cano J, Díez F (2002) Dynamic mechanical analysis of an epoxy/thermoplastic blend: polymerization induced phase separation. *Polym Int* 51:1100–1106
- Luo X, Mather PT (2010) Triple-shape polymeric composites (TSPCs). *Adv Funct Mater* 20:2649–2656
- Luo X, Mather PT (2013) Shape memory assisted self-healing coating. *ACS Macro Lett* 2:152–156
- Luo X, Ou R, Eberly DE, Singhal A, Vyratyaporn W, Mather PT (2009) A thermoplastic/thermoset blend exhibiting thermal mending and reversible adhesion. *ACS Appl Mater Interfaces* 1:612–620
- Lützen H, Gesing TM, Kyu Kim B, Hartwig A (2012) Novel cationically polymerized epoxy/poly(3-caprolactone) polymers showing a shape memory effect. *Polymer* 53:6089–6095
- Mackinnon AJ, Jenkins SD, McGrail P, Pethrick RA (1995) Cure and physical properties of the thermoplastic modified epoxy resins based on polyethersulfone. *J Appl Polym Sci* 58:2345–2355
- Mather PT, Luo X, Russeau IA (2009) Shape memory polymer research. *Annu Rev Mater Sci* 39:445–471
- May CA (1988) *Epoxy resins: chemistry and technology*, 2nd edn. Marcel Dekker, New York
- McGarry FJ (1996) In: Arends CB (ed) *Polymer toughening*. Marcel Dekker, New York, pp 175–188
- McGarry FJ, Rosner RB (1993) Epoxy rubber interactions. In: Riew CK, Kinloch AJ (eds) *Toughened plastics I. Science and engineering*, Advances in Chemistry Series. American Chemical Society, Washington, DC, pp 305–315
- Meister JJ (2000) *Polymer modification. Principles, techniques and applications*. Marcel Dekker, New York
- Mimura K, Ito H, Fujioka H (2000) Improvement of thermal and mechanical properties by control of morphologies in PES-modified epoxy resins. *Polymer* 41:4451–4459

- Mimura K, Ito H, Fujioka H (2001) Toughening of epoxy resin modified with in situ polymerized thermoplastic polymers. *Polymer* 42:9223–9233
- Mondragon I, Remiro PM, Martin MD, Valea A, Franco M, Bellenguer V (1998) Viscoelastic behavior of epoxy resins modified with poly(methyl methacrylate). *Polym Int* 47:152–158
- Oyanguren PA, Galante MJ, Andromaque K, Frontini PM, Williams RJJ (1999) Development of bicontinuous morphologies in polysulfone–epoxy blends. *Polymer* 40:5249–5255
- Parameswaranpillai J, Woo EM, Hameed N, Piontek J (2015) *Handbook of epoxy blends*. Switzerland, Springer
- Pethrick RA, Hollins EA, McEwan I, MacKinnon JA, Hayward D, Cannon LA (1996) Dielectric, mechanical and structural, and water absorption properties of a thermoplastic-modified epoxy resin: poly(ether sulfone)-amine cured epoxy resin. *Macromolecules* 29:5208–5214
- Prolongo MG, Arribas C, Salom C, Masegosa RM (2010) Dynamic mechanical properties and morphology of poly(benzyl methacrylate)/epoxy thermoset blends. *Polym Eng Sci* 50:1820–1830
- Qipeng, G., Huang J, Binyao L, Tianlu C, Hongfang Z, Zhiliu F (1991) Blends of phenolphthalein Poly (ether ether ketone) with phenoxy and epoxy resin. *Polymer* 32:58–65
- Remiro PM, Cortazar MM, Calahorra ME (1999) A study of the degradation of uncured DGEBA/PVP blends by thermogravimetry and their miscibility state. *J Appl Polym Sci* 54:2627–2633
- Robeson LM (2007) *Polymer blends. A comprehensive review*. Carl Hansen Verlag, Munich
- Romo-Urbe A, Arcos-Casarrubias JA, Flores A, Valerio-Cardenas C, Gonzalez AE (2014) Influence of rubber on the curing kinetics of DGEBA epoxy and the effect on the morphology and hardness of the composites. *Polym Bull* 71:1241–1261
- Santiago D, Fernandez-Franco X, Ferrando F, de la Flor S (2015) Shape memory effect in hyperbranched poly(ethyleneimine)-modified epoxy thermosets. *J Polym Sci Polym Phys*. doi:10.1002/polb.23717
- Saxena A, Francis B, Rao VL, Ninan KN (2006) Epoxy-*tert*-butyl poly(cyanoarylene ether) blends: phase morphology, fracture toughness, and mechanical properties. *J Appl Polym Sci* 100:3536–3544
- Song X, Zheng S, Huang J, Zhu P, Guo Q (2000) Miscibility, morphology and fracture toughness of tetrafunctional epoxy resin/poly (styrene-co-acrylonitrile) blends. *J Appl Polym Sci* 35:5613–5619
- Song X, Zheng S, Huang J, Zhu P, Guo Q (2001) Miscibility and mechanical properties of tetrafunctional epoxy resin/phenolphthalein poly(ether ether ketone) blends. *J Appl Polym Sci* 79:598–607
- Sultan JN, McGarry FJ (1973) Effect of rubber particle size on deformation mechanisms in glassy epoxy. *J Polym Eng Sci* 13:29–34
- Torbati AH, Birjandi Nejad H, Ponce M, Sutton JP, Mather PT (2014) Properties of triple shape memory composites prepared via polymerization-induced phase separation. *Soft Matter* 10:3112–3121
- Vanden Poel G, Goossens S, Goderis B, Groeninckx G (2005) Reaction induced phase separation in semicrystalline thermoplastic/epoxy resin blends. *Polymer* 46:10758–10771
- Velisaris CN, Seferis JC (1986) Crystallization kinetics of polyetheretherketone matrices. *Polym Eng Sci* 26:1574–1581
- Vyas A, Iroh JO (2013) In situ growth of multilayered crystals in amorphous matrix: thermal, dynamic mechanical, and morphological analysis of nylon-6/epoxy composites. *J Appl Polym Sci* 130:3319–3327
- Xie T, Rousseau IA (2009) Facile tailoring of thermal transition temperatures of epoxy shape memory polymers. *Polymer* 50:1852–1856
- Yamanaka K, Inoue T (1989) Structure development in epoxy resin modified with poly(ether sulfone). *Polymer* 30:662–667

- Yu Y, Zhang Z, Gan W, Wang M, Li S (2003) Effect of polyethersulfone on the mechanical and rheological properties of polyetherimide-modified epoxy systems. *Ind Eng Chem Res* 42:3250–3256
- Zhang Y, Shi W, Chen F, Han CC (2011) Dynamically asymmetric phase separation and morphological structure formation in the epoxy/polysulfone blends. *Macromolecules* 44:7465–7472
- Zhong Z, Zheng S, Huang J, Cheng X, Guo Q, Wei J (1998) Phase behavior and mechanical properties of epoxy resin containing phenolphthalein poly(ether ether ketone). *Polymer* 39:1075–1080

Thermal Properties of Epoxy/Thermoplastic Blends 24

Irthasa Aazem, Aklesh Kumar, Manisha Mohapatra, Jung Hwi Cho, Jarin Joyner, Peter Samora Owuor, Jyotishkumar Parameswaranpillai, Vijay Kumar Thakur, Jinu Jacob George, and Raghavan Prasanth

Abstract

Incorporation of thermoplastics into the epoxy resin is a potential route for the development of toughened epoxy thermoset with augmented properties. The ultimate properties of the blend depend on the various transitions and transformations during epoxy polymerization such as the viscoelastic phase separation, secondary phase separation, gelation, and vitrification. In this chapter, it is aimed to give a detailed description on the various approaches for improving the fracture toughness of epoxy by blending with thermoplastics, the toughening mechanisms involved, and their effects on the thermal properties of the

I. Aazem • A. Kumar • M. Mohapatra • J. Parameswaranpillai • J.J. George (✉)
Department of Polymer Science and Rubber Technology, Cochin University of Science and Technology, Cochin, Kerala, India
e-mail: jinu@cusat.ac.in

J.H. Cho
School of Engineering, Materials Science, Brown University, Providence, Rhode Island, USA

J. Joyner • P.S. Owuor
Department of Materials Science and NanoEngineering, Rice University, Houston, TX, USA
Department of Mechanical Engineering and Materials Science, Rice University, Houston, TX, USA

V.K. Thakur
School of Aerospace, Transport and Manufacturing, Cranfield University, Cranfield, Bedfordshire, UK

R. Prasanth (✉)
Department of Polymer Science and Rubber Technology, Cochin University of Science and Technology, Cochin, Kerala, India
Department of Materials Science and NanoEngineering, Rice University, Houston, TX, USA
Department of Mechanical Engineering and Materials Science, Rice University, Houston, TX, USA
e-mail: dr.prasanthr@gmail.com

blends. All the systems have been analyzed with a special attention on their thermal properties. Thus, the thermoplastic-modified epoxy resins with improved fracture toughness along with the inherent properties of epoxy resins fall in the class of engineering materials, which is eligible for many high-end applications.

Keywords

Epoxy thermoset • Thermal transitions • Thermoplastics • Thermal mending • Glass transition temperature

Abbreviations

3D	Three dimensional
ABS	Poly(acrylonitrile- <i>block</i> -butadiene- <i>block</i> -styrene)
AFM	Atomic force microscopy
AN	Acrylonitrile
BCP	Block copolymers
°C	Degree Celsius
DDM	4,4'-Diamino diphenyl methane
DDS	4,4'-Diamino diphenyl sulfone
DEB	Differential expansive bleeding
DGEBA	Diglycidyl ether of bisphenol-A
DMA	Dynamic mechanical analysis
DMTA	Dynamic mechanical thermal analysis
DSC	Differential scanning calorimetry
E''	Loss modulus
ECN	Epoxy cresol novolac
EP	Epoxy
EPN	Epoxy phenol novolac
ER	Epoxy resin
eSBS	Epoxidized styrene butadiene styrene
G'	Storage modulus
HDT	Heat deflection temperature
HTPB	Hydroxyl-terminated polybutadiene
LED	Light emitting diode
MCDEA	4,4'-Methylene <i>bis</i> (3-chloro-2,6-diethyl aniline)
MDA	Methylene dianiline
MF	Melamine formaldehyde
MMA	Methyl methacrylate
MOCA	4,4'-Methylene <i>bis</i> (2-chloraniline)
MWCNT	Multiwalled carbon nanotube
NBR	Poly(acrylonitrile) rubber
NG	Nucleation and growth
NMR	Nuclear magnetic resonance spectroscopy

OM	Optical microscopy
P(MMA-VAc)-PEGDA	Poly(methyl methacrylate-vinyl acetate)- <i>co</i> -poly(ethylene glycol) diacrylate
PB	Polybutadiene
PCL	Poly(ϵ -caprolactone)
PCL-PPC-PCL	Poly(ϵ -caprolactone)- <i>block</i> -poly(propylene carbonate)- <i>block</i> -poly(ϵ -caprolactone)
PDMS	Poly(dimethyl siloxane)
PEGDA	Poly(ethylene glycol) diacrylate
PEI	Poly(ether imide)
PEO	Poly(ethylene oxide)
PEP	Poly(ethylene- <i>alt</i> -propylene)
PF	Phenol formaldehyde
PGA	Poly(glycolic acid)
phr	Parts per hundred resin
PMMA	Poly(methyl methacrylate)
POM	Polyoxymethylene
PPC	Poly(propylene carbonate)
PPE	Poly(2,6-dimethyl-1,4-phenylene ether)
PPO	Poly(propylene oxide)
PS	Polystyrene
P-SBMMA	Poly(styrene- <i>block</i> -butadiene- <i>block</i> -methyl methacrylate)
PS- <i>b</i> -PGA	Polystyrene- <i>block</i> -poly(glycolic acid)
PVAc	Poly(vinyl acetate)
RIPS	Reaction-induced phase separation
SALLS	Small-angle laser light scattering
SAN	Styrene-acrylonitrile
SAXS	Small-angle X-ray scattering
SBS	Poly(styrene- <i>block</i> -butadiene- <i>block</i> -styrene)
SEM	Scanning electron microscopy
SIS	Epoxidized poly(styrene- <i>block</i> -isoprene- <i>block</i> -styrene)
Sn(Oct) ₂	Stannous octoate
tan δ	Loss tangent
TEM	Transmission electron microscopy
T_g	Glass transition temperature
T_{g0}	T_g of unreacted epoxy resin
TGA	Thermo gravimetric analysis
TGAP	Triglycidyl- <i>p</i> -amino phenol
TGDDM	Tetraglycidyl-4,4''-diamino diphenyl methane
$T_{g\alpha}$	Transition temperature of fully cured epoxy resin
Tm	Crystalline melting temperature
TMA	Thermomechanical analysis
TP	Thermoplastic
TS	Thermoset

TTT	Isothermal time versus temperature transformation
UCST	Upper critical solution temperature
UF	Urea formaldehyde
VAc	Vinyl acetate

Contents

Introduction	710
Epoxy Resins	712
Epoxy/Thermoplastic Blends (Homo- and di-block Copolymer)	715
Epoxy/Poly(ethylene oxide) (PEO)/Poly(ethylene glycol) (PGA) Blends	715
Epoxy/Poly(ϵ -caprolactone) (PCL) Blends	719
Epoxy/Poly(methyl methacrylate) (PMMA) Blends	722
Epoxy/Poly(ether sulfone) (PES) Blends	723
Epoxy/Poly(2,6 dimethyl 1,4 phenylene ether) (PPE) Blends	724
Epoxy/Terpolymer or Tri-block Copolymer Blends	725
Epoxy/Poly(acrylonitrile- <i>block</i> -butadiene- <i>block</i> -styrene) (ABS) Blends	725
Epoxy/Polyoxymethylene (POM) Blends	728
Epoxy/PCL-PPC/PB-PCL Blends	728
Epoxy/Poly(ether imide) (PEI) Blends	730
Epoxy/Poly(styrene- <i>block</i> -butadiene- <i>block</i> -methyl methacrylate) (P-SBMMA) Blends	732
Epoxy/Poly(styrene- <i>block</i> -butadiene- <i>block</i> -styrene) (SBS) Blends	733
Conclusions	736
References	736

Introduction

Polymer blending is a simple and versatile method to develop structurally advanced polymeric materials. The ultimate properties of the polymer blends can be manipulated according to the end use by the proper selection of constituent polymers and processing method. Polymer blending can simply be done by proper mixing of two or more miscible or immiscible constituent polymers to reactive multicomponent systems based on thermosetting resin/thermoplastic (TS/TP) polymers. The latter system has recently gained much fundamental as well as practical interest from the scientific community and industrialist towards the development of new high-performance materials. Thermosetting polymers that include epoxy, unsaturated polyester, phenolics, or melamine formaldehyde are being increasingly used in diverse applications, ranging from aerospace structures to simple dental fillers. By the formation of a covalently cross-linked and thermally stable network through cross-linking reaction, the thermoset materials undergo a permanent change under the influence of heat, even if they possess good processability and excellent chemomechanical properties. The reactive oligomers grow in molecular weight to form tough and strong three-dimensional structure during cross-linking.

Due to the exceptionally good mechanical properties and chemical and/or degradation resistance, high tensile and impact strength, stiffness, environmental stability,

insulating and adhesion properties, ease of processing, low-temperature cure, cost-effectiveness, and easiness in fabrication of complex and very large shapes thermoset-based polymer systems are preferred over thermoplastics for high-performance structural applications. Among the thermosets, for example, phenol formaldehyde (PF), urea formaldehyde (UF), or melamine formaldehyde (MF) and epoxy resin (ER) based on diglycidyl ether of bisphenol-A (DGEBA) are versatile groups which find structural and adhesive applications in various fields such as aerospace, electronics, construction, submarine, etc. (May 1988).

Epoxy is a common term representing both the basic components and the cured products of epoxy resins. This thermosetting resins are a class of reactive pre-polymers which contain epoxide groups capable of reacting (cross-linking) either with themselves through catalytic homopolymerization or with a variety of co-reactants which are generally called as hardeners or cross-linking agents. Cross-linking reaction of polyepoxides with polyfunctional curing agents, for example, polyfunctional amines, acids/acid anhydrides, phenols, or thiols etc., forms a thermosetting polymer, often having high mechanical, thermal, and chemical properties. Epoxy has a wide range of applications, including metal coatings, electronics/electrical components, light-emitting diodes (LED), high tension electrical insulators, fiber-reinforced plastics, flooring and casting, protective coatings, high-performance composite, bonding, and structural adhesives.

Compared to other thermosetting resins, primary advantage of epoxy resins is that it can cross-link with the reactive functional groups of cross-linking agents without the evolution of any volatile products. The cross-linked epoxy possesses excellent thermomechanical and chemical properties. Their unique properties are primarily obtained from the cross-linked 3D-network structures and the presence of highly stable epoxide groups. Eventhough they possess high degree of chemical cross-linking, epoxy resins are highly brittle which is one of their major drawbacks. Low fracture toughness and brittleness also limit their use in many advanced high-performance applications (Kinloch 1986); hence, it has caught the attention of researchers globally to modify the brittle epoxy resins by blending with elastomers (Zhang and Berglund 1993; Hsich 1990), thermoplastics (Bucknall et al. 1994; Riccardi et al. 1996; Yu et al. 2004), block copolymers (Mijovic et al. 2000; Ritzenthaler et al. 2002), etc. Among the above mentioned methods, incorporation of thermoplastics into the epoxy resin is a potential route for the development of toughened epoxy thermosets with augmented properties. Blending the brittle epoxy resins with suitable thermoplastics, having high elastic modulus and high glass transition temperature (T_g), with an aim to enhance their fracture toughness and thermal resistance (higher T_g) has been a topic of interest for the researchers for the past two decades (Natarajan and Rao 1994; Pena et al. 2003; Das et al. 1994; Schauer et al. 2002; Paul and Bucknall 2000; Tribut et al. 2007; Blanco et al. 2004). These blends are generated by a reaction-induced phase separation process determined by cure conditions, compositions, nature of modifier, molecular weights, and molecular weight distribution of tougheners. The ultimate properties were dependent on the various transitions and transformations during epoxy polymerization such as the viscoelastic phase separation, secondary phase separation, gelation, and vitrification.

Morphological structures thus formed by blending the epoxy with thermoplastics are classified into three: (i) sea-island structure formed with low thermoplastic loadings, (ii) nodular structure formed at high thermoplastic concentrations, and (iii) bicontinuous, salami, or layered structure formed in the middle thermoplastic concentration range (Park and Kim 1996; Francis et al. 2006; Kim et al. 2008; Zhang et al. 2011). Backbone structure, molecular weight, and the end-group chemistry of the thermoplastic are the influencing factors which determine the morphology of the blend. Each of these three aspects influences the thermomechanical properties of the epoxy-thermoplastic blend in a unique way (Williams et al. 1996; Girard-Reydet et al. 1997, 1998; Pearson 1993). As the molecular weight of epoxy increases, phase separation will be induced which gradually slows down and finally stops as the gelation increases. Hence, curing reaction and phase separation play critical roles in the development of structure and morphology of the final blend (Bonnet et al. 1999a, b; Swier and Mele 2003; Swier et al. 2005; Liu et al. 2010). Epoxy-thermoplastic blends thus made have been used as engineering materials for aircraft, electronic, and automobile applications where they have modified epoxy resin with poly(ether sulfone) (PES), poly(ether imide) (PEI), poly(propylene oxide) (PPO), etc. (Paul and Bucknall 2000; Tribut et al. 2007; Blanco et al. 2004). In this chapter, it is intended to give a detailed description on the various approaches for toughening epoxy with thermoplastics and the toughening mechanism with special attention to the thermal properties of the blends.

Epoxy Resins

Epoxy resin is a commercially important thermosetting resin, which has molecule with multiple epoxy groups capable of being hardened into a usable product. After commercial launching in 1946, epoxy resin industry has undergone a fast development and presently has taken up a substantial share of (nearly 35%) the world's total thermoset market with an yearly consumption of around 90 k tones (Analysis 2004). Figure 1 shows the major market consumption and application of epoxy resins. When cured, the epoxy resins form a highly cross-linked 3D infinite network with unique microstructure which impart the desirable engineering properties. The superior chemical, environmental, and corrosion resistance; good mechanical and thermal properties; outstanding adhesion to various substrates including ceramics and metals; low shrinkage upon cure; durability, toughness, and flexibility in processing; good electrical and electronic properties; and ability to be processed under a variety of conditions make them an attractive candidate for the high-performance engineering applications (Mc Adams and Gannon 1986).

Epoxy resins contain more than one α -epoxy group, which can be converted to a useful thermoset form. Epoxide group is usually a 1,2- or α -epoxide (epoxy group) as shown in Scheme 1, called the glycidyl group. The glycidyl group firmly attached to the rest of the functional molecules by an oxygen, nitrogen, or carboxyl linkage, which is called as glycidyl ether, glycidyl amine, or glycidyl ester, respectively. Epoxy resins are available in various physical forms ranging from low viscosity liquids to tack free solids which greatly depends on the molecular weight of the resin.

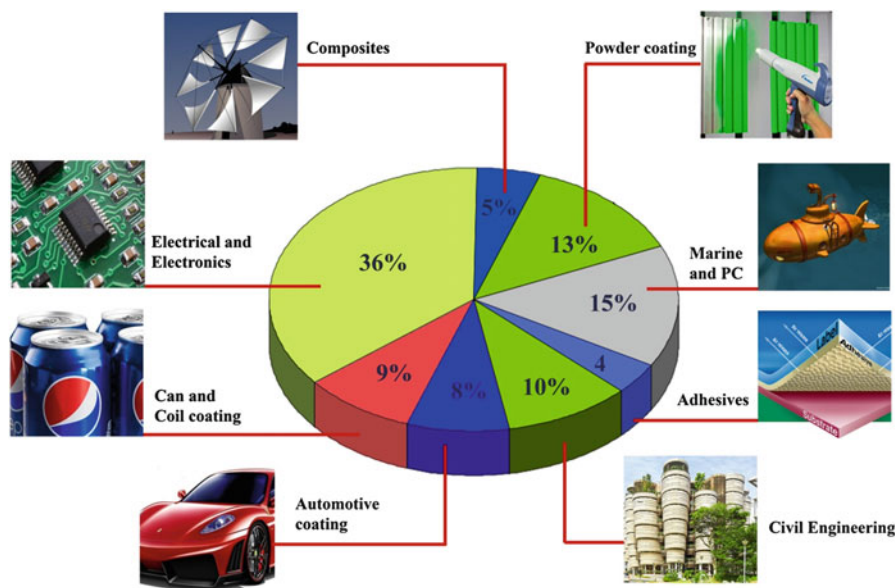
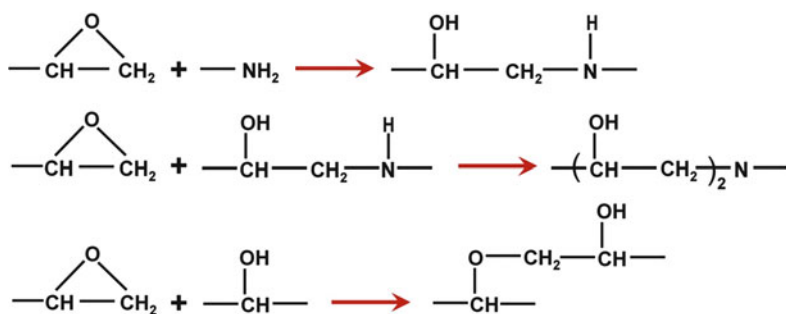


Fig. 1 The global market share of epoxy consumption in different applications



Scheme 1 Reaction between amine curing agent and epoxy resin

The most popular commercial grade bifunctional epoxy resin is DGEBA. Specific multifunctional aromatic glycidyl ether resins such as epoxy phenol novolac (EPN) as well as epoxy cresol novolac (ECN) resins impart excellent thermal and chemical resistance owing to the high functionality. Because of the aromatic backbone, multifunctional glycidyl amine resins like triglycidyl-*p*-aminophenol (TGAP) and tetraglycidyl-4,4'-diaminodiphenyl methane (TGDDM) offer excellent elevated temperature properties and are used as binders in graphite reinforced composites. The transformation of epoxy resins from liquid or semisolid monomers into infusible and insoluble thermoset 3D network is taking place through the cross-linking reaction and/or polymerization by thermal, ultraviolet, or microwave radiation.

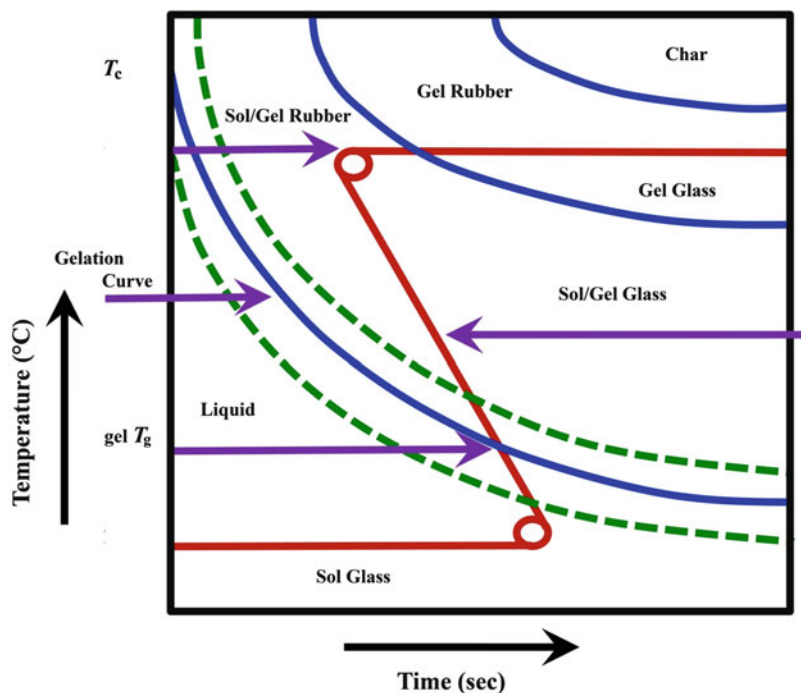


Fig. 2 Time-temperature-transformation diagram of polymers (Adopted from Gillham 1986)

Cross-linking initially leads to chain extension and branching due to molecular weight buildup, and finally the individual clusters join to form a 3D network of infinite molecular weight. Gel point is defined as the point where irreversible transformation from viscous to elastic gel takes place. Beyond gel point, the uninhibited polymerization reaction proceeds toward the formation of infinite network assuming the shape of the reaction vessel with tremendous hike in cross-link density, glass transition temperature (T_g), and ultimate physical properties. The isothermal time versus temperature transformation (TTT) cure diagram is a very useful tool for studying cross-linking processes of epoxy-based polymer systems (Fig. 2) (Gillham 1986). In the TTT cure diagram, the times to gelation and vitrification are plotted as a function of the isothermal cure temperature. The “S”-shaped gelation and vitrification curves of liquid, gelled rubber, sol-glass, and gelled glass (the four intermediate states of epoxy resins curing process) divide TTT diagram into four distinct stages of the thermosetting curing process. At a temperatures below the T_g of unreacted epoxy resin (T_{g0}), the cross-linking process occurs in slow reaction rate and kinetics as it is confined to the solid state. The storage temperature for unreacted resins is defined by T_{g0} . The resin start to react above T_{g0} which leads to the vitrification. Between T_{g0} and gel T_g , the resin will react until T_g becomes equal to the cure temperature; thereafter, the reaction becomes diffusion controlled. At this stage, the vitrification is complete, and the resin is eventually quenched. Between gel T_g and glass transition

temperature of fully cured epoxy resin ($T_{g\alpha}$), gelation precedes vitrification and a cross-linked rubbery network forms, which continues until its T_g coincides with the cure temperature and the reaction will be quenched. $T_{g\alpha}$ is defined as the minimum cure temperature required for the complete curing of the resin. Above this temperature ($T_{g\alpha}$), the resin will be in the rubbery state after gelation, if there is no other cure reactions like oxidative cross-linking or chain scission. The handling, processing, and properties of the cured resins are greatly influenced by the rate of gelation and vitrification.

The strained three-membered ring structure of an epoxy group is highly reactive toward many nucleophilic and electrophilic reagents. Because of their effectiveness and availability, compounds with active hydrogen atoms such as amines, phenols, alcohols, thiols, carboxylic acids, and acid anhydrides have been used as curatives. The ultimate cured resin properties are highly influenced by the nature of the cross-linker. Epoxies cured by aromatic amine offer excellent resistance to water absorption (Wu and Xu 2007). Epoxy resins cured with anhydrides have excellent outdoor weathering resistance. Some of them have high heat deflection temperature (HDT) and excellent retention of strength at high temperature. These systems have low viscosity and long pot life. Polyamines are among the most commonly used curing agents for epoxy resins and make up around 22% of the commercial market (Ashcroft 1993). All primary, secondary, and tertiary amines can be employed to initiate cure in epoxy systems. The reaction between epoxy resin and an amine curing agent is given in Scheme 1.

The reaction of primary amine with epoxy leads to the formation of a secondary amine and secondary hydroxyl group. The secondary amine reacts with epoxy group to form a tertiary amine and two secondary hydroxyl groups. Depending on the reaction temperature, the tendency of the etherification reaction takes place (Lunak and Dusek 1975; Riccardi and Williams 1986), and the basicity of the diamine increases with increase of epoxy/amine ratio. For primary and secondary amines, stoichiometric amounts are generally employed, while the tertiary amines are used in catalytic quantities (Riccardi and Williams 1986). The selection of amine is crucial that it influences the formation of polymer networks (cross-link density and hence glass transition temperature) which, in turn, has great effect on the resin performance. For ambient temperature curing, low viscosity aliphatic amine was preferred and, for high-temperature properties, chemical resistance, long pot life, and low moisture absorption aromatic amine are employed as the curing agent.

Epoxy/Thermoplastic Blends (Homo- and di-block Copolymer)

Epoxy/Poly(ethylene oxide) (PEO)/Poly(ethylene glycol) (PGA) Blends

Blends of epoxy resin with poly(ϵ -caprolactone) (PCL) and poly(ethylene oxide) (PEO) have been a topic of high interest for the researchers working on TS/TP blends. Poly(ethylene oxide) has been widely studied as a versatile polymer for

preparing polymer blends, due to its good thermomechanical properties and solubility characteristics in water (Prasanth et al. 2014). It has ether linkages, with oxygen atoms present at a suitable interatomic separation to allow segmental motion of the polymeric chain which is beneficial for many electrochemical and electrochromic applications (Prasanth et al. 2014; Shubha et al. 2014). The effect of blending PEO with different polymers to improve the segmental motion, dissociation of ionic salts, and improve the electrochemical performance of the resulting blend has been reported (Prasanth et al. 2014). Meltzer (1979) showed that the presence of ether linkage in the main chain of the polymer is beneficial for preparing compatible blends with different thermoplastic and thermosetting resins. PEO-based polymer blend led to a significant refinement in morphology due to reactive compatibilization with hydroxyl ends of PEO.

Formation of a fine phase-separated morphology by reaction-induced microphase separation mechanism of a novel amphiphilic polystyrene-*block*-poly(glycolic acid) (PS-*b*-PGA)₃ three-arm star copolymer upon blending with epoxy precursor has been systematically demonstrated by Francis and Baby (2014). The translucent film formed was characterized by scanning electron microscopy (SEM), atomic force microscopy (AFM), and transmission electron microscopy (TEM), and the creation of nanodomains of the PS phase was evident from these analyses. After curing, the miscible PGA block was observed to be well dispersed in the epoxy matrix. The formation of the PS nanodomains in the epoxy-PGA matrix enhanced the toughness and tensile properties of the final epoxy thermoset formed. The AFM micrographs (Fig. 3), SEM, and TEM of the epoxy thermosets containing (PS-*b*-PGA)₃ of block copolymer showed ordered nanostructure in the thermoset, which resulted from the star-shaped architecture of the block copolymer as presented in Fig. 4 on the reaction-induced phase separation.

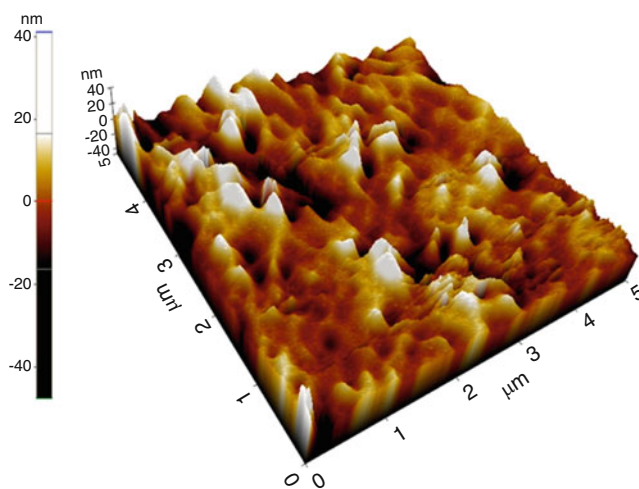


Fig. 3 AFM image of epoxy thermoset containing 10% of (PS-*b*-PGA)₃ block copolymer (topography) (Adopted from Francis and Baby 2014)

He et al. (2014) have blended epoxy with block copolymers containing epoxy resin-miscible PEO or PCL blocks. In their investigation, they have observed an interesting structure and dynamics of the interphase and cross-linked network and the intermolecular interactions between epoxy resin and block copolymers (BCP) with the aid of multiscale solid-state NMR techniques. Interphase thickness of PEO-containing blends was observed to be smaller than that of PCL-containing blends. Furthermore, it is anticipated that the mechanical properties of the blends may be enhanced by the improved rigidity of cross-linked network due to the high

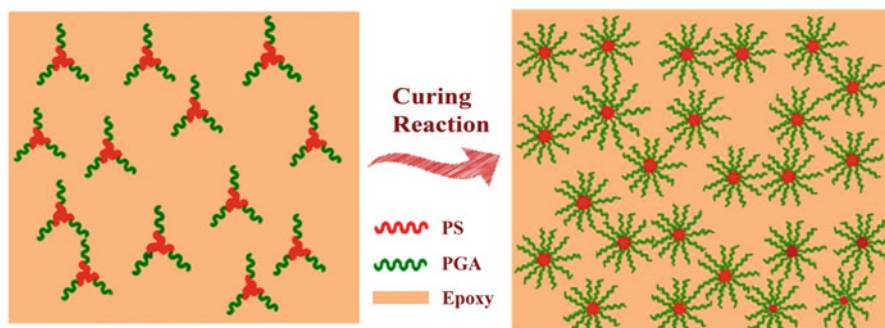


Fig. 4 Formation of nanostructures in epoxy thermoset by reaction-induced microphase separation (Adopted from Francis and Baby 2014)

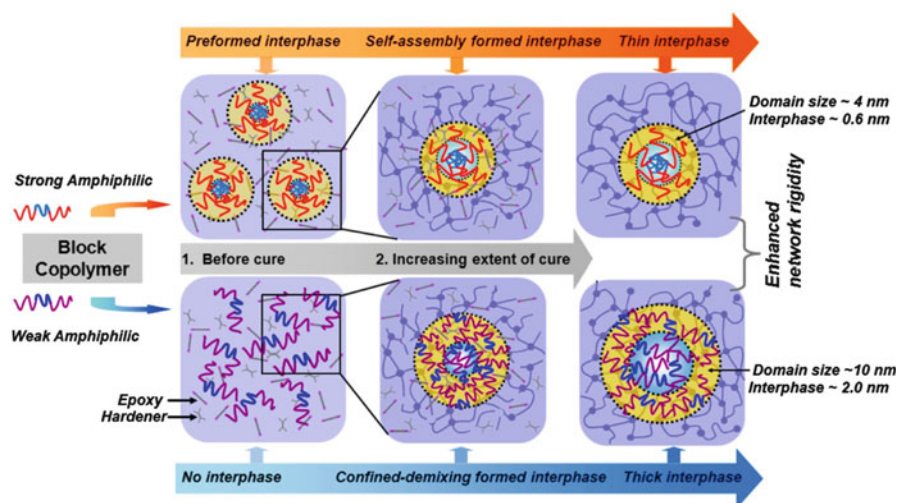
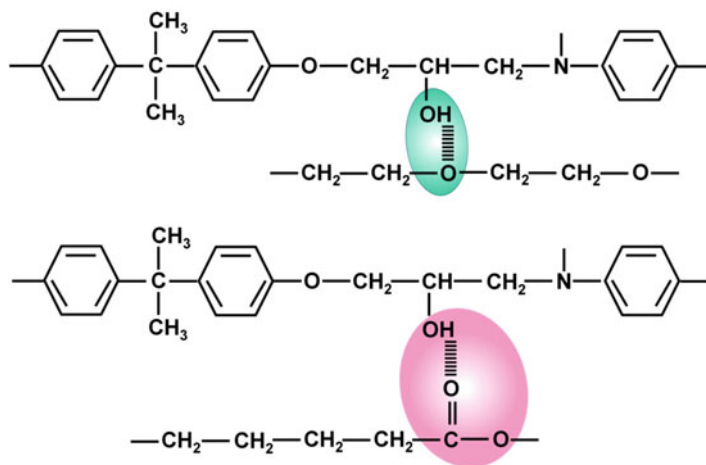


Fig. 5 Schematic illustration of the model describing two different types of unique structures and dynamics of the interphase and cross-linked network and their underlying formation mechanism in epoxy/BCP blends* (Adopted from He et al. 2014). *The interphase is indicated between two dotted circles and filled with yellow



Scheme 2 Intermolecular hydrogen bonding between cross-linked epoxy and **a** PCL and **b** PEO (Adopted from He et al. 2014)

mobility of BCPs. The unique structure and dynamics of the interphase and cross-linked network and their formation mechanism in epoxy/BCP blends have been demonstrated by a proposed scheme as in Fig. 5. In this model, amphiphilic BCPs are mainly divided as strong and weak amphiphilic BCPs. Strong amphiphilic BCPs indicate that there is large difference in thermodynamic interaction parameter χ between each of the amphiphilic BCP blocks and epoxy before curing, generally shown as large difference in miscibility, and vice versa for weak amphiphilic BCPs. Also it has been suggested that PEO and PCL have intermolecular hydrogen bonding interactions between hydroxyl groups of reacted epoxide-amine, and oxygen of PEO or carbonyl groups of PCL, as shown in Scheme 2, is to be considered as the driving force for the miscibility in thermoset blends.

Hillmyer et al. and Lipic et al. (Hillmyer et al. 1997; Lipic et al. 1998) blended a poly(ethylene oxide)-*block*-poly(ethylene-*alt*-propylene) (PEO-*b*-PEP) symmetrical di-block copolymer of low molar mass with an epoxy system and methylene dianiline as hardener (MDA). The selected epoxy prepolymer, the classical DGEBA, is initially a selective solvent for the PEO chains. During cross-linking, DGEBA was reacted with MDA to form 3D-network structures. The evolution of the morphology during reaction was recorded by small-angle X-ray scattering (SAXS). No macrophase separation could be observed between the di-block and the epoxy during the whole reaction process. As PEO is expelled from the epoxy network only at a local scale, the fully cured material presents a well-defined ordered nanostructure. This phenomenon is explained by a synergy between the curing reaction, local phase separation, and energy barriers to nucleation of block copolymer-rich domains. Recently, there are few studies reported on block copolymers having an epoxy-reactive functionality, for example, poly(epoxy isoprene)-*block*-polybutadiene or poly(methyl acrylate-*co*-glycidyl methacrylate)-*block*-polyisoprene as chain

modifier for epoxy thermosets (Grubbs et al. 2000). In the same way, nanostructured phenolic networks have been obtained with the use of poly(2-vinylpyridine)-*block*-polyisoprene (Kosonen et al. 2001).

Epoxy/Poly(ϵ -caprolactone) (PCL) Blends

Poly(ϵ -caprolactone) is a well-known biodegradable polymer having glass transition temperature (T_g) of about -60 °C and low melting point of around 60 °C. This polymer is being popularly used as a biopolymer; however, it is also used as an additive for resins to improve the processing characteristics and end-use properties of epoxy system (e.g., impact resistance). As PCL is economically viable, having good processing characteristics and compatible with organic materials, it could be mixed with many polymers such as starch or PEO, which lower its cost and increase biodegradability. It is also reported as a polymeric plasticizer to both thermoplastic and thermosets. Recently, the blend of PCL and epoxy is widely attracted by the scientific community due to its unique thermal and mechanical properties. The differences in miscibility for both anhydride and amine cross-linked epoxy-PCL blends and the effects on mechanical properties have been investigated by Clark et al. (1984) and Hameed and Guo (2008). Chen and Chang studied immiscibility of the blends when an aromatic amine was used as the curing agent (Chen and Chang 1999). This effect is due to the intrachain-specific interaction on the phase behavior. Miscibility and hydrogen bonding interaction between PCL and epoxy resin were frequently reported in the literature (Williams et al. 1996; Meng et al. 2006a). Wu et al. (2012) recently reported the effect of PCL as a modifier on the mechanical properties of epoxy thermosetting resin. They found that with increase in PCL composition, the tensile strength and the elongation at break of the modified epoxy thermoset decreased due to the lack of intermolecular force of attraction in the blend. The primary demerit of PCL is its plasticization effect in the blend. Alternative block copolymers have been developed to modify epoxy resin to overcome this problem

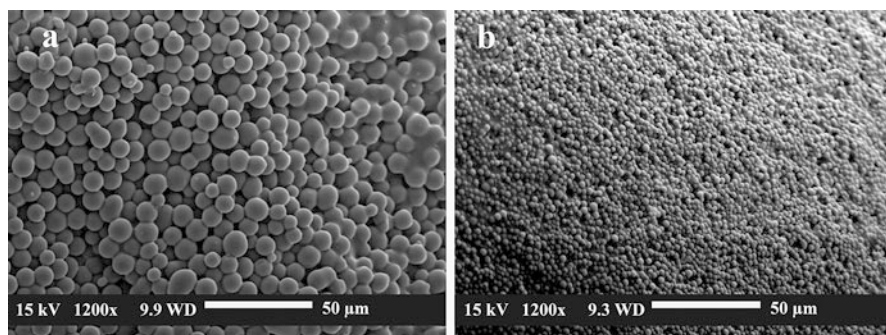


Fig. 6 SEM images showing the bulk morphologies of fully cured epoxy/PCL blends of different compositions: **a** epoxy/PCL(27.0); **a** epoxy/PCL(34.9) (Adopted from Xiaofan et al. 2009)

(Engelberg and Kohn 1991; Park et al. 2006; Boland et al. 2001; Aghdam et al. 2012). A new broadly applicable strategy to produce thermally mendable polymeric materials, demonstrated with an epoxy/PCL phase-separated blend, has been reported by Xiaofan et al. (2009). A series of morphologies (Fig. 6) produced by varying the weight ratio of DGEBA to PCL. The study reported that PCL is miscible initially in the epoxy matrix; however, PCL undergoes polymerization-induced phase separation during cross-linking reaction, which yields a “bricks and mortar” morphology. As a result, the epoxy phase exists as interconnected spheres (bricks) interpenetrated within the percolating PCL matrix (mortar) (Fig. 7). The cross-linked composite material is tough, strong, and durable. The thermal studies witnessed heating-induced “bleeding” behavior in the form of spontaneous wetting of all free surfaces by the molten PCL phase in the epoxy matrix. Hence, it was observed that thermally induced bleeding is capable of repairing damage by crack wicking and subsequent recrystallization with only minor concomitant softening during the aforementioned process. This bleeding process is attributed to volumetric thermal expansion of PCL in the epoxy brick due to the influence of temperature above the crystalline melting point of PCL, which is termed as differential expansive bleeding (DEB) (Xiaofan et al. 2009). It is reported that, even above the melting temperature of PCL, the blend behaves as a stiff elastic solid, given the relatively low loss modulus (E'') and loss tangent ($\tan \delta$) values. Melting the PCL fraction does not fluidize the blend inducing dimensional changes, and this is in line with the microscopic observations of interconnectivity. This is just opposite behavior to that of pure PCL as well as epoxy/PCL blends with high PCL content, which lose mechanical properties or even flow if heated above the melting temperature (Barone et al. 2006). In fact, the material remains stiff until the T_g of the epoxy (203 °C). The composition

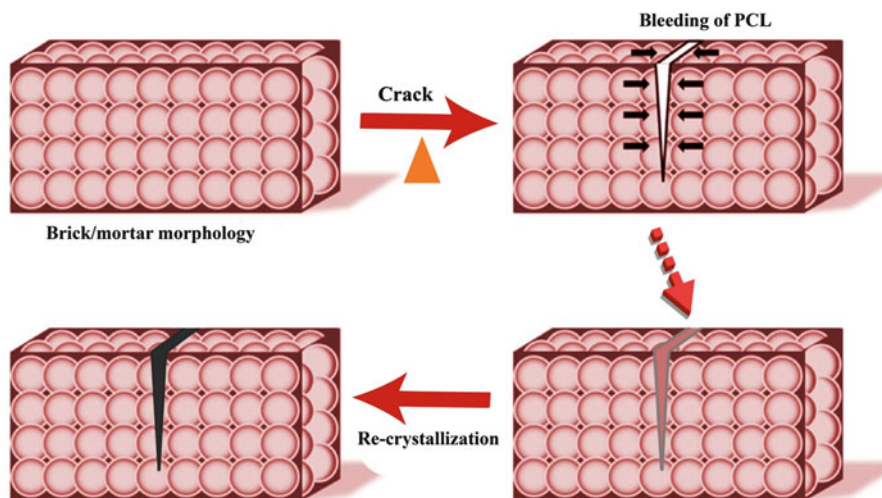


Fig. 7 Schematic illustration of the overall mechanism of thermal mending (Adopted from Xiaofan et al. 2009)

and morphology of epoxy/PCL blend with 15.5% PCL content display excellent mechanical properties that are caused by the interconnected epoxy “bricks,” making the material suitable for various structural applications.

Fractured epoxy when subjected to the same thermal treatment at 190 °C or even higher temperatures of 200–240 °C does not thermally mend. Hence, the thermal-mending ability of epoxy/PCL (15.5) is not due to the curing of epoxy and is due to incorporation of PCL. Finally, it was concluded that the thermal-mending performance is closely related to a “bleeding” phenomenon (Fig. 7).

Heating specimens to a temperature within the range $T_m \text{ PCL} < T < T_g$ epoxy resulted in spontaneous surface wetting of samples by molten PCL “bleeding” (DEB). Bleeding is initiated with temperature and small liquid droplets formed on the surface, and then the droplets grow and coalesce by contact line motion and impingement of adjacent growing droplets. Eventually (>20 min), a thin layer of fluid PCL covers a large area on the surface. It was reported that the bleeding phenomenon is a consequence of differential thermal expansion between the two interpenetrating phases, with the minor but continuous PCL phase expanding at least 10% more than the epoxy phase because of the melting transition and the large expansivity of the fluid phase (Fig. 8) (Rodgers 1993).

The kinetics of PCL flow to the surface expansion is mainly determined by heat transfer, with visible flow occurring in system with the temperature rise (Fig. 9) (heating-induced “bleeding” behavior). The process of heating-induced “bleeding” behavior was characterized by hot-stage stereomicroscopy coupled with surface temperature monitoring. Images were taken at various time points during heating. As the temperature stabilizes, bleeding completes. PCL displays large bulk modulus (less compressible) and a large liquid expansivity; as a result, a large transient pressure is generated which drives the flow of liquid PCL through the network of epoxy spheres onto the surface within a short period of time. The flow time of PCL is

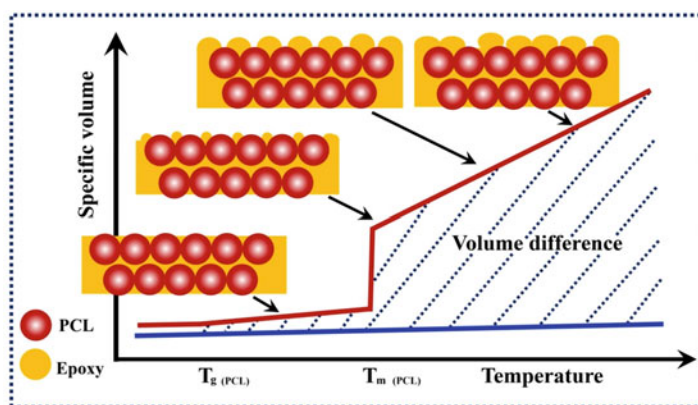


Fig. 8 Schematic illustration of DEB indicating its origin in differential thermal expansion between PCL and epoxy (Adopted from Xiaofan et al. 2009)

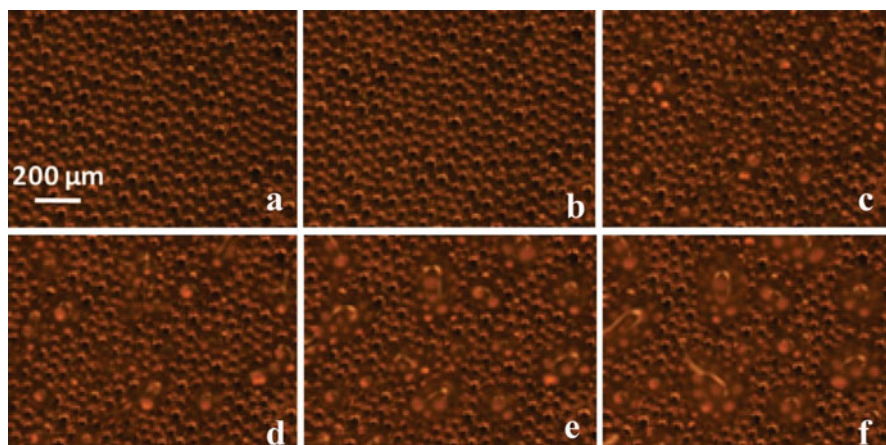


Fig. 9 Heating-induced “bleeding” behavior of epoxy/PCL blend. Images were taken at various time points during heating, time/temperature (sec.:°C); **a** 0:30, **b** 30:60, **c** 150:120, **d** 200:130, **e** 260:130, **f** 360:130 (Adopted from Xiaofan et al. 2009)

small compared to the time required for heat transfer (Xiaofan et al. 2009). In summary, the “bricks and mortar” morphology of epoxy/PCL blend exhibits unique thermal properties, e.g., differential expansive “bleeding” which enables excellent thermal mending and applicability as a rigid and reversible adhesives. This sort of morphologies can be obtained in many other systems, where a thermoset is blended with an amorphous (Cabanelas et al. 2005; Meynie et al. 2004; Oyanguren et al. 1999; Wang et al. 2004) or semicrystalline (Goossens and Groeninckx 2006; Johnsen et al. 2005) thermoplastic polymer. This in turn leads to broad applicability of this strategy to the design of DEB polymers and polymer composites, based on low raw material cost and ease of manufacturing, for those applications requiring long-lasting material performance and facile repair. Further, the reversible adhesive properties of DEB polymer composites should enable a new paradigm in adhesives as reusable bonding “blocks” that can adhere to or be removed from virtually any surface with a simple heat treatment (Xiaofan et al. 2009).

Epoxy/Poly(methyl methacrylate) (PMMA) Blends

Poly(methyl methacrylate) (PMMA) is a polar polymer with exceptional transparency, biocompatibility, and weather resistance. The properties of PMMA can be easily designed by changing the polymerization conditions and polymerization technique during its synthesis. PMMA has wide applications in building and construction; optical, automotive, consumer goods; and medical applications. Recently, many epoxy/PMMA blends having unique properties are reported. Natarajan and Rao (1994) modified the

epoxy resin based on DGEBA with PMMA and nitrile rubber (NBR). The resulting blend is cured with a stoichiometric quantity of 4,4'-diaminodiphenyl methane (DDM). The effect of adding PMMA and NBR on the morphology, mechanical properties, and thermal properties of the modified epoxy network is investigated. It has been observed that the modified epoxy network showed an enhancement in thermomechanical properties (elongation, tensile strength, ductility, impact strength, toughness, and glass transition temperature). The improvement in mechanical strength is due to the inclusion of NBR, while the shifting of T_g to the higher end (T_g) is due to the inclusion of PMMA into the blend. The improvement in tensile strength and thermal properties is due to the incorporation of PMMA into the blend, while the addition of rubbery particles is effective in increasing the fracture toughness of epoxy resin. The phase separation at elevated temperature and the thermal stability of the blend were addressed by using PMMA as the chain modifier in the blend system (Natarajan and Rao 1994; Pena et al. 2003; Das et al. 1994; Schauer et al. 2002). It has been shown that the thermoplastic-modified epoxies exhibit various types of morphology and unique thermal properties which is crucially dependent on the backbone structure, molecular weight, molecular weight distribution, and the end-group chemistry of the thermoplastic chain modifier. Recently, there are many reports on the thermal properties of the epoxy/NBR blend. The dynamic mechanical thermal analysis (DMTA) showed that as temperature increases, damping goes through a maximum in the transition region and then decreases in the rubbery region. The structure and extent to which the polymer is cross-linked is examined by the position and height of the $\tan \delta$ peaks. They observed that $\tan \delta$ peak is shifted from higher region to lower region in the unmodified blend (without PMMA). This may be due to lowering of cross-linking density in the unmodified cured sample. During the curing of epoxy resin, phase-separated thermoplastic domains may occupy the space in between the reaction sites, thereby impairing the cross-linking reaction. This, in turn reduces the cross-link density of the cured systems. It is reported that the T_g of modified blend is 164 °C, which is ~16.5% higher than the T_g value of unmodified blend (Padma and Natarajan 2014).

Epoxy/Poly(ether sulfone) (PES) Blends

Linear, high molecular weight thermoplastics are inherently tough and may be expected to reduce the brittleness of a thermoset without affecting their other properties significantly. Alessi et al. (2009) studied the epoxy resin/thermoplastic blends cured by ionizing radiation. The blend of difunctional epoxy resin and poly(ether sulfone) is cured by electron beam (e-beam) at about 60 °C using strong acid salt as initiator. Selected cured samples have been subjected to post-irradiation thermal curing. Both e-beam cured and thermally post-cured samples are aged hydrothermally before the thermal characterization.

From the DMTA, only irradiated sample exhibits two relaxation peaks, corresponding to the glass transitions of clusters with different network densities.

This is attributed to the vitrification phenomenon occurring during irradiation at low temperature. On contrary, the second peak is due to the relaxation of both high cross-linked portions of materials (resulted by irradiation) and increase in cross-link density due to the transformation from lower to higher cross-linking by the thermal treatment happening in the DMTA itself. From the cross-linking degree point of view, it is reasonable that post-curing treatment (after e-beam curing) at a higher temperature which is sufficiently high to overcome vitrification effects (between the two relaxations) is able to make the system more homogeneous. The $\tan \delta$ curve for such condition shows only one peak at a temperature almost corresponding to the second peak of the only irradiated system.

The accelerated hydrothermal aging on the irradiated sample causes a significant change in the $\tan \delta$ curve with a “homogenization” of the cross-linking density due to both plasticization and thermal curing effects, while for the post-irradiation thermally cured sample, a not dramatic decrease of T_g is observed, justified by its lower water absorption.

Epoxy/Poly(2,6 dimethyl 1,4 phenylene ether) (PPE) Blends

Poly(2,6-dimethyl-1,4-phenylene ether) (PPE) is one of the polymers having wide applications in electronic industry due to its low dielectric constant(2.45), dissipation factor (7×10^{-4}), and high T_g (210 °C). Because of the unique properties, PPE gained great interest for modifying epoxy resins to improve its toughness and ductility. The high T_g of PPE makes its processing difficult and limits practical applications. To reduce the viscosity of PPE, solvents have been introduced during processing, which incurs the following disadvantages during and after processing:

- (a) Requires the disposal or discharge of organic solvent.
- (b) Volatilization of the solvent from the material.
- (c) Causes the presence of voids and irregularities in the material.
- (d) Considerable amount of time and energy is required for the solvent removal.
- (e) Causes environmental issues.
- (f) Increases the post-processing cost.

These problems could be addressed by using thermosetting monomers as the solvents. If then instead of solvent removal during and post-processing, thermosets monomers can be polymerized into a constituent of the final material, which gives a uniform blend of thermoplastic and thermosetting polymers. In addition, by choosing an appropriate thermoset monomer as a solvent, reduction in T_g of thermoplastics during processing can be prevented.

Venderbosch et al. (1994a) reported that the DGEBA is an excellent reactive solvent for making epoxy/PPE resin system. Also PPE/DGEBA epoxy system observed an upper critical solution temperature (UCST) phase diagram. During processing, the DGEBA (act as solvent in the system) significantly reduce the processing temperature and viscosity of the polymer. After the molding process,

DGEBA is converted into the interpenetrating network by polymerization reaction. It is reported that in 20–50 wt.% of PPE content in the blend system, phase separation is accompanied by phase inversion, leads to a unique morphology of epoxy-rich spheres uniformly dispersed in PPE matrix. The phenomenon of locking the original solvent by the phase inversion (polymerizing to thermosetting resins) inside the thermoplastic matrix material is termed as “reaction-induced or chemically induced phase separation (Williams et al. 1996). In 2000, Yoshiyuki and Ryan (2000) investigated the reaction-induced phase separation of epoxy/PPE blends using a specially constructed time-resolved light scattering camera equipped with DSC and observed the chemical gel point not being a true phase transition; however, the reaction remains homogeneous throughout matrix. Because of this, the thermodynamics of the mixture (monomers inside the homopolymer matrix) is considered to be a pseudo-binary system, in which one phase is the homopolymer and the other is the reactant mixture (Venderbosch et al. 1994b; Cahn and Hilliard 1958).

The thermal analysis of epoxy/PPE system revealed the demixing and vitrification of the blend. It was reported that after quenching, the epoxy/PPE blend behaves as a two-component system which gives two separate T_g which are associated with the T_g of the PPE-rich phase and epoxy-rich phase. For example, the blend having 60 wt.% PPE shows two transition temperatures at -5 and 110 °C, which corresponds to the T_g of PPE and epoxy, respectively. When thermal analysis is performed on a 20% solution of PPE, only the lower T_g is observed (Yoshiyuki and Ryan 2000). The thermal studies showed that the vitrification of the PPE-rich phase occurs when the phase reaches the Berghmans point (Callister et al. 1990), which is the intersection between the coexistence curve and T_g composition line defined by the Fox equation (Fox and Loshaek 1955), and no phase separation is possible thereafter. It is also reported that due to the small heat of mixing, there is no thermal transition in association with phase separation (Vandwerdt et al. 1991).

Epoxy/Terpolymer or Tri-block Copolymer Blends

Epoxy/Poly(acrylonitrile-*block*-butadiene-*block*-styrene) (ABS) Blends

Terpolymers are a special class of macromolecules from three species of monomers to exploit the advantageous properties of different polymers, which are not easy to make the miscible blends. Terpolymers of poly(methyl methacrylate-acrylonitrile-vinyl acetate) {P(MMA-AN-VAc)} (Liao et al. 2009; Chen et al. 2011; Kim 1998, 2000; Kim and Yang-Kook 1998) and poly(methyl methacrylate-vinyl acetate)-*co*-poly(ethylene glycol) diacrylate {P(MMA-VAc)-PEGDA} (Liao et al. 2011) have been reported for different applications. It is found that the comprehensive performances of terpolymer are much better than that of copolymer or its blends. The tri-block copolymers have been widely used as modifiers to toughen epoxy resins. One of the most important properties of these block copolymers is its ability to self-assemble into different nanoscale structures in the thermosetting matrix via interpenetration or phase separation. The unique nanoscale morphologies of the thermoplastic tri-block polymers are

generally formed before or during the curing process. These microphase-separated or interpenetrated network structures result from the competition between chain connectivity and block immiscibility. For such tri-block copolymers, e.g., poly(styrene-*block*-butadiene-*block*-methyl methacrylate) (P-SBMMA) or poly(acrylonitrile-*block*-butadiene-*block*-styrene) tri-block copolymers abbreviated as ABS, the morphology is influenced by the repulsive forces between the polybutadiene (PB) mid-block and both polystyrene (PS) and poly(acrylonitrile) end blocks.

In an earlier work (Finaz et al. 1967), block copolymers are limited to soluble polymers which are dissolved in reactive solvents like styrene; however, the method is revalorized recently using thermoset precursors like epoxy (Mijovic et al. 2000; Lipic et al. 1998) and phenolic systems (Kosonen et al. 2001). In a classical thermoplastic linear homopolymer-modified thermosetting system, the thermoplastic chain modifier and the thermosets prepolymer are initially miscible. During curing process, the molar mass of the epoxy resin and its increase involves a decrease in the conformational entropy of mixing, which leads to the phase separation between the thermoplastic and the step-growing thermoset network, generally well before gelation (Pascault and Williams 2000). On contrary to the classical linear homopolymer-modified thermosetting system, macroscopic phase separation can be suppressed or avoided with block copolymers due to the fact that amphiphilic di-block or tri-block thermoplastic copolymers, with one block miscible with the thermoset, are not only dispersible in a reactive prepolymer thermosetting system but also able to order themselves on the micrometer to nanometer scale in both the thermoset prepolymer and cross-linked states, which is successfully demonstrated by different research groups (Mijovic et al. 2000; Hillmyer et al. 1997; Kosonen et al. 2001). Inspiration from di-block copolymer system, tri-block thermoplastic polymers such as ABS (Jyotishkumar et al. 2009, 2011), poly(ϵ -caprolactone)-*block*-PPC-*block*-poly(ϵ -caprolactone) (PCL-PPC-PCL) (Fanliang et al. 2006), and polystyrene-*block*-polybutadiene-*block*-poly(methyl methacrylate) tri-block copolymers (Ritzenthaler et al. 2002) have been investigated as chain modifier in the epoxy thermosetting systems.

Poly(acrylonitrile butadiene styrene) (chemical formula, $C_8H_8)_x \cdot (C_4H_6)_y \cdot (C_3H_3N)_z$) is a common thermoplastic polymer having glass transition temperature of approximately 105 °C. ABS is an amorphous terpolymer prepared from styrene and acrylonitrile monomers polymerized in the presence of polybutadiene and has no true melting point. Recently, the thermal properties of ABS-modified epoxy blends are reported by Jyotishkumar et al. (2009). The study showed complex phase separation in ABS-modified epoxy/4,4'-diaminodiphenyl sulfone (DDS) blends. The amount of ABS in the blends was kept from 5 to 20 parts per hundred parts of epoxy resin (phr). At a lower concentration of ABS (<10 phr), the phase separation of the system takes place through nucleation and growth (NG), while at higher concentrations (>15 phr), the phase separation occurs due to both NG and spinodal decomposition. It is reported that the epoxy blend is heterogeneous in nature.

In DMA studies, the authors observed a higher relaxation peak around 210 and lower relaxation peak at 110 °C, which corresponds to the T_g of the epoxy-rich and SAN-rich phase of ABS, respectively, in the modified blends. The $\tan \delta$ curve of the unmodified epoxy network and the cross-linked epoxy blends however showed a

relaxation peak of very low amplitude at around $-65\text{ }^{\circ}\text{C}$ which caused by the segmental motions of glycidyl units in the network (Guo et al. 2001). The dynamic mechanical spectrum of pristine ABS ($\tan \delta$ vs. temperature plot) has two sharp relaxation peaks at $-88\text{ }^{\circ}\text{C}$ and $107\text{ }^{\circ}\text{C}$ corresponding to the T_g of the polybutadiene and SAN-rich phase, respectively. For the unmodified epoxy network, there is a well-defined sharp relaxation peak centered at $216\text{ }^{\circ}\text{C}$ and corresponds to the T_g of the amine-cured epoxy resin which is in well agreement with the T_g of the cross-linked epoxy/DDS system in the literature (Grillet et al. 1989). The modification of epoxy with ABS caused a slight shift in T_g of epoxy-rich phase to the lower side. The shifting of T_g to the lower end is explained by the following reasons:

- (a) The decrease in the cross-link density of the cured blends, due to the increase in viscosity by the addition of thermoplastic material in to the epoxy system, in turn result in an incomplete cross-linking due to the kinetic factors.
- (b) The addition of thermoplastic causes dilution effect, which may also result in an incomplete cross-linking.
- (c) The addition of thermoplastics into the epoxy cause the formation of substructures, which results in subinclusions of the ABS-rich phase in the continuous cross-linked epoxy region, leading to increased miscibility between both the epoxy and ABS phases.

The T_g of the SAN phase of ABS remains the same for 5 and 10 phr in epoxy/ABS blends. For 15 and 20 phr ABS-modified epoxy blends, however, the T_g of the SAN phase increases to a higher temperature. The intensity of $\tan \delta$ peak for cross-linked epoxy/ABS blends is reported to be higher than for the unmodified amine cross-linked epoxy resin which is associated with changes in the cross-link density. This may also be due to a small amount of ABS molecules dissolved in the epoxy system. Rao et al. (2005) also reported that the addition of the thermoplastic to the epoxy resin increases the viscosity of the material, and hence, the cross-link density decreases upon curing, which results in higher segmental mobility, thereby higher peak intensity. The peak areas and peak widths of the epoxy blends, however, are comparable to those of the unmodified epoxy cross-linked resin. There are two inflection points observed for the ABS-modified cross-linked epoxy blend, one at the T_g of the SAN phase of ABS and the other at the T_g of the cross-linked epoxy resin, while the unmodified cross-linked epoxy resin has only one inflection. The storage modulus of the blends (ABS content $\leq 15\%$) is higher than unmodified epoxy network for the entire spectrum of temperature. As the ABS content increase from 10 phr, the storage modulus of the cross-linked epoxy blends is higher than the unmodified epoxy network up to $110\text{ }^{\circ}\text{C}$; thereafter, it goes down to that of the unmodified epoxy network, which may be due to the bicontinuous nature of the blends (Jyotishkumar et al. 2009).

Jyotishkumar et al. (2011) studied the stress relaxation and thermomechanical properties of poly(acrylonitrile butadiene styrene)-modified epoxy-amine systems. Epoxy networks based on DGEBA cured with DDS (both ABS modified and unmodified) were prepared according to two different cure schedules. One set of

samples were prepared through a single-step and the other through a two-step curing process. The lower concentration of ABS (≤ 6.9 wt.%) in the epoxy resin resulted in more than 100% increase in tensile toughness compared to neat cross-linked epoxy. The presence of internal stress affects the dimensional stability of the blends at high temperatures (above the T_g of ABS). The internal stress however can be removed by two-step curing. The impact of the cure schedules and the increasing ABS concentration on properties were carefully analyzed. Irrespective of the cure schedule, the thermal and mechanical properties remain comparable. On the other hand, the mechanical and morphological properties are affected by blending with the thermoplastic (Jyotishkumar et al. 2011).

Epoxy/Polyoxymethylene (POM) Blends

The mutual influence between isothermal crystallization and reaction-induced phase separation in epoxy/polyoxymethylene (POM) blends is recently reported by Sara and Gabriël (2006). The development of phase morphology in blends of DGEBA/POM/DDS was studied at cure temperatures between 140 and 150 °C, which is lower than the melting temperature of POM. The phase separation behavior of the blends varying from 5 to 30 wt.% POM content was examined with optical microscopy (OM), small-angle laser light scattering (SALLS), and SEM. Different demixing mechanisms were observed depending on the blend composition. At a high curing temperature (150 °C), a reaction-induced phase separation (RIPS) followed by crystallization inside the POM-rich matrix phase was observed. When the sample was cured at 145 °C, all blends showed spherulitic crystallization starting before the RIPS which leads to a gradient of phase-separated structures. This characteristic of the blend is attributed to the inter-spherulitic demixing that may be suppressed by the increase in the nucleation density. In brief, the properties of the blend can be altered by changing the thermal history of the thermoplastic in the blends or by lowering the cure temperature to 140 °C. The increase of the growth rate has been attributed to the increase of the super cooling due to the decrease of the melting point depression caused by the polymerization of the epoxy resin (Sara and Gabriël 2006).

Epoxy/PCL-PPC/PB-PCL Blends

Recently, it is reported that interactions between thermoset matrix and modifiers can further be optimized by the formation of ordered (disordered) nanostructures in thermosets, which endow the materials with improved properties (Hillmyer et al. 1997; Lipic et al. 1998). Based on the catch, there are few reports on epoxy-based nanostructures formed with thermoplastic modifiers. Epoxy blended with PCL-PPC-PCL or PC-PB-PCL is a tri-block copolymer caught attention recently due to the miscibility of PCL in epoxy. The use of PCL-PPC-PCL or PCL-PB-PCL enables innovative application of PPC as a toughening agent of epoxy thermosets. Fenget

et al. (Fanliang et al. 2006) reported the application of sustainable PPC copolymer for toughening epoxy thermosets. PPC is used as a novel initiator for ϵ -caprolactone polymerization to produce the tri-block copolymer.

PCL-PPC-PCL (Chen et al. 2015) and PCL-PB-PCL (Fanliang et al. 2006) were synthesized via the ring-opening polymerization of ϵ -caprolactone in the presence of a hydroxyl-terminated polybutadiene (HTPB), and the polymerization reaction is catalyzed by stannous octoate [$\text{Sn}(\text{Oct})_2$]. The resulting amphiphilic PCL-PPC-PCL or PCL-PB-PCL tri-block copolymer is used to prepare the nanostructured epoxy thermosets via blending with epoxy resin (Chen et al. 2015) or in situ polymerization (Fanliang et al. 2006). The epoxy monomers are polymerized in the presence of PCL-PB-PCL or PCL-PPC-PCL, which is dissolved in THF at the temperature above the upper critical solution temperature of DGEBA and HTPB blends, and 4,4'-methylene *bis* (2-chloroaniline) (MOCA) is used as the cross-linking agent.

When amphiphilic tri-block copolymer PCL-PPC-PCL or PCL-PB-PCL tri-block thermoplastic polymer is used to prepare the nanostructured epoxy thermosets, the PCL blocks in the terpolymer are miscible with the cross-linked epoxy networks, i.e., the PCL subchains in the tri-block copolymer are easily interpenetrated into the cross-linked epoxy network at the segmental level; hence, the interfacial interaction between PPC modifiers and epoxy was enhanced significantly. Due to the miscibility of PCL blocks with epoxy matrix, the size of phase-separated PPC modifiers decreased dramatically as the amphiphilic block copolymer formed nanophases in epoxy host. The miscibility of PCL in epoxy facilitates the easy incorporation of 30 wt.% PCL-PPC-PCL modifier in the epoxy thermoset without the formation of any microdomains. For the lower concentration of PCL-PPC-PCL, it is observed that epoxy-rich components are composed of the cross-linked epoxy networks which are interpenetrated by the PCL blocks of the copolymer, whereas the PB domains form the nano-islands due to its incompatibility with epoxy resin. Depending on the content of the block copolymer in the thermosets, the PB domains exhibit spherical and interconnected nano-objects having the particle size varying from 10 to 20 nm. For the TS/TP blend containing 10 wt.% of PCL-PB-PCL tri-block, the nanosized phase-separated PB particles were imbedded in the continuous epoxy matrix at the average size of ca. 10 nm in diameter. When the thermoplastic content increases beyond 10 wt.%, the nanosized phase-separated PB particles began to coagulate in the continuous epoxy matrix resulted in the formation of some PB domains (worm-like objects in the epoxy matrix), and while the concentration of PCL-PB-PCL increased to ≥ 30 wt.%, the epoxy component began to form some separated nanosized particles or wormlike objects. The number of the spherical objects increased, whereas the average distance between adjacent domains decreased with increasing the content of PCL-PB-PCL in the thermosets; however, the size of the nanoparticles almost remains invariant. When the content of PCL-PB-PCL is 20 wt.%, the spherical particles began to interconnect to some extent; hence, the thermoset at this composition possesses a combined morphology, in which both spherical PB domains and few interconnected PB domains were simultaneously present. When the content of PCL-PB-PCL was increased up to 30 wt.%, the domains of PB were highly interconnected, forming interconnected objects at the nanometer scales. This

morphology is a typical structure of bicontinuous microphase separation. The formation of nanostructures takes place on the basis of the mechanism of polymerization-induced microphase separation. The morphology of nanostructures is controlled by the microphase separation of PB blocks, which is induced during the polymerization of epoxy other than by fixing the preformed self-assembly microphases in the mixtures of the block copolymer and the epoxy precursors. The reaction-induced microphase separation of PB blocks in the thermosets predominated due to its lower entropic contribution to free energy of mixing for the mixing of PB blocks with cross-linked epoxy networks (Fanliang et al. 2006).

The thermal properties of cross-linked epoxy networks with PCL and PPC blocks studied by DMA (Chen et al. 2015) showed that the pristine epoxy exhibited a well-defined T_g (α -transition) at 146 °C. It is also reported that, apart from α -transition, it exhibits a secondary relaxation peak (β - transition) from about -50 to -60 °C, which is predominantly attributed to the motion of hydroxyl ether structural units and diphenyl groups in epoxy (Xu et al. 2007a). Since the T_g of PPC is about -53 °C, the α -transition of PPC nanodomains is overlapped with the β - transition of epoxy in epoxy/PCL-PPC-PCL thermosets, which leads to make difficulties to distinguish T_g of PPC in the DMA analysis of thermosets containing the PCL-PPC-PCL tri-block copolymer. Upon incorporating the thermoplastics PCL-PPC-PCL tri-block copolymer into the thermosets, the T_g of the matrix shifts to a lower temperature, which indicates the miscibility of the PCL subchains and epoxy matrix. The effect is more predominant with increasing PLCL-PPC-PCL tri-block content. As a result of interpenetrating morphology of PCL and the formation of nanodomain of PB in the thermoset, the PCL-PPC-PCL modifier possesses an excellent toughening effect for epoxy thermosets in spite of sacrificing part of the strength and thermal property of the matrix (Chen et al. 2015).

Before curing, all the epoxy precursors, curing agents, and PCL-PPC-PCL (or PPC) were transparent at room and elevated temperatures. After curing at a setting temperature, the thermosetting blend containing PPC and PCL homopolymers becomes cloudy (losing its transparency), implying the occurrence of macroscopic phase separation. All the thermosets containing the PCL-PPC-PCL tri-block copolymer are homogeneous and transparent, which suggests that there is no macroscopic phase separation at least on the scale exceeding the wavelength of visible light (Fig. 10) (Chen et al. 2015). Li et al. also reported that PPC is miscible with EP precursors; however, reaction-induced phase separation occurs during the curing (Li et al. 2010).

Epoxy/Poly(ether imide) (PEI) Blends

Bonnet and coworkers (1999a) reported the similar thermal behavior in epoxy/Poly(ether imide) (PEI) blends discussed in earlier section “Epoxy/PCL-PPC/PB-PCL Blend” for epoxy/tri-block thermoset thermoplastic blends. In 1999, Bonnet et al. (1999b) studied the rates of epoxy-amine reactions in TS/TP blends with different thermoplastic concentrations. The thermoset system selected for the study was

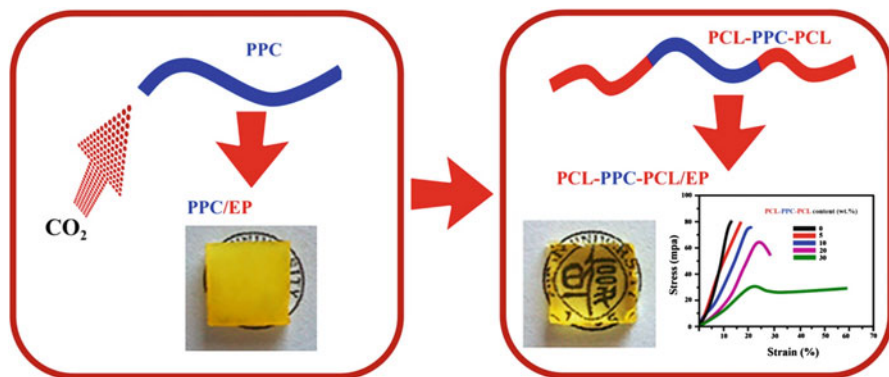


Fig. 10 The effect of PCL in the transparency of epoxy blend system (Adopted from Chen et al. 2015)

DGEBA-based epoxy cured with 4,4'-methylene bis(3-chloro-2,6-diethylaniline) in the presence of varying PEI concentrations (10-64 wt.%). The studies reported the rates of reaction in amorphous thermoplastic-modified epoxy systems depending on the initial concentrations of thermoplastic, and the authors highlighted two specific behaviors of the system as follows:

- (i) For thermoplastic concentration ≤ 10 wt.%, no sudden change in the kinetic rates was detected when phase separation occurred, due to the low quantity of dispersed phase.
- (ii) For thermoplastic concentrations higher than 30%, an increase of the reaction rate is observed when phase separation occurred, due to the appearance of a less dilute epoxy-amine phase.

It is well known that block copolymers have the ability to form micelles in the selected nonreactive organic solvents. For instance, poly(styrene acrylonitrile) di-block copolymer in a selective solvent (e.g., acetone) is a good solvent for styrene block but poor for acrylonitrile; hence, the block copolymer molecules tend to associate into acrylonitrile core/styrene shell spherical micelles (Chu et al. 1997).

Buchholz et al. and Könczöl et al. (Buchholz and Mülhaupt 1992; Könczöl et al. 1994) incorporated low molar weight poly(ϵ -caprolactone)-*block*-poly(dimethyl siloxane), $(PCL)_2$ -*b*-PDMS-*b*-(PCL)₂, and branched tri-block copolymers in epoxy matrix. The aim was to improve mechanical properties of epoxy network with the immiscible elastomeric PDMS blocks compatibilized by the PCL segments, initially miscible in epoxy precursors. Even if the structure obtained before reaction is not detailed, elastomeric particles of 20 nm in diameter, uniformly dispersed in the epoxy matrix, are generated at the end of the curing process. Addition of tri-block copolymer (>5 wt.%) leads to an increase in the toughness by a factor of more than two, without reduction of the strength at break and Young's modulus when compared to the neat epoxy system.

Epoxy/Poly(styrene-*block*-butadiene-*block*-methyl methacrylate) (P-SBMMA) Blends

Ritzenthaler et al. (2002) studied the tri-block copolymers/epoxy-diamine blends. The tri-block polymer used is P-SBMMA tri-block copolymers. The tri-block copolymer (P-SBMMA) has been selected in the study due to the following reasons.

- (a) When looking in to the literature which are devoted to tri-block copolymers, the most important theoretical (Zheng and Wang 1995) and experimental studies (Auschra and Stadler 1993; Abetz and Goldacker 2000) have been carried out on (P-SBMMA).
- (b) More recently, the morphological behavior of a polystyrene-*block*-polybutadiene-*block*-poly(ethylene oxide) tri-block copolymer also has been studied (Bailey et al. 2001).
- (c) Polybutadiene (PB) is immiscible with the epoxy precursor, which leads to an initial macrophase separation between PB and epoxy monomers (Chen et al. 1994).
- (d) In the initial stage, the homo-polystyrene is partially miscible with the epoxy precursors (a homogeneous solution can obtained at a temperature higher than 90 °C, whereas decreasing temperature involves phase separation between homo-polystyrene and the epoxy monomers).
- (e) The homo-poly(methyl methacrylate) was previously shown to be completely miscible with epoxy prepolymer (Ritzenthaler et al. 2000).

Epoxy thermoset blended with P-SBMMA tri-block copolymers (10–50 wt.%) is synthesized anionically and has been investigated for its morphological and thermo-mechanical properties before and after the epoxy-amine reaction. Before the cross-linking reaction, the three blocks self-organize on a nanometer scale, in such a way that PS spheres surrounded by PB nodules, while the PMMA blocks are solubilized with the epoxy precursors, forming a swollen corona. When the PB blocks aggregate into spherical domains at the interface between the epoxy-rich matrix and PS block nanospheres, the epoxy components swells the MMA blocks, thereby inducing a morphological transition from PB helices around PS cylinders (the morphology of the neat tri-block) to PB spheres on PS spheres. This indicates that the PS blocks are microphase separated from the epoxy system even before reaction. Also even after using MCDEA as hardener, the domain sizes of the thermoplastic chain modifiers remain unaffected throughout the network frames, and the final structure of the blend system has “spheres on spheres” morphology of undiluted PS block sphere formed on PB blocks spheres, while most of the PMMA chain remaining embedded in the epoxy network frames. The thermal behavior of PMMA blocks in the blend system is investigated on the fully reacted sample in different temperature from room temperature to 250 °C using DMA and found that there are three different relaxations that correspond to the T_g of epoxy-rich phase, relaxation of pristine PMMA blocks, and pristine PS microdomains in the blend. The relaxation observed for the epoxy/tri-block blend at 163 °C is associated

with the glass transition temperature of the epoxy-rich phase. The shift of relaxation temperature from 163 °C to lower temperature compared to the one of the neat DGEBA-MCDEA network (187 °C) is ascribed to the plastification effect induced by the incorporation of PMMA blocks in the epoxy network. Ritzenthaler et al. (2000) also has reported same phenomena for miscible DGEBA-MCDEA/PMMA homopolymer blends. The high-temperature relaxation at 130 °C (T_g of PMMA homopolymer) and the low-temperature relaxation at 97 °C (T_g of PS homopolymer) ascribed to the chain relaxation of microphase-separated pristine PMMA units from the epoxy-rich matrix and pristine PS domains in the epoxy matrix, respectively.

Epoxy/Poly(styrene-*block*-butadiene-*block*-styrene) (SBS) Blends

Sajeev et al. (2014) recently (in 2014) reported the blend of epoxidized poly(styrene-*block*-butadiene-*block*-styrene) (SBS) tri-block copolymer and epoxy based on DGEBA with 4,4'-diaminodiphenylmethane (DDM) curing agent. Before blending with epoxy, SBS tri-block copolymer is epoxidized to a 47 mol% (denoted as eSBS47, having degree of epoxidation 47%) by hydrogen peroxide in a water/dichloroethane biphasic system, and the thermal properties of the modified system are analyzed using differential scanning calorimetry (DSC), DMA, thermo-mechanical analysis (TMA), and thermogravimetric analysis (TGA). The epoxy/tri-block copolymer blends with 10–20 wt.% eSBS were prepared by simple solvent casting technique. The onset temperature of molecular chain relaxation, i.e., T_g , and heat flow (ΔH) is studied by DSC in a temperature range of –30 to 300 °C on the samples cured for different cure times varying from 0 to 360 min at 90 °C to understand the thermal behavior of epoxy/eSBS tri-block blend system under dynamic conditions. DSC studies revealed that in the case of neat epoxy or blends cured in the shortest times, an exothermic peak was observed in the DSC thermograms which indicates that the curing reaction was not completed during cross-linking reaction, which in turn leave some cross-linking sites in the epoxy/eSBS tri-block blend system. A broad exothermic peak is observed on the DSC thermograms of uncured epoxy blend system (cure time $t = 0$) which is the direct measure for the enthalpy of cross-linking reaction. There is no exothermic peak observed for the completely cured epoxy/eSBS tri-block blend system (cure time ≥ 90 min) and enthalpy of the reaction found to be decreasing with increasing cure time from 0 to 90 min. This does not indicate that all of the entire epoxide groups and amino hydrogen atoms were involved in the formation of 3D-network structures during the cross-linking reactions; however, the mobility of some of the reactive sites might have been frozen, which stops the polymerization reaction. Recently, other than epoxy/amine hardener system, similar exothermic peaks in the DSC thermograms are observed by Garate et al. (2013) for the epoxidized poly(styrene-*block*-isoprene-*block*-styrene) (SIS)/hardener reaction. This behavior, however, is not observed in George et al. (2012) studies for the same epoxy resin and epoxidized styrene-*block*-butadiene-*block*-styrene tri-block copolymer blend systems.

In Sajeev et al. (2014) studies on the blend of eSBS tri-block copolymer and epoxy polymer blend system, upon addition of eSBS to the epoxy matrix, the fracture toughness of the nanostructured thermosets is improved, while the thermal stability was retained; however, the dimensional stability was slightly decreased. The storage modulus (G') versus temperature curves of the pristine amine-cured epoxy resin showed a higher G' value compared to the nanostructured epoxy thermosets blends with 10 and 20 wt.% eSBS tri-block copolymer. The lower G' value of nanostructured epoxy/eSBS tri-block copolymer blends ascribed to the plasticizing effect of less stiff eSBS tri-block copolymer, basically resulted from its miscibility with the epoxy-rich phase, which in turn resulted in reduction in modulus of the TS/TP blends (Xu et al. 2007b). It is also reported that the cross-linked epoxy phase exhibited a well-defined α -transition centered at 130 °C and a weak relaxation at around 40 °C, which is called the ω -relaxation peak due to the lower cross-link density in the epoxy network. On the other hand, in addition to the α and ω transitions, the eSBS nanostructured tri-block thermoplastic blends exhibited an additional minor transition at around 90 °C (T_g of PS) that corresponds to the molecular relaxation of phase-separated PS nanodomains. Also for all the epoxy/eSBS tri-block blend system, the $\tan \delta$ profile showing a sharp relaxation peak centered at around 150 °C corresponds to the T_g of the amine-cured epoxy resin. A broadening of the $\tan \delta$ peak is observed for the nanostructured blends and is slightly overlapped with the T_g of the PS domains in the tri-block blend system. The T_g value of the pristine epoxy system was found to be 10 to 20 °C higher than epoxy/tri-block thermoplastic blend with 10 and 20 wt.% eSBS chain modifier. The decrease in T_g in the blend system is due to the:

- (a) Plasticizing effect of the nanodispersed eSBS copolymer in epoxy system
- (b) Miscibility of eSBS tri-block copolymer with epoxy resin
- (c) Uniform dispersion/distribution of eSBS nanodomains in the epoxy
- (d) Reduction in crystallinity or enthalpy due to the plasticizing effect of eSBS

The lower T_g of the epoxy/tri-block polymer system indicates that the eSBS tri-block subchains were effectively interpenetrated into the cross-linked epoxy matrix at the segmental level (Meng et al. 2006b). In addition to the main relaxation peak, there were two other minor relaxation peaks of very low amplitude also reported, the one at around -65 and other at 65 °C, called β -relaxation corresponds to the motion of glycidyl units in the epoxy network (Guo et al. 2001) and ω -relaxation peak, which is due to the lower cross-link density in the epoxy network, respectively (Francis et al. 2006).

The thermal stability study of the epoxy/tri-block copolymer blend system showed there is no weight loss or release of any small molecular weight molecules from the host upon heating, and the whole spectrum of the TS/TP blends was thermally stable up to 350 °C. Above 350 °C, considerable weight loss is observed due to the chain scission of polymer molecules. The temperature of the maximum rate of decomposition (T_{peak}) was found to be 377–383 with eSBS tri-block copolymer content of 0–20 wt.%. The T_{max} shows an increasing trend with nanodispersed

eSBS tri-block nanodomains, and no drastic change in thermal stability is observed for the TS/TP blend system which in turn indicates that the thermal stability of cross-linked epoxy system is not adversely affected by the incorporated eSBS tri-block copolymer chain modifiers.

The influence of temperature on dimensional stability (studied by TMA) is studied and reported that the dimensional changes with temperature for the epoxy/eSBS tri-block copolymer blend system are greater than pristine epoxy system over the complete range of temperature due to the higher molecular vibration at higher temperatures. The increase in molecular vibration in eSBS tri-block copolymer may be due the availability of increased intermolecular distance resulted from the plasticizing effect of tri-block eSBS soft polymer chains, which leads to the increased thermal expansion for the blends. In the case of the pristine epoxy system, a drop in the dimensional change near T_g is observed due to relaxation of nonequilibrium states of the cured samples that are frozen below T_g . Similar phenomenon is also recently reported for epoxy/multiwalled carbon nanotube (MWCNT) composites cured with DDS (Jyotishkumar et al. 2013a, b). At a temperature close to the T_g , the motion capacity of the chain segment is high enough to unfreeze the frozen chains, so that the vacant spaces will be lost which results in a drop in dimensional change. The schematic (Fig. 11) represents the mechanism behind the freezing of such local sites in the nanostructured thermosets due to the insertion of tri-block

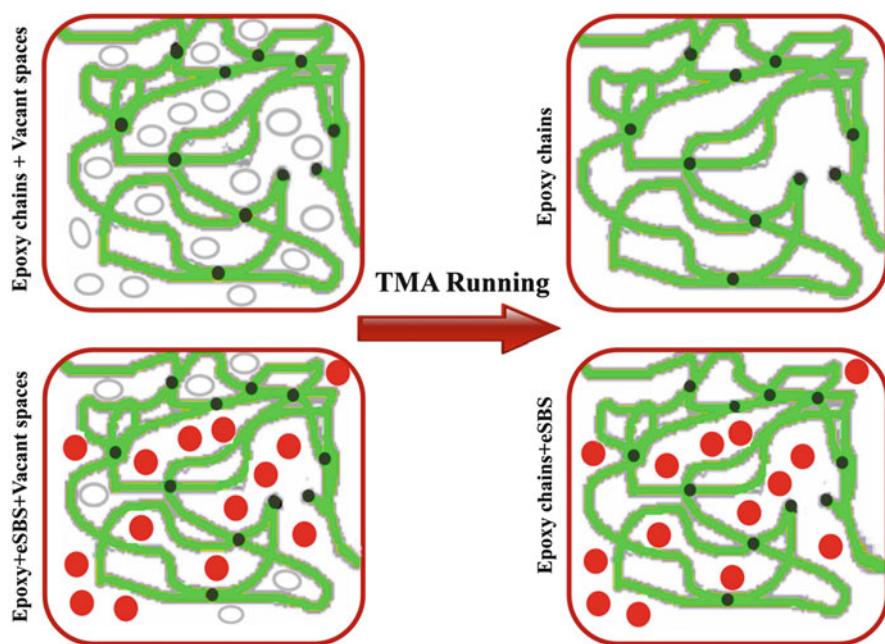


Fig. 11 Schematic of the mechanism for the drop in dimension change near T_g . (Adopted from Sajeev et al. 2014)

thermoplastics or associated mixing in pristine and blend epoxy system (Sajeev et al. 2014).

Recently, it was reported that epoxidized butadiene block of a di-block copolymer poly(styrene–butadiene) and a tri-block copolymer SBS and SIS and isoprene block of SIS for developing the nanostructured thermosets/tri-block copolymer thermoplastic blends (Garate et al. 2013; Serrano et al. 2006, 2007; Ramos et al. 2012; Ocando et al. 2013). The effects of the eSBS tri-block copolymers, however, on the rheological, viscoelastic, thermal, dimensional, and fracture toughness properties in the epoxy/eSBS tri-block copolymer blend system cured with DDM have never been reported.

Conclusions

Blending of brittle epoxy resins with suitable thermoplastics, having high elastic modulus and high glass transition temperature (T_g), with an aim to enhance their fracture toughness and thermal resistance, has been a relevant topic in the current research scenario. Various studies which were carried out using different thermoplastic systems such as ABS, P(MMA-VAc)-PEGDA, PB, PCL-PPC-PCL, PEI, PEO, PGA, PPO, and P-SBMMA for toughening the epoxy resin have been thoroughly analyzed. In this chapter, the authors have tried to give a detailed overview on the various approaches and methods adopted for toughening epoxy resin with thermoplastics and the mechanisms of toughening of epoxy with special attention to the thermal properties of the blends. The important factors which control the thermomechanical behavior and morphology of the epoxy/thermoplastic blend are the backbone structure, molecular weight, and the end-group chemistry of the thermoplastics. Epoxy/thermoplastic blends thus produced find many applications such as engineering materials for aircraft, electronic, construction, and automobile industries.

References

- Abetz V, Goldacker T (2000) Formation of superlattices via blending of block copolymers. *Macromol Rapid Commun* 21:16–34
- Aghdam RM, Najarian S, Shakhesi S, Khanlari S, Shaaban K, Sharifi S (2012) Investigating the effect of PGA on physical and mechanical properties of electrospun PCL/PGA blend nanofibers. *J Appl Polym Sci* 124:123–129
- Alessi S, Dispenza C, Conduruta D, Pitarresi G, Spadaro G (2009) Epoxy resin-thermoplastic blends cured by ionising radiation. Structure/properties relationships, Proceedings, 17th International Conference on Composite Materials (ICCM-17), The British composite society, pp D10.7
- Analysis of Plastics Consumption and Recovery in Western Europe (2003) APME, Brussels, 2004
- Ashcroft WR (1993) Curing agents for epoxy resins. In: Ellis B (ed) *Chemistry and technology of epoxy resins*. Blackie Academic and Professional, Glasgow, pp. 37–71

- Auschra C, Stadler R (1993) New ordered morphologies in ABC triblock copolymers. *Macromolecules* 26:2171–2174
- Bailey TS, Pham HD, Bates FS (2001) Morphological behavior bridging the symmetric AB and ABC states in the poly(styrene-*b*-isoprene-*b*-ethylene oxide) triblock copolymer system. *Macromolecules* 34:6994–7008
- Barone L, Carciotto S, Cicala G, Recca A (2006) Thermomechanical properties of epoxy/poly(ϵ -caprolactone) blends. *Polym Eng Sci* 46:1576–1582
- Blanco I, Cicala G, Motta O, Recca A (2004) Influence of a selected hardener on the phase separation in epoxy/thermoplastic polymer blends. *J Appl Polym Sci* 94:361–371
- Boland ED, Wnek GE, Simpson DG, Pawlowski KJ, Bowlin GL (2001) Tailoring tissue engineering scaffolds using electrostatic processing techniques: a study of poly(glycolic acid) electrospinning. *J Macromol Sci* 38:1231–1243
- Bonnet A, Pascault JP, Sautereau H, Camberlin Y (1999a) Epoxy-diamine thermoset/thermoplastic blends 2 rheological behaviour before and after phase separation. *Macromolecules* 32:8524–8530
- Bonnet A, Pascault JP, Sautereau H, Taha M, Camberlin Y (1999b) Epoxy–diamine thermoset/thermoplastic blends. 1. Rates of reactions before and after phase separation. *Macromolecules* 32:8517–8523
- Buchholz U, Mühlaupt R (1992) Contributions to the dynamic-mechanical thermoanalysis of adhesives. *ACS Polym Prepr* 33:205–206
- Bucknall CB, Gomez CM, Quintard I (1994) Phase separation from solutions of poly(ether sulfone) in epoxy resins. *Polymer* 35:353–359
- Cabanelas JC, Serrano B, Baselga J (2005) Development of cocontinuous morphologies in initially heterogeneous thermosets blended with poly(methyl methacrylate). *Macromolecules* 38:961–970
- Cahn JW, Hilliard JE (1958) Free energy of a nonuniform system. I. Interfacial free energy. *J Chem Phys* 28:258–267
- Callister S, Keller A, Hikmet RM (1990) Introductory lecture. Aspects of polymer gels. *Makromol Chem Makromol Symp* 39:19–20
- Chen JL, Chang FC (1999) Phase separation process in poly(ϵ -caprolactone)-epoxy blends. *Macromolecules* 32:5348–5356
- Chen S, Chen B, Fan J, Feng J (2015) Exploring the application of sustainable poly(propylene carbonate) copolymer in toughening epoxy thermosets. *ACS Sustain Chem Eng* 3:2077–2083
- Chen D, Pascault JP, Bertsch RJ, Drake RS, Siebert AR (1994) Synthesis, characterization, and properties of reactive liquid rubbers based on butadiene–acrylonitrile copolymers. *J Appl Polym Sci* 51:1959–1970
- Chen L, Rao MM, Li WS, Xu MQ, Liao YH, Tan CL, Yi J (2011) Performance improvement of polyethylene-supported PAMS electrolyte using urea as foaming agent. *Acta Phys Chim Sin* 27:1689–1694
- Chu B, Liu T, Wu C, Zhou Z (1997) *Makromol Symp* 118:221–227 <http://pubs.acs.org/doi/abs/10.1021/bm015574q?src=recsys&journalCode=bomaf6>
- Clark JN, Daly JH, Garton A (1984) Hydrogen bonding in epoxy resin/poly(ϵ -caprolactone) blends. *J Appl Polym Sci* 29:3381–3390
- Das B, Chakraborty D, Hajra AK, Sinha S (1994) Epoxy/poly(methyl methacrylate) interpenetrating polymer networks- morphology, mechanical and thermal properties. *J Appl Polym Sci* 53:1491–1496
- Engelberg I, Kohn J (1991) Physico-mechanical properties of degradable polymers used in medical applications: a comparative study. *Biomaterials* 12:292–304
- Fanliang M, Sixun Z, Weian Z, Huiqin L, Qi L (2006) Nanostructured thermosetting blends of epoxy resin and amphiphilic poly(ϵ -caprolactone)-*block*-polybutadiene-*block*-poly(ϵ -caprolactone) triblock copolymer. *Macromolecules* 39:711–719
- Finaz G, Skoulios A, Sadron CCR (1967) *Acad Sci Paris* 253:565–569

- Fox TG, Loshaek S (1955) Fiber lubricant properties and dynamic mechanical properties of polyoxyalkylene fluids. *J Polym Sci* 15:371–390
- Francis R, Baby DK (2014) Toughening of epoxy thermoset with polystyrene-block-polyglycolic acid star copolymer: nanostructure–mechanical property correlation. *Ind Eng Chem Res* 53:17945–17951
- Francis B, Rao VL, Poel GV, Psaada F, Groeninckx G, Ramaswamy R (2006) Cure kinetics, morphological and dynamic mechanical analysis of diglycidyl ether of bisphenol-A epoxy resin modified with hydroxyl terminated poly(ether ether ketone) containing pendent tertiary butyl groups. *Polymer* 47:5411–5419
- Garate H, Mondragon I, D'Accorso NB, Goyanes S (2013) Exploring microphase separation behavior of epoxidized poly(styrene-*b*-isoprene-*b*-styrene) block copolymer inside thin epoxy coatings. *Macromolecules* 46:2182–2187
- George SM, Puglia D, Kenny JM, Jyotishkumar P, Thomas S (2012) Cure kinetics and thermal stability of micro and nanostructured thermosetting blends of epoxy resin and epoxidized styrene-block-butadiene-block-styrene triblock copolymer systems. *Polym Eng Sci* 52:2336–2347
- Gillham JK (1986) Formation and properties of thermosetting and high T_g polymeric materials. *Polym Eng Sci* 26:1429–1433
- Girard-Reydet E, Sautereau H, Pascault JP, Keates P, Navard P, Thollet G, Vigier G (1998) *Polymer* 39:2269–2279
- Girard-Reydet E, Vicard V, Pascault JP, Sautereau H (1997) Polyetherimide-modified epoxy networks: influence of cure conditions on morphology and mechanical properties. *J Appl Polym Sci* 65:2433–2445
- Goossens S, Groeninckx G (2006) Mutual influence between reaction-induced phase separation and isothermal crystallization in POM/epoxy resin blends. *Macromolecules* 39:8049–8059
- Grillet AC, Galy J, Pascault JP, Bardin I (1989) Effects of the structure of the aromatic curing agent on the cure kinetics of epoxy networks. *Polymer* 30:2094–2103
- Grubbs RB, Dean JM, Broz ME, Bates FS (2000) Reactive block copolymers for modification of thermosetting epoxy. *Macromolecules* 33:9522–9534
- Guo Q, Figueiredo P, Thomann R, Gronski W (2001) Phase behavior, morphology and interfacial structure in thermoset/thermoplastic elastomer blends of poly(propylene glycol)-type epoxy resin and polystyrene-*b*-polybutadiene. *Polymer* 42:10101–10110
- Hameed N, Guo Q (2008) Nanostructure and hydrogen bonding in interpolyelectrolyte complexes of poly(ϵ -caprolactone)-block-poly(2-vinyl pyridine) and poly(acrylic acid). *Polymer* 49:5268–5275
- He X, Liu Y, Zhang R, Wu Q, Chen T, Sun P (2014) Unique interphase and cross-linked network controlled by different miscible blocks in nanostructured epoxy/block copolymer blends characterized by solid-state NMR. *J Phys Chem C* 118:13285–13299
- Hillmyer MA, Lipic PM, Hadjuk DA, Almdal K, Bates FS (1997) Self-assembly and polymerization of epoxy resin-amphiphilic block copolymer nanocomposites. *J Am Chem Soc* 119:2749–2750
- Hsieh H (1990) Morphology and properties control on rubber-epoxy alloy systems. *Polym Eng Sci* 30:493–510
- Johnsen BB, Kinloch AJ, Taylor AC (2005) Toughness of syndiotactic polystyrene/epoxy polymer blends: microstructure and toughening mechanisms. *Polymer* 46:7352–7369
- Jyotishkumar P, Abraham E, George SM, Elias E, Pionteck J, Moldenaers P, Thomas S (2013a) Preparation and properties of MWCNTs/poly(acrylonitrile-styrene-butadiene)/epoxy hybrid composites. *J Appl Polym Sci* 127:3093–3103
- Jyotishkumar P, Jürgen R, Rüdiger H, George SM, Uroš C, Thomas S (2011) Studies on stress relaxation and thermomechanical properties of poly(acrylonitrile-butadiene-styrene) modified epoxy–amine systems. *Ind Eng Chem Res* 50:4432–4440
- Jyotishkumar P, Koetz J, Brigitte T h, Veronika S, Ceren Ö, Paula M, Rudiger H, Thomas S (2009) Complex phase separation in poly(acrylonitrile–butadiene–styrene)-modified epoxy/

- 4,4'-diaminodiphenyl sulfone blends: generation of new micro- and nanostructures. *J Phys Chem B* 113:5418–5430
- Jyotishkumar P, Logakis E, George SM, Pionteck J, Haussler L, Haßler R, Pissis P, Thomas S (2013b) Preparation and properties of multiwalled carbon nanotube/epoxy-amine composites. *J Appl Polym Sci* 127:3063–3073
- Kim DW (1998) Electrochemical characteristics of a carbon electrode with gel polyelectrolyte for lithium-ion polymer batteries. *J Power Sources* 76:175–179
- Kim DW, Yang-Kook S (1998) Polymer electrolytes based on acrylonitrile-methyl methacrylate-styrene terpolymers for rechargeable lithium-polymer batteries. *J Electrochem Soc* 145:1958–1963
- Kim DW, Bookeun O, Jin-Hwan P, Yang-Kook S (2000) Gel-coated membranes for lithium-ion polymer batteries. *Solid State Ionics* 138:41–49
- Kim JT, Kim HC, Kathi J, Rhee KY (2008) Double-phase morphology of high molecular weight poly(methyl methacrylate)-epoxy blend. *J Mater Sci* 43:3124–3129
- Kinloch AJ (1986) Structural adhesives, development in resins and primers. Elsevier, New York
- Könczöl L, Döll W, Buchholz U, Muöl R (1994) Ultimate properties of epoxy resins modified with a polysiloxane–polycaprolactone block copolymer. *J Appl Polym Sci* 54:815–826
- Kosonen H, Ruokolainen J, Nyholm P, Ikkala O (2001) Self-organized thermosets: blends of hexamethyl tetramine cured novolac with poly(2-vinylpyridine)-*block*-poly(isoprene). *Macromolecules* 34:3046–3049
- Li J, Du Z, Li H, Zhang C (2010) Chemically induced phase separation in the preparation of porous epoxy monolith. *J Polym Sci B Polym Phys* 48:2140–2147
- Liao YH, Li XP, Fu CH, Xu R, Rao MM, Zhou L, Hu SJ, Li WS (2011) Performance improvement of polyethylene-supported poly (methyl methacrylate-vinyl acetate)-co-poly (ethylene glycol) diacrylate based gel polymer electrolyte by doping nano- Al_2O_3 . *J Power Sources* 196:6723–6728
- Liao YH, Zhou DY, Rao MM, Li WS, Cai ZP, Liang Y, Tan CL (2009) Self-supported poly (methyl methacrylate–acrylonitrile–vinyl acetate)-based gel electrolyte for lithium ion battery. *J Power Sources* 189:139–144
- Lipic PM, Bates FS, Hillmyer MA (1998) Nanostructured thermosets from self-assembled amphiphilic block copolymer/epoxy resin mixtures. *J Am Chem Soc* 120:8963–8970
- Liu Y, Zhong XH, Yu YF (2010) Gelation behavior of thermoplastic-modified epoxy systems during polymerization-induced phase separation. *Colloid Polym Sci* 288:1561–1570
- Lunak S, Dusek KJ (1975) *Polym Sci Polym Symp* 53:45–55
- May CA (1988) *Epoxy resins chemistry and technology*, 2nd edn. Marcel Dekker, New York
- Mc Adams LV, Gannon JA (1986) *Encyclopedia of polymer science and engineering*, Vol. 6, 2nd edn. Wiley Interscience, Hoboken, p. 322
- Meltzer YL (1979) *Water-soluble polymers, recent developments, (chemical technology review)*. Noyes Data Corp, London ISBN-10: 0815507429
- Meng F, Zheng S, Zhang W, Li H, Liang Q (2006a) Nanostructured thermosetting blends of epoxy resin and amphiphilic poly(ϵ -caprolactone)-*block*-polybutadiene-*block*-poly(ϵ -caprolactone) triblock copolymer. *Macromolecules* 39:711
- Meng F, Zheng S, Li H, Liang Q, Liu T (2006b) Formation of ordered nanostructures in epoxy thermosets: a mechanism of reaction-induced microphase separation. *Macromolecules* 39:5072–5080
- Meynie L, Fenouillot F, Pascault JP (2004) A phenomenological modification of rheological models for concentrated two-phase systems: application to a thermoplastic/thermoset blend. *Polymer* 45:1867–1877
- Mijovic J, Shen M, Sy JW, Mondragon I (2000) Dynamics and morphology in nanostructured thermoset network/block copolymer blends during network formation. *Macromolecules* 33:5235–5244
- Natarajan K, Rao RMVGK (1994) Toughening studies on an ABS/PC blend-modified epoxy resin system, high perform. *Polymer* 6:241–248

- Ocando C, Fernandez R, Tercjak A, Mondragon I, Eceizá A (2013) Nanostructured thermoplastic elastomers based on SBS triblock copolymer stiffening with low contents of epoxy system. *Morphol Behav Mech Prop Macromol* 46:3444–3451
- Oyanguren PA, Galante MJ, Andromaque K, Frontini PM, Williams RJJ (1999) The use of load separation criterion and normalization method in ductile fracture characterization of thermoplastic *polymers*. *Polymer* 40:5249–5255
- Padma CB, Natarajan K (2014) Mechanical and morphological studies of modified epoxy resin matrix for composite applications. *Int J Emerg Technol Adv Eng* 4:105–112
- Park JW, Kim SC (1996) Phase separation during synthesis of polyetherimide/epoxy semi-IPNs. *Polym Adv Technol* 7:209–220
- Park KE, Kang HK, Lee SJ, Min BM, Park WH (2006) Biomimetic nanofibrous scaffolds: preparation and characterization of PGA/chitin blend nanofibers. *Biomacromolecules* 7:635–643
- Pascault JP, Williams RJJ (2000) In: Paul D, Bucknall CB (eds) *Polymer blends; volume I: formulation*, vol 1. Wiley, New York, pp. 379–415
- Paul DR, Bucknall CB (2000) *Polymer blends*, vol 1. Wiley, New York.
- Pearson RA (1993) In: Kinloch CK, Edns AJ (eds) *Rubber toughened plastics I-riew*, *Adv Chem Ser*, vol 233, p 407
- Pena G, Eceiza A, Valea A, Remiro P, Oyanguren P, Mondragon I (2003) Control of morphologies and mechanical properties of thermoplastic- modified epoxy matrices by addition of a second thermoplastic. *Polym Int* 52:1444–1453
- Prasanth R, Shubha N, Hng HH, Madhavi S (2014) Effect of poly(ethylene oxide) on ionic conductivity and electrochemical properties of poly(vinylidene fluoride) based polymer gel electrolytes prepared by electrospinning for lithium ion batteries. *J Power Sources* 245:283–291
- Ramos JA, Esposito LH, Fernández R, Zalakain I, Goyanes S, Avgeropoulos A, Zafeiropoulos NE, Kortaberria G, Mondragon I (2012) Block copolymer concentration gradient and solvent effects on nanostructuring of thin epoxy coatings modified with epoxidized styrene–Butadiene–Styrene block copolymers. *Macromolecules* 45:1483–1491
- Rao BS, Reddy KR, Pathak SK, Pasala AR (2005) Benzoxazine epoxy copolymers: effect of molecular weight and crosslinking on thermal and viscoelastic properties. *Polym Int* 54:1371–1376
- Riccardi CC, Williams RJJ (1986) A kinetic scheme for an amine-epoxy reaction with simultaneous etherification. *J Appl Polym Sci* 32:3445–3456
- Riccardi CC, Borrajo J, Williams RJJ, Girard-Reydet E, Sautereau H, Pascault JP (1996) Thermodynamic analysis of the phase separation in polyetherimide-modified epoxies. *J Polym Sci B Polym Phys* 34:349–356
- Ritzenthaler S, Court F, David L, Girard-Reydet E, Leibler L, Pascault JP (2002) ABC triblock copolymers/epoxy-diamine blends. 1. Keys to achieve nanostructured thermosets. *Macromolecules* 35:6245–6254
- Ritzenthaler S, Girard-Reydet E, Pascault JP (2000) Influence of epoxy hardener on miscibility of blends of poly(methyl methacrylate) and epoxy networks. *Polymer* 41:6375–6386
- Rodgers PA (1993) Pressure–volume–temperature relationships for polymeric liquids: a review of equations of state and their characteristic parameters for polymers. *J Appl Polym Sci* 48:1061–1080
- Sajeev MG, Debora P, Jose MK, Jyotishkumar P, Thomas S (2014) Reaction-induced phase separation and thermomechanical properties in epoxidized styrene-block-Butadiene-block-styrene triblock copolymer modified epoxy/DDM system. *Ind Eng Chem* 53:6941–6950
- Sara G, Gabriël G (2006) Mutual influence between reaction-induced phase separation and isothermal crystallization in POM/epoxy resin blends. *Macromolecules* 39:8049–8059
- Schauer E, Berglund L, Pena G, Marieta C, Mondragon I (2002) Morphological variations in PMMA- modified epoxy mixtures by PEO addition. *Polymer* 43:1241–1248
- Serrano E, Tercjak A, Kortaberria G, Pomposo JA, Mecerreyes D, Zafeiropoulos NE, Stamm M, Mondragon I (2006) Nanostructured thermosetting systems by modification with epoxidized

- styrene–Butadiene star block copolymers, effect of epoxidation degree. *Macromolecules* 39:2254–2261
- Serrano E, Tercjak A, Ocando C, Larrañaga M, Parellada MD, Galvan SC, Mecerreyes D, Zafeiropoulos NE, Stamm M, Mondragon I (2007) Curing behavior and final properties of nanostructured thermosetting systems modified with epoxidized styrene–Butadiene linear di-block copolymers. *Macromol Chem Phys* 208:2281–2292
- Shubha N, Prasanth R, Hng HH, Madhavi S (2014) Study on effect of poly (ethylene oxide) addition and in-situ porosity generation on poly (vinylidene fluoride)-glass ceramic composite membranes for lithium polymer batteries. *J Power Sources* 267:48–57
- Swier S, Mele BV (2003) Mechanistic modeling of the epoxy–amine reaction in the presence of polymeric modifiers by means of modulated temperature DSC. *Macromolecules* 36:4424–4435
- Swier S, Assche GV, Vuchelen W, Mele BV (2005) Role of complex formation in the polymerization kinetics of modified epoxy–amine systems. *Macromolecules* 38:2281–2288
- Tribut L, Fenouillot F, Carrot C, Pascault JP (2007) Rheological behavior of thermoset/thermoplastic blends during isothermal curing: experiments and modeling. *Polymer* 48:6639–6647
- Vandwerdt P, Berghmans H, Tervoort Y (1991) Processing of Poly(2,6-dimethyl-1,4-phenylene ether) with epoxy resin. 1. Reaction-induced phase separation. *Macromolecules* 24:3547
- Venderbosch RW, Meijer HEH, Lemstra P (1994a) Processing of intractable polymers using reactive solvents: 3. Mechanical properties of poly(2,6-dimethyl-1,4-phenylene ether) processed by using various epoxy resin systems. *Polymer* 36:2903–2913
- Venderbosch RW, Meijer HEH, Lemstra P (1994b) Processing of intractable polymers using reactive solvents: 1. Poly(2,6-dimethyl-1,4-phenylene ether)/epoxy resin. *Polymer* 35:4349–4357
- Wang M, Yu Y, Wu X, Li S (2004) Enhanced mechanical and thermal properties of epoxy with hyperbranched polyester grafted perylene diimide. *Polymer* 45:1253–1259
- Williams RJJ, Rozenberg BA, Pascault JP (1996) Reaction-induced phase separation in modified thermosetting polymers. *Adv Polym Sci* 128:95–156
- Wu C, Xu W (2007) Atomistic simulation study of absorbed water influence on structure and properties of crosslinked epoxy resin. *Polymer* 48:5440–5448
- Wu S, Guo Q, Peng S, Hameed N, Kraska M, Stühn B, Mai YW (2012) Toughening epoxy thermosets with block ionomer complexes: a nanostructure-mechanical property correlation. *Macromolecules* 45:3829
- Xiaofan L, Runqing O, Daniel EE, Amit S, Wantinee V, Patrick TM (2009) A thermoplastic/thermoset blend exhibiting thermal mending and reversible adhesion. *ACS Appl Mater Interfaces* 3:612–620
- Xu Z, Zheng S (2007a) Reaction-induced microphase separation in epoxy thermosets containing poly(ϵ -caprolactone)-block-poly(*n*-butyl acrylate) di-block copolymer. *Macromolecules* 40:2548–2558
- Xu Z, Zheng S (2007b) Morphology and thermomechanical properties of nanostructured thermosetting blends of epoxy resin and poly(ϵ -caprolactone)-block-poly(dimethyl siloxane)-block-poly(ϵ -caprolactone) triblock copolymer. *Polymer* 48:6134
- Yoshiyuki I, Ryan AJ (2000) Processing of poly(2,6-dimethyl-1,4-phenylene ether) with epoxy resin. 2 Gelation Mechanism. *Macromolecules* 33:158–166
- Yu Y, Wang M, Gan W, Tao Q, Li S (2004) Polymerization-induced viscoelastic phase separation in polyethersulfone-modified epoxy systems. *J Phys Chem B* 108:6208–6215
- Zhang H, Berglund LA (1993) Deformation and fracture of glass bead/CTBN-rubber/epoxy composites. *Polym Eng Sci* 33:100–107
- Zhang Y, Shi WC, Chen FH, Han CC (2011) Dynamically asymmetric phase separation and morphological structure formation in the epoxy/polysulfone blends. *Macromolecules* 44:7465–7472
- Zheng W, Wang ZG (1995) Morphology of ABC triblock copolymers. *Macromolecules* 28:7215–7223

Ana M. Díez-Pascual

Abstract

Thermoset (TS) epoxy resins have drawn a lot of attention over the last years in several fields including transportation, construction, and electronics owed to their excellent combination of mechanical properties, ease of processing, and low cost. However, their brittleness is a main disadvantage that limits their applications. Incorporation of thermoplastic (TP) polymers, i.e., poly(phenylene oxide) (PPO), polysulfone (PSF), or polyetherimide (PEI), has found to overcome this drawback. In this chapter, the phase separation and mechanical properties of selected TS/TP blends will be described, and the toughening mechanisms that have been proposed will be discussed. Further, the morphology and mechanical properties of TS/TP-based ternary nanocomposites, with special emphasis on those containing carbon-based nanofillers such as carbon nanotubes (CNTs), carbon black (CB), or graphene oxide (GO), will be addressed. These blends typically undergo reaction-induced phase separation upon curing, leading to different morphologies such as dispersed, co-continuous, dendritic, or phase inverted. Examples have been selected to demonstrate the importance of the asymmetric distribution of the nanofillers for developing new materials with enhanced properties, superior than those attained in the corresponding nanofiller-reinforced binary samples. These multifunctional materials are expected to have a wide range of applications, particularly in sensing devices, shape memory, and self-healing materials.

A.M. Díez-Pascual (✉)

Analytical Chemistry, Physical Chemistry and Chemical Engineering Department, Faculty of Biology, Environmental Sciences and Chemistry, Alcalá University, Alcalá de Henares, Madrid, Spain

e-mail: am.diez@uah.es

Keywords

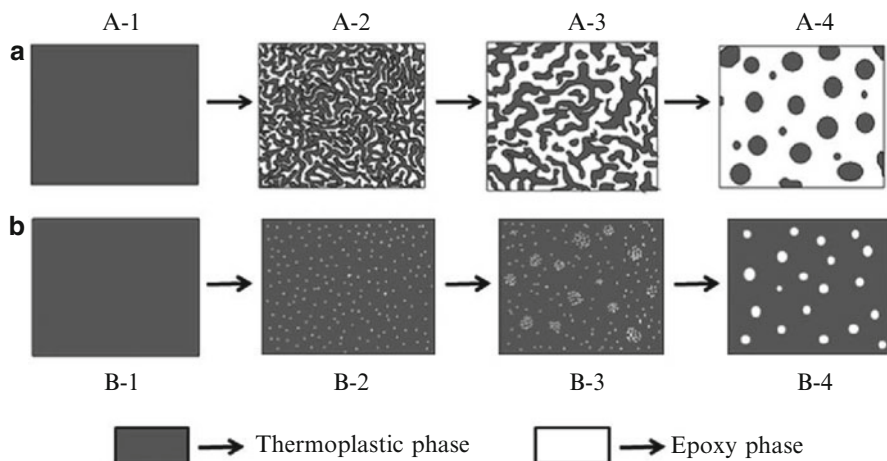
Epoxy resin • Polymer blends • Phase separation • Morphology • Carbon nanofiller • Asymmetric distribution

Contents

Introduction	744
Morphology	749
Morphology of Binary TS/TP Mixtures	749
Morphology of Ternary TS/TP-Based Composites	751
Mechanical Properties	758
Mechanical Performance of Binary TS/TP Mixtures: Dynamic Mechanical Properties ...	758
Mechanical Performance of Binary TS/TP Mixtures: Static Mechanical Properties	758
Mechanical Performance of Nanofiller-Reinforced TS/TP Blends: Dynamic Mechanical Properties	764
Mechanical Performance of Nanofiller-Reinforced TS/TP Blends: Static Mechanical Properties	767
Conclusions and Outlook	769
References	771

Introduction

Epoxy resins are thermosetting polymers that were first commercialized in 1946 and are currently widely used in many applications such as adhesives, coatings, construction, and polymer matrices of composites for the aerospace, automotive, electric, and electronic industries. This is due to their good mechanical and thermal properties, excellent chemical and corrosion resistance, outstanding adhesion properties, good dimensional stability, versatile processing, and low cost. However, their inherent brittleness due to their high cross-link density is a major drawback and limits their use in high-performance applications. To overcome this weakness, many strategies have been employed to toughen epoxy resins by introducing rubbers (Frigione et al. 1999; Konnola et al. 2015a) or engineering thermoplastics such as poly(phenylene oxide) (PPO) (Rutnakornpituk 2005), polyetherimide (PEI) (Ma et al. 2013a), polysulfone (PSF) (Huang et al. 1997), or polyethersulfone (PES) (Shi et al. 2013). The incorporation of rubber usually leads to a decrease in the glass transition temperature (T_g) of cured epoxy resins, which is detrimental for the mechanical and thermal properties of the composites. In contrast, modifying epoxy resins with thermoplastics that have a high T_g and modulus like PEI, PSF, or PES can increase toughness without reducing T_g or other properties. In 1986, Bucknall and Partridge first developed high-performance thermoplastic modified epoxy networks (Bucknall and Partridge 1986). These new materials showed outstanding advantages over the elastomeric modified systems: their fracture toughness was improved without sacrificing the mechanical properties of the systems. Even though thermoplastic modified epoxies have been significantly developed in the past years, the fracture and toughening mechanisms of epoxy/thermoplastic blends are not perfectly clear yet (Rutnakornpituk 2005).

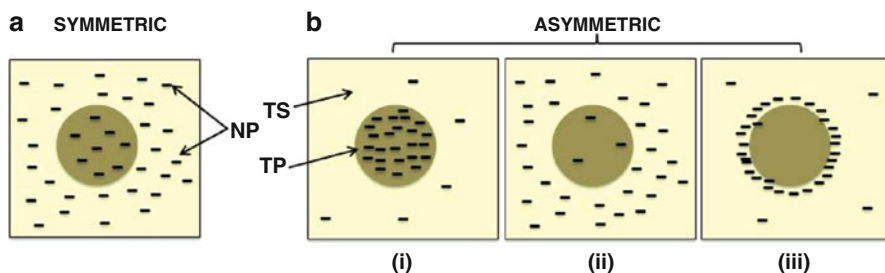


Scheme 1 Schematic representation of the *spinodal decomposition* (SD) (a) and the *nucleus growth* (NG) (b) mechanisms in an epoxy/thermoplastic binary system (Taken from Yu and Wu (2014), with permission from the Royal Society of Chemistry)

Many thermoset/thermoplastic (TS/TP) binary systems are homogeneous before curing, like those incorporating amorphous TPs such as polystyrene (PS), PEI, PSF, or PES, since the TP phase is miscible with the epoxy resin. However, as the curing reaction progresses, the molar mass of TS increases, and phase separation is induced up to the gel point. This phenomenon is known as cure-reaction-induced phase separation (CRIPS) (Yu and Wu 2014) and can occur via two possible mechanisms: *spinodal decomposition* (SD) or *nucleus growth* (NG), as depicted in Scheme 1. In the SD mechanism, the mixture is initially a single phase, and as the cure reaction proceeds, the TP begins to separate out, leading to a co-continuous structure (A-2 in Scheme 1). Subsequently, the TS regions grow and connect with each other (coarsening), leading to the destruction of the continuous TP-net (A-3). The TS becomes a continuous phase with the TP particles, irregular or regular in shape, forming islands (A-4). An inverted structure with TS particles distributed in the continuous TP phase may occur if the TP content is high enough (i.e., ≥ 30 wt%). In the NG mechanism, the mixture starts homogeneous, but as curing advances phase separation takes place forming small spherical particles within the TS (B-2), which aggregate into larger particles (B-3), leading also to an island in the sea structure with regularly distributed TP particles (B-4). The type of CRIPS mechanism depends on many factors, such as curing temperature, concentration of the TP, and curing agent, and the SD mechanism is more common. On the other hand, there are some TS/TP blends that are immiscible even before the curing reaction, basically those incorporating semicrystalline TPs such as PP or polyethylene (PE), where the TP forms a dispersed phase within the epoxy. These systems do not undergo CRIPS and remain phase separated after the cross-linking process.

On the other hand, the development of polymer nanocomposites incorporating nanofillers has become a key area in the field of nanoscience and nanotechnology due

to their high potential for advanced technological applications ranging from structural materials, through electronic devices to regenerative medicine, to mention but a few (Ajayan et al. 2003). Among the many attributes of nanofillers, their outstanding electrical, thermal, and mechanical properties are noteworthy when compared to conventional fillers. Carbon nanotubes (CNTs), for example, display a very high aspect ratio ($>1,000$), large surface area, and low density ($\sim 1.8 \text{ g/cm}^3$) and are much more flexible and resilient than carbon fibers, while demonstrating a superior elastic modulus (up to 1.2 TPa) and fracture strength, excellent thermal stability ($>800 \text{ }^\circ\text{C}$ in inert atmospheres), superior thermal conductivity ($\sim 3,500 \text{ W/m}\cdot\text{K}$), and outstanding electrical conductivity with high current densities ($4 \times 10^9 \text{ A/cm}^2$) (Popov 2004; Thostenson et al. 2001). Carbon black (CB) is the most widely used conductive filler because of its abundant source, low density ($\sim 2 \text{ g/cm}^3$), high electrical conductivity (in the range of 10–100 S/cm), high surface area (typically $\sim 1,250 \text{ m}^2/\text{g}$), and low cost (Donnet et al. 1993). It contains at least 97% of carbon in grape-like clustered aggregates, the smallest indivisible CB units having various sizes, morphology, degree of porosity, and surface chemistry. On the other hand, graphene (G) is a bidimensional monolayer of sp^2 carbon atoms arranged in a honeycomb structure that, when isolated, can display extraordinary electronic, thermal, optical, and mechanical properties (Novoselov et al. 2004), with some values that exceed those obtained in any other material. G has excellent thermal conductivity ($\sim 5,000 \text{ W/m}\cdot\text{K}$), the highest electrical conductivity known at room temperature (6,000 S/cm), a Young's modulus of $\sim 1 \text{ TPa}$, and ultimate strength of 130 GPa (Lee et al. 2008). Numerous methods have been described to prepare exfoliated graphene from readily available graphite, a highly active research area at present. Graphene oxide (GO) is the oxidized state of G and contains several oxygenated species including hydroxyl and epoxide groups on the basal plane and carbonyl and carboxyl groups located at the sheet edges. Many examples are already emerging where these unique properties can be exploited by successfully incorporating G (or GO) into polymeric matrices (Li and Zhong 2011), with applications in areas such as electromagnetic interference shields, electrostatic charge dissipaters, compact microelectronics, and fuel and solar cells, to name but a few. One of the fundamental issues in optimizing the properties of these nanocomposites, particularly mechanical and electrical properties, is the efficient dispersion of the nanofillers within the host matrix. Nonetheless, almost all nanoparticles appear naturally in an aggregated or agglomerated state because of strong attractive forces such as *van der Waals* interactions that hinder homogenous dispersion in, or good interfacial adhesion with, the polymer, and the subsequent effective transfer of their unique properties to the matrix (Moniruzzaman and Winey 2006). To overcome the aforementioned drawbacks, different strategies have been employed ranging from conventional melt phase, solid state or solution mixing, and sonication to the introduction of chemical functionalities on the nanofiller surface, including grafting to polymer chains or grafting from routes via in situ polymerization (Spitalsky et al. 2010; Konnola et al. 2015b). However, since no universal solution is available, nanoparticle agglomeration and particle migration are generally blamed for properties falling below expectation. Nanoparticle migration phenomena have mainly



Scheme 2 Schematic representation of possible nanoparticle distribution scenarios in TS/TP blend nanocomposites (see text)

been discussed for layered silicates (Ray et al. 2004), and also for CNTs (Gödel et al. 2009), but in most cases it is undesirable.

Regarding immiscible polymer-blend multiphase composites, the location of the nanofiller throughout the material is seldom homogeneous, and generally three possible scenarios can be contemplated, Scheme 2, whereby the nanofiller is preferentially located in one of the polymeric phases (Scheme 2b(i), (ii)), or at the interface between them (Scheme 2b(iii)) (Gödel et al. 2011). Indeed, the factors affecting nanofiller distribution are very complex and include kinetic and thermodynamic factors, dimensionality (shape, aspect ratio) and surface properties (roughness, chemical composition, etc.) of the nanofiller, and the viscosity of the polymer matrix. From a thermodynamics viewpoint, the localization of the nanofiller will depend on the balance of interfacial energies that can be predicted using the wetting coefficient, ω_a , defined as (Sumita et al. 1991) $\omega_a = (\gamma_{\text{filler-polymer1}} - \gamma_{\text{filler-polymer2}}) / \gamma_{\text{polymer1-polymer2}}$, where, γ_x represents the interfacial tension between the filler and polymers 1 and 2 and that between the two polymers, respectively. They predicted that when $\omega_a < -1$, the nanofiller tends to locate in polymer 1, when $\omega_a > 1$ it tends to locate in polymer 2, and when $-1 < \omega_a < 1$, it is more likely to locate at the interface. So, this coefficient can be used to indicate the preferential location of the nanofiller in an immiscible polymer blend. Several groups (Gödel et al. 2011; Zhang et al. 2009) have shown that the nature of the polymers also has a notable influence on the nanofiller distribution, especially when intermolecular interactions occur between the polymer and the nanoparticles, in such case the location in one or other polymer phase can, in principle, be driven by the relative degree of interaction. In this respect, the nanoparticle location can be tuned by tailoring affinity via functionalization (Li et al. 2011) or by the addition of reactive components that modify the polymer–nanofiller interaction (Gültner et al. 2011).

Nanoparticle shape and dimensions also condition the morphology of the composite material. Gödel et al. (2011) compared CB with multiwalled carbon nanotubes (MWCNTs) in a blend containing poly(styrene acrylonitrile) and polycarbonate (PC). The MWCNTs (very high aspect ratio) could migrate easily from one phase to the other, whereas CB (low aspect ratio spherical shape) found more

stability at the interface. Composition is also an important factor. Sun et al. (2010) and Xiong et al. (2013) prepared (PC)/acrylonitrile-butadiene-styrene (ABS)/MWCNT nanocomposites with varying ABS contents and found that the MWCNT localization changed from the PC to the ABS phase on increasing the ABS content from 5 to 60 wt%, also resulting in increased electrical conductivity of the composite. Recently, Chen et al. (2012) reported the selective distribution of CNTs at the interface of PC/ABS by using maleic anhydride-grafted ABS (ABS-g-MA) and an appropriate processing methodology. They showed that by adjusting both kinetic (i.e., shear forces, mixing procedure or sequence, blending time) and thermodynamic factors (i.e., controlling the interfacial energy through careful choice of the composite components) and/or applying an electrical or magnetic field, the morphology of the composites, hence their final properties, could be tuned.

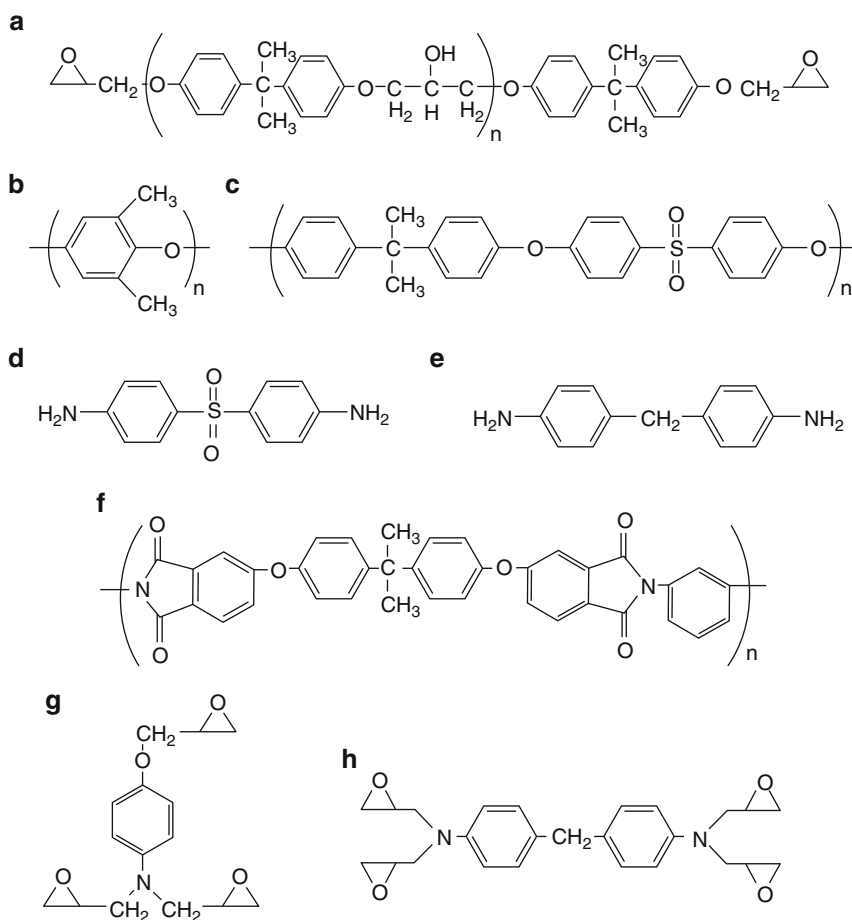
Further, it has been shown that the uneven or “asymmetric” distribution of nanofillers can lead to significant improvements in key properties. For instance, Li and Shimizu (2008) described the preparation of co-continuous poly(vinylidene fluoride) (PVDF)/polyamide-6 (PA-6)/MWCNT nanocomposites where MWCNTs were homogeneously and selectively located in the PA-6 phase, and the materials exhibited a unique combination of high electrical conductivity, ductility, and stiffness. Liu and coworkers (2009) demonstrated an important improvement in the fracture toughness of immiscible polypropylene (PP)/ethylene-co-vinyl acetate (EVA) blends upon addition of functionalized MWCNTs, which they ascribed to a bridging effect of the nanofillers at the interphase and the formation of a dual-network structure between the MWCNTs and EVA. However, to date experimental studies of the thermodynamic properties of mixtures of nanofillers and binary polymer blends are relatively scarce, and as a result little quantitative information is available about the influence of fundamental factors such as nanoparticle size and form, volume fraction, chemical architecture, or surface chemical structure on the phase behavior of the composites. Therefore, a critical challenge lies in predicting how the morphology of the nanoparticle-filled blends can affect the macroscopic properties of the resulting nanocomposites, in particular the mechanical performance.

To date, most of the literature on multiphase polymer-blend composites incorporating nanofillers refers to TP blends (Gültner et al. 2011; Ray et al. 2004; Göldel et al. 2009, 2011; Li et al. 2011, etc.), and work on TS/TP-based ternary nanocomposites is very recent and relatively scarce (Ma et al. 2013a, b; Shi et al. 2013; Díez-Pascual et al. 2014; Li et al. 2006; Abdel-Aal et al. 2008a, b; Ma and Liu 2013; Wang et al. 2012). In this chapter, the phase separation and mechanical properties of selected epoxy/thermoplastic blends will be described. In addition, the morphology and mechanical properties of TS/TP-based ternary nanocomposites, with special emphasis on those containing carbon-based nanofillers (i.e., CNTs, CB, GO), will be addressed. Examples have been selected to emphasize the effect of asymmetric distribution of nanofillers on the material properties, and an effort has been made to correlate the morphology with the final material performance. Finally, future perspectives for potential applications of these multiscale composites will be discussed.

Morphology

Morphology of Binary TS/TP Mixtures

Morphological information is typically probed using scanning electron microscopy (SEM) images of cryofractured surfaces. Pearson and Yee (1993) developed a series of diglycidyl ether of bisphenol A (DGEBA) composites with different PPO content (Scheme 3a, b). A particulate morphology was attained by first dissolving PPO in the hot epoxy and then precipitating spherical particles upon curing with piperidine at



Scheme 3 Chemical structure of (a) diglycidyl ether of bisphenol A (DGEBA), (b) poly(phenylene oxide) (PPO), (c) polysulfone (PSF), (d) diaminodiphenyl sulfone (DDS), (e) diaminodiphenylmethane (DDM), (f) polyetherimide (PEI), (g) triglycidyl-p-aminophenol (TGAP), and (h) tetraglycidyl-diaminodiphenyl methane (TGDDM)

160 °C for 2 h. Since the solubility parameters of PPO and the DGEBA matrix differ sufficiently, it is possible to develop microphase-separated PPO-modified DGEBA networks. Therefore, small domains of PPO phase, which was the minority component, were dispersed in the continuous matrix composed of the epoxy resin. Transmission electron microscopy (TEM) micrographs revealed a two-phase morphology containing discrete PPO particles. However, the morphology was not uniform, and some large heterogeneous PPO particles containing occlusions of smaller epoxy particles were observed throughout the materials. In order to eliminate the occluded PPO particles, styrene-maleic anhydride (SMA) copolymers were employed as compatibilizing agents for PPO–DGEBA blends. The addition of SMA copolymers with a 10:1 ratio of styrene to maleic anhydride significantly improved the uniformity of these two-phase materials, leading to spherical PPO particles (2 nm in diameter) embedded within the continuous DGEBA matrix. Similar results were reported by Wu and coworkers for DGEBA/PPO blends cured with cyanate ester (Wu et al. 2000). In contrast, the blends of DGEBA with poly(ethylene oxide) (PEO)/PPO block copolymers led to completely homogeneous materials (Larrañaga et al. 2007).

The morphology of DGEBA networks modified with hydroxyl-terminated polysulfone (PSF) in the presence of 4,4'-diaminodiphenylsulfone (DDS) as a hardener (Scheme 3c, d) for different PSF contents has been reported by Min and coworkers (1993a, b). The required amounts of DGEBA, PSF, and DDS were blended at 140 °C, cured in an oven at 140 °C for 2 h and postcured at 180 °C for 2 h. SEM micrographs revealed that the microstructure changed from the characteristic particulate structure (spherical PSF particles in epoxy matrix) at 5 and 10 wt% PSF concentration to the partial phase-inverted structure at 15 wt% PSF and to the complete phase-inverted structure at 20 wt% PSF. Similar results were reported by Zengli and Yishi (1989) for DGEBA/PSF blends cured with piperidine (Fig. 1). When the content of PSF was lower than 15 wt% (Fig. 1a), small spherical TP

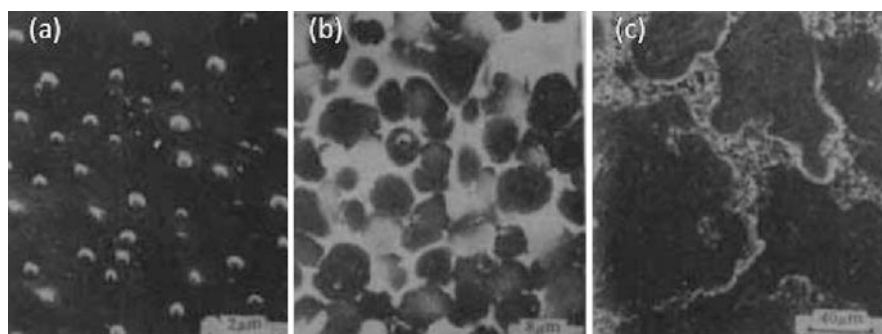


Fig. 1 Fracture surface of DGEBA/PSF blends cured with piperidine and DDS for different PSF contents: (a) 10 wt%, (b) 20 wt% (DDS cured), and (c) 20 wt% (Adapted from Zengli and Yishi (1989), with permission from Springer)

particles well dispersed within the epoxy were found. For PSF content is 20%, PSF is the continuous phase and the thermoset resin is the dispersed phase (Fig. 1c).

Yoon et al. (1995) studied the morphology of DGEBA networks toughened with aminophenyl terminated or *t*-butyl terminated PSF. The samples were prepared by blending DGEBA with PSF loadings in the range of 5–30 wt% and cured upon addition of DDS at 130 °C for 4 h and postcured at 220 °C for 2 h. SEM micrographs also evidenced a change from a particulate structure with PSF spheres (~0.5 μm in diameter) within the epoxy matrix at low PSF contents (up to 10 wt%) to a phase-inverted morphology at high loadings (≥15 wt%). A completely different morphology was found for PSF-modified DGEBA networks cured with diaminodiphenylmethane (DDM) (Scheme 3e), as demonstrated by Huang and coworkers (1997). DGEBA, PSF, and DDM were first cured at 80 °C for 2 h, then at 150 °C for 2 h, and finally postcured at 200 °C for 2 h. In this case, the blends were found to be homogenous as revealed by SEM, and differential scanning calorimetry (DSC) studies showed that all the DDM-cured DGEBA/PSF blends had only one T_g .

Gilbert and Bucknall (1991) investigated the phase separation of PEI-modified epoxy networks (Scheme 3f). A tetrafunctional epoxy resin, tetraglycidylethylamine-diphenyl methane (TGDDM) (Scheme 3h), was blended with PEI using DDS as curing agent and then cured at 120 °C for 16 h, 150 °C for 2 h, 180 °C for 2 h, and finally postcured at 200 °C for 4 h. SEM micrographs revealed spherical PEI domains in the epoxy matrix at 5 wt% PEI content, and these domains became larger as the PEI content increased up to 20 wt%. At 30 wt% loading, the phase inversion took place. Murakami et al. (1992) examined the morphology of PEI-modified DGEBA networks as a function of PEI concentration. The polymers were blended with dicyanodiamide as a curing agent at 15 °C for 4 h and postcured at 200 °C for 2 h. According to SEM, no phase separation at 10 wt% PEI loading was found, but as the PEI content increased to 20 wt%, a particulate morphology with PEI spheres within the epoxy matrix was observed, and at 30 wt% PEI content the phase inversion also occurred. Li et al. (1999) investigated the morphology of DGEBA/PEI blends cured with DDS (Fig. 2). Samples with 5 and 10 wt% PEI loading exhibited fine dispersed PEI particles surrounded by the continuous epoxy phase (Fig. 2a, b), while for those with 15 and 20 wt%, co-continuous phases were observed (Fig. 2c, d). With the increase in PEI molecular weight, the morphology of the modified system changes from a PEI spherical domain dispersed in the epoxy matrix to a phase-inverted epoxy domain dispersed in the PEI matrix.

Morphology of Ternary TS/TP-Based Composites

Several studies have examined the morphology of ternary systems in which the TS and the TP form a single phase before curing and undergo CRIPS. In this regard, Yu and Wu (2014) recently analyzed the morphology of DGEBA+DDS/PEI (13 wt%)/methylendianiline-modified graphene oxide (GO-MDA) composites after curing at 170 °C for 4 h (Fig. 3). The samples, with 0, 1, 2, and 3 wt% GO-MDA (designated as G-0, G-1, G-2, and G-3, respectively), were etched in CH_2Cl_2 to remove the PEI

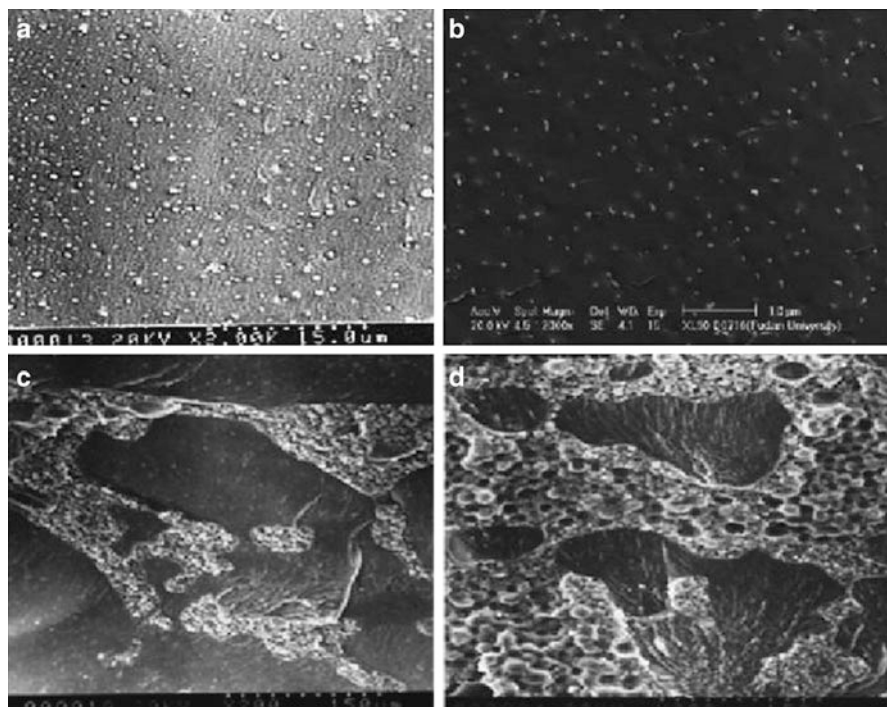


Fig. 2 Fracture surface of DGEBA/PEI blends cured with DDS for different PEI contents: (a) 5 wt%, (b) 10 wt%, (c) 15 wt%, and (d) 20 wt% (Reprinted from Li et al. (1999), with permission from Elsevier)

phase. The SEM images reveal CRIPS for the four samples following the SD mechanism since both the PEI-rich phase and the epoxy-rich phase are irregular in shape, showing a co-continuous structure. As the GO-MDA concentration increased, the domain size of the TS-rich phase was reduced (the coarsening was suppressed), and for 3.0 wt% no large epoxy particles ($>100\ \mu\text{m}$) were detected (Fig. 3, G-3). In this sample, no secondary phase separation occurred; the addition of GO-MDA increased the complex viscosity and the curing rate of the composites, which considerably suppressed the development of phase separation and helped freezing the final composite morphology at an earlier stage of development of the co-continuous structure.

Ma et al. (2013b) investigated the morphology of a system comprising a bisphenol A-type epoxy cured with methyl tetrahydrobenzene-anhydride (MTHPA) as matrix, 16 wt% PEI as a thermoplastic modifier, and CNTs in the range of 0.1–3.0 wt% as reinforcements. All the nanocomposites displayed an inverted-phase structure, as revealed by SEM (Fig. 4). The dark globular areas in Fig. 4a, b correspond to the TS-rich phase, while the bright regions penetrating the TS globules constitute the PEI-rich phase where the CNTs (1.0 wt%) are selectively

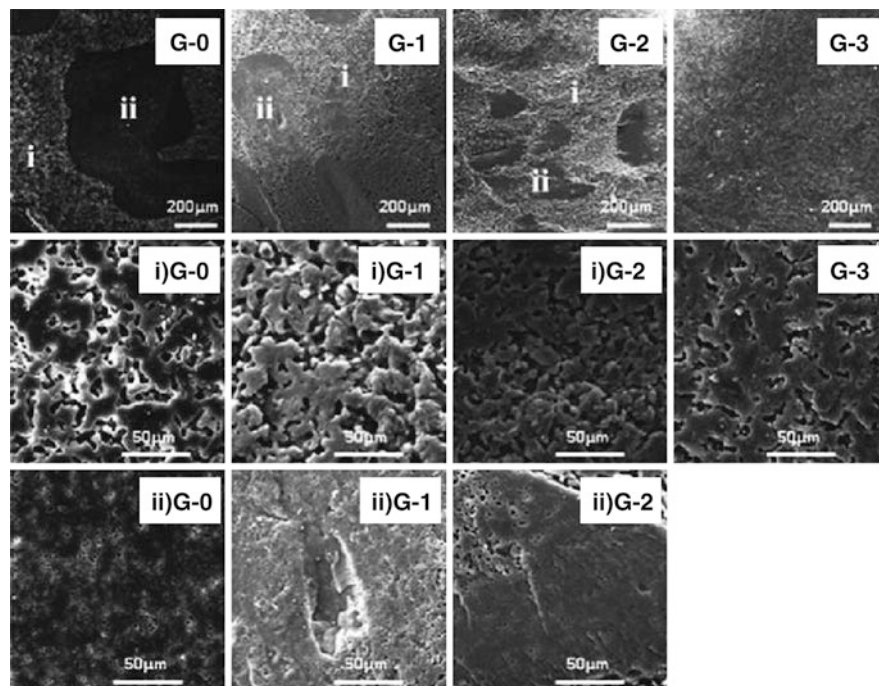


Fig. 3 SEM images of fractured surfaces of DGBA+DDS/PEI (13 wt%)/GO-MDA composites with GO-MDA contents of 0, 1, 2, and 3 wt% (designated as G-0, G-1, G-2, and G-3, respectively). *i* denotes the PEI-rich phase and *ii* the epoxy-rich phase (Reprinted from Yu and Wu (2014), with permission from the Royal Society of Chemistry)

dispersed forming a three-dimensional continuous network structure. An inverted phase structure is typically formed in immiscible TS/TP blends only when the content of the minor component approximates to 30 wt%. However, an almost complete phase reverse was attained in this system for a relatively low PEI content. The morphology of the nanocomposites was also observed by optical microscopy (Fig. 4c, d). Before curing (Fig. 4c), the CNTs were uniformly dispersed in the blend, and phase separation between TS and PEI did not occur. Upon curing (Fig. 4d), a phase-reverse structure was formed with bright TS globules and a black continuous PEI/CNTs network, in agreement with SEM analysis. This selective distribution of the CNTs was predicted considering the dispersive and polar components of surface energy for the different composite constituents, which were used to estimate the CNT/TS, CNT/PEI, and TS/PEI interfacial tensions by applying Wu's harmonic mean average equation (Wu 1982). Overall, the CNTs were found to preferentially locate in the TP phase as a consequence of the lower interfacial tension between CNTs and PEI.

The same authors (Ma et al. 2013a; Shi et al. 2013) also compared the dispersion of CB in similar epoxy-based composites incorporating PS, PES, or PEI (Fig. 5a–c,

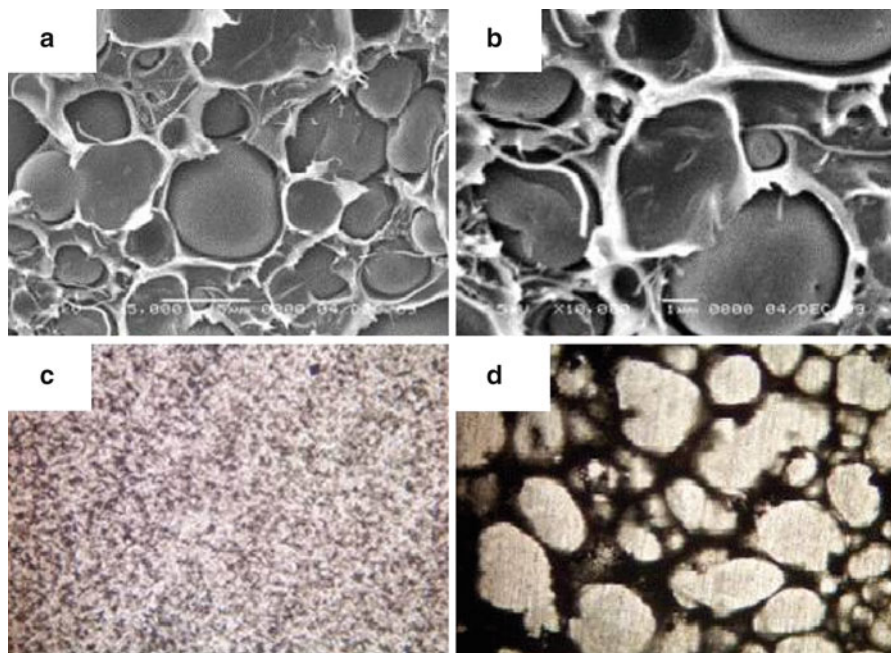


Fig. 4 (a, b) SEM micrographs at different magnifications of bisphenol A-type epoxy+MTHPA/PEI (16 wt%)/CNT (1.0 wt%) nanocomposite. (c, d) OM images of the nanocomposite before and after the curing reaction, respectively (Adapted from Ma et al. (2013b), with permission from Trans Tech Publications)

respectively). For TS/PS (16 wt%)/CB (1.0 wt%), with co-continuous phase structure, CB particles were found to be located both in the epoxy-rich phase and the PS-rich phase, as shown in the magnified images 1 and 2, respectively. However, for TS/PES (16 wt%)/CB (1.0 wt%), with a kind of inverted phase structure, as well as for TS/PEI (16 wt%)/CB (1.0 wt%), with perfect inverted phase morphology, CB was selectively situated in the TP-rich phase, and several agglomerates were detected. The authors calculated the wetting parameter, ω_a , for the three systems and obtained values of -0.4 , -3.6 , and -2.8 , respectively. According to the wetting coefficient criterion explained in the introduction, CB should be located at the interface for TS/PS while in the TP phase for the other two systems. Overall, the predicted distribution of CB particles was consistent with the real distribution shown by SEM analysis, which indicates that the nanofiller location is mainly controlled by thermodynamics. CB particles have stronger affinity for PEI or PES than for epoxy, while the interfacial surface energy between CB particles and PS is close to that between CB particles and epoxy; hence, the nanofiller is not selectively dispersed in that composite.

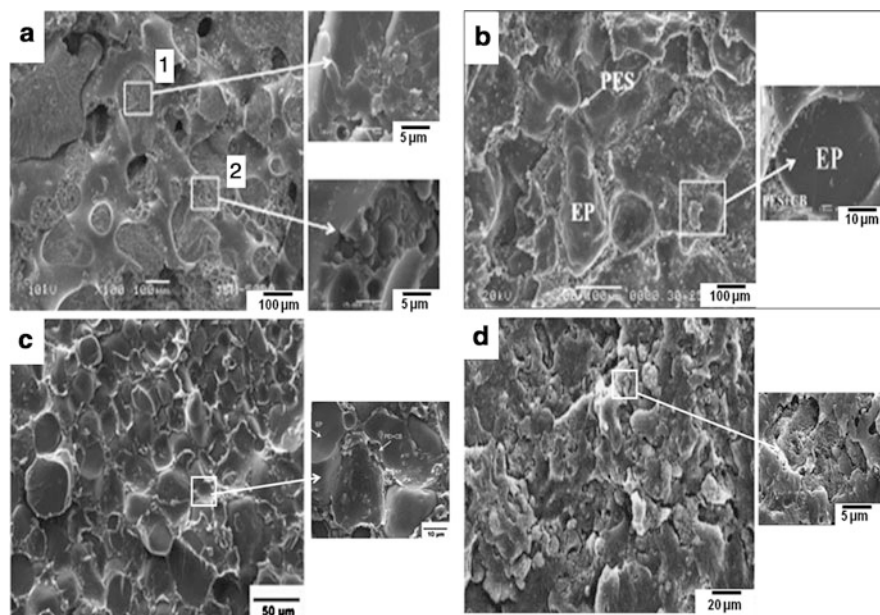


Fig. 5 SEM micrographs of fractured surfaces of (a) bisphenol A-type epoxy/PS (16 wt%)/CB (1.0 wt%); (b) bisphenol A-type epoxy/PES (16 wt%)/CB (1.0 wt%); (c) bisphenol A-type epoxy/PEI (16 wt%)/CB (1.0 wt%); (d) DGEBA/PP (70 wt%)/CB (6.0 wt%) (Adapted from Ma et al. (2013a), Shi et al. (2013), and Li et al. (2006))

The morphology of ternary systems based on TS/TP blends that are immiscible even before the curing reaction has also been investigated. In this regard, Li et al. (2006) characterized DGEBA/PP/CB composites. In binary DGEBA (30 wt%)/PP (70 wt%) blends, the epoxy resin disperses in the PP phase forming spherical particles of 3–20 μm diameter. A similar morphology is found for the ternary composites incorporating 6 wt% CB (Fig. 5d), where preferential localization of CB was observed in the epoxy phase, attributed to the higher polarity of the epoxy enabling easy wetting of the CB surface. Furthermore, these composites were prepared by melt blending at 190 $^{\circ}\text{C}$, where the lower melt viscosity of the epoxy also promotes the incorporation of CB into the thermoset phase. These findings are in agreement with previous studies on CB-reinforced immiscible thermoplastic blends, such as PP/PA-6 (Tchoudakov et al. 1996a) or PP/PC (Tchoudakov et al. 1996b), that showed preferential location of the nanofiller in the phase with higher polarity or surface tension (PA-6 or PC). In CB-filled DGEBA (40 wt%)/PP (60 wt%) blends, the morphology of the dispersed epoxy phase changed from spherical domains to elongated structures, resulting in very narrow gaps between adjacent epoxy domains, with CB also located in the TS phase. Further increasing DGEBA content, the elongation deformation of the epoxy phase

became more evident and a co-continuous structure developed. The authors also showed that the processing sequence also conditions the composite morphology. By blending CB with epoxy then adding PP, the CB was preferentially distributed within the epoxy phase, similar to the single-step composites. However, by initially blending with PP followed by the addition of the epoxy, partial migration of CB particles from the TP to the TS phase was observed, demonstrating a strong influence of kinetic parameters on the final morphology.

Díez-Pascual et al. (2014) studied the morphology of ternary nanocomposites comprising triglycidyl-p-aminophenol (TGAP) epoxy resin and DDS curing agent as TS matrix, 5.0 wt% of a semicrystalline thermoplastic (TP), an ethylene/1-octene copolymer as a toughness modifier, and 0.5 or 1.0 wt% MWCNTs as nanoreinforcements. In this system, the polymers were completely immiscible before and after curing, and a strong dependence of the morphology on the CNT concentration was detected, as shown in Fig. 6. Ternary nanocomposites with 0.5 wt% MWCNTs displayed a matrix-dispersed droplet-type morphology of the TP (Fig. 6a), with randomly and homogeneously dispersed domains within the matrix, and a uniform, aggregate-free CNT dispersion was found throughout the examined areas. However, some evidence for preferential location of MWCNTs near the TS/TP interphase was found (circles on Fig. 6b, c), attributed to higher affinity of the MWCNTs for the TP due to their hydrophobic nature. One explanation for this phenomenon may be the reduction of the interfacial tension due to the distribution of the nanofiller at the interface (Fenouillot et al. 2009) acting as a kind of interfacial agent or surfactant, a mechanism well known in polymer blends that results in domain size reduction of the minor polymer phase. In contrast, SEM micrographs of the nanocomposite with 1.0 wt% revealed a completely different morphology. Considerably larger TP domains were observed that appeared interconnected owed to the coalescence of several particles, resulting in a coarse dendritic morphology (Fig. 6d, e). In this case the MWCNTs were generally encountered within the TP phase (Fig. 6f), where several nanotube aggregates were found. The authors suggested that higher CNT concentration provoked an increase in viscosity of the phases that hindered nanotube diffusion and migration in the composite (Díez-Pascual et al. 2014), resulting in coalescence of the TP domains and redistribution of the nanofillers that were incorporated into the large TP domains. Thus, a noteworthy change in the phase morphology of TGAP/poly(ethylene-1-octene) blends from droplet-dispersed type to agglomerated TP domains with dendritic structures was found when the CNT concentration was increased from 0.5 to 1.0 wt%, these differences arising from a fine balance between nanoparticles affinity and the viscosity of the ternary system. An analogous phase-modifying behavior was reported for TP blend nanocomposites such as PVDF/PA6/CNT (Li and Shimizu 2008), where the morphology changed from sea island to co-continuous when more than 1.2 wt% CNTs were added to the blends, as well as in PS/poly(methyl methacrylate) (PMMA) blends, where the addition of 10 wt% nanoclay changed the PMMA domains from isolated spherical-like droplets to a co-continuous structure (Si et al. 2006).

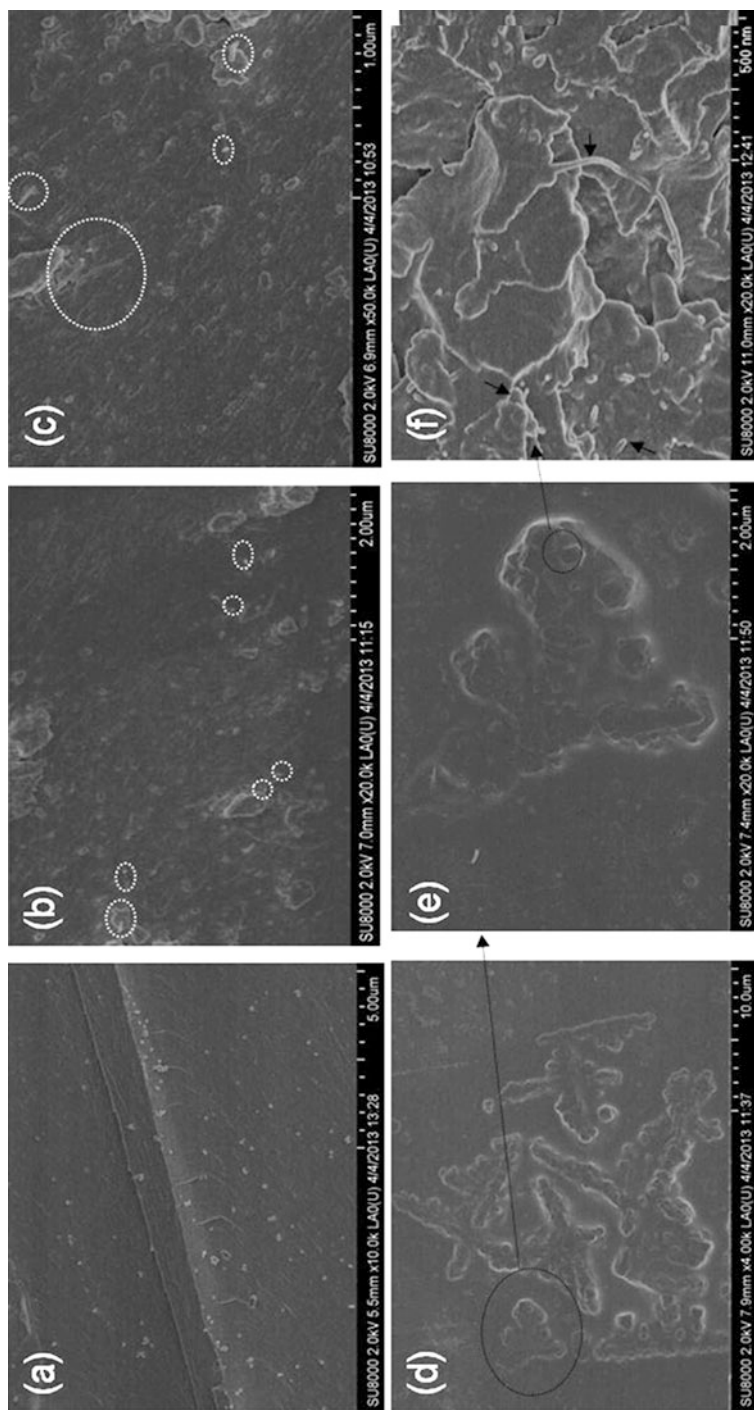


Fig. 6 (a–c) SEM micrographs at different magnifications of TGAP+DDS/poly(ethylene-1-octene) (5 wt%)/MWCNT (0.5 wt%)/nanocomposite. The *dashed circles* in (b) and (c) show MWCNTs located close to the TP particles. (d–f) SEM images of TGAP+DDS/poly(ethylene-1-octene) (5 wt%)/MWCNT (1.0 wt%) nanocomposite showing the dendritic morphology of the TP phase. The *solid arrows* in (f) show MWCNTs situated inside the TP domains (Adapted from Diez-Pascual et al. (2014), with permission from John Wiley & Sons, Inc.)

Mechanical Properties

Mechanical Performance of Binary TS/TP Mixtures: Dynamic Mechanical Properties

The mechanical properties of TS/TP blends are frequently investigated by dynamic mechanical analysis (DMA), a technique that provides information about the stiffness of the composites and the transition and relaxation processes that take place as a function of temperature. The storage modulus (E') indicates the load-bearing capacity of the material. E' generally decreases with increasing temperature, showing a sharp decline in the vicinity of the glass transition region. This behavior is attributed to the increase in the molecular mobility of the polymer chains above T_g . The loss modulus (E'') is a measure of the energy dissipated as heat per cycle under deformation, that is, the viscous response of the material. The ratio of the loss modulus to the storage modulus is named as the mechanical loss factor or $\tan \delta$. The damping properties of the material give the balance between the elastic and viscous phases in a polymeric material. The glass transition temperature can be determined from the maximum of $\tan \delta$.

Brooker et al. (2010) recorded the DMA spectra of a mix of diglycidyl ether of bisphenol F (DGEBA) and TGAP cured with an amine hardener, 4,4'-methylenebis-(3-chloro 2,6-diethylaniline) (MCDEA), toughened with different amount of PES. Hardly change in E' was detected with the incorporation of the thermoplastic, which had a similar T_g to that of the epoxy (about 200 °C). Conversely, a decrease in E' was detected upon addition of 2.5–10 wt% ultrahigh molecular weight polyethylene (UHMWPE) to DGEBA (Fig. 7), indicative of a plasticizing effect that results in higher flexibility for the blends (Pashaei et al. 2010). Further, a drop in the T_g of epoxy (~108 °C) was also observed upon increasing TP concentration, attributed to the low cross-link density and poor interaction between the epoxy and UHMWPE. A completely opposite behavior was found for epoxy phenol novolac resin (EPN) +DDS system blended with PEI (Kandpal et al. 2013), where a noticeable rise in E' was found as the TP loading increased, showing a maximum at 7.5 wt% PEI. The enhancement in E' was attributed to the increase in the matrix stiffness upon addition of the amorphous thermoplastic. A single T_g (ranging between 179 °C and 183 °C) was observed in all blends due to the close proximity of the T_g s of the individual components, which increased slightly as the PEI content raised, indicative of the restrictions in the matrix chain mobility with the incorporation of the TP.

Mechanical Performance of Binary TS/TP Mixtures: Static Mechanical Properties

The static mechanical properties of TS/TP blends are frequently characterized by tensile and fracture toughness tests carried out at room temperature. Tensile tests are used to determine the Young's modulus (E), tensile strength (σ_y), and elongation at

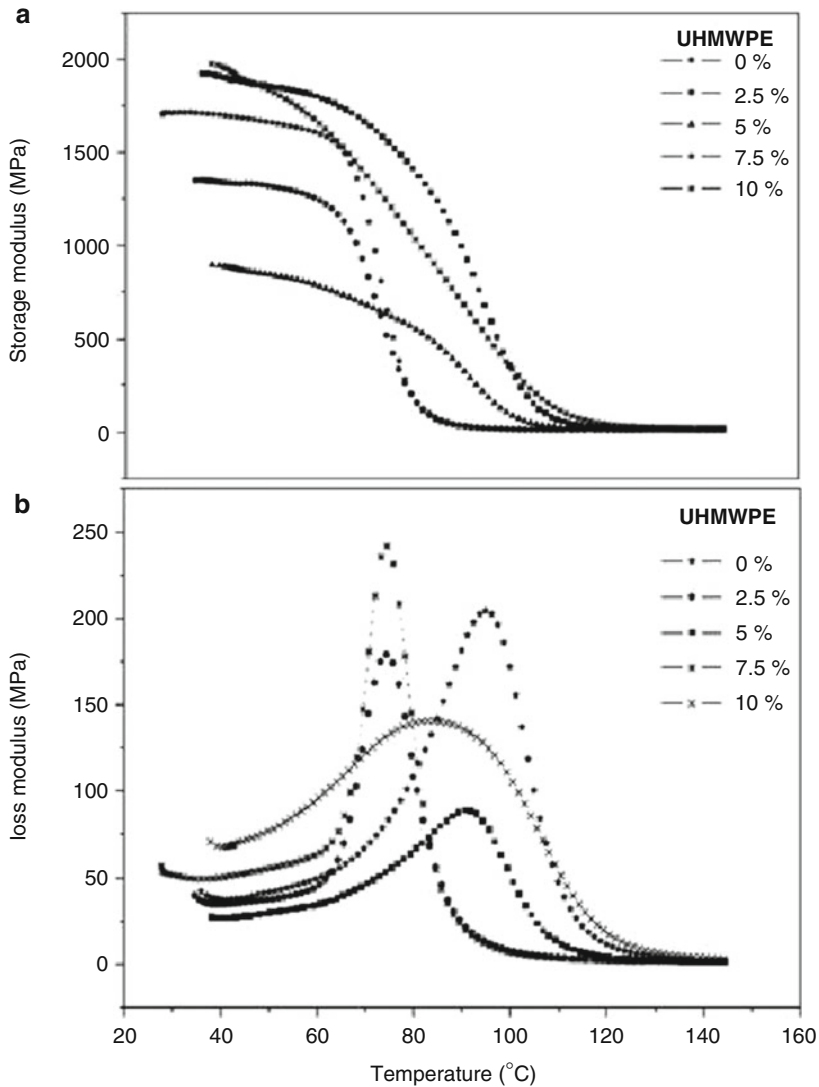
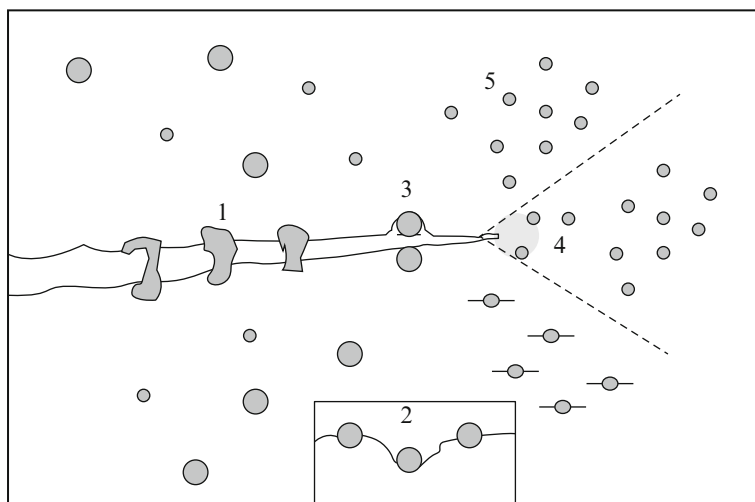


Fig. 7 DMA spectra of DGEBA/UHMWPE blends with different thermoplastic content Adapted from Pashaei et al. (2010).

break (ϵ_b), which give information about the rigidity, strength, and ductility of the materials. Fracture toughness is a property that describes the ability of a material containing a crack to resist fracture and is one of the most important properties for design applications. The stress intensity factor at which a thin crack in the material begins to grow is denoted as K_{Ic} . High values of K_{Ic} indicate high fracture toughness.

Several mechanisms of toughening of epoxy systems by rigid thermoplastic particles have been proposed, namely, particle bridging, crack pinning, crack path



Scheme 4 Schematic representation of toughening mechanisms in TP-modified epoxies: (1) particle bridging, (2) crack pinning, (3) crack path deflection, (4) particle-yielding-induced shear banding, and (5) particle yielding (Reprinted from Pearson and Yee 1993)

deflection, particle yielding-induced shear banding, particle yielding, and microcracking (Pearson and Yee 1993), as depicted in Scheme 4. In the particle bridging mechanism, the proposed role of the rigid plastic particles is to distance two crack surfaces and apply surface tractions that efficiently alleviate the stress applied at the crack tip. An alternate explanation for this toughening via crack bridging takes into account the energy consumed when the crack deforms and tears the rigid plastic particles. In the crack pinning mechanism, the role of the rigid thermoplastic particles is to behave as impenetrable objects that slow down the crack, resulting in consuming extra energy as the crack propagates, while in the crack path deflection, the thermoplastic causes the crack to deviate from its original direction; hence, the surface area of the crack is increased resulting in increasing energy to propagate such crack. In the particle-yielding-induced shear banding mechanism, the rigid plastic particles would yield and produce a significant stress concentration, which initiates shear banding in the matrix.

Table 1 compares the mechanical properties of TS/TP blends with those of neat epoxy systems. Insignificant change in E and σ_y of DGEBA was found upon addition of increasing PPO contents (Pearson and Yee 1993). However, a remarkable improvement in fracture toughness was detected as PPO started to form the continuous phase (20 wt% PPO or more). It is believed that the particle-yielding-induced shear banding of the PPO continuous phase was the main toughness mechanism in this system.

Larrañaga et al. (2007) investigated the mechanical properties of DGEBA/DDM blended with PEO/PPO copolymer. In this case, a strong decrease in stiffness and strength as well as in T_g values was detected with increasing copolymer

Table 1 Percentage of change in the mechanical properties of thermoset/thermoplastic blends compared to the neat epoxy

TS	TP (wt%)	ΔE^a (%)	$\Delta \sigma_y^b$ (%)	T_g^c (°C)	ΔK_{Ic}^d (%)	Ref.
DGEBA+piperidine	PPO (5)	0	1		9	Pearson and Yee (1993)
	PPO (10)	3	1		27	
	PPO (20)	-3	0		64	
DGEBA+DDM	PEO-PPO (10)	-11	-14	-27	56	Larrañaga et al. (2007)
	PEO-PPO (20)	-26	-28	-35	17	
	PEO-PPO (30)	-61	-60	-46	6	
DGEBA+piperidine	PSF (15)	3		-1	110	Zengli and Yishi (1989)
DGEBA+DDM	PSF (15)	9	7	-5	20	Huang et al. (1997)
TGDMM+DDS	PEI (30)	10	6		218	Gilbert and Bucknall (1991)
DGEBA+dicyanodiamide	PEI (10)	3		0	0	Murakami et al. (1992)
	PEI (20)	4		1	153	
	PEI (30)	6		-0	112	
EPN+DDS	PEI (2.5)	-7	6	1	33°	Kandpal et al. (2013)
	PEI (5)	-7	10	1	112°	
	PEI (7.5)	-7	19	3	175°	
	PEI (10)	-8	23	4	138°	
DGEBF+TGAP+MCDEA	PES (15)	-5	9	0	1	Brooker et al. (2010)
	PES (20)	15	27	1	24	
	PES (25)	13	30	2	41	
	PES (35)	15	33	0	63	

^aYoung's modulus, ^btensile strength, ^cglass transition temperature, ^dstress intensity factor, ^eCharpy impact strength

concentration, due to the plasticizing effect of the TP, while the fracture toughness was significantly increased, since the spherical TP particles homogeneously dispersed within the matrix acted as efficient crack barriers.

The influence of PSF content on the mechanical properties of PSF-modified DGEBA/DDM networks was investigated by Huang et al. (1997). Both tensile modulus and strength of the blends slightly improved compared to those of neat DGEBA/DDM. More importantly, K_{Ic} increased by ~20% with the addition of 15 wt% PSF to the system. Unfortunately, the toughening mechanism for this system has not been investigated. Similar behavior has been reported for DGEBA cured with piperidine (Zengli and Yishi 1989), where the addition of 15 wt% PSF led to 110% increase in K_{Ic} without sacrificing the epoxy stiffness and strength. It seems that the fracture toughness was improved as the morphology changed from particulate to

phase-inverted structure. SEM micrographs suggested that particle bridging combined with shear banding was the main toughening mechanism.

The mechanical properties of TGDDM/PEI blends with DDS curing agent have also been investigated (Gilbert and Bucknall 1991). An unprecedented improvement of 218% in fracture toughness was found for blends with 30 wt% PEI, concentration at which the phase inversion occurred, and the TP phase was effectively continuous throughout the materials. Furthermore, there was a slight increase in modulus upon addition of PEI compared with that of the neat epoxy. According to SEM, it seemed that particle bridging was the major toughening mechanism, while crack pinning was a minor toughening mechanism in this system. Murakami et al. (1992) also studied the mechanical properties of PEI-modified DGEBA with dicyanodiamide as a curing agent. No increase in K_{Ic} was found for the composite with 10 wt% of PEI, while in the blend with 20 wt% loading, the fracture toughness increased drastically, showing a maximum augment of about 150%. In the blends with 30 wt% PEI, the increase was slightly smaller, around 110%. According to SEM, there was no phase separation in the sample with the lowest TP loading, thereby K_{Ic} remained unchanged. When the PEI content was increased to 20 wt%, a particulate morphology with TP spheres dispersed within the epoxy matrix was observed, and it seems that the ductile PEI spheres provided the particle bridging toughening mechanism. However, as the PEI loading increased to 30 wt%, the phase inversion took place and formed PEI-based materials, causing a decrease in fracture toughness. More interestingly, in the PEI-modified blends, a high T_g was retained and the stiffness was increased compared with the unmodified epoxy.

Kandpal et al. (2013) explored the mechanical properties of EPN/PEI blends cured with DDS. The stiffness of the epoxy resin remained merely unchanged upon addition of PEI, while the tensile strength moderately improved. More importantly, the Charpy impact strength strongly increased, by up to 175% at 7.5 wt% TP content. These results can be explained taking into account that PEI could effectively reduce the entanglement of the polymer chains which resulted in higher molecular mobility and improved the toughness of the cured epoxy resin without lowering its strength. At higher PEI concentrations, the composite composition became uncompatibilized due to stoichiometric disbalance, and PEI is phase separated out via crystallization leading to a deterioration in the mechanical properties. The toughening effect was confirmed by SEM images of the fractured surfaces of the samples. The neat resin (Fig. 8a) displayed a smooth and featureless surface characteristic of the brittle failure of a homogenous material. In the PEI-modified epoxy (2.5 wt%), a homogeneous morphology was also observed, and many river markings appeared (Fig. 8b), which became more extensive and deeper at 5 wt% PEI concentration (Fig. 8c). However, in the composites with higher PEI content, a heterogeneous morphology was developed due to CRIPS; phase separation occurred by SD, producing bicontinuous morphologies that resulted in a rougher surface (Fig. 8d, e), which has been correlated with improved toughness.

Brooker et al. (2010) investigated the mechanical properties of DGEBA+TGAP mixture with 4,4'-methylenebis-(3-chloro 2,6-diethylaniline) (MCDEA) as curing agent blended with PES with reactive end groups. Tensile tests were carried out to

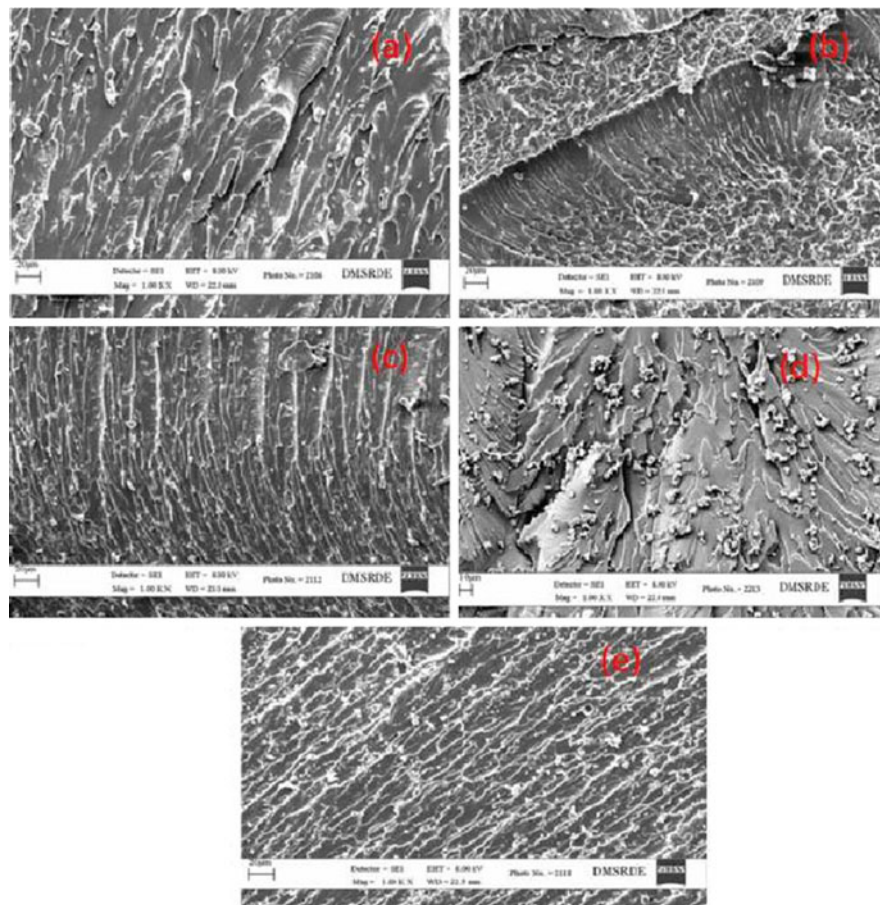


Fig. 8 SEM micrographs of (a) EPN, (b) EPN/PEI (2.5 wt%), (c) EPN/PEI (5.0 wt%), (d) EPN/PEI (7.5 wt%), and (e) EPN/PEI (10.0 wt%) (Taken from Kandpal et al. (2013), with permission from the VBRI press)

determine the changes in stiffness and strength as a function of PES content (Fig. 9). A steady increase in the value of σ_y was found as the content of PES increased, as shown in Table 1. This confirms the existence of good adhesion between the epoxy and the thermoplastic phases. The modulus values for the samples containing 0 and 15 wt% of the thermoplastic toughener were the same within the experimental error. However, when 20 wt% PES was added, the modulus was somewhat higher. The moduli for the composites incorporating 25 and 35 wt% PES were similar to that of the sample containing 20 wt%. Therefore, there was no progressive increase in modulus with increasing TP content. In contrast, the strain at break increased considerably as the percentage of TP in the composite rose (Fig. 9). The epoxy and TP-modified epoxies had similar T_g values and moduli, but the modified epoxies showed higher ductility. The comparison of the stress–strain curves for the

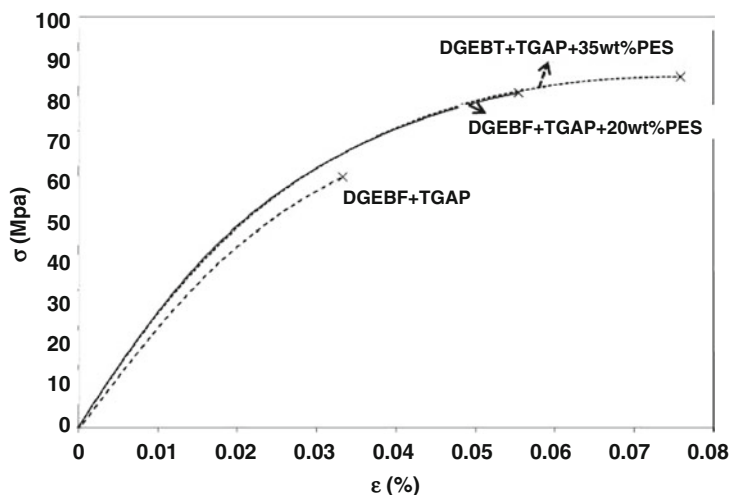


Fig. 9 Stress–strain curves for DGEBF/TGAP mixture containing 0, 20, and 35 wt% PES content

composites with 20 and 35 wt% PES revealed that the traces were almost identical, except that the sample with 20 wt% loading failed before that with 35 wt%. Both composites had a particulate morphology, with spherical particles of about 1 μm in diameter. However, at 20 wt% the TP showed a particulate morphology in a continuous epoxy-rich phase, while at 35 wt.% phase inversion occurred, yielding particles of epoxy in a continuous PES-rich phase. On another note, the fracture toughness increased steadily with increasing percentage of the thermoplastic toughener, by up to 63% at 35 wt% PES. Nonetheless, there was no sudden increase in the fracture properties which coincided with a change in morphology. According to SEM images, the fracture surface of the unmodified epoxy was relatively smooth, flat, and featureless with only a few river lines indicating a brittle failure. The composite with 15 wt% PES displayed a spherical particulate morphology, albeit during fracture the TP particles were plastically deformed, being drawn into peaks in the direction of crack growth. Further, some “tails” were found on the far side of the thermoplastic spheres. These tails suggested that the crack has passed more slowly through the TP than through the epoxy, and the crack fronts met up again on the far side of the PES particles at different levels, giving rise to “tails.” The plastic deformation of the TP-rich phase for the blends containing 15 and 20 wt% PES would result in an increase in the fracture toughness.

Mechanical Performance of Nanofiller-Reinforced TS/TP Blends: Dynamic Mechanical Properties

The influence of MWCNTs and GO on the dynamic mechanical performance of epoxy resins has been explored by DMA. Figure 10 compares DMA data reported for

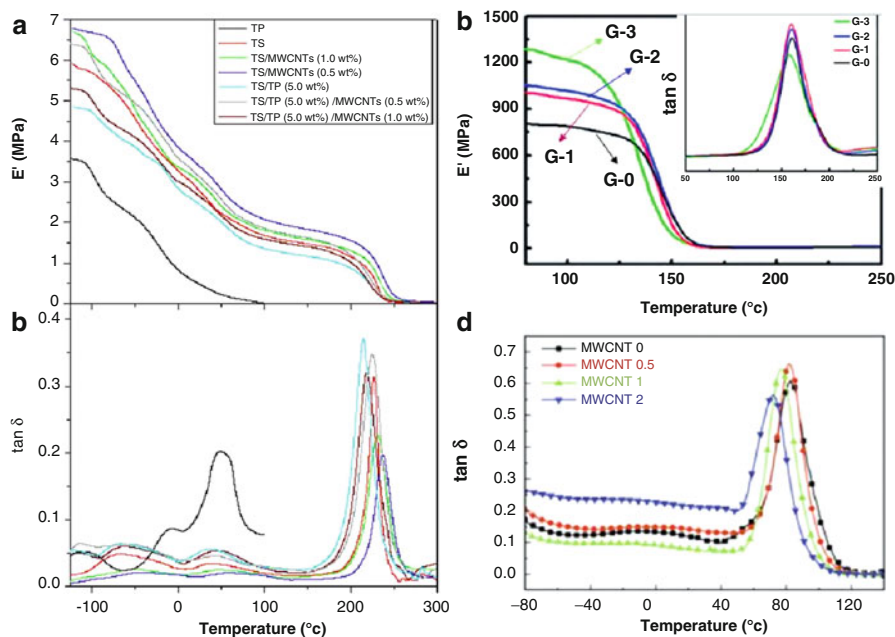


Fig. 10 Storage modulus (E') and $\tan \delta$ data obtained from DMA measurements of TGAP+DDS/poly(ethylene-1-octene)/MWCNT (a, b), DGEBA+DDS/PEI/GO-MDA (c), and DGEBA+Jeffamine/CTBN/MWCNT-COOH (d) composites (Adapted from Diez-Pascual et al. (2014), Yu and Wu (2014), and Wang et al. (2012))

TGAP+DDS/poly(ethylene-1-octene)/MWCNT composites (a and b), DGEBA+DDS/PEI/GO-MDA (c), and DGEBA+Jeffamine/CTBN/MWCNT-COOH (d). Regarding the former system (Diez-Pascual et al. 2014), E' of the epoxy decreased upon addition of the TP (Fig. 10a), attributed to the plasticizing role of the semicrystalline copolymer, in agreement with the observations reported for the same thermoset system blended with PEO-based amphiphilic block copolymer (Gonzalez-Domínguez et al. 2011). In contrast, the addition of MWCNTs provoked a remarkable increase in E' , by up to 13% for the ternary composite with 0.5 wt% loading, indicating that the reinforcement effect of the nanofiller outweighs the plasticizing effect of the TP. However, the composite with 1.0 wt% MWCNT showed similar modulus to that of the neat TS, related to a poorer nanofiller distribution, as revealed by SEM, and the preferential MWCNT location within the TP phase (Fig. 6). In contrast, it was found that the addition of GO-MDA to a DGEBA/PEI blend (Yu and Wu 2014) led to a strong increase in E' (Fig. 10c), by about 25% and 58% at 1.0 and 3.0 wt% loading. This enhanced behavior was ascribed to the homogenous nanofiller dispersion and its strong interaction with both DGEBA and PEI via functionalization with MDA, which is one of the monomers for the polycondensation of PEI. Thus GO-MDA can interact with PEI via non-covalent bonds, and with DGEBA through the remaining amino groups provided by MDA, forming covalent bonds and efficiently transferring the high modulus of GO to the matrix.

The evolution of $\tan \delta$ (ratio of the loss to storage modulus, a measure of the damping within the system) as a function of temperature (Fig. 10b) showed three transition peaks for neat TGAP+DDS (Diez-Pascual et al. 2014): that at the lowest temperature (β transition) was ascribed to crankshaft rotation of hydroxyl ether segments ($-\text{CH}_2-\text{CH}(\text{OH})-\text{CH}_2-\text{O}-$) of the cross-linked network in the glassy state, while the other relaxations were associated with α transitions of the cured network. In particular, at the highest temperature (α_1 transition or T_g) was associated to Brownian motions of the chains and the relaxation of associated dipoles. Three relaxation peaks were also detected for neat TP at -110 , -5 °C, and 48 °C, corresponding to the γ , β , and α transitions, respectively. The γ relaxation was ascribed to localized motion of the methylene units of the PE chain and considered as the T_g although this assignment is controversial. Regarding the composites, it was found that the T_g of the TS/TP blend was ~ 13 °C lower than that of neat TS, and the other transition temperatures also shifted to lower values, confirming the strong plasticizing effect of the TP. In the ternary composite with 1.0 wt% MWCNTs, T_g was ~ 8 °C lower, while that with 0.5 wt% loading displayed similar T_g to that of the neat TS, suggesting that the plasticizing effect is compensated by the stiffening effect of the CNTs mostly located around the TS/TP interphase (Fig. 6). Similar behavior was reported for DGEBA+DDS/PEI/GO-MDA composites (Yu and Wu 2014), where the T_g of samples with low nanofiller loading was similar to that of the matrix (Fig. 10c), while that of the composite with 3.0 wt% GO-MDA decreased slightly, or for DGEBA+Jeffamine/CTBN/MWCNT-COOH nanocomposites (Fig. 10d), where the T_g of the composite with 0.5 wt% loading was similar to that of the neat resin but decreased markedly with the CNT content (Wang et al. 2012). The authors suggested that the addition of MWCNT-COOH could cause over-stoichiometric active hydrogen that can react with the epoxy groups, while the stoichiometric ratio of curing agent to epoxide group is known to lead to the maximum T_g . Further, the nanofiller increases the viscosity of the system resulting in a rapid decrease of the degree of cure in the diffusion-controlled stage and finally the presence of CNT agglomerates (as revealed by SEM), all these issues being responsible for the drop in T_g .

On another note, the height of the $\tan \delta$ peak reflects the extent of mobility of the polymer chain segments. Figure 10b reveals an increase in the peak maximum for samples incorporating the TP compared to TGAP+DDS (Diez-Pascual et al. 2014), indicating enhanced mobility of the polymeric segments. Moreover, the higher $\tan \delta$ value in the nanocomposites suggests that when the stress is eliminated the energy stored during the deformation process recuperates at a slower rate in comparison to the neat epoxy. In contrast, a decrease in height is found upon addition of GO-MDA to DGEBA/PEI (inset of Fig. 8c), suggesting reduced chain mobility in the presence of this 2D functionalized nanofiller (Yu and Wu 2014). Regarding the area under the $\tan \delta$ peak, which is indicative of the energy dissipated in the viscoelastic relaxations, it was found that ternary TGAP+DDS/poly(ethylene-1-octene)/MWCNT nanocomposites exhibited higher value, hence improved toughness, since energy dissipation processes enhance the impact resistance of polymeric systems (Diez-Pascual et al. 2010). Similar behavior was found upon addition of GO-MDA to DGEBA/PEI blends, indicating a clear toughening effect (Yu and Wu 2014).

However, a reduction in the area under the $\tan \delta$ was found for DGEBA+Jeffamine/CTBN blends with MWCNT-COOH ≥ 1.0 wt% (Fig. 8d), indicating poorer impact strength for these composites compared to that of the neat resin (Wang et al. 2012). Here the presence of nanotube agglomerates cause cracks to initiate and propagate easily.

Mechanical Performance of Nanofiller-Reinforced TS/TP Blends: Static Mechanical Properties

The static mechanical properties of multiphase composites have been also characterized by tensile and Charpy impact strength tests. Table 2 summarizes the percentage of variation reported in the mechanical properties of nanofiller-reinforced TS/TP hybrid composites with respect to the corresponding binary blends: E , σ_y , elongation at break (ϵ_b), and impact strength (G). The results indicate that, in general, MWCNTs can be considered as the most effective filler for improving the composite stiffness and strength, albeit the enhancement depends strongly on the type and concentration of nanotubes. Thus, the addition of 0.5 wt% MWCNTs to TGAP+DDS/poly(ethylene-1-octene) resulted in a 34% E increase (Diez-Pascual et al. 2014), while the incorporation of 1.0 wt% only increased the modulus by 8%, behavior related to the poorer nanofiller dispersion in the composite with higher loading. In contrast, at 0.5 wt% loading, the MWCNTs were predominantly located around the TS/TP interphase and might improve the matrix-TP interfacial adhesion. Another plausible explanation for the improved mechanical performance could be the formation of droplet-type TP domains and their reduction in size as a result of the localization of the CNTs at the TS/TP interphase. Moreover, this composite exhibited higher crystallinity and smaller crystal size than TS/TP (Diez-Pascual et al. 2014), facts that result in improved rigidity. On the other hand, for the same nanofiller loading, the reinforcement attained upon addition of pristine MWCNTs to TGAP+DDS/poly(ethylene-1-octene) blends was about double that reported on incorporation of MWCNT-COOH to DGEBA+Jeffamine/CTBN (Wang et al. 2012). Despite the fact that the functionalized CNTs showed strong interactions with both the epoxy and CTBN, their dispersion was only relatively uniform, leading to limited property improvements. As expected, composites reinforced with CB displayed the lowest reinforcement effect (Ma et al. 2013a), likely related to the lower modulus of this nanofiller compared to CNTs or GO and the aggregation of CB within the TP phase (Fig. 5). Intermediate E improvements were found upon addition of functionalized GO to DGEBA+DDS/PEI blends (Yu and Wu 2014), where good nanofiller dispersion and strong interaction with both TS and TP were attained, which could be related to a decrease in the nanofiller modulus on functionalization. In this system, E increments grew gradually with increasing nanofiller loading, associated with the morphology of the composites (Fig. 3); thus, the phase separation behavior was hindered with the incorporation of GO-MDA and completely suppressed at 3.0 wt% loading, fact that was beneficial for the mechanical properties.

Regarding σ_y , the trends observed are qualitatively similar to those described above for the modulus (Table 2); pristine MWCNTs led to the highest strength

Table 2 Percentage of change in the mechanical properties of nanofiller-reinforced thermoset/thermoplastic multiphase composites compared to the corresponding binary blends

TS	TP (wt%)	Nanofiller type	Nanofiller content (wt%)	ΔE^a (%)	$\Delta \sigma_y^b$ (%)	$\Delta \varepsilon_b^c$ (%)	ΔG^d (%)	Ref.
TGAP+DDS	Poly(ethylene-1-octene) (5)	MWCNT	0.5	34	37	-25	15	Díez-Pascual et al. (2014)
DGEBA+Jeffamine	CTBN (15)	MWCNT-COOH	0.5	8	18	-13	-20	Wang et al. (2012)
			1.0	15	5	-3		
			2.0	10	-3	-29		
DGEBA+DDS	PEI (13)	GO-MDA	1.0	10	8	0		Yu and Wu (2014)
			2.0	22	8	13		
			3.0	23	40	28		
DGEBA+MTHPA	PEI (16)	CB	1.0	3	-29		-66	Ma et al. (2013a)

^aYoung's modulus, ^btensile strength, ^celongation at break, ^dimpact strength

improvements (Diez-Pascual et al. 2014), while the incorporation of CB resulted in considerable σ_y decrements (Ma et al. 2013a), hinting that the strength is even more sensitive to the nanofiller agglomeration than the stiffness. Focusing on ϵ_b , significant reductions were found for MWCNT-reinforced composites (Diez-Pascual et al. 2014; Wang et al. 2012), which is the typical behavior reported for composites reinforced with rigid nanofillers. Accordingly, the ductility drop became more pronounced with increasing nanotube loading since agglomerates strongly obstruct plastic deformation of the matrix. Surprisingly, ϵ_b of DGEBA+DDS/PEI blends increased upon addition of 2 or 3 wt% GO-MDA (Yu and Wu 2014), explained in terms of the almost perfect co-continuous structure attained in these composites that improves their ductility and toughness.

More interesting are the toughness data derived from Charpy impact strength tests (Table 2). The incorporation of 1.0 wt% MWCNTs to TGAP+DDS/poly(ethylene-1-octene) provoked a moderate toughness reduction, since the agglomerates nucleated cracks and promoted dimple formation, resulting in premature failure. In contrast, the nanocomposite with 0.5 wt% showed ~15% higher value than that of TS/TP, suggesting a toughening effect arising from a synergistic action between the TP and the MWCNTs. Moreover, this improved performance could be related to the matrix-dispersed droplet-type morphology observed for this composite (Fig. 6), where small TP domains were found to be regularly dispersed within the matrix. In fact, previous researchers working with immiscible polymer blends that showed droplet morphology demonstrated improved toughness for samples with smaller and more uniformly distributed drops (Wu 1988). For instance, Lee et al. (2005) observed a super-toughness behavior for PP/PP-g-MA/poly(ethylene-co-octene)/montmorillonite nanocomposites containing more than 20 wt% copolymer, explained by the morphological change in the presence of the nanofiller that reduced the size of the copolymer domains. Conversely, a strong drop in impact strength was found for DGEBA+MTHPA/PEI blends reinforced with CB (Ma et al. 2013a), also associated to the formation of large CB aggregates that nucleate cracks and provoke premature failure, hence poor impact strength. Overall, results demonstrate that the TGAP+DDS/poly(ethylene-1-octene) composite incorporating 0.5 wt% MWCNTs displays an optimal balance between stiffness, strength, and toughness.

Conclusions and Outlook

In this chapter, the morphology and mechanical properties of selected TS/TP blends have been discussed. The addition of TPs to epoxy resins is a promising alternative to improve their toughness without sacrificing their stiffness and strength. At low TP contents (i.e., 5–10 wt%), a particulate morphology (TP domains within the epoxy matrix) typically predominates. However, as the toughening agent concentration increases (i.e., 15–30 wt%), phase inversion takes place. The toughness of the systems generally improves as the amount of TP rises. In other terms, the toughness increases when the morphology changes from the homogeneity of the epoxy phase to the particulate and to the phase-inverted morphology eventually. Many possible

toughening mechanisms have been proposed to explain this behavior such as particle bridging, crack pinning, crack path deflection, particle-yielding-induced shear banding, particle yielding, and microcracking.

More importantly, recent studies on TS/TP-based composites incorporating carbon nanofillers have been described, analyzing in detail the correlation between their morphology and mechanical properties. Many different morphologies can be developed such as dispersed, co-continuous, dendritic, or phase-inverted morphologies, and it has been clearly shown that uneven or asymmetric distribution of nanofillers can lead to important improvements in key properties, generally higher than those attained in the corresponding nanofiller-reinforced binary samples, due to synergistic effects. Thus, tuning the preferential distribution of the nanofillers can result in remarkable improvements in composite rigidity and strength and becomes an important tool for the development of materials with an optimum combination of properties. In particular, samples with matrix-dispersed droplet-type morphology of the TP and selective distribution of the nanofillers at the TS/TP interphase display an optimal balance of stiffness, strength, and toughness.

Nevertheless, although the morphological control of nanofiller-reinforced TS/TP multiphase composites has attracted significant attention due to the key role that morphology plays on the final composite properties, the progress has been relatively slow, and several challenges still need to be addressed. The factors affecting nanofiller distribution within polymer blends are very complex, including thermodynamic and kinetic parameters, the aspect ratio and surface roughness of the nanofiller, and the viscosity of the polymers. Theoretically, by adjusting kinetic issues (shear forces during processing, fabrication methodology, mixing procedures and sequence, blending time, etc.), as well as thermodynamic issues (controlling the interfacial energy through careful choice of the composite components), the morphology of the composites can be tuned. However, to put these principles into practice is a very hard task due to the high complexity of the systems, involving various phases with different physical properties that must be controlled simultaneously. Furthermore, the successful industrial use of such multiphase composites requires property stability and reproducibility as well as ease of preparation. However, a continued effort in this area has the potential to generate interesting and exciting materials.

These multifunctional materials are expected to have numerous applications, primarily in the aeronautics, automobile, and energy sectors. In particular, they are suitable for aircraft parts such as wing elements and landing gear hubcaps, wind turbine blades, and solar panels and can be employed in energy storage devices, as the load-carrying structural body. They can also be used for defense applications where high-temperature susceptible and lightweight structures are required and as matrix material for manufacturing of lightweight military shoes and bulletproof jackets. On the other hand, they can be employed in strain/damage sensing. In this regard, new strategies such as the use of conductive fillers with different aspect ratio have to be considered, and the filler–matrix interfacial stress transfer needs to be carefully analyzed. The sensitivity and selectivity of such sensors can be improved by grafting functional groups or polymer molecules onto the filler surface. They also

show great potential for the development of shape memory materials (Rousseau and Xie 2010) that can be deformed and fixed into a temporary shape and then recover their original shape in response to external stimuli, which can be provided by electricity-induced heating. In addition, the replacement of petroleum-based epoxies by biobased thermosets like epoxidized vegetable oils combined with the use of biothermoplastics would lead to biocompatible and biodegradable materials that could be employed for the development of sustainable devices or “green electronics” (Irimia-Vladu 2014). More importantly, they are suitable as self-healing materials, a class of smart materials that have the ability to repair damage caused by mechanical usage over time (Luo et al. 2009; Pingkarawat et al. 2012). In particular, thermally triggered self-healing materials can be prepared by blending a high-temperature epoxy resin with a TP and CNTs (Hayes et al. 2007). When the CNTs sense a crack within the structure, they can be used as thermal transports to heat up the resin so that the molten TP can diffuse to fill the cracks in the epoxy matrix, thus healing the material. This self-healing composite displays improved performance due to a synergistic effect of the three components: good load-bearing capability, given by the TS; fracture toughness improvement, given by the TP; and this thermal healing possibility after a curing cycle when the material is damaged due to the superior thermal conductivity of the CNTs.

References

- Abdel-Aal N, El-Tantawy F, Al-Hajry F, Bououdina M (2008a) Epoxy resin/plasticized carbon black composites. Part I. Electrical and thermal properties and their applications. *Polym Compos* 29:511–517
- Abdel-Aal N, El-Tantawy F, Al-Hajry F, Bououdina M (2008b) Epoxy resin/plasticized carbon black composites. Part II. Correlation among network structure and mechanical properties. *Polym Compos* 29:804–808
- Ajayan PM, Schadler LS, Braun PV (2003) *Nanocomposite science & technology*. Wiley-VCH, Germany
- Brooker RD, Kinloch AJ, Taylor AC (2010) The morphology and fracture properties of thermoplastic-toughened epoxy polymers. *J Adhesion* 86:726–741
- Bucknall CB, Partridge IK (1986) Phase-separation in cross-linked resins containing polymeric modifiers. *Polym Eng Sci* 26:54–62
- Chen J, Shi YY, Yang JH et al (2012) A simple strategy to achieve very low percolation threshold via the selective distribution of carbon nanotubes at the interface of polymer blends. *J Mater Chem* 22:22398–22404
- Diez-Pascual AM, Naffakh M, González-Domínguez JM, Anson-Casaos A, Martínez-Rubi Y, Martínez MT, Simard B, Gómez M (2010) High performance PEEK/carbon nanotube composites compatibilized with polysulfones-II. Mechanical and electrical properties. *Carbon* 48:3500–3511
- Diez-Pascual AM, Shuttleworth PS, González-Castillo EI, Marco C, Gómez-Fatou MA, Ellis G (2014) Polymer blend nanocomposites: effect of selective nanotube location on the properties of a semicrystalline thermoplastic-toughened epoxy thermoset. *Macromol Mater Eng* 299:1430–1444
- Donnet JB, Bansal RC, Wang MJ (1993) *Carbon black: science and technology*. Marcel Dekker, New York

- Fenouillot F, Cassagnau P, Majesté JC (2009) Uneven distribution of nanoparticles in immiscible fluids: morphology development in polymer blends. *Polymer* 50:1333–1350
- Frigione M, Acierno D, Mascia L (1999) Miscibilization of low molecular weight functionalized polyethylenes in epoxy resins. I. Effects of composition and modifications chemistry. *J Appl Polym Sci* 73:1457–1470
- Gilbert AH, Bucknall CB (1991) Epoxy-resin toughened with thermoplastic. *Makromol Chem Macromol Symp* 45:289–298
- Gödel A, Kasaliwal G, Pötschke P (2009) Selective localization and migration of multiwalled carbon nanotubes in blends of polycarbonate and poly(styrene-acrylonitrile). *Macromol Rapid Commun* 30:423–429
- Gödel A, Marmur A, Kasaliwal GR, Pötschke P, Heinrich G (2011) Shape-dependent localization of carbon nanotubes and carbon black in an immiscible polymer blend during melt mixing. *Macromolecules* 44:6094–6102
- Gonzalez-Domínguez JM, Anson-Casaos A, Díez-Pascual AM, Ashrafi B, Naffakh M, Backman D, Stadler H, Johnston A, Gómez M, Martínez MT (2011) Solvent-free preparation of high-toughness epoxy-SWNT composite materials. *ACS Appl Mater Interfaces* 3:1441–1450
- Gültner M, Gödel A, Pötschke P (2011) Tuning the localization of functionalized MWCNTs in SAN/PC blends by a reactive component. *Compos Sci Technol* 72:41–48
- Hayes SA, Jones FR, Marshiya K, Wang W (2007) A self-healing thermosetting composite material. *Compos Part A* 38:1116–1120
- Huang P, Zheng S, Huang J, Guo Q, Zhu W (1997) Miscibility and mechanical properties of epoxy resin/polysulfone blends. *Polymer* 38:5565–5574
- Irimia-Vladu M (2014) “Green” electronics: biodegradable and biocompatible materials and devices for sustainable future. *Chem Soc Rev* 43:588–610
- Kandpal J, Yadaw SB, Nagpal A (2013) Mechanical properties of multifunctional epoxy resin/glass fiber reinforced composites modified with poly(ether-imide). *Adv Mater Lett* 4:241–249
- Konnola R, Parameswaranpillai J, Joseph K (2015a) Mechanical, thermal, and viscoelastic response of novel in situ CTBN/POSS/epoxy hybrid composite system. *Polym Compos*. doi:10.1002/pc.23390
- Konnola R, Parameswaranpillai J, Joji J, Joseph K (2015b) Structure and thermo-mechanical properties of CTBN-grafted-GO modified epoxy/DDS composites. *RSC Adv* 5:61775–61786
- Larrañaga M, Mondragon I, Riccardi CC (2007) Miscibility and mechanical properties of an amine-cured epoxy resin blended with poly(ethylene oxide). *Polym Int* 56:426–433
- Lee HS, Fasulo P, Rodgers WR, Paul DR (2005) TPO based nanocomposites. Part 1. Morphology and mechanical properties. *Polymer* 46:11673–11689
- Lee C, Wei X, Kysar JW, Hone J (2008) Measurement of the elastic properties and intrinsic strength of monolayer graphene. *Science* 321:385–388
- Li Y, Shimizu H (2008) Conductive PVDF/PA6/CNTs nanocomposites fabricated by dual formation of cocontinuous and nanodispersion structures. *Macromolecules* 41:5339–5344
- Li B, Zhong W-H (2011) Review on polymer/graphite nanoplatelet nanocomposites. *J Mater Sci* 46:5595–5614
- Li S, Hsu BL, Li F, Li CY, Harris FW, Cheng SZD (1999) A study of polyimide thermoplastics used as tougheners in epoxy resins-structure, property and solubility relationships. *Thermochim Acta* 340:221–229
- Li Y, Wang S, Zhang Y, Zhang Y (2006) Carbon black-filled immiscible polypropylene/epoxy blends. *J Appl Polym Sci* 99:461–471
- Li CQ, Zhao QN, Deng H et al (2011) Preparation, structure and properties of thermoplastic olefin nanocomposites containing functionalized carbon nanotubes. *Polym Int* 60:1629–1637
- Liu L, Wang Y, Li YL, Wu J, Zhou ZW, Jiang CX (2009) Improved fracture toughness of immiscible polypropylene/ethylene-co-vinyl acetate blends with multiwalled carbon nanotubes. *Polymer* 50:3072–3078
- Luo X, Ou R, Eberly DE, Singhal A, Viratyaporn W, Mather PT (2009) A thermoplastic/thermoset blend exhibiting thermal mending and reversible adhesion. *ACS Appl Mater Interfaces* 1:612–620

- Ma C-G, Liu M (2013) Carbon black selective dispersion and electrical properties of epoxy resin/polystyrene/carbon black ternary composites. *Adv Mater Res* 548:94–98
- Ma C-G, Xi DY, Liu M (2013a) Epoxy resin/polyetherimide/carbon black conductive polymer composites with a double percolation structure by reaction-induced phase separation. *J Compos Mater* 47:1153–1160
- Ma C-G, Xi DY, Liu M, Shi R (2013b) Electrical property of carbon nanotubes/epoxy resin/polyetherimide composites with inverted-phase structure. *Adv Mater Res* 652–654:56–59
- Mi BG, Hodgkin JH, Stachurski ZH (1993a) Reaction mechanisms, microstructure, and fracture properties of thermoplastic polysulfone-modified epoxy resin. *J Appl Polym Sci* 50:1065–1073
- Mi BG, Hodgkin JH, Stachurski ZH (1993b) Microstructural effects and the toughening of thermoplastic modified epoxy resins. *J Appl Polym Sci* 50:1511–1518
- Moniruzzaman M, Winey KI (2006) Polymer nanocomposites containing carbon nanotubes. *Macromolecules* 39:5194–5205
- Murakami A, Saunders D, Ooishi K, Yoshiki T, Saitoo M, Watanabe O, Takezawa M (1992) Fracture-behavior of thermoplastic modified epoxy resins. *J Adhesion* 39:227–242
- Novoselov KS, Geim AK, Morozov SV, Jiang D, Zhang Y, Dubonos SV, Grigorieva IV, Firsov AA (2004) Electric field effect in atomically thin carbon films. *Science* 306:666–669
- Pashaei S, Siddaramaiah, Avval MM, Syed AA (2010) Investigation on thermal, mechanical and morphological properties of epoxy/UHWPE blends. *J Eng Appl Sci* 5:26–37.
- Pingkarawat K, Wang CH, Varley RJ, Mouritz AP (2012) Self-healing of delamination fatigue cracks in carbon fibre–epoxy laminate using mendable thermoplastic. *J Mater Sci* 47:4449–4456
- Popov VN (2004) Carbon nanotubes: properties and application. *Mater Sci Eng R* 43:61–102
- Ray SS, Pouliot S, Bousmina M, Utracki LA (2004) Role of organically modified layered silicate as an active interfacial modifier in immiscible polystyrene/polypropylene blends. *Polymer* 45:8403–8413
- Rousseau IA, Xie T (2010) Shape memory epoxy: composition, structure, properties and shape memory performances. *J Mater Chem* 20:3431–3441
- Rutnakornpituk M (2005) Thermoplastic toughened epoxy networks and their toughening mechanisms in some systems. *Naresuan Univ J* 13:73–83
- Shi R, Ma C-G, Liu M (2013) Selective distribution of carbon black in epoxy resin/thermoplastic multiphase composites. *Adv Mater Res* 652–654:73–76
- Si M, Araki T, Ade H et al (2006) Compatibilizing bulk polymer blends by using organoclays. *Macromolecules* 39:4793–4801
- Spitalsky Z, Tasis D, Papagelis K, Galiotis C (2010) Carbon nanotube–polymer composites: chemistry, processing, mechanical and electrical properties. *Prog Polym Sci* 35:357–401
- Sumita M, Sakata K, Asai S, Miyasaka K, Nakagawa H (1991) Dispersion of fillers and the electrical conductivity of polymer blends filled with carbon black. *Polym Bull* 25:265–271
- Sun Y, Guo ZX, Yu J (2010) Effect of ABS rubber content on the localization of MWCNTs in PC/ABS blends and electrical resistivity of the composites. *Macromol Mater Eng* 295:263–268
- Tchoudakov R, Breuer O, Narkis M, Siegmann A (1996a) Conductive polymer blends with low carbon black loading: polypropylene/polyamide. *Polym Eng Sci* 36:1336–1346
- Tchoudakov R, Breuer O, Narkis M, Siegmann A (1996b) Conductive polymer blends with low carbon black loading: polypropylene/polycarbonate. *Polym Netw Blends* 6:1–8
- Thostenson ET, Ren Z, Chou T-W (2001) Advances in the science and technology of carbon nanotubes and their composites: a review. *Compos Sci Technol* 61:1899–1912
- Wang YT, Wang CS, Yin HY, Wang LL, Xie HF, Cheng RS (2012) Carboxyl-terminated butadiene-acrylonitrile-toughened epoxy/carboxyl-modified carbon nanotube nanocomposites: thermal and mechanical properties. *eXPRESS Polym Lett* 6:719–728
- Wu S (1982) Polymer interface and adhesion. Marcel Dekker, New York
- Wu SH (1988) A generalized criterion for rubber toughening – the critical matrix ligament thickness. *J Appl Polym Sci* 35:549–561
- Wu SJ, Lin TK, Shyu SS (2000) Cure behavior, morphology, and mechanical properties of the melt blends of epoxy with polyphenylene oxide. *J Appl Polym Sci* 75:26–34

- Xiong ZY, Wang L, Sun Y, Guo ZX, Yu J (2013) Migration of MWCNTs during melt preparation of ABS/PC/MWCNT conductive composites via PC/MWCNT masterbatch approach. *Polymer* 54:447–455
- Yoon TH, Priddy DH, Lyle GD, McGrath JE (1995) Hydrolytically stable thermo plastic and thermosetting poly(arylene phosphine oxide) material systems. *Macromol Symp* 98:673–686
- Yu G, Wu P (2014) Effect of chemically modified graphene oxide on the phase separation behaviour and properties of an epoxy/polyetherimide binary system. *Polym Chem* 5:96–104
- Zengli F, Yishi S (1989) Epoxy resin toughened by thermoplastics. *Chin J Polym Sci* 7:367–378
- Zhang L, Wan C, Zhang Y (2009) Morphology and electrical properties of polyamide 6/polypropylene/multi-walled carbon nanotubes composites. *Compos Sci Technol* 69:2212–2217

Gianluca Cicala and Salvatore Mannino

Abstract

The present chapter deals with the applications and drawbacks of epoxy/thermoplastic blends. The fundamentals of epoxy/thermoplastic blends are discussed. The different toughening technologies applied to epoxy resins for advanced composites are thoroughly discussed and their commercial outcomes presented. Some applications like adhesives and self-healing are also introduced. For each application field, when appropriate, examples of commercial exploitation for the epoxy/thermoplastic blends are given to present the reader to the practical down to earth applications. In some cases, i.e., self healing, the future applications are presented.

Keywords

Epoxy • Thermoplastic • Blends • Application • Commercial systems

Contents

Introduction	776
Fundamentals of Thermoplastic/Epoxy Blends	776
Applications	781
Matrices for Composites	781
Adhesive Bonding	788
Future Applications	793
Conclusions	797
References	798

G. Cicala (✉) • S. Mannino

Department for Industrial Engineering, University of Catania, Catania, Italy

e-mail: gcicala@unict.it; salvatoremannino@hotmail.com

© Springer International Publishing AG 2017

J. Parameswaranpillai et al. (eds.), *Handbook of Epoxy Blends*,

DOI 10.1007/978-3-319-40043-3_28

775

Introduction

Epoxy resins are the most used chemicals among thermoset materials (Cicala and Lo 2012). This is due to their versatility which comes from their low viscosity as monomers and, at the same time, the good mechanical and thermal properties once curing reaction is completed. The main drawback of epoxies is the brittleness in the cured state. Other limitations are the shrinkage upon curing, the poor recyclability and, for some formulations, the low thermal resistance.

Most applications require for improvements of the brittleness. In order to satisfy this requirement, epoxy resins can be toughened by adding a dispersed second phase material, which can be either a rubber or a thermoplastic. This dispersed material “slows down” the crack propagation leading to much higher energy to fracture values. The main areas of interest for toughened epoxy resins are matrix for composites, adhesive bonding, and coatings and corrosion protection. The addition of thermoplastic leads to improvements in toughness that were exploited in several commercial systems. Blending thermoplastics with epoxy can also serve as a mean to develop smart functions like self-healing and shape memory effects.

In the present chapter the fundamentals of thermoplastic/epoxy blends will be recalled first and the main applications will be treated thereafter.

Fundamentals of Thermoplastic/Epoxy Blends

A lot of research has been carried out for the development of polymeric systems to increase the fracture toughness of epoxides without decreasing their thermal and mechanical properties. Back in 1983 Bucknall and Partridge proposed the use of polyaromatics like polyether sulfones (PES) as modifiers for epoxy resins as a solution to overcome the limitation of rubber toughening. The choice of this class of polymers is due to their high modulus and glass transition temperature, which are comparable to those of the epoxide resins. Tables 1 and 2 summarize some common amorphous and semicrystalline thermoplastic polymers used for thermoset/thermoplastic blends.

When thermoplastic is added to epoxy, homogenous or not homogenous blends can be obtained. Upon curing three different scenarios can happen that result in different phase morphology (Fig. 1). All the scenarios have been exploited in commercial systems as described in Fig. 1.

In the first case, if the thermoplastic is soluble in the resin, a homogeneous mixture is obtained. When curing starts, the mixture can either remain homogenous or phase separate. This is the case for some commercial toughened epoxy prepreg systems like CYCOM[®] 977 series and Hexcel 8552. When phase separation happens, it can lead to several types of morphologies, i.e., particulate, cocontinuous, and inverted. In the particulate morphology a thermoplastic-rich phase is dispersed in the epoxy-rich matrix; on the contrary, in the phase-inverted morphology an epoxy-rich phase is dispersed in the thermoplastic-rich phase. In the cocontinuous morphology, the two phases are segregated and interpenetrated altogether (Williams et al. 1997).

Table 1 Examples of amorphous thermoplastic polymers

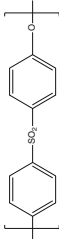
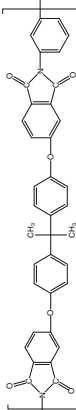
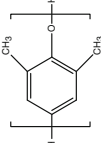
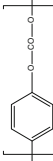
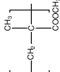
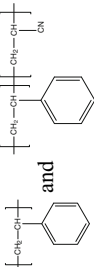
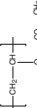
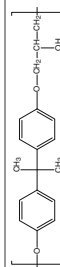
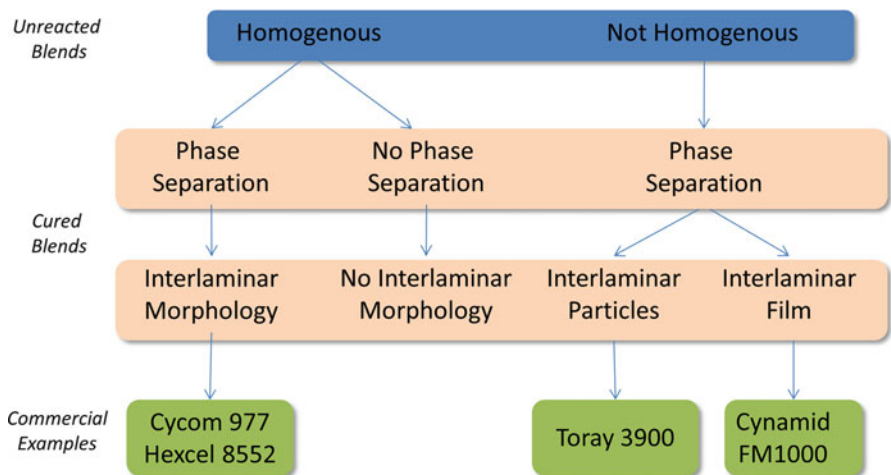
Acronym	Name	Formula	Tg (°C)	Some commercial references
PES	Polyether sulfone		220	Solvey Virantage VW-10200, Mn _{GPC} : 46,500 Virantage VW-10300, Mn _{GPC} : 55,000 Virantage VW-10700, Mn _{GPC} : 21,000 Virantage VW-30500, Mn _{GPC} : 14,000
PEI	Polyether imide		210	Sabic Ultem 1000, Mn = 26,000 1040, Mn = 9,900
PPE	Poly(2,6 dimethyl-1,4-phenylene ether)		210	Sabic 820, Mn = 12,000
PC	Polycarbonate		140	Saic Lexan
PMMA	Polymethylmetacrylate		110	Numerous
PS and SAN	Polystyrene and Poly(styrene-co-acrylonitrile)		11	Numerous
PVAc	Polyvinylacetate		40	Union Carbide LP40A, Mn = 40,000
Phenoxy	Poly(hydroxy) ether of bisphenol A		90	Union Carbide Mn = 20,000

Table 2 Example of semicrystalline thermoplastic polymers

Acronym	Name	Formula	Tg (°C)	Tm (°C)
PE	Polyethylene	$\left[\text{CH}_2 - \text{CH}_2 \right]$		110–140
PVDF	Polyvinylidene fluoride	$\left[\text{CH}_2 - \text{CF}_2 \right]$	-50	170
PET PBT	Polyethylene terephthalate Polybutylene terephthalate	$\left[\text{C}(=\text{O}) - \text{C}_6\text{H}_4 - \text{C}(=\text{O}) - \text{O}(\text{CH}_2)_i\text{O} \right]$ i = 2 i = 4	60 60	270 220
PA6 PA11 PA12	Polyamide	$\left[(\text{CH}_2)_i \text{C}(=\text{O}) \text{N}(\text{H}) \right]$ i = 5 i = 10 i = 11	40 43 42	216 185 177

**Fig. 1** Toughening technologies of epoxy/thermoplastic blends

As described in Fig. 2 the initial thermoplastic concentration controls, among other parameters, the resulting morphology. Under particular circumstances, other special morphologies can be obtained (Fig. 3). Bimodal particulate morphology is one of the cases, in which the thermoplastic-rich particle presents two average diameter values. Another case is the secondary phase inversion, which is the result of demixing of the epoxy phase inside the thermoplastic-rich domains occurring in postcuring conditions.

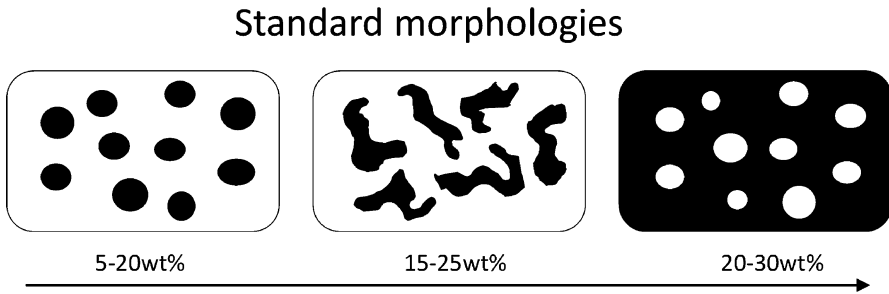


Fig. 2 Effect of the thermoplastic concentration on the interlaminar morphologies of thermoset/thermoplastic blends

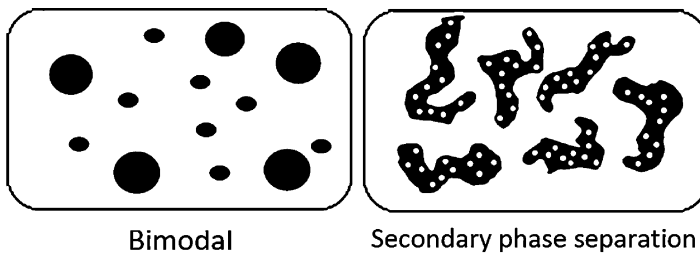


Fig. 3 Special interlaminar morphologies for epoxy/thermoplastic blends

When the initial mixture is homogeneous but no phase separation occurs during the cure of the resin, the final composite is a homogeneous transparent material. This can be due to the low concentration of the thermoplastic or due to the chemical affinity between the thermoplastic and the epoxy hardener. Polycarbonate/epoxy and polycaprolactone (PCL)/epoxy are an example of blend which do not phase separate upon curing.

If the thermoplastic polymer is not soluble in the epoxy resin, the initial mixture is not homogeneous and the thermoplastic particles remain dispersed in the epoxy before and after the cure. Examples of these are polyamides (PA), polybutylene terephthalate (PBT), and polyvinylidene fluoride (PVDF) (Yee et al. 2000). Commercially speaking, this is the principle used by Toray Industries for toughening their Toray 3900 epoxy system.

In general, to achieve toughening effects the thermoplastic phase should act as an obstacle for crack propagation resulting in crack deviation or crack bridging. However, to a certain extent, homogenous blends can also be toughened by the presence of the thermoplastic chains within the epoxy network. The limitation of this approach can be that less energy is dissipated and that the thermal properties of the blend depend linearly on the relative amounts of the two components. This can

be a limitation when the wrong thermoplastic is chosen. Thermoplastic-epoxy blends were developed to obtain materials with improved properties, like thermomechanical and solvent resistance. The thermoplastics reported in Table 1 have high glass transition temperatures, high modulus, and good solvent resistance. The choice to use this type of thermoplastic was largely due to their superior properties compared to traditional reactive rubbers. The latter are performing much better in terms of toughening improvements but they also result in reduction of glass transition, modulus, and solvent resistance for the epoxy blends. Other properties are influenced by the blending of thermoplastic with epoxy.

For example, thermoplastic polymers can be used as low-profile additives to improve the dimensional stability of thermoset resins. Often, they are used in polyester blends to have a better surface quality and to compensate the resin shrinkage. One of the most common polymer for this specific use is the polyvinyl acetate (PVAc). The mechanism works with a continuous thermoplastic rich phase that promotes cavitation in response to tensile stresses coming from internal deformation in the presence of mechanical constraints (Lucas et al. 1993). In epoxy prepregs, thermoplastics are used both as tougheners and as modifiers in order to keep a high elastic modulus of the composite during the cure of the thermoset at low temperatures, lower than the T_g of the thermoplastic polymer. This property of thermoplastic is particularly useful to counteract the warpage in composite manufacturing due to resin shrinkage. Exact values of the amount of thermoplastic added is not released by companies as it is covered by trade secret. In most cases, it ranges from 15% to 30% by weight with respect to the resin matrix, depending on the specific application of the material.

Another application of epoxy-thermoplastic blends is the case of epoxy-phenolic coatings for magnetic disks. Porosity (macro or micro) is needed in the coating to enhance the retention of a lubricant used to increase the durability of the head-disk interface (Prime 1997). A well-known thermoplastic polymer used for this purpose is polyvinylmethyl ether (PVME) which, once is blended with the thermoset resins, phase separates. Then, PVME is degraded by annealing at 220 °C in oxidative atmosphere (air). The emission of volatile products leads to the formation of macro- or microporosity as shown in Fig. 4.

Finally, in some cases, the epoxy is not the matrix of interest but thermoplastic/epoxy blending is used to enhance thermoplastic processing. Thermoplastic polymers can be unprocessable. A common example is poly(2,6-dimethyl-1,4-phenylene ether) (PPE), an amorphous thermoplastic with a glass transition temperature of 220 °C. It softens at around 300–350 °C, but at this temperatures it starts degrading as well. In order to overcome this issue, PPE is processed by blending with a small amount of an epoxy resin acting as a reactive solvent. Upon curing of the epoxy, when phase separation occurs, PPE matrix is obtained reinforced by a dispersed thermoset-rich phase (Vendersbosch and Meijer 1997).

In the following paragraphs, the main applications down to earth are presented and some insights on future application under development or recent exploitation are also given. For commercial applications in relevant fields, like as matrices for composites, an extensive database of properties from producer is offered.

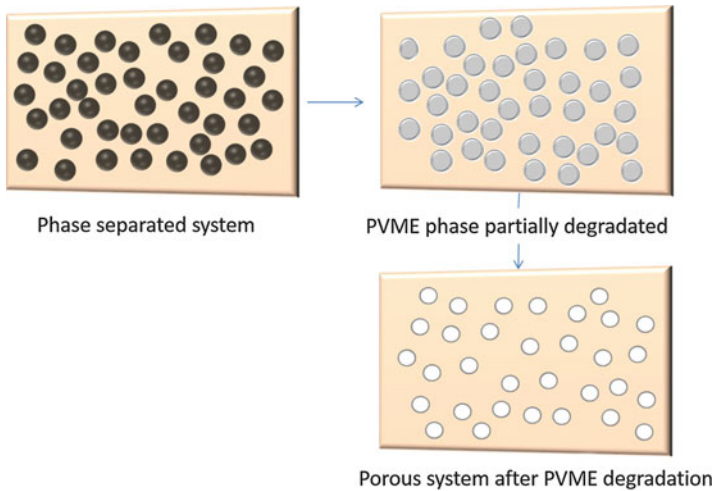


Fig. 4 Steps to obtain a porous system from a PVME/epoxy blend

Applications

Matrices for Composites

The business of epoxy/thermoplastic blends is well consolidated in the field of composite matrices for aerospace applications. Aircraft manufacturers are increasingly using composites because these materials offer great performances at a lower weight compared with metals, resulting in increased fuel efficiency, reduced maintenance, and longer service life. Two examples of aircrafts with massive use of composites for primary structures are the Boeing 787 (Fig. 5) and the Airbus A380. The use of composites for primary structures requires tough systems; therefore, thermoset/thermoplastic blends are the choice. The leading prepreg manufacturing companies (i.e., Cytec Engineered Materials, Hexcel, and Toray Industries) are selling different systems based on thermoset/thermoplastic blends which are qualified for primary structures.

One of the largest supplier, in terms of volume, for the Boeing 787 is Toray Industries. The material used is Torayca 3900 series which is a highly toughened carbon fiber-reinforced epoxy prepreg for the primary structures. The advantages of the use of composites are not limited to weight/economy benefits but extends to improved cabin pressure, bigger windows, less corrosion, and extended maintenance schedules. The 787 incorporates also key components made with out-of-autoclave molding processes. Cytec Engineered Materials, now part of Solvay, offers a whole range of prepreg systems for out of clave curing ranging from the Cycom 5320 to the MTM series.

Hexcel has several new materials on the 787 as well. One is the HexMC. This product was selected for the 787s larger window frames, which are considered as

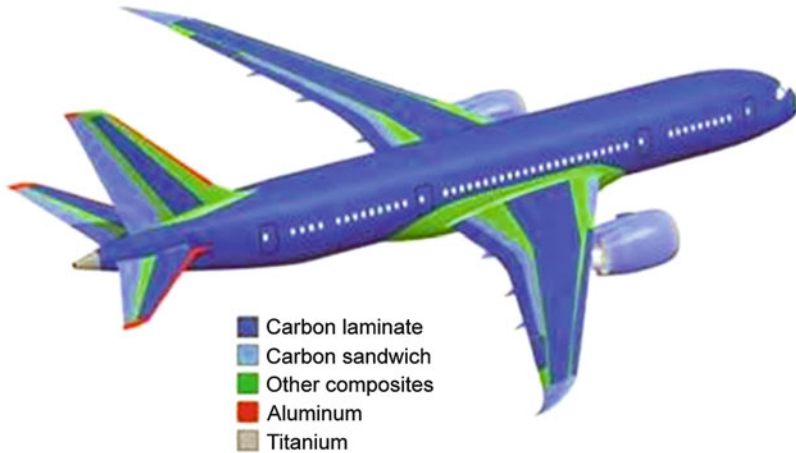


Fig. 5 Boeing 787 “Dreamliner”

Table 3 Impact resistance and failure modes of some CYCOM systems used in racing cars

Resin system	Resin toughness (kJ/m ²)	SEA (J/g)	Predominant micro failure mode	Predominant macro failure mode
977-6	0.64	63	Fiber breakage	Splaying/fragmentation
977-2	0.62	61	Fiber breakage	Splaying/fragmentation
949	0.51	54	Mixed	Splaying
759	0.39	49	Delamination	Splaying
950-1	0.36	48	Delamination	Splaying
5250-4	0.24	44	Delamination	Splaying

primary structure. For other window frames Hexcel proposed the use of the aerospace-qualified 177 °C-cure 8552 epoxy prepreg resin. This system is also used for the engine nacelles made by GE and Rolls Royce. The 8552 epoxy resin is an example of toughened epoxy blend containing aromatic engineering thermoplastic.

The use of toughened thermoset/thermoplastic blends is not limited to aircraft structures. Several applications exist in the field of racing and exotic cars. The crashworthiness is the main benefit offered by these blends in these applications (Lo Faro et al. 2003). The use of high toughness prepreps results in better specific energy absorption as required by FIA (Federation Internationale de l’Automobile) rules. The study by Lo Faro et al. was focused on the effect of prepreg parameters like resin matrix and carbon fiber type on the crush behavior of composite tubes used as crush absorber in F1 cars. The data (Table 3) shows a clear correlation between SEA (Specific Energy Absorption) and resin toughness values. Similar requirements are needed for structures like the nose cone (Fig. 6) and the rear crash structure (Fig. 7).

The use of impact resistant resin is transferred into exotic cars as demonstrated by several applications like Ferrari LaFerrari, Lamborghini Aventador, etc. For the

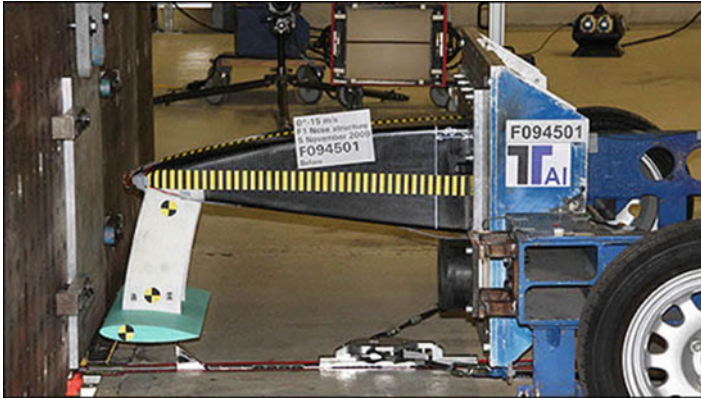
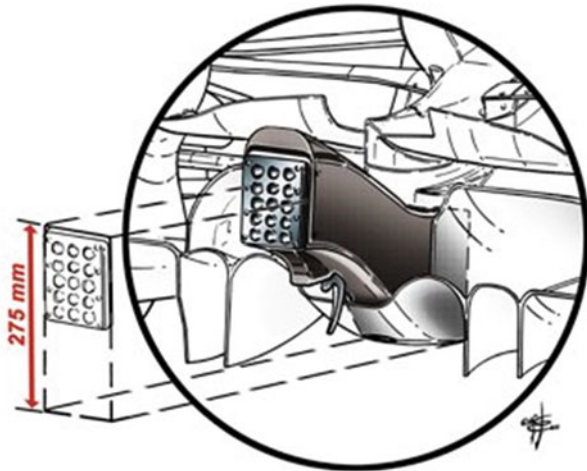


Fig. 6 Impact test for a nose cone made by composite materials (From http://www.formula1-dictionary.net/crash_test.html)

Fig. 7 Rear crash structure made in composites for F1 cars (from http://leonardasfl.narod.ru/F1_Challenge/2011/2011_DEVELOPMENTS.html)



Ferrari “LaFerrari,” Dr. Lo Faro, VP of Cytec, revealed the use of four different types of carbon fiber, all labor-intensively hand-laminated, before being cured in the autoclave (sources <http://www.topgear.com/uk/car-news/new-ferrari-laFerrari-f150-revealed-geneva-2013-03-05>).

Cytec Engineered Materials, now part of Solvay, is one of the leading suppliers of composite materials for the aerospace applications. Its product portfolio (Table 4) includes prepregs and resin systems, adhesives and surfacing, carbon fibers, ancillary materials, tooling portfolio, and process materials.

The CYCOM[®] 977 series, for example, include a number of epoxy prepregs toughened with aromatic thermoplastic. The formulation and structure of this thermoplastic is proprietary but the principle is based on the homogenous uncured blend turning into a phase separated cured blend. The toughening mechanism

Table 4 Overview of commercial polymer matrixes for automotive and aircraft structures

	Features and applications	Processing conditions	Toughness	Service temperature dry [°C]	Out-life at 25 °C
CYCOM 2020	Modified epoxy-based prepreg system which displays excellent retention of mechanical performance at elevated temperatures	10 h at 80 °C + optional 1 h at 150 °C postcure	High	–	8 weeks
CYCOM 759	Modified epoxy prepreg. Provides superb surface finish with good hot/wet performance	14 h at 70 °C	Medium	91	4 weeks
CYCOM 761	Modified epoxy prepreg. Designed for use as thermal barriers (nonload bearing) in motor sport applications	14 h at 79 °C or 45 min at 121 °C	Low	212	2 weeks
CYCOM 919	Modified epoxy prepreg. 919 is widely recognized as the industry standard in race car construction. High toughness with mechanical performance and flame retardant. Self-adhesive with 4 weeks tack life, suitable for sandwich panel construction. Also available in high flow version	1.5 h at 121 °C	Medium	143	4 weeks
CYCOM 950-1	Modified epoxy prepreg. A 121 °C curing system with the performance of a 177 °C curing epoxy. A toughened system exhibiting excellent mechanical properties	2 h at 127 °C	Medium	177	4 weeks
CYCOM 985	Modified epoxy prepreg. Suitable for the manufacture of carbon composite block for use in machining of solid carbon inserts	2 h at 127 °C	Low	193	10 day

(continued)

Table 4 (continued)

	Features and applications	Processing conditions	Toughness	Service temperature dry [°C]	Out-life at 25 °C
CYCOM 977-2	Modified epoxy prepreg. Excellent hot/wet properties. Controlled flow, good surface characteristics	3 h at 177 °C	High	200	10 day
CYCOM 977-6	Modified epoxy prepreg. Excellent hot/wet properties. Also used for primary aircraft structures	2 h at 154 °C	High	180	10 day
CYCOM 5215	Modified epoxy prepreg. Curable at 66°C with only vacuum bag pressure. The cured part will yield <1% void content. Mechanical property and service temperature range equivalent to first generation epoxy prepreg after post-cure at 177°C. The resin can be used for prototyping, repairing, tooling and structural application where controlled cost processing is desired	14 h at 66 °C + 2 h at 177 °C post cure	Low	191	10 day

Table 5 Typical neat resin properties of the CYCOM 977-2 at room temperature

Tensile strength, ksi (MPa)	11.8 ± 1.6 (81.4 ± 11)
Tensile modulus, msi (GPa)	0.51 ± 0.02 (3.52 ± 0.14)
Flexural strength, ksi (MPa)	28.6 ± 1.0 (197 ± 7)
Flexural modulus, msi (GPa)	0.50 ± 0.01 (3.45 ± 0.07)
G _{1C} , in-lb/in ² (J/m ²)	2.73 ± 0.48 (478 ± 84)
K _{1C} , ksi · in ^{1/2} (MPa · m ^{1/2})	1.34 ± 0.15 (1.22 ± 0.14)
T _g , °C (RDS, 10 °C/min)	212
Density, g/cm ³	1.31

works with a cocontinuous morphology and shows excellent impact resistance. CYCOM[®] 977 prepregs are certified both for civil and military aircraft and used for several primary and secondary structures. CYCOM[®] 977-2 is a 177 °C toughened epoxy resin (Table 5). Commercially speaking, it is the most important

977 system, being used for primary structures of commercial and military aircrafts and helicopters.

Most commercial prepregs are formulated to be cured in autoclaves. The autoclave manufacturing has led in the past to very efficient composite and it is a well-consolidated process. However, it has some main drawbacks. The first limitation is the high investment costs required for acquisition of the plant. Then the operation costs and the complexity of tooling have pushed the interest toward out-of-autoclave (OoA) manufacturing. OoA has been developed and suitable prepregs have been introduced leading to parts with autoclave-quality properties, by using vacuum-bag-only (VBO) consolidation. In the VBO prepreg, the fabric is just partially impregnated in order to leave vacuum channels that let air escape during the consolidation in the vacuum bag. In this way, the amount of vacuums is reduced to very low values. Unlike the autoclave process, where the external applied pressure (≈ 7 atms) prevents the formation of volatile gasses leaving them dissolved in the resin, the VBO process works with only 1 atm. This means that all the volatile gasses must be taken out before the resin starts curing. The laminate composites produced from VBO prepregs have shown fiber volume content of about 65% for UD tapes and of about 55% for fabrics (Cytec Engineered Materials). This is the main way to reduced operation costs since only conventional ovens and heating toolings are needed.

Among the resins for OoA Cytec's CYCOM[®] 5320-1 OoA prepreg is a toughened epoxy prepreg system. It can be processed by vacuum-bag-only but its performances are equivalent to primary-structure-capable autoclaved prepregs (Table 6). The system is characterized by a very low porosity. With a wet glass transition temperature of 163 °C, an average water uptake of 0.55 wt%, and because of its low temperature curing capability, it is also suitable for prototyping where low cost tooling or vacuum-bag-only curing is desired.

However, one main drawback of adding a toughening agent to epoxies is the very high increases of the resin's viscosity. This makes most of the toughened commercial prepregs unsuitable for infusion techniques. To overcome such limitation, Cytec has developed the PRIFORM[®] technology. Manufacturing primary structure composite parts through liquid resin infusion requires the addition of the toughening agents to resin to assure performance standards are met. In Cytec's PRIFORM, the toughening agent is not blended with the resin but is woven into the textile preform. Figure 8 puts on evidence the scheme of the Priform fabric principle, showing the warp and

Table 6 Resin characteristics of the CYCOM 5320-1

Shelf life	1 year at < 10 °F (− 12 °C)
Tack life	20 days at room temperature
Shop life	30 days minimum at room temperature
Cured resin density, g/cm ³	1.31
Wet glass transition temperature, °F (°C) ^a	324 (163)
Average moisture uptake, wt% ^b	0.55

^aExposure: 24-h water boil; Test method: DMA, E'

^bExposure: 48-h water boil; Dry at 250 °F (121 °C) for 24 h.

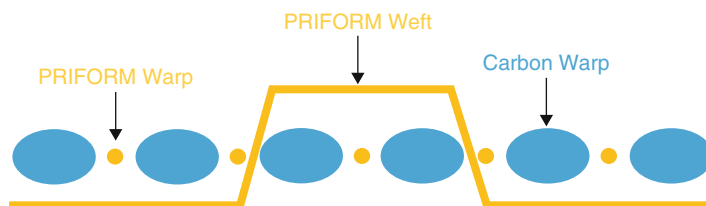


Fig. 8 Scheme of the PRIFORM's weaving

Table 7 PRISM EP2400 neat resin characteristics

Property	Specimen conditioning	Value
Cured resin density, g/cm ³ (lb/ft ³)	Room temperature, Dry	1.24 (77.4)
Tensile strength, MPa (ksi)	Room temperature, Dry	95 (13.8)
Tensile modulus GPa, (msi)	Room temperature, Dry	3.4 (0.49)
Tensile strain, %	Room temperature, Dry	7.2
Flexural strength, MPa (ksi)	Room temperature, Dry	164 (23.8)
Flexural modulus, GPa (msi)	Room temperature, Dry	3.6 (0.52)
Strain energy release, GIC, J m ⁻²	Room temperature, Dry	279
Fracture toughness, KIC, MPa m ^{1/2}	Room temperature, Dry	0.96
CTE, ×10 ⁻⁶ C ⁻¹	Room temperature, Dry	60.5
T _g , °C (°F)	Room temperature, Dry	179 (354)
T _g , °C (°F)	Wet, 48 h water boil	163 (325)

the weft of the thermoplastic woven together among the carbon fibers. This solution allows resin infusion. The thermoplastic filaments are designed to be soluble in the resin at certain temperatures giving raise to homogeneous dispersion in the epoxy first and, secondly, to phase separation. This unconventional approach leads to excellent structural performance coupled with infusion processability. The use of Priform in some airbus center fittings led to the international JEC awards for Cytec. The Priform technology has also some relevant side applications due to the self-binding aspect of PRIFORM reinforcements. This means that the soluble fibers dispersed in the Priform fabrics can replace the use of binders helping to stabilize and process high quality preforms.

Cytec's PRISM[®] resin infusion systems represent a new step in to the resin infusion capability, delivering primary structure level performance without limitation in reinforcement or processing type. PRISM[™] EP2400 is a single part, 180 °C curing, toughened liquid epoxy resin system offering simple and flexible processing with the damage tolerance required for composite primary and secondary structure. PRISM EP2400 offers a dry T_g of 179 °C and an exceptional wet T_g of 163 °C following a 2 h cure at 180 °C. It shows also very good mechanical properties, like a flexural strength of 164 MPa, flexural modulus of 3.6 GPa, and a fracture toughness of 279 Jm⁻². More characteristics of the neat resin are reported in Table 7.

As already said, aerospace is not the only application field for toughened epoxy. The serial automotive market needs light-weight, low-temperature, press-curable

Table 8 Physical properties of MTM45-1

Test	Sample/test conditions	Results
Cured resin density	2 h at 180 °C	1.18 g/cm ³
DMA E' onset T _g , SACMA	2 h at 180 °C, dry 2 h at 180 °C, wet ^a	180 °C 160 °C
Resin gel time	At 80 °C At 130 °C At 180 °C	16.5 h 90 min 10 min

^aWet – 14 days immersion in water at 70 °C

materials to meet legislative requirements for lower emissions, high safety, and end-of-life recycling (Centea et al. 2015).

MTM[®]45-1 is a flexible curing temperature, high performance toughened epoxy matrix system optimized for low pressure, vacuum bag processing. This system offers a combination of properties (Table 8) that make it an ideal candidate for the OoA production. A whole range of the products available for OoA is presented in Table 9.

The other big player for epoxy/thermoplastic for composites is the French company Hexcel. This company provides a wide range of prepregs for civil aircraft, military jets, helicopters, aeroengines or space satellite and launchers. Its range of resin formulations for aerospace prepregs includes a wide range of epoxies for highly loaded parts and toughness (Table 10).

HexPly M91 is the very latest aerospace primary structure prepreg from Hexcel. With excellent toughness including very high residual compression after impact (see Table 11), HexPly M91 can meet the growing needs of aerospace industry to manufacture lighter, faster, and more efficient aircraft. This system is also suitable to be processed with both automated tape laying (ATL) and advanced fiber placement (AFP). These processing technologies are the choice to manufacture big composite parts like the three sectors of the 787 fuselage.

Another widely commercialized system is the HexPly[®] 8552. HexPly[®] 8552 is a high performance tough epoxy matrix for use in primary aerospace structures. It exhibits good impact resistance and damage tolerance for a wide range of applications. It is an amine cured, toughened epoxy resin system supplied with unidirectional or woven carbon or glass fibers. The typical neat resin data are reported in Table 12.

Toray Group is the Japanese company that developed one of the most used thermoplastic/epoxy blend based on preformed particles. The full commercial product, T800H/3900-2, has heterogeneous interlayer including fine thermoplastic particles (Fig. 9), and it is used in the primary structures of Boeing 777.

Adhesive Bonding

One drawback about composites is their cost of manufacturing and assembly. This is basically a problem for high volume production. In particular, the joining cost of composite components is one of the major cost drivers. One way to reduce cost of

Table 9 Current-generation aerospace grade OoA/VBO prepreg resin systems

Manufacturer	Resin family	Resin type	Description
ACG (now Cytec)	MTM44-1 MTM45-1 MTM45-1FR MTM47-1	Epoxy Epoxy Epoxy Epoxy	Medium temperature molding (MTM) toughened epoxy. Qualified by Airbus for secondary and tertiary structure Lower temperature cure system optimized for compression performance Variant of MTM45-1 optimized for flame retardation Variant of MTM45-1 optimized for hot/wet notched performance up to 130 °C
Cytec	Cycom 5320 Cycom 5320-1	Epoxy Epoxy	Toughened epoxy designed for primary structure application Variation on 5320 system, formulated for increased out life
Gurit	Sprint ST94	Epoxy	Single-sided moulding prepreg for parts requiring resistance to impact damage and microcracking
Hexcel	Hexply M56	Epoxy	High performance VBO epoxy system
Toray	2510	Epoxy	Formulated to meet the requirements of general aviation primary structure
Tencate	BT250E TC250 TC275 TC350-1 TC420 TC800 BMI	Epoxy Epoxy Epoxy Epoxy Cyanate ester Bismaleimide	Standard VBO system used in Cirrus aircraft and unmanned vehicles. Variations for fatigue and fracture resistance for helicopter rotor blades Second generation VBO system with increased toughness and higher service temperatures Third generation system with greater inspectability, resistance to hot/wet conditioning, and curable at 135 °C Third generation system with increased out life (45+ days), high toughness, and ability to cure at 135 °C with 177 °C required postcure High temperature system (service temperatures up to 315 °C) High-temperature, toughened BMI prepreg formulated for cure out-of-autoclave
Henkel	Loctite BZ	Benzoxazine	VBO prepreg based on a blended epoxy-benzoxazine resin formulation

production is to apply specific joining technologies. Using epoxies as adhesive bonding is the main way to assemble composite components. Mechanical fastening, adhesive bonding, and fusion bonding (welding) are the other developed joining technologies.

The disadvantages of epoxies as adhesive bonding are the need for surface preparation and, sometimes, long curing time. Composite welding is carried out by melting a thermoplastic polymer using it as adhesive. Usually a pretreatment of surfaces is needed. By doing this, it is possible to achieve a very performant joint for

Table 10 Main commercially available Hexcel's toughened systems

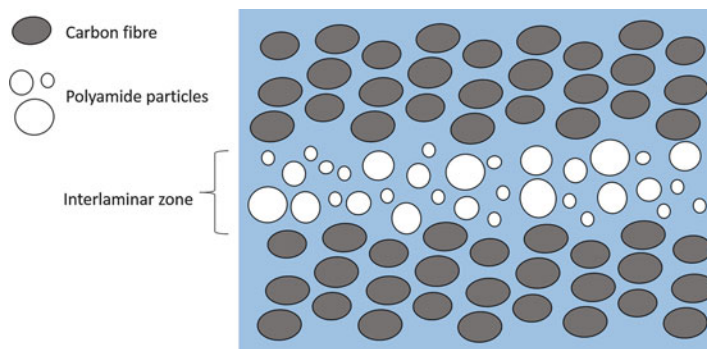
Hexply resin system	Attributes	Typical application	Commercial aircraft	Interiors	Helicopters	Military jets	Nacelles engines	Space	Uav's
M26T	Self adhesives, self extinguishing	Fairings / sandwich structures	✓		✓				
M76	High toughness, self adhesive, flexible cure	Space applications	✓					✓	
913	Versatile system with high environmental resistance	Structural components / fairings / helicopter blades	✓		✓				✓
M92	Self adhesive, self extinguishing versatile system with high environmental resistance	Fairings / sandwich structures / structural components	✓		✓				
M20	High temperature performance from low temperature cure	Composite repair	✓			✓			
8551-7	Extreme damage resistance, very high toughness	Structural components / engine parts / fan blades	✓				✓		
M91	Latest product for aerospace structure and aeroengine, excellent toughness with very high residual compression strength after impact	Aircraft and aeroengine primary structure	✓				✓		
M21	Preferred product for aerospace structures, high toughness, and excellent translation of IM fiber	Primary structure	✓				✓		
8552	Preferred product for aerospace structures	Structural parts	✓		✓	✓	✓	✓	

Table 11 Mechanical properties of Hexcel's M91

Mechanical properties	Units	Temp °C	M91/34%/UD194/IM10-12 K
T_g	°C		185–190
Tensile strength	MPa	23	3520
Tensile modulus	GPa	23	176
Compression strength	MPa	23	1880
Compression modulus	GPa	23	156
ILSS	MPa	23	105
CAI @ 30.5 J	MPa	23	350

Table 12 Hexcel's 8552 neat resin properties

Color	Yellow
Density	1.301 g/cm ³
Glass transition temperature, T_g dry	200 °C
Glass transition temperature, T_g wet	154 °C
Tensile strength	121 MPa
Tensile modulus	4670 MPa

**Fig. 9** Interlaminar toughening particles at interlayer region for T800H3900-2 laminates (schematic drawing)

composites, even better than adhesively bonded or mechanically fastened joints. Unfortunately, because of cross-linked nature, it is not possible to apply welding directly onto the thermoset surface of the composite. The use of a thermoplastic-thermoset blend as adhesive is a solution to indirectly overcome this issue, otherwise it is also possible to use a thermoplastic film incorporated onto the cured thermoset surface. The thermoplastic and thermoset polymers partially blend before totally curing the thermoset resin. This leads to a thermoset surface with a thermoplastic attached on it. Therefore, it is possible to achieve fusion bonding of thermoset composites by means of various methods. The simultaneous application of heating and pressure, for example, causes the thermoplastic layers to soften, leading to a better contact between the adherent surfaces. Temperature also allows the thermoplastic chains to interdiffuse across the contact area thus leading to the disappearance of the interface due to the

chains' interdiffusion. This process leads to the strong welding of the surface layers forming a strong joint with less sensitivity to aggressive environments.

Cytec is among the world-leading suppliers of top quality adhesives specifically designed for bonding composites. Its products are qualified for use on aircrafts, having a portfolio ranging from high-performance adhesives to surfacing films and primers in a variety of product forms to enable manufacturing flexibility. Cytec's aerospace adhesives and surfacing portfolio includes:

- Adhesives for aerospace
- Composite surfacing films
- Foam cores and potting compounds
- Sealants, fire resistant
- Primers

HT[®] 424 is an aluminum-filled, modified epoxy-phenolic resin coated on a glass carrier which meets the federal and military requirements. It was developed for bonding metal-to-metal and sandwich composite structures requiring long-term exposure to 149 °C and short-term exposure to 260 °C. HT 424 has adaptability to many bonding procedures. FM[®] 300, which is one of the bestselling product, is a toughened epoxy film adhesive available with different polyester carriers. It is designed for bonding metal-to-metal and sandwich composite structures. FM 300 has unique properties that drastically reduce time-consuming sanding and filling operations. Moreover, it has high elongation and toughness with high ultimate shear strength. This makes it particularly suitable for redistributing the high shear stress concentrations of graphite epoxy-to-metal bonds, and allows it to accommodate the low interlaminar shear strength of the composite. It is particularly good in fatigue resistance in these joints. Table 13 shows some properties of the FM 300 adhesive.

Hexcel formulates and manufactures a comprehensive range of structural film adhesives too. The Redux[®] film adhesives range includes epoxy, phenolic, and bismaleimide (BMI) adhesives. The cured adhesives form a permanent structural bond which is able to withstand harsh environments, including elevated temperatures. The range includes adhesives for metal-to-metal and composite bonding which find wide application in transportation, recreation, and construction industries.

Redux 319, an hot melt film, is a high performance modified epoxy film adhesive curing at 175 °C. It is available in both supported and unsupported versions at areal weights between 180 and 400 g/m². The supported versions contain a woven nylon carrier for glueline thickness control and improved handle ability. Redux 319 is free from solvents and consequently it has a very low volatile content.

Future Applications

Self-healing materials are defined as those that have properties of repairing themselves after a damage has occurred, without losing their main functionalities. The growing interest in the development of polymer nanocomposites with enhanced

Table 13 Properties of the FM 300 adhesive

Product number	Weight, psf (gsm) ^a	Nominal thickness, inches (mm)	Color	Carrier	Characteristics
FM 300 film adhesive	0.08 (390) 0.10 (490)	0.013 (0.32) 0.015 (0.38)	Blue Blue	Tight knit	Enhanced bondline thickness control. Good blend of structural and handling properties
FM 300 K film adhesive	0.05 (244) 0.08 (390)	0.008 (0.20) 0.013 (0.32)	Green Green	Wide open knit	Highest overall performance
FM 300 M film adhesive	0.03 (150) 0.08 (390)	0.005 (0.13) 0.013 (0.32)	Green Green	Random mat	Provides the best bondline and flow control. Reduces tendency to trap air during layup
FM 300U film adhesive	0.03 (150) 0.055 (268)	0.005 (0.13) 0.008 (0.20)	Green Green	Unsupported film	Can be reticulated

^aWeight tolerance equals nominal weight ± 0.005 psf (± 25 gsm)

performance is parallel to the increasing number of applications of neat polymers or polymer matrix composites. Damage and failure are unavoidable in material lives thus the damage resistance is one of the main topics to address in material development. Among thermoset materials, epoxy resins present a number of well-known advantages including high electrical resistance and thermal stability and ease of fabrication but, as outlined before, brittleness is one of their main drawbacks. Epoxy resins are used in applications ranging from electric and electronic devices to automotive parts, aircraft components, biocompatible implants, protective coatings, and adhesives. All these applications lead material to experience cyclic loads and requires, in many case, tribological good behavior. The tribological performance of epoxy resins are extremely poor due to their inherent brittleness and lack of self-lubricating behavior. The severe wear, due to crack propagation and fracture under sliding conditions, can lead to premature and catastrophic failure which must be avoided. The presence of cracks or defects in biological materials (like human tissues for example) activates healing mechanism which extends the useful life of the material itself. Similar approaches are to be transferred in engineering materials in order to reduce damage during use.

Self-healing materials exhibit the ability to repair themselves and to recover functionality using the resources inherently available to them. Whether the repair process is autonomic or externally assisted, the recovery process is activated by damage to the material. Self-healing materials aim to offer a new route toward safer, longer-lasting products and components.

Brostow et al. (2002) described the increase in scratch recovery of epoxy resin by the addition of a fluoropolymer. There exist numerous precedents (Yuan et al. 2008;

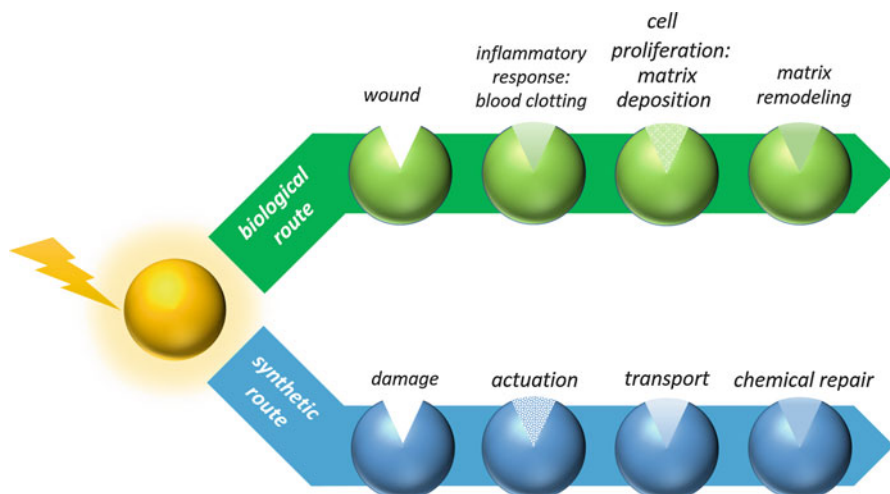


Fig. 10 Autonomic healing (i.e., syntetich route) mimics the biological route of wound healing. Damages in the matrix can break the microcapsules, releasing the healing agent into the crack plane through capillary action (transport). The healing agent bonds the crack repairing the material

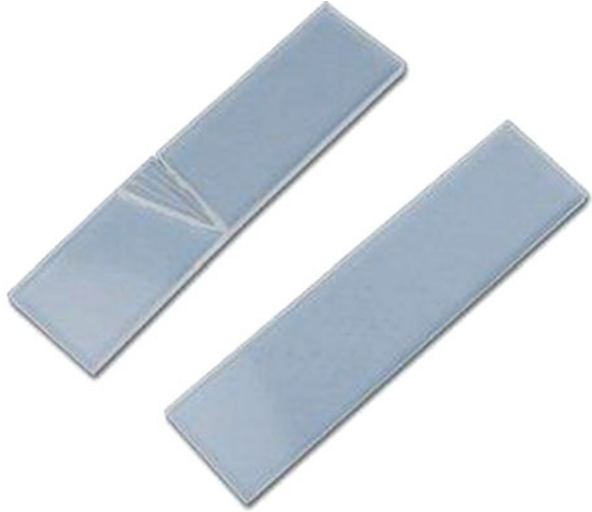
Ratna and Karger-Kocsis (2008) of self-repairing or self-healing epoxy resin systems, usually by the addition of encapsulated curing agents which tend to be released from the microencapsulating capsules in the presence of fracture cracks, following the mechanism described in Fig. 10.

Liu et al. (2012) demonstrated that it is possible to achieve self-healing properties by introducing epoxy microcapsules containing a healing agent into an epoxy resin. The microcapsules were introduced by simply dispersion into the resin at ambient temperature. These microcapsules, made by interfacial polymerization of epoxy resin droplets with ethylenediamine, can be broken by the propagation of a crack. This is very useful for coatings, so that when surfaces are scratched, the microcapsules break and release the healing agent repairing the composite material. The experimental results showed that the artificial scratches were successfully healed in about 4 h after made. The self-healing coatings loaded with epoxy microcapsules are promising for applications in the coatings and the self-healing coatings but, as reported in the following, other approaches well designed for composite laminates as well have been studied.

Epoxy/thermoplastic blend with self-healing properties have been reported. For example, Fejős et al. (2013) studied epoxy/polycaprolactone (PCL) systems with triple-shape memory effect. To set the temporary shapes, the glass transition temperature (T_g) of the epoxide and the melting temperature (T_m) of PCL were used for the shape memory cycle. This approach has the merit to use epoxy/thermoplastic blends thus ensuring a uniform dispersion of the healing agent (i.e., the PCL) rather than confining it into localized microcapsules.

The Cornerstone Research Group (<http://www.crgroup.com>) developed a self-healing version of shape memory polymer (SMP) called Veriflex[®] EH (Fig. 11).

Fig. 11 Damaged (*top*) and self-healed Veriflex EH epoxy



This healable SMP resin was tested to increase survivability for manned and unmanned air vehicles, spacecraft, habitats for space exploration missions, automobiles, and more.

Veriflex EH is an epoxy-based resin that will be a direct replacement for current aerospace-grade epoxy resins. Veriflex EH is available in grades that can be processed using vacuum-assisted resin transfer molding, resin transfer molding, or wet lay-up techniques. Veriflex EH uses two healing mechanisms to restore up to 85% of original mechanical performance. The first healing mechanism, shape recovery, brings the cracked or damaged area back into intimate physical contact. The second healing mechanism, polymer diffusion, allows long polymer chains to diffuse across the failure line and restore mechanical integrity. Both healing mechanisms are thermally activated and are achieved in less than 3 min. The system is claimed to reach 85% recovery of flexural strength. Further details on the composition of the Veriflex systems are not disclosed by the company for intellectual property (IP) reasons. However, the self healing mechanism, such as described, resembles those found for epoxy/thermoplastic blends described in the literature.

Such developments are relevant in the field of epoxy/thermoplastic blends because, as noted by Prof. Ratna and Prof. Karger-Kocsis, “by creating a semi-interpenetrating network composed of a crosslinked thermoset and a thermoplastic, both shape memory and self-healing functions can be combined (Ratna and Karger-Kocsis 2008). In such an intelligent material, the thermoplastic polymer (amorphous or semicrystalline) could offer “switching” and “healing” effects, whereas the crosslinked thermoset could act as the fixing phase.”

The development of shape memory epoxy/thermoplastic blends might be of interest in composite processing technology. The Veriflex system, for example, was developed to allow easy demolding of complex composite parts by using the shape memory effects. Thermal shape memory effect (Fig. 12) is the property of

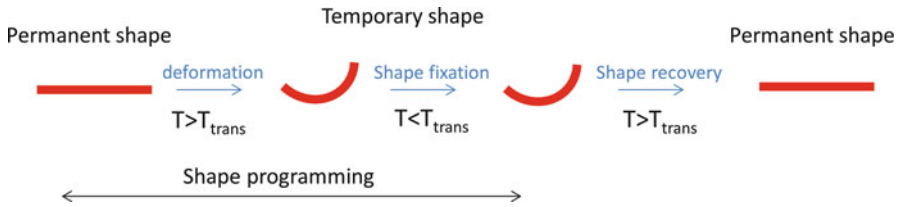


Fig. 12 Thermally induced shape memory effect

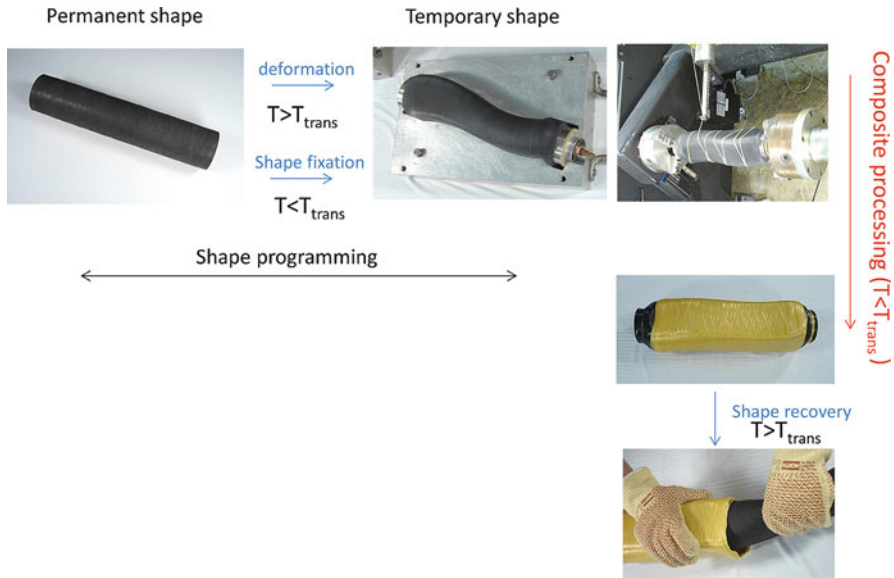


Fig. 13 Application of thermally induced shape memory effects for smart mandrels used in composites processing as introduced by Spintech LLC (photos adapted from <http://www.smarttooling.com/investigate/smart-mandrels>)

certain material to recover their original shape (i.e., permanent) when a different shape (i.e., temporary) is induced by a deformation applied at temperatures over the so-called transition temperature. The shape recovery is induced by heating the material over its transition temperature. The thermal shape memory effects is at the working principle for the Smart Mandrel epoxy composites developed by Spintech llc (<http://spintechllc.com/smart-tooling>) (Fig. 13).

Conclusions

The present chapter offered an updated overview of the applications and drawbacks of epoxy/thermoplastic blends. The development of epoxy/thermoplastic blends dates back to 1980s, but their use is widespread today in advanced applications.

The benefits of adding a thermoplastic phase to epoxy were demonstrated to rely on the combination of good toughness increments with overall good thermal and solvent resistance. In the application paragraphs, many examples of commercial systems which rely on epoxy/thermoplastic blending were presented giving references of their practical uses in aircraft structures and automotive applications.

Despite being a well-consolidated novel application field for epoxy/thermoplastic blends are still emerging. For example, the use for smart self-healing or shape memory systems. Such novel systems might find applications in several different fields ranging from structural composites to intelligent materials. Shape memory blends were discussed as a fruitful example of application of blends for novel processing methods.

References

- Brostow W, Bujard B, Cassidy PE, Hagg HE, Montemartini PE (2002) Effects of fluoropolymer addition to an epoxy on scratch depth and recovery. *Mater Res Innov* 6:7–12
- Centea T, Grunenfelder LK, Nutt SR (2015) A review of out-of-autoclave prepregs – material properties, process phenomena, and manufacturing considerations. *Compo Part A* 70:132–154
- Cicala G, Lo Faro C (2012) Polymeric matrixes: materials type and modification strategies. In: *Wiley encyclopedia of composites*. Wiley
- Cytec Engineered Materials, Unpublished data
- Fejős M, Molnár K, Karger-Kocsis J (2013) Epoxy/polycaprolactone systems with triple-shape memory effect: electrospun nanoweb with and without graphene versus co-continuous morphology. *Materials* 6:4489–4504
- Liu XX, Zhang HR, Wang JX, Wang Z, Wang SC (2012) Preparation of epoxy microcapsule based self-healing coatings and their behavior. *Surf Coat Technol* 206:4976–4980
- Lo Faro C, Cicala G, Recca A, Sanders D (2003) Crash behaviour of composite materials: a DOE and fracture mechanics approach. In: *Sampe international conference 2003*, Paris
- Lucas JC, Borrajo J, Williams RJJ (1993) Cure of unsaturated polyester resins: 2. Influence of low-profile additives and fillers on the polymerization reaction, mechanical properties and surface rugosities, *Polymer* 34:1886
- Prime RB (1997) *Thermoset*. In: Turi EA (ed) *Thermal characterization of polymeric materials*, 2nd edn. Academic, San Diego
- Ratna D, Karger-Kocsis J (2008) Recent advances in shape memory polymers and composites: a review. *J Mater Sci* 43:254–269
- Vendersbosch RW, Meijer HEH (1997) Processing of polymers using reactive solvents. In: Cahn RW, Haase P, Kramer EJ (eds) *Material science and technology*, vol. 18. Processing of polymers. Wiley-VCH-Weinheim, New York
- Williams RJJ, Rozenberg BA, Pascault JP (1997) Reaction-induced phase separation in modified thermosetting polymers. *Adv Poly Sci* 128:95
- Yee AF, Du J, Thouless MD (2000) Toughening of epoxies in polymer blends, vol 2. Wiley, New York, p 225
- Yuan YC, Yin T, Rong MZ, Zhang MQ (2008) Self healing in polymers and polymer composites. Concepts, realization and outlook: a review *eXPRESS. Polym Lett* 2:238–258

pVT Analysis of the Effect of Addition of Thermoplastics, Block-Copolymers, or Rubbers on the Curing Behavior and Shrinkage of Epoxy Resins

27

Jürgen Pionteck

Abstract

During curing of epoxy resins shrinkage of the material appears. As long the resin is in the liquid or gel state, the material can easily relax and no stresses appear caused by shrinkage. After vitrification, the mobility of the polymer units is hampered and internal stresses develop. Thus, the shrinkage may cause problems during processing and in the final properties and application. One strategy to reduce the shrinkage is the addition of nonshrinking additives. Favorable is the addition of thermoplastics or rubbers, which in addition to the reduction of cure shrinkage often exhibit a toughening effect to the material. This chapter focuses on the influence of added thermoplastics, hyperbranched polymers, block-copolymers, or rubbers on the cure shrinkage and kinetics. The efficiency of the additives in reduction of shrinkage depends not only on their type and amount but also on their reactivity and the morphology of the blends which develops during the cure process. Beside the shrinkage, also other volumetric properties are discussed like changes in the thermal expansivity.

Keywords

Epoxy blends • pVT analysis • Rubbers • Thermoplastics • Volume shrinkage

Contents

Introduction	800
Cure Shrinkage of Epoxy Resins	801
Methods to Analyze Cure Shrinkage	804
Modification of Cure Shrinkage Due to Addition of Thermoplastics	809
Modification of Cure Shrinkage Due to Addition of Hyperbranched Polymers and Star Polymers	812
Modification of Cure Shrinkage Due to Addition of Rubbers	814

J. Pionteck (✉)

Leibniz-Institut für Polymerforschung Dresden e.V., Dresden, Germany

e-mail: pionteck@ifdd.de

© Springer International Publishing AG 2017

J. Parameswaranpillai et al. (eds.), *Handbook of Epoxy Blends*,

DOI 10.1007/978-3-319-40043-3_44

799

Modification of Cure Shrinkage Due to Addition of Block-Copolymers	819
Conclusions	820
References	821

Introduction

Beside all the advantageous properties of epoxy thermosets one major drawback is their shrinkage during cure, which can be detrimental in processing and application of thermosets. When one discusses shrinkage the type of shrinkage has to be defined. Chemical shrinkage starts directly with starting the cure reaction. As long as the resin is in the liquid or gel state, the material easily can relax and no stress develops. However, after gel formation and especially after vitrification, when the glass transition temperature T_g raises above the cure temperature T_{cure} , the growing polymer network cannot relax completely and internal stresses develop. The volumetric material properties are not in equilibrium and the specific volume V_{sp} becomes more or less frozen, thus V_{sp} may not correlate to the network density anymore. The stress which is created during chemical shrinkage after gelation and vitrification can cause serious problems in dimensional accuracy and stability of epoxides and its composites, in surface quality of coatings, or the performance of joints when epoxides are used as adhesives. Post annealing can be helpful to heal up some stresses, but it may also alter the network structure.

Furthermore, during cure also the thermal expansivity and the compressibility will reduce compared to the noncured resin, properties which are very important in application as composites material, coatings, adhesives, etc. Thus, also during cooling from the cure temperature to room temperature and during application at changing outer conditions, stress will develop when the thermal expansion coefficient α and compressibility κ do not fit to the other components in the final application as coatings, laminates, or composites, where warpage and delamination are serious problems. Thus, it is often necessary to reduce the shrinkage below a certain degree or to fit it to certain values.

Since the cure shrinkage, gelation, and vitrification are dependent on the chemical structure of the epoxy resin, the content of reacting sites and cure mechanism and conditions, the choice of proper epoxy system is the easiest way to control the volumetric properties (Klaus and Knowles 1966). In general, as lower the content of reacting sites is, as lower is the shrinkage, and less crosslinked systems exhibit better ductility. Otherwise, low crosslink density results in lower T_g , lower heat deflection temperature, reduced heat stability, as well as lower moduli and strength. On the other hand, highly crosslinked epoxy resins are often very brittle, and they may even break already at very small deformations.

To overcome this dilemma, different strategies have been developed. A simple approach is the partly substitution of resin with inert compounds like fillers or flexibilizing agents, which do not participate at cure shrinkage. In a first approximation, the overall shrinkage follows the additivity rule. In this regard, the use of

nonreactive rubbers or thermoplastics, which can act parallel as toughener, is very successful.

In this chapter, the effect of addition of such modifiers on the curing behavior of epoxides, the cure mechanism, kinetics, and the final shrinkage and volumetric properties will be discussed in detail and correlated to the morphology development and some final thermal and mechanical properties of the epoxy blends containing rubbers or thermoplastics including block-copolymers and hyperbranched polymers.

Cure Shrinkage of Epoxy Resins

During cure, epoxy resins undergo polymerization and crosslinking reactions and shrinkage occurs. The cure shrinkage of epoxy resins is caused by the ring opening of oxirane rings of the resin and its reaction with hydrogen active hardeners like alcohols, phenols, amines, carboxylic acids, and others (Scheme 1). Also the catalyzed homopolymerization under the formation of ether bonds results in shrinkage.

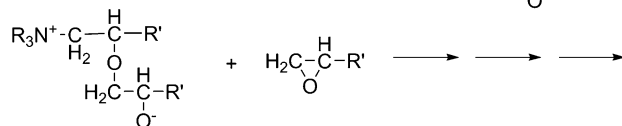
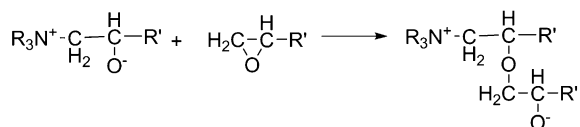
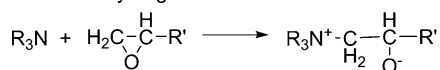
Generally, it is believed that the reason for the shrinkage is the replacement of secondary van der Waals bonds of around 0.2–0.5 nm by primary covalent C–O or C–N bonds with bonding lengths of around 0.14 nm (Haynes 2016–2017). The van der Waals radius of atoms is determined by the outer electron shell. When atoms approach each other, the sum of the van der Waals radii determines their closest distance. This distance reduces when a chemical reaction occurs under formation of covalent bonds. Similarly, the van der Waals volume of two molecules reduces when they react with each other.

The van der Waals volumes V_W , which can be calculated from group additive methods (Van Krevelen and te Nijenhuis 2009; Barton 1991), of the reacting functionalities of the epoxy resin (oxirane ring) and hardeners and the resulting new structures in the coupling product (see Scheme 1) are not changing within the accuracy limit of the method. However, calculations of the overall volume of the corresponding chemical structures before and after reaction by the group contribution parameters, given in (Fedors 1974) for liquids at room temperature, result in a strong loss in molar volume.

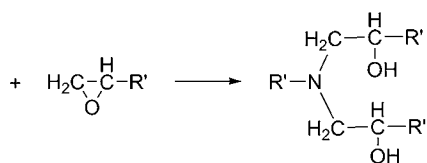
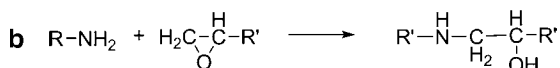
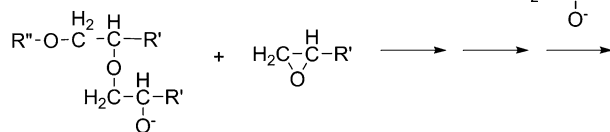
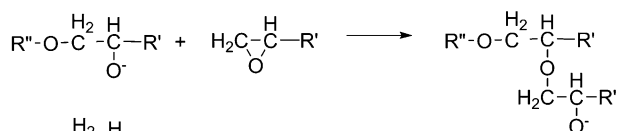
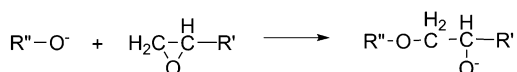
The shrinkage during polymerization and crosslinking comes mainly from changes in the free volume. Scheme 2 presents a draft of the composition of the volume of polymers in dependence on glass transition temperature T_g . The van der Waals volume is under normal thermal energy impenetrable by other molecules and nearly independent of temperature and is closely related to the volume at $T = 0$ K. Thus, the macroscopic volume at $T = 0$ K consist of the van der Waals volume and an interstitial free volume V_{if} , that is free volume existing in between the molecules due to geometric reasons even when perfect packing the molecules like in crystals ($V_{c(T=0K)}$) (Van Krevelen and te Nijenhuis 2009):

$$\frac{V_{(T=0K)}}{V_W} \cong \frac{V_{c(T=0K)}}{V_W} \cong 1.3 \quad (1)$$

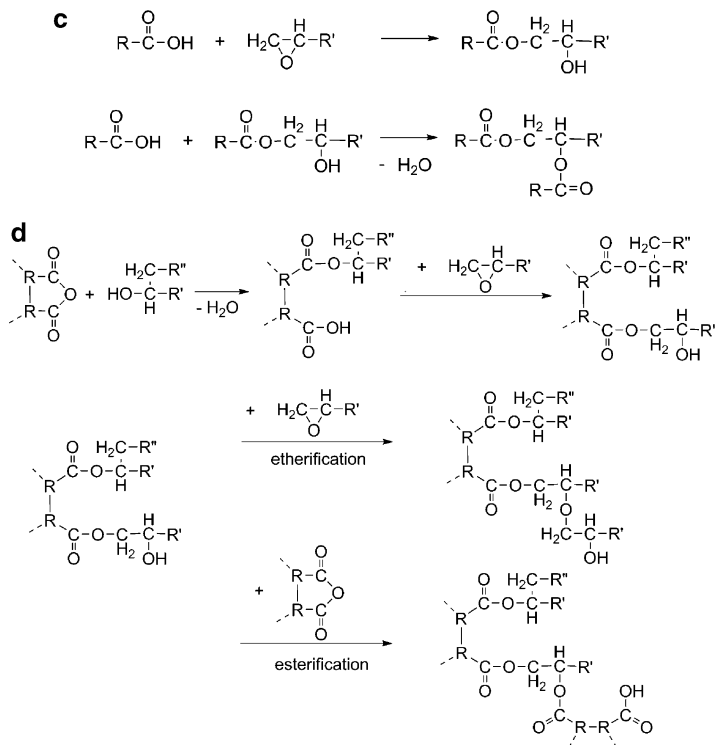
a Without hydrogen donors



In presence of hydrogen donors

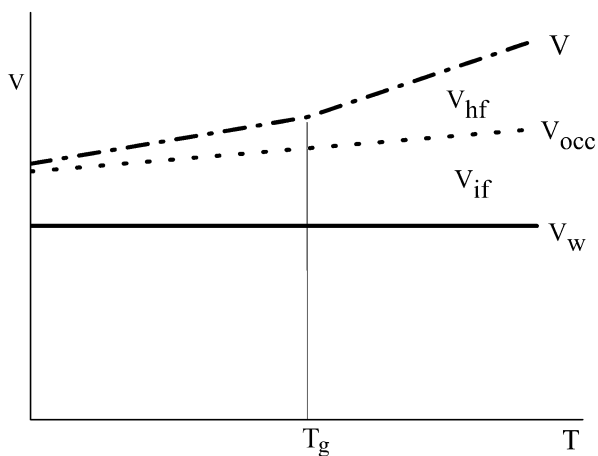


Scheme 1 (continued)



Scheme 1 Typical curing reactions of epoxy resins (a) Catalyzed homopolymerization. (b) Primary amines. (c) Carboxylic acids. (d) Carboxylic acid anhydrides

Scheme 2 Schematic presentation of contribution of free volume V_f to overall volume V



With raising temperature the interstitial volume increases slightly. In addition an excess volume, the so-called hole free volume V_{hf} , develops, resulting from static or dynamic disorder of the molecules. Thus, V is the sum of the occupied volume V_{occ} plus the hole free volume V_{hf} :

$$V = V_W + V_{if} + V_{hf} = V_{occ} + V_{hf} \quad (2)$$

At T_g the slope of the V-T dependence changes to higher value, and the gain in volume due to temperature increase is dominated by the gain in hole free volume. In (Dlubek et al. 2006, 2007) the free and occupied volumes of the diglycidyl ether of bisphenol A (DGEBA) monomer and a DGEBA oligomer are compared, clearly showing that the difference in specific volume because of polymerization comes from changes in free volume, which also dominates the thermal expansion and compressibility of the material above glass transition. The reduction in the free volume finally correlates with the transition from liquid/rubbery state of the noncured/partially cured resin to the glassy state of the cured epoxy resin.

In Fig. 1a, a simplified presentation of volume changes during typical curing regimes is given. When heating the noncured resin from room temperature RT to the curing temperature T_{cure} , the volume (please note that this presentation is independent of the use of absolute or specific volumes) increases from $V_{noncured}$ at RT to $V_{noncured}$ at T_{cure} due to thermal expansion. At T_{cure} the chemical shrinkage occurs reducing the volume to V_{cured} at T_{cure} . This shrinkage is the real chemical shrinkage. When cooling now thermal contraction results eventually in V_{cured} at RT. Considering only the volume values at room temperature, the cure shrinkage is underestimated since the thermal expansivity of the cured sample is much reduced compared to the noncured resin (Kulawik et al. 1989). Thus, when providing data for cure shrinkage always the temperature at which it was measured has to be given. In Li et al. (2004) for a catalyzed system consisting of DGEBA and methyltetrahydrophthalic anhydride values of chemical shrinkage at 100 °C of 6.1% are given, compared to shrinkage of 1.2% measured at room temperature.

The change in the slope in the V-T plot corresponds to the glass transition temperature of the cured sample. In that case during heating the curing starts already, the volume starts to shrink at $T_{cure, onset}$ until complete curing, which can be reached before reaching the actual curing temperature (represented in the plot of Fig. 1a by the filled symbols, adopted from a real experiment) or which can be partially during heating and continues at T_{cure} . In both cases, $V_{noncured}$ will not be reached experimentally. The degree of cure during heating depends on the balance between heating rate and cure kinetics.

Methods to Analyze Cure Shrinkage

The simplest method for analyzing the volume shrinkage ΔV is the determination of the densities of the noncured and cured systems by pycnometric methods. For defined conditions (commonly room temperature and atmospheric pressure), the values of chemical shrinkage can be calculated by

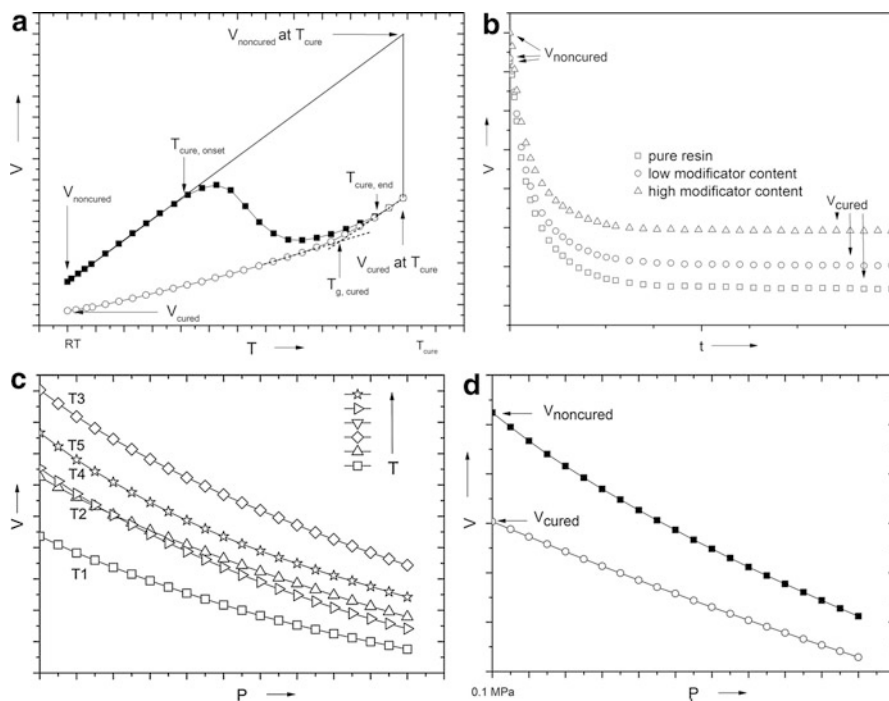


Fig. 1 Progress of volume changes during curing an epoxy resin in different curing regimes. (a) isobaric heating and cooling; (b) isothermal cure of blends with different contents of modifier; (c) isothermal pressurization with stepwise increase of temperature; (d) comparison of compressibility of epoxy resin before and after cure

$$\Delta V_{sp} \text{ (in \%)} = \left(\frac{V_{sp(\text{noncured})} - V_{sp(\text{cured})}}{V_{sp(\text{noncured})}} \right) \times 100 \% \quad (3)$$

Typically, this method does not allow conclusions about the cure kinetics, gelation, or vitrification but can detect different degrees of cure, e.g., due to changing crosslinking conditions. Otherwise, a helium pycnometer was used to follow the cure shrinkage kinetics of an amine-cured epoxy resin at room temperature (Schoch et al. 2004; Shah and Schubel 2010).

Linear or volumetric dilatometry measures changes in the dimension or specific volume caused by shrinkage. Linear dilatometry is often restricted to solid states and standard pressure. Thus, e.g., thermo-mechanical analysis is not applicable to analyze the whole cure process starting from liquid to solid form since always a tiny force is applied to the sample, but after solidification post curing and thermal expansion can be followed reliably (Zarrelli et al. 2002). Optical methods can follow cure shrinkage over the whole process time. All the linear dilatometric methods are very useful for analyzing cure shrinkage in anisotropic systems like coatings, adhesives, or composites, where the shrinkage in one or two dimensions is restricted because of contacts with the substrate or anisotropically dispersed fillers.

To conclude on the volume change of anisotropic materials, the linear dimension changes must be analyzed in two or three directions, depending on the type of anisotropy.

Using pycnometer flasks, Chen et al. investigated the kinetic of shrinkage of an epoxy/caprolactam system by analyzing the density (the inverse of the specific volume) of the mixture in defined time intervals until the resin gelled (Chen et al. 1997). Continuous measurement of volume shrinkage or thermal expansion of a liquid is possible by connecting a reservoir of known dimension to a precise calibrated capillary. The change of the volume of the liquid in dependence on temperature (since also the volume of the reservoir is dependent on temperature, its V-T dependence has to be calibrated) or cure can be read on the scale of the capillary. Of course this method is restricted to the very early stage of cure before viscosity increases too much or vitrification occurs. To overcome this dilemma, the confining liquid technique can be used. In this method, a defined amount of the resin to be analyzed is placed in the reservoir and all the remaining volume is filled with the confining liquid. Necessary conditions are that the liquid is inert to the resin and immiscible and thus any change in volume due to changed temperature and/or cure shrinkage can then be recalculated to the epoxy part. Typically, mercury is used in this technique as confining liquid (mercury dilatometer). All these methods are working typically at standard pressure. In Holst et al. (2005) instead of the capillary dilatometer a calibrated laser dilatometer is used to measure the volume shrinkage of the epoxy resin filled in a cylindrical glass tube (either directly, covered by, or embedded in silicon oil as confining fluid) by accurate determination of the position of the sample surface with time.

Dilatometers of the cylinder-piston type are useful for determination of the pressure influence on volume cure shrinkage and cure kinetics (Holst et al. 2005; Ramos et al. 2005; Nawab et al. 2012). The advantage of this method is the possibility of fast pressurizations of the sample to be analyzed, necessary, e.g., for studying fast kinetics. As long as the material is in the liquid or pasty state, the volume of the resin in dependence on pressure, temperature, and time can be analyzed by determination of the distance of the piston from the bottom of the cylinder with known diameter. The cylinder geometry itself will be affected by T and p changes, and a calibration of the actual cylinder diameter is necessary. After vitrification of the resin, no homogeneous pressurization of the sample is possible anymore and reliable pVT are not accessible. Another problem of cylinder-piston type dilatometers is the possible leakage of material at the piston end which has to be excluded strictly. Contrary to this, the friction between piston and cylinder must be low enough so that the pressure acting on the piston is completely transmitted onto the sample to be analyzed.

Very accurate is the analysis of pVT parameter by means of bellows-type dilatometers like the GNOMIX pVT apparatus, which measure volume changes of a substance directly as a function of temperature, pressure, and time (Zoller 1986; Zoller and Walsh 1995). Since the volume of the pVT cell will be dependent on pressure and temperature, the system has to be calibrated over the whole temperature and pressure range using a liquid with known pVT parameters, typically mercury.

Fluids can be measured directly, but when measuring solids or materials which change the state from liquid to solid (like epoxy resins during cure) the confining fluid technique must be used. This ensures hydrostatic pressure at any time of analysis giving reliable results also for the solidified materials. For the curing analysis of epoxy resins, a defined amount of resin is filled in a cell of known volume, which is closed at one end by a movable bellows. The remaining cell volume is filled with mercury as confining fluid. Now, any volume change due to changing temperature, pressure, phase transitions, or chemical reactions in dependence on time of the completely filled cell is recorded by analyzing the deflection of the bellows. Knowing the pVT behavior of the confining liquid and the amount of confining liquid and resin in the cell, the changes in the specific volume of the resin can be calculated. Since the apparatus records only the volume changes, the actual volume of the material has to be determined externally for defined conditions, typically room temperature and standard pressure (Zoller and Walsh 1995).

pVT analyses using the bellows-type dilatometer is widely used to determine the specific volume V_{sp} of polymers, blends, or composites in dependence on temperature T and pressure p as well as phase transitions like melting, crystallization, and glass transition (Pionteck and Pyda 2014; Zoller and Walsh 1995). As long as the material is in the molten or liquid state, relaxation is fast and the measured values are equilibrium data. When the material is in the glassy state, the relaxation processes may be too slow to follow changes of the outer conditions so that the measured values are nonequilibrium data. For curing systems this means that as long as the glass transition temperature T_g is below the cure temperature T_{cure} , equilibrium data can be determined by pVT analysis (Zarrelli et al 2002), while when T_g increases above T_{cure} , the resin is in nonequilibrium. Thus, under these conditions no further shrinkage may be observed even if the crosslinking reaction still continuous, and thus no reliable conclusions on the crosslinking density from the volume data can be drawn. Nevertheless, pVT analysis is the most accurate method to analyze volume shrinkage in curing systems.

Using pVT analysis different modes for curing are possible. Most common is the isobaric curing regime at constant temperature or with stepwise increase of cure temperature. Assuming that there is a linear correlation between the shrinkage and epoxide conversion X ($\Delta V \propto X$), this mode allows the detection of polymerization and crosslinking kinetics, setting the final specific volume $V_{t \rightarrow \infty}$ to 100% conversion:

$$X \text{ (in \%)} = \left(\frac{\Delta V_{sp(t)}}{\Delta V_{sp(t \rightarrow \infty)}} \right) \times 100 = \left(\frac{V_{sp(t=0)} - V_{sp(t)}}{V_{sp(t=0)} - V_{tsp(t \rightarrow \infty)}} \right) \times 100 \quad (4)$$

This is certainly only an approximation since in practice the cure reaction stops when the vitrification is reached and the hampered mobility of chains hinders further reactions. When a value for “complete” conversion is known, incomplete cure due to changed processing conditions, additives, etc. can be detected.

Continuous heating at defined pressure gives the possibility to detect the begin of cure ($T_{cure, onset}$), where the nearly linear increase of V_{sp} due to thermal expansion is

changing to slower slopes or even reduced due to overlapping the thermal expansion with cure shrinkage. When the cure is completed ($T_{\text{cure, end}}$), the thermal expansion is reflected by a further nearly linear increase of V_{sp} with raising temperature, giving the thermal expansion coefficient of the cured resin. This ideal case is only working when the cure reaction is fast enough to follow the temperature rise and the glass transition temperature of the cured system $T_{\text{g (cured)}}$ is below the decomposition temperature $T_{\text{decomposition}}$. If the rate of temperature increase is properly chosen, this mode allows maximum conversion and the proper determination of $V_{t \rightarrow \infty}$. When cooling, the change of the slope in the V-T plot characterizes the glass transition of the completely cured sample $T_{\text{g (cured)}}$.

When the temperature is stepwise increased and at each temperature an isothermal pressurization is performed (so-called isothermal standard mode, ITS (Zoller and Walsh 1995)), beside changes in thermal expansion coefficients also changes in the compressibilities due to cure can be detected. In this mode also $T_{\text{cure, onset}}$, $T_{\text{cure, end}}$ and $V_{t \rightarrow \infty}$ can be determined but kinetics hardly can be quantified. In Fig. 1 a graphical presentation of the different pVT modes is given. Figure 1a shows the isobaric heating curve with the cure shrinkage overlapping the thermal expansion due to cure shrinkage (between $T_{\text{cure, onset}}$ and $T_{\text{cure, end}}$, filled symbols). The slope between room temperature RT and $T_{\text{cure, onset}}$ represents the thermal expansion of the noncured mixture and the slope above $T_{\text{cure, end}}$ the thermal expansion cured sample in the rubbery state (above T_{g}). The cooling curve (open symbols) gives the thermal expansion in the glassy state (below T_{g}). Further heating and cooling should not alter the V-T dependence of completely cured samples, except some physical aging. The exponents of thermal expansion are calculated as

$$\alpha_V = \frac{1}{V} \left(\frac{\partial V}{\partial T} \right)_p \quad (5)$$

The subscript V stays for volumetric thermal expansion coefficient in contrast to the linear thermal expansion coefficient, which is determined by measuring one-dimensional changes in the length of a sample in dependence on temperature:

$$\alpha_L = \frac{1}{V} \left(\frac{\partial V}{\partial T} \right)_p \quad (6)$$

For isotropic materials and small dimensional changes α_V equals 3 α_L . Epoxide composites, compounds, coatings, or adhesives, however, behave typically anisotropic, since shrinkage in one or two dimensions is restricted because of immobilization at the anisotropic fillers or substrates.

In Fig. 1a below $T_{\text{cure, onset}}$ the differences between the two lines are the loss in volume due to shrinkage. In practice, often only the values at room temperature and standard pressure are determined. In Fig. 1b the isothermal cure shrinkage is shown. Addition of modifiers can reduce the shrinkage and alter the cure mechanism and

kinetics. However, the main mechanism for reducing the shrinkage is just the bulk replacement with an inert modifier, as indicated in the plot.

Figure 1c, d shows the isothermal compression at defined temperatures. The compressibility can be calculated for each T-p pair in the plot by

$$\kappa = \frac{1}{V} \left(\frac{\partial V}{\partial p} \right)_T \quad (7)$$

In Fig. 1c one can see that the compressibility is strongly dependent on temperature and cure. With rising temperature, as long as no curing occurs (T1 to T3), the specific volumes and compressibilities at defined pressure increases. Between T3 and T4 curing occurs resulting in reduction in V_{sp} values and with further rising temperature V_{sp} increases again (T5). The seemingly higher compressibility of the cured sample is caused by the higher temperature (compare T4 to T2). With rising temperatures typically the free volume increases and thus the compressibility. However, Fig. 1d shows clearly that at same temperature the compressibility of noncured resin is much higher than that of cured one. Since the compression occurs mainly in the free volume, noncrosslinked material has higher response to pressure than crosslinked material because crosslinking consumes much of the free volume of the starting material.

Other methods, which will not be discussed in detail in this chapter are, e.g., the gravimetric method measuring the change in buoyancy of a resin in a known fluid at a controlled cure temperature (e.g., Li et al. (2004)) or the rheometer method which measures the change in the gap between the two plates of a plate-plate rheometer (Zarrelli et al 2002; Schoch et al. 2004; Khoun and Hubert 2010; Shah and Schubel 2010). While the first method can follow the change in density over the full cure process, the rheometer can measure the shrinkage only in between gelation and vitrification. Advantageous is that the rheometer method allows the determination of the gelation time that allows correlation between conversion and gelling and thus, in combination with other methods, one can determine the shrinkage before and after gelation, which is important for many applications.

Modification of Cure Shrinkage Due to Addition of Thermoplastics

When adding thermoplastics to epoxy resins one can assume that the nonreactive additive in a first approach reduces the shrinkage by replacing some volume of the shrinking epoxide $V_{epoxy(t=0)}$ by nonshrinking thermoplastic ($V_{thermoplastic(t=0)}$). Thus, in a first approach one can estimate the shrinkage of the epoxy/thermoplastic blend ΔV_{blend} from its composition, assuming that the observed shrinkage is due to shrinkage of the epoxy phase (ΔV_{epoxy}) only:

$$\Delta V_{blend} (\text{in } \%) = \left(\frac{V_{epoxy(t=0)}}{V_{epoxy(t=0)} + V_{thermoplastic(t=0)}} \right) \times \Delta V_{epoxy} \quad (8)$$

However, in reality, the change in overall volume shrinkage does not follow necessarily linearity in regard to composition.

Many thermoplastics are miscible with epoxy resins in the noncured state. That means that the epoxy resin is a solvent for the thermoplastic. During epoxy curing, the molecular weight of the resins increases and solubility of the thermoplastic decreases; the thermoplastic becomes insoluble and phase separation occurs (reaction induced phase separation, RIPS). As long as both phases are liquids, the domain size of the separating thermoplastic can grow due to continuous increase in insolubility and due to secondary processes like coalescence of the growing domain. These processes slow down with increase in viscosity and gelation and stop because of vitrification. Overall, the phase separation is thermodynamically driven but kinetically controlled. Thus, composition, chemical structure, temperature, and molecular weights control the viscosity, the reaction rate, the phase separation kinetics, and the final epoxy/thermoplastic blend morphology. These complex processes affect differently the cure shrinkage and final thermal behavior of the blends.

Acrylonitrile-butadiene-styrene-copolymer (ABS) is an amorphous impact resistant thermoplastic and often used to modify the toughness of epoxy resins. The toughness of ABS results from the phase separated polybutadiene phase embedded in the poly(styrene-co-acrylonitrile) (SAN) matrix as small particles. The morphology and performance of ABS depends on the terpolymer composition and grafting degree between the rubber phase and SAN phase. The SAN phase of ABS is at least partially miscible with epoxy resins and when curing RIPS occurs.

The curing of a DGEBA/DDS (4,4'-diaminodiphenylsulfone) system is accelerated when adding 5–20 wt% ABS, as determined by pVT analysis at 157 °C and a pressure of 10 MPa (Müller et al. 2007) (Fig. 2). This increased rate of epoxy conversion is surprising since the addition of ABS increases the viscosity of the noncured resin and dilutes the concentration of reactive sites. Thus, a catalyzing

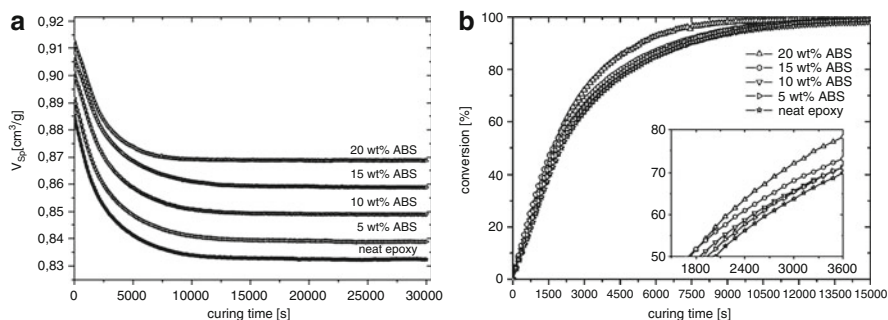


Fig. 2 Effect of ABS on curing of DGEBA/DDS (*left*) detected as specific volume changes by pVT analysis (10 MPa, 157 °C) and (*right*) calculated conversion curves (Reproduced from Müller et al. (2007) with permission from John Wiley and Sons)

effect of ABS and differences in the morphology development mechanism with phase inversion and secondary phase separation are considered as reasons for the cure acceleration. The final crosslinking density of the epoxy seems to be not effected by presence of ABS, as concluded from glass transition temperatures of both the epoxy (ca. 200 °C) and SAN phase (105 °C), which are independent on ABS content. When analyzing the specific volume over cure time in dependence on ABS content (Fig. 2), it becomes clear that due to ABS addition the specific volumes at $t = 0$ and $t \rightarrow \infty$ increase and the shrinkage decreases from 6% to <5%, estimated from $V_{sp(t=0)}$ and $V_{sp(t \rightarrow \infty)}$ values in Fig. 2.

Changes in the type of ABS and the curing regime can alter the findings described above. A detailed analysis of the V_{sp} data during curing at 180 °C and 10 MPa in presence of up to 12.9 wt% ABS exhibited a nonlinear shrinkage dependence on the SAN content (Fig. 3).

When up to 20 g SAN is mixed into a high temperature epoxy-diamine system (100 g DGEBA plus 32 g DDS) as toughener, the blend shrinkage is reduced from ca. 7.3% (pure epoxy resin) to 5.4% at 20 g SAN addition (Jose et al. 2008). However, the shrinkage is governed by viscoelastic phase separation kinetics and not linear with composition. Kinetics analysis has shown that before phase separation the shrinkage is reduced due to the diluent effect of SAN and its reduction correlates with the SAN content. Beyond phase separation a coupling between phase

Fig. 3 Effect of ABS on shrinkage (*top*) and conversion (*bottom*) of DGEBA/DDS (pVT analysis, 10 MPa, 180 °C) (Reproduced from Jyotishkumar et al. (2011) with permission from the Royal Society of Chemistry)

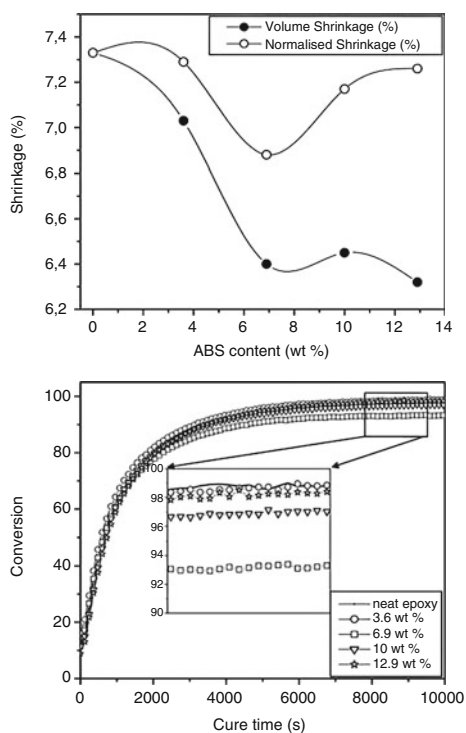
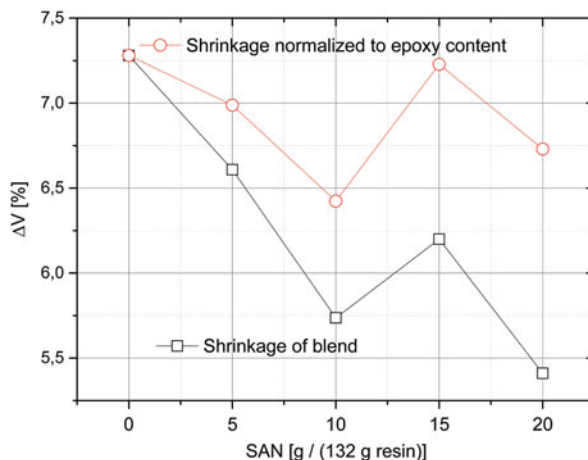


Fig. 4 Shrinkage of epoxy/SAN blends having different SAN contents after curing at 160 °C at 10 MPa for 8 h (Reprinted with permission from Jose et al. (2008), American Chemical Society)



coarsening and reaction kinetics decides the shrinkage behavior. When a double phase separated co-continuous morphology is formed, the thermoplastic rich phase contributes to the overall shrinkage, visible as local maximum in the shrinkage dependence on SAN content (Fig. 4).

The modification of epoxy resin with poly(methyl methacrylate) (PMMA) failed in reducing the cure shrinkage when the blend is prepared by the in-situ method (Alcantara et al. 2003). The hardening of the epoxy resin was done in-situ with the polymerization of methyl methacrylate (MMA) to obtain pseudo-interpenetrating polymer networks based on epoxy matrix and dispersed PMMA. Low amounts of MMA were favorable for mechanical strength. However, in this method, also the polymerization of MMA contributes to shrinkage, thus increasing the contraction of the final product and the thermal expansion coefficients increase as well with raising PMMA content.

Modification of Cure Shrinkage Due to Addition of Hyperbranched Polymers and Star Polymers

Hyperbranched polymers (HBP) are variable in chemical structure, degree in branching, functionality, and reactivity. They have been used successfully in improving toughness of epoxides and processibility. Their effect on cure shrinkage depends on chemical structure, degree of crosslinking, and reactivity of the terminal sites.

The influence of the polymer topology on the effectivity in reducing epoxy shrinkage was analyzed by comparing a linear poly(ϵ -caprolactone) (*l*-PCL) with a multi-arm star poly(ϵ -caprolactone) having > 100 arms (*s*-PCL) (Morell et al. 2011a). As epoxy system the anionic homopolymerization of DGEBA was

chosen and 5 or 10 wt% thermoplastic polymer was added. The cure process is less affected by addition of *s*-PCL and both polymers improved the impact strength but the *s*-PCL to a higher degree. The post-gelation shrinkage was determined by rheometer technique and is reduced when *s*-PCL is added (from 6% to <4%) and much less reduced in case of linear polymer addition. While these shrinkage values are determined at T_{cure} the gross shrinkage determined at 30 °C by pycnometer method is much less and can be as small as 0.77% at *s*-PLA content of 10 wt% compared to 1.6% for the pure resin (Morell et al. 2011b). The efficiency of the *s*-PCL in reducing the shrinkage is dependent on the PCL arm lengths.

In an amino-catalyzed DGEBA/anhydride system, the addition of an aliphatic hyperbranched polyester with terminal OH-groups did not contribute to reduction in overall shrinkage, at higher HBP loadings the shrinkage even increased (Foix et al. 2009) from 4.3 to ca. 6% at 15 wt% HBP, calculated from the densities before and after cure. However, the part of shrinkage which takes place after gelation was reduced, thus reducing internal stress. The OH-groups cause a covalent incorporation of the HBP into the epoxy network.

When DGEBA is cationically homopolymerized, hyperbranched polyester based on pure 4,4-bis(4-hydroxyphenyl) valeric acid (HPhVA) and 3-(4-hydroxyphenyl) propionic acid (HPhPA) will be incorporated in the epoxy network due to the reactivity of the terminal phenolic groups to the oxirane rings of the epoxides (Foix et al. 2012). As lower the amount of HPhPA in the HBP is, as higher is the degree in branching and the number of terminal OH-groups. Thus, with increase in branching more dense networks are formed when reacting with DGEBA. Caused by the dense structure of HBP the shrinkage due to cure is reduced with raising amount of HBP (up to 10 wt%) and degree of branching (DB) (Table 1). Very small shrinkage or even an expansion instead of contraction during curing of DGEBA is

Table 1 Effect of reactive hyperbranched polyester on density and shrinkage of DGEBA during catalyzed cure in dependence on HBP content and its degree of branching (Data taken from Foix et al. (2012))

Composition ^a	[OH]/[epoxy] molar ratio	$\rho_{\text{noncured}}^{\text{b}}$ (g cm ⁻³)	$\rho_{\text{cured}}^{\text{b}}$ (g cm ⁻³)	$\Delta V^{\text{b, c}}$ (%)
DGEBA	0	1.163	1.227	5.2 (3.2)
DGEBA HBP(50) 5 wt%	0.035	1.185	1.214	2.4 (2.5)
DGEBA HBP(40) 5 wt%	0.017	1.171	1.215	3.6
DGEBA HBP(30) 5 wt%	0.011	1.159	1.216	4.7
DGEBA HBP(50) 10 wt%	0.075	1.184	1.208	2.0 (2.2)
DGEBA HBP(40) 10 wt%	0.037	1.179	1.209	2.4
DGEBA HBP(30) 10 wt%	0.024	1.164	1.212	4.0

^aNumber in brackets: Degree of branching (HBP(50) is the pure poly(HPhVA))

^bDensities of noncured ρ_{noncured} and cured samples ρ_{cured} determined pycnometrically at 30 °C

^cValues in bracket from (Foix et al. 2010)

observed in other HBP containing systems, strongly depending on the amount of reactive hydroxyl groups present in the HBP (Morell et al. 2010; Foix et al. 2011).

Modification of Cure Shrinkage Due to Addition of Rubbers

Rubbers are the most suitable modifiers for toughness of brittle matrices like epoxy resins by nature. The effect of the rubber on the shrinkage during cure depends on the epoxy/rubber blend composition, on the reactivity of the rubber to the epoxy, morphology of the blend, and on changes in curing mechanism due to present catalyst, which can have drastic effects on the resulting network structure and morphology and thus material properties.

In Bittmann and Ehrenstein (1998), a cycloaliphatic epoxy resin was modified with silicon elastomers in two different concepts, one resulting in dispersed silicon elastomer particles of fixed size (dispersion) and the other in homogeneous mixture (mixing). The hardening at 120 °C resulted in a shrinkage from ca. 4% in the pure resin to around 1% with 20 or 35 wt% silicon when the dispersion method was applied, while no reduction in shrinkage was observed with the mixing approach, analyzed as gross values at ambient conditions. Parallel the modification by particle dispersion reduced the thermal expansion coefficient α by ca. 20% at 35 wt% silicon content (low silicon contents have had no effect), while in the homogeneous mixed system α drastically increased with increasing silicon content (about doubled with 15 wt% silicon). Both modification methods reduce the modulus and increase the fracture toughness, but since the T_g of the epoxy phase is not reduced by the dispersion method and because of the reduced shrinkage and thermal expansion coefficient this method is favorable for the production of materials and components with low internal stresses.

When the liquid rubber CTBN (carboxylic-terminated butadiene-acrylonitrile rubber) is mixed with a DGEBA/DDS system, due to interphase reaction resulting in incorporation of rubber into the epoxy network and vice versa, the typical cure shrinkage can be drastically reduced, and a transition from heterogeneous to more or less homogeneous morphology can occur, depending on the reactivity (Pionteck et al. 2011). To show the effect of reactivity on cure shrinkage, CTBN was converted into a nonreactive ester form (CTBN-ester) and, in addition, partially dimethyl benzyl amine (DMBA) was added to the blend to change the reactivity and cure mechanism. The curing was performed within a pVT apparatus at 157 °C under a pressure of 10 MPa.

In the noncatalyzed system, after 4 h the cure reaction is finished and a plateau value in V_{sp} is visible (Fig. 5, left; please note that at high rubber content further treatment under cure conditions results in slight increase in V_{sp} properly due to some degradation of the rubber phase). Due to dissolution with the lower dense rubber, the starting and final specific volumes ($V_{sp(t=0)}$ and $V_{sp(t \rightarrow \infty)}$, respectively) are increased with raising rubber content. Up to 10 wt% rubber addition no differences in shrinkage are seen depending on rubber reactivity, but at higher rubber contents the reactivity of CTBN results in lower shrinkage compared to the nonreactive

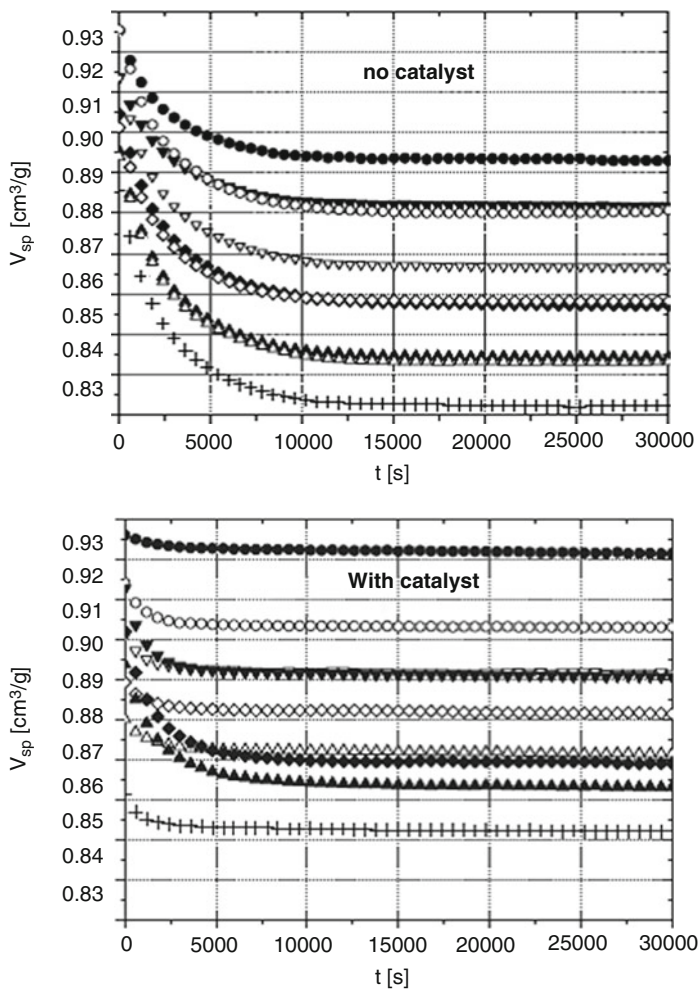


Fig. 5 Influence of the rubber content and rubber reactivity on the shrinkage during curing of DGEBA/DDS without catalyst (*top*) and with 1 mol% DMBA (*bottom*). Rubber content: 0 (+), 5 (Δ), 10 (\diamond), 15 (∇), and 20 wt% (\circ); *full symbols* CTBN, *open symbols*: CTBN-ester (Reproduced from Pionteck et al. (2011) with permission from John Wiley and Sons)

CTBN-ester. It was assumed that the increasing amount of carboxylic groups catalyzes more and more the ether formation resulting in reduced network density. However, the network changes must be small since the T_g was not affected. Analyzing the shrinkage normalized to the epoxy phase content, the shrinkage of the CTBN containing resin is about the same as the pure epoxy resin, while the normalized epoxy shrinkage of the CTBN-ester containing blend is even slightly increased by trend. Overall, as well the carboxylic terminated as the ester-terminated rubber exhibited a slight catalyzing effect causing faster cure shrinkage.

Table 2 Chemical volume shrinkage of DGEBA/DDS-rubber blends in dependence on rubber content, rubber reactivity, and present catalyst (values taken from (Pionteck et al. 2011))

Rubber content (wt%)	Nocatalyzed		Catalyzed	
	ΔV_{sp} %	ΔV_{sp} (normalized) %	ΔV_{sp} %	ΔV_{sp} (normalized) %
CTBN				
0	5.8	5.8	3.5	3.5
5	5.7	6.1	3.7	3.9
10	5.7	6.5	4.4	5.0
15	4.3	5.3	3.4	4.2
20	4.3	5.7	1.4	1.8
CTBN-ester				
0	5.8	5.8	3.5	3.5
5	5.7	6.1	2.6	2.8
10	5.2	5.9	2.7	3.1
15	5.5	6.7	2.9	3.5
20	4.8	6.3	2.7	3.5

In the catalyzed systems a very complex behavior is observed. As expected the curing is much faster and happens partially already during sample preparation and before reaching the cure temperature during heating the pVT cell. Therefore, the $V_{sp(t=0)}$ values in the plot (Fig. 5, right) are not the real one and for determination of the gross chemical shrinkage $V_{sp(t=0)}$ values have to be calculated from the composition of the starting mixture. The plateau values of V_{sp} are reached much faster than in the noncatalyzed system, with the tendencies of fastest kinetics in rubber-free systems and at high rubber contents, and faster kinetics in case of addition of nonreactive rubber compared to reactive rubber addition. At low amounts of rubber the catalyst results in higher shrinkage in the reactive system, at 15 wt% both rubber modified resins behave similar, and at high rubber contents the addition of reactive rubber results in much lower shrinkage as compared to addition of the nonreactive rubber. Table 2 summarizes the absolute shrinkage and the shrinkage normalized to the epoxy phase content. Also in the epoxy resin devoid of rubber addition of DMBA catalyst reduces the shrinkage. This is certainly due to a change in the reaction mechanism to amino-catalyzed homopolymerization of the epoxy units, resulting in increased linear ether formation (Scheme 1a).

All the differences between reactive and nonreactive rubber and between catalyzed and noncatalyzed systems have been explained by quaternary ammonium salt formation of the amino catalyst with the carboxylic endgroups of the reactive rubber, which hampers the catalytic activity of the catalyst and thus the epoxy homopolymerization as well the reactivity of the carboxylic groups to the epoxy units and thus the incorporation of the rubber into the epoxy network. The very low shrinkage of only 1.8% in case of the catalyzed system with 20 wt% CTBN is explained by an excess of carboxylic groups, allowing a high degree of CTBN incorporation into the

epoxy phase and vice versa. In this way, a total change in the morphology occurred from a strongly phase separated epoxy matrix/rubber particle system in all noncatalyzed systems to co-continuous structures of phases with different epoxy/rubber compositions in catalyzed systems with high reactive rubber contents (Pionteck et al. 2011).

In the nonreactive rubber containing systems no salt formation is possible, and the DMBA catalyst is active in all compositions causing some epoxy homopolymerization. Thus, independent on compositions all catalyzed systems exhibit lower shrinkage than the noncatalyzed one. The normalized shrinkage of the epoxy phase is nearly independent on CTBN-ester content and slightly higher than that of the pure resin, possibly due to some pressure induced volume shrinkage of the dispersed rubber particles embedded within the shrinking epoxy matrix. The systems did not show co-continuous phase morphologies but secondary phase separation at higher CTBN-ester concentration. There are no signs for incorporation of rubber into the epoxy phase or vice versa.

Attractive for combining toughening with strengthening is the use of mixed systems of rubber and filler for modification of epoxy resins. In Vijayan et al. (2014) a mixture of CTBN and silicon carbide (SiC) nanofibers is used for analyzing their effects on cure shrinkage and the results have been compared with thermal and mechanical properties. The epoxy resin was based on DGEBA, nadic methyl anhydride (NMA) as hardener, and DMBA as catalyst. The composition of the epoxy resin was constant with equimolar amounts of DGEBA and NMA and addition of 15 phr CTBN, 0.25 phr SiC fibers, or both of them. Two different preparation methods have been used. Premixing the SiC fibers with DGEBA under sonication before adding CTBN resulted in better dispersion of the fibers (labeled as M_2), faster reaction kinetics, higher T_g and thermal stability, and changed fracture structure, when compared to mixing the SiC fibers in the DGEBA/CTBN mixture before adding hardener and accelerator (labeled as M_1). However, the impact strength is synergistically increased in both methods of the blend composite.

CTBN is miscible in the noncured state with the resin, and RIPS occurs during polymerization and crosslinking forming a typical epoxy matrix/rubber particle structure. Analyzing the cure shrinkage kinetics at 100 °C and 10 MPa by pVT analysis, an accelerating effect of SiC fibers and a retarding effect of CTBN is visible. In the mixed system containing both SiC and CTBN the degree of SiC dispersion decides on its activity, which is better in the system labeled as M_2 (Fig. 6). The plateau value is reached when the vitrification occurs, i.e., the T_g raises above T_{cure} , freezing in this way the state of the cure shrinkage, even if some cure may continue.

In all samples roughly 2 vol% shrinkage occur already during sample preparation and heating the pVT to the cure temperature. The final shrinkage of the differently modified resins is rather similar to that of the nonmodified resin, even if ca. 13 vol% of the system are substituted by phase separated CTBN. However, the shrinkage normalized to the epoxy volume is higher for all modified resins (Table 3). Principally, the carboxylic-terminated rubber can be incorporated into the epoxy resin, which would result in a reduced network density and reduced shrinkage, as shown

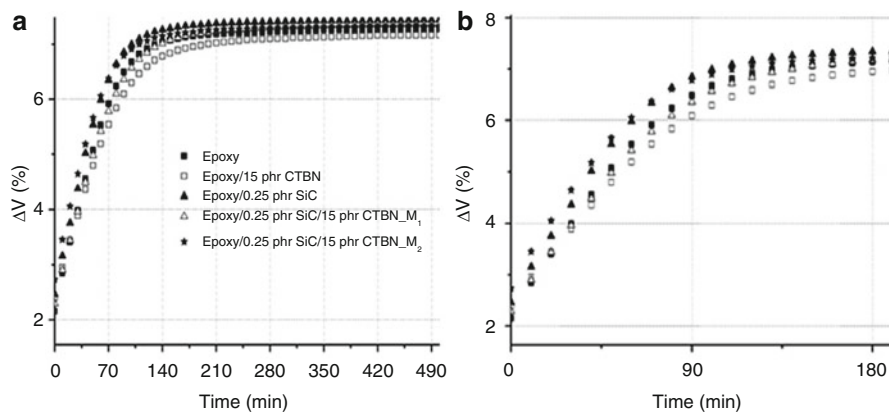


Fig. 6 Influence of rubber and SiC fiber addition on cure shrinkage behavior of DGEBA/methyl nadic anhydride system catalyzed by DMBA (Reprinted from Vijayan et al. (2014) with permission from Elsevier)

Table 3 Chemical volume shrinkage of DGEBA/MNA epoxy resins in dependence on added modifier and preparation method (values taken from (Vijayan et al. 2014, 2015a))

Additive	ΔV_{sp}	ΔV_{sp} (normalized)
	%	%
Pure epoxy resin	7.27	7.27
15 phr CTBN	7.16	8.23
0.25 phr SiC	7.44	7.44
15 phr CTBN + 0.25 phr SiC M ₁	7.36	8.46
15 phr CTBN + 0.25 phr SiC M ₂	7.32	8.41
3 phr clay	7.76	7.99
15 phr CTBN + 3 phr clay	7.69	9.07

above (Pionteck et al. 2011). Here, the nonreduced shrinkage counts for the formation of the quaternary ammonium salts of DMBA with the present carboxylic units of the rubber. These salts cannot react with the oxirane rings, hindering the incorporation of CTBN into the network. The increased shrinkage in the CTBN containing epoxy resin can be explained by a mobilization of the reacting sites due to partial dissolved CTBN in the epoxy phase or by a pressure densification of the CTBN particles due to shrinkage of the surrounding epoxy matrix. The volume fraction of SiC nanofibers is too small to influence significantly the cure shrinkage by the volume substitution effect. The observed fastening of the cure kinetics and increased shrinkage in presence of SiC fibers can be explained by some moisture at the SiC fiber surfaces, which can accelerate the esterification reaction between the oxirane rings and anhydride.

Also nanoclay modified with a quaternary ammonium salt alters the cure kinetics and final cure shrinkage of DGEBA/NMA epoxy resins containing 15 phr liquid CTBN (Vijayan et al. 2015b). In presence of 3 phr clay, polymerization and crosslinking (catalyzed by 1 phr DMBA) are accelerated and the shrinkage is slightly increased compared to the corresponding resin systems devoid of clay (Table 3). The increase in curing rate and final normalized shrinkage is due to the catalyzing effect

of the used modifier for the clay, trimethyl stearyl ammonium, which is unable to catalyze the epoxy homopolymerization (etherification) but the epoxy-anhydride reaction. There are no signs of changes in the cure mechanism. Traces of water in the system undergo auto-pyrolysis and the formed OH-anions thermally cleave the N-C bond of the quaternary ammonium forming in this way the catalytic active form, the tertiary amine. The conversion-time plot calculated from the shrinkage kinetics (Eq. 4) using the theoretically $V_{sp}(t=0)$ values exhibits a large degree of conversion already during sample preparation and heating to T_{cure} in the pVT apparatus (Fig. 7), that is higher in case of clay containing composites. The pVT results are verified by FTIR analysis of the cure kinetics and DSC measurements. The effect of clay addition and of different preparation methods on the thermal and mechanical properties is studied elsewhere (Vijayan et al. 2015b).

Modification of Cure Shrinkage Due to Addition of Block-Copolymers

Block-copolymers are efficient tougheners for epoxides because of self-assembling forming nanostructures in the epoxy matrix. Typically they are assigned in such a way that one block is miscible with the epoxy matrix, while the other block forms

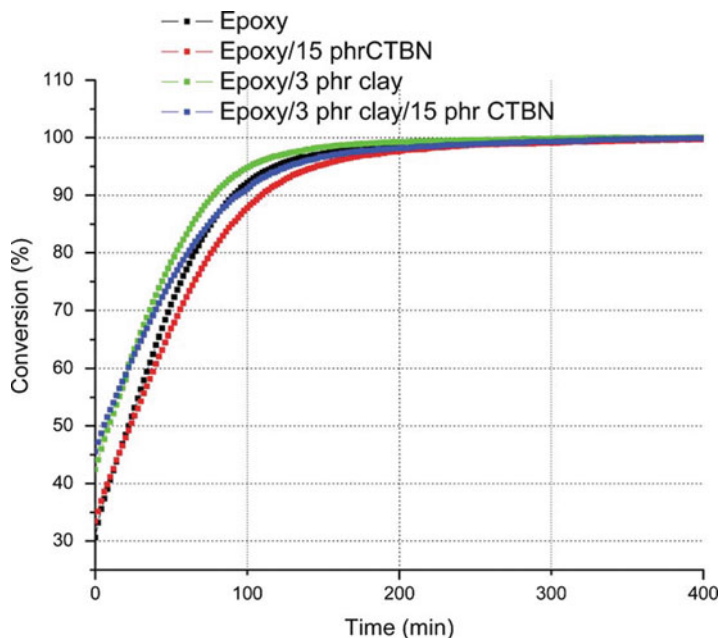


Fig. 7 Influence of rubber and organo-modified clay on epoxy conversion of DGEBA/methyl nadic anhydride system catalyzed by DMBA (Reprinted from Vijayan et al. (2015a) by permission of the publisher (Taylor & Francis Ltd, <http://www.tandfonline.com>))

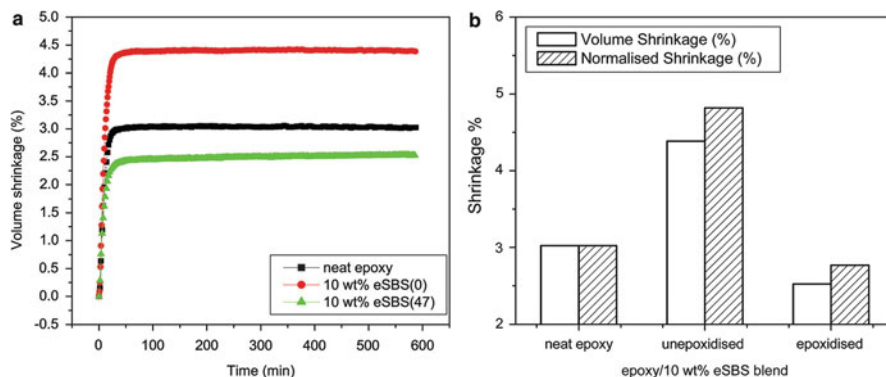


Fig. 8 Effect of epoxidation of SBS on the volume shrinkage during curing of epoxy/DDM blends at 110 °C, 10 MPa (*left*); eSBS(0): nonepoxidized SBS; SBS(47): 47 mol% epoxidation of the polybutadiene block: The *right images* gives the final shrinkage after 10 h and normalized values to the epoxy phase content (Reproduced from George et al. (2015) with permission from the PCCP Owner Societies)

ordered or disordered nanoscale morphologies. The miscibility of the one block hinders macroscopic phase separation.

A DGEBA/DDM (4,4'-diaminodiphenylmethane) system in the noncured state is miscible with epoxidized styrene-*block*-butadiene-*block*-styrene (eSBS) terpolymer and polymerization induced phase separation occurs during cure resulting in nanophase separation. The resulting morphology as well as the shrinkage depends on the degree of epoxidation of the polybutadiene blocks (George et al. 2015). Nonepoxidized or SBS with low epoxidation degrees form microphase separated domains. At high epoxidation degrees the polybutadiene block remains miscible with the polymerizing and crosslinking matrix, thus forcing the formation of nanoseparated domains of the immiscible polystyrene. When analyzing the specific volume changes in dependence on the curing time it was found that the addition of highly epoxidized SBS caused a reduced shrinkage, while nonmodified SBS caused increased shrinkage (Fig. 8). The shrinkage kinetics is fastest with SBS and reduced with eSBS and after ca. 2 h ΔV remains constant because of vitrification, even if the curing may gradually continue. The higher shrinkage in the epoxy/SBS blend is explainable by a higher mobility of the epoxy-amine system in presence of SBS allowing a higher conversion, and a pressure induced shrinkage of the microphase separated SBS can also contribute to the overall shrinkage. The reduced shrinkage in presence of eSBS is explained by plasticization and miscibility of the epoxidized polybutadiene blocks, that is higher in case of nanoseparated eSBS compared to microphase separated SBS.

Conclusions

For analyzing the shrinkage of epoxy resins different methods are available. The density measurement of the noncured sample and of the cured sample gives values of the gross shrinkage. These values are much smaller than the chemical shrinkage

which occurs when the curing is performed at elevated temperature. Only when analyzing the volume changes directly during the cure process one can conclude on the chemical shrinkage which is caused by the formation of covalent bonds between the epoxy components, resulting in crosslinked polymer network structures. The volume change can be measured very accurately by bellow-type goniometers. Other methods are suitable to analyze the cure process before gelation and vitrification or after gelation separately, giving thus important information about the portion of the overall shrinkage which is responsible for stress development in final applications.

The direct observation of volume changes during the cure process is a very practical way to analyze the effects of added components on changes in cure kinetics and – in combination with other analytical tools – cure mechanism. The addition of rubbers and thermoplastics, including hyperbranched and block-copolymers, typically reduces the shrinkage of the epoxy blends. The reduction is not necessarily linear dependent on the volumetric composition of the blends. Most drastically is the effect of polymer addition in case of reactive systems, where the added component can react with the resin, thus changing the network structure and density. If the added components exhibit catalytic activity or if they interfere with the catalyst, the kinetic and mechanism of polymerization and network formation can be changed drastically, not only reducing in this way the chemical shrinkage but also affecting the final mechanical and thermal properties of the epoxy blends. Also in case that no changes in cure mechanism occur, changes in the viscosity of the resin system due to added miscible polymeric components can affect the cure kinetics, and in the final stage of cure the mobilization of the hardened network structure by flexible additives can increase the mobility of the reacting components, thus causing the formation of more dense epoxy networks compared to the neat epoxide.

Many of the commonly used rubbers and thermoplastics are initially miscible in the noncured resin and during cure reaction induced phase separation occurs. The resulting morphology of this process also affects the shrinkage. For example, embedded rubber particles can be pressurized because of shrinkage of the surrounding epoxy matrix, thus contributing to additional shrinkage. This is not possible when the rubber forms the matrix.

Overall, the effects of added polymers on the cure process and shrinkage of epoxy resins are very complex but effective not only in regard to the shrinkage reduction but also for toughening the epoxy resin.

References

- Alcantara RM, Pires ATN, de Barros GG, Belfiore LA (2003) Pseudo-interpenetrating polymer networks based on tetrafunctional epoxy resins and poly(methyl methacrylate). *J Appl Polym Sci* 89:1858–1868
- Barton AFM (1991) *CRC handbook of solubility parameters and other cohesion parameters*, 2nd edn. CRC Press, Boca Raton
- Bittmann E, Ehrenstein GW (1998) Optimierung cycloaliphatischer Epoxidharzsysteme mit Silikonkautschuk. *Angew Makromo Chem* 258:93–98

- Chen LW, Twu C-H, Cho C-S (1997) Physical properties and shrinkage of epoxy resins cured with lactams. *J Polym Res* 4:65–72
- Dlubek G, Hassan EM, Krause-Rehberg R, Pionteck J (2006) Free volume of an epoxy resin and its relation to structural relaxation: evidence from positron lifetime and pressure-volume-temperature experiments. *Phys Rev E* 73:031803-1–031803-14
- Dlubek G, Pionteck J, Shaikh MQ, Hassan EM, Krause-Rehberg R (2007) Free volume of an oligomeric epoxy resin and its relation to structural relaxation: evidence from positron lifetime and pressure-volume-temperature experiments. *Phys Rev E* 75:021802–1–021802–13
- Fedors FF (1974) A method for estimating both the solubility parameters and molar volumes of liquids. *Polym Eng Sci* 14:147–154
- Foix D, Yu Y, Serra A, Ramis X, Salla JM (2009) Study on the chemical modification of epoxy/anhydride thermosets using a hydroxyl terminated hyperbranched polymer. *Eur Polym J* 45:1454–1466
- Foix D, Erber M, Voit B, Lederer A, Ramis X, Mantecon A, Serra A (2010) New hyperbranched polyester modified DGEBA thermosets with improved chemical reworkability. *Polym Degrad Stab* 95:445–452
- Foix D, Fernandez-Francos X, Salla JM, Serra A, Morancho JM, Ramis X (2011) New thermosets obtained from bisphenol A diglycidyl ether and hydroxyl-ended hyperbranched polymers partially blocked with benzoyl and trimethylsilyl groups. *Polym Int* 60:389–397
- Foix D, Khalyavina A, Morell M, Voit B, Lederer A, Ramis X, Serra A (2012) The effect of the degree of branching in hyperbranched polyesters used as reactive modifiers in epoxy thermosets. *Macromol Mater Eng* 297:85–94
- George SM, Puglia D, Kenny JM, Parameswaranpillai J, Vijayan PP, Pionteck J TS (2015) Volume shrinkage and rheological studies of epoxidised and unepoxidised poly(styrene-*block*-butadiene-*block*-styrene) triblock copolymer modified epoxy resin–diamino diphenyl methane nanostructured blend systems. *Phys Chem Chem Phys* 17:12760–12770
- Haynes WM (2016–2017) CRC handbook of chemistry and physics, 97th edn. CRC Press, Boca Raton
- Holst M, Schänzlin K, Wenzel M, Xu J, Lellinger D, Alig I (2005) Time-resolved method for the measurement of volume changes during polymerization. *J Polym Sci B* 43:2314–2325
- Jose J, Joseph K, Pionteck J, Thomas S (2008) PVT behavior of thermoplastic poly(styrene-co-acrylonitrile)-modified epoxy systems: relating polymerization-induced viscoelastic phase separation with the cure shrinkage performance. *J Phys Chem B* 112:14793–14803
- Jyotishkumar P, Pionteck J, Özdilek C, Moldenaers P, Cvelbar U, Mozetic M, Thomas S (2011) Rheology and pressure–volume–temperature behavior of the thermoplastic poly(acrylonitrile-butadiene-styrene)-modified epoxy-DDS system during reaction induced phase separation. *Soft Matter* 7:7248–7256
- Khoun L, Hubert P (2010) Cure shrinkage characterization of an epoxy resin system by two in situ measurement methods. *Polym Compos* 31:1603–1610
- Klaus IS, Knowles WS (1966) Reduction of shrinkage in epoxy resins. *J Appl Polym Sci* 10:887–889
- Kulawik J, Szeglowski Z, Mireia Morell C, Fernández-Francos X, Ramis X, Serrazapla AT, Kulawik JP (1989) Determination of glass transition temperature, thermal expansion and shrinkage of epoxy resins. *Colloid Polym Sci* 267:970–975
- Li C, Potter K, Wisnom MR, Stringer G (2004) In-situ measurement of chemical shrinkage of MY750 epoxy resin by a novel gravimetric method. *Compos Sci Technol* 64:55–64
- Morell M, Fernandez-Francos X, Ramis X, Serra A (2010) Synthesis of a new hyperbranched polyaminoester and its use as a reactive modifier in anionic curing of DGEBA thermosets. *Macromol Chem Phys* 211:1879–1889
- Morell M, Ramis X, Ferrando F, Serra A (2011a) Effect of polymer topology on the curing process and mechanical characteristics of epoxy thermosets modified with linear or multiarm star poly(ϵ -caprolactone). *Polymer* 52:4694–4702

- Morell M, Lederer A, Ramis X, Voit B, Serra À (2011b) Multiarm star poly(glycidol)-block-poly (ε-caprolactone) of different arm lengths and their use as modifiers of diglycidylether of bisphenol a thermosets. *J Polym Sci A Polym Chem* 49:2395–2406
- Müller Y, Häußler L, Pionteck J (2007) ABS-modified epoxy resins – curing kinetics, polymerization induced phase separation, and resulting morphologies. *Macromol Symp* 254:267–273
- Nawab Y, Tardif X, Boyard N, Sobotka V, Casari P, Jacquemin F (2012) Determination and modelling of the cure shrinkage of epoxy vinylester resin and associated composites by considering thermal gradients. *Compos Sci Technol* 73:81–87
- Pionteck J, Pyda M (2014) Thermodynamic properties – pVT data and thermal properties. In: Arndt K-F, Lechner, MD (eds). *Landolt-Börnstein: numerical data and functional relationships in science and technology – new series; VIII 6 A: polymer solids and polymer melts, part 2*. Springer, Berlin/Heidelberg
- Pionteck J, Müller Y, Häußler L (2011) Reactive epoxy-CTBN rubber blends: reflection of changed curing mechanism in cure shrinkage and phase separation behaviour. *Macromol Symp* 306–307:126–140
- Ramos JA, Pagani N, Riccardi CC, Borrajo J, Goyanes SN, Mondragon I (2005) Cure kinetics and shrinkage model for epoxy-amine systems. *Polymer* 46:3323–3328
- Schoch KF Jr, Panackal PA, Frank PP (2004) Real-time measurement of resin shrinkage during cure. *Thermochim Acta* 417:115–118
- Shah DU, Schubel PJ (2010) Evaluation of cure shrinkage measurement techniques for thermosetting resins. *Polym Test* 29, 629-3-639
- Van Krevelen DW, te Nijenhuis K (2009) *Properties of polymers, their correlation with chemical structure; their numerical estimation and prediction from additive group contributions*, 4th edn. Elsevier, Amsterdam
- Vijayan PP, Pionteck J, Huczko A, Puglia D, Kenny JM, Thomas S (2014) Liquid rubber and silicon carbide nanofiber modified epoxy nanocomposites: volume shrinkage, cure kinetics and properties. *Compos Sci Technol* 102:65–73
- Vijayan PP, Pionteck J, Thomas S (2015a) Volume shrinkage and cure kinetics in carboxyl-terminated poly(butadiene-co-acrylonitrile) (CTBN) modified epoxy/clay nanocomposites. *J Macromol Sci Part A: Pure Appl Chem* 52:353–359
- Vijayan PP, Puglia D, Pionteck J, Kenny JM, Thomas S (2015b) Liquid-rubber-modified epoxy/clay nanocomposites: effect of dispersion methods on morphology and ultimate properties. *Polym Bull* 72:1703–1722
- Zarelli M, Skordos AA, Partridge IK (2002) Investigation of cure induced shrinkage in unreinforced epoxy resin. *Plast Rubber Compos Process Appl* 31:377–384
- Zoller P (1986) Dilatometry. In: Mark HF, Bikales NM, Overberger CG, Menges G, Kroschwitz JI (eds) *Encyclopedia of polymer science and engineering*, vol 5, 2nd edn. John Wiley & Sons, New York, pp 69–78
- Zoller P, Walsh DJ (1995) *Standard pressure-volume-temperature data for polymers*. Technomic Publishing, Lancaster

Part III

Epoxy/Block-Copolymer Blends

Seno Jose, Sajeev Martin George, and Jyotishkumar Parameswaranpillai

Abstract

Formation of nanostructures inside epoxy thermosets by the inclusion of appropriate block copolymers (BCPs) has been emerged as a promising approach to optimize epoxy thermoset material properties for potential applications. For the last two decades, tremendous efforts have been made by researchers to create ordered or disordered nanostructures in epoxy thermosets by the incorporation of reactive or nonreactive BCPs in an attempt to develop toughened thermosets suitable for specific applications. This chapter briefly reviews the different mechanisms of phase separation in epoxy/BCP systems, such as self-assembly and reaction-induced microphase separation (RIMPS), and outlines some of the important features of nanostructured morphologies and their influence on fracture toughness of fabricated products.

Keywords

Epoxy resins • Block copolymers • Self-assembly • Reaction-induced microphase separation • Nanostructured morphology • Fracture toughness

S. Jose (✉)

Department of Chemistry, Government College Kottayam, Kottayam, Kerala, India
e-mail: senojose@gmail.com

S.M. George

Department of Chemistry, St. Thomas College, Palai\Arunapuram, Kerala, India
e-mail: martin.v.george@gmail.com

J. Parameswaranpillai

Department of Polymer Science and Rubber Technology, Cochin University of Science and Technology, Cochin, Kerala, India
e-mail: jyotishkumarp@gmail.com

Contents

Introduction	828
Mechanism of Phase Separation	829
Self-Assembly	829
Reaction-Induced Microphase Separation	830
Morphology: Formation of Nanostructures	832
Toughening by Nanostructures: Structure-Property Correlation	835
Conclusions	836
References	837

Introduction

Epoxy resins, probably the most versatile family of structural adhesives, are extensively used as matrices for the fabrication of high-performance polymeric materials for engineering applications, especially in automobile and aerospace industries (Pascault and Williams 2010). Their global market size is forecasted to reach ca. US\$ 10.55 billion in 2020 from US\$ 7.1 billion in 2014, registering an increase of ca. 50% in a 6-year period (www.transparencymarketresearch.com/epoxy-resins-market.html). It is widely recognized that the intrinsic brittleness, considered as the main limitation which restricts epoxy thermosets to be used as potential materials for many engineering applications, can be alleviated by the incorporation of appropriate amount of judiciously selected functionalized elastomers and engineering thermoplastics but at the expense of stiffness and/or use temperature. Nowadays, researchers and industrialists are more interested in block copolymer (BCP) modified tough thermosetting systems, which neither compromise with stiffness nor with T_g . In general, amphiphilic BCPs have at least one of their blocks miscible with epoxy thermoset while reactive BCPs contain functional groups in one of the blocks to facilitate specific interactions which enhance chemical compatibility with the matrix.

The pioneering work of Hillmyer et al. (1997) on the self-assembly and polymerization of epoxy resin/BCP system reported that the cross-linking of the epoxy matrix without macrophase separation of BCP yields optically homogenous materials containing nanoscopic core/shell-like morphology. In the following year, Hillmyer and coworkers (Lipic et al. 1998) established that a sequence of morphologies such as lamellar, cylindrical, cubic, and disordered micelles could be achieved by varying the composition of epoxy/BCP system without a curing agent, while cured system retains nanostructure without undergoing macrophase separation. This remarkable discovery instigates enormous interest among researchers and opens a fundamentally new class of nanostructured epoxy/BCP systems, using a novel method of templating ordered structures in thermosetting matrix on a nanometer scale. This fascinating property of BCP to self-assemble into highly ordered nanostructures in thermosetting matrix make them suitable candidates for the fabrication of nanoporous materials having many potential applications including templating, surface patterning, support for catalysts, and size-selective separation. Figure 1 shows the TEM micrographs of various nanostructured morphologies generated in epoxy/BCP blends (Dean et al. 2003).

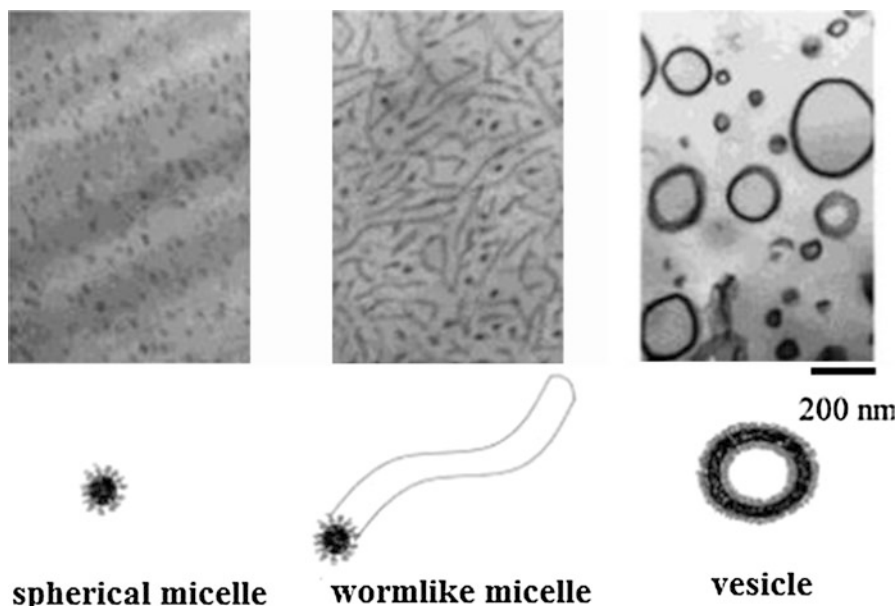


Fig. 1 TEM images showing various nanostructured morphologies generated in epoxy/BCP blends (Reprinted with permission) (Dean et al. 2003)

Eventually, various researchers have attempted several interesting variations to this protocol and revealed that significant improvements in fracture toughness can be achieved without compromising the stiffness, modulus, and T_g by incorporation of a small amount of microphase-separated amphiphilic BCP into epoxy thermoset. In the succeeding years, researchers were successful to develop another promising approach to generate nanostructures in thermosetting matrix through a mechanism called reaction-induced microphase separation (RIMPS). These two approaches, viz., self-assembly and RIMPS, now regarded as convenient and time-proven means to create nanostructures in thermosetting matrix, could be employed to develop epoxy system with remarkably enhanced toughness.

Mechanism of Phase Separation

Self-Assembly

The creation of self-assembly nanostructures discovered by Hillmyer and colleagues is regarded as one of the most outstanding achievements in this field. In this approach, precursors of epoxy form a selective solvent for BCPs, which usually contain “epoxy-philic” and “epoxy-phobic” blocks. Before curing reaction, depending on the blend composition, BCPs self-assemble into micellar structures so that the mixture exhibits distinct morphologies with lamellar, bicontinuous, wormlike,

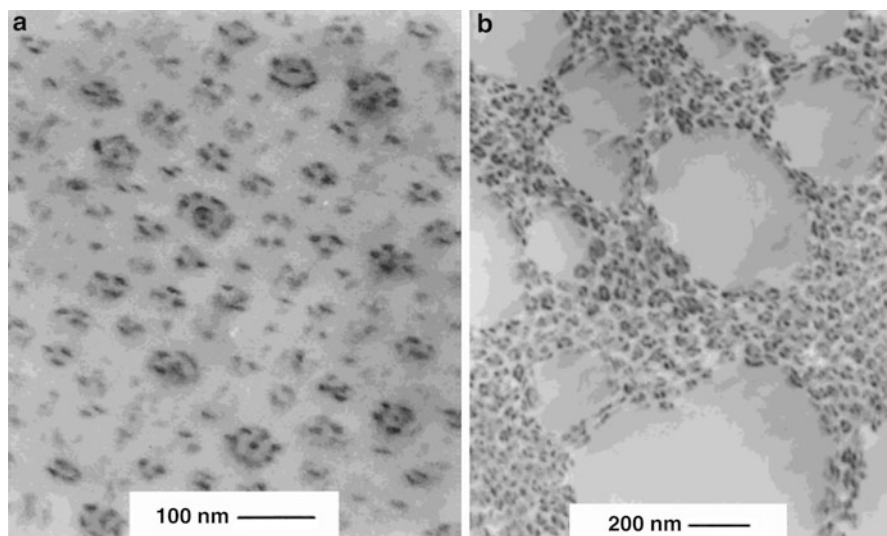


Fig. 2 TEM images (a) showing “raspberry-like” morphology for epoxy/SBM cured with MCDEA (b) the same system cured with DDS showing macrophase separation (Reprinted with permission) (Ritzenthaler et al. 2002)

spherical, and other interesting structures. Figure 2 shows the morphologies derived from the self-assembly of BCP in epoxy thermosets (Ritzenthaler et al. 2002).

In addition to blend composition, other parameters like molecular weights, block length, and block-block and block-matrix interaction parameters have profound influence on the type of self-organized structures. These preformed structures are fixed through the subsequent cross-linking with the introduction of hardeners, when curing reaction lock in the generated morphology. Note that there may be small changes in the nanostructures before and after curing reaction. Table 1 displays some of the epoxy/BCP systems which form nanostructured morphology via self-assembly.

Reaction-Induced Microphase Separation

In contrast to self-assembly approach, the RIMPS technique does not necessitate the formation of self-organized micellar structures before curing reaction. In this case, BCP will be miscible with the epoxy precursors before curing reaction, and a part of BCP gets microphase separated during curing because the polymerization increases the molecular weight of the epoxy thermoset and thereby reduces the combinatorial entropy contribution towards the free energy of mixing.

It turned out that the formation of nanostructured morphologies in particular is affected by the competitive kinetics between polymerization and phase separation and the confinement of miscible polymer chains of BCP on the phase-separated sub-chains. Finally, it is worth noting that the difference in block architecture of BCP

Table 1 Epoxy/BCP systems which form nanostructured morphology via self-assembly

Block copolymer	Hardener	References
Poly(ethylene oxide)- <i>b</i> -poly(ethylene-alt-propylene) (PEO- <i>b</i> -PEP)	4,4'-methylenedianiline (MDA)	Lipic et al. (1998)
PEO- <i>b</i> -PEP, poly(methyl methacrylate- <i>ran</i> -glycidyl methacrylate)-poly(2-ethylhexyl methacrylate) (P(MMA- <i>ran</i> -GMA)-PEHMA)	Phenol novolac (PN)	Dean et al. (2003)
Polystyrene- <i>b</i> -polybutadiene- <i>b</i> -poly(methyl methacrylate) (SBM)	4,4'-Methylenebis(3-chloro-2,6-diethylaniline) (MCDEA), 4,4'-diaminodiphenyl sulfone (DDS)	Ritzenthaler et al. (2002)
SBM	MCDEA	Ritzenthaler et al. (2003)
Poly(ethylene glycol- <i>co</i> -propylene glycol) (PEO- <i>b</i> -PPO), poly(ethylene glycol)- <i>block</i> -poly(propylene glycol)- <i>block</i> -poly(ethylene glycol) (PEO- <i>b</i> -PPO- <i>b</i> -PEO)	MDA	Mijovic et al. (2000)
Poly(methyl acrylate- <i>co</i> -glycidyl methacrylate- <i>b</i> -polyisoprene)	MDA	Guo et al. (2003)
Poly(ethylene oxide)- <i>block</i> -poly(dimethylsiloxane) (PEO-PDMS)	MDA	Guo et al. (2006a)
PEO- <i>b</i> -PPO	MDA	Guo et al. (2006b)
Poly(hexylene oxide)- <i>b</i> -poly(ethylene oxide) (PHO-PEO)	PN	Thio et al. (2006)
Epoxidised styrene- <i>b</i> -butadiene (SepB)	MCDEA	Serrano et al. (2006)
Poly(ϵ -caprolactone)- <i>b</i> -polydimethylsiloxane- <i>b</i> -poly(ϵ -caprolactone) (PCL- <i>b</i> -PDMS- <i>b</i> -PCL)	4,4'-Methylene bis(2-chloroaniline) (MOCA)	Xu and Zheng (2007a)
Poly(hydroxyether of bisphenol A)- <i>b</i> -polydimethylsiloxane (PH- <i>alt</i> -PDMS)	4,4'-Diaminodiphenylmethane (DDM)	Gong et al. (2008)
PEO- <i>b</i> -PEP	1,1,1-tris(4-hydroxyphenyl)ethane (THPE)	Thompson et al. (2009) and Liu et al. (2008, 2010)
Poly(2,2,2-trifluoroethyl acrylate)- <i>block</i> -poly(ethylene oxide) (PTFEA- <i>b</i> -PEO)	MOCA	Yi et al. (2009)
Polystyrene- <i>block</i> -poly(methyl methacrylate) (PS- <i>b</i> -PMMA)	DDM	Blanco et al. (2010)
Poly(ϵ -caprolactone)- <i>block</i> -poly(ethylene-coethylethylene)- <i>block</i> -poly(ϵ -caprolactone) (PCL- <i>b</i> -PEEE- <i>b</i> -PCL)	MOCA	Hu et al. (2010)

(continued)

Table 1 (continued)

Block copolymer	Hardener	References
Poly (methyl methacrylate)- <i>b</i> - poly (n-butyl acrylate) - <i>b</i> - poly (methyl methacrylate) (PMMA- <i>b</i> -PnBA- <i>b</i> -PMMA)	DDS, PN, methyl nadic anhydride (MNA), and 2, 4, 6-tris (dimethylaminomethyl) phenol (DMP)	Kishi et al. (2011)
Poly(2,2,2-trifluoroethyl acrylate)- <i>b</i> -poly(glycidyl methacrylate) (PTFEA- <i>b</i> -PGMA)	MOCA	Yi et al. (2011)
Poly(styrene- <i>b</i> -isoprene- <i>b</i> -styrene) (SIS)	Ancamine 2500	Garate et al. (2011)
Block complex of sulfonated polystyrene-block-poly(ethylene-ran-butylene)-block-polystyrene (SSEBS) and a tertiary amine-terminated poly(ϵ -caprolactone), SSEBS- <i>c</i> -PCL	MDA	Wu et al. (2012)
Poly(styrene- <i>b</i> -butadiene- <i>b</i> -styrene) (SBS)	Ancamine 2500	Ramos et al. (2012)
Poly(ϵ -caprolactone)-block-polyethylene-block-poly(ϵ -caprolactone) (PCL- <i>b</i> -PE- <i>b</i> -PCL)	MOCA	Zhang et al. (2013)
SBS	MCDEA	Ocando et al. (2013)
Epoxidized poly-(styrene- <i>b</i> -isoprene- <i>b</i> -styrene) (eSIS-AEP)	Ancamine 2500	Garate et al. (2014)
PEO- <i>b</i> -PPO- <i>b</i> -PEO	m-xylylenediamine (MXDA)	Cano et al. (2014)
PEP- <i>b</i> -PEO, polystyrene- <i>b</i> -poly(ethylene oxide) (PS- <i>b</i> -PEO)	Polyether triamine	Redline et al. (2014)
PS- <i>b</i> -PEO	4,4'-methylenebis(2,6-diethylaniline) (MDEA)	Leonardi et al. (2015)
Poly-(heptadecafluorodecyl acrylate)- <i>b</i> -poly(caprolactone) (PaF- <i>b</i> -PCL)	MCDEA	Ocando et al. (2007)

leads to quite different RIMPS behavior. Table 2 shows some of the epoxy/BCP systems, which follow RIMPS for the generation of nanostructured morphology.

Morphology: Formation of Nanostructures

Immense contributions from researchers during the last several years have unequivocally established that a wide range of morphologies can be generated by self-assembly or RIMPS approaches. It is worth emphasizing that the shape, size, and distribution of nanostructures in thermosetting matrix depend on a number of parameters related to the epoxy precursors, curing agents, and BCPs. As mentioned

Table 2 Epoxy/BCP systems which form nanostructured morphology via RIMPS

Block copolymer	Hardener	References
PS- <i>b</i> -PEO	MOCA	Meng et al. (2006a)
Poly(ϵ -caprolactone)- <i>block</i> -poly-(<i>n</i> -butyl acrylate) (PCL- <i>b</i> -PBA)	MOCA	Xu and Zheng (2007b)
PS- <i>b</i> -PCL, PS- <i>b</i> -PCL- <i>b</i> -PS, and PCL- <i>b</i> -PS- <i>b</i> -PCL	MOCA	Yu et al. (2012)
PCL- <i>b</i> -PS	MOCA	Meng et al. (2008)
Epoxidized poly(styrene- <i>b</i> -isoprene- <i>b</i> -styrene) (eSIS)	Ancamine 2500	Garate et al. (2013)
PS- <i>b</i> -PMMA	Tertiary amine (benzyltrimethylamine, BDMA), DDS	Girard-Reydet et al. (2002)
Polydimethylsiloxane- <i>block</i> -poly(ϵ -caprolactone)- <i>block</i> -polystyrene (PDMS- <i>b</i> -PCL- <i>b</i> -PS)	MOCA	Fan et al. (2009) ^a
Polystyrene- <i>block</i> -poly(ϵ -caprolactone)- <i>block</i> -poly(<i>n</i> -butyl acrylate) (PS- <i>b</i> -PCL- <i>b</i> -PBA)	MOCA	Fan et al. (2010)
Poly(ethylene oxide)- <i>block</i> -poly(ϵ -caprolactone)- <i>block</i> -polystyrene (PEO- <i>b</i> -PCL- <i>b</i> -PS)	MOCA, DDS	Yu and Zheng (2011)
PS- <i>b</i> -PMMA	MDEA	Romeo et al. (2013)
SBS	DDM	George et al. (2015)
PEO- <i>b</i> -PCL	MOCA, DDS	Meng et al. (2006b)
Polyisoprene- <i>b</i> -poly(4-vinyl pyridine) (PI- <i>b</i> -P4VP)	MDA	Guo et al. (2008)
PS- <i>b</i> -PMMA	MOCA	Fan and Zheng (2008)
Poly(ϵ -caprolactone)- <i>block</i> -poly(butadiene- <i>co</i> -acrylonitrile)- <i>block</i> -poly(ϵ -caprolactone) triblock copolymer (PCL- <i>b</i> -PBN- <i>b</i> -PCL)	MOCA	Yang et al. (2009)
Poly(ethylene glycol)- <i>b</i> -carboxyl terminated butadiene-acrylonitrile rubber (PEG- <i>b</i> -CTBN)	MOCA	Heng et al. (2015)
Epoxidized poly(styrene- <i>b</i> -butadiene) (SepB)	MCDEA	Serrano et al. (2009)
PS- <i>alt</i> -PEO	MOCA	Hu and Zheng (2009)
PEO- <i>b</i> -PPO- <i>b</i> -PEO	DDS	Parameswaranpillai et al. (2017)

^aBoth self-assembly and RIMPS

earlier, concentration of BCP, block length, block-block interaction, molecular weights of blocks, the type of matrix, matrix-matrix interactions, the type of curing agent, cure cycle, etc. are the important factors which influence the nature of final nanostructured morphology. AFM images given in Fig. 3 show that as the concentration of BCP changes, morphology of epoxy/BCP blends shifts from spherical nanodomains to interconnected nanoobjects at intermediate concentrations and then

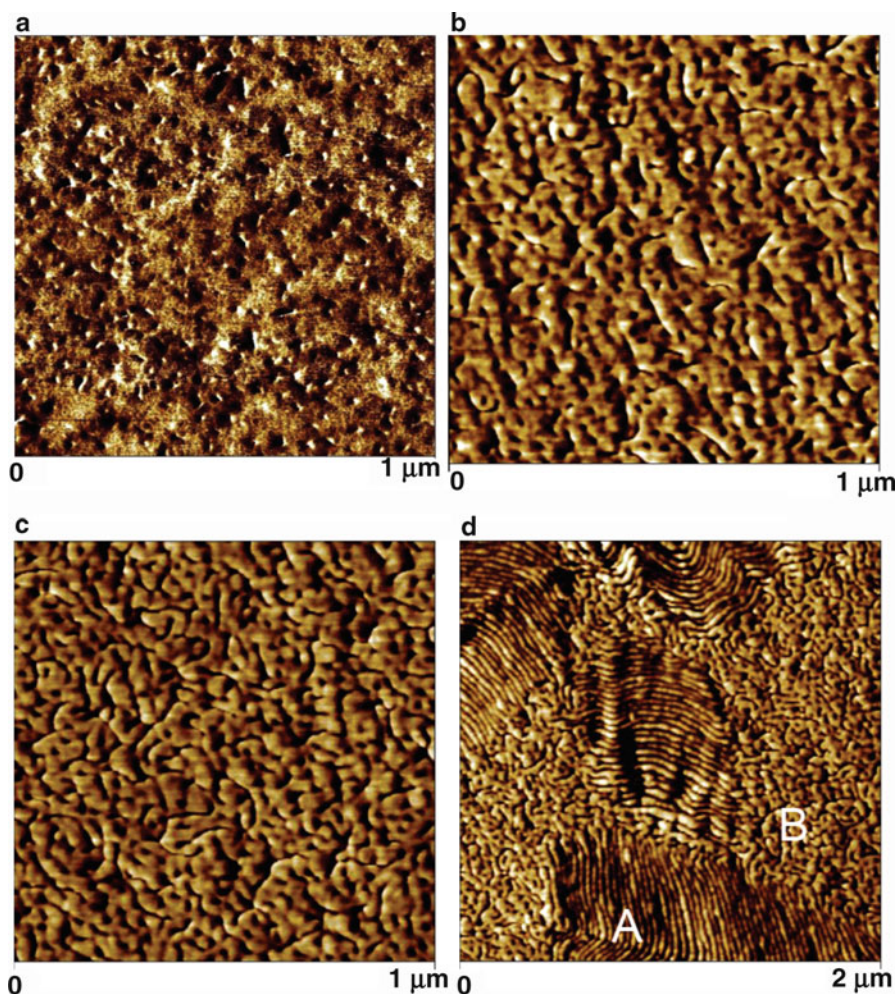


Fig. 3 AFM images of epoxy/BCP/MOCA blends containing (a) 10, (b) 20, (c) 30, and (d) 40 wt.% of BCP. Increasing the concentration of the BCP shifted the morphology from spherical domains to lamellar nanostructures besides the interconnected nanoobjects (Reprinted with permission) (Xu and Zheng 2007b)

to lamellar nanostructures besides the interconnected nanoobjects at higher concentrations (Xu and Zheng 2007b).

In addition, the competitive dynamics between the curing reaction, phase separation, and thermodynamic factors including hydrogen bonding interactions are some other important aspects which should be considered to evaluate the development of final micro- or nanostructured morphology. The following schematic model (Fig. 4) illustrates the unique structure and dynamics of thermoset/BCP interphase and the underlying principle of formation of final-phase structure in epoxy resin/

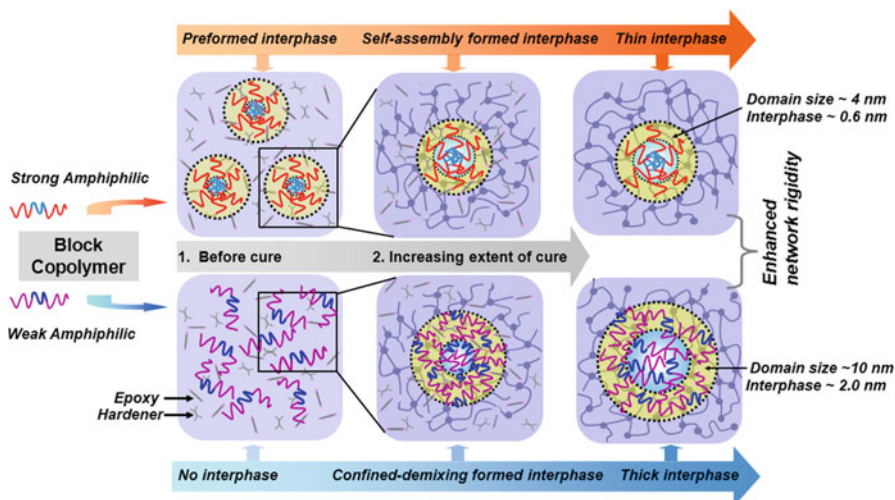


Fig. 4 Schematic representation of the model describing two different types of interphase structures and their underlying formation mechanism in epoxy resin/BCP blends (Reprinted with permission) (He et al. 2014)

BCP blends. This model displays two types of interphase structures generated by self-assembly and RIMPS and provides microlevel information about the morphology (He et al. 2014).

Toughening by Nanostructures: Structure-Property Correlation

Since the intrinsic brittleness of epoxy thermosets makes them susceptible to fracture failure, the extent of improvement in toughness and the related mechanisms in BCP-modified epoxy systems are of greatest importance in terms of scientific and technological perspective. The final nanostructured morphology governed by self-assembly and RIMPS differ in terms of size, shape, and distribution of nanodomains, and therefore the correlation between nanostructure parameters and fracture toughness will provide an intuitive insight on the structure property correlation in other toughened thermosets as well.

Researchers have shown that improvement in toughness without compromising stiffness and modulus of thermoset can be explained in terms of various mechanisms including crack-tip blunting, debonding, crack bridging, shear yielding, cavitation, etc. Attention should be paid to the fact that the enhancement of toughness in epoxy thermosets modified with BCP depends on nanodomain morphology, which in turn depends on the nature and thickness of epoxy/BCP interphase. Despite the fact that there are still unsettled issues and unresolved problems in this regard, different nanostructures lead to different levels of toughening improvement (Fig. 5). For example, irrespective of the same basic shape of

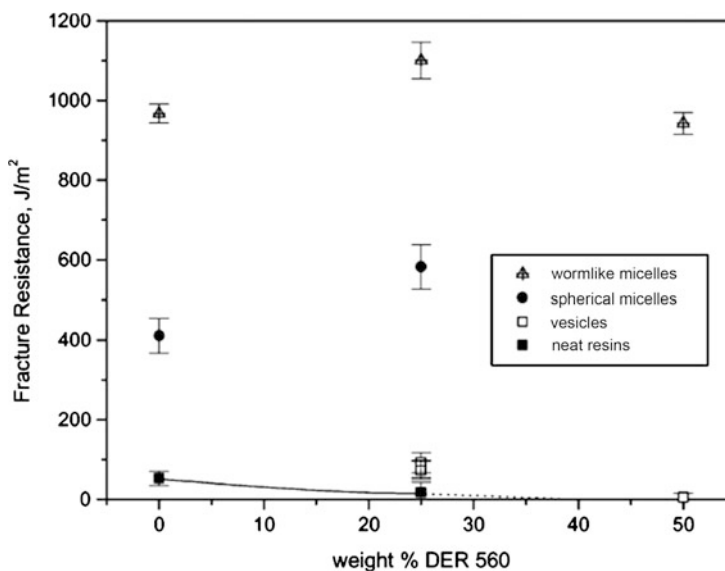


Fig. 5 Fracture resistance for DER383/DER560/PN containing 5 wt.% BCP; spherical and wormlike micelles were obtained from PEO-*b*-PEP-9 and PEO-*b*-PEP-15 BCPs, respectively, while vesicles were generated with the P(MMA-*ran*-GMA)-PEHMA compounds (Reprinted with permission) (Dean et al. 2003)

the spherical micelles and vesicles, larger size of vesicles results in greater fracture toughness. Similarly, wormlike micelles can produce greater improvement in fracture toughness compared to spherical micelles, mainly because of the crack-tip blunting and crack-bridging mechanisms whereas spheres are more effective in deflecting the progressive crack away from the original crack plane.

Conclusions

Block copolymers (BCPs) are extensively used for enhancing fracture toughness of brittle epoxies, without compromising modulus, stiffness, and use temperature. BCPs form wide variety of structures at nanometer scale in thermosetting matrix via self-assembly and reaction-induced microphase separation mechanisms. The formation of nanostructured morphology depends on several factors including blend composition, type of BCP, molecular weights of blocks, block architecture, matrix-block and block-block interactions, type of curing agent, and curing cycle. Since the end-use structural applications of epoxy thermosets are assessed in terms of the toughness of the product by judicious selection BCPs and optimization of curing conditions, nanostructured morphology could be tuned in such a way that tough polymeric materials with attractive thermomechanical properties suitable for demanding applications can be developed.

References

- Blanco M, Lopez M, Kortaberria G, Mondragon I (2010) Nanostructured thermosets from self-assembled amphiphilic block copolymer/epoxy resin mixtures: effect of copolymer content on nanostructures. *Polym Int* 59:523–528
- Cano L, Builes DH, Tercjak A (2014) Morphological and mechanical study of nanostructured epoxy systems modified with amphiphilic poly(ethylene oxide-*b*-propylene oxide-*b*-ethylene oxide)triblock copolymer. *Polymer* 55:738–745
- Dean JM, Verghese NE, Pham HQ, Bates FS (2003) Nanostructure toughened epoxy resins. *Macromolecules* 36:9267–9270
- Fan W, Zheng S (2008) Reaction-induced microphase separation in thermosetting blends of epoxy resin with poly(methyl methacrylate)-block-polystyrene block copolymers: effect of topologies of block copolymers on morphological structures. *Polymer* 49:3157–3167
- Fan W, Wang L, Zheng S (2009) Nanostructures in thermosetting blends of epoxy resin with polydimethylsiloxane-block-poly(ϵ -caprolactone)-block-polystyrene ABC triblock copolymer. *Macromolecules* 42:327–336
- Fan W, Wang L, Zheng S (2010) Double reaction-induced microphase separation in epoxy resin containing polystyrene-block-poly(ϵ -caprolactone)-block-poly(*n*-butyl acrylate) ABC triblock copolymer. *Macromolecules* 43:10600–10611
- Garate H, Mondragon I, Goyanes S, D'Accorso NB (2011) Controlled epoxidation of poly(styrene-*b*-isoprene-*b*-styrene) block copolymer for the development of nanostructure epoxy thermosets. *J Polym Sci Part A Polym Chem* 49:4505–4513
- Garate H, Mondragon I, D'Accorso NB, Goyanes S (2013) Exploring microphase separation behavior of epoxidized poly(styrene-*b*-isoprene-*b*-styrene) block copolymer inside thin epoxy coatings. *Macromolecules* 46:2182–2187
- Garate H, Goyanes S, D'Accorso NB (2014) Controlling nanodomain morphology of epoxy thermosets modified with reactive amine-containing epoxidized poly(styrene-*b*-isoprene-*b*-styrene) block copolymer. *Macromolecules* 47:7416–7423
- George SM, Puglia D, Kenny JM, Parameswaranpillai J, Vijayan P, Pionteck J, Thomas S (2015) Volume shrinkage and rheological studies of epoxidised and unepoxidised poly(styrene-block-butadiene-block-styrene) triblock copolymer modified epoxy resin-diamino diphenyl methane nanostructured blend systems. *Phys Chem Chem Phys* 17:12760–12770
- Girard-Reydet E, Sevignon A, Pascault JP, Hoppe CE, Galante MJ, Oyangueren PA, Williams RJJ (2002) Influence of the addition of polystyrene-block-poly(methyl methacrylate) copolymer (PS-*b*-PMMA) on the morphologies generated by reaction-induced phase separation in PS/PMMA/epoxy blends. *Macromol Chem Phys* 203:947–952
- Epoxy Resins Market – Global Industry Analysis, Size, Share, Growth, Trends and Forecast, 2014–2020. <http://www.transparencymarketresearch.com/epoxy-resins-market.html>
- Gong W, Zeng K, Wang L, Zheng S (2008) Poly(hydroxyether of bisphenol A)-block-polydimethylsiloxane alternating block copolymer and its nanostructured blends with epoxy resin. *Polymer* 49:3318–3326
- Guo Q, Dean JM, Grubbs RB, Bates FS (2003) Block copolymer modified novolac epoxy resin. *J Polym Sci Part B Polym Phys* 41:1994–2003
- Guo Q, Chen F, Wang K, Chen L (2006a) Nanostructured thermoset epoxy resin templated by an amphiphilic poly(ethylene oxide)-block-poly(dimethylsiloxane) diblock copolymer. *J Polym Sci Part B Polym Phys* 44:3042–3052
- Guo Q, Wang K, Chen L, Zheng S, Halley PJ (2006b) Phase behavior, crystallization, and nanostructures in thermoset blends of epoxy resin and amphiphilic star-shaped block copolymers. *J Polym Sci Part B: Polym Phys* 44:975–985
- Guo Q, Liu J, Chen L, Wang K (2008) Nanostructures and nanoporosity in thermoset epoxy blends with an amphiphilic polyisoprene-block-poly(4-vinyl pyridine) reactive diblock copolymer. *Polymer* 49:1737–1742

- He X, Liu Y, Zhang R, Wu Q, Chen T, Sun P, Wang X, Xue G (2014) Unique interphase and cross-linked network controlled by different miscible blocks in nanostructured epoxy/block copolymer blends characterized by solid-state NMR. *J Phys Chem C* 118:13285–13299
- Heng Z, Chen Y, Zou H, Liang M (2015) Simultaneously enhanced tensile strength and fracture toughness of epoxy resins by a poly(ethylene oxide)-block-carboxyl terminated butadiene-acrylonitrile rubber diblock copolymer. *RSC Adv* 5:42362–42368
- Hillmyer MA, Lipic PM, Hajduk DA, Almdal K, Bates FS (1997) Self-assembly and polymerization of epoxy resin-amphiphilic block copolymer nanocomposites. *J Am Chem Soc* 119:2749–2750
- Hu D, Zheng S (2009) Reaction-induced microphase separation in epoxy resin containing polystyrene-block-poly(ethylene oxide) alternating multiblock copolymer. *Eur Polym J* 45:3326–3338
- Hu D, Zhang C, Yu R, Wang L, Zheng S (2010) Self-organized thermosets involving epoxy and poly(ϵ -caprolactone)-block-poly(ethylene-co-ethylthylene)-block-poly(ϵ -caprolactone) amphiphilic triblock copolymer. *Polymer* 51:6047–6057
- Kishi H, Kunimitsu Y, Imade J, Oshita S, Morishita Y, Asada M (2011) Nano-phase structures and mechanical properties of epoxy/acryl triblock copolymer alloys. *Polymer* 52:760–768
- Leonardi AB, Zucchi IA, Williams RJJ (2015) Generation of large and locally aligned wormlike micelles in block copolymer/epoxy blends. *Eur Polym J* 65:202–208
- Lipic PM, Bates FS, Hillmyer MA (1998) Nanostructured thermosets from self-assembled amphiphilic block copolymer/epoxy resin mixtures. *J Am Chem Soc* 120:8963–8970
- Liu J, Sue H, Thompson ZJ, Bates FS, Dettloff M, Jacob G, Verghese N, Pham H (2008) Nanocavitation in self-assembled amphiphilic block copolymer-modified epoxy. *Macromolecules* 41:7616–7624
- Liu J, Thompson ZJ, Sue H, Bates FS, Hillmyer MA, Dettloff M, Jacob G, Verghese N, Ha P (2010) Toughening of epoxies with block copolymer micelles of wormlike morphology. *Macromolecules* 43:7238–7243
- Meng F, Zheng S, Li H, Liang Q, Liu T (2006a) Formation of ordered nanostructures in epoxy thermosets: a mechanism of reaction-induced microphase separation. *Macromolecules* 39:5072–5080
- Meng F, Zheng S, Liu T (2006b) Epoxy resin containing poly(ethylene oxide)-block-poly(ϵ -caprolactone) diblock copolymer: effect of curing agents on nanostructures. *Polymer* 47:7590–7600
- Meng F, Xu Z, Zheng S (2008) Microphase separation in thermosetting blends of epoxy resin and poly(ϵ -caprolactone)-block-polystyrene block copolymers. *Macromolecules* 41:1411–1420
- Mijovic J, Shen M, Sy JW, Mondragon I (2000) Dynamics and morphology in nanostructured thermoset network/block copolymer blends during network formation. *Macromolecules* 33:5235–5244
- Ocando C, Serrano E, Tercjak A, Pena C, Kortaberria G, Calberg C, Grignard B, Jerome R, Carrasco PM, Mecerreyes D, Mondragon I (2007) Structure and properties of a semifluorinated diblock copolymer modified epoxy blend. *Macromolecules* 40:4068–4074
- Ocando C, Fernández R, Tercjak A, Mondragon I, Eceiza A (2013) Nanostructured thermoplastic elastomers based on SBS triblock copolymer stiffening with low contents of epoxy system. Morphological behavior and mechanical properties. *Macromolecules* 46:3444–3451
- Parameswaranpillai J, Sidhardhan SK, Jose S, Siengchin S, Pionteck J, Magueresse A, Grohens Y, Hameed N (2017) Reaction-induced phase separation and resulting thermomechanical and surface properties of epoxy resin/poly(ethylene oxide)-poly(propylene oxide)-poly(ethylene oxide) blends cured with 4,4'-diaminodiphenylsulfone. *J Appl Polym Sci* 134:44406
- Pascault JP, Williams RJJ (2010) General concepts about epoxy polymers. In: Pascault J-P, Williams RJJ (eds) *Epoxy polymers: new materials and innovations*. Wiley-VCH Verlag GmbH & Co. KGaA, Weinheim. doi:10.1002/9783527628704.ch1
- Ramos JA, Espósito LH, Fernández R, Zalakain I, Goyanes S, Avgeropoulos A, Zafeiropoulos NE, Kortaberria G, Mondragon I (2012) Block copolymer concentration gradient and solvent effects

- on nanostructuring of thin epoxy coatings modified with epoxidized styrene–butadiene–styrene block copolymers. *Macromolecules* 45:1483–1491
- Redline EM, Declet-Perez C, Bates FS, Francis LF (2014) Effect of block copolymer concentration and core composition on toughening epoxies. *Polymer* 55:4172–4181
- Ritzenthaler S, Court F, David L, Girard-Reydet E, Leibler L, Pascault JP (2002) ABC triblock copolymers/epoxy-diamine blends. 1. Keys to achieve nanostructured thermosets. *Macromolecules* 35:6245–6254
- Ritzenthaler S, Court F, Girard-Reydet E, Leibler L, Pascault JP (2003) ABC triblock copolymers/epoxy-diamine blends. 2. Parameters controlling the morphologies and properties. *Macromolecules* 36:118–126
- Romeo HE, Zucchi IA, Rico M, Hoppe CE, Williams RJJ (2013) From spherical micelles to hexagonally packed cylinders: the cure cycle determines nanostructures generated in block copolymer/epoxy blends. *Macromolecules* 46:4854–4861
- Serrano E, Tercjak A, Kortaberria G, Pomposo JA, Mecerreyes D, Zafeiropoulos NE, Stamm M, Mondragon I (2006) Nanostructured thermosetting systems by modification with epoxidized styrene-butadiene star block copolymers. Effect of epoxidation degree. *Macromolecules* 39:2254–2261
- Serrano E, Kortaberria G, Arruti P, Tercjak A, Mondragon I (2009) Molecular dynamics of an epoxy resin modified with an epoxidized poly(styrene–butadiene) linear block copolymer during cure and microphase separation processes. *Eur Polym J* 45:1046–1057
- Thio YS, Wu J, Bates FS (2006) Epoxy toughening using low molecular weight poly(hexylene oxide)-poly(ethylene oxide) diblock copolymers. *Macromolecules* 39:7187–7189
- Thompson ZJ, Hillmyer MA, Liu J, Sue H, Dettloff M, Bates FS (2009) Block copolymer toughened epoxy: role of cross-link density. *Macromolecules* 42:2333–2335
- Wu S, Guo Q, Peng S, Hameed N, Kraska M, Stühn B, Mai Y (2012) Toughening epoxy thermosets with block ionomer complexes: a nanostructure–mechanical property correlation. *Macromolecules* 45:3829–3840
- Xu Z, Zheng S (2007a) Morphology and thermomechanical properties of nanostructured thermosetting blends of epoxy resin and poly(ϵ -caprolactone)-block-polydimethylsiloxane-block-poly(ϵ -caprolactone) triblock copolymer. *Polymer* 48:6134–6144
- Xu Z, Zheng S (2007b) Reaction-induced microphase separation in epoxy thermosets containing poly(ϵ -caprolactone)-block-poly(*n*-butyl acrylate) diblock copolymer. *Macromolecules* 40:2548–2558
- Yang X, Yi F, Xin Z, Zheng S (2009) Morphology and mechanical properties of nanostructured blends of epoxy resin with poly(ϵ -caprolactone)-block-poly(butadiene-co-acrylonitrile)-block-poly(ϵ -caprolactone) triblock copolymer. *Polymer* 50:4089–4100
- Yi F, Zheng S, Liu T (2009) Nanostructures and surface hydrophobicity of self-assembled thermosets involving epoxy resin and poly(2,2,2-trifluoroethyl acrylate)-block-poly(ethylene oxide) amphiphilic diblock copolymer. *J Phys Chem B* 113:1857–1868
- Yi F, Yu R, Zheng S, Li X (2011) Nanostructured thermosets from epoxy and poly(2,2,2-trifluoroethyl acrylate)-block-poly(glycidyl methacrylate) diblock copolymer: demixing of reactive blocks and thermomechanical properties. *Polymer* 52:5669–5680
- Yu R, Zheng S (2011) Morphological transition from spherical to lamellar nanophases in epoxy thermosets containing poly(ethylene oxide)-block-poly(ϵ -caprolactone)-block-polystyrene triblock copolymer by hardeners. *Macromolecules* 44:8546–8557
- Yu R, Zheng S, Li X, Wang J (2012) Reaction-induced microphase separation in epoxy thermosets containing block copolymers composed of polystyrene and poly(ϵ -caprolactone): influence of copolymer architectures on formation of nanophases. *Macromolecules* 45:9155–9168
- Zhang C, Li L, Zheng S (2013) Formation and confined crystallization of polyethylene nanophases in epoxy thermosets. *Macromolecules* 46:2740–2753

Miscibility, Phase Separation, and Mechanism of Phase Separation of Epoxy/Block-Copolymer Blends

29

Hernan Garate, Noé J. Morales, Silvia Goyanes, and Norma B. D'Accorso

Abstract

Incorporating block copolymers into epoxy systems has emerged as a versatile and effective methodology not only to enhance their mechanical properties, but also as an intriguing strategy to design advanced materials with tailored properties. Knowledge of microphase separation mechanisms operating during the development of these materials is essential due to the straight relationship between block copolymer characteristics, epoxy system formulation, and curing conditions with the final nanodomain morphology. This chapter is focused on the thermodynamic and kinetic fundamentals describing microphase separation mechanisms by which the nanodomains are obtained. Moreover, key parameters affecting phase separation mechanisms and morphologies are discussed,

H. Garate (✉)

YPF Tecnología S.A., Ensenada, Buenos Aires, Argentina

IFIBA-CONICET, LP&MC, Departamento de Física, FCEyN-UBA, Ciudad Universitaria, Ciudad Autónoma de Buenos Aires, Argentina

CIHIDECAR-CONICET, Departamento de Química Orgánica, FCEyN-UBA, Ciudad Universitaria, Ciudad Autónoma de Buenos Aires, Argentina

e-mail: hgarate001@gmail.com

N.J. Morales

YPF Tecnología S.A., Ensenada, Buenos Aires, Argentina

e-mail: noe.jmorales@gmail.com

S. Goyanes

IFIBA-CONICET, LP&MC, Departamento de Física, FCEyN-UBA, Ciudad Universitaria, Ciudad Autónoma de Buenos Aires, Argentina

e-mail: goyanes@df.uba.ar

N.B. D'Accorso

CIHIDECAR-CONICET, Departamento de Química Orgánica, FCEyN-UBA, Ciudad Universitaria, Ciudad Autónoma de Buenos Aires, Argentina

e-mail: norma@qo.fcen.uba.ar

explaining how different material properties can be tuned by controlling the nanostructure morphology.

Keywords

Block copolymers • Epoxy system • Polymerization-induced microphase separation • Self-assembly • Miscibility

Contents

Introduction	842
Macro- Versus Microphase Separation Behavior	843
Microphase Separation Mechanisms	848
Microphase Separation During Curing	849
Microphase Separation Before Curing	852
“Tandem-Like” Mechanisms	853
Experimental Strategies to Follow Microphase Separation Mechanism	857
Key Parameters Affecting Mechanisms and Morphologies	859
Epoxy/BCP Composition	859
Number of Block Types	860
Block Sequence	861
Influence of BCP Reactivity	863
Influence of the Hardener	864
Influence of Curing Conditions	866
Impact of Morphology in the Epoxy/BCP Blend Properties	872
Mechanical Properties	873
Thermal Properties	873
Surface Properties	876
Conclusions	877
References	877

Introduction

Block copolymers are a unique class of polymers capable of structuring epoxy systems down to molecular scales (few tens of nanometers). This intriguing ability can be used to design advanced nanostructured polymers with potential technological applications as multifunctional coatings (Esposito et al. 2014), transparent materials with high refractive indices for optical applications (Caseri 2000), low dielectric constant films for microelectronic industry (Hedrick et al. 1998), nanostructured templates for composite materials (Esposito et al. 2013) and porous polymers (Guo et al. 2008), and toughening of polymer networks (Karger-Kocsis et al. 2004; Zhu et al. 2004; Declet-Perez et al. 2015), among others.

With the aim to obtain novel materials with tuned properties, it is crucial to first understand the nanostructuring mechanisms operating during thermoset formation and how these are related to the thermodynamics of epoxy/BCP blends and kinetic conditions dictated by viscosity and curing kinetics. It is possible to adjust the nature of the selected epoxy/BCP blend and establish curing conditions that enable obtaining controlled nanodomain morphologies. Moreover, since there is a close

relationship between morphology, size, dispersion state, and interfacial adhesion between the phases and the ultimate properties of the blends, knowledge of phase separation mechanism in these systems is essential to gain access a myriad of well-defined morphologies and therefore controlled final properties, by tuning epoxy/BCP formulation and curing conditions.

This chapter provides an insight into thermodynamic and kinetic fundamentals of nanodomain formation mechanisms in epoxy/BCP blends which are essential to understand how it is possible to control nanodomain size, shape, and morphology by selecting proper blend formulation and curing conditions. It also provides a discussion of key factors that control the obtained morphologies and describes how a given nanodomain morphology further dictates material properties based on state-of-the-art literature examples.

Macro- Versus Microphase Separation Behavior

Block copolymers are capable of microphase separation on nanometer length scales into well-defined ordered nanophases both in the undiluted state and in blends (Matsen and Bates 1996; Bates and Fredrickson 1999). These morphologies are determined mainly due to the balance between enthalpic penalty arising from association between different blocks and the restrictions imposed by covalent bonds linking blocks. Block copolymer morphologies are dictated by polymer length, block symmetry, and interblock repulsion strength. Furthermore, when BCP are blended with homopolymers and copolymers or are in solution, other parameters as solvent-block interaction parameters and blend composition further determine block copolymer morphology.

Phase behavior of epoxy/BCP blends can be roughly modeled by considering each system as a solution of a BCP in a block-selective solvent (epoxy precursors) which evolves during the curing process, through a BCP/block-selective polymer blend, into a cross-linked epoxy network bearing BCP-separated domains.

There are two possible scenarios when blending block copolymer with epoxy precursors: (a) *microphase-separated system*, where the block copolymer induces nanodomain inclusions within the epoxy matrix, and (b) *macrophase-separated system* consisting of a multiphase system with a well-defined epoxy phase and block copolymer-rich phase in the submicron length scale.

A simple and approximate approach to anticipate whether micro- or macrophase separation will take place for a given epoxy/BCP blend is by direct comparison between solubility parameters (δ) of each block and those for the epoxy precursors, which can be considered as reactive solvents before curing.

The solubility between a polymer and a solvent is determined by the polymer-solvent interaction parameter $\chi_{\text{polymer-solvent}}$, defined by Eq. 1:

$$\chi_{\text{polymer-solvent}} = \frac{Z\chi_{\text{polymer}} \Delta w_{\text{polymer-solvent}}}{k_B T} = \chi_H + \chi_S \quad (1)$$

Here, Z is the lattice coordination number, χ_{polymer} is the number of polymer segments per solvent molecule (usually assumed as one), $\Delta w_{\text{polymer-solvent}}$ is the interaction free energy associated with the formation of an unlike contact pair between segments of a solvent and a polymer molecule, k_B is the Boltzmann constant, and $k_B T$ is the thermal energy. $\chi_{\text{polymer-solvent}}$ is expressed in terms of an enthalpic, χ_H , and an entropic contribution, χ_S . The enthalpic component χ_H can be calculated in terms of the solubility parameters as by Eq. 2:

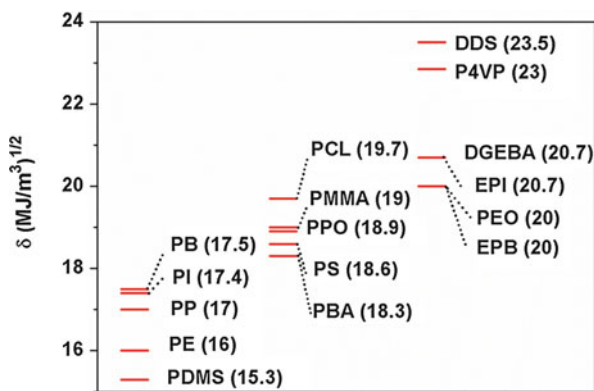
$$\chi_H = \frac{V_{\text{solvent}}}{RT} \left((\delta_{\text{polymer}} - \delta_{\text{solvent}})^2 + 2I_{\text{polymer-solvent}} \delta_{\text{polymer}} \delta_{\text{solvent}} \right) \approx \frac{V_1 (\delta_{\text{polymer}} - \delta_{\text{solvent}})^2}{RT} \quad (2)$$

where V_{solvent} is the solvent molar volume; R is the gas constant; δ_{polymer} and δ_{solvent} are the solubility parameters of polymer and solvent, respectively; and I is a binary parameter between solvent and polymer, which can be approximated to a zero value (Mikos and Peppas 1988).

Therefore, those polymer-solvent systems with similar δ values tend to be miscible with one another ($\delta_{\text{polymer}} - \delta_{\text{solvent}} \rightarrow \text{zero}$). Solubility parameters (δ) for selected polymers diglycidyl ether of bisphenol A (DGEBA) and hardener are given in Fig. 1.

Following the previous analysis, it can be anticipated that interactions between ePI ($\delta_{\text{ePI}} = 20.7 \text{ (MJ/m}^3)^{1/2}$) and epoxy monomer DGEBA ($\delta_{\text{DGEBA}} = 20.7 \text{ (MJ/m}^3)^{1/2}$) are favorable enough to enable miscibility. Grubbs et al. (2000) calculated the solubility parameters for epoxidized polyisoprene of poly(butadiene-*b*-isoprene-*ran*-epoxidizedisoprene) with epoxidation degrees of 75% and 46%. By doing so, it was determined that interactions between epoxidated BCP in 75% and epoxy precursors are favorable enough to enable miscibility of these highly epoxidized systems, while at lower epoxidation degree (46%), the interactions between BCP and the epoxy component are sufficiently unfavorable. Since polybutadiene block is also immiscible with the epoxy precursors, macrophase separation occurs for the BCP with epoxidation degree of 46%.

Fig. 1 Solubility parameter for different polymers and epoxy precursors (Barton 1990; Van Krevelen 1990; Ng and Chee 1997; Yu et al. 1997; Bordes et al. 2010; O'Driscoll et al. 2011)

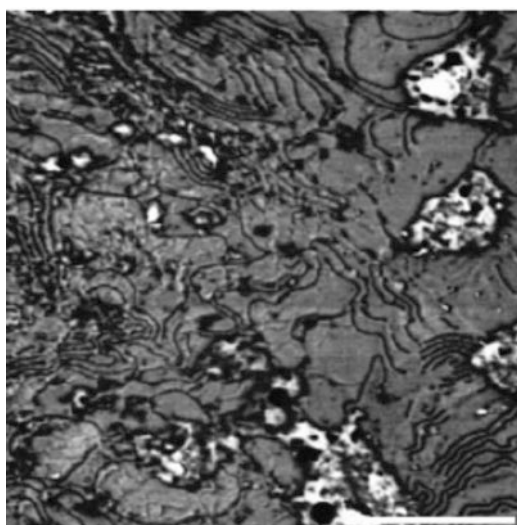


Macrophase-separated epoxy/BCP blends are characterized by opaque aspect due to light scattering of separated domains with dimensions comparable to the wavelength of visible light. On the contrary, the nanometer length domain size in microphase-separated systems avoids this effect, and therefore such materials are transparent. For this reason, a practical and simple strategy to anticipate whether micro- or macrophase separation occurs is by direct inspection of the system or by optical microscopy. Macrophase-separated systems are composed by separated epoxy-rich phase and copolymer-rich phase with domain lengths on the order of several hundred nanometers. These copolymer-rich domains are almost pure copolymer regions that involve separate compartments of ordered features similar to those encountered in the corresponding parent copolymer, as shown in Fig. 2 for an immiscible epoxy/poly(styrene-*b*-butadiene) blend (Serrano et al. 2004).

As the cure process begins, the molecular weight of the growing epoxy matrix diverges, and the correspondingly large increase in the copolymer degree of polymerization N overcomes the favorable interaction parameter value and drives χN (the strength of interblock repulsion), where χ is the Flory-Huggins interaction parameter, to values large enough to exceed critical phase separation condition and therefore promotes phase separation.

Following this analysis, it might be thought that the final system after curing epoxy/BCP blends should always be macrophase separated, as for the case of traditional epoxy/homopolymer blends. However, this is not the case because the highly cross-linked epoxy network substantially reduces chain mobility of the copolymer, and therefore the tendency toward macrophase separation is greatly retarded, as the cure process progresses. This kinetic restriction due to the increase in molecular weight and cross-linking avoids the possibility of coarsening and growth of phase-separated domains and is responsible for the evolution of the epoxy/BCP blends to a microphase-separated state. Therefore, both thermodynamic

Fig. 2 TEM micrograph of macrophase-separated epoxy/poly(styrene-*b*-butadiene) blend. Scale bar = 1 μm (Reprinted with permission from Serrano et al. (2004). Copyright (2004). John Wiley and Sons)



and kinetic effects compete during the cure process of epoxy/BCP blends as manifested in the phase behavior of partially epoxidized poly(styrene-*b*-butadiene) (SB) within epoxy system studied by Serrano et al. (2007). Epoxidized SB block copolymers with epoxidation degree in the range of 37–46% are suitable candidates to understand the phase behavior of epoxy/BCP blends, since the incorporation of oxirane ring to the immiscible polybutadiene block gives access to BCP with tuned miscibility with epoxy precursors. In this regard the epoxidized block of SB with an epoxidation degree of 37% (SB37) and 46% (SB46) are both initially miscible with the epoxy precursors, but epoxidized polybutadiene block of SB46 is more miscible than the corresponding epoxidized block of SB37 due to a similar solubility parameter with the epoxy precursors. Transmission electron microscopy (TEM) images of cured epoxy/SB37 and epoxy/SB46 showed the nanostructured pattern of both systems. Epoxy/SB37 presented a combination of spherical and wormlike structures, while epoxy/SB46 system consisted of ordered spherical micelles, as presented in Fig. 3. These morphological differences suggest that the epoxybutadiene blocks with epoxidation degrees of 37% are only barely miscible with the uncured epoxy resin. As the molecular weight of the epoxy resin increases during cure, the miscibility between epoxy resin and epoxybutadiene block decreases to the point where phase separation begins at much lower conversions than for the case of highly epoxidized epoxybutadiene block of SB46. When phase separation begins at this lower conversion, the viscosity of the growing epoxy network is low enough to allow nucleation and growth of block copolymer domains, allowing the shift from spherical micelles to aggregated micelles in the form of wormlike structures. On the contrary, growth of phase-separated domains in epoxy/SB46 blends is arrested because the gelation of the curing resin occurs at a

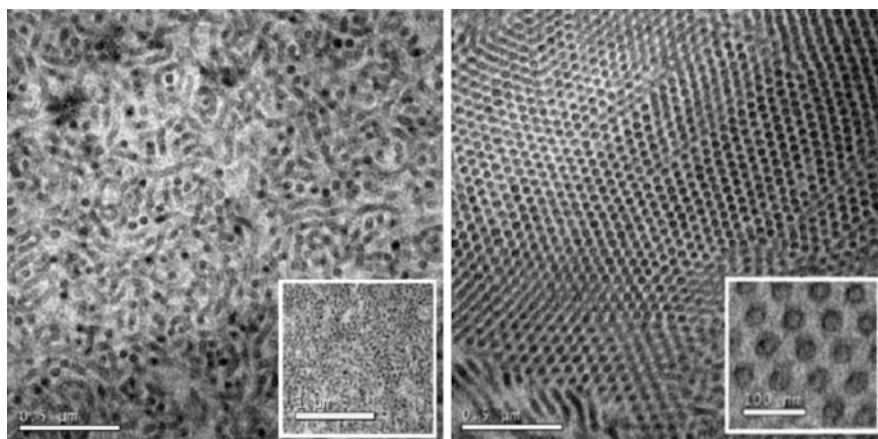
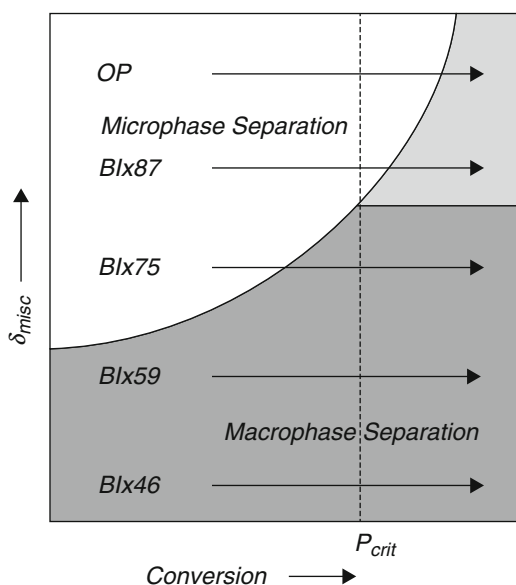


Fig. 3 TEM micrographs of microphase-separated epoxy/partially epoxidized poly(styrene-*b*-butadiene) blend. The epoxidation degree is 37% (*left*) and 46% (*right*). Scale bars = 0.5 μm . Scale bars in the inset = 1 μm (*left*) and 100 nm (*right*) (Reprinted with permission from Serrano et al. (2007). Copyright (2007). John Wiley and Sons)

similar curing conversion or prior to the critical segregation limit χN_{crit} . Since χ is related with the segregation strength, being lower for epoxy/epoxypolybutadiene 46 than the corresponding parameter for epoxy/epoxypolybutadiene 37, the product χN overcomes critical phase separation limit χN_{crit} at lower N , or lower epoxy conversion for SB37 than for SB46.

In this regard, Grubbs et al. (2000) synthesized poly(butadiene-*b*-isoprene) (BI) block copolymers selectively epoxidized in the isoprene units (BIe) with epoxidation degrees ranging from 46% to 87%, in order to classify each epoxy/BCP blend according to their phase separation behavior (micro- or macrophase separation) as a function of miscibility and epoxy conversion. As a result of their analysis, the authors proposed a phase separation behavior map, which is shown in Fig. 4 and contains valuable information on how a given epoxy/BIE blend evolves during curing. Dark gray regions in the map correspond to macrophase-separated systems. For instance, the epoxidation degree of BI46 is low enough to prevent miscibility from the initial uncured system, and therefore it is situated in the macrophase-separated region, regardless of the epoxy conversion. For the case of BI75, the initial epoxy/BCP blend is miscible, and it situates in the microphase separation region (white region). However, as the polymerization reaction proceeds, the system evolves to the macrophase separation region (dark gray) before reaching the critical epoxy conversion (p_{crit}), after which the system is kinetically hindered to phase separate. On the contrary, by further increasing initial miscibility between epoxidized polyisoprene blocks and epoxy precursors, epoxy/BI87 blend surpasses the critical epoxy conversion in the microphase-separated region (white), indicating that the final material is nanostructured. It is worth noting that if the epoxy conversion is further increased, the system should situate in the macrophase-separated region as the product $\chi N > \chi N_{crit}$.

Fig. 4 Proposed mapping of phase separation in epoxy/BCP blends as a function of miscibility and epoxy conversion (Reprinted with permission from Grubbs et al. (2000). Copyright (2000). American Chemical Society)



This thermodynamically stable region is however not accessible due to the increased viscosity of the cross-linked system as the epoxy conversion exceeds p_{crit} , which fixes the material in the microphase-separated state as indicated by light gray color. A similar scenario occurs for the more miscible epoxy/poly(ethylene oxide-*b*-ethylene-*alt*-propylene) (OP) blend.

While the absence of macrophase separation in epoxy/BCP blend systems is the result of both thermodynamic and kinetic factors, not all microphase-separated epoxy/BCP systems are obtained by the same sequence of events. The following section describes the possible operating mechanisms that lead to epoxy/BCP nanostructured systems, as well as practical considerations to follow and determine which mechanism occurs and the key parameters affecting nanostructured systems.

Microphase Separation Mechanisms

Blends between BCP and epoxy precursors can be considered as a special case of microphase separation of BCP in solution (Grubbs et al. 2000; Ritzenthaler et al. 2002; Maiez-Tribut et al. 2007). General procedures to obtain nanostructured epoxy/BCP systems involve the use of solvents, and in many cases the epoxy precursors can be considered as reactive solvents in the uncured state. In this section it will be discussed how the interplay between each block of the selected BCP and the epoxy precursors play a key role in the evolution of the nanostructuring mechanisms. Fully characterization of the actual sequence of events by which a given epoxy/BCP blend microphase separates is of great interest because it has significant impact not only in the final morphological pattern displayed by the material, but also and more importantly in the material properties.

The sequence of events by which block copolymers microphase separate within epoxy systems can be classified by two major mechanisms:

1. Polymerization-induced microphase separation
2. Self-assembly

The main difference between both general mechanisms is the initial thermodynamic condition in the uncured state which dictates the epoxy conversion at which the nanoscopic objects are formed.

The polymerization-induced microphase separation (PIMPS) mechanism consists of an initially miscible epoxy/BCP precursor blend which evolves to a nanostructured system in the course of the epoxy precursor polymerization. On the other hand, if an epoxy/BCP blend follows a self-assembly (SA) mechanism, there is at least one block that is not miscible with the epoxy precursors in the uncured state and at least one block which is miscible with the epoxy precursors. The immiscible block self-assembles due to the enthalpic energy contribution gained by contacts of identical subchains which overcomes the mixing entropy of the nonsegregated system. SA mechanism consists of an initially preformed nanostructure that is subsequently fixed by network formation.

Although there are many epoxy/BCP systems whose nanostructure formation can be explained by these proposed mechanisms, many others are quite more complicated and cannot be interpreted by simply considering isolated SA or PIMPS mechanisms. In fact, it is possible that the actual mechanism taking place in the formation of nanostructured epoxy/BCP blends corresponds to a “tandem-like” sequence which combines more than one mechanism, such as SA, followed by PIMPS, or PIMPS followed by a second PIMPS.

In this section, a detailed description of each basic mechanism will be given, as well as examples following “tandem-like” mechanisms.

The introduction of solvents increases the level of complexity to understand microphase separation of BCP with epoxy systems. For example, the microphase separation of a general AB block copolymer in a mixture of epoxy monomer (em) and hardener (h) involves six χ parameters: χ_{AB} , χ_{A-em} , χ_{A-h} , χ_{B-em} , χ_{B-h} , and χ_{em-h} . Of course that by increasing the number of blocks of the BCP or using more solvents in the formulation, the complexity of the BCP self-assembly further increases. For simplicity, but without loss of generality, in this section the discussion will be focused on the possible microphase separation mechanisms for a system composed by AB block copolymer, epoxy monomer and hardener.

Depending on the solubility of the blocks in the epoxy monomer and hardener at the curing conditions, the block copolymer AB can be characterized into amphiphilic with one epoxy-philic segment and one epoxy-phobic segment, double “epoxy-philic” or double “epoxy-phobic.” Of course double “epoxy-phobic” BCP are not the subject of the present section as they will macrophase separate due to the lack of miscibility of both blocks with the epoxy precursors, as already discussed in the previous section. Therefore, herein we will focus on amphiphilic BCP and double “epoxy-philic” AB BCP (Amendt et al. 2012; May and Eisenberg 2012).

Nanostructuring mechanism for BCP bearing at least one “epoxy-phobic” block starts before curing and proceeds during curing, while BCP with block solubility parameters very similar to those for the epoxy precursors undergo microphase separation only during curing and thus will be discussed first.

Microphase Separation During Curing

Epoxy/BCP blend nanostructure can be formed in situ during the curing reaction when all blocks are miscible with the epoxy precursors in the uncured state. For diblock copolymers, this situation occurs for “double epoxy-philic” BCP at the curing condition temperature. Although there might be not many BCP completely miscible with an epoxy system at room temperature, it is well known that many epoxy system/homopolymer blends (PS, PMMA, epoxidized polybutadiene, among others) display upper critical solution temperature (UCST), above which the epoxy/polymer blend is miscible (homogeneous phase). Therefore, if the curing temperature for a given epoxy/BCP blend is above the UCST, then such system meets the initial conditions. At epoxy conversion 0% these systems are homogeneous, and no phase-separated domains are formed (stable system, ΔG mixing < 0). During the

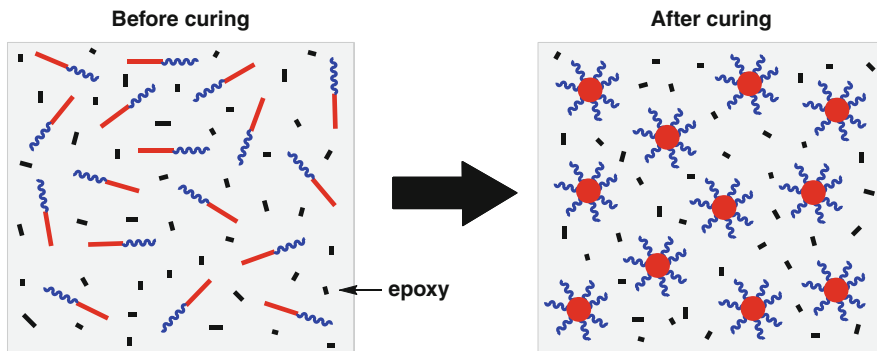


Fig. 5 Schematic of the development of nanoscopic structures by PIMPS in epoxy/BCP blends

course of the polymerization, there are thermodynamic factors which drive microphase separation of the BCP (Fig. 5). Such mechanism is called *polymerization-induced microphase separation* and is a particular case of the more general reaction-induced phase separation (RIPS) mechanism, where the chemical reaction taking place is the polymerization of the epoxy precursors (i.e., epoxy/amine polycondensation). The RIPS mechanism is well known to occur in thermosetting blends containing homopolymers (and/or random copolymers) where structures of the order of magnitude of micrometers in size can be formed via spinodal decomposition and/or nucleation and growth mechanism. A vast literature is available in the field of rubber-modified epoxies (Verchère et al. 1989; Chen et al. 1994; Williams et al. 1997).

Events involved in microphase separation induced by polymerization process are determined by thermodynamic and kinetic factors. A thermodynamic analysis enables to determine the regions where the system is stable (no phase separation occurs), metastable (phase separation may occur), or unstable (phase separation takes place). The following thermodynamic analysis proposed by Williams et al. (Williams et al. 1997) is based on a Flory-Huggins model and is valid for a monodisperse constituent. This is a simple approach that serves to get a qualitative insight into the reaction-induced microphase separation in the pregel stage.

In this model the entropy of mixing per unit volume is given by Eq. 3:

$$\Delta S = -R \left(\frac{\phi_P}{V_P} \ln \phi_P + \frac{\phi_M}{V_M} \ln \phi_M \right) \quad (3)$$

where R is the gas constant, ϕ_P is the volume fraction for the epoxy thermoset, ϕ_M is the volume fraction of the miscible block, and V_i is the molar volume of component i in the mixture. Here, $\phi_P + \phi_M = 1$.

The enthalpy of mixing per unit volume is given by Eq. 4:

$$\Delta H = \left(\frac{RT}{V_r} \right) \chi \phi_P \phi_M \quad (4)$$

where χ is the Flory-Huggins interaction parameter between the epoxy and the block under consideration and V_r is the volume of the unit cell usually referred to as the reference volume.

This leads to a Gibbs free energy per unit volume given by Eq. 5:

$$\Delta G = \Delta H - T\Delta S = \left(\frac{RT}{V_r}\right) \left(\frac{\phi_P}{V_P/V_r} \ln\phi_P + \frac{\phi_M}{V_M/V_r} \ln\phi_M + \chi\phi_P\phi_M \right) \quad (5)$$

At this point two important considerations must be highlighted.

First, during the curing reaction, the ratio V_P/V_r increases as the volume of the thermosetting polymer increases. On the other hand, the ratio V_M/V_r is constant. Therefore, the entropic contribution to the free energy of mixing decreases during polymerization. In particular, at the gel point, where the viscosity of the system and the molecular weight of the polymer network diverge, the entropic contribution is minimal. Therefore, this aspect highlights the chain growth effect on the free energy of mixing. A second important contribution to the free energy is that, as the curing reaction progresses, the conversion of oxirane rings of the epoxy precursor is transformed to more polar functional groups. For example, when the used hardener is a diamine, the obtained β -aminoalcohols are more polar than the epoxide precursors. By this transformation, the epoxy/block copolymer interaction parameter χ increases in the course of the polymerization, contributing positively to the free energy enthalpic term.

It is possible to anticipate that the above factors may cause the system to cross thermodynamic phase boundaries and result in a transition from an initial homogeneous state to a microphase-separated state. In the case of the thermosets containing block copolymers, the surface tension of domains of phase-separated blocks is reduced by the presence of the miscible block within the epoxy system giving rise to phase separation at the nanoscale (microphase separation).

In order to achieve nanostructured epoxy/BCP systems by PIMPS, it might be of great importance to select a proper combination of blocks and epoxy precursors so that the critical phase separation occurs before gelation for one block and after the gel point for the other block (high conversion). If the critical phase separation of both blocks occurs at a similar conversion, it might be possible to produce simultaneous PIMPS of both blocks that lead to a macrophase-separated state.

Apart from the thermodynamic factors that dictate phase separation in epoxy/BCP blends during the course of the reaction, it is also very important to consider kinetic aspects of this process. The possibility to achieve nanostructured systems is also governed by the competition between the phase separation rate (k_{psep}) and the polymerization rate (k_{pol}). Let's consider a system that crosses the thermodynamic boundaries in the pregel stage where the k_{psep} tends to be infinite and k_{pol} is near zero. Under these conditions, phase separation will occur instantly with no considerable increase in the conversion. At this point, if the phase-separated domains have enough time to coarsen and grow, they could even lead to undesirable aggregated domains and shift in the morphological pattern. If the opposite scenario

takes place (k_{pol} tends to be infinite and k_{psep} near zero), phase separation process may have not enough time to occur, and the immiscible block may remain trapped within the growing cross-linked network, precluding a nanostructured system. In real systems, the actual behavior might be in the middle of these extreme conditions. For instance, Fan et al. reported a partially demixing process of poly(ϵ -caprolactone) (PCL) block of polystyrene-*block*-poly(ϵ -caprolactone)-*block*-poly(*n*-butyl acrylate) based on glass transition temperature analysis of the nanostructured materials (Fan et al. 2010). Typical variables that can be adjusted to tune the rate k_{pol} and k_{psep} will be discussed in the next section (Fig. 5).

In summary, the driving forces governing PIMPS mechanism in epoxy/BCP blends are attributed to the following aspects:

- The increased molecular weight owing to polymerization (curing reaction), which gives rise to the decreased contribution of mixing entropy to the free energy of mixing
- The typical increase of the intercomponent interaction parameters (χ) with epoxy conversion
- Competitive kinetics of curing reaction and microphase separation

It should be mentioned that the effect of the increased molecular weight is much more significant than any change produced in the interaction parameter due to modification of chemical structures (Williams et al. 1997).

Microphase Separation Before Curing

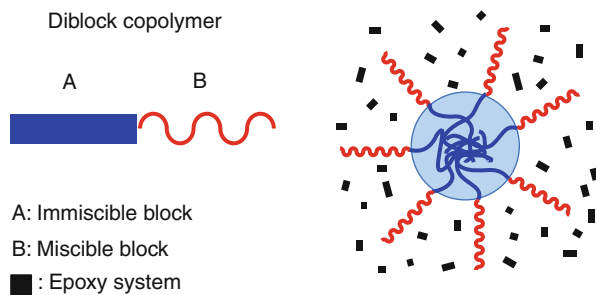
First Step: Morphologies Initiated by Self-Assembly

Self-assembly (SA) is one of the most studied microphase separation mechanisms for epoxy/BCP blends (Hillmyer et al. 1997, Xu and Zheng 2007). BCP following this type of mechanism are generally amphiphilic BCP, since the condition for SA is that at least one block is miscible with the epoxy and at least one block is immiscible in the uncured epoxy precursors. Under these conditions, the initial self-assembly process of the immiscible block is driven by the unfavorable mixing enthalpy coupled with a small mixing entropy, with the covalent bond connecting the blocks preventing macroscopic phase separation. The immiscible block self-assembles into a wide range of morphologies such as spheres, cylinders, wormlike, and lamellae, among others, depending on different formulation characteristics which will be discussed in the following section. The epoxy-miscible B block subchains extend from the A-B interface to the epoxy-rich region in a brushlike configuration as pictured in Fig. 6.

Second Step: Immobilization by Polymerization

The SA mechanism is followed by a stabilization step in which the aggregated nanostructures are immobilized by network formation during the epoxy curing

Fig. 6 Self-assembly of AB diblock copolymer. Self-assembled A blocks into spherical domains and B blocks in a brush-like configuration



process. This step is absolutely important to preserve the initially obtained nanostructure.

In order to highlight the relevance of this step in the mechanism, it can be useful to compare the following two hypothetical systems:

1. Amphiphilic AB block copolymer blended with the epoxy precursors that act as selective solvents for B before (*state a*) and after curing (*state b*)
2. Amphiphilic AB block copolymer with a selective solvent for B block (*state a*), which is gradually replaced by a more polar solvent (*state b*)

In the corresponding *state a* for both systems, it is expected that A subchains form aggregates by self-assembly in both systems, due to the amphiphilic nature of AB block copolymer. In the *b state* for both systems, there will be an increase in the product $\chi N_{B\text{-epoxy}}$ once the curing reaction begins in system 1 and an increase in product $\chi N_{B\text{-solvent}}$ for system 2, as the polarity of the solvent increases. Although the initial self-assembly and the subsequent increase in χN may anticipate a similar phase behavior for both systems in *state b*, they will actually behave completely different. System 1 will evolve to a microphase-separated material, while system 2 will end up in a macroscopically separated system (polymer and solvent). The reason for this difference, even when the thermodynamic may seem to be very similar, is that in system 1, the viscosity increases with the polymerization reaction and this reduces chain mobility and domain growth mechanism. Therefore, the size of the BCP domains are limited to the nanoscale, as determined by the initial self-assembly. On the other hand, in system 2 the initial nanodomains have no restriction to move and grow and will finally end up in the micrometric length scale.

Although the previous systems are hypothetical, they are helpful to get an approximate picture of the importance of the BCP chain immobilization process given by the epoxy/hardener polymerization during curing.

“Tandem-Like” Mechanisms

The preservation of the morphologies obtained by PIMPS or SA mechanisms requires that the block copolymer entering in the composition has to be compatible

with the matrix at any stage of the curing. Since the chemical nature of the material is varying with time during curing, a block copolymer selected for a given curable composition may become completely inappropriate once curing is completed. In practice, this condition is hardly reached, and therefore there are additional steps occurring after PIMPS or SA mechanisms, which are generally a combination of these mechanisms. Thus, the whole sequence of events operating in the nanostructuration process will be referred to as “tandem-like” mechanisms.

Self-Assembly Followed by Immobilization by Polymerization + Demixing

This combined mechanism is generally the case for amphiphilic block copolymers that first self-assemble into ordered morphologies, but in the course of the curing process, the miscible block undergoes a demixing process based on the PIMPS mechanism. For instance, Lipic et al. studied blends of poly(ethylene oxide)-poly(ethylene-*alt*-propylene) (PEO-PEP) diblock copolymer with an epoxy system (BPA348/MDA) and tracked the evolution of morphology during the cross-linking by means of small angle X-ray spectroscopy (SAXS) (Lipic et al. 1998). The authors found that in the uncured state the sample presented a cylindrical morphology which was retained during curing (SA followed by immobilization by reaction). However, SAXS measurements evidenced an increase in the principal spacing (d^*) of around 15% as the epoxy cures, as pictured in Fig. 7.

Of course the final morphology cannot be explained only by SA followed by immobilization, and therefore the actual mechanism operating in this system is likely to be a combination of SA followed by immobilization and a local expulsion of the initially miscible PEO blocks by PIMPS mechanism.

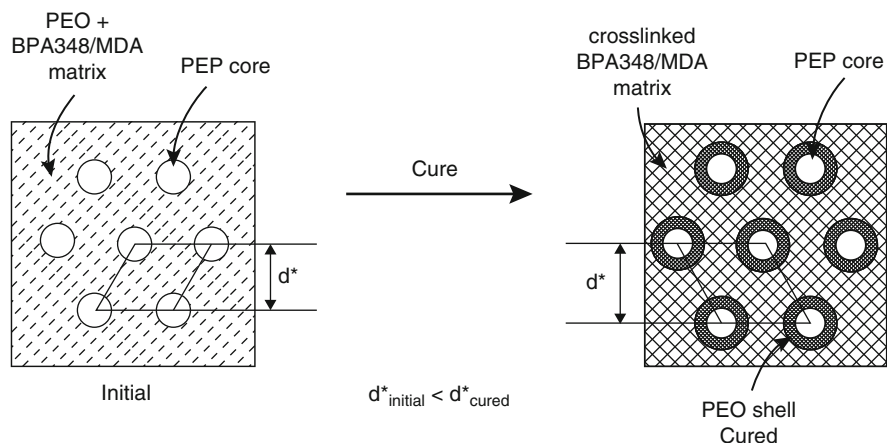


Fig. 7 Structural changes that accompany curing of an epoxy/OP system blend with a hexagonally packed cylindrical microstructure. Cross-linking the epoxy resin leads to a core and shell structure and an increase in the principal spacing d^* (Reprinted with permission from Lipic et al. (1998). Copyright (1998). American Chemical Society)

Self-Assembly Followed by Immobilization by Polymerization + Reaction

Gelation of the epoxy matrix is effective to attain a microphase-separated material, but as detailed in the previous mechanism, maintaining the same nanodomain dimensions and morphology than that for the initially uncured state is almost impossible because the initially miscible block cannot be miscible with the growing thermoset throughout the entire curing cycle. In this regard, Grubbs et al. (2000) implemented a different approach by incorporating functional groups into the block copolymer capable of reacting with the amine end group of the hardener so that the block copolymer could cure within the epoxy network without phase separation. In a subsequent work by Rebizant et al. (2004), the authors showed that it is possible to use any functional group, preferably located in the structuring block and able to react with epoxy, amine groups, or both of them. By doing so, these authors introduced the concept of reactive block copolymers, which are BCP bearing miscible blocks capable to react in a competitive way toward the epoxy precursors during curing. Figure 8 shows TEM images of a poly(styrene-*b*-butadiene-*b*-methyl methacrylate-*b*-glycidyl methacrylate) (SBMG) BCP blended with DGEBA and 4,4'-diaminodiphenylsulfone (DDS) as epoxy precursors before (a) and after

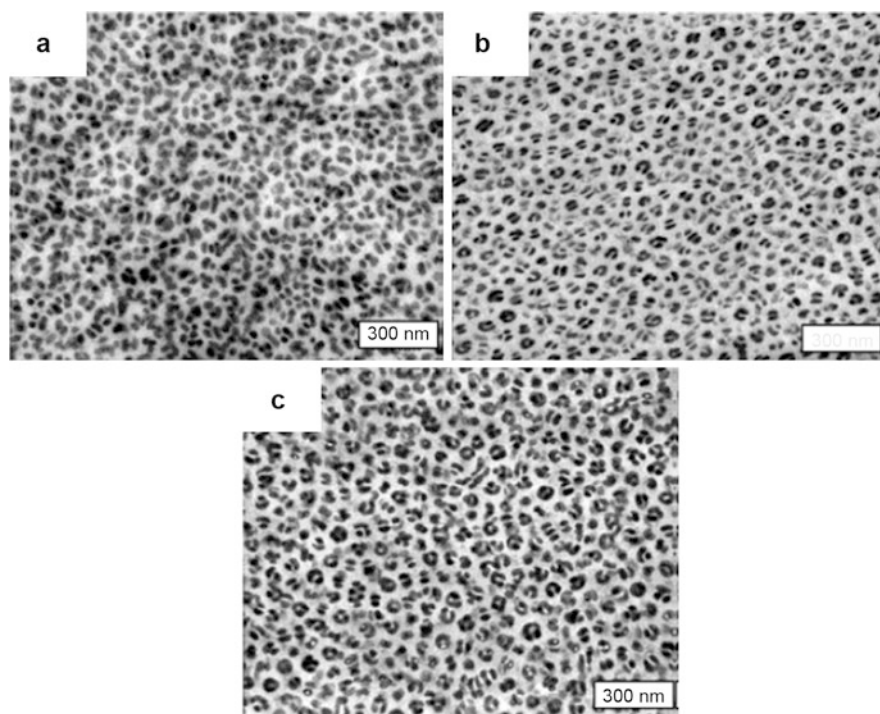


Fig. 8 TEM micrographs of DGEBA/DDS blends with 30 wt.% of (a) SBMG before curing, (b) SBMG after curing 5 h at 135 °C, and (c) SBMG after curing 5 h at 220 °C. Scale bar = 300 nm (Reprinted with permission from Rebizant et al. (2003). Copyright (2003). American Chemical Society)

(b) curing (Rebizant et al. 2003). In this system, oxirane groups of glycidyl methacrylate block are capable to react with the DDS at a similar rate than that for the DGEBA/DDS reaction.

The initial nanostructured pattern before curing was characterized by a raspberry-like morphology with dark spheres of polybutadiene on light spheres of polystyrene within DGEBA-DDS prepolymer mixture (Fig. 8a). After curing the system under different conditions, it was observed that the morphology was retained almost unchanged, whatever the curing temperature. In particular, the size of included objects remained smaller than 70 nm, in agreement with the visual aspect of the films.

Grubbs et al. (2000) proposed three possible curing scenarios for epoxy/BCP blends following initial self-assembly, which are summarized in Fig. 9. If the epoxy-miscible block is not reactive toward the epoxy precursors, it undergoes local expulsion from the epoxy network to the surrounding self-assembled nanodomain during curing (Fig. 9a). On the contrary, the incorporation of reactive functional groups in the BCP avoids local expulsion if the reaction epoxy precursor/BCP competes against the reaction between the epoxy precursors (Fig. 9b) or undergoes local expulsion followed by interfacial reaction if the reactivity of the BCP against the epoxy precursor is lower than that for epoxy/hardener (Fig. 9c).

Multiple Polymerization-Induced Microphase Separation

The nanostructuring mechanisms of epoxy/BCP blends bearing three or more blocks are much richer than that for the corresponding two-component diblocks or triblocks because multiple interaction parameters ($\chi_{\text{block } i\text{-epoxy}}$) result from the presence of more than two-component BCP. In this regard, the mechanistic studies reported by Fan et al. (2010) about the microphase separation behavior of epoxy/ABC BCP blend are of particular interest. The authors used a polystyrene-*block*-poly(ϵ -caprolactone)-*block*-poly(*n*-butyl acrylate) (PS-PCL-PBA) ABC triblock

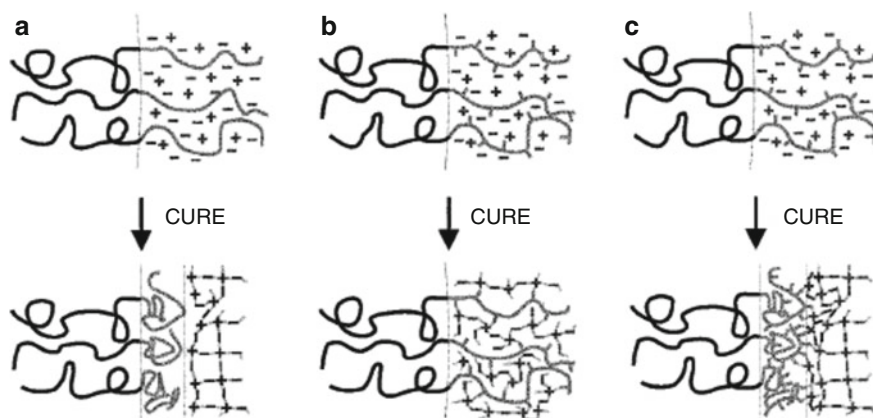


Fig. 9 Comparison of microphase separation process during cure of nonreactive BCP (a) and reactive copolymer: copolymer cures within epoxy matrix (b) or copolymer cures interfacially after expulsion from epoxy phase (c) (Reprinted with permission from Grubbs et al. (2000). Copyright (2000). American Chemical Society)

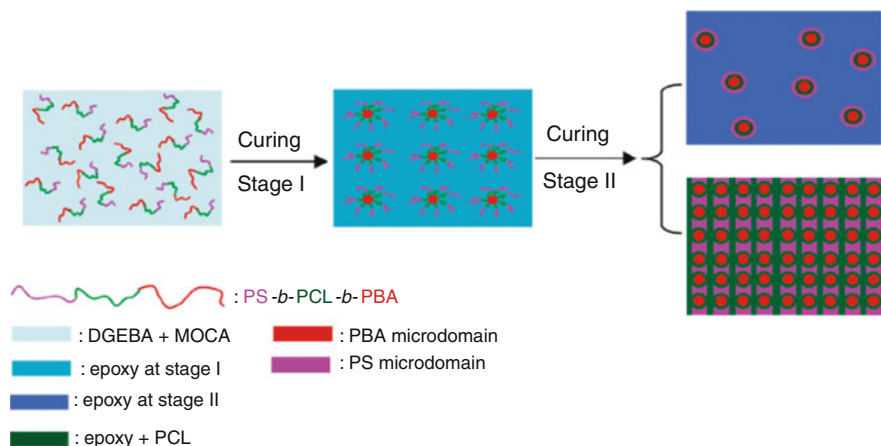


Fig. 10 Double reaction-induced microphase separation in thermosetting blends of epoxy with PS-*b*-PCL-*b*-PBA triblock copolymer

copolymer, where the three blocks were initially miscible in the epoxy precursors. By employing epoxy/PS and epoxy/PBA binary models, it was determined that the phase separation of PBA subchains occurred before than the PS subchains during the curing reaction. Moreover, the preformed PBA nanophases could act as the template of the polymerization-induced microphase separation of PS subchains and confine PS block nanophases around the PBA nanodomains. The sequential demixing of PBA and PS subchains resulted from the higher intermolecular interaction parameter for epoxy/PBA than for epoxy/PS. Figure 10 depicts the multicomponent morphologies that can be obtained by multiple PIMPS mechanisms (Fan et al. 2010). Recent studies by Yu et al. (Yu and Zheng 2011) on epoxy/BCP blends using a PS-*b*-PCL-*b*-PEO block copolymer and DDS as hardener described a similar microphase separation mechanism consisting of double polymerization-induced microphase separation of PS subchains followed by PCL subchain demixing.

In this context, the actual mechanism operating for epoxy/BCP blends, where the BCP contains more than two components, can be a combination of simpler mechanisms occurring in a sequential or simultaneous fashion. By taking these considerations into account, the complexity of the obtained morphologies highly increases with the number of blocks.

Experimental Strategies to Follow Microphase Separation Mechanism

The most convenient way to establish if a phase separation mechanism occurs by PIMPS is to use different experimental techniques giving different size scales of the generated morphology, i.e., SAXS, and to observe the evolution of morphologies by scanning electron microscopy (SEM), TEM, or atomic force microscopy (AFM) at the

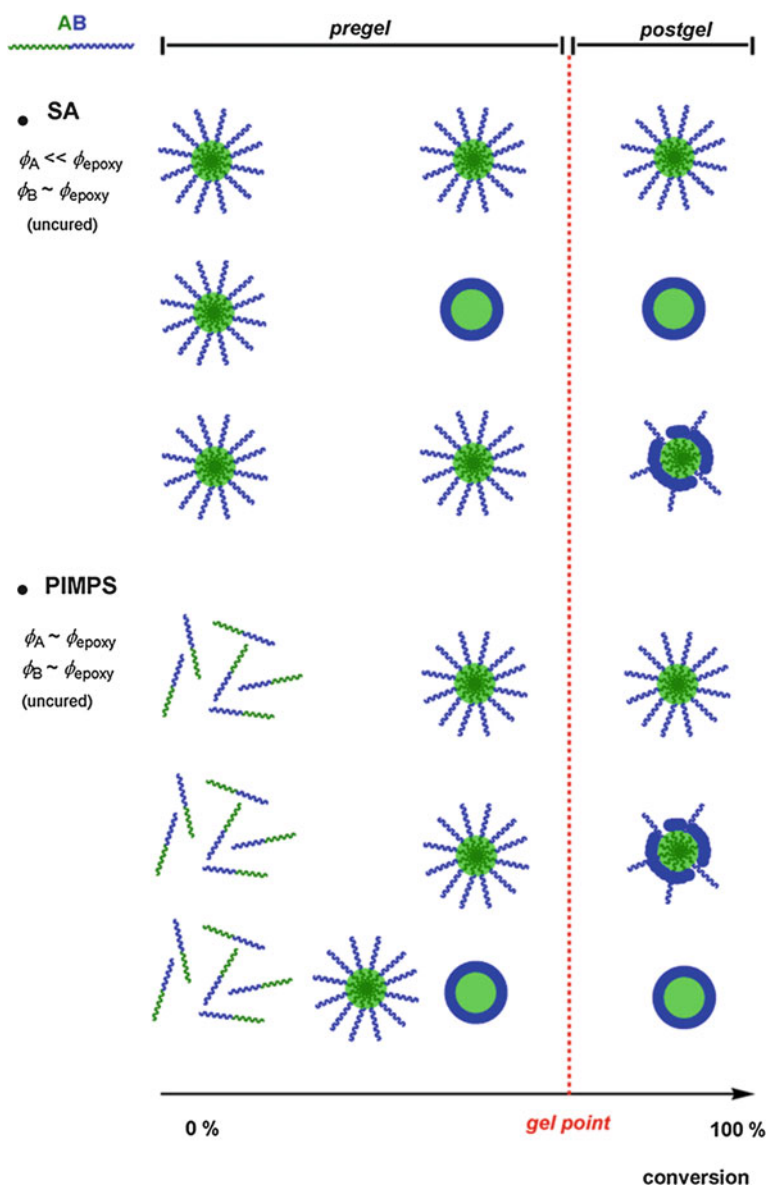


Fig. 11 Schematic representation of the possible sequence of events occurring during microphase separation of AB diblock copolymers within epoxy systems depending on block and epoxy precursors solubility parameters as a function of epoxy conversion

same curing times as SAXS and light scattering (LS) observations (Lipic et al. 1998; Mijovic et al. 2000; Fan and Zheng 2008; Hu and Zheng 2009). Figure 11 summarizes the possible sequence of events occurring during microphase separation of AB diblock copolymers within epoxy systems as a function of the epoxy conversion.

Key Parameters Affecting Mechanisms and Morphologies

This section explores more in detail the underlying factors controlling the morphology of epoxy/BCP blends in both the unreacted and the reacted states.

Epoxy/BCP Composition

One of the main parameters that determines the morphology in epoxy/BCP blends is the overall blend composition (ϕ) expressed in terms of epoxy precursors of block copolymer.

Let's consider a symmetric AB diblock copolymer, where A block is immiscible in the epoxy precursors and B block is fully miscible. The progression of morphologies can be rationalized by considering B subchains as brushes extending from A to B interface. B block exists as a "dry" brush in the neat block copolymer (lamellar morphology), leading to an interfacial curvature controlled by the block symmetry.

The incorporation of epoxy monomers in the uncured state (0% epoxy conversion) results in selective solubilization of the epoxy monomers in the B domains producing a swollen "wet" B brush, leading to an increased volume per B subchain, while the volume per A subchain remains constant. If the value of $\phi_{\text{epoxy monomers}}$ is increased, then the epoxy monomers may ultimately change the packing arrangement of chains along the interface and consequently induce a change in the interfacial curvature. In the swollen state, the lamellar morphology cannot support interfacial curvature, and therefore, the system shifts to the gyroid, cylinder, and spherical morphologies as the amount $\phi_{\text{epoxy monomers}}$ is increased (Fig. 12).

By doing so, it is then possible to effect a transition from one morphology to another by varying the epoxy monomer fraction in the epoxy/BCP blend. Figure 13 presents a composition-conversion diagram showing changes in morphology for epoxy/PEP-*b*-PEO blends proposed by Lipic et al. (1998). Phase behavior in the uncured state corresponds well with the behavior predicted and observed for blends of block copolymers with a solvent selective for one block, with a progression of morphologies from lamellar to G, C, and S as the epoxy monomer content

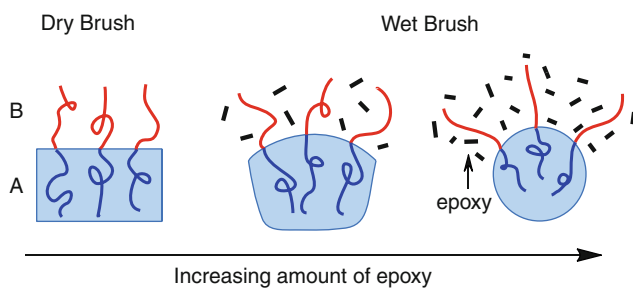
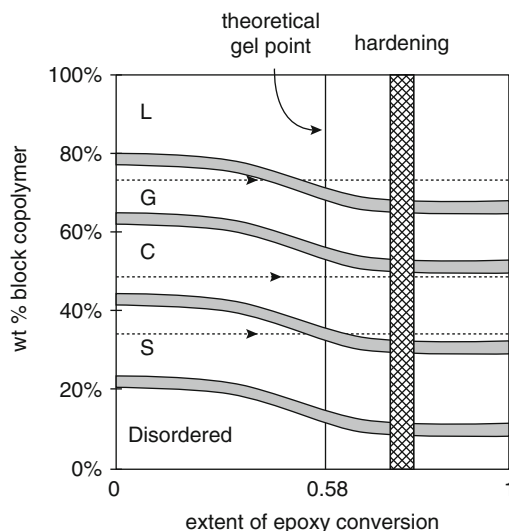


Fig. 12 Illustration of swelling-induced change in the interfacial curvature for epoxy/A-B (epoxy selective) blends

Fig. 13 Proposed composition-conversion diagram showing changes in morphology with cure. The two-phase coexistence windows are shaded, and the dotted lines indicate the path taken by certain conditions. At high degrees of epoxy conversion, the tightly cross-linked matrix prevents further changes in the morphology, and the phase boundaries no longer shift (Adapted with permission from Lipic et al. (1998). Copyright (1998). American Chemical Society)



increases. During curing at a constant BCP%, indicated by the trajectories of dotted lines, PEO blocks are demixed by the growing of epoxy network, as discussed in the previous section. This creates conformational strain which induces order-order phase transitions to the “dry brush” (gyroid (G) to lamellar (L), cylinder (C) to G, and spherical (S) to C), as the nanostructured epoxy network forms.

Number of Block Types

One of the principal molecular variables that influences BCP microphase separation within an epoxy system is the number of block types. Obviously, by increasing the number of block types, the number of events increases too and so does the complexity of the nanostructuring mechanism.

BCP with two different blocks (AB and ABA) typically can adopt four different nanodomain morphologies (lamellae, gyroid, cylinders, and spheres) when blended with epoxy systems. Introduction of a third block type (ABC) expands the spectrum of possible nanostructured morphologies. Figure 14 shows different nanodomain inclusions observed in epoxy/BCP system using poly(styrene-*b*-butadiene-*b*-methacrylate) ABC terpolymer, depending on the BCP composition (Ritzenthaler et al. 2003)

Introduction of a fourth different block (ABCD) provides an extra level of complexity to the epoxy/BCP systems not even realized in epoxy/ABC terpolymer blends. Difficulty to control microphase separation of such complex systems may explain why there are only few works on epoxy/ABCD BCP blends. Rebizant et al. (2003) explored epoxy/BCP blends using PS-*b*-PB-PMMA-*b*-PGMA tetrablock copolymer. The authors succeeded to characterize raspberrylike morphologies bearing multi-domain microphase-separated structures.

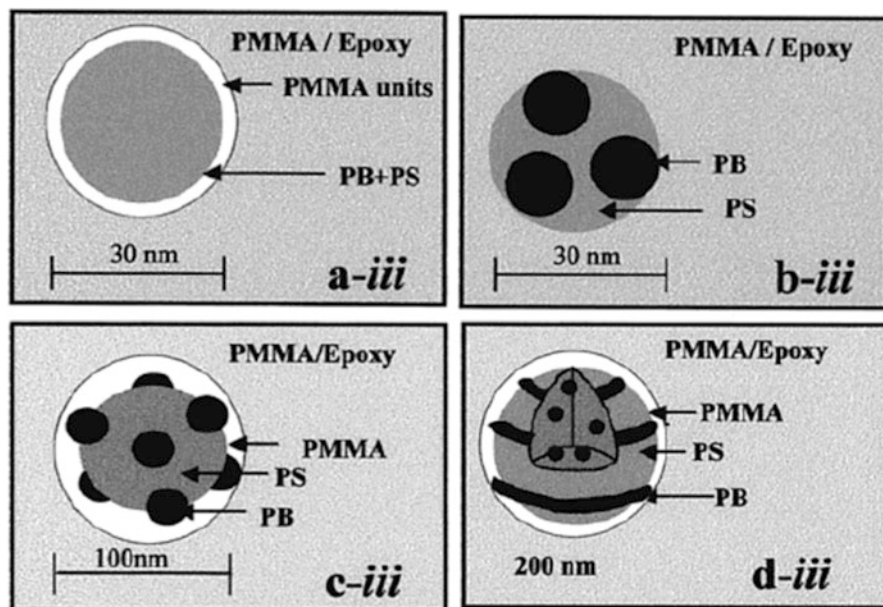


Fig. 14 Nanostructures obtained when ABC block copolymer (PS-*b*-PB-*b*-PMMA), where PMMA is the miscible block, in DGEBA/MCDEA system. (a) Spherical micelle, (b) sphere on sphere, and (c) core shell onion (Adapted with permission from Ritzenthaler et al. (2003). Copyright (2015). American Chemical Society)

Block Sequence

BCP architecture may influence the mechanism by which the BCP microphase separates within the epoxy system and, therefore, affect the final morphological pattern. For instance, Yu et al. (2012) investigated the morphological evolution of epoxy/BCP blends using PS-*b*-PCL (AB) diblock copolymer and PS-*b*-PCL-*b*-PS (ABA) triblock copolymer bearing identical block length. After systematic analysis by SAXS and AFM, the authors found that AB diblock copolymer formed spherical nanophases, whereas ABA triblock copolymer displayed vesicular nanodomains. Morphological differences were accounted to the different degrees of swelling of PCL blocks at the interfaces, as a consequence of changing the BCP architecture. PCL swelling with the epoxy precursors is associated with the PCL subchain conformation. In the AB configuration, PCL blocks displayed the conformation in which each PCL subchain is along the normal direction to the interface of PS nanodomains. In contrast, for the ABA architecture, PCL blocks adopted the loop-like conformation at the interface of PS microdomains, as depicted in Fig. 15. Therefore, the free-end PCL subchains in the AB diblock copolymer could accommodate epoxy precursors more than those for the ABA system, owing to the difference in the PCL subchain conformation. To meet this requirement of the interfacial curvature, AB block copolymer displayed sphere-like nanodomains while ABA block copolymer formed vesicular nanophases.

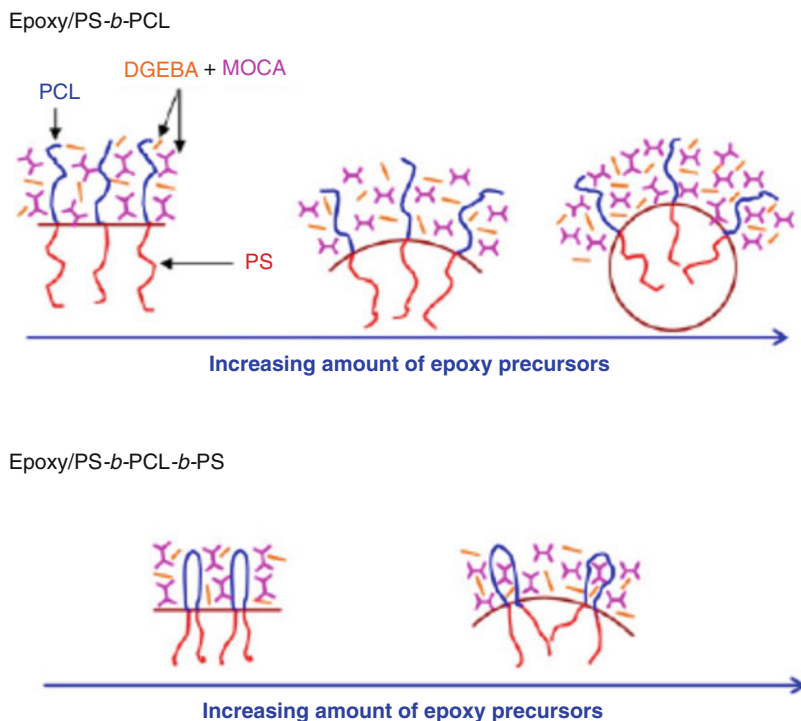


Fig. 15 Formation of nanophases in the thermosets containing PS-*b*-PCL diblock and/or PS-*b*-PCL-*b*-PS triblock copolymer in the process of curing reactions

Another interesting consequence of the block copolymer architecture is that described by Garate et al. for an epoxy/BCP blend using highly epoxidized SIS block copolymer (eSIS) (ABA architecture) (Garate et al. 2013). By following the morphological evolution of the system as the curing progressed, the authors observed that the initially spherical nanodomains became gradually distorted shifting to bigger and less organized nanostructures as a consequence of epoxidized poly(isoprene) (ePI) subchain local expulsion. Before curing, PS block self-assembled into spherical nanodomains, while ePI block remained swollen by the epoxy precursors. In this case, the configuration of ePI subchains was a combination of “loop-like” and “bridge-like” conformation due to the BCP composition (23 wt.%). In “bridge-like” conformation, ePI subchains are connecting two adjacent PS spherical nanodomains, as shown in Fig. 16 before curing. Under these conditions, “loop-like” ePI subchains were locally demixed to the surroundings of PS nanodomains, while “bridge-like” ePI subchains were not able to do so due to mobility restrictions imposed by PS blocks at each extreme. Therefore, “bridge-like” ePI subchains were partially demixed into the region between two interconnected PS nanodomains, as depicted in Fig. 16 after curing. These differences in local expulsion of ePI subchains with different configurations could explain the morphological shift from spherical to distorted sphere-like nanodomains in the systems investigated by Garate et al. (2013).

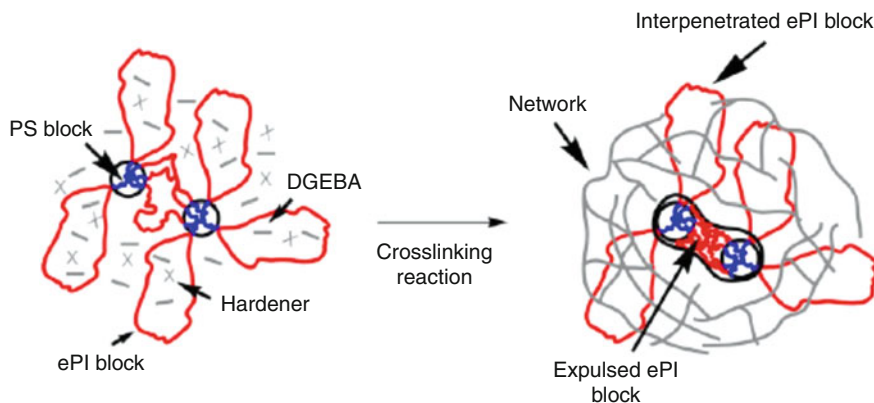


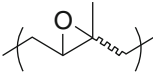
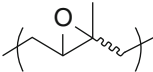
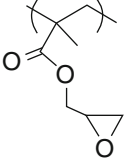
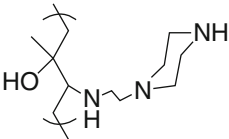
Fig. 16 Scheme of uncured (*left*) and cured (*right*) states for epoxy/eSIS85 blend

Influence of BCP Reactivity

Based on the nanostructuring mechanisms proposed by Grubbs et al. (2000), the reactivity of the BCP toward the epoxy precursors has great influence in the way the BCP microphase separates within the cross-linked matrix. The incorporation of any chemical group to the miscible block of the BCP capable of reacting with the thermosetting polymer during the curing cycle is a key parameter to control not only the morphology of the nanostructured nanocomposite, but also the interfacial adhesion between dispersed nanophases and the matrix. To obtain an optimum adhesion between the epoxy matrix and the block copolymer, Grubbs et al. and Dean et al. (Grubbs et al. 2000, 2001; Dean et al. 2003a, b) employed a different approach by incorporating functional groups into the block copolymer. The epoxy groups of glycidyl methacrylate in a poly(methyl acrylate-*stat*-glycidyl methacrylate-*block*-isoprene) block copolymer were able to react with the amine end groups of the hardener 4,4'-methylenedianiline (MDA), so that the block copolymer could cure within the epoxy network. In these works, glycidyl derivatives were considered as well as other oxiranes, since the reactivity of such units can enter in competition with the one of DGEBA. Of course that when incorporating reactive BCP, it is very important to adjust the stoichiometric balance between epoxy groups and $-NH$ groups of the hardener.

Following this idea, Rebizant et al. extended the possible functional spectrum by incorporating carboxylic reactive group after hydrolysis of *tert*-butyl methacrylate repeating units of a poly(styrene)-*b*-polybutadiene-*b*-poly[(methyl methacrylate)-*stat*-(*tert*-butyl methacrylate)] (Rebizant et al. 2004). This group was able to react with both epoxy and amine groups of the epoxy precursors. Rebizant et al. found that the formation of ether links by addition of $-COOH$ onto the oxirane ring is quick enough to prevent phase separation at the early stage of cure. The authors concluded that the formation of small amounts of graft in the early stage of the curing is sufficient to stabilize the interfaces and preserve the nanostructure until

Table 1 Reactive groups of block copolymers

Group	Reactive toward	Reaction conditions	References
	4,4'-methylenedianiline	55 °C for 48 h + 200 °C for 1 h	Grubbs et al. 2000
	1,3-bis(aminomethyl)benzene/1-(2-aminoethyl)piperazine (2:1 mol/mol)	80 °C for 3 h	Garate et al. 2013
	4,4'-methylenebis-(3-chloro 2,6-diethylaniline)	140 °C for 24 h + 165 °C for 2 h	Serrano et al. 2006
	4,4'-methylenedianiline	100 °C for 24 h + 210 °C for 1 h	Grubbs et al. 2000
	4,4'-diaminodiphenyl sulfone	135 °C for 5 h or 220 °C for 5 h	Rebizant et al. 2003
	4,4'-methylenedianiline	150 °C for 12 h + 180 °C for 2 h	Hameed et al. 2010
	4,4'-diaminodiphenyl sulfone	135 °C for 5 h	Rebizant et al. 2004
DGEBA	135 °C for 5 h		
	DGEBA	80 °C for 3 h	Garate et al. 2014

the gel point. More recently, Garate et al. arrived to a similar conclusion by blending an epoxy system with poly(styrene-*b*-epoxyisoprene-*b*-styrene) (eSIS) block copolymer bearing terminal amine groups (A-eSIS) (Garate et al. 2014). By this approach A-eSIS was more reactive toward the epoxy precursors compared to epoxidized SIS. By employing A-eSIS, sphere-like nanodomain morphology could be controlled, whereas eSIS displayed wormlike nanostructures by local expulsion of partially reactive ePI subchains.

These results demonstrate that the obtained nanostructure in an epoxy thermoset can be modulated by incorporating a BCP containing an epoxy-miscible block with enhanced reactivity toward the epoxy system (Table 1).

Influence of the Hardener

Selection of the hardener of an epoxy system is very important because it has great impact on the final properties of the cross-linked network. Epoxy systems are generally cured using difunctional nucleophilic molecules capable of reacting

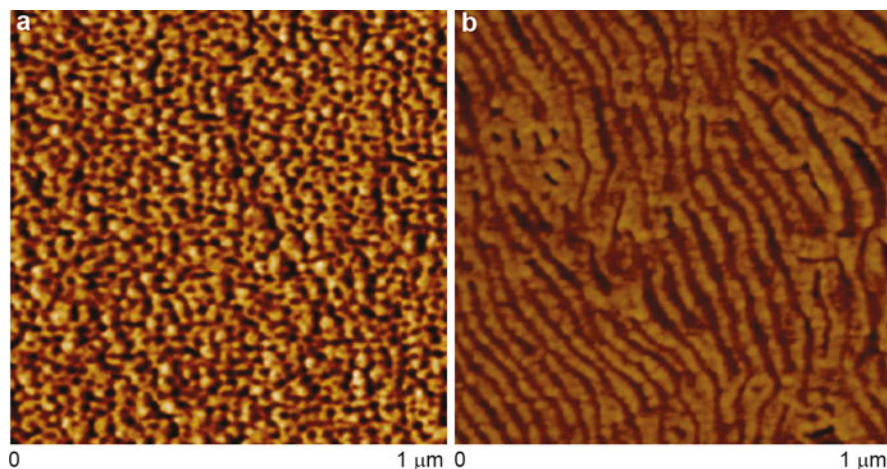


Fig. 17 AFM-phase contrast images of epoxy thermosets containing 30 wt.% of PEO-*b*-PCL-*b*-PS triblock copolymer with MOCA (a) and DDS (b) as hardener. Images correspond to $1 \mu\text{m} \times 1 \mu\text{m}$ area (Adapted with permission from Yu and Zheng (2011). Copyright (2011). American Chemical Society)

toward oxirane groups of the epoxy monomer (diamines, anhydrides, diphenols, among others). This section focuses on diamines, which are the most common hardeners employed for epoxy/BCP blends.

The nanostructures within epoxy/BCP blends can be modulated by the use of different hardener. In this regard, Yu et al. (Yu and Zheng 2011) investigated the impact of using 4,4'-methylenebis(2-chloroaniline) (MOCA) or 4,4'-diaminodiphenylsulfone as hardeners on the microphase separation behavior of epoxy/PEO-*b*-PS-*b*-PCL triblock copolymer blends. The authors found strong differences on the morphological pattern of the cured nanocomposites, as shown in Fig. 17. Thermosets cured with MOCA (Fig. 17a) presented a combination of spherical and wormlike PS microdomains, while for the samples cured with DDS (Fig. 17b), the thermosets displayed lamellar nanostructures.

In order to rationalize how the hardener influenced the final morphologies, the authors considered the following aspects: first, the impact of the selected hardener on the epoxy precursor solubility parameter. It is well known that the selection of the amine can increase the solubility of a BCP with the epoxy monomer (Fan et al. 2009) or, on the contrary, reduce the solubility of the BCP with the epoxy precursor (Garate et al. 2013), as for the case of amines with increased polarity. By means of SAXS the authors determined that epoxy/BCP blends in the uncured state were homogeneous when the hardener was 4,4'-methylene-bis-(2-chloroaniline). On the contrary, epoxy/BCP blends self-assembled into nanophases in the uncured state when the hardener was DDS. However, by heating the samples to the curing temperature, self-assembled structures disappeared due to UCST behavior of PS block in the mixture of epoxy precursors.

The second important aspect addressed by Yu et al. (Yu and Zheng 2011) is the ability of the cross-linked epoxy to establish intermolecular specific interactions with the miscible block of the BCP that stabilize the cross-linked network (i.e., hydrogen bonds). The authors stated that hydrogen bonds between carbonyl of PCL subchains and hydroxyl ether structural units of the epoxy network could be significantly suppressed by replacing MOCA for DDS due to the presence of considerable intramolecular hydrogen bonds between sulfonyl groups from DDS moieties and hydroxyl ether structural units of epoxy network. This stabilization difference would in turn give access to control whether PCL subchains remain in the wet-brush state or undergoes phase separation (dry brush) by PIMPS.

For the case of epoxy/BCP blends with reactive BCP, special consideration must be taken. In such systems, it is strongly recommended to perform separated analysis to determine the relative reactivity of BCP/hardener against epoxy monomer/hardener. To this end, depending on the nature of the amine (primary, secondary, aromatic, aliphatic), it is possible to tune the BCP/hardener reaction and therefore the phase separation behavior of the BCP within the epoxy matrix. For instance, George et al. (2014) investigated the system DGEBA-BCP blend using epoxidized poly(styrene-*b*-butadiene-*b*-styrene) eSBS block copolymer with an epoxidation degree of 47% and 4,4'-diaminodiphenylmethane (DDM) (*p*-substituted aniline) as hardener. Although epoxidized polybutadiene subchains contain secondary oxirane rings, the authors stated that no reaction occurred during curing between eSBS and DDM. On the contrary, Garate et al. (2013) employed a DGEBA/BCP blend using a highly epoxidized poly(styrene-*b*-isoprene-*b*-styrene) (eSIS85) block copolymer with an epoxidation degree of 85 wt.% cured with a more nucleophilic hardener than the *p*-substituted aniline used by George et al. (Kanzian et al. 2009). The hardener consisted of a mixture of 1,3-bis(aminomethyl)benzene (*m*-XDA) (primary diamine) and 1-(2-aminoethyl) piperazine (AEP) (primary-secondary-tertiary amine) (2:1 mol/mol). By means of fourier transform infrared spectroscopy (FT-IR) and differential scanning calorimetry (DSC) experiments, the authors found that the tertiary oxirane rings of epoxidized isoprene (ePI) units partially reacted with the hardener at the curing conditions, precluding a complete ePI subchain demixing process. Therefore, the nucleophilicity of the selected hardener is a very important aspect that has to be carefully considered to ascribe the correct microphase separation behavior of epoxy-reactive BCP blends.

Blending formulations to obtain nanostructured epoxy/BCP blends by the different microphase separation mechanisms detailed in this section is given in Table 2 (Fig. 18).

Influence of Curing Conditions

The possibility of trapping one of the evolving nanostructures generated during polymerization by control of the curing conditions can be of interest to modulate final properties of the material such as transparency and toughness, among others. The nanostructuring mechanism and the morphologies generated during polymerization of a specific blend may be strongly influenced by the presence of solvents or cosolvents and the selection of the curing temperature and the cure cycles.

Table 2 Epoxy/BCP blend formulation, microphase separation mechanism, cure cycle and morphology

Block copolymer	Epoxy system	Mechanism	Curing cycle	Morphology	BCP wt. %	References
No reactive, the miscible block is in bold						
PS- <i>b</i> -PMMA	DGEBA +MOCA	PIMPS	150 °C for 2 h + 180 °C for 2 h	S	10%	Fan and Zheng 2008
<i>star</i> -PS- <i>b</i> -PMMA	DGEBA +MOCA	PIMPS	150 °C for 2 h + 180 °C for 2 h	S+C	20%	Romeo et al. 2013
PEP- <i>b</i> -PEO	DGEBA +THPE	SA	200 °C for 2 h/60 °C for 40 min + 80 °C for 1 h + 120 °C for 2 h	L	40%	Fan and Zheng 2008
PEP- <i>b</i> -PEO	DER383, DER560 +PN	SA	200 °C for 2 h	S	5%	Liu et al. 2008; Thompson et al. 2009; Redline et al. 2014
			100 °C for 1 h + 125 °C for 1 h + 150 °C for 2 h	W	5%	Liu et al. 2010
PS- <i>b</i> -PEO	DGEBA +MOCA	PIMPS	150 °C for 2 h + 180 °C for 2 h	S+W	5%	Hermel-Davidock et al. 2007
PS- <i>b</i> -PEO	DGEBA +MDA	PIMPS	135 °C for 4 h	S	10%	Meng et al. 2006
<i>star</i> -PS- <i>b</i> -PCL	DGEBA +MOCA	PIMPS	150 °C for 2 h + 180 °C for 2 h	W	20%	Leonardi et al. 2015
				S	10%	Meng et al. 2008
PS- <i>b</i> -PCL	DGEBA +MOCA	PIMPS	150 °C for 2 h + 180 °C for 2 h	W	20–30%	Meng et al. 2008
				L	40%	
PEO- <i>b</i> -PCL	DGEBA +MDA	SA	80 °C for 8 h + 150 °C for 2 h + 175 °C for 1 h	S	40%	He et al. 2014
PS- <i>b</i> -PB- <i>b</i> -PMMA	DGEBA +MCDEA	SA	135 °C for 24 h + 190 °C for 4 h	SS	50%	Ritzenthaler et al. 2002

(continued)

Table 2 (continued)

Block copolymer	Epoxy system	Mechanism	Curing cycle	Morphology	BCP wt. %	References
PS- <i>b</i> -PB- <i>b</i> -PMMA	DGEBA +MCDEA	SA	135 °C for 14 h (for 10% of BCP, for other BCB content 20, 24, or 185 h) + 190 °C for 4 h	S SS SS/CS	10% 15% ≥30%	Ritzenthaler et al. 2003
PEO- <i>b</i> -PCL- <i>b</i> -PS	DGEBA +MOCA	PIMPS	150 °C for 4 h + 180 °C for 2 h	S W	10% 30%	Yu and Zheng 2011
PEO- <i>b</i> -PCL- <i>b</i> -PS	DGEBA +DDS	PIMPS	150 °C for 4 h + 180 °C for 2 h	S L	20% ≥30%	Yu and Zheng 2011
PDMS- <i>b</i> -PCL- <i>b</i> -PS	DGEBA +MOCA	SA +PIMPS	150 °C for 2 h + 180 °C for 2 h	CS L	≤20% ≥30%	Fan et al. 2009
PCL- <i>b</i> -PEEES- <i>b</i> -PCL	DGEBA +MOCA	SA	150 °C for 3 h + 180 °C for 2 h	S W	10% ≥30%	Cong et al. 2014
PCL- <i>b</i> -PBS- <i>b</i> -PCL	DGEBA +MOCA	PIMPS	150 °C for 3 h + 180 °C for 2 h	S W	10% 40%	
PS- <i>b</i> -PCL- <i>b</i> -PBA	DGEBA +MOCA	PIMPS	150 °C for 4 h	S W	10–20% 30–40%	Fan et al. 2010
		PIMPS	150 °C for 4 h + 180 °C for 2 h	CS L	10–20% 30–40%	
PS- <i>b</i> -PB- <i>b</i> -P (MMA- <i>stat</i> -BMA)	DGEBA +MCDEA	SA	135 °C for 5 h	S	10%	Rebizant et al. 2004
PS- <i>b</i> -PB- <i>b</i> -P (MMA- <i>stat</i> -BMA)	DGEBA +DDS	SA	135 °C for 5 h	SS	30%	
PS- <i>b</i> -PB- <i>b</i> -P (MMA- <i>stat</i> -MAA)	DGEBA +DDS	SA	135 °C for 5 h	SS	30%	

Reactive, the reactive block is in bold								
PI-<i>b</i>-P4VP	DGEBA +MDA	PIMPS	100 °C for 20 h + 150 °C for 2 h + 175 °C for 1 h	S	5%			Guo et al. 2008
PS-<i>b</i>-ePB	DGEBA +MCDEA	SA +PIMPS	140 °C for 24 h + 165 °C for 2 h	V	10%			Ocando et al. 2009
				W	30%			
PS-<i>b</i>-ePB	DGEBA +MCDEA	PIMPS	140 °C for 24 h + 165 °C for 2 h	C	30%			Serrano et al. 2006
PB-<i>b</i>-ePI	BPA +MDA	SA +PIMPS	55 °C for 48 h + 200 °C for 1 h +	S	10–30%			Grubbs et al. 2000
				L	≥65%			
PI-<i>b</i>-P(MA-<i>co</i>-GMA)	BPA +MDA	PIMPS	100 °C for 24 h + 210 °C for 1 h	S	5%			
PS-<i>b</i>-PB-<i>b</i>-P(MMA-<i>stat</i>-MAA)	DGEBA +MCDEA	SA	135 °C for 5 h	S	10%			Rebizant et al. 2004
PS-<i>b</i>-PB-<i>b</i>-P(MMA-<i>stat</i>-MAA)	DGEBA +DDS	SA +PIMPS	135 °C for 5 h	S	30%			

S spherical, C cylinder, L lamellar, W wormlike, SS spheres on spheres, CS core shell, V vesicle

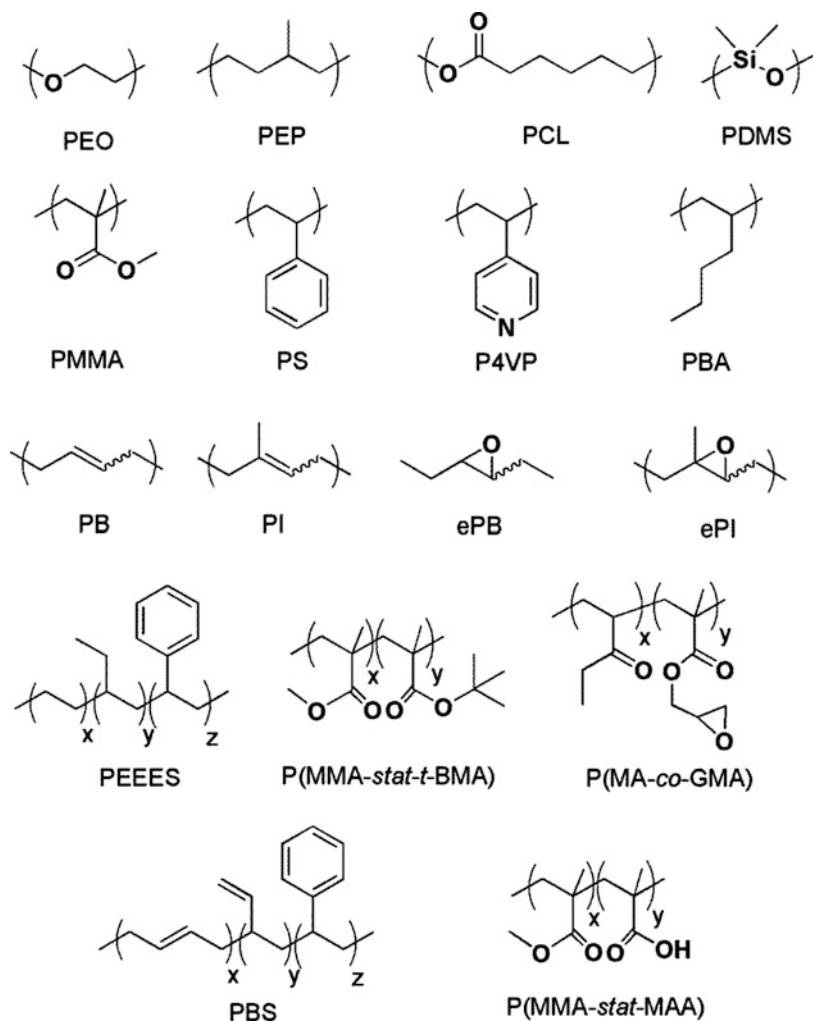


Fig. 18 Chemical structures of different blocks referred in Table 2

Solvents or Cosolvents

Epoxy/BCP blends can be prepared in bulk or as films depending on the application purpose. Protocols employed to obtain bulk or film samples generally require the use of a good solvent for the epoxy system and the BCP in order to attain a homogeneous mixture before curing. For bulk samples, it is essential to perform an intermediate of step solvent evaporation before curing (Serrano et al. 2006). Thus, volatile solvent are the preferred choice for this step. Of course that if the solvent is not adequately removed from the blend, the viscosity of the system could be low enough to allow an increase in the nanodomain coarsening rate. This may in turn alter the morphology dimensions and eventually could lead to macrophase

separation. A similar situation occurs for the case of coating applications (film samples). In this case solvents are generally needed to allow a good application of the material over the substrate. Once the material is applied, it is necessary to evaporate the solvent before curing for the same reasons explained for bulk samples (Dean et al. 2003a; Garate et al. 2011; Li et al. 2014).

Temperature

Curing temperature of course will affect the polymerization rate and the viscosity of the medium. On the one hand, increasing the polymerization rate may substantially reduce the available time for phase separation before reaching the gel point, and this can be beneficial for mechanisms initiated by SA, where it is desirable to preserve the original morphology. However, an increase in temperature also leads to a decrease in viscosity and therefore an increase in the coarsening rate of the self-assembled nanodomains.

The curing temperature will also determine whether a BCP undergoes SA or PIMPS mechanism. This is the case for those BCP bearing a block which displays UCST (i.e., polystyrene). If the selected curing temperature is below the UCST, SA mechanism may take place. On the contrary, if the curing temperature is above the UCST, the uncured state will be homogeneous, and the nanodomains will eventually be obtained by PIMPS mechanism.

Curing temperature selection is also critical for those epoxy/BCP blends where the BCP is reactive toward the epoxy precursor. For this case, it is very important to study which is the optimum reaction temperature for the epoxy precursors (i.e., DGEBA/hardener) and to compare this with the reaction between BCP and the epoxy precursor. Grubbs et al. (2000) studied the system poly(bisphenol A-*co*-epichlorohydrin)/4,4'-methylenedianiline modified by poly(1,2-butadiene)-*block*-poly(epoxy-1,4-isoprene-*ran*-1,4-isoprene) (BI87) BCP. By performing DSC experiments, the authors determined that the reaction exothermic peak between the epoxy monomer and MDA was between 131 °C and 145 °C, while the reaction exothermic peak between the BCP and MDA was 263–287 °C. Therefore, by setting the curing temperature at 55 °C for 48 h and 200 °C for 1 h, the authors concluded that the reaction of BCP with the hardener did not occur simultaneously with the cure of the epoxy precursors. In fact, during the first curing step, BCP/MDA reaction was practically neglected, and therefore it was suggested that the epoxidized block could undergo local expulsion followed by interfacial reaction during the second curing step. More recently, Garate et al. (2011) studied by DSC experiments the system DGEBA with a mixture of 1-(2-aminoethyl)piperazine and 1,3-bis(aminomethyl)benzene as the curing agent modified with eSIS85. The authors found that the exothermic peak for DGEBA/hardener was 80 °C, while for eSIS85/hardener was in the range of 65–105 °C. Therefore, they stated that even though the reactivity of the epoxy system is higher than that for the epoxidized block, at the curing temperature (80 °C) the BCP could react simultaneously with the epoxy precursors.

These examples evidence that the selection of the curing temperature for a given epoxy/BCP blend may have strong consequences on the nanostructuration mechanism and therefore on the morphological features displayed after curing.

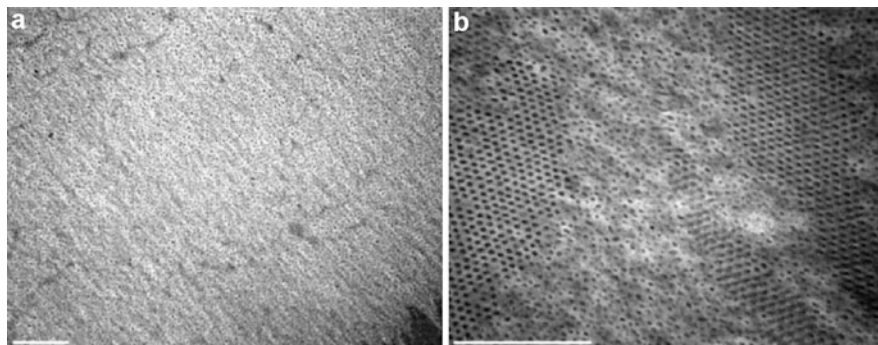


Fig. 19 TEM images of an epoxy/BCP blend reacted for 7 h at 135 °C and 4 h at 190 °C: (a) without the intermediate cooling to room temperature and (b) with intermediate cooling to room temperature. Scale bars = 1 μm (Reprinted with permission from Romeo et al. (2013). Copyright (2013). American Chemical Society)

Cure Cycle

The curing cycle can also be used to control the mechanism by which the BCP leads to the final morphology. In this regard, recent work by Romeo et al. (2013) pointed out the strong influence that the cure cycle may have on epoxy/BCP blends. The authors used an epoxy system formulated with DGEBA and 4,4'-methylenebis(2,6-diethylaniline) as the hardener modified with poly(styrene-*b*-methyl methacrylate). They employed two different curing cycles: (a) curing at 135 °C for 7 h followed by 190 °C for 4 h and (b) curing at 135 °C for 7 h followed by cooling to room temperature and 190 °C for 4 h. When the cure cycle was the condition *a*, a dispersion of spherical micelles and micellar chains were obtained (Fig. 19a). The introduction of a cooling step in the cure cycle (condition *b*) led to a dual-phase morphology consisting of microdomains of the hexagonal phase and regions exhibiting a dispersion of spherical micelles and micellar chains (Fig. 19b). The differences encountered were explained by the decrease of the miscibility of the PMMA block produced during the cooling step which produced partial phase separation of PMMA from the epoxy/amine network. Without the intermediate cooling step, the PMMA block remained interpenetrated within the cross-linked network and after the postcure was kinetically trapped in the final nanocomposite.

Impact of Morphology in the Epoxy/BCP Blend Properties

The obtained nanostructures in epoxy/amine matrix like sphere, cylindrical, worm-like micelle, and vesicle, among others, have an influence in the mechanical, thermal, and hydrophobic properties of the epoxy/BCP blends (Guo et al. 2002; Hameed et al. 2010; Cano et al. 2014; Zheng et al. 2014).

Mechanical Properties

One of the main interests of BCP to be used as epoxy modifiers relies in that they can improve fracture resistance of brittle epoxies even when they are added in relatively small amounts (<5 wt.%) (Dean et al. 2003a). Depending on to final morphology of the BCP in epoxy/amine matrix (vesicle, spherical micelles, or wormlike micelles), the improvement in the fracture resistance might be different. The fracture resistance, critical stress intensity factor (K_{Ic}), and the strain energy release rate have a strong dependence with the morphology of the BCP in the epoxy/amine matrix (Dean et al. 2003b; Cano et al. 2014).

Among the morphologies, vesicles are found to be more effective than spherical micelle to improve mechanical properties (Dean et al. 2001). Vesicles can be effective in toughening epoxy at relatively low loadings (2.5 wt.% block copolymer). Vesicles are closed, spherical objects consisting of a thin (ca. 10 nm) bilayer membrane that encases the epoxy resin. Given that the block copolymer forms only the shell and the volume of the vesicle phase consists of both the shell and the encapsulated epoxy, a small amount of block copolymer possess a large effective modifier volume fraction (Dean et al. 2003a).

In addition to vesicles and spherical micelles, block copolymers can also self-assemble into wormlike micelles according to the block copolymer architecture (Dean et al. 2003a). However, the improvement is bigger when wormlike micelle is employed (Dean et al. 2003b; Liu et al. 2010). Remarkably, addition of 5 wt.% block copolymer transforms the virtually useless fragile glassy material into a tough resistant plastic suitable for practical applications (Fig. 20). Wormlike micelles act as microcavities within the epoxy system, allowing more facile deformation of the matrix and therefore contributing to energy absorption. Additionally, it is possible to obtain a network of interconnected wormlike micelles which further enhances energy absorption in these materials (Wu et al. 2005).

The addition of BCP to an epoxy matrix produces generally a drop of Young's modulus while the fracture toughness increased. For similar BCP contents, vesicle morphology produces the largest decrease in Young's modulus which could be attributed to the large effective volume fraction of vesicles. A significant fraction of the cured epoxy resides inside the vesicle and does not fully contribute to the bulk Young's modulus of the blend (Thio et al. 2006).

Another important aspect to take into account is the nanoinclusion size developed during the BCP microphase separation. Small micelles neither induced plastic deformation nor contributed to surface roughness significantly whereas larger micelles acted as local defects resulting in early failure (Thio et al. 2009). There is an optimum inclusion length scale at which the toughening effect is maximized (Fig. 21), and this will depend on the particular system used (BCP, epoxy formulation, etc.).

Thermal Properties

Addition of BCP to the epoxy system may considerably alter the material glass transition temperature (T_g) value, and these changes depend on the BCP content

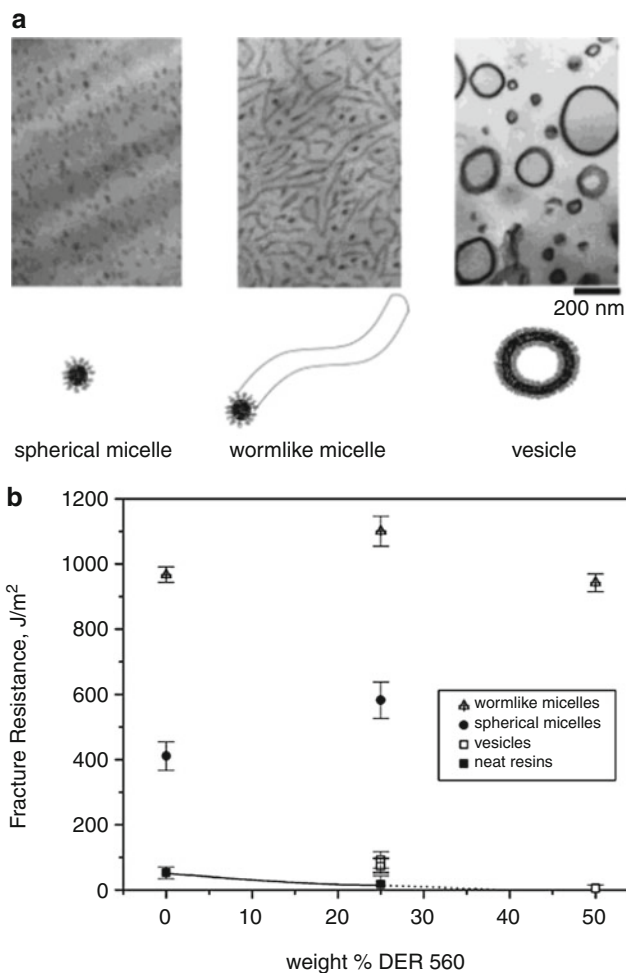


Fig. 20 (a) Different morphologies obtained for epoxy/amine network reinforced with PEO-PEP block copolymer, (b) fracture resistance of this mixtures containing 5 wt.% of block copolymer in diglycidyl ether of bisphenol A (DER383)/brominated diglycidyl ether of bisphenol A (DER560) epoxy system (Reprinted with permission from Dean et al. (2003b). Copyright (2003). American Chemical Society)

and the nanodomain morphology. For instance, by increasing BCP content, it is possible to shift the T_g to lower temperatures by means of the plasticization effect generated by nonreactive interpenetrated BCP subchains (Guo et al. 2002; Zhang et al. 2013; Cano et al. 2014). This effect seems to be more dependent on the BCP content than on the block ratio, as presented in Fig. 22 for epoxy/PEO-PPO-PEO blends with different EO contents and could be related with local decrease of epoxy cross-linking density as a consequence of the interpenetration of the miscible block.

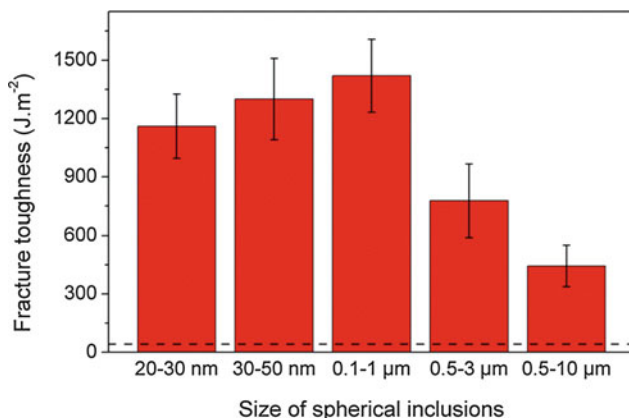


Fig. 21 Effect of the vesicle size morphology of poly(hexylene oxide-*b*-ethylene oxide) on the fracture toughness. The *dash line* corresponds to the epoxy system value

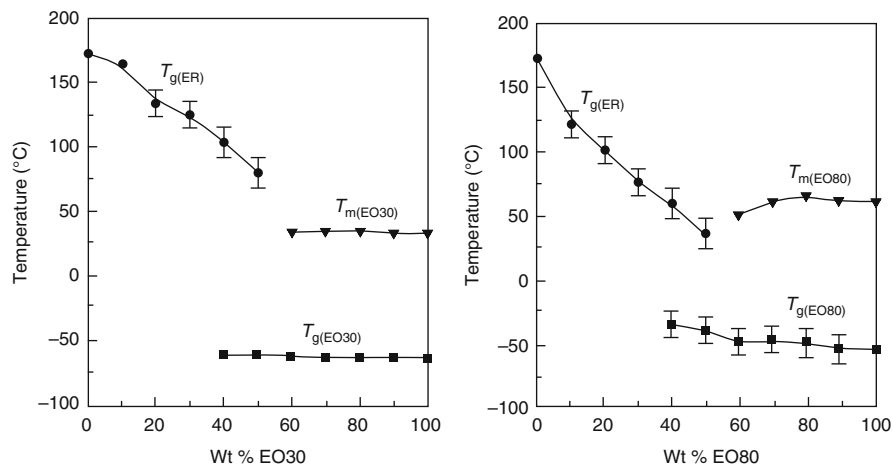
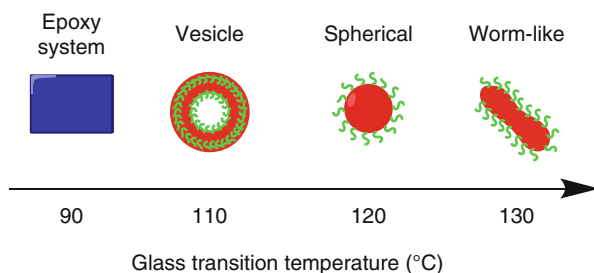


Fig. 22 T_g values for PEO-PPO-PEO blend epoxy resin ($T_{g(ER)}$) with different content of EO: 30 wt.% (*left*) and 80 wt.% (*right*). $T_m(EO)$ is the melting temperature, and $T_{g(EO)}$ is the T_g of the block copolymer, respectively (Reprinted with permission from Guo et al. (2002). Copyright (2002). American Chemical Society)

Other authors (Hameed et al. 2010; Garate et al. 2013) found that the incorporating reactive BCP to the epoxy system conducted to the opposite trend, shifting the T_g to higher values than that for the epoxy matrix. This effect occurs due to interpenetration and fixation of reactive BCP subchains. Once the BCP subchains are covalently linked to the epoxy matrix, demixing process is avoided, and therefore interpenetrated blocks can either fill matrix-free volume or increase the cross-linking density of the matrix. By doing so, the glass transition temperature is increased.

Fig. 23 Influence of the nanodomain morphology in the T_g of epoxy system for 5 wt.% of PBO-PEO modified epoxy



For the case of constant BCP content, the epoxy T_g value may have significant variations depending on the nanodomain morphology. Wu et al. (2005) observed that wormlike and spherical micelles conducted to a larger increment in T_g value than for the case of incorporating vesicles (Fig. 23). To rationalize this effect, it is important to consider that BCP addition perturbs the local concentration of epoxy precursors, because a little quantity of these components is solubilized inside the nanodomains. As long as the curing process occurs, the incorporated epoxy precursors are expelled from the swollen nanodomains to the epoxy-rich phase. This mass transport process depends on the interfacial area between the nanodomains and the continuous epoxy phase and therefore on the nature of the nanodomain morphology. This effect in combination with local expulsion of epoxy-miscible block at higher epoxy conversion is likely to alter the network topology and therefore constitute evident sources of variation in T_g , as pictured in Fig. 23.

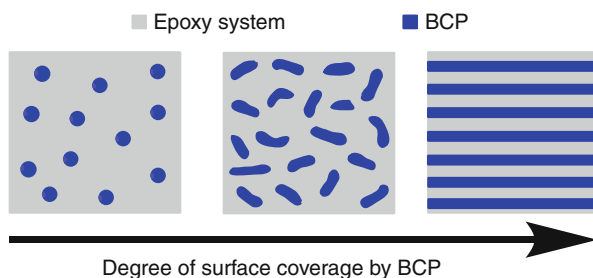
Surface Properties

Another important application of BCP as epoxy system modifier is the possibility of tuning material surface properties which is particularly relevant for coating applications. By properly selecting the BCP, the material surface property may be changed to more hydrophilic or hydrophobic for a specific application. This change in the epoxy system surface is gradual and increase with BCP content. The increment in BCP content produces two effects: (i) increment in epoxy covers area for the BCP and (ii) changes in the nanoinclusion morphology (Fig. 24).

The first effect determines the net change on hydrophobicity or hydrophilicity of epoxy system surface which depends of the block copolymer nature. For instance, the use of PDMS-PGMA (PDMS consists of a methacrylate siloxane hydrophobe) modifies the surface to more hydrophobic (Hameed et al. 2010). On the other hand, the use of PEO-PPO-PEO or PTFEMA-PCL-PTFEMA (PEO and PTFEMA have strong hydrophilic character) changes the surface to more hydrophilic (Cano et al. 2014; Zheng et al. 2014).

The second effect attains a nanoinclusion morphological shift from spheres to wormlike and from wormlike to lamellar structures, which in turn increases the BCP cover area exposed to the polymer/air interface.

Fig. 24 Epoxy system with different BCP contents



Conclusions

Different methods for generating nanostructured epoxy/BCP blends are discussed in this chapter. A general classification was proposed based on whether the solubility parameters of each block of the block copolymer are similar to those for epoxy precursors and therefore, on the basis of PIMPS mechanism, phase separation occurs during curing. On the other hand, if at least one block has a solubility parameter similar to those for the epoxy precursors but the other does not, microphase separation initiates before curing by self-assembly mechanism. Under the later condition, well-defined nanoinclusions are generated within the epoxy system, which are subsequently fixed by the growing epoxy network during curing. It was also discussed that by employing complex BCP other than simple symmetric diblock copolymers, the actual phase separation pathway may correspond to a combination of the previous mechanisms in a *tandem-like* way or simultaneously.

Both thermodynamics and kinetics of epoxy/BCP blends can be controlled by finely tuning epoxy formulation, BCP characteristics, and adequate curing conditions such as curing cycle and curing temperature, among others. These considerations must be carefully taken into account in order to gain control over the microphase separation mechanism and therefore over the nanodomain morphology displayed by the nanostructured system, as well as the final desired material properties.

References

- Amendt MA, Pitet LM, Moench S, Hillmyer MA (2012) Reactive triblock polymers from tandem ring-opening polymerization for nanostructured vinyl thermosets. *Polym Chem* 3:1827–1837
- Barton AFM (1990) Handbook of polymer-liquid interaction parameters and solubility parameters. CRC Press, Boca Raton
- Bates FS, Fredrickson GH (1999) Block copolymers-designer soft materials. *Phys Today* 52:32–38
- Bordes C, Fréville V, Ruffin E, Marote P, Gauvrit JY, Briançon S, Lantéri P (2010) Determination of poly(ϵ -caprolactone) solubility parameters: application to solvent substitution in a microencapsulation process. *Int J Pharm* 383:236–243

- Cano L, Builes DH, Tercjak A (2014) Morphological and mechanical study of nanostructured epoxy systems modified with amphiphilic poly(ethylene oxide-*b*-propylene oxide-*b*-ethylene oxide) triblock copolymer. *Polymer* 55:738–745
- Caseri W (2000) Nanocomposites of polymers and metals or semiconductors: historical background and optical properties. *Macromol Rapid Commun* 21:705–722
- Chen D, Pascault JP, Bertsch RJ, Drake RS, Siebert AR (1994) Synthesis, characterization, and properties of reactive liquid rubbers based on butadiene–acrylonitrile copolymers. *J Appl Polym Sci* 51:1959–1970
- Cong H, Li L, Zheng S (2014) Formation of nanostructures in thermosets containing block copolymers: from self-assembly to reaction-induced microphase separation mechanism. *Polymer* 55:1190–1201
- Dean JM, Lipic PM, Grubbs RB, Cook RF, Bates FS (2001) Micellar structure and mechanical properties of block copolymer-modified epoxies. *J Polym Sci Pol Chem* 39:2996–3010
- Dean JM, Grubbs RB, Saad W, Cook RF, Bates FS (2003a) Mechanical properties of block copolymer vesicle and micelle modified epoxies. *J Polym Sci Pol Chem* 41:2444–2456
- Dean JM, Verghese NE, Pham HQ, Bates FS (2003b) Nanostructure toughened epoxy resins. *Macromolecules* 36:9267–9270
- Declet-Perez C, Francis LF, Bates FS (2015) Deformation processes in block copolymer toughened epoxies. *Macromolecules* 48:3672–3684
- Esposito LH, Ramos JA, Mondragon I, Kortaberria G (2013) Nanostructured thermosetting systems modified with poly(isoprene-*b*-methyl methacrylate) diblock copolymer and polyisoprene-grafted carbon nanotubes. *J Appl Polym Sci* 129:1060–1067
- Esposito LH, Ramos JA, Kortaberria G (2014) Dispersion of carbon nanotubes in nanostructured epoxy systems for coating application. *Prog Org Coat* 77:1452–1458
- Fan W, Zheng S (2008) Reaction-induced microphase separation in thermosetting blends of epoxy resin with poly(methyl methacrylate)-*block*-polystyrene block copolymers: effect of topologies of block copolymers in morphological structures. *Polymer* 47:3157–3167
- Fan W, Wang L, Zheng S (2009) Nanostructures in thermosetting blends of epoxy resin with polydimethylsiloxane-*block*-poly(*ε*-caprolactone)-*block*-polystyrene ABC triblock copolymer. *Macromolecules* 42:327–336
- Fan W, Wang L, Zheng S (2010) Double reaction-induced microphase separation in epoxy resin containing polystyrene-*block*-poly(*ε*-caprolactone)-*block*-poly(*n*-butyl acrylate) ABC triblock copolymer. *Macromolecules* 43:10600–10611
- Garate H, Mondragon I, Goyanes S, D'Accorso N (2011) Controlled epoxidation of poly(styrene-*b*-isoprene-*b*-styrene) block copolymer for the development of nanostructured epoxy thermosets. *J Polym Sci Pol Chem* 49:4505–4515
- Garate H, Mondragon I, D'Accorso N, Goyanes S (2013) Exploring microphase separation behavior of epoxidized poly(styrene-*b*-isoprene-*b*-styrene) block copolymer inside thin epoxy coatings. *Macromolecules* 46:2182–2187
- Garate H, Goyanes S, D'Accorso N (2014) Controlling nanodomain morphology of epoxy thermosets modified with reactive amine-containing epoxidized poly(styrene-*b*-isoprene-*b*-styrene) block copolymer. *Macromolecules* 47:7416–7423
- George SM, Puglia D, Kenny JM, Parameswaranpillai J, Thomas S (2014) Reaction-Induced phase separation and thermomechanical properties in epoxidized styrene-*block*-butadiene-*block*-styrene triblock copolymer modified epoxy/DDM system. *Ind Eng Chem Res* 53:6941–6950
- Grubbs RB, Dean JM, Broz ME, Bates FS (2000) Reactive block copolymers for modification of thermosetting epoxy. *Macromolecules* 33:9522–9534
- Grubbs RB, Dean JM, Bates FS (2001) Methacrylic block copolymers through metal-mediated living free radical polymerization for modification of thermosetting epoxy. *Macromolecules* 34:8593–8595
- Guo Q, Thomann R, Gronski W (2002) Phase behavior, crystallization, and hierarchical nanostructures in self-organized thermoset blends of epoxy resin and amphiphilic poly

- (ethylene oxide)-*block*-poly(propylene oxide)-*block*-poly(ethylene oxide) triblock copolymers. *Macromolecules* 35:3133–3144
- Guo Q, Liu J, Chen L, Wang K (2008) Nanostructures and nanoporosity in thermoset epoxy blends with an amphiphilic polyisoprene-*block*-poly(4-vinyl pyridine) reactive diblock copolymer. *Polymer* 49:1737–1742
- Hameed N, Guo Q, Xu Z, Hanley TL, Mai Y-W (2010) Reactive block copolymer modified thermosets: highly ordered nanostructures and improved properties. *Soft Matter* 6:6119–6129
- He X, Liu Y, Zhang R, Wu Q, Chen T, Sun P, Wang X, Xue G (2014) Unique interphase and cross-linked network controlled by different miscible blocks in nanostructured epoxy/block copolymer blends characterized by solid-state NMR. *J Phys Chem C* 118:13285–13299
- Hedrick JL, Miller RD, Hawker CJ, Carter KR, Volksen W, Yoon DY, Trollsås M (1998) Templating nanoporosity in thin-film dielectric insulators. *Adv Mater* 10:1049–1053
- Hermel-Davidock TJ, Tang HS, Murray DJ, Hahn S (2007) Control of the block copolymer morphology in templated epoxy thermosets. *J Polym Sci Pol Phys* 45:3338–3348
- Hillmyer MA, Lipic PM, Hajduk DA, Almdal K, Bates FS (1997) Self-assembly and polymerization of epoxy resin-amphiphilic block copolymer nanocomposites. *J Am Chem Soc* 119:2749–2750
- Hu D, Zheng S (2009) Reaction-induced microphase separation in epoxy resin containing polystyrene-*block*-poly(ethylene oxide) alternating multiblock copolymer. *Eur Polym J* 45:3326–3338
- Kanzian T, Nigst TA, Maier A, Pichl S, Mayr H (2009) Nucleophilic reactivities of primary and secondary amines in acetonitrile. *Eur J Org Chem* 2009:6379–6385
- Karger-Kocsis J, Frölich J, Gryshchuk O, Kautz H, Frey H, Mülhaupt R (2004) Synthesis of reactive hyperbranched and star-like polyethers and their use for toughening of vinylurethane hybrid resins. *Polymer* 45:1185–1195
- Leonardi AB, Zucchi IA, Williams RJJ (2015) Generation of large and locally aligned wormlike micelles in block copolymer/epoxy blends. *Eur Polym J* 65:202–208
- Li T, Heinzer MJ, Redline EM, Zuo F, Bates FS, Francis LF (2014) Microstructure and performance of block copolymer modified epoxy coatings. *Prog Org Coat* 77:1145–1154
- Lipic PM, Bates FS, Hillmyer MA (1998) Nanostructured thermosets from self-assembled amphiphilic block copolymer/epoxy resin mixtures. *J Am Chem Soc* 120:8963–8970
- Liu J, Sue HJ, Thompson ZJ, Bates FS, Dettloff M, Jacob G, Verghese N, Pham H (2008) Nanocavitation in self-assembled amphiphilic block copolymer-modified epoxy. *Macromolecules* 41:7616–7624
- Liu J, Thompson ZJ, Sue H-J, Bates FS, Hillmyer MA, Dettloff M, Jacob G, Verghese N, Pham H (2010) Toughening of epoxies with block copolymer micelles of wormlike morphology. *Macromolecules* 43:7238–7243
- Mai Y, Eisenberg A (2012) Self-assembly of block copolymers. *Chem Soc Rev* 41:5969–5985
- Maiez-Tribut S, Pascault JP, Soule ER, Borrajo J, Williams RJJ (2007) Nanostructured epoxies based on the self-assembly of block copolymers: a new miscible block that can be tailored to different epoxy formulations. *Macromolecules* 40:1268–1273
- Matsen MW, Bates FS (1996) Unifying weak-and strong-segregation block copolymer theories. *Macromolecules* 29:1092–1098
- Meng F, Zheng S, Li H, Liang Q, Liu T (2006) Formation of ordered nanostructures in epoxy thermosets: a mechanism of reaction-induced microphase separation. *Macromolecules* 39:5072–5080
- Meng F, Xu Z, Zheng S (2008) Microphase separation in thermosetting blends of epoxy resin and poly(ϵ -caprolactone)-*block*-polystyrene block copolymers. *Macromolecules* 41:1411–1420
- Mijovic J, Shen M, Wing Sy J, Mondragon I (2000) Dynamics and morphology in nanostructured thermoset network/block copolymer blends during network formation. *Macromolecules* 33:5235–5244
- Mikos AG, Peppas NA (1988) Flory interaction parameter χ for hydrophilic copolymers with water. *Biomaterials* 9:419–423

- Ng SC, Chee KK (1997) Solubility parameters of copolymers as determined by turbidimetry. *Eur Polym J* 33:749–752
- O'Driscoll S, Demirel G, Farrell RA, Fitzgerald TG, O'Mahony C, Holmes JD, Morris MA (2011) The morphology and structure of PS-*b*-P4VP block copolymer films by solvent annealing: effect of the solvent parameter. *Polym Adv Technol* 22:915–923
- Ocando C, Tercjak A, Martín MD, Ramos JA, Campo M, Mondragon I (2009) Morphology development in thermosetting mixtures through the variation on chemical functionalization degree of poly(styrene-*b*-butadiene) diblock copolymer modifiers. *Thermomech Prop Macromol* 42:6215–6224
- Rebizant V, Abetz V, Tournilhac F, Court F, Leibler L (2003) Reactive tetrablock copolymers containing glycidyl methacrylate. Synthesis and morphology control in epoxy-amine networks. *Macromolecules* 36:9889–9896
- Rebizant V, Venet A-S, Tournilhac F, Girard-Reydet E, Navarro C, Pascault J-P, Leibler L (2004) Chemistry and mechanical properties of epoxy-based thermosets reinforced by reactive and nonreactive SBMX block copolymers. *Macromolecules* 37:8017–8027
- Redline EM, Declat-Perez C, Bates FS, Francis LF (2014) Effect of block copolymer concentration and core composition on toughening epoxies. *Polymer* 55:4172–4181
- Ritzenthaler S, Court F, David L, Girard-Reydet E, Leibler L, Pascault JP (2002) ABC triblock copolymers/epoxy-diamine blends. 1. Keys to achieve nanostructured thermosets. *Macromolecules* 35:6245–6254
- Ritzenthaler S, Court F, David L, Girard-Reydet E, Leibler L, Pascault JP (2003) ABC triblock copolymers/epoxy-diamine blends. 2. Parameters controlling the morphologies and properties. *Macromolecules* 36:118–126
- Romeo H, Zucchi I, Rico M, Hoppe CE, Williams RJJ (2013) From spherical micelles to hexagonally packed cylinders: the cure cycle determines nanostructures generated in block copolymer/epoxy blends. *Macromolecules* 46:4854–4861
- Serrano E, Larrañaga M, Remiro PM, Mondragon I, Carrasco PM, Pomposo JA, Mecerreyes D (2004) Synthesis and characterization of epoxidized styrene-butadiene block copolymers as templates for nanostructured thermosets. *Macromol Chem Phys* 205:987–996
- Serrano E, Tercjak A, Kortaberria G, Pomposo JA, Mecerreyes D, Zafeiropoulos NE, Stamm M, Mondragon I (2006) Nanostructured thermosetting systems by modification with epoxidized styrene-butadiene star block copolymers. Effect of epoxidation degree. *Macromolecules* 39:2254–2261
- Serrano E, Tercjak A, Ocando C, Larrañaga M, Parellada MD, Corona-Galván S, Mecerreyes D, Zafeiropoulos NE, Stamm M, Mondragon I (2007) Curing behavior and final properties of nanostructured thermosetting systems modified with epoxidized styrene-butadiene linear diblock copolymers. *Macromol Chem Phys* 208:2281–2292
- Thio YS, Wu J, Bates FS (2006) Epoxy toughening using low molecular weight poly (hexylene oxide)-poly (ethylene oxide) diblock copolymers. *Macromolecules* 39:7187–7189
- Thio YS, Wu J, Bates FS (2009) The role of inclusion size in toughening of epoxy resins by spherical micelles. *J Polym Sci Pol Chem* 47:1125–1129
- Thompson ZJ, Hillmyer MA, Liu J, Sue H-J, Dettloff M, Bates FS (2009) Block copolymer toughened epoxy: role of cross-link density. *Macromolecules* 42:2333–2335
- Van Krevelen DW (1990) *Properties of polymers*, 3rd edn. Elsevier, Amsterdam
- Verchère D, Sautereau H, Pascault JP, Moschiar SM, Riccardi CC, Williams RJJ (1989) *Polymer* 30:107–115
- Williams RJJ, Rozenberg BA, Pascault J-P (1997) Reaction-induced phase separation in modified thermosetting polymers. In: Abe A, Albertsson AC, Coates GW, Genzer J, Kobayashi S, Lee K-S, Leibler L, Long TE, Möller M, Okay O, Percec V, Tang BZ, Terentjev EM, Vicent MJ, Voit B, Wiesner U, Zhang X (eds) *Advances in polymer science*. Springer, Berlin, pp 95–156
- Wu J, Thio YS, Bates FS (2005) Structure and properties of PBO-PEO diblock copolymer modified epoxy. *J Polym Sci Pol Chem* 43:1950–1965

- Xu Z, Zheng S (2007) Morphology and thermomechanical properties of nanostructured thermosetting blends of epoxy resin and poly(ϵ -caprolactone)-*block* polydimethylsiloxane-*block*-poly(ϵ -caprolactone) triblock copolymer. *Polymer* 48:6134–6144
- Yu R, Zheng S (2011) Morphological transition from spherical to lamellar nanophases in epoxy thermosets containing poly(ethylene oxide)-*block*-poly(ϵ -caprolactone)-*block*-polystyrene triblock copolymer by hardeners. *Macromolecules* 44:8546–8557
- Yu R, Zheng S, Li X, Wang J (2012) Reaction-induced microphase separation in epoxy thermosets containing block copolymers composed of polystyrene and poly(ϵ -caprolactone): influence of copolymer architectures on formation of nanophases. *Macromolecules* 45:9155–9168
- Yu Y, Dubois P, Teyssié P, Jérôme R (1997) Difunctional initiator based on 1,3-diisopropenylbenzene.6. Synthesis of methyl methacrylate – butadiene – methyl methacrylate triblock copolymers. *Macromolecules* 30:4254–4261
- Zhang C, Li L, Zheng S (2013) Formation and confined crystallization of polyethylene nanophases in epoxy thermosets. *Macromolecules* 46:2740–2753
- Zheng Y, Xue Q, Zhu L, Xin Z, Sheng Y, Ren W (2014) Copolymer architecture effects on the morphology and surface performance of epoxy thermosets containing fluorinated block copolymers. *J Polym Sci Pol Phys* 52:1037–1045
- Zhu B, Katsoulis DE, Keryk JR, McGarry FJ (2004) Toughening of polysilsesquioxane network by simultaneous incorporation of short and long PDMS chain segments. *Macromolecules* 37:1455–1462

Galder Kortaberria

Abstract

The ability of block copolymers to generate nanostructures when mixed with epoxy thermosetting systems is deeply analyzed. Both amphiphilic and chemically modified di- or triblock copolymers have been used with this purpose. In both cases, one of the blocks is miscible with epoxy system (or even can react with it) before and after curing, while the other one is immiscible before or after curing, leading to morphology development by self-assembly (SA) or reaction-induced phase separation (RIPS), respectively. In some cases, nanostructure development can occur by a combination of both mechanisms or even some demixing of the miscible block can also happen, generating different morphologies. Depending on that and on other parameters like employed hardener, cure cycle, copolymer block ratio, and topology among others, different morphologies such as spherical or wormlike micelles, hexagonally packed cylinders, bilayer micelles, or mixtures of them can be obtained. The effect of nanofillers on morphologies of ternary systems based on epoxy systems nanostructured with block copolymers is also analyzed.

Keywords

Block copolymer • Micelles • Cylinders • Wormlike • Nanostructures

Contents

Introduction	884
Morphologies in Epoxy/Block Copolymer Blends	887
Epoxy/Amphiphilic Block Copolymer Blends	887
Epoxy/Chemically Modified Block Copolymer Blends	901

G. Kortaberria (✉)

'Materials + Technologies' Group, Universidad del Pais Vasco/Euskal Herriko Unibertsitatea, Donostia, Spain

e-mail: galder.kortaberria@ehu.eus

Ternary Systems Based on Nanostructured Epoxy and Inorganic Nanoparticles	905
Conclusion	913
References	915

Introduction

Block copolymers (BC) are the focus of a great deal of research activity because of their intrinsic ability to self-assemble into different nanoscale structures. This intriguing ability can be used to design new polymeric nanostructures with potentially interesting properties. Self-assembly of block copolymers can be maintained in their blends with different homopolymers. In this way, block copolymers have been widely used and are still being used, as templates for generating nanostructured epoxy matrices with long-range order in both uncured and cured states during last decades (Hillmyer et al. 1997; Ritzenthaler et al. 2002; Rebizant et al. 2004; Yi et al. 2011; Wang et al. 2013; Francis and Baby 2014). The control over morphology of those multicomponent thermosets is important for the improvement of their properties. The formation of nanostructures in thermosets can further optimize the inter-component interactions, improving their properties.

The concept of incorporating amphiphilic block copolymers into thermosets has widely been accepted to prepare materials with ordered or disordered nanostructures. During the last years of 1990 decade, a strategy of creating the nanostructures in thermosets using amphiphilic block copolymers by the mechanism of self-assembly was proposed (Lipic et al. 1998). In the protocol, precursors of thermosets act as selective solvents of block copolymers, and some self-organized structures such as lamellar, bicontinuous, cylindrical, and spherical can be accessed in the mixtures depending on fraction of block copolymers before the curing reaction. In this approach, the role of the curing reaction is to lock in the preformed self-organized nanostructures although it has been identified that the nanostructures could undergo some small changes with the occurrence of the curing reaction.

However, self-organization of amphiphilic block copolymers in the precursors of thermosets does not always occur. In many circumstances all the subchains of block copolymers are actually miscible with the precursors of thermosets. The miscibility (or solubility) is ascribed to the nonnegligible entropic contribution (ΔS_m) to free energy of mixing (ΔG_m) in the mixtures of block copolymers since the precursors (or monomers) of thermosets are generally compounds of low molecular weights. In addition, the presence of the self-organized microphases formed at lower temperatures does not assure the survival of these structures at elevated temperatures that are required for curing of some thermosets, since the mixtures of polymers with precursors of thermosets generally displayed upper critical solution temperature (UCST) behaviors.

Under this circumstance, it has been pointed out that ordered and/or disordered nanostructures can be alternatively formed by reaction-induced microphase separation in thermosets (Larrañaga et al. 2005; Meng et al. 2006a; Ocando et al. 2007;

Sinturel et al. 2007). In this approach, it is not required that the amphiphilic block copolymers are self-organized into nanostructures before curing reaction; all the subchains of block copolymers are miscible with precursors of thermosets, and only a part of subchains of block copolymers are microphase-separated out upon curing.

Formation of nanostructures by self-assembly is based on the equilibrium thermodynamics in the mixtures of precursors of thermosets and amphiphilic block copolymers, which is governed by the nature of precursors of thermosets and block copolymers. On the other hand, the morphological control by reaction-induced microphase separation is quite dependent on the competitive kinetics between polymerization and microphase separation. Compared to reaction-induced phase separation in the blends of thermoset and homopolymers or random copolymers, reaction-induced microphase separation of block copolymers in the thermosets occurs in a confined fashion and on the nanometer scale, owing to the presence of miscible blocks.

Nowadays, with the synthesis of versatile block copolymers, the possibility to control the formation of nanostructures has been clearly favored. Ordered and disordered nanostructures have been obtained by incorporating AB-type amphiphilic diblock copolymers (Yi and Zheng 2009; Blanco et al. 2010; Romeo et al. 2013; Cano et al. 2014) ABA-type triblock copolymers (Yang et al. 2009; Hu et al. 2010; Cong and Zheng 2014) or ABC-type triblock copolymers (Ritzenthaler et al. 2002; Yu and Zheng 2011) into thermosets.

Moreover, a second generation of block copolymers has been developed using the concept of chemical compatibilization. This approach incorporates reactive groups into one block in order to promote covalent bonding with the forming epoxy network without loss of ordering in the resulting blends (Grubbs et al. 2000a, b; Rebizant et al. 2003; Serrano et al. 2006; Hameed et al. 2010; Yi et al. 2011; Garate et al. 2013). This pathway could lead to an improvement in mechanical properties and stability of nanostructured materials.

Many different morphologies such as spherical or wormlike micelles, hexagonally packed cylinders, bilayer micelles, or mixtures of them, among others, have been obtained when nanostructuring epoxy matrices with block copolymers. Many factors affect obtained morphologies, being the nature of the copolymer the most important one. This effect will be deeply analyzed through this chapter. Topology and block sequence (Guo et al. 2006; Fan and Zheng 2008; Meng et al. 2008; Wang et al. 2013), together with block composition (Serrano et al. 2005a), also showed a great effect on obtained morphologies. In that way, for epoxy thermosets containing the linear PCL-*b*-PS diblock copolymer (Meng et al. 2008), spherical PS nanophases were arranged into cubic lattice, whereas the PS nanophases were arranged into lamellar lattice when tetra-armed PCL-*b*-PS block copolymer was added. The difference in nanostructures was interpreted on the basis of the restriction of topological structures of the block copolymers on the formation of nanophases. For PS-*b*-PMMA copolymer (Fan and Zheng 2008), different morphologies were obtained depending on subchain sequence. Both linear (*l*-PS-*b*-PMMA) and star-shaped copolymers with two sequential structures (denoted *s*-PS-*b*-PMMA and *s*-PMMA-*b*-PS) were used. Nanostructures were found in the

thermosets containing *l*-PS-*b*-PMMA and *s*-PS-*b*-PMMA, consisting on spherical and wormlike micelles, being the long-range order of the nanostructures higher for the system containing the linear copolymer. This difference was interpreted on the basis of the effects of topological structure of the miscible subchains (PPMA in this case) on the surface free energy of PS nanodomains. For systems with *s*-PMMA-*b*-PS copolymer, however, the phase separation occurred at the scale of micrometer, due to the insufficient suppression of the PMMA chains of macroscopic phase separation of the tetra-armed PS at shell in the block copolymer. For PEO-*b*-PPO copolymer (Guo et al. 2006), it was found that PEO content and block sequence (different four-arm star-shaped copolymers with different PEO contents) determined final morphology, avoiding macroscopic phase separation by increasing PEO content. Similar conclusions were obtained for PEO-*b*-PPO-*b*-PEO triblock copolymer (Serrano et al. 2005a).

On the other hand, together with the amount of block copolymer in the mixture (Blanco et al. 2010), the hardener employed for curing the epoxy matrix and cure cycle (Ritzenthaler et al. 2002; Serrano et al. 2005a; Meng et al. 2006b; Yu and Zheng 2011; Romeo et al. 2013) also would determine the final morphology of those nanomaterials. The hardener shows a great importance because it can determine the miscibility of blocks with epoxy system before and after cure, affecting nanostructuring mechanism or obtained morphology. In that way, different mechanisms and morphologies have been found depending on the hardener: for PEO-*b*-PCL-*b*-PS (Yu and Zheng 2011), spherical PS domains were formed when cured with 4,4'-methylenebis-(2-chloroaniline) (MOCA), while lamellar morphology was obtained by tandem RIPS of PS and PCL blocks when cured with diaminodiphenylsulfone (DDS). For PEO-*b*-PCL copolymer (Meng et al. 2006b), spherical morphology was obtained when cured with DDS, while homogeneous mixtures were achieved when cured with methylenebis-(3-chloro-2,6-diethylaniline) (MCDEA). For PS-*b*-PB-*b*-PMMA copolymer (Ritzenthaler et al. 2002), "spheres on spheres" morphology was obtained when cured with MCDEA by SA mechanism with partial deswelling of PMMA, and flocculated, elongated nanostructures were obtained by RIPS of PMMA when cured with DDS. Cure temperatures and cycle also can determine obtained morphologies because it affects to the miscibility of blocks in epoxy system. For PS-*b*-PMMA (Romeo et al. 2013), different morphologies (from spherical micelles to a dual morphology consisting on hexagonally packed cylinders and spherical micelles) were obtained depending on cure cycle, due to the change of PMMA miscibility with temperature. For PCL-*b*-PB-*b*-PCL copolymer (Meng et al. 2006c), it was found that PCL was miscible with epoxy monomers before curing and also miscible with MOCA-cured epoxy and that the blend system composed of low molecular weight PB and epoxy precursors displayed an upper critical solution temperature (UCST) behavior. RIPS of PB occurred when blends were cured at elevated temperatures. Therefore, the curing reaction was initiated from a homogeneous solution at a temperature above the UCST of the system to ensure that the curing reactions were carried out without the presence of SA structures, altering morphologies.

Nowadays, in order to reach new requirements in nanotechnology, ternary thermosetting systems modified with inorganic nanoparticles and block copolymers have attracted attention (Tercjak et al. 2009, 2012; Ocando et al. 2010; Gutierrez et al. 2010a; Esposito et al. 2014). Nanostructured thermosetting systems designed using different block copolymers are challenging to obtain multifunctional hybrid inorganic/organic materials, since block copolymers can act as template for the incorporation of inorganic nanoparticles or other components. In the case of these multifunctional thermosetting systems modified with nanoparticles, the main objective has been the control of the distribution and size of nanoparticles due to these parameters limit possible applications of the designed materials. Additionally, the selective confinement of nanoparticles in one of the microphase-separated domains, playing with the capability of block copolymers to nanostructuring epoxy resins, has been investigated by several researchers. In summary, the effect of nanoparticles on the morphologies generated by block copolymers when nanostructuring epoxy matrices and their selective placement on the desired domains are the main challenges for those multifunctional materials.

In the present work the most significant morphologies obtained for epoxy/block copolymer mixtures are presented, as characterized by different microscopical techniques such as atomic force microscopy (AFM), transmission electron microscopy (TEM), or scanning electron microscopy (SEM). The effect of all cited parameters on them are also deeply analyzed, showing the versatility of those systems for giving different nanostructures, offering the possibility to design nanostructured materials with different patterns by controlling the mixture components and cure process.

Morphologies in Epoxy/Block Copolymer Blends

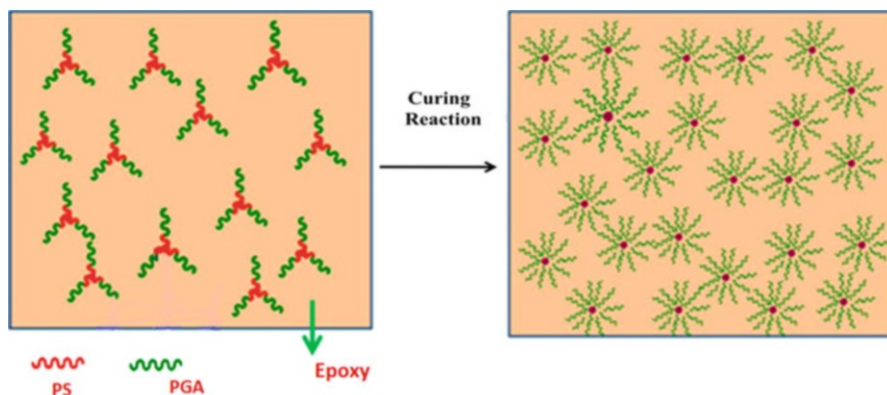
As it was previously pointed out, two main types of copolymers have been used for preparing thermosetting blends with epoxy resins: amphiphilic block copolymers and chemically modified ones.

Epoxy/Amphiphilic Block Copolymer Blends

Many different morphologies can be obtained with the use of amphiphilic diblock or triblock copolymers (ABA or ABC type) by both self-assembly (SA) or reaction-induced phase separation (RIPS) mechanisms.

Amphiphilic Diblock Copolymers

Different morphologies have been obtained for amphiphilic diblock copolymers by both mechanisms. Starting from those diblock copolymers that separate by RIPS mechanism, as was previously pointed out, both blocks are miscible with epoxy precursor and hardener before curing reaction, and one of the blocks becomes immiscible with cure reaction advance, separating from the continuous epoxy



Scheme 1 Formation of nanostructures in epoxy thermoset by reaction-induced microphase separation (Reproduced with permission of (Francis and Baby), copyright 2014 American Chemical Society)

phase in which the other block remains miscible (or even reacts with the matrix), as it can be seen in Scheme 1, where the poly(glycolic acid) (PGA) block remains miscible during curing, while polystyrene (PS) separates forming its phase at the nanoscale. Both blocks were miscible with epoxy precursors before curing reaction.

Many different diblock copolymers presenting this behavior can be found: poly(styrene-*block*-glycolic acid) (PS-*b*-PGA) with PGA as miscible block (Francis and Baby 2014), poly(isoprene-*block*-methyl methacrylate) (PI-*b*-PMMA) with PMMA as miscible block (Esposito et al. 2013), poly(styrene-*block*-methyl methacrylate) (PS-*b*-PMMA) with PMMA as miscible block (Fan and Zheng 2008), poly(isoprene-*block*-4-vinyl pyridine) (PI-*b*-P4VP) with P4VP as miscible block (Guo et al. 2008), poly(ϵ -caprolactone-*block*-styrene) (PCL-*b*-PS) with PCL as miscible block (Meng et al. 2006), poly(heptadecafluorodecyl acrylate-*block*-caprolactone) (PaF-*b*-PCL) with PCL as miscible block (Ocando et al. 2007), poly(styrene-*block*-ethylene oxide) (PS-*b*-PEO) with PEO as miscible block (Meng et al. 2006a; Gutierrez et al. 2011), and poly(dimethylsiloxane-*block*-glycidyl methacrylate) (PDMS-*b*-PGMA) with PGMA as miscible block (Hameed et al. 2010). The typical morphology obtained by RIPS mechanism consists on spherical domains of the immiscible block dispersed in a continuous epoxy matrix in which the other block remains miscible, especially for low copolymer contents of around 10 wt.%, as it can be seen in Fig. 1 for PI-*b*-PMMA copolymer as an example.

Increasing block copolymer amount, for many copolymers like PS-*b*-PMMA (Fan and Zheng 2008), PCL-*b*-PS (Meng et al. 2008), and PS-*b*-PEO (Meng et al. 2006a), spherical domains start to coagulate, in which some interconnected domains together with spherical ones appear. Generally the amount of spherical domains increases, maintaining their size almost constant. In some cases, by increasing copolymer content even lamellar morphologies (Gutierrez et al. 2011) can be obtained, as it can be seen in Fig. 2 for PS-*b*-PEO (also called SEO)

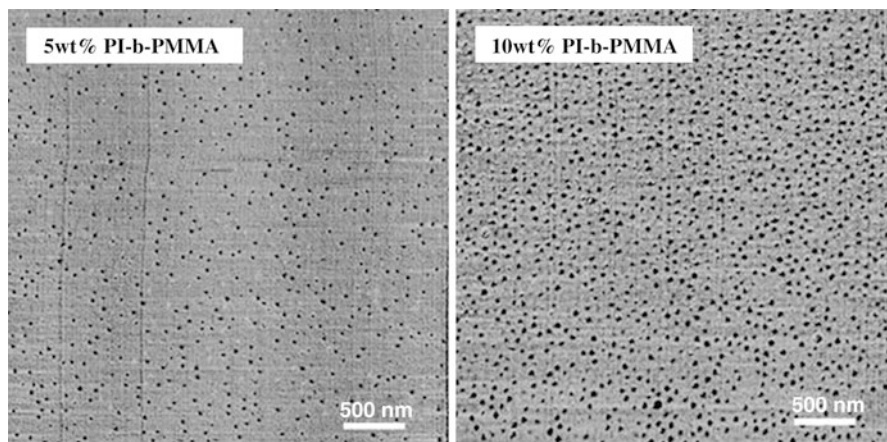


Fig. 1 AFM-phase images of DGEBA/MCDEA with 5 and 10 wt.% of PI-*b*-PMMA

copolymer. Depending on the copolymer and its amount, other morphologies can also be obtained such as mixtures of spherical and wormlike micelles of the separating block (Ocando et al. 2007) as it can be seen in Fig. 3 or morphologies in which the nanophase can be arranged into the epoxy matrix in cubic lattices (Hameed et al. 2010).

An interesting phenomenon that can occur with some copolymers is that, for high contents, even some miscible subchains can demix from the matrix upon curing, generating corona-like domains with an external layer formed from the partial demixing of the miscible block (Fan and Zheng 2008). This phenomenon has also been found for epoxy/copolymer systems in which nanostructure is generated by self-assembly mechanism (Lipic et al. 1998; Blanco et al. 2010; Yi et al. 2011) and will be analyzed below.

On the other hand, several copolymers have been found to nanostructure epoxy matrix by SA mechanism. As was pointed out previously, precursors of thermosets act as selective solvents of block copolymers accessing self-organized structures, depending on fraction of block copolymers, before the curing reaction. The role of the curing reaction is to lock in those self-organized nanostructures. Many diblock copolymers presenting this behavior can be found: poly(styrene-*block*-2-vinyl pyridine) (PS-*b*-P2VP) with P2VP as miscible block; poly(caprolactone-*block*-2,2,2-trifluoroethyl acrylate) (PCL-*b*-PTFEA) with PCL as miscible block; poly(styrene-*block*-methyl methacrylate) (PS-*b*-PMMA) with PMMA as miscible block (Blanco et al. 2010); poly(ethylene oxide-*block*-dimethylsiloxane) (PEO-*b*-PDMS) with PEO as miscible block; and poly(2,2,2-trifluoroethyl acrylate-*block*-glycidyl methacrylate) (PTFEA-*b*-PGMA) with PGMA as miscible block, among others.

Different self-organized structures such as lamellar, bicontinuous, cylindrical, and spherical can be accessed in the mixtures depending on fraction of block copolymers before the curing reaction. Most common morphology for cured systems with copolymer contents up to 20 wt.% is that composed by spherical micelles

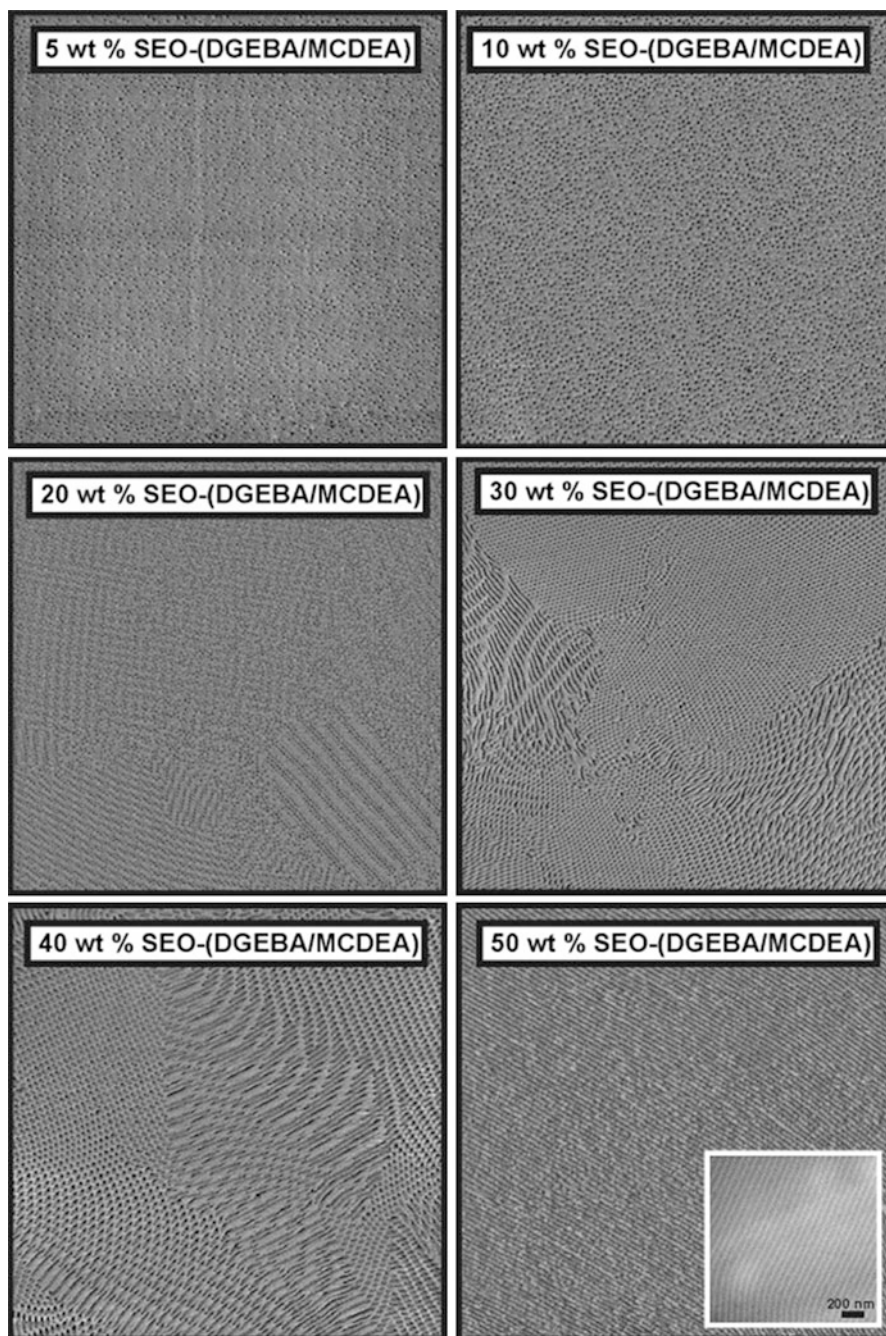


Fig. 2 AFM-phase images ($5 \times 5 \mu\text{m}$) of binary systems. TEM image of 50 wt.% copolymer inset at the bottom of the corresponding AFM-phase image (Reproduced with permission of (Gutierrez et al.), copyright 2011 Elsevier Ltd)

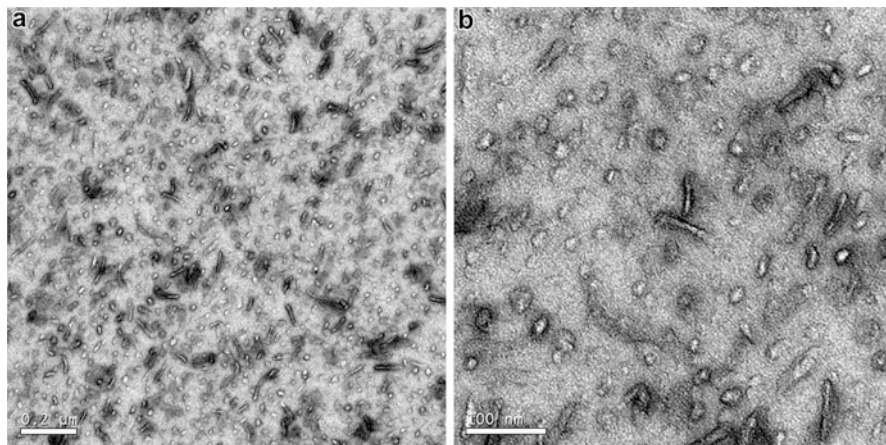


Fig. 3 TEM images at different magnifications for DGEBA/MCDEA cured blend containing 35 wt.% PaF-*b*-PCL. The samples have been stained with RuO₄ for 4 min. Scale bar: (a) 0.2 μm and (b) 100 nm (Reproduced with permission of (Ocando et al.), copyright 2007 American Chemical Society)

that has been obtained for different copolymers: for PCL-*b*-PTFEA (Wang et al. 2013), PTFEA spherical nanodomains dispersed in a continuous epoxy matrix in which PCL remained miscible; for PEO-*b*-PDMS (Guo et al. 2006), spherical PDMS micelles in a continuous epoxy matrix in which PEO block remained miscible; and for PTFEA-*b*-PGMA (Yi et al. 2011), spherical PTFEA domains in a continuous epoxy matrix in which PGMA remained miscible. Increasing block copolymer content, in many cases spherical domains start to coagulate, increasing their size and generating morphologies composed by spherical and wormlike micelles, as it was found for PEO-*b*-PDMS, PTFEA-*b*-PGMA, or PS-*b*-PMMA copolymers. Examples can be seen in Figs. 4, 5, and 6 for PEO-*b*-PDMS, PCL-*b*-PTFEA, and PTFEA-*b*-PGMA copolymers, respectively. Commonly, for high copolymer contents (from 40 to 60 wt.% depending on the copolymer) macroscopic phase separation is obtained.

However, depending on the copolymer some other morphologies like cylinders can also be obtained. For epoxy mixtures with PS-*b*-P2VP copolymer (Casaban et al. 2013), a morphology consisting on PS cylinders dispersed in a continuous epoxy phase in which P2VP block remained miscible was obtained, for 30 wt.% of copolymer. For epoxy mixtures with PEO-*b*-PEP copolymer (Lipic et al. 1998), a morphology consisting on cylindrical PEP cores surrounded by a PEO shell enclosed by the epoxy matrix was found.

Moreover, as was also described for RIPS mechanism, the partial demixing of the miscible block has also been found to occur, affecting obtained morphologies. In that way, for PS-*b*-PMMA copolymer (Blanco et al. 2010), it was found that micellar self-assembled PS block chains formed the micelle nucleus. This micellar nanostructure was stabilized by the partial demixing of PMMA block close to

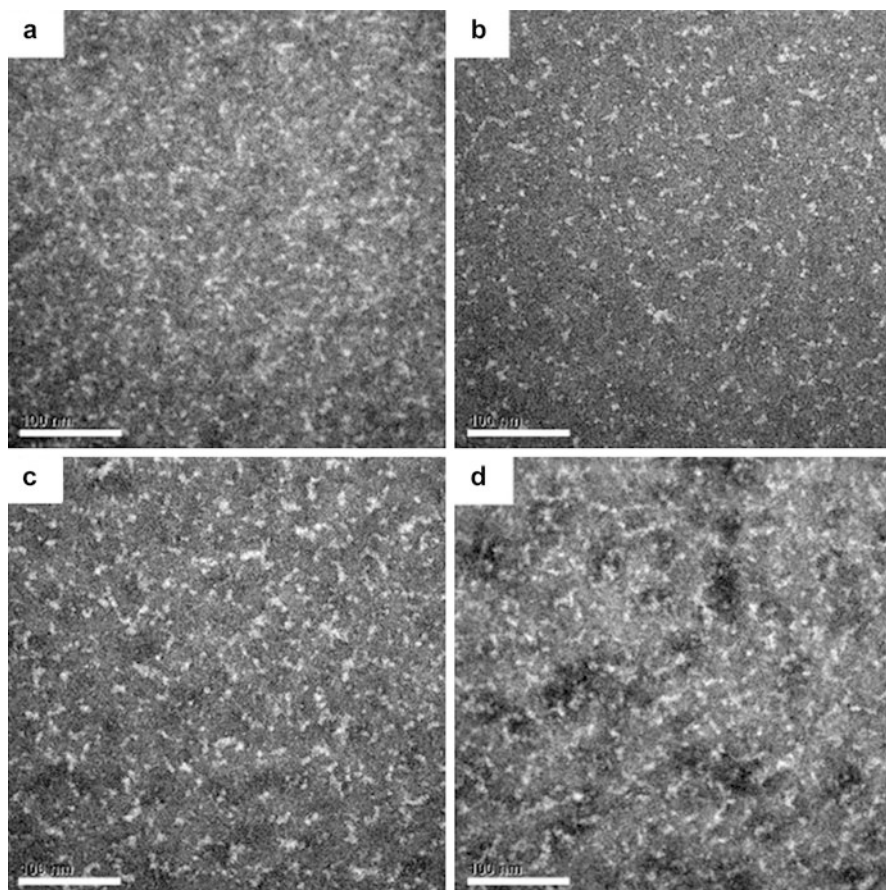


Fig. 4 TEM micrographs of (a) 80/20, (b) 70/30, (c) 60/40, and (d) 50/50 MDA-cured ER/PEO-PDMS blends. The scale bars represent 100 nm (Reproduced with permission of (Guo et al.), copyright 2006 Wiley Periodicals Inc)

gelation of epoxy matrix. For PTFEA-*b*-PGMA copolymer mixtures with epoxy (Yi et al. 2011), the spherical nanodomains obtained for low copolymer contents started to be interconnected, appearing some wormlike micellar morphology. As their size decreased with copolymer content, it can be concluded that a demixing of PGMA block at the surface of PTFEA nanodomains occurred. The miscible block demixed from epoxy matrix during curing process, as it can be seen in Scheme 2.

A similar behavior was found for mixtures of epoxy with PEO-*b*-PEP copolymer (Lipic et al. 1998). The epoxy resin has selectively swollen the PEO chains. As the amount of epoxy added to the block copolymer was increased, the microstructure evolved from lamellar to gyroid, to cylinders, and to body-centered cubic-packed spheres and ultimately disordered micelles. When hardener was added and the epoxy cured, the system retained the nanostructure and macrophase separation

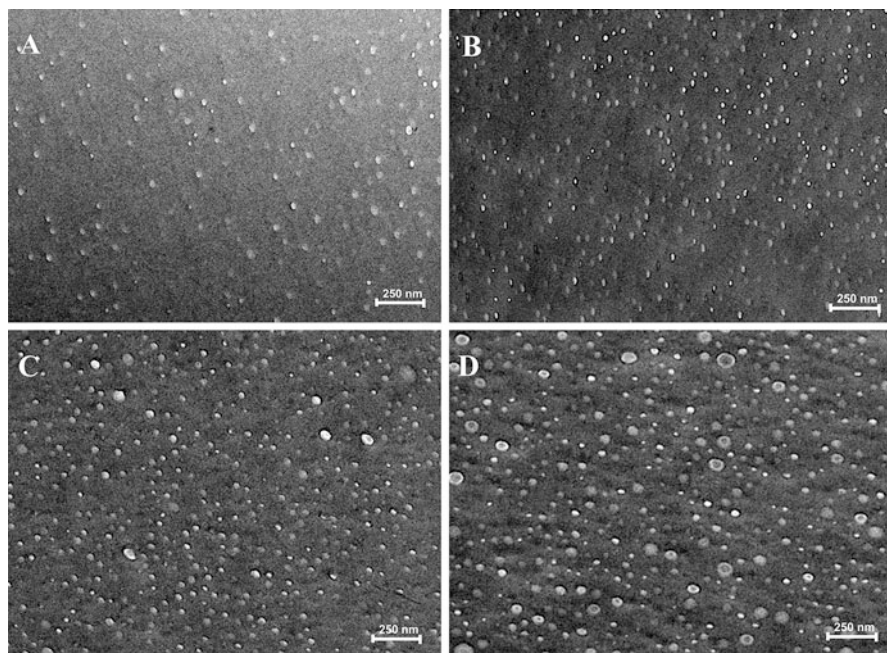


Fig. 5 TEM micrographs of the thermosets containing (a) 10, (b) 20, (c) 30, and (d) 40 wt.% of PCL-*b*-PTFEA diblock copolymer (Reproduced with permission of (Wang et al.), copyright 2013 American Chemical Society)

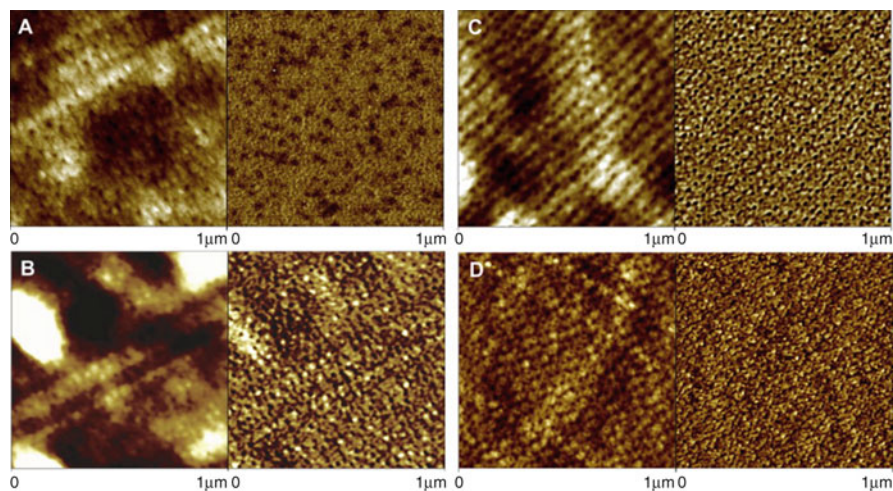
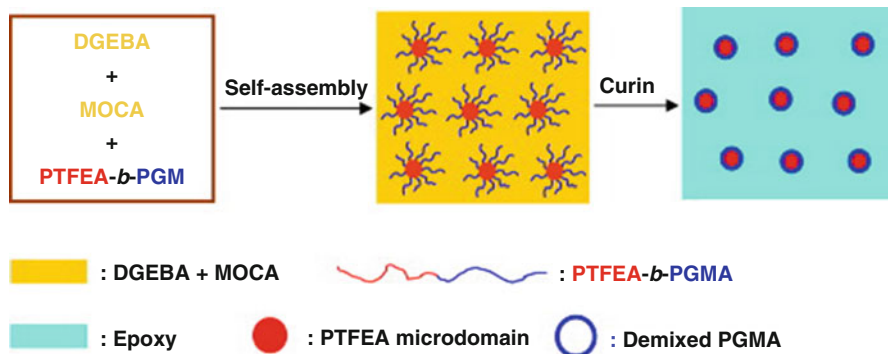


Fig. 6 AFM images of epoxy thermosets containing: (a) 10, (b) 20, (c) 30, and (d) 40 wt.% of PTFEA-*b*-PGMA diblock copolymer. *Left*, topography; *right*, phase contrast images (Reproduced with permission of (Yi et al.), copyright 2011 Elsevier Ltd)



Scheme 2 Formation of nanostructures in epoxy thermosets and demixing of PGMA blocks out of epoxy-amine matrix (Reproduced with permission of (Yi et al.), copyright 2011 Elsevier Ltd)

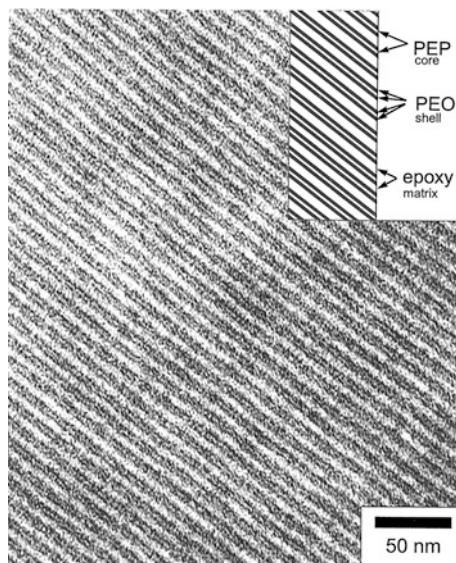
between the block copolymer and epoxy was avoided. However, the PEO block was expelled from the reactive matrix on a local level as the molecular weight of the epoxy increased, leading to cure-induced phase transitions and regions of relatively pure crystalline PEO. There was a transition from an equilibrium morphology to a chemically pinned metastable state as the cross-linking reaction progressed through the gel point.

Expulsion of PEO by the epoxy network was restricted to a local scale, and there was no disruption of long-range order. Chemical curing, and the associated increase in molecular weight, ejected the PEO from the curing epoxy. A “wet” brush to “dry” brush transition with cure was depicted, as it can be seen in Fig. 7.

Amphiphilic ABA-Type Triblock Copolymers

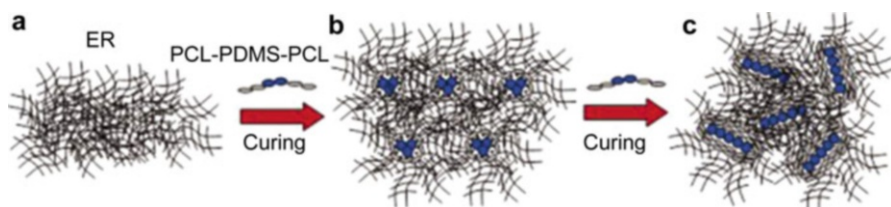
Different morphologies have been obtained for amphiphilic ABA-type triblock copolymers by both mechanisms. Usually A block is miscible with epoxy matrix, while B block separates before (SA mechanism) or during cure (RIPS). Several ABA copolymers have been found to generate nanostructures in their mixtures with epoxy systems by RIPS mechanism: poly(ϵ -caprolactone-*block*-(styrene-*co*-acrylonitrile)-*block*- ϵ -caprolactone) (PCL-*b*-PBS-*b*-PCL) with PCL as miscible block (Cong and Zheng 2014), poly(ϵ -caprolactone-*block*-dimethylsiloxane-*block*- ϵ -caprolactone) (PCL-*b*-PDMS-*b*-PCL) with PCL as miscible block (Hameed et al. 2010), poly(ϵ -caprolactone-*block*-polybutadiene-*block*- ϵ -caprolactone) (PCL-*b*-PB-*b*-PCL) with PCL as miscible block (Meng et al. 2006c), poly(ϵ -caprolactone-*block*-(butadiene-*co*-acrylonitrile)-*block*- ϵ -caprolactone) (PCL-*b*-PBN-*b*-PCL) with PCL as miscible block (Yang et al. 2009), poly(methyl methacrylate-*block*-butyl acrylate-*block*-methyl methacrylate) (PMMA-*b*-PbuA-*b*-PMMA) with PMMA as miscible block (Bashar et al. 2014), and poly(ethylene oxide-*block*-propylene oxide-*block*-ethylene oxide) (PEO-*b*-PPO-*b*-PEO) with PEO as miscible block (Guo et al. 2002; Serrano et al. 2005a). As it can be seen in most of cases, PCL has

Fig. 7 TEM image of the OP5/BPA348/MDA blend (52 wt.% OP5). The inset provides an interpretation of the morphology; cylindrical PEP cores (*thin white lines*) surrounded by a PEO shell (*black*), enclosed by the epoxy matrix (Reproduced with permission of (Lipic et al.), copyright 1998 American Chemical Society)



been chosen as the miscible block. The typical morphology obtained by RIPS mechanism with ABA copolymers, especially for those containing PCL blocks, consists on spherical domains of the immiscible block dispersed in a continuous epoxy matrix in which the other block remains miscible, especially for low copolymer contents of around 10 wt.%. By increasing copolymer content, spherical domains (usually increasing in number and/or size) start to coagulate, resulting in interconnected domains, obtaining morphologies composed by a mixture of spherical and interconnected domains (for mixtures with around 20–30 wt.% of copolymer). For higher copolymer contents (around 40 wt.% and higher), wormlike morphologies are usually obtained. This behavior has been found for ABA copolymers in which PCL is the A block, such as PCL-*b*-PDMS-*b*-PCL, PCL-*b*-PBS-*b*-PCL, PCL-*b*-PB-*b*-PCL, and PCL-*b*-PBN-*b*-PCL. As an example, Scheme 3 shows the schematic representation of different morphologies for PCL-*b*-PDMS-*b*-PCL copolymer, while Fig. 8 shows the described evolution of nanostructures with copolymer content for PCL-*b*-PBS-*b*-PCL copolymer.

Some other morphologies like bilayer vesicles or bicontinuous have also been found with other ABA-type triblock copolymers. For PMMA-*b*-PBuA-*b*-PMMA copolymer, a morphology consisting in randomly dispersed bilayer vesicles has been found (Bashar et al. 2014), being PBuA the immiscible block. For PEO-*b*-PPO-*b*-PEO copolymers with different PEO contents (Guo et al. 2002), different morphologies have been found, as it can be seen in Fig. 9 for the copolymer with the lower PEO content of 30 wt.%, EO30. For the copolymer with higher PEO amount (80 wt.% of PEO, called EO80 and not shown in the figure), a behavior quite similar to that described above (spherical domains that coagulate resulting in wormlike



Scheme 3 Schematic representation of different phase morphologies in ER/PCL-*b*-PDMS-*b*-PCL blends: (a) MDA-cured ER, (b) spherical microdomains at 5–20 wt.% PCL-*b*-PDMS-*b*-PCL concentration, and (c) wormlike microdomains at 30–50 wt.% PCL-*b*-PDMS-*b*-PCL concentration (Reproduced with permission of (Hameed et al.), copyright 2010 Wiley Interscience)

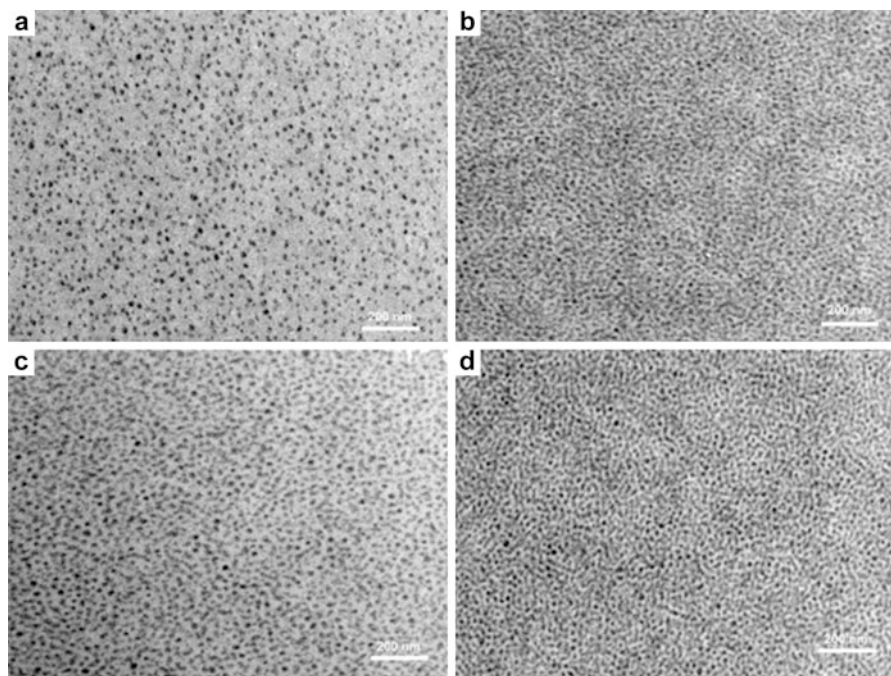


Fig. 8 TEM images of the thermosets containing: (a) 10, (b) 20, (c) 30, and (d) 40 wt.% of PCL-*b*-PBS-*b*-PCL triblock copolymer (Reproduced with permission of (Cong and Zheng), copyright 2014 Elsevier Ltd)

morphology) was found. For the copolymer with lower PEO amount (EO30), hierarchical nanostructures were found with bicontinuous morphology or mixtures of wormlike and bicontinuous. For 20 wt.% of copolymer, a structural inhomogeneity was found: microphases composed of cross-linked epoxy network swollen with small amount of miscible PEO block, areas of PPO domains shielded by coronae of PEO blocks, and areas with insufficient cross-linked epoxy and more PEO blocks. Because of unfavorable interactions of PPO with the epoxy network as

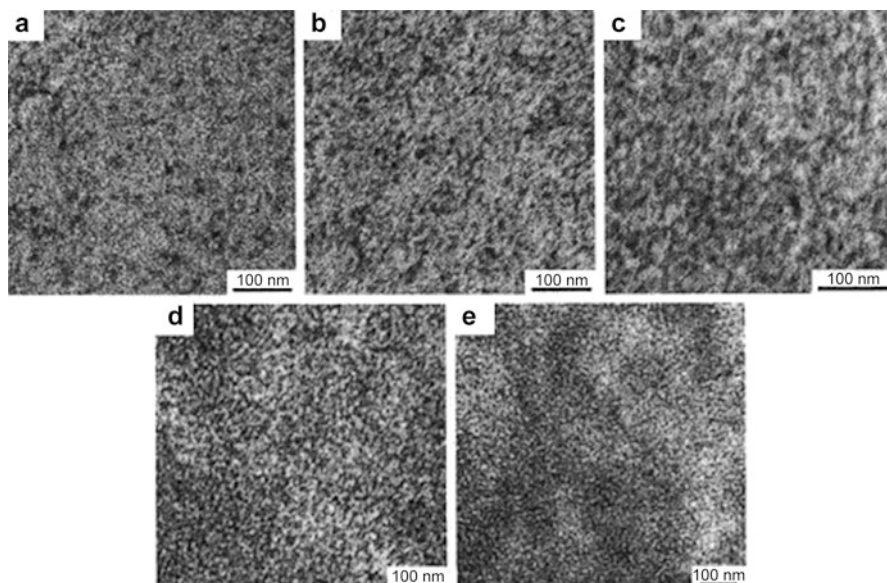


Fig. 9 TEM micrographs of (a) 90/10, (b) 80/20, (c) 70/30, (d) 60/40, and (e) 50/50 MDA-cured ER/EO30 blends (Reproduced with permission of (Guo et al.), copyright 2002 American Chemical Society)

well as with the insufficiently cured epoxy, microphase separation took place within both the phases to form the PPO spherical domains. For mixtures with 50 wt.% of copolymer, bicontinuous microphase structure was achieved, with both spherical and wormlike micelles of PPO.

Regarding ABA triblock copolymer that nanostructure epoxy systems via RIPS mechanism, the most important ones have been those copolymers obtained by chemical modification of one of the blocks in previously cited copolymers. In that way, PBS block in PCL-*b*-PBS-*b*-PCL has been converted into poly(ethylene-*co*-ethyl ethylene) (PEEES) (Cong and Zheng 2014), and PB block in PCL-*b*-PB-*b*-PCL has been converted into PEEE by hydrogenation (Hu et al. 2010). In both cases, the nanostructuring mechanism changed from RIPS to SA. The driving force for the RIPS of PBS or PB blocks is the decrease in entropic contribution to free energy of mixing with the occurrence of cross-linking reactions. It is proposed that the following two factors affect the formation of PBS or PB nanophases: (i) the immiscibility of PBS and PB with the cross-linked epoxy and (ii) the competitive kinetics between polymerization and microphase separation. The former is governed by the factors of thermodynamics in the blends of epoxy with PBS or PB, whereas the latter affected the morphologies of the thermosets since the PBS or PB nanophases were formed under the nonequilibrium condition. As the curing reaction proceeds, the mixtures underwent a series of structural changes involving chain extension, branching, and cross-linking in succession, and the viscosity of system was significantly increased and the system was converted into

the three-dimensional networks due to the occurrence of gelation. For the systems containing PCL-*b*-PEEES-*b*-PCL or PCL-*b*-PEEE-*b*-PCL, the curing reaction was started from the self-organized mixtures composed of epoxy system and the copolymer. The formation of PEEES or PEEE nanophases was governed by the equilibrium thermodynamics of the triblock copolymer in the precursors of epoxy, i.e., the size and shape of the micelles were dependent on the establishment of epoxy-phobic and epoxy-philic balances with PEEES or PEEE and PCL blocks, respectively. With identical concentrations of the copolymers, the size of PEEES or PEEE nanophases is larger than that of PBS or PB under the same curing conditions. In both cases, the morphologies obtained and their evolution were very similar than that explained above for RIPS mechanism: spherical micelles for low content, interconnected domains by increasing block copolymer amount, and wormlike micelles for higher contents. Very similar evolution of morphology generated by SA was found for PCL-*b*-PDMS-*b*-PCL (Xu and Zheng 2007) and PCL-*b*-PE-*b*-PCL (Zhang and Zheng 2013) copolymers. In the last case, besides described morphology, the crystallization of PE was found to occur in confined manner.

Amphiphilic ABC-Type Triblock Copolymers

The presence of three different blocks with different solubility in epoxy precursors and cured systems complicates obtained morphologies and mechanisms for their obtention. A combination of RIPS and SA mechanisms (Fan et al. 2009), a tandem RIPS mechanism (Yu and Zheng 2011), and SA with partial deswelling of one of the blocks (Ritzenthaler et al. 2002) during cure have been described. For mixtures of epoxy with PDMS-*b*-PCL-*b*-PS copolymer, a combination of RIPS and SA mechanism has been found. PDMS block is immiscible with epoxy precursors before cure, forming spherical or wormlike micelles before cure. During cure, RIPS of PS subchains occurred in the presence of PDMS nanophases, while PCL remained miscible. Preformed PDMS nanophases acted as template of the RIPS of PS, confining PS subchains around PDMS nanophases. Obtained morphologies can be seen in Fig. 10 for different block copolymer contents. For 10 and 20 wt.% of copolymer, spherical nanodomains were found, assignable to the immiscible components (i.e., PDMS and PS), whereas the continuous matrix to epoxy is miscible with PCL subchain. Dispersed nanodomains were not homogeneous and displayed a “core-shell” structure. The “core” could be ascribed to PDMS subchain, whereas the “shell” could be attributed to PS subchain. For higher copolymer contents different morphologies were found.

Thermosets containing 30 wt.% PDMS-*b*-PCL-*b*-PS showed large-scaled circled and lamellar structures, and all the features were concentric circled (Fig. 9c). This was the first observation of the formation of concentric-circled nanostructures in epoxy thermosets. With increasing the content of triblock copolymer, the concentric-circled lamellar morphology was transformed into the large-scaled lamellar nanostructures (Fig. 9d).

For PEO-*b*-PCL-*b*-PS copolymer (Yu and Zheng 2011), a tandem RIPS mechanism was found. When cured with MOCA hardener, morphologies consisting on

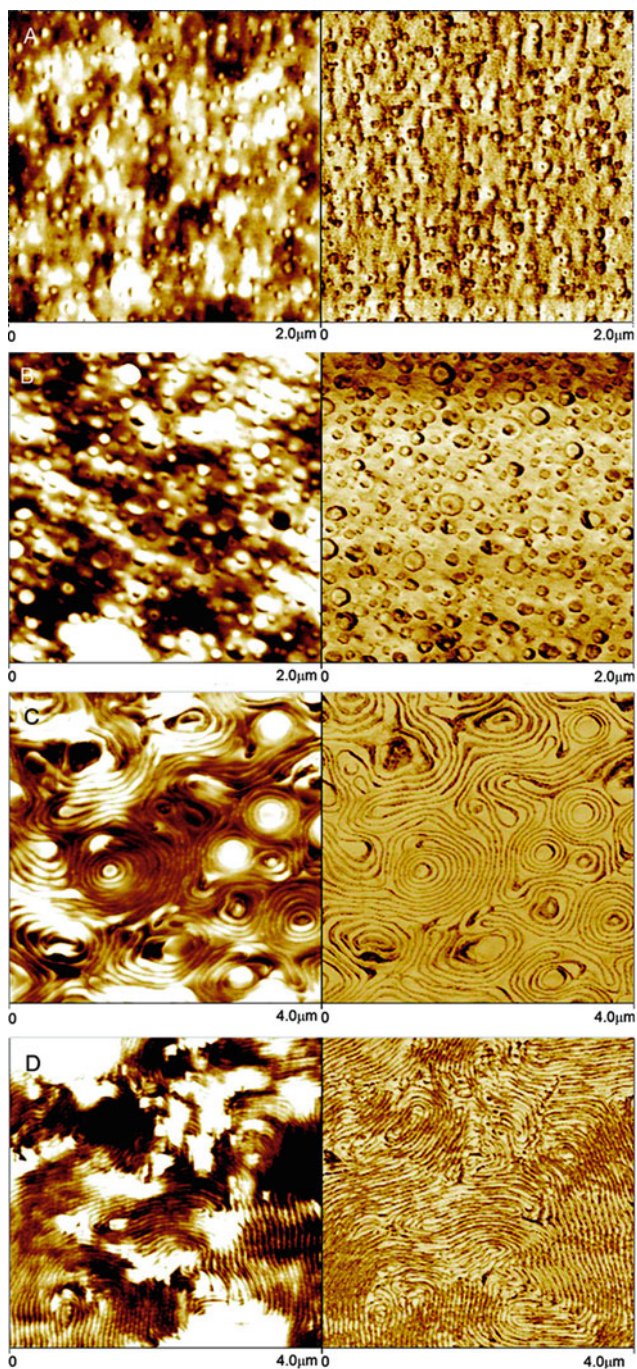
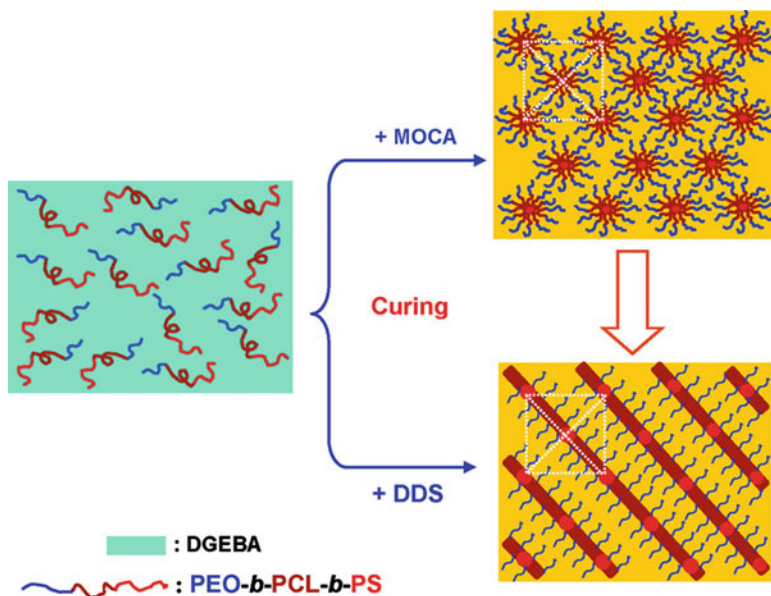


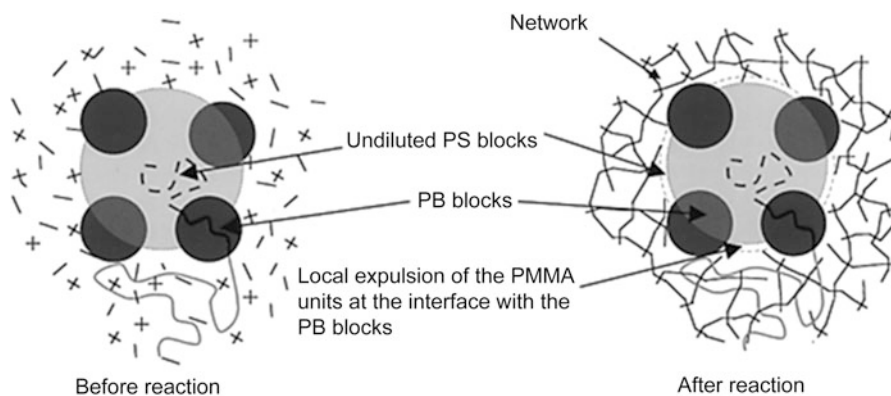
Fig. 10 AFM images of epoxy thermosets containing PDMS-*b*-PCL-*b*-PS triblock copolymer. *Left*, height image; *right*, phase image. (a) 10, (b) 20, (c) 30, and (d) 40 wt.% of PDMS-*b*-PCL-*b*-PS triblock copolymer (Reproduced with permission of (Fan et al.), copyright 2009 American Chemical Society)



Scheme 4 Formation of spherical and lamellar nanophases in epoxy thermosets containing PEO-*b*-PCL-*b*-PS triblock copolymer (Reproduced with permission of (Yu and Zheng), copyright 2011 American Chemical Society)

spherical nanophases of PS arranged into body-centered cubic lattice were found, formed by RIPS of PS subchains. Increasing copolymer content, spherical domains began to interconnect, resulting finally in wormlike micellar morphology. When DDS was used as hardener, due to the immiscibility of PCL with cured epoxy/DDS system, a RIPS of PS and PCL occurred, resulting in spherical nanodomains of PS and PCL (for copolymer contents less than 20 wt.%) dispersed in a continuous epoxy phase where PEO was solved. For 30 wt.% of copolymer and higher, lamellar morphology was obtained, being each nanolayer composed by PS and PCL. The scheme of this mechanism can be seen in Scheme 4.

Finally, for PS-*b*-PB-*b*-PMMA copolymer, Ritzenthaler et al. (2002) found that morphologies when mixed with an epoxy system depended on hardener. Before cure, three block self-organized in PS spheres surrounded by PB nodules while PMMA remained soluble forming a swollen corona. So SA mechanism was followed for nanostructuring. When cured with MCDEA, undiluted PS and PB blocks formed a “spheres on spheres” morphology, while most of PMMA was embedded in the matrix, but with a partial deswelling of PMMA resulting in a pure PMMA phase at the interface with PB blocks. Scheme 5 shows the process of nanostructure formation. If cure was carried out with DDS, the RIPS of PMMA occurred at early stages of cure, leading to flocculated, micrometer-size elongated nanostructures.



Scheme 5 Schematic description of the evolution of the triblock organization in the DGEBA–MCDEA thermoset system before and after reaction (Reproduced with permission of (Ritzentaler et al.), copyright 2002 American Chemical Society)

Epoxy/Chemically Modified Block Copolymer Blends

A second generation of block copolymers has been developed using the concept of chemical compatibilization that consists on chemical modification of one of the blocks in the copolymer in order to compatibilize and react with epoxy matrix. In this way, the epoxidation of the elastomeric block in thermoplastic elastomer (TPE) di- and triblock copolymers has been the main trend: epoxidation of poly(isoprene) block in poly(styrene-*block*-isoprene-*block*-styrene) (PS-*b*-PI-*b*-PS) copolymer (Garate et al. 2011, 2013, 2014) and epoxidation of poly(butadiene) block in poly(styrene-*block*-butadiene-*block*-styrene) (PS-*b*-PB-*b*-PS) or poly(styrene-*block*-butadiene) (PS-*b*-PB) copolymers (Serrano et al. 2005b, 2006, 2007; Ocando et al. 2008a, 2009; George et al. 2012, 2013).

Starting with triblock copolymers, for epoxidized PS-*b*-PI-*b*-PS (Garate et al. 2011, 2013, 2014), epoxidation degree has been found to determine obtained nanostructured pattern. In the uncured state, PS blocks self-assembled in sphere-like nanodomains with a short-range order, while epoxidized polyisoprene (ePI) subchains were initially miscible with the epoxy precursors. As cure proceeded the PS nanodomains became gradually distorted switching to bigger and less organized structures, due to RIPS of ePI subchains which became immiscible with the epoxy system as the curing process occurs. However, this demixing process was partial because of the reaction between ePI subchains and the epoxy matrix, which reduced ePI subchains mobility. The higher the epoxidation degree was, the lower the demixing process was, and therefore less interconnected sphere-like structures were formed. For high epoxidation degrees, nanostructured pattern changed from distorted and interconnected sphere-like nanodomains when the epoxidation degree was 65% to sphere-like nanostructures for 100% of epoxidation. Figure 11 shows obtained morphologies and a schematic representation of their obtention. When an epoxidized PS-*b*-PI-*b*-PS copolymer incorporating amine-reactive functionalities

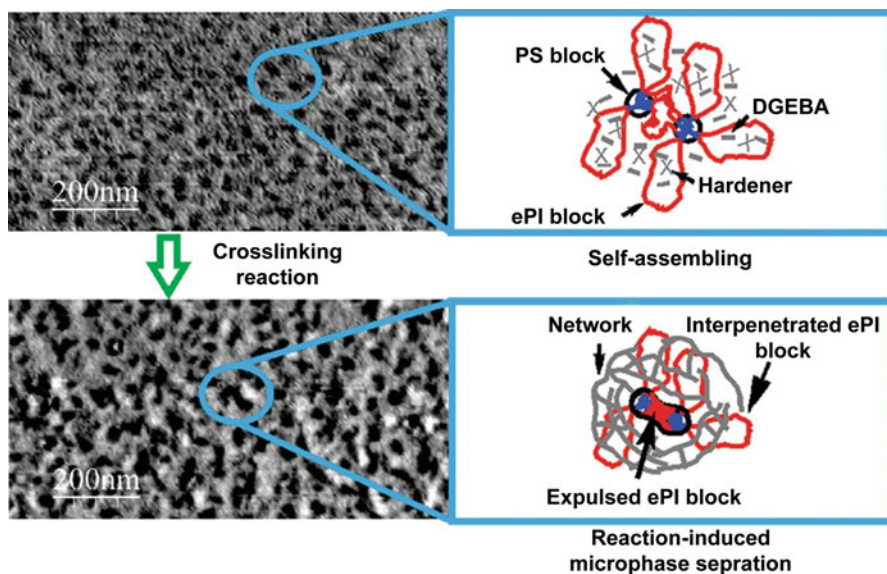


Fig. 11 AFM images and schematic description of morphologies obtained for epoxy mixtures with 23% of PS-*b*-PI-*b*-PS 100% epoxidized (Reproduced with permission of (Garate et al.), copyright 2013 American Chemical Society)

(eSIS-AEP) in the epoxidized block was used, nanostructured materials with sphere-like nanodomains were formed before curing by SA of PS blocks. Conversely to the typical ePI demixing process previously cited, for the case of eSIS-AEP, the nanodomain morphology was preserved, which indicated that no ePI-AEP demixing process occurred as a consequence of the enhanced reactivity of eSIS-AEP with epoxy matrix.

Regarding epoxidized PS-*b*-PB-*b*-PS copolymer (George et al. 2012, 2013), it was found that nanostructures were generated for epoxidation degrees of 39% and higher. Without epoxidation and with lower epoxidation degrees (25%), macroseparation or generation of microstructures was obtained. So epoxidized copolymers at high degree of epoxidation (39% and 47%) could be able to create nanostructured templates in epoxy resins, as it can be seen in Fig. 12.

For the copolymer 39% epoxidized, wormlike micellar morphology was obtained. The reduced compatibility of epoxidized PB blocks in epoxy matrix was due to the presence of unepoxidized PB block that produced a tendency toward aggregation of vesicles and hence a wormlike micelle morphology. For the copolymer 47% epoxidized, these interconnected wormlike micelle morphologies changed to long-range ordered nanostructured spherical micelles. Regarding the mechanism that led to described morphologies, since PB subchains remained immiscible in the epoxy resin, the formation of PB core by SA before curing followed by RIPS of PS phase over the PB phase could be expected. However, there was a small unepoxidized PB phase present in the mixture. During cure, a part

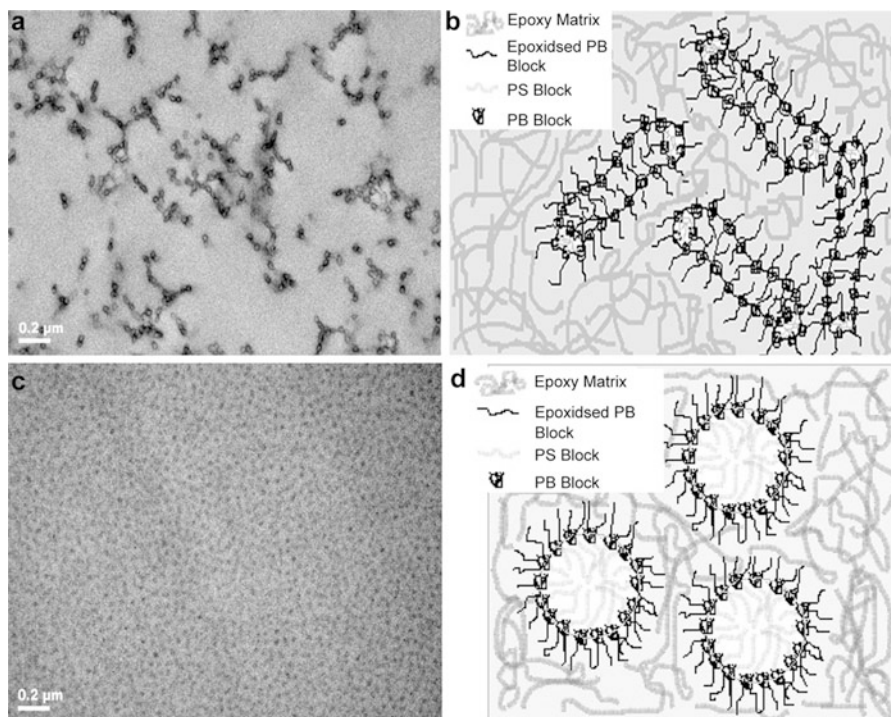


Fig. 12 TEM images of epoxy/eSBS/DDM blends containing 10 wt.% eSBS epoxidized at (a) 39 and (c) 47 mol%, schematic representation of epoxy/eSBS/DDM blends containing 10 wt.% eSBS epoxidized at (b) 39 and (d) 47 mol% (Reproduced with permission of (George et al.), copyright 2013 American Chemical Society)

of the PS subchain phase is separated to form nanosized PS core, followed by reaction-induced self-assembly of most of the unepoxidized PB phase to form a shell of PB chains over the PS core.

The minimum degree of epoxidation needed for nanostructuring epoxy system with PS-*b*-PB-*b*-PS copolymer has also been investigated, together with the effect of PS block content (Ocando et al. 2008b). A minimum of 27 mol% of epoxidation, which corresponds to 4.8 wt.% of epoxidized PB units in the overall mixture, was needed to ensure nanostructuring of final mixtures. Generated morphologies were found to be very dependent on PS content. PS contents between 16 and 20 wt.% in the overall mixture were needed to obtain hexagonally ordered nanostructures. Additionally, as the amount of block copolymer added to the epoxy matrix increased, the morphologies in the mixtures develop from micelles to vesicles, to wormlike and finally to hexagonally ordered nanostructures. Morphologies were generated by RIPS of PS block, together with some local demixing of PB block. An increase of epoxidation produced a decrease in domains size, probably due to a smaller amount of phase-separated non-epoxidized PB units around PS domains.

PS-*b*-PB diblock copolymer (both linear and star shape) has also been epoxidized in order to obtain nanostructured mixtures with epoxy systems (Serrano et al. 2005, 2006, 2007; Ocando et al. 2009). For linear PS-*b*-PB (Serrano et al. 2007), depending on the block copolymer content and its epoxidation degree, the PS domains can display micellar, wormlike, or hexagonally packed cylinder structures. Independent of the copolymer percentage and epoxidation degree used (37% and 46%), cured blends containing epoxidized copolymers were nanostructured. With 30 wt.% of copolymer, morphology consisting on wormlike or cylindrical irregular domains of PS was obtained for lower epoxidation degree, while hexagonally ordered structure was obtained for the copolymer 46% epoxidized. With 10 wt.% of copolymer, micellar structures were obtained for both epoxidation degrees. Morphology development was by RIPS of PS block, while reactive epoxidized PB block remained mostly miscible with the growing thermosetting epoxy system during the polymerization reaction (among some local expulsion). Nanostructuring occurred through an epoxy-miscible block.

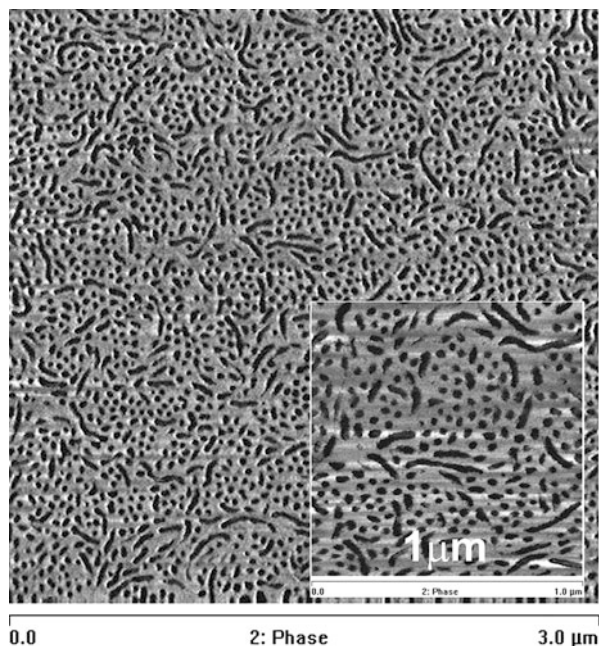
The critical epoxidation threshold to achieve nanostructuring of epoxy systems with PS-*b*-PB copolymer has also been investigated (Ocando et al. 2009). Different mechanisms are involved through morphology development, depending on the content of epoxidized PB (PBep) in the initial mixture.

A minimum threshold of around 27% was found. Near this threshold, microphase separation was obtained through SA mechanism of PBep and RIPS of PS block. New bilayered structures developed by the occurrence of these two mechanisms, leading to vesicles or long wormlike micelles depending on the concentration of block copolymer in the overall mixture. When the epoxidation degree was considerable lower than the minimum threshold, macrophase separation occurred as expected. Nevertheless, at higher epoxidation degree, long-range order microstructures of PS were obtained as a consequence of RIPS because the initial miscibility of both blocks with the epoxy resin before curing, as it can be seen in Fig. 13.

In the AFM image, a morphology consisting in hexagonally packed PS cylinders oriented parallelly and perpendicularly to the cutting surface can be seen. The schematic representation of morphology development for different epoxidation degrees can be seen in Scheme 6.

Epoxidation of PS-*b*-PB star block copolymer has also been developed (Serrano et al. 2007) in order to analyze the effect of epoxidation degree on the ability of these copolymers to produce nanostructures inside the epoxy matrix. The epoxidation threshold was found to be around 40%, higher than that of linear copolymer. As epoxidation of PB block enhanced the miscibility of copolymers and the epoxy resin, nearly nanoordered structures were obtained for uncured blends, even for high epoxy resin content. So SA mechanism is followed for morphology development. For epoxidation degrees lower than 40%, copolymer macrophase separated, forming an inverted morphology, with epoxy particles dispersed in a continuous copolymer matrix. For epoxidation degrees higher than the threshold, a morphology consisting on PS cylinders arranged in the epoxy-rich phase was obtained, with the presence of PB units in both the epoxy-rich phase and near to the PS cylinders. For

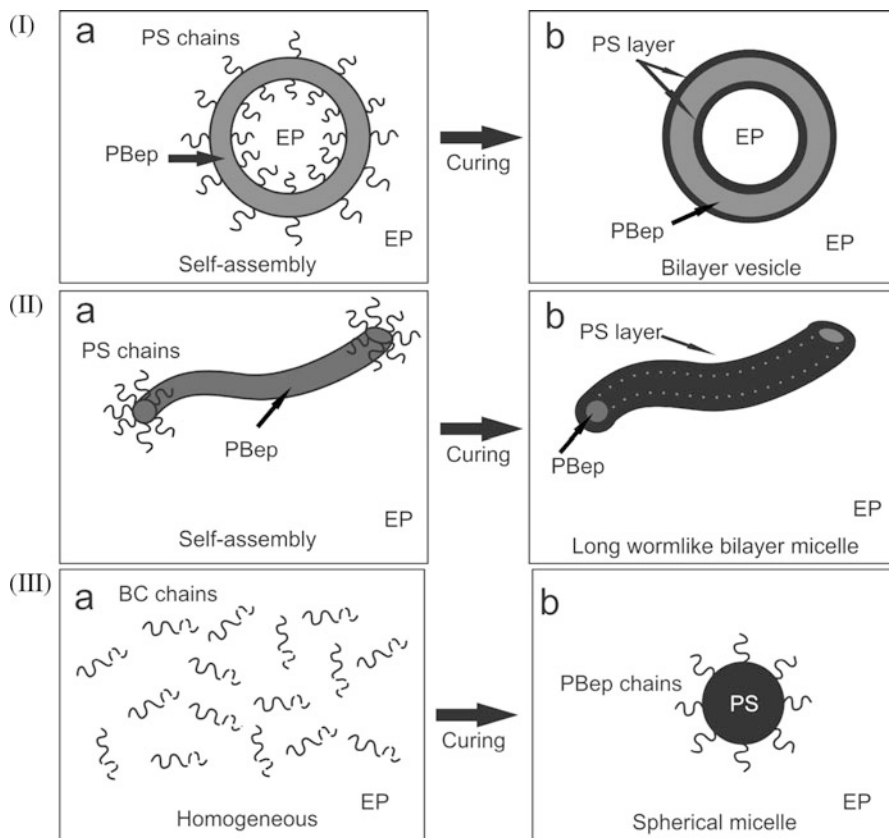
Fig. 13 TM–AFM-phase image for epoxy mixture containing 30 wt.% SB50(1) ep35. PS block appears *dark* in AFM images (Reproduced with permission of (Ocando et al.), copyright 2009 American Chemical Society)



an epoxidation degree of 61%, a morphology consisting in PS cylinders arranged in an epoxy-rich phase containing both epoxidized and non-epoxidized PB segments was obtained, which indicate at least some partial miscibility of the epoxidized PB block with the cured epoxy matrix as a consequence of the non-epoxidized segments of PB block. For the highest epoxidation degree achieved (76%), a long-order hexagonal structure was obtained. Obtained morphologies can be seen in Fig. 14.

Ternary Systems Based on Nanostructured Epoxy and Inorganic Nanoparticles

The development of new materials based on ternary systems composed by epoxy matrices nanostructured with block copolymers in which inorganic nanoparticles can be placed has received the attention of several authors during the last years. Nanoparticles can be synthesized in situ during nanocomposite preparation (Gutierrez et al. 2010a; Tercjak et al. 2012) by techniques like sol–gel or previously synthesized nanoparticles can be added during nanocomposite preparation (Ocando et al. 2010; Esposito et al. 2014). Several reasons can be found for this strategy. From one side, the poor fracture toughness of thermosetting polymers has represented an important drawback for many potential engineering applications. In order to overcome this problem, the preparation of nanostructured materials via SA or RIPS of block copolymers modified epoxy matrices has been one of the most important approaches. This



Scheme 6 Schematic representations of blocks organization for the thermosetting mixtures containing: (I) 10 wt.% SBep22, (II) 30 wt.% SBep22, and (III) 10 wt.% SBep28 block copolymers before (a) and after curing (b) (Reproduced with permission of (Ocando et al.), copyright 2009 American Chemical Society)

strategy can further optimize the fracture toughness of brittle epoxy matrices and in the same time can retain their transparency because phase separation in these systems generally occurs at nanometer scale (Thio et al. 2006; Larrañaga et al. 2007; Liu et al. 2008). Block copolymers with one block chemically modified in order to make it compatible with the epoxy matrix, such as epoxidized SBS, have been used for this purpose (Serrano et al. 2005a, 2007; Ocando et al. 2009). Nevertheless, one disadvantage of block copolymers is the risk of sacrificing the stiffness of the epoxy matrix (Ocando et al. 2008b). An approach to avoid this behavior can be the addition of inorganic nanoparticles into the epoxy matrix to enhance its mechanical behavior by lowering the plasticization effect obtained by inorganic additives and also preserving an optical transparency (Johnsen et al. 2007; Ocando et al. 2010).

On the other hand, the fabrication of inorganic/organic epoxy-based materials modified with nanoparticles is an active research field due to optic, magnetic,

conductive, photonic, and other properties of the inorganic filler (Tercjak et al. 2009; Tercjak and Mondragon 2010; Pethrick et al. 2010; Gutierrez et al. 2010a). Nanostructured epoxy-based materials can act as templates for nanoparticles and allow the control of their distribution and size playing with

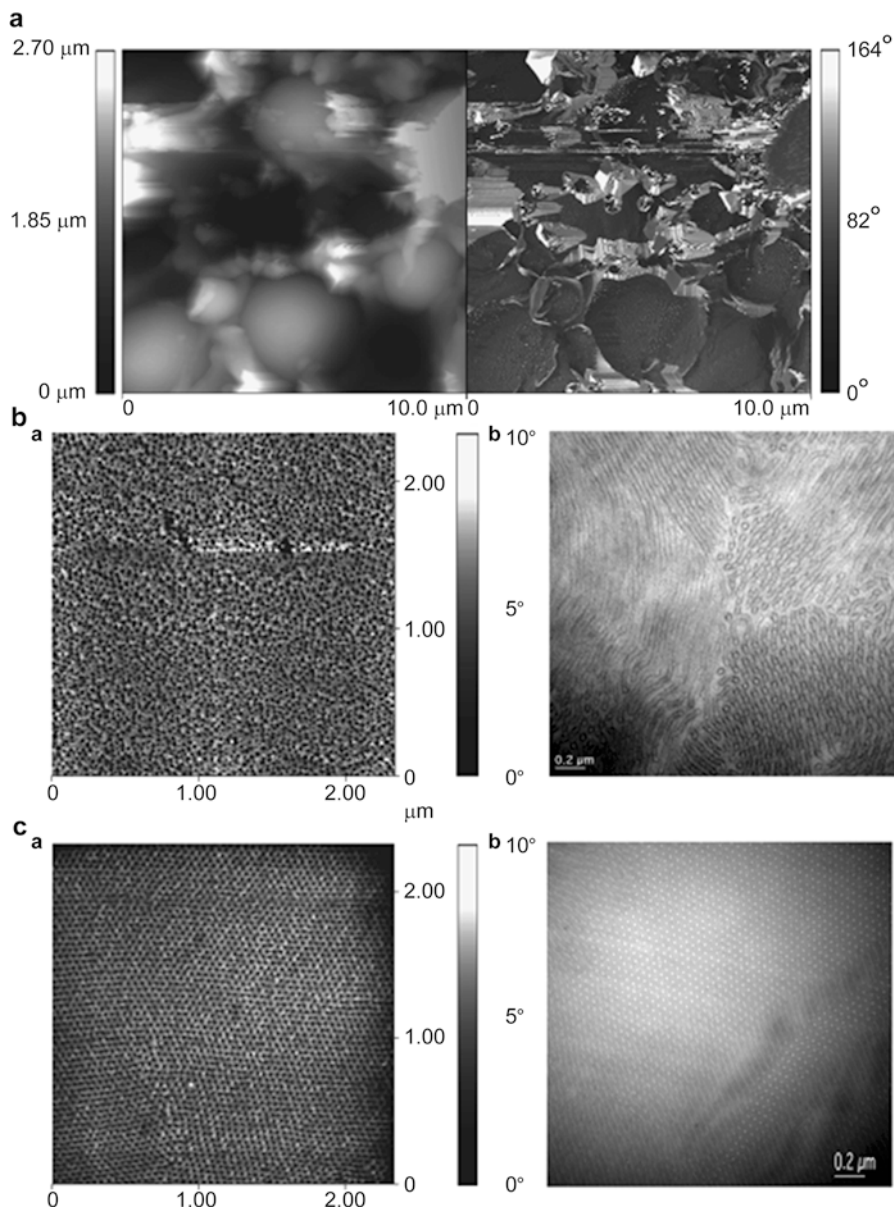


Fig. 14 (continued)

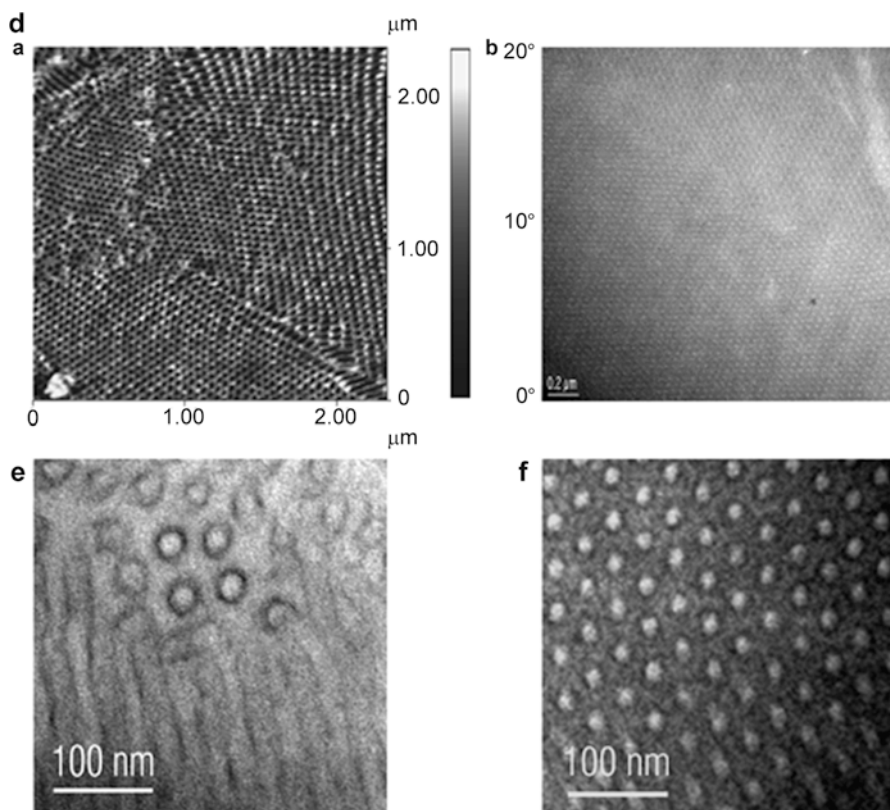


Fig. 14 TM–AFM-phase (I) and TEM (II) images for DGEBA/MCDEA blends containing 30 wt.% of: (a) SepB15, (b) SepB40, (c) SepB61, and (d) SepB76 copolymers. (e, f) Figures show higher magnification of TEM images for SepB40- and SepB61-modified systems, respectively (Reproduced with permission of (Serrano et al.), copyright 2006 American Chemical Society)

preparation conditions, concentration of nanoparticles, type of matrix used as a template, and others (Tercjak et al. 2009; Tercjak and Mondragon 2010; Pethrick et al. 2010; Gutierrez et al. 2010b).

Besides mechanical, electric, or magnetic properties incorporated by inorganic nanoparticles, the morphology or nanostructures obtained for epoxy/block copolymer blends may be altered or not by the presence of nanoparticles. Regarding the main interest of this chapter, how different nanoparticles such as TiO_2 , Al_2O_3 , or carbon nanotubes (CNT) affect morphologies obtained for epoxy/block copolymer mixtures will be analyzed below, also pointing out the positioning of inorganic nanofillers in the generated nanodomains.

Starting with ternary systems based on epoxy matrices nanostructured with block copolymers and inorganic nanofillers in situ synthesized, nanocomposites with TiO_2 nanoparticles obtained by sol–gel must be underlined. Multifunctional hybrid nanostructured thermosetting materials obtained by using poly(styrene-*b*-

ethylene oxide) (SEO) as a template for selective location of TiO₂ nanoparticles (Gutierrez et al. 2010a; Tercjak et al. 2012) have shown some morphological changes when compared with the corresponding binary systems, especially for high inorganic contents. Binary epoxy/SEO systems with 40 wt.% of copolymer resulted in a hexagonally ordered structure with PS block cylinders mainly perpendicularly oriented, since PEO block is miscible with the epoxy matrix and segregation of PS block-rich phase took place during network formation (Gutierrez et al. 2010a). For ternary systems, similar morphologies were obtained but with PS cylinders arranged parallel and perpendicular. Nanoparticles appeared in the interface between PEO-modified epoxy matrix and microphase-separated PS block domains. By increasing inorganic content, morphology changed to spherical PS domains uniformly dispersed in the continuous epoxy matrix where PEO block remained miscible. Moreover, a higher amount of uniformly distributed nanoparticles was detected in the epoxy-rich matrix, due to their interaction.

As it is interesting to check the effect of block content in the copolymer, let us have a look at ternary systems that were prepared with a SEO copolymer with low PEO content and TiO₂ nanoparticles (Tercjak et al. 2012). No many morphological changes have been detected with the addition of nanoparticles. However, nanoparticles appeared placed mainly in the PEO-/epoxy-rich phase. Starting with epoxy/SEO binary systems, it has to be pointed out that by using a SEO copolymer with low PEO content, unusual morphologies can be obtained, for systems containing less than 30 wt.% SEO. This is explained by the UCST behavior of PS in the epoxy system (at around 100 °C, while cure is carried out at 190 °C) and also by the short PEO block, which results in difficulties to stabilize PS domains by PEO block. For 40 wt.%, phase inversion takes place. Morphologies obtained for those systems can be seen in Fig. 15.

For systems with 5 wt.% of SEO (Fig. 15a), a morphology consisting of spherical PS block domains dispersed in epoxy/PEO matrix is formed. PEO remains miscible due to the intermolecular hydrogen bonding interactions between the hydroxyl groups of amine-cured epoxy and ether oxygen atom of PEO. Increasing SEO content, morphology changes to long wormlike micelles passing through-out vesicle-like morphology. For 10 wt.% SEO (Fig. 15b), vesicles of PS with different size can be seen dispersed in the continuous epoxy/PEO phase. This vesicles present layered structure, with two separated phases in each vesicle domain: outer layers of PS block phase confining between them an inner layer of PEO/epoxy phase forming the vesicle shell with the core being related to the epoxy-rich phase. Some vesicles can appear interconnected forming wormlike micelles. With 20 wt.% PEO (Fig. 15c), a morphology change is detected, with long interconnected wormlike micelles (with bilayered structure) well dispersed in the epoxy/PEO continuous phase. The system with 30 wt.% SEO shows a very similar morphology (Fig. 15d). Addition of 40 wt.% SEO provokes phase inversion, in which PEO/epoxy phase is macrophase separated into continuous PS-rich phase (Fig. 15e). The effect of sol-gel solution adding (and thus TiO₂ nanoparticles) on morphologies is analyzed next. Independently on the generated morphology, nanoparticles are confined into PEO-/epoxy-rich phase near the microphase-

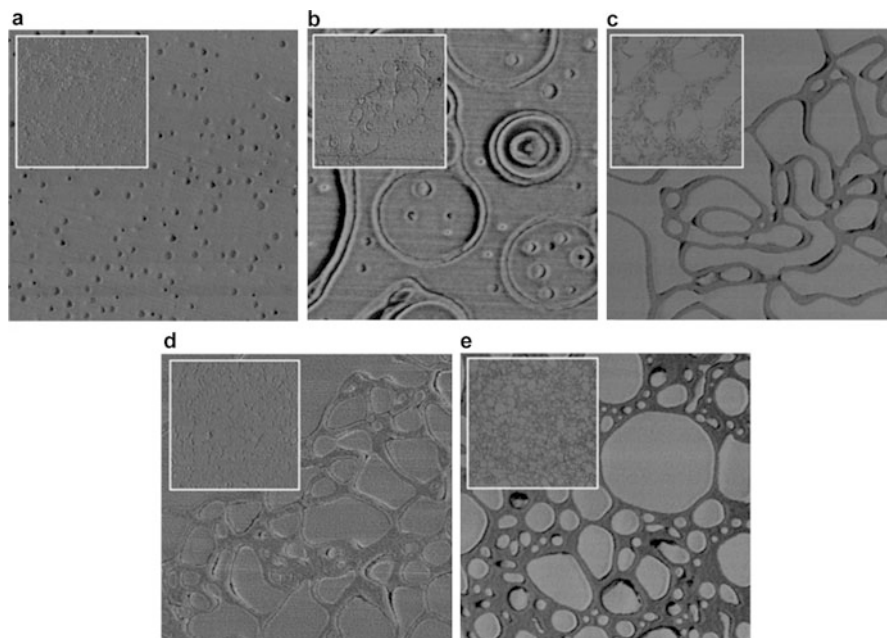


Fig. 15 TM-AFM-phase image ($5 \times 5 \mu\text{m}$) of different SEO-(DGEBA/MCDEA) systems containing: (a) 5 wt.%, (b) 10 wt.%, (c) 20 wt.%, (d) 30 wt.%, (e) 40 wt.% SEO block copolymer. *Left, top inset* in each figure corresponds to $15 \times 15 \mu\text{m}$ (Reproduced with permission of (Tercjak et al. 2012), copyright 2012 Elsevier Ltd)

separated PS block. For the nanocomposite based on the system with 5 wt.% of SEO, separated domains have been found to be much bigger than those of the binary system, due to the nanoparticles confinement in the interphase between PS block-rich phase and epoxy/PEO phase. Similar behavior can be found for the nanocomposite with 10 wt.% SEO with nanoparticles located into the epoxy-rich phase confined between the bilayered PS-rich phases formed vesicle structure. For the nanocomposite with 20 wt.% of SEO, when compared with the binary system, nanoparticles were located in some of the separated PEO/epoxy-rich domains and confined between microphase-separated long PS block wormlike micelles.

Regarding the ternary systems based on epoxy matrices nanostructured with block copolymers and previously synthesized inorganic nanofillers, it is worth to note that morphologies obtained for binary systems have not been very affected by the presence of nanofillers such as metal oxide nanoparticles (Ocando et al. 2010) or carbon nanotubes (Esposito et al. 2014). However, the dispersion of the nanofiller has been clearly improved when compared with epoxy/nanofiller binary systems, acting the copolymer as nanostructuring agent and surfactant. In this way, the nanostructuring of epoxy matrix with epoxidized SBS block copolymer has been found to improve the dispersion of Al_2O_3 nanoparticles (Ocando et al. 2010). Nanostructured thermosets have been obtained through RIPS microphase

separation of PS block from the epoxy-/PB-rich phase, showing spherical micelles of PS nanodomains dispersed in the epoxy-rich phase for 30 wt.% of copolymer. With the addition of Al_2O_3 nanoparticles, morphologies have maintained unaffected, with the same spherical micelles than in the binary system but with the presence of well-dispersed individual nanoparticles embedded in the epoxy matrix containing PS microphase-separated nanodomains. In this case, the microphase separation of PS block prevents the agglomeration of nanoparticles. In the same way, the nanostructuring of an epoxy matrix with epoxidized SBS copolymer has been found to be unaltered after the addition of carboxylic acid-modified multiwalled carbon nanotubes (a-MWCNT) (Esposito et al. 2014). With 5, 10, and 20 wt.% of epoxidized SBS, different morphologies can be obtained: spherical micelles of PS in epoxy matrix for 5 wt.% and wormlike ones for 10 and 20 wt.%, respectively. Obtained morphologies have not been affected by the addition of a-MWCNT, but their dispersion has been clearly improved when compared with binary epoxy/a-MWCNT systems: copolymer acted as dispersing agent, due to the π - π stacking interactions between MWCNT walls and aromatic rings into microphase-separated PS nanodomains, as well as the interactions between the carboxylic acid groups and epoxy matrix. Those interactions seemed to act synergistically to improve a-MWCNT dispersion.

Going further in the preparation and characterization of hybrid inorganic/organic thermosetting materials, quaternary systems based on nanostructured epoxy with nanoparticles and low molecular weight liquid crystals also have been developed (Tercjak et al. 2009), analyzing the effect of both liquid crystal and nanoparticles on generated morphologies. Firstly the effect of liquid crystal on nanostructured epoxy/block copolymer systems has been analyzed (Tercjak and Mondragon 2008). Different morphologies can be obtained depending on the amount of block copolymer and liquid crystal. Preparing ternary systems based on epoxy modified with SEO copolymer and a liquid crystal such as 4'-(hexyloxy)-4-biphenylcarbonitrile (HOBC) different morphologies has been found (Tercjak and Mondragon 2008), as it can be seen in Fig. 16.

Depending on SEO and HOBC amounts, different morphologies have been obtained: for epoxy system modified with 5, 10, and 15 wt.% SEO, PS block microseparated forming spherical or wormlike micelles as was previously pointed out. For ternary systems with 30 wt.% of liquid crystal, HOBC was within these micelles (increase of microphase-separated domains in the ternary systems when compared with binary ones). When 30 wt.% of HOBC was added, neither systems containing 5 wt.% SEO nor those containing 10 or 15 wt.% SEO presented macrophase-separated domains of the liquid crystal phase. If a SEO copolymer with lower PEO content was used, macrophase-separated domains appeared, thus indicating that the higher PEO content, partially miscible with epoxy resin, led to more stable HOBC/PS block microphase-separated thermoset systems. In the case of the addition of 50 wt.% HOBC to the system with 5 wt.% SEO (Fig. 16c), an almost continuous microstructure was obtained, the liquid crystal clearly altering the morphology of epoxy/SEO system. The effect of adding 50 wt.% of HOBC to the system with 10 or 15 wt.% SEO is the macrophase separation, which included

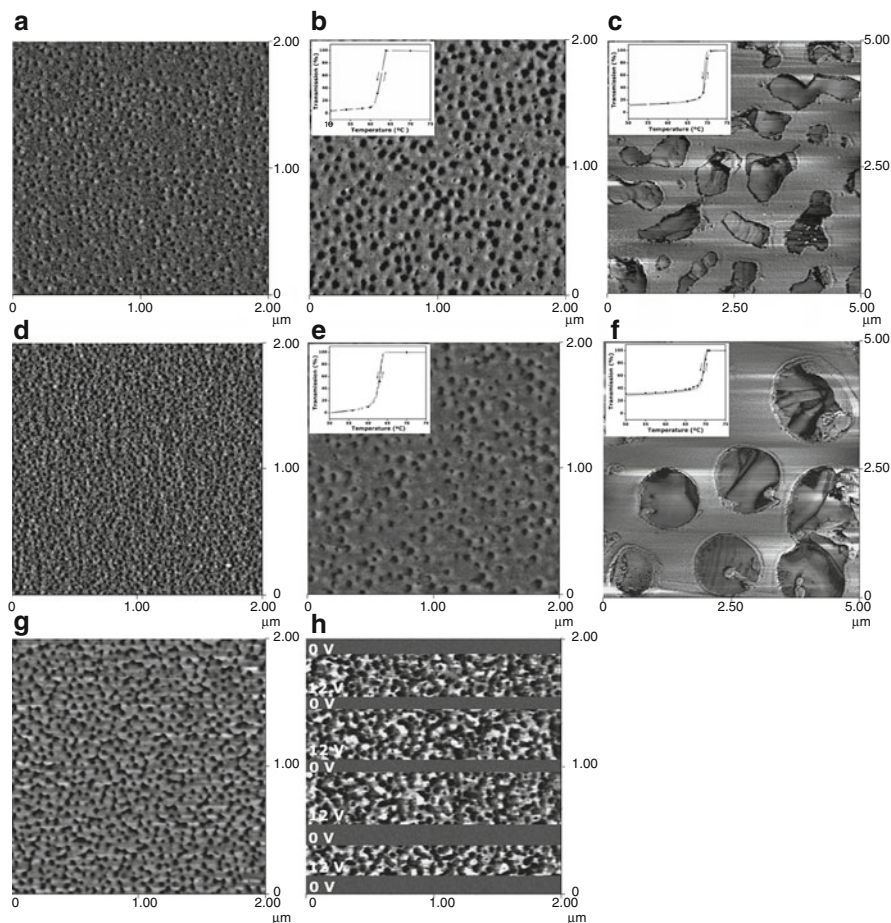


Fig. 16 TM–AFM-phase images of DGEBA/MXDA systems modified with different SEO or/and HOBC contents: (a) 5 wt.% SEO, (b) 5 wt.% SEO–30 wt.% HOBC, (c) 5 wt.% SEO–50 wt.% HOBC, (d) 10 wt.% SEO, (e) 10 wt.% SEO–30 wt.% HOBC, (f) 10 wt.% SEO–50 wt.% HOBC, and (g) 15 wt.% SEO–30 wt.% HOBC. (h) AFM-phase images of 15 wt.% SEO–30 wt.% HOBC. The insets show thermo-optical curves during the heating/cooling cycle (Reproduced with permission of (Tercjak and Mondragon 2008), copyright 2008 American Chemical Society)

PS blocks within. This behavior is very similar to that showed by the SEO copolymer with lower amount of PEO block. As morphologies generated in those ternary systems influenced the thermoresponsive behavior of the HOBC provoked by applying an external field such as temperature gradient and electrical field, it can be concluded that those properties can be tuned by controlling obtained morphologies.

After analyzing the effect of liquid crystal, quaternary systems were prepared by adding commercial TiO_2 nanoparticles (Tercjak et al. 2009), obtaining multiphase

novel materials with interesting properties. 15 wt.% SEO, 40 wt.% HOBC, and 1 wt.% nanoparticles were used for preparing nanocomposites, whose morphologies can be seen in Fig. 17. Ternary system without nanoparticles resulted in a morphology consisting on HOBC/PS nanodomains microseparated from the PEO-/epoxy-rich phase. In quaternary systems, nanoparticles were confined within HOBC/PS nanodomains, increasing their size in an amount very similar to their size (around 20 nm). HOBC acted as surfactant for nanoparticle dispersion. The presence of nanoparticles in HOBC/PS nanodomains was confirmed by electrostatic force microscopy (EFM) measurements and by removing HOBC/PS organic phase by UV irradiation.

Conclusion

Block copolymers have been widely used and are still being used, as templates for generating nanostructured epoxy matrices. The control over morphology of those multicomponent thermosets is important for the improvement of their properties.

The concept of incorporating amphiphilic di- or triblock copolymers into thermosets has widely been accepted to prepare the materials with ordered nanostructures, achieved by both self-assembly or reaction-induced phase separation mechanisms, in which one of the blocks is miscible with the epoxy system, while the other one separates before or after curing process.

A second generation of di- or triblock copolymers has been developed using the concept of chemical compatibilization. This approach incorporates reactive groups (usually epoxy groups obtained by epoxidation) into one block in order to promote covalent bonding with the forming epoxy network without loss of ordering in the resulting blends.

Many different morphologies, such as spherical or wormlike micelles, hexagonally packed cylinders, bilayer micelles, or mixtures of them, among others, have been obtained when nanostructuring epoxy matrices with block copolymers.

Obtained nanostructures or morphologies depend on many factors apart from the copolymer type, such as cure temperature and hardener employed (affecting the miscibility of blocks in epoxy systems before and/or after cure), copolymer amount in the mixture, and topography or block sequence and composition, which also will determine the affinity with epoxy precursors and cured systems, determining the nanostructure and the mechanism for their formation.

Moreover, ternary or even quaternary systems can be prepared by adding nanoparticles and/or low molecular weight molecules such as liquid crystals in order to prepare novel materials with interesting specific properties. New components can affect somehow the morphology, but in most of cases morphologies of nanostructured epoxy matrices are almost unaltered or can be controlled by component amount or preparation conditions. New components usually give new electrical, magnetic, or optical properties depending on the morphologies, so controlling the former implies to control generated nanostructures.

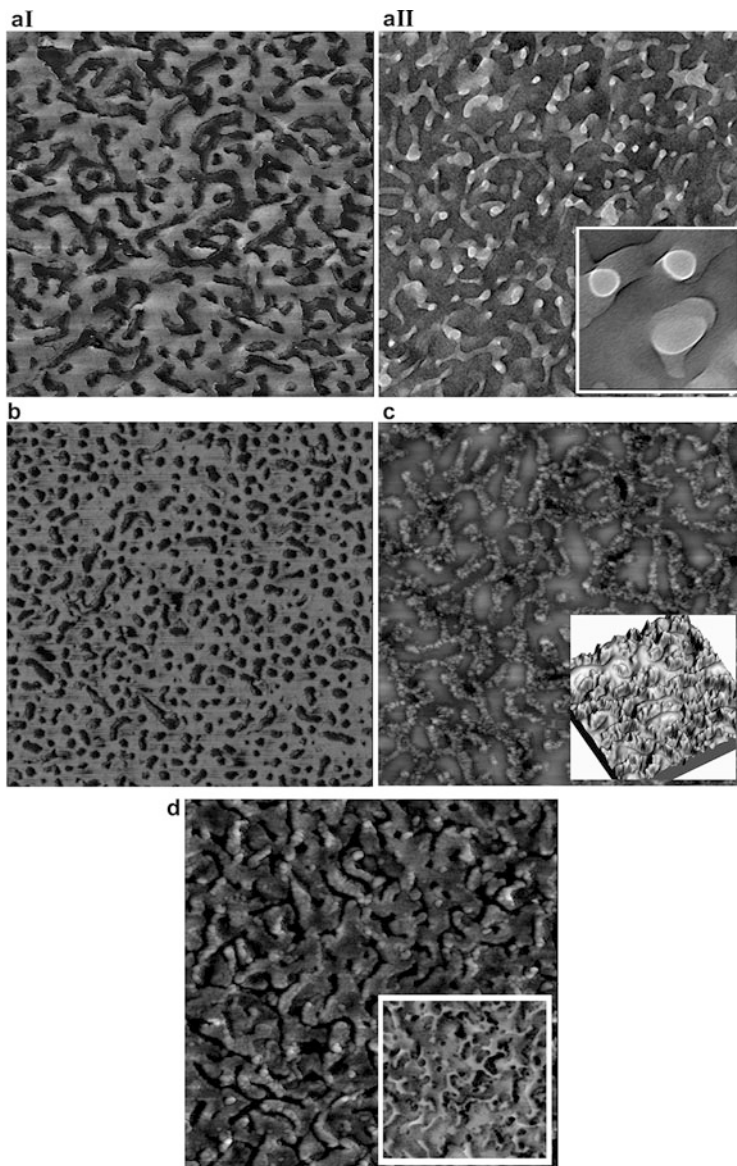


Fig. 17 (aI) TM-AFM-phase image ($2 \times 2 \mu\text{m}^2$) of 1 wt.% TiO_2 , 15 wt.% PSEO, 40 wt.% HBC-(DGEBA/MXDA) epoxy system. (aII) TEM image ($2 \times 2 \mu\text{m}^2$) of 1 wt.% TiO_2 , 15 wt.% PSEO, 40 wt.% HBC-(DGEBA/MXDA) epoxy system; *inset*: a higher magnification detail. TM-AFM-phase images ($2 \times 2 \mu\text{m}^2$) of (b) 15 wt.% PSEO, 40 wt.% HBC-(DGEBA/MXDA) epoxy system; (c) 1 wt.% TiO_2 , 15 wt.% PSEO, 40 wt.% HBC-(DGEBA/MXDA) epoxy system after 3 h of UV light exposure; *inset*, 3D image; (d) 1 wt.% TiO_2 , 15 wt.% PSEO, 40 wt.% HBC-(DGEBA/MXDA) epoxy system after 3 h of applying 12 V by using EFM tip; *inset*, negative image

The versatility of those systems for giving different nanostructures, offering the possibility to design nanostructured materials with different patterns by controlling the mixture components and cure process, has been demonstrated.

Acknowledgments Financial support from the Basque Country Government (Grupos Consolidados, IT-776-13) and the Ministry of Economy and Competitiveness – Spain (MAT MAT2015-66149-P) is gratefully acknowledged.

References

- Bashar MT, Sundaraj U, Mertiny P (2014) Morphology and mechanical properties of nanostructured acrylic triblock copolymer modified epoxy. *Polym Eng Sci* 54:1047–1055
- Blanco M, Lopez M, Kortaberria G, Mondragon I (2010) Nanostructured thermosets from self-assembled amphiphilic block copolymer/epoxy resin mixtures: effect of copolymer content on nanostructures. *Polym Int* 59:523–528
- Cano L, Builes DH, Tercjak A (2014) Morphological and mechanical study of nanostructured epoxy systems modified with amphiphilic poly(ethylene oxide-*b*-propylene oxide-*b*-ethylene oxide) triblock copolymer. *Polymer* 55:738–745
- Casaban L, Kirsten M, Pegel S, Carrasco PM, Garcia I, Stamm M, Kenny JM (2013) Shear induced orientation of phase-segregated copolymer/epoxy blends. *Eur Polym J* 49:3359–3365
- Cong H, Zheng S (2014) Formation of nanostructures in thermosets containing block copolymers: from self-assembly to reaction-induced microphase separation mechanism. *Polymer* 55:1190–1201
- Esposito LH, Ramos JA, Mondragon I, Kortaberria G (2013) Nanostructured thermosetting epoxy systems modified with poly(isoprene-*b*-methyl methacrylate) diblock copolymer and polyisoprene-grafted carbon nanotubes. *J Appl Polym Sci* 129:1060–1067
- Esposito LH, Ramos JA, Kortaberria G (2014) Dispersion of carbon nanotubes in nanostructured epoxy systems for coating application. *Prog Org Coat* 77:1452–1458
- Fan W, Zheng S (2008) Reaction induced microphase separation in thermosetting blends of epoxy resin with poly(methylmethacrylate)-block-poly(styrene) block copolymers: effect of topology of block copolymer on morphological structures. *Polymer* 49:3157–3167
- Fan W, Wang L, Zheng S (2009) Nanostructures in thermosetting blends of epoxy resin with polydimethylsiloxane-block-poly(*ε*-caprolactone)-block-polystyrene ABC triblock copolymer. *Macromolecules* 42:327–336
- Francis R, Baby DK (2014) Toughening of epoxy thermoset with polystyrene-*b*-polyglycolic acid star copolymer: nanostructure-mechanical property correlation. *Ind Eng Chem Res* 53:19945–19951
- Garate H, Mondragon I, Goyanes S, D'Accorso N (2011) Controlled epoxidation of poly(styrene-*b*-isoprene-*b*-styrene) block copolymer for the development of nanostructured epoxy thermosets. *J Polym Sci A Polym Chem* 49:4505–4513
- Garate H, Mondragon I, D'Accorso NB, Goyanes S (2013) Exploring microphase separation behavior of epoxidized poly(styrene-*b*-isoprene-*b*-styrene) block copolymer inside thin epoxy coatings. *Macromolecules* 46:2182–2187
- Garate H, Goyanes S, D'Accorso N (2014) Controlling nanodomain morphology of epoxy thermosets modified with reactive amine-containing epoxidized poly(styrene-*b*-isoprene-*b*-styrene) triblock copolymer. *Macromolecules* 47:7416–7423
- George SN, Puglia D, Kenny JM, Jyotishkumar P, Thomas S (2012) Cure kinetics and thermal stability of micro and nanostructured thermosetting blends of epoxy resin and epoxidized styrene-*block*-butadiene-*block*-styrene triblock copolymer systems. *Polym Eng Sci* 52:2336–2347

- George SN, Puglia D, Kenny JM, Causin V, Jyotishkumar P, Thomas S (2013) Morphological and mechanical characterization of nanostructured thermosets from epoxy and styrene-*block*-butadiene-*block*-styrene triblock copolymer. *Ind Eng Chem Res* 52:9121–9129
- Grubbs RB, Dean JM, Broz ME, Bates FS (2000a) Reactive block copolymers for modification of thermosetting epoxy. *Macromolecules* 33:9522–9534
- Grubbs RB, Dean JM, Broz ME, Bates FS (2000b) Selectively epoxidized polyisoprene-*b*-polybutadiene block copolymers. *Macromolecules* 33:2308–2310
- Guo Q, Thomann R, Gronski W (2002) Phase behavior, crystallization and hierarchical nanostructures in self organised thermoset blends of epoxy resin and amphiphilic poly(ethylene oxide)-*block*-poly(propylene oxide)-*block*-poly(ethylene oxide) triblock copolymers. *Macromolecules* 35:3133–3144
- Guo Q, Wang K, Chen L, Zheng S, Halley PJ (2006) Phase behavior, crystallization and nanostructures in thermoset blends of epoxy resin with amphiphilic star-shaped block copolymers. *J Polym Sci B Polym Phys* 44:975–985
- Guo Q, Liu J, Chen N, Wang K (2008) Nanostructures and nanoporosity in thermoset epoxy blends with an amphiphilic poly(isoprene)-*b*-poly(4-vinyl pyridine) reactive block copolymer. *Polymer* 49:1737–1742
- Gutierrez J, Tercjak A, Mondragon I (2010a) Transparent nanostructured thermoset composites containing well-dispersed TiO₂ nanoparticles. *J Phys Chem C* 114:22424–22430
- Gutierrez J, Tercjak A, Mondragon I (2010b) Conductive behavior of high TiO₂ nanoparticle content of inorganic/organic nanostructured composites. *J Am Chem Soc* 132:873–878
- Gutierrez J, Mondragon I, Tercjak A (2011) Morphological and optical behavior of thermoset matrix composites varying both polystyrene-*block*-poly(ethylene oxide) and TiO₂ nanoparticle content. *Polymer* 52:5699–5707
- Hameed N, Guo Q, Xu Z, Hanley TL, Mai YW (2010) Reactive block copolymer modified thermosets: highly ordered nanostructures and improved properties. *Soft Matter* 6:6119–6129
- Hillmyer MA, Lipic PM, Hadjuk DA, Almdal K, Bazer F (1997) Self assembly and polymerization of epoxy resin-amphiphilic block copolymer nanocomposites. *J Am Chem Soc* 119:2749–2750
- Hu D, Zhang C, Yu R, Wang L, Zheng S (2010) Self-organized thermosets involving epoxy/poly(ϵ -caprolactone)-*b*-poly(ethylene-co-ethylene) *b*-poly(ϵ -caprolactone) amphiphilic triblock copolymer. *Polymer* 51:6047–6057
- Johnsen BB, Kinloch AJ, Mohammed RD, Taylor AC, Sprenger S (2007) Toughening mechanisms of nanoparticle-modified epoxy polymers. *Polymer* 48:530–541
- Larrañaga M, Gabilondo N, Kortaberria G, Serrano E, Remiro P, Riccardi CC, Mondragon I (2005) Micro- or nanoseparated phases in thermoset blends of an epoxy resin and PEO-PPO-PEO triblock copolymer. *Polymer* 46:7082–7093
- Larrañaga M, Serrano E, Martin MD, Tercjak A, Kortaberria G, De la Caba K, Mondragon I (2007) Miscibility and mechanical properties of an amine-cured epoxy resin blended with block copolymer. *Polym Int* 56:1392–1403
- Lipic PM, Bates FS, Hillmyer MA (1998) Nanostructured thermosets from self-assembled block copolymer/epoxy resin mixtures. *J Am Chem Soc* 120:8963–8970
- Liu JD, Sue HJ, Thompson ZJ, Bates FS, Dettloff M, Jacob G (2008) Nanocavitation in self-assembled amphiphilic block copolymer-modified epoxy. *Macromolecules* 41:7616–7624
- Meng F, Zheng S, Li H, Liang Q, Liu T (2006a) Formation of ordered nanostructures in epoxy thermosets: a mechanism of reaction-induced microphase separation. *Macromolecules* 39:5072–5080
- Meng F, Zheng S, Liu T (2006b) Epoxy resin containing poly(ethylene oxide)-*block*-poly(ϵ -caprolactone) diblock copolymer: effect of curing agents on nanostructures. *Polymer* 47:7590–7600
- Meng F, Zheng S, Zhang W, Li H, Liang Q (2006c) Nanostructured thermosetting blends of epoxy resin and amphiphilic poly(ϵ -caprolactone)-*block*-polybutadiene-*block*-poly(ϵ -caprolactone) triblock copolymer. *Macromolecules* 39:711–719

- Meng F, Xu Z, Zheng S (2008) Microphase separation in thermosetting blends of epoxy resin and poly(ϵ -caprolactone)-block-poly(styrene) block copolymers. *Macromolecules* 41:1411–1420
- Ocando C, Serrano E, Tercjak A, Peña C, Kortaberria G, Calberg C, Grignard B, Jerome R, Carrasco PM, Mecerreyes D, Mondragon I (2007) Structure and properties of a semifluorinated diblock copolymer modified epoxy blend. *Macromolecules* 40:4068–4074
- Ocando C, Tercjak A, Martin MD, Ramos JA, Campo M, Mondragon I (2008a) Morphology development in thermosetting mixtures through the variation of chemical functionalization degree of poly(styrene-*block*-butadiene) diblock copolymer modifiers. *Thermomechanical properties*. *Macromolecules* 42:6215–6224
- Ocando C, Tercjak A, Martin MD, Ramos JA, Corona-Galvan S, Perellada MD, Mondragon I (2008b) Micro- and macrophase separation of thermosetting systems modified with epoxidized poly(styrene-*block*-butadiene-*block*-styrene) linear triblock copolymers and their influence on final mechanical properties. *Polym Int* 57:1333–1342
- Ocando C, Tercjak A, Martin MD, Ramos JA, Campo M, Mondragon I (2009) Morphology development in thermosetting mixtures through the variation on chemical functionalization degree of SB diblock copolymer modifiers. *Thermomechanical properties*. *Macromolecules* 42:6215–6224
- Ocando C, Tercjak A, Mondragon I (2010) Nanostructured systems based on SBS epoxidized triblock copolymers and well-dispersed alumina/epoxy matrix composites. *Compos Sci Technol* 70:1106–1112
- Pethrick RA, Miller C, Rhoney I (2010) Influence of nanosilica particles on the cure and physical properties of an epoxy thermoset resin. *Polym Int* 59:236–241
- Rebizant V, Abetz V, Tournillac F, Leibler L (2003) Reactive block copolymers containing glycidyl methacrylate. Synthesis and morphology control in epoxy-amine networks. *Macromolecules* 36:9889–9896
- Rebizant V, Venet AS, Tournillac F, Girard-Reydet E, Navarro C, Pascault JP, Leibler L (2004) Chemistry and mechanical properties of epoxy-based thermosets reinforced by reactive and non-reactive SBMX block copolymers. *Macromolecules* 37:8017–8027
- Ritzenthaler S, Court F, David L, Girard-Reydet E, Leibler L, Pascault JP (2002) ABC triblock copolymer/epoxy diamine blends. 1. Keys to achieve nanostructured thermosets. *Macromolecules* 35:6245–6254
- Romeo HE, Zucchi IA, Rico M, Hoppe CE, Williams RJJ (2013) From spherical micelles to hexagonally packed cylinders: the cure cycle determines nanostructures generated in block copolymer/epoxy blends. *Macromolecules* 46:4854–4861
- Serrano E, Larrañaga M, Kortaberria G, Remiro PM, Mondragon I (2005a) Towards nanostructured materials by modification of thermosetting matrices with block copolymers. In: Zaikov GE, Jimenez A (eds) *New developments in polymer analysis, stabilization and degradation*. Nova Science, Moscow, pp 45–55
- Serrano E, Martin MD, Tercjak A, Pomposo J, Mecerreyes D, Mondragon I (2005b) Nanostructured thermosetting systems from epoxidized styrene butadiene block copolymers. *Macromol Rapid Commun* 26:982–985
- Serrano E, Tercjak A, Kortaberria G, Pomposo JA, Mecerreyes D, Zafeiropoulos NE, Stamm M, Mondragon I (2006) Nanostructured thermosetting systems by modification with epoxidized styrene-butadiene star block copolymers. Effect of epoxidation degree. *Macromolecules* 39:2254–2261
- Serrano E, Tercjak A, Ocando C, Larrañaga M, Perellada MD, Corona-Galvan S, Mecerreyes D, Zafeiropoulos NE, Stamm M, Mondragon I (2007) Curing behavior and final properties of nanostructured thermosetting systems modified with epoxidized styrene butadiene linear diblock copolymers. *Macromol Chem Phys* 208:2281–2292
- Sinturel C, Vayer M, Erre R, Amenitsch H (2007) Nanostructured polymers obtained from polyethylene-*b*-poly(ethylene oxide) block copolymer in unsaturated polyester. *Macromolecules* 40:2532–2538

- Tercjak A, Mondragon I (2008) Relationships between the morphology and thermoresponsive behavior in micro/nanostructured thermosetting matrixes containing a 4'-(hexyloxy)-4-biphenylcarbonitrile liquid crystal. *Langmuir* 24:11216–11224
- Tercjak A, Mondragon I (2010) Polymer dispersed liquid crystal, thermotropic and other responsive epoxy polymers. In: Pascault JP (ed) *Epoxy polymers*, Wiley, Berlin, pp 124–136
- Tercjak A, Gutierrez J, Peponi L, Rueda L, Mondragon I (2009) Arrangement of conductive TiO₂ nanoparticles in hybrid inorganic/organic thermosetting materials using liquid crystal. *Macromolecules* 42:3386–3390
- Tercjak A, Gutierrez J, Martin MD, Mondragon I (2012) Transparent titanium dioxide/block copolymer modified epoxy-based systems in the long-scale microphase separation threshold. *Eur Polym J* 48:16–25
- Thio YS, Wu J, Bates FS (2006) Structure and properties of PBO-*b*-PEO diblock copolymer modified epoxy. *J Polym Sci B Polym Phys* 43:1950–1965
- Wang L, Zhang C, Cong H, Li L, Zheng S (2013) Formation of nanophases in epoxy thermosets containing amphiphilic block copolymers with linear and star-like topologies. *J Phys Chem B* 117:8256–8268
- Xu Z, Zheng S (2007) Morphology and thermomechanical properties of nanostructured thermosetting blends of epoxy resin and poly(ϵ -caprolactone)-block-(polydimethyl siloxane)-block-poly(ϵ -caprolactone) triblock copolymer. *Polymer* 48:6134–6144
- Yang X, Yi F, Xin Z, Zheng S (2009) Morphology and mechanical properties of nanostructured blends of epoxy resin with poly(ϵ -caprolactone)-*b*-poly(butadiene-co-acrylonitrile)-*b*-poly(*i*;-caprolactone) triblock copolymer. *Polymer* 50:4089–4100
- Yi F, Zheng S (2009) Nanostructures and surface hydrophobicity of self-assembled thermosets involving epoxy resin and poly(2,2,2-trifluoroethyl acrylate)-*b*-poly(ethylene oxide) amphiphilic diblock copolymer. *J Phys Chem B* 113:1857–1868
- Yi F, Yu R, Zheng S, Li X (2011) Nanostructured thermosets from epoxy and poly(2,2,2-trifluoroethyl acrylate)-*b*-poly(glycidyl methacrylate) diblock copolymer: demixing of reactive blocs and thermomechanical properties. *Polymer* 52:5669–5680
- Yu R, Zheng S (2011) Morphological transition from spherical to lamellar nanophases in epoxy thermosets containing poly(ethylene oxide)-*b*-poly(ϵ -caprolactone)-*b*-poly(styrene) triblock copolymer by hardeners. *Macromolecules* 44:8546–8557
- Zhang C, Zheng S (2013) Formation and confined crystallization of polyethylene nanophases in epoxy thermosets. *Macromolecules* 46:2740–2753

Fenfen Wang, Xin He, Qinqin Dang, Tao Li, and Pingchuan Sun

Abstract

Epoxy/block copolymer blends exhibit unique nanostructure, morphologies, phase behavior, and physical properties, which are determined by the cross-linking reaction of the thermosetting resin, the self-assembly of the block copolymer, and the process of phase separation. Understanding of the influence of different types of ER-miscible blocks on the microdomain structure and dynamics, as well as the underlying molecular mechanism responsible for the structure formation and evolution in these blends is still lacking at a molecular level. In this chapter, a variety of advanced multiscale solid-state NMR techniques were used to characterize the heterogeneous dynamics, miscibility, microdomain, and interphase structure, as well as the cross-linked network in nanostructured epoxy/block copolymer (ER/BCP) blends, focusing on the role of ER-miscible blocks containing poly(ϵ -caprolactone) (PCL) or poly(ethylene oxide) (PEO) blocks having different intermolecular interactions with ER. ^1H static and magic-angle spinning (MAS) experiments were used to detect the molecular mobility in these blends, and then detailed dynamic behavior and the miscibility of the BCPs with the cured-ER network were obtained by ^1H dipolar filter experiments. Two-dimensional ^{13}C - ^1H WISE experiment was used to gain information about the heterogeneous dynamics of individual components and to determine the extent of phase separation in the blends. ^1H dipolar filter spin-diffusion experiments were used to quantitatively determine the evolution of interphase thickness. High-resolution ^1H DQ filter and ^1H - ^1H spin-exchange experiments under fast MAS were utilized to detect interphase composition and detailed intermolecular proximity between ER and BCPs in the interphase region. High-resolution ^{13}C CPMAS experiments were employed to probe the driving force for the interphase

F. Wang • X. He • Q. Dang • T. Li • P. Sun (✉)

Key Laboratory of Functional Polymer Materials of the Ministry of Education, College of Chemistry, Nankai University, Tianjin, China

e-mail: spclbh@nankai.edu.cn

© Springer International Publishing AG 2017

J. Parameswaranpillai et al. (eds.), *Handbook of Epoxy Blends*,

DOI 10.1007/978-3-319-40043-3_34

919

formation and miscibility associated with the intermolecular interactions between ER and ER-miscible blocks. Finally, ^{13}C T_1 spin–lattice relaxation experiments were used to quantitatively determine the amount of local destroyed network and dynamics of cross-linked network in all blends. On the basis of these NMR results, we proposed a model to describe the unique structure and dynamics of the interphase and cross-linked network, as well as the underlying mechanism responsible for the nanostructure formation in ER/BCP blends with different ER-miscible blocks.

Keywords

Epoxy • Block copolymer • Cross-link • Blend • Miscibility • Phase behavior • Nanostructure • Interphase • Microdomain • Solid-state NMR • Dynamics • Relaxation

Contents

Introduction	920
Advanced Multiscale Solid-State NMR Technique for ER/BCP Blends	924
Heterogeneous Dynamics and Phase Behavior Determined by ^1H Static and MAS Experiment	926
Correlation of Mobility and Domain Structure by 2D ^{13}C - ^1H WISE Experiment	930
Characterization of the Interphase and Domain Size by Proton Spin Diffusion Experiment	930
Interfacial Mixing Between ER and BCP Determined by 2D ^1H - ^1H Spin-Exchange MAS Experiment	936
Interphase Composition and Heterogeneous Dynamics of Epoxy Network Determined by Double-Quantum-Filtered ^1H MAS Experiment	943
Hydrogen Bonding Interactions in PCL-Containing Blends Determined by ^{13}C CPMAS Experiment	945
Unique Structure and Dynamics of Cross-Linked Network Determined by ^{13}C T_1 Experiment	949
A Model to Describe the Unique Structure and Dynamics of Interphase and Microdomain, Cross-Linked Network as well as Their Underlying Formation Mechanism	950
Conclusion	952
References	953

Introduction

Because of the ability to integrate excellent properties of individual components and well-controlled microdomain structure on the scale of nanometers, the preparation and characterization of nanostructured multiphase polymer blends have been extensively studied and have gained wide applications in industry in the past decades (Paul et al. 2000; Ruiz-Perez et al. 2008). Recently, toughening of the thermosetting resin, such as epoxy (ER) and unsaturated polyester, by means of block copolymer (BCP) assembly has attracted significant attention (Lipic et al. 1998; Mijovic et al. 2000; Guo et al. 2002; Thio et al. 2006; Li et al. 2008). For ER/BCP blends, the amphiphilic block copolymer generally contains an ER-miscible block, such as PEO

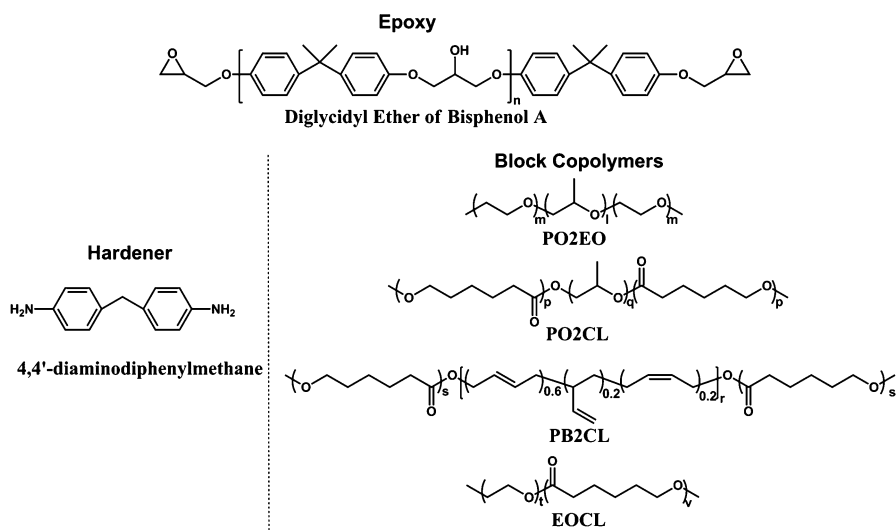
and PCL, and epoxy-immiscible block, such as PPO, polybutadiene (PB), poly(ethylene-*alt*-propylene) (PEP), and polystyrene (PS), and thus it is able to obtain a variety of nanostructured epoxy blends with controlled size, shape, and dispersion of nanoparticles in the cross-linked blends (Declet-Perez et al. 2012; Mijovic et al. 2000; Zheng et al. 2003; Meng et al. 2006). It has been reported that the nanostructured thermoset blends exhibit unique nanostructure, morphologies, phase behavior, and physical properties. In the block copolymer/thermoset blend, the final structure and morphologies of the blend are determined by several factors including the cross-linking reaction of the thermosetting resin, the self-assembly of the block copolymer, and the phase separation of the blend. Naturally such intrinsic competing interactions would have an impact on the final structures and properties of the blend.

The interphase between adjacent phases is an important factor in determining the final properties in such materials. For ER/BCP blends, due to the complex composition and small volume fraction of the interphase, it is always a great challenge to understand the detailed interphase composition of individual components and their intermolecular interactions, as well as the evolution of interphase thickness at a scale from a few angstroms to tens of nanometers (Fu et al. 2010). The miscibility of the miscible block with the cured-ER network driven by specific intermolecular interactions is considered to be a crucial factor to control the interphase structures and final properties of the blends (Hameed et al. 2010). Recently, the role of the ER/BCP interphase and its contribution to the toughening mechanism was highlighted by Bates' work, which demonstrated that the block copolymer can effectively disrupt the local properties of the interfacial epoxy network (Declet-Perez et al. 2012). Although ER/BCP blends have been extensively studied by many groups, the miscibility of BCP with cured-ER network, the component dynamics, and the formation of the interphase and domain structure in these thermoset blends have not been well understood so far. Till now, two different mechanisms about the formation of the nanostructure in ER/BCP blends with ER-miscible PEO and PCL blocks have been proposed in previous work, including preformed self-organized microphase before curing (Lipic et al. 1998) and polymerization-induced microphase separation starting from a homogenous solution of all components (Meng et al. 2006; Xu et al. 2007). It is expected that different interphase structures will be formed as a result of different initial equilibrium states before curing. Meanwhile, two different models describing structures formed in epoxy with block copolymers containing ER-miscible blocks have been proposed, and there are still two competing viewpoints concerning the interphase structure of the miscible block and the cured-ER network in the interphase. One viewpoint is that ER-miscible blocks were considered to be only partially miscible with the cured-ER phase, and partial ER-miscible blocks mixed with partially cured-ER forming the interphase region, while partial ER-miscible blocks expelled from the growing network formed the dispersed domain in conjunction with immiscible blocks (Lipic et al. 1998; Sun et al. 2005). The other viewpoint is that ER-miscible blocks were completely dissolved in the cured-ER network, and thus ER-miscible blocks were considered to be completely miscible with the cured-ER in the interphase due to the possible specific intermolecular interactions (Hameed et al. 2010; Xu et al. 2007). Despite numerous

advances, complete understanding of the influence of different types of ER-miscible blocks on the interphase structure and the underlying molecular mechanism responsible for the structure formation and evolution in these blends is still lacking at a molecular level.

A variety of experimental techniques including differential scanning calorimetry (DSC), transmission electron microscopy (TEM), and small-angle X-ray scattering (SAXS) were utilized to investigate the phase behavior and nanostructure of multiphase polymers. Solid-state nuclear magnetic resonance (SSNMR) provides another nondestructive and powerful multiscale technique to study the interfacial intermolecular interactions, microdomain structure, and componential dynamics (Asano et al. 2002; Brus et al. 2000; Schmidt-Rohr 1994; Sun et al. 2005; Yu et al. 2013); usually, high-resolution ^1H or ^{13}C NMR experiments provide useful information of the intermolecular interaction due to their sensitivity to local chemical environments. Furthermore, it can also be used to probe heterogeneous dynamics and monitor morphology changes. Based on the differences in molecular mobility of different phases, the length scales in nanoscopic heterogeneities from several nm up to 100 nm and the interface between different microdomains can be determined by measuring the time scale of proton spin diffusion from ^1H dipolar filter spin-diffusion NMR experiments (Mellinger et al. 1999). Besides, 2D ^1H - ^{13}C wide-line separation (WISE) and heteronuclear correlation (HETCOR) with spin-diffusion experiments were found to be effective methods for quantitative measurement of the length scales of mixing region in amorphous macromolecules and their blends (Brus et al. 2000; Schmidt-Rohr et al. 1994; Zhu et al. 2010). These advanced multiscale NMR techniques allow us to address many unresolved issues mentioned above in ER/BCP blends.

In this chapter, a variety of advanced multiscale SSNMR techniques were utilized to characterize five typical thermoset epoxy blends containing 40 wt% BCPs with ER-miscible blocks of PEO and PCL. The structure of the epoxy systems and block copolymers are presented in Scheme 1, and the detailed information of polymers is summarized in Table 1. We want to address the following questions to elucidate the influence of different ER-miscible blocks on the structure and dynamics of the interphase and cross-linked network: (1) the evolution of the heterogeneous dynamics; (2) microdomain structure and interphase thickness; (3) detailed composition and formation mechanism of the interphase; (4) miscibility and specific intermolecular interactions between interfacial ER and BCP; (5) experimental evidence of local destroyed cross-linked ER network. To achieve these goals, ^1H static and magic-angle spinning (MAS) NMR was first used to detect the molecular mobility in these blends, then detailed dynamic behavior and the miscibility of PEO block with the cured-ER network were obtained by ^1H dipolar filter experiments. 2D WISE NMR was used to gain information about the heterogeneous dynamics of individual components and to determine the extent of phase separation in the ER/PO2EO blends. ^1H dipolar filter with spin-diffusion experiment was further employed to quantitatively determine the domain size and the evolution of interphase thickness. High-resolution ^1H double-quantum (DQ) filter and ^1H - ^1H spin-exchange experiments under fast MAS were utilized to detect interphase composition and detailed intermolecular proximity between ER and BCPs in the interphase region. ^{13}C CPMAS



Scheme 1 Structure of epoxy, hardener and block copolymers

Table 1 Information of polymers

Polymers	M_n^a (g/mol)	Composition ^b	T_g^c (°C)	T_m^d (°C)
Poly(ethylene oxide)- <i>b</i> -Poly(propylene oxide)- <i>b</i> -Poly(ethylene oxide) (PO2EO, EO80)	8400 5800	21 wt% PPO, 79 wt% PEO	-59 -65	56 39
Poly(ethylene oxide)- <i>b</i> -Poly(propylene oxide)- <i>b</i> -Poly(ethylene oxide) (EO30)		64 wt% PPO, 36 wt% PEO		
Poly(ε-caprolactone)- <i>b</i> -Poly(propylene oxide)- <i>b</i> -Poly(ε-caprolactone) (PO2CL)	9500	21 wt% PPO, 79 wt% PCL	-67	53
Poly(ε-caprolactone)- <i>b</i> -Polybutadiene- <i>b</i> -Poly(ε-caprolactone) (PB2CL)	25000	17 wt% PB, 83 wt% PCL	-80	54
Poly(ethylene oxide)- <i>b</i> - Poly(ε-caprolactone) (EOCL)	10400	52 wt% PCL, 48 wt% PEO	-59	54
Poly(ε-caprolactone) (PCL)	2000	100 wt% PCL	-63	48

^{a,b}Were determined by ¹H solution NMR experiments and product information of the supplier

^{c,d}Were determined by DSC experiments

experiments were employed to probe the intermolecular interactions between ER and ER-miscible blocks at a molecular level. Finally, ¹³C T₁ spin-lattice relaxation experiments were used to quantitatively determine the amount of local destroyed network and dynamics of cross-linked network in all blends. Based on these NMR studies, we proposed a model to describe the unique structure and dynamics of the interphase and microdomain, cross-linked network, as well as the underlying mechanism responsible for the nanostructure formation in these blends with different ER-miscible blocks.

Advanced Multiscale Solid-State NMR Technique for ER/BCP Blends

A variety of multiscale solid-state NMR techniques were utilized to characterize the heterogeneous structure and dynamics in nanostructured ER/BCP blends. Figure 1 shows the pulse sequences for various SSNMR experiments used in the present work, and brief introductions of these experiments are given below (Schmidt-Rohr et al. 1994; Sun et al. 2005; He et al. 2014).

1. ^1H static and MAS experiments: Among solid-state NMR techniques, ^1H static wide-line NMR is a simple but efficient method to investigate the heterogeneous dynamics and estimate phase behavior of multiphase polymers, because the line widths of different components reflect the nature of dipolar interaction among protons associated with dynamics and phase separation. In order to assess the chemical nature of different components, ^1H high-resolution MAS experiment can be used.
2. ^1H dipolar filter experiments: In this experiment (Fig. 1a), several cycles (N_{cycle}) of a 12-pulse dipolar filter sequence is first used to select the ^1H magnetization from the mobile phases which have longer transverse relaxation times than those of rigid phase. A 90° pulse is then used to detect the ^1H signals. For polymer blends composed of rigid and mobile phases, with the increasing of the dipolar filter strength, the ^1H magnetization from the rigid phase will be suppressed due to its shorter transverse relaxation time than that of the mobile phase. The peak intensity as a function of the dipolar filter strength provides useful information about the dynamics heterogeneity. In addition, subtle structure information can also be obtained under MAS, because the resolution of ^1H MAS spectrum will be further improved due to the suppression of the broad peaks arising from protons in the rigid region.
3. ^1H dipolar filter spin-diffusion NMR experiment: This experiment (Fig. 1b) is used to measure the domain size and interphase thickness of multiphase polymers composed of rigid and mobile components, as well as immobilized interphase. At the start of the mixing period, the signals arising from the rigid region is suppressed by 12-pulse dipolar filter, only protons from relative mobile region have a net magnetization depending on the filter strength. A pair of 90° pulses was then placed immediately after the dipolar filter with 0° and 180° phase-cycled in order to eliminate the effect of T_1 relaxation during the mixing period. During the mixing time, this magnetization of mobile components is transferred to rigid components by spin diffusion. Since the rate of spin diffusion is related to internuclear distance and the extent of molecular mobility, this NMR method not only allows one to estimate the interphase thickness but also provides detailed information about structures and composition in interfacial regions. Detailed treatments of ^1H spin-diffusion experiments will be discussed in the following section.
4. Two-dimensional (2D) ^{13}C - ^1H WISE experiment: WISE experiment (Fig. 1c) correlates the ^{13}C CP/MAS spectrum (F2 dimension) with the proton wide-line spectrum (F1 dimension) due to ^1H - ^1H and ^{13}C - ^1H interactions. Generally, the

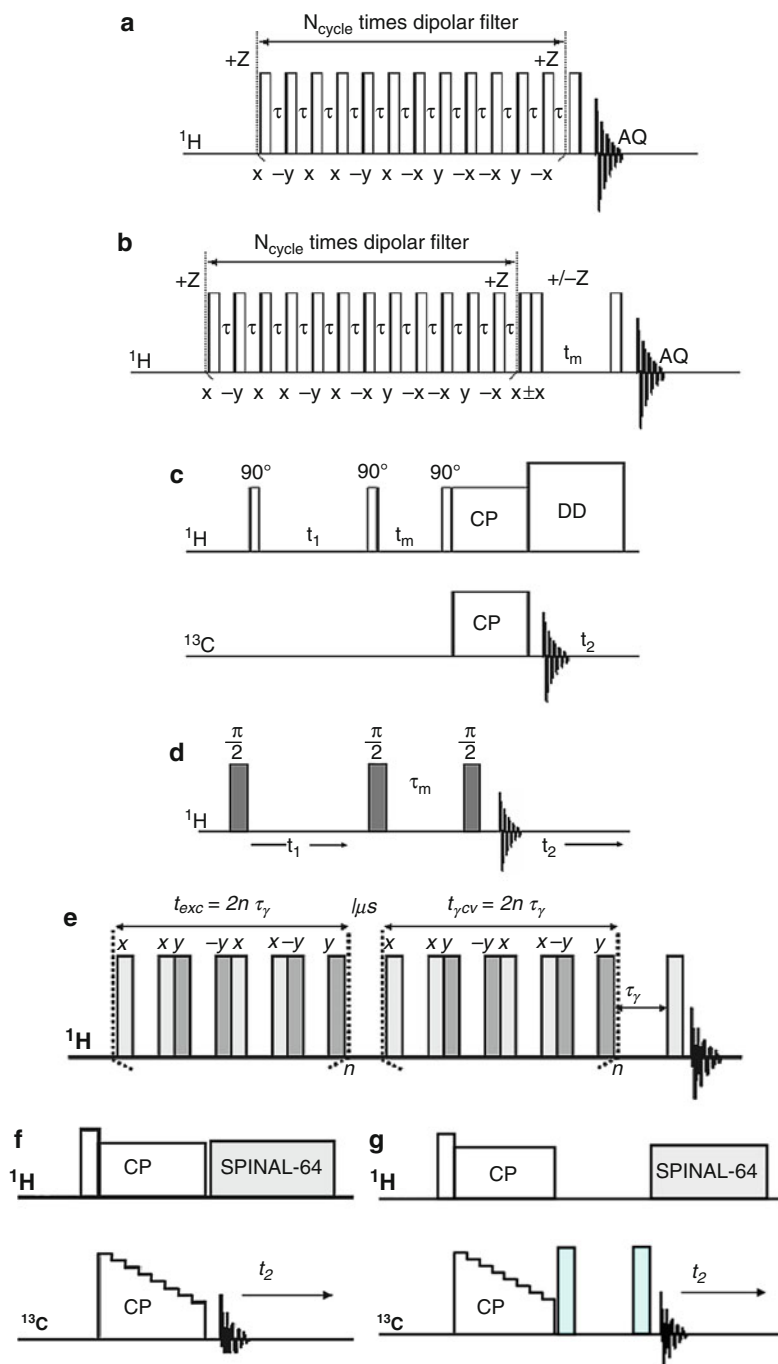


Fig. 1 Solid-state NMR pulse sequences used in the current study: (a) Pulse sequence with a 12-pulse dipolar filter for ^1H dipolar filter experiment. (b) ^1H spin-diffusion measurement with only ^1H magnetization of the mobile phases selected. (c) Pulse sequence for the 2D ^{13}C - ^1H WISE

mixing time (t_m) is set to zero without spin diffusion. This technique is useful for the characterization of polymers with complex morphology that include hard and soft domains, such as polymer blends and block copolymers. Different domains are distinguished by ^1H wide-line spectrum in the indirect dimension. At the same time, the directly observed ^{13}C chemical shifts indicate the segmental composition of the regions. This method can be used to determine the degree of phase separation qualitatively, and it allows one to characterize whether there is an extended interphase between the two phases in phase-separated blends.

5. ^1H - ^1H spin-exchange experiment under fast MAS: This high-resolution 2D experiment (Fig. 1d) is utilized to detect detailed intermolecular proximity between ER and BCPs in the interphase region. In principle, with increasing the mixing time (t_m), the proximity of different groups can be detected through observing their through space ^1H - ^1H spin-exchange. Therefore, by using this technique, the interfacial mixing and proximity of ER with different blocks in the interphase region at different length scale can be well elucidated.
6. ^1H DQ-filter experiment under fast MAS: In general, the interphase in a two-component system is the region with gradual change in structure and molecular mobility between different phases. In the case of mobility gradient arising from gradient of composition, dipolar coupling also exhibits a gradual change between the values of the pure phases. This DQ experiment (Fig. 1e) is a powerful high-resolution method to detect the componential heterogeneous dynamics, isolate the signal of interphase, and determine the interphase composition by means of varying the DQ excitation time (t_{exc}).
7. ^{13}C experiments: High-resolution ^{13}C CPMAS experiment (Fig. 1f) is used to probe the driving force for the interphase formation and miscibility associated with the intermolecular interactions between ER and ER-miscible blocks. ^{13}C T_1 spin-lattice relaxation experiment (Fig. 1g) is used to quantitatively determine the amount of local destroyed network and dynamics of cross-linked network in all blends.

Heterogeneous Dynamics and Phase Behavior Determined by ^1H Static and MAS Experiment

Heterogeneous dynamics and phase behavior of multiphase polymers can be monitored by simple ^1H static wide-line NMR experiments, because the line widths of different components reflect the nature of dipolar interaction among protons associated with dynamics and phase separation. For glass and crystalline polymers, the



Fig. 1 (continued) experiment, including an optional mixing time t_m . CP and DD stand for cross-polarization and dipolar decoupling, respectively. (d) The 2D ^1H - ^1H spin-exchange experiment under fast MAS. Variation in the mixing time t_m allows monitoring of ^1H - ^1H spin diffusion within the material. (e) ^1H DQ-filtered MAS experiment utilizing the rotor-synchronized BABA excitation/conversion sequence. The excitation period t_{exc} is an even multiple of the rotor period t_r . (f) ^{13}C CPMAS experiment. (g) ^{13}C T_1 spin-lattice relaxation times experiment

chain segments are rigid, and the dipolar couplings of protons for these polymers are generally on the order of 30–50 kHz. For polymers above T_g , such as PPO, PB, and amorphous PEO and PCL at room temperature, the dipolar couplings are partially averaged by chain motion, and a high-resolution spectrum can be obtained with moderate MAS. For ER/BCP blends containing mobile blocks, if the block copolymers were completely dissolved in the rigid cross-linked ER network, all the ^1H signals of the copolymer would be remarkably broadened. If they were phase-separated, narrow lines arising from mobile blocks in dispersed domain could be obtained under moderate MAS condition. In the following discussion, the word “immobilized” polymer means that the polymer is in the regime of intermediate mobility between “rigid” and “mobile,” and generally it relates to the interphase component.

Figure 2a shows the ^1H static wide-line NMR spectra of the four blends and MDA-cured ER, where heterogeneous dynamics and phase behavior can be clearly observed. It is noted that the line-shape obviously changes with different types of block copolymers. For MDA-cured ER, a broad Gaussian line (~ 40 kHz fwhm) indicates that the cured network is very rigid. For all blends, the spectra show overlapping peaks containing a narrowed line at the center of the spectra and a broad hump at the bottom. The broad hump can be assigned to cross-linked ER network, and the relative narrow peaks (2–7 kHz fwhm) are assigned to block copolymers. Furthermore, a third component with line width between the narrow line and broad hump can be found from the deconvolution of these spectra, indicating the existence of interphase (Inset in Fig. 2a for ER/PO2CL). In principle, the better the miscibility, the larger the ^1H line width and smaller the dispersed domain size. ^1H static NMR spectra in Fig. 2 also clearly indicate the extent of phase separation in all blends because of the remarkable molecular mobility differences between the cross-linked ER and the copolymers. For blends with amphiphilic BCP, the line-shapes of PCL-containing blends (ER/PB2CL and ER/PO2CL) are obviously sharper than that of PEO-containing blend (ER/PO2EO, i.e., EO80). In addition, the observed line width of ER/EOCL is the broadest among all blends because of the incorporation of two ER-miscible blocks. Therefore, the above results imply that the BCPs containing PEO block have better miscibility with ER than that containing PCL block, and the phase separation is weaker for ER/BCPs containing PEO block.

Figure 2b shows the expanded region of ^1H NMR spectra of all samples under 4 kHz low MAS condition. Only the mobile components of BCP related to dispersed domain can be clearly detected, and the signal of cross-linked ER only shows a flat baseline. The resolution of the signals of the mobile PB2CL and PO2CL in corresponding blends obviously increase, while those from EOCL and PO2EO in corresponding blends are still poor, indicating that PEO block should have stronger interaction and better miscibility with cured-ER than PCL block. This result will be further confirmed by the following ^{13}C CPMAS NMR experiments.

Proton dipolar filter experiment shown in Fig. 1a can provide detailed information about the structure, heterogeneous dynamics, and miscibility in polymer blends. Figure 3 shows the effect of increasing dipolar filter strength (N_{cycle}) on the spectra

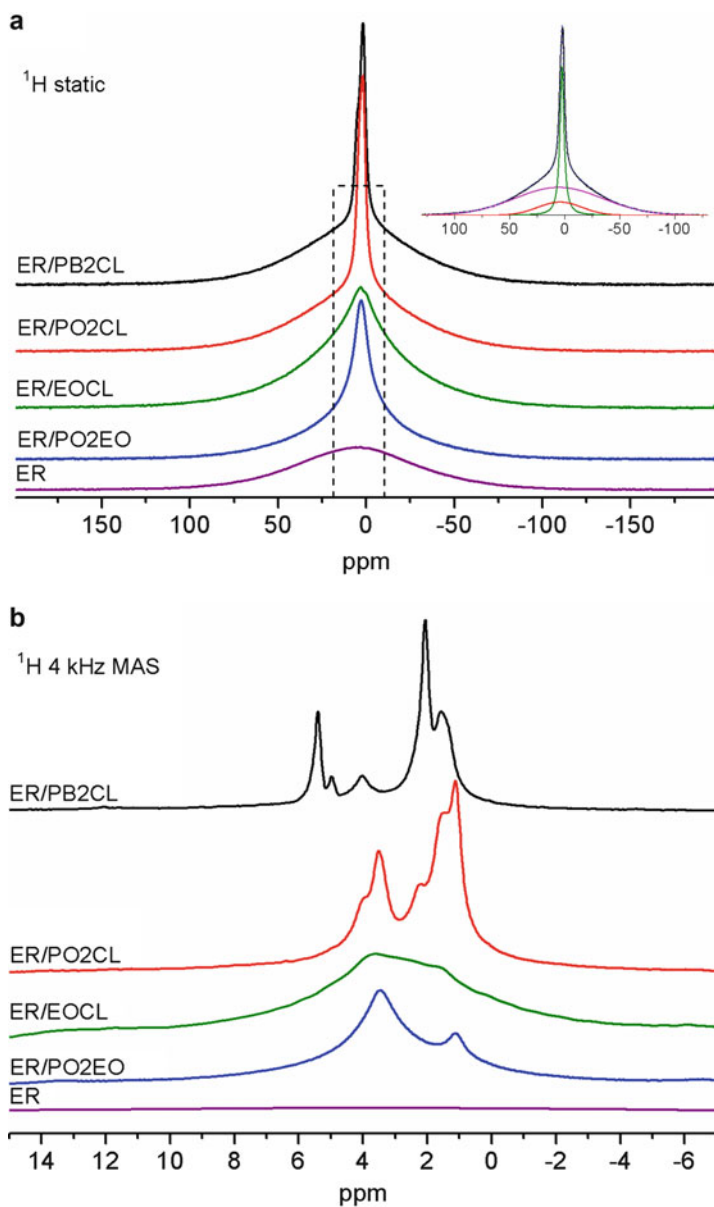


Fig. 2 ^1H NMR spectra of all MDA-cured ER/BCP blends and ER under (a) static and (b) 4 kHz MAS condition. Dashed line in (a) indicates the expanded display region in (b). The inset in (a) is the deconvolution of ^1H static spectrum of ER/PO2CL, where the red line indicates the existence of interphase (Reprinted with permission from He et al. (2014), copyright American Chemical Society 2014)

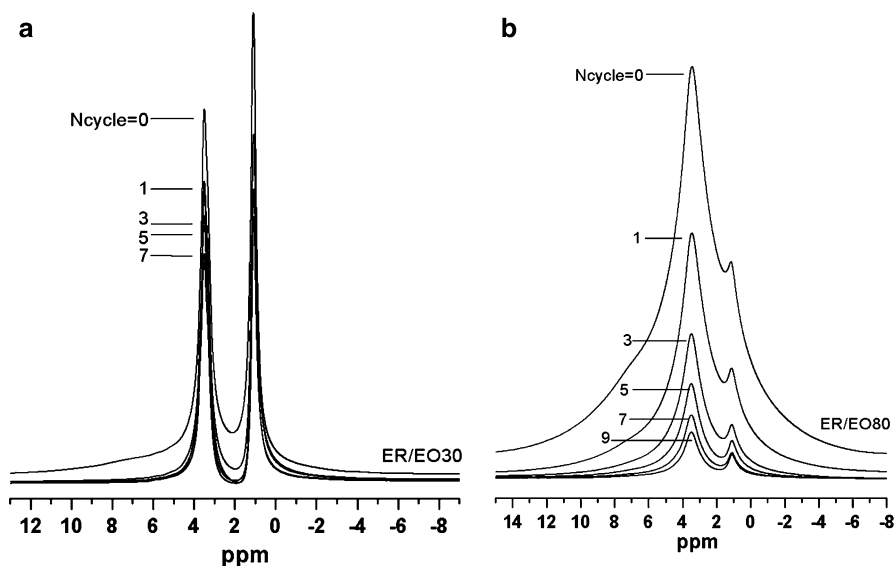


Fig. 3 Effect of dipolar filter strength on the ^1H MAS spectra for (a) ER/EO30, (b) ER/EO80 at 8 kHz MAS (Reprinted with permission from Sun et al. (2005), copyright American Chemical Society 2005)

of ER/EO30 and ER/EO80 blends. In Fig. 3a for ER/EO30, the MAS spectrum without dipolar filter ($N_{\text{cycle}} = 0$) exhibits both broad and narrow components. The broad component at the bottom of the spectrum was suppressed by using one cycle of 12-pulse dipolar filter, the line width of this broad component was far less than that of the rigid ER phase (~ 40 kHz fwhm). Therefore it is reasonably to assign this broad signal to the interphase. The remaining signals after the strong dipolar filter ($N_{\text{cycle}} > 7$) should be attributed to the mobile BCP. In Fig. 3b for the ER/EO80 blend, a significant decrease in the signal intensity for the peak at 3.5 ppm was found with increasing dipolar filter strength from $N_{\text{cycle}} = 1-9$, indicating that the broad hump (in the spectra when $N_{\text{cycle}} = 0$) could result from the immobilized PEO protons as well. The ^1H MAS NMR spectrum with a strong dipolar filter ($N_{\text{cycle}} = 9$) was deconvoluted with two overlapping Lorentzian lines. The above observations confirm that the PEO blocks are only partially miscible with the cured-ER network. The line widths of ER/EO80 were obviously broader than those of ER/EO30 under strong filter strength, indicating that the chain motion of the mobile phase (PPO and PEO) in ER/EO80 was more restricted than in ER/EO30. In Fig. 3, we can also observe a weak shoulder at about 7 ppm for the two samples without dipolar filter ($N_{\text{cycle}} = 0$). This weak signal can be completely suppressed by gradually increasing dipolar filter strength, and which might be attributed to the “mobilized” partially cured-ER.

Correlation of Mobility and Domain Structure by 2D ^{13}C - ^1H WISE Experiment

To achieve a better understanding of the detailed dynamics and the phase behavior in the ER/BCP blends, we employed 2D ^{13}C - ^1H WISE NMR experiment (Fig. 1c) that has been widely used for the determination of heterogeneous dynamics in solid polymers. Figure 4 displays the ^{13}C - ^1H WISE spectra of ER/EO30 and ER/EO80 as an example, which clearly show distinctly different mobility for the individual component and confirm the existence of phase separation in the blends. The appearance of three strong and narrow peaks of PPO at 72.0, 74.0, and 16.5 ppm on ^{13}C dimension implies that the PPO blocks are mobile and segregated from the rigid ER matrix, whereas the ER matrix which exhibits remarkably broadened NMR lines. From the slice projection of PEO peak at 70 ppm, it was found that the PEO blocks exhibited both narrow and broader lines corresponding to mobile and immobilized components, respectively. This result confirms again that the PEO blocks are only partially miscible with the cured-ER network and the narrow component could be assigned to the mobile PEO blocks segregated from the cured-ER matrix. Since PEO was completely amorphous in this blend from the DSC results, it is reasonable to assume that the broad component should be attributed to the immobilized PEO in the interphase region. The WISE NMR results are in good agreement with those obtained by ^1H NMR experiments.

Characterization of the Interphase and Domain Size by Proton Spin Diffusion Experiment

Interphase of polymer blends has been an attractive subject in the past decades. Understanding the nanoscale interphase property is crucial, because it plays an important role in controlling the final structure and property of the blends. Due to the extremely small volume fraction of interphases in a typical polymer blend, experimental determination of interphase property has been a challenging subject. It is important to have a method which enables a quantitative determination of the fine structures of the interface on the scale of 0.1–20 nm. TEM and X-ray scattering techniques have been successfully applied to detect the existence of an interfacial region. Due to the obvious molecular mobility differences between the cross-linked ER network and BCP in these blends, the phase behavior and microdomain structure of these blends can be well determined by ^1H dipolar filter spin-diffusion NMR experiment under static condition. Figure 5a shows schematic spin-diffusion curves after the application of different dipolar filter strength for a blend containing a rigid (black) and a mobile (white) component. The interphase (gray) with mobility gradient is also illustrated. The signal intensity I of retained ^1H signals is plotted as a function of mixing time $t_m^{1/2}$. The characteristic mixing time of spin diffusion, $t_m^{s,0}$, detected at certain filter strength reflects the initial slope of the curve (dot line) and depends directly on the domain size. The end (plateau) value of the curve contains important information about the interphase. For certain filter

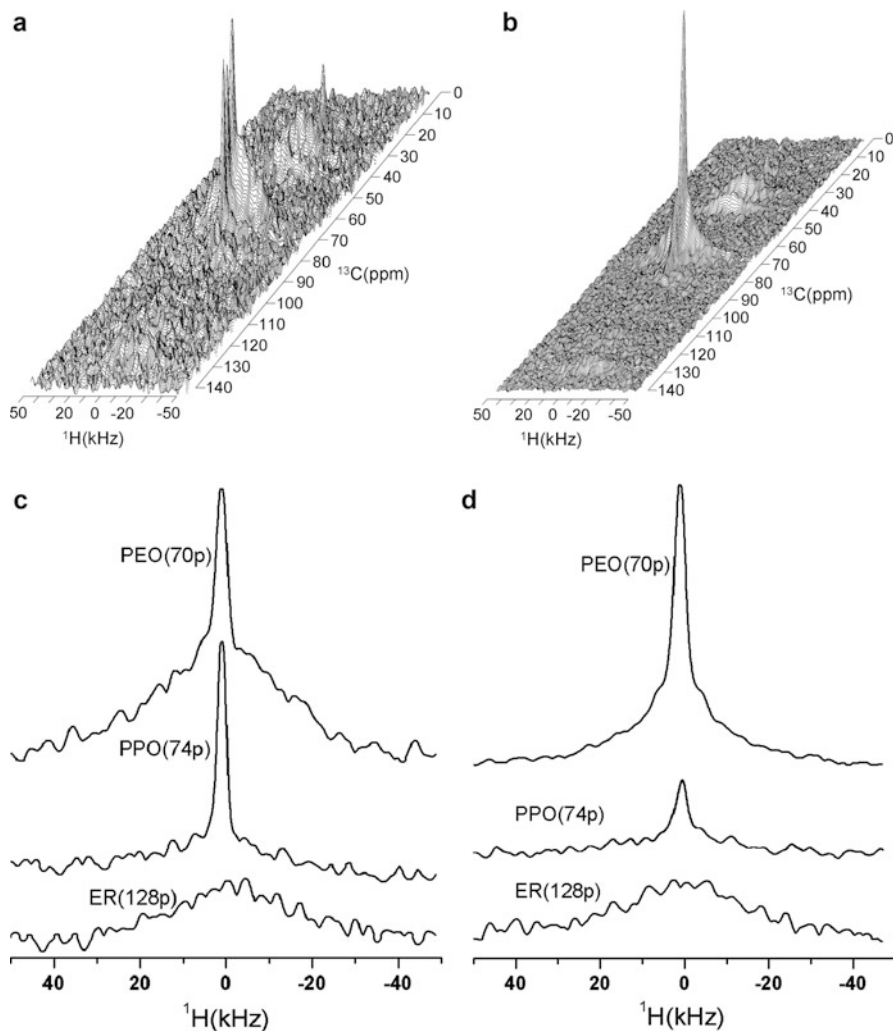


Fig. 4 2D ^{13}C - ^1H WISE spectra for (a) ER/EO30, (b) ER/EO80, and corresponding ^1H projection of (c) ER/EO30 and (d) ER/EO80 (Reprinted with permission from Sun et al. (2005), copyright American Chemical Society 2005)

strength, the end value corresponds to the selected fraction of protons in the blend and it decreases with increasing filter strength. For the ER/BCP, the contributions from the protons in the rigid cured-ER region are too broad to be observed. In case of weak dipolar filters, the mobile phase and the interphase with the partially cured (mobilized) ER could be selected, and the end value might be higher than expected from the stoichiometric proton ratio (curve A). With a strong filter, only the mobile phase near the interfacial region is selected. The end value is lower than expected from the stoichiometric proton ratio (curve B). The selected mobile component can

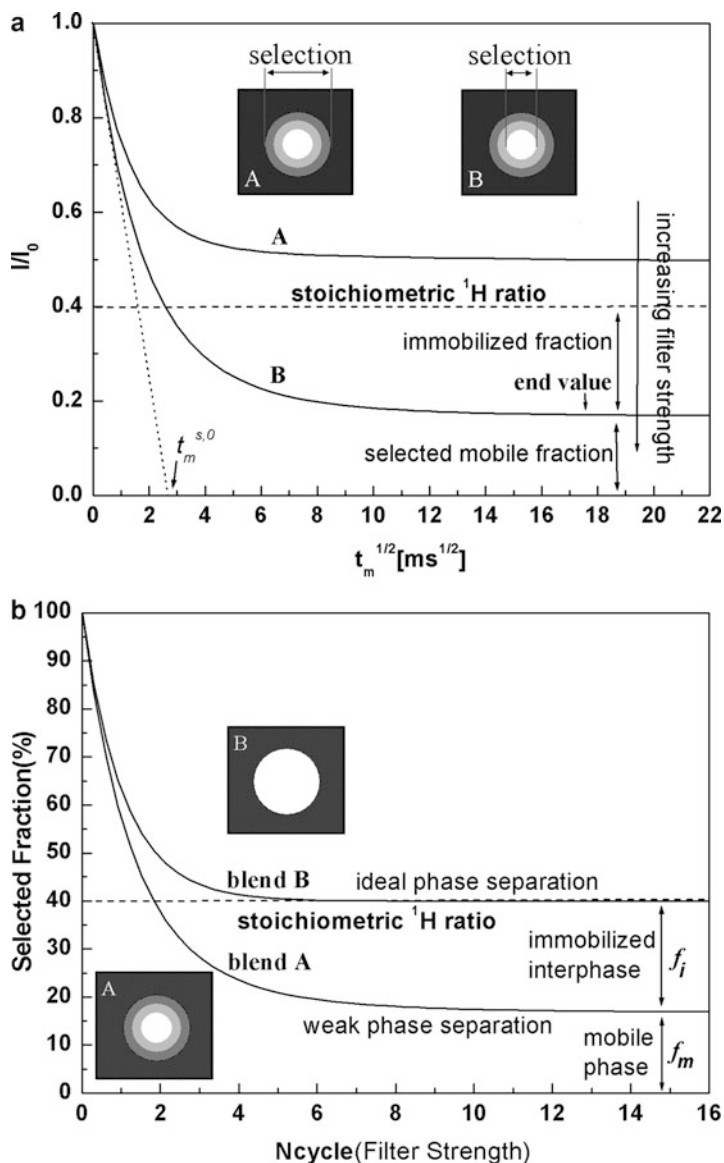


Fig. 5 (a) Schematic spin-diffusion curves showing the significance of the end (plateau) value and the effect of different dipolar filter strength. The end value of the spin-diffusion curve represents the selected fraction of protons in the blend. The suppressed rigid fraction can be calculated from $(1 - \text{selected mobile fraction})$. The immobilized fraction represents the difference between the stoichiometric ratio and the selected mobile fraction. With increasing filter strength the end value decreases. A weak filter selects both the mobile phase and the immobilized interphase; a strong filter selects only the mobile phase. The description of curve A and B is given in the text. (b) Schematic curve of the selected fraction (end value) in spin-diffusion experiment with increasing filter strength (N_{cycle}). The interphase, as well as the extent of phase separation in blends containing rigid and mobile components can be determined from the curves (Reprinted with permission from Sun et al. (2005), copyright American Chemical Society 2005)

be directly determined from the end value of the spin-diffusion curve. The difference of the measured end value to the expected stoichiometric one is the amount of immobilized fraction in the interphase region. In the case of ideal phase separation, only the separated mobile phase is selected, the end value should directly reflect the proton ratio of the components denoted as the stoichiometric end value as shown in Fig. 5a.

A detailed analysis for the evolution of the selected fraction (end value) with increasing dipolar filter is very important to quantitatively determine the interphase thickness and distinguish blends with different phase separation. Based on the work of Spiess et al., we propose a new and useful representation for spin-diffusion experimental results used to determine the interphase thickness (Sun et al. 2005). Figure 5b shows the schematic curve of the selected fraction (end value) in a spin-diffusion experiment with increasing filter strength (N_{cycle}). Although this curve is similar with the spin-diffusion curve shown in Fig. 5a, it has different meaning. The significance of the equilibrium selected fraction at stronger filter strength (denoted as “final value”), e.g., $N_{\text{cycle}} > 10$, represents the fraction of the mobile phase. This final value is very important to quantitatively determine the immobilized component and its fraction in interphase region. In Fig. 5b, two blends with different interphase can be well distinguished and the fraction of the interphase in the blend can be quantitatively determined. For blend A with weak phase separation, the final value must be lower than that expected from the stoichiometric ratio, indicating the presence of an immobilized interphase, the fraction of the interphase protons can be determined from the difference of the stoichiometric ratio with the final value. For blend B with ideal phase separation, the final value should be the same as the stoichiometric ratio that indicates the absence of the interphase. From the above discussions, we can conclude that the spin-diffusion experiment is a powerful and convenient method to elucidate the structure and dynamics of the interphase in blends.

Because the proton fraction of the interphase and the mobile phase, f_i and f_m , can be quantitatively determined from the curves shown in Fig. 7b, the thickness of the interphase for blend A, d_{itp} , can be directly estimated. In our recent work (Li et al. 2008), a strict mathematical relationship between the interphase thickness, d_{itp} , and the domain size of dispersed phase, d_{dis} , in multiphase polymers was established as

$$d_{\text{itp}} = \left(\sqrt[\varepsilon]{2 - \lambda_{DFS}} - \sqrt[\varepsilon]{\lambda_{DFS}} \right) d_{\text{dis}}/2 \quad (1)$$

where the parameter $\lambda_{DFS} = f_m/(f_i + f_m)$ represents the residual proton fraction of mobile phase (f_m) in stoichiometric mobile phase ($f_i + f_m$, i.e., the percent of BCP proton content), which can be directly measured by ^1H dipolar filter spin-diffusion NMR experiments as shown in Fig. 6a for ER/PO2CL. It should be emphasized that f_i provides important and quantitative information of the fraction of BCP in the interphase region. $\varepsilon = 1, 2$, and 3 for lamellar, cylindrical, and spheres (or cubes), respectively.

The domain size of the dispersed phase A in the two-phase A/B mixture (d_{dis}) can be determined by the following equation

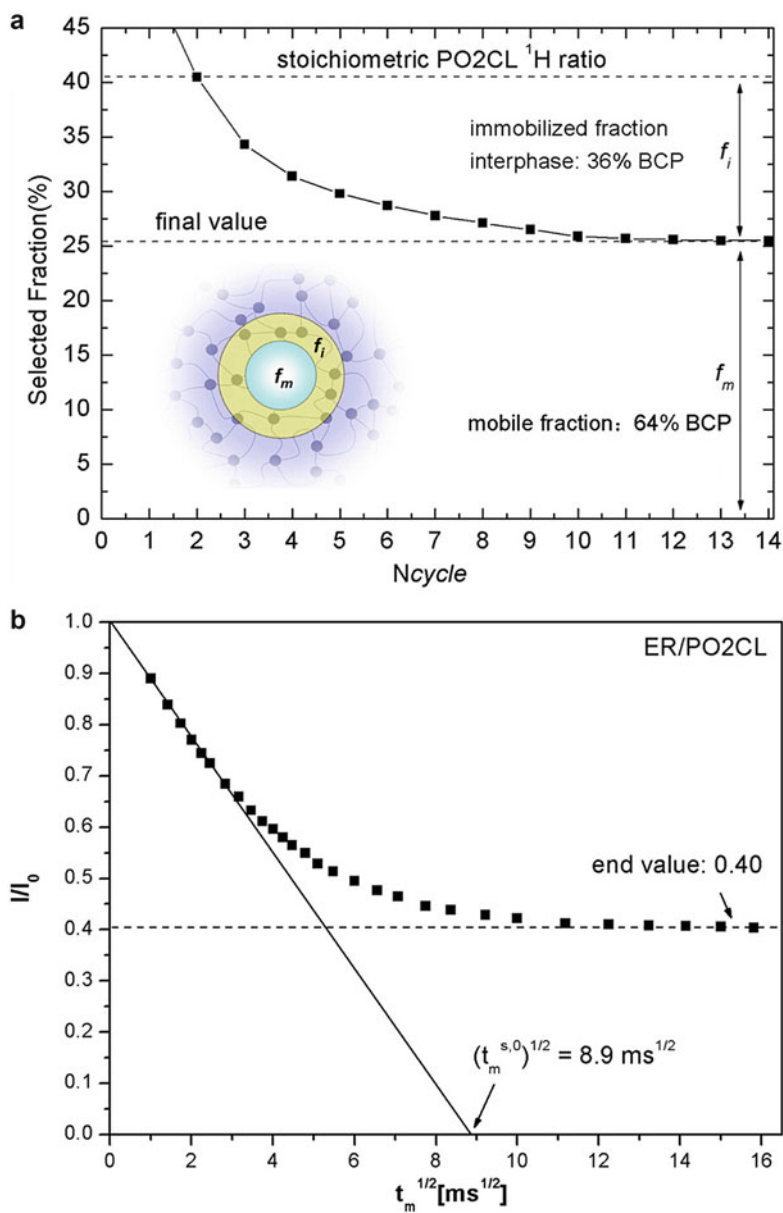


Fig. 6 ^1H dipolar filter spin-diffusion NMR experiments of ER/PO2CL, (a) selected ^1H fraction as the function of filter strengths (N_{cycle}) and (b) spin-diffusion curves, plotted as the normalized intensity I/I_0 against the square root of the mixing time (t_m) (Reprinted with permission from He et al. (2014), copyright American Chemical Society 2014)

Table 2 Domain size (d_{dis}) and interphase thickness (d_{ip}) for ER/BCP blends determined by proton spin-diffusion experiments

Samples	ER/PO2EO	ER/EO30	ER/EOCL	ER/PO2CL	ER/PB2CL
Proton fraction of copolymer (stoichiometric proton ratio) (%) ($f_i + f_m$)	39.9	41.4	40.0	40.5	39.7
Immobilized protons in interphase (%) f_i	15.8	10.6	10.8	14.9	15.7
Mobile protons in dispersed domain (%) f_m	24.1	30.8	29.2	25.6	24.0
λ_{DFS}	0.60	0.74	0.73	0.63	0.60
$(t_m^{s,0})^{1/2}$ (ms ^{1/2})	4.2	10.4	3.7	8.9	13.5
d_{dis} (nm)	3.9	8.9	3.4	8.3	12.2
d_{ip} (nm)	0.8	1.2	0.5	1.7	2.5

$$d_{dis} = \phi_A / \phi_B \times \varepsilon \times \sqrt{4D_{eff} t_m^{s,0} / \pi} \quad (2)$$

where ϕ_m ($m = A, B$) is the volume fraction of the mobile phase A or rigid phase B. $t_m^{s,0}$ is the characteristic mixing time of spin diffusion introduced by Spiess et al., and it can be determined by the intercept of the extrapolated linear initial decay with the X-axis in the spin-diffusion curves, as shown in Fig. 6b for ER/PO2CL as an example, and the initial linear portion of the curves are extrapolated to give a $(t_m^{s,0})^{1/2}$ value of 8.9 ms^{1/2}. By adjusting the dipolar filter strength, the selected proton fraction by dipolar filter for measuring $t_m^{s,0}$ equals to the stoichiometric proton ratio of BCP. The effective spin-diffusion coefficient D_{eff} is defined according to the following equation

$$\sqrt{D_{eff}} = \frac{2\sqrt{D_A D_B}}{(\rho_A^H / \rho_B^H) \sqrt{D_A} + \sqrt{D_B}} \quad (3)$$

where ρ_A^H and ρ_B^H are proton densities.

Table 2 lists the calculated fraction of BCP in the interphase, domain size of dispersed phase, interphase thickness of all blends from ¹H dipolar filter spin-diffusion experiments. In this study for blends with 40% BCP, cylindrical domains are assumed on the basis of previous work and TEM micrograph (not shown). These spin-diffusion experiments provide convincing evidences for the existence of microphase separation on the nanoscale of 3 ~ 15 nm in these ER/BCP blends. Compared to blends with PCL block except ER/EOCL with two ER-miscible blocks, a certain amount of BCP exist in the interphase, and smaller dispersed domain size was detected in blends containing PEO block. This could be attributed to the better miscibility of PEO with ER than that of PCL block with ER. Furthermore, the above results also indicate that more PEO blocks were repelled

from the ER phase in ER/EO80 as compared with ER/EO30, although the weight fraction of PEO increased from 36% in EO30 to 79% in EO80 and PEO has a good miscibility with ER before curing. It is interesting to notice that the domain size in ER/EO80 is much smaller than that in ER/EO30, which could be attributed to the good miscibility of the PEO block with ER matrix and higher PEO content in EO80. SAXS is generally used for systems with a good electron density contrast between components. In previous reported work on ER/EO80 (Guo et al. 2002), SAXS was unable to determine the length scale in this blend due to the low contrast of the sample, whereas spin-diffusion NMR experiment can still quantitatively determine the domain size on a scale of several nanometers. It is also interesting to notice that, despite the domain size of ER/EO30 is remarkably larger than that of ER/EO80, the interphase thickness of the two blends is only slightly different. The NMR results clearly indicate that, although the PEO volume fraction of the block copolymer can significantly affect the domain size of the blend, it has only small effect on the interphase thickness in the blend. It is well known that the interphase thickness strongly depends on the binary polymer-polymer interaction. Therefore, it could be expected that the interphase thickness of blends will decrease when the ER-miscible block is changed from PEO to PCL due to the poorer miscibility between PCL and ER. Our previous comparative work on blends of ER and UPR with the same BCP also confirmed such a conclusion (Li et al. 2008). However, in Table 2, we surprisingly found that the interphase thicknesses of blends containing BCP with PCL blocks (ER/PO2CL and ER/PB2CL) are unexpected obviously larger than that containing PEO blocks (ER/PO2EO and ER/EOCL), especially for ER/PO2EO and ER/PO2CL blends containing similar fraction of miscible and immiscible blocks. To understand the above unusual evolution of the interphase thickness in ER/BCP blends with different miscible blocks, detailed information of interphase composition and interfacial intermolecular interactions at a molecular level need to be further elucidated. In the following section, the distribution of different blocks in the interphase and dispersed domain will be further examined by NMR experiments. Although TEM image of ER/PB2CL shows some spherical domains, the calculated interphase thicknesses of all blends do not depend on their morphologies of either cylinder or sphere, thus the morphology has no effect on the above result about the unusual evolution of the interphase thickness.

Interfacial Mixing Between ER and BCP Determined by 2D ^1H - ^1H Spin-Exchange MAS Experiment

Although ER/BCP blends have been extensively investigated in the past decade, due to the complex composition and heterogeneous dynamics of the interphase, the detection of the interfacial mixing of individual components is still a great challenge. Recently, 2D high-resolution ^1H - ^1H spin-exchange experiments have been successfully used to elucidate the proximity among protons from different groups in organic solids and water-polymer interaction in polymers. To understand the obtained unusual evolution of interphase thickness in ER/BCP blends with

different miscible blocks, 2D high-resolution ^1H - ^1H spin-exchange experiment under fast MAS was further employed. Because a certain mixing time corresponds to a certain distance related to spin-exchange, we can roughly estimate specific ^1H - ^1H distance in typical blends for a given mixing time according to Eq. 2. As the effective spin-diffusion coefficient D_{eff} under fast MAS frequency of 26 kHz is only 20% of that at static condition, the estimated characteristic length scale with 3 ms mixing time is about 1 nm, corresponding well to the length scale of interphase for all samples as shown in Table 2, which will be used in the following discussion.

Figure 7 shows the high-resolution ^1H NMR spectra of all samples under 26 kHz fast MAS condition. The signals of aromatic groups of the cross-linked ER network and those of all BCP components can be well distinguished. Because the signals of aliphatic groups of ER (ranging from 0 to 5 ppm) only show a broadened line-shape as shown in Fig. 7, and thus they do not influence the detection of overlapped narrowed BCP signals. Therefore, 2D high-resolution ^1H - ^1H spin-exchange experiment with different mixing time (t_m) is available to probe the interfacial mixing and proximity of ER with BCPs in the interphase region by observing the ^1H - ^1H spin-exchange between the aromatic protons and BCP protons.

Figure 8 shows the typical 2D ^1H - ^1H spin-exchange spectra of ER/PO2EO and ER/PO2CL observed at mixing time of 2 ms using normalized heights of aromatic

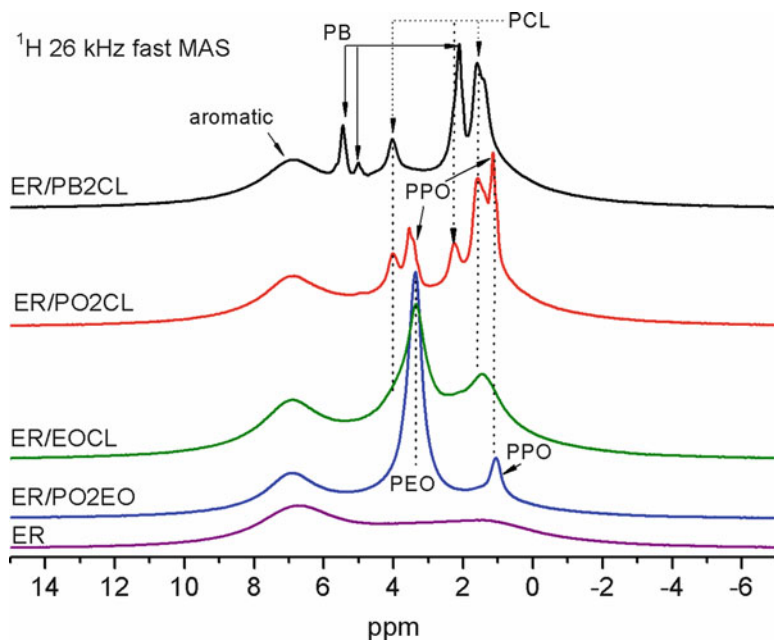


Fig. 7 ^1H MAS NMR spectra under 26 kHz fast MAS condition of all MDA-cured ER/BCP blends and ER (Reprinted with permission from He et al. (2014), copyright American Chemical Society 2014)

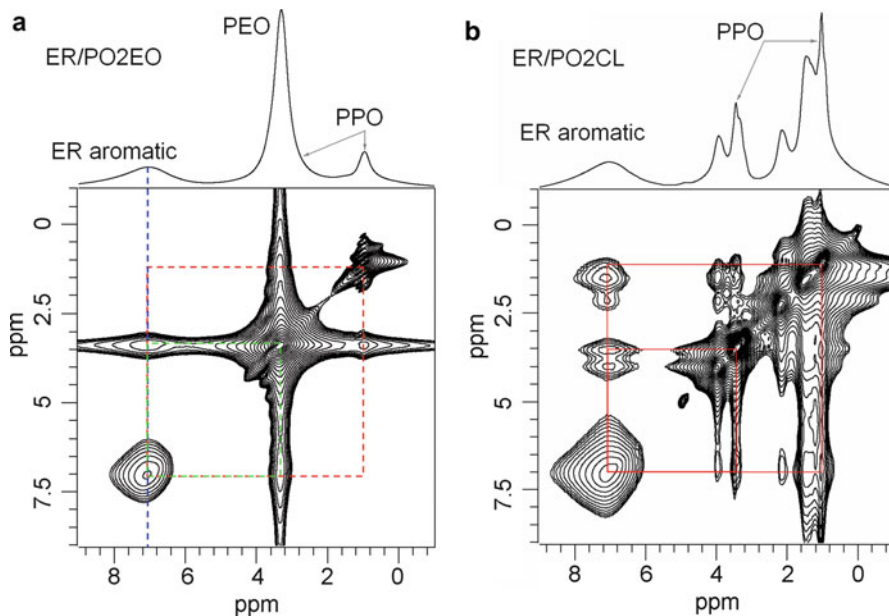


Fig. 8 2D ^1H - ^1H spin-exchange MAS NMR spectra of (a) ER/PO2EO and (b) ER/PO2CL acquired at mixing time (t_m) of 2 ms. ^1H projection is shown on top of the figure. The exchanges of magnetization due to spatial connectivity between aromatic BCP protons within these two blends are indicated by *solid square*. For ER/PO2EO, the cross-peak between ER aromatic and PEO at 3.4 ppm (overlapped with PPO CH_2 groups) can be clearly observed, while that with PPO CH_3 protons at 1.2 ppm cannot be observed (*dashed square*). For ER/PO2CL, the cross-peak between ER aromatic and PPO protons can be clearly observed (Reprinted with permission from He et al. (2014), copyright American Chemical Society 2014)

signals. The cross-peak associated with ER aromatic groups and different groups of BCP can be clearly observed, indicating the proximity of different groups. Detailed information of the interfacial mixing between ER and BCP in all blends can be extracted from the F1 slice of 2D spin-exchange spectrum at the signal of ER aromatic groups (7.0 ppm) as shown in Fig. 9. For comparison, the F1 slices of all blends and cured-ER at mixing times of 0.2 and 3 ms are displayed in Fig. 10. With increasing the mixing time of spin diffusion, the signal intensity of the ER aromatic groups in all samples decreases and that of the BCP groups increases. In previous work, it was reported that generally only one type of interfacial mixing exists for ER/BCP blends, where the ER-immiscible blocks are completely expelled from ER network upon curing and form the dispersed phase with partial ER-miscible blocks. However, we surprisingly found that two different types of interfacial mixing in the interphase region can be identified from Fig. 9. For PEO-containing blends at a short mixing time of 0.2 ms, it is noteworthy that only the spin-exchange between ER aromatic groups and PEO (3.4 ppm) can be observed for ER/PO2EO, and no spin-

exchange between ER aromatic groups and CH_3 groups of PPO is detected, implying that PPO is either too mobile to have spin-exchange with ER or nearly completely expelled from the cross-linked network and in dispersed domain. Because the T_g of

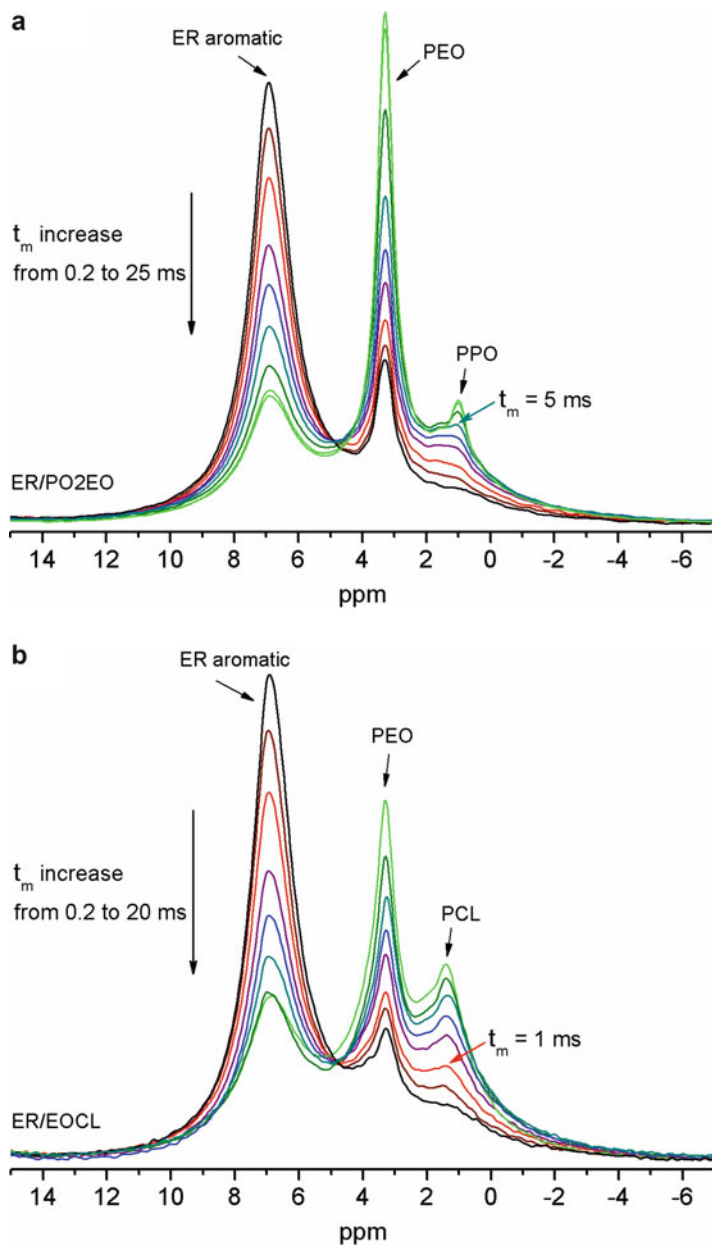
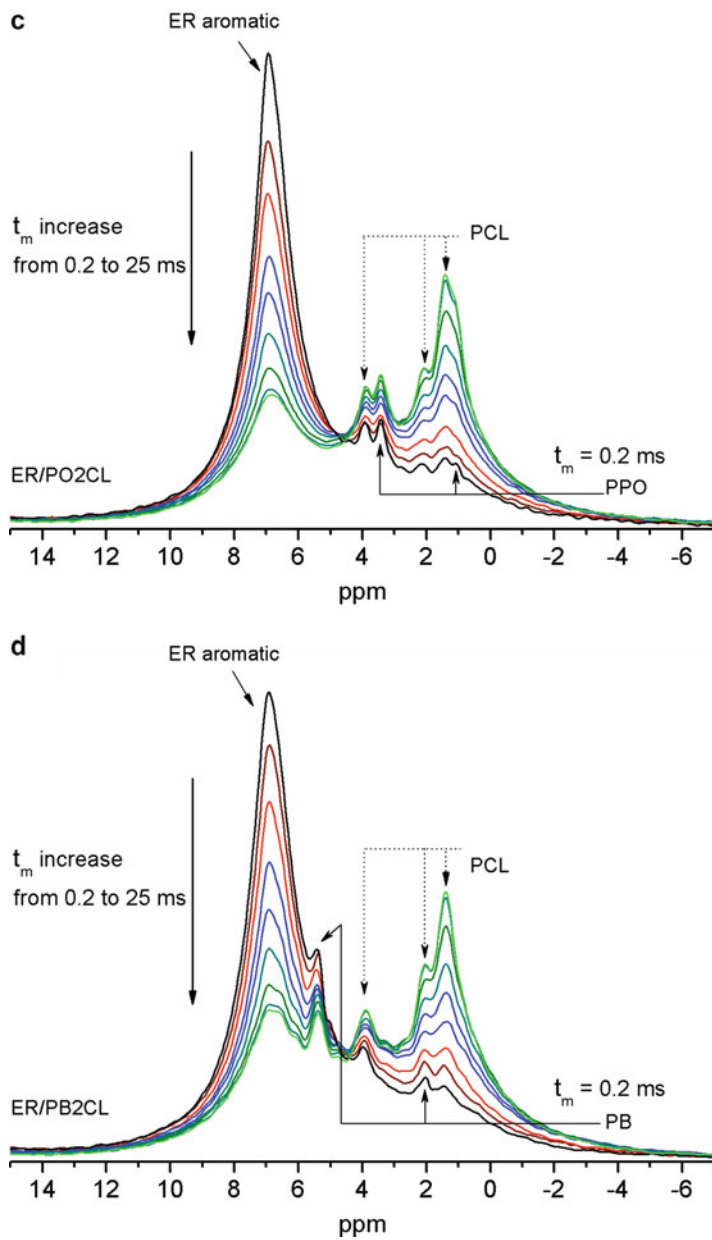


Fig. 9 (continued)

**Fig. 9** (continued)

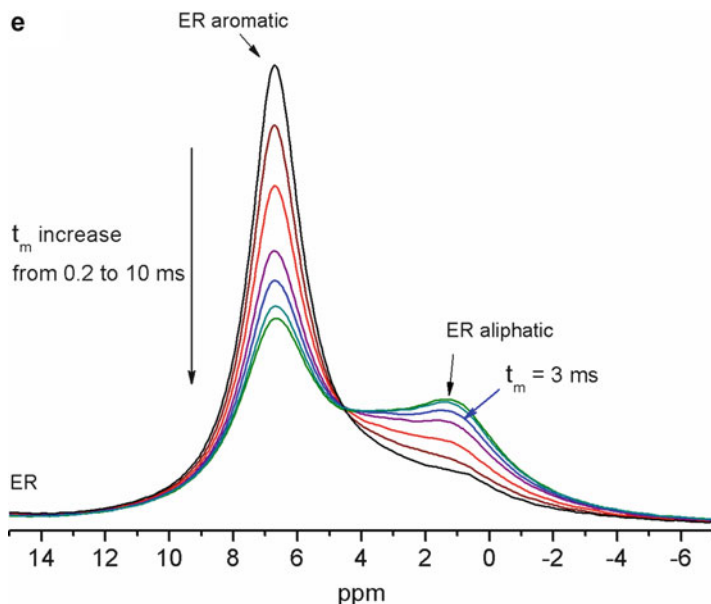


Fig. 9 A series of ^1H - ^1H spin-exchange spectra sliced along F1 of 2D NMR spectra corresponding to the aromatic groups (7.0 ppm) with increasing ^1H spin diffusion times (t_m) for blends: (a) ER/PO2EO, (b) ER/EOCL, (c) ER/PO2CL, (d) ER/PB2CL, and (e) ER. The aromatic protons transfer magnetization to BCP in the interphase and remote dispersed phases during different spin-diffusion mixing time in ER/BCP blends (Reprinted with permission from He et al. (2014), copyright American Chemical Society 2014)

PB ($-80\text{ }^\circ\text{C}$) is remarkably lower than that of PPO ($-59\text{ }^\circ\text{C}$), and the line width of PB is obviously smaller than that of CH_3 groups of PPO as shown in Fig. 2b, therefore, PB should have higher mobility than that of CH_3 groups of PPO at room temperature. As the spin-exchange between ER aromatic groups and PB can be obviously observed in ER/PB2CL at very short mixing time of 0.2 ms (Fig. 9d), which indicates that nearly no PPO locates in the interphase.

While for ER/EOCL, only a very weak spin-exchange between ER aromatic groups and PCL is observed, implying that only a small amount of PCL mixed with ER in the interphase. With increasing mixing time, the signals of PPO and PCL in these two PEO-containing blends begin to show up at mixing time greater than 3 and 0.5 ms, respectively. These results indicate that PEO should be the dominating component intimately mixing with ER in the interphase and also imply that the intermolecular interactions between PEO and cured-ER are stronger than those between PCL and cured-ER. These results further confirm that the miscibility is better between ER and BCP in blends containing PEO block than that in blends containing PCL block as also revealed by ^1H static NMR experiments in Fig. 2.

However, for PCL-containing blends except ER/EOCL, it is quite interesting to note that the spin-exchange between ER aromatic groups and all BCP (both miscible

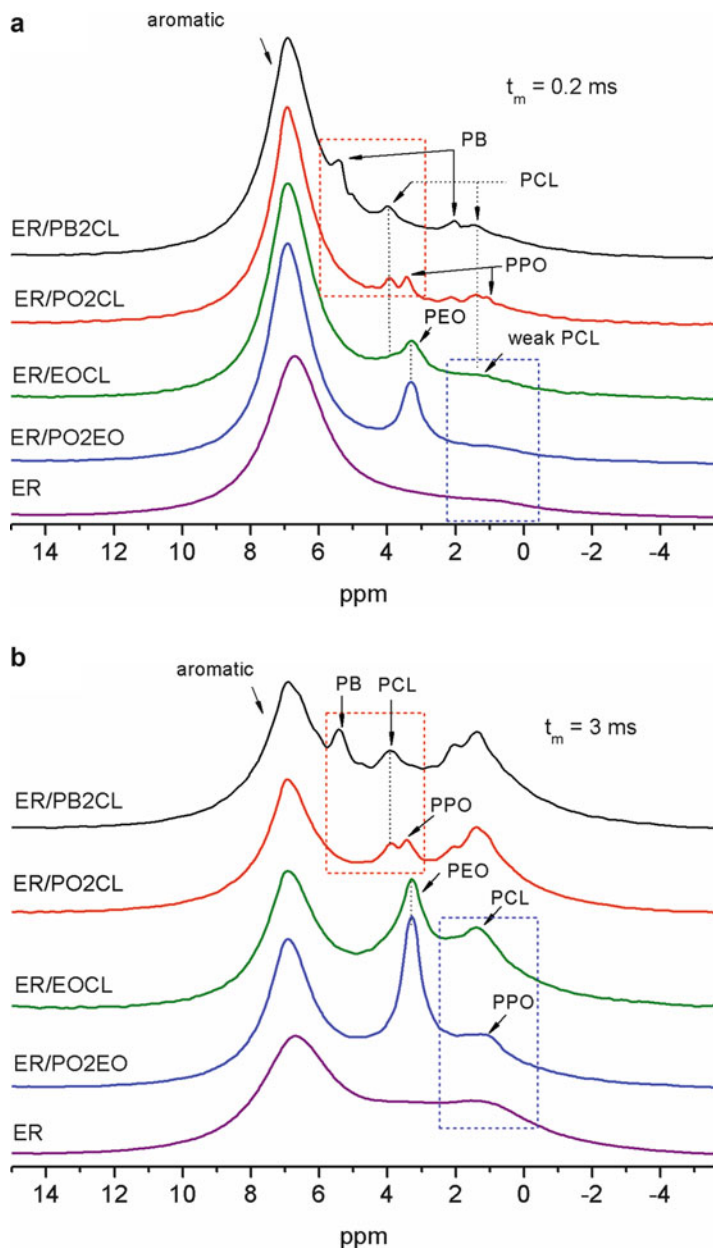


Fig. 10 $1D\ ^1H-^1H$ spin-exchange spectra sliced along F1 of 2D NMR spectra corresponding to the aromatic groups at 7.0 ppm for all blends at mixing times (t_m) of (a) 0.2 ms and (b) 3 ms. At a short spin-diffusion time of 0.2 ms, the signal of interfacial BCP intimately mixed with ER aromatic protons is observed selectively. The aromatic protons transfer magnetization to the more remote BCP in dispersed phase during the longer (ca. 3 ms) spin-diffusion mixing time (Reprinted with permission from He et al. (2014), copyright American Chemical Society 2014)

and immiscible) blocks can be simultaneously observed for ER/PO2CL and ER/PB2CL from a very short mixing time of 0.2 ms to a long time (25 ms), indicating that a certain amount of immiscible blocks should be intimately mixed with cured-ER in interphase besides the miscible PCL blocks. This unexpected finding challenges previous models describing the structures formed in ER/BCP blends, where the immiscible blocks were thought to be completely expelled out of the cured-ER network upon curing. The observed remarkable difference of the interfacial mixing in blends containing different miscible blocks provides clear evidence that the mechanism of the structure formation and phase separation in ER blends with different miscible blocks should be quite different. In previous works, two different mechanisms about the formation of the nanostructure in ER/BCP blends with ER-miscible PEO and PCL blocks were proposed, including preformed self-organized microphase before curing and polymerization-induced microphase separation starting from a homogenous solution of all components. Our above spin-exchange experiments suggest that different interphase structure should be formed as a result of different initial equilibrium states before curing.

Interphase Composition and Heterogeneous Dynamics of Epoxy Network Determined by Double-Quantum-Filtered ^1H MAS Experiment

Although the above ^1H - ^1H spin-exchange experiments have successfully determined the detailed interfacial mixing between ER and BCP, the interphase composition has not been obtained due to the overlap of signals from different components. Because of the extremely small volume fraction of the interphase in a typical polymer blend, experimental determination of the interphase composition at a molecular level has always been a challenging subject. Recently, a novel NMR method was proposed to directly observe the mobile interphase composition in phase-separated styrene-butadiene-styrene block copolymers by double-quantum-filtered proton spin-diffusion NMR experiments performed under low MAS (4 kHz) conditions. The broad signal of the rigid PS phase is removed by baseline-correction using a second-order polynomial. For ER/BCP blends, the above method cannot be applied because of the low resolution of cross-linked blends under low MAS as shown in Fig. 2b.

2D DQ correlation under MAS is a powerful method to provide information of ^1H - ^1H proximity for organic solids, on the other hand, ^1H DQ-filter experiment under fast MAS condition (Fig. 1e) is a powerful high-resolution method to detect the componential heterogeneous dynamics by means of varying the DQ excitation time. To isolate the signal of interphase and determine the interphase composition, we performed ^1H DQ-filter experiment for all samples. Figure 11a shows the ^1H DQ spectra at different excitation time, t_{exc} , for ER/PO2CL as an example. At a shorter excitation time, t_{exc} (ca. 76.9 μs), both the broad DQ signals of rigid network and immobilized interphase can be detected. At a longer excitation time (ca. 769 μs), only the narrow signals from the mobile phase exist. Herein, we propose a new

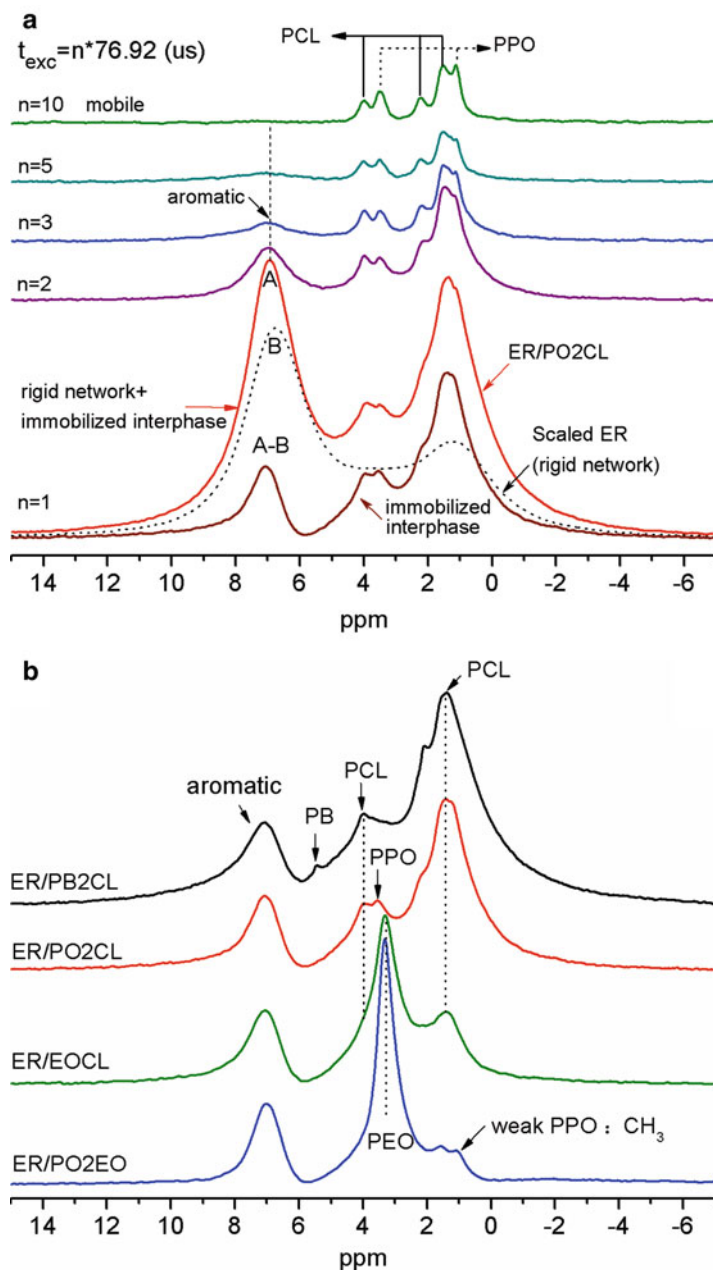
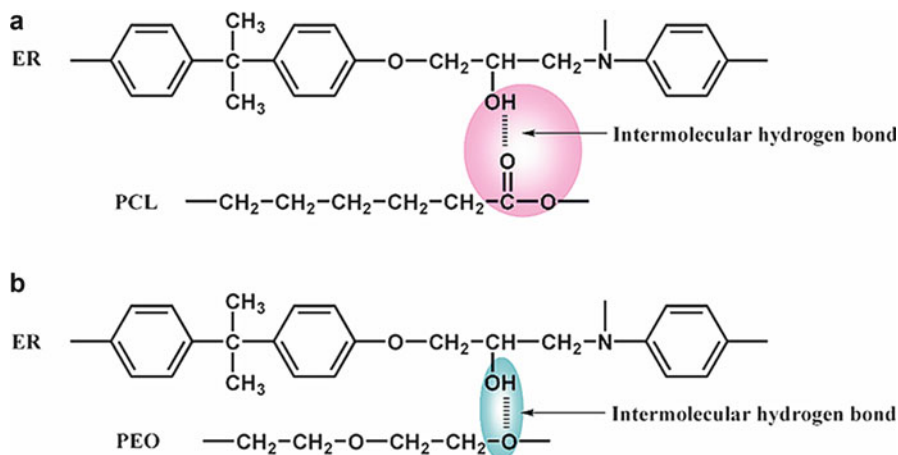


Fig. 11 High-resolution ^1H DQ-filter spectra under 26 kHz MAS of (a) ER/PO2CL at different excitation time from 76.9 to 769 μs , where the *dot line* indicated the DQ signal of pure ER with $n = 1$ as indicated. (b) Obtained interphase DQ signal of all samples at a short excitation time of 76.9 μs by subtracting the scaled DQ signal of pure rigid ER network of cured-ER without BCP (Reprinted with permission from He et al. (2014), copyright American Chemical Society 2014)

approach to obtain the interphase DQ signals in blends by subtraction of a properly scaled DQ signal of pure cured-ER without BCP at a short excitation time of 76.9 μ s. This scaling factor is chosen to be the largest number satisfying the criterion that the difference spectrum contains no regions with negative intensity. One example of this method is also shown in Fig. 11a for ER/PO2CL. Figure 11b shows the obtained interphase signals for all samples. It is noteworthy that a residual narrowed aromatic peak at 7.0 ppm is obtained, which should be attributed to the immobilized aromatic groups of partially cured-ER in the interphase region, and this NMR result provides a clear evidence of the local destroyed ER cross-linked network as suggested by Bates et al. It is also noted that strong and broad signals of ER-miscible blocks (PEO and PCL) are obviously detected in all samples due to the interfacial intermolecular interaction. In addition, weak DQ signals of interfacial ER-immiscible blocks (PPO and PB) are also detected; this should be ascribed to the lower efficiency of DQ excitation for these relative mobile components at a short excitation time. For ER/PO2EO, a small peak at 1.6 ppm is assigned to the interfacial aliphatic protons of partially cured-ER, while the weak peak at 1.2 ppm could be assigned to PPO methyl group or to the aliphatic protons of partially cured-ER. In consideration of 2D ^1H - ^1H spin-exchange experiments indicating that all PPO should be in dispersed phase, the weak DQ signal of PPO should be in dispersed phase and adjacent (in proximity) to the interphase.

Hydrogen Bonding Interactions in PCL-Containing Blends Determined by ^{13}C CPMAS Experiment

Intermolecular interactions were considered to be the driving force for the miscibility in thermoset blends. Therefore, they have a crucial effect on the structure and properties of the blends, especially the formation of interphase structure. In previous work (Hameed et al. 2010; Xu et al. 2007), it has been suggested that PEO and PCL have intermolecular hydrogen bonding interactions between hydroxyl groups of reacted epoxide-amine and oxygen of PEO or carbonyl groups of PCL as shown in Scheme 2. Fourier transform infrared spectroscopy (FTIR) is usually used to investigate the hydrogen bonding interactions in polymer blends by observing the frequency difference between the free and hydrogen-bonded hydroxyl bands. The FTIR spectra of all ER/BCP samples indicate possible hydrogen bonding interactions between ER and ER-miscible blocks (not shown). However, a strict and quantitative detection of hydrogen bonds in ER blends containing PCL or PEO is still lacking. High-resolution ^{13}C CPMAS experiment is a powerful method to investigate the intermolecular interactions due to its sensitivity to local chemical environments. Especially the carboxyl group of polymers is very sensitive to the formation of hydrogen bonds and can be directly detected by ^{13}C CPMAS techniques. Because of a great number of carbonyl groups in PCL, thus ^{13}C CPMAS method can be used to determine the formation of hydrogen bonds in ER/BCP blends containing PCL. While for ER blends containing PEO, due to the overlap of PEO and hydroxyl groups of reacted epoxide-amine at about 70 ppm, ^{13}C CPMAS



Scheme 2 Intermolecular hydrogen bonding between cross-linked epoxy and (a) PCL, as well as (b) PEO (Reprinted with permission from He et al. (2014), copyright American Chemical Society 2014)

method is not suitable to be adopted. However, by preparing the blend containing two ER-miscible blocks (EOCL) and determining the relative fraction of hydrogen-bonded PCL in interphase by ^{13}C NMR, the relative strength of the hydrogen bonding interactions between ER and PEO can be evaluated.

To investigate the specific intermolecular interactions between ER and PCL, and examine the miscibility of the thermosetting blends at the molecular level, we performed ^{13}C CPMAS NMR experiments on PCL-containing blends as shown in Fig. 12. For comparison of the chemical shift of carboxyl groups without cured-ER, ^{13}C CPMAS spectrum of block copolymer PO2CL is also shown in this figure, where the signal of PPO is very weak due to its high mobility and low cross-polarization efficiency. It is noteworthy that carbonyl groups in all blends show two overlapping peaks, while those of pure BCP just show a narrow peak at 173.8 ppm, as shown in Fig. 12b. The carbonyl peaks are broadened in all blends when PCL-containing BCPs were mixed with ER, and the deconvolution of these carbonyl signals (not shown) gives two peaks at about 176 and 174 ppm, respectively. It is reasonable to assign the low field peak at 175.6 ppm to hydrogen-bonded carbonyl groups of PCL in interfacial region and the peak at 173.8 ppm to free carbonyl groups of PCL in dispersed domain. The presence of peak at 175.6 ppm is a clear and direct evidence of the intermolecular interactions between ER and PCL. More importantly, the relative fraction of this peak provides information about the proportion of PCL interacting with ER in interphase. Therefore, this peak is a direct and sensitive probe to quantitatively detect the interfacial mixing of PCL with ER. In previous work on PCL-containing ER blends, solid-state ^{13}C CPMAS NMR experiments were also employed to investigate the specific intermolecular interactions between 2,2-bis[4-(4-aminophenoxy)-phenyl] propane-cross-linked ER and PCL. It

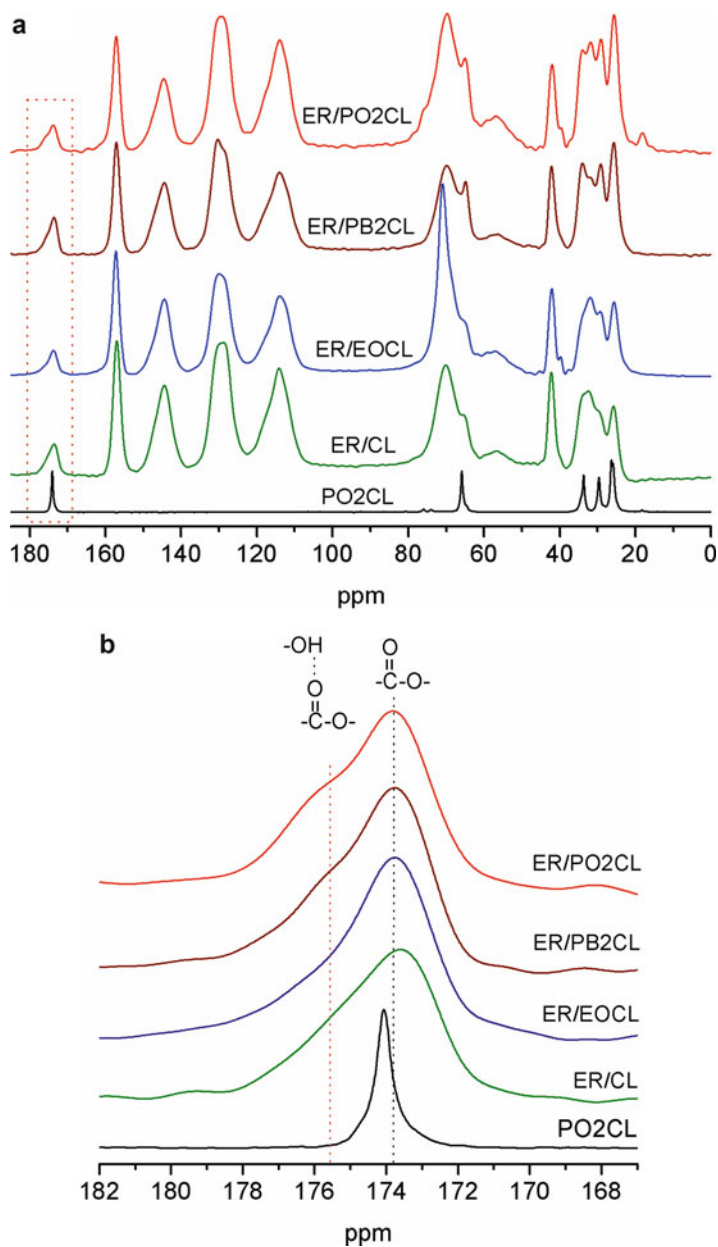


Fig. 12 (a) Standard ^{13}C CPMAS NMR spectra of all samples as indicated. (b) The ^{13}C peaks for the carbonyl groups in the samples (Reprinted with permission from He et al. (2014), copyright American Chemical Society 2014)

was found that the line widths of ^{13}C CPMAS spectra decreased with increasing PCL contents, and the chemical shift of carbonyl carbon resonance of PCL shifted to low field with increasing epoxy content in the blends. The shift and broadening of carbonyl peak also indicate the presence of intermolecular interactions, although the signal of hydrogen-bonded carbonyl group cannot be identified. The reason might be attributed to the lower resolution of the spectra in that work, which can be clearly seen by comparing the resolution of the two aromatic peaks at 128 and 115 ppm with those in our present work shown in Fig. 12a.

From the deconvolution of carbonyl peaks, the calculated fractions of hydrogen-bonded carbonyl groups of PCL in the interphase are 42.3%, 46.1%, 20.4%, and 56.3% for ER/PO2CL, ER/PB2CL, ER/EOCL, and ER/CL, respectively. It is worth noting that the fraction of hydrogen-bonded carbonyl groups in ER/EOCL is the lowest in all samples because of the competing H-bonding interactions of PEO and PCL with ER, and large fraction of PCL ($\sim 79\%$) is expelled from the ER network, indicating that PEO has stronger interaction with cured-ER than PCL. On the basis of the above determined distribution of BCP and that of ER-miscible PCL blocks by ^1H spin diffusion and ^{13}C CPMAS experiments, respectively, we can propose a quantitatively calculation method to determine the distribution of ER-immiscible blocks in the interphase and dispersed phase. In principle, for BCP containing A and B blocks, if the fraction of block B in the interphase, φ_{ip}^B , can be determined, and thus the fraction of A block in interphase, φ_{ip}^A , can be calculated from the following equation:

$$\frac{\varphi_{ip}^A + k\varphi_{ip}^B}{1 + k} = \frac{f_i}{f_i + f_m} = 1 - \lambda_{DFS} \quad (3)$$

Thus, we have

$$\varphi_{ip}^A = (1 - \lambda_{DFS})(1 + k) - k\varphi_{ip}^B \quad (4)$$

Where k is the stoichiometric proton ratio of block B to A determined from the BCP chemical structure, λ_{DFS} can be determined by ^1H spin-diffusion experiment as mentioned in the foregoing discussion. The fraction of block A or B in the dispersed phase equals to $1 - \varphi_{ip}^A$ or $1 - \varphi_{ip}^B$.

Table 3 lists the calculated distribution of different blocks in the interphase and dispersed phase for all blends. It is noteworthy that a certain amount of ER-immiscible blocks (PPO and PB) in ER/PO2CL and ER/PB2CL still exist in the interphase, which is in good agreement with the results obtained by ^1H - ^1H spin-exchange experiments. These two experiments unambiguously demonstrate that partially ER-immiscible blocks intimately mixed with ER in the interphase. For ER/EOCL, a larger amount of PEO and smaller amount of PCL simultaneously exist in interphase, indicating the competition of hydrogen bonding interactions for these two ER-miscible blocks, and the H-bonding interactions of PEO are stronger than those of PCL. For ER/PO2EO, the fraction of PPO in interphase is set to zero

Table 3 Quantitative distribution of different blocks of BCP in interphase determined by combined ^{13}C CPMAS and ^1H spin-diffusion experiments

Samples	ER/PO2EO	ER/EOCL	ER/PO2CL	ER/PB2CL
k	0.31	0.20	0.31	0.31
$\lambda_{\text{DFS}}^{\text{a}}$	0.60	0.73	0.63	0.60
$\phi_{\text{ip}}^{\text{B}}$ ^b	0 (PPO) ^c	0.20 (PCL)	0.42 (PCL)	0.46 (PCL)
$\phi_{\text{ip}}^{\text{A}}$	0.51 (PEO)	0.35 (PEO)	0.19 (PPO)	0.14 (PB)

^aDetermined by ^1H spin-diffusion experiments

^bDetermined by ^{13}C CPMAS experiments except ER/PO2EO

^cDetermined by ^1H - ^1H spin-exchange experiments

according to the result of ^1H - ^1H spin-exchange experiments, and as a result a large amount of PEO was found in interphase. On the foregoing discussion, we conclude that two different types of interphases can be formed: a thin interphase formed from dominating PEO for PEO-containing blends due to the stronger PEO-ER interaction, while thick interphase formed from all miscible and immiscible blocks for PCL-containing blends due to the weaker PCL-ER interaction. The underlying mechanism should be closely related to the difference of phase separation process in these blends. The above examples demonstrate that the combination of ^1H spin diffusion and ^{13}C CPMAS NMR is an efficient method to determine detail information of the interfacial mixing of ER/BCP blends.

Unique Structure and Dynamics of Cross-Linked Network Determined by ^{13}C T_1 Experiment

The structure and dynamics of cross-linked network play an important role in controlling the final property of ER/BCP blends. A recent work by Bates et al. suggested that the block copolymer effectively disrupts the local properties of the interfacial epoxy network, thus enhancing the toughness of ER/BCP blends (Declat-Perez et al. 2012). To quantitatively detect the dynamics of the bulk and interfacial damaged epoxy network, ^{13}C T_1 spin-lattice relaxation experiments were also performed. Two ^{13}C T_1 spin-lattice relaxation times ($T_{1,C}$) including fast- and slow-relaxing components of the ER aromatic carbons are observed for all blends, clearly indicating the heterogeneous dynamics of cross-linked network. The decomposed $T_{1,C}$ are listed in Table 4. The fast-relaxing component should be ascribed to the immobilized interphase related to the local damaged epoxy network suggested by Bates et al. The slow-relaxing component should be ascribed to the rigid cross-linked network. It is noted that $T_{1,C}$ of the fast-relaxing component is 5 ~ 8 times smaller than that of slow-relaxing component, indicating enhanced mobility of these damaged epoxy network in the interphase, and this could be a significant factor related to interphase contribution to the toughening mechanism. It is generally accepted that the blending of BCPs containing epoxy-miscible blocks inevitably

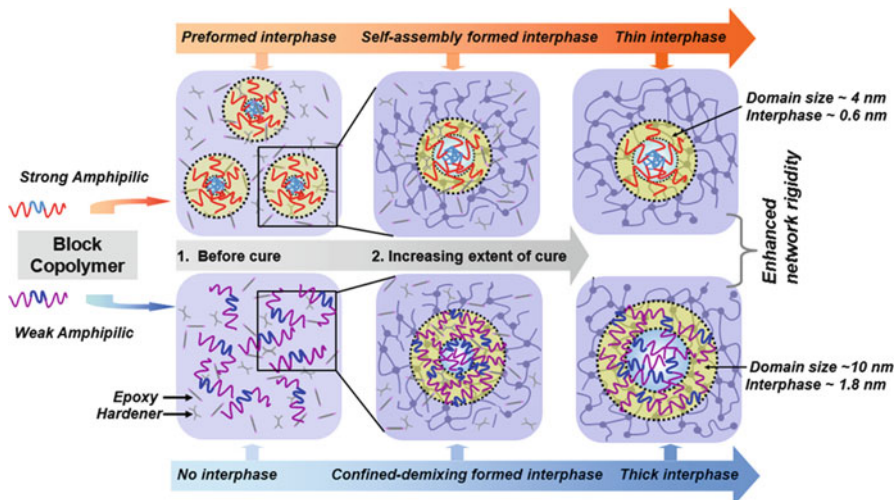
Table 4 ^{13}C $T_{1,C}$ values of cured-ER and ER/BCP blends

Samples	$T_{1,C}$ (fast) (s)	$T_{1,C}$ (slow) (s)	Fast fraction (%)	Slow fraction (%)
ER	1.9 ± 0.3	14.5 ± 0.6	27.7 ± 2.4	72.3 ± 2.5
ER/EOCL	3.9 ± 0.5	22.0 ± 3.2	54.4 ± 6.2	45.6 ± 6.5
ER/PO2EO	3.2 ± 0.3	21.6 ± 2.2	50.1 ± 4.3	49.9 ± 4.6
ER/PO2CL	2.0 ± 0.2	19.4 ± 1.1	44.6 ± 2.3	55.4 ± 2.5
ER/PB2CL	2.9 ± 0.4	21.1 ± 1.3	34.9 ± 3.4	64.3 ± 3.6

induces the decrease of T_g of cured-ER, thus the decrease of ER network rigidity. However, we surprisingly find that the $T_{1,C}$ of slow-relaxing component in all blends is obviously larger than that of cured-ER without BCP, implying that incorporation of BCPs induces enhanced rigidity of cross-linked network. This unexpected enhancement of network rigidity may influence the mechanical properties of the blends and might be attributed to the more ordered ER network upon curing. Similar phenomenon can be observed, where the polymer crystallization is enhanced from large molecule solvent or when the crystalline polymer is co-blocked with mobile ones (such as PB). We also observe that the incorporation of 40 wt% BCPs remarkably increases the amount of fast-relaxing component related to the interphase from 28% to 35 ~ 54%, due to the increased hydrogen bonding interaction between ER and ER-miscible blocks. Because the hydrogen bonding interactions between ER and PEO are stronger than those with PCL as discussed above, therefore, the determined content of fast-relaxing component in the interphase of PEO-containing blends (ER/EOCL and ER/PO2EO) is greater than that of blends without PEO (ER/PO2CL and ER/PB2CL).

A Model to Describe the Unique Structure and Dynamics of Interphase and Microdomain, Cross-Linked Network as well as Their Underlying Formation Mechanism

Based on the NMR experiments discussed above, a comprehensive understanding of the unique structure and dynamics of the microphase structure and interphase, cross-linked network, and their underlying formation mechanism in ER/BCP blends can be achieved, and a model could be proposed as shown in Scheme 3 (He et al. 2014). Depending on the strength of hydrogen bonding interactions between cured-ER and ER-miscible blocks in ER/BCP blends, there are two different processes of phase separation and interphase formation in these blends. In this model, amphiphilic BCPs are mainly divided as strong and weak amphiphilic BCPs, respectively. Strong amphiphilic BCPs indicate that there is large difference in thermodynamic interaction parameter χ between each of the amphiphilic BCP blocks and epoxy before curing, generally shown as large difference in miscibility, and vice versa for weak amphiphilic BCPs. It should be noted that strong and weak can be altered as the temperature changes.



Scheme 3 Schematic illustration of the model to describe two different types of unique structure and dynamics of interphase and microdomain, cross-linked network and their underlying formation mechanism in ER/BCP blends (Reprinted with permission from He et al. (2014), copyright American Chemical Society 2014)

For blends with strong amphiphilic BCPs, such as ER/PO₂EO, a preformed self-organized microphase structure containing “wet brush” interphase before curing is formed as proposed by Bates et al. (Lipic et al. 1998), ER-immiscible blocks form the “core,” and ER-miscible blocks are dissolved in epoxy. Upon curing, the cross-linked rigid ER formed a separated microphase, while partial mobile BCP was locally expelled from the cured-epoxy matrix and formed mobile phase. “Wet brush” changes to “dry brush” due to the strong hydrogen bonding interaction between ER-miscible block and cured-ER and is not disturbed by the cross-linking reactions. A portion of miscible BCP block is intimately mixed with the partially cured-ER phase and formed an interphase region. Thus a complete interphase is formed and no ER-immiscible blocks exist in interphase. With an increased volume fraction of miscible BCP block, the domain size decreases, whereas the interphase thickness is only slightly changed.

However, for blends with weak amphiphilic BCPs, such as ER/PO₂CL and ER/PB₂CL, a quasi-homogenous solution of all components will form before curing, and then polymerization-induced microphase separation starts from this solution. Thus, the diffusion of all BCP blocks separated from the cross-link network is controlled by the competition of the microphase separation and cross-linking reaction during a relative short time scale. The presence of hydroxyl groups from cured-ER interact with ER-miscible block, which prohibits the segregation of ER-miscible block from the cured-ER network, and a considerable amount of BCP will be trapped in the partially cured-ER network in the interphase, thus a thicker interphase containing a considerable amount of BCPs could be formed.

For the blends containing double epoxyphilic block copolymer, such as ER/EOCL, the above two scenarios are probably included in this system. Before curing, partial double epoxyphilic BCP dissolves in the epoxy while partial double epoxyphilic BCP self-assembles into aggregation as the case of double hydrophilic BCP in water (Casse et al. 2012). Upon curing, the blends go through both the above two processes. Besides, the competing intermolecular interactions between epoxy and each block of BCP will reduce the proportion of each block in the interphase.

Our forgoing NMR results unambiguously demonstrate the above underlying molecular mechanism of structure formation model. Thus we come to the conclusion that two different types of interphase structures can form depending on the different initial equilibrium states before curing. Upon curing, the cross-linked rigid ER forms a separated microphase, while some of the BCPs were locally expelled out of the cured-ER network and forms another microphase. The residual immobilized BCPs were intimately mixed with some partially cured-ER matrix and formed the interphase region. Due to the high mobility of BCP blocks, the incorporation of BCPs induces enhanced rigidity of cross-linked ER network. On the basis of this model, unique structure and dynamics of interphase and cross-linked network and their underlying formation mechanism in ER/BCP blends can be well understood, and more importantly, the detailed and quantitative information of the interphase and cross-linked network provides new insight into the toughening mechanism for developing advanced thermoset blends.

Conclusion

Using a variety of multiscale solid-state NMR techniques, we have shown that detailed information about the componential miscibility, unusual structure and dynamics of the interphase and microdomain, cross-linked network, as well as the intermolecular interactions between ER and BCPs in these nanostructured ER/BCP blends with different types of ER-miscible blocks can be obtained. A distinct dynamic difference between the cured-ER matrix and BCPs was observed by 1D and 2D NMR experiments, indicating that these blends underwent phase separations. Detailed interfacial mixing between ER and BCPs was revealed and two different types of interphase structure are found. SSNMR provides a fast and convenient detection of interphase composition, including immobilized BCPs and partially cured or local damaged ER network, which unambiguously demonstrate that ER-miscible blocks are not completely dissolved in the cured-ER matrix. Rather, the ER-miscible blocks are partially miscible with the cured-ER matrix. Upon curing, the cross-linked rigid ER formed a separated microphase, while the part of mobile ER-miscible blocks was locally expelled from the cured-ER matrix and formed another microphase with the immiscible blocks. The residual immobilized ER-miscible blocks were intimately mixed with the partially cured-ER phase, and they formed an interphase region. It was found that the interphase thickness of PEO-containing blends is obviously smaller than that of PCL-containing blends.

The driving force for the interphase formation and miscibility in PCL-containing blends was successfully determined by SSNMR, demonstrating the formation of hydrogen bonds between PCL and ER; competing hydrogen bonding interactions were also found when ER was blended with PEO-*b*-PCL. We also propose a new method to quantitatively determine the distribution of different blocks in the interphase and dispersed phase for PCL-containing blends. NMR relaxation experiment provides a quantitative determination of the amount of local destroyed network in the interphase. Furthermore, it is found that incorporation of BCPs induces unexpected enhanced rigidity of the cross-linked network. On the basis of SSNMR results, we propose a model to describe the unique structure and dynamics of the interphase and cross-linked network as well as their underlying formation mechanism in ER/BCP blends.

References

- Asano A, Eguchi M, Shimizu M, Kurotsu T (2002) *Macromolecules* 35(23):8819–8824
- Brus J, Dybal J, Schmidt P, Kratochvil J, Baldrian J (2000) *Macromolecules* 33(17):6448–6459
- Casse O, Shkilnyy A, Linders J, Mayer C, Häussinger D, Völkel A, Thünemann AF, Dimova R, Cölfen H, Meier W, Schlaad H, Taubert A (2012) *Macromolecules* 45(11):4772–4777
- Declet-Perez C, Redline EM, Francis LF, Bates FS (2012) *ACS Macro Lett* 1:338–342
- Fan WC, Wang L, Zheng SX (2010) *Macromolecules* 43:10600–10611
- Fu W, Jiang R, Chen T, Lin H, Sun P, Li B, Jin Q, Ding D (2010) *Polymer* 51(9):2069–2076
- Guo QP, Thomann R, Gronski W, Thurn-Albrecht T (2002) *Macromolecules* 35:3133–3144
- Hameed N, Guo QP, Hanley T, Mai YW (2010) *J Polym Sci Part B: Polym Phys* 48:790–800
- He X, Liu Y, Zhang R, Wu Q, Chen T, Sun P, Wang X, Xue G (2014) *J Phys Chem C* 118:13285–13299
- Li X, Fu W, Wang Y, Chen T, Liu X, Lin H, Sun P, Jin Q, Ding D (2008) *Polymer* 49:2886–2897
- Lipio PM, Bates FS, Hillmyer MA (1998) *J Am Chem Soc* 120:8963–8970
- Mellinger F, Wilhelm M, Spiess HW (1999) *Macromolecules* 32:4686
- Meng FL, Zheng SX, Liu TX (2006a) *Polymer* 47(21):7590–7600
- Meng FL, Zheng SX, Zhang W, Li HQ, Liang Q (2006b) *Macromolecules* 39(2):711–719
- Mijovic J, Shen M, Sy JW, Mondragon I (2000) *Macromolecules* 33(14):5235–5244
- Paul D, Bucknall C (2000) *Polymer blends*. Wiley, New York
- Ruiz-Perez L, Royston GJ, Fairclough JPA, Ryan AJ (2008) Toughening by nanostructure. *Polymer* 49:4475–4488
- Schmidt-Rohr K, Spiess HW (1994) *Multiple dimensional NMR and polymers*. Academic, San Diego
- Sun PC, Dang QQ, Li BH, Chen TH, Wang YN, Lin H, Jin QH, Ding DT, Shi AC (2005) *Macromolecules* 38:5654–5667
- Thio YS, Wu JX, Bates FS (2006) *Macromolecules* 39:7187–7189
- Xu Z, Zheng S (2007) *Macromolecules* 40:2548–2558
- Yu S, Zhang RC, Wu Q, Chen TH, Sun PC (2013) *Adv Mater* 25(35):4912–4917
- Zheng SX, Guo QP, Chan CMJ (2003) *Polym Sci Pt B-Polym Phys* 41(10):1099–1111
- Zhu HJ, Graf R, Hou GJ, Zhao Y, Wang DJ, Spiess HW (2010) *Macromol Chem Phys* 211(10):1157–1166

Junkal Gutierrez, Laida Cano, and Agnieszka Tercjak

Abstract

The rheology of the epoxy/block copolymer blends is an important learning tool to understand the microphase separation of one of the blocks of block copolymer during the curing process. The knowledge about the viscoelastic changes during the thermosetting network formation allows to better understand the processes such as gelation, vitrification, and microphase separation. Different methods can be employed to determine the gelation point of the epoxy/block copolymer blends. The first method is related to the extrapolation of the complex viscosity (η^*) to infinite, the second to the intersection of dynamic storage modulus (G') and dynamic loss modulus (G'') curves, and the third one to the fact that $\tan \delta$ is independent on frequency at gelation point. In this chapter, a few examples of rheology of epoxy/block copolymer blends will be presented with the main aim of showing the correlation between rheological behavior and final properties of thermosetting systems.

Keywords

Rheology • Phase separation • Epoxy based blends • Block copolymers • Viscoelastic properties

Contents

Introduction	956
Rheology of Epoxy/Block Copolymer Blends	959
Gelation point	959
Rheology of the Uncured Epoxy/PS-b-PMMA and PB-b-PMMA Block Copolymer Blends	961

J. Gutierrez • L. Cano • A. Tercjak (✉)

Group 'Materials + Technologies', Department of Chemical and Environmental Engineering, Engineering College of Gipuzkoa, University of the Basque Country, UPV/EHU, Donostia-San Sebastián, Spain

e-mail: juncal.gutierrez@ehu.eus; laida.cano@ehu.eus; agnieszka.tercjaks@ehu.eus

Rheology of the Epoxy/Epoxidized SB Block Copolymer Blends	963
Rheology of the Epoxy/Epoxidized SBS Block Copolymer Blends	966
Rheology of the Epoxy/PS-b-PEO Block Copolymer Blends Modified with Low-Molecular-Weight Liquid Crystals	971
Conclusions	974
References	975

Introduction

Rheology of polymer blend based on epoxy type resins modified with block copolymers is an important tool for better understanding of the processes such as gelation, vitrification, and microphase separation of one of the blocks of block copolymer during the thermosetting network formation. This point is essential to know more about the mechanism of phase separation of block copolymers since epoxy/block copolymer blends have been a topic of many research works due to their variety of potential applications; however, the microphase separation mechanism of block copolymers during the polymerization reaction is still not fully understood (Macosko 1994; Winter 2000, 2007; Pascault and Williams 2010).

Rheological behavior of epoxy/block copolymer blends depends strongly on the length of polymeric chains, being strongly related with molar mass and its distribution (Macosko 1994). During polymerization reaction of thermosetting systems, viscosity tends to infinity value during gelation process in which formation of the three-dimensional network takes place (Winter 2000, 2007; Mortimer et al. 2001; Pascault and Williams 2010). In other words, gelation is a transition which takes place during thermosetting network formation, resulting in the change from a liquid to a solid state.

Taking the above into account, it is essential to gain a complete understanding of the rheological behavior of epoxy/block copolymer blends during network formation in order to control the viscosity variation and gelation time (Poncet et al. 1999; Mustata and Bicu 2001; Pichaud et al. 1999; Byutner and Smith 2002), which is crucial for fabrication of thermosetting systems modified with block copolymer.

In the literature, one can find different methods, which allow to determine the gelation point from rheological measurements. The simplest one is based on the extrapolation of the complex viscosity (η^*) to infinite (Macosko 1994). In this case, it should be taken into account that the fluctuation of viscosity during thermosetting network formation can also take place due to phenomena like phase separation (Castro et al. 1984) and/or vitrification (Harran and Laudouard 1986) and care must be taken to not mistake these phenomena with chemical gelation.

The second method used to describe the gelation point is to define it as the point of intersection of dynamic storage modulus (G') and dynamic loss modulus (G'') curves in small-amplitude oscillatory shear experiments. This definition was proposed by Tung and Dynes (1982). Nonetheless, Winter and Chambon (1986, 1987) and Chambon et al. (Chambon and Winter 1985; Chambon et al. 1986; Chambon and Winter 1987) proved that this definition depends strongly on the formulation of

the thermosetting system with stoichiometric balance. The third method for detecting the gelation point from dynamic moduli data is based on the observation that at the gelation point $\tan \delta$ is independent on frequency. Consequently, the gelation point is defined as the reaction time at which $\tan \delta$ becomes independent of the frequency. Here it should be pointed out that this criterion is often not applicable for epoxy/block copolymer blends due to the nonsimultaneity of the measurements for different frequencies and the formulation of the thermosetting system (Eloundou et al. 1996; Bonnet et al. 1999; Tercjak et al. 2005).

Taking the above into account, rheological behavior of epoxy/block copolymer blends leads to better understanding of the thermosetting network formation during polymerization process and controls the fabrication of these blends by optimization of the curing conditions. From this point of view, many research groups investigated rheology of epoxy/thermoplastic blends. Bonnet et al. (1999) have studied the effect of polyetherimide (PEI) content on the rheological behavior of the epoxy/amine system being epoxy low-molecular-weight diglycidyl ether of bisphenol A (DGEBA), and they used 4,4'-methylenebis(3-chloro 2,6-diethylaniline) (MCDEA) as amine. The authors have found that reaction-induced phase separation leads to local rapid decrease of the viscosity for the PEI-(DGEBA/MCDEA) systems with low PEI content. For the PEI contents closed to the phase inversion composition (higher than 15 wt%), authors have reported the rheological behavior characteristic for a bicontinuous systems with a strong dependence of the shape of the curves on the frequency of rheology measurement. They observed that before phase separation process, a continuous increase in complex viscosity took place due to the formation of bicontinuous structure. Nevertheless, after some time a slight decrease of complex viscosity occurred, which can be related to local destruction of bicontinuous structure and their reappearance in short interval of time when the complex viscosity start to increase gradually again. The decrease of the complex viscosity during the formation of bicontinuous structure depended strongly on frequency in which measurement was performed. Additionally, they reported that for PEI-(DGEBA/MCDEA) systems with PEI content higher than 30 wt%, reaction-induced phase separation led to a gradual increase in viscosity. The authors have confirmed also a strong relation between the viscoelastic behavior of this system during curing and final morphology, which is visualized in Fig. 1.

Kim et al. (Kim and Char 2000) have examined the rheological behavior of epoxy/poly(ether sulfone) (PES) during the curing of the epoxy-based system with 4,4'-diaminodiphenylmethane (DDM) as curing agent. They have detected some variations in viscosity before an abrupt viscosity increase due to the gelation. They have attributed this phenomenon to the phase separation of PES from the epoxy matrix during the isothermal curing. Similar results have been reported by Yu et al. (2004) using the same epoxy/PES system cured with methyl tetrahydrophthalic anhydride (MTHPA). The authors have found that both the complex viscosity and the storage modulus increased during reaction-induced phase separation. Additionally, similar to Bonnet et al. (1999), they have reported that for bicontinuous phase structured PES-(DGEBA/MTHPA) systems, the complex viscosity showed strong dependency on the frequency of the rheology measurement.

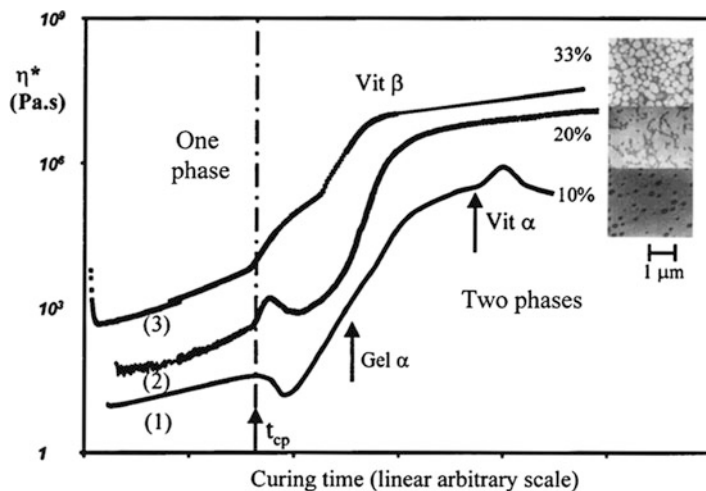


Fig. 1 Influence of PEI concentration on the rheological behavior of (1) 10 wt%, (2) 20 wt%, and (3) 33 wt%. TEM images correspond to the final morphologies obtained for each investigated thermosetting system cured 5 h at 135 °C and postcured 7 h at 220 °C (Reproduced with permission of (Bonnet et al.), copyright 1999 American Chemical Society)

Rheology of epoxy/thermoplastic blends has been also studied by Tercjak et al. (2005, 2006). The authors have monitored the rheological behavior of DGEBA/MCDEA system modified with syndiotactic polystyrene (sPS) during thermosetting network formation at different curing isothermal conditions. A rheological analysis of various sPS-(DGEBA/MCDEA) systems has been performed using ARES rheometer. The authors have applied the Winter–Chambon criterion in order to determinate the gelation point. Moreover, gelation point obtained from Winter–Chambon criterion was in good agreement with that recorded by following the G' and G'' crossing criterion. The authors have concluded that the addition of less than 7.5 wt% sPS into the DGEBA/MCDEA system shifted the gelation point towards longer cure times, which means that the addition of sPS resulted in a delay of the curing reactions. For sPS contents higher than 7.5 wt%, when morphology is changing from particulate to co-continuous, the gelation time decreased at increasing sPS contents. It can be noted a strong influence of crystallization-induced phase separation (CIPS) on a liquid–solid transition of sPS-(DGEBA/MCDEA) systems. Here it should be pointed out that sPS homopolymer is a semicrystalline, and consequently in this particular case, phase separation during network formation can be provoked by crystallization process of sPS. Tercjak et al. (2005, 2006) have studied also the influence of the curing temperature on the viscoelastic behavior and on the final morphology of 5% sPS-(DGEBA/MCDEA) systems. They proved that the high curing temperature led to faster gelation process before RIPS and CIPs and that reaction- and crystallization-induced phase separation (RIPS and CIPS,

respectively) showed strong influence on the shape of the rheology curves. The rheological behavior of the same sPS-(DGEBA/MCDEA) system contains 5 wt% sPS during curing at 210 °C, 220 °C, and 240 °C, which is shown in Fig. 2

As observed by Tercjak et al. (2006), sPS-(DGEBA/MCDEA) system cured at lower curing temperatures (210–220 °C) showed an increase in G' , G'' , and η^* before gelation process. This phenomenon was attributed to the CIPS since as confirmed by authors the final morphology of this thermosetting system showed sPS spherulites embedded in a continuous matrix as clearly observed in Fig. 3. The spherulites formed at 220 °C were smaller than those crystallized at 210 °C. This can be related to the fact that the initial increase of η^* at 220 °C was slower compared to the increase at 210 °C.

On the contrary, at high curing temperature, no fluctuation in G' , G'' , and η^* before gelation was found. As visualized in Fig. 3c and in more detail in Fig. 3d, no sPS spherulites were detected in these cases. The authors have found good correlation of the viscoelastic behavior of the 5% sPS-(DGEBA/MCDEA) system at different curing temperatures (210 °C, 220 °C, and 240 °C) with the final morphologies. Both sPS spherulites and sPS particles, formed by CIPS and RIPS, respectively, dispersed in DGEBA/MCDEA matrix were found for the systems cured at 210 °C and 220 °C; however, only sPS particles dispersed in DGEBA/MCDEA matrix (RIPS) were found for the system cured at 240 °C.

In this chapter, different examples of the rheological behavior of epoxy/block copolymer blends are presented. Relationship between the rheology and reaction-induced phase separation is shown using Advanced Rheometric Expansion Systems (ARES, TA Instruments). Knowledge related to viscoelastic behavior of epoxy resin blends modified with block copolymers during network formation allows authors to understand the final morphology and final properties of thermosetting systems nanostructured by block copolymers.

Rheology of Epoxy/Block Copolymer Blends

Gelation point

The continuous monitoring of the rheological behavior of a neat DGEBA/MCDEA mixture during thermosetting network formation permits following the transitions that take place during curing such as gelation, vitrification, and others. As is well known during reaction time, the epoxy/amine systems undergo a phase transition changing their state from liquid to solid during network formation process. The gelation point of a chemically cross-linked system is defined as the time at which the weight-average molecular weight diverges (Winter and Chambon 1986; Chambon and Winter 1985, 1987). During this phase transition, covalent bonds connect across the whole volume of the curing thermosetting system and a macroscopic network is formed. Based on the Winter–Chambon criterion, the chemically cross-linking

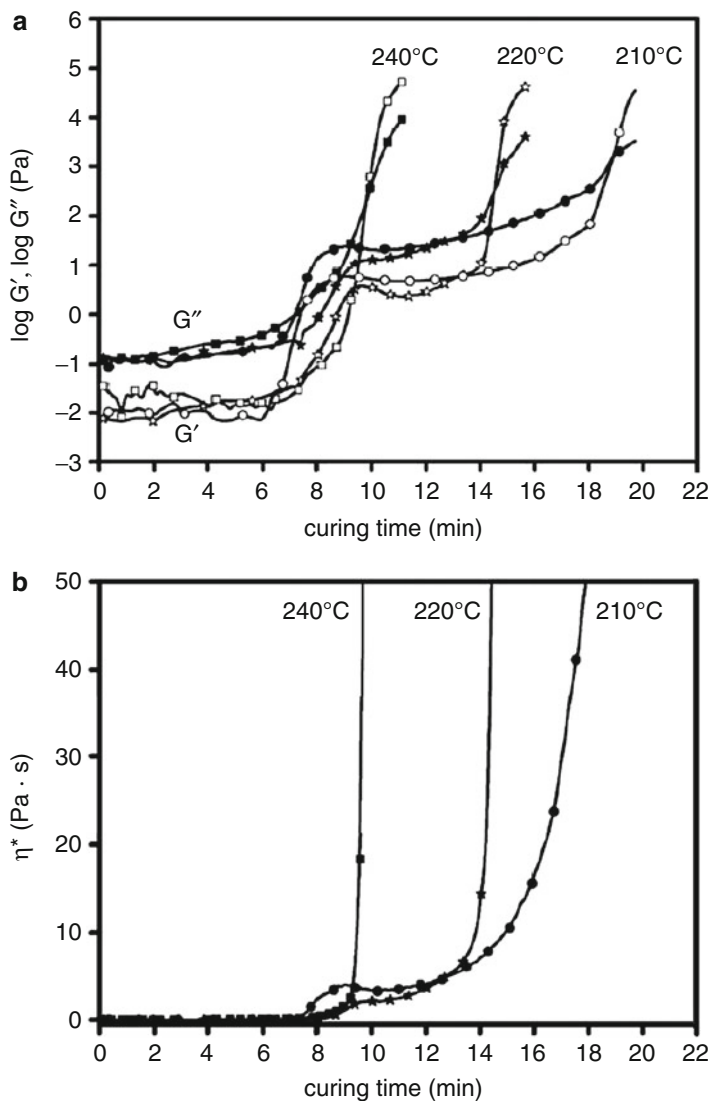


Fig. 2 (a) Evolution of G' (open symbols) and G'' (full symbols) versus the curing time for the 5 wt% sPS-(DGEBA/MCDEA) system cured at different temperatures and (b) evolution of η^* versus the curing time for the 5 wt% sPS-(DGEBA/MCDEA) system cured at different temperatures at 1 Hz (Reproduced with permission of (Tercjak et al.), copyright 2006 Wiley-VCH Verlag GmbH & Co. KG)

systems display the following behavior at the gelation point (Winter and Chambon 1986; Ishii and Ryan 2000; Chambon et al. 1986):

$$\tau(t) = S \int_{-\infty}^t (t - t')^{-n} \gamma(t) dt' \quad (1)$$

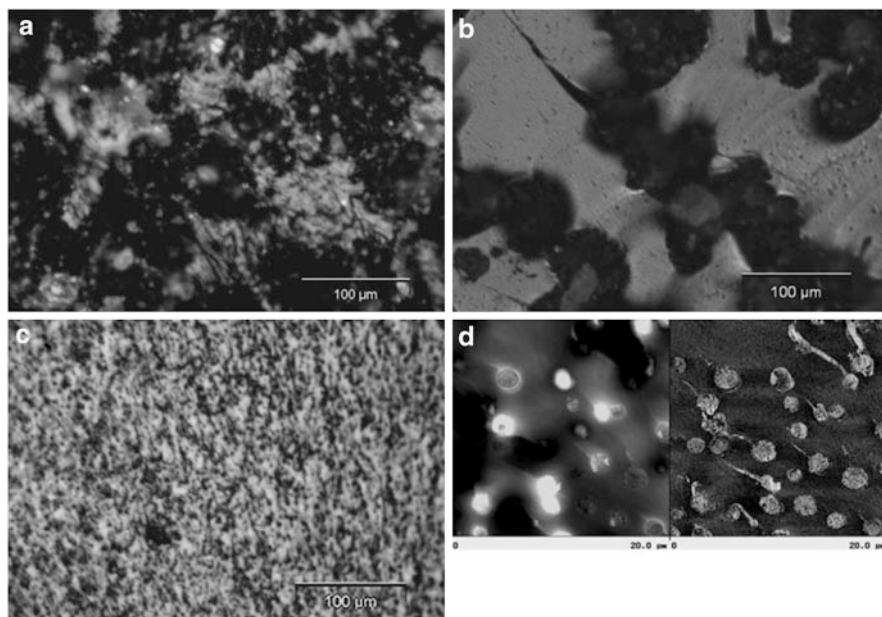


Fig. 3 Cross-section OM images of 5 wt% sPS-(DGEBA/MCDEA) system cured 2 h at (a) 210 °C, (b) 220 °C, and (c) 240 °C. (d) Height and phase AFM image of the system cured at 240 °C (Reproduced with permission of (Tercjak et al.), copyright 2006 Wiley-VCH Verlag GmbH & Co. KG)

where $\tau(t)$ is the time-dependent shear stress and $\gamma(t)$ is the time-dependent shear strain. Equation 1 describes the shear stress in a critical gel which is being deformed at a rate $\dot{\gamma}(t)$, for a time t' ranging from $-\infty$ to t . As a consequence, at the gelation point:

$$G'(\omega) \approx G''(\omega) \approx \omega^n \quad (2)$$

and the loss tangent will be:

$$\tan\delta = G'(\omega)/G''(\omega) = \tan(n\pi/2) \quad (3)$$

Consequently, at the gelation point, $\tan\delta$ is independent of frequency, and G' and G'' have the same power-law frequency dependence.

Rheology of the Uncured Epoxy/PS-*b*-PMMA and PB-*b*-PMMA Block Copolymer Blends

The self-organization of the poly(styrene-*b*-methyl methacrylate) (PS-*b*-PMMA) and poly(butadiene-*b*-methyl methacrylate) (PB-*b*-PMMA) block copolymers in

DGEBA solution has been investigated by Fine et al. (2005). The authors have correlated the rheology results with the results obtained from X-ray scattering (SAXS). They have proved that the microphase separation of PS and PB block of PS-*b*-PMMA and PB-*b*-PMMA, respectively, takes place at room temperature in DGEBA solution, while PMMA blocks of both block copolymers remains soluble in DGEBA acting as stabilizer of the microphase separation. SAXS patterns of both PS-*b*-PMMA/DGEBA and PB-*b*-PMMA/DGEBA solutions indicated the existence of highly ordered structures at room temperature. The relative positions of the higher-order peaks corresponded with a hexagonally packed cylinder structure. Here it should be also pointed out that the authors have recorded the temperature dependences of the SAXS profiles of the nonannealed and annealed PS-*b*-PMMA/DGEBA and PB-*b*-PMMA/DGEBA solution from room temperature to 180 °C. They have concluded that investigated systems maintain their highly ordered structures up to 100 °C. They have also proved that the high-order peaks disappeared when temperature is raised to 120 °C for both annealed and solvent evaporation. Here, it is worth to note that temperature dependence phase separation of PS or PB blocks took place since PS, PMMA, and PB block show different miscibility with DGEBA, being PMMA block partially miscible with DGEBA and both PS and PB block immiscible once. The different miscibility of each block of PS-*b*-PMMA/DGEBA and PB-*b*-PMMA/DGEBA with DGEBA leads to phase separation of PS or PB blocks as a function of the thermal treatment.

The effect of the structural transition observed by temperature dependences of the SAXS profiles of both PS-*b*-PMMA/DGEBA and PB-*b*-PMMA/DGEBA solutions has been also studied by rheology in the linear viscoelastic regime since this technique is also a useful tool for studying the order–disorder transition (ODT). The authors collected frequency dependences of the store modulus G' and lost modulus G'' at different temperatures for both PS-*b*-PMMA/DGEBA and PB-*b*-PMMA/DGEBA solutions. They have corroborated that the threshold temperature for which $\log G'$ versus $\log G''$ becomes linear with a slope of 2 independent of temperature was indicative for disorder of the system. The rheology measurement performed by the authors indicated that PS-*b*-PMMA/DGEBA solution followed four regimes. Below 60 °C, the G' and G'' curves were superimposed and a low frequency and the elastic plateau were exhibited. For the range of the temperature from 60 °C to 110–120 °C, an intermediate regime was observed. This regime corresponded to a softening of the investigated system. As pointed out by Fine et al. (2005), this phenomenon can be related to both the migration of DGEBA in the PS core (DGEBA plasticize the PS domains) and the fact that the temperature is reaching a value close to the T_g of the microsegregated PS-rich domains. The increase of the temperature to 140 °C led to a viscoelastic regime with a Maxwellian behavior (slope of 2) which was visualized by lack of superimposability of the G' and G'' curves. This means that the system contains persistent micelles or heterogeneities. Once the temperature is higher than 140 °C, all the curves are perfectly superimposed with a slope of 2, indicating that the solution is homogeneous. Similarly, the relation between the morphology investigated by temperature

dependences SAXS patterns of PB-*b*-PMMA/DGEBA solutions was related to their temperature dependences rheological curves. In this case, the PB block stays microsegregated independently on the temperature. The relaxation times of the chains are not affected significantly in the temperature range 20–180 °C and no ODT was observed.

Rheology of the Epoxy/Epoxidized SB Block Copolymer Blends

The curing behavior of epoxy/poly(styrene-*b*-butadiene) (SB) block copolymer epoxidized with 37 and 46 mol% degree of epoxidation (eSB37 and eSB46, respectively) was analyzed using a Rheometrics Ares rheometer equipped with parallel plates of 50 and 25 mm diameter (upper and lower plate, respectively). Dynamic oscillatory shear measurements were performed at 140 °C as a function of curing time at a constant frequency of 1 Hz. The selected thermosetting system was the diglycidyl ether bisphenol-A (DGEBA) as epoxy resin cured with 4,4'-methylenebis(3-chloro,2,6-diethylaniline) (MCDEA) as a curing agent. Investigated systems were prepared just before loading the sample in the rheometer. The parallel plates were preheated to 140 °C before a zero gap was set. The upper plate was then raised, always ensuring that the normal force was close to zero, and the liquid, uncured sample was put on the lower plate. The gap between the plates was about 1 mm, and the applied strain was changed during the experiment to ensure a linear viscoelastic response. Serrano et al. (2007) reported the evolution of the storage (G') and loss (G'') moduli as a function of curing reaction time. Consequently, they studied also the complex viscosity magnitude (η^*) from the complex modulus (G^*) through the relation $\eta^* = G^*/\omega$, being ω the frequency. The evolution of the viscoelastic behavior versus curing time for the neat DGEBA/MCDEA system at 140 °C, measured at 1 Hz, is shown in Fig. 4.

It is well known that the simplest method for the estimation of gelation times from rheological measurements is the divergence of the η^* (Tercjak et al. 2006). As can be clearly observed in Fig. 4, the divergence of the η^* magnitude occurs at about 250 min, which is in good agreement with the gelation time reported for the DGEBA/MCDEA system (Eloundou et al. 1996, 1998; Girard-Reydet et al. 1995). The gelation time is also in good agreement with the gelation time determined by Serrano et al. (2007) using differential scanning calorimetry (DSC) measurement (following the protocol described by Eloundou et al. (1996, 1998) and by Girard-Reydet et al. (1995)) at a degree of conversion of 0.59 by fitting the experimental conversion evolution to the model used by Eloundou et al. (1996) at 140 and 160 °C. Similar results were also obtained by Girard-Reydet et al. (1995). Here it should be pointed out that the divergence of the complex viscosity is in good agreement with the intersection of the G' and G'' . As was mentioned in the Introduction section, the use of this intersection like a criterion for the precise determination of the gelation process, according with the Winter and Chambon criterion (Winter 1987; Winter and Chambon 1986; Chambon et al. 1986; Chambon and Winter 1985, 1987), is valid only for some kind of stoichiometrically balanced networks.

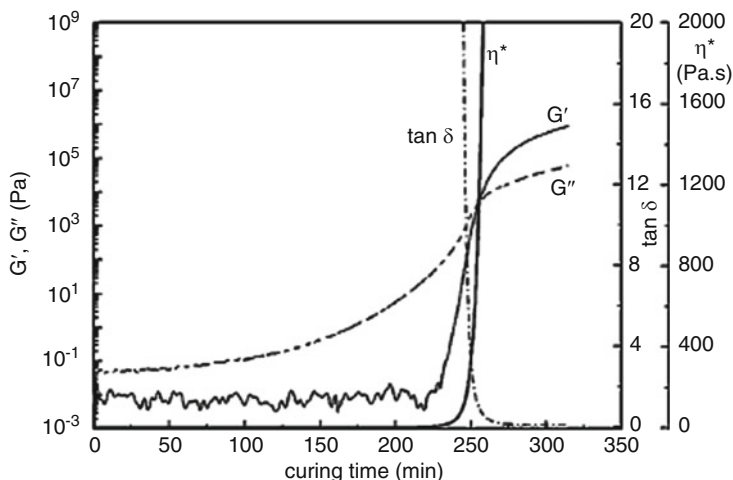


Fig. 4 Viscoelastic properties measured at 1 Hz during isothermal curing at 140 °C for the neat DGEBA/MCDEA system: storage shear modulus, G' , loss shear modulus, G'' , complex viscosity, η^* , and loss tangent ($\tan \delta$) profiles versus curing time (Reproduced with permission of (Serrano et al.), copyright 2007 Wiley-VCH Verlag GmbH & Co. KGaA)

The complex viscosity profiles and the evolution of the storage and loss moduli as a function of curing reaction time measured at 1 Hz during isothermal curing at 140 °C for the neat DGEBA/MCDEA system and its epoxy/block copolymer blends containing 10 and 30 wt% eSB46 and 30 wt% SB block copolymer are shown in Fig. 5a, b, respectively. As can be clearly observed, the gelation process of SB-(DGEBA/MCDEA) systems is slightly faster (around 10 min) compared to the gelation process of neat DGEBA/MCDEA system.

Moreover, an increase in the magnitude of both η^* (inset in Fig. 5a) and the G' and G'' moduli (Fig. 5a) can be clearly detected before gelation (at around 120 min) and can be directly linked with macrophase separation of SB block copolymer in SB-(DGEBA/MCDEA) system modified with SB block copolymer without epoxidation. The rheological behavior of the SB-(DGEBA/MCDEA) system reported by Serrano et al. (2007) was in good agreement with the final morphology of this system. Thus, the addition of 30 wt% SB without previous epoxidation of PB block led to opaque epoxy/block copolymer blends with macrophase separated an inverted morphology, where epoxy-cured particles are dispersed in a continuous SB block copolymer matrix, which could explain the acceleration of the epoxy polymerization rate in this system, in comparison with the neat epoxy system, and also the increase of the viscosity profile upon phase separation. These results are in good agreement with those published by Tercjak et al. (2006), Meynie et al. (2004) and Cassagnau et al. (Cassagnau and Fenouillot 2004).

Similarly to the SB-(DGEBA/MCDEA) system, an increase in the magnitude of both η^* and the G' and G'' moduli was also detected for eSB-(DGEBA/MCDEA) systems just before chemical gelation of these systems. This fluctuation in the complex viscosity and G' and G'' moduli before gelation can be associated with microphase separation of the PS block of SB block copolymer, thus confirming the

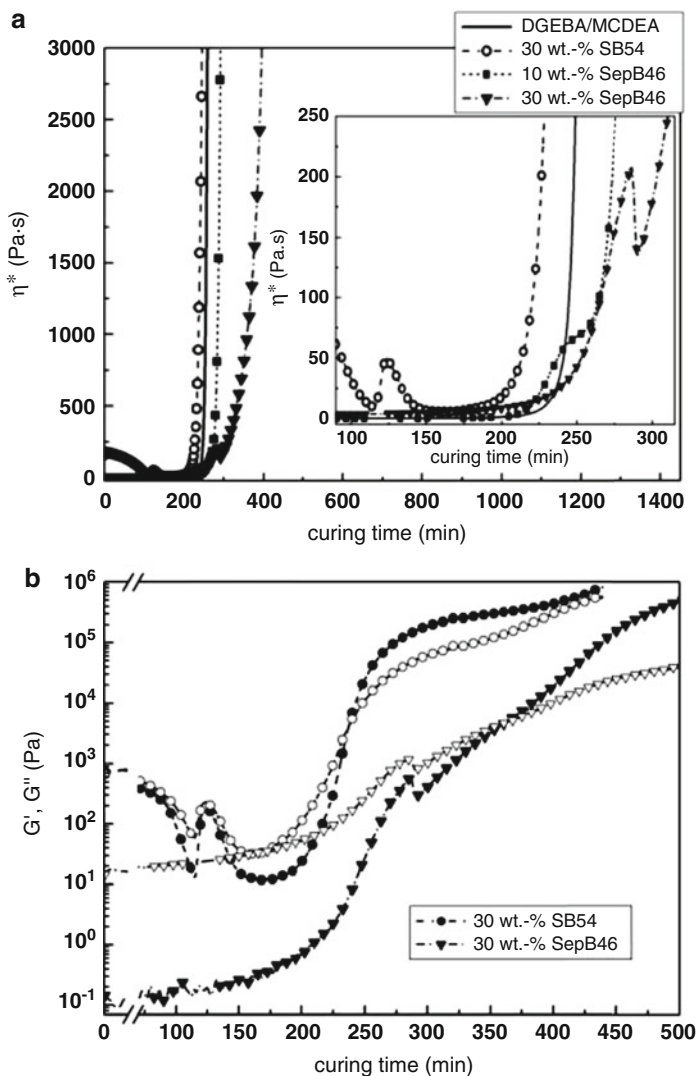


Fig. 5 Viscoelastic properties measured at 1 Hz during isothermal curing at 140 °C for the neat DGEBA/MCDEA system and its epoxy/block copolymer blends containing 10 and 30 wt% eSB46, as well as 30 wt% SB block copolymers: (a) complex viscosity, η^* , profile versus curing time and (b) evolution of storage shear modulus, G' , (full symbols) and loss shear modulus, G'' , (open symbols) versus curing time for 30 wt% modified systems (Reproduced with permission of (Serrano et al.), copyright 2007 Wiley-VCH Verlag GmbH & Co. KGaA)

formation of nanostructures in eSB-(DGEBA/MCDEA) systems occurs through reaction-induced microphase separation. The onset of the phase separation in the rheological measurement takes place at around 220 and 270 min for DGEBA/MCDEA system modified with 10 and 30 wt% eSB, respectively.

The driving force for the reaction-induced microphase separation of PS blocks is the decrease in the entropic contribution to the free energy of mixing with the occurrence of cross-linking reactions, that is to say, the microphase separation of the PS block was driven by the increased molecular weight of the system due to polymerization.

As reported for PS-(DGEBA/MCDEA) systems, the formation of an inverted morphology of a PS-rich matrix through a nucleation and growth mechanism (Meynie et al. 2004; Cassagnau and Fenouillot 2004) provokes an acceleration of the polymerization process. In the case when amphiphilic diblock copolymers are used instead of the thermoplastic homopolymer, phase separation of the PS domains takes place at the nanoscale level. Consequently, the reaction-induced microphase separation could be different from the analogue case of macroscopic phase separation. It is proposed that the formation of nanostructures through reaction-induced phase separation could be governed by two factors: the competitive kinetics (or dynamics) between phase separation and polymerization and the confinement of the miscible block with microphase separated block of the block copolymers (Meng et al. 2006). Moreover, an increase in η^* has been detected for epoxy/PS homopolymer blends as a consequence of an inverted morphology (Meng et al. 2006). Here it should be pointed out that for PS microseparated thermosetting blends, this increase in η^* can be related to the fact that the compatibilization effect of the epoxidized PB block is a competition between the PS and epoxy chains, due to their affinity with the epoxidized PB chains, which can reduce the mobility of the epoxy chains.

Rheological behavior of eSB-(DGEBA/MCDEA) systems modified with 30 wt% eSB37 and eSB46 block copolymers, reported by Serrano et al. (2007), is in good agreement with the morphology of this systems detected by transmission electron microscopy (TEM) shown in Fig. 6. TEM images of these epoxy/block copolymer blends confirmed the microphase separation of the PS block of eSB block copolymer leading to nanostructured epoxy systems.

Additionally, both rheology and TEM results are supported by the results obtained by dynamic-mechanical analysis (DMA) shown in Fig. 7. DMA measurements allow to detect three transitions with an increase of the temperature: β relaxation of the epoxy-rich phase in the low-temperature range (not shown in Fig. 7) and two α relaxations associated with the T_g of the PS block of SB block copolymer and the epoxy-rich phase, thus supporting the self-assembly due to the microphase separation of the PS block (Serrano et al. 2006). The interesting point is that α relaxation of the epoxy-rich phase in 30 wt% eSB-(DGEBA/MCDEA) systems appears at temperatures slightly higher than expected by assuming exclusively miscibility between the epoxy-rich and epoxidized PB block, thus suggesting some reactivity of the epoxidized PB units with the thermosetting formulation.

Rheology of the Epoxy/Epoxidized SBS Block Copolymer Blends

The rheology of the epoxy/poly(styrene-*b*-butadiene-*b*-styrene) (SBS) triblock copolymer epoxidized with 47 mol% degree of epoxidation (eSBS47) was studied by George et al. (2014). In this case, diglycidyl ether of bisphenol A (DGEBA) was

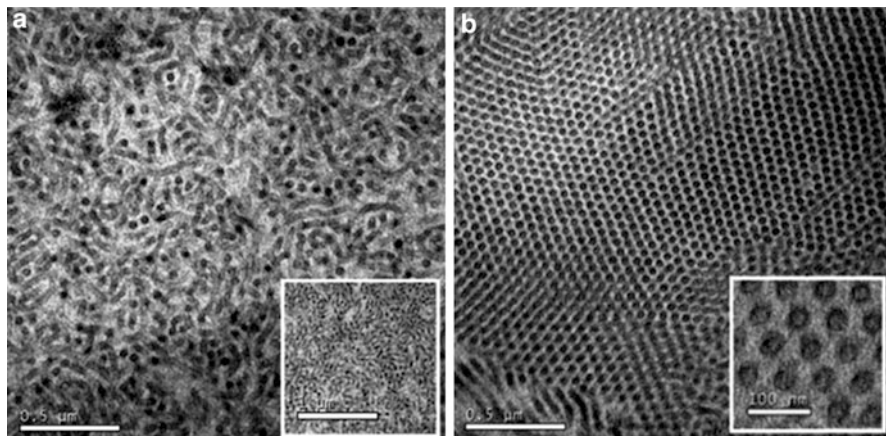


Fig. 6 TEM images of eSB-(DGEBA/MCDEA) cured systems containing 30 wt% of (a) eSB37 and (b) SepB46 block copolymer. The samples were stained with RuO₄ for 4 min (scale bar = 0.5 μm). The insets in parts (a) and (b) show TEM images at lower (scale bar = 1 μm) and high (scale bar = 100 nm) magnification for eSB-(DGEBA/MCDEA) cured systems modified with 30 wt% eSB37 and eSB46, respectively (Reproduced with permission of (Serrano et al.), copyright 2007 Wiley-VCH Verlag GmbH & Co. KGaA)

used as epoxy resin and 4,4'-diaminodiphenylmethane (DDM) as a curing agent. The rheological characterization of these systems was carried out using an ARES Rheometric Scientific, and the authors studied the rheological behavior of the investigated eSBS47-(DGEBA/DDM) systems at 130 °C during thermosetting network formation. Time dependences of the complex viscosity (η^*), storage modulus (G'), and loss modulus (G'') at 130 °C are shown in Fig. 8.

As clearly visualized in Fig. 8a, 10 and 20 wt% eSBS47-(DGEBA/DDM) systems showed additional fluctuation in the η^* before gelation point compared to the η^* of neat DGEBA/DDM system. This increase in the viscosity can be related to the phase separation of eSBS47 induced by curing reaction during increase of the curing reaction time. Thus, variation in η^* and G' and G'' before gelation can be used as criteria for the identification of phase separation (Tercjak et al. 2006; Serrano et al. 2007; Jyotishkumar et al. 2011, 2012; Liu et al. 2012). Consequently, rheology of the DGEBA/DDM systems modified with eSBS47 suggested that initially miscible eSBS47 phase separated before gelation and the final morphologies of the systems were fixed by a cross-linking reaction. In order to prove and better understand the phase separation of eSBS47 phase in eSBS47-(DGEBA/DDM) systems during network formation, $\log G'$ and $\log G''$ in the function of the curing reaction time was also analyzed (Fig. 8b).

At the beginning of the curing reaction time of neat DGEBA/DDM system, values of $\log G'$ were lower than values of $\log G''$, indicating that investigated system was in a liquid state. An increase of the curing reaction time led to an increase of $\log G'$ and $\log G''$ up to their intersection when chemical gelation took place. At chemical gelation, $\log G'$ was equal to $\log G''$ and the DGEBA/DDM system

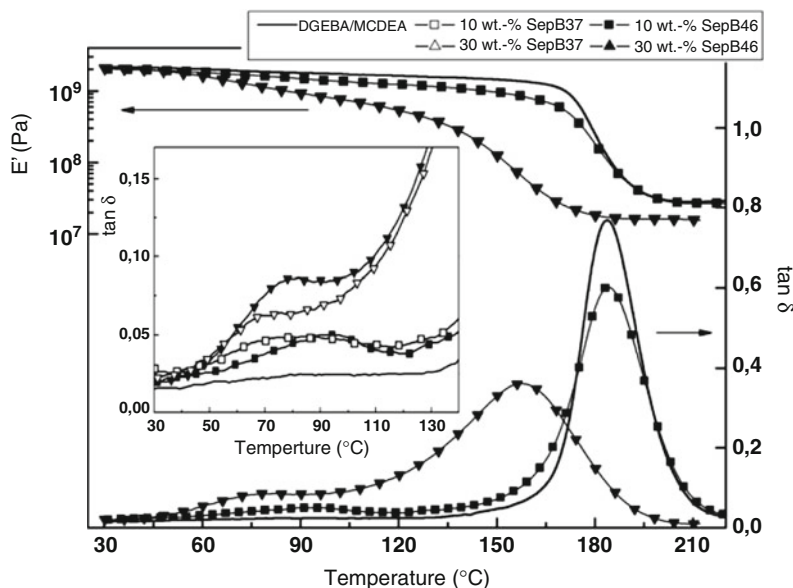


Fig. 7 Dynamic mechanical spectra in the high-temperature range obtained at 1 Hz for the neat DGEBA/MCDEA system and its epoxy/block copolymer blends containing 10 and 30 wt% eSB37 and eSB46 diblock copolymers. The inset shows a higher magnification of the $\tan\delta$ curve. The full spectrum, corresponding to eSB37-(DGEBA/MCDEA) systems, is only shown in the inset for clarity (Reproduced with permission of (Serrano et al.), copyright 2007 Wiley-VCH Verlag GmbH & Co. KGaA)

acted as both elastic and viscous phases, storing (elastic phase) and dissipating (viscous phase) equal amounts of energy (Jyotishkumar et al. 2012). After the crossover point, the epoxy behaved as a solid material as a result of the formation of three-dimensional cross-linked thermosetting network. On the contrary to rheological profile of neat DGEBA/DDM system, the system modified with eSBS47 followed a different trend. As clearly observed in Fig. 8b, the $\log G'$ and $\log G''$ correspond to 20 wt% eSBS47-(DGEBA/DDM) system started to increase before the chemical gelation. In other words, the crossover point shifted to a shorter time for 20 wt% eSBS47-(DGEBA/DDM) system compared to neat DGEBA/DDM system. One can attribute the crossover of $\log G'$ and $\log G''$ of the epoxy/eSBS47 blend systems not to chemical gelation but to physical gelation, which took place due to phase separation confirming the formation of nanostructures as a consequence of reaction-induced phase separation. Here it should be pointed out that both $\log G'$ and $\log G''$ crossed over only once for 20 wt% eSBS47-(DGEBA/DDM) system, suggesting that the chemical gelation of these system might be overlapped by the physical gelation process.

The rheology of neat DGEBA/DDM system and the eSBS47-(DGEBA/DDM) systems modified with 10 and 20 wt% eSBS47 is in good agreement with their final morphologies studied by transmission electron microscopy (TEM), as shown in

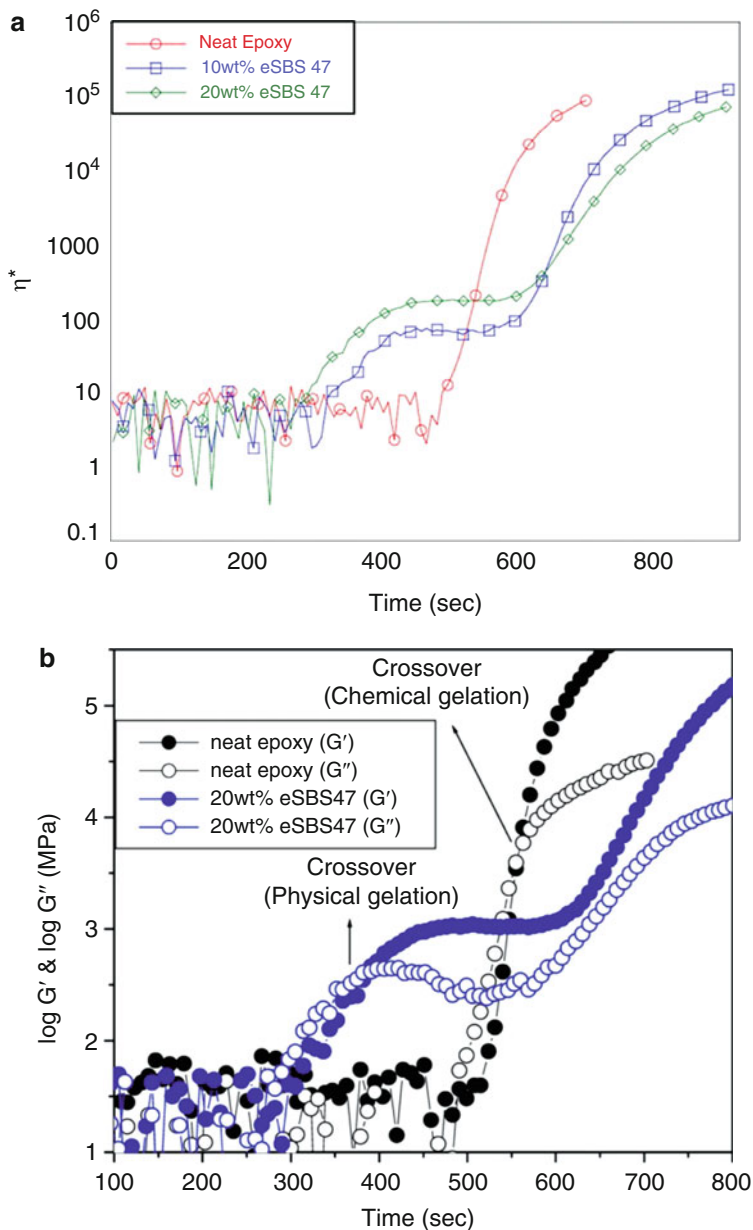


Fig. 8 (a) Changes in the complex viscosities of neat epoxy and eSBS47-modified epoxy blends at 130 °C. (b) Storage and loss modulus curves of neat DGEBA/DDM epoxy and eSBS47-modified epoxy blends at 130 °C (Reproduced with permission of (George et al.), copyright 2014 American Chemical Society)

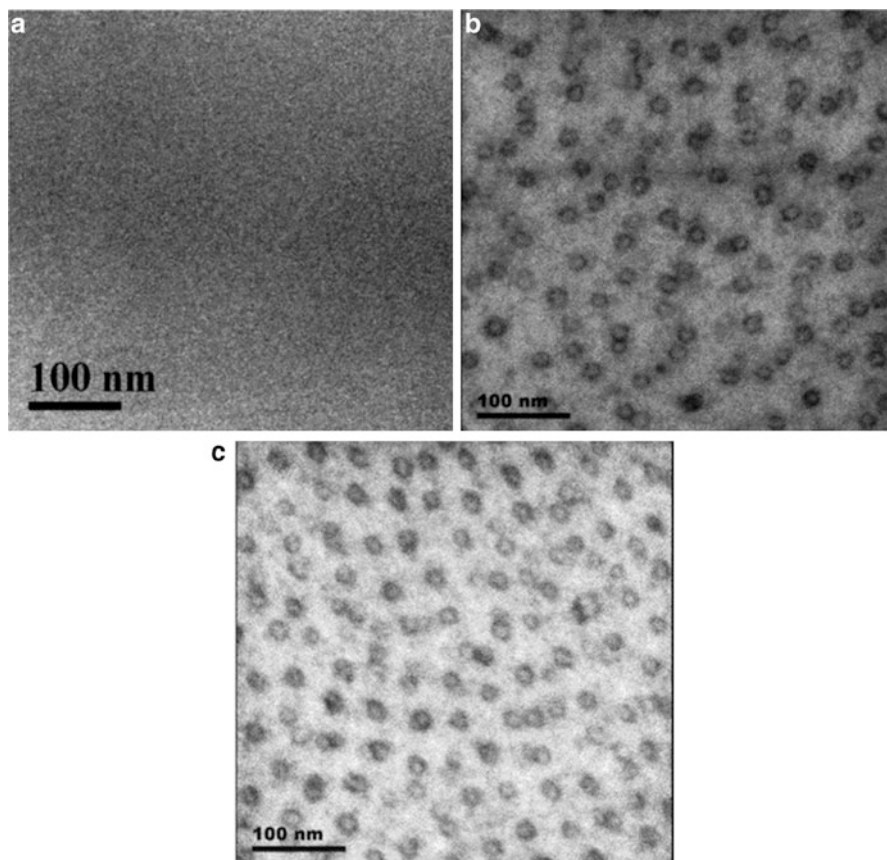


Fig. 9 HR-TEM images of (a) neat DGEBA/DDM system and (b) 10 and (c) 20 wt% eSBS47-(DGEBA/DDM) (Reproduced with permission of (George et al.), copyright 2014 American Chemical Society)

Fig. 9. As expected, neat DGEBA/DDM system showed the homogenous morphology on the contrary to the 10 and 20 wt% eSBS47-(DGEBA/DDM) system where microphase-separated domains with an average diameter of around 15 nm in size are clearly visualized. As pointed out by George et al. (2014), the microphase-separated domains correspond to PS block-rich phase. The authors have proved a strong relation between the rheological behavior of eSBS47-(DGEBA/DDM) systems during the curing reaction and the final morphology of systems investigated by them.

George et al. (2015) have studied also rheology of 10 wt% eSBS-(DGEBA/DDM) systems with eSBS triblock copolymer with different epoxidation degree (0, 26, 39, and 47% mol). The authors performed both dynamic and isothermal measurement using ARES rheometer to better understand the effect of epoxidation of eSBS triblock copolymer on the viscoelastic behavior of 10 wt% eSBS-(DGEBA/DDM) systems during thermosetting network formation. They have monitored changes in η^* as a

function of temperature. At the beginning of the curing reaction time, the viscosity of the eSBS/epoxy blends increased with the increase of the epoxidation degree. This phenomenon can be related to the fact that using the high-molecular-weight-epoxidized SBS led to an increase in their compatibility with DGEBA/DDM epoxy matrix due to the formation of the hydrogen bonds between unreacted epoxy group and the epoxidized PB block of SBS block copolymer (Serrano et al. 2007, 2009; George et al. 2012). At around 160 °C, an abrupt increase in viscosity occurred due to the gelation. In this case, authors have detected small fluctuation in viscosity prior to the sharp increase related to the gelation of thermosetting network. This fluctuation related to microphase separation of PS block of SBS with 39 and 47 mol% epoxidation degrees appeared just before gelation point as was also proved in other reported works (Tercjak et al. 2006; Serrano et al. 2007; Jyotishkumar et al. 2011, 2012; Liu et al. 2012). Thus, the viscosity behavior of the epoxy/block copolymer blends depends strongly on the reaction-induced phase separation process of immiscible block of block copolymer and vice versa. The authors have also confirmed that similar trends can be observed for DGEBA/DDM system modified with different content of eSBS47 triblock copolymer (10, 20 and 30 wt%) (George et al. 2014, 2015). Increase of eSBS47 in the epoxy/block copolymer blends led to an increase of the fluctuation in the viscosity around 160 °C priori to gelation of investigated eSBS47-(DGEBA/DDM) system. The viscosity fluctuations have a strong influence on the final morphology of epoxy/block copolymer blends as proved also by Tercjak et al. (2006) and Serrano et al. (2007). In order to better understand this correlation between viscoelastic behavior of epoxy/block copolymers and final morphology of thermosetting systems, George et al. (2015) have also studied the isothermal time dependence η^* as a widely accepted method to comprehend the structure generated in epoxy blends during thermosetting network formation. In their previous work, they performed rheology measurement at three different temperatures 90 °C, 110 °C, and 130 °C (George et al. 2014, 2015). At the beginning, the η^* slowly increased with the curing reaction time, and then a very rapid increase was detected as a consequence of chemical gelation of investigated thermosetting networks. Here it should be mentioned that as was expected, the gelation point shifted to shorter reaction times with an increase in the curing temperature. This phenomenon can be related to the fact that at higher curing temperature the epoxy amine reaction is faster leading to shorter gelation times. These results are in good agreement with calorimetric measurement, which proved that addition of the block copolymers to the epoxy systems delays curing reaction (Gutierrez et al. 2010, 2011; Ocando et al. 2007; Serrano et al. 2006; Tercjak et al. 2008; Cano et al. 2014).

Rheology of the Epoxy/PS-b-PEO Block Copolymer Blends Modified with Low-Molecular-Weight Liquid Crystals

Tercjak et al. (2008) have studied the rheology of epoxy/poly(styrene-b-ethylene oxide) block copolymer (PS-b-PEO) blends. The selected thermosetting system was the diglycidyl ether bisphenol-A (DGEBA) as epoxy resin cured with 4,4'-methylenebis (3-chloro,2,6-diethylaniline) (MCDEA) as a curing agent.

Additionally, this system was modified also with 4'-(hexyl)-4-biphenyl-carbonitrile (HBC) low-molecular-weight liquid crystal. The rheology measurement was performed using a Rheometrics Ares rheometer equipped with parallel plates

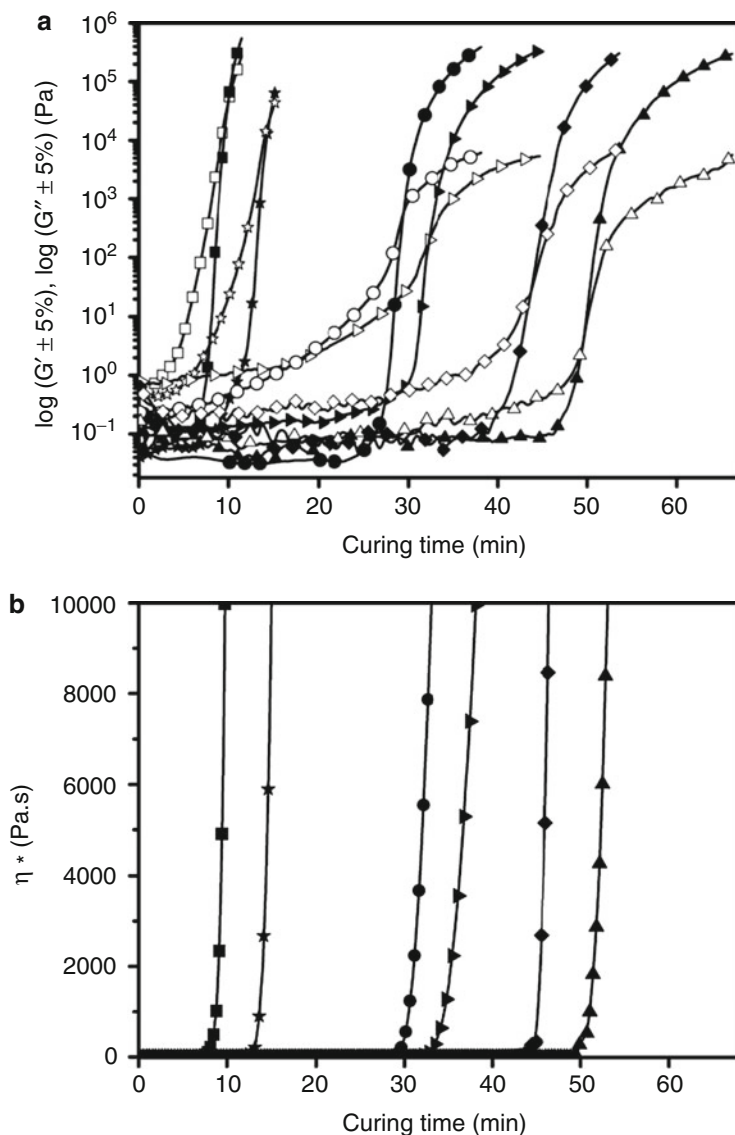


Fig. 10 Viscoelastic properties of neat DGEBA/MXDA system and its blends containing different PS-b-PEO or/and HBC contents. (a) Storage shear modulus, G' (filled symbols), and loss shear modulus, G'' (open symbols), versus curing time and (b) complex viscosity profile versus curing time (Reproduced with permission of (Tercjak et al.), copyright 2008 Elsevier)

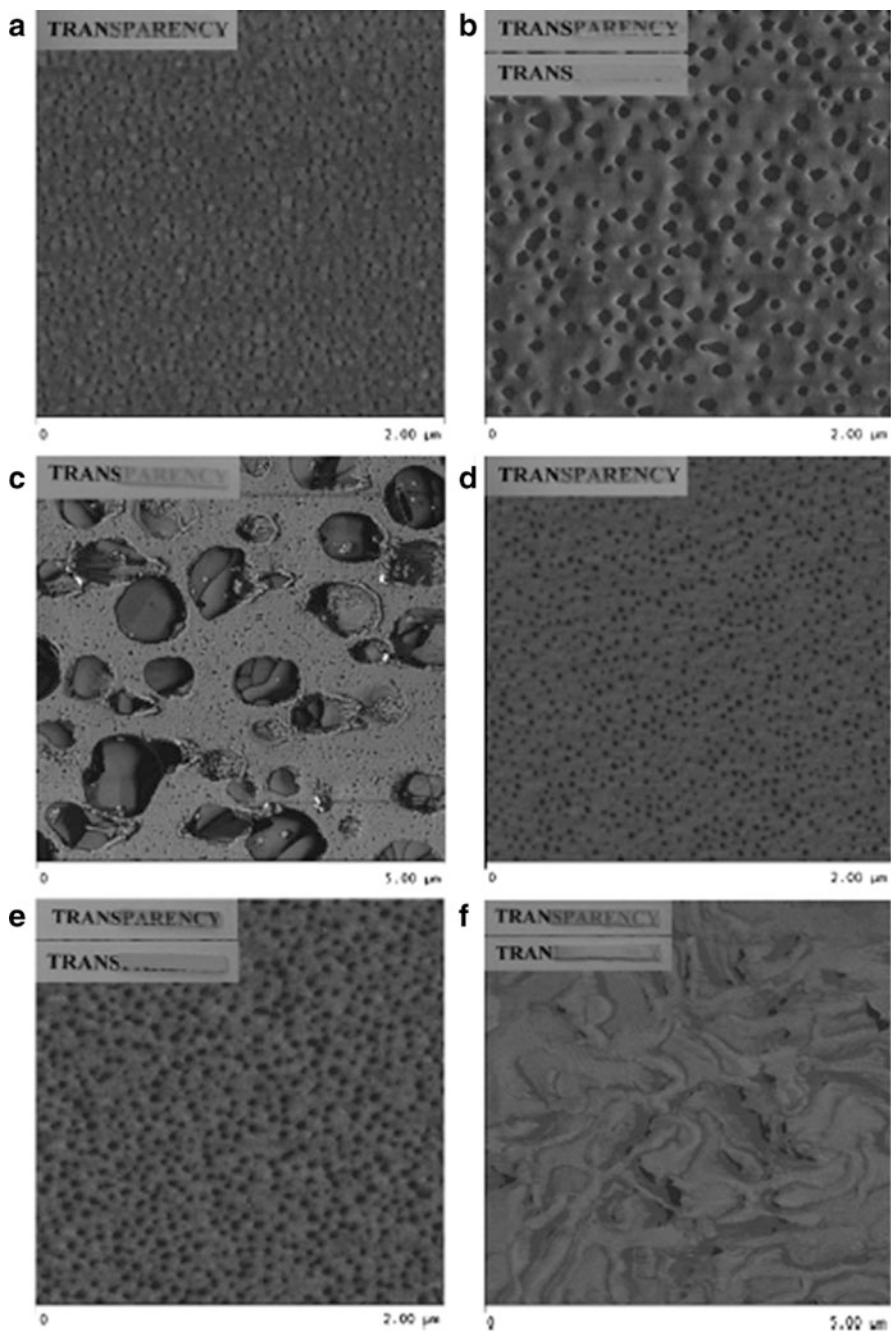


Fig. 11 AFM phase images of the DGEBA/MXDA systems modified with different PS-b-PEO or/and HBC contents: (a) 5 wt% PS-b-PEO, (b) 5 wt% PS-b-PEO-30 wt% HBC, (c) 5 wt%

of 50 and 25 mm diameter (upper and lower plate, respectively). Dynamic oscillatory shear measurements were performed at 80 °C as a function of curing time at a constant frequency of 1 Hz.

The evolution of G' and G'' moduli and complex viscosity profiles measured for the neat DGEBA/MXDA system and its epoxy/PS-*b*-PEO block copolymer or/and HBC liquid crystal are shown in Fig. 10. As can be clearly observed, for neat DGEBA/MXDA system, the magnitude of both G' and G'' moduli intersected at around 9 min. This time was in good agreement with the abrupt increase of complex viscosity and slightly shorter than those determined by DSC, which clearly indicates that the system reaches the gel point. Similar tendency of epoxy/block copolymer blends is described in sections “[Rheology of the Epoxy/Epoxidized SB Block Copolymer Blends](#)” and “[Rheology of the Epoxy/Epoxidized SBS Block Copolymer Blends](#).”

As is mentioned in Introduction section, even if various methods are available to determine the gelation point, the simplest one is based on an extrapolation of η^* to infinity (Macosko 1994) and the point of intersection of the dynamic storage and dynamic loss moduli (Tung and Dynes 1982; Winter 1987; Winter and Chambon 1986; Chambon et al. 1986; Chambon and Winter 1985, 1987), the last one valid only for some stoichiometric balanced networks.

The addition of PS-*b*-PEO block copolymers does not significantly hinder the gelation process of DGEBA/MXDA epoxy system. As is well known, microphase separation of PS-block can affect the viscoelastic behavior of PS-*b*-PEO-(DGEBA/MXDA) system during curing formation resulting in an increase of values of both G' and G'' moduli and complex viscosity magnitudes. However, for the investigated system, polymerization-induced microphase separation does not have influence on the viscoelastic behavior probably due to both low content of PS-*b*-PEO block copolymer with respect to whole composition and low molecular weight of the PS-block in the PS-*b*-PEO block copolymers. Here it should be pointed out that even if the phase separation of the PS block of PS-*b*-PEO block copolymer was not detected during rheological measurement, the 5 wt% PS-*b*-PEO-(DGEBA/MCDEA) investigated system was microphase separated as shown in Fig. 11 by means of atomic force microscopy (AFM).

Conclusions

This chapter deals with rheology of the epoxy/block copolymer blends showing different examples of use of a rheology measurement to determine viscoelastic behavior of epoxy blends during thermosetting network formation. Time or



Fig. 11 (continued) PS-*b*-PEO-50 wt% HBC, (d) 10 wt% PS-*b*-PEO, (e) 10 wt% PS-*b*-PEO-30 wt% HBC, and (f) 10 wt% PS-*b*-PEO-50 wt% HBC. The inset shows digital images of the transparency of the blends at room temperature and, in case of the thermoreversible blends, at room temperature and at -10 °C, top and bottom, respectively (Reproduced with permission of (Tercjak et al.), copyright 2008 Elsevier)

temperature dependence complex viscosity, η^* , dynamic storage modulus, G' , and dynamic loss modulus, G'' , allow to better understand the phase separation of immiscible block of the block copolymer during reaction-induced phase separation. Moreover, rheology of the epoxy/block copolymer blends provided also information about gelation, vitrification, and others.

Strong relationship between phase separation detected following the viscoelastic behavior of the epoxy/block copolymer blends during curing reaction, and the final morphology of these epoxy blends was also showed. The correlation between block copolymer content in epoxy/block copolymer blends and the ability to detect the microphase separation during monitoring of viscoelastic behavior of epoxy-based blends was showed.

Finally, we proved that knowledge about the rheology of epoxy/block copolymer blends is crucial to understand phase separation of the blocks of block copolymer during thermosetting network formation.

References

- Bonnet A, Pascault JP, Sautereau H, Camberlin Y (1999) Epoxy-diamine thermoset/thermoplastic blends. 2. Rheological behavior before and after phase separation. *Macromolecules* 32:8524–8530
- Bytner O, Smith GD (2002) Viscoelastic properties of polybutadiene in the glassy regime from molecular dynamic simulations. *Macromolecules* 35:3769–3771
- Cano L, Builes DH, Tercjak A (2014) Morphological and mechanical study of nanostructured epoxy systems modified with amphiphilic poly(ethylene oxide-b-propylene oxide-b-ethylene oxide)triblock copolymer. *Polymer* 55:738–745
- Cassagnau P, Fenouillot F (2004) Rheological study of mixing in molten polymers: 2-mixing of reactive systems. *Polymer* 45:8031–8040
- Castro JM, Macosko CW, Perry SJ (1984) Viscosity changes during urethane polymerization with phase separation. *Polym Commun* 25:82–87
- Chambon F, Winter HH (1985) Stopping of crosslinking reaction in a PDMS polymer at the gel point. *Polym Bull* 13:499–503
- Chambon F, Winter HH (1987) Linear viscoelasticity at the gel point of a crosslinking PDMS with imbalanced stoichiometry. *J Rheol* 31:683–697
- Chambon F, Petrovic ZS, Mac Knight WJ, Winter HH (1986) Rheology of model polyurethanes at the gel point. *Macromolecules* 19:2146–2149
- Eloundou JP, Gerard JF, Harran D, Pascault JP (1996) Temperature dependence of the behavior of a reactive epoxy-amine system by means of dynamic rheology. 2. High-Tg epoxy-amine system. *Macromolecules* 29:6917–6927
- Eloundou JP, Ayina O, Nga NH, Gerard JF, Pascault JP, Boiteux G, Seytre G (1998) Simultaneous kinetic and microdielectric studies of some epoxy-amine systems. *J Polym Sci Part B Polym Phys* 36:2911–2921
- Fine T, Lortie F, David L, Pascault J-P (2005) Structures and rheological properties of reactive solutions of block copolymers. Part I. Diblock copolymers in a liquid epoxy monomer. *Polymer* 46:6605–6613
- George SM, Puglia D, Kenny JM, Jyotishkumar P, Thomas S (2012) Cure kinetics and thermal stability of micro and nanostructured thermosetting blends of epoxy resin and epoxidized styrene-block-butadiene-block-styrene triblock copolymer systems. *Polym Eng Sci* 52:2336–2347

- George SM, Puglia D, Kenny JM, Parameswaranpillai J, Thomas S (2014) Reaction-induced phase separation and thermomechanical properties in epoxidized styrene-block-butadiene-block-styrene triblock copolymer modified epoxy/DDM system. *Ind Eng Chem Res* 53:6941–6950
- George SM, Puglia D, Kenny JM, Parameswaranpillai J, Vijayan PP, Pionteck J, Thomas S (2015) Volume shrinkage and rheological studies of epoxidised and unepoxidised poly(styrene-blockbutadiene-block-styrene) triblock copolymer modified epoxy resin–diamino diphenyl methane nanostructured blend systems. *Phys Chem Chem Phys* 17:12760–12770
- Girard-Reydet E, Riccardi CC, Sautereau H, Pascault JP (1995) Epoxy-aromatic diamine kinetics. Part 1. Modeling and influence of the diamine structure. *Macromolecules* 28:7599–7607
- Gutierrez J, Tercjak A, Mondragon I (2010) Transparent nanostructured thermoset composites containing well-dispersed TiO₂ nanoparticles. *J Phys Chem C* 114:22424–22430
- Gutierrez J, Mondragon I, Tercjak A (2011) Morphological and optical behavior of thermoset matrix composites varying both polystyrene-block-poly(ethylene oxide) and TiO₂ nanoparticle content. *Polymer* 52:5699–5707
- Harran D, Laudouard A (1986) Rheological study of the isothermal reticulation of an epoxy resin. *J Appl Polym Sci* 32:6043–6062
- Ishii Y, Ryan AJ (2000) Processing of poly(2,6-dimethyl-1,4-phenylene ether) with epoxy resin. 1. Reaction-induced phase separation. *Macromolecules* 33:158–166
- Jyotishkumar P, Pionteck J, Ozdilek C, Moldenaers P, Thomas S (2011) Rheology and pressure-volume-temperature behavior of the thermoplastic poly(acrylonitrile-butadiene-styrene)-modified epoxy-DDS system during reaction induced phase separation. *Soft Matter* 7:7248–7256
- Jyotishkumar P, Moldenaers P, George SM, Thomas S (2012) Viscoelastic effects in thermoplastic poly(styrene-acrylonitrile)-modified epoxy-DDM system during reaction induced phase separation. *Soft Matter* 8:7452–7462
- Kim H, Char K (2000) Effect of phase separation on rheological properties during the isothermal curing of epoxy toughened with thermoplastic polymer. *Ind Eng Chem Res* 39:955–959
- Liu Y, Zhong XH, Zhan GZ, Yu YF, Jin JY (2012) Effect of mesoscopic fillers on the polymerization induced viscoelastic phase separation at near- and off-critical compositions. *J Phys Chem B* 116:3671–3682
- Macosko CW (1994) *Rheology: principles, measurements and applications*. Wiley-VCH, New York
- Meng F, Zheng S, Zhang W, Li H, Liang Q (2006) Nanostructured thermosetting blends of epoxy resin and amphiphilic poly(ϵ -caprolactone)-block-polybutadiene-block-poly(ϵ -caprolactone) triblock copolymer. *Macromolecules* 39:711–719
- Meynie L, Fenouillot F, Pascault JP (2004) Polymerization of a thermoset system into a thermoplastic matrix. Effect of the shear. *Polymer* 45:1867–1877
- Mortimer S, Ryan AJ, Stanford JL (2001) Rheological behavior and gel-point determination for a model lewis acid-initiated chain growth epoxy resin. *Macromolecules* 34:2973–2980
- Mustata F, Bicu J (2001) Rheological and thermal behaviour of DGEBA/EA and DGEHQ/EA epoxy systems crosslinked with TETA. *Polym Testing* 20:533–538
- Ocando C, Serrano E, Tercjak A, Pena C, Kortaberria G, Calberg C, Grignard B, Jerome R, Carrasco PM, Mecerreyes D, Mondragon I (2007) Structure and properties of a semifluorinated diblock copolymer modified epoxy blend. *Macromolecules* 40:4068–4074
- Pascault JP, Williams RJJ (2010) *Epoxy polymers: new materials and innovations*. Wiley-VCH, Weinheim
- Pichaud S, Duteurtre X, Fit A, Stephan F, Maazouz A, Pascault JP (1999) Chemorheological and dielectric study of epoxy-amine for processing control. *Polym Int* 48:1205–1218
- Poncet S, Boiteux G, Pascault JP, Sautereau H, Seytre G, Rogozinski J, Kranbuehl D (1999) Monitoring phase separation and reaction advancement in situ in thermoplastic/epoxy blends. *Polymer* 40:6811–6820
- Serrano E, Tercjak A, Kortaberria G, Pomposo JA, Mecerreyes D, Zafeiropoulos NE, Stamm M, Mondragon I (2006) Nanostructured thermosetting systems by modification with epoxidized

- styrene-butadiene star block copolymers. Effect of epoxidation degree. *Macromolecules* 39:2254–2261
- Serrano E, Tercjak A, Ocando C, Larrañaga M, Parellada MD, Corona-Galván S, Mecerreyes D, Zafeiropoulos NE, Stamm M, Mondragon I (2007) Curing behaviour and final properties of nanostructured thermosetting systems modified with epoxidized styrene-butadiene linear diblock copolymers. *Macromol Chem Phys* 208:2281–2292
- Serrano E, Kortaberria G, Tercjak A, Mondragon I (2009) Molecular dynamics of an epoxy resin modified with an epoxidized poly(styrene-butadiene) linear block copolymer during cure and microphase separation processes. *Europ Polym J* 45:1046–1057
- Tercjak A, Remiro PM, Mondragon I (2005) Phase separation and rheological behavior during curing of an epoxy resin modified with syndiotactic polystyrene. *Polym Eng Sci* 45:303–313
- Tercjak A, Serrano E, Remiro PM, Mondragon I (2006) Viscoelastic behavior of thermosetting epoxy mixtures modified with syndiotactic polystyrene during network formation. *J Appl Polym Sci* 100:2348–2355
- Tercjak A, Serrano E, Garcia I, Mondragon I (2008) Thermoresponsiveness/nanostructured thermosetting materials based on PS-*b*-PEO block copolymer-dispersed liquid crystal: curing behavior and morphological variation. *Acta Mater* 56:5112–5122
- Tung CYM, Dynes PJ (1982) Relationship between viscoelastic properties and gelation in thermosetting systems. *J Appl Polym Sci* 32:569–574
- Winter HH (1987) Can the gel point of a crosslinking polymer be detected by the G' - G'' crossover? *Polym Eng Sci* 27:1698–1702
- Winter HH (2000) *Experimental methods in polymer science*. Academic, San Diego
- Winter HH (2007) Evolution of rheology during chemical gelation. *Prog Colloid Polym Sci* 75:104–110
- Winter HH, Chambon F (1986) Analysis of linear viscoelasticity of a crosslinking polymer at the gel point. *J Rheol* 30:367–382
- Yu Y, Wang M, Gan W, Tao Q, Li K (2004) Polymerization-induced viscoelastic phase separation in polyethersulfone-modified epoxy systems. *J Phys Chem B* 108:6208–6215

Connie Ocando, Raquel Fernandez, M^a Angeles Corcuera,
and Arantxa Eceiza

Abstract

This chapter deals with the study of the cure kinetics of epoxy/block copolymer blends in order to give a comprehensive account about the effect of adding this kind of modifier on the reaction rate of the network formation. Non-isothermal runs at constant heating rates and isothermal runs at constant temperature were carried out in order to determine the total heats of reaction released during curing for the epoxy blends modified with different contents of block copolymers. It was found a clearly delay of cure kinetics with the increase of block copolymer content. In order to understand the parameters affecting epoxy curing kinetics, the influence of block copolymer blocks chemical structure, and the molar ratio between blocks on the curing rate was also analyzed. Fourier transform infrared spectroscopy was used for this purpose. The experimental curves of isothermal curing were fitted to a phenomenological autocatalytic model and also to mechanistic model. Kinetics parameters were calculated from the previous models. The increase observed in activation energy values with the increase of block copolymer content corroborated that the physical interactions between the block copolymer and the epoxy significantly affect the curing behavior, agreeing with the observed delay.

C. Ocando (✉)

Laboratoire De Physique Des Surfaces Et Des Interfaces, Université De Mons-UMONS, Mons, Belgium

e-mail: connie.ocandocordero@umons.ac.be

R. Fernandez • M.A. Corcuera • A. Eceiza

Group 'Materials + Technologies', Department of Chemical and Environmental Engineering, Polytechnic School, University of the Basque Country, Donostia-San Sebastián, Spain

e-mail: raquel.fernandez@ehu.eus; marian.corcuera@ehu.eus; arantxa.eceiza@ehu.eus

Keywords

Epoxy blends • Block copolymer • Cure kinetics • Phenomenological model • Mechanistic model

Contents

Introduction	980
Non-isothermal DSC Analyses	983
Isothermal DSC Analyses	988
Conclusions	999
References	1002

Introduction

During the curing process of a modified epoxy system, the cross-linking reactions involve a number of chemical and physical changes, while the material turns from a viscous liquid to a solid. The comprehension of the cure kinetic behavior related to the network formation permits a clear analysis of the structure/property/processing relationships that will determine the proper set of process parameters for the development of high-performance blends and composites with the best structural and morphological properties. Differential scanning calorimetry (DSC) has been widely employed to study the curing process of epoxy systems. This technique is very effective for monitoring the network formation since it permits the measurement of the amount of heat that is either absorbed or evolved during the course of polymerization reactions (i.e., epoxy–amine systems are well known as exothermic reactions). Several works have been published about DSC studies, both isothermal and non-isothermal heating mode, to determine the reaction rate curves and kinetic parameters for epoxy/amine systems (Grillet et al. 1989; Verchere et al. 1990; Cole 1991; Serier et al. 1991; Deng and Martin 1994; Girard-Reydet et al. 1995; Vyazovkin and Sbirrazzuoli 1996; Ghaemy and Khandani 1998; Karkanis and Partridge 2000; Vinnik and Roznyatovsky 2006) and their blends with thermoplastics (Bonnet et al. 1999; Varley et al. 2000; Bonnaud et al. 2000; Swier and Van Mele 2003a; Swier et al. 2005; Bejoy et al. 2006; Varley 2007; Zhang et al. 2009), rubbers (Kim and Kim 1994; Calabrese and Valenza 2003; Raju et al. 2007), and block copolymers (Swier and Van Mele 2003b, c; Larrañaga et al. 2004, 2005; Kim et al. 2005; Larrañaga et al. 2006a; George et al. 2012, 2014; Cano et al. 2014; Hu et al. 2015), among others.

Diverse mathematical models have been also applied in order to obtain a comprehensive description and simulation of the experimental cure profiles taking into account the catalytic effects and the influence of the diffusion phenomena. Modeling of the curing behavior of epoxy–amine systems can be approached both mechanistically (Mijovic et al. 1992; Mijovic and Wijaya 1994; Blanco et al. 2005; Zvetkov 2005) and phenomenologically (Ryan and Dutta 1979; Barton 1985; Roşu

et al. 2002; Du et al. 2004; Cai et al. 2008). Mechanistic models consider a complete scheme of consecutive and competitive reactions that take place during the curing process. As the cross-linking reaction of epoxy systems is very complex due to the close relationship between the chemical kinetics and changes in their physical properties, it is difficult to derive an accurate mechanistic model. Moreover, phenomena such as autocatalysis in the early stages or the effect of diffusion on the kinetic rate constants at later stages can further complicate modeling. Consequently, phenomenological approaches are preferred to study the curing kinetics of these thermosetting polymers. Phenomenological models are based on empirical or semi-empirical equations which explain the autocatalytic behavior of the epoxy–amine reaction. It should be pointed out that the unmodified epoxy–amine curing reaction is well known as an autocatalytic mechanism (Smith 1961; Riccardi et al. 1984; Xu et al. 1994). The autocatalysis in epoxy–amine reaction is attributed to a termolecular intermediate with hydroxyl groups produced during curing. On the other hand, the referred phenomenological models have been widely employed to study the cure kinetics because they are simple and fit experimental data with relative success.

The blending of an epoxy resin with block copolymers consisted of an epoxy phobic block and another epoxy phyllic, and/or reactive blocks that are capable to control self-assembling at the nanometer scale in the uncured and cured state have been widely explored due to their excellent properties that can be tailored after the complete network formation, such as good mechanical behavior. As it is well known, the final self-assembled morphology of epoxy/block copolymer blends depends principally on both kinetics and thermodynamic factors, such as the curing rate, the change of the viscosity during the phase separation, as well as the modifier concentration, volume fraction of each block, architecture, and molecular weight of the blocks (Lipic et al. 1998; Girard-Reydet et al. 1999, 2002; Mijovic et al. 2000; Grubbs et al. 2000; Ritzenthaler et al. 2002, 2003, Rebizant et al. 2004; Dean et al. 2003; ; Serrano et al. 2005, 2006, 2007; Meng et al. 2006; Larrañaga et al. 2006a, b; Tercjak et al. 2006; Maiez-Tribut et al. 2007; Hermel-Davidock et al. 2007; Ruiz-Pérez et al. 2008; Liu et al. 2008, 2010; Ocando et al. 2008, 2013; Garate et al. 2011, 2013; Wu et al. 2013; Liu 2013; Xu et al. 2015).

In particular, the effect of blending an epoxy–amine system with different amounts of amphiphilic block copolymers, consisted on poly(ethylene oxide)-b-poly(propylene oxide)-b-poly(ethylene oxide) (PEP–PPO–PEO) with differing volume fractions of PEO block, on the cure kinetics during the network formation has been systematically studied (Larrañaga et al. 2004, 2005, 2006a). It is possible to point out that epoxy–amine systems blended with poly(ethylene oxide) homopolymer (PEO) lead to a miscible material owing to the fact that the OH groups, developed during the network formation of the growing epoxy matrix, interact by hydrogen bonding with the ether oxygen of PEO avoiding phase separation (Larrañaga et al. 2007), whereas the poly(propylene oxide) (PPO) tends to phase separate from the forming epoxy network as the molecular weight is increased by curing reaction. Nevertheless, as the miscibility between polymers is also governed

by the temperature of blending and composition, the control of both the reaction and the phase separation rate for a given modifier through the selection of an appropriate curing cycle (temperature vs. time) permits a fine-tune of the self-assembled morphologies (Liu 2013). Concerning this last argument, it was found that the phase separation in epoxy/PEO–PPO–PEO block copolymer blends at micro- or nanoscale depends mainly on the PEO content and curing temperature (Larrañaga et al. 2005). In addition, the cure kinetics curves obtained from DSC experiments of epoxy/PEP–PPO–PEO block copolymer blends were successfully fitted to an autocatalytic (Larrañaga et al. 2004) and mechanistic kinetic model (Larrañaga et al. 2005, 2006a). It was found that PEO–PPO–PEO slows the reaction rate both by acting as a diluent and by interfering with the autocatalytic process. This delay was related to a preferential hydrogen bonding interaction between the hydroxyl groups of the growing epoxy network and the PEO oxygens, which inhibit the autocatalysis process. Another finding was that the curing rate decreases with increasing block copolymer content in the epoxy blend as well as increasing PEO content in the block copolymer. This last fact also proved that the delaying of cure kinetics is mainly due to physical interactions between components (Larrañaga et al. 2006a).

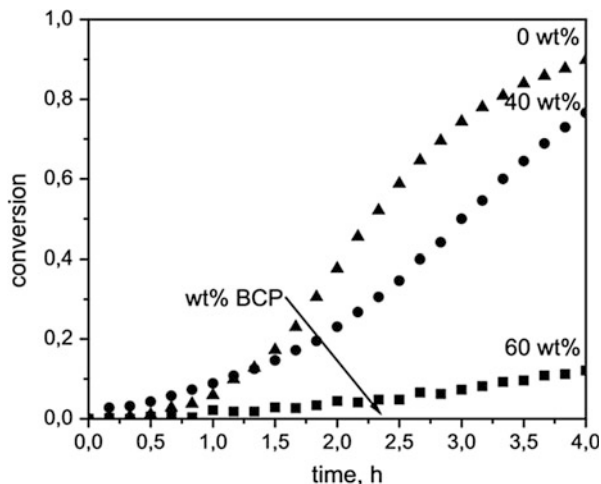
Similar results about the delay on the cross-linking reaction of epoxy groups were obtained for epoxy/poly(styrene)-*b*-poly(ethylene oxide) (PS–PEO) block copolymer blends (Leonardi et al. 2015a). It is possible to emphasize that in these blends, the PS block was phase separated at low conversions, while the PEO block remained miscible up to very high conversions (Leonardi et al. 2015b). The lowering on reaction rate produced by block copolymer addition, illustrated in Fig. 1, was explained as a dilution effect by the large amount of miscible PEO block present in this copolymer as well as by a partial segregation of reactive monomers and short oligomers to the PS-rich phase. Regarding this last fact, it was established that a differential segregation of reactive components in both epoxy–amine-rich and block-rich phase can occur (Williams et al. 1997).

Interestingly, it was published a study about the cure kinetics of epoxy/poly(butadiene-co-acrylonitrile) (PS-PAN) blends. This study took into account the contribution of diffusion phenomena on the reaction rate after gelation and crosslinking of epoxy-amine systems in order to fit the experimental data near to vitrification using the autocatalytic model (Kim et al. 2005).

Finally, the kinetics of curing of an epoxy system and their blends with epoxidized poly(styrene)-*b*-poly(butadiene)-*b*-poly(styrene) (eSBS) was studied using isothermal and non-isothermal DSC analyses (George et al. 2012, 2014). The experimental cure kinetics curves were phenomenologically modeled with success. It is possible to emphasize that the eSBS used for this study was a block copolymer with high degree of epoxidation (eSBS 47 mol%) to ensure the nanostructuring of these blends (Ocando et al. 2008).

The most relevant results about the effect of block copolymer addition on cure behavior of epoxy–amine blends by DSC analyses, as well as a comprehensive understanding of the kinetic parameters by applying mathematical models to describe the obtained experimental data, will be addressed in this chapter.

Fig. 1 Conversion of epoxy groups at 135 °C for blends containing 0, 40, and 60 wt% BCP (Reprinted with permission Leonardi et al. (2015a))



Non-isothermal DSC Analyses

In general, the heat released during the network formation determined by non-isothermal or dynamic DSC measurements is assumed to be directly proportional to the extent of consumption of the reactive groups in epoxy–amine systems. Non-isothermal runs at constant heating rates were carried out in order to determine the total heats of reaction (ΔH_T) released during dynamic curing for the epoxy blends modified with 10, 20, and 30 wt% of PEO–PPO–PEO (EP) block copolymer ($M_{EO} = 1088$ and $M_{PO} = 1794$ g mol⁻¹) with a molar ratio between blocks, PEO:PPO, of 0.8:1 (EP-0.8:1) (Larrañaga et al. 2004). The epoxy–amine system used for this study was a diglycidylether of bisphenol A (DGEBA)/4,4-diaminodiphenylmethane (DDM) system. From the dynamic curing profiles (Fig. 2), it was concluded that the curing reaction for the studied systems was kinetically affected by the modifier content. This fact was proved by a displacement of exothermic polymerization temperature peaks (T_p) to higher values as the concentration of block copolymer in the blend increases. Regarding the ΔH_T , it was observed that the presence of block copolymer did not affect the reaction pathway due to this value decrease in proportion to the block copolymer content in the blend (Table 1). In addition, as can be seen from dynamic curing profiles (Fig. 2), a shoulder appeared (T_{sh}) after the exothermic polymerization peak for the epoxy blends. This last behavior was attributed to the phase separation of the block copolymer, and it was corroborated by light transmission dynamic scan by the same authors. Table 1 summarizes the obtained values of ΔH_T , T_p , and T_{sh} determined by DSC as well as the cloud point temperature (T_{cp}) determined by transmission optical microscopy (TOM), a temperature where the phase separation occurs, and it was in agreement with T_{sh} .

Fig. 2 DSC dynamic scans carried out at a rate of $10\text{ }^{\circ}\text{C min}^{-1}$, for epoxy mixtures containing various PEO-PPO-PEO contents (Reprinted with permission Larrañaga et al. (2004))

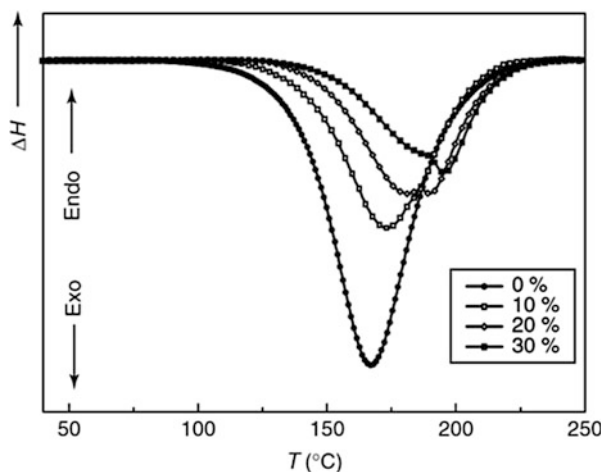


Table 1 Thermal properties and TOM measurements of the PEO-PPO-PEO-modified epoxy mixtures (Reprinted with permission Larrañaga et al. (2004))

PEO-PPO-PEO content (wt%)	H_T (kJ (epoxy equivalent) $^{-1}$)	T_p ($^{\circ}\text{C}$)	T_{cp} ($^{\circ}\text{C}$)	T_{sh} ($^{\circ}\text{C}$)
0	101	171	–	–
10	87	174	173	180
20	75	179	180	184
30	65	185	187	188

The observed delaying behavior on curing reaction was related to dilution effects, due to a reduction in the density of the reactive groups as the block copolymer content increased. Nevertheless, the authors also pointed out that in this epoxy/PEO-PPO-PEO blend, the delay on curing reaction was higher than the one observed in other epoxy blends containing other modifiers (Jenninger et al. 2000). Therefore, this observed behavior could not be explained only by a dilution effect. This fact suggested that the OH groups (developed in the cure reactions) interact through hydrogen bonding with ether oxygen of PEO, so decreasing the autocatalytic process, and therefore delaying the curing process (Larrañaga et al. 2007). Fourier transform infrared spectroscopy (FTIR) analyses (Fig. 3a) confirmed this hypothesis, revealing that the associated hydroxyl group bands shifted to lower wave numbers. In addition, from Fig. 3b, it was noticed that the intensity ratio between the associated hydroxyl band and the free hydroxyl band around 3570 cm^{-1} in the modified system increased with the increment of the conversion, and this increment is more significant compared with the unmodified systems (Larrañaga et al. 2004).

The influence on the delaying of cure rate with the molar ratio between blocks of diverse PEO-PPO-PEO (EP-0.33:1, EP-0.8:1, and EP-3:1) block copolymers was also demonstrated by DSC analyses (Larrañaga et al. 2006a). Figure 4b shows the

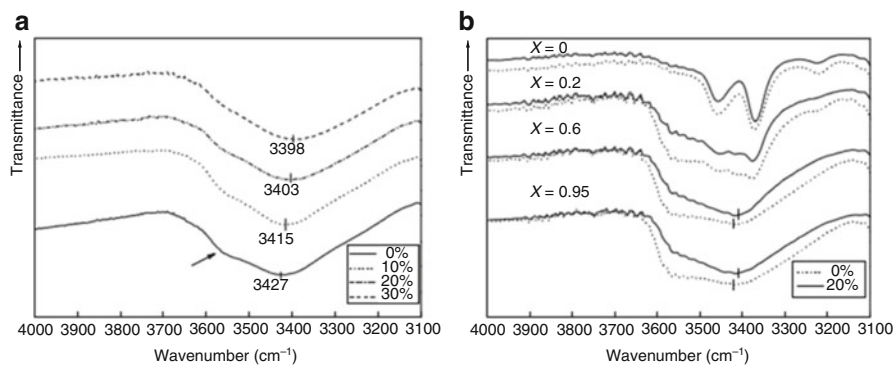


Fig. 3 FTIR spectra for (a) all cured samples with various contents of modifier and (b) for neat epoxy and a 20 wt% PEO-PPO-PEO-modified mixture at different conversions (Reprinted with permission Larrañaga et al. (2004))

Fig. 4 DSC dynamic scans for (a) epoxy systems with various EP-0.33:1 contents and (b) neat epoxy and 30 wt% PEO-PPO-PEO-modified systems (Reprinted with permission Larrañaga et al. (2006a))

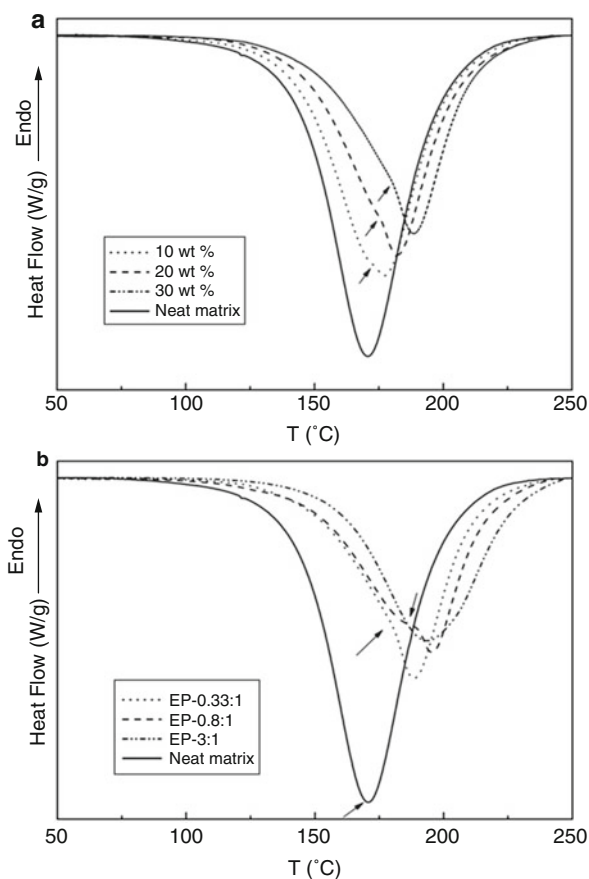


Table 2 Heat of reaction and T_{peak} values of neat epoxy and with various contents of eSBS (Reprinted with permission George et al. (2012))

wt% of eSBS in DGEBA/eSBS(47 mol%)/DDM	Heating rate ($^{\circ}\text{C min}^{-1}$)	ΔH_0 (J/g)	$T_{\text{peak}}(^{\circ}\text{C})$
0	2.5	558.7	128.3
	5	534.6	143.8
	7.5	485.8	154.8
	10	470.8	162.1
10	2.5	575.2	130.6
	5	526.1	148.4
	7.5	454.2	160.0
	10	449.6	166.4
20	2.5	532.5	129.8
	5	496.7	147.7
	7.5	455.7	163.1
	10	434.6	170.5
30	2.5	488.5	138.2
	5	485.1	153.4
	7.5	434.6	163.4
	10	364.8	171.1

dynamic thermograms for a neat epoxy–amine system and its blends containing 30 wt% of EP-0.33:1, EP-0.8:1, and EP-3:1. It was found that the displacement of exothermic peak was higher for the modified epoxy blend with high PEO content. This behavior was attributed to the occurrence of more physical interactions between the epoxy and PEO block in the blend modified with EP-3:1. The occurrence of more physical interactions was also confirmed by FTIR analyses. In addition, the shoulder in the dynamic heating profiles attributed to the macrophase separation process was observed in EP-0.33:1 and EP-0.8:1 modified epoxy blends but not for the block copolymer with high PEO content.

A recent work was published about the effect of the addition of different amounts of eSBS block copolymer with 47 mol% of polybutadiene block epoxidation (eSBS47) on the cure kinetics of epoxy blends (George et al. 2012). The epoxy–amine system used in this study was DGEBA/DDM. Dynamic DSC experiments were carried out at different heating rates for the epoxy systems modified with 0, 10, 20, and 30 wt% of eSBS. It was observed that the exothermic peak maximum (T_{peak}) undergoes a displacement to higher temperatures when heating rate was increased. This behavior was also observed at different blend composition. The average of enthalpy values obtained at different heating rate was used to estimate the total heat of the reaction (Table 2). From these results, it was noticed that the minimum in the exothermic curve corresponding to the maximum heat flow of the epoxy–amine reaction increases as the weight percentage of eSBS in the epoxy blend increases. This behavior was related to a plasticization effect and interactions between the epoxidized PB segments with the epoxy resin that causes retardation

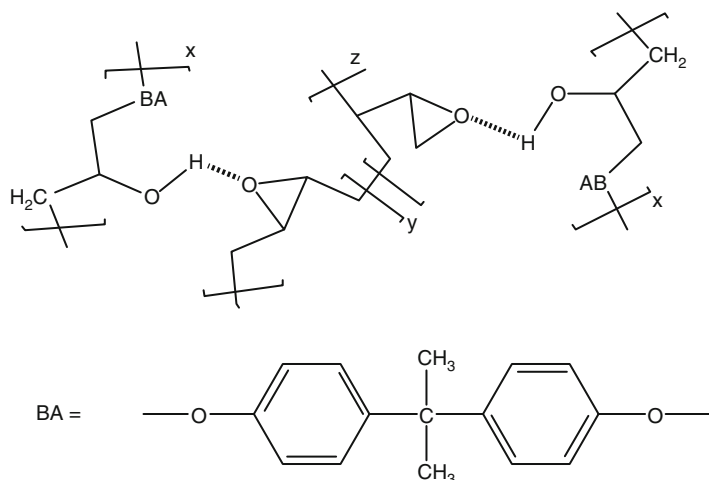


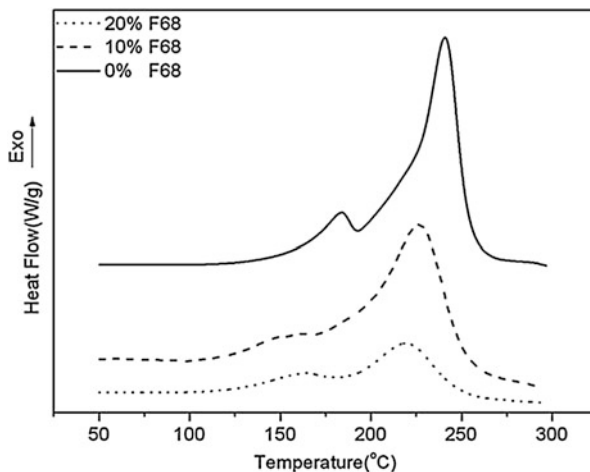
Fig. 5 Schematic representation of hydrogen bonding interaction between hydroxyl hydrogen in DGEBA and epoxy oxygen atom of epoxidized SBS (1,4- and 1,2-epoxidized PB) (Reprinted with permission George et al. (2012))

in cure reaction. FTIR studies carried out by the same authors corroborated the presence of interactions between the hydroxyl group of the growing epoxy network and oxirane groups of the epoxidized polybutadiene. The schematic representation of hydrogen bonding interaction between the epoxy resin and eSBS is illustrated in Fig. 5.

In a subsequent work, the same authors studied the evolution of the total heats of reaction of an epoxy blend modified with 10 wt% of eSBS47 at different cure times by dynamic DSC measurements. For the kinetic studies, the epoxy blends were cured in an air oven for different periods at 90 °C prior to DSC analyses. From this study, it was observed that the evolution of the total heats of reaction for the 10 wt% eSBS47-modified epoxy blend decreased as a function of cure time, as a result of the epoxy–amine reaction, and essentially no exothermic reaction was observed when the cure time reached 90 min. This behavior was related to the fact that the mobility of some reactive sites could be frozen, causing an ending of the polymerization (George et al. 2014).

Interestingly, a recent study about the curing behavior of a cyanate ester/epoxy system and its blends containing PEO–PPO–PEO with molecular weight $M_w = 8600$ (F68) was published (Hu et al. 2015). For this purpose, the authors developed a series of mixtures varying the matrix composition (cyanate ester/epoxy ratio) and the block copolymer contents (up to 20 wt%). The matrix composition was varied, and some differences about the hydrogen bonding interactions and chemical reaction resulting from the cross-linked network structures were observed. DSC analyses (Fig. 6) revealed an exothermic polymerization peak at lower temperature that was related to homopolymerization reactions of cyanate ester groups. On the other hand,

Fig. 6 Differential scanning calorimetry dynamic scans for a cyanate ester/epoxy resins with various F68 contents (Reprinted with permission (Hu et al. (2015)))



the exothermic polymerization peak observed at higher temperature was related to the formation of oxazolidinone groups (reaction between epoxy–cyanate ester). On the contrary to the results described above, this study indicated that cure reaction was accelerated by the incorporation of a small amount of block copolymer. In addition, the exothermic polymerization peak at lower temperature was less notorious in the case of higher block copolymer contents. Therefore, it was concluded that the presence of hydroxyl groups in block copolymers had a significant catalytic effect on the curing of cyanate ester/epoxy resins. This catalytic behavior was also corroborated by FTIR analyses, where it was clearly observed that the disappearing rate of both cyanate and epoxy groups was faster for the modified system than that of the neat resin.

Isothermal DSC Analyses

The curing rate of different contents of PEO–PPO–PEO block copolymer with 30wt% of PEO (EPE) blended with a DGEBA/m-xylylenediamine system was studied using DSC under isothermal conditions (Cano et al. 2014). The curing temperature for this purpose was chosen taking into account the lower critical solution temperature (LCST) behavior of this block copolymer. In this sense, isothermal runs at 25 °C were performed to the epoxy blends, and the resulting thermograms are shown in Fig. 7. The curing reaction between the epoxy resin and the amine was indicated as the drop in heat flow, and the reaction was considered complete when the isothermal DSC traces leveled off to the baseline. In agreement with the non-isothermal studies previously shown in this chapter, from these results, a clear delay in the curing reaction with the increment of the block copolymer content was also found. This behavior on curing reaction time was again related to the dilution effect in the blends that makes the reaction between the epoxy and the amine groups more difficult.

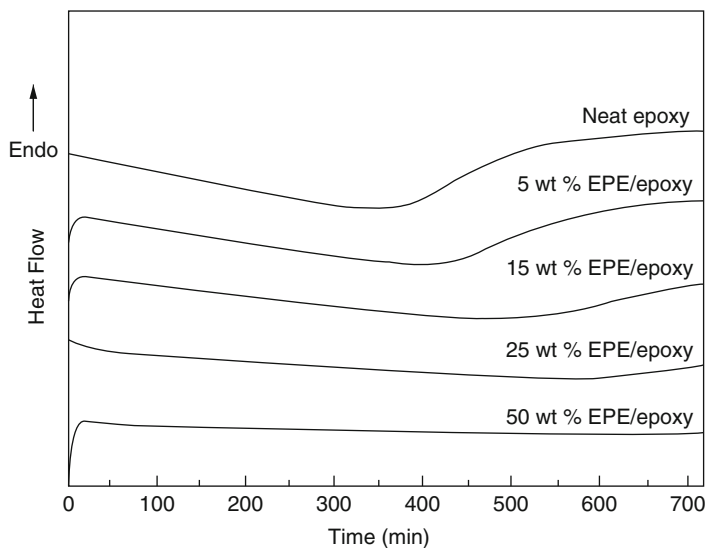


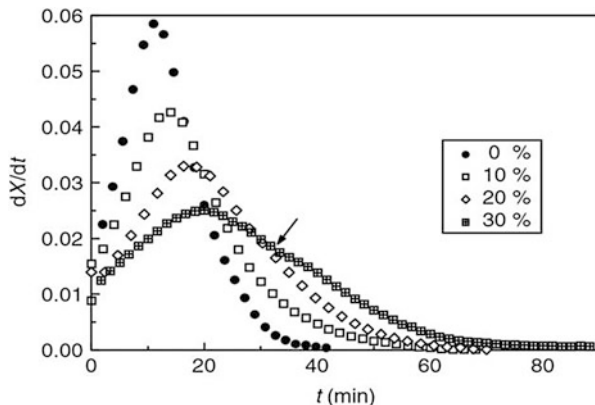
Fig. 7 Isothermal DSC thermograms of the neat epoxy system and all EPE/epoxy systems at 25 °C (Reprinted with permission Cano et al. (2014))

In addition, it was also pointed out that the presence of more physical interactions between the epoxy resin and the PEO–PPO–PEO block copolymer by an increment on the amount of modifier, from 5 to 50 wt%, can be also responsible for the delay on curing rate.

Similar results about the curing rate of epoxy blends depending on the amount of PEO–PPO–PEO block copolymer were obtained at an isothermal cure temperature of 120 °C (Larrañaga et al. 2004). It was observed from the reaction rate curves (dX/dt vs. time) that the peak for the maximum reaction rate decreased and the time at which this maximum takes places increase with the block copolymer content (Fig. 8). In addition, the authors related the shoulder observed in the reaction rate trace of the modified system with 30 wt% block copolymer with the occurrence of a macroseparation at the curing temperature of 120 °C. This last behavior was corroborated by the measurement of the cloud point by light transmission analysis at 120 °C.

Interestingly, the influence of the curing temperature and block copolymer content on cure kinetics of epoxy/PEO–PPO–PEO block copolymer blends analyzed by isothermal DSC experiments was correctly fitted to a phenomenological autocatalytic model assuming equal reactivity of primary and secondary amino hydrogens with the epoxy groups (Larrañaga et al. 2004). The epoxy–amine system used for this study was a diglycidylether of bisphenol A (DGEBA)/4,4-diaminodiphenylmethane (DDM) system. This phenomenological autocatalytic approach employs empirical or semiempirical equations (Kamal and Sourour 1973; Sourour and Kamal 1976). Explained in a more detailed way, this model takes into account the reactions of the oxirane groups with the primary and

Fig. 8 Reaction rate curves of the epoxy mixtures containing various amounts of block copolymer cured at 120 °C (Reprinted with permission Larrañaga et al. (2004))



secondary amines, as well as catalytic and autocatalytic effects. The generalized equation for this autocatalytic model is described by (Eq. 1):

$$\frac{dX}{dt} = (k_1 + k_2 X^m)(1 - X)^n \quad (1)$$

where k_1 and k_2 correspond to the rate constant for the reaction catalyzed by proton donors initially present in the system (e.g., α -glycols present in the epoxy monomer) and proton donors that are produced during cure, respectively; X denotes the conversion of the epoxy groups, m and n are the kinetic exponents of the reactions, and $m + n$ is the overall reaction order. The rate constants k_1 and k_2 are dependent on the temperature with an Arrhenius-type relationship: $k_1 = A_1 \exp(-E_{a1}/RT)$ and $k_2 = A_2 \exp(-E_{a2}/RT)$, where A_i denotes the collision frequency or Arrhenius frequency factor, E_{ai} its corresponding activation energy, R the gas constant, and T the absolute temperature. In order to obtain accurate values of Eq. 1 parameters from isothermal curve data, a simple iterative method can be utilized until an apparent convergence of the m and n values is obtained, and Eq. 1 can be rewritten as

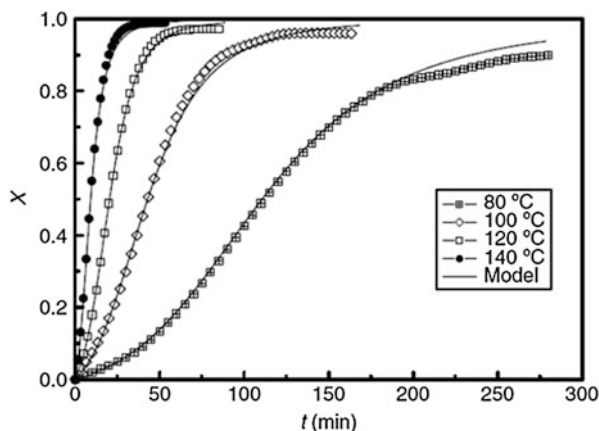
$$\ln\left(\frac{dX}{dt}\right) - \ln(k_1 + k_2 X^m) = n \ln(1 - X) \quad (2)$$

This equation takes into account the autocatalytic nature of the curing process with the term $k_2 X^m$, while the uncatalyzed process is represented by k_1 . The values of E_{a1} and E_{a2} were obtained by plotting $\ln k_1$ and $\ln k_2$, respectively, versus $1/T$. Therefore, Arrhenius plots of the rate constants from isothermal runs were characterized for straight lines where the slope is E_{a1}/RT and E_{a2}/RT and the intercept is $\ln A_1$ and $\ln A_2$, respectively. The summarized kinetics parameters, reaction constants, and activation energy, obtained for the epoxy/PEO–PPO–PEO blends, are shown in Table 3. From these results, it was pointed out that the reaction orders did not change very much with the content of block copolymer in the blend as well as with the cure

Table 3 Kinetic constants obtained for the PEO-PPO-PEO-modified epoxy mixtures (Reprinted with permission Larranaga et al. (2004))

PEO-PPO-PEO content (wt%)	T_{cure} (°C)	m	n	$k_1 \times 10^3$ (min ⁻¹)	$k_2 \times 10^3$ (min ⁻¹)	E_{a1} (kJ mol ⁻¹)	E_{a2} (kJ mol ⁻¹)	$\ln A_1$	$\ln A_2$
	80	0.98	1.11	1.5	45.6				
	100	0.97	1.12	5.1	107.7				
0	120	0.95	1.18	11.0	198.5	57.9	44.6	13.29	12.16
	140	0.93	1.22	28.0	427.4				
	80	0.99	1.40	1.4	37.0				
	100	0.97	1.42	4.9	85.0				
10	120	0.93	1.39	10.5	174.2	58.5	44	13.41	11.71
	140	0.93	1.37	26.0	326.8				
	80	0.91	1.37	1.3	28.6				
	100	0.91	1.29	4.5	56.8				
20	120	0.97	1.26	10.0	126.6	58.6	44.4	13.38	11.51
	140	0.91	1.35	25.0	246.2				
	80	0.93	1.23	1.1	19.4				
	100	0.91	1.22	4.2	39.1				
30	120	0.87	1.25	9.5	82.5	58.8	42.7	13.33	10.58
	140	0.81	1.34	21.0	158.6				

Fig. 9 Comparisons between the autocatalytic model and experimental data for the mixture modified with a 20 wt% block copolymer at various cure temperatures (Reprinted with permission Larrañaga et al. (2004))



temperature. On the other hand, k_2 decreased at all temperatures as the block copolymer content increases. This reduction in k_2 was related to the decrease in the autocatalytic effect by specific interactions between the hydroxyl groups and the block copolymer. As discussed before these interactions were demonstrated by FTIR analyses (Fig. 3).

Figure 9 presents a comparison between the autocatalytic model and the experimental data for epoxy blends modified with 20 wt% of PEO-PPO-PEO. It is possible to emphasize that the experimental conversion values at a given temperature were defined as the ratio between the enthalpy of reaction at time t , $(\Delta H_{\text{iso}})_t$, and the sum of the total enthalpy from the isothermal and residual scans $((\Delta H_{\text{iso}}) + (\Delta H_{\text{res}}))$. As can be seen, the model fitted quite well with the experimental conversion curves; small variations between experimental and theoretical values were related to vitrification effects (Larrañaga et al. 2004). Similar results about cure kinetics studies of epoxy blends, by the use of isothermal DSC analyses and a modified autocatalytic kinetic model, were obtained for the same group when an epoxy resin was modified with different amounts of two kinds of thermoplastics polymers (Fernández et al. 2001). It is possible to point out that the conversion increases in the initial stages of reaction, and then the cure reaction rate decreases at later stages because the blends became vitrified. This decrease in the cure reaction rate is related to the cross-linking density. In addition, the maximum in reaction rate against time plot is typical of autocatalytic mechanism. Therefore, it was concluded that the presence of block copolymer in the epoxy blends does not affect the autocatalytic nature of the reaction.

In a later work, the same authors (Larrañaga et al. 2005) used a mechanistic model to fit the experimental results obtained by DSC for the DGEBA/DDM system modified with PEO-PPO-PEO block copolymer. The employed

mechanistic kinetic model considers a scheme of consecutive and competitive reactions that can take place during the curing process (Riccardi et al. 2001). As mentioned before, the curing process of epoxy–amine systems is a very complex procedure due to the chemical reactions and changes in the physical properties which are closely related; in this sense it is difficult to obtain an accurate mechanistic model (Riccardi and Williams 1986a, b; Mijovic et al. 1992; Mijovic and Wijaya 1994; Urbaczewski et al. 1990; Blanco et al. 2005; Zvetkov 2005). Nevertheless, Riccardi et al. (2001) introduced a simple mechanistic model that encloses an equilibrium reaction that produces an epoxy–hydroxyl complex established as the only intermediate species as well as two possible mechanisms for the use of amine hydrogens. It was found that this simple mechanism model provided a good fitting with respect to the experimental results obtained by DSC for the DGEBA/ethylenediamine (EDA) system, under both isothermal and constant heating rate conditions. It is possible to emphasize that the main advantage of this mechanistic model with respect to the phenomenological model is that the mechanistic model offers more predictive capability due to the results obtained from its equations which can be extrapolated to account for variations in the initial formulations (Chiao 1990; Chiao and Lyon 1990). In addition, this model can give an insight about the network structure. As a result, the evolution of different statistical parameters during the network formation can be predicted (Riccardi and Williams 1986b).

In this sense, following the work presented by Riccardi et al. about epoxy–amine systems (Riccardi et al. 2001), Larrañaga et al. proposed a mechanistic approach that includes the following alternatives for the curing reaction steps (Larrañaga et al. 2005): (1) epoxy activation by hydrogen bonding with hydroxyl groups in the pre-equilibrium to form an epoxy–hydroxyl complex, (2) uncatalyzed addition reactions of primary and secondary amine hydrogens with epoxy groups, (3) and parallelly, autocatalyzed reactions by the OH groups produced during curing reactions. In this sense, the mechanistic kinetic model, assuming different reactivities of primary and secondary amine hydrogens, was defined by the following equations:

$$\left(\frac{dX}{dt}\right) = [K'_1(1-x-y) + K_1y] \left[\frac{2(1-r)z_1 + rz_1^{r/2}}{2-r}\right] \quad (3)$$

$$\left(\frac{dz_1}{dt}\right) = -2z_1 [K'_1(1-x-y) + K_1y] \quad (4)$$

where

$$y = 0.5 \left\{ A - [A^2 - 4[C_0 + x(1-C_0) - x^2]]^{0.5} \right\} \quad (5)$$

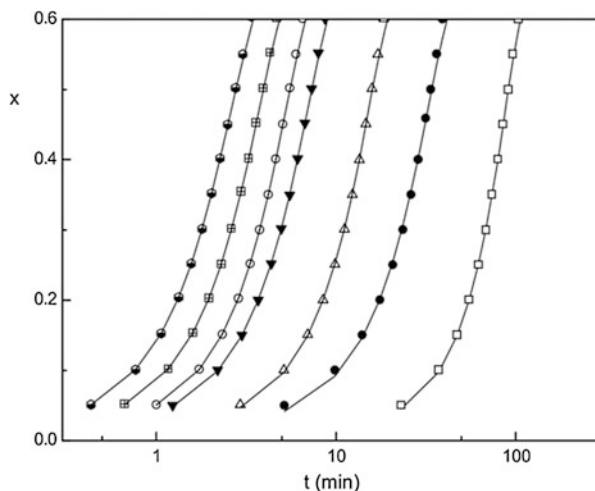


Fig. 10 Comparison between the mechanistic model (—) and experimental data at (□) 80 °C, (●) 100 °C, (Δ) 120 °C, (▼) 140 °C, (○) 150 °C (⊞), 160 °C, and (◄) 170 °C for the blend modified with a 10 wt% block copolymer (Reprinted with permission Larrañaga et al. (2005))

Table 4 Values of the ratios of kinetic constants and the initial ratio of the epoxy group concentrations in blends and neat system (Reprinted with permission Larrañaga et al. (2005))

PEO–PPO–PEO (wt%)	$K_{\text{Blend}}/K_{\text{Neat}}$	$K_{1\text{Blend}}/K_{1\text{Neat}}$	$K'_{1\text{Blend}}/K'_{1\text{Neat}}$	$c_{0\text{Blend}}/c_{0\text{Neat}}$
10	0.75	0.72	1.86	0.89
20	0.68	0.55	1.98	0.79
30	0.60	0.43	2.23	0.68

$$A = 1 + C_0 + \frac{1}{K} \quad (6)$$

$$x = \frac{e_0 - [e + (e - OH)]}{e_0} \quad (7)$$

and

$$z_1 = \frac{a_1}{a_0} \quad (8)$$

where e_0 and e denote the concentration of epoxy at time 0 and t , respectively, a_1 is the concentration of primary amino hydrogens, and r is the ratio of secondary to primary amino-hydrogen rate constants. The epoxy–hydroxyl complex formation is represented with the dimensionless equilibrium constants K . The autocatalyzed and uncatalyzed reactions are represented by the dimensionless kinetic constants K_1 and

K'_1 , respectively; $e\text{-OH}$ is the epoxy–hydroxyl complex concentration. C_0 is OH-equivalent/epoxy-equivalent and y is $e\text{-OH}/e_0$.

Figure 10 shows the fit of experimental curves with this mechanistic model for the epoxy system modified with 10 wt% PEO–PPO–PEO block copolymer at different curing temperatures. As can be seen, this model presented a satisfactory match with the experimental curves.

From the analyses of the kinetic parameters summarized in Table 4, it was found a hindering in the formation of epoxy–hydroxyl complex and the autocatalytic process by blending compared with neat epoxy. On the contrary, it was observed that the constant for the uncatalyzed reaction of epoxy with amine increases with copolymer content. The diminution in K and K_1 values was ascribed to the fact that the interactions between the OH groups formed during curing with the block copolymer are more favored. In the case of K'_1 , its increment was related to the fact that at early stages of reaction, less oxirane groups can interact with OH groups as the block copolymer content increases. In this sense, more oxirane groups are available for direct reaction with the amine. Therefore, from these results it was concluded that the influence of K and K_1 kinetics constants on curing rate is higher than the influence of K'_1 because even though the uncatalyzed process was favored, the block copolymer delayed the curing reaction.

On the other hand, the effect of the interactions between the epoxy–amine system and the PEO–PPO–PEO block copolymers on the reaction rate depending on the molar ratio between blocks was also proved by isothermal DSC analyses (Larrañaga et al. 2006). Figure 11 shows conversion of epoxy groups vs. time curves obtained for the epoxy blends containing different amounts of EP-0.33:1, EP-0.8:1, and EP-3:1 block copolymers cured at 140 °C. From these curves, it was noticed that the epoxy blends modified with copolymers containing different block molar ratio present a different delay even at the same content of modifier. This last fact proved that the delaying of cure kinetics is mainly due to physical interactions between the epoxy (OH groups initially existing and developed during the network formation) and PEO block (ether groups) than a dilution effect due to the content of modifier in the growing network system. As a result, the system that presented the higher delay on the curing reaction was the system modified with the block copolymer with higher PEO content. FTIR analyses corroborated these results because it was observed that when the PEO molar ratio in the block copolymer is higher, the associated hydroxyl group band appears at lower wave numbers. In addition, the intensity ratio between associated and free hydroxyl bands also increases. It was also pointed out that the hydroxyl–ether interactions modified the autocatalytic process causing a delay on the curing process. Figure 11b also shows the predicted curve from the kinetic model and the theoretical curve obtained taking into account the dilution effect for the epoxy system modified with 20 wt% of EP-0.8:1, an appropriate agreement was pointed out. In addition, it was also noticed that the curing reactions occur at a lower rate than when just the dilution effect was taken into account for the estimation. This last fact also corroborated the hypothesis that the interactions between the block copolymer and the epoxy significantly affect the curing behavior.

Fig. 11 Cure kinetics curves for epoxy systems cured at 140 °C containing 0 wt% (■), 10 wt% (○), 20 wt% (▲), and 30 wt% (□) of (a) EP-0.33:1, (b) EP-0.8:1, and (c) EP-3:1. In subpanel (b), *solid lines* show predicted curves from kinetic model for neat and 20 wt% EP-0.8:1, while *dashed lines* show a theoretical curve obtained by modeling dilution effect for 20 wt% EP-0.8:1 (Reprinted with permission Larrañaga et al. (2006a))

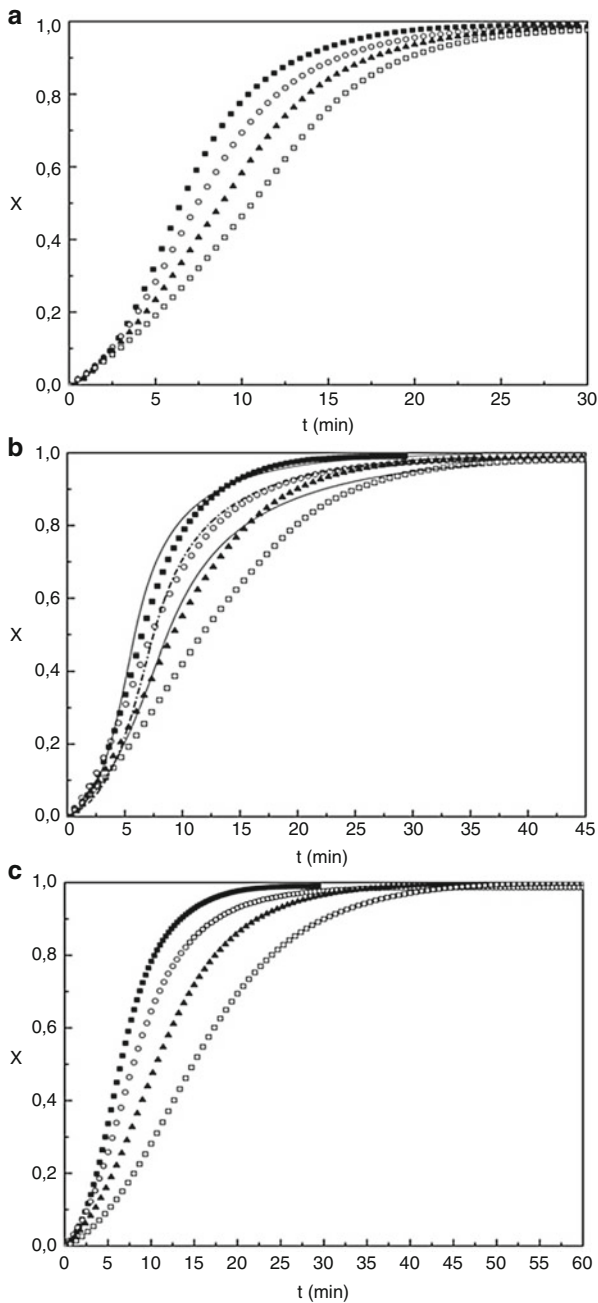


Table 5 Kinetic constants and concentrations of epoxy at initial time of block copolymer-modified epoxy systems with respect to those values for the neat system (Reprinted with permission Larrañaga et al. (2006a))

Modifier	Content (wt%)	$K_{\text{Blend}}/K_{\text{Neat}}$	$K_{1\text{Blend}}/K_{1\text{Neat}}$	$K'_{1\text{Blend}}/K'_{1\text{Neat}}$	$e_{0\text{Blend}}/e_{0\text{Neat}}$
EP-0.33:1	10	0.80	0.73	1.45	0.89
	20	0.77	0.61	1.69	0.78
	30	0.62	0.51	1.49	0.68
EP-0.8:1	10	0.75	0.72	1.86	0.89
	20	0.68	0.55	1.98	0.79
	30	0.60	0.43	2.23	0.68

Table 6 Activation energy and frequency factor values of block copolymer-modified epoxy systems (Reprinted with permission Larrañaga et al. (2006a))

Modifier	Content (wt%)	E_1 (kJ mol ⁻¹)	E'_1 (kJ mol ⁻¹)	$\ln(A_1 \text{ min}^{-1})$	$\ln(A'_1 \text{ min}^{-1})$
Neat matrix	0	49.0	61.8	13.9	13.2
	10	48.7	61.9	13.5	13.6
EP-0.33:1	20	49.6	62.0	13.6	13.7
	30	49.5	62.4	13.4	13.8
	10	49.7	62.1	13.8	13.9
EP-0.8:1	20	49.7	62.3	13.5	14.1
	30	49.7	62.5	13.3	14.2

The kinetics constants obtained by the use of this mechanistic approach, as average values in the 80–170 °C range, for epoxy blends with EP-0.8:1 and EP-0.33:1 compared with the corresponding epoxy system are summarized in Table 5. From these results, it was pointed out that in addition to the dilution effect, the interactions between components play an important role. This finding was ascribed to the fact that the ratio between the kinetic constants of the blend and the neat epoxy is different if they are compared with the ratio between the initial concentration of epoxy equivalents of the blend and the neat epoxy. From K and K_1 values, it was concluded that the formation of epoxy–hydroxyl complex and the autocatalytic processes are less restricted for the epoxy blends containing EP-0.33:1 than for the epoxy blend containing EP-0.8:1 when they are compared with the neat epoxy system. This behavior corroborated the fewer occurrences of physical interactions between components presented on the epoxy blend modified with the block copolymer containing lower PEO block content. Another finding was the increment of uncatalyzed kinetic parameter, K'_1 , in the modified systems, and it is more evident in the case of the epoxy system modified with EP-0.8:1 due to its higher PEO content.

The activation energy and frequency factor values of the epoxy system modified with EP-0.8:1 and EP-0.33:1 compared with the corresponding epoxy system are summarized in Table 6. It was noticed that the activation energy values yield similar

values for all the systems. On the contrary, the frequency factors presented a slight variation, being higher for EP-0.8:1 than for EP-0.33:1 modified systems. In addition, the observed decrease of A_1 values was attributed to the delay of the autocatalytic process as a consequence of physical interactions between the components, while the increase of A'_1 values was related to the increase of epoxy groups that can react with the amine (Larrañaga et al. 2006).

The cure kinetic parameters of an epoxy system blended with ATPEI (amine terminated polyetherimide)–CTBN (carboxyl terminated poly(butadiene-co-acrylonitrile)) block copolymer, denoted as AB, were evaluated using isothermal DSC measurements and an autocatalytic model (Kim et al. 2005). Similar results to those discussed above about the effect on heat of reaction and final conversion of epoxy groups with the content of block copolymer were observed. Interestingly, this work proposed to take into account a rate equation with a diffusion control factor to explain the delay on curing process in the later stages of the reaction and to obtain a better match between the experimental values and the theoretical ones. The diffusion control factor $f(X)$ is represented by the next equation:

$$f(X) = \frac{1}{1 + \exp[C(X - X_c)]} \quad (9)$$

where C denotes the parameter of diffusion control and X_c is the critical value of cure conversion where reaction becomes controlled by diffusion. Therefore the final rate equation was rewritten as follow:

Table 7 Kinetic constants of the autocatalytic model for epoxy/DDS/AB blend systems (Reprinted with permission Kim et al. (2005))

Temp. (°C)	m	n	m + n	k_1 (min ⁻¹)	k_2 (min ⁻¹)
Epoxy/AB (0 wt%)					
160	1.0110	2.5410	3.5520	0.0070	0.0563
175	1.0213	2.3883	3.4096	0.0183	0.1241
190	1.0012	2.0346	3.0358	0.0274	0.1688
Epoxy/AB (10 wt%)					
160	1.0179	3.1792	4.1971	0.0069	0.0834
175	1.4494	2.8137	4.0610	0.0208	0.2027
190	1.4115	2.3171	3.7286	0.0366	0.2611
Epoxy/AB (20 wt%)					
160	1.0100	3.4210	4.4310	0.0042	0.0995
175	1.3213	3.0072	4.3285	0.0120	0.2288
190	1.2194	2.4750	3.6944	0.0245	0.2404
Epoxy/AB (30 wt%)					
160	1.0898	3.7662	4.8560	0.0050	0.1052
175	1.5328	3.1938	4.7266	0.0173	0.2432
190	1.4628	2.5251	3.9879	0.0287	0.3605

$$\frac{dX}{dt} = \frac{(k_1 + k_2 X^m)(1 - X)^n}{1 + \exp[C(X - X_c)]} \quad (10)$$

Table 7 summarized the kinetic parameters calculated using this autocatalytic model including the diffusion phenomena. It was noticed that the values of n increased as the reaction rate decreased. This behavior was explained by the fact that for the epoxy blends, the reaction can be hindered by the phase separation process. On the other hand, the values of m oscillated around 1.0 even though when the block copolymer content was increased. This last fact revealed that neither the curing reaction nor the vitrification process has a significant effect on the autocatalytic behavior.

Figure 12 depicts the conversion versus reaction time at 160 °C, 175 °C, and 190 °C of the epoxy blends containing different amounts of AB. The calculated solid and dashed traces were obtained from Eqs. 1 and 10 with and without the diffusion control factor, respectively. From this study, it was noticed that the model including the diffusion control factor fitted quite well with the experimental data at the later stage of reaction, while the differences between the predicted values without the diffusion control factor and the experimental data were pronounced. This result indicated that, at the later stage of reaction, the diffusion control factor in the rate expression should be considered. It was also observed that the differences became more pronounced when the curing temperature used is low.

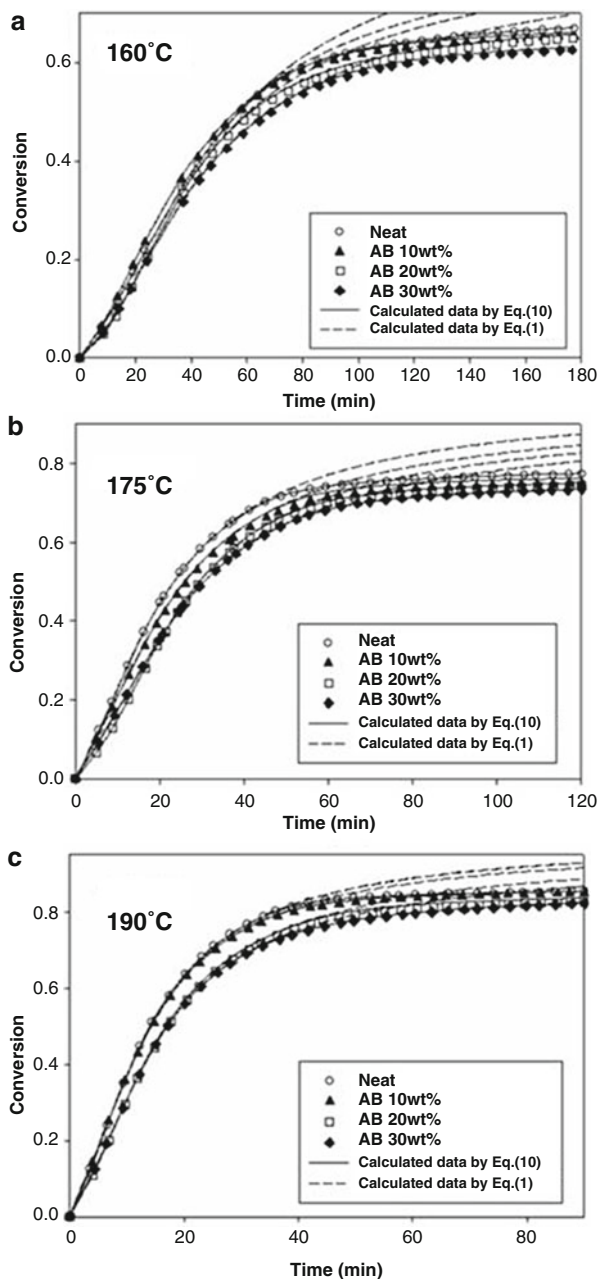
Finally, the curing kinetics studies for the epoxy system and its corresponding blends with 10, 20, and 30 wt% of eSBS (47 mol%) were conducted at different isothermal temperatures. The corresponding plot of conversion rate versus time is shown in Fig. 13. Similar results to those observed with the PEO–PPO–PEO block copolymer about the reaction rate delay with the increment of the block copolymer content in the blends were observed. This delay in this case was also attributed to a differential distribution of the epoxy–amine components in the epoxy-rich phase and in the block copolymer-rich phase, as a result of the phase separation process. The observed behavior on the extent of reaction with the time corroborated that the autocatalytic nature of the curing process was not affected by the inclusion of the block copolymer.

The kinetics parameters were calculated by the autocatalytic model (Eq. 1). The activation energy values and frequency factors are summarized in Table 8. It was found that the activation energy values increased with the amount of eSBS. This last fact was pointed out as another sign of cure reaction delay of epoxy system by the addition of eSBS. In addition, the same behavior of k_1 and k_2 with the content of block copolymer and temperature than that observed in Table 2 for the epoxy system modified with PEO–PPO–PEO was found.

Conclusions

Differential scanning calorimetry, both non-isothermal and isothermal mode, has demonstrated to be a very effective technique to study the curing process of epoxy/block copolymer blends. The experimental cure kinetics curves of epoxy/block

Fig. 12 Degree of conversion vs. time plot for the cure process of epoxy/DDS/AB systems; experimental data (symbols) and calculated data (lines) at various isothermal conditions, at 160 °C (a), 175 °C (b), and 190 °C (c) (Reprinted with permission Kim et al. (2005))



copolymer blends can be successfully fitted to both phenomenological autocatalytic and mechanistic kinetic models. It has been observed that the cure kinetics during the network formation of epoxy/block copolymer blends is affected by modifier concentration, volume fraction, chemical structure, and molecular weight of the blocks,

Fig. 13 Conversion rate vs. time curve for DGEBA/eSBS (47 mol%)/DDM (0, 10, 20, and 30 wt%) blends at 110 °C (Reprinted with permission George et al. (2012))

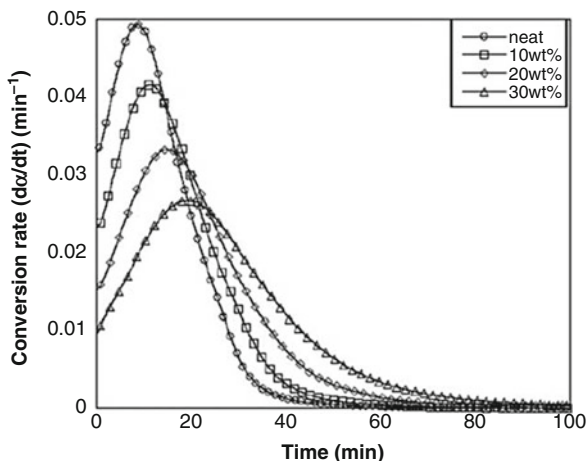


Table 8 The values of activation energy and frequency factor obtained for DGEBA/eSBS (47 mol%)/DDM system by Kamal approach (Reprinted with permission George et al. (2012))

wt% of eSBS in DGEBA/eSBS (47 mol%)/DDM	$\ln A_1$	$\ln A_2$	E_{a1} (kJmol ⁻¹)	E_{a2} (kJmol ⁻¹)
0	15.76	9.93	62.16	38.14
10	15.94	13.16	63.48	48.87
20	16.31	15.01	65.59	54.93
30	17.58	14.85	70.16	54.58

among others. Both DSC modes demonstrated that curing rate decreases as block copolymer content increases. The delay in reaction rate of epoxy/block copolymer blends can be attributed to the dilution effect due to a reduction in the density of reactive groups as the block copolymer content increases, interactions between blocks and the growing epoxy network which inhibits autocatalytic process, as well as a partial segregation of reactive monomers and oligomers to the block copolymer-rich phase. The delay in cure rate attributed to interactions between epoxy and block copolymer blocks was corroborated by FTIR analyses. However, it was observed that the presence of hydroxyl groups in block copolymers had a significant effect on the curing reaction. Isothermal curing was successfully fitted to a phenomenological autocatalytic model based on a semiempirical equation which takes into account catalytic and autocatalytic effects and also to mechanistic model accounting an epoxy–hydroxyl complex, uncatalyzed and parallel catalyzed reactions. Phenomenological autocatalytic model fitted quite well with the experimental conversion curves, and the observed small deviations at high conversion values were related to vitrification effects. The autocatalytic model including diffusion phenomena fitted quite well with the experimental data in the later stage of the reaction. Mechanistic model corroborated that in addition to dilution effect, the physical

interactions between components play an important role, and the observed delay is mainly due to these physical interactions than dilution effects. The kinetic parameters calculated from these mathematical models showed an increase in activation energies as block copolymer contents increase in agreement with the delay on curing rate observed.

References

- Barton JM (1985) The application of differential scanning calorimetry (DSC) to the study of epoxy resin curing reactions. In: *Epoxy resins and composites I*. Springer, Berlin/Heidelberg, pp 111–154
- Bejoy F, Rao VL, Poel GV, Posada F, Groeninckx G, Ramaswamy R, Thomas S (2006) Cure kinetics, morphological and dynamic mechanical analysis of diglycidyl ether of bisphenol-A epoxy resin modified with hydroxyl terminated poly (ether ether ketone) containing pendent tertiary butyl groups. *Polymer* 47:5411–5419
- Blanco M, Corcuera MA, Riccardi CC, Mondragon I (2005) Mechanistic kinetic model of an epoxy resin cured with a mixture of amines of different functionalities. *Polymer* 46:7989–8000
- Bonnaud L, Pascault JP, Sautereau H (2000) Kinetic of a thermoplastic-modified epoxy-aromatic diamine formulation: modeling and influence of a trifunctional epoxy prepolymer. *Eur Polym J* 36:1313–1321
- Bonnet A, Pascault JP, Sautereau H, Taha M, Camberlin Y (1999) Epoxy-diamine thermoset/thermoplastic blends. 1. Rates of reactions before and after phase separation. *Macromolecules* 32:8517–8523
- Cai H, Li P, Sui G, Yu Y, Li G, Yang X, Ryu S (2008) Curing kinetics study of epoxy resin/flexible amine toughness systems by dynamic and isothermal DSC. *Thermochimica Acta* 473:101–105
- Calabrese L, Valenza A (2003) Effect of CTBN rubber inclusions on the curing kinetic of DGEBA-DGEBF epoxy resin. *Eur Polym J* 39:1355–1363
- Cano L, Builes DH, Tercjak A (2014) Morphological and mechanical study of nanostructured epoxy systems modified with amphiphilic poly (ethylene oxide-b-propylene oxide-b-ethylene oxide) triblock copolymer. *Polymer* 55:738–745
- Chiao L (1990) Mechanistic reaction kinetics of 4,4'-diaminodiphenyl sulfone cured tetraglycidyl-4, 4'-diaminodiphenylmethane epoxy resins. *Macromolecules* 23:1286–1290
- Chiao L, Lyon RE (1990) A fundamental approach to resin cure kinetics. *J Compos Mater* 24:739–752
- Cole KC (1991) A new approach to modeling the cure kinetics of epoxy/amine thermosetting resins. 1. Mathematical development. *Macromolecules* 24:3093–3097
- Dean JM, Verghese NE, Pham HQ, Bates FS (2003) Nanostructure toughened epoxy resins. *Macromolecules* 36:9267–9270
- Deng Y, Martin GC (1994) Diffusion and diffusion-controlled kinetics during epoxy-amine cure. *Macromolecules* 27:5147–5153
- Du S, Guo ZS, Zhang B, Wu Z (2004) Cure kinetics of epoxy resin used for advanced composites. *Polym Inter* 53:1343–1347
- Fernández B, Corcuera MA, Marieta C, Mondragon I (2001) Rheokinetic variations during curing of a tetrafunctional epoxy resin modified with two thermoplastics. *Eur Polym J* 37:1863–1869
- Garate H, Mondragon I, Goyanes S, D'Accorso NB (2011) Controlled epoxidation of poly (styrene-b-isoprene-b-styrene) block copolymer for the development of nanostructured epoxy thermosets. *J Polym Sci Part A: Polym Chem* 49:4505–4513
- Garate H, Mondragon I, D'Accorso NB, Goyanes S (2013) Exploring microphase separation behavior of epoxidized poly(styrene-b-isoprene-b-styrene) block copolymer inside thin epoxy coatings. *Macromolecules* 46:2182–2187

- George SM, Puglia D, Kenny JM, Jyotishkumar P, Thomas S (2012) Cure kinetics and thermal stability of micro and nanostructured thermosetting blends of epoxy resin and epoxidized styrene-block-butadiene-block-styrene triblock copolymer systems. *Polym Eng Sci* 52:2336–2347
- George SM, Puglia D, Kenny JM, Parameswaranpillai J, Thomas S (2014) Reaction-induced phase separation and thermomechanical properties in epoxidized styrene-block-butadiene-block-styrene triblock copolymer modified epoxy/DDM system. *Ind Eng Chem Res* 53:6941–6950
- Ghaemy M, Khandani MH (1998) Kinetics of curing reaction of DGEBA with BF₃-amine complexes using isothermal DSC technique. *EurPolym J* 34:477–486
- Girard-Reydet E, Riccardi CC, Sautereau H, Pasault JP (1995) Epoxy-aromatic diamine kinetics. Part 1. Modeling and influence of the diamine structure. *Macromolecules* 28:7599–7607
- Girard-Reydet E, Sautereau H, Pascault JP (1999) Use of block copolymers to control the morphologies and properties of thermoplastic/thermoset blends. *Polymer* 40:1677–1687
- Girard-Reydet E, Sévignon A, Pascault JP, Hoppe CE, Galante MJ, Oyanguren PA, Williams RJJ (2002) Influence of the addition of polystyrene-block-poly(methyl methacrylate) copolymer (PS-*b*-PMMA) on the morphologies generated by reaction-induced phase separation in PS/PMMA/epoxy blends. *Macromol Chem Phys* 203:947–952
- Grillet AC, Galy J, Pascault JP, Bardin I (1989) Effects of the structure of the aromatic curing agent on the cure kinetics of epoxy networks. *Polymer* 30:2094–2103
- Grubbs RB, Dean JM, Broz ME, Bates FS (2000) Reactive block copolymers for modification of thermosetting epoxy. *Macromolecules* 33:9522–9534
- Hermel-Davidock TJ, Tang HS, Murray DJ, Hahn SF (2007) Control of the block copolymer morphology in templated epoxy thermosets. *J Polym Sci Part B: Polym Phys* 45:3338–3348
- Hu C, Yu J, Huo J, Chen Y, Ma H (2015) Nanostructures and thermal-mechanical properties of cyanate ester/epoxy thermosets modified with poly(ethylene oxide)-poly(propylene oxide)-poly(ethylene oxide) triblock copolymer. *Polym Adv Technol* 26:907–916
- Jenninger W, Schawe JEK, Alig I (2000) Calorimetric studies of isothermal curing of phase separating epoxy networks. *Polymer* 41:1577–1588
- Kamal MR, Sourour S (1973) Kinetics and thermal characterization of thermoset cure. *Polym Eng Sci* 13:59–64
- Karkanis PI, Partridge IK (2000) Cure modeling and monitoring of epoxy/amine resin systems. I. Cure kinetics modeling. *J Appl Polym Sci* 77:1419–1431
- Kim DS, Kim SC (1994) Rubber modified epoxy resin. I: cure kinetics and chemorheology. *Polym Eng Sci* 34:625–631
- Kim D, Beak JO, Choe Y, Kim W (2005) Cure kinetics and mechanical properties of the blend system of epoxy/diaminodiphenyl sulfone and amine terminated polyetherimide-carboxyl terminated poly (butadiene-co-acrylonitrile) block copolymer. *Korean J Chem Eng* 22:755–761
- Larrañaga M, Martin MD, Gabilondo N, Kortaberria G, Corcuera MA, Riccardi CC, Mondragon I (2004) Cure kinetics of epoxy systems modified with block copolymers. *Polym Int* 53:1495–1502
- Larrañaga M, Gabilondo N, Kortaberria G, Serrano E, Remiro P, Riccardi CC, Mondragon I (2005) Micro- or nanoseparated phases in thermoset blends of an epoxy resin and PEO-PPO-PEO triblock copolymer. *Polymer* 46:7082–7093
- Larrañaga M, Martin MD, Gabilondo N, Kortaberria G, Eceiza A, Riccardi CC, Mondragon I (2006a) Toward microphase separation in epoxy systems containing PEO-PPO-PEO block copolymers by controlling cure conditions and molar ratios between blocks. *Colloid Polym Sci* 284:1403–1410
- Larrañaga M, Arruti P, Serrano E, De la Caba K, Remiro P, Riccardi C, Mondragon I (2006b) Towards microphase separation in epoxy systems containing PEO/PPO/PEO block copolymers by controlling cure conditions and molar ratios between blocks. Part 2. Structural characterization. *Colloid Polym Sci* 284:1419–1430
- Larrañaga M, Mondragon I, Riccardi CC (2007) Miscibility and mechanical properties of an amine-cured epoxy resin blended with poly (ethylene oxide). *Polym Int* 56:426–433

- Leonardi AB, Zucchi IA, Williams RJ (2015a) The change in the environment of the immiscible block stabilizes an unexpected HPC phase in a cured block copolymer/epoxy blend. *Eur Polym J* 71:164–170
- Leonardi AB, Zucchi IA, Williams RJ (2015b) Generation of large and locally aligned wormlike micelles in block copolymer/epoxy blends. *Eur Polym J* 65:202–208
- Lipic PM, Bates FS, Hillmyer MA (1998) Nanostructured thermosets from self-assembled amphiphilic block copolymer/epoxy resin mixtures. *J Am Chem Soc* 120:8963–8970
- Liu Y (2013) Polymerization-induced phase separation and resulting thermomechanical properties of thermosetting/reactive nonlinear polymer blends: a review. *J Appl Polym Sci* 127:3279–3292
- Liu J, Sue HJ, Thompson ZJ, Bates FS, Dettloff M, Jacob G, Verghese N, Pham H (2008) Nanocavitation in self-assembled amphiphilic block copolymer-modified epoxy. *Macromolecules* 41:7616–7624
- Liu J, Thompson ZJ, Sue HJ, Bates FS, Hillmyer MA, Dettloff M, Jacob G, Verghese N, Pham H (2010) Toughening of epoxies with block copolymer micelles of wormlike morphology. *Macromolecules* 43:7238–7243
- Maiez-Tribut S, Pascault JP, Soule ER, Borrajo J, Williams RJJ (2007) Nanostructured epoxies based on the self-assembly of block copolymers: a new miscible block that can be tailored to different epoxy formulations. *Macromolecules* 40:1268–1273
- Meng F, Zheng S, Li H, Liang Q, Liu T (2006) Formation of ordered nanostructures in epoxy thermosets: a mechanism of reaction-induced microphase separation. *Macromolecules* 39:5072–5080
- Mijovic J, Wijaya J (1994) Reaction kinetics of epoxy/amine model systems. The effect of electrophilicity of amine molecule. *Macromolecules* 27:7589–7600
- Mijovic J, Fishbain A, Wijaya J (1992) Mechanistic modeling of epoxy-amine kinetics. 1. Model compound study. *Macromolecules* 25:979–985
- Mijovic J, Shen M, Sy JW, Mondragon I (2000) Dynamics and morphology in nanostructured thermoset network/block copolymer blends during network formation. *Macromolecules* 33:5235–5244
- Ocando C, Tercjak A, Serrano E, Ramos JA, Corona-Galván S, Parellada MD, Fernández-Berridi MJ, Mondragon I (2008) Micro- and macrophase separation of thermosetting systems modified with epoxidized styrene-block-butadiene-block-styrene linear triblock copolymers and their influence on final mechanical properties. *Polym Int* 57:1333–1342
- Ocando C, Fernández R, Tercjak A, Mondragon I, Eceiza A (2013) Nanostructured thermoplastic elastomers based on SBS triblock copolymer stiffening with low contents of epoxy system. Morphological behavior and mechanical properties. *Macromolecules* 46:3444–3451
- Raju T, Durix S, Sinturel C, Omonov T, Goossens S, Groeninckx G, Moldenaers P, Thomas S (2007) Cure kinetics, morphology and miscibility of modified DGEBA-based epoxy resin—effects of a liquid rubber inclusion. *Polymer* 48:1695–1710
- Rebizant V, Venet AS, Tournilhac F, Girard-Reydet E, Navarro C, Pascault JP, Leibler L (2004) Chemistry and mechanical properties of epoxy-based thermosets reinforced by reactive and nonreactive SBMX block copolymers. *Macromolecules* 37:8017–8027
- Riccardi CC, Williams RJ (1986a) A kinetic scheme for an amine-epoxy reaction with simultaneous etherification. *J Appl Polym Sci* 32:3445–3456
- Riccardi CC, Williams RJ (1986b) Statistical structural model for the build-up of epoxy-amine networks with simultaneous etherification. *Polymer* 27:913–920
- Riccardi CC, Adabbo HE, Williams RJJ (1984) Curing reaction of epoxy resins with diamines. *J Appl Polym Sci* 29:2481–2492
- Riccardi CC, Fraga F, Dupuy J, Williams RJJ (2001) Cure kinetics of diglycidylether of bisphenol A-ethylenediamine revisited using a mechanistic model. *J Appl Polym Sci* 82:2319–2325
- Ritzenthaler S, Court F, David L, Girard-Reydet E, Leibler L, Pascault JP (2002) ABC triblock copolymers/epoxy-diamine blends. 1. Keys to achieve nanostructured thermosets. *Macromolecules* 35:6245–6254

- Ritzenthaler S, Court F, Girard-Reydet E, Leibler L, Pascault JP (2003) ABC triblock copolymers/epoxy-diamine blends. 2. Parameters controlling the morphologies and properties. *Macromolecules* 36:118–126
- Roşu D, Caşcaval CN, Mustăţ F, Ciobanu C (2002) Cure kinetics of epoxy resins studied by non-isothermal DSC data. *Thermochimica Acta* 383:119–127
- Ruiz-Pérez L, Royston GJ, Fairclough JPA, Ryan AJ (2008) Toughening by nanostructure. *Polymer* 49:4475–4488
- Ryan ME, Dutta A (1979) Kinetics of epoxy cure: a rapid technique for kinetic parameter estimation. *Polymer* 20:203–206
- Serier A, Pascault JP, Lam TM (1991) Reactions in aminosilane-epoxy prepolymer systems. I. Kinetics of epoxy-amine reactions. *J Polym Sci Part A: Polym Chem* 29:209–218
- Serrano E, Martin MD, Tercjak A, Pomposo JA, Mecerreyes D, Mondragon I (2005) Nanostructured thermosetting systems from epoxidized styrene butadiene block copolymers. *Macromol Rapid Commun* 26:982–985
- Serrano E, Tercjak A, Kortaberria G, Pomposo JA, Mecerreyes D, Zafeiropoulos NE, Stamm M, Mondragon I (2006) Nanostructured thermosetting systems by modification with epoxidized styrene-butadiene star block copolymers. Effect of epoxidation degree. *Macromolecules* 39:2254–2261
- Serrano E, Tercjak A, Ocando C, Larrañaga M, Parellada MD, Corona-Galván S, Mecerreyes D, Zafeiropoulos NE, Stamm M, Mondragon I (2007) Curing behavior and final properties of nanostructured thermosetting systems modified with epoxidized styrene-butadiene linear diblock copolymers. *Macromol Chem Phys* 208:2281–2292
- Smith IT (1961) The mechanism of the crosslinking of epoxide resins by amines. *Polymer* 2:95–108
- Sourour S, Kamal MR (1976) Differential scanning calorimetry of epoxy cure: isothermal cure kinetics. *Thermochim Acta* 14:41–59
- Swier S, Van Mele B (2003a) Mechanistic modeling of the epoxy-amine reaction in the presence of polymeric modifiers by means of modulated temperature DSC. *Macromolecules* 36:4424–4435
- Swier S, Van Mele B (2003b) In situ monitoring of reaction-induced phase separation with modulated temperature DSC: comparison between high-T_g and low-T_g modifiers. *Polymer* 44:2689–2699
- Swier S, Van Mele B (2003c) The heat capacity signal from modulated temperature DSC in non-isothermal conditions as a tool to obtain morphological information during reaction-induced phase separation. *Polymer* 44:6789–6806
- Swier S, Van Assche G, Vuchelen W, Van Mele B (2005) Role of complex formation in the polymerization kinetics of modified epoxy-amine systems. *Macromolecules* 38:2281–2288
- Tercjak A, Larrañaga M, Martin M, Mondragon I (2006) Thermally reversible nanostructured thermosetting blends modified with poly (ethylene-b-ethylene oxide) diblock copolymer. *J Therm Anal Calorim* 86:663–667
- Urbaczewski E, Pascault JP, Sautereau H, Riccardi CC, Moschiar SS, Williams RJ (1990) Influence of the addition of an aliphatic epoxide as reactive diluent on the cure kinetics of epoxy/amine formulations. *Die Makromolekulare Chemie* 191:943–953
- Varley RJ (2007) Reaction kinetics and phase transformations during cure of a thermoplastic-modified epoxy thermoset. *Macromol Mater Eng* 292:46–61
- Varley RJ, Hodgkin JH, Hawthorne DG, Simon GP, McCulloch D (2000) Toughening of a trifunctional epoxy system Part III. Kinetic and morphological study of the thermoplastic modified cure process. *Polymer* 41:3425–3436
- Verchere D, Sautereau H, Pascault JP (1990) Buildup of epoxy cycloaliphatic amine networks. Kinetics, vitrification and gelation. *Macromolecules* 23:725–731
- Vinnik RM, Roznyatovsky VA (2006) Kinetic method by using calorimetry to mechanism of epoxy-amine cure reaction. *J Therm Anal Calorim* 85:455–461
- Vyazovkin S, Sbirrazzuoli N (1996) Mechanism and kinetics of epoxy-amine cure studied by differential scanning calorimetry. *Macromolecules* 29:1867–1873

- Williams RJJ, Rozenberg BA, Pascault JP (1997) Reaction-induced phase separation in modified thermosetting polymers. In: *Polymer analysis polymer physics*. Springer, Berlin/Heidelberg, pp 95–156
- Wu S, Guo Q, Kraska M, Stühn B, Mai YW (2013) Toughening epoxy thermosets with block ionomers: the role of phase domain size. *Macromolecules* 46:8190–8202
- Xu L, Fu JH, Schlup JR (1994) In situ near-infrared spectroscopic investigation of epoxy resin-aromatic amine cure mechanisms. *J Am Chem Soc* 116:2821–2826
- Xu Q, Zhou Q, Shen K, Jiang D, Ni L (2015) Nanostructured epoxy thermoset templated by an amphiphilic PCL-b-PES-b-PCL triblock copolymer. *J Polym Sci Part B: Polym Phys*. doi:10.1002/polb.23917
- Zhang J, Guo Q, Fox BL (2009) Study on thermoplastic-modified multifunctional epoxies: influence of heating rate on cure behaviour and phase separation. *Comp Sci Tech* 69:1172–1179
- Zvetkov VL (2005) Mechanistic modeling of the epoxy-amine reaction: model derivations. *Thermochimica Acta* 435:71–84

Sajeev Martin George, Nishar Hameed, Seno Jose, Jinu Jacob George, and Jyotishkumar Parameswaranpillai

Abstract

Dynamic mechanical thermal analysis (DMTA) is one of the most powerful techniques to investigate the phase separation dynamics of block-copolymer (BCP)-modified epoxy systems as it provides information such as phase separation, compatibility/miscibility between the BCP blocks and epoxy matrix, specific interactions among various phases, damping characteristics, and stiffness and toughness of the system. In this chapter, we focus on the dynamic mechanical properties of epoxy thermosets modified with diblock and triblock copolymers. The type of block copolymers and the effects of different curing agents, cure temperature, hardeners, etc. on the phase structure and phase separation dynamics of epoxy thermosets are discussed. An extremely fascinating feature of DMTA is that direct information about the phase structure could be derived from the $\tan \delta$

S.M. George

Department of Chemistry, St. Thomas College, Palai/Arunapuram, Kerala, India
e-mail: martin.v.george@gmail.com

N. Hameed

Carbon Nexus, Institute for Frontier Materials, Deakin University, Geelong, VIC, Australia
Factory of the Future, Swinburne University of Technology, Melbourne, VIC, Australia
e-mail: nishar.hameed@deakin.edu.au

S. Jose

Department of chemistry, Government College Kottayam, Kottayam, Kerala, India
e-mail: senojose@gmail.com

J.J. George • J. Parameswaranpillai (✉)

Department of Polymer Science and Rubber Technology, Cochin University of Science and Technology, Cochin, Kerala, India
e-mail: jinujac@gmail.com; jyotishkumarp@gmail.com

peaks. Shift in the T_g , broadening of glass transition peaks, superimposition of two or more peaks, height and width of various transition peaks, etc. furnish ample evidence for the type and nature of the phase structure and an intuitive understanding of the related mechanism.

Keywords

Compatibility • Viscoelastic properties • Phase structure • Toughness • Glass transition temperature

Contents

Introduction	1008
Dynamic Mechanical Analysis of Nanostructured Epoxy Thermosets	1010
Epoxy System Modified with Diblock Copolymer	1010
Epoxy System Modified with Triblock Copolymer	1015
Reactive Block Copolymers	1031
Epoxidation of Immiscible Blocks	1031
Conclusion	1037
References	1037

Introduction

Epoxy resins are important thermosetting resins widely used as matrix for high-performance composites in aerospace and automobile industries, and in adhesives, coating, and insulation applications (Pham et al. 2007; Bagheri et al. 2009; Veena et al. 2011; Prolongo et al. 2012; Pethrick 2014). For developing composites for advanced applications, cured epoxy resins should be tough. However, cured epoxy systems are highly brittle which limits their applications in different areas. A number of methods are available for improving the toughness of epoxy resin. The most widely used method is the blending of epoxy resin with another polymer, such as rubber, thermoplastic, and block copolymer (Jyotishkumar et al. 2011; Parameswaranpillai et al. 2012, 2013; Vijayan et al. 2012; Mathew et al. 2012; George et al. 2013, 2014, 2015; Konnola et al. 2015a, b). Although blending of epoxy resins with rubbery inclusions improves toughness, quite often the glass transition temperature (T_g) considerably decreases, which leads to reduction of stiffness. Functionalized liquid rubbers such as carboxyl-terminated-butadiene-acrylonitrile (CTBN), amine-terminated-butadiene-acrylonitrile (ATBN), and epoxidized natural rubber (ENR) are the most widely used rubbers for improving toughness (Bucknall and Yoshii 1978; Verchere et al. 1990; Chikhi et al. 2002; Mathew et al. 2014). Alternatively, the incorporation of high-performance engineering thermoplastics enhances toughness without much reduction in T_g of epoxy matrix, but often results in only marginal improvement in toughness (Bucknall and Gilbert 1989; Hourston and Lane 1992; Pearson and Yee 1993; Jyotishkumar et al. 2013).

Recently, it has been shown that epoxy-based thermosets can be made tougher by introducing structural inhomogeneities at the nanoscales by the generation of nanovesicles, wormlike micelles, spherical micelles, and core-shell nanodomains from self-assembling block copolymers (Hillmyer et al. 1997; Lipic et al. 1998; Liu et al. 2008, 2010; Amendt 2010). One of the fascinating features of nanostructured thermosets is that there exists strong relationship between nanostructured morphology and end-use properties so that their ultimate properties can be tuned by controlling the morphology. Traditionally, amphiphilic block copolymers are used for epoxy modification, where one of the blocks is miscible with epoxy resin due to the specific interaction between the block copolymer (BCP) and the epoxy resin, while the other phase remains immiscible before and after cure.

It is well established that BCPs phase separate to nanostructures in the epoxy matrix by two different approaches, viz., self-assembly and reaction-induced phase separation (RIPS) (Amendt 2010). Self-assembly is typically observed in epoxy systems with amphiphilic block copolymers (Fig. 1), where immiscible block self-assembled in the epoxy resin and nanostructures are fixed by epoxy/hardener reaction, while the miscible block remains miscible before and after cure (Hillmyer et al. 1997; Lipic et al. 1998). Although the selection of the miscible block depends on the type of the curing agent used, the most widely accepted miscible blocks include poly(ethylene oxide) (PEO), poly(ϵ -caprolactone) (PCL), and poly(methyl methacrylate) (PMMA) (Hillmyer et al. 1997; Lipic et al. 1998; Xu and Zheng 2007a; Ocando et al. 2007; Liu et al. 2008; Fan and Zheng 2008; Amendt 2010; Liu et al. 2010; Kishi et al. 2011). These blocks are miscible with epoxy phase due to intermolecular hydrogen bonding with epoxy thermoset.

In the RIPS approach, the blocks are initially miscible with the epoxy resin, up on curing one block remains miscible with epoxy, while the other blocks get phase separated. The phase separation is limited to nanoscale since the blocks are covalently bonded. Polystyrene (PS), poly(ϵ -caprolactone) (PCL), poly(*n*-butyl acrylate) (PBA), etc. blocks undergo RIPS. However, RIPS of these blocks depends on the type of curing agent and curing temperature (Meng et al. 2006; Xu and Zheng 2007; Meng et al. 2008; Shen et al. 2015). Figure 2 illustrates the general scheme for formation of nanostructured thermosets by RIPS. Reactive block copolymers such as poly-glycidyl methacrylate, epoxidized polybutadiene, etc. are also widely used as a toughener for epoxy resin (Serrano et al. 2007; Yi et al. 2011), because the reactive blocks present in these block copolymers react with the curing agent and become a

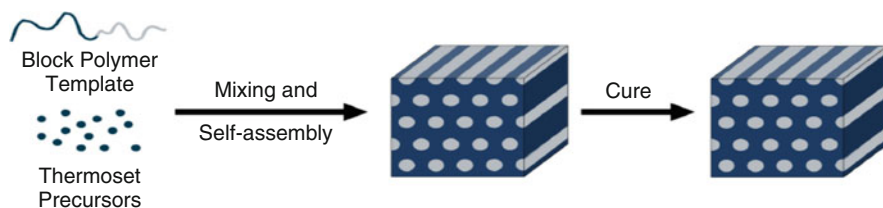


Fig. 1 Formation of nanostructures by self-assembly approach (Amendt 2010)

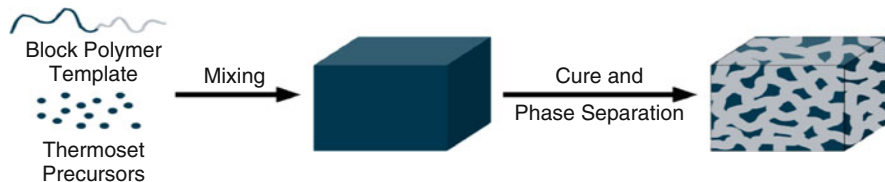


Fig. 2 Formation of nanostructures by RIPS (Amendt 2010)

part of the cured network. The other block may undergo self-assembly or RIPS depending on the nature of the block copolymer with respect to the epoxy resin.

The present chapter focuses on the dynamic mechanical properties of block copolymer-modified epoxy system. Dynamic mechanical thermal analysis (DMTA) is a widely recognized tool for the interpretation and evaluation of the performance of polymeric material as it measures response of a material to vibrational forces. The investigation of storage modulus, loss modulus, and $\tan \delta$ (internal friction or damping) over a wide range of temperatures and frequencies has proven to be very useful in studying the structural features of polymer blends and composites including miscibility, phase separation, morphological changes, stability of the phases, glass transition temperature, degree of crystallinity, and energy dissipation. The chapter is organized in such a way that the DMTA profile of epoxy systems modified with diblock copolymer, triblock copolymer, and reactive block copolymer is carefully examined, discussed, and compared.

Dynamic Mechanical Analysis of Nanostructured Epoxy Thermosets

DMTA may be considered as one of the best methods to investigate the phase separation dynamics of BCP-modified epoxy systems. Various researchers employed DMTA as a powerful tool to analyze the energy dissipation capacity (toughness), stiffness, and extent of interpenetration of BCP with epoxy resin. The physical structures of various systems, effects of cure conditions, hardeners, functionalization of epoxy, extent of specific interactions between various phases, etc. can be analyzed from dynamic mechanical spectra.

Epoxy System Modified with Diblock Copolymer

It is unequivocally established that incorporation of diblock copolymer into epoxy resin changes its phase structure and thereby the end use properties like fracture toughness. For example, the interpenetration of BCP chains into epoxy network may enhance the energy dissipation capacity of epoxy matrix, which indeed shifts the T_g of epoxy phase and broadens the glass transition peak. Quite often, the miscible component of the BCP may plasticize the epoxy matrix and reduce its T_g . The extend of peak broadening and reduction of T_g depend on various factors like nature of

miscible block, type of interaction, concentration of the BCP, etc. On the other hand, the immiscible component of BCP self-assembles into nanostructures, the shape and internal structure of which depend on the factors such as the nature and amount of immiscible block.

Poly(ethylene oxide)-Based Block Copolymer

Liu et al. (2008) studied the effect of amphiphilic BCP, poly(ethylene-*alt*-propylene)-*b*-poly(ethylene oxide) (PEO-PEP), on epoxy/1,1,1-tris(4-hydroxyphenyl)ethane (THPE) matrix. PEO was the epoxy-miscible block and PEP the epoxy-immiscible block, the immiscible block self-assembled to form spherical micelles with size of 15 nm. Figure 3 shows the DMA profile of neat epoxy system and the 5 wt% BCP-modified epoxy thermoset. The $\tan \delta$ values are slightly higher than that of neat polymer for all the temperatures. Moreover, BCP-toughened epoxy exhibits a broader T_g peak, which suggests that BCP gets well interpenetrated into the epoxy network and thereby enhances the damping characteristics of the system. This implies that the incorporation of the BCP enhances the energy dissipation capacity of the epoxy matrix and provides better toughness. It is worthwhile to mention that three relaxations are observed for the neat epoxy system, viz., α -relaxation at 110 °C (related to the relaxation of the epoxy phase), β -transition (secondary transition) at -60 °C (derived from the motions of glycidyl units in cross-linked epoxy), and ω -relaxation at 60 °C (due to the lower cross-link density sites in the epoxy network). The T_g of the epoxy phase decreases slightly for the modified thermoset due to the plasticization effect of miscible PEO sub-chains of BCP in the epoxy matrix. The ω -relaxation is not observed for the modified thermoset due to the

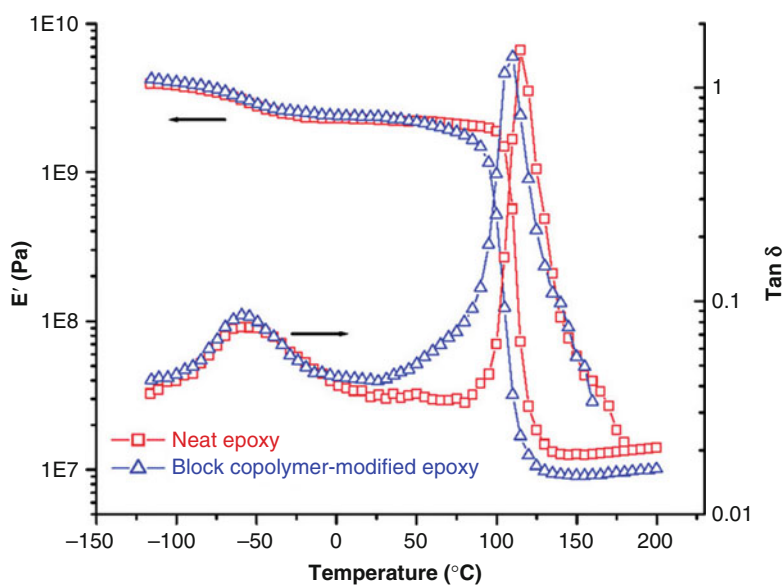
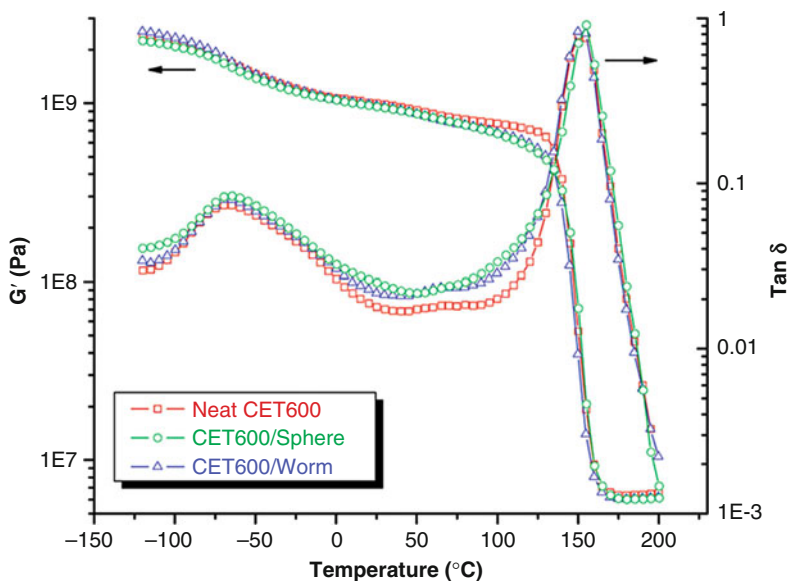


Fig. 3 Dynamic mechanical spectra of neat epoxy and PEO-PEP-toughened epoxy (Reprinted with permission (Liu et al. 2008))

Table 1 Storage modulus and fracture toughness values of neat epoxy and BCP-toughened epoxy (Reprinted with permission (Liu et al. 2008))

	Neat epoxy ($T_g = 115\text{ }^\circ\text{C}$)	BCP-toughened epoxy ($T_g = 110\text{ }^\circ\text{C}$)
Storage modulus (Pa)		
At low temperature ($-100\text{ }^\circ\text{C}$)	3.86×10^9	4.04×10^9
At room temperature	2.25×10^9	2.36×10^9
At rubbery plateau	1.41×10^7	1.01×10^7
Fracture toughness, K_{IC} ($\text{MPa m}^{1/2}$)	0.96 ± 0.04	2.73 ± 0.08

**Fig. 4** Dynamic mechanical spectra of CET600, CET600/sphere, and CET600/worm (Reprinted with permission (Liu et al. 2010))

overlapping of broader relaxations of T_g of the nanostructured thermoset. The storage modulus at different temperatures and fracture toughness of the epoxy system and nanostructured thermoset are shown in the Table 1. The table reveals that the storage modulus of epoxy system increases with the incorporation of BCP up to room temperature, and beyond that it drops below the modulus of neat control epoxy.

Investigations on the viscoelastic properties of PEP-PEO BCP blended with epoxy/1,1,1-tris(4-hydroxyphenyl)ethane (THPE) system showed that the immiscible PEP self-assembled into a wormlike and spherical micelle structures (Liu et al. 2010). The neat epoxy, BCP wormlike micelle-modified epoxy, and BCP spherical micelle-modified epoxy are designated as CET600, CET600/worm, and CET600/sphere, respectively. Figure 4 displays the DMA profile of neat epoxy

system and the BCP-modified epoxy thermoset. The T_g 's of the epoxy phase for the neat epoxy and nanostructured thermosets are almost same. However, for both CET600/sphere and CET600/worm samples, the storage modulus is slightly lower, while $\tan \delta$ values are slightly higher than that of neat polymer between 0 °C and the T_g of the epoxy phase. This suggests that both the spherical and wormlike BCP micelles get intimately interpenetrated into epoxy networks and enhanced fracture toughness of epoxy system. Moreover, it indicates that the incorporation of the BCP enhances the energy dissipation capacity of the epoxy matrix, rendering the matrix more viscoelastic at temperatures above 0 °C.

In another study, these authors (Liu et al. 2009) performed the DMA of epoxy/THPE system (three different model epoxies having different cross-link density) with 5 wt% PEP-PEO diblock copolymer (Fig. 5). The neat and modified epoxy samples with different M_c (molecular weight between cross-links) are designated as CET900, CET1550, CET2870, CET900/BCP, CET1550/BCP, and CET2870/BCP. The storage moduli at low temperature, room temperature, and rubbery plateau are given in Table 2. For the control epoxy, T_g decreases with decreasing cross-link density. The $\tan \delta$ peak height is minimum indicating lower damping for systems with higher cross-link density. This implies that the epoxy sites with higher cross-link density are least capable of dissipating fracture energy. Moreover, it implies that the toughening ability of epoxies can be correlated with the magnitude of $\tan \delta$ curve. The storage modulus is greater for the BCP-modified epoxies than the control epoxy at room temperature indicating that the modulus of the epoxy is not compromised by the incorporation of BCP. Additionally, enhanced damping for BCP-modified epoxies implies better toughness of nanostructured thermosets.

Poly(ϵ -caprolactone)-Based Block Copolymer

Xu and Zheng (2007a) developed nanostructured PCL-*b*-PBA/epoxy by RIPS of poly(ϵ -caprolactone)-block-poly-(*n*-butyl acrylate)/(PCL-*b*-PBA)-epoxy system cured with 4,4'-methylenebis(2-chloroaniline) (MOCA). PCL remains miscible with epoxy before and after cure, while PBA gets phase separated. The dynamic mechanical spectra of the nanostructured thermoset are shown in Fig. 6. The cured neat epoxy system shows T_g of the epoxy phase (α -transition) at 160 °C. Attention should be paid to the fact that the addition of PCL-*b*-PBA into the thermosets significantly decreases the T_g of epoxy phase. In fact, addition of 40 wt% of BCP diminishes the T_g of the epoxy phase from 160 °C to 136 °C due to the plasticization of miscible PCL sub-chains of the BCP in the epoxy matrix. Note that the miscibility of PCL with epoxy resin is due to intermolecular hydrogen bonding. Interestingly, another transition at -34 °C is observed with increasing the concentration of PCL-*b*-PBA, assignable to the T_g of the PBA microdomains in the nanostructured thermosets.

In a similar study, Mondragon and coworkers (Ocando et al. 2007) investigated the dynamic mechanical properties of neat epoxy and PCL- and PaF-*b*-PCL-modified epoxy/MCDEA (aromatic diamine). PCL phase remains miscible with epoxy before and after cure. However, PaF block remains immiscible in the epoxy phase and self-assembles into wormlike and spherical micelles in the thermoset system.

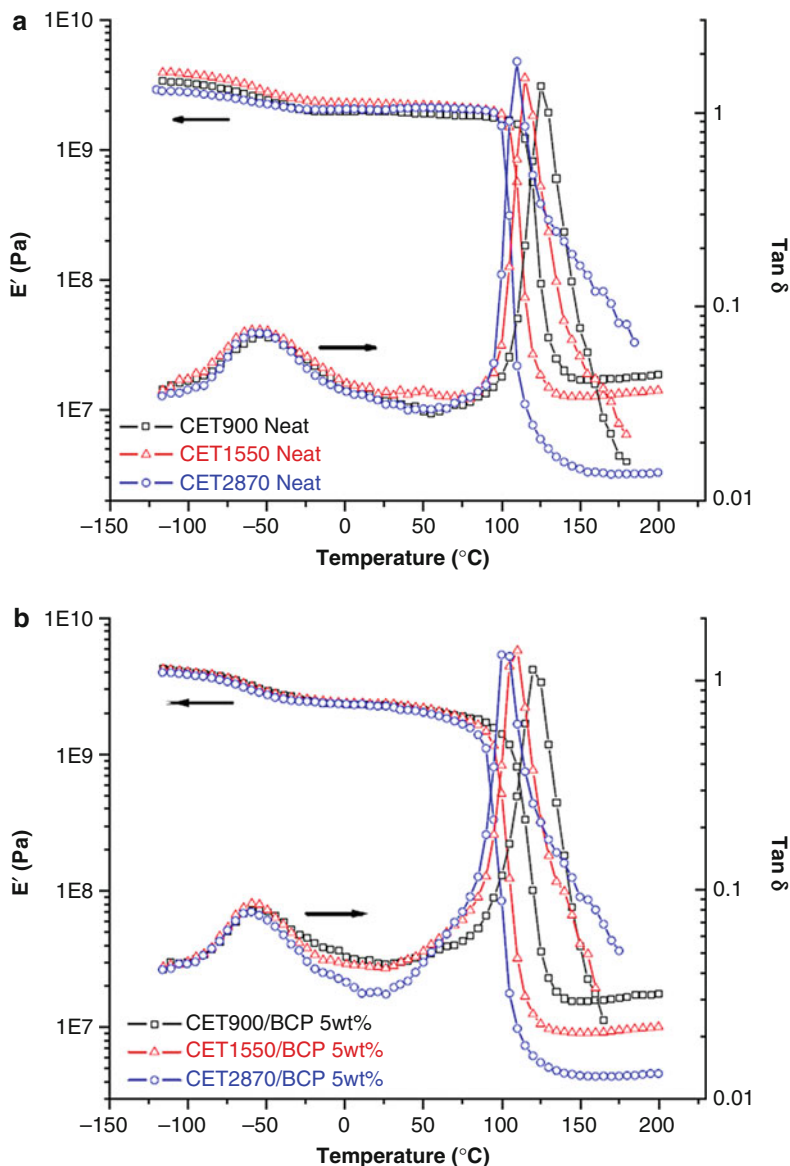


Fig. 5 Dynamic mechanical spectra of (a) neat epoxies and (b) BCP-modified epoxies with different cross-link densities (Reprinted with permission (Liu et al. 2009))

DMA profile at high-temperature range (RT to 240 $^{\circ}\text{C}$) and low-temperature range (-150 $^{\circ}\text{C}$ to RT) is shown in Fig. 7. The neat epoxy exhibits two relaxation peaks, a β -relaxation at around -80 $^{\circ}\text{C}$ and an α -relaxation at 190 $^{\circ}\text{C}$. The spectra associated with 20 wt% PCL and 35 wt% PaF-*b*-PCL-modified epoxy systems show shift of T_g

Table 2 Storage modulus (E'), glass transition temperature (T_g), and fracture toughness (K_{IC}) of neat and toughened epoxy samples (Reprinted with permission (Liu et al. 2009))

Sample	E' (MPa)			T_g (°C)	K_{IC} (MPa m ^{1/2})
	At low temp	At room temp	At rubbery plateau		
CET900	3270	1990	17.9	125	0.82 ± 0.05
CET1550	3860	2250	13.3	115	0.96 ± 0.04
CET2870	2800	2040	32	110	0.92 ± 0.03
CET900/ BCP	4070	2310	16.8	120	1.95 ± 0.03
CET1550/ BCP	4040	2360	9.4	110	2.73 ± 0.08
CET2870/ BCP	3870	2270	4.4	100	3.02 ± 0.17

of the epoxy-rich phase to lower temperatures, probably due to the partial dissolution of PCL and PaF-*b*-PCL in epoxy matrix. However, the T_g of the epoxy phase for the epoxy/BCP system is slightly higher than PCL-modified blends resulting from the restriction in the mobility of PCL chains in the copolymer and de-swelling of a part of PCL chains near the PaF block, due to the microphase separation of PaF block.

Wu et al. (2012) studied the effect of addition of SSEBS-*c*-PCL (block ionomer complexes based on sulfonated polystyrene-block-poly(ethylene-*ran*-butylene)-block-polystyrene, SSEBS, and a tertiary amine-terminated poly(ϵ -caprolactone)) with various PCL compositions in epoxy/MDA system. Nanostructured spherical domains of SSEBS dispersed in epoxy matrix are obtained. The storage modulus and $\tan \delta$, measured at five different frequencies (0.1, 0.4, 1.0, 2.0, and 4.0 Hz), are shown in Fig. 8. The T_g of the epoxy matrix decreases by the addition of SSEBS-*c*-PCL. Interestingly, the change in T_g of epoxy phase depends on the wt% PCL in SSEBS-*c*-PCL block copolymer. The T_g decreases with increasing PCL content in BCP, due to the increased miscibility of PCL phase at higher PCL content. Furthermore, for a given epoxy blend, T_g moves toward higher temperature with increasing test frequency.

Epoxy System Modified with Triblock Copolymer

It is well recognized that addition of a triblock copolymer into epoxy resin changes the phase structure of the matrix in a way similar to that observed for diblock copolymer-modified epoxy systems. For example, incorporation of triblock copolymer decreases the T_g of epoxy phase, due to the plasticization effect of miscible blocks in epoxy matrix. Note that immiscible blocks get self-assemble to generate nanostructures. Generally, with increase in concentration of copolymer, T_g decreases. In contrast, formation of chemical linkages between epoxy matrix and reactive BCP may increase the T_g of epoxy phase (Yi et al. 2011). Broadening of transition peaks of epoxy phase due to the superimposition of two or more peaks (not necessarily transition peaks) also

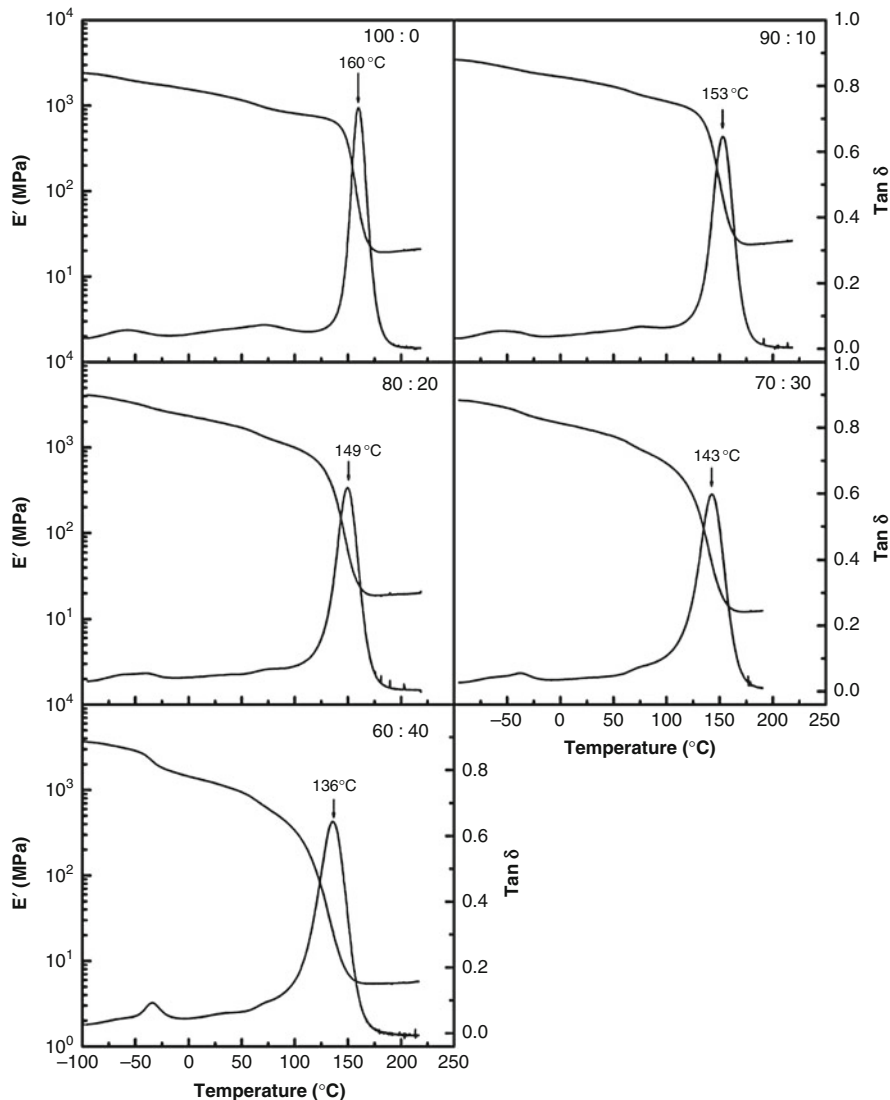


Fig. 6 Dynamic mechanical spectra of PCL-*b*-PBA-modified nanostructured thermosets (Reprinted with permission (Xu and Zheng 2007a))

can be expected. It is important to mention that cure temperature has a prominent role in phase separation dynamics as different phase structures can be re-melted at different cure temperatures. Further, hardeners also play a distinct role in deciding the final phase structure, irrespective of the triblock copolymer as they influence the phase separation phenomena and thereby the T_g of various phases. Attention should be paid to the fact that systems having different phase structures, viz., microstructures and nanostructures,

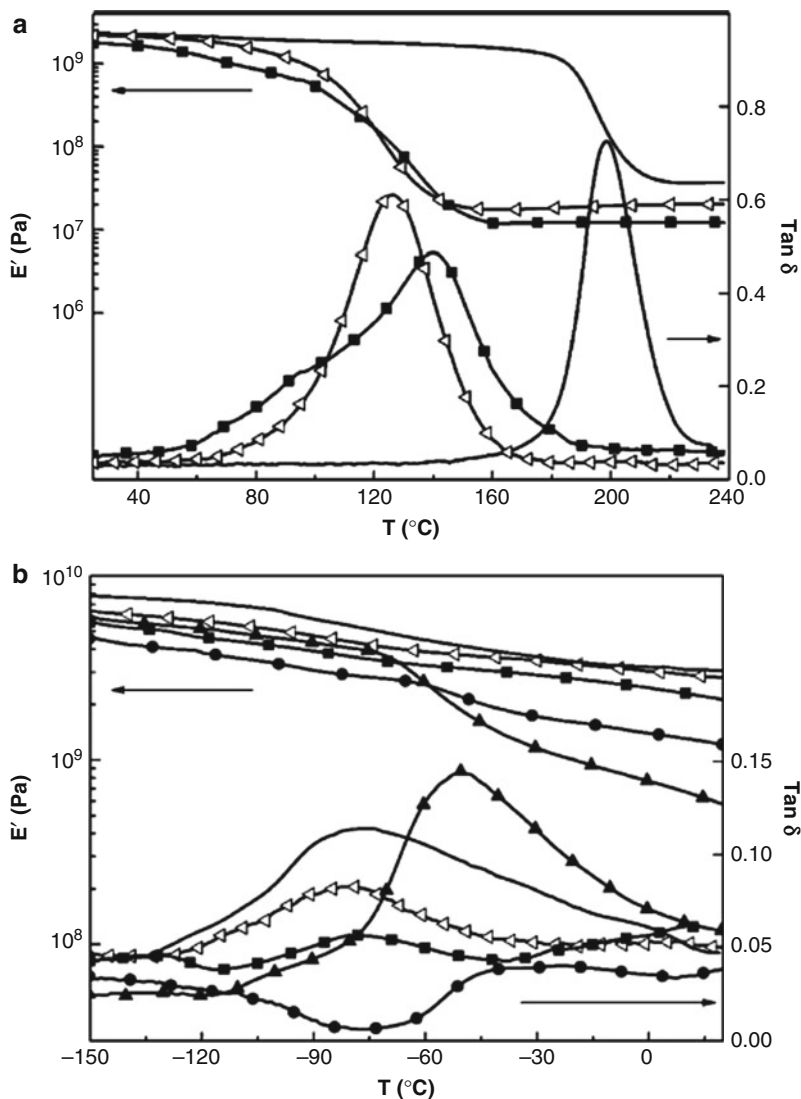


Fig. 7 Dynamic mechanical spectra obtained at 1 Hz of neat DGEBA/MCDEA system (—) and its blends containing 20 wt% PCL (Δ) and 35 wt% PaF-*b*-PCL (\blacksquare). (a) High- and (b) low-temperature range (Reprinted with permission (Ocando et al. 2007))

exhibit marked difference in T_g 's, even if other factors remain almost unaffected. Cross-link density also plays a crucial role as the molecular motions at T_g are related to the cross-link density of epoxy thermoset. Convincing experimental evidence has been emerged to establish the importance of epoxidation of BCP to improve the compatibility between BCP and epoxy matrix. Presence of epoxy groups in the system, indeed, changes T_g , favorably affect damping characteristics and enhance end use properties.

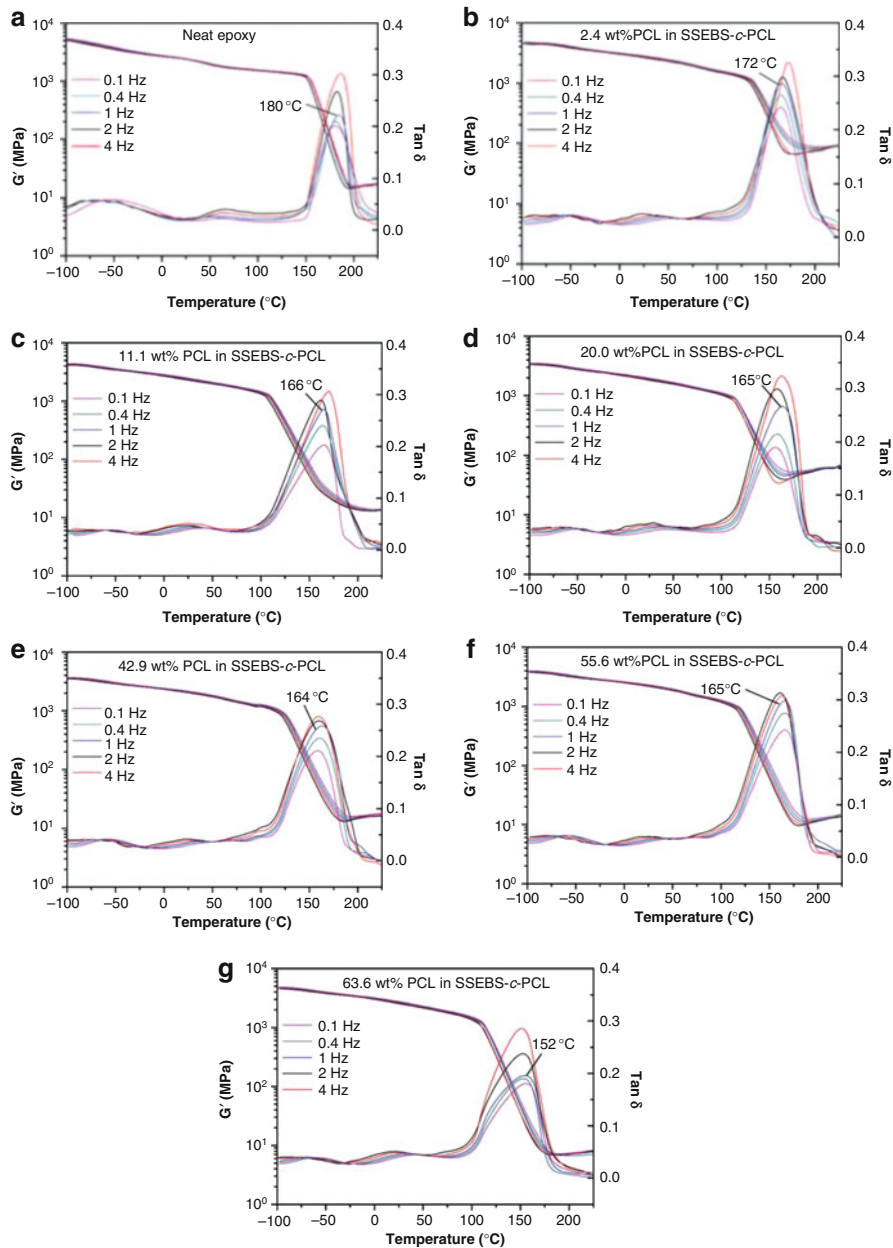


Fig. 8 Dynamic mechanical spectra of (a) neat epoxy and epoxy blends with 10 wt% SSEBS-c-PCL containing (b) 2.4, (c) 11.1, (d) 20.0, (e) 42.9, (f) 55.6, and (g) 63.6 wt% PCL (Reprinted with permission (Wu et al. 2012))

Poly(ϵ -caprolactone)-Based BCP

Zheng and coworkers (Hu et al. 2010) investigated the self-assembly behavior of amphiphilic poly(ϵ -caprolactone)-block-poly(ethylene-co-ethylethylene)-block-poly(ϵ -caprolactone) (PCL-b-PEEE-b-PCL) triblock copolymer in epoxy thermosets. Note that PCL is miscible in epoxy due to the hydrogen bonding interaction, the extent of which could be understood from the changes in T_g with respect to the neat epoxy system. The authors found the self-assembly of PEEE block in epoxy resin before curing, and the self-assembled structure is fixed by epoxy/MOCA reaction. Moreover, the cured blends reveal spherical or wormlike nanodomains of PEEE blocks in the epoxy matrix phase depending on the content of the triblock copolymer in the epoxy thermosets. Figure 9 shows the DMA profile of epoxy resin modified with different amounts of PCL-b-PEEE-b-PCL triblock copolymers. The control epoxy shows T_g at around 160 °C. On the other hand, modified epoxy thermosets show lower values of T_g for the epoxy phase due to the plasticization of miscible PCL sub-chains of the BCP on the epoxy matrix. The T_g of the epoxy phase decreases from 159 °C to 135 °C, 120 °C, 106 °C, and 92 °C by the addition of 10%, 20%, 30%, and 40% BCP, respectively. A new transition, due to the T_g of the PEEE microdomains in the nanostructured thermosets, appears at -40 °C for the thermoset containing 40 wt% BCP. It should be emphasized that this peak is not discernible for the thermosets with less than 40 wt% BCP possibly due to too low content of amorphous PEEE.

In another study, Xu and Zheng (2007b) investigated the nanostructured thermosets containing PCL-b-PDMS-b-PCL-modified epoxy/MOCA. Figure 10 shows the dynamic mechanical spectra of this system. The neat cross-linked system shows two transitions, an α -transition at 148 °C and a secondary β -transition at -50 °C. As observed for the other epoxy/BCP systems, the T_g of the epoxy phase decreases by the addition of PCL-b-PDMS-b-PCL, due to the plasticization of miscible PCL phase on the epoxy matrix. Note that PCL remains miscible with epoxy/MOCA, before and after cure. On the other hand, PDMS remains immiscible before cure and gets self-assembled to nanodomains dispersed in the epoxy matrix. It is interesting to note that the transition of PDMS nanodomains is not pronounced in the DMA profile.

Zheng and coworkers (2013) used DMTA to study the compatibility of PCL-b-PE-b-PCL with epoxy/MOCA system and observed self-assembly of PE block in epoxy resin before curing, while the self-assembled structure was fixed by epoxy/MOCA reaction. From the DMA profile (Fig. 11), it is obvious that T_g of the epoxy phase (159 °C) decreases with increasing the concentration of PCL-b-PE-b-PCL triblock copolymer indicating plasticizing effect of PCL in epoxy matrix. It is worth noting that the melting of PE nanophase at 125 °C is observed for nanostructured thermoset containing 10 and 50 wt% of PCL-b-PE-b-PCL triblock copolymer and is superimposed with the T_g of the epoxy phase in other nanostructured thermosets.

Wang and coworkers (Yu et al. 2012) employed DMTA to compare the phase separation phenomena in epoxy/MOCA system modified with PS-b-PCL diblock and PS-b-PCL-b-PS triblock copolymers. The dynamic mechanical spectra of these

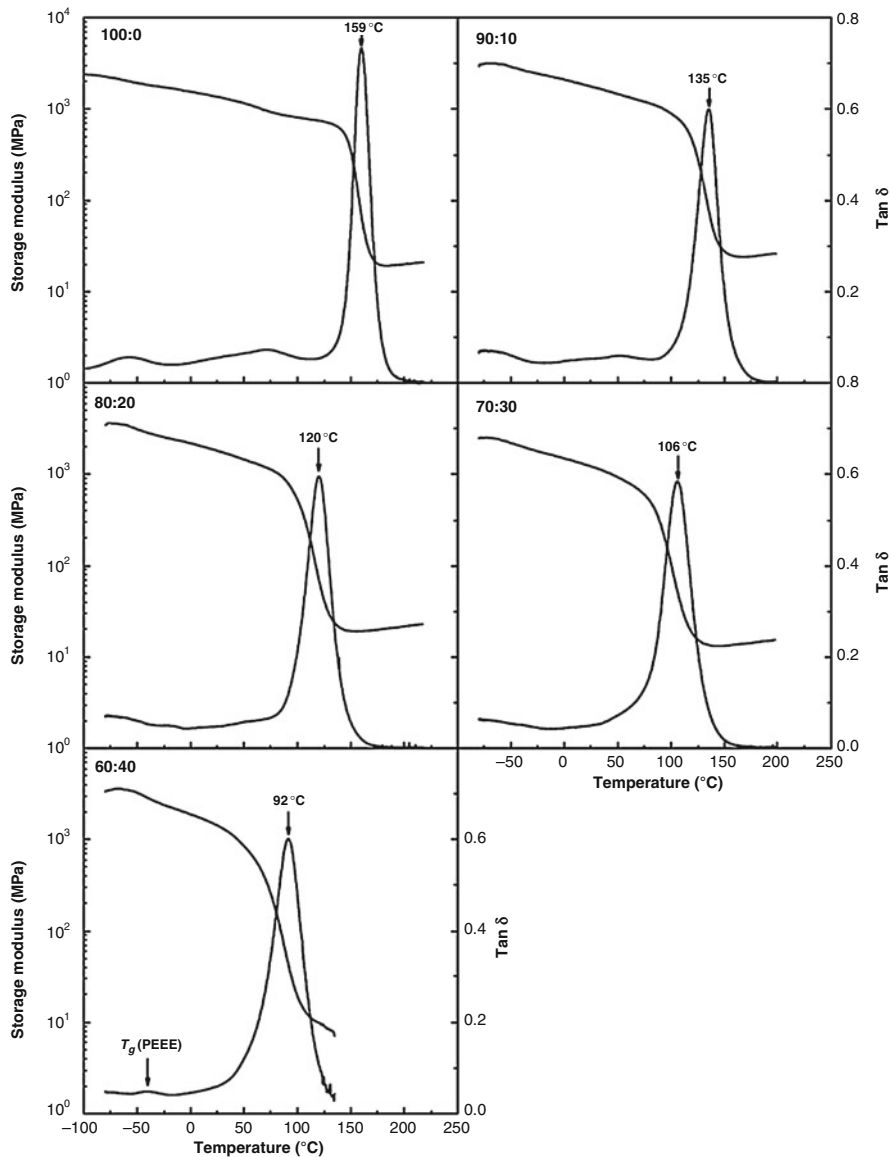


Fig. 9 Dynamic mechanical spectra of epoxy resin containing PCL-b-PEEE-b-PCL triblock copolymer (Reprinted with permission (Hu et al. 2010))

nanostructured thermosets are given in Figs. 12 and 13. The T_g of epoxy phase decreases from 159 °C to 151 °C by the addition of 10 wt% PS-b-PCL diblock copolymer (Fig. 12). The T_g of the PS microdomains visible in the range of 60–80 °C indicates the phase separation of the PS phase from the epoxy matrix. It is interesting

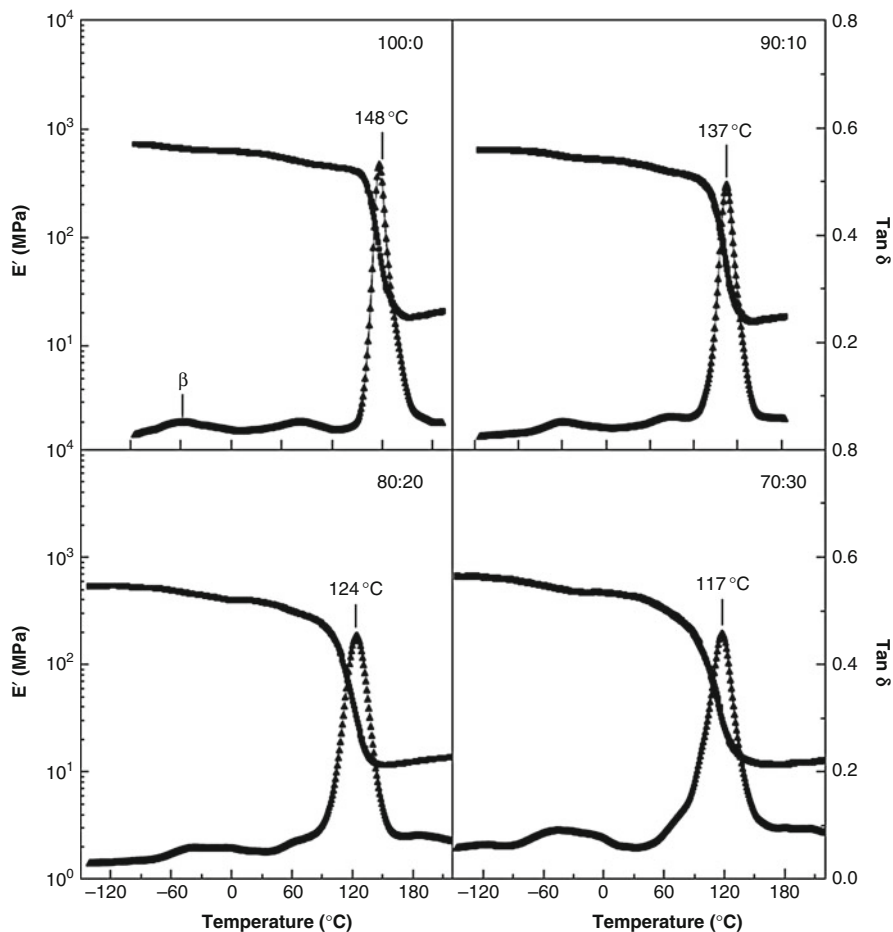


Fig. 10 Dynamic mechanical spectra of neat epoxy and PCL-b-PDMS-b-PCL-modified epoxy thermosets (Reprinted with permission (Xu and Zheng 2007a))

to note that another transition is visible at 104 °C for system with 30 wt% PS-b-PCL BCP, due to the RIPS of miscible PCL, which forms a shell over the PS nanodomains. A similar observation can be deduced from Fig. 13, for epoxy system modified with PS-b-PCL-b-PS triblock copolymer. However, in this case, a relaxation is visible at 104 °C even at 10% PS-b-PCL-b-PS triblock copolymer-modified epoxy system, probably due to the looped conformation of PCL chains at the surface of PS microdomains.

The miscibility and morphology of nanostructured thermoset containing PCL-b-PBN-b-PCL cured with MOCA was compared with ternary microstructured thermosets composed of epoxy, PBN, and PCL cured with MOCA by Zheng and coworkers (Yang et al. 2009). The dynamic mechanical spectra of these systems with the identical composition are shown in Fig. 14. The control epoxy shows a T_g at

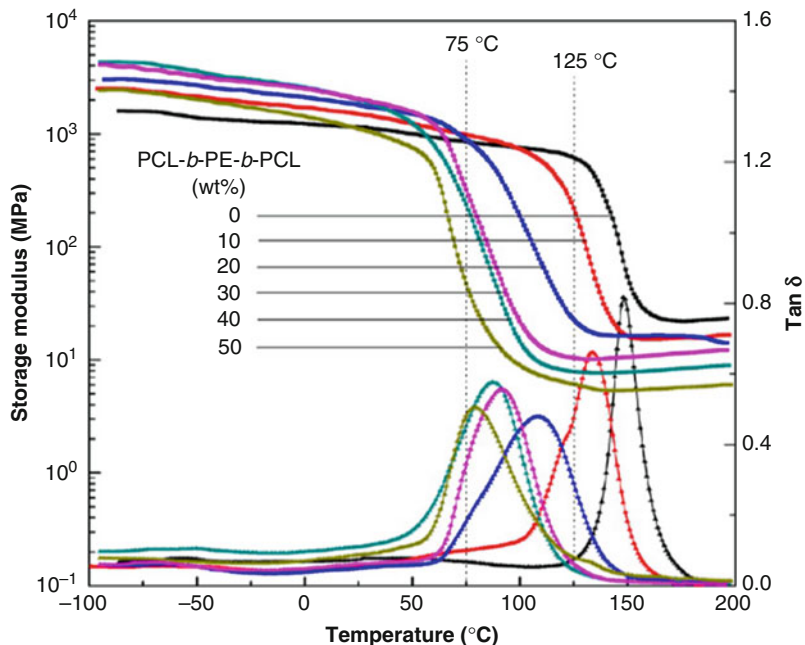


Fig. 11 Dynamic mechanical spectra of neat epoxy and PCL-*b*-PE-*b*-PCL-modified epoxy thermosets (Reprinted with permission (Zhang et al. 2013))

160 °C, while the epoxy system modified with PCL-*b*-PBN-*b*-PCL copolymer shows a decrease in T_g with increasing copolymer content, due to the plasticization of miscible PCL phase in epoxy matrix. As observed in other cases, the PCL block remains miscible with epoxy resin before and after cure, while PBN phase remains miscible in the epoxy phase before curing but gets reaction-induced phase separated to form nanostructures, after curing. It is interesting to note that for the same composition, the T_g of the epoxy matrix for the nanostructured thermoset is significantly higher than that of ternary blends composed of epoxy, PCL, and HTBN, probably due to the complete dissolution of PCL in the epoxy matrix. It should be emphasized that for the epoxy system modified with 40 wt% modifier, the rubbery plateau is not observed for ternary blends, indicating the occurrence of phase inversion. On the other hand, a well-defined rubbery plateau is visible for nanostructured thermosets. The marked difference in DMA profile is due to the difference in morphology generated for the nanostructured thermosets.

PEO-Based Triblock Copolymer

Mondragon and coworkers (Larrañaga et al. 2005) performed DMTA to investigate the influence of cure conditions on phase separation of epoxy resin in the presence of PPO, PEO, and PEO-PPO-PEO triblock copolymer. They reported the dynamic mechanical properties of DGEBA/DDM modified with 10 and 20 wt% of

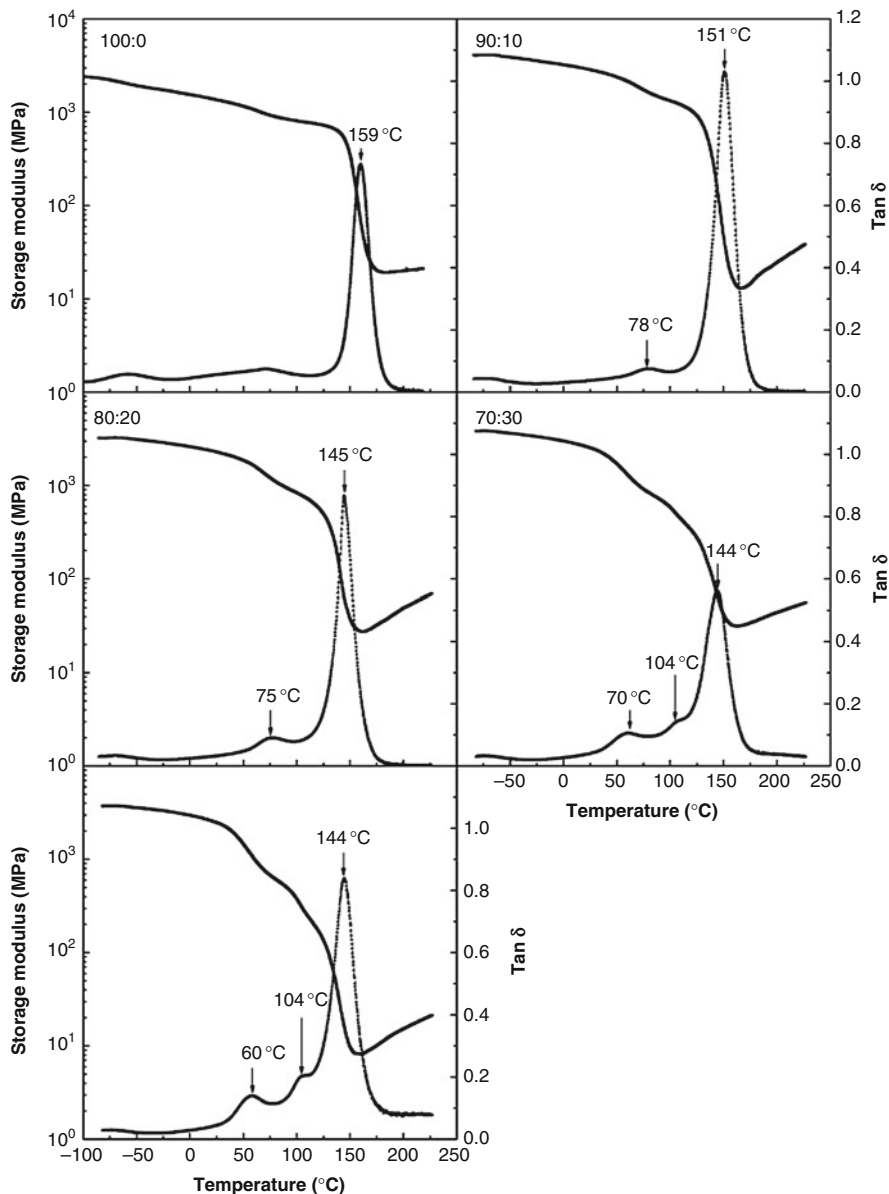


Fig. 12 Dynamic mechanical spectra of the nanostructured epoxy thermosets containing PS-b-PCL diblock copolymer (Reprinted with permission (Yu et al. 2012))

PEO-PPO-PEO, PPO, and PEO cured at (a) 80 °C and (b) 140 °C and postcured at 190 °C to examine the microstructure of the modified epoxy system with respect to cure temperatures. Figure 15 shows the variation of storage modulus and $\tan \delta$ with temperature for modified epoxy systems. For the samples cured at 80 °C and

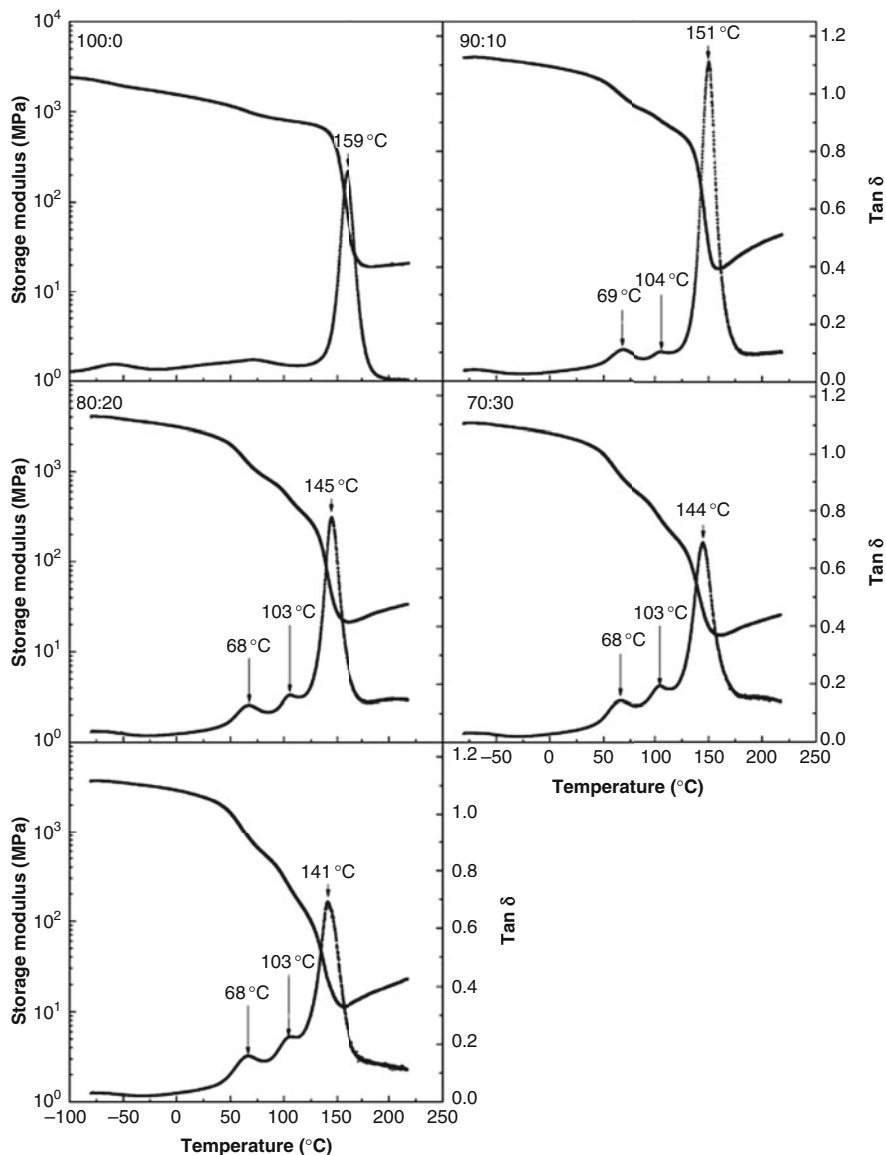


Fig. 13 Dynamic mechanical spectra of the nanostructured epoxy thermosts containing PS-*b*-PCL-*b*-PS triblock copolymer (Reprinted with permission (Yu et al. 2012))

postcured at 190 °C, neat epoxy system shows T_g at 190 °C, while PPO-modified system shows T_g at 180 °C. However, a drop in storage modulus at 100 °C due to α -relaxation is observed for the PEO-PPO-PEO- and PEO-modified systems. It is important to mention that both PEO and PEO-PPO-PEO are miscible with epoxy system before and after cure reactions since gelation occurs before nano- or

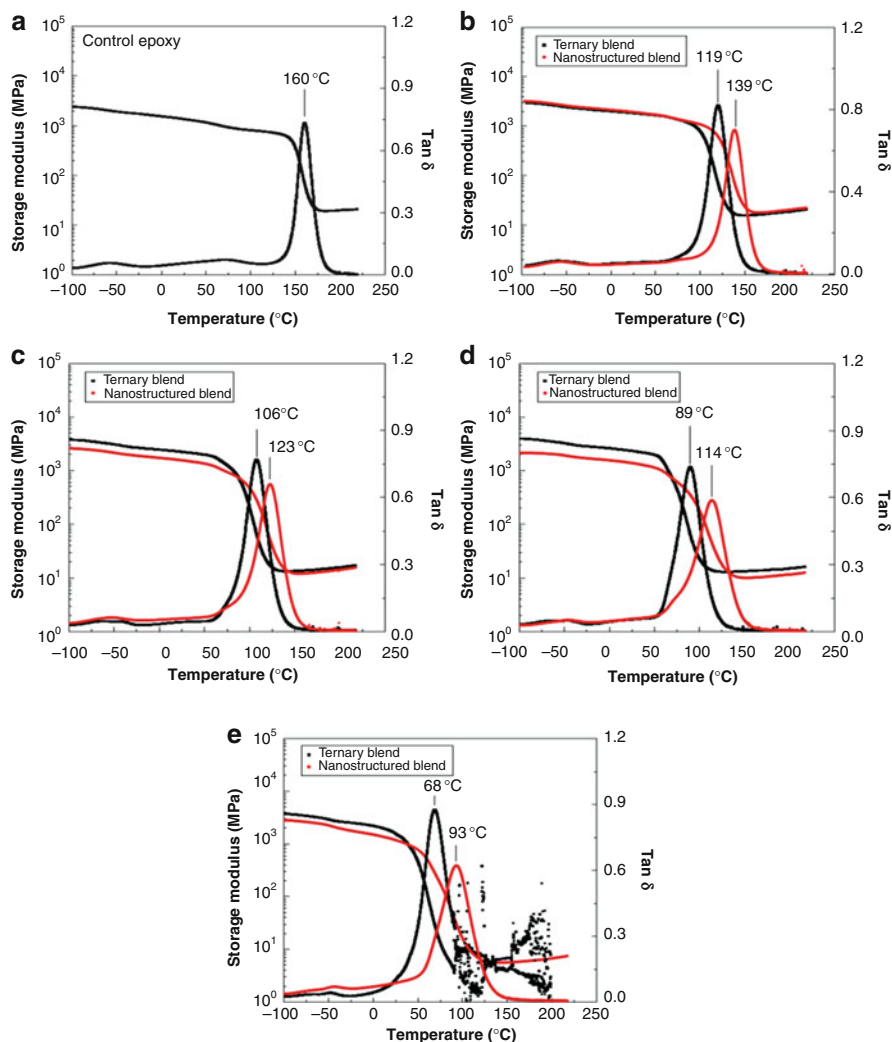
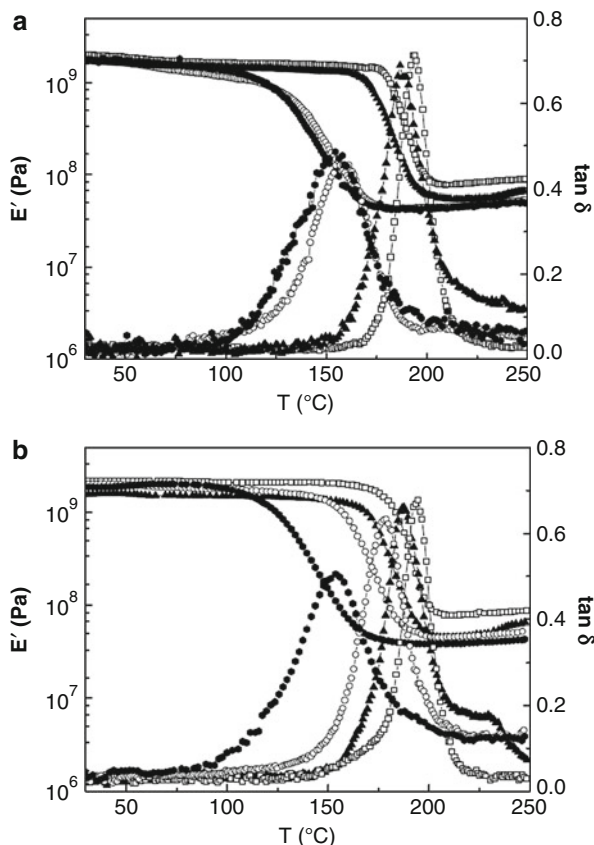


Fig. 14 The dynamic mechanical spectra of control epoxy, ternary blends, and nanostructured thermosets containing PCL-b-PBN-b-PCL (a) control epoxy, (b) 10 wt%, (c) 20 wt%, (d) 30 wt%, and (e) 40 wt% modifiers (Reprinted with permission (Yang et al. 2009))

microseparation of the system, which leads to a miscible system and hence lower T_g . The maximum in $\tan \delta$ peak for these systems is observed at 145 °C. On the other hand, for the samples cured at 140 °C and postcured at 190 °C, the α relaxation for PEO-PPO-PEO-modified blend takes place very close to with PPO, confirming the microstructure. The study signifies the importance of using DMA for a better understanding of phase separation dynamics. The peak that corresponds the T_g of the epoxy phase for nanostructured thermoset is not very intense compared with

Fig. 15 Dynamic mechanical spectra of DGEBA/DDM system modified with 10 wt% of (●) PEO, (▲) PPO, (○) PEO–PPO–PEO, and (□) neat matrix, cured at (a) 80 °C and (b) 140 °C and postcured at 190 °C (Reprinted with permission (Larrañaga et al. 2005))



microphase-separated thermoset. The depression in the peak height is due to the miscibility imparted by the block copolymer.

The extent of phase separation can be further understood from the DMA curves of samples cured at 80 °C and 140 °C and postcured at 190 °C (Fig. 16). For the systems cured at high temperature, T_g of PEO–PPO–PEO for the 20 and 30 wt% modified systems is observed at around -80 °C. However, the T_g of BCP is not intense for the system cured at low temperature, thus confirming nanophase-separated structure. The displacement of this peak to higher temperature can be related to physical interactions between PEO blocks and epoxy matrix. The physical structure of different systems and T_g of epoxy-rich phase as a function of modifier concentration and cure temperature (T_{cure}) are given in Table 3.

In general, the miscibility depends on the type of the hardener used. Yu and Zheng (2011) studied the effect of different hardeners on the modification of epoxy resin with PEO-b-PCL-b-PS triblock copolymer and observed phase separation in epoxy-modified PEO-b-PCL-b-PS triblock copolymer in the presence of hardeners, MOCA and DDS. For MOCA-cured system, both PCL and PEO remain miscible with epoxy system before and after cure and PS block gets phase separated in to

Fig. 16 Dynamic mechanical spectra of DGEBA/DDM system modified with PEO-PPO-PEO, cured at (a) 80 °C and (b) 140 °C and postcured at 190 °C (Reprinted with permission (Larrañaga et al. 2005))

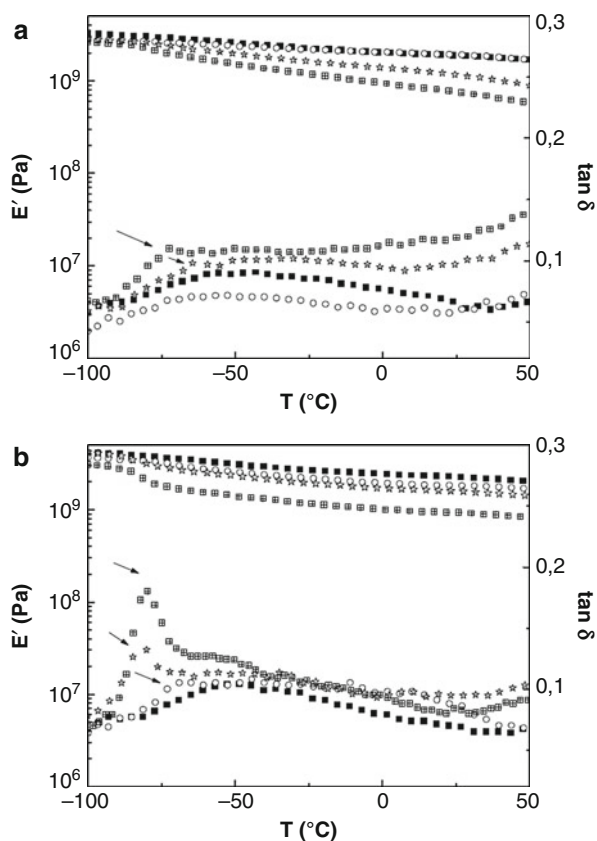


Table 3 Physical structure of different systems and T_g of epoxy-rich phase as a function of modifier concentration and cure temperature (T_{cure}) (Reprinted with permission (Larrañaga et al. 2005))

PEO-PPO-PEO (Wt%)	T_{cure} (°C)	Structure	T_g (°C)
0	80	Homogeneous	194
10	80	Homogeneous	159
10	140	Microseparated	178
20	80	Nanoseparated	155
20	140	Microseparated	180
30	80	Nanoseparated	159
30	140	Microseparated	183

nanoscale. On the other hand, when DDS is used, both PS and PCL are phase separated by RIPS. For MOCA-cured system (Fig. 17), the control epoxy exhibits T_g at 159 °C. The T_g of the epoxy phase decreases from 159 °C to 116 °C by the addition of 40 wt% PEO-b-PCL-b-PS, while the T_g of the PS phase is detected at 65 °C for all the modified nanostructured epoxy system, indicating that PS phase is

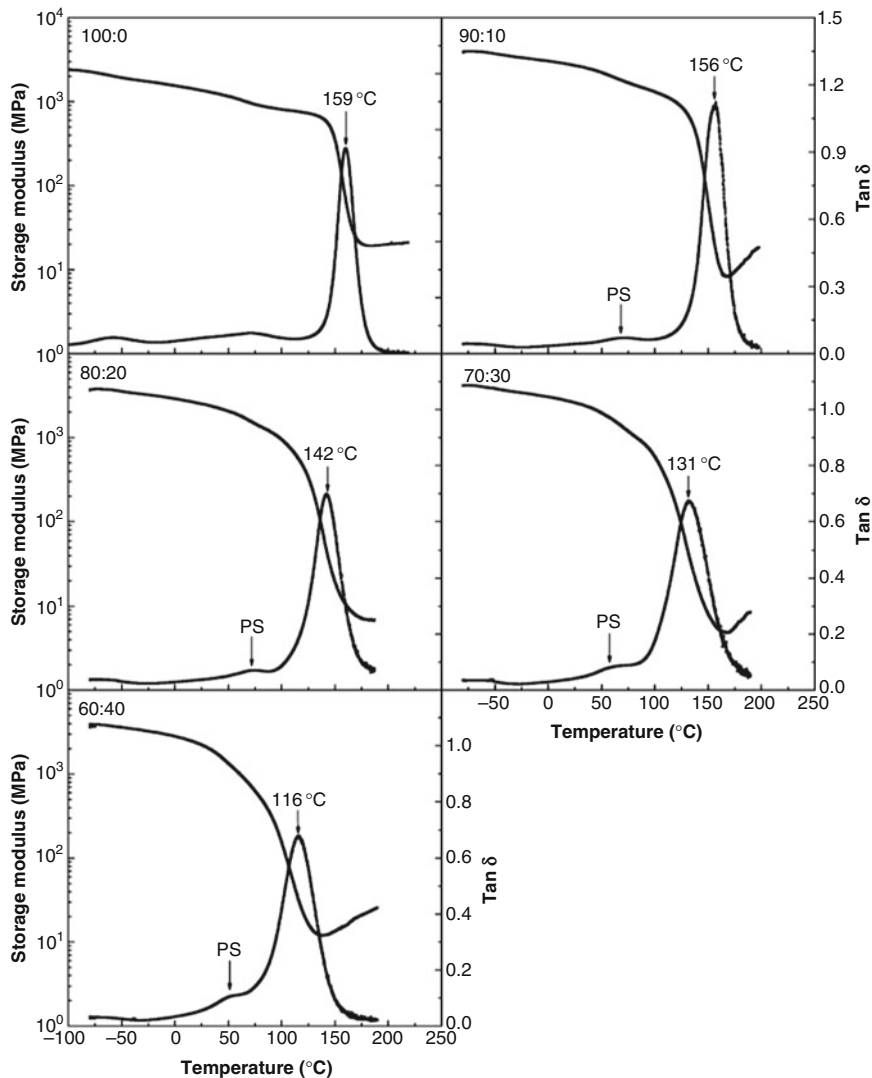


Fig. 17 Dynamic mechanical spectra of the nanostructured epoxy thermostets cured with MOCA (Reprinted with permission (Yu and Zheng 2011))

separated out of the epoxy matrix. Attention should be paid to the fact that there is no transition for PEO or PCL indicating that both PEO and PCL remain miscible with the epoxy matrix.

DDS-cured epoxy system (Fig. 18), on the other hand, shows a different behavior. The control epoxy exhibits α -transition at 199 °C. The 10 wt% of PEO-b-PCL-b-PS triblock copolymer-modified epoxy system exhibits two T_g 's; one at 190 °C (for the epoxy matrix phase) and the other at 65 °C (for the PS nanodomains dispersed in the

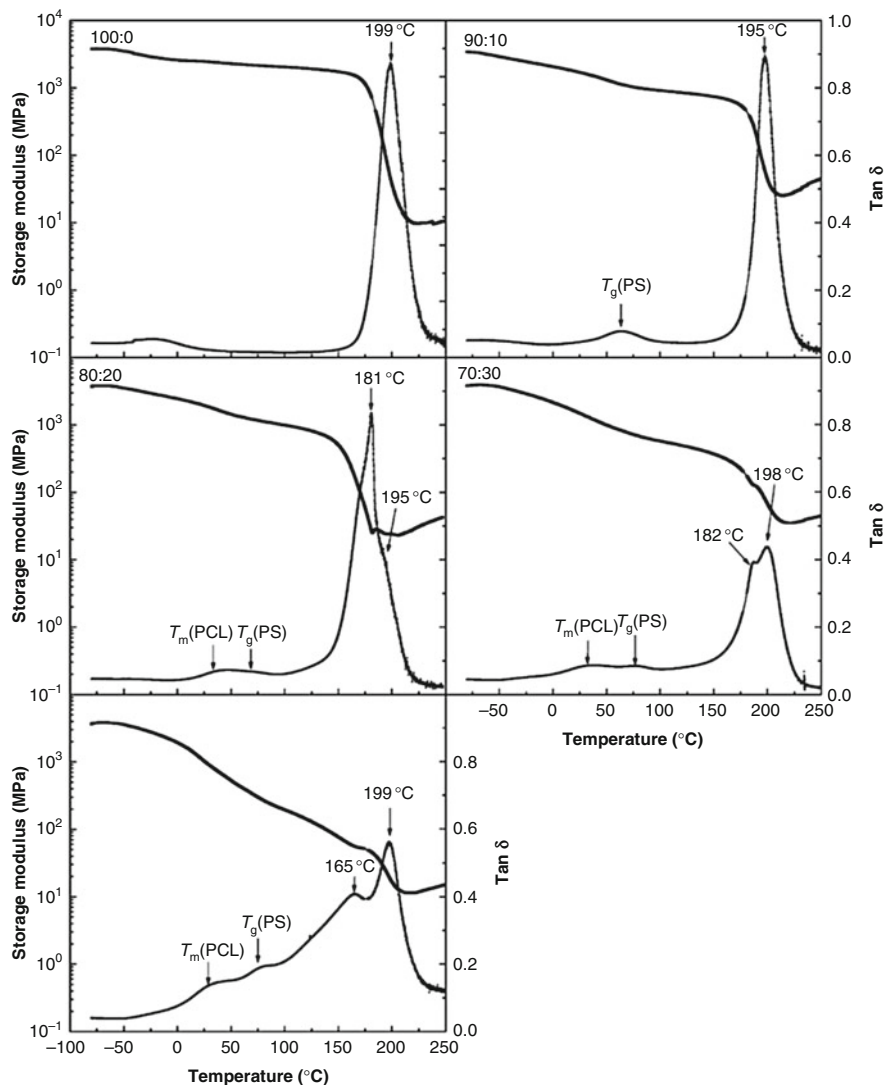


Fig. 18 Dynamic mechanical spectra of the nanostructured epoxy thermostets cured with DDS (Reprinted with permission (Yu and Zheng 2011))

matrix). The T_m of PCL microdomains is visible at 27 °C for epoxy system modified with 20 wt% PEO-b-PCL-b-PS triblock copolymer. These observations are clear indication of phase separation of both PS and PCL in epoxy/PEO-b-PCL-b-PS/DDS system, while the PEO phase remains miscible with the epoxy phase. Note that the epoxy phase shows two T_g 's at higher PEO-b-PCL-b-PS content because the epoxy matrix close to the surface of the PCL and PS dispersed microdomains are mixed with miscible PEO blocks and thus possess lower T_g , whereas the epoxy matrix far

from the surface of the dispersed microdomains remains unmixed with PEO blocks and exhibits T_g as high as the control epoxy.

PMMA-Based Triblock Copolymer

Kishi et al. (2011) employed DMTA to study the nanophase structures and mechanical properties of epoxy/PMMA-*b*-PnBA-*b*-PMMA thermosets. Four different curing agents, viz., DDS, phenol novolac (PN), methyl nadic anhydride (MNA), and 2,4,6-tris(dimethyl amino methyl)phenol (DMP), are used. The use of DDS, MNA, and DMP results in macro-phase separation in the epoxy/PMMA-*b*-PnBA-*b*-PMMA triblock-copolymer blends during curing. On the other hand, PN-cured epoxy/triblock-copolymer system leads to nanophase structures in the epoxy blends. DMA profile of four kinds of epoxy/PMMA-*b*-PnBA-*b*-PMMA blends is shown in Fig. 19a–d. Only one T_g observed at 120 °C due to the epoxy matrix for the PN-cured epoxy/BCP system suggests nanophase separation in this system. In contrary, epoxy/BCP blends using DDS, MNA, and DMP show two or three T_g 's. For the DDS-cured nanostructured thermosets, the first T_g observed at –50 °C corresponding to the T_g of PnBA segments of the BCP confirms the phase separation of PnBA segments from the epoxy matrix. The second T_g observed at 120 °C derives from the phase-separated PMMA segments of the BCP and the third T_g at 210 °C is for the epoxy-rich phase. For MNA-cured epoxy system, the first T_g observed at –50 °C corresponds to the T_g of PnBA segments of the BCP, the second T_g at 110 °C derives from the segmental motion of PMMA, and the third T_g at 160 °C corresponds

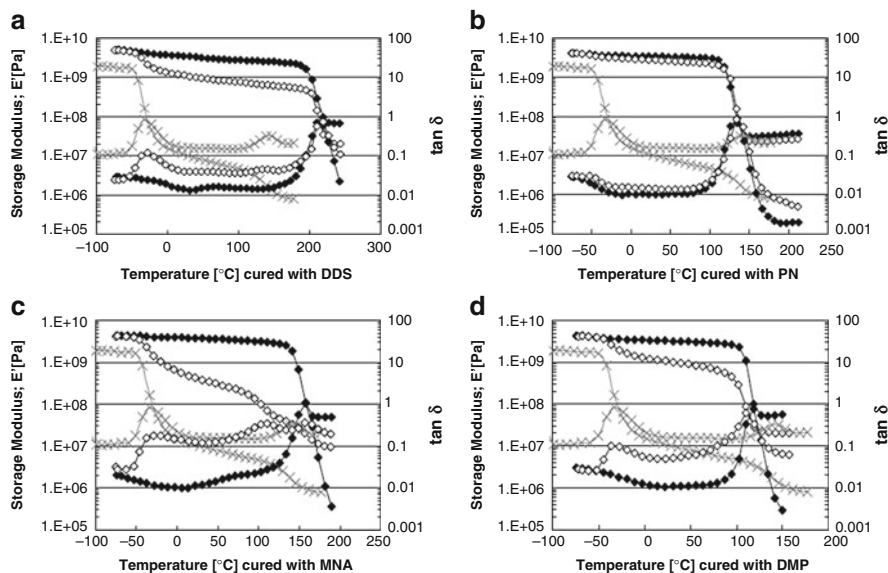


Fig. 19 Dynamic mechanical spectra of epoxy/PMMA-*b*-PnBA-*b*-PMMA blends: (a) cured with DDS; (b) cured with PN; (c) cured with MNA; (d) cured with DMP, (■) pure DGEBA, (□) DGEBA/BCP (20 wt%) blend, (×) pure BCP (Reprinted with permission (Kishi et al. 2011))

to epoxy networks. The three T_g 's confirm the phase separation of both PnBA and PMMA from the epoxy matrix. In the DMP-cured epoxy, the first T_g at -50 °C corresponds to PnBA phase and the second T_g at 110 °C to PMMA phase and epoxy networks as the relaxation of PMMAs and epoxy networks are overlapped.

Reactive Block Copolymers

Yi et al. (2011) studied Poly(2,2,2-trifluoroethylacrylate)-block-poly(glycidyl methacrylate) (PTFEA-b-PGMA)-modified epoxy/MOCA system and established the role of DMA in determining the rate of the reaction between PGMA blocks with MOCA and between epoxy with MOCA. Since PTFEA remains immiscible with epoxy, the system phase separates through self-assembly. The DMA profile given in Fig. 20 shows two T_g 's for the nanostructured thermoset. The T_g of PTFEA observed at -9 °C, irrespective of the PTFEA-b-PGMA content, represents complete phase separation of PTFEA from epoxy matrix. The T_g of the control epoxy observed at 159 °C decreases to 142 °C by the addition of 10 wt% PTFEA-b-PGMA and to 135 °C by the incorporation of 20 wt% PTFEA-b-PGMA. Interestingly, T_g of the epoxy phase increases to 151 °C and 177 °C, respectively, for systems containing 30 and 40 wt% PTFEA-b-PGMA. Note that PGMA is miscible with epoxy and capable of forming cross-linking reaction with hardener, while PTFEA is immiscible with epoxy before and after curing reaction. The authors argued that the increase in T_g is due to the formation of chemical linkages between PGMA blocks and epoxy matrix since reaction between PGMA and MOCA is faster than that between DGEBA and MOCA. On the other hand, if the reaction between PGMA and MOCA is slower than that between DGEBA and MOCA, de-mixing of PGMA blocks will occur.

Epoxidation of Immiscible Blocks

Certain BCPs containing PB blocks are immiscible with epoxy resin. They form macro-phase-separated structures in the epoxy matrix after curing, which lead to inferior properties. In order to prevent macroscopic phase separation, one of the blocks in the BCP should be miscible with epoxy phase. This can be actualized by epoxidation of PB phase, which introduces epoxy functional groups that impart miscibility and are also able to react with the curing agent to form a part of the cross-linked network. For example, George et al. epoxidized SBS at different degrees as a modifier for epoxy resin (George et al. 2013, 2014, 2015). Epoxidation was carried out to achieve nanostructured thermosets (for better compatibility with epoxy resin). A comparison of DMA profile to neat epoxy and modified epoxy which contains 47 mol% epoxidation (eSBS47) can be made in Fig. 21. The storage modulus decreases by the addition of eSBS47 due to the plasticization of miscible eSBS phase in the epoxy matrix. The control epoxy exhibits the T_g at 130 °C. Other than α -transition, a weak ω -relaxation peak at 40 °C is observed. For the nanostructured

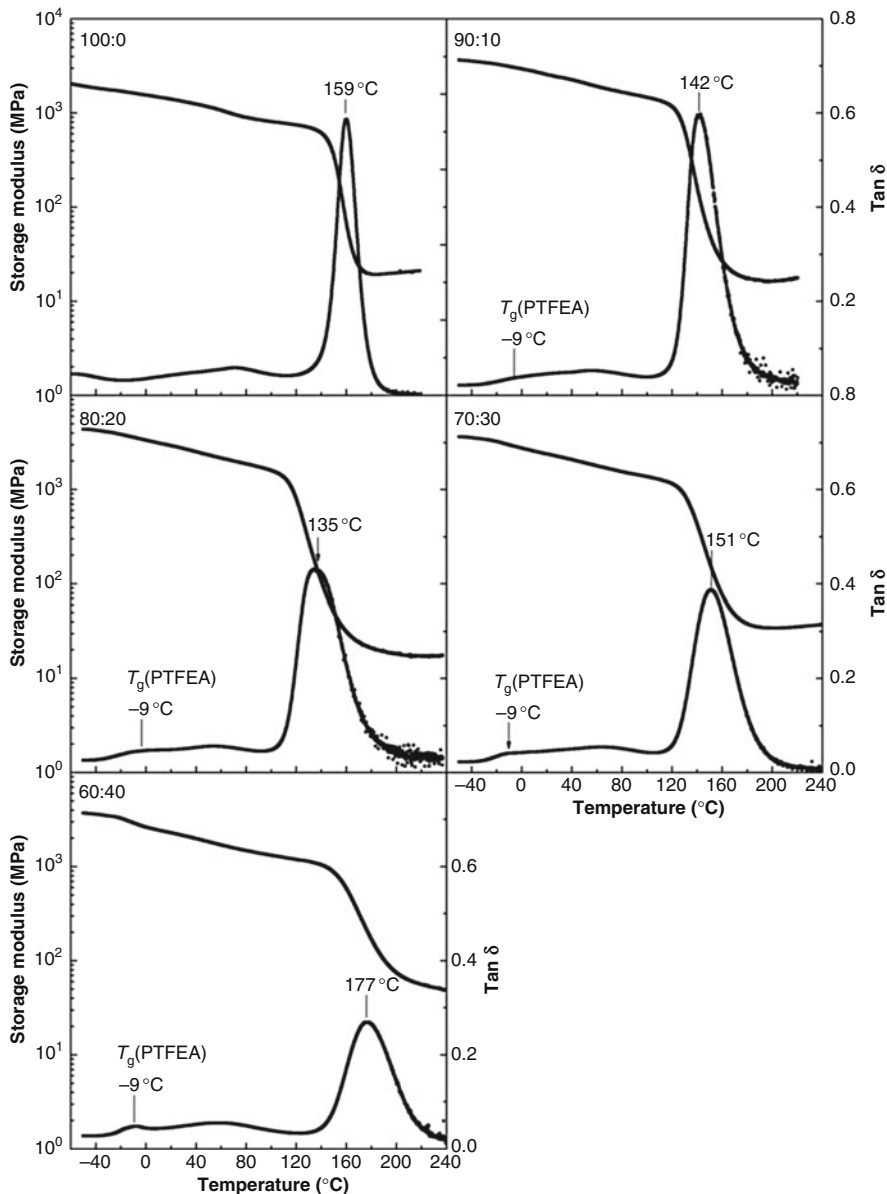
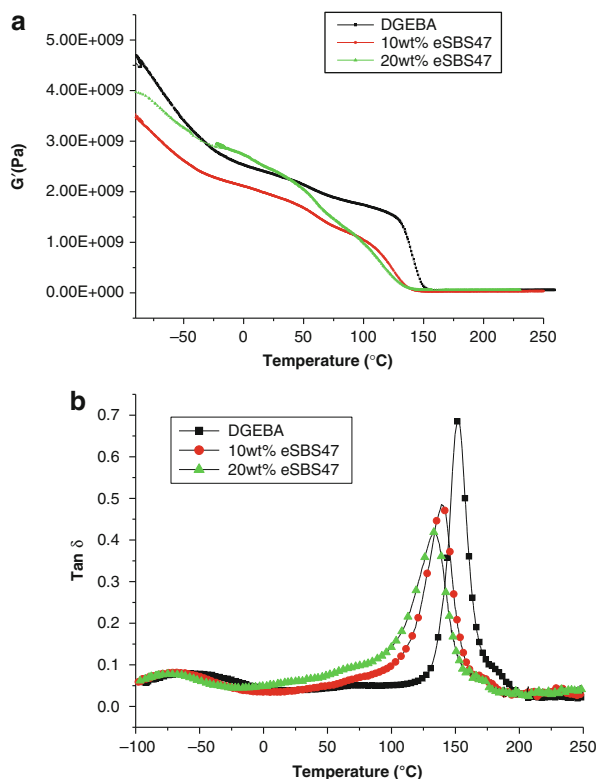


Fig. 20 The dynamic mechanical spectra of PTFEA-b-PGMA-modified epoxy/MOCA system (Reprinted with permission (Yi et al. 2011))

thermosets, a minor relaxation at around 90 °C due to PS nanodomains is noted, which confirms the phase separation of epoxy-miscible PS blocks. It is important to mention that the T_g of epoxy phase decreases by the addition of miscible BCP. The decrease in T_g is due to the compatibility between eSBS and epoxy matrix as a result

Fig. 21 Dynamic mechanical spectra of neat epoxy and eSBS47-modified epoxy blends plotted against temperature (Reprinted with permission (George et al. 2014))



of hydrogen bonding. The T_g of epoxy phase in nanostructured thermoset decreases by 10–20 °C when compared with the control epoxy system. This suggests that eSBS47 sub-chains are effectively interpenetrated into the cross-linked epoxy matrix at the segmental level.

The dynamic mechanical spectra of DGEBA/MCDEA system and its blends containing 30 wt% of styrene-*b*-butadiene BCPs epoxidized at several degrees (SepB), SepB15, SepB40, SepB61, and SepB76, were analyzed by Mondragon and coworkers (Serrano et al. 2006). The samples SepB15, SepB40, SepB61, and SepB76 correspond to 15, 40, 61, or 76 mol% epoxidation. Figure 22 represents the storage modulus profile at (a) low-temperature range and (b) high-temperature range, respectively. The neat DGEBA/MCDEA system shows two relaxations, β -relaxation at -65 °C and α -relaxation at 162 °C, due to the glass transition of the epoxy matrix.

From the low-temperature profile, relaxations at -85 °C and -70 °C for the 30 wt% SB- and SepB15-modified systems can be observed. These relaxations derive from the glass transition of SepB block in neat SB and SepB15 copolymers which overlap with the β -relaxation at -65 °C. The α -relaxation for this blend is observed at 90 °C. For higher degrees of epoxidation, for example, SepB40-, SepB61-, and SepB76 BCP-modified epoxy systems, the β -relaxations corresponding to SepB phase are observed at around -50 °C, -30 °C, and -23 °C, respectively. The

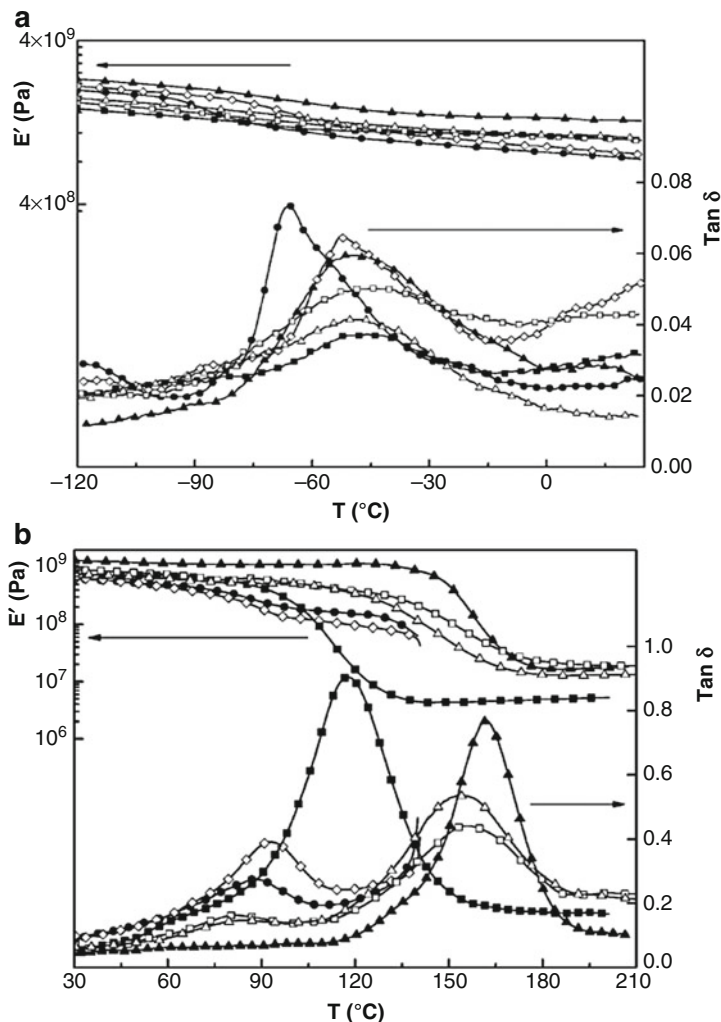


Fig. 22 Dynamic mechanical spectra obtained at 1 Hz for neat DGEBA/MCDEA system (▲) and its blends containing 30 wt% of (●) SB, (◇) SepB15, (■) SepB40, (□) SepB61, and (△) SepB76 copolymers: (a) low-temperature range and (b) high-temperature range (Reprinted with permission (Serrano et al. 2006))

increase in T_g with increasing epoxidation reveals the enhanced compatibility between SepB and epoxy. This suggests that SepB units are not separated from the epoxy matrix. For SepB40-modified epoxy system, the T_g of the epoxy phase is observed at 120 °C and slightly overlapped with the T_g for the phase-separated PS block. The increased height of the $\tan \delta$ curve indicates a plasticization effect induced by the incorporation of the SepB block in the epoxy network, which could be attributed to miscibility or to some degree of reaction between SepB40 and

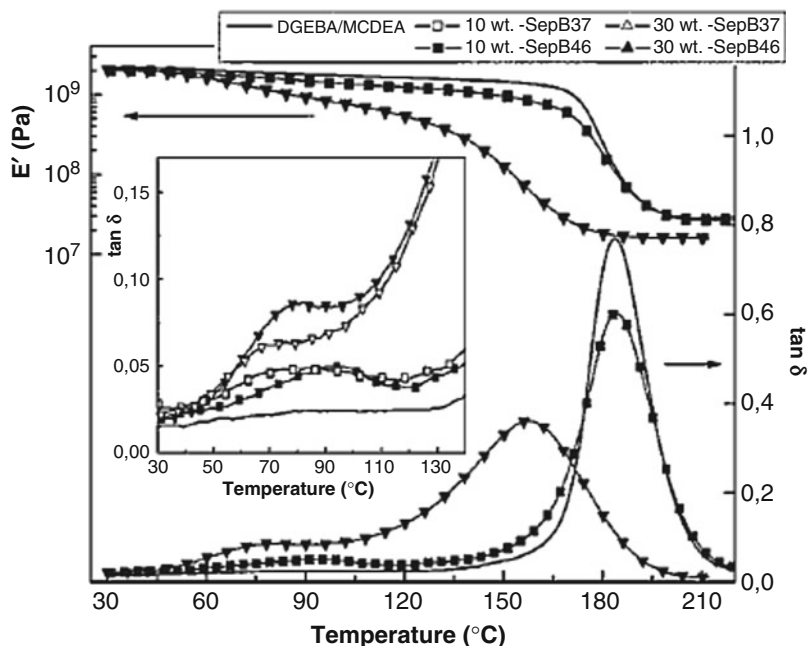


Fig. 23 Dynamic mechanical spectra of neat epoxy and epoxidized SB plotted against temperature (Reprinted with permission (Serrano et al. 2007))

MCDEA. On the other hand, for SepB61 and SepB76, the glass transition of PS is visible at 80 °C and that of epoxy phase at 155 °C, suggesting the phase separation of PS from the epoxy network. The epoxy systems modified with 30 wt% SepB40, SepB61, and SepB76 exhibit elastomer-like behavior after the T_g of the epoxy phase, indicating the continuous epoxy matrix for these systems. The lower rubbery modulus values for SepB40-modified system are consistent with a lower cross-link density for this system, which indicate that higher epoxidation rates are needed to retain the stiffness at higher temperatures. The difference in behavior between epoxy systems modified with 30 wt% SepB40, SepB61, and SepB76 arises due to the difference in the reactivity of the BCPs with MCDEA.

In another study, these authors (Serrano et al. 2007) epoxidized SB linear diblock copolymers with different epoxidation degrees (37 and 46 mol%) for better compatibility with epoxy resin. DMA profile of neat epoxy and epoxidized SB are shown in the Fig. 23. The T_g of the phase-separated PS phase is observed from the DMA profile. The T_g of the epoxy phase slightly decreases for the nanostructured thermosets indicating the miscibility between the epoxy-rich and SepB phases, thus suggesting some reactivity of the SepB units with the thermosetting formulation.

Recently, Ocando et al. (2013) studied the effect of epoxidation of PB block of poly(styrene-*b*-butadiene-*b*-styrene)/epoxy/MCDEA system by keeping a maximum of 30 wt% epoxy. The phase miscibility of 90SBSep46/10epoxy, 80SBSep46/20epoxy, and 70SBSep46/30 epoxy systems was investigated by DMA. Figure 24

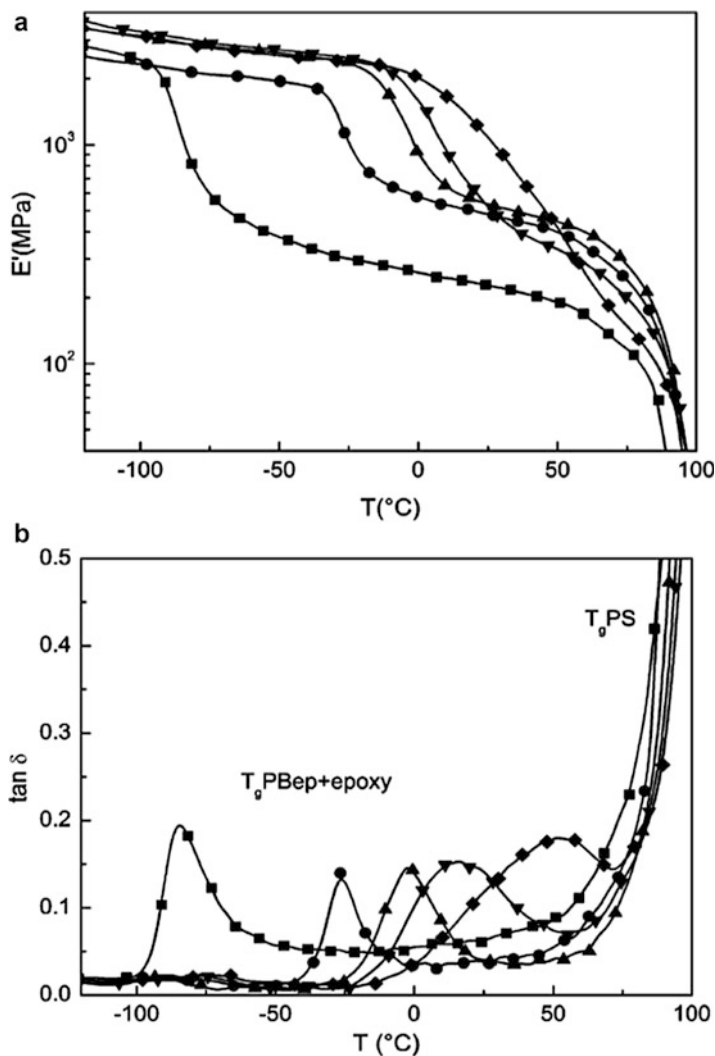


Fig. 24 Dynamic mechanical spectra of (■) neat SBS, (●) SBSep46, (▲) 90SBSEp46/10epoxy, (▼) 80SBSEp46/20epoxy, and (◆) 70SBSEp46/30epoxy systems after curing (Reprinted with permission (Ocando et al. 2013))

shows the DMA profiles of SBS, SBSep46, 90SBSEp46/10epoxy, 80SBSEp46/20epoxy, and 70SBSEp46/30epoxy systems. The SBS shows two relaxation peaks, one corresponds to the T_g of PB at -84 °C and the other corresponds to that of PS phase around 80 °C. It is interesting to note that there is dramatic increase in the T_g of PB phase (from -84 °C to -26 °C) for the 46 mol% epoxidized SBS.

All the epoxy blends reveal two T_g 's. The T_g of the epoxidized PB was -2 °C, 15 °C, and 54 °C for 90SBSEp46/10epoxy, 80SBSEp46/20epoxy, and 70SBSEp46/30epoxy

systems, respectively. The second T_g is that of the PS block phase which remains almost unchanged with respect to neat BCP (83 °C). As the content of epoxy phase increases, the T_g of epoxidized PB block phase shifts toward higher temperatures due to a larger restriction of epoxidized PB molecular motion by the presence of epoxy polymer network. The width and peak height of $\tan \delta$ peaks are enlarged with the increase of epoxy content. The broadening and increase in peak height of the $\tan \delta$ relaxation is due to the presence of epoxy networks in the epoxidized PB-rich phase.

Conclusion

Introduction of structural inhomogeneities at the nanoscales by the incorporation of block copolymers (BCP) is one of the most promising methods for enhancing the toughness of thermosetting epoxy systems. BCPs phase separate to nanostructures in the epoxy matrix either by self-assembly or reaction-induced phase separation. Dynamic mechanical analysis (DMA) has proven to be a very useful method to investigate the phase separation dynamics of BCP-modified epoxy systems. A prominent feature of DMA profile is that direct information about the phase structure could be derived from the $\tan \delta$ peaks. The interpenetration of BCP chains into epoxy thermoset enhances the energy dissipation capacity of the matrix and shifts the T_g of epoxy phase and broadens the glass transition peak. Further, the miscible component of the BCP may plasticize the epoxy matrix. In general, incorporation of BCP decreases the T_g of epoxy matrix. Nonetheless, in some cases, reactive BCP may increase the T_g of epoxy phase due to the chemical reactions between epoxy and BCP phases. Cure conditions and type of hardeners play crucial roles in the generation of final phase structure of BCP-modified epoxy systems, and a basic insight into their influence on the phase structure of epoxy thermosets can be elucidated from DMA profile.

References

- Amendt MA (2010) Nanoporous thermosetting membranes using reactive block polymer templates. PhD thesis, University of Minnesota
- Bagheri R, Marouf BT, Pearson RA (2009) Rubber-toughened epoxies: a critical review. *Polym Rev* 49:201–225
- Bucknall CB, Gilbert AH (1989) Toughening tetrafunctional epoxy resins using polyetherimide. *Polymer* 30:213–217
- Bucknall CB, Yoshii T (1978) Relationship between structure and mechanical properties in rubber toughened epoxy resins. *Br Polym J* 10:53–59
- Chikhi N, Fellahi S, Bakar M (2002) Modification of epoxy resin using reactive liquid (ATBN) rubber. *Eur Polym J* 38:251–264
- Fan W, Zheng S (2008) Reaction-induced microphase separation in thermosetting blends of epoxy resin with poly(methyl methacrylate)-*block*-polystyrene block copolymers: effect of topologies of block copolymers on morphological structures. *Polymer* 49:3157–3167

- George SM, Puglia D, Kenny JM, Causin V, Parameswaranpillai J, Thomas S (2013) Morphological and mechanical characterization of nanostructured thermosets from epoxy and styrene-block-butadiene-block-styrene triblock copolymer. *Ind Eng Chem Res* 52:9121–9129
- George SM, Puglia D, Kenny JM, Parameswaranpillai J, Thomas S (2014) Reaction-induced phase separation and thermomechanical properties in epoxidized styrene-block-butadiene-block-styrene triblock copolymer modified epoxy/DDM system. *Ind Eng Chem Res* 53:6941–6950
- George SM, Puglia D, Kenny JM, Parameswaranpillai J, Vijayan PP, Pionteck J, Thomas S (2015) Volume shrinkage and rheological studies of epoxidised and unepoxidised poly(styrene-block-butadiene-block-styrene) triblock copolymer modified epoxy resin–diaminodiphenyl methane nanostructured blend systems. *Phys Chem Chem Phys* 17:12760–12770
- Hillmyer MA, Lipic PM, Hadjuk DA, Almdal K, Bates FS (1997) Self assembly and polymerization of epoxy resin-amphiphilic block copolymer nanocomposites. *J Am Chem Soc* 119:2749–2750
- Hourston DJ, Lane JM (1992) The toughening of epoxy resins with thermoplastics: 1. Trifunctional epoxy resin-polyetherimide blends. *Polymer* 33:1379–1383
- Hu D, Zhang C, Yu R, Wang L, Zheng S (2010) Self-organized thermosets involving epoxy and poly(ϵ -caprolactone)-block-poly(ethylene-co-ethylethylene)-block-poly(ϵ -caprolactone) amphiphilic triblock copolymer. *Polymer* 51:6047–6057
- Jyotishkumar P, Pionteck J, Hassler R, George SM, Cvelbar U, Thomas S (2011) Studies on stress relaxation and thermomechanical properties of poly(acrylonitrile-butadiene-styrene) modified epoxy-amine systems. *Ind Eng Chem Res* 50:4432–4440
- Jyotishkumar P, Abraham E, George SM, Elias E, Pionteck J, Moldenaers P, Thomas S (2013) Preparation and properties of MWCNTs/poly(acrylonitrile-styrene-butadiene)/epoxy hybrid composites. *J Appl Polym Sci* 127:3093–3103
- Kishi H, Kunimitsu Y, Imade J, Oshita S, Morishita Y, Asada M (2011) Nano-phase structures and mechanical properties of epoxy/acryl triblock copolymer alloys. *Polymer* 52:760–768
- Konnola R, Parameswaranpillai J, Joseph K (2015a) Mechanical, thermal, and viscoelastic response of novel in situ CTBN/POSS/Epoxy hybrid composite system. *Polym Compos.* doi:10.1002/pc.23390
- Konnola R, Joji J, Parameswaranpillai J, Joseph K (2015b) Structure and thermo-mechanical properties of CTBN-grafted-GO modified epoxy/DDS composites. *RSC Adv* 5:61775–61786
- Larrañaga M, Gabilondo N, Kortaberria G, Serrano E, Remiro P, Riccardi CC, Mondragon I (2005) Micro- or nanoseparated phases in thermoset blends of an epoxy resin and PEO–PPO–PEO triblock copolymer. *Polymer* 46:7082–7093
- Lipic PM, Bates FS, Hillmyer MA (1998) Nanostructured thermosets from self-assembled amphiphilic block copolymer/epoxy resin mixtures. *J Am Chem Soc* 120:8963–8970
- Liu J, Sue H, Thompson ZJ, Bates FS, Dettloff M, Jacob G, Verghese N, Pham H (2008) Nanocavitation in self-assembled amphiphilic block copolymer-modified epoxy. *Macromolecules* 41:7616–7624
- Liu J, Sue H, Thompson ZJ, Bates FS, Dettloff M, Jacob G, Verghese N, Pham H (2009) Effect of crosslink density on fracture behavior of model epoxies containing block copolymer nanoparticles. *Polymer* 50:4683–4689
- Liu J, Thompson ZJ, Sue H, Bates FS, Hillmyer MA, Dettloff M, Jacob G, Verghese N, Pham H (2010) Toughening of epoxies with block copolymer micelles of wormlike morphology. *Macromolecules* 43:7238–7243
- Mathew VS, Jyotishkumar P, George SC, Gopalakrishnan P, Delbreilh L, Saiter JM, Saikia PJ, Thomas S (2012) High performance HTLNR/epoxy blend – phase morphology and thermo-mechanical properties. *J Appl Polym Sci* 125:804–811
- Mathew VS, George SC, Parameswaranpillai J, Thomas S (2014) Epoxidized natural rubber/epoxy blends: phase morphology and thermomechanical properties. *J Appl Polym Sci.* doi:10.1002/APP.39906

- Meng F, Zheng S, Li H, Liang Q, Liu T (2006) Formation of ordered nanostructures in epoxy thermosets: a mechanism of reaction-induced microphase separation. *Macromolecules* 39:5072–5080
- Meng F, Xu Z, Zheng S (2008) Microphase separation in thermosetting blends of epoxy resin and poly(ϵ -caprolactone)-block-polystyrene block copolymers. *Macromolecules* 41:1411–1420
- Ocando C, Serrano E, Tercjak A, Peña C, Kortaberria G, Calberg C, Grignard B, Jerome R, Carrasco PM, Mecerreyes D, Mondragon I (2007) Structure and properties of a semifluorinated diblock copolymer modified epoxy blend. *Macromolecules* 40:4068–4074
- Ocando C, Fernández R, Tercjak A, Mondragon I, Eceiza A (2013) Nanostructured thermoplastic elastomers based on SBS triblock copolymer stiffening with low contents of epoxy system. Morphological behavior and mechanical properties. *Macromolecules* 46:3444–3451
- Parameswaranpillai J, Pionteck J, Häbler R, Sinturel C, Mathew VS, Thomas S (2012) Effect of cure conditions on the generated morphology and viscoelastic properties of a poly(acrylonitrile – butadiene – styrene) modified epoxy – amine system. *Ind Eng Chem Res* 51:2586–2595
- Parameswaranpillai J, Moldenaers P, Thomas S (2013) Rheological study of the SAN modified epoxy–DDM system: relationship between viscosity and viscoelastic phase separation. *RSC Adv* 3:23967–23971
- Pearson RA, Yee AF (1993) Toughening mechanisms in thermoplastic-modified epoxies: 1. Modification using poly(phenylene oxide). *Polymer* 34:3658–3670
- Pethrick RA (2014) Applications of toughened epoxy resins, Chapter 17. In: Thomas S, Sinturel C, Thomas R (eds) *Micro and nanostructured epoxy/rubber blends*. Wiley, Weinheim, pp 339–362
- Pham H, Aguirre F, Dettloff M, Verghese N (2007) Development of novel toughening technology for fusion-bonded-epoxy (FBE) powder coatings. *Paint Coat Ind Mag* 23(10):64
- Prolongo SG, Gude MR, Ureña A (2012) Adhesive strength and toughness improvement of epoxy resin modified with polystyrene-*b*-polybutadiene-*b*-poly(methylmethacrylate) block copolymer. *J Mater Sci Eng* 1:2. doi:10.4172/2169-0022.1000109
- Serrano E, Tercjak A, Kortaberria G, Pomposo JA, Mecerreyes D, Zafeiropoulos NE, Stamm M, Mondragon I (2006) Nanostructured thermosetting systems by modification with epoxidized styrene – butadiene star block copolymers. Effect of epoxidation degree. *Macromolecules* 39:2254–2261
- Serrano E, Tercjak A, Ocando C, Larrañaga M, Parellada MD, Corona-Galván S, Mecerreyes D, Zafeiropoulos NE, Stamm M, Mondragon I (2007) Curing behavior and final properties of nanostructured thermosetting systems modified with epoxidized styrene-butadiene linear diblock copolymers. *Macromol Chem Phys* 208:2281–2292
- Shen K, Zhou Q, Xu Q, Jiang NL (2015) Reaction-induced microphase separation in DDS-cured TGDDM thermosets containing PCL-*b*-PES-*b*-PCL triblock copolymer. *RSC Adv* 5:61070–61080
- Veena MG, Renukappa NM, Raj JM, Ranganathaiah C, Shivakumar KN (2011) Characterization of nanosilica-filled epoxy composites for electrical and insulation applications. *J Appl Polym Sci* 121:2752–2760
- Verchere D, Sautereau H, Pascault JP, Moschiar SM, Riccardi CC, Williams RJJ (1990) Rubber-modified epoxies. I. Influence of carboxyl-terminated butadiene-acrylonitrile random copolymers (CTBN) on the polymerization and phase separation processes. *J Appl Polym Sci* 41:467–485
- Vijayan PP, Puglia D, Jyotishkumar P, Kenny JM, Thomas S (2012) Effect of nanoclay and carboxyl-terminated (butadiene-coacrylonitrile) (CTBN) rubber on the reaction induced phase separation and cure kinetics of an epoxy/cyclic anhydride system. *J Mater Sci* 47:5241–5253
- Wu S, Guo Q, Peng S, Hameed N, Kraska M, Stühn B, Mai Y (2012) Toughening epoxy thermosets with block ionomer complexes: a nanostructure–mechanical property correlation. *Macromolecules* 45:3829–3840

- Xu Z, Zheng S (2007a) Reaction-induced microphase separation in epoxy thermosets containing poly(ϵ -caprolactone)-block-poly(*n*-butyl acrylate) diblock copolymer. *Macromolecules* 40:2548–2558
- Xu Z, Zheng S (2007b) Morphology and thermomechanical properties of nanostructured thermosetting blends of epoxy resin and poly(ϵ -caprolactone)-block-polydimethylsiloxane-block-poly(ϵ -caprolactone) triblock copolymer. *Polymer* 48:6134–6144
- Yang X, Yi F, Xin Z, Zheng S (2009) Morphology and mechanical properties of nanostructured blends of epoxy resin with poly(ϵ -caprolactone)-block-poly(butadiene-co-acrylonitrile)-block-poly(ϵ -caprolactone) triblock copolymer. *Polymer* 50:4089–4100
- Yi F, Yu R, Zheng S, Li X (2011) Nanostructured thermosets from epoxy and poly(2,2,2-trifluoroethyl acrylate)-*block*-poly(glycidyl methacrylate) diblock copolymer: demixing of reactive blocks and thermomechanical properties. *Polymer* 52:5669–5680
- Yu R, Zheng S (2011) Morphological transition from spherical to lamellar nanophases in epoxy thermosets containing poly(ethylene oxide)-*block*-poly(ϵ -caprolactone)-*block*-polystyrene triblock copolymer by hardeners. *Macromolecules* 44:8546–8557
- Yu R, Zheng S, Li X, Wang J (2012) Reaction-induced microphase separation in epoxy thermosets containing block copolymers composed of polystyrene and poly(ϵ -caprolactone): influence of copolymer architectures on formation of nanophases. *Macromolecules* 45:9155–9168
- Zhang C, Li L, Zheng S (2013) Formation and confined crystallization of polyethylene nanophases in epoxy thermosets. *Macromolecules* 46:2740–2753

Nisa V. Salim, Jyotishkumar Parameswaranpillai, Bronwyn L. Fox,
and Nishar Hameed

Abstract

New ways to improve the thermal properties of epoxy systems have been interesting topic for polymer researchers for several years. The block copolymer-modified epoxy matrix has received a great deal of attention and is still being intensely studied. Differential scanning calorimetry (DSC) is the most commonly used technique to investigate the thermal properties of epoxy/block copolymer systems. It can generally provide information such as phase behavior, miscibility, glass transition temperature, melting temperature, etc. between the block copolymer blocks and the epoxy matrix. In this chapter, we have mainly focused on the changes in the glass transition properties of the thermosets modified with block copolymers. The influence of the type of block copolymers and curing agents used and the effects of cure time and temperature on the phase behavior and microphase separation of epoxy thermosets are also discussed.

N.V. Salim (✉)

Carbon Nexus, Institute for Frontier Materials, Deakin University, Geelong, VIC, Australia
e-mail: nisavs@deakin.edu.au

J. Parameswaranpillai

Department of Polymer Science and Rubber Technology, Cochin University of Science and
Technology, Cochin, Kerala, India
e-mail: jyotishkumarp@gmail.com

B.L. Fox

Factory of the Future, Swinburne University of Technology, Melbourne, Australia
e-mail: blfox@swin.edu.au

N. Hameed

Carbon Nexus, Institute for Frontier Materials, Deakin University, Geelong, VIC, Australia
Factory of the Future, Swinburne University of Technology, Melbourne, VIC, Australia
e-mail: nisharhameed@swin.edu.au

Keywords

Glass transition temperature • Crystallinity • Melting temperature • Miscibility

Contents

Introduction	1042
Thermal Properties of Epoxy Thermosets Modified with Block Copolymers	1045
Epoxy Thermosets with Poly(ethylene oxide) (PEO)-Based Block Copolymers	1045
Epoxy Thermosets with PMMA-Based Block Copolymers	1051
Nanostructured Epoxy Thermosets with Chemically Modified/Reactive Block Copolymers	1055
Nanostructured Epoxy Thermosets via RIPS Approach	1057
Conclusions	1062
References	1063

Introduction

Epoxy resin composites exhibit numerous advantageous properties which allow them to be used as structural materials since the 1940s. Thermosetting polymers, in general, and epoxy resins, in particular, have been characterized by excellent properties such as mechanical strength, thermal stability, high chemical and corrosion resistance, good adhesion, and brittleness and have poor crack growth resistance. These characteristics, along with a long service life, make epoxies an important material necessary for the future growth of new technologies. Presently, there is high potential for more sophisticated application of high-performance epoxies in both automotive and aerospace industries. However, the high cross-link density of these materials makes them less ductile and poor resistant to crack propagation which constraint many of its applications. Several approaches have been undertaken to improve the feasibility of these materials particularly thermal properties of resins for practical applications. Since the early works of McGarry and the pioneering advances at B. F. Goodrich Company, the technology of rubber toughening has been applied to epoxy resins (McGarry and Willner 1968; McGarry and Sultan 1968). The common approaches for toughening epoxies include the incorporation of rubbers (mainly copolymers of butadiene and acrylonitrile with different acrylonitrile contents ranging from 0% to 26%), thermoplastics (such as poly(phenyleneoxide) (PPO), polysulfone (PSF), polystyrene (PS), polycarbonate, poly(ether ether ketone)), and rigid particle fillers like silica (Young and Beaumont 1977) glass beads, alumina trihydrate, etc. (Lange and Radford 1971). Among these, the most successful methods comprise the toughening of epoxies with rubber such as carboxyl-terminated butadiene acrylonitrile (CTBN) (Bascom et al. 1975), and acrylonitrile–butadiene rubber (NBR) showed impressive toughening effect. During curing reactions, thermoplastics and rubber get phase separated from the epoxy matrix. Normally, these additives act as stress concentrators and prevent the epoxy matrix from catastrophic failure on application of load. However, there was a significant deterioration in the glass transition temperature, modulus, and cross-link

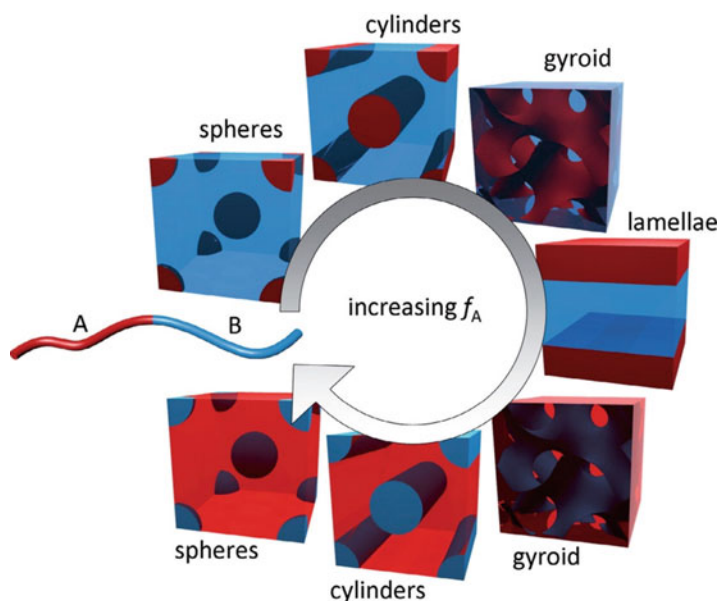


Fig. 1 Schematics of equilibrium morphologies observed for a stable A-b-B block copolymer as an increasing volume fraction of A (Botiz and Darling 2010)

density of cured epoxy resins that makes them not ideal for high-performance structural applications.

The improvement in the fracture toughness of the epoxy blends without affecting the glass transition temperatures is considered as a major challenge in composite industries. To enable this, block copolymers have been emerged as effective candidates for toughening epoxies (Hydro and Pearson 2007; Liu et al. 2010; Guo et al. 2003a, 2006; Mijovic et al. 2000; Wu et al. 2005; Lipic et al. 1998; Sun et al. 2005; Grubbs et al. 2003). The nanoscale self-organization of block copolymers is extensively investigated to create periodic structures in epoxy thermosets. The most common periodic morphologies of block copolymer comprise of spheres, hexagonal cylinders, gyroid, and lamellae with dimensions from 10 to 100 nm, which are detailed in Fig. 1 (Botiz and Darling 2010). Combining these ordered geometries within the thermoset matrix by the addition of small amounts of block copolymers can phase separate on the scale of nanometers, in particular they have capability to improve the mechanical properties and T_g s without sacrificing the optical transparency.

Generally, AB- and ABC-type di- and triblock copolymers with epoxy miscible and immiscible blocks can generate complex nanostructured phases by self-assembly within the uncured epoxy network to form different morphologies (Helfand 1975). Addition of relatively small amount of such block copolymers has been shown to give remarkable improvement in the toughness of epoxies with a minimal impact on the glass transition temperature and modulus. This strategy of creating nanostructures via the mechanism of self-assembly was primarily proposed

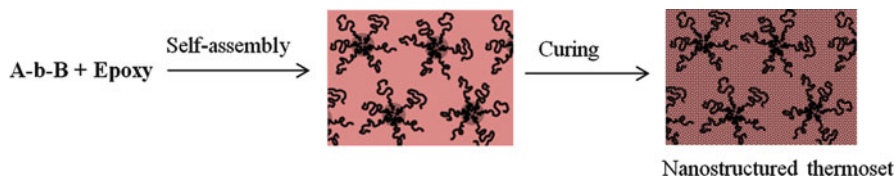


Fig. 2 Formation of nanostructured epoxy thermosets via self-assembly approach

by Hillmayer and co-workers (Lipic et al. 1998) using amphiphilic block copolymers which is shown in Fig. 2. In this mechanism, the preformed self-assembled nanostructures were locked with the introduction of hardeners followed by curing reactions; thus, the nanostructured thermosets can be prepared. The properties and final morphology of a thermoset/block copolymer system are determined by several factors including the cross-linking reaction of the thermoset resin, self-assembly of the block copolymer, and the phase separation of the blend.

The reaction-induced phase separation (RIPS) denotes a method in which the initial homogeneous mixture undergoes a phase separation during the curing reaction. Conventionally, the RIPS occurs at macroscopic scale. Some recent reports identified that the thermosetting polymer blends with an amphiphilic block copolymer with ordered and/or disordered nanostructures can be prepared alternatively through the mechanism of so-called reaction-induced microphase separation (RIMPS) (Xu and Zheng 2007). Here, the nanostructures are accessed by the control of microphase separation of a part of sub-chains of the block copolymer, while the other sub-chains remain miscible with the cross-linked thermosets. In this method, it is not necessary that the amphiphilic block copolymers should phase separate into the nanophases before the curing reaction. The blocks in the block copolymers may be miscible with precursors of thermosets. Generally in any of the abovementioned cases, the self-assembled morphologies in the thermosets are not formed until the curing reaction proceeds with a sufficient conversion of monomers. In comparison to the self-assembly type, the RIPS can apply additional variables to influence the formation of nanophases in thermosets, which are mainly associated with the thermodynamic and kinetic factors such as competitive kinetics between the cure and the microphase separation. A general mechanism of RIPS by block copolymer thermosets is shown in Fig. 3.

RIPS and self-assembly have their own advantages and disadvantages. By knowing the characteristics of these two procedures, one can design the architectures of a block copolymer which may be used to prepare nanostructured thermosets by the combination of these two mechanisms. The incorporation of these materials into epoxies often modifies the thermal properties of the epoxy-based thermosets (Ellis 1993). This chapter discusses the thermal properties of epoxy/block copolymer blends where the knowledge on these properties is very crucial in the processing stage as well as in diverse applications. Differential scanning calorimetry (DSC) is employed to measure the thermal properties of the polymer materials as a direct function of time or temperature. In this technique, the uncured and cured epoxy samples are exposed to heat in a calibrated closed furnace where the heat flow of the epoxy sample is measured in comparison to a blank reference cell. The heat flow data

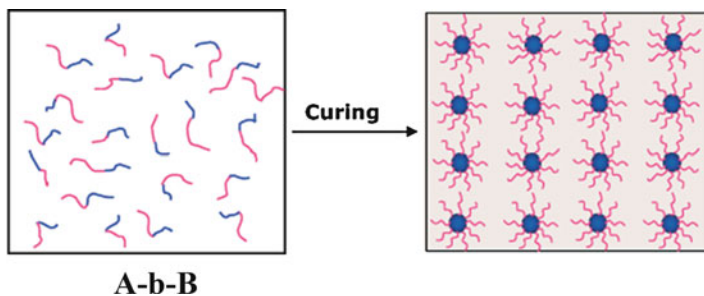


Fig. 3 Formation of nanostructured epoxy thermosets via RIPS approach

provide a direct method for determining cure kinetics, changes in T_g with respect to cure time, curing temperature, crystallization, and enthalpy of fusion of the samples. Glass transition temperature (T_g) is a unique property of an amorphous polymer which determines the transition from hard glassy to soft rubbery states. The polymer becomes very brittle when the temperature drops below its T_g whereas it attains a rubbery behavior when the temperature rises. Generally, the T_g s of the epoxy matrix can be assessed by means of differential scanning calorimetry (DSC) and dynamic mechanical analysis (DMA). The chapter provides the detailed information and techniques regarding the DSC analysis of epoxy/block copolymer blends.

Thermal Properties of Epoxy Thermosets Modified with Block Copolymers

The thermal properties of epoxy blends with block copolymers are very different from that of homopolymer or random copolymers. The T_g s of the epoxy/block copolymers are connected with the nanostructures of the epoxy systems as well as the miscibility of the block copolymer blocks with the thermosets before and after curing though it can be affected by the addition of the hardener and the curing processes. Generally, the influence of thermal properties by the incorporation of block copolymer in epoxy matrix can be related with the following factors such as epoxy miscible blocks, epoxy immiscible blocks, and the demixing of partial epoxy miscible blocks. In the following, we will discuss the nanostructured thermosets with block copolymer having commonly used blocks in detail. Generally amphiphilic compounds are selected in such a way that at least one of these blocks promotes sufficient miscibility with thermoset matrix so as to produce toughened thermosets with nanosized inclusions.

Epoxy Thermosets with Poly(ethylene oxide) (PEO)-Based Block Copolymers

Following the pioneer works of Hillmayer et al. (1998), Mijovic et al. (2000), and Guo et al. (2003), different strategies for creating nanostructures using amphiphilic

block copolymers have been proposed. Here, the uncured epoxy resin acts as a solvent to dissolve block copolymers and form nanostructures such as lamellar, cylindrical, and spherical structures, depending on the blend composition. As formed block copolymer morphologies will have effect both on the mechanical and the glass transition temperatures (T_g s) of the block copolymer-modified epoxy systems. Bates and co-workers have pioneered in this field, investigating the effect of block copolymer morphologies on the T_g of modified and unmodified epoxies. Two amphiphilic block copolymers, namely, poly(ethylene oxide)-*block*-poly(ethylene-alt-propylene) (PEO-*b*-PEP) and poly(methyl methacrylate-ran-glycidyl methacrylate)-*block*-poly(2-ethylhexyl methacrylate) ((PMMA-ran-GMA)-*b*-PEHMA), were blended with brominated and non-brominated epoxies cured with phenol novolac (Dean et al. 2003). The system exhibited morphological transitions from spherical micelles to vesicles with the increasing length of the PEP block with regard to PEO blocks. In this study, block copolymers self-assembled into vesicles resulted an increase in T_g of epoxy blends from 89 °C to 109 °C. The self-assembled spherical and wormlike micelles demonstrated a significant increase in T_g along with fracture toughness. The increase in temperature may be due to the high cross-link density of epoxy and hardener when blended with block copolymers. Though diluents normally degrade T_g , the rise in temperature was prominent with wormlike micelles. This indicates that the added block copolymer has an impact on the rate of cross-linking reactions during curing reactions. They concluded that the nanostructures play a critical role in the enhancement of mechanical as well as thermal properties.

In another study, Dean et al. reported (Dean et al. 2001) the changes in the thermal properties of the thermosetting blends by modifying epoxy with symmetric or asymmetric poly(ethylene oxide)-*block*-poly-(ethylene-alt-propylene) (PEO-*b*-PEP) block copolymer with PEO volume fractions of 0.5 and 0.26, respectively. These resins exhibited an increased fracture toughness without large reduction in T_g at low block copolymer concentrations (<5 wt%).

In another study, Bates and co-workers have reported that BADGE epoxy resin and poly(hexylene oxide)-*block*-poly(ethylene oxide) (PHO-*b*-PEO) block copolymers curing under phenol novolac resins have shown to be effective in improving T_g and fracture toughness (Thio et al. 2006).

Wu et al. (2005) detailed the experimental methods to establish the morphological features of cured epoxy thermosets with its thermal properties by modifying with bisphenol A-based resin/phenol novolac (PN) curing agent/poly(*n*-butylene oxide)-*block*-poly(ethylene oxide) (PBO-*b*-PEO) mixtures. The neat epoxy resin exhibits a T_g at 89 °C, while addition of 5% by weight PBO-PEO-2 (vesicles) results in T_g of 109 °C. The incorporation of PBO-PEO-6 (spherical micelles) and PBO-PEO-4 (wormlike micelles) leads to even greater glass transition temperatures, such as 122 °C and 127 °C, respectively. More details are displayed in Fig. 4 and Table 1.

Another major system that has been investigated by Hillmayer and co-workers (Liu et al. 2010) is the modification of epoxy resin with poly(ethylene-alt-propylene)-*b*-poly(ethylene oxide) (PEP-*b*-PEO) block copolymer self-assembled into wormlike micelles with improvements in tensile properties without sacrificing its T_g . In these studies, the epoxy resin that selectively dissolves with the PEO block and

Fig. 4 DSC scans obtained from (a) the unmodified epoxy resin and modified with (b) PBO–PEO-2 (vesicles), (c) PBO–PEO-6 (spherical micelles), and (d) PBO–PEO-4 (wormlike micelles) at a concentration of 5% by weight (Wu et al. 2005)

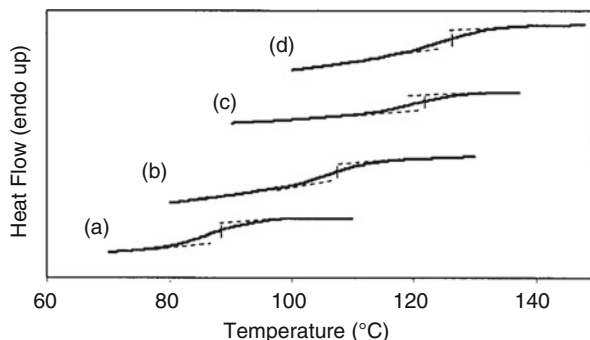


Table 1 Properties of epoxy/PN modified by 5% PBO–PEO block copolymer (Wu et al. 2003, 2005)

Polymer ^a	Morphology in epoxy ^b	T_g^c (°C)
None		89
PBO–PEO-1	Clustered vesicles	91
PBO–PEO-2	Vesicles	109
PBO–PEO-3	Branched cylinders	122
PBO–PEO-4	Cylinders	127
PBO–PEO-5	Cylinders + spheres	116
PBO–PEO-6	Spheres	122

^aPBO–PEO block copolymers varying ethylene oxide repeat units and mass fractions of the PEO blocks

^bDetermined from TEM images

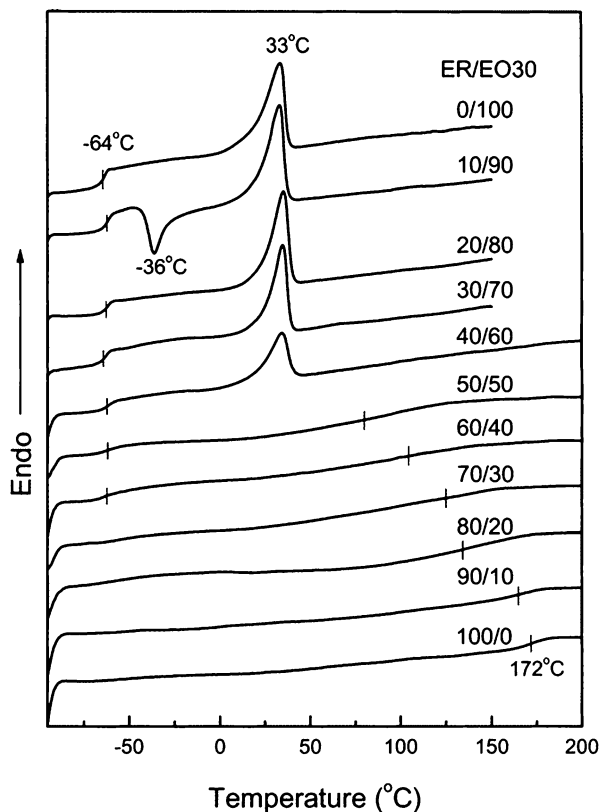
^cDetermined from DSC analysis

could swell the PEO domains in the block copolymers without macroscopic phase separation leads to stable nanostructures, thus reducing polymer segment mobility by increasing cross-link density.

Guo et al. (2002) explored new principles for creating nanostructures in DGEBA-type epoxy resin (ER) with amphiphilic poly(ethylene oxide)-*block*-poly(propylene oxide)-*block*-poly(ethylene oxide) PEO-*b*-PPO-*b*-PEO triblock copolymers by carefully choosing the curing condition. PEO-*b*-PPO-*b*-PEO triblock copolymers with different ethylene oxide contents, such as 30 wt% EO content (EO30) and with 80 wt% EO content (EO80), lead to stable nanostructures in DGEBA-type epoxy using 4,4'-methylenedianiline (MDA) as curing agent.

Figure 5 shows DSC curves of the second scan of the MDA-cured epoxy, EO30, and the MDA-cured epoxy/EO30 thermosetting blends. The block copolymer shows a melting temperature at 33 °C and a T_g at –64 °C. In Fig. 5, it can be seen that the cured epoxy displays T_g at 172 °C, which shifts down to lower temperature with increasing EO30 content. When the EO30 content in the blends increases, T_g of the thermosets decreases which means EO30/epoxy components are miscible or at least partially miscible at these compositions. The reduction in T_g of the cured blends suggests the combination of internal and external plasticization effects. Figure 5 also shows the T_m (EO30) values from the second scans as a function of the blend

Fig. 5 DSC thermograms of the second scan of the MDA-cured ER/EO30 blends (Guo et al. 2002)



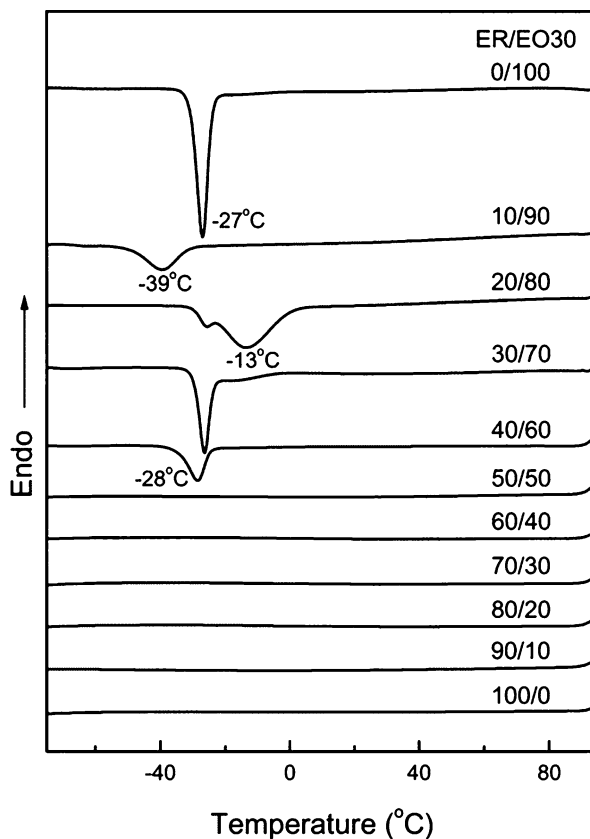
composition. The T_m values remain unchanged up to 50 wt% of EO30 showing immiscible or partially miscible blends with a crystalline component.

Figure 6 displays the DSC cooling scan of epoxy/EO30 blends. From the cooling scan, pure EO30 copolymer displays a crystallization peak at -27°C that remains unchanged until 60 wt% EO30 which indicates an immiscible blend. There is another crystallization peak observed at -13°C for 80 wt% of block copolymer and that becomes a shoulder peak for blends with 70 wt% of EO30. This is due to the higher content of epoxy which acts as a nucleation agent in ER/EO30 blends. At 90 wt% of EO30, the crystallization peak shifts down to lower values representing a reduced crystallization rate.

In a study, Guo et al. (2003) investigated the nanoscale confinement on the crystallization kinetics in MDA-cured epoxy resin with a low molecular weight polyethylene-*block*-poly(ethylene oxide) (PE-*b*-PEO) diblock copolymer. DSC measurements show two melting peaks at 23°C and 106°C representing crystalline PEO blocks and the crystalline PE blocks.

Figure 7 shows that the thermosets with up to 40 wt% of block copolymer did not display melting peak for the PEO blocks. This indicates the miscibility of PEO blocks with epoxy resins. The T_g of the cured epoxy shifts down from 177°C to

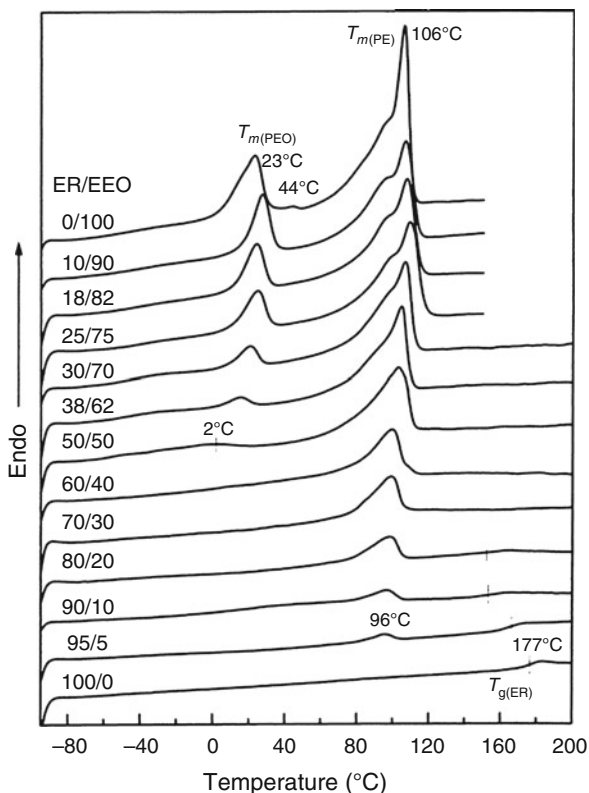
Fig. 6 DSC thermograms of crystallization curves of the MDA-cured ER/EO30 blends (Guo et al. 2002)



lower temperatures with increase in the PE-*b*-PEO content up to 20 wt% and finally disappears at high content of the block copolymer. This again confirms the miscibility or at least partial miscibility between epoxy resin and PEO blocks in the block copolymer. The reduction in T_g is due to the dilution effect of the PEO component that causes a reduction in cross-linking density of the network.

Figure 8 shows DSC thermograms of the cooling scan for the cured ER/EEO blends. The crystallization peak (T_c), at 3 °C, denotes the crystallization of the PEO blocks which shifts down to lower values with increasing ER content in the cured blends. At 18/82 ER/EEO blend composition, PEO showed a crystallization exotherm at -11 °C beyond the crystallization peak at -5 °C which can be attributed to heterogeneous and homogeneous nucleation, respectively. The homogeneous nucleation of PEO slowly becomes dominant when the epoxy content in the blends increases from 25 to 50 wt%, whereas at 50 wt% the peak becomes small and shifts down to -31 °C, indicating a declined crystallization rate. At very high epoxy content, PEO becomes completely miscible with the matrix; hence, no crystallization exotherm is observed for EEO. The major crystallization peak observed at 93 °C denotes the T_c of PE which does not disappear even with very low content of EEO in the blends.

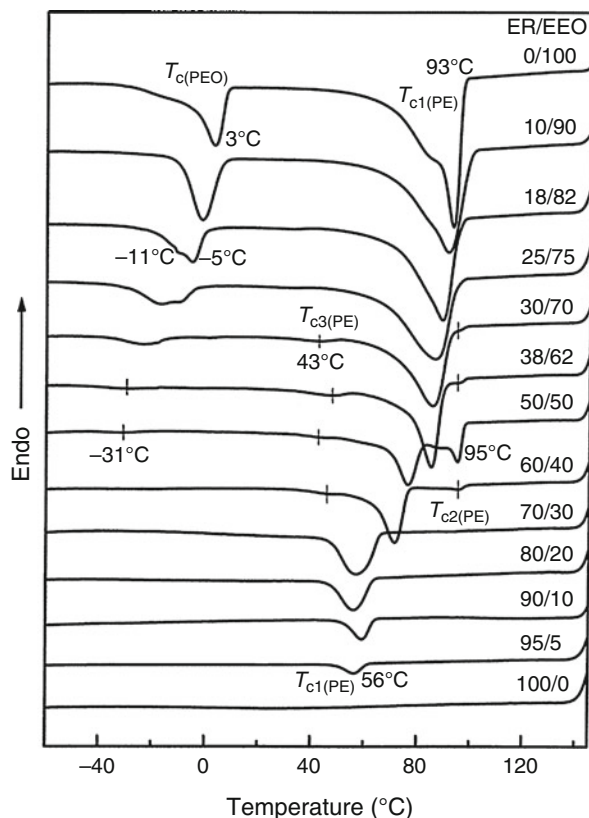
Fig. 7 DSC thermograms of the second scan of the MDA-cured ER/EEO blends after the cooling scan. The heating rate is 20 °C/min (Guo et al. 2003)



There are a number of studies reported with various morphologies from PEO-based block copolymers with nanostructures controllably produced in diglycidyl ether of bisphenol A (DGEBA)-type epoxy resin. Mijovic et al. (2000) reported preliminary investigation on DGEBA with PEO-*b*-PPO diblock copolymer and PEO-*b*-PPO-*b*-PEO triblock copolymer. The DSC curves of the epoxy resins with both PEO triblock copolymer and diblock copolymer are detailed in Figs. 9 and 10. It can be seen in Fig. 9 that the T_g of the thermosets broadens and shifts to higher temperature whereas the triblock copolymers showed a phase separation with two distinct T_g s. PEO, being a crystalline polymer, its addition to DGEBA suppress the crystallization and increase its T_g (Mijovic et al. 2000). They observed macrophase separation for epoxy blends with PEO-*b*-PPO-*b*-PEO triblock copolymer in contrast to the microphase separation.

The DSC thermograms of 50/50 DGEBA–MDA/PEO–PPO–PEO blend measured at various times during cure at 120 °C are shown in Fig. 9. Originally the mixture has a single T_g at –41 °C. It is observed that the phase separation occurred between 45 and 60 min giving rise to two glass transitions. The low temperature one belongs to the block copolymer and the higher one related primarily with the DGEBA–MDA phase. Phase separation starts between 45 and 60 min and is

Fig. 8 Crystallization curves of the MDA-cured ER/EEO blends during the cooling at $-20\text{ }^{\circ}\text{C}/\text{min}$ (Guo et al. 2003)



accompanied by the emergence of two transitions: the lower one related mostly to the block copolymer and the higher one associated primarily with the DGEBA–MDA network. As the network continues to grow, the higher T_g increases. Figure 9 shows the thermograms of 50/50 DGEBA–MDA/PEO–PPO blend where it was observed that the T_g broadens, shifts slightly to higher temperature, and flattens out considerably as the curing progresses.

Epoxy Thermosets with PMMA-Based Block Copolymers

Pascault and co-workers (Ritzenthaler 2000) studied the blends of polystyrene-block-polybutadiene-block-poly(methylmethacrylate) (SBM) copolymer with DGEBA by using 4,4'-diaminodiphenyl sulfone (DDS) and 4,4'-methylenebis(3-chloro-2,6-diethylaniline) (MCDEA) as hardeners. Transparent nanostructured thermosets were obtained with MCDEA as hardener, and PMMA remained soluble during curing. They concluded that the solubility of SBM blocks with epoxy is crucial for the formation of nanostructures in the thermosets. The studies have shown that the formation of nanostructured morphologies in PMMA-modified epoxy thermosets depends on the

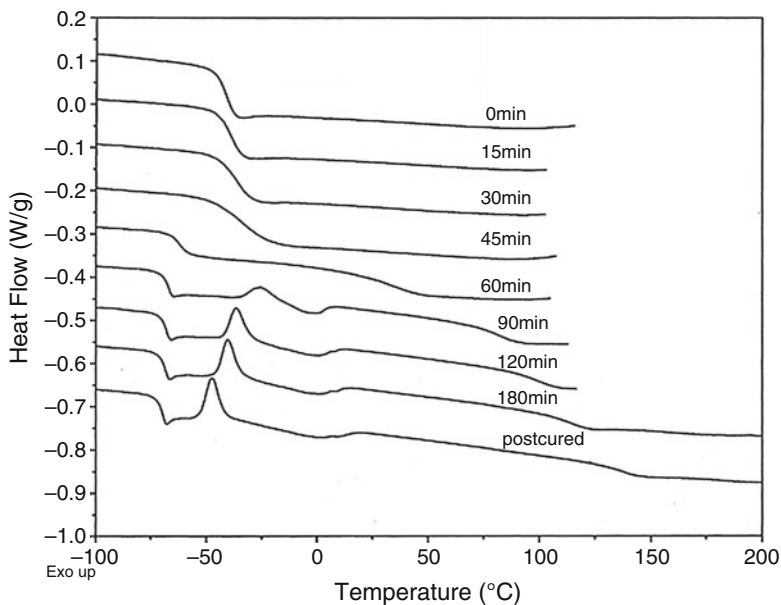


Fig. 9 DSC thermograms of 50/50 DGEBA-MDA/PEO-PPO-PEO blend at various times during reaction at 120 °C (Mijovic et al. 2000)

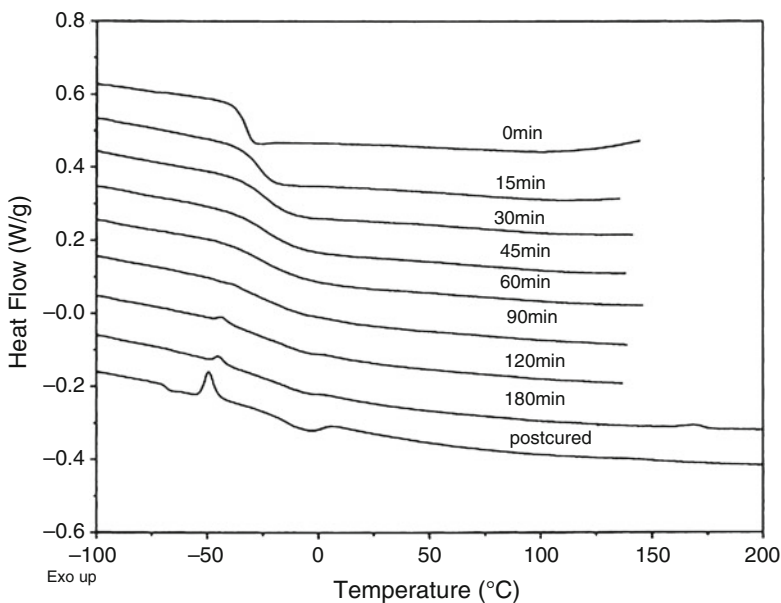
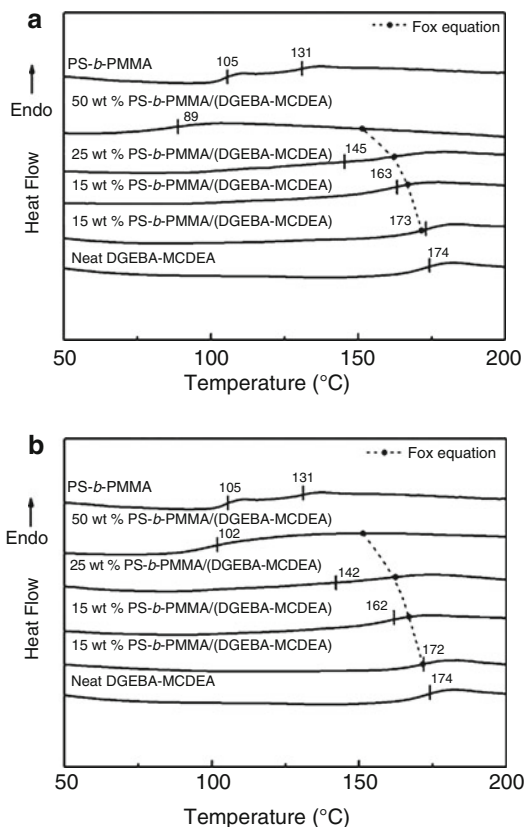


Fig. 10 DSC thermograms of 50/50 DGEBA-MDA/PEO-PPO-PEO blend at various times during reaction at 150 °C (Mijovic et al. 2000)

Fig. 11 DSC curves of the DGEBA–MCDEA-cured PS-*b*-PMMA systems prepared by the non-solvent method (**a**) and by the solvent method (**b**). The dotted line in each graph indicates the theoretical T_g values calculated by the Fox equation (Cano et al. 2015)



nature of curing agents used. Macrophase separation could take place when hardeners such as 4,4'-diaminodiphenyl sulfone (DDS) or 4,4'-methylenedianiline (MDA) are used. Going from homo-PMMA to triblock SBM, similar trends have been observed (Court et al. 2001; Ritzenthaler et al. 2000, 2002, 2003; Girard-Reydet et al. 2003).

Tercjak (Cano et al. 2015) investigated the nanostructure morphologies in a DGEBA epoxy monomer-based thermosetting system modified with polystyrene-block-polymethyl methacrylate (PS-*b*-PMMA) block copolymer and MCDEA as the curing agent. The thermosets were prepared by two different preparation methods such as solvent and non-solvent methods.

Figure 11 summarizes the thermal properties of the PS-*b*-PMMA modified with MCDEA-cured epoxy resins. The T_g s of the neat epoxy, the block copolymers, are 174 °C, 105 °C, and 131 °C, respectively. As the composition of block copolymer in the epoxy increases, the T_g of the epoxy decreases indicating the miscibility between the block copolymer and epoxy (Blanco et al. 2010; Cano et al. 2014). It has been proven that the PMMA is miscible with epoxy up to the end of curing whereas PS block phase separates before the gel point. Figure 11b represents the theoretical

values of the glass transitions of the thermosets, calculated using Fox equation which is represented as (Larránaga et al. 2007)

$$\frac{1}{T_g} = \frac{w_1}{T_{g1}} + \frac{w_2}{T_{g2}} \quad (1)$$

where w_1 and w_2 are weight fractions of components 1 and 2, respectively. By analyzing the T_g values under with or without solvent conditions, systems prepared by the solvent method showed slightly lower T_g values than that of without solvent up to a 25 wt% PS-*b*-PMMA block copolymer content. This denotes that a better miscibility was obtained under solvent method. It was interesting to note that at 50 wt% block copolymer content, the blends prepared under two different conditions showed a lower T_g . This low T_g of the thermosets pointed out that the high amount of the block copolymer content creates the dilution effect in the matrix which significantly delays the curing reaction (Cano et al. 2014; George et al. 2012).

Guo et al. (2001) reported an existence of three different glass transition temperatures when blending DDM-cured epoxy with an immiscible polystyrene-*block*-polybutadiene (PS-*b*-PB) block copolymer. DSC thermograms of the blends, cured epoxy, and pure block copolymer are shown in Fig. 12. The blends show a T_g around

Fig. 12 DSC thermograms of the second scan of ER/SB blends (Guo et al. 2001)

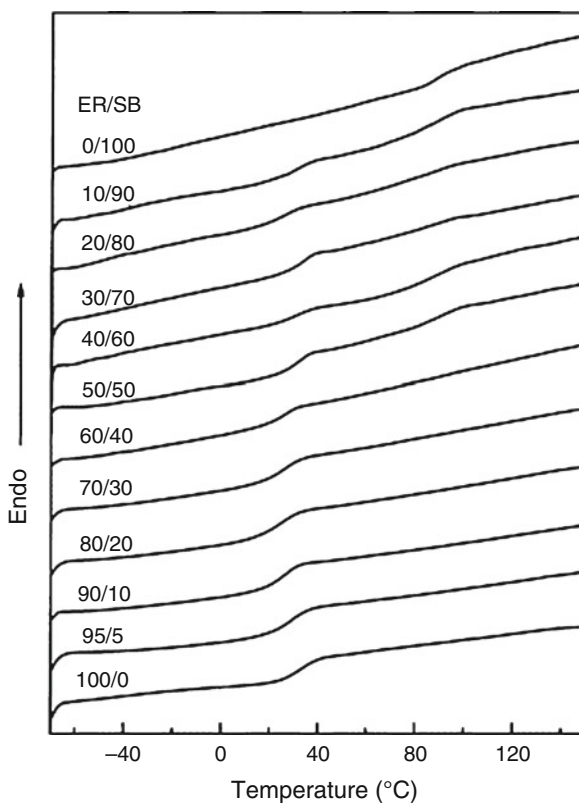


Table 2 T_g s of epoxidized PB-rich phase in the SBSEp46 and their mixtures with 10, 20, and 30 wt% epoxy before and after curing determined by DSC

System	T_g ePB (°C)		ΔT_g epoxy matrix (°C)
	Before curing	After curing	
SBSEp46	-31		
90SBSEp46/10epoxy	-23	-12	11
80SBSEp46/20epoxy	-18	4	22
70SBSEp46/30epoxy	-14	33	47

30 °C represents the cured epoxy. At high content of block copolymer, there is a T_g observed at 90 °C that corresponds to the PS blocks in the blends. But the T_g of the PB block was not detectable under the used experimental conditions.

Nanostructured Epoxy Thermosets with Chemically Modified/Reactive Block Copolymers

The formation of nanostructures in epoxy thermosets by the chemical modification of block copolymers is a viable method for inducing the compatibility of at least one block with the epoxy resin. Ocando et al. (2013) reported the design of such a nanostructured system with poly(styrene-*block*-butadiene-*block*-styrene) (SBS) and epoxy by epoxidation of PB blocks. The microphase separation of epoxidized SBS with epoxy was confirmed by DSC and the results are detailed in Table 2. DSC results show that before curing, all the blends show the presence of two glass transition temperatures due to the microphase separation between the components of the mixtures. The T_g of the PS blocks remains constant around 80 °C for all mixtures, whereas the T_g of epoxidized PB blocks shows at lower temperatures. After the addition of 10, 20, and 30 wt% of epoxy content, the T_g of epoxidized PB phase shifts from around -31 °C to higher temperatures. This shows the miscibility of the SBSEp46 with epoxy matrix before curing. After curing reaction, the T_g of epoxidized PB shifts to even high temperatures suggesting the cross-linking formation of DGEBA/MCDEA which gets interact with oxirane groups present in epoxidized PB block and that can enhance the T_g .

Hameed et al. (2010) reported the modification of epoxy with a highly ordered poly(dimethyl siloxane)-*block*-poly(glycidyl methacrylate) (PDMS-*b*-PGMA) block copolymer where PGMA reactive block can involve in with epoxy in the network formation.

The DSC scans of the MDA-cured epoxy/PDMS-*block*-PGMA blends are shown in Fig. 13. Pure PDMS-*b*-PGMA block copolymer shows a T_g at 64 °C and after curing with MDA, the T_g shifted to 107 °C. By blending the block copolymer with epoxy, the T_g of the cured blends is shifted to higher temperatures. It can be seen that the T_g of the cured blends increased approximately 28 °C by adding 10 wt% of the reactive diblock copolymer. But, the T_g s of the blends decrease above the 10 wt% of the reactive diblock copolymer composition. This can be attributed to the presence of

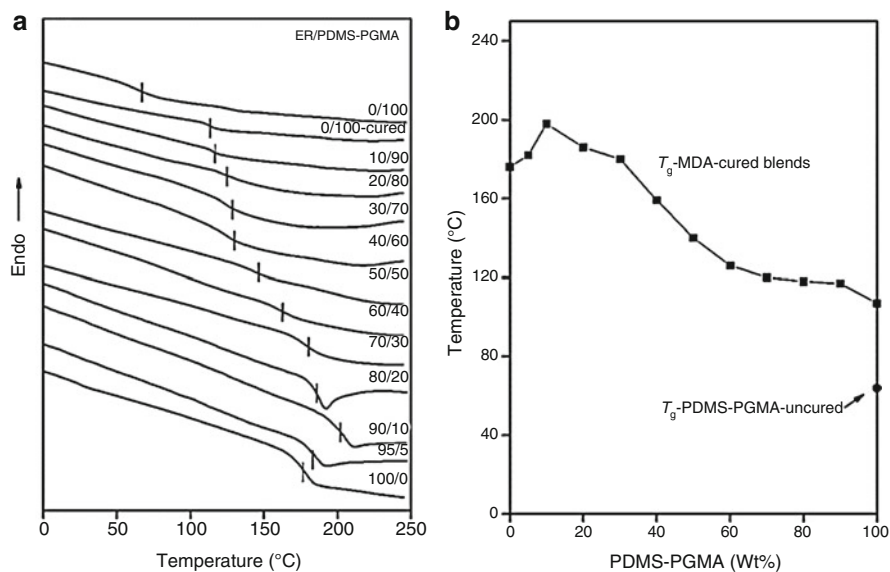


Fig. 13 (a) DSC curves of the second scan of ER/PDMS-*b*-PGMA blends and (b) glass transition temperature (T_g) versus blend composition from the second scans of ER/PDMS-PGMA blends (Hameed et al. 2010)

microphase-separated rubbery PDMS blocks. There is a reduction in the T_g of nanostructured epoxy with the modification of additives due to the external or internal plasticization of the soft polymer chains, which can take part in the network formation with epoxy by hydrogen-bonding interactions.

Xu et al. (2010) reported an increase in the glass transition temperature of the thermosets by blending epoxy with reactive polystyrene-*block*-poly(glycidyl methacrylate) diblock copolymer (PS-*b*-PGMA). The DSC curves of cross-linked epoxy and nanostructured epoxy/PS-*b*-PGMA thermosets are shown in Fig. 14. It can be seen from the graph that the neat epoxy displays a T_g at 174 °C and the PS-*b*-PGMA diblock copolymer shows that at 100 °C, which indicates PS blocks of the diblock copolymer. The T_g s of the blends are significantly increasing with the addition of block copolymer content in the epoxy. The introduction of the glycidyl methacrylate blocks in the block copolymers can react spontaneously with MDA and form covalent linkages between the reactive copolymers and the cross-linked epoxy matrix. As a result, microphase separation of the other blocks will be restricted because of strong chemical covalent interaction; thereby, the cross-link density of the matrix increases and the T_g of the blends moves to high values.

Mai and co-workers (Wu et al. 2012) reported a novel method for preparing nanostructured thermosets by introducing block ionomer polystyrene-*block*-poly(ethylene-*ran*-butylene)-*block*-polystyrene (SEBS) with a tertiary amine terminated PCL, which is represented as SSEBS-*c*-PCL in the block copolymers for modifying epoxies. The thermal studies of cured epoxy/SSEBS-*c*-PCL thermosets are given in

Fig. 14 The DSC thermograms of epoxy resin and epoxy/PS-*b*-PGMA-blended thermosets (Xu et al. 2010)

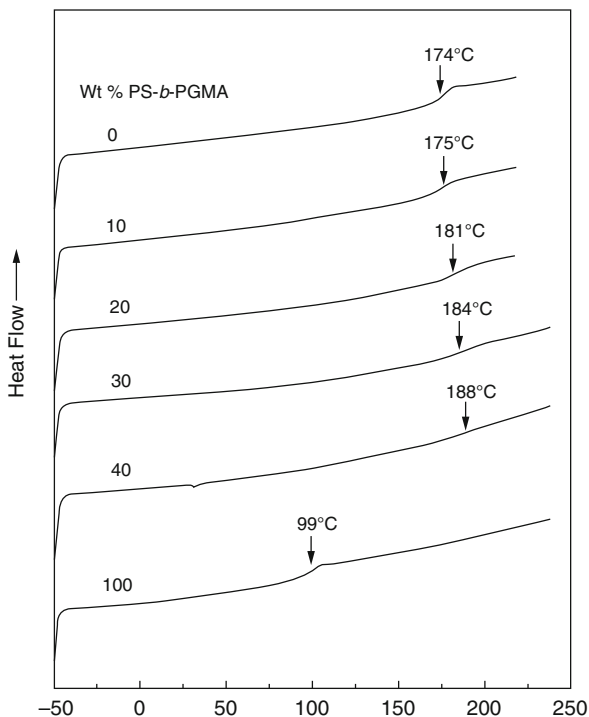
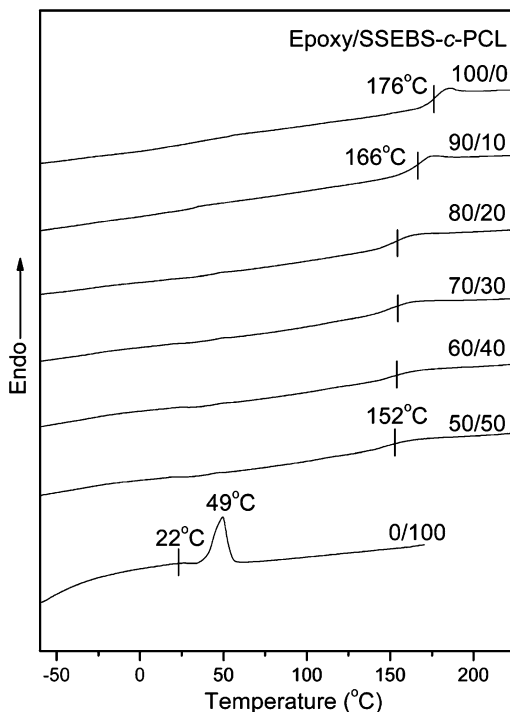


Fig. 15. The DSC data shows a sharp peak at 49 °C denotes the melting temperature of the PCL blocks in ionomer SSEBS. Melting point depression is the characteristic of a miscible polymer blend involving hydrogen-bonding interactions. It can be seen that the T_m of the PCL side chains in the PCL side chains in the block ionomer SSEBS-*c*-PCL disappears with increasing epoxy compositions. This depression in T_g of the epoxy-rich phase indicates the miscibility between the PCL side chains and the epoxy matrix. It has already been reported that the epoxy/PCL blends cured with aromatic amine are miscible with aromatic amine-cured epoxy matrix and interpenetrated into the cross-linked epoxy networks (Guo and Groeninckx 2001; Wang et al. 2001). The cured epoxy shows a T_g at 176 °C and is substantially shifted down to lower temperatures with increasing content of the SSEBS-*c*-PCL which is due to the plasticization effect of the PCL side chains on the epoxy matrix (Guo et al. 2001).

Nanostructured Epoxy Thermosets via RIPS Approach

Zheng (Xu and Zheng 2007) reported ordered nanostructures via RIPS method by blending epoxy and poly(ϵ -caprolactone)-*block*-poly(*n*-butyl acrylate) (PCL-*b*-PBA) in 4,4'-methylenebis(2-chloroaniline) (MOCA). DSC has used to reveal the miscibility and phase behavior of these systems. Here, PCL blocks were miscible

Fig. 15 DSC curves of second scan of epoxy/SSEBS-*c*-PCL blends



with epoxy before and after curing reaction whereas the mixtures of PBA and epoxy precursors displayed an upper critical solution temperature (UCST) behavior. In Fig. 16, it has been confirmed that the cured blends showed a single, composition-dependant T_g indicating a miscible blend. Pure epoxy shows a T_g at 153 °C and the block copolymer shows a melting peak at 56 °C and T_g at around -51 °C. As the block copolymer composition in the blend increases, lower T_g range is observed due to the miscibility of PCL blocks with epoxy resin.

In another study, Zheng detailed (Yi et al. 2009) nanostructured epoxy by blending poly(2,2,2-trifluoroethyl acrylate)-block-poly(ethylene oxide) amphiphilic diblock copolymer with epoxy resin where PEO is miscible whereas PTFEA is immiscible with epoxy after and before curing. DSC studies in Fig. 17 confirm the miscibility of these blocks with epoxy resins. At higher compositions of epoxy, a depression in T_g was observed which also confirms the miscibility of PEO blocks in the matrix. Though pure block copolymer exhibited an endotherm peak at 54 °C, the blends did not show the melting peak. This is due to the miscible PEO blocks which get trapped into the epoxy network. The broadening of the glass transition range could be attributed to the enrichment of soft PEO chains in the epoxy matrix.

Recently, Gong et al. (2008) have studied the effect of miscibility of block copolymer block with epoxy matrix by analyzing the glass transition behavior of all blend compositions. In their study, they used PH-alt-PDMS alternating block copolymer with epoxy miscible PH blocks and immiscible PDMS blocks with epoxy

Fig. 16 DSC curves of the control epoxy, PCL-*b*-PBA, and their nanostructured blends

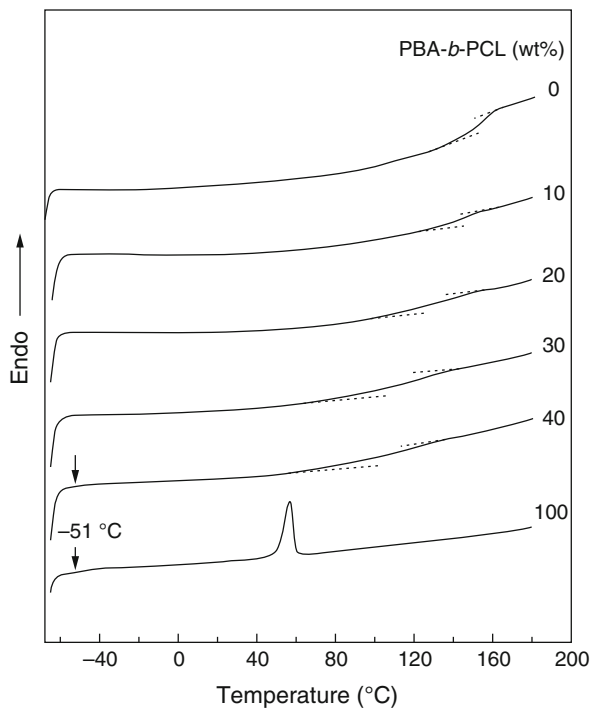


Fig. 17 DSC curves of the nanostructured thermosets containing PTFEA-*b*-PEO diblock copolymer

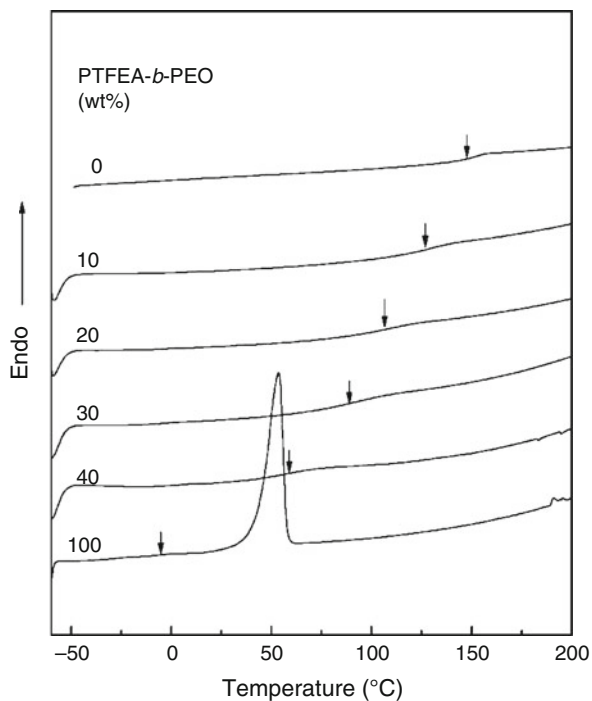
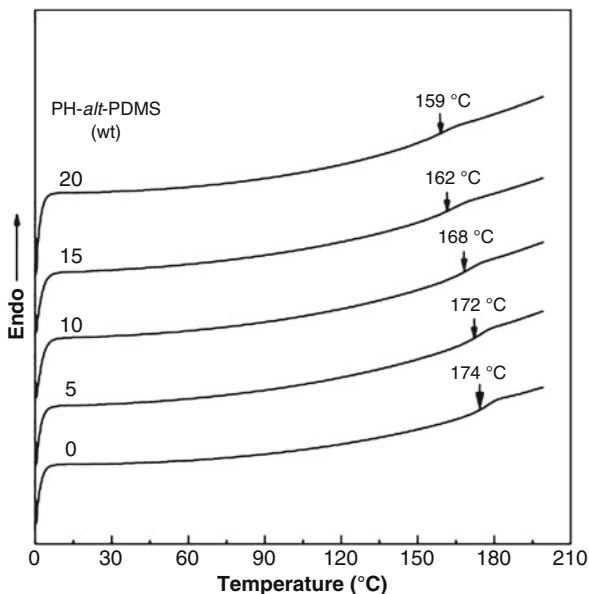


Fig. 18 DSC curves of the epoxy thermosts containing PH-alt-PDMS alternating block copolymer



before and after curing. Figure 18 shows the DSC thermograms of the PH-alt-PDMS with epoxy cured with 4,4'-diaminodiphenylmethane (DDM). The PH of the PH-alt-PDMS exhibited a glass transition at 52 °C, and epoxy thermost shows a T_g at 174 °C and is much higher than the T_g corresponding to PH blocks as displayed in Fig. 18. The T_g s of the blends shift to lower temperatures with increasing block copolymer content which is due to the plasticization effect of the PH blocks on the epoxy matrix. In addition to this, the hydrogen-bonding interactions of the phenolic hydroxyl groups of the block copolymers with DGEBA are responsible for the miscibility of PH in the epoxy matrix that causes a decrease in T_g .

Hu et al. (2010) investigated the self-assembly behavior of poly(ϵ -caprolactone)-*block*-poly(ethylene-coethylene)-*block*-poly(ϵ -caprolactone) (PCL-*b*-PEEE-*b*-PCL) triblock copolymer in epoxy thermosts. Figure 19 shows the blends of epoxy with PCL-*b*-PEEE-*b*-PCL triblock copolymer. The blends displayed T_g s in the range of 60–160 °C, which shows increasing with the content of PCL-*b*-PEEE-*b*-PCL triblock copolymer. The peak at 73 °C corresponds to the melting peak of the nanostructured thermost which indicates the fusion of PEEE blocks. It is not assigned to the melting transition of PCL since the PCL blocks were not crystalline in the nanostructured thermosts. When the block copolymer content increases in the blends, the intensity of this peak increases.

For understanding the demixing behavior of PCL sub-chains, the glass transition values of PCL/epoxy are considered. Couchman equation (Couchman 1978) is used out of many theoretical equations (Fox 1956; Gordon and Taylor 1952) in this study to understand the dependence of T_g on composition in miscible polymer blends. The

Fig. 19 DSC curves of the nanostructured thermosets containing PCL-b-PEEE-b-PCL triblock copolymer

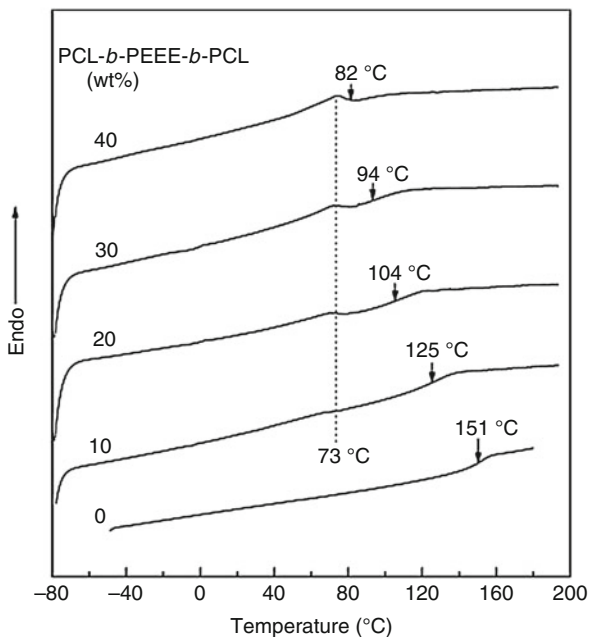
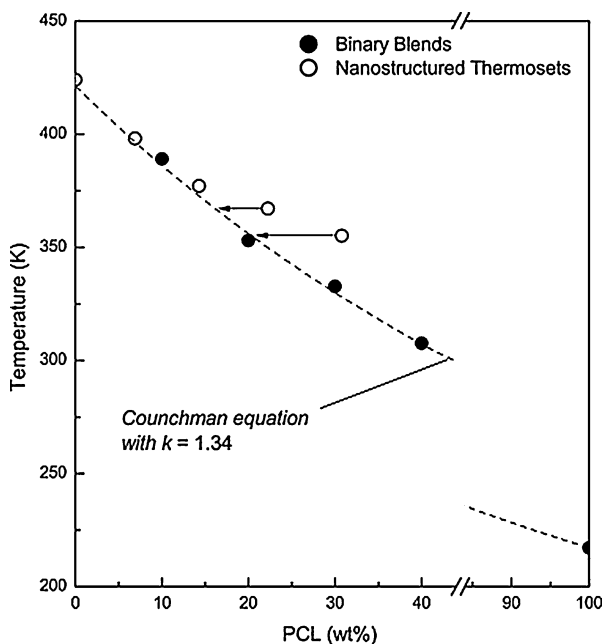


Fig. 20 Plots of T_g s as functions of concentration of PCL for epoxy thermosets containing the block copolymers



plots of T_g s as functions of the concentration of PCL for the nanostructured thermosets are shown in Fig. 20:

$$T_g = \frac{w_1 T_{g1} + k w_2 T_{g2}}{w_1 + k w_2} \quad (2)$$

where W_1 is the weight fraction of component 1 and T_g is the glass transition temperature of blend; the parameter k is Couchman coefficient defined by

$$k = \frac{\Delta C_{p1}}{\Delta C_{p2}} \quad (3)$$

where ΔC_p represents the increase in the heat capacity of the material. Figure 20 shows the T_g s of epoxy with PCL-*b*-PEEE-*b*-PCL triblock copolymer as well as binary blends of epoxy/PCL where PCL blocks are having the same molecular weight with length of the PCL block in the triblock copolymer. The results pointed out that the thermosets containing 30 and 40 wt% of the block copolymer exhibited higher T_g s than the epoxy/PCL blends with the same compositions of PCL blocks. In the binary blends, homogenous dispersion of PCL blocks takes place via intermolecular hydrogen-bonding interactions with epoxy networks. But in triblock copolymer, due to the steric hindrance, the PCL blocks remain at the surface of PEEE domains. Hence, the miscibility of PCL blocks with epoxy diminishes which weakens the effect of plasticization of PCL blocks with epoxy and increases the T_g of the thermosets.

Moreover, improving the thermal stability and thermal conductivity of epoxy thermosets while maintaining other important physical properties has attracted significant research interest. In general, most of the additives (polymers/fibers/nanoparticles) tend to slightly reduce the thermal stability of epoxy. However, the thermal conductivity of thermosets tends to increase with nanoparticle additives such as carbon nanotubes, graphene, etc.

Conclusions

The modification of epoxy thermosets by block copolymer nanostructures has a tremendous impact on epoxy toughening with some enhancement in thermal and mechanical properties. The nanostructure formation in the thermosets by block copolymers can take place in two approaches, namely, self-assembly and reaction-induced microphase separation (RIMPS). DSC is the primary technique to measure the heat flow of the epoxy/block copolymer materials to investigate the thermal properties such as T_g , T_m , T_c , cure kinetics, phase separation, etc. Most of the works performed to date on nanostructured thermosets with an epoxy miscible chains show a depression in T_g which is due to the plasticization effects of the miscible chains. However, there are several interesting reports addressing the unusual increase in glass transition temperature which is an important finding. These changes in T_g

whether increase or decrease in the epoxy matrix depend mainly on the miscibility, reactivity, and the T_g s of the blocks in the block copolymers with epoxy thermosets.

References

- Bascom WD, Cottingham RL, Jones RL, Peyser PJ (1975) The fracture of epoxy- and elastomer-modified epoxy polymers in bulk and as adhesives. *J Appl Polym Sci* 19:2545–2562
- Blanco M, L'opez M, Kortaberria G, Mondragon I (2010) Nanostructured thermosets from self-assembled amphiphilic block copolymer/epoxy resin mixtures: effect of copolymer content on nanostructures. *Polym Int* 59:523–528
- Botiz I, Darling SB (2010) Optoelectronics using block copolymers. *Mater Today* 13:42–51
- Cano L, Builes DH, Tercjak A (2014) Morphological and mechanical study of nanostructured epoxy systems modified with amphiphilic poly(ethylene oxide-*b*-propylene oxide-*b*-ethylene oxide)triblock copolymer. *Polymer* 55:738–745
- Cano L, Gutierrez J, Tercjak A (2015) Enhancement of the mechanical properties at the macro and nanoscale of thermosetting systems modified with a polystyrene-block-polymethyl methacrylate block copolymer. *RSC Adv* 5:102085–102095
- Couchman PR (1978) Compositional variation of glass-transition temperatures. 2. application of the thermodynamic theory to compatible polymer blends. *Macromolecules* 11:1156–1161
- Court F, Leibler L, Pascault JP, Ritzenthaler S (2001) Patent WO 01 92415 (PCT/FR 01 01517) (ATOFINA)
- Dean JM, Lipic PM, Grubbs RB, Cook RF, Bates FS (2001) Micellar structure and mechanical properties of block copolymer modified epoxies. *J Polym Sci Part B: Polym Phys* 39:2996–3010
- Dean JM, Vergheese NE, Pham HQ, Bates FS (2003) Nanostructure toughened epoxy resins. *Macromolecules* 36:9267–9270
- Ellis B (1993) Chemistry and technology of epoxy resins. Blackie Academic Professional, Glasgow
- Fox TG (1956) Influence of diluent and of copolymer composition on the glass temperature of a polymer system. *Bull Am Phys Soc* 1:123–125
- George SM, Puglia D, Kenny JM, Jyotishkumar P, Thomas S (2012) Cure kinetics and thermal stability of micro and nanostructured thermosetting blends of epoxy resin and epoxidized styrene-block-butadiene-block-styrene triblock copolymer systems. *Polym Eng Sci* 52:2336–2347
- Girard-Reydet E, Pascault JP, Bonnet A, Court F, Leibler L (2003) A new class of epoxy thermosets. *Macromol Symp* 198:309–322
- Gong W, Zheng K, Wang L, Zheng S (2008) Poly(hydroxyether of bisphenol A)-block-polydimethylsiloxane alternating block copolymer and its nanostructured blends with epoxy resin. *Polymer* 49:3318–3326
- Gordon M, Taylor JS (1952) Ideal copolymers and the second-order transitions of synthetic rubbers. i. non-crystalline copolymers. *J Chem Tech Biotech* 2:493–500
- Grubbs RB, Dean JM, Broz ME, Bates FS (2003) Reactive block copolymers for modification of thermosetting epoxy. *Macromolecules* 33:9522–9534
- Guo Q, Groeninckx G (2001) Crystallization kinetics of poly(ϵ -caprolactone) in miscible thermosetting polymer blends of epoxy resin and poly(ϵ -caprolactone). *Polymer* 42:8647–8655
- Guo Q, Figueiredo P, Thomann R, Gronski W (2001a) Phase behavior, morphology and interfacial structure in thermoset/thermoplastic elastomer blends of poly(propylene glycol)-type epoxy resin and polystyrene-*b*-polybutadiene. *Polymer* 42:10101–10110
- Guo Q, Harrats C, Groeninckx G, Reynaers H, Koch MHJ (2001b) Miscibility, crystallization and real-time small-angle X-ray scattering investigation of the semicrystalline morphology in thermosetting polymer blends. *Polymer* 42:6031–6041
- Guo Q, Thomann R, Gronski W, Thurn-Albrecht T (2002) Phase behavior, crystallization, and hierarchical nanostructures in self-organized thermoset blends of epoxy resin and amphiphilic

- poly(ethylene oxide)-*block*-poly(propylene oxide)-*block*-poly(ethylene oxide) triblock copolymers. *Macromolecules* 35:3133–3144
- Guo Q, Dean JM, Grubbs RB, Bates FS (2003a) Block copolymer modified novolac epoxy resin. *J Polym Sci Part B: Polym Phys* 41:1994–2003
- Guo Q, Thomann R, Gronski W, Staneva R, Ivanova R, Stuhn B (2003b) Nanostructures, semicrystalline morphology, and nanoscale confinement effect on the crystallization kinetics in self-organized block copolymer/thermoset blends. *Macromolecules* 36:3635–3645
- Guo Q, Wang K, Chen L, Zheng S, Halley PJ (2006) Phase behavior, crystallization, and nanostructures in thermoset blends of epoxy resin and amphiphilic star-shaped block copolymers. *J Polym Sci Part B: Polym Phys* 44:975–985
- Hameed N, Guo Q, Xu Z, Hanley TL, Mai YW (2010) Reactive block copolymer modified thermosets: highly ordered nanostructures and improved properties. *Soft Matter* 6:6119–6129
- Helfand E (1975) Block copolymer theory. III. Statistical mechanics of the microdomain structure. *Macromolecules* 8:552–556
- Hillmayer MA, Lipic PM, Hajduk D, Almdal K, Bates FS (1998) Self-assembly and polymerization of epoxy resin-amphiphilic block copolymer nanocomposites. *J Am Chem Soc* 119:2749–2750
- Hu D, Zhang C, Yu R, Wang L, Zheng S (2010) Self-organized thermosets involving epoxy and poly(ϵ -caprolactone)-*block*-poly(ethylene-co-ethylethylene)-*block*-poly(ϵ -caprolactone) amphiphilic triblock copolymer. *Polymer* 51:6047–6057
- Hydro RM, Pearson RA (2007) Epoxies toughened with triblock copolymers. *J Polym Sci A* 45:1470–1481
- Lange FF, Radford KC (1971) Fracture energy of an epoxy composite system. *J Mater Sci* 6:1197–1203
- Larránaga M, Serrano E, Martin MD, Tercjak A, Kortaberria G, de la Caba K, Riccardi CC, Mondragon I (2007) Mechanical properties–morphology relationships in nano-/microstructured epoxy matrices modified with PEO–PPO–PEO block copolymers. *Polym Int* 56:1392–1403
- Lipic PM, Bates FS, Hillmyer MA (1998) Nanostructured thermosets from self-assembled amphiphilic block copolymer/epoxy resin mixtures. *J Am Chem Soc* 120:8963–8970
- Liu J, Thompson ZJ, Sue HJ, Bates FS, Hillmyer MA, Dettloff M, Jacob G, Verghese N, Pham H (2010) Toughening of epoxies with block copolymer micelles of wormlike morphology. *Macromolecules* 43:7238–7243
- McGarry FJ, Sultan NJ (1968) *ACS Div Org Coat Plast Chem* 28:526
- McGarry FJ, Willner AM (1968) *ACS Div Org Coat Plast Chem* 28:512
- Mijovic J, Shen M, Sy JW, Mondragon I (2000) Dynamics and morphology in nanostructured thermoset network/block copolymer blends during network formation. *Macromolecules* 33:5235–5244
- Ocando C, Fernández R, Tercjak A, Mondragon I, Eceiza A (2013) Nanostructured thermoplastic elastomers based on SBS triblock copolymer stiffening with low contents of epoxy system. Morphological behavior and mechanical properties. *Macromolecules* 46:3444–3451
- Ritzenthaler S (2000) PhD thesis, INSA Lyon
- Ritzenthaler S, Girard-Reydet E, Pascault JP (2000) Influence of epoxy hardener on miscibility of blends of poly(methyl methacrylate) and epoxy networks. *Polymer* 41:6375–6386
- Ritzenthaler S, Court F, David L, Girard-Reydet E, Leibler L, Pascault JP (2002) ABC triblock copolymers/epoxy – diamine blends. 1. Keys to achieve nanostructured thermosets. *Macromolecules* 35:6245–6254
- Ritzenthaler S, Court F, Girard-Reydet E, Leibler L, Pascault JP (2003) ABC triblock copolymers/epoxy – diamine blends. 2. Parameters controlling the morphologies and properties. *Macromolecules* 36:118–126
- Sun P, Dang Q, Li B, Chen T, Wang Y, Lin H, Jin Q, Ding D (2005) Mobility, miscibility, and microdomain structure in nanostructured thermoset blends of epoxy resin and amphiphilic poly(ethylene oxide)-*block*-poly(propylene oxide)-*block*-poly(ethylene oxide) triblock copolymers characterized by solid-state NMR. *Macromolecules* 38:5654–5667

- Thio YS, Wu J, Bates FS (2006) Epoxy toughening using low molecular weight poly(hexylene oxide)-*block*-poly(ethylene oxide) diblock copolymers. *Macromolecules* 39:7187–7189
- Wang Y, Shen JS, Long CF (2001) The effect of casting temperature on morphology of poly(styrene-ethylene/butylene-styrene) triblock copolymer. *Polymer* 42:8443–8446
- Wu J, Thio YS, Bates FS (2005) Structure and properties of PBO–PEO diblock copolymer modified epoxy. *J Polym Sci Part B: Polym Phys* 43:1950–1965
- Wu S, Peng S, Hameed N, Guo Q, Mai YW (2012) A new route to nanostructured thermosets with block ionomer complexes. *Soft Matter* 8:688–698
- Xu Z, Zheng S (2007) Reaction-induced microphase separation in epoxy thermosets containing poly(ϵ -caprolactone)-*block*-poly(*n*-butyl acrylate) diblock copolymer. *Macromolecules* 40:2548–2558
- Xu Z, Hameed N, Guo Q, Mai YW (2010) Nanostructures and thermomechanical properties of epoxy thermosets containing reactive diblock copolymer. *J Appl Polym Sci* 115:2110–2118
- Yi F, Zheng S, Liu T (2009) Nanostructures and surface hydrophobicity of self-assembled thermosets involving epoxy resin and poly(2,2,2-trifluoroethyl acrylate)-*block*-poly(ethylene oxide) amphiphilic diblock copolymer. *J Phys Chem B* 113:1857–1868
- Young RJ, Beaumont PWR (1977) Failure of brittle polymers by slow crack growth: Part 3 Effect of composition upon the fracture of silica particle-filled epoxy resin composites. *J Mater Sci* 12:684–692

Lei Li and Sixun Zheng

Abstract

In this chapter, we summarized the recent progress in the studies of mechanical properties of epoxy/block copolymer blends. It is recognized that nanostructures can be formed in epoxy/block copolymer blends via either self-assembly or reaction-induced microphase separation mechanism. The formation of nanostructures in the epoxy thermosets can more effectively improve the toughness of the epoxy thermosets, which has been called “toughening by nanostructures.” The toughening of nanostructured epoxy thermosets is quite dependent on type and shape of dispersed nanophases and the interactions between nanophases and epoxy matrix. In terms of the mechanism for energy dissipation, toughening mechanisms of the epoxy/block copolymer blends involve shear band, microcracking, crack pinning, and particle bridging. Depending on the inherent features of materials and operating conditions (e.g., applied loading), improvement of toughness can be achieved by the function of a single mechanism or through a complex combination of simultaneous and successive actions of different processes.

Keywords

Epoxy/block copolymer blends • Toughness • Crosslinking density • Curing condition and curing agents • Nanophase formation mechanism • Nanophase morphologies • Block copolymer reactivity • Strain condition

L. Li • S. Zheng (✉)

Department of Polymer Science and Engineering and the State Key Laboratory of Metal Matrix Composites, Shanghai Jiao Tong University, Shanghai, China
e-mail: szheng@sjtu.edu.cn

Contents

Introduction	1068
Formation of Nanophases in Epoxy Thermosets	1069
Fracture Toughness of Nanostructured Epoxy Thermosets	1070
Factors to Influence Toughness of Nanostructured Thermosets	1071
Mechanisms of Toughness Improvement	1086
Conclusions	1091
References	1091

Introduction

Epoxy polymers, a class of important thermosets, have been widely used as high-performance materials such as coatings, adhesives, electronic encapsulating materials, and matrices of composites. The performance of epoxy resins is often dictated by the mechanical properties. However, epoxy thermosets are inherently of low impact resistance due to their high cross-linking density. In the past decades, considerable efforts have been made to improve the toughness of epoxy thermosets (Cooper and Estes 1979; Yee and Pearson 1986; Sultan and McGarry 1973). The incorporation of a diverse range of polymeric modifiers such as elastomers (Bucknall and Partridge 1983; Bucknall and Gilbert 1989; Yorkgitis et al. 1985) and thermoplastics (Meijerink et al. 1994; Raghava 1988; Hwang et al. 1997) into the epoxy resins is the successful approaches to achieve the enhanced toughness. Although elastomers (and/or thermoplastics) can be used effectively to toughen the thermosets, the resulting thermosets would suffer from various deficiencies. For example, the incorporation of liquid rubbers such as carboxyl (and/or amino)-terminated acrylonitrile butadiene (CTBN) (and/or ATBN) can significantly improve the toughness of the materials; however, the unsaturated bonds in these modifiers brought the modified thermosets with thermal instability and low oxidation resistance. It has been realized that the modification with elastomers is not suitable for the thermosets with high cross-linking density (Yee and Pearson 1986; Kinloch et al. 1983a, b; Pearson and Yee 1989, 1991). For the modification with high-performance thermoplastics, the toughness improvement of the thermosets would be at the expense of sacrificing the processing properties of thermosetting systems.

Generally, the modified thermosets are prepared starting from the homogeneous solution composed of precursors of thermosets and the modifiers. With the occurrence of curing reaction, the modifiers were demixed out of the initial homogeneous mixtures. This process is called reaction-induced phase separation (RIPS). The driving force of RIPS is the unfavorable entropic contribution (ΔS_m) to the mixing free energy (ΔG_m), which results in the dramatic increase of the epoxy network during the process of the curing reaction. If there exist the favorable inter-component specific interactions (e.g., hydrogen bonding, ionic bond) between the thermosets and the modifiers, which result in the negative enthalpy (Utracki and Favis 1989), the thermosetting blends of epoxy with the modifiers could still remain homogeneous or miscible. In the RIPS systems, there were the competitive kinetics between the phase separation and the curing reaction (viz., polymerization), which can be employed to modulate the morphological

structures of epoxy thermosets to improve the fracture toughness of epoxy thermosets. In the past years, the improvement of fracture toughness of epoxy thermosets has been well understood, which would follow the mechanisms including shear yielding (Gilbert and Bucknall 1991), particle bridging (Cho et al. 1993), crack pinning (Iijima et al. 1991), and microcracking (Francis et al. 2006). Depending on the material systems and operating conditions (e.g., applied loading), toughness improvement is achieved through a single mechanism or the complex combination of simultaneous and successive actions of different processes. The fine heterogeneous morphology is crucial for the improvement of toughness in terms of the above-known toughening mechanisms. Recently, it is realized that formation of microphase separation (or nanostructures) in the thermosets can further significantly improve the toughness of epoxy thermosets. Such an effect has been called “toughening by nanostructures” (Ruiz-Pérez et al. 2008). Compared to the conventional modification of epoxy thermosets, the toughness improvement of epoxy thermosets via the formation of the nanostructures could display the following specific features: (i) the nanostructures (i.e., the formation of microphase separation) can significantly optimize the interactions between the modifiers and the thermosetting matrix; (ii) the interface interactions between the thermosetting matrix and the nanodomains are significantly increased. Therefore, the toughness of epoxy thermosets can be further significantly improved.

Formation of Nanophases in Epoxy Thermosets

It is critical to control the formation of the nanostructures in epoxy thermosets. In the past decade, there has been a great progress in the studies as evidenced by rapid increase in the quantity of literature (Ruiz-Pérez et al. 2008; Zheng 2010). Herewith, we briefly summarized the main clues in chronological order. In 1970s, de Gennes (1969, 1979) first proposed that the formation of well-defined nanostructures in thermosets can be achieved by locking in the performed ordered mesoscopic structures in the process of curing reaction (or polymerization). As one of the successful applications, liquid crystalline epoxy resins have been developed to obtain the materials with ordered mesomorphic structures, which thus endow the materials with improved properties (Barclay et al. 1992; Hikmet 1992; Broer et al. 1993; Litt et al. 1993; Hikmet et al. 1993; Kishore 1993; Lin et al. 1994). In 1997, Bates and coworkers (Hillmyer et al. 1997; Lipic et al. 1998) proposed that the nanophases in epoxy thermosets can be formed through a self-assembly approach by the use of amphiphilic block copolymers. The basic idea of this protocol is to use the precursors of thermosets as the selective solvents of the amphiphilic block copolymers, and some nanoobjects with spherical, cylindrical, bicontinuous, and lamellar morphologies are generated via self-assembly approach prior to curing reaction. These self-assembled nanostructures are then fixed (or locked in) with the subsequent curing reaction. This approach is in reality a templating method based on the self-assembly behavior of block copolymers in selective solvents. Nonetheless, the self-assembly approach is not exclusive for the formation of nanophases in thermosets by the use of block copolymers. In 2006, Zheng and coworkers

(Meng et al. 2006) reported that ordered or disordered nanostructures in thermosets can be alternatively accessed via reaction-induced microphase separation (RIMPS) mechanism. In this mechanism, a part of subchains of the block copolymers were demixed with the occurrence of polymerization, whereas the other subchains still remained miscible with the matrix of the thermosets. In this approach, all the blocks of the copolymers are miscible with precursors of thermosets, and no self-organized nanophases are generated prior to curing reaction. The nanostructures in the thermosetting systems are not formed until the polymerization reaction (*viz.*, curing) occurs with a sufficient conversion of monomers. The formation of nanophases in the thermosets is due to the demixing of the thermoset-phobic subchains of the block copolymers out of the thermosetting matrix in the process of curing reaction. Since Bates et al. (Hillmyer et al. 1997; Lipic et al. 1998) reported the nanostructured epoxy thermosets by using amphiphilic block copolymers, many investigators have been involved with the studies on the formation of the nanostructures in epoxy thermosets, which have been summarized in the previous chapters of this book.

Fracture Toughness of Nanostructured Epoxy Thermosets

It is well known that toughness improvement of epoxy thermosets can be achieved by incorporating liquid rubbers (Meeks 1974; Ratna and Simon 2001; Thomas et al. 2008; Kong et al. 2008). In the multicomponent blends, phase-separated morphologies were formed via reaction-induced phase separation mechanism. In the macroscopically phase-separated thermosets, cavitation around the rubber particles with shear yielding of epoxy matrix could cause energy dissipation and thus toughen the thermosets. In addition, microvoiding and tearing of the rubber particles may also occur. It is expected that the toughness of the materials would be further improved if the particles can be dispersed into the thermosetting matrix at the nanometer scale due to (i) the further optimization of the interactions between the thermosetting matrix and the modifier and (ii) the increased interface interactions between thermosetting matrix and the modifiers. Dean et al. (2001) first investigated the effect of nanostructures on the mechanical properties of the epoxy thermosets. The nanostructured epoxy thermosets were prepared on the basis of poly(ethylene oxide)-*block*-poly(ethylene-*alt*-propylene) (PEO-*b*-PEP) block copolymer containing 50 or 26 vol% PEO, poly(bisphenol-A-*co*-epichlorohydrin) (BPA), and 4,4'-methylenedianiline (MDA). It was found that the formation of nanostructure can significantly improve the toughness of the epoxy thermosets. Spherical micelles improved the strain energy release rate (G_{IC}) by 25–35%, whereas the vesicle morphology displayed the most significant impact on G_{IC} (177% increase).

Yang et al. (2009) reported a comparative investigation on the mechanical properties of microphase- and macrophase-separated blends of epoxy thermosets. In their work, an amphiphilic triblock copolymer, poly(ϵ -caprolactone)-*block*-poly(butadiene-*co*-acrylonitrile)-*block*-poly(ϵ -caprolactone) (PCL-*b*-PBN-*b*-PCL), was synthesized and incorporated into epoxy thermosets. The nanostructured thermosets were obtained via RIMPS mechanism since PCL subchains are miscible with epoxy

after and before curing reaction (Yin and Zheng 2005; Ni and Zheng 2005) whereas PBN subchains underwent RIPS process in epoxy thermosets (Riew and Kinloch 1993; Hsich 1990; Morgan et al. 1984). For comparison, the ternary blends containing epoxy resin, plain poly(butadiene-*co*-acrylonitrile), and plain PCL with the same composition as the above-nanostructured blends were also prepared. The morphologies of the above two systems were explored by the combination of transmission electron microscope (TEM) and small-angle X-ray scattering (SAXS). It was found that the epoxy thermosets containing PCL-*b*-PBN-*b*-PCL triblock copolymer displayed microphase-separated morphologies, whereas the ternary blends containing plain PBN and PCL were macroscopically phase separated (Fig. 1). The fracture toughness of both epoxy thermosets was investigated in terms of the critical stress intensity factor (K_{IC}). It is seen that the K_{IC} values of all the thermosetting blends are higher than that of the control epoxy ($K_{IC} = 0.8 \text{ MN/m}^{3/2}$), indicating that epoxy thermoset was significantly toughened with the inclusions of the modifiers (i.e., PCL-*b*-PBN-*b*-PCL and/or HTBN + PCL), and the values of K_{IC} increased with increasing the content of the modifiers. For the nanostructured thermosets containing PCL-*b*-PBN-*b*-PCL triblock copolymer, the value of K_{IC} attained its maximum (i.e., $1.98 \text{ MN/m}^{3/2}$) at the concentration of the triblock copolymer of 20 wt%. For the ternary blends (viz., the macroscopically phase-separated blends), in contrast, the value of K_{IC} did not attain the maximum (i.e., $1.6 \text{ MN/m}^{3/2}$) until the concentration of modifier (i.e., HTBN + PCL) reached 30 wt%. In addition, the fracture toughness of the nanostructured blends was much higher than that of the macroscopically phase-separated thermosets with the identical content of modifiers. The effect of the nanostructures on the toughness improvement is attributable to the formation of the nanophases in the thermosets containing block copolymers.

Factors to Influence Toughness of Nanostructured Thermosets

Reactivity of Block Copolymers

It has been realized that the block copolymers that can be used to prepare the nanostructured thermosets must contain both thermoset-phobic and thermoset-philic blocks. The epoxy-phobic subchains are immiscible with the thermosets and occur phase separation from the epoxy matrix after curing reaction. The epoxy-philic blocks are initially miscible with precursors of thermosets and remained mixed with the thermoset after curing reaction up to high conversions. The covalent linkages between epoxy-phobic and epoxy matrix are critical to suppress the macroscopic phase separation in the process of curing reaction. The affinity of the block copolymers with epoxy can be achieved through physical interactions and/or chemical reactivity of the blocks with the thermoset. It is proposed that the reactivity of copolymer blocks with epoxy is favorable to the enhancement of adhesion between epoxy matrix and the microdomains.

The block copolymers containing glycidyl methacrylate (Yi et al. 2011; Grubbs et al. 2000; Dean et al. 2003a) and methacrylic acid (Rebizant et al. 2004) have been

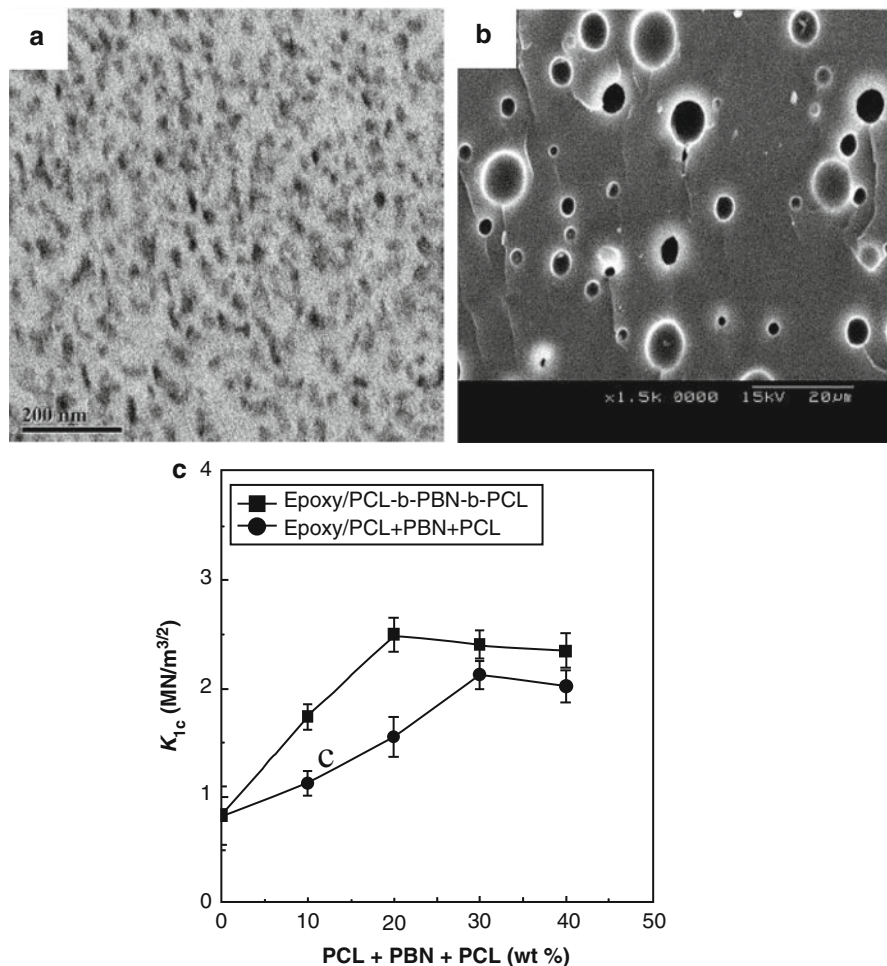


Fig. 1 TEM images of nanostructured epoxies containing PCL-*b*-PBN-*b*-PCL triblock copolymer (a) and ternary blends containing PBN and PCL (b). Plots of K_{1C} as function of modifiers for both above blends (c) (Reprinted with permission from Yang et al. (2009). Copyright 2009 Elsevier)

often used to prepare the nanostructured epoxy thermosets and improve the toughness of the materials. For example, Grubbs et al. (2000) reported the modification of epoxy thermosets by incorporating reactive poly(epoxyisoprene)-*block*-polybutadiene (BIXn) copolymers and poly(methyl acrylate-*co*-glycidyl methacrylate)-*block*-polyisoprene (MG-I) copolymers. It was demonstrated that the reactivity of the block copolymers enabled them to form the well-dispersed nanostructures (spheres, vesicles) in the epoxy thermosets with the occurrence of the curing reaction. In addition, they (Dean et al. 2003b) further investigated the effect of the reactivity of the block copolymer on the toughness of the epoxy thermosets by the use of BIXn copolymers and poly(methyl methacrylate-*co*-glycidyl methacrylate) (PMA-*co*-PGMA). The results of the

strain energy release rate (G_{IC}) indicated that the reactive vesicles provided higher toughness than the nonreactive ones.

Rebizant et al. (2004) have investigated the mechanical properties of the different epoxy networks alone and blended with polystyrene-*block*-polybutadiene-*block*-poly-[(methyl methacrylate)-*stat*-(*tert*-butyl methacrylate)] [S-*b*-B-*b*-(MT)] and its derivative of hydrolysis [S-*b*-B-*b*-(MA)]. It was found the inclusion of reactive block copolymer improved the fracture toughness of the epoxy thermosets. For example, in DGEBA/dicyandiamide (*N*-cyanoguanidine) (DICY) networks, the incorporation of 3 wt% [S-*b*-B-*b*-(MT)] block copolymer leads to a 1.5-fold increase of critical stress field intensity factors (K_{IC}), whereas [S-*b*-B-*b*-(MA)] block copolymer with reactive methacrylic acid groups promoted a higher value of K_{IC} (1.7-fold).

Yi et al. (2011) investigated the nanostructured epoxy thermosets by the use of a reactive block copolymer poly(2,2,2-trifluoroethyl acrylate)-*block*-poly(glycidyl methacrylate) (PTFEA-*b*-PGMA). The formation of nanostructure was followed by self-assembly mechanism since PTFEA was phase-separated in the epoxy matrix after and before curing reaction while PGMA was miscible with epoxy. It was found that the fracture toughness of the nanostructured thermosets was much higher than plain epoxy and that the value of critical stress field intensity factors (K_{IC}) reached the maximum with $K_{IC} = 2.42 \text{ MN/m}^{3/2}$ while the concentration of the diblock copolymer was 10 wt%. The improvement in fracture toughness could be associated with the following factors. First, the formation of the nanostructure could greatly optimize the interactions between block copolymer and the thermosetting matrix. Second, the spherical and interconnected nano-objects of PTFEA were obtained in the epoxy thermosets containing PTFEA. It is proposed that the energy-dissipation mechanisms could be related to on the formation of shearing bands induced by the nanocavitation of PTFEA microdomains in the nanostructured epoxy thermosets containing PTFEA. Third, there were the chemical bonds between epoxy matrix and PTFEA microphases because the block copolymer was reactive. In addition, the demixing behavior of PGMA subchains decreased in cross-linking density of thermoset matrix, leading to the improvement of fracture toughness.

Polystyrene-*block*-polybutadiene-*block*-polystyrene (SBS) triblock copolymer with 60–80 wt% soft phase fraction is one of the main commercial thermoplastic elastomers (TPE) due to their excellent mechanical properties. Therefore, SBS block copolymer is a kind of very potential modifier to improve the toughness of epoxy thermosets. Due to the immiscibility of the blocks (*viz.*, PB and PS block) with epoxy, SBS block copolymers must be chemically modified in order to obtain a new block copolymer which contains an epoxy-philic (or reactive) blocks. Ocando et al. (2008, 2013) have succeeded in toughening epoxy thermosets by using the modified SBS block copolymers. They (Ocando et al. 2013) reported the preparation of nanostructured epoxy thermosets with epoxidized SBS triblock copolymers. It was found that microphase separation at nanoscale from disordered to well-ordered self-assembled morphologies occurred in epoxy thermosets containing the modified SBS triblock copolymer. The nanostructures were quite dependent on the mixture compositions, showing a transition from short cylinders to lamellae. The formation of the nanostructures gives rise to a

significant increase on strength and stiffness in the system with well-ordered lamellar morphology.

Morphologies of Nanophases

Bates and coworkers (Dean et al. 2001, 2003a, b) have systemically investigated the formation of various nanostructures such as spherical micelle, vesicles, or wormlike micelle in the epoxy/block copolymer thermosets and found that the toughening of nanostructured epoxy thermosets was quite dependent on the type and shape of dispersed nanophases and the interactions between the nanophases and the thermosetting matrix. For example, they (Dean et al. 2001) investigated the effect of morphological structure on the mechanical properties of the epoxy/block copolymer [viz., poly(ethylene oxide)-*block*-poly(ethylene-*alt*-propylene) (PEO-*b*-PEP)] thermosets. Spherical micelles were found to improve the toughness, and the fracture resistance has no statistically significant dependence on the micelle radius (the fracture resistance of the system containing the largest micelle radius was just slightly higher than that with the lowest micelle radii). In addition, there was no discernible concentration effect on fracture resistance for the epoxies containing spherical micelles between 5 and 10 wt% block copolymer. The vesicular morphology displayed the most significant impact on G_{IC} (177% increase), even though at half the diblock copolymer concentration of the micelle forming thermosets. The formation of vesicular nanophases was recognized to be one of the most effective approaches for improving the fracture resistance of the epoxy thermosets (Grubbs et al. 2000, 2001). Liu et al. (2010) also reported the formation of wormlike micelle resulted in the improved toughness of the epoxy/block copolymer thermosets. Poly(ethylene oxide)-*block*-poly(ethylene-*alt*-propylene) (PEO-*b*-PEP) diblock copolymer was still used in this work. By tuning the molecular weight of the block copolymer, the fraction of PEO block in the PEO-PEP diblock copolymer, and the cross-link density of the epoxy matrix, wormlike micelles were obtained in the epoxy/block copolymer thermosets. An improvement in K_{IC} by 106% over plain epoxy was found for the wormlike micelle-modified thermosets. In contrast, the same epoxy thermoset formulation containing PEO-*b*-PEP diblock copolymer that self-assembled into spherical micelles displayed relatively less effective improvement in toughness. It was proposed that wormlike micelles in the epoxy thermosets produced enhanced toughness, which is attributed to a combination of mechanisms including crack tip blunting, cavitation, particle debonding, limited shear yielding, and crack bridging (see Fig. 2).

Dean et al. (2003b) further investigated the nanophase effect on the mechanical properties of the epoxy blends with a wide variety of block copolymers, such as poly(ethylene oxide)-*block*-poly(1,2-butadiene) (PEO-*b*-PB), poly(ethylene oxide)-*block*-poly(1,4-isoprene) (PEO-*b*-PI), poly(ethylene oxide)-*block*-poly(ethylene-*alt*-propylene) (PEO-*b*-PEP), and poly(methyl methacrylate-*co*-glycidyl methacrylate) (PMA-*co*-PGMA). It was also demonstrated that vesicle-modified epoxy/block copolymer thermosets displayed much higher G_{IC} (a maximum of sixfold for the improved toughness) than spherical micelles or wormlike micelle-modified thermosets at an identical block copolymer concentration (see Fig. 3). The relationship of

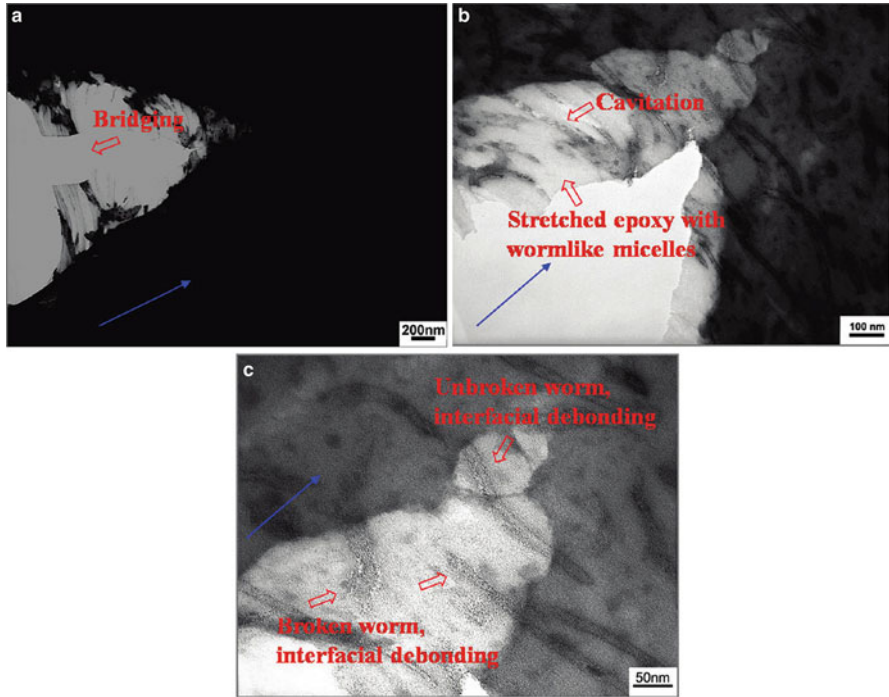
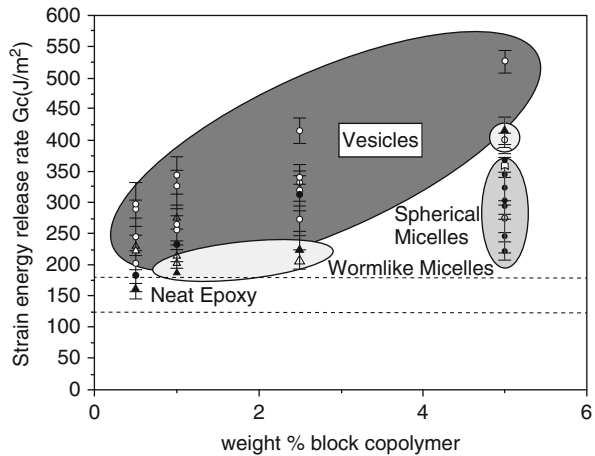


Fig. 2 TEM micrographs of the crack tip DN-4 PB specimen of BCP-toughened epoxy: overview of the crack tip (a), evidence of wormlike structure cavitation or fragmentation after severe stretching (b), and evidence of interfacial debonding or voiding (c). The blue arrows in the micrographs indicate the direction of crack propagation (Reprinted with permission from Liu et al. (2010). Copyright 2010 American Chemical Society)

Fig. 3 G_{IC} as a function of the weight percentage of the block copolymer in the blends (Reprinted with permission from Dean et al. (2003a). Copyright 2003 John Wiley & Sons)



between G_{IC} and the separated vesicle size was systematically illustrated. It was found that a continual increase in G_{IC} as D_i/D_p decreases (where D_i/D_p is ratio of the interparticle distance to the average vesicle (or spherical micelle) diameter). At high values of D_i/D_p (smaller vesicles further apart), the improvement in G_{IC} is small, but there is a measurable effect of the degree of adhesion on the mechanical properties. The beneficial effects of vesicle-matrix adhesion disappear as D_i/D_p decreases (larger vesicles closer together) and G_{IC} of the blends increases. Therefore, G_{IC} is most dependent on the morphology and is not dependent on the specific nature of the block copolymers.

Block Copolymer Architectures

In the past years, there have been a great number of reports on the formation of nanostructures in epoxy thermosets by the use of block copolymers with various architectures. Linear (e.g., di-, tri-, alternating) and nonlinear (star-shaped, hyperbranched) block copolymers have been used (Dean et al. 2003b; Yu and Zheng 2011; Thio et al. 2006; Ritzenthaler et al. 2003; Gong et al. 2008; Hu and Zheng 2011; Francis and Baby 2014; Könczöl et al. 1994; Zhang et al. 2014; Li et al. 2015). Depending on the molecular weights, composition, and architectures of block copolymers, the content of the block copolymer in the epoxy thermosets, the epoxy/block copolymer thermosets, displayed various morphologies, such as spherical micelle, vesicle, and wormlike micelle. For example, Bates and coworkers (Dean et al. 2003b) studied the toughening effect of PEO-*b*-PEP diblock copolymers at low concentration on a poly(bisphenol-A-*co*-epichlorohydrin)/tetrafunctional aromatic amine hardener (BPA/MDA) system. It was demonstrated that a vesicular morphology was observed to generate higher improved toughness than the spherical micelle morphologies. Yu (Yu and Zheng 2011) and Thio (Thio et al. 2006) et al. have extended this work on toughening the epoxy thermosets by the use of poly(ethylene oxide)-*block*-poly(butylene oxide) (PBO-*b*-PEO) and poly(ethylene oxide)-*block*-poly(hexylene oxide) (PEO-*b*-PHO) diblock copolymers. It was found that the wormlike morphology gave the best improvement in K_{IC} and G_{IC} , while vesicles were found to give greater improvements than spherical micelles. In addition, the fracture surfaces of each epoxy/block copolymer blend significantly related to the mechanisms of crack propagation. For the thermosetting blends containing small spherical micelles, there was no significant deformation of the epoxy matrix prior to fracture. In contrast, for the thermosetting blends containing larger wormlike micelles or bilayer vesicles, the surface roughness increased, for instance, the blend with wormlike micelles displayed a surface with steps and “leaflike” structures indicating some small-scale plastic deformation of the matrix.

The addition of triblock copolymer polystyrene-*block*-polybutadiene-*block*-poly(methyl methacrylate) (SBM) in the epoxy resins was also found to be an effective approach to solve the problem of poor toughness of epoxy thermosets without the drawback of phase inversion, which usually occurred in the liquid rubber-modified thermosets. Pascault and coworkers (Ritzenthaler et al. 2003) investigated the toughening of the epoxy thermosets by the incorporation of SBM triblock copolymers. The SBM triblock copolymer can self-assemble into nanostructure in the

epoxy thermosets: (i) PB is immiscible with the epoxy precursor, leading to an initial macrophase separation between PB rubber and epoxy monomers, (ii) PS can cause reaction-induced phase separation, and (iii) PMMA is previously shown to be completely miscible with epoxy precursors. Depending on the content and molecular weight of each block, the as-obtained epoxy/SBM blends displayed various nanostructures, such as spheres, vesicles, and spheres on spheres (Fig. 4). The formation of nanostructure leads to the improved toughness of the epoxy/block copolymer thermosets. At lower concentration of the triblock copolymer, toughness was observed to linearly increase with the fraction of PB block in the triblock copolymer. SB diblock was demonstrated to behave as toughness “boosters” as long as a transparent nanostructured epoxy thermosets was preserved. Alternatively, in the epoxy/SBM thermosets with higher SBM concentrations (30 wt%), the “spheres on spheres” morphology displayed, which was more efficient than the “core-shell” morphology to improve the toughness of the epoxy thermosets. However, when the content of SB diblock is higher than 45%, the SBM triblock copolymer was no more able to fully stabilize the SB diblocks which were partially macrophase-separated from the epoxy matrix and thus the toughness of the materials accordingly decreased.

Zheng and coworkers (Gong et al. 2008; Hu and Zheng 2011) designed and synthesized epoxy/block copolymer blends by the use of alternating block copolymer [viz., poly(hydroxyether of bisphenol-A)-*alt*-polydimethylsiloxane (PH-*alt*-PDMS)] and multiblock copolymer [polysulfone-*block*-polydimethylsiloxane (PSF-*b*-PDMS)]. The incorporation of PH-*alt*-PDMS produced spherical or worm-like micelles in the epoxies depending on the content of the block copolymer in the thermosets. The formation of the nanostructure induced improved fracture toughness, and the K_{IC} value in the epoxy thermoset containing 20 wt% PH-*alt*-PDMS increased up to $3.0 \text{ MN/m}^{3/2}$, which is almost threefold of the control epoxy thermoset. For the epoxy/PSF-*b*-PDMS thermosets, the spherical particles with the size of 50–200 nm in diameter were displayed into the continuous epoxy matrices. The nanostructured thermosets also exhibited the enhanced toughness. The maximum value of K_{IC} value was found about $2.8 \text{ MN/m}^{3/2}$ while the content of PSF-*b*-PDMS was 5 wt%.

It is proposed that the nonlinear architectures of block copolymers could exert additional variables to influence the formation of the nanophases in the epoxy thermosets, and thus the nanostructures of thermosets can be modulated by the topologies of these copolymers. Under this condition, the nonlinear block copolymers such as starlike and brushlike polymers also can be used as the modifiers for the toughness improvement of the epoxies. Francis et al. (Francis and Baby 2014) reported on the toughening of epoxy thermoset by an amphiphilic polystyrene-*block*-polyglycolic acid three-arm star copolymer (PS-*b*-PGA)₃. The chemically different nature of the blocks in the star polymer is responsible for the nanodomain formation. It was found that the nanodomains of the PS phase were dispersed in the epoxy matrix which was miscible with PGA blocks. The tensile strength of the thermoset increased with the incorporation of 10% and 20% (PS-*b*-PGA)₃ block copolymer. The value of tensile strength was approximately 52 MPa and elongation

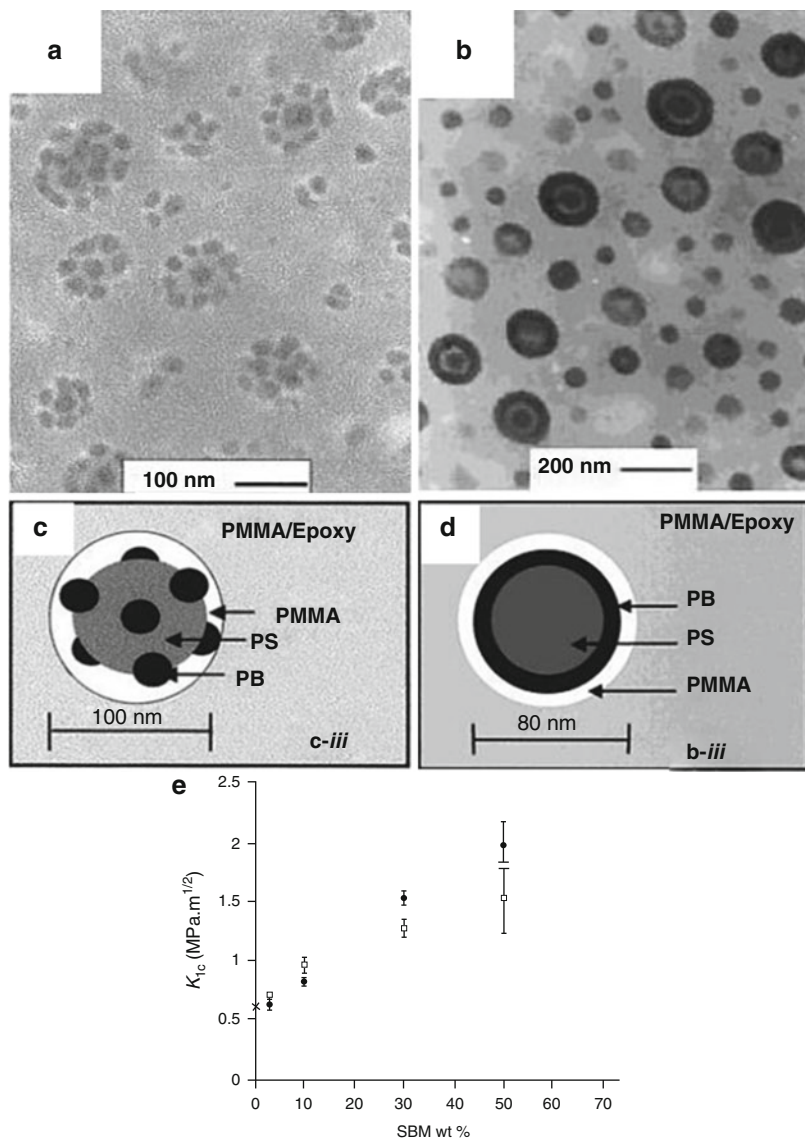


Fig. 4 TEM images of epoxy thermostets containing 30 wt% $S_{22}^{27}B_{69}M_{69}$ -SB21 (a) and $S_{12}^{14}B_{18}M_{70}$ -SB10 copolymer (b). Schematic representations of the above blocks' organization for 30 or 50 wt% blend after epoxy reaction (c, d). Plots of K_{1c} as function of modifiers for both above blends (e) (Reprinted with permission from Ritzenthaler et al. (2003). Copyright 2003 American Chemical Society)

at break was 51% (compared to that of neat epoxy, 28%). The mechanical properties of the thermostet are enhanced because of the presence of uniform nanostructures formed by the reaction-induced microphase separation of PS blocks and high miscibility of PGA blocks. Könczöl et al. (1994) synthesized low molecular weight

branched triblock copolymers poly(ϵ -caprolactone)-*block*-polydimethylsiloxane (PCL)₂-*b*-PDMS-*b*-(PCL)₂ with controlled composition. The aim was to improve mechanical properties of epoxy network with the immiscible elastomeric PDMS blocks compatibilized by the PCL segments, initially miscible in epoxy precursors. Elastomeric particles of 20 nm in diameter were uniformly dispersed in the epoxy matrix. The formation of nanostructure resulted in an increase of the toughness for copolymer contents of 5 wt% or more, without reduction of the strength at break and Young's modulus by comparison with the neat epoxy system. Zhang et al. (2014) reported toughening the epoxy thermosets by nanostructure by the uses of a novel macromolecular miktobrush, which is composed of a poly(2-hydroxyethyl methacrylate) (PHEMA) backbone and both poly(ϵ -caprolactone) (PCL) and polydimethylsiloxane (PDMS) side chains. It is seen that the K_{IC} values of all the nanostructured thermosets were higher than that of the control epoxy and that the value of K_{IC} increased with increasing the content of PHEMA-*g*-[PCL-*r*-PDMS]. While the content of miktobrush was 40 wt%, the value of K_{IC} was increased up to 3.48 MN/m^{3/2}, which was more than four times that of control epoxy.

Block Ionomer Complexes

Recently, Wu et al. (2012) reported a new type of modifier, block ionomer complex, [sulfonated polystyrene-*block*-poly(ethylene-*ran*-butylene)-*block*-polystyrene]-*co*-poly(ϵ -caprolactone) (SSEBS-*c*-PCL), and investigated the toughness of epoxy thermosets by the use of SSEBS-*c*-PCL samples with different PCL contents. It was seen that all the epoxy blends with 10 wt% SSEBS-*c*-PCL exhibited the nanoscaled spherical microdomains [(poly(ethylene-*ran*-butylene) (EB) cores surrounded by a thin sulfonated polystyrene (SPS) shell)]. In addition, with increasing PCL content, the number and average diameter of the spherical microdomains decrease gradually while the distance between the microdomains increases. This kind of specific nanostructure endowed the epoxy blends with improved mechanical properties. It was found that the fracture toughness of the thermosetting blends increases gradually with decreasing PCL content, and the best improvement comes with the blends with SSEBS-*c*-PCL containing 2.4 wt% PCL where G_{IC} (0.71 kJ m⁻²) is more than three times that of neat epoxy. It was notable that both K_{IC} and G_{IC} depend on the core radius R_c , shell thickness T_s , and effective hard sphere radius R_{hs} of the spherical nanostructures. The blend containing largest R_c and R_{hs} displayed the highest K_{IC} and G_{IC} , and they decrease with decreasing R_c and R_{hs} of the spherical microdomains. SEM observations of the fracture surfaces suggested that the toughening mechanisms of these block ionomer complex modified epoxies with spherical nanostructures were formation of crack front damage regions and interfacial debonding of spherical microdomains, followed by matrix void expansion and coalescence and small-scale matrix shear deformation.

Formation Mechanisms of Nanophases

The incorporation of block copolymers into epoxy resins has been proved to be an efficient approach to improve the toughness of the epoxy due to the nano-effect in the epoxy/block copolymer blends. The nanostructure in the epoxy/block copolymer

blends can be modulated via self-assembly or RIMPS mechanism. The former approach is in reality a templating method based on the self-assembly behavior of block copolymers in selective solvents. That is to say, the precursors of thermosets (e.g., DGEBA) are considered as the selective solvents of the amphiphilic block copolymers and the nanostructures can be generated before curing reaction. With the subsequent curing reaction, the self-assembled nanostructures are then fixed (or locked in). In this approach, the formation of nanostructure of the block copolymers in selective solvents is governed by the equilibrium thermodynamics of the multicomponent mixtures, and the morphologies of the nanostructures are dependent on the balance between the solvent-philic and the solvent-phobic subchains of the block copolymers. However, in the latter approach (viz., RIMPS), no self-assembled nanophases are generated prior to curing reaction since all the blocks of the copolymers may be miscible with precursors of thermosets. With the proceeding of curing reaction, one subchain of the block copolymers demixes out of the thermosetting matrix and thus the nanostructures are formed. In contrast to the self-assembly approach, the formation of nanostructure via RIMPS could be significantly affected by the competitive kinetics between curing reaction and phase separation in the thermosets. The formation mechanism of nanophases (i.e., self-assembly or RIMPS) has been demonstrated to be a great influence on the mechanical properties of the nanostructured epoxy thermosets. Recently, Cong et al. (2014) reported the nano-toughening of epoxy/block copolymer thermosets via two different formation mechanisms (self-assembly and RIMPS) of the nanophases in the epoxy thermosets. In this work, two block copolymers [viz., poly(ϵ -caprolactone)-*block*-poly(butadiene-*co*-styrene)-*block*-poly(ϵ -caprolactone) (PCL-*b*-PBS-*b*-PCL) and poly(ϵ -caprolactone)-*block*-poly(ethylene-*co*-ethylethylene-*co*-styrene)-*block*-poly(ϵ -caprolactone) (PCL-*b*-PEEES-*b*-PCL)] were synthesized and prepared the nanostructured thermosets. Both block copolymers possessed the same architecture, identical composition, and molecular weights, and the latter block copolymer (PCL-*b*-PEEES-*b*-PCL) was obtained by the hydrogenation of the former one (PCL-*b*-PBS-*b*-PCL). As evidenced by the results of SAXS, the formation of nanophases in the thermosets containing PCL-*b*-PEEES-*b*-PCL followed self-assembly mechanism whereas that in the thermosets containing PCL-*b*-PBS-*b*-PCL the formation of nanophases followed RIMPS mechanism. The difference in formation mechanism of nanophases leads to the different morphological structure of the epoxy/block copolymer thermosets. It was found that the nanophases (viz., PBS) in the thermosets containing PCL-*b*-PBS-*b*-PCL had larger number and smaller size than the thermosets containing PCL-*b*-PEEES-*b*-PCL (See Fig. 5). The morphological difference can be accounted for with the following factors: (i) the immiscibility of PBS (and/or PEEES) with epoxy and (ii) the competitive kinetics between polymerization and microphase separation. For the PCL-*b*-PBS-*b*-PCL-containing system, the mixtures (DGEBA, MOCA and PCL-*b*-PBS-*b*-PCL) were homogeneous before curing reaction. With the curing reaction proceeding, the PBS block was gradually demixed out of epoxy/PCL matrix. The driving force for the microphase separation of PBS blocks is the decrease in entropic contribution to free energy of mixing during the process of curing reaction. In contrast, for the PCL-*b*-PEEES-*b*-PCL-containing system, the block copolymers were self-assembled into the

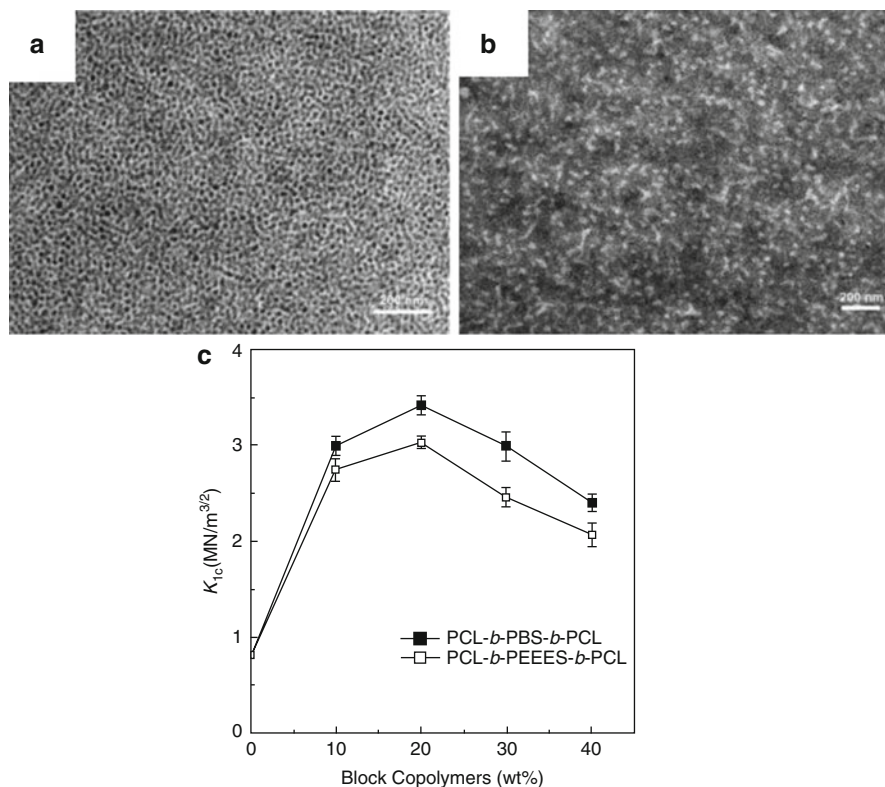


Fig. 5 TEM images of nanostructured epoxies containing 40 wt% PCL-*b*-PBS-*b*-PCL (a) and PCL-*b*-PEEES-*b*-PCL triblock copolymer (b). Plots of K_{IC} as function of modifiers for both above blends (c) (Reprinted with permission from Cong et al. (2014). Copyright 2014 Elsevier)

nanostructure in the mixtures (DGEBA, MOCA, and PCL-*b*-PBS-*b*-PCL) before curing reaction. The morphological structure (i.e., the size and shape) of PEEES nanophases was governed by the equilibrium thermodynamics of the triblock copolymer in the precursors of epoxy. The preformed nanostructure would be fixed after curing reaction. It was notable that with the occurrence of curing reaction, some minor changes could occur, which allowed the size of PEEES nanophases larger than that of PBS nanophases under the same curing conditions. The uniform dispersion of microdomains (PBS or PEEES) in the matrix could greatly optimize the interactions between the block copolymers and the epoxy matrix, and thus the nanostructured thermosets displayed the improved fracture toughness compared to the unmodified epoxy. The difference in morphological structures between both the thermosetting systems had a profound impact on the mechanical properties of the nanostructured thermosets. It was observed that the values of critical stress field intensity factors (K_{IC}) of the nanostructured epoxy/PCL-*b*-PBS-*b*-PCL thermosets were higher than that of the epoxy/PCL-*b*-PEEES-*b*-PCL thermosets with the same contents of the block

copolymers. This phenomenon can be explored by the energy-dissipation mechanisms in the nanostructured epoxy thermosets. The energy dissipation is associated with the formation of shearing bands induced by the cavitation of microdomains; therefore, the specific surface areas of the nanophases are largely responsible for the energy dissipation in the nanostructured epoxy thermosets. As shown in TEM images, the epoxy/PCL-*b*-PBS-*b*-PCL thermoset displayed smaller size of nanodomains, and thus, the specific surface area of the dispersed microdomains (PBS) in this material is larger than that in the epoxy/PCL-*b*-PEEES-*b*-PCL thermoset with the identical contents of the block copolymer. As a consequence, the nanostructures of epoxy/PCL-*b*-PBS-*b*-PCL thermosets were more favorable to the dissipation of fracture energy than epoxy/PCL-*b*-PEEES-*b*-PCL thermosets. It was notable that the maximum values of K_{IC} values in both nanostructured epoxy thermosets were displayed while the content of the block copolymers were 20 wt%. This observation can be attributed to the different viscoelasticity and stress status of the epoxy matrices and dispersed microdomains (viz., PBS or PEEES), which are significantly dependent on the composition of the nanostructured epoxy/block copolymer thermosets.

Curing Conditions and Curing Agents

The nanostructured thermosets are obtained via in situ polymerization of the precursors (i.e., curing reaction) in the presence of block copolymers. Therefore, toughening by nanostructure for the epoxy/block copolymer blends is significantly influenced by curing conditions, especially for the formation of nanophases via RIMPS mechanism. It is known that during the curing process, the chemical nature of the matrix varies with time, and thus, a block copolymer with one of the blocks miscible in the reactive mixtures may become completely incompatible with the matrix once curing is completed, which is due to the increase in the average molar mass before gelation (decrease in the entropic contribution to the free energy of mixing) and the increase in cross-link density after gelation. The variation of miscibility of the block copolymers in the thermosets largely influences the morphological nanostructures, as shown in phase diagrams of solutions of block copolymers in selective solvents of different feature. It is possible to modulate the mechanical properties of the epoxy/block copolymer blends by controlling the curing conditions.

Rebizant et al. (2004) have investigated the chemistry and mechanical properties of epoxy/block copolymer blends with the different curing agents. Polystyrene-*block*-polybutadiene-*block*-poly-[(methyl methacrylate)-*stat*-(*tert*-butyl methacrylate)] [S-*b*-B-*b*-(MT)] was chosen in this work since the miscibility of the PMMA block in precursor (viz., DGEBA) was adjusted by a very accurate choice of the diamine hardener. For example, the macrophase separation occurred in the epoxy/PMMA blends when 4,4'-diaminodiphenyl sulfone (DDS) or 4,4'-methylenedianiline (MDA) was used as the curing agent, whereas the use of 4,4'-methylenebis(3-chloro-2,6-diethylaniline) (MCDEA) as curing agent does not generate noticeable phase separation. The effective dispersion of PMMA block in the epoxy matrix may affect the final properties of the materials. In this work, the cure of the epoxy/block

copolymer blends has been explored by using six different curing processes: 2-phenylimidazole (2-PI), alone or in the presence of methyltetrahydrophthalic anhydride (MTHPA) as comonomer, dicyandiamide (DICY), and three different diamines as comonomers without accelerator: 4,4-methylenebis(3-chloro-2,6-diethylaniline) (MCDEA), 4,4'-methylenedianiline (MDA), and 4,4'-diaminodiphenyl sulfone (DDS). It was found that in DGEBA/MCDEA/SB(MT) system, PB microdomains of approximately 30 nm in size were evenly dispersed in the thermosetting matrix. It was explained that the nanostructure of the initially miscible system remains unchanged during the curing process. In contrast, MDA and DDS were used as the curing agents; the epoxy/block copolymer blends were unstable and flocculate whenever the system was reacted. After curing reaction, SB(MT)-rich domains were detected in the form of elongated aggregates with the length of more than 200 nm. While 2-PI, MTHPA, or DICY were used as the curing agents, flocculation soon occurred at the primary stage of curing process, which generated larger aggregates with the sizes of 100–500 nm. The mechanical properties of the different epoxy networks alone and blended with block copolymers have been systemically investigated. It was noted that all the block copolymer-containing epoxy blends displayed higher fracture toughness than that of the neat epoxy whatever the nature of the curing agents and the curing process. The inclusions of 10 wt% block copolymers lead to 1.8- [in the epoxy-anhydride system (MTHPA)] to 2.6-fold [in anionically polymerized DGEBA (2-PI)] improvements in critical stress field intensity factors (K_{IC}). In epoxy/aromatic diamine systems, the value of K_{IC} is multiplied by a 1.15–1.6 factor, and the level of toughness with MCDEA as curing agent is higher than that with DDS and MDA as curing agents. Notably, in epoxy/DICY systems, the 1.5-fold increase of K_{IC} was found when only 3% of SB(MT) block copolymer was incorporated in the epoxy matrix, even though the thermosetting blends were macrophase-separated after curing reaction. It was proposed that this may be correlated with the appearance of the vesicular morphology. Such organization of the block copolymer in vesicular and other types of core-shell morphologies has been demonstrated to accompany with the improved toughness in epoxy materials.

Cross-Linking Density

Although the formation of nanostructures in the epoxy/block copolymers blends has been recognized as an effective toughening approach, not all epoxy resins can be toughened to great extent. Toughening of the epoxy thermosets has been found to be related to the cross-link density of epoxy networks (Pearson and Yee 1986; Iijima et al. 1992). The cross-link density generally influences the intrinsic ductility of the cured thermosets, and the deformation of the ductility requires the conformational arrangements of polymer chains. It was demonstrated that the matrix shear banding of thermosets was the major dissipation process in the rubber-toughened epoxy resins, that is, the toughness of the epoxy thermosets can be varied by altering the ductility of the matrix. The function of rubber particle cavitation is to relieve the triaxial stress at the crack tip and consequently to facilitate matrix shear banding. Thus, the thermoset matrix ductility (i.e., cross-link density of the thermosetting

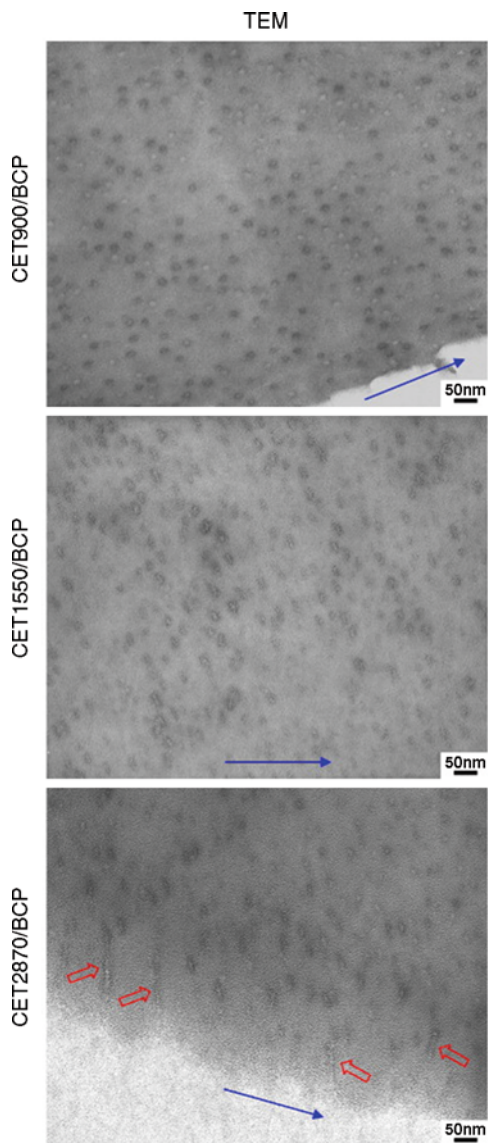
matrix) plays an important role in improving fracture toughness of rubber-modified thermosets. For the block copolymer-modified epoxy thermosets, cross-link densities of the matrix also affect the toughness of the thermosets.

Liu et al. (2009a) investigated the toughening effect of block copolymer (PEP-*b*-PEO)-modified epoxy thermosets with variation in cross-link densities on fracture behavior. DGEBA was used as the epoxy monomer, bisphenol-A (BPA) was used as chain extender, and the ratio of DGEBA and BPA was altered to vary the cross-link density. The cross-link densities of epoxy matrix in this system were designed with theoretical M_c being 900, 1550, and 2870 g mol⁻¹, respectively, and the modified epoxy samples with different M_c are designated as CET900/BCP, CET1550/BCP, and CET2870/BCP. The concentration of block copolymer in all final epoxy products was controlled to be 5 wt%, and the block copolymer self-assembles into well-defined and well-dispersed spherical micelles with an average diameter of *c.a.* 15 nm in all epoxy/block copolymer blends. It was noted that the presence of the block copolymer reduced the cross-link density of the epoxy matrix for CET900 and CET1550 systems, due to the hydrogen bonding between the OH groups generated during the cure reaction and the ether oxygen in the PEO backbone. In addition, the fracture toughness of the block copolymer-modified epoxy thermosets is strongly dependent on the cross-link density of epoxy matrix. The higher the epoxy M_c , the higher the K_{IC} value becomes. However, this phenomenon was not found in the neat epoxy resins. The optical microscopy (OM) and TEM were performed to examine the difference in major toughening effects from the influence of the matrix cross-link density. The OM images of the subcritical crack tip damage zones in the modified epoxies under both bright field and cross-polars displayed that the lower the cross-link density, the larger the damage zone size that is formed in front of the crack tip. It was also found that a shear banding process occurred due to the presence of a birefringent zone under cross-polarized light. The TEM images (Fig. 6) showed the micromechanical deformation process upon fracture by the observation of the specific location in the vicinity of the subcritical crack tips. For the epoxy/block copolymer blends with lower cross-link density (*viz.*, CET900/BCP), some cavitated nanoparticles have been found to remain spherical in shape, even in the regions immediately beneath the crack path. With increasing the cross-link density, the cavitation phenomenon becomes more uniform and the degree of particle deformation is more pronounced, indicating the shear plastic deformation of the matrix around those particles. Both OM and TEM results demonstrated that the particle cavitation and matrix shear banding mechanisms were highly suppressed for the epoxy thermosets with high cross-link density.

Strain Conditions

Incorporation of a small amount of block copolymers to form the nanostructure in the epoxy thermosets can produce improvements in fracture toughness without compromising other desirable physical and mechanical properties (e.g., T_g and Young's modulus of the cured epoxy). It was also demonstrated that upon adding block copolymer (e.g., PEP-*b*-PEO diblock copolymer) an obvious viscoelastic damping behavior appeared above room temperature, indicating that the final

Fig. 6 TEM micrographs taken in the vicinity of subcritical crack tips in CET900/BCP, CET1550/BCP, and CET2870/BCP. The crack propagating directions are indicated in the images. In the CET2870/BCP image, the *arrows* point to the BCP nanoparticles that are severely stretched (Reprinted with permission from Thompson et al. (2009). Copyright 2009 Elsevier)



mechanical properties might be significantly determined by the strain rate. It is known that mechanical properties of polymers have been demonstrated to be strain rate dependent (Webb and Aifantis 1997; Barry and Delatycki 1989). A lower strain rate usually leads to a higher fracture toughness due to the viscoelastic feature of polymer chains (Kinloch et al. 1983a). In other words, the reduction of strain state increases the molecular mobility, and thus dissipates the applied mechanical energy more effectively (Raghavan et al. 2002).

Liu et al. (2009b) reported the strain rate effect on the mechanical properties of poly(ethylene-*alt*-propylene)-*b*-poly(ethylene oxide) (PEP-*b*-PEO) block copolymer-modified epoxy thermosets with 1,1,1-tris(4-hydroxyphenyl)ethane (THPE) as the curing agents. The content of PEP-*b*-PEO block copolymer in the epoxy thermosets was controlled to be 5 wt%, and the molecular weight between cross-links of the epoxy matrix (M_c) was designed to be around 1550 Da. In this case, the block copolymer can self-assemble into spherical micelles in epoxy with an average diameter of 15 nm. According to the DMA spectra, a pronounced increase was displayed in the $\tan\delta$ curves of block copolymer-modified epoxy at temperature above 0 °C compared to the plain epoxy thermoset, indicating that the incorporation of PEP-*b*-PEO diblock copolymer causes the epoxy network to be more flexible. One proposed explanation was that the epoxy-philic corona blocks (PEO) at the boundary demixed from the cross-linked epoxy matrix, and thus, a gradient in composition in the vicinity of the micelle corona may have occurred. As a result, the BCP-toughened epoxy is likely to become more strain rate dependent at a given range of tested temperature. The fracture and tensile behaviors of the block copolymer-modified epoxy thermosets were investigated at the loading rates 0.51, 15.84, and 508 mm min⁻¹, respectively. It was found that BCP-toughened epoxy displayed mechanical properties that are significantly more loading rate dependent than the neat epoxy material. A higher strain rate leads to lower fracture toughness and a more brittle behavior in tension. The investigation further demonstrated significant strain rate dependence on the toughening mechanisms. TEM was performed to investigate the micromechanical deformation mechanisms of the block copolymer-modified epoxy materials by examining the crack tip damage zone of the double-notch four-point-bending (DN-4 PB) specimens at higher magnifications (see Fig. 7). It was shown that a higher test rate reduced to a lesser degree of block copolymer cavitation and plastic deformation at the identical relative locations; in other words, the increase of test rate dissipates the fracture energy, leading to a low K_{IC} value. Here, it was notable that yielding and localized necking mechanisms were found at slower test rate conditions (viz., 0.51, 5.08, and 50.8 mm min⁻¹) when the specimen broke before yielding, whereas shear banding or crack tip blunting dominated at higher test rate (508 mm min⁻¹). It can be explained by the following aspects: (i) at higher test rates, the volumetric dilatation of the microphase-separated domains is relatively low at the early stage of brittle failure in the epoxy matrix; (ii) there is not extensive cavitation around the crack tip to trigger massive plastic deformation of the epoxy matrix; and (iii) shear banding behavior of the matrix is highly suppressed at high rates due to increased critical stress for yielding. Therefore, care should be taken when toughening the epoxy thermosets by the use of the block copolymer is applied at a high strain state.

Mechanisms of Toughness Improvement

Traditionally, the toughening of the epoxy materials is to restrict the propagation of a sharp crack of the matrix, which can be achieved by the inclusion of the second

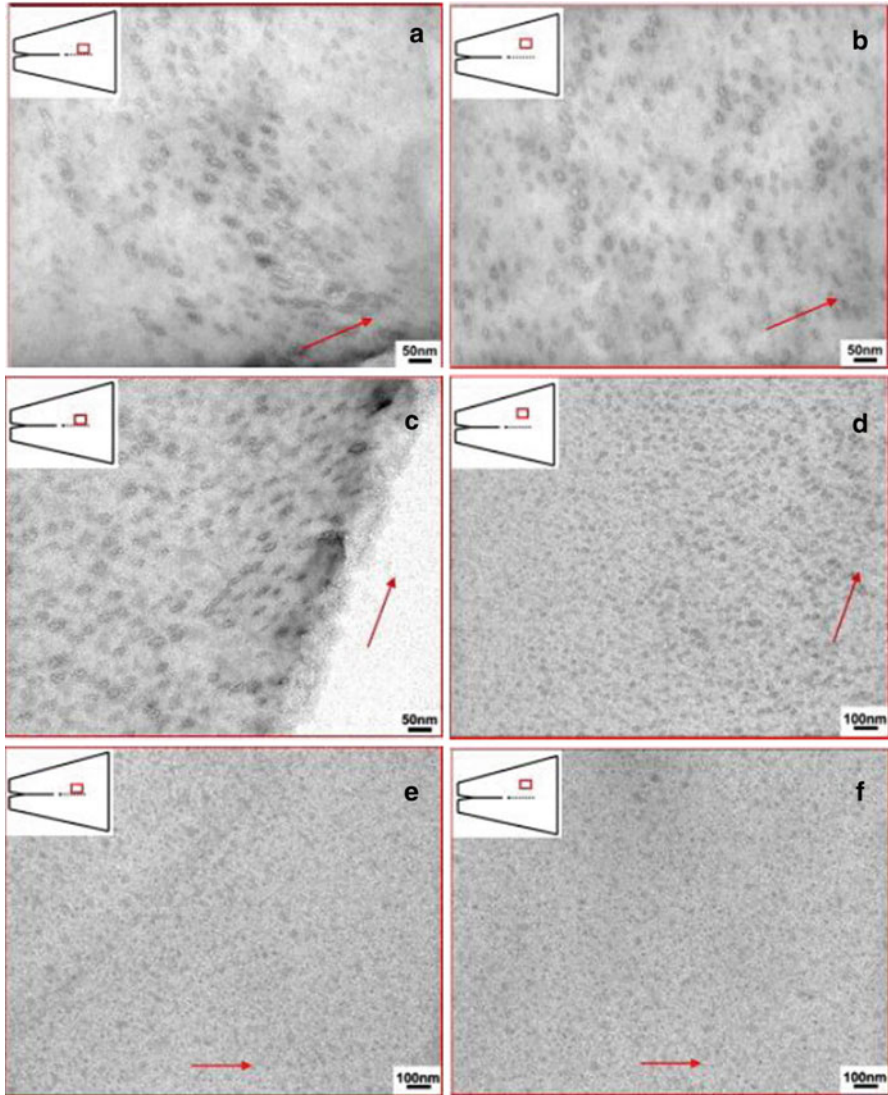


Fig. 7 TEM micrographs of BCP-toughened epoxy after DN-4 PB test with different strain states: at 0.51 mm min^{-1} at locations close to the crack tip (a) and some distance away from the crack (b), at $15.24 \text{ mm min}^{-1}$ at locations close to the crack tip (c) and some distance away from the crack (d), and at 508 mm min^{-1} at locations close to the crack tip (e) and some distance away from the crack (f). The insets show the spots where the micrographs were taken. The arrows indicate the crack propagation direction (Reprinted with permission from Liu et al. (2009b). Copyright 2009 Elsevier)

modifiers, such as the inorganic particles, rubbery polymers, block copolymers, etc. The theoretical understanding regarding toughening mechanisms has been advanced in the recent years, and the detailed descriptions of the toughening mechanisms for

modified epoxy thermosets have been described in some reviews (Kinloch et al. 1983a; Riew et al. 1976; Sigl et al. 1988; Lange and Radford 1971; Evans et al. 1985; Ortiz 1987). Here, we briefly describe the main toughening mechanisms (viz., shear yielding, particle bridging, crack-pinning, microcracking mechanism). Shear yielding (Gilbert and Bucknall 1991; Chen and Chang 1999) is a major mechanism for the second phase-modified thermosets, which involves matrix deformation and cavitations of the micro-/macrodomains in response to the stresses near the crack tip. It is known that in rubber-modified epoxy thermosets, cavitation of elastomeric phase is critical in promoting shear banding in the thermosetting materials (Cho et al. 1993; Yorkgitis et al. 1985). Considerable research work demonstrated that the major toughening mechanisms of rubber-modified thermosets are cavitation of rubber particles, followed by shear banding of the matrix. Particle bridging (Yorkgitis et al. 1985) is also recognized as the persuasive mechanism for most of the improvements in toughness. On the one hand, the incorporated rigid or flexible particles can act as the bridging particles to guarantee the compressive grip in the crack path. On the other hand, the ductile particles deform plastically in the material surrounding the crack tip providing additional crack shielding. A crack-pinning mechanism (Francis et al. 2006) supposes that the incorporated second phases restrict the propagation of the crack through the resin and thus improve the toughness of the thermosets. The microcracking mechanism (Gilbert and Bucknall 1991; Iijima et al. 1991) proposes that incorporating the second phases into polymers creates stress concentration effects, resulting in the formation of microcracks in the thermosets. Such microcracks provide tensile yielding, and the following generate a large tensile deformation. When the microcracks propagate, voids and large strains produce. The modulus in the frontal zone around the crack tip is significantly reduced, and therefore, the stress intensity is also reduced. It is notable that all the toughening mechanisms have their unique features but they are complementary in the wide applications.

In the past few years, considerable work has been done to study the fundamentals of structure–property relationships between the epoxy matrix and the modifiers for toughening the epoxy thermosets. Block copolymers, a new type of toughening agent, have been revealed to improve the toughness of the thermosets without sacrificing other mechanical properties. For example, the addition of relatively small amount (~5 wt%) of block copolymers has been shown to give remarkable improvement in fracture toughness (Dean et al. 2001). Compared to the traditional modification by the use of liquid rubber, the toughness improvement of epoxy/block copolymer thermosets via the formation of the nanostructures could mainly display the following features: (i) the elastomeric component (epoxy-phobic block) is homogeneously dispersed in the thermosetting matrix at the nanometer scale and thus greatly optimizes the interactions between the thermosetting matrix and the modifiers; ii) the interface interactions between thermosetting matrix and the modifiers are significantly increased due to the presence of epoxy-miscible blocks. Depending on various aspects, such as the type of the block copolymers and the formation mechanism of nanostructure, toughening by nanostructure in the epoxy/block copolymer thermosets displayed different toughening mechanisms.

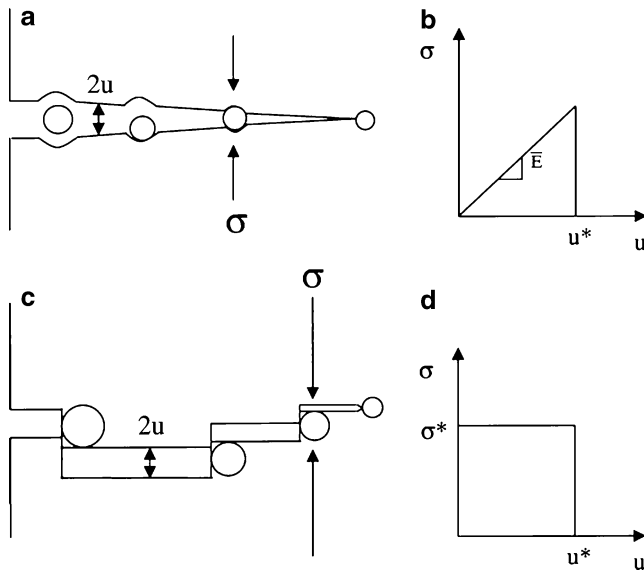


Fig. 8 Schematics of vesicle bridging as a toughening mechanism (a), the stress-displacement response of an elastic vesicle bridge (b), frictional-interlock crack wake vesicle bridges separating terraces on a fracture surface (c), and the stress-displacement response of a frictional-interlock bridge (d). 2μ is the crack-opening displacement, $\sigma(\mu)$ is the stress-displacement response, and E is the effective modulus of the bridging particle (Reprinted with permission from Dean et al. (2001). Copyright 2001 John Wiley & Sons)

Bates and coworkers (Dean et al. 2001, 2003a; Wu et al. 2012) have systemically investigated the formation of various nanostructures in the epoxy/block copolymer thermosets and found that the toughening of nanostructured epoxy thermosets was quite dependent on the type and shape of dispersed nanophases and the interactions between the nanophases and the thermosetting matrix, in which the following affected the debonding of the microdomains (i.e., micelle or vesicles) in the thermosetting matrix and crack deflection for the thermosets with gradient morphologies. For example, they (Dean et al. 2001) investigated toughening mechanism of the nanostructured epoxy/block copolymer (PEO-PEP) thermosets. The vesicle morphology displayed more significant impact on G_{IC} than spherical morphology. In the vesicle-modified epoxies, the energy-dissipation mechanism was identified as debonding followed by localized matrix deformation, crack deflection resulting in the terraced fracture surface, and possibly crack bridging by the larger vesicles (see Fig. 8). It was demonstrated the debonding followed by localized matrix deformation was likely the dominant mode of energy dissipation. In the spherical micelle-modified epoxies, the lower improvement in fracture resistance is attributed to the smaller size of the micelles in the matrix. The energy-dissipation mechanism is also likely to be debonding (or cavitation) of the micelles followed by limited matrix deformation, which is similar to that in the vesicle-modified epoxies. However, the

size of the micelles in the thermosets is very small, which precludes crack bridging as a toughening mechanism (Grubbs et al. 2000, 2001).

Liu et al. (2008) investigated toughening mechanism by the direct experimental evidence of nanocavitation of the nanosized spherical micelles in the epoxy thermosets. Poly(ethylene oxide)-*b*-poly(ethylene-*alt*-propylene) (PEO-PEP) diblock copolymer which self-assembles as nanoscale spherical micelles with a size of about 15 nm in diameter was chosen as a toughening agent for a commercially available epoxy resin, and 1,1,1-tris(4-hydroxyphenyl)ethane (THPE) was used as the curing agent. It was found that incorporation of 5 wt% block copolymer in the epoxy resins led to a significant improvement in K_{IC} (by 180%) over neat epoxy. Toughening mechanisms were investigated by the double-notch four-point bending (DN-4 PB) test and TEM observation. It was suggested that the micelles with the size of 15 nm in the epoxy/block copolymer thermosets could cavitate to induce matrix shear banding, which mainly accounted for the significant toughening effect. Other mechanisms, such as crack tip blunting, may also play a role in the toughening. Apart from the toughening of spherical micelles in the epoxy/block copolymer thermosets, Liu et al. (2010) also reported toughening mechanisms from the wormlike micelle-modified epoxy thermosets. Poly(ethylene oxide)-*b*-poly(ethylene-*alt*-propylene) (PEO-PEP) diblock copolymer was still used in this research work. By tuning the molecular weight of the block copolymer, the fraction of PEO block in the PEP-PEO diblock copolymer, and the cross-link density of the epoxy matrix, wormlike micelles were obtained in the epoxy/block copolymer thermosets. An improvement in K_{IC} by 106% over the neat epoxy was found for the wormlike micelles-modified thermosets. In contrast, the same epoxy thermoset formulation containing PEO-PEP diblock copolymer that self-assembled into spherical micelles displayed relatively less effective in toughness. It was proposed that wormlike micelles in the epoxy thermosets produced enhanced toughness, which is attributed to a combination of mechanisms including crack tip blunting, cavitation, particle debonding, limited shear yielding, and crack bridging.

Declet-Perez and coworker (Declet-Perez et al. 2012, 2013, 2015) investigated the toughening mechanism by means of in situ SAXS. In contrast to the common techniques such as TEM and SEM, in situ SAXS technique provides two advantages. First, morphological changes, which provide real-time information about deformation events in the epoxy systems, can be trace. Second, the macroscopic volumes of the material can be probed. Polystyrene-*block*-poly(ethylene oxide) (PS-*b*-PEO) and poly(ethylene-*alt*-propylene)-*b*-poly(ethylene oxide) (PEP-PEO) block copolymers have been used as the modifiers in the epoxy resins to detect the real-time deformation processes of epoxy/block copolymer blends. It was found that before the yield point, both systems displayed similar deformation behaviors, whereas after the yield point, significant differences in deformation were detected. The cavitation in 30 nm rubber particles (viz., PEP nanodomains) was displayed. The extent of void growth after cavitation is significantly dependent on the cross-link density of the epoxy matrix. These differences in the mode of deformation between the rubbery (viz., PEP) and the glassy (viz., PS) micelles were related to the different constraint relief provided by the toughening mechanisms that promote shear yielding: cavitation in rubbery micelles and network disruption in glassy micelles.

Conclusions

The control over morphology of multicomponent epoxy thermosets is crucial for the improvement of mechanical properties of the materials. Incorporation of block copolymers in the epoxy resins can achieve ordered or disordered nanostructures via either self-assembly or reaction-induced microphase separation (RIMPS) approaches. It is recognized that the formation of nanostructures in thermosets can further optimize the inter-component interactions and thus significantly enhance the toughness of the epoxy thermosets. The factors to influence toughness of nanostructured thermosets involve the reactivity and architecture of the block copolymer, the morphology of the nanophases, curing agents, cross-link density, strain state, etc. There is a general agreement that the toughness mechanism for the epoxy/block copolymer blends can illustrate either the debonding of the nanodomains from thermosetting matrix or crack deflection and frictional interlocking for the thermosets possessing the terraced morphology. Despite many successful examples of using block copolymers to toughen epoxy thermosets, there are still some issues to be explored. It is expected that the studies in the future would be directed to (i) the better understanding of the correlation of nanostructures with the mechanical properties of the epoxy thermosets, (ii) the thorough description of the toughening mechanisms of epoxy/block copolymer blends, and (iii) the exploration of the utilization of toughening epoxy thermosets in other materials.

References

- Barclay G, Ober C, Papathomas K, Wang D (1992) Rigid-rod thermosets based on 1, 3, 5-triazine-linked aromatic ester segments. *Macromolecules* 25:2947–2954
- Barry DB, Delatycki O (1989) The strain rate dependency of fracture in polyethylene: fracture initiation. *J Appl Polym Sci* 38:339–350
- Broer D, Lub J, Mol G (1993) Synthesis and photopolymerization of a liquid-crystalline diepoxide. *Macromolecules* 26:1244–1247
- Bucknall CB, Gilbert AH (1989) Toughening tetrafunctional epoxy resins using polyetherimide. *Polymer* 30:213–217
- Bucknall CB, Partridge IK (1983) Phase separation in epoxy resins containing polyethersulphone. *Polymer* 24:639–644
- Chen J, Chang F (1999) Phase separation process in poly (ϵ -caprolactone)-epoxy blends. *Macromolecules* 32:5348–5356
- Cho J, Hwang J, Cho K, An J, Park C (1993) Effects of morphology on toughening of tetrafunctional epoxy resins with poly (ether imide). *Polymer* 34:4832–4836
- Cong H, Li L, Zheng S (2014) Formation of nanostructures in thermosets containing block copolymers: from self-assembly to reaction-induced microphase separation mechanism. *Polymer* 55:1190–1201
- Cooper SL, Estes GM (1979) *Advances in chemistry series*. American Chemical Society, New York
- de Gennes PG (1969) Scaling concepts in polymer physics. *Phys Lett* 28A:725–726
- de Gennes PG (1979) *Scaling concepts in polymer physics*. Cornell University Press, New York
- Dean JM, Lipic PM, Grubbs RB, Cook RF, Bates FS (2001) Micellar structure and mechanical properties of block copolymer-modified epoxies. *J Polym Sci Part B: Polym Phys* 39:2996–3010

- Dean JM, Grubbs RB, Saad W, Cook RF, Bates FS (2003a) Mechanical properties of block copolymer vesicle and micelle modified epoxies. *J Polym Sci Part B: Polym Phys* 41:2444–2456
- Dean JM, Verghese NE, Pham HQ, Bates FS (2003b) Nanostructure toughened epoxy resins. *Macromolecules* 36:9267–9270
- Declet-Perez C, Redline EM, Francis LF, Bates FS (2012) Role of localized network damage in block copolymer toughened epoxies. *ACS Macro Lett* 1:338–342
- Declet-Perez C, Francis LF, Bates FS (2013) Cavitation in block copolymer modified epoxy revealed by in situ small-angle X-ray scattering. *ACS Macro Lett* 2:939–943
- Declet-Perez C, Francis LF, Bates FS (2015) Deformation processes in block copolymer toughened epoxies. *Macromolecules* 48:3672–3684
- Evans A, Williams S, Beaumont P (1985) On the toughness of particulate filled polymers. *J Mater Sci* 20:3668–3674
- Francis R, Baby DK (2014) Toughening of epoxy thermoset with polystyrene-block-polyglycolic acid star copolymer: nanostructure-mechanical property correlation. *Ind Eng Chem Res* 53:17945–17951
- Francis B, Rao VL, Poel GV, Posada F, Groeninckx G, Ramaswamy R, Thomas S (2006) Cure kinetics, morphological and dynamic mechanical analysis of diglycidyl ether of bisphenol-A epoxy resin modified with hydroxyl terminated poly (ether ether ketone) containing pendent tertiary butyl groups. *Polymer* 47:5411–5419
- Gilbert A, Bucknall C (1991) Epoxy resin toughened with thermoplastic, vol 45. Wiley Online Library, Amsterdam, pp 289–298
- Gong W, Zeng K, Wang L, Zheng S (2008) Poly(hydroxyether of bisphenol A)-block-polydimethylsiloxane alternating block copolymer and its nanostructured blends with epoxy resin. *Polymer* 49:3318–3326
- Grubbs RB, Dean JM, Broz ME, Bates FS (2000) Reactive block copolymers for modification of thermosetting epoxy. *Macromolecules* 33:9522–9534
- Grubbs RB, Dean JM, Bates FS (2001) Methacrylic block copolymers through metal-mediated living free radical polymerization for modification of thermosetting epoxy. *Macromolecules* 34:8593–8595
- Hikmet R (1992) Piezoelectric networks obtained by photopolymerization of liquid crystal molecules. *Macromolecules* 25:5759–5764
- Hikmet R, Lub J, Higgins J (1993) Anisotropic networks obtained by in situ cationic polymerization of liquid-crystalline divinyl ethers. *Polymer* 34:1736–1740
- Hillmyer MA, Lipic PM, Hajduk DA, Almdal K, Bates FS (1997) Self-assembly and polymerization of epoxy resin-amphiphilic block copolymer nanocomposites. *J Am Chem Soc* 119:2749–2750
- Hsich HS (1990) Morphology and properties control on rubber-epoxy alloy systems. *Polym Eng Sci* 30:493–510
- Hu D, Zheng S (2011) Morphology and thermomechanical properties of epoxy thermosets modified with polysulfone-block-polydimethylsiloxane multiblock copolymer. *J Appl Polym Sci* 119:2933–2944
- Hwang J, Park S, Cho K, Kim J, Park C, Oh T (1997) Toughening of cyanate ester resins with cyanated polysulfones. *Polymer* 38:1835–1843
- Iijima T, Tomoi M, Tochimoto T, Kakiuchi H (1991) Toughening of epoxy resins by modification with aromatic polyesters. *J Appl Polym Sci* 43:463–474
- Iijima T, Yoshioka N, Tomoi M (1992) Effect of cross-link density on modification of epoxy resins with reactive acrylic elastomers. *Euro Polym J* 28:573–581
- Kinloch A, Shaw S, Hunston D (1983a) Deformation and fracture behaviour of a rubber-toughened epoxy: 2. Failure criteria. *Polymer* 24:1355–1363
- Kinloch A, Shaw S, Tod D, Hunston D (1983b) Deformation and fracture behaviour of a rubber-toughened epoxy: 1. Microstructure and fracture studies. *Polymer* 24:1341–1354

- Kishore K (1993) Novel photocrosslinkable liquid-crystalline polymers: poly [bis (benzylidene)] esters. *Macromolecules* 26:2995–3003
- Könczöl L, Döll W, Buchholz U, Mühlaupt R (1994) Ultimate properties of epoxy resins modified with a polysiloxane-polycaprolactone block copolymer. *J Appl Polym Sci* 54:815–826
- Kong J, Tang Y, Zhang X, Gu J (2008) Synergic effect of acrylate liquid rubber and bisphenol A on toughness of epoxy resins. *Polym Bull* 60:229–236
- Lange F, Radford K (1971) Fracture energy of an epoxy composite system. *J Mater Sci* 6:1197–1203
- Li J, Xiang Y, Zheng S (2015) Hyperbranched block copolymer from AB₂ macromonomer: synthesis and its reaction-induced microphase separation in epoxy thermosets. *J Polym Sci Part A: Polym Chem*. doi:10.1002/pola.27784
- Lin Q, Yee AF, Earls JD, Hefner RE Jr, Sue HJ (1994) Phase transformations of a liquid crystalline epoxy during curing. *Polymer* 35:2679–2682
- Lipic PM, Bates FS, Hillmyer MA (1998) Nanostructured thermosets from self-assembled amphiphilic block copolymer/epoxy resin mixtures. *J Am Chem Soc* 120:8963–8970
- Litt M, Whang W, Yen K, Qian X (1993) Crosslinked liquid crystal polymers from liquid crystal monomers: synthesis and mechanical properties. *J Polym Sci Part A: Polym Chem* 31:183–191
- Liu JD, Sue HJ, Thompson ZJ, Bates FS, Dettloff M, Jacob G, Verghese N, Pham H (2008) Nanocavitation in self-assembled amphiphilic block copolymer-modified epoxy. *Macromolecules* 41:7616–7624
- Liu JD, Sue HJ, Thompson ZJ, Bates FS, Dettloff M, Jacob G, Verghese N, Pham H (2009a) Effect of crosslink density on fracture behavior of model epoxies containing block copolymer nanoparticles. *Polymer* 50:4683–4689
- Liu JD, Sue HJ, Thompson ZJ, Bates FS, Dettloff M, Jacob G, Verghese N, Pham H (2009b) Strain rate effect on toughening of nano-sized PEP-PEO block copolymer modified epoxy. *Acta Mater* 57:2691–2701
- Liu JD, Thompson ZJ, Sue HJ, Bates FS, Hillmyer MA, Dettloff M, Jacob G, Verghese N, Pham H (2010) Toughening of epoxies with block copolymer micelles of wormlike morphology. *Macromolecules* 43:7238–7243
- Meeks AC (1974) Fracture and mechanical properties of epoxy resins and rubber-modified epoxy resins. *Polymer* 15:675–681
- Meijerink J, Eguchi S, Ogata M, Ishii T, Amagi S, Numata S, Sashima H (1994) The influence of siloxane modifiers on the thermal expansion coefficient of epoxy resins. *Polymer* 35:179–186
- Meng F, Zheng S, Li H, Liang Q, Liu T (2006) Formation of ordered nanostructures in epoxy thermosets: a mechanism of reaction-induced microphase separation. *Macromolecules* 39:5072–5080
- Morgan RJ, Kong FM, Walkup CM (1984) Structure–property relations of polyethertriamine-cured bisphenol-A-diglycidyl ether epoxies. *Polymer* 25:375–386
- Ni Y, Zheng S (2005) Influence of intramolecular specific interactions on phase behavior of epoxy resin and poly (ϵ -caprolactone) blends cured with aromatic amines. *Polymer* 46:5828–5839
- Ocando C, Tercjak A, Serrano E, Ramos JA, Corona-Galván S, Parellada MD, Fernández-Berridi MJ, Mondragon I (2008) Micro- and macrophase separation of thermosetting systems modified with epoxidized styrene-block-butadiene-block-styrene linear triblock copolymers and their influence on final mechanical properties. *Polym Int* 57:1333–1342
- Ocando C, Fernández R, Tercjak A, Mondragon I, Eceiza A (2013) Nanostructured thermoplastic elastomers based on SBS triblock copolymer stiffening with low contents of epoxy system. Morphological behavior and mechanical properties. *Macromolecules* 46:3444–3451
- Ortiz MJ (1987) A continuum theory of crack shielding in ceramics. *J Appl Mech* 54:54–58
- Pearson RA, Yee AF (1986) Toughening mechanisms in elastomer-modified epoxies. *J Mater Sci* 21:2475–2488

- Pearson RA, Yee AF (1989) Toughening mechanisms in elastomer-modified epoxies: part 3. The effect of cross-link density. *J Mater Sci* 24:2571–2580
- Pearson RA, Yee AF (1991) Influence of particle size and particle size distribution on toughening mechanisms in rubber-modified epoxies. *J Mater Sci* 26:3828–3844
- Raghava R (1988) Development and characterization of thermosetting-thermoplastic polymer blends for applications in damage-tolerant composites. *J Polym Sci Part A: Polym Chem* 26:65–81
- Raghavan D, He J, Hunston D, Hoffman D (2002) Strain rate dependence of fracture in a rubber-toughened epoxy system. *J Adhes* 78:723–739
- Ratna D, Simon G (2001) Mechanical characterization and morphology of carboxyl randomized poly (2-ethyl hexyl acrylate) liquid rubber toughened epoxy resins. *Polymer* 42:7739–7747
- Rebizant V, Venet AS, Tournilhac F, Girard-Reydet E, Navarro C, Pascault JP, Leibler L (2004) Chemistry and mechanical properties of epoxy-based thermosets reinforced by reactive and nonreactive SBMX block copolymers. *Macromolecules* 37:8017–8027
- Riew CK, Kinloch AJ (1993) Toughened plastics I: science and engineering. American Chemical Society, Washington, DC
- Riew CK, Rowe E, Siebert A (1976) Rubber toughened thermosets. *Adv Chem Ser* 154:326
- Ritzenthaler S, Court F, Girard-Reydet E, Leibler L, Pascault J (2003) ABC triblock copolymers/epoxy-diamine blends. 2. Parameters controlling the morphologies and properties. *Macromolecules* 36:118–126
- Ruiz-Pérez L, Royston GJ, Fairclough JPA, Ryan AJ (2008) Toughening by nanostructure. *Polymer* 49:4475–4488
- Sigl LS, Mataga P, Dalgleish B, McMeeking R, Evans A (1988) On the toughness of brittle materials reinforced with a ductile phase. *Acta Metall* 36:945–953
- Sultan JN, McGarry FJ (1973) Effect of rubber particle size on deformation mechanisms in glassy epoxy. *Polym Eng Sci* 13:29–35
- Thio YS, Wu J, Bates FS (2006) Epoxy toughening using low molecular weight poly (hexylene oxide)-poly (ethylene oxide) diblock copolymers. *Macromolecules* 39:7187–7189
- Thomas R, Yumei D, Yuelong H, Le Y, Moldenaers P, Weimin Y, Czigany T, Thomas S (2008) Miscibility, morphology, thermal, and mechanical properties of a DGEBA based epoxy resin toughened with a liquid rubber. *Polymer* 49:278–294
- Thompson ZJ, Hillmyer MA, Liu J, Sue HJ, Dettloff M, Bates FS (2009) Block copolymer toughened epoxy: role of cross-link density. *Macromolecules* 42:2333–2335
- Utracki L, Favis B (1989) Polymer alloys and blends. Marcel Dekker, New York
- Webb TW, Aifantis EC (1997) Loading rate dependence of stick-slip fracture in polymers. *Mech Res Commun* 24:115–121
- Wu S, Guo Q, Peng S, Hameed N, Kraska M, Stühn B, Mai YW (2012) Toughening epoxy thermosets with block ionomer complexes: a nanostructure-mechanical property correlation. *Macromolecules* 45:3829–3840
- Yang X, Yi F, Xin Z, Zheng S (2009) Morphology and mechanical properties of nanostructured blends of epoxy resin with poly (ϵ -caprolactone)-block-poly (butadiene-co-acrylonitrile)-block-poly (ϵ -caprolactone) triblock copolymer. *Polymer* 50:4089–4100
- Yee AF, Pearson RA (1986) Toughening mechanisms in elastomer-modified epoxies. *J Mater Sci* 21:2462–2474
- Yi F, Yu R, Zheng S, Li X (2011) Nanostructured thermosets from epoxy and poly (2, 2, 2-trifluoroethyl acrylate)-block-poly (glycidyl methacrylate) diblock copolymer: demixing of reactive blocks and thermomechanical properties. *Polymer* 52:5669–5680
- Yin M, Zheng S (2005) Ternary thermosetting blends of epoxy resin, poly (ethylene oxide) and poly (ϵ -caprolactone). *Macromol Chem Phys* 206:929–937
- Yorkgitis E, Eiss N Jr, Tran C, Wilkes G, McGrath J (1985) In: Dušek K (eds) Epoxy resins and composites. Springer-Verlag Berlin, pp 79–109

- Yu R, Zheng S (2011) Morphological transition from spherical to lamellar nanophases in epoxy thermosets containing poly (ethylene oxide)-block-poly (ϵ -caprolactone)-block-polystyrene triblock copolymer by hardeners. *Macromolecules* 44:8546–8557
- Zhang C, Yi Y, Li L, Zheng S (2014) Morphology and fracture toughness of nanostructured epoxy thermosets containing macromolecular miktobrushes composed of poly(ϵ -caprolactone) and polydimethylsiloxane side chains. *J Mater Sci* 49:1256–1266
- Zheng S (2010) In: Pascault J, Williams R (eds) *Epoxy polymers: new materials and innovations*. Wiley-VCH, Weinheim, pp 79–108

Water Sorption and Solvent Sorption of Epoxy/Block-Copolymer and Epoxy/Thermoplastic Blends

37

Anbazhagan Palanisamy, Nisa V. Salim, Jyotishkumar Parameswaranpillai, and Nishar Hameed

Abstract

Epoxy polymers are well known for their superior barrier properties in various environmental conditions. Block copolymers and thermoplastics were added to these epoxy polymers to modify their hydrophilic/hydrophobic balance and control various macroscopic physical properties such as moisture absorption, cross-linking, and degradation. The hydrophilic/hydrophobic balance is an important property of any material that determines their fate in the real-world application. Here, in this chapter, water and solvent sorption in various epoxy blends were discussed. Specifically, the change in hydrophilic/hydrophobic balance in the presence of various amounts of block copolymers and thermoplastics were discussed. Contact angle and surface free energy measurements in these blends gave an indication of change in surface properties with respect to blend compositions. Additionally, the nano/micro channels produced by microphase separation of block copolymers and their bulk phase separated morphologies had a greater influence on the sorption behavior of the epoxy blends. This chapter would give an overview of water and solvent sorption behavior of various epoxy/block copolymer and epoxy/thermoplastic blends studied in recent years.

A. Palanisamy (✉)

Institute for Frontier Materials, Deakin University, Geelong, Australia

e-mail: psabchem@gmail.com

N.V. Salim

Carbon Nexus, Institute for Frontier Materials, Deakin University, Geelong, VIC, Australia

J. Parameswaranpillai

Department of Polymer Science and Rubber Technology, Cochin University of Science and Technology, Cochin, Kerala, India

N. Hameed (✉)

Carbon Nexus, Institute for Frontier Materials, Deakin University, Geelong, VIC, Australia

Factory of the Future, Swinburne University of Technology, Melbourne, VIC, Australia

e-mail: nishar.hameed@deakin.edu.au

Keywords

Epoxy • Epoxy blends • Water absorption • Solvent absorption • Permeability • Microphase separation • Block copolymer • Homopolymer • Thermoplastic • Surface free energy • Contact angle • Morphology • Hydrophilic • Hydrophobic • Cross-linking • Degradation • Adhesive • Hydrogen bonding • Nanostructure

Contents

Introduction	1098
Epoxy/PCL-PDMS-PCL Blend	1099
Epoxy/PS- <i>b</i> -PEO/TiO ₂ Blend	1102
Epoxy/PTFEA- <i>b</i> -PGMA Blend	1102
Epoxy/PEO- <i>b</i> -PPO- <i>b</i> -PEO Blend	1104
Epoxidized PS-PI-PS Blend	1105
Epoxy/PEI Blend	1106
Epoxy/PES Blend	1106
Epoxy/Polycarbonate (PC) Blend	1108
Epoxy/Polysulfone Blend	1109
Conclusions	1109
References	1110

Introduction

Epoxy polymers are well known for their excellent engineering properties such as high strength, high thermal, electrical and chemical resistance, and good adhesiveness to many surfaces. Hence epoxy resins are widely used in composite, electronic, adhesives, and coating applications. Improving various properties of epoxy resins by synthesis of new epoxy polymers, incorporating additives, and introducing new curing agents and processes is one of the important areas of research in recent years (Jin et al. 2015). Especially, the brittleness in cross-linked epoxy resin was improved by adding block copolymer additives of various architectures and engineering thermoplastics with high modulus and high T_g (glass transition temperature). Since Hillmyer et al. first reported toughening of epoxy polymers via block copolymer (BCP) blending (Hillmyer et al. 1997), considerable attention has been given towards nanostructuring of epoxies. Depending on the type of block copolymer and epoxy components used, self-assembled morphology of block copolymers within epoxy resin can be tuned by adjusting a number of parameters (Pandit et al. 2014). Due to this flexibility, materials with novel properties were developed from epoxy/block copolymer blends (Dean et al. 2003).

In addition to nanostructuring of epoxies, surface properties such as water and solvent repellency, absorption, and surface tension can also be improved remarkably by introducing block copolymers. Due to relatively high surface free energy of epoxies, the coatings made of epoxy resins are more prone to contamination. Furthermore, epoxy coatings are affected by water due to presence of hydroxyl and amine groups in their molecular structure that can form hydrogen bonding with water molecules (Sharpe 1996). These limitations can be circumvented by introducing

block copolymers and thermoplastics via appropriate blending technique. The added block copolymer or homopolymer, the second component in epoxy, generates microphase separation of chemically dissimilar polymer domains into various morphologies within epoxy-rich phase. The phase-separated morphology can be controlled via varying the composition (Hameed et al. 2010b; Liu et al. 2010). Hence, in epoxy blends, water or solvent absorption primarily depends on phase-separated morphology and chemical structure of the blend components (Nam et al. 2014).

Epoxy polymers are generally hydrophilic due to the presence of polar epoxy groups. Hydrophilic or hydrophobic polymers are either copolymerized or blended with epoxy polymers to change the hydrophobic/hydrophilic balance (Liu et al. 2013; Wu et al. 2014). The epoxy polymers blended with various homopolymers and fillers exhibit varying adhesion strength depending on the substrate polarity and glass transition temperature (Mansourian-Tabaei et al. 2014; Wang et al. 2014; Kishi et al. 2016). In addition to polarity-dependent adhesion, polarity plays important role in overall performance of the epoxy blends. Particularly, water or solvent absorption properties greatly depend on the blend composition and polar functional group density (Bouvet et al. 2016; Zhang et al. 2014). Furthermore, introduction of block copolymers into epoxy may further help in regulating liquid permeation or sorption via phase-separated nano/micro channels (Lekatou et al. 1997). In this chapter, the surface properties, polarity, and sorption properties of epoxy/block copolymer and epoxy/thermoplastic blends are discussed.

Epoxy/PCL-PDMS-PCL Blend

PDMS-based block copolymers were primarily investigated for phase separation and toughening of epoxy resins at various compositions (Xu and Zheng 2007; Könczöl et al. 1994). In addition to microphase separation, the hydrophobic PDMS blocks were also found to change the surface properties such as wettability and surface energy. Hameed et al. studied hydrogen bonding interactions, crystallization, and surface hydrophobicity in diglycidyl ether of bisphenol A (DGEBA)/poly(ϵ -caprolactone)-*block*-poly(dimethyl siloxane)-*block*-poly(ϵ -caprolactone) (PCL-PDMS-PCL) triblock copolymer blends cured with 4,4'-methylenedianiline (MDA) (Hameed et al. 2010a). The miscibility between epoxy and block copolymer was due to hydrogen bonding interaction between cured epoxy and PCL blocks (Fig. 1). In this system, the surface hydrophobicity was found to increase with increasing block copolymer content. It can be evidenced from contact angle measurements showing an increase in contact angle (θ) values upon addition of PCL-PDMS-PCL block copolymer containing hydrophobic PDMS blocks (Fig. 2). Here, the surface free energies of the blends were lower than pure epoxy irrespective of their composition. Upon increasing PDMS concentration in blends, the contact angle increased with a gradual decrease in surface free energy. This straightforward method of tuning surface hydrophobicity can be used in the development of water-repellent coatings, adhesives, and corrosion-resistant surfaces.

Fig. 1 Schematic representation of the hydrogen bonding interaction between cured epoxy resin and PCL blocks of the triblock copolymer (Hameed et al. 2010a) (Reproduced with permission of John Wiley and sons)

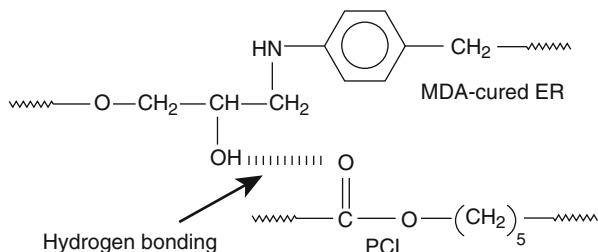
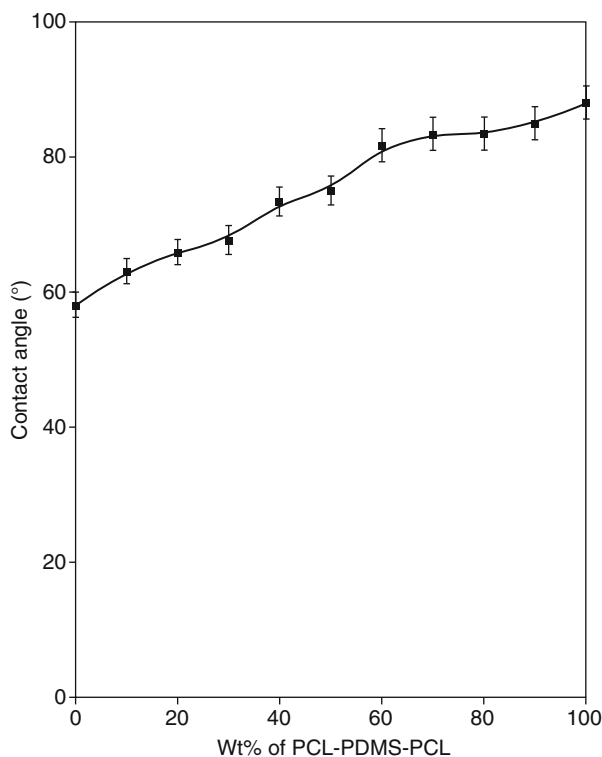


Fig. 2 The change in contact angle (θ) values with respect to block copolymer concentration in epoxy/PCL-PDMS-PCL blends (Hameed et al. 2010a) (Reproduced with permission of John Wiley and sons)



The same authors have studied surface properties of DGEBA/poly(dimethyl siloxane)-poly(glycidyl methacrylate) (PDMS-PGMA) blends at various block copolymer compositions (Hameed et al. 2010b). The PGMA is the reactive block that can form covalent bond with epoxy, while PDMS (epoxy-immiscible) block phase separated into various morphologies upon curing. This system followed the same trend of increase in hydrophobicity with decrease in surface free energy upon increasing PDMS content. The increase in hydrophobicity can be evidenced from the contact angle measurements (Fig. 3) and photographs of water droplets on the surfaces of the blends (Fig. 4).

Fig. 3 The change in contact angle (θ) values with respect to block copolymer concentration in epoxy/PDMS-PGMA blends (Hameed et al. 2010b) (Reproduced with permission of The Royal Society of Chemistry)

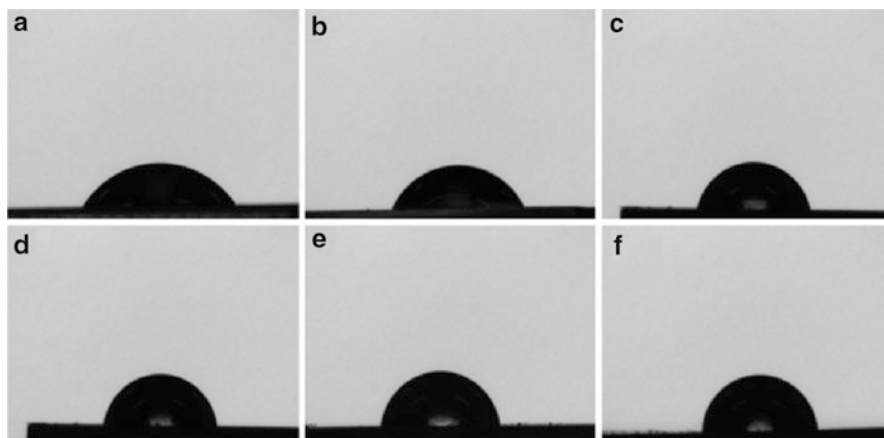
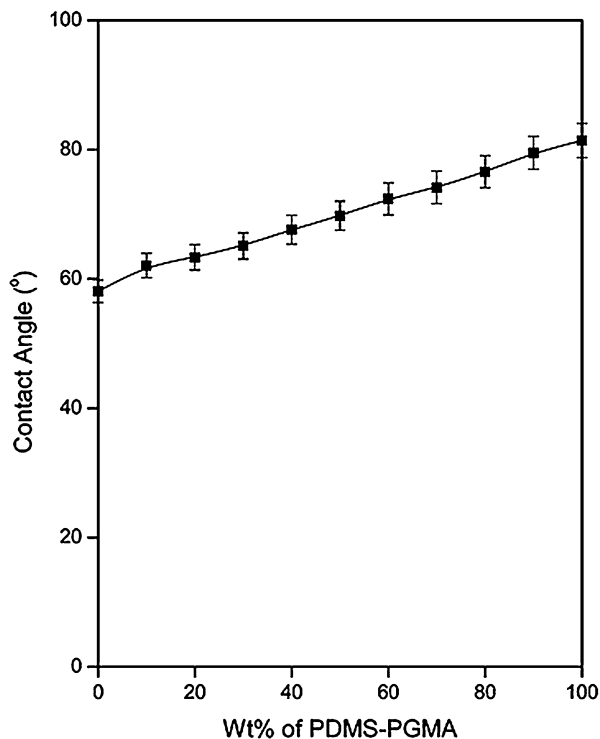


Fig. 4 The images of water droplet on surfaces of epoxy/PDMS-PGMA blends at (a) 0, (b) 20, (c) 40, (d) 60, (e) 80, and (f) 100 wt% PDMS-PGMA diblock copolymer (Hameed et al. 2010b) (Reproduced with permission of The Royal Society of Chemistry)

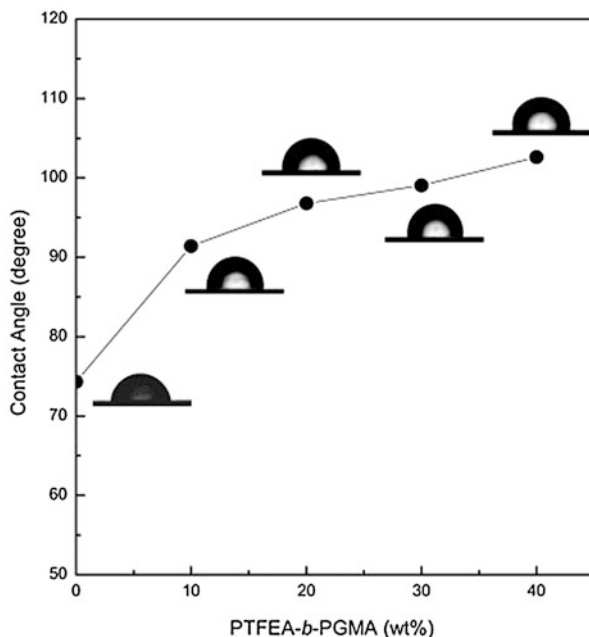
Epoxy/PS-*b*-PEO/TiO₂ Blend

The amphiphilic diblock copolymer poly(styrene-*b*-ethylene oxide) (PS-*b*-PEO) was blended with diglycidyl ether of bisphenol A (DGEBA) epoxy resin and cured with aromatic amine hardener 4,4'-methylene bis(3-chloro-2,6-diethylaniline) (MCDEA). The hydrophilic PEO block is miscible in the epoxy component, and phase separation of PS blocks into various morphologies at different block copolymer concentration was studied (Tercjak et al. 2012). Additionally, the TiO₂ nanoparticles synthesized via sol-gel method were added to the pure epoxy system DGEBA/MCDEA and epoxy block copolymer blends DGEBA/MCDEA/PS-*b*-PEO. Both the block copolymer and TiO₂ nanoparticles of predetermined quantity were added to epoxy before curing. Here, the highly transparent multiphase inorganic/organic epoxy-based material was envisaged with high UV shielding efficiency and water repellence character. The hydrophobic PS block was found to phase separate into various morphologies from spherical micelles to long wormlike structures. As it is well known that epoxy polymers are hydrophilic, in this system, the content of hydrophobic PS blocks dictates the water sorption behavior. Static contact angle technique was used to study the surface properties of the blends. The hydrophilicity of the surface was found to decrease with increasing PS-*b*-PEO content, and this behavior was further strongly correlated to the phase-separated morphology. Particularly, in DGEBA/MCDEA/PS-*b*-PEO blends with 5 wt% of PS-*b*-PEO block copolymer exhibited comparatively higher water repellence due to the spherical morphology of PS domains in the epoxy matrix. In DGEBA/MCDEA/PS-*b*-PEO/TiO₂ blends, compositions with 10 wt% of PS-*b*-PEO and 10 wt% TiO₂ showed higher water repellence. Generally, the hydrophilic/hydrophobic balance in epoxy was governed by PS-*b*-PEO/TiO₂ content along with the phase-separated morphologies.

Epoxy/PTFEA-*b*-PGMA Blend

Fluorinated polymers with low surface energy are widely used to improve the hydrophobicity of polymers via blending. However, macrophase separation was observed due to their incompatibility with most of other polymers. The macrophase separation of these polymers in epoxy resin was prevented by copolymerizing with epoxy compatible polymers. For instance, an reactive fluorinated amphiphilic block copolymer poly(2,2,2-trifluoroethyl acrylate)-*block*-poly(glycidyl methacrylate) (PTFEA-*b*-PGMA) with epoxy compatible PGMA was mixed with DGEBA-type epoxy resin at various compositions and cured with 4,4'-Methylenebis(2-chloroaniline) (MOCA) (Yi et al. 2011). The surface properties of these blends were studied using contact angle measurement and atomic force microscopy. The water contact angle increased from 74.3° for neat epoxy to 102° for 40 wt% PTFEA-*b*-PGMA block copolymer content in epoxy (Fig. 5). Also, the total surface free

Fig. 5 The change in water contact angles at various PTFEA-*b*-PGMA block copolymer contents (Yi et al. 2011) (Reproduced with permission of Elsevier)



energy of the blends decreased from 29.2 to 16.4 mN/m upon increasing block copolymer concentration. It has been suggested that the PTFEA blocks may have migrated to the surface, thereby screening the polar groups of the epoxy that lead to a dramatic increase in hydrophobicity.

Furthermore, in surface AFM images, PTFEA domains (dark region) were detected on the surface even at 10 wt% of PTFEA-*b*-PGMA block copolymer. The PTFEA domains were highly interconnected on the surface (Fig. 6), which may also be the contributing factor for surface hydrophobicity. A similar phenomenon was reported in another study, where a semifluorinated block copolymer poly(heptadecafluorodecyl acrylate)-*b*-poly(caprolactone) (PaF-*b*-PCL), was blended with DGEBA-type epoxy (Ocando et al. 2007). The contact angle measurements showed higher surface hydrophobicity (109°) and low surface energy (17 mN/m) upon adding PaF-*b*-PCL block copolymer. The hydrophobicity of surface of the blends even at low concentrations of fluorinated polymer was due to migration of fluorinated chains to the uppermost surface. However, in blends containing fluorinated triblock block copolymer with PCL segments, the water diffusion coefficient depends on the PCL block content in spite the presence of fluorinated blocks. As expected, the water diffusion decreased upon increasing fluorinated block copolymer that contains low to moderate PCL content. In case of block copolymer with comparatively higher PCL content, water diffusion coefficient was higher due to PCL phase segregation and surface reorganization of block copolymer chains while in water (Messori et al. 2001).

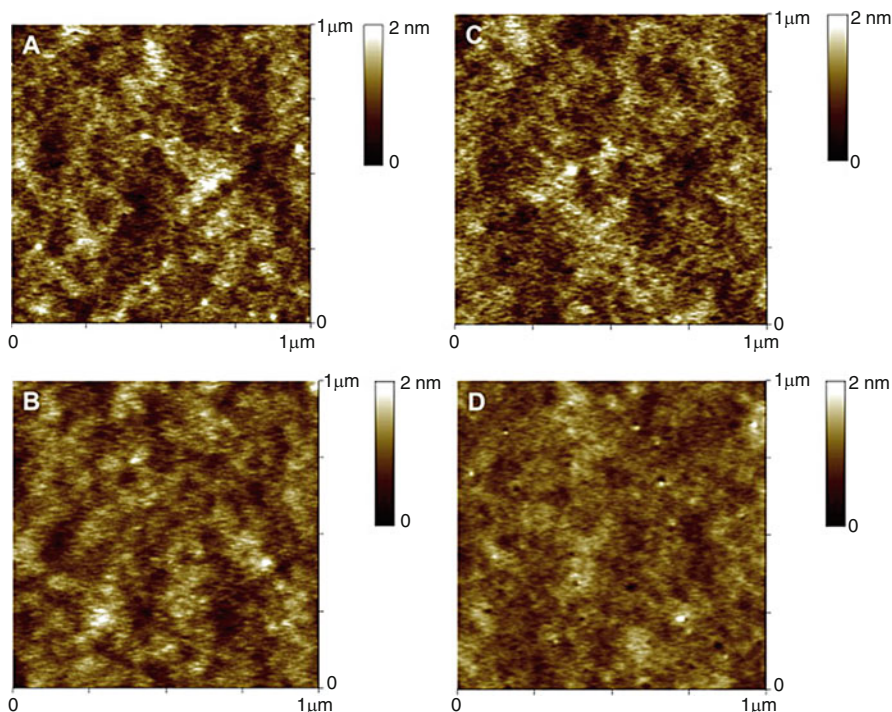


Fig. 6 AFM images of epoxy blends containing (a) 10, (b) 20, (c) 30, and (d) 40 wt% of PTFEA-*b*-PGMA block copolymer. The darker and lighter regions correspond to the PTFEA and epoxy phases, respectively (Yi et al. 2011) (Reproduced with permission of Elsevier)

Epoxy/PEO-*b*-PPO-*b*-PEO Blend

Block copolymers containing epoxy immiscible hydrophobic blocks such as PS, PDMS, and PTFEA were mostly studied for phase separation in epoxy resins. In contrast, Cano et al. studied various properties of epoxy blends containing hydrophilic polyethylene oxide-based block copolymer (Cano et al. 2014). Here, the blends of DGEBA/poly(ethylene oxide-*b*-propylene oxide-*b*-ethylene oxide) (PEO-*b*-PPO-*b*-PEO) were prepared at various compositions and cured with *m*-Xylylenediamine (MXDA). The contact angle measurement was used to study the hydrophilic nature of the blends at different copolymer contents (Fig. 7). Additionally, the surface free energies were also calculated from the contact angle data. As expected, the contact angle of the blends decreased with increase in surface free energy upon addition of block copolymer. The surface becomes hydrophilic due to the hydrophilic nature of the PEO blocks and also due to their existence at the surface of the samples. In this system, the most hydrophobic one was the neat epoxy sample, while the blend containing 50 wt% of PEO-*b*-PPO-*b*-PEO showed comparatively higher hydrophilicity.

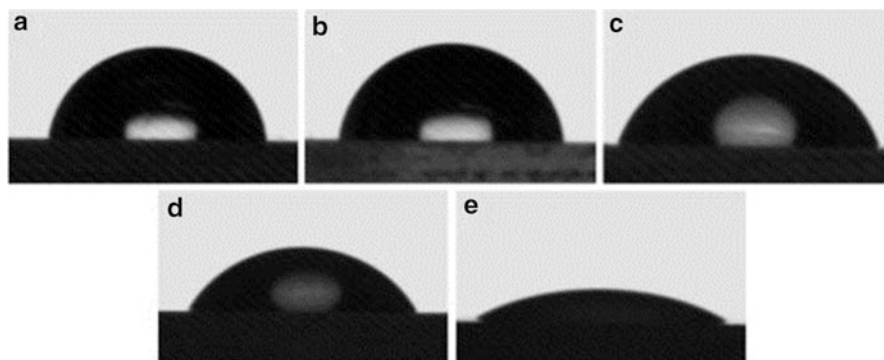


Fig. 7 The images of water droplet on (a) neat epoxy, (b) 5, (c) 15, (d) 25, and (e) 50 wt% PEO-b-PPO-b-PEO/epoxy blends (Cano et al. 2014) (Reproduced with permission of Elsevier)

Epoxidized PS-PI-PS Blend

Thermoplastic block copolymers such as styrene-butadiene-styrene, styrene-isoprene-styrene (PS-PI-PS), and ethylene vinyl acetate copolymer were used as hot-melt-pressed pressure-sensitive adhesives which carry no solvent or water. The adhesion property depends on the polarity of the surfaces. Those abovementioned nonpolar polymers are disadvantaged when polar surfaces come into play. Hence, polar epoxide groups were incorporated via post-polymer modification technique and then blended with either parent polymer or other nonpolar polymers to increase adhesion strength. In one particular study, three different surfaces, polyethylene (PE), polyvinyl chloride (PVC), and steel with different polarity ($PE < PVC < steel$) were coated with blends of epoxidized PS-PI-PS and peel strength studied (Li et al. 2008). For polar materials PVC and steel, the peel strength was higher with epoxidized PS-PI-PS blends depending on the composition and total epoxide content, while PE showed comparatively lower peel strength. This behavior was due to higher wettability of the polar adhesives on the polar surfaces. Furthermore, glass transition temperature (T_g) of the adhesives played important role in determining adhesion while using higher concentrations of epoxidized polymers with lower chain mobility or higher T_g . The same epoxidized PS-PI-PS based polymers were also subjected for drug delivery experiments. The melt pressed hydrophobic PS-PI-PS block copolymer could not be used directly as a carrier for hydrophilic drugs due to its incompatibility. The epoxidized PS-PI-PS was successfully employed as a drug carrier for hydrophilic drugs with good adhesive and drug release performance (Wang et al. 2012). In polyethylene glycol (PEG) containing PS-PI-PS based blends, the water absorption and drug release were based on morphology of phase-separated domains and PEG content. For instance, water absorption was higher when PEG domains form hydrophilic channels during phase separation (Tong et al. 2014). Hence, melt-pressed pressure-sensitive adhesives with different polarity can be used in applications such as drug delivery and preparation of solvent free adhesives.

Epoxy/PEI Blend

Poly (ether imide) (PEI) is an important industrial thermoplastic blended with epoxy resins to improve their toughness (Bucknall and Gilbert 1989). Presence of water in epoxy blends greatly affects their mechanical properties and limits their potential application. The water diffusion in blends depends on the nature of blend components and phase-separated morphologies. Attenuated total reflection Fourier transfer infrared (ATR-FTIR) technique has been developed for in situ measurements of polymer-water interaction. ATR-FTIR coupled with scanning electron microscopy (SEM) was used to monitor the dynamic water sorption in blends of PEI/DGEBA cured with (4,4'-diaminodiphenyl)sulfone (DDS). Based on 2D correlation spectra and SEM data, the process of water diffusion in blends at various PEI concentration was explained. From the asynchronous correlation spectra (Fig. 8), it can be observed that the water vibration bands at 3200–3600 cm^{-1} were separated into two bands which correspond to strong (water mixed with hydrophilic groups of polymer) and less (water in voids) hydrogen bonded water molecules in the system. At lower PEI concentrations (epoxy EP, 10-phr and 15-phr), the water diffuses into free volumes in epoxy before interacting with hydrophilic groups of the polymer. However, at 20-phr, water molecules first diffuse into PEI rich region and then into epoxy domains. Additionally, the co-continuous morphology at 15-phr and 20-phr may be responsible for controlling water diffusion sequence due to formation of long percolation path between the components. Hence, the water diffusion sequence in PEI/DGEBA blends depends on both composition and phase-separated morphologies.

Water absorption behavior was studied again in the same PEI/DGEBA/DDS system, and the equilibrium water uptake by the blends was found to be strong composition dependent rather than the free volume factor (Li et al. 2004). Additionally, the phase-separated morphology due to addition of thermoplastic was also responsible for the anomalous diffusion behavior at the beginning of the co-continuous phase. The fractional free volume was found to decrease with increasing PEI content, also drop of free volume was related to specific morphology and hence the decrease in water uptake (Fig. 9). Hence, the water molecules in the epoxy blends are mainly located within the epoxy phase, and water uptake depends on the total epoxy content and morphology of the blends. Epoxy films prepared via curing epoxy resin with a reactive polyimide showed good solvent resistance even though the polyimide component was soluble in the corresponding solvents such as DMF, NMP, THF, and DCM. The network structure formation between the polyimide and epoxy resin was responsible for providing the cured films with excellent solvent resistance (Agag and Takeichi 1999).

Epoxy/PES Blend

The aging process of epoxy blends when exposed to the environmental agents such as temperature, moisture, and solvents is important from an engineering and application perspective. The moisture absorption in epoxy resins leads to plasticization and molecular changes such as degradation and cross-linking. These changes in the

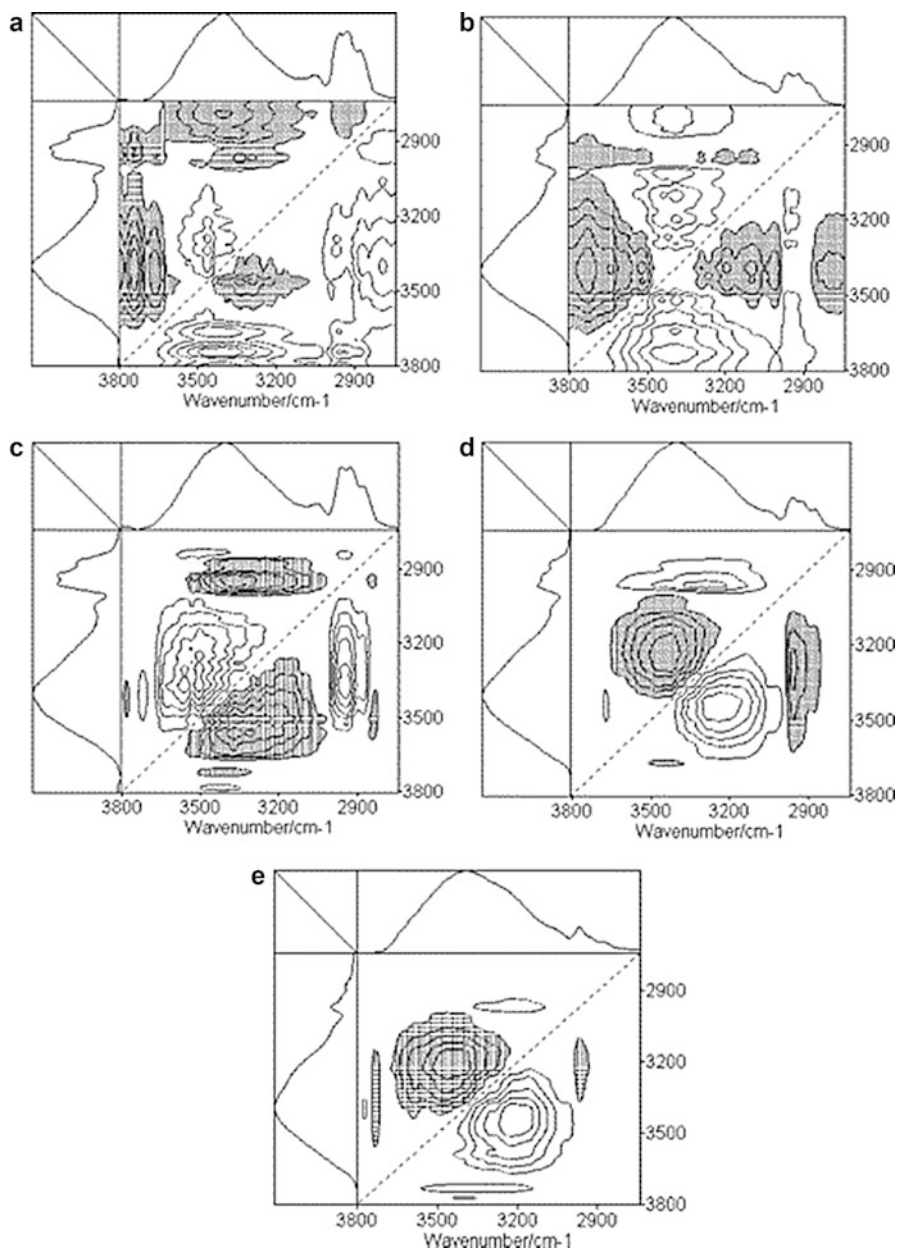


Fig. 8 Asynchronous 2D-correlation spectra showing band splitting due to presence of strong and less hydrogen-bonded hydroxyl groups representing two different states of water in these blends. (a) EP, (b) 10-phr, (c) 15-phr, (d) 20-phr, and (e) PEI (Bucknall and Gilbert 1989) (Reproduced with permission of Elsevier)

Fig. 9 Normalized equilibrium water uptake curve of PEI/DGEBA blends at different PEI and corresponding epoxy contents showing decrease in fractional free volume and water uptake upon increasing PEI content (Li et al. 2004) (Reproduced with permission of Elsevier)

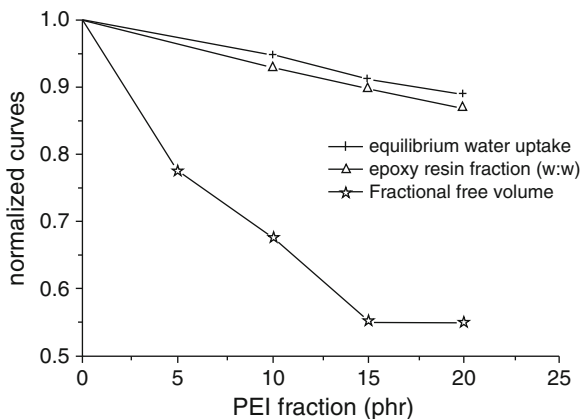
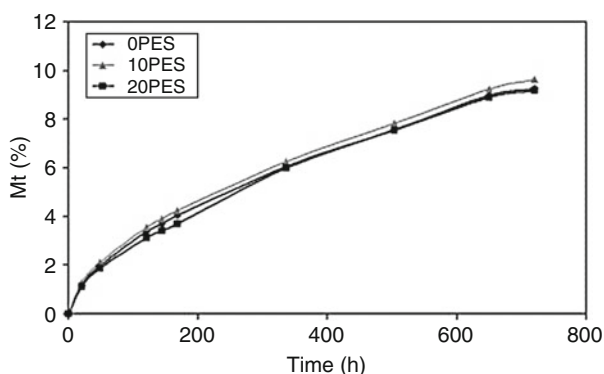


Fig. 10 Water absorption curves for epoxy/PES blends at different PES contents 0PES (0 phr PES), 10PES (10 phr PES), and 20PES (20 phr PES). The graph shows the percentage weight increase (M_t) with time (Alessi et al. 2011) (Reproduced with permission of Elsevier)



physiochemical properties of the constituent polymers may lead to material failure. In an epoxy/polyethersulfone (PES) blend system, progressive segregation effects were observed with formation of domains of different cross-linking degrees upon exposing the blends to hot water for a prolonged period of time (Alessi et al. 2011). Here, blends with different PES content was subjected to water absorption experiments and at the end of 1 month about 9.5–10% W water was absorbed. The absorbed water was expected to form single or double hydrogen bonding within the epoxy networks that lead to segregation of domains and cross-linking. Figure 10 shows the water absorption curves for blends with different PES contents (0–20 phr, per hundred of resin).

Epoxy/Polycarbonate (PC) Blend

The unique properties such as good mechanical strength and high chemical and solvent resistance of epoxy/thermoplastic blends were exploited to prepare bamboo fiber composites containing epoxy/PC as coating material (Rajulu et al. 2001). The

fibers were coated with epoxy/PC blend with different PC content. The coated fibers showed high tensile strength and resistance to acids and alkalis. Particularly, the uncoated fibers absorbed high quantity of water, while the epoxy blend coated fibers showed comparatively good water resistance. Even though the epoxy blend coated fibers showed resistance to acids, alkalis, and water, the coating was not effective against solvents such as benzene and toluene due to solubility of PC in those solvents.

Epoxy/Polysulfone Blend

The interpenetrating polymer networks (IPNs) of DGEBA/DDS and functionalized polysulfone were prepared, and curing behavior and resulting physical properties of these blends were investigated (Tanaka et al. 1997). The polysulfone was modified with pendant vinyl benzyl groups and also with benzyl groups as reactive and nonreactive modifiers, respectively. The epoxy blends containing reactive vinyl benzene modified polysulfone showed higher solvent resistance than the blends with nonreactive polysulfone. This behavior was ascribed to the higher entanglement of epoxy matrix and cross-linked reactive polysulfone and also the difference in phase-separated morphology of the blend.

Conclusions

Nanostructuring of epoxy polymers using block copolymers and thermoplastics to improve their mechanical property is an important area of research in epoxies. Blending epoxy polymers with homo or block copolymers of various compositions and functional groups is a convenient handle to tune the macroscopic properties of epoxies. The water sorption or hydrophilicity of these epoxy blends were controlled via choosing appropriate block copolymer or a thermoplastic component. Generally, epoxy polymers were blended with various homo or block copolymers of varying hydrophilic/hydrophobic degrees to enhance their environmental stability. The adhesiveness of epoxy polymers was also improved via blending block copolymers with appropriate polarity and glass transition temperature. The block copolymers containing polyethylene glycol blocks were found to phase separate into hydrophilic channels that enhanced water sorption properties. On the other hand, incorporation of thermoplastics into epoxies improved their solvent resistance. In general, most of the studies involving epoxy blends have focused on composition-dependent morphology evolution and improving thermal and mechanical properties. The water and solvent sorption properties have been given comparatively less attention particularly in epoxy/block copolymer and epoxy/thermoplastic blends. Understanding water or solvent permeation in epoxy blends may help in developing high thermal and chemical-resistant polymer membranes. The availability of variety of epoxy compatible polymers synthesized via modern polymerization techniques may stimulate

further research in development of nanostructured membranes, adhesives, and coatings.

References

- Agag T, Takeichi T (1999) Synthesis and characterization of epoxy film cured with reactive polyimide. *Polymer* 40(23):6557–6563. doi:10.1016/S0032-3861(99)00026-9
- Alessi S, Conduruta D, Pitarresi G, Dispenza C, Spadaro G (2011) Accelerated ageing due to moisture absorption of thermally cured epoxy resin/polyethersulphone blends. Thermal, mechanical and morphological behaviour. *Polym Degrad Stab* 96(4):642–648. doi:10.1016/j.polymdegradstab.2010.12.027
- Bouvet G, Dang N, Cohendoz S, Feaugas X, Mallarino S, Touzain S (2016) Impact of polar groups concentration and free volume on water sorption in model epoxy free films and coatings. *Progr Org Coat*. doi:10.1016/j.porgcoat.2015.12.011
- Bucknall CB, Gilbert AH (1989) Toughening tetrafunctional epoxy resins using polyetherimide. *Polymer* 30(2):213–217
- Cano L, Builes DH, Tercjak A (2014) Morphological and mechanical study of nanostructured epoxy systems modified with amphiphilic poly(ethylene oxide-b-propylene oxide-b-ethylene oxide)triblock copolymer. *Polymer* 55(3):738–745. doi:10.1016/j.polymer.2014.01.005
- Dean JM, Grubbs RB, Saad W, Cook RF, Bates FS (2003) Mechanical properties of block copolymer vesicle and micelle modified epoxies. *J Polym Sci B* 41(20):2444–2456. doi:10.1002/polb.10595
- Hameed N, Guo Q, Hanley T, Mai Y-W (2010a) Hydrogen bonding interactions, crystallization, and surface hydrophobicity in nanostructured epoxy/block copolymer blends. *J Polym Sci B* 48(7):790–800. doi:10.1002/polb.21950
- Hameed N, Guo Q, Xu Z, Hanley TL, Mai Y-W (2010b) Reactive block copolymer modified thermosets: highly ordered nanostructures and improved properties. *Soft Matter* 6(24):6119–6129. doi:10.1039/C0SM00480D
- Hillmyer MA, Lipic PM, Hajduk DA, Almdal K, Bates FS (1997) Self-assembly and polymerization of epoxy resin-amphiphilic block copolymer nanocomposites. *J Am Chem Soc* 119(11):2749–2750. doi:10.1021/ja963622m
- Jin F-L, Li X, Park S-J (2015) Synthesis and application of epoxy resins: a review. *J Ind Eng Chem* 29:1–11. doi:10.1016/j.jiec.2015.03.026
- Kishi H, Tanaka S, Nakashima Y, Saruwatari T (2016) Self-assembled three-dimensional structure of epoxy/polyethersulphone/silver adhesives with electrical conductivity. *Polymer* 82:93–99. doi:10.1016/j.polymer.2015.11.043
- Könczöl L, Döll W, Buchholz U, Mülhaupt R (1994) Ultimate properties of epoxy resins modified with a polysiloxane–polycaprolactone block copolymer. *J Appl Polym Sci* 54(6):815–826. doi:10.1002/app.1994.070540612
- Lekatou A, Faidi SE, Ghidaoui D, Lyon SB, Newman RC (1997) Effect of water and its activity on transport properties of glass/epoxy particulate composites. *Compos A Appl Sci Manuf* 28(3):223–236
- Li L, Liu M, Li S (2004) Morphology effect on water sorption behavior in a thermoplastic modified epoxy resin system. *Polymer* 45(8):2837–2842. doi:10.1016/j.polymer.2004.02.002
- Li H, Zeng X, Wu W (2008) Epoxidation of styrene-isoprene-styrene block copolymer and its use for hot-melt pressure sensitive adhesives. *Polym-Plast Technol Eng* 47(10):978–983. doi:10.1080/03602550802274696
- Liu J, Thompson ZJ, Sue H-J, Bates FS, Hillmyer MA, Dettloff M, Jacob G, Verghese N, Pham H (2010) Toughening of epoxies with block copolymer micelles of wormlike morphology. *Macromolecules* 43(17):7238–7243. doi:10.1021/ma902471g

- Liu M, Mao X, Zhu H, Lin A, Wang D (2013) Water and corrosion resistance of epoxy–acrylic–amine waterborne coatings: effects of resin molecular weight, polar group and hydrophobic segment. *Corros Sci* 75:106–113. doi:10.1016/j.corsci.2013.05.020
- Mansourian-Tabaei M, Jafari SH, Khonakdar HA (2014) Lap shear strength and thermal stability of diglycidyl ether of bisphenol A/epoxy novolac adhesives with nanoreinforcing fillers. *J Appl Polym Sci* 131(6). doi:10.1002/app.40017
- Messori M, Toselli M, Pilati F, Tonelli C (2001) Unsaturated polyester resins modified with poly(ϵ -caprolactone)–perfluoropolyethers block copolymers. *Polymer* 42(25):09877–09885. doi:10.1016/S0032-3861(01)00521-3
- Nam KH, Kim D, Seo K, Han H (2014) Effect of tetrapod ZnO whiskers on the physical and moisture barrier properties of transparent polyimide/TZnO-W composite films. *Macromol Res* 22(12):1243–1252. doi:10.1007/s13233-014-2187-6
- Ocando C, Serrano E, Tercjak A, Peña C, Kortaberria G, Calberg C, Grignard B, Jerome R, Carrasco PM, Mecerreyes D, Mondragon I (2007) Structure and properties of a semifluorinated diblock copolymer modified epoxy blend. *Macromolecules* 40(11):4068–4074. doi:10.1021/ma070585i
- Pandit R, Michler GH, Lach R, Grellmann W, Saiter JM, Berkessel A, Adhikari R (2014) Epoxidation of styrene/butadiene star block copolymer by different methods and characterization of the blends with epoxy resin. *Macromol Symp* 341(1):67–74. doi:10.1002/masy.201400001
- Rajulu AV, Rao GB, Reddy RL, Sanjeevi R (2001) Chemical resistance and tensile properties of epoxy/polycarbonate blend coated bamboo fibres. *J Reinf Plast Compos* 20(4):335–340. doi:10.1177/073168401772678788
- Sharpe LH (1996) *Adhesion international 1993*. Taylor & Francis. Emmaplein 5, 1075 AW Amsterdam, The Netherlands
- Tanaka N, Iijima T, Fukuda W, Tomoi M (1997) Synthesis and properties of interpenetrating polymer networks composed of epoxy resins and polysulphones with cross-linkable pendant vinylbenzyl groups. *Polym Int* 42(1):95–106. doi:10.1002/(SICI)1097-0126(199701)42:1<95::AID-PI679>3.0.CO;2-C
- Tercjak A, Gutierrez J, Martin MD, Mondragon I (2012) Transparent titanium dioxide/block copolymer modified epoxy-based systems in the long scale microphase separation threshold. *Eur Polym J* 48(1):16–25. doi:10.1016/j.eurpolymj.2011.10.004
- Tong X, Wang Q, Wang H-x, Li X-H, Wu W, Che X-y (2014) Fabrication of pH sensitive amphiphilic hot-melt pressure sensitive adhesives for transdermal drug delivery system. *Int J Adhes Adhes* 48:217–223. doi:10.1016/j.ijadhadh.2013.09.025
- Wang Q, Wang Y-z, Zhao Z-f, Fang B (2012) Synthesis of SIS-based hot-melt pressure sensitive adhesives for transdermal delivery of hydrophilic drugs. *Int J Adhes Adhes* 34:62–67. doi:10.1016/j.ijadhadh.2011.12.002
- Wang L, Shui X, Zheng X, You J, Li Y (2014) Investigations on the morphologies and properties of epoxy/acrylic rubber/nanoclay nanocomposites for adhesive films. *Compos Sci Technol* 93:46–53. doi:10.1016/j.compscitech.2013.12.023
- Wu TH, Foyet A, Kodentsov A, van der Ven LGJ, van Benthem RATM, de With G (2014) Wet adhesion of epoxy–amine coatings on 2024-T3 aluminum alloy. *Mater Chem Phys* 145(3):342–349. doi:10.1016/j.matchemphys.2014.02.022
- Xu Z, Zheng S (2007) Morphology and thermomechanical properties of nanostructured thermosetting blends of epoxy resin and poly(ϵ -caprolactone)-block-polydimethylsiloxane-block-poly(ϵ -caprolactone) triblock copolymer. *Polymer* 48(20):6134–6144. doi:10.1016/j.polymer.2007.07.072
- Yi F, Yu R, Zheng S, Li X (2011) Nanostructured thermosets from epoxy and poly(2,2,2-trifluoroethyl acrylate)-block-poly(glycidyl methacrylate) diblock copolymer: demixing of reactive blocks and thermomechanical properties. *Polymer* 52(24):5669–5680. doi:10.1016/j.polymer.2011.09.055
- Zhang Y, Adams RD, Silva LFM (2014) Absorption and glass transition temperature of adhesives exposed to water and toluene. *Int J Adhes Adhes* 50:85–92. doi:10.1016/j.ijadhadh.2014.01.022

Index

A

ABC terpolymer, 860
ABS blends. *See* Poly(acrylonitrile-*block*-butadiene-*block*-styrene) (ABS) blends
Absorption models, 327, 328, 334
Adhesives, 1105
Amino-terminated butadiene-acrylonitrile (ATBN), 6–7
Amphiphilic block copolymers, 852, 854
Anti-Stokes scattering, 169
Applications, 203, 204, 206
 epoxy-rubber blend, 207
 epoxy/thermoplastic blends, 781–793
Asymmetrical system, 497
Asymmetric distribution, 748, 770
Atomic-force microscopy (AFM), 385, 386
Autocatalytic process, 995

B

BCP. *See* Block copolymer (BCP)
Bicontinuous structure, 488, 491, 500, 503, 506, 508, 510, 512, 515, 518
Binodal curve, 71, 72, 74, 75, 81
Blend(s)
 composition, 859
 cured, 462, 464, 469
 diglycidyl ether of bisphenol A (DGEBA), 468, 473
 DMTA (*see* Dynamical mechanical thermal analysis (DMTA))
 epoxy/thermoplastic (*see* Epoxy/thermoplastic blends)
 ER/BCP, 924–926
 poly(hydroxyl amino ether) (PHAE), 473
 poly(phenylene ether) (PPE), 467
 poly(trimethylene terephthalate) (PTT), 468
 PVME/epoxy, 781

 thermoset/thermoplastic, 776, 779, 781, 782, 792
Block copolymer (BCP), 13, 22–23, 405–406, 413, 417, 558, 828, 836, 842, 851, 859, 873, 920, 921, 923, 926, 927, 936, 946, 952
 architecture, 861
 amphiphilic ABA-type triblock copolymers, 894–900
 amphiphilic diblock copolymers, 887–894
 blend (*see* Epoxy/block-copolymer blends)
 chemical compatibilization, 901–905
 epoxy/poly(styrene-*b*-butadiene), 963–966
 epoxy/poly(styrene-*b*-butadiene-*b*-styrene), 966–971
 epoxy/poly(styrene-*b*-ethylene oxide), 971–974
 gelation point, 959
 hyperbranched, 213
 morphologies, 887
 PCL–PDMS–PCL, 1099
 polystyrene based, 563
 poly(styrene-*b*-caprolactone), 577
 poly(styrene-*b*-ethylene oxide), 1102
 poly(styrene-*b*-methyl methacrylate), 961–963
 poly(2,2,2-trifluoroethyl acrylate)-*block*-poly(glycidyl methacrylate), 1102
 PS-*b*-PCL, 568
 reactivity, 863–864
 ternary systems, 905–913
 thermoplastics, 1105
Bridge-like conformation, 862

C

Carbon nanofiller, 770
Carboxyl-terminated butadiene-acrylonitrile (CTBN), 5–6, 23, 285

- Carboxyl-terminated butadiene-acrylonitrile (CTBN) (*cont.*)
 and ATBN, 6, 7
 and ETBN, 7
- Carboxyl-terminated poly(2-ethyl hexyl acrylate) (CTPEHA), 14
- Chemical characterization, 584
- Chemorheology, 190, 622, 644
- Cloud-point curve (CPC), 489, 491
- Cloud-point temperature, 80, 81, 86
- ¹³C-NMR spectrum, 167
- Coalescence, 383, 500, 510
- Coating applications, 871
- Commercial systems, 776, 798
- Compatibility, 698, 1017, 1019, 1032, 1034, 1035
- Composition, 489, 491, 504, 506, 514, 515
- Concentration, 489, 495, 496, 503, 506, 507, 512, 514, 515, 518
 profiles, 320, 334
 of thermoplastic, 449
- Contact angle, 1099, 1100, 1103
- Conversion, 489, 495, 496
- Core-shell particles (CSPs), 10, 11
- Core-shell rubber (CSR), 10–13
- Critical conditions, phase separation, 73
- Critical interaction parameter, 78, 82
- Critical segregation limit, 847
- Critical stress intensity factor, 873
- Crosslink, 946, 950–952, 1108
 epoxy network, 845
 network, 864
- Crystallinity, 1048, 1050
- Cure(ing), 584, 589, 591, 595, 601, 602, 604, 608
 agent, 82, 83, 85–87
 conversion, 847
 kinetics, 216, 980, 982, 986, 989, 992, 996, 998, 999
 process, 853
 protocols, 87–88
 reaction, 351
 shrinkage, 225–226, 231, 332–333, 642, 804–821
 temperature, 871
- Cycloaliphatic amine cured resins, 652
- Cylinders, 891, 904, 909
- D**
- Degradation, 1106
- Degree of polymerization, 845
- Demixing process, 854
- 4,4-diaminodiphenylmethane (DDM) system, 983, 986, 989, 992
- Dielectric relaxation spectroscopy, 605–606
- Differential expansive bleeding (DEB), 720
- Differential scanning calorimetry (DSC), 218–224, 287, 355, 658–659
- Diffusion, 323, 592
 ambipolar, 326
 characterization, 320
 coefficient, 326
 Fickian and non-Fickian, 330
 Fick's first law, 325
 models and mechanisms, 327–331
 random walk, 325
- Diglycidyl ether of bisphenol A (DGEBA), 148, 844, 855, 983, 986, 988, 989, 992
- Double polymerization, 857
- Dry-brush, 860, 866
- Ductility, 174
- Dynamic(s), 922, 924
 asymmetric phase separation, 507, 518
 asymmetry, 492, 494, 503, 505, 506, 510, 513, 515, 518
 cross-linked network, 949–950
 heterogeneous, 926
 interphase composition and heterogeneous, 943
 microphase structure, 950–952
- Dynamic mechanical thermal analysis (DMTA), 723
 ATBN rubber, 240–241
 CTBN rubber, 241–243
 liquid natural rubber, 243–244
 nanostructured epoxy rubber blends, 244–246
- E**
- Einstein's equation, 378
- Electron microscopy, 92–94
- Endgroups, 435, 447, 448–449, 455
- Endothermic peak, 354
- Energy of mixing, 851
- Epoxidation degrees, 847
- Epoxidation reaction, 170
- Epoxidized hydroxyl-terminated polybutadiene (ETPB), 8–9
- Epoxidized natural rubber (ENR), 20, 22
- Epoxidized soybean oil (ESO), 20
- Epoxy, 70, 921, 923, 943–945
 based blends, 809, 810, 812, 814, 820, 1099–1109 (*see also* Block copolymer (BCP))

- conversion, 847, 849, 860
- liquid rubber-modification, 416
- prepolymer, 31, 53, 58
- system, 842, 849, 858, 860, 864, 872, 873, 876, 877
- Epoxy-amine system, 983, 986, 989
- Epoxy based particulate composites
 - preparation of, 373–374
 - silicone modifiers and core-shell rubber particles, 387–390
- Epoxy/block copolymer
 - nanostructured morphology
 - (*see* Nanostructured morphology)
 - phase separation mechanism, 829–830
 - reaction induced microphase separation (RIMPS), 830–832
- Epoxy/block copolymer blends
 - architectures, 1076–1079
 - block ionomer complexes, 1079
 - crosslinking density, 1083–1084
 - curing conditions and agents, 1082–1083
 - epoxy/poly (butadiene-co-acrylonitrile) (PS-PAN) blends, 982
 - fracture toughness, 1070–1071
 - isothermal DSC analyses, 988–999
 - non-isothermal DSC analyses, 983–988
 - nanophases formation, 1069–1070
 - nanophases mechanism, 1079–1082
 - nanophases morphologies, 1074–1076
 - reactivity, 1071–1074
 - strain conditions, 1084–1086
 - toughness improvement, 1086–1090
- Epoxy/clay nanocomposite, 350–353
- Epoxy/liquid rubber blends
 - crosslinking density, 291
 - curing agent, 292–294
 - curing times and temperatures, 286–289
 - fracture and impact test, 294–305
 - glass transition, matrix and rubbery phase, 291
 - interfacial adhesion, 286
 - rubber concentration, particles size, and distribution, 284–285
 - tensile properties, 306–310
 - test temperature and rate, 289–291
 - toughening mechanism, 282–284
 - volume fraction, 294
- Epoxy-philic segment, 849
- Epoxy resin(s), 4, 39–59, 148, 155–156, 375–376, 385–387, 434–437, 462, 481, 524–525, 584, 590, 601, 650, 659, 712–715, 744, 750, 751, 755, 756, 762, 764, 769, 771, 828, 835, 1042, 1098
- amine curing agent, 713
- curing, 650–654
- diglycidyl ether of bisphenol A-based, 148
- fracture toughness of, 435
- gel point, 714
- glycidyl group, 712
- hydroxyl-terminated silicone oligomer-bridged, 153
- molar mass, 440, 441
- molecular weight, 440
- PES in, 434
- thermoplastic modification of, 430
- trifunctional and tetrafunctional epoxy resins, 432
- market consumption and application, 712, 713
- physical forms, 712
- terpolymer/tri-block copolymer blends
 - (*see* Terpolymer/tri-block copolymer blends)
- three-membered ring structure, 715
- TP blends (*see* Thermoplastic (TP) blends)
- TTT, 714 (*see also* Epoxy/thermoplastic blends)
- Epoxy-rubber blends, 186, 321, 324, 326, 329
- applications, 207
- atomic force microscopy, 127–133
- DMTA (*see* Dynamic mechanical thermal analysis (DMTA))
- evolution, phases, 200–201
- linear thermal expansion behavior, 263–267
- optical microscopy, 103–113
- phase separation, 82–83
- phase separation, techniques for, 88–94
- scanning electron microscopy, 113–127
- thermal conductivity and heat capacity, 262–263
- thermal properties, 251–262
- thermodynamics, 201–202
- transmission electron microscopy, 135–140
- viscoelastic models, 194–195
- Epoxy-rubber networks, 52
- Epoxy/rubber system
 - adduct, 416
 - adhesives, 419
 - autocatalytic kinetics model, 220
 - biocompatible, 420
 - block copolymers, 405–406
 - carbon-fiber, 412
 - chemorheological models, 227
 - coatings, 406–411
 - commercial product, 415
 - complex viscosity versus time plot, 230

- Epoxy/rubber system (*cont.*)
- composites, 411–414
 - core/shell, 213
 - covalent interactions, 212
 - cross-linking process, 215
 - cure characteristics, 224
 - cure kinetics, 216
 - di-block copolymer, 414
 - DSC, 218–224
 - fiber-reinforced, 411
 - FORTEGRA™, 408
 - glass-fiber, 412
 - kinetics analysis, 218–224
 - micrographs, 223
 - modifiers, 402
 - nanoparticulate composites, 214
 - oligomer with liquid rubber, 77–82
 - optimal curing, 219
 - phase separation, factors, 83
 - preformed particles, 404–405
 - PVT measurements, 224–226
 - reactive oligomers, 403–404
 - real time FTIR spectroscopy, 224–226
 - rheological studies, 226–232
 - rubber toughening, 401–402
 - thermosetting materials, 212
 - thermosetting polymers, 214, 228
- Epoxy-terminated butadiene-acrylonitrile (ETBN), 7
- Epoxy/thermoplastic blends
- adhesive bonding, 788–793
 - batch mixers, 463–469
 - composite matrices, 781–788
 - continuous mixers, 469–476
 - continuous polymerization reactor, 476–478
 - cure reaction induced phase separation, 461
 - dielectric relaxation spectroscopy, 605–606
 - dynamic kinetic analysis, 660–662
 - energy dispersive X-ray spectroscopy, 604–605
 - fluorescence spectroscopy, 599–602
 - infrared spectroscopy, 588–592
 - in-situ dissolution, 482–483
 - in-situ polymerization, 480–482
 - interlaminar morphologies, 779
 - isothermal kinetic analysis, 662–669
 - morphology, 525
 - nuclear magnetic resonance (NMR) spectroscopy, 595–599
 - phase separation, 524
 - polymerization-induced phase separation (*see* Polymerization-induced phase separation)
- positron annihilation lifetime spectroscopy, 606
- Raman spectroscopy, 593–595
- resonant acoustic mixer (RAM), 480
- self-healing materials, 793
- self-healing properties, 795
- small-angle X-ray scattering, 608
- solvent casting, 479
- thermal properties, 779
- thermal shape memory effect, 796
- thermoplastic polymers, 780
- toughening technologies, 778
- Veriflex EH, 796
- vibrational spectroscopy, 585–588
- viscoelastic effect, 550–554
- viscoelastic phase separation, 540–550
- wide angle X-ray diffraction, 608
- Etherification, 652
- Ethylene glycol dimethacrylate (EG-DMA), 12
- F**
- Finite element modeling, 386
- Flexural modulus, 352
- Flory-Huggins interaction parameter, 845, 851
- Flory-Huggins model, 850
- Fluorescence spectroscopy, 599–602
- Flynn–Wall–Ozawa method, 657
- Formation, 491, 494, 511
- Fourier transform infrared spectroscopy (FTIR), 154–163, 984, 986, 987, 995, 1001
- Fracture resistance, 873
- Fracture toughness, 381, 430, 432, 434, 435, 437, 447, 448, 829, 835, 836, 875
- Fractured surface, 500, 502, 504, 507, 508, 514
- Free energy, 851
- G**
- Gelation, 496, 499, 502, 515
- Gel point, 622, 623, 636, 637, 714, 851, 864
- Glass transition temperature (T_g), 251, 494, 505, 507, 514, 516, 518, 678–681, 1008, 1010, 1011, 1013, 1015, 1019, 1020, 1022, 1026, 1027, 1030, 1031, 1034, 1036, 1043, 1045, 1054, 1056, 1062
- epoxy/natural rubber blends, 251–252
 - epoxy/nitrile rubber blends, 253–256
 - epoxy/polybutadiene rubber blends, 252–253
 - epoxy/polyurethane rubber blends, 256–259
 - epoxy/silicon rubber blends, 260–262
- Glycidoxypropyl triethoxy silane (GPTS), 393
- Glycidyl group, 712
- Glycidyl methacrylate (GMA), 12, 13

H

- Halpin and Tsai model, 379
- Hardener(s), 651, 864–866
- HPB
 - (hyperbranched epoxy), 353
 - (hyperbranched polymers), 105, 694, 701, 812–814
- HBPU (hyperbranched polyurethane), 258, 272
- Heat distortion temperature (HDT), 373
- Heating-induced “bleeding” behavior, 721
- ¹H-NMR spectra
 - carboxyl-terminated butadiene acrylonitrile copolymer, 166
 - epoxy siloxane, 164
 - PCL-*b*-PBN-*b*-PCL triblock copolymer, 166
- Homopolymer, 1099
- Hydrodynamic flow, 494, 504, 506, 513
- Hydrogen bonding, 1100
- Hydrophilic polymer, 876, 1099, 1102, 1104
- Hydrophobic polymer, 876, 1099, 1102, 1104
- Hydroxy-terminated polybutadiene (HTPB), 7–8
- Hygrothermal conditioning, 321–323
- Hyperbranched epoxy (HBP), 353
- Hyperbranched polymer (HBP), 105, 694, 701, 812–814
- Hyperbranched polyurethane (HBPU), 258, 272

I

- Impact strength
 - epoxy-rubber blends, 349, 350
 - ternary systems, 362
- Infrared spectroscopy, 588–592
- Interaction parameter, 851
- Interfacial curvature, 859
- Interpenetrating polymer networks (IPNs), 150, 151
- Interphase, 921, 922, 926, 927
 - characterization, 930–936
- Isothermal kinetic model, 655–656

K

- Kamal model, 655–656
- Kinetic analysis, 657–659
- Kinetic modeling, 655
- Kissinger method, 656–657

L

- Lap shear strength (LSS), 21
- Layered structure, 502, 504, 506, 508, 510, 512–517

- Light scattering, 81, 87, 91, 92, 95, 491, 492, 496, 499, 508, 509, 526, 527, 559, 560, 570
- Light transmittance, 80
- Liquid rubber, 33–34, 57–59, 70, 102, 108, 110, 137, 149–150
 - epoxy oligomer, 77–82
- Loop-like conformation, 861
- Lower critical solution temperature (LCST), 72

M

- Macrophase separation, 843, 844
- Mechanistic model, 981, 992, 994, 1001
- Melting temperature, 1047, 1057
- Micelles, 885, 886, 889, 897, 898, 903, 909, 911
- Microdomain, 920, 922, 930, 950–952
- Micro modifier, 411
- Microphase separation mechanisms, 843, 856, 1099
 - experimental strategies, 857–858
 - immobilization by polymerization, 852–853
 - multiple polymerization, 856–857
 - polymerization and demixing process, 854
 - polymerization and reaction, 855–856
 - self-assembly (SA), 852
 - “Tandem-like” mechanisms, 853
- Micro-rheology, 191
- Microscopic techniques
 - atomic force microscopy, 127–133
 - optical microscopy, 103–113
 - scanning electron microscopy, 113–127
 - transmission electron microscopy, 135–140
- Miscibility, 70, 71, 80, 81, 83, 86, 88, 96, 150, 153, 164, 489, 518, 846, 872, 921, 922, 926, 927, 935, 941, 946, 952, 1045, 1048, 1053, 1055, 1057, 1058, 1062
 - epoxy oligomer with liquid rubber, 77
- Miscible block, 854, 867
- von Mises stresses, 376, 377
- Mixing
 - continuous mixers, 469–476
 - internal mixers, 465–467
 - low shear liquid batch mixer, 463–465
 - resonant acoustic mixer (RAM), 480
 - rheo mixing (RMX), 467–469
 - solvent casting, 479
- Mobility, 493, 504, 515, 518
- Modulus, 615, 620, 621, 637, 644
- Moisture uptake, 318, 329
- Molecular deformation theories, 191–195
- Molecular weight, 431, 440, 449–451

- Montmorillonite, 342, 350, 362
- Mooney's equation, 379
- Morphology, 70, 84, 85, 87, 89, 92, 97, 488, 494, 495, 499, 503, 511, 514, 517, 573, 574, 577, 578, 595, 604, 616–617, 626, 628, 631, 644, 764, 852, 1099, 1106
- of binary TS/TP mixtures, 749–751
 - pattern, 865
 - of ternary TS/TP-based composites, 751–756
- Multiple polymerization, 856–857
- m-Xylylenediamine system, 988
- N**
- Nanoclay, 342
- Nanocomposites
- rubber modified epoxies, 391–392
 - sol–gel process, 392–395
- Nanodomain, 862, 871, 876
- Nano-modifier, 409, 411
- Nanostructure(s), 884, 885, 888, 894, 896, 904, 913
- ER/BCP blends, 943
 - formation, 923
- Nanostructured morphology
- formation, 832–835
 - reaction induced microphase separation (RIMPS), 833
 - self assembly, 831–832
 - toughening, structure property correlation, 835–836
- Natural rubber, 343
- Neilson's equation, 379
- Nuclear magnetic resonance (NMR)
- epoxy/rubber blends, 164–168
 - sample preparation, 163
 - spectrometer, 163
 - spectroscopy, 595–599
- Nucleation and growth (NG), 491
- Nucleation and growth separation, 76
- O**
- Optical microscopy, 89–91, 170–174
- sample preparation, 171
 - synthesis and application, 171–174
- Organoclay, 351
- Osmosis, 323, 330
- P**
- Particulate composites, 395–396
- definition, 372
 - fracture toughness, 381
- rubber modified epoxy resin (*see* Rubber modified epoxy resin)
 - theories of strength, 379–381
- Petrographic polishing technique, 171
- Phase behavior, 921, 922, 926–929
- Phase composition, 585
- Phase contrast optical microscope (PCOM), 497, 499, 500, 503, 508
- Phase diagram, 490, 491, 494, 512
- polymer-polymer system, 71–72
- Phase inversion, 491, 492, 513
- Phase separation, 200, 202, 204, 207, 344, 346–350, 461, 462, 558, 562, 745, 751, 753, 762, 843–857, 957, 958, 962, 966
- behavior, 847
 - critical conditions, 73–74
 - DGEBA/phenoxy bends, 574
 - epoxy/poly(acrylonitrile-*block*-butadiene-*block*-styrene) (ABS) blends, 570
 - epoxy/polycarbonate blends, 577
 - in epoxy/polyetherimide/SiO₂ blend, 568, 577
 - epoxy resin/poly(ether sulfone), 559
 - epoxy/rubber blends, 82–83
 - factors, epoxy/rubber system, 83–88
 - limit, 847
 - mechanisms, 74–77, 829–830
 - nematic EBBA liquid crystal, 566
 - polystyrene, 565
 - rate, 851
 - process, 171
 - reaction induced, 560
 - techniques, 88–94
 - thermodynamics, 71–77
- Phase structure, 688, 1010, 1015, 1037
- Phenomenological model, 981, 993
- Plasticization, 874
- Polyacrylate rubber, 151–152
- Poly(acrylonitrile-*block*-butadiene-*block*-styrene) (ABS) blends, 725–728
- Poly(acrylonitrile-*block*-butadiene-*block*-styrene), 726
- Poly(butyl acrylate) (PBA), 12
- Poly(2,6-dimethyl-1,4-phenylene ether) (PPE), 724
- Polydimethylsiloxane (PDMS), 152, 387
- Poly(ϵ -caprolactone) (PCL) blends, 719–722
- PCL-PPC/PB-PCL blend, 728–730
- Polyetherimide (PEI) blends, 730
- Poly(ether sulphone) (PES) blends, 723
- Poly(ethylene glycol) (PGA) blends, 715
- Poly(ethylene oxide) (PEO), 715–718
- Polymer blends, 559, 747, 748, 756, 769, 770
- See also* Block copolymer
- Polymerization, 848, 850, 852–854

- Polymerization induced microphase separation, 848, 850, 857
- Polymerization-induced phase separation
- curing agent, 539
 - light scattering, 526, 527
 - linear block copolymers, 537–539
 - molecular weight, 530–532
 - physical and chemical properties, 525
 - preure temperature, 534–536
 - reactive end group, 532–534
 - SEM, 527
 - thermoplastics concentration, 528–530
 - viscoelastic phase separation, 541–550
- Polymerization rate, 851, 871
- Polymer nanocomposites, 342
- Polymer-solvent interaction parameter, 843
- Poly(methyl methacrylate) (PMMA), 12, 722
- Polyoxymethylene (POM) blends, 728
- Polyoxypropylene diamine (POPDA), 661
- Poly(styrene-*block*-butadiene-*block*-methyl methacrylate) (PSBMMMA) blends, 732
- Poly(styrene-*block*-butadiene-*block*-styrene) (SBS) blends, 733–736
- Positron annihilation lifetime studies (PALS), 385
- PPE/DGEBA epoxy system, 724
- Processing, 190, 199, 202–206
- Property degradation, 316, 321
- pVT analysis, 199, 217, 224–226, 231, 804–821
- R**
- Raman spectroscopy, 168–170, 593–595
- Rayleigh scattering, 168
- Reaction-induced/chemically induced phase separation, 725
- Reaction induced microphase separation (RIMPS), 829–832, 835, 836, 850
- Reaction-induced phase separation (RIPS), 439–446, 491, 492, 494, 602, 663
- Refractive index (RI), 491, 508, 509
- Relaxation, 493, 495, 497, 503, 506, 515, 923, 924, 926, 949
- Rheology, 186, 229, 231
- chemo-rheology, 190
 - epoxy/poly(styrene-*b*-butadiene) block copolymer, 963–966
 - epoxy/poly(styrene-*b*-butadiene-*b*-styrene) block copolymer blends, 966–971
 - epoxy/poly(styrene-*b*-ethylene oxide) block copolymer blends, 971–974
 - epoxy/thermoplastic blends, 958
 - fluids, 187
 - gelation point, 959
 - micro-rheology, 191
 - poly(styrene-*b*-methyl methacrylate), 961–963
- Rheotriology, 206
- Rubber(s), 810, 814–819
- ATBN, 408
 - automotive coatings, 406
 - barrier coatings, 409
 - blends, coatings, 406–411
 - can coatings, 406
 - coil coatings, 407
 - core-shell modifiers, 213, 404
 - CTBN, 408
 - Kissinger method, 221
 - liquid, 149
 - marine coatings, 407
 - modification, 416
 - modified epoxy, 216
 - modifying agent, 217
 - morphological parameters, 215
 - phenomenological approach, 218
 - powder coatings, 407
 - protective coatings, 407
 - second phase particles, 402
 - sequential processes, 214
 - silicon-based, 411
 - urethane, 150
- Rubber blends, DMTA. *See* Dynamic mechanical thermal analysis (DMTA)
- Rubber/epoxy blends. *See* Epoxy/rubber blends
- Rubber modified epoxy resin
- 2-D models, 375
 - mechanical properties, 377–378
 - nanoparticles, 390–391
 - stress distribution, 376
 - volume fraction, 377
- Rubber particles, 35–37
- Rubber-polybutadiene blend, 382
- Rubber toughened epoxy, 343–346, 353–354
- Rubber toughened epoxy polymers
- ATBN, 6–7
 - BCPs, 13, 22–23
 - bio-based tougheners, 19–22
 - CSR, 10–13
 - CTBN, 5–6
 - ETBN, 7
 - functionalized polybutadiene rubber, 7–9
 - matrix characteristics, 15–16
 - particle size, 15
 - rubber content, effect of, 14–15
 - toughening mechanisms, 16–19
- Rubber toughened epoxy/clay nanocomposite, 353–354

S

- SBM triblock copolymer, 1076
- Scanning electron microscopy (SEM), 87, 88, 92, 93
- Secondary phase separation, 491, 492
- Self-assembly, 852
- Self-assembly, nanostructured morphology, 829–830
- Shear, 186, 187, 191, 193, 197, 203, 205
- Shrinkage. *See* Cure shrinkage
- Shrinking, 502–503, 505–506, 512
- Silicone rubber, 152
- Small angle laser light scattering (SALLS) technique, 179
- Small-angle light scattering (SALS) technology, 179
- Small-angle X-ray scattering (SAXS), 175–177
- Sol–gel process, 390, 392–395
- Solid-state NMR technique
 - ER/BCP blends, 924–926
- Solid-state ²⁹Si-NMR spectrum, 168
- Solubility parameter(s), 77, 78, 80, 81, 86, 844, 865
- Solvent absorption, 1099
- Solvent sorption, 333
- Specific intermolecular interactions, 595, 598
- Spectroscopic techniques, epoxy/thermoplastic blends. *See* Epoxy/thermoplastic blends
- Spinodal curve, 74, 76
- Spinodal decomposition (SD), 491, 508, 534
- Spinodal separation, 75
- Star polymer(s), 812–813, 1077
- Static light scattering, 346
- Stokes scattering, 169
- Strain energy, 873
- Stress distribution, 376
- Structural relaxation, 608
- Surface free energy, 1099, 1100, 1102

T

- Tandem-like mechanisms, 853
- Ternary systems
 - glass transition temperature, 359–362
 - impact strength, 362–364
 - morphology, 356–359
- Terpolymer/tri-block copolymer blends
 - ABS, 725
 - PCL-PPC/PB-PCL Blends, 728
 - PEI, 730
 - POM, 728
 - P-SBMMA, 732–733
 - SBS, 733
- Thermal conductivity
 - CTBN and HTPB volume fraction, 264
 - heat capacity, epoxy/rubber blends, 262–263
- Thermal expansion behavior
 - epoxy/rubber blends, 263–267
 - quenched samples and strained samples, 266
- Thermal stability
 - epoxy and silicon rubber blends, 272–274
 - epoxy/natural rubber, 267–268
 - epoxy/nitrile rubber blends, 268–270
 - epoxy/polybutadiene rubber blends, 268
 - epoxy/polyurethane rubber blends, 270–272
- Thermodynamics
 - epoxy-rubber blend, 201–202
 - of phase separation, 71
- Thermoplastic based nanocomposite, 342–343
- Thermoplastic (TP) blends, 558, 569, 573, 574, 579, 809–813, 1099, 1105
 - See also* Epoxy/thermoplastic blends
 - PCL, 719
 - PEO/PGA, 715
 - PES, 723
 - PMMA, 722–723
 - PPE, 724–725
- Thermoset(s), 46, 55
 - based nanocomposite, 343
- Thermoset/thermoplastic (TS/TP) blends
 - mechanical properties, 758–769
 - morphology (*see* Morphology)
- Thermosetting curing process, 714
- Thermosetting (TS) polymers, 709
- Thermosetting resins, 711
- Time resolved light scattering, 562, 563, 567, 572
- Time-resolved small-angle light scattering (TRSALS), 346
- Time-temperature superposition (TTS)
 - principle, 624, 634, 644
- Time-temperature-transformation (TTT), 489, 714
- Toughening mechanisms, 451–455, 873
- Toughness, 173, 677, 684, 686, 688, 1008, 1010, 1012, 1015, 1037
- Transamidation reaction, 662
- Transmission electron microscopy (TEM), 88, 92, 94
- Transmission optical microscopy (TOM), 984
- Triblock copolymer, 861, 862, 865
- Trifluoropropyl siloxane (TFP), 390
- 1,1,1-Tris(4-hydroxyphenyl)ethane (THPE), 1086

U

Upper critical solution temperature (UCST), 72, 849, 865, 871
Urethane rubber, 150

V

Velocity, 493, 494
Viscoelastic effect, 550–554
Viscoelastic models, 194–195
Viscoelastic phase separation (VPS), 492, 494, 503, 506, 615, 617, 625, 630
 modeling, 632–635
 polymerization-Induced, 541–550
 rheological analysis, 630–632
Viscoelastic properties, 684, 964, 965, 972, 1012
Viscosity, 615, 620, 622, 625, 629, 634, 638
 molding, 641–643
 prepreg materials, 640–641
Vitrified state, 651

Volume fraction, 492, 502, 505, 512
Volume shrinkage, 502, 506, 804, 808, 816, 818, 820

W

Water absorption, 1105, 1106, 1108
Water uptake, 606
Wet-brush state, 866
Wide-angle X-ray scattering (WAXS), 177–179
Williams–Landel–Ferry (WLF) equation, 624
Worm-like micelles, 886, 892, 895, 897, 900, 902, 909, 913

X

X-ray spectroscopy, 604–605

Y

Young's modulus, 376